power systems

F. Kiessling · P. Nefzger
J. F. Nolasco · U. Kaintzyk

Overhead Power Lines

Planning
Design
Construction

Springer

Power Systems

F. Kiessling · P. Nefzger · J. F. Nolasco · U. Kaintzyk
Overhead Power Lines

Springer
Berlin
Heidelberg
New York
Hong Kong
London
Milan
Paris
Tokyo

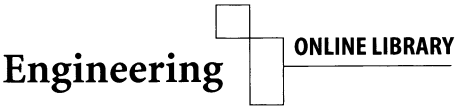

F. Kiessling · P. Nefzger · J.F. Nolasco · U. Kaintzyk

Overhead Power Lines

Planning, Design, Construction

With 402 Figures and 193 Tables

Springer

Dr.-Ing. Friedrich Kiessling

Rosenstraße 18
91083 Baiersdorf
Germany

E-mail: fr.kiessling@easynet.de

Dipl.-Ing. Peter Nefzger

Koenigsberger Weg 2
30966 Hemmingen
Germany

peter.nefzger@t-online.de

Dipl.-Ing. João Felix Nolasco

Rua Rodrigues Caldas 726/s905
30190-120 Belo Horizonte
MG
Brasil

E-mail: jfnolasc@bis.com.br

Dipl.-Ing. Ulf Kaintzyk

Siemens AG
Power Transmission and Distribution
Paul-Gossen-Straße 1
91052 Erlangen/Germany

E-mail: ulf.kaintzyk@siemens.com

ISBN-13: 978-3-642-05556-0 e-ISBN-13: 978-3-642-97879-1
DOI: 10.1007/978-3-642-97879-1

Cataloging-in-Publication Data applied for
Bibliographic information published by Die Deutsche Bibliothek.
Die Deutsche Bibliothek lists this publication in the Deutsche Nationalbibliografie;
detailed bibliographic data is available in the Internet at <http://dnb.ddb.de>

This work is subject to copyright. All rights are reserved, whether the whole or part of the material is concerned, specifically the rights of translation, reprinting, reuse of illustrations, recitation, broadcasting, reproduction on microfilm or in other ways, and storage in data banks. Duplication of this publication or parts thereof is permitted only under the provisions of the German Copyright Law of September 9, 1965, in its current version, and permission for use must always be obtained from Springer-Verlag. Violations are liable for prosecution act under German Copyright Law.

Springer-Verlag Berlin Heidelberg New York
a member of BertelsmannSpringer Science+Business Media GmbH

http://www.springer.de

© Springer-Verlag Berlin Heidelberg 2003
Softcover reprint of the hardcover 1st edition 2003

The use of general descriptive names, registered names, trademarks, etc. in this publication does not imply, even in the absence of a specific statement, that such names are exempt from the relevant protective laws and regulations and therefore free for general use.

Typesetting: Camera ready by authors
Cover-design: deblik, Berlin
Printed on acid-free paper 62 / 3020 hu - 5 4 3 2 1 0 -

Foreword

It is a great honour to be asked by the authors to prepare a foreword to this book on overhead lines.

Electricity has been used as a major energy source since the late 19th century. In 1891, three-phase alternating current transmission started, when a 175 km long line was commissioned to supply electricity to an international electrical engineering exhibition held in Frankfurt am Main (Germany). Since electric energy cannot be stored, generation in power plants and consumption need to be permanently balanced requiring powerful transmission systems. Such systems were installed in many parts of the world in the 20th century utilising step by step rising voltages. The 110 kV voltage was used in Germany in 1912; lines adopting 220 kV were opened there in 1929; in 1952, 400 kV transmission started in Sweden; the first 750 kV line was installed in Canada in 1965 and a 1200 kV line in the former Soviet Union in 1985.

Even in developing countries such as South Africa, electric streetlights were used in Kimberly already in 1882, a time when London still relied on gas. As in other parts of the world, industrial development such as mining activities, resulted in many independent power producers being formed to supply small networks in South Africa. Transmission voltages of up to 44 kV were used in the 1930's. As development grew, it became apparent that it was more cost effective to transmit energy over long distances in the form of electricity than to transport coal or gas and generate at the load. This led to developments of higher and higher voltages generally 275 kV in the 1950's, 400 kV in the 1960's and 765 kV in the 1980's.

Transmission lines form the backbones in power networks, being the installations which transmit power over long distances. They are the most valuable constituents of the network often costing as much as or more than an entire substation. In addition, lines are uniquely designed for every application. Other devices such as breakers and transformers can be standardized to a large extent. Each line has a different number of towers, foundation types and unique problems that need to be solved. Lines are installations that can be tailor made to the requirements on the individual network. Thus, specific conductor, tower and foundation combinations can be used to provide for the optimum impedance and power transfer characteristics of the line. The lines determine the power flow and influence the ability to control the network under normal and emergency conditions. Thus, designing and installing incorrect lines can have serious impacts on the viability of the network. In the deregulated environment, this is even more important and inappropriate designs can affect trading ability as well as economic profitability of asset owners and traders.

It could be argued that overhead transmission lines are but one solution to transmit power over long distances, the other being underground cables. However, overhead lines have distinct advantages over cables. The costs of cables vary between three and ten times the costs of overhead lines, the higher ratios being found at higher voltages. Overhead lines are a lot more forgiving when it comes to overloading than cables. In most cases, the integrity of a line is not at all affected with short-term overloads and catastrophic failures are extremely rare. Line damage can be more easily discovered and repaired rapidly, e. g. with emergency structures being put in place. Transmission lines can be altered in situ to accommodate the change in requirements of the network being especially important in the light of the deregulation of the industry and power trading. On the other hand, an overhead line could be a fragile system constituent

where one failed joint or such a component would render ineffective the entire line, stretching over many kilometres. This is why line operation and maintenance practices are so important to the integrity of systems and gain growing significance in ageing networks.

A line is thus the result of solving a complex combination of mechanical, electrical and civil design, construction, operation and maintenance issues. As such, there are very few persons who are knowledgeable in the entire ambit of line design and implementation. This new book covers all aspects of overhead line planning, design, construction, operation and maintenance and allows engineers to understand the complexity as well as the interdependence between its components. An example is that in order to improve the power transfer ability of a line, phases may need to be brought closer together. This impacts the tower and foundation loading as well as the corona inception voltage etc. Exactly how and to what extent the one option affects the other components takes long periods of study to determine. The book has been written pursuing a three step procedure, with the theory been dealt with initially and followed then by the main components. The third area covers the planning, construction, operation and maintenance of specific lines.

The study of all aspects of transmission lines has been the subject of International Council on Large Electric Systems (Cigré) for many years. In the 1960's, the Study Committee SC22 was formed devoted entirely to the study of all aspects of transmission lines. Over the years, SC22 has presented papers in the open sessions, developed and published reports in Electra as well as numerous brochures. These formed the basis for preparing the book together with standards from IEC and CENELEC. The authors have participated and contributed actively in Cigré for many years. They have been recognised as experts in their fields by being appointed in some cases as Special Reporters on more than one occasion. The book can, therefore, be considered a result of SC22's activities as well.

To my knowledge, there is no book on the market that so comprehensively covers all aspects relating to overhead lines. In this regard, this book is a must for all design, maintenance and construction engineers that are in any way linked to overhead lines.

With more than two billion people still not having access to electricity in the world, the need for optimum line design, construction and maintenance practices will continue if not increase. The need for sharing the expert knowledge, as is to be found in this book, is thus critical for sustainable development in the future.

Therefore, I would like to thank the authors for their efforts to gather all the details and prepare the text for printing. I hope and wish that the book will be well received by the overhead power line community.

Johannesburg,
September 2002

Robert Stephen
Chairman of Cigré Study Committee "Transmission Lines"

Preface

Overhead transmission lines are the highways to transport electric energy within power supply systems, which have extended across national borders already for a long while. With the expansion of economic regions beyond national borders, the conditions were established for long distance transport of electric energy and, therefore, for liberalization of the electric energy market. Overhead transmission lines are very long lasting assets that require long-term investment of a large amount of money. Electric power supply systems have reached an outstanding technical status in the industrialized countries guaranteeing supply of electric energy with very high reliability. This is not the case in all parts of the world. In some countries, many inhabitants do not have any access to reliable electric energy. There, electric supply networks will be installed or improved in the near future and new overhead lines constructed as well. Raising the supply quality requires the reliability of overhead power lines to be increased further.

The transition from smaller regional to larger national and international economic entities is described by the term of globalization. This trend also has led to new and bigger organisational units within the electric power industry as well as to modified targets and, as a consequence, also to the adjustment of international technical stipulations and of standards resulting thereof. These new stipulations comply also with the requirement on elimination of trading restrictions within the enlarged economic region. European and international standards have been introduced. Nationally oriented engineering practices will be replaced by more and more internationally adopted engineering solutions. The consumers, especially those from producing industries, expect from more liberalization and globalization of the electric energy market in addition to economic advantages an enhanced reliability of supply, an expectation which requires to increase further the reliability of overhead power lines.

Politics have become increasing influence through approval of rights-of-way and by establishing many stipulations and requirements, e. g. concerning environmental protection.

The basic elements of overhead power lines technology have been known for many years and can be considered to a high extent as mature. Technological progress, therefore, is achieved in small steps. Overhead power lines technology has been continuously developing, e. g. to adjust the line design to restrictedly available rights-of-way and to the limited environmental resources, to take efficiently care of the interdependence with environment and landscape and to transport the electric energy at lower costs. Economical solutions are of paramount interest for further development, since the costs for energy transport are a considerable share of the total expenditures for energy. Many existing overhead line installations have reached an age of 50 years and more and, therefore, are approaching their economic and technical lifetime. Many overhead line operators are developing strategies for maintenance with the target to extend the operational life of a line depending on its condition. Investments will be necessary for replacement, when an increased transmission capability is stipulated. Many lines designed and constructed in the past become much more important and require an increased reliability now. These requirements should be met without the need of additional rights-of-way.

Standard EN 50 341-1 sets general requirements and EN 50 341-3 contains supplemental National Normative Aspects for many European countries, which take care of any climatic conditions within these countries. Through the introduction of the new standards, the basis of design and verification for all aspects and steps in overhead line planning and construction have changed throughout Europe. For many years, standards for overhead line components have been based on international rules prepared by

the International Electrotechnical Commission (IEC), e. g. for insulators. This situation has applied increasingly to all other components of overhead lines such as conductors, fittings, vibration dampers and supports. Design and construction procedures require the responsibility of line owners and contractors concerning stipulations for individual lines, e. g. regarding the climatic loads. A wider background knowledge is, therefore, necessary for the application of the new standards.

The new international standards and technological innovations in the overhead line subject are the result of a long period of developments within international technical committees such as the International Council on Large Electric Systems (Cigré) and the International Electrotechnical Commission (IEC). Some important innovations should be mentioned, such as: The introduction of Flexible Alternating Current Transmission Systems (FACTS), the replacement of conventional earth wires by optical ground wires, an increasing utilization of existing conductors by innovative real-time monitoring of climatic data, the more precise design of supports by means of computer-based procedures and the survey of overhead lines using global positioning systems and laser scanning and the use of modern diagnostic tools for maintenance. More capable machinery for the installation of foundations and for stringing of conductors is increasingly adopted for overhead line construction. Scientific research has expanded the knowledge on climatic processes and effects which nowadays are predominantly described by probabilistic methods.

This publication **"Overhead Power Lines"** is based on the 5th and completely revised German edition with the title **"Freileitungen"** published by the authors F. Kießling, P. Nefzger and U. Kaintzyk in the autumn 2001. The latter describes the further developed technical rules and current legal basis for overhead line planning by using examples from Central Europe in particular. Current developments from South America and applications to the 500 kV voltage level not used in Europe so far were added by J. F. Nolasco acting as additional co-author. Therefore, the English edition of the book considers the changing economic and technical environment of the overhead power line business from an international perspective.

The book is designed as a reference and a documentation of the current engineering state of the art of overhead power lines. It also presents the basic ideas for technical stipulations and designs. It intends to introduce students and beginners employed by overhead line operators, contractors and consulting companies into the subject and should assist those active in the business to carry out their daily tasks. The book is further addressed to all people involved in the electric energy supply industry who are not daily confronted with overhead line issues.

The overhead line business comprises many engineering subjects and detailed questions which are discussed in many publications. The volume of the book did not allow all details to be tackled very deeply. Concerning special aspects, the reader is referred to the quoted references. The selected examples reflect in particular international developments and their publication within Cigré in addition to the well documented overhead line engineering in Central Europe.

The draft of a such an extensive reference book cannot be prepared without financial sponsoring by entities interested in the subject. Therefore, the authors would like to thank Siemens AG, Power Transmission and Distribution Group, and RWE Net AG for their generous fundings. In addition, the companies Richard Bergner GmbH, Schwabach, Germany, and Pfleiderer Verkehrstechnik, Neumarkt, Germany, supported the preparation and layout of the book. Many experts active in the overhead line subject prepared contributions for detailed clauses and checked the completeness of the draft. In an alphabetic series, there should be mentioned R. P. Guimaraes, Belo Horizonte, Eng. Hildebrando, Belo Horizonte, W. P. Johnson, P. Eng., Vancouver, Dipl.-Ing. C. Jürdens, Dortmund, Dipl.-Ing. R. Kliegel, Erlangen, Dipl.-Ing. H. Lorenz, Erlangen,

Dipl.-Ing. D. Lutter, Neumarkt, Dr.-Ing. L. Möcks, Schwabach, Dipl.-Ing. H. Schramm, Erlangen, Dr.-Ing. J. Seifert, Wunsiedel and H. Veith, Erlangen. The authors and the publisher would like to thank them at this opportunity for their valuable contributions. H. Stöver and M. Schwarz prepared the desktop draft for printing and were responsible for the figures. The authors would like to acknowledge their remarkable efforts. The publisher came to meet with the authors concerning the volume and the arrangement of the book generously.

The authors would like to ask all the readers to advise them on mistakes which they will surely find in the book and to stimulate further additions and updates.

Erlangen, Hannover, Belo Horizonte
October 2002

Friedrich Kießling
Peter Nefzger
Joao F. Nolasco
Ulf Kaintzyk

Contents

1 Overall planning

1.0 Symbols

Symbols	Signification
A_{Al}	Aluminium cross section of the conductor
I_{AC}, I_{DC}	Current of AC or DC line
K_{2C}	Investment of a double circuit overhead line
K_{1C}	Investment of a single circuit overhead line
K_{4C}	Investment of a four-circuit overhead line
n_2	Number of subconductors per bundle
U_N	Rated voltage
U_{AC}, U_{DC}	Voltage of an AC or DC line
P_{AC}	Power of a three-phase AC line
P_{DC}	Power of a DC bipolar line
δ	Power angle

1.1 Development stages of a transmission project

Overhead transmission of electric power has been along the years and will still continue one of the most important elements of today's electric power systems. *Power transmission* from generating stations to industrial sites and to substations is the fundamental object of the transmission systems. This function is accomplished by overhead transmission lines that connect the power plants into the transmission network, interconnect various areas of transmission networks, interconnect one electric utility with another, or deliver the electric power from various areas within the transmission network to the distribution substations, from which the distribution systems supply residential and commercial consumers.

The *planning studies* take a leading role in the definition of an electric system or in its expansion. Due to the several variables involved in the process, the planning activities have to start several years before a new installation or an expansion of an existing one is planned to be implemented.

So, a transmission line project may be considered as being initiated with some planning activities long before its execution can be started. Several stages are usually necessary inside a power utility before a new transmission system from its conception until its completion is energized. The conception of a transmission line and of the associated substations starts in the *long-term planning* with initial system evaluations and continues with further steps of *medium-term planning* and finally with the detailed definition of the line and then the granting of operation licence and approval.

For completing the preliminary studies of a new line, some complementary studies of performance assessment are carried out such as (see [1.1, 1.2, 1.3]):

- *Reactive compensation* needs,
- *Load flows* and *stability*,
- *Transposition* needs,
- *Switching surge overvoltages* and
- *Reliability* evaluation.

Finally, the line owner proceeds to the line basic design and then the detailed design, with all associated activities. The last stages consist in establishing the rights-of-way, performing and approving *environmental impact studies* and providing indemnification to the landowners affected by the new line in order to obtain their agreement. Only

Table 1.1: Classification of transmission planning

	Long-term planning	Medium-term planning	Operation (short-term) planning
Horizon (years)	15	10	3
Problems to be considered	required power, overloads, stability.	required power, overloads, stability, voltage levels, short circuit.	required power, overloads, stability, voltage levels, short circuit.
Parameters to be defined	capacity (ratings), voltage levels, terminal areas, approximate years.	capacity (ratings), losses, operative voltages, terminal substations, years of operation.	list of operational constrains, needs to uprate or upgrade lines, anticipating of programmed facilities.
Model size	area or supply region.	interconnected system.	utility system.

then survey and construction can legally be started and carried out until completion. The commissioning of the line and start-up of operation ends the process.

1.2 Transmission planning

1.2.1 Objective

The *transmission planning* is purposed to define a transmission system or its expansions so as to comply with the electric energy demand at specified quality and reliability criteria at a minimum cost. The characteristics of the *planning process* should be continuous as every plan represents a set of existing perspectives at the moment as far as future evolution is concerned. Beside that the process has an interactive structure because the medium-term needs of a system have to be fulfilled so as to make an optimized future evolution possible.

1.2.2 Planning stages

Table 1.1 shows a summary of the different kinds of planning and the main variables that are defined in each of them. It should be emphasized that the definition of planning stages is somehow arbitrary and can vary according to reality of each system, utility or transmission operator.

Long-term planning
Long-term planning is an important tool inside a power utility as it defines the basic future structure of an electric system, including transmission links. It comprises a long-term horizon for the system planning in the range of 15 to 30 years.
The long-term planning allows identifying the main variables of system development, the expected composition of the generating plants and the needs of introducing new transmission backbones and of developing new technologies. This planning should be dynamic and should be subjected to revisions when significant changes occur in the strategic or macroeconomic variables. Deregulation and restructuring of the electric energy industry make long-term planning more difficult (see [1.4]).

Medium-term planning
Medium-term planning comprising a *target horizon* in the range of 10 to 15 years usually defines basic characteristics of a system such as voltages, main transmission

lines and substations. A reference expansion program is established, depending upon complementary studies for some areas or specified links.
As in the preceding case, such planning should be continuously revised depending on the variations that can occur in the economic environment, the energy market, energy industry or in the generation program.

Operation or short-term planning
Operation or *short-term planning* is a continuous operational tool that a utility or any system owner should manage in order to keep the quality of the energy supply inside the requirements of the consumers or according to the contracts of public or private service. Therefore, the horizon to be analysed is usually below three years and urgent requirements of the system are established, such as anticipation of operation dates of new facilities, needs to uprate or upgrade existing lines etc.

1.2.3 Planning aspects regarding transmission lines

Answers should be obtained from planning studies to the following questions:
- When a new transmission line or the *uprating* or *upgrading* of existing lines will be required?
- Where is it required and what *quality of supply* or *reliability* is required?
- What normal and emergency ratings are required?
- What type of transmission should be used? Overhead lines or underground cables, DC or AC lines?
- What voltage and how many circuits will be needed?

1.3 Planning methods

1.3.1 Data acquisition and preparation

Market forecast
The period of time required to obtain sites for constructing new power plants as well as new substations and overhead lines varies from three to ten or more years. These long lead times require that decisions need to be made based on long-term *load forecasts.* Welfare and progress of a modern society depend so heavily on the availability of electric energy that a utility has to ascertain that sufficient generating capacity will be available at the required sites when the clients need it. So a good *market forecast* should establish:
- Total energy market and load distribution at busbars,
- Reactive power requirements (not required in long-term studies) (see [1.1]).

Generation
Regarding the generating capacity of a utility, long- and medium-term studies should establish:
- List of power plants considered inside the study horizon,
- Number of generating units, their ratings and operational limits,
- Active power to be supplied by every machine,
- Rotating reserves and units at maintenance or at stand-still and
- Power interchange among companies or regions.

Existing network and preferential characteristics
Other data to be gathered include:
- Configuration and general characteristics of the existing system,

- Preferential line routes, considering availability, investments and environmental impacts and
- Preferential characteristics: Voltages, frequencies, type of transmission, parameters.

1.3.2 Formulation and preselection of alternatives

Alternatives for expansion of a transmission system inside the horizon of the study under consideration are brought about as far as boosting or reinforcement of the existing system is concerned. A simplified technical and economical evaluation of the alternatives for the horizon covered by the investigation is carried out to reduce the number of alternatives to be detailed and to preselect most promising alternatives.

1.3.3 Electrical studies

The basic electric design of an AC system involves the following *electrical studies* or definitions:

- Power flow requirements,
- *System stability* and *dynamic performance*,
- Selection of *voltage level* and optimization studies,,
- Voltage and *reactive power flow control*,
- Conductor selection,
- *Losses*,
- *Corona performance* (audible, radio and television noise),
- *Electromagnetic field* effects,
- Reliability evaluation,
- Insulation and overvoltage design,
- Switching arrangements,
- Circuit breaker duties and
- Short circuit and *protective relaying*.

1.3.4 Economic studies and final evaluation

The preselected alternatives that satisfied the basic electric criteria are evaluated in cost and the *present worth of investment* and *annual losses* is determined in order to obtain the most economical alternatives.
A final study of economic feasibility and a *sensitivity analysis* are carried out on the preselected alternatives, taking into account a cost-benefit evaluation comprising:

- Investment,
- Maintenance,
- Availability of energy,
- Load market and revenues and
- Losses and reliability benefits.

Finally, the optimum alternative is selected based not only on technical and economic analysis but often considering also subjective points such as experience of the utility, local standards, availability of spare parts etc. (see also [1.5]).

1.4 Planning criteria

1.4.1 General

One of the basic criteria that should be established in a system planning is that no load can be lost under occurrence of a simple contingency in the system being studied

or in another neighbouring interconnected system. It should be differentiated between steady-state and transient conditions of a system, when designing it.

1.4.2 Criteria for steady-state conditions

The system should be tested for heavy-load and light-load conditions and should support the non-simultaneous outage of any one of its components what is known as the *(n−1) criterion.*
The first and more important study to be carried out is the execution of *load flow* runs that are performed to evaluate voltages on the bus bars, loads in transmission lines and transformers and losses. The usual ranges of the relevant parameters are:

- *voltage range*: between 0,95 and 1,05 p.u.,
- *transformer loads*:
  - Normal conditions: no overload,
  - Loss of a transmission line or generator unit: 20 % overload,
  - Loss of a transformer: 40 % overload.

1.4.3 Criteria for temporary and transient conditions

Stability
System stability is required under any load condition in case of phase to ground short circuit without reclosing, considering the loss of one of the system components.

Overvoltages
Temporary overvoltages should not cause damage to any system equipment. The following cases are analysed: *load rejection, unbalanced fault, closing operations, line dropping* and load switching.
The maximum allowable *temporary overvoltages* are in the ranges of:

- 140 % in points with saturable equipment and
- 150 % in other points.

Short circuit
Short circuit powers and currents have to be assessed as accurately as possible in order to prevent exceeding the equipment capacity of the system and installations.

1.5 Evolution and selection of voltage levels

1.5.1 Evolution of transmission voltages

In 1891, Oskar von Miller built the first three-phase transmission line between Lauffen and Frankfurt in Germany on the occasion of inauguration of an electrotechnical exhibition. A power of about 200 kW was transmitted by a 175 km long 15 kV line at 40 Hz [1.6, 1.7].
Figure 1.1 shows the *evolution of voltage levels.* Some important milestones can be mentioned:

- 1891: first three-phase transmission between Lauffen and Frankfurt, in Germany;
- 1911: 110 kV transmission line between Lauchhammer and Riesa, in Germany;
- 1929: 220 kV transmission between Brauweiler and Hoheneck, in Germany;
- 1932: 287 kV transmission between Boulder dam and Los Angeles, in USA;
- 1952: 380 kV transmission between Harspranget and Halsberg, in Sweden;
- 1965: 725 kV transmission between Manicouagan and Montreal, in Canada;
- 1985: 1200 kV transmission between Ekibastuz and Kokchetav, in the former Soviet Union.

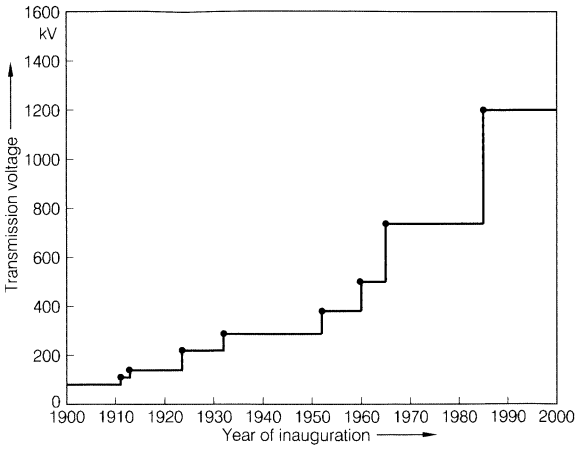

Figure 1.1: Development of transmission voltages of three-phase AC networks

According to EN 60 071 [1.8] and general use, the following *voltage classification* is considered:

- Below 1 kV: *Low Voltage* (LV),
- Between 1 kV and 45 kV: *Medium Voltage* (MV),
- Between 45 kV and 300 kV: *High Voltage* (HV),
- Between 300 kV and 750 kV: *Extra-High Voltage* (EHV),
- Above 800 kV: *Ultra-High Voltage* (UHV).

While in Central and West Europe the highest operating transmission voltage is 400 kV, as shown above, 500 kV and 800 kV have been extensively used in other countries of the world, as in Canada, China, USA, Brazil, Russia, South Africa and India. The transmission voltage 1200 kV has been used in the former Soviet Union and today in Kasachstan, while in Japan transmission lines with that voltage are under construction [1.9]. There are presently no plans for AC transmissions with voltages above 1200 kV.

1.5.2 Introduction of transmission voltages

The transmission lines are the connecting links between the generating station and the distribution systems, as well as links between transmission systems. The distribution systems supply individual consumers or localities. The voltage levels of transmission lines, either overhead or cables, are selected according to the power to be transmitted to a certain area or supplied to a consumer.

The advantage of higher levels of transmission line voltage clearly appears when consideration is given to the transmitting capability of a line, which increases with the square of the voltage.

Table 1.2 shows the voltage levels according to [1.10]. The voltages in the range of 2 to 30 kV are predominantly used for supply of distribution loads until around 10 MVA for one circuit. The range between 60 to 145 kV is especially appropriate for *regional transmission* or for the supply of large individual consumers, as well as for carrying power from medium-size power plants. The upper power capacity of such voltage levels is around 100 to 150 MVA per circuit.

The voltage levels from 145 to 300 kV are considered as *intermediate transmission links* and are extensively used for interconnecting regional systems in areas with high-load concentration. Furthermore, they are also used for transmitting medium-size powers (range of 150 to about 400 MVA) for relatively long distances, especially in large-size countries, like in USA, Canada, Russia and large countries in South America and Asia.

Voltages of 380, 500 and 765 kV are *extra-high voltage* (EHV) with an already extensive

Table 1.2: Nominal voltages and corresponding highest system voltages according to IEC 60 038

Nominal voltage (kV)	Highest system voltage (kV)
3	3,6
6	7,2
10	12
15	17,5
20	**24**
30	36
45	**52**
50	72,5
60	72,5
63	72,5
66	**72,5**
70	82,5
90	100
110	**123**
132	**145**
150	**170**
220	**245**
225	245
275	300
380	**420**
400	420
480	525
700	765

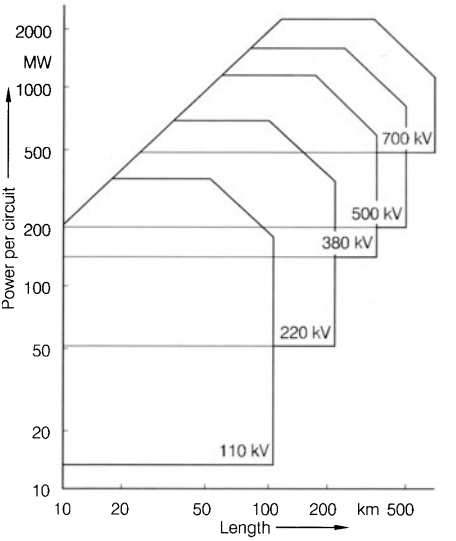

Figure 1.2: Voltage selection for transmission of electric energy

Table 1.3: Electric characteristics of AC lines

Rated voltage kV	20	110	220	380	500	750
Highest operation voltage in kV	24	123	245	420	525	765
Rated aluminum area in mm^2	50	230	435	Bundle 2 × 572	Bundle 3 × 483	Bundle 4 × 658
Conductor diameter in mm	9,6	21,5	28,8	2 × 32,9	3 × 29,6	4 × 35,2
Steady state current (at 80°C conductor temperature) in A	210	630	900	2100	2850	4380
Thermal limit power in MVA	7	120	340	1380	2470	5690
Surge impedance in Ω	400	375	365	284	276	259
Surge impedance load in MW	—	32	135	500	910	2170

use for transmitting high blocks of power, ranging from 500 until 4000 MVA per circuit, as well as for interconnecting grids. Besides the voltages standardized by IEC, the nominal voltage 500 kV, having the highest system voltage 550 kV has a widespread use in several countries.

Standards IEC 60 038 [1.10] and IEC 60 071-1 [1.8] establish two ranges of standard voltages (see Table 1.2), namely

- Range I : highest operating voltage between 1 and 245 kV;
- Range II: highest operating voltages between 300 and 765 kV (see also [1.11]).

The ultra-high voltages (UHV) as established and preliminarily studied in [1.12] are in the range of 800 to 1500 kV. For supply of the great metropolis of Tokyo in Japan a 1100 kV grid is being constructed and will start operation between 2003 and 2005 [1.13], while in Russia a 1200 kV 2500 km overhead line is already in operation for transmitting a large power block from North Kasachstan to Ural [1.14]. Figure 1.2 and Table 1.3 depict main characteristics of AC transmission lines for the specified voltage levels.

When selecting the voltage for a line, especially in the EHV level, attention should be given to the aspects related to interconnection of systems, reliability and availability. Interconnection increases the amount of current flowing when a short circuit occurs and requires an accurate and selective design of relays, circuit breakers and control to avoid major disturbances.
Furthermore, the use of special schemes, such as series capacitors, static compensation, *flexible alternating current transmission systems* (FACTS), as well as *high-surge impedance load* lines can play a role in the selection of the most appropriate voltage for a line.
It should also be considered the possibility of selecting *high-voltage direct current* (HVDC) *transmission* for both carrying large power blocks over long distances or for interconnecting systems with different frequencies. DC voltages have had an increasing use in the last decades and lines with voltages in the range of $\pm$ 200 to $\pm$ 600 kV are already in operation (see [1.12]). The two $\pm$ 600 kV lines bipolar of Itaipu are examples able to carry a power of 3000 MVA per bipole (see [1.15]).

1.6 Conductor selection

The *selection of the conductors*, their cross section and arrangements is a keypoint for a transmission line, because the conductors represent between 30 to 35 % of the total line investments. The choice of the optimum conductor is a compromise between its mechanical and electric properties, as well as the investment and the cost of the losses along the life time of the line.
Copper conductors were the first ones to be employed in overhead lines, but soon they proved to be technically difficult to be used for long spans due to their high weight to strength ratio. Besides, the costs of copper conductors were high. The *aluminium conductors* that have lower conductivity than copper conductors (about 62 %) were introduced around 1900 for reasons of lower costs. However, they were also inappropriate for using in long spans because of low strength. The introduction of *aluminium conductor steel reinforced* (ACSR) combined the relatively good electric properties of aluminium with the high strength of the steel, at reasonable investments.
Other conductor types have been developed along the years such as the *aluminium alloy conductors* that have a similar behaviour as the ACSR conductors and have no problems of corrosion as it happens sometimes with the core of ACSR conductors when installed in aggressive environments (see [1.16]).
Corona performance is another point that has to be considered for the selection of the conductors for overhead lines. It is a function of the voltage level and depends also on the line and conductor configuration.
The conductors should be selected so as to reduce *impacts of electric origin* on the environment. Such impacts as electrical and magnetic fields, radio interference and audible noise have been of growing concern during the last years. Attention should, therefore, be given to the reduction of such effects to tolerable limits.
Under the consideration of all the effects and variables described above and taking into account the required period of life for the line, an optimization study can be carried out for selecting the best technical and economic conductor (see [1.5]).
Such a study takes into account the *initial investments* and also the *cost of losses* along the life period of the line, reducing such costs to the *present value*, in order to have the same base to compare numbers for different alternatives.
It should be emphasised that other variables of subjective nature are sometimes also important such as standardization, difficulties of obtaining right-of-ways for new lines in the future, political reasons etc.

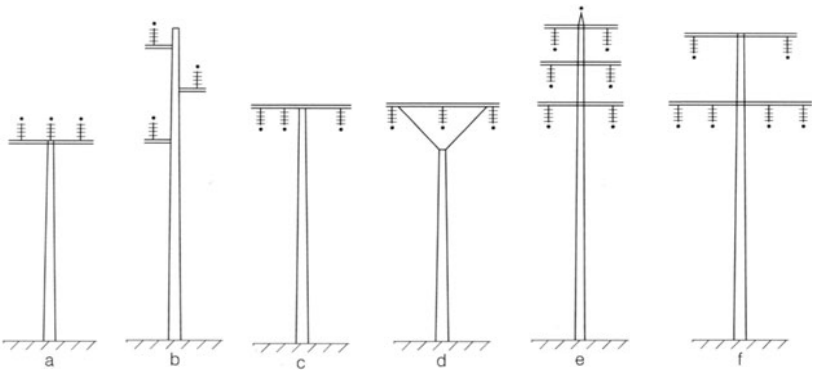

Figure 1.3: Towers for medium-voltage lines

1.7 Selection of line configuration

The *selection of* the basic *tower configuration* for an overhead line depends on various parameters starting with the voltage, the number of circuits per tower, including the type of conductors or bundles to be used. If required, the use and positioning of wires to shield the conductors against direct lightning strokes will increase the line reliability. For selecting tower configuration for high-voltage lines with reduced environmental criteria, consideration should be given to the maximum acceptable electrical and magnetic fields, radio interference and audible noise, as well as to aesthetics and *visual perception* of the line and its insertion into the landscape. The need of compaction for obtaining high surge impedance load and reducing *right-of-way* width is also a determinant factor. In case of medium voltages, the selection of the towers or supports is dependent on the number of circuits per tower, as the acquisition of new rights-of-way is becoming increasingly difficult.

In medium-voltage lines consideration is usually given to lattice towers, concrete poles, steel poles and even wood poles. The investment and reliability requirements as well as the assessed life time form the most important parameters in this case.

When dealing with lines in densely populated areas such as urban and suburban regions where cables are not a must, *compact structures*, generally with double circuit vertical conductor configuration, have been generally adopted. *Steel polygonal poles* or *concrete poles* are in general a good option in such cases. Figure 1.3 shows silhouettes for medium-voltage lines (see [1.17]).

For high and extra-high voltage lines a wide variety of line configuration is in use worldwide. Depending on the requirements for availability and necessary right-of-way single circuit, double circuit or multi-circuit lines are erected. In densely populated areas like Central Europe and Japan bundling of circuits is required resulting in lines comprising four and more circuits also with different voltages and different owners although *multi-circuit lines* result in considerable operational and economic disadvantages [1.18, 1.19]. Multi-circuit lines are more extensive and high investments have to be made for fulfilling present and future system requirements (see clause 1.10).

Some line configurations used in Central Europe are shown Figure 1.4. Most line configurations shown have been also used in other regions with two shield wires to improve protection against direct lightning strokes. Mainly I-strings are used at suspension structures. When *single-circuit lines* are erected configuration 1.4 a is preferred due to narrower right-of-way requirements while configuration 1.4 b is very often adopted in other regions. This arrangement results in relatively low foundation loads. For double-circuit 110, 220 and 380 kV lines in Europe the Danube type (Figure 1.4 d) or vertical

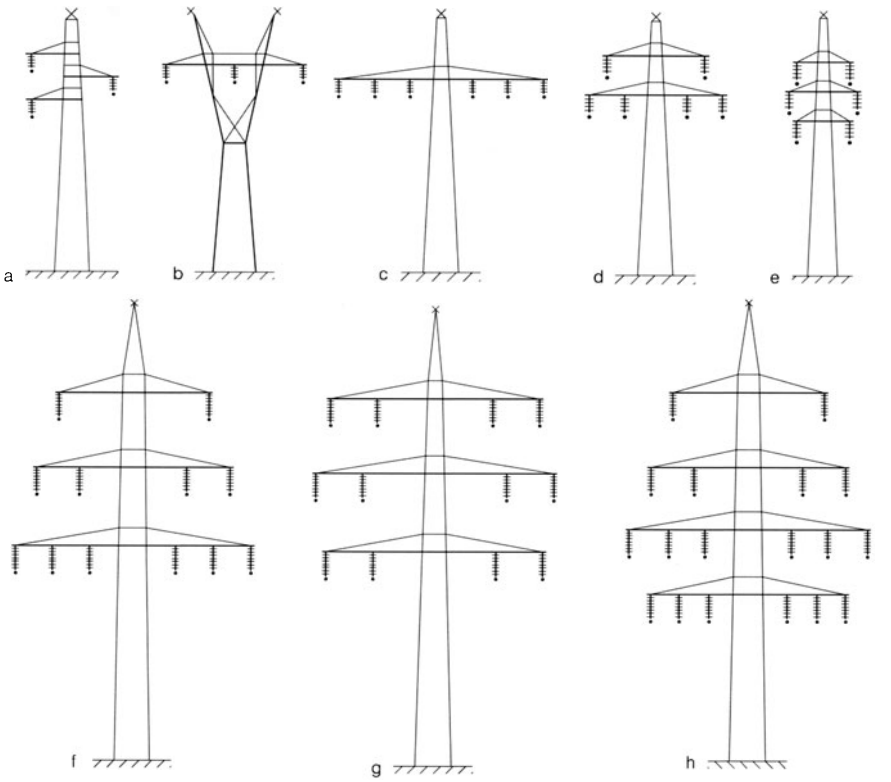

Figure 1.4: Towers for high-voltage and extra-high-voltage lines

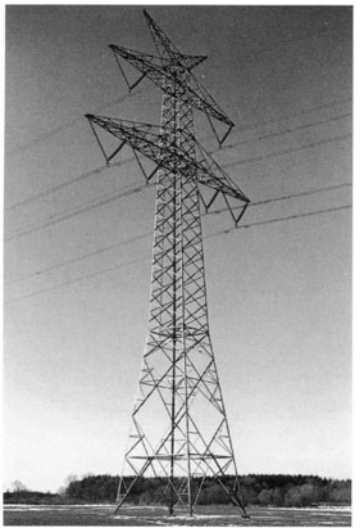

Figure 1.5: Suspension tower of a double circuit 380 kV line in Germany

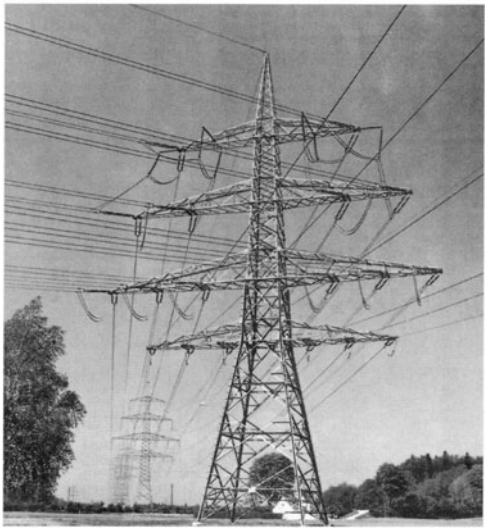

Figure 1.6: Strain tower of a 380/220/110 kV six-circuit line in Germany

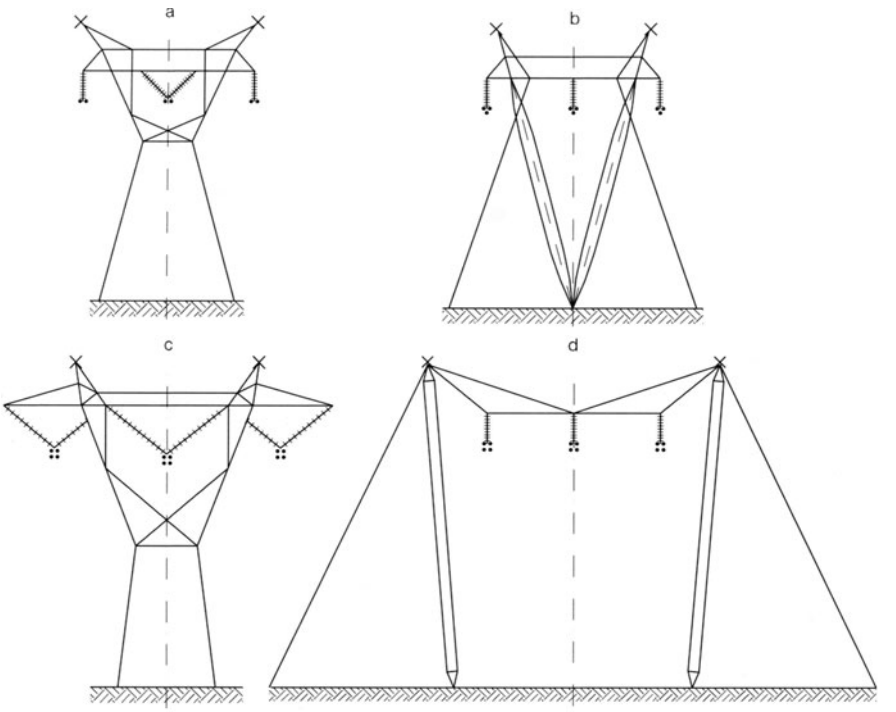

Figure 1.7: Tower configurations for 500 kV (a and b) and 750 kV lines (c and d)

configurations (1.4 e) are preferred nowadays. Figure 1.5 shows a suspension tower of a double circuit 380 kV line. The *Danube configuration* provides a compromise between width of right-of-way, tower height and investments with sufficient protection against direct lightning strokes. The vertical configuration according to Figure 1.4 e results in a narrow right-of-way but increases the tower height and the visibility of the line. The effect of the tower configuration on investments depends on the specific conditions of the line route.

For multi-circuit lines a manifold of configurations is used. In combination with 220 or 380 kV circuits the 110 kV circuits are arranged horizontally below the circuits of higher voltages (see Figure 1.4 f). This arrangement is advantageous in view of reducing electrical and magnetic fields under the line [1.20]. Four circuits having the same voltage level can be arranged like in Figure 1.4 g. The three phases placed vertically or two phases of the upper crossarm and one phase of the middle crossarm are forming one circuit. Six circuits are arranged as in Figure 1.4 h, being two circuits of 380 kV, two of 220 kV and two of 110 kV, see also [1.21] and [1.19].

A 380/220/110 kV six-circuit line, which was erected in Germany due to lack of separate rights-of-way is shown in Figure 1.6.

For the range of 500 kV and above, and especially for long lines the use of *guyed structures* has become more and more common. Either the guyed V, Y or portal types have been used extensively (Figure 1.7), see [1.12].

It should be mentioned that the use of crossarmless towers with different tower top geometries (*Chainette* or *crossrope towers*, Figure 1.7 d) has also been considered in several countries. Such towers present good technical and economic performance, especially if there are no major constraints regarding right-of-way acquisition (see [1.22]). A guyed V-tower of a 500 kV line in Brazil is shown in Figure 1.8.

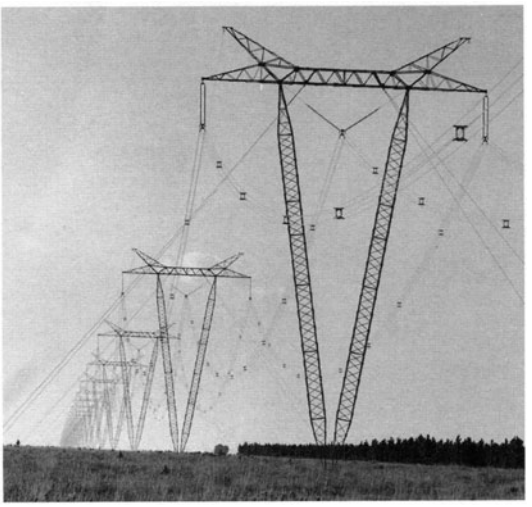

Figure 1.8: Suspension tower of a 500 kV line in Brazil

1.8 Direct current transmission

1.8.1 Aspects of DC transmission components

Attempts to develop *DC transmission* have been initiated in the end of 19th century. Since the beginning, the main technical challenge posed to the electrical industry has been the design of reliable and economic installations that transform AC current into DC and vice-versa. DC power is really not very appropriate for large scale use as most industrial and domestic applications require AC power. Thus, DC transmission would only be considered as a valid alternative to AC if it offered technical and economic advantages for the electric system as a whole.

1.8.2 Economic comparison of DC and AC lines

As a starting point, a simple *economic comparison between a DC and an AC line* can be carried out under the following premises:

- It is assumed that the same power will be transmitted by a three-phase AC line (three-phase conductors) and a DC line (two pole conductors).
- The DC voltage (U_{DC}), equals the AC peak voltage to ground (U_{AC}), i. e. $U_{DC} = \sqrt{2} \cdot U_{AC}$.
- DC current in every pole conductor equals effective (RMS) AC current in each three-phase conductor, i. e. $I_{DC} = I_{AC}$.

For the three-phase AC system the power will be, therefore:

$$P_{AC} = 3 \cdot U_{AC} \cdot I_{AC} \cdot \cos\varphi \quad . \tag{1.1}$$

Similarly for a bipolar DC line the total power is

$$P_{DC} = 2 \cdot U_{DC} \cdot I_{DC} \quad . \tag{1.2}$$

The ratio between P_{DC} and P_{AC} will, therefore, result in

$$\frac{P_{DC}}{P_{AC}} = \frac{2 \cdot U_{DC} \cdot I_{DC}}{3 \cdot U_{AC} \cdot I_{AC} \cdot \cos\varphi} \quad . \tag{1.3}$$

Since $U_{DC} = \sqrt{2} \cdot U_{AC}$ and $I_{DC} = I_{AC}$, therefore,

$$\frac{P_{DC}}{P_{AC}} = \frac{2\sqrt{2} \cdot U_{AC} \cdot I_{AC}}{3 \cdot U_{AC} \cdot I_{AC} \cdot \cos\varphi} = \frac{2\sqrt{2}}{3\cos\varphi} \quad . \tag{1.4}$$

If $\cos\varphi$ is taken equal to 0,945, it results

$$\frac{P_{DC}}{P_{AC}} \cong 1 \quad . \tag{1.5}$$

Thus a DC *bipolar line* having the same voltage as the peak phase-to-ground voltage of an AC three-phase line can transport with the same current approximately the same power. However, the DC line requires only two pole conductors of the same size as the three-phase conductors required by the equivalent AC line. Furthermore, a DC line presents a reduction between 25 and 35 % in the ohmic losses for the transmission of the same power at the same distance as compared with an equivalent AC line as shown in the example.

So, through a simple comparison it can be seen that the DC line will require about two third of conductor investments and, therefore, lighter towers and foundations, besides lower construction costs. However, due to the electrostatic attraction, pollution is a great problem for DC insulation so that much higher specific creepage distances than for AC lines are required. In case of the mentioned example the total creepage path of the DC insulation would be approximately 30 % longer than that for the equivalent AC line (see also [1.23, 1.24]).

In general, the practice shows that a DC line needs around 70 % of the investment of the equivalent AC line for the same power capacity.

1.8.3 Technical comparison of AC and DC transmission

The main advantages of the DC lines towards AC lines when operating isolated or when inserted in an electric system are:

- DC lines present lower power losses;
- DC lines present lower switching overvoltages and, therefore, require lower clearances to towers;
- DC lines introduce no problem of stability as the interconnected systems do not operate in synchronism (see [1.25]);
- DC lines have the great ability to interconnect systems of different frequencies through back-to-back converter stations [1.26];
- DC lines present reduced levels of short-circuit powers and do not contribute to increase short-circuit levels of neighbouring systems.

Disadvantages of DC against AC transmission are due to the lack of simple voltage transformation into DC voltages and vice-versa:

- DC lines cannot directly supply loads. They require converter stations – a rectifying station at the sending end and an inverting station at the receiving end. Such converter stations are usually very expensive;
- DC lines cannot economically be tapped with intermediate substations to supply consumers;
- The converter stations need a high reactive power for supplying the commutation equipment reaching until 60 % of the active power.

1.8.4 Practical use of DC transmission

DC lines only provide a more economic alternative than AC lines if the transmission distance is long enough to offset the investment for the converter stations. There is no universal break-even distance beyond which the DC transmission can be considered as advantageous. Local conditions and system requirements can play a major role in the decision to adopt a DC transmission. As a rough indication a transmission distance of more than 800 km could be considered as a threshold beyond which the DC transmission alternative can be taken into account. The decrease in investments of converter stations,

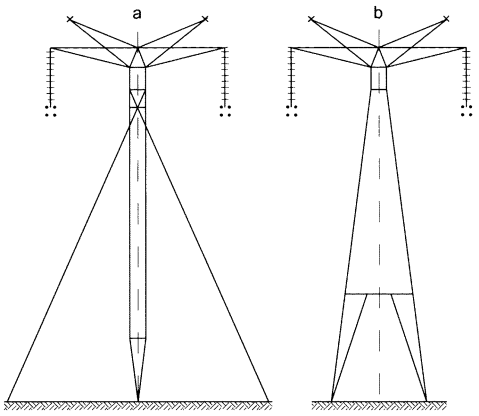

Figure 1.9: Tower configurations for DC ± 600 kV line (Itaipu, Brazil)

Table 1.4: Phase-to-phase voltages, as compared with phase-to-ground voltages for multiple phase systems in kV

Phase-to-ground voltage	Phase-to-phase voltage				
N	3	6	12	24	36
80	138	80	41	21	14
133	230	133	69	35	23
199	345	199	103	52	35
289	500	289	149	75	50
433	750	433	224	113	75

if achieved, may change the mentioned threshold to lower distance in the future. DC transmission is frequently adopted for underwater crossings, such as [1.27, 1.28]. So far DC transmission as a whole has been competitive with equivalent AC systems only in specific cases due to the high investments of converter stations.
The tower configurations for a DC ± 600 kV line according to [1.15] is shown in Figure 1.9. For this case it is usually preferred to employ guyed towers according to Figure 1.9 a, as they result in lower investments.

1.9 Transmission with higher order phase lines

1.9.1 Options

Difficulties in siting new transmission lines and the need for increased transmission capacity have forced power utilities and line owners to maximize power density in existing transmission corridors. One of the ways to achieve this increased capacity is the use of more than three phases, presently in the stage of research and testing. Theoretical and experimental studies have considered up to 36-phase systems. The six-phase and twelve-phase systems have been the presumably more attractive alternatives to substitute for the three-phase systems [1.29, 1.30].
Phase-to-phase voltages (U_{pp}) for *multiple-phase systems* up to 36 phases are shown in Table 1.4 as compared with the corresponding phase-to-ground voltages.
The key points of *multiple-phase lines* can be observed as:

- In hexaphase (six-phase) systems, phase-to-phase voltages are equal to phase-to-ground voltages.
- For phase orders higher than six, phase-to-phase voltages between adjacent phases are lower than phase-to-ground voltages. That is the reason why in multiple-phase

Table 1.5: Comparison of technical data of a twelve-phase 138 kV with a 345 kV three-phase transmission. Conductor at 138 kV: 434-AL1/63-ST1A, conductor at 345 kV: 2 × 806-AL1/102-ST1A

Parameter	Dodecaphase (12-phase) line	Three-phase line horizontal configuration (7,3 m)
Surge impedance (Ω)	502	274
Surge impedance load (MW)	455	434
Thermal limit (MW)	1648	1625
Electric field (kV/m)	3,6	6
Magnetic field (μT/kA)	10	50

systems, phase-to-ground voltages are taken as reference.
- Whereas in three-phase systems phase-to-phase voltages are always equal, phase-to-phase voltages in multiple-phase systems depend on the selected conductor combination.

1.9.2 Properties of multiple-phase systems

Comparing with conventional three-phase system, the *characteristics of multiple-phase systems* can be reported as:
- Lower voltages for the same power transmitted, resulting in lower phase-to-phase and phase-to-ground clearances and, therefore, in shorter towers and narrower rights-of-way.
- Lower phase-to-phase spacing; they require, therefore, in several cases *phase-to-phase spacers*, in order to utilize the same tower configuration in long spans as well.
- Lower voltage gradients, allowing smaller conductors to be used, as far other electric limits (RI, AN etc.) are attained. This is, however, connected with higher electrical fields at ground level. In comparison with adequate three-phase systems, such electrical fields can result in lower values as shown by the example presented in clause 1.9.3.
- Since the probability of flashovers between phases increases with increasing number of phases, special attention should be paid to the design of insulation between the phases.
- Transmission with more than three phases, for instance six phases, requires corresponding transformers and circuit breakers, switchgear and bus bars for six poles as well, what is more expensive and results in difficult protection (relaying), when interconnected with three-phase lines. Therefore, the use of multiple-phase transmission is presently restricted to some few lines.

1.9.3 Present experience

Experimental hexaphase (six-phase) and dodecaphase (twelve-phase) lines have had a relative success in the USA, where the main technical problems have already been overcome [1.30]. Multiple-phase lines are, therefore, considered to be technically and economically attractive alternatives for uprating existing three-phase lines as well as for construction of new lines.

As a practical *application of the multiple-phase concept*, a 138 kV (phase-to-ground) dodecaphase (twelve-phase) line was constructed and tested through 1987 at Power Technologies, Inc's, Saratoga, NY, test site. This line was designed to have equivalent thermal and surge impedance load to a 345 kV three-phase line. Table 1.5 shows the comparison of electric characteristics of both lines.

It can be noted that with the twelve-phase transmission the electrical field at ground level is reduced from 6,0 kV/m to 3,6 kV/m.
The magnetic field is reduced approximately 20 % when compared with the values of conventional three-phase transmission. In [1.31] it is reported about the conversion of a 115 kV three-phase line into a six-phase line aiming at increasing the transmission capacity. Keeping the same six conductors an increase of 40 % in the transmission capacity has been obtained. The right-of-way could be kept the same but the uprating of the switching equipment required significant investments.

1.10 Investments

The *investment* to construct an *overhead transmission line* depends on several factors. Line voltage, number of circuits and conductor cross section are the most important items. However, other factors contribute significantly to increase or decrease the required investments such as tower heights, characteristics of the line route and resulting relation between suspension towers to strain towers and the external loads, for instance wind and/or ice loads. The degree of reliability and security required can play a significant role in the total investments. In addition, the indemnities to be paid to landowners have been increasing sharply during recent years reaching in some cases approximately the investments for the line itself.
Equations for rough *estimation of investments* for transmission lines had been established in [1.32] depending on rated voltage, cross-sections of aluminium and number of subconductors per phase as parameters. Based on these equations the factors were updated to adjust the relations to the investment level in Central Europe nowadays. For double circuit lines an estimate for the investment without indemnities can be obtained

$$K_{2C} \sim 60 + 0{,}4\,U_N + 0{,}4\sqrt[3]{n_2} \cdot A_{Al} \quad \text{(kEUR/km)} \quad , \tag{1.6}$$

where U_N is the rated voltage in kV, n_2 the number of subconductors and A_{Al} the total aluminium or aluminium alloy cross section in mm^2. The investment necessary for single circuit lines may be obtained from

$$K_{1C} \approx 0{,}45 \text{ to } 0{,}5\,K_{2C} \quad . \tag{1.7}$$

The investment for a single circuit line is less than half of double circuit line, as it has been experienced. Therefore, single circuit lines are the favoured solution in many countries.
The investments for a double circuit line with one circuit initially installed are estimated as

$$K_{2D(1)} \approx 0{,}75 \text{ to } 0{,}8\,K_{2C} \quad , \tag{1.8}$$

and that for a line comprising four circuits are

$$K_{4C} \approx 2{,}1 \text{ to } 2{,}2\,K_{2C} \quad . \tag{1.9}$$

Economic data for 110 kV to 380 kV double circuit lines as well as for 500 kV and 750 kV single circuit lines are given in Table 1.6, which indicates the most important parameters.
Investments for an individual line may be considerably higher than those given, depending on the environment and special conditions. Useful data of cost component of overhead lines are given in [1.33].
The separation of investments for the main line components is given in Table 1.7. Since for a line with four circuits the investment for the circuits will be double and those for towers will be more than twice, the total investments for lines with four circuits will be more than twice. This relation is confirmed by executed projects. An economic advantage may result, however, since indemnities will not double.

Table 1.6: Economic data for transmission lines: 110 kV to 380 kV double circuit lines, 500 kV and 750 kV single circuit lines with self-supporting towers

Rated voltage in kV	110	220	380	500	750
Thermal limit[1)] (MVA)	100 to 350	300 to 1000	1400 to 2700	1800 to 3000	3000 to 5000
Economic power (MVA)	20 to 100	120 to 350	500 to 1200	700 to 1500	2000 to 3000
Right-of-way (m)	40 to 50	55 to 60	60 to 70	60 to 70	80 to 120
Tower weight (t/km)	15 to 25	25 to 35	45 to 65	16 to 25	28 to 50
Concrete volume (m^3/km)	100 to 200	120 to 250	150 to 300	120 to 250[3)]	150 to 250
Investment[2)] (kEUR/km)	125 to 200	150 to 400	650 to 1200	250 to 400	350 to 4500

[1)] for one circuit [2)] without indemnities [3)] 20 m^3/km for guyed towers

Table 1.7: Separation of investment in %

Rated voltage in kV	110	220	380	500	750
Circuits	35 to 45	40 to 50	45 to 55	45 to 60	45 to 60
Towers	35 to 45	35 to 45	35 to 45	30 to 45	30 to 45
Foundations	15 to 25	10 to 20	7 to 15	7 to 15	7 to 15
Engineering	5	4	3	3	3

1.11 Licences and permit procedures

Studies carried out inside Cigré [1.34] show that practically all countries require *environmental impact studies* for constructing a new overhead line. Regulatory controls vary from country to country but they generally present common features and similarities regarding the obtainment of approvals and licences. The efficient management of the *permit process* is vital. For instance it is important to consult public and individuals involved in the process in adequate time.

Regarding the preparation of environmental impact studies, specialists should be involved in advance for studying all kinds of impacts and present reports in due time for approval by the authorities in charge. The various concerns and issues that belong to the process comprise among others

- *Project justification*,
- *EMF effects*,
- *Visual impact* of the line,
- Interests of communities and
- *Effect on land use* and on property value.

In some cases, communication programmes or centres explaining the use of electricity and the environmental effects of the overhead line help to ease approval.

Regarding the relation with the landowners, early communication is vital. They need to be informed on all aspects of the project, including the financial compensation criteria, and criteria for *route selection* and location of towers.

Standards should be established for the communication process including personal contacts. Landowners should be adequately informed on *access roads* required for the construction works, maintenance and possible changes in land use.

Another aspect to be covered refers to the *visual impact*, especially for the routing guidelines. Qualitative systems of assessment of visual impacts are preferable to quantitative systems. When dealing with the general public quantitative systems should be used only for expert assessment.

Visualization methods should be understandable by the audience to which they are directed. *Photomontages* are usually the most suitable method for visual presentation to the public, also to illustrate *camouflage techniques* and different designs.

Consideration should also be given to impact of construction and maintenance. Examples are:

- Sensitive areas should be avoided and removal of vegetation mitigated so far as possible.
- Access road should follow natural contours and avoid erosion or impact on watercourses.

If an *environmental management plan* is prepared, attention should be given to specific quality plans in advance of construction. Guidelines of [1.34] have been drafted on the basis of the best practices which appear to be in use in many countries in quite a broad range of utilities. Which procedures or practices to adopt, however, will depend on prevailing regulatory regimes in each country or region and on their unique cultural and environmental climates and it may depend also on the particular features of each project.

1.12 Underground transmission versus overhead lines

1.12.1 Application and planning aspects

Underground cable systems are usually installed in urban or suburban areas where overhead lines are not approved, in locations such as airport approaches because of safety issues, or water crossings where overhead lines are not feasible. Other applications include substation getaways, crossings under major overhead line conductors and other installations where technical considerations favour underground cables. *Submarine cables* offer also a valuable alternative to overhead transmission or are even the only possible solution for the interconnection of electric systems physically separated by ocean waters [1.35].

Anyway, the introduction of underground cables in an electric transmission system is part of the planning and depends on technical and economic variables [1.24].

In [1.36] a comparison of overhead lines with underground cables has been carried out, based on a questionnaire issued by the Cigré Study Committee 22.

System planning and operation has the objective of developing a transmission network of sufficient capacity and high availability and reliability at minimum cost. A requirement to underground partly or completely a circuit causes significant system planning and operational implications.

Long-term overloads are more critical for cables than for overhead lines. A long-term overload can be defined as an overload current of such magnitude that the circuit protection does not operate, and of such duration that the conductor temperature of an overhead line does not exceed the specified emergency operating temperature. If a cable is operated with such an overload, it ages faster and may be damaged. Similar conditions are not so critical for an overhead line. This is why system planning must be modified once cables are introduced in meshed transmission networks consisting primarily of overhead lines.

System planning is subjected to design criteria. In many cases, the *(n −1) criterion* is applied which means that any one circuit or busbar can be disconnected due to a fault without customer interruptions and without any network component overload. It is assumed that the repair time is so short that no other fault will occur in the network before the faulty component is taken into operation again. This is generally the case with overhead lines but may not apply for cables which have significantly longer repair times.

The impact of *cable faults* on the operation of a transmission network can be minimized by:

- Installing a spare phase cable;
- Installing a double circuit cable;
- Applying the *(n − 2) design criterion.*

Each of the above options has additional investment implications.
The replacement of an existing overhead line by a cable in a meshed transmission network has to be analysed not only from a cable but also from a system planning viewpoint. The impact of the insertion of a cable on the surrounding network must be carefully assessed for both normal and fault under operation.
If an existing overhead line is replaced by a cable, the fault current level in the network will increase due to the lower impedance of the cable. The resulting fault currents must be calculated and the fault current capacity for each component in the network and the protection settings checked.

1.12.2 Environmental constraints

Environmental constraints cover statutory requirements, utility policy with regard to environmental matters and also public and private views and concerns. These constraints are of increasing importance.
The permanent and temporary effects of a new overhead line or underground cable can usually be quantified but public reaction to the project may sometimes be emotional. Therefore, the evaluation of the *environmental impact* of such projects is fairly complicated and involves many aspects, most of which can be considered and analysed only from a qualitative point of view.
The major constraints likely to be encountered – in the design and planning authorisation phase and during subsequent construction and operation – are magnetic fields and to a less extent electrical fields, with relevant exposure limits; land occupation and depreciation, and limitations to land use. *Visual impact* is important for overhead power lines and some impact may also be produced by the exterior installations of a cable circuit, such as terminations and reactive power compensation equipment. In many cases, remedial actions can be taken to reduce the effects on the environment.

1.12.3 Technical limitations

Technical limitations of underground cable use have an important influence on the feasibility of alternatives. Technical limitations can make some alternatives impracticable. High-voltage underground cables, due to their longer fault repair times are on average out of service for periods significantly longer than that for overhead lines. The impact on security of electricity supplies is relatively small because of the limited lengths of high-voltage underground cables on the present day systems. This situation could change if there were proportionally more underground systems and additional circuits would be required to preserve the same reliability of supply.
High-voltage cables are more restricted in their ability to be uprated. The transmission capability of an overhead line can be increased by reconductoring. This is not so simple with a cable where the route would have to be re-excavated and larger cables installed and/or the heat dissipation would have to be improved. Thus the high-voltage cable section virtually fixes the rating of a circuit and future rating increase can only be achieved at considerable expense.

1.12.4 Comparative investments

In Table 1.8 a summary of *international investment data* is presented, according to a survey made by a questionnaire prepared by Cigré SC22 JWG 21/22-01 [1.36]. *Comparative investments* are very important in achieving economical electricity transmission. The investment ratio of underground cable to overhead line can vary from project to project because of differing terrain and soil conditions and varying investments for additional planning and design, authorisation procedures, environmental impact assessment

Table 1.8: Summary of international investment data of overhead lines and underground cables

Voltage range kV	110 to 219	220 to 362	363 to 764
Mean power MVA/circuit	220	600	1800
Mean overhead line investments EUR/(km· MVA)	820	390	185
Mean underground cable investments EUR/(km· MVA)	6100	4900	3700
Mean ratio	7	13	20
Spread	3.4 to 16	5,1 to 21,1	14,6 to 33.3

and remedial works. The capitalized costs of losses are also project specific and should be included to refine the comparisons. Transmission of electricity at high voltage by underground cables is significantly more costly than by overhead lines. The disparity in investments increases with the voltage and in the high-voltage range, it is on average 20 times more expensive to go underground rather than overhead. This ratio is decreased somewhat once the cost of losses is included, which are less in underground cables due to the larger conductive cross sections.

It is inevitable, therefore, that utilities will seek to plan new transmission links using overhead lines and to reserve undergrounding to those situations where it is either impracticable to deploy overhead lines or where amenity considerations are so overwhelming that serious consideration needs to be given to undergrounding. In both cases, experience indicates that undergrounding is confined to relatively short lengths because of economic viability.

1.12.5 Perspectives

The present perspectives are that the following items will assume even greater importance for transmission projects in future years

- Land use and availability of right-of-way;
- Availability of licences and legal obstructions;
- Environmental factors;
- New technologies;
- Financial aspects.

The expectation is that the amount of land available for transmission projects will decrease due to both increasing population density and increasing land prices. Since overhead lines need much larger areas than equivalent cables, the future tendency will give greater consideration to building *compact overhead lines* and to undergrounding new and in some cases existing medium-voltage connections.

Objections to the construction of overhead lines will increase. In many countries, it is increasingly difficult to build an overhead line below 220 kV. Environmental issues will continue to be a significant factor in the comparison of overhead lines and underground cables.

New technologies should lead to both less complicated and, from the financial point of view, more attractive cable types. Solid dielectric insulated cables are now available for 400 kV and above. Using this cable type, the maintenance costs are generally lower and technical disadvantages such as electric capacitance are minimized. Use of special stabilized *thermal backfills* results in increased power transfer capability and lower life cycle cost. Higher power transfer capabilities are already available using SF_6 insulated and forced cooled cable systems, and there are some perspectives for super-conductive cables.

Relatively high investment is the major impediment to the use of high-voltage underground cables. However, due to the application of modern cable laying techniques such as directional drilling, and the development of less expensive cables and prefabricated accessories, these investments will decrease. The investment ratio underground cable versus overhead line is expected to decrease although the reduction will not be sufficient to bridge the significant difference, particularly at the highest voltages.
To summarize, it could be said that overhead lines will remain the most economic and reliable means of high-voltage transmission. In most cases, they can be harmoniously integrated into the environment. It can be further affirmed that in future, for both new and replacement circuits, greater consideration will be given to the use of underground cables, particularly at the lower transmission voltages.

1.13 Results of overall planning

Regarding transmission line construction, the *planning stages* usually established inside the power utilities or line operators, either public or independent entities, should define the following characteristics for a new transmission line or for an existing line to be refurbished, uprated or upgraded.
Items to be defined are:

- Required *data for commissioning*;
- Terminal substations and *line length*;
- *Power to be transmitted* in normal and emergency conditions;
- *Type of transmission*; AC versus DC;
- Conductors, voltage, necessity of shield wires ;
- *number of circuits*;
- Tower type, phase configuration;
- Use of earth wires such as optical ground wires for communication purpose;
- *Maximum* allowable *losses*;
- Required *availability* and *reliability*;
- Maximum acceptable values of electrical and magnetic fields, as well as of other electric impacts on the environment;
- Work *schedule.*

Based on these items, special studies and complementary evaluations are performed concerning:

- *Overvoltages* for defining insulation and clearances and tower dimensions;
- *Short-circuit levels*, definition of shield wires and earthing schemes;
- Transposition needs;
- Reactive compensation needs;
- Eventual future intermediate switching stations;
- Future lines in the same corridor;
- Required *electric performance*;
- Evaluation of impacts of electric origin on the environment;
- Static and dynamic stability see also [1.37] and [1.12]).

Based on the results of the overall planning, detailed survey and planning have to follow regarding the different components of individual lines. Plans have to be carried out to determine the tower locations and types, the design of foundations and for establishing a bill of quantity for materials to be purchased. Details are dealt with in chapter 15.

1.14 References

1.1 Hütte Energietechnik, Band 3: Netze. (Power engineering, Volume 3: Electric networks). Berlin, Heidelberg, New York: Springer Verlag 1987

1.2 Stevenson, H. F.: Elements of power system analysis. New York, Mc Graw Hill, 2nd edition 1987

1.3 Clark, E.: Circuit analysis of AC power systems. Cigré. New York, John Wiley & Sons, 1943

1.4 Drapper, E. L.: 21th Century power systems – Perspectives from the threshold. Cigré Session 2000 Opening – August 2000

1.5 Nolasco, J. F.: Conductor optimization for 220 kV line. University of Lima, 1996.

1.6 Kahnt, R.: Development of high-voltage technology – 100 years of AC transmission. Elektrizitätswirtschaft 90 (1991), pp. 558 to 576

1.7 Bauer, K.-H.; Paschen, R.; Schlayer, G.: 100 Jahre Drehstrom-Fernübertragung (100 years of AC transmission). Elektrizitätswirtschaft 90 (1991), pp. 1119 to 1126

1.8 IEC 60071-1: Insulation Coordination. Part I: Definitions, Principles and Rules. Geneva 1993

1.9 Nanita, J.; Yamagata, Y.; Tanabe, T.: UHV transmission project in Tokyo Electric Power Company. 11th CEPSI. Kuala Lumpur, 1996

1.10 IEC 60038: IEC standard voltages. Geneva, IEC, 1983

1.11 EN 50341-1: Overhead electrical lines exceeding AC 45 kV. Part 1: General Requirements – Common specifications. Brussels, CENELEC, 2001

1.12 EPRI: Transmission line reference book: 345 kV and above. Palo Alto, Electric Power Research Institute, 2nd edition 1982

1.13 Plan and general design for 1000 kV transmission in Japan. Tokio Electric Power Company, 1983

1.14 Djakow, A.F. et al.: USSR 1200 kV line connects three power systems. T & D International, March 1991

1.15 Fadini, H. A. M.; Motta, S. S. G.: Sistema de transmissas de Itaipu – A experiência de FURNAS (Transmission systems of Itaipu – the experience of FURNAS). Rio de Janeiro, FURNAS, 1995

1.16 Overhead conductor manual. Southwire: 1994

1.17 EPRI: Transmission line reference book: 115/138 kV compact line design. Palo Alto, Electric Power Research Institute, 1978

1.18 Barbarito, M. et al.: Compact versus conventional EHV lines: Technical and economical comparison. Cigré Report 22-13,

1.19 Boos, K. V. et al.: Experiences gained in the operation of multiple circuit high-voltage overhead lines of compact design. Cigré Report 22-12, 1986

1.20 Kießling, F.; Hussels, D.; Jürdens, C.; Ruhnau, J.: Upgrading high-voltage lines to increase their capacity and mitigate environmental impacts. Cigré Report 22-208, 1998

1.21 Kießling, F.; Meier, P.: The 380 kV power lines of Bayernwerk AG exemplify the development of overhead line construction in Germany. Elektrizitätswirtschaft 76 (1977), pp. 637 to 642

1.22 Leconte, D.; Meyère, P.: Evolution of the design for the 735 kV Transmission Lines of Hydro-Quebec. Cigré Report 22-08, 1990

1.23 Bowles, J. P. et al.: AC-DC Economics and alternatives – 1987 Panel session report. IEEE Transactions on Power Delivery, Vol. 5, No. 4, pp. 1956 to 1976

1.24 Fink, D.G.; Beaty, H. W.: Standard handbook for electrical engineers. New York, Mc Graw-Hill, 12th edition, 1987

1.25 Brumshagen, H. et al.: East-West European high hower transmission system. Cigré Report 37-304, 1996

1.26 da Silva, J. B. et al.: First interconnection Brazil-Argentina - Design of the AC 500/525 kV, 50 Hz/60 Hz line, Rinion-Garabi-Ita. IX South American Cigré regional meeting, Foz do Iguazu, May 2001

1.27 Nymann, A. et al.: The Baltic Cable HVDE Project. Cigré Report 14-105, 1996

1.28 Poulsen, S. H. et al.: 400 kV flat-type oil-filled cables for Kontek, HVDC interconnection Denmark/Germany. Cigré Report 21-204, 1994

1.29 Barthold, L. O.; Barnes, H. C.: High-phase order power transmission. Electra 24 (1973), pp. 139 to 153

1.30 Grant, J. et al.: Higher-phase order transmission line research. Cigré Symposium SC22-81 Report 220-02, 1981

1.31 Brown, R. et al.: Six-phase successfully applied to utility transmission systems. Cigré Report 22/33/36-01, 1998

1.32 Technische und wirtschaftliche Kenndaten von Freileitungen bei DHÜ und HGÜ (Technical and economic characteristics of HVAC and HVDC transmissions with overhead lines). etz-A 98 (1977), pp. 711 to 715

1.33 Cigré SC22, WG09: International survey of component costs of overhead transmission lines. Electra No. 137 (1991), pp. 60 to 79

1.34 Cigré SC 22 WG 14: Environmental concerns, procedures, impacts and mitigations. Paris, Cigré Brochure No. 147, 2000

1.35 Gazzana-Priaroggia, P. et al.: Long Island Sound submarine cable interconnection. IEEE Transactions on Power Apparatus and Systems, July/Aug. 1971, Vol. 90, pp.

1.36 Cigré SC21/22: Comparison of high-voltage lines and underground cables. Report and guidelines. Paris, Cigré Brochure 110, 1997

1.37 Happoldt, H., Oeding, D.: Elektrische Kraftwerke und Netze (Electric power stations and networks). Berlin, Springer Verlag, 5th edition, 1978

Nich mehr im Text erwähnt:

1.38 Busch, H. G.: Aspects of the future of AC-EHV transmission in Germany, model analysis. Cigré Report 31-13, 1978

2 Electric requirements and design

2.0 Symbols

Symbols	Signification
a	Span length
a_{g}	Weight span
a_{som}	Minimum straight line distance between live and earthed parts
a_{W}	Wind span
B	Magnetic flux density
c_{min}	Minimum clearance between conductors and earthed parts
C	Capacitance
C'	Capacitance per unit length
C_{C}	Drag factor for conductors
d	Air gap distance, clearance distance
d_{ins}	Flashover distance of an insulator string
D	Conductor diameter
D_{AB}, D_{AC}, D_{BC}	Phase-to-phase distance
D_{add}	Additional clearance component
D_{el}	Minimum air clearance required to prevent a disruptive discharge between conductors and objects at earth potential during fast-front or slow-front overvoltages
$D_{\mathrm{el\_ff}}$	Minimum air clearance required to prevent a disruptive discharge between conductors and objects at earth potential during fast-front overvoltages
$D_{\mathrm{el\_sf}}$	Minimum air clearance required to prevent a disruptive discharge between conductors and objects at earth potential during slow-front overvoltages
$D_{\mathrm{L}i}$	Distance between source of interference and measuring point
D_{M}	Mean geometric distance
$D_{\mathrm{pf\_pe}}$	Minimum air clearance required to prevent a disruptive discharge between live conductors and objects at earth potential at power frequency voltage
$D_{\mathrm{pf\_pp}}$	Minimum air clearance required to prevent a disruptive discharge between phase conductors at power frequency voltage
D_{pp}	Minimum air clearance required to prevent a disruptive discharge between phase conductors during fast-front or slow-front overvoltages
$D_{\mathrm{pp\_ff}}$	Minimum air clearance required to prevent a disruptive discharge between phase conductors during fast-front overvoltages
$D_{\mathrm{pp\_sf}}$	Minimum air clearance required to prevent a disruptive discharge between phase conductors during slow-front overvoltages
E	Voltage gradient, electrical field strength
$\overline{E}$	Mean voltage gradient of a circuit
E_{aV}	Voltage gradient along conductor surface
E_{I}	Radio or audible noise interference intensity
E_i	Maximum voltage gradient at conductor i
E_{e}	Energy stored in the electrical field of an overhead line
E_{m}	Energy stored in the magnetic field of an overhead line
E_ϑ	Voltage gradient angle ϑ
f	Frequency
f_{C}	Conductor sag
F_{WI}	Wind load on insulator string
g	Gravitational acceleration
G_{L}	Span factor
h_{al}	Altitude above sea level

Symbols	Signification
h_{M}	Mean conductor height above ground
H	Magnetic field strength
I	Current; rms current
$k_1,\ k_2$	Factors to calculate voltage gradients
k_{C}	Factor to determine minimum conductor clearances
k_{hm}	Humidity voltage correction factor
k_{w}	Factor for conductor swing
K_{a}	Altitude factor
K_{cs}	Statistical coordination factor
K_{g}	Gap factor
$K_{\mathrm{g\_ff}}$	Lightning impulse gap factor
$K_{\mathrm{g\_ff\_ins}}$	Lightning impulse gap factor of the insulator strings
$K_{\mathrm{g\_pf}}$	Power frequency gap factor
$K_{\mathrm{g\_sf}}$	Switching impulse air gap factor
K_{z}	Deviation factor
$K_{\mathrm{z\_ff}}$	Deviation factor of the air gap withstand voltage distribution for fast-front overvoltages
$K_{\mathrm{z\_pf}}$	Deviation factor of the air gap withstand voltage distribution for power frequency voltages
$K_{\mathrm{z\_sf}}$	Deviation factor of the air gap withstand voltage distribution for slow-front overvoltages
l_{k}	Length of insulator set
L	Inductance
m_{c}	Conductor mass per unit length
n	Exponent
n_2	Number of subconductors
N_{x}	Number of standard deviations
NP	Interference level
NP_{A}	Audible noise level
NP_{I}	Radio interference
$NP_{\mathrm{I\,perm}}$	Permissible radio interference level
$\mathrm{p}(U)$	Discharge probability function
p	Probability of occurrence
P_{G}	Power limit of electric stability
P_{j}	Ohmic loss
P_{nat}	Surge impedance load, natural power
q_{C}	Effective wind pressure on conductor
q_{z}	Wind pressure depending on height above ground
Q	Electric charge
Q_{WC}	Wind force on conductor
Q_{Wins}	Wind force on insulator
r_0	Radius of bundle circle
r_{e}	Equivalent radius
r_{B}	Bundle conductor equivalent radius
r	Subconductor radius
R	Ohmic resistance
RIS	Relative insulation strength
s	Subconductor distance within a bundle
t	Period of time
t_2	Time to half value
t_{p}	Front time

Symbols	Signification
T	Absolute air temperature
U	Electric voltage
$U_{100\%}$	100 % withstand voltage of the air gap
$U_{2\%}$	Overvoltage having a 2 % probability of being exceeded
$U_{2\%\_sf}$	Slow-front overvoltage having a 2 % probability of being exceeded
$U_{50\%}$	50 % withstand voltage of the air gap
$U_{50\%rp}$	50 % withstand voltage of a rod-plane gap
$U_{50\%rp\_sf}$	50 % withstand voltage of a rod-plane gap for slow-front overvoltages
$U_{50\%rp\_ff}$	50 % withstand voltage of a rod-plane gap for fast-front overvoltages
$U_{50\%rp\_pf}$	50 % withstand voltage of a rod-plane gap for power frequency overvoltages
$U_{50\%real}$	Critical discharge voltage in the line
$U_{90\%}$	90 % withstand voltage of the air gap
$U_{90\%ff\_ins}$	90 % lightning withstand voltage of the installed insulator strings
U_{A}	Voltage at the line sending end
U_{cw}	Coordination withstand voltage
U_{DC}	Highest voltage of a DC line
U_{e}	Voltage at the line receiving end
$U_{e2\%\_sf}$	2 % slow-front phase-to-earth overvoltage
U_{max}	Maximum overvoltage
$U_{p2\%\_sf}$	2 % slow-front phase-to-phase overvoltage
U_{pp}	Voltage between phases
U_{rp}	Representative overvoltage
U_{rw}	Required withstand voltage of the air gap
U_{s}	Highest system voltage (kV rms)
U_{sAC}	Highest system voltage of an AC line
U_{W}	Insulation withstand voltage
U_{x}	Truncated voltage
v_{u}	Coefficient of variation of a voltage
V	Wind velocity
$\overline{V}$	Mean wind velocity
V_{2a}	Wind velocity having a two year return period
V_{R}	Reference wind velocity
V_{z}	Wind velocity at height z above ground
V_{η}	Wind velocity parameter
V_{τ}	Wind velocity having a return period τ
W_{C}	Effective conductor weight
W_{ins}	Weight of insulator set
X_{C}	Capacitive reactance
X_{L}	Inductive reactance
z	Height above ground
z_{R}	Reference height above ground
Z_{C}	Surge impedance
α	Terrain roughness parameter
β	Exponent
δ	Power angle
ε_{0}	Dielectric constant
θ	Angle around conductor periphery
μ_{0}	Magnetic constant
μ_{r}	Relative permeability
ϱ'	Air density

Symbols	Signification
ϱ'_{r}	Relative air density
ϕ	Swing angle
ϕ_{ins}	Swing angle of insulator sets
ϕ_{C}	Swing angle of conductors
σ_{u}	Standard deviation of a voltage
σ_{V}	Standard deviation of a wind velocity
σ_{ϕ}	Standard deviation of a swing angle
τ	Return period
θ	Variable angle at subconductor surface
ω	Angular frequency

2.1 Overhead lines as components of electric systems

2.1.1 Surge impedance and surge impedance load (natural power)

The energy stored in the electrical field of an overhead line can be equated as

$$E_{\mathrm{e}} = 1/2 \cdot C \cdot U^2 \quad , \tag{2.1}$$

where C is the *capacitance* and U the voltage. In a similar way, the energy stored in the magnetic field is

$$E_{\mathrm{m}} = 1/2 \cdot L \cdot I^2 \quad , \tag{2.2}$$

where L is the *inductance* and I the current.
At the threshold condition where the same energy is stored in both fields, that is if $E_{\mathrm{e}} = E_{\mathrm{m}}$, it results from (2.1) and (2.2)

$$U/I = \sqrt{L/C} = Z_{\mathrm{C}} \quad . \tag{2.3}$$

The ratio above has dimensions of an impedance and is called *surge impedance* of the line. It can further be deduced

$$Z_{\mathrm{C}} = \sqrt{L/C} = \sqrt{X_{\mathrm{L}} \cdot X_{\mathrm{C}}} \quad , \tag{2.4}$$

where $X_{\mathrm{L}} = 2\pi \cdot f \cdot L$ is the *inductive reactance* and $X_{\mathrm{C}} = 1/(2 \cdot \pi \cdot f \cdot C)$ the *capacitive reactance*. The surge impedance Z_{C} of a transmission line is also called the *characteristic impedance* with the ohmic resistance set equal to zero, i. e. the ohmic resistance R is assumed to be small as compared with the inductive reactance. The power which flows in a transmission line without reactive power losses is denoted as the *surge impedance load* "SIL" or *natural power* of the line. Under these conditions, the sending end voltage U_{A} and the receiving end voltage U_{e} differ by an angle δ corresponding to the travel time on the line. For a three-phase line, the *surge impedance load* P_{nat} is

$$P_{\mathrm{nat}} = U_{\mathrm{pp}}^2 / Z_{\mathrm{C}} \quad , \tag{2.5}$$

where U_{pp} is the phase-to-phase voltage of the line. Since Z_{C} has no reactive component, there is no reactive power requirement in the line. This indicates that for P_{nat} the reactive losses due to the line inductance are exactly offset by the reactive power supplied by the *shunt capacitance*, or

$$I^2 \omega L = U^2 \cdot \omega C \quad . \tag{2.6}$$

The surge impedance load is a useful quantity to measure transmission line capability even for practical lines with resistance, as it indicates a loading when the line reactive requirements are small. For power transfer significantly above P_{nat}, *shunt capacitors*

Table 2.1: Surge impedance load (SIL) of typical overhead lines (MW)

Number of conductors per phase bundle	Z_C Ω	Operating voltage kV					
		69	138	230	400	500	765
1	400	12	48	132	—	—	—
2	320	—	60	165	557	781	—
3	280	—	—	—	602	893	—
4	240	—	—	—	627	1042	2230

may be needed to minimize the *voltage drop* along the line, to improve the *power factor* and to increase the line capacity. For operation significantly below P_{nat}, *shunt reactors* may be needed. Efforts have been made by electric industry nowadays towards increasing the surge impedance load of overhead lines, especially considering the growing difficulties to acquire rights-of-way for new lines. The surge impedance load of an overhead line can be increased by:

- Voltage increase;
- Reduction of surge impedance Z_C through:
  - Reducing phase spacing (*compact overhead lines*);
  - Increasing number of conductors per phase bundle;
  - Increasing conductor diameter;
  - Increasing bundle radius;
  - Introducing *bundle expansion* along the span.

In Table 2.1, the *surge impedance load* of typical overhead lines is shown. It illustrates loading limits and is useful as an estimating tool. Long EHV lines according to range II of Table IEC 60 071 tend to be voltage-drop and stability-limited. This corresponds to a lower loading limit in case of short lines, which tend to be limited by conductor ampacity.

2.1.2 Stability

A power system made up of interconnected dynamic elements may be said to have stability if it will regain stable operation after a system disturbance.

- *Steady-state stability* is associated with small perturbations such as slow variation on loads or generation and line dropouts. It depends fundamentally on the state of the system, i. e. the operating conditions, at the instant of the perturbation.
- *Transient stability* is associated with great perturbations (periodic disturbances), such as line faults, loss of a generating unit, sudden application of a big load, fault in equipment. It strongly depends on the magnitude and site of the perturbation and less on the initial state of the system.

The stability limit is defined as:

$$P_G = (U_A \cdot U_e)/X_L \sin\delta \quad , \tag{2.7}$$

where P_G is the power limit in MW, U_A and U_e are the voltages at sending end and receiving end terminals, respectively, X_L is the *inductive reactance* and δ the *power angle* of stability.

As far as dynamic stability is concerned, the power angle δ is limited to the range below 45°. A value near 90° is required to maintain stability after power oscillations resulting from perturbations. The transient stability criterion usually requires lower limits for the power angle than the steady-state stability. The reduction of the series reactance X_L is, therefore, considered by planning engineers as a convenient alternative to increase the power transmission capacity of a line.

2.1.3 Voltage regulation and maximum permissible losses

Voltage regulation

The transmission capacity of radial lines, especially medium and long lines up to 150 kV is often limited by *voltage drop* or *voltage regulation*. The highest limit practically recommended for line regulation is in the range of 5 to 10 %, depending on the line voltage and on the reactive power compensation available. Table 1.2 contains the highest system operation voltages. For extra-high voltage lines, voltage regulation is usually not the governing limit as these lines either belong to interconnected systems or are controlled by other criteria (see clause 2.1.4).

Line losses

Regarding *line losses*, line owners or power utilities generally establish maximum acceptable limits, considering the economic aspects associated with long-term operation of the line and the amount of power and energy that can be wasted within this period. The following types of losses have to be considered when designing overhead transmission lines:

- Losses by "*Joule heat*" (*ohmic losses*) in the conductors: Those are the main losses that occur in the overhead conductors and correct conductor selection is decisive for obtaining an economical line. The losses are like energy thrown in the basket as they represent consumption of primary energy without the corresponding generation of useful work. The power $R \cdot I^2$ dissipated in the conductors and joints reduces the efficiency of the electric system and its ability to supply new loads. The energy $R \cdot I^2 \cdot \Delta t$ is dissipated as heat.
- *Dielectric losses* and *corona losses*: For a careful design of conductors and accessories, maximum conductor gradients have to be limited so as to generate negligible corona losses under fair and foul weather conditions. On the other hand, a careful design of accessories and insulators can reduce the amount of leakage currents and the resulting losses to negligible values.

2.1.4 Capability of a line

The *capability of a line* is the degree of power that can be transmitted by a line, considering the limitations imposed by voltage regulation and conductor temperature, as well as limitations inherent to system constraints such as stability, maximum capacities of substation terminal equipment, circuit breakers, current transformers etc. The capability of lines of range II ($U_s \geq 245$ kV, see Table 2.12), is usually governed by *thermal limit* for lengths up to 80 km, by *voltage regulation* in the 80 to 320 km range and by *stability* for lines longer than 320 km. The numbers above are generally valid for radial lines or lines interconnecting a generating terminal with a weak system. In case of lines interconnecting strong systems, other limits such as reactive power available or terminal equipment limitations may prevail.

2.1.5 Reliability and availability

Consideration of the two important aspects of *continuity of supply* and *quality of supply*, together with other relevant elements in the planning, design, control, operation and maintenance of an electric power system network, is usually designated as *reliability assessment*. Generally, the past performance of a system is calculated according to some performance indices, such as the *Average Customer Interruption Frequency Index* and the *Customer Average Interruption Duration Index*. The *unavailability* of transmission lines is measured in terms of hours per year or percent of time while the lines have been out of operation. Two main reasons can be distinguished:

- *Mechanical unavailability* of the weakest component, mostly the supports, equal to the inverse of twice the return period of the design wind velocity or climatic loads, as per [2.1]. The unavailability of all other components together usually doesn't exceed 25 % of that one for the supports.
- *Electric unavailability* related to failure of electric origin. Three main causes of electric failures exist, namely:
  - Failures due to unsuccessful reclosing operation, when a lightning flashover occurred, amounting to about 30 to 35 % of all reclosing operations. Each of those permanent failures lasts in average two to four hours and represents an appreciable part of the line unavailability in regions of high keraunic activity.
  - Failures due to switching surge overvoltages, mainly caused by line energization or reclosing. The probability of flashover (PFO) is usually very low (around 10^{-3} to 10^{-4}) and contributes little to the line unavailability.
  - Failures caused by power frequency voltages, when *adverse weather conditions* or other circumstances, such as fire under a line or touching of conductors by tree branches, occur, can add about 0,3 outages per year with an average duration below 10 hours in general according to international statistics.

Documentation of the following indices is usual for an electric system as well as for an overhead line [2.2]:

- *Forced Energy Unavailability (FEU)* is an index that measures the percent ratio between the unplanned out-of-service hours of a line during one year divided by the total number of hours of one year (8760).
- *Scheduled Energy Unavailability (SEU)* is an index that measures the percent ratio between planned out-of-service hours of a line during one year divided by the total number of hours of one year (8760).
- *Forced Outage Rate (FOR)* is the ratio between the mean time to repair the line after automatic or emergency taking out-of-service of a line and the total number of hours of one year (8760).
- *Mean Time Between Failures (MTBF)* is an index that measures the average time elapsed between two consecutive failure events.
- *Mean Time To Repair (MTTR)* is an index that measures the average time for repairing non-scheduled failures.

2.1.6 Reactive power compensation

There are two basic types of compensation required by an electric system as a consequence of the *reactive power requirements*, namely:

- *Series compensation*, made up of capacitor banks connected in series with the line, off-setting part of the inductive reactance and thus reducing the electrical line length. Its main advantages are
  - Improving the steady-state and transient stability;
  - Allowing for a more economic power loading;
  - Reducing reactive power requirements of the system;
  - Reducing the voltage drop;
  - Distributing the load better between circuits.

  When using series compensation, especial attention should be given to other factors affecting technically and economically the system, such as capacitor protection, line protection and sub-synchronous resonance.
- *Shunt compensation.* The main shunt compensation schemes used in electric systems are:
  - *Reactors*, for compensating capacitive powers of long EHV lines in periods

of light load *(Ferranti Effect)*;
- Capacitors for voltage control and power factor correction during periods of high load demand;
- Synchronous condensers, that can perform the functions of reactors as well as of capacitors, depending on the instantaneous system needs;
- Static compensators, performing the function of synchronous condensers without moving parts.
- *Flexible alternating current transmission system (FACTS)* facilities.

2.1.7 Power transmitted versus right-of-way width

The need to transmit the highest possible power in a line corridor makes it important to increase the power carried by the lines inside. This originates the concept of *efficiency ratio* [2.3] of a line corridor expressed as power transmitted related to the width of right-of-way (ROW):

$$\text{Efficiency ratio} = \frac{\text{Power transmitted}}{\text{ROW width}} \quad . \tag{2.8}$$

The power transmitted is proportional to the square of the voltage, while the ROW width is nearly proportional to the voltage. Table 2.2 shows typical values. The efficiency ratio is measured in MVA/m. There are several ways to increase the efficiency ratio basically by increasing the power transmitted in a given corridor, such as:
- Use of higher voltage compatible with the required loads;
- Use of double- or multiple-circuit lines, where acceptable by reliability or environmental considerations;
- *Line compaction*;
- Uprating of lines (series compensation, use of FACTS, reconductoring, voltage increase);
- Use of DC transmission.

2.2 Current-related phenomena

2.2.1 Normal and emergency conditions

An overhead line can be designed for carrying a maximum level of power under normal or emergency conditions. As a function of that, the conductor design temperature will depend on the resulting current for the above conditions and on meteorological parameters, such as ambient temperature, wind velocity etc. The line design itself should take into account the sags resulting from the conductor design conditions together with the applicable safety clearances.
Normal condition is herein considered as a situation in which the conductor will not lose its mechanical properties along the line life (30 to 40 years as a minimum). *Emergency condition* can be considered, according to [2.4], as a condition in which the conductor will not lose more than 10 % of its mechanical strength along the line life.
For aluminium and ACSR conductors, normal operation temperatures will be until 80°C while emergency temperatures would be in the range of 100 to 120°C as specified in national standards, project specifications or utility experience.

2.2.2 Ohmic losses

The *ohmic* or *Joule losses* of a three-phase line can be calculated using the equation

$$P_j = 3\,R_{AC} \cdot I^2 \quad , \tag{2.9}$$

Table 2.2: Typical values of efficiency ratios of rights-of-way

Voltage (kV)	230	500	765
Power (MVA)	165	1000	2500
ROW width (m)	45	65	95
Efficiency ratio (MVA/m)	3,7	15,4	26,3

where R_{AC} is the AC phase conductor resistance at the operating temperature and I the *rms current* flowing on the line, as a function of the power being transmitted (see subclause 7.2.3).

2.2.3 Short circuit condition

Overhead lines and their components should be designed so as to remain sound after the occurrence of *short circuits*, either three-phase, phase-to-phase or phase-to-earth. The duration of the short-circuit currents depends on the system design, especially on the protective schemes and on the respective break time. Typical values of short-circuit duration for designing conductors, shield wires and accessories are:

- Operation of first zone or second zone relays: 0,1 to 0,2 s;
- Operation of back-up protection and eventual reclosing operation during a remaining short-circuit: 0,5 to 1 s at voltages up to 300 kV (range I according to IEC 60 071-1) and 0,2 to 0,5 s at voltages above 300 kV (range II according to IEC 60 071-1).

2.3 Voltage and current-related phenomena

2.3.1 Introduction

The *electric effects* on the *environment* produced by an overhead line turned out to be a matter of concern in the last decades. Several studies were carried out on possible harmful consequences that the electrical and magnetic fields produced by overhead lines could cause on humans, animals and plants. Interference on communication systems have been since long time another matter of pre-occupation. In view of that, the electric industry as well as international or national regulations used to establish maximum acceptable limits for such effects, which should be complied with when a new overhead transmission line is designed and constructed.

2.3.2 Electrical and magnetic fields

2.3.2.1 Effects on humans and animals

Ground level *electric and magnetic field* effects of overhead power lines became of increasing concern as transmission voltages have been increased. The effects of such fields are especially important because their influence on human beings and animals have been under investigation in the last decades [2.5, 2.6, 2.7] and [2.8]. The latter contains an extended list of references. Suspicions still exist that exposure to electrical and magnetic fields could be associated with adverse health effects or with increased risks. But the studies performed so far in this sense failed to prove such risks in case of fields occurring close to overhead power lines. Therefore, it is not appropriate to consider unlikely conditions when setting and applying electrical field safety criteria because of possible consequences.

The magnitude of electrical and magnetic fields in proximity to a transmission line results from the superposition of the fields due to the three-phase conductors. Usually,

Table 2.3: Effects of low-frequency electrical and magnetic fields on the human body

Current density thresholds mA/m^2	Consequences in case of exceeding the thresholds	Body current	Field gradients corresponding to the thresholds at $f = 50/60$ Hz	
			E	B
		mA	kV/m	mT
1	no biological effects	0,07	4 to 5	0,025 to 0,070
10	stimulation (eye flickering)	0,7	40 to 50	0,25 to 0,70
100	stimulation of muscles and nerves (hazards possible)	7	400 to 500	2,5 to 70
1000	damage (heart fibrillation)	70	4000 to 5000	250 to 700

Table 2.4: Precaution values for low-frequency electrical fields in kV/m (rms)

Source	Occupational exposure		General public exposure	
	permanently	few hours per day	permanently	few hours per day
ICNIRP [2.8]	10	10	5	5
IRPA/WHO [2.10]	10	30	5	10
Europe [2.11] (50 Hz)	–	–	5	5
Germany [2.12]	–	–	5	10
United Kingdom [2.13]	12,3	–	12,3	–
USA [2.14]	8 to 11,8[1)]	7 to 11[2)]	1 to 3[3)]	–
Belgium [2.14]	10[1)]	7[2)]	5	–

[1)] Overhead power lines in general

[2)] Road crossings

[3)] Edge of right-of-way

limitations, originated from the practice or researches, are imposed to the maximum electrical field at the edge of or within the right-of-way.

The *electrical field strength* E, measured in kV/m, is used to describe the electrical field. The *magnetic induction* or *magnetic flux density* B is often used to determine the magnetic field instead of the *magnetic field strength* H, because it can be measured more easily. The relation between both quantities is

$$B = H \cdot \mu_0 \cdot \mu_r \quad , \tag{2.10}$$

where H is measured in A/m, μ_0 is the permeability of the vacuum $\mu_0 = 4 \cdot \pi \cdot 10^{-7}$V·s/(A· m) and μ_r the relative permeability being equal 1 in air. Since the magnetic field strength is measured in A/m, the magnetic flux density is given in V·s/m^2 or Tesla (T), where 1 T = 1 V·s/m^2. From (2.10) it is obtained in air

$$1\text{A/m} = 4 \cdot \pi \cdot 10^{-7}\,\text{T} \quad \text{or} \quad 1\text{A/m} = 1,256\,\mu\text{T} \quad \text{and} \quad 1\mu\text{T} = 0,7962\,\text{A/m} \tag{2.11}$$

for the homogenous magnetic field.

The electrical field influences electric charges on the body surface affecting the current flow within the body. From numerous measurements it is known that an electrical field of 1 kV/m causes a current of approximately 0,015 mA within the human body [2.9], the current density being between 0,2 and 0,3 mA/m^2. The *body currents* caused by the electrical field do not depend on the body conductivity nor on the body size [2.9]. However, the magnetic field induces currents in the human body which depend on the dimensions, as well as on the conductivity of the different parts of the human body. According to [2.9], a conductivity of 1 S/m is assumed for the physiological serum and 0,1 S/m for other parts. Therefore, an induction of 1 μT leads to current densities between 0,0016 mA/m^2 and 0,016 mA^2 in the head as well as 0,004 mA/m^2 to 0,04 mA/m^2 in the thorax.

It is further well-proved knowledge that with current densities up to 1 mA/m^2 no biological effects can be detected within the body. Current densities above 10 mA/m^2

Table 2.5: Precaution values for low-frequency magnetic induction in μT (rms)

Source	Occupational exposure		General public exposure	
	permanently	few hours per day	permanently	few hours per day
ICNIRP [2.8]	500	500	100	100
IRPA/WHO [2.10]	500	5 000; 25 000[1)]	100	1 000
Europe [2.11]	–	–	100	100
Germany [2.12]	–	–	100	200
United Kingdom [2.13]	2 000	–	2 000	–
USA [2.14]	1 000	–	20[2)]	–

[1)] For limbs only

[2)] Edge of right-of-way

Table 2.6: Range of maximum electrical and magnetic fields below overhead lines

Voltage (kV)	Electrical field at ground level under a line (kV/m)	Magnetic induction at ground level[1)] (μT)
765	8 to 13	28 to 32
525	5 to 9	25 to 30
420	4 to 8	22 to 28
245	2 to 3,5	20 to 25
123	1 to 2	12 to 15
70	1 to 1,5	2 to 2,5

[1)] for 1000 A current per circuit

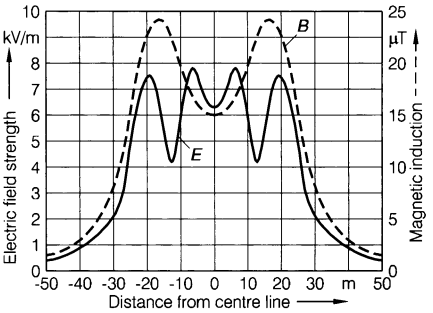

Figure 2.1: Electrical (E) and magnetic fields (B) below a 380 kV double-circuit overhead line. Current 1000 A per circuit

may cause *eye flickering* and up to 100 mA/m^2 stimulation of nerves and muscles. The *threshold of hazards* is 100 mA/m^2. Harms must be expected from 1000 mA/m^2 and above, e. g. ventricular fibrillation. The average cross section of the human body is between 0,06 and 0,07 m^2. In Table 2.3 these values are related to the corresponding field strengths.

Although there is no evidence of harmful effects of the magnetic fields on humans or animals, there are certain limitations imposed by practice and good sense. International organisations like Cigré and ICNIRP (International Commission on Non-Ionizing Radiation Protection) have undertaken extensive investigations on that issue, as it can be seen in [2.6, 2.8] and [2.15]. In Table 2.4, precaution values are shown for electrical fields and in Table 2.5 for magnetic fields. The usual range of maximum intensities of electrical and magnetic fields below overhead lines is shown in Table 2.6.

In Figure 2.1, a typical graph with the electrical and magnetic field profiles across a right-of-way is presented. The evaluation of the electrical and magnetic fields across the right-of-way of an overhead transmission line can nowadays be made with high accuracy, so that the established limits can be well checked.

Although medical examinations of linemen, performed in various countries, have so far failed to scientifically prove health problems ascribable to electrical and magnetic fields produced by overhead lines, precaution values have been established for exposures, from which the numbers presented in Table 2.4 give an indication of the order of magnitude of electrical fields accepted by different standards. As can be seen, the more recent recommendations according to [2.8] and [2.11] do no longer distinguish permanent and temporary exposure since there is an indication for a difference between permanent and temporary exposure. The precaution value of 5 kV/m stipulated in [2.8, 2.11] and [2.12] corresponds under worst case conditions to an induced current density of about

2 mA/m^2. The recommendation for occupational exposure of 10 kV/m is equivalent, therefore, to a current density of 4 mA/m^2. Both limits are well within the safe range where no biological effects occur.

In Table 2.5 precaution values are listed for magnetic fields. Regarding the *acceptable limits for* the *magnetic fields*, there is some controversy still existent world-wide, especially about their real effects on the health of human beings and animals. While in some countries the regulations are more permissible, in others very stringent rules have been established under a subjective basis. As in case of electrical fields, the precaution values for the magnetic field are no longer stipulated differently for permanent and temporary exposure. The flux density limit of 100 μT (0,1 mT) for general public exposure corresponds again to a current density of approximately 2 mA/m^2. In [2.8] and [2.10], limits for occupational exposure are set to 500 μT (0,5 mT) aiming at restricting the current density to 10 mA/m^2.

As can be concluded from a comparison with the data given in Table 2.6 for electrical and magnetic fields below overhead lines, the limits for magnetic field will not affect the design of overhead lines while the stipulations for electrical fields could be relevant for 420 kV and above.

2.3.2.2 Effects on electronic devices

Magnetic fields under overhead power lines can disturb sensitive electronic devices such as screen tubes of monitors and television sets, as measurements close to railway installations have demonstrated [2.16]. Limits for protection of electrical devices have been still under consideration, however, interference can occur at flux densities above 1 μm.

2.3.3 Corona phenomena and related effects

2.3.3.1 General

Corona effects on conductors are generated by the disruption of air dielectrics around the conductor, when the electrical field reaches the *critical surface gradient.* The critical gradient for smooth round cylinders with 10 mm radius is about 27 kV_{rms}/cm, falling to 21 kV_{rms}/cm for stranded conductors.

As the *corona discharges* are not permanent but occur in form of sparks around the conductor, electromagnetic radiation are emitted from the conductor, causing different types of undesirable effects.

The main nuisances of a too high conductor surface gradient are the emission of *radio interference* (RIV) at the AM band and the production of *audible noise* (AN) in the vicinity of the line, besides the generation of *corona losses.* In view of that, the maximum conductor surface gradient has to be kept below certain limits in order to avoid undue impacts of electric origin. In practice, it is recommended that the conductor surface gradient of overhead conductors should be limited to around 17 kV_{rms}/cm.

2.3.3.2 Calculation of voltage gradients on individual conductors

Several methods have been developed for calculating *conductor surface gradients* and in general they present a reasonable degree of accuracy [2.17]. The method of multiple images is considered by [2.18] as providing the most accurate calculations of conductor surface gradients. According to this method, every conductor or subconductor is considered as a cylinder and the influence of its charge is taken into account on other conductors or subconductors through its images and vice-versa. In application to practical bundle configuration, consideration of images until the second order is sufficient.

A *charge matrix* [**Q**] and a *potential coefficient matrix* [**P**] are correlated and the following matrix equation results:

$$[\mathbf{Q}] = [\mathbf{P}]^{-1}[\mathbf{V}] \quad , \tag{2.12}$$

where [**V**] is the matrix of *charge voltages*. The solution of this equation is made through computer programs. The gradient in any point of the space outside the conductors (subconductors) is then computable.
When dealing with three-phase conductors separated by relatively large distances, an approximation can be made, considering that the charge is concentrated in the centre of the conductor. For this case, the *maximum voltage gradient* E_i at the conductor surface will be

$$E_i = Q_i/(2\,\pi\,\varepsilon_0 \cdot r_\mathrm{B}) \quad , \tag{2.13}$$

where r_B is the equivalent bundle conductor radius according to (2.19) and ε_0 the *dielectric constant*. The charge Q can be expressed by

$$Q_i = C_i \cdot U_\mathrm{s}/\sqrt{3} \quad , \tag{2.14}$$

where C_i is the capacitance and U_s the highest system voltage. The variation around the subconductor periphery may be obtained by

$$E_\theta = E_i\,[1 + (2\,r/s) \cdot (n_2 - 1) \cdot \sin\,(\pi/n_2) \cdot \cos\,\theta] \quad , \tag{2.15}$$

where r is the radius of the bundle circle, s the subconductor distance, n_2 the number of subconductors and θ the angle at the subconductor surface.
Alternatively, E_θ can be expressed through

$$E_\theta = \overline{E}\,[1 + (r/r_0) \cdot (n_2 - 1) \cdot \cos\,\theta] \quad , \tag{2.16}$$

where r_0 is the bundle conductor perimeter radius. The maximum voltage E_i was replaced by the mean $\overline{E}$ of maximum voltage gradients of the three conductors. Equation (2.22) represents the value $\overline{E}$.
The maximum voltage gradient around the subconductor periphery is obtained by setting $\theta = 0$. Calculation of conductor voltage gradients by this method requires the use of computer programs for taking into account all necessary matrix operations.

2.3.3.3 Calculation of voltage gradient by approximate formulae

The maximum *voltage gradient* of a phase conductor i can be obtained according to [2.17] from

$$E_i = \frac{C_i'}{2\,\pi\varepsilon_0 \cdot n_2 \cdot r}\,[1 + 2 \cdot r/s\,(n_2 - 1) \cdot \sin(\pi/n_2)]\,\frac{U}{\sqrt{3}} \tag{2.17}$$

with
C_i' positive-sequence capacitance per unit length of the conductor i;
ε_0 dielectric constant = $8{,}854 \cdot 10^{-12}$ F/m;
n_2 number of subconductors;
r subconductor radius;
s subconductor distance;
U rated voltage.

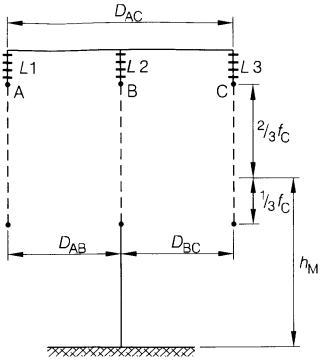

Figure 2.2: Geometric data for conductor arrangement to determine the voltage gradient

Table 2.7: Coefficients to determine the voltage gradients

Number of subconductors n_2	1	2	3	4	5	6	8
k_1	1	1	1	1,12	1,27	1,43	1,76
$k_2 = 2 \cdot (n_2 - 1) \cdot \sin(\pi/n_2)$	1	2	3,48	4,24	4,70	5,00	6,07

Table 2.8: Voltage gradients for some conductor arrangements. U_s = 420 kV

Conductor	562-AL1/ 49-ST1A			389-AL1/ 34-ST1A	264-AL1/ 34-ST1A
Number of subconductors	2	3	4	3	4
Subconductor diameter in mm	32,2	32,2	32,2	26,7	22,4
Total cross section in mm^2	1222	1836	2445	1260	1191
Voltage gradient in kV/cm	17,2	13,7	11,5	15,9	15,4

The capacitances per unit length have to be determined from the geometric data of conductors and earth wires and their arrangement on the supports. The procedure is given in [2.17] and can be carried out by computer programs. Accepting some approximations, mean capacitances per unit length can be evaluated. It applies to the line presented in Figure 2.2 having one circuit without earth wires (see clause 3.5):

$$C' = 2\pi\varepsilon_0 / \ln \frac{D_M}{r_B \sqrt{1 + (D_M/2h_M)^2}} \tag{2.18}$$

where r_B is the equivalent bundle conductor radius according to

$$r_B = (n_2 \cdot r \cdot r_0^{n_2-1})^{1/n_2} = r\,(k_1 \cdot s/r)^{(n_2-1)/n_2} \quad , \tag{2.19}$$

(for k_1 see Table 2.7)
D_M is the mean conductor distance (see Figure 2.2)

$$D_M = (D_{AB} \cdot D_{AC} \cdot D_{BC})^{1/3} \quad , \tag{2.20}$$

h_M is the mean conductor height above ground (see Figure 2.2)

$$h_M = (h_A \cdot h_B \cdot h_C)^{1/3} \quad . \tag{2.21}$$

The value r_0 in (2.19) represents the radius of the bundle conductor circle and can be obtained from $r_0 = s/\sin(\pi/n_2)$ being s the subconductor distance. For other phase conductor and earth wire arrangements, the positive-sequence capacitances can be computed according to clause 3.5. With these data, the mean voltage gradient of a single-circuit line results from (see also [2.19])

$$\overline{E} = \frac{1 + k_2 \cdot r/s}{n_2 \cdot r} \cdot \frac{1}{\ln\left[D_M \Big/ \left(r_B \cdot \sqrt{1 + (D_M/2h_M)^2}\right)\right]} \cdot \frac{U}{\sqrt{3}} \quad . \tag{2.22}$$

The coefficients k_1 and k_2 are presented in Table 2.7. In (2.22) $(D_M/2h_M)^2$ can be neglected against 1 in many cases. For double-circuit lines D_M/r_B is to be replaced by $(D_M \cdot D_{M2}/r_B \cdot D_{M1})$ (see (3.30) and (3.35)).
Due to $r_B = r$ it is obtained for a single conductor

$$\overline{E} = \frac{1}{r \ln(D_M/r)} \frac{U}{\sqrt{3}} \quad . \tag{2.23}$$

Table 2.9: Reception quality of radio signals

Reception class	Signal to noise ratio (dB)	Reception quality
A	32	Entirely satisfactory
B	27 to 32	Very good, background noise unobtrusive
C	22 to 27	Fairly satisfactory, background noise plainly evident
D	16 to 22	Background noise very evident, speech easily understood
E	6 to 16	Speech understandable only with severe concentration
F	7	Speech unintelligible

Example: For a 400 kV line with the phase arrangement according to Figure 2.2 the mean voltage gradient should be determined.
The data are: $D_{AB} = D_{BC} = 7{,}5$ m; $D_{AC} = 15$ m; $h = 15{,}0$ m.
Conductors: Twin bundle 562-AL1/49-ST1A (see Table 2.7). Bundle spacing 400 mm.

$r \quad = 32{,}2/2 \qquad\qquad = 16{,}1$ mm $= 1{,}61$ cm;
$r_B \quad = 16{,}1 \cdot (1 \cdot 400/16{,}1)^{1/2} \quad = 80{,}25$ mm $= 0{,}08025$ m (see (2.19));
$D_M \quad = (7{,}5 \cdot 7{,}5 \cdot 15{,}0)^{1/3} \quad = 9{,}45$ m (see (2.20));
$h_M \quad = \mathrm{h} \qquad\qquad = 15{,}00$ m

$$\overline{E} = \frac{1 + 2(16{,}1/400)}{2 \cdot 1{,}61 \cdot \sqrt{3}} \cdot \frac{420}{\ln\left[9{,}45/\left(0{,}08025\sqrt{1 + (9{,}45/(2 \cdot 15{,}0))^2}\right)\right]} =$$

$$= \frac{1{,}0805 \cdot 420}{5{,}577 \cdot 4{,}72} = 17{,}2 \text{ kV/cm}.$$

Table 2.8 depicts voltage gradients for circuits equipped with typical 420 kV conductor alternatives.

2.3.3.4 Radio noise or radio interference (RI)

General considerations

Radio noise or radio interference (RI) is a disturbance by undesired electric waves within the radio frequency band in any transmission channel or device. The phenomenon becomes even more evident in the frequency band of 500 to 1500 kHz (AM band). The frequency of 1000 kHz (1 MHz) is usually taken as reference for RI calculation.
Radio interference (RI) decreases with lateral distance from the line axis. It is normally quoted in dB above 1 μV/m and its maximum value is usually established for the edge of the right-of-way. Its significance, however, will depend upon the population density and the signal strengths of the various radio stations in a particular area. Usually, people living near to overhead lines are quite aware of their rights and require a strict observation of standardized RI levels from the line owner. In the vicinity of urban areas, the high intensity of radio signal strength is generally enough to offset the radio noise produced by overhead lines.
The noise level alone is not sufficient to determine the severity of interference, but when combined with signal strength to indicate the *signal-to-noise ratio*, it has much more significance. According to signal-to-noise ratio, a reception quality scale is prescribed, as the so-called IEEE scale, which shows the results of subjective listening tests correlating the quality of reception to the signal-to-noise ratio. The IEEE scale according to [2.18] is shown in Table 2.9.
The right-of-way may be sometimes defined by RI criteria, provided a minimum signal to be protected is specified. In general, signals in AM frequency in the range of 65 to 75 dB should be protected, according to different national regulations. So if, for example, a reception class C is required and the radio signal to be protected is 66 dB, the maximum RI acceptable to be generated by the line at the edge of the right-of-way will be $NP_I = 66 - 22 = 44$ dB.

Calculation of RI levels

Several utilities have so far adopted for their EHV lines rough estimates of *RI levels* through the use of design curves that provide positive or negative adders to a base-case design. Quick indication of the effects in variation of phase spacing, conductor size, conductor height, etc. can be obtained and are added to RI of a base case [2.18].

An empirical method for *calculating the RI level* at fair weather conditions is as follows: The RI level [2.20, 2.21], measured in dB above 1 μV/m, can be determined by

$$NP_{\mathrm{I}i} = 3{,}5\,E_i + 12\,r_{\mathrm{i}} - 33\log(D_{\mathrm{L}i}/20) - 30 \qquad \text{in dB} \quad , \tag{2.24}$$

where E_i is the voltage gradient of the conductor i in kV/cm, r_i the radius of the conductor or subconductor in cm and $D_{\mathrm{L}i}$ the distance from the conductor to the measuring point in m.

In a three-phase AC system, where the RI level of one of the three phases is at least 3 dB higher than the RI levels of the other two phases, the lower two can be neglected then [2.20]. Otherwise, the resulting RI level at the measuring point is

$$NP_{\mathrm{I\,total}} = (NP_{\mathrm{I1}} + NP_{\mathrm{I2}})/2 + 1{,}5 \quad \text{in dB} \quad , \tag{2.25}$$

where NP_1 and NP_2 represent the two higher values of the three phases. For multiple-circuit lines, all RI levels NP_i are determined by (2.24). Then, the RI levels of the corresponding phases are added squarely. The resulting or total RI is determined by (2.25). The relationship between RI level in dB and the field intensity E_{I} in μV/m is

$$NP_{\mathrm{I}} = 20\,\log E_{\mathrm{I}} \quad \text{and} \quad E_{\mathrm{I}} = 10^{(NP_{\mathrm{I}}/20)} \quad . \tag{2.26}$$

Field measurements

Background RI noises are relevant as they are present even before the line is constructed. In this case, the insertion of a well designed line may not significantly affect the overall radio noise level. *Field measurements* of background (ambient) noise, as well as of AM signal intensities, should be performed along the routes of EHV lines, before their construction. The results of the measurements generally show, that in many non-populated and remote areas, no AM stations can be tuned during the day, while, in other cases, signal-to-noise ratio even without any line is already very low.

2.3.4 Audible noise (AN)

General conditions

Audible noise (AN) produced by corona of transmission line conductors has emerged as a matter of concern having to be considered duly. In dry conditions, the conductors usually operate below the *corona inception level* and only few corona sources are present. Audible noise from transmission lines occurs primarily in foul weather. However, in general it can be said that transmission systems contribute little as compared with the audible noise produced by other sources. In case of rural lines, the importance of the audible noise (AN) may be still lower, as the population density beside the line is low.

It is complex to define how much audible noise can be tolerated from a transmission line. However, as voltage levels increase, audible noise becomes one of the limiting factors in the design of transmission lines. To define the acceptable noise levels, the best guide is the experience with EHV transmission lines.

It is difficult in general to permanently comply with 45 dB(A) required for residential areas according to [2.22]. In general, complaints on audible noise will be avoided if the noise level does not exceed 50 dB(A). However, complaints have to be expected, if noise with more than 55 dB(A) will be produced by a line. This can occur close to 420 kV

lines showing high voltage gradients under adverse weather conditions. If an overhead line does not cause concerns in adverse weather no problems will be realized in dry weather. There is a close correlation between the audible noise, measured in dB(A), and the radio interference at 1 MHz (see [2.18]).

Calculation

According to [2.23], in order to determine the audible noise (AN) of an overhead line, the *noise potential* of every conductor should be first calculated as follows

$$NP_{\mathrm{A}i} = -164{,}6 + 120 \log E_i + 55 \log r_{\mathrm{e},i} \quad , \tag{2.27}$$

where E_i is the voltage gradient in kV/cm and r_{e} the equivalent radius according to

$$r_{\mathrm{e}} = r \qquad \text{for } n_2 \leq 2$$

and

$$r_{\mathrm{e}} = 0{,}58 \cdot n_2^{0{,}48} \cdot r \qquad \text{for } n_2 \geq 3 \quad , \tag{2.28}$$

where n_2 is the number of subconductors and r the subconductor radius in mm. Equation (2.27) was obtained from evaluation of tests.

The audible noise (AN) at any point close to a line can be determined by

$$NP_{\mathrm{A}} = 10 \log \left\{ \sum_{i=1}^{n} \exp[0{,}23\,(NP_{\mathrm{A}i} - 11{,}4\,\log D_{\mathrm{L}i} - 5{,}8)] \right\} \quad , \tag{2.29}$$

where n is the number of phase conductors and $D_{\mathrm{L}i}$ the distance (in m) between conductor i and the reference point (measuring point).

Example: Referring to Table 2.8 and equations (2.24) and (2.29), the RI and AN levels at a point 40 m far from a 420 kV circuit will be determined as an example as follows:

RI level of a twin bundle is obtained from (2.24)

$$NP_{\mathrm{I}i} = 3{,}5 \cdot 17{,}2 + 12 \cdot 1{,}61 - 33 \log 2 - 30 = 39{,}6 \text{ dB} \quad ,$$

and the RI level of a quadruple bundle

$$NP_{\mathrm{I}i} = 3{,}5 \cdot 11{,}5 + 12 \cdot 1{,}61 - 33 \log 2 - 30 = 19{,}6 \text{ dB} \quad .$$

Considering that the higher RI levels are assumed to be the same for three phases it results from (2.20) for:

Twin bundle: $NP_{\mathrm{total}} = 39{,}6 + 1{,}5 = 41{,}1$ dB corresponding to $E_{\mathrm{I}} = 10^{(41{,}1/20)} = 113{,}5\ \mu$V/m

Quadruple bundle: $NP_{\mathrm{total}} = 19{,}6 + 1{,}5 = 21{,}1$ dB corresponding to $E_{\mathrm{I}} = 10^{(21{,}1/20)} = 11{,}4\ \mu$V/m.

Similarly, the AN levels can be determined as follows:

For the twin bundle

$$NP_{\mathrm{A}i} = -164{,}6 + 120 \log 17{,}2 + 55 \log 32{,}2 = 66{,}6 \text{ dB} \quad ,$$

and for the quadruple bundle

$$NP_{\mathrm{A}i} = -164{,}6 + 120 \log 11{,}5 + 55 \log 36{,}3 = 48{,}5 \text{ dB} \quad .$$

From equation (2.29) it results:

Twin bundle

$$NP_{\mathrm{A}} = 10 \log\{3 \cdot \exp[0{,}23\,(66{,}6 - 11{,}4 \log 40 - 5{,}8)]\} = 47{,}3 \text{ dB(A)} \quad ,$$

Quadruple bundle

$$NP_{\mathrm{A}} = 10 \log\{3 \cdot \exp[0{,}23\,(48{,}5 - 11{,}4 \log 40 - 5{,}8)]\} = 29{,}2 \text{ dB(A)} \quad .$$

The audible noise level is reduced by approximately 18 dB(A) when using a quadruple bundle instead of a twin bundle. Other references, e. g. [2.20] and [2.24], weigh the voltage gradient to a lower extent. Thus, the audible noise level would drop to a smaller extent only. Equation (2.27) is confirmed also through measurements carried out in the field and by experience with existing lines (see [2.25]).

Table 2.10: Impact of line design and conductor configuration on fields, radio interference and audible noise

Parameter	Electrical field	Magnetic field	Radio interference	Audible noise
Increase of phase conductor distance	↑	↑	↓	↓
Increase of clearance to ground	↓	↓	↓	↓
Increase of subconductor number of bundles	↑	→	↓	↓
Increase of conductor cross section	→	→	↓	↓
Increase of subconductor distance in bundles	→	→	→	↑
Inverse sequence of phases to achieve a low impedance of double-circuit lines	↓[1)]	↓[1)]	→	→

Comments: ↑ means increasing the effect
↓ means reducing the effect
→ has no substantial impact
1) substantial reduction outside the right-of-way

2.3.5 Impact of line design on voltage- and current-depending phenomena

The described relationships between line configuration and the *voltage- and current-depending phenomena* and the effects on the environment resulting thereof play a steadily increasing role in the design and configuration of overhead power lines. While electrical field strength is perceived by persons, e. g. by straightening up the hair or by causing weak electrostatic shocks, magnetic fields cannot be perceived directly by persons; however, both are quoted to affect health and wellness of human beings and animals. Radio interference and audible noise are perceived and may not exceed stipulated limits. The *design* and *configuration of lines* should, so far as possible, keep all the mentioned phenomena on a low level. This cannot be achieved completely since the variation of some design parameters affect the emissions in opposite directions. The effective essential parameters are:

- Distance and arrangement of phase conductors;
- Height of phase conductors above ground;
- Number of subconductors in bundles;
- Subconductor spacing in bundles and
- Conductor cross section.

Table 2.10 according to [2.26] depicts the results due to parameter variation. Since the effects of several simultaneous parameter variations may tend in opposite directions, it is important to design each individual line such that those design targets having priority will be achieved.

Increasing the subconductor spacing reduces radio interference and audible noise but rises electrical and magnetic fields. Increasing the clearance to ground reduces all the considered phenomena, however, involves substantially higher investments. A higher *number of subconductors* within a bundle results in lower *radio interference* and *audible noise*, even at the same over-all cross sections but also in higher electrical field strength at the ground level. A bigger conductor cross section decreases radio interference and audible noises but has low effect on *electrical* and *magnetic field* intensities. The subconductor spacing within a bundle is of minor influence only by increasing the audible noise level. An asymmetrical arrangement of phase conductors of lines equipped with

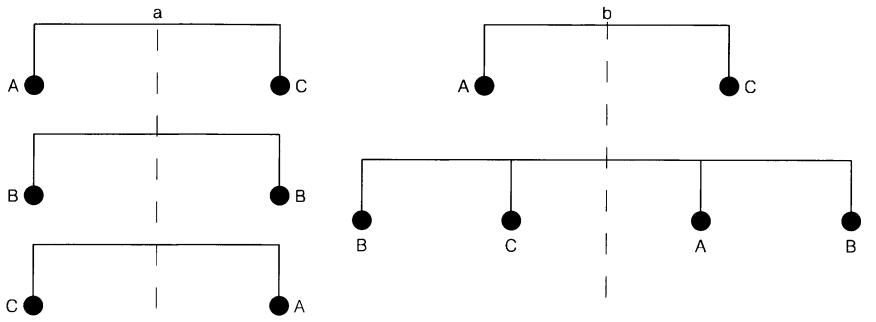

Figure 2.3: Configuration of phase conductors with respect to low electrical and magnetic fields. a) vertical conductor configuration, b) Danube configuration

two circuits (Figure 2.3) contributes to reduce substantially the field strengths outside the right-of-way.

2.4 Line performance and insulation requirements

2.4.1 Introduction

The performance of a transmission line is an important factor to assure the *reliability* and *security* of an electric system. Besides the *mechanical behaviour* of its components, attention should be given to the *electric performance* that plays a main role either in the design and investment of transmission components or in the outage rates (permanent or transient) of the specific transmission line. For attaining such objectives, optimum insulation clearances of the towers should be selected; in other words, the insulation levels, depending on different voltage stresses that reach the air gaps, should be chosen as to result in a compromise between a satisfactory electric performance and reasonable investments.

Regarding insulation, it is important to understand the basic difference between stresses caused by *system power frequency voltage* and stresses caused by *overvoltages*. Overvoltages are rare and of limited duration, but the system power frequency voltage, even though relatively low in amplitude, permanently stresses the insulation while the system is in operation.

To define the tower top geometry, the following voltage stresses are considered: Power frequency voltage; fast-front and slow-front overvoltages. Additionally, towers are potentially designed to permit live-line maintenance, so that clearances for such a work should be considered as well.

2.4.2 Power frequency voltages and temporary overvoltages

System voltage is the rms, phase-to-phase power frequency voltage of an electric system. The system is usually designed by a *nominal system voltage* to which certain operating characteristics of the system are related. For instance, nominal system voltage is used as a base for load flow and some other system studies. Generally, most systems are specified for operating near the nominal system voltage. Some systems, however, are required to operate near or at the maximum system voltage, which is usually 5 to 10 % higher than the nominal. *Highest system voltage* is the highest rms phase-to-phase system voltage that occurs under normal operating conditions at any time and at any point in the system.

Table 2.11: Standard insulation levels for range I (1 kV $\leq U_s \leq$ 245 kV) according to IEC 60071-1

Highest voltage for equipment U_s [1] kV (rms value)	Standard short-duration power frequency withstand voltage kV (rms value)	Standard lightning impulse withstand voltage kV (peak value)
3,6	10	20
		40
7,2	20	40
		60
12	28	60
		75
		95
17,5	38	75
		95
24	50	95
		125
		145
36	70	145
		170
52	95	250
72,5	140	325
123	(185)[2]	(450)
	230	550
145	(185)	(450)
	230	550
	275	650
170	(230)	(550)
	275	650
	325	750
245	(275)	(650)
	(325)	(750)
	360	850
	395	950
	460	1050

[1] The highest voltage for equipment is desigated by U_m in [2.29].

[2] If values in parenthesis are considered insufficient to prove that the required phase-to-phase withstand voltages are met, additional phase-to-phase withstand tests are needed.

Temporary overvoltages are of oscillatory nature at a given location, normally of relatively long duration and which are undamped or weakly damped. They usually originate from switching operation, such as load rejection or resonant conditions. In directly earthed neutral systems with earth fault factors of 1,3 or below, temporary overvoltages are usually not considered for determining electrical clearances for a line.

In this case, consideration should be given only to the highest system voltage U_s that characterizes the electric systems as in [2.27]. Two voltage ranges are established as range I and range II, as it can be seen in Tables 2.11 and 2.12 , respectively.

In case of *power frequency overvoltages*, the continuous stress due to voltage is also of concern if the insulation itself changes with time. Flashover may occur if insulation strength is reduced sufficiently. Weather conditions may lead to such reductions in strength. As an example, the wind might blow a conductor to one side, hence reducing the air gap between it and the support structure. Because air gaps are stressed perma-

Table 2.12: Standard insulation levels for range II (U_s > 245 kV) according to IEC 60071-1

Highest voltage for equipment U_s[1] kV (rms value)	Standard switching impulse withstand voltage			Standard lightning impulse withstand voltage kV (peak value)
	Longitudinal insulation[2] kV (peak value)	Phase-to-earth kV (peak value)	Phase-to-phase (ratio to the phase-to-earth peak value)	
300	750	750	1,50	850
				950
	750	850	1,50	950
				1050
362	850	850	1,50	950
				1050
	850	950	1,50	1050
				1175
420	850	850	1,60	1050
				1175
	950	950	1,50	1175
				1300
	950	1050	1,50	1300
525[3]	950	950	1,70	1175
				1300
	950	1050	1,60	1300
				1425
	950	1175	1,50	1425
				1550
765[3]	1175	1300	1,70	1675
				1800
	1175	1425	1,70	1800
				1950
	1175	1550	1,60	1950
				2100

[1] The highest voltage for equipment is designated by U_m in [2.29].

[2] Value of the impulse component of the relevant combined test.

[3] The introduction of U_s = 550 kV (instead of 525 kV), 800 kV (instead of 765 kV) and of a value between 765 kV and 1200 kV, and of the associated standard withstand voltages is under consideration.

nently, there is more risk of a flashover if a conductor is blown close to the structure than if the insulators were loaded by an overvoltage.

Insulation strength may also change over longer periods, e. g. due to *contamination* built up, or within minutes as the insulators are alternately wetted by fog or rain and dried by surface leakage. In either case, only the continuous system voltage lasts long enough for changes in strength to become evident. Effects of contamination may be evaluated through laboratory testing (see clause 9.9.4).

Usually, power frequency voltages as described govern the design of the insulator strings as far as the pollution levels along the line route are concerned. The total insulating length along the surface of the insulators is the basic parameter that is specified to define the number of insulators required for a line. As a function of the individual creepage distances of each insulator type, it is possible to determine the type and number of insulators required for the region crossed by the line. In Table 9.8, the classification of the pollution level is shown together with the required specific creepage distances according to IEC recommendations [2.28]. It is possible, therefore, to determine the type and umber of insulators required for a certain line provided that a previous investigation is carried out to assess the pollution levels along the line route.

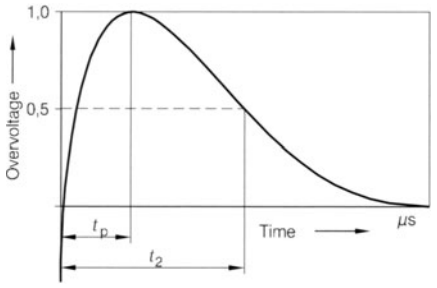

Figure 2.4: Standard slow-front impulse voltage. $t_p = 250\ \mu s$; $t_2 = 2500\ \mu s$

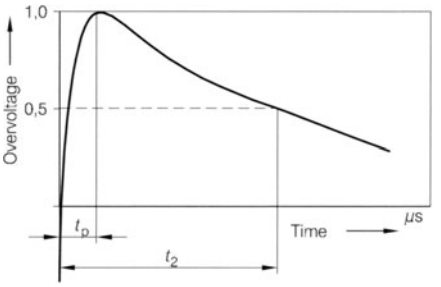

Figure 2.5: Standard fast-front impulse voltage. $t_p = 1{,}2\ \mu s$; $t_2 = 50\ \mu s$

2.4.3 Slow-front overvoltages

The *slow-front overvoltages* can be produced by switching overvoltages or distant direct lightning strokes and depend basically on system parameters, system configuration and system condition, e. g. load release. However, switching overvoltages may attain different values even for the same system and the same switching operation. The overvoltages of this type in an overhead line are mainly produced by energization or by reclosing operations of the line.

The voltage stress is characterized in this case by a standard wave shape of 250/2500 μs, as it can be seen in Figure 2.4. The values of the overvoltages depend on the relative timing of the switching event with respect to the power frequency system voltage sine wave. Generally, the closing time of the breaker is not synchronized with the power frequency voltage wave shape. It is random, and each switching operation will result in a different overvoltage.

By finding the worst-case combination of breaker closing times through trial and error on a *transient network analyser* (TNA) in general or with a computer program, it is possible to determine the maximum overvoltages associated with a given switching operation in a certain system. A random evaluation of different cases can be used to determine a statistical distribution that will represent the probability function of occurrence of slow-front overvoltages.

2.4.4 Fast-front overvoltages

Fast-front overvoltages at a given location in a system are mainly caused by a lightning discharge that hit directly on the phase conductors or by *back-flashovers*, the shape of which can be regarded, for insulation coordination purposes, as similar to that of the standard impulse used for lightning impulse tests. Such overvoltages are usually unidirectional and of very short duration. The *standard lightning impulse* has a front time of 1,2 μs and a time-to-half-value of 50 μs, as it can seen in Figure 2.5. For a simplified analysis, lightning may be considered as a current source, so that the overvoltage developed by lightning is the product of lightning current and the impedance through which it flows.

2.4.5 Principles of insulation coordination

2.4.5.1 General principles

According to [2.29], the *insulation coordination* comprises the adequacy of the dielectric strength of an equipment or any other insulating arrangement, such as line insulation, to the voltages that can appear in the system, for which the equipment has been designed.

This procedure takes into account the characteristics of the protective devices, aiming at reducing to an economically and operationally acceptable level the probability that resulting voltage stresses would cause damage or hinder the continuity of service of the equipment or of the overhead line. The determination of insulation requirements of a transmission line is given by *steady-state conditions*, as well as by *transient conditions* that can occur in the system. The line design should be adequate, inside the system reality, to generate a satisfactory performance. The way for protecting a system against overvoltages is fundamentally an economic issue. It would be unfeasible to insulate the whole system, so as to withstand any kind of electric stress. On the other hand, it would be nonsense to insulate the system for withstanding only the normal operating voltage accepting failures for all transient electric stresses.
The basic purpose of *insulation coordination* consists in adequately treating several information such as the electric stresses applied to the equipment, the insulation withstand capability, the applicable protection devices, the minimum acceptable performance and the global investments involved in the process.

2.4.5.2 Insulation design for permanent power frequency voltages

The power frequency performance of transmission lines consists basically of two considerations:
The first one is the *electric strength of insulator strings* under contaminated conditions and the second one is the *clearance to tower* under extreme swing conditions of conductors and insulators. In both cases, only power frequency voltages are considered; in fact, when considering the air gap requirements under conditions of extreme swing, the probability of occurrence of a switching or lightning surge is so small as to be negligible. According to the present experience, insulators, that are contaminated and the power frequency voltage is very close to flashover voltage can sustain significant switching or lightning surges without increasing the probability of flashovers.
The first step is, therefore, to select the insulator type and string length and the number of insulators as a function of the pollution levels of the area to be crossed by the line. Table 9.8 reproduces the IEC definitions of pollution levels and creepage distances required for each pollution level. Clause 9.9 deals with insulation design in view of pollution.
For unrestrainedly swinging insulator set only the air gap strength for power frequency voltages should be considered under conditions of extreme swinging.
The swing angle should be calculated as a function of the wind speed, of weight span to wind span ratio and of diameter and weight of the conductor. The required *power frequency clearance* can be determined for the maximum power frequency stress. The return period associated with maximum swing angle can also be considered as *mean recurrence interval* (MRI) of a flashover at power frequency voltage, e. g. once in 50 years.

2.4.5.3 Insulation design for slow-front overvoltages

There are two basic methods for studying the insulation coordination of an overhead line considering *slow-front overvoltages.*
The first one, designated as deterministic or conventional method of insulation coordination, assumes that there is a known, definite *maximum overvoltage*, $U_{\max}$, that may stress the insulation. It is also assumed that there is a definite *minimum insulation withstand voltage*, U_{w}. The insulation is designed so that U_{w} is larger than $U_{\max}$ by a safety margin, as shown in Figure 2.6. The withstand voltage is called in this case *basic surge insulation level* (BSIL) as it refers to slow-front or switching overvoltages. In Tables 2.11 and 2.12, the most common insulation levels are shown as adopted for each voltage level. This approach has been used in traditional insulation coordination

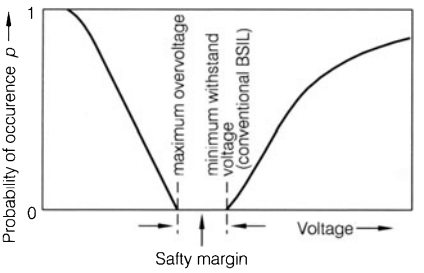

Figure 2.6: Conventional insulation coordination

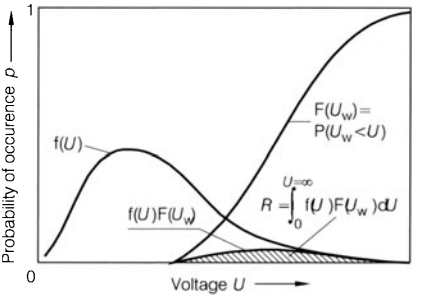

Figure 2.7: Statistical approach for insulation coordination.
$f(U)$ density distribution of overvoltages; $F_{(Uw)}$ probability function of withstand voltage; R risk of flashover

procedure; the corresponding overvoltage is called *conventional maximum switching overvoltage.*

The conventional method is usually more conservative, as the maximum overvoltages occur seldom and, likewise, the insulation strength rarely decreases to its lowest values. Moreover, the likelihood of both events occurring simultaneously is limited.

Nowadays, it is a common and more adequate practice to use statistical methods for determining the *probability of flashover* of a certain insulation or specifically of a line. The statistical methods do not predict the specific overvoltages produced by any particular switching operation, but they give the probability with which a certain overvoltage may be expected or, more practically, the probability of exceeding a certain overvoltage value. The overvoltage would be fully described if its probability density function or cumulative distribution function were given.

In contrast with the solid insulation, that is not allowed to flashover, the air insulation of structures is so selected as to permit a certain number of flashovers, corresponding to the desired performance. The coordination of stresses (overvoltages) and the strengths (clearances) to obtain the desired performance is by nature a statistical procedure, as both the strengths and stresses have no fixed values but vary within ranges, that constitute probability distributions of stresses and strengths, whose integrated probability constitutes the performance or *probability of flashover* (PFO) or *risk of failure* (Figure 2.7).

For determining the withstand strength of the different structural gaps, their shapes should be taken into account and the rod to plane gap is usually taken as reference. The *critical flashover voltage* $U_{50\%}$ is calculated using empirical formulae. Equation (2.42) applies for slow-front overvoltages, equation (2.43) for fast-front overvoltages. However, the statistical procedure, as presented here, is in practice only applied to slow-front overvoltages.

The critical voltage is calculated for standard atmospheric conditions and it is also necessary to take into account the influence of the real atmospheric conditions. The critical voltage $U_{50\%\text{real}}$ in the real atmospheric conditions is calculated as a function of $U_{50\%}$ in standard conditions by:

$$U_{50\%\,\text{real}} = U_{50\%} \cdot (\varrho_r'/k_{\text{hm}})^n = U_{50\%} \cdot \text{RIS} \quad . \tag{2.30}$$

There, ϱ_{r}' is the relative air density, depending on the absolute air temperature T and

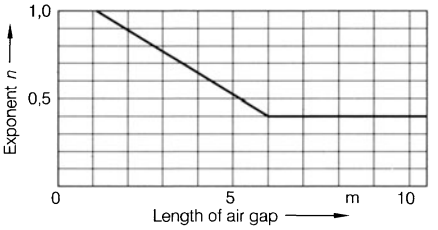

Figure 2.8: Exponent n for temperature- altitude- and humidity-depending correction of critical flashover voltage according to equation (2.30)

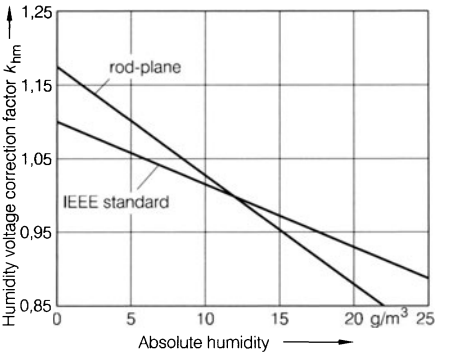

Figure 2.9: Nomogram to determine the humidity voltage correction factor

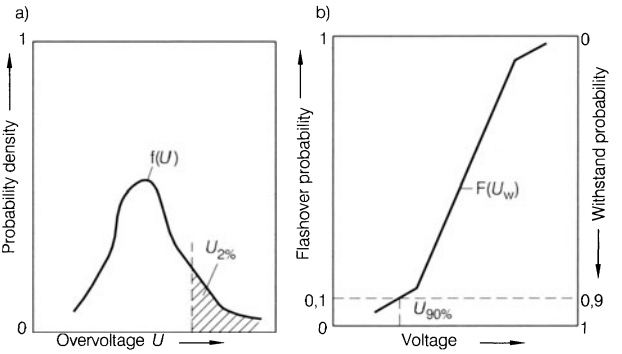

Figure 2.10: Simplified statistical approach:
a) probability density function of overvoltages;
b) cumulative distribution function of impulse withstand voltage

the altitude h_{al} in m above sea level. According to [2.30]

$$\varrho'_r = \varrho_T/\varrho_{15} = (288/T) \cdot \exp(-0{,}00012\, h_{al}) \quad . \tag{2.31}$$

For $T = 288$ K (+15°) and $h_{al} = 0$, ϱ'_r will be 1,0.
The quantity k_{hm} is a *humidity voltage correction factor* depending on the absolute air humidity according to Figure 2.9; n is an exponent depending on the air gap distance as in Figure 2.8 [2.18]. The term $(\varrho'_r/k_{hm})^n$ is named *relative insulation strength* (RIS).

Example: The relative insulation strength (RIS) should be evaluated for $h_{al} = 1000$ m; $T = 293$ K; length of rod-plane air gap 4,0 m and a humidity of 15 g/m^3. From (2.31), it is obtained $\varrho'_r(288/293)\exp(-0{,}12) = 0{,}983 \cdot 0{,}887 = 0{,}87$. $k_{hm} = 0{,}95$ results from Figure 2.9 and $n = 0{,}64$ from Figure 2.8. Then RIS $= (0{,}87/0{,}95)^{0{,}64} = 0{,}95$.
If the actual distribution of overvoltages and withstand strengths are not known, an approximation of the risk may be obtained by a simplified statistical approach (Figure 2.10). This approach is based on the premise that the actual shape of the low-voltage end of the overvoltage distribution is not too important because those low overvoltages will not cause failures. Likewise, there is little need to keep accurate track of how likely it is that the insulation strength is greater than normal. Therefore, the actual distributions are replaced by simple distributions, generally Gaussian distributions, that can be characterized by the standard deviation and by one defined point. This point belongs to the overvoltage distribution and is characterized as the *statistical overvoltage*, $U_{2\%}$, this being the overvoltage at the 2 % point.

The distribution of withstand voltages is described by $U_{90\%}$, the statistical withstand voltage, measured at the 90 % withstand or 10 % breakdown point. These points are illustrated in Figure 2.10. The task would be, therefore, to coordinate the two distributions of slow-front or switching surge overvoltages at one side with the distribution of withstand voltages at the other side. This can be reached by adequate selection of the air gap and the corresponding cumulative distribution adjusting the right curve in Figure 2.10.

The *maximum switching overvoltage* mentioned above should be combined with the minimum withstand voltage of narrowest gaps for one tower in order to determine the risk of failure for one typical tower. Using the appropriate statistical formulae it is then possible to determine the risk of failure, also called probability of flashover, for the number of towers that are supposed to be reached by the overvoltages.

Considering, therefore, the statistical method of insulation coordination for determining the insulation of a certain line, the practice consists in specifying a *maximum risk of failure* or *probability of flashover* (PFO) that a line can accept. The figures specified for the PFO usually are in the range of 10^{-2} to 10^{-4}, meaning that one line outage will be accepted in the range of 100 to 10 000 switching operations.

2.4.5.4 Insulation design for fast-front overvoltage

Fast-front overvoltages are responsible for the *lightning performance* of an overhead transmission line. Fast-front overvoltages or lightning overvoltages produce overvoltages on transmission lines through two main mechanisms, namely:

- Overvoltages due to lightning strokes that bypass the overhead shield wires and terminate directly upon phase conductors. These overvoltages are called *shielding failures.*
- *Back-flashovers*, when the lightning strokes reach the shield wire or a tower and the stroke current flows through a transmission line tower, elevating its potential above that of the more remote earth. A voltage difference develops between the tower and phase conductors and a flashover from tower to conductor may occur. If the lightning overvoltage is high enough to cause a flashover along an insulator set, it is likely that a *power arc* will be established needing to be extinguished by switching off the line.

It has to be considered that the circuit breakers of the line terminals are often provided with *automatic reclosing operations*, so that in general 60 to 70 % of the flashovers caused by lightning are usually of transient nature and the line is reclosed without suffering a permanent outage. Among several factors affecting line performance, it can be mentioned:

- Lightning ground flash density or, alternatively, lightning stroke frequency or *keraunic levels* that measure the average number of thunderstorm days per year along the line route (see Chapter 4);
- Stroke magnitude and wave shapes (see Chapter 4);
- Tower type, height and geometry;
- Shielding angles of earth wires (see Chapter 4);
- System voltage;
- Earthing resistance and soil characteristics (see Chapter 5);
- Type of terrain and natural shielding through trees or mountains and
- Installation of surge arresters in parallel to the insulator sets along the line.

The basic parameter used to measure the *lightning performance* is the number of outages per 100 km per year. The lightning performance is dealt with in Chapter 4.

The withstand voltage to be used should be taken as higher than or equal to the overvoltage which can propagate beyond a few towers from the point of the lightning

stroke. If no more accurate means of calculation is available, the phase-to-earth fast-front overvoltage can be taken as the withstand voltage of the insulator set, that is the 90 % *lightning withstand voltage* of the insulator strings $U_{90\%\text{ff\_ins}}$. The withstand voltage in this case is called *basic insulation level* (BIL) as it refers to fast-front or lightning overvoltages.

2.4.6 Live-line maintenance

The overhead transmission lines are frequently required to be designed for accepting live-line maintenance, either with the bare-hand method or with the hot-stick method. In view of that, it is necessary to establish clearances in the towers big enough so as to offer total safety for the linemen that will work in the energized line. Such clearances can in some cases govern some parts of the insulation of the towers and should, therefore, be taken into account when designing the towers.

2.5 Clearances

2.5.1 Clearance requirements

2.5.1.1 Types of electrical clearances

According to [2.27], five types of requirements are considered for determining the *minimum electrical clearance* distances, namely:

- Prevention of disruptive discharges between phase conductors and objects at earth potential when fast-front or slow-front overvoltages occur. The required clearance distances are designated as D_{el} and can be either internal clearances between conductors and earthed tower components, or external clearances between a conductor and an obstacle.
- Prevention of disruptive discharges between phase conductors when fast-front or slow-front overvoltages occur. The minimum required clearance distances are of internal nature and are designated as D_{pp}.
- Prevention of disruptive discharges between a live conductor and an object with earth potential at power frequency voltage. The minimum required clearance distances are of internal nature and are designated as $D_{\text{pf\_pe}}$.
- Prevention of disruptive discharges between live conductors at power frequency voltage. The required clearance distances are of internal nature and are designated as $D_{\text{pf\_pp}}$.
- Setting of *minimum air clearance* distances to *obstacles* or crossed objects, in order to achieve that potential disruptive discharges occur inside the overhead line and not to obstacles. In view of that, the minimum air clearance distances should be higher than the lowest value a_{som}, among the shortest straight lines between live and earthed parts of the overhead line.

The values D_{el}, D_{pp}, $D_{\text{pf\_pe}}$ and $D_{\text{pf\_pp}}$ are determined from the electric stresses considering the respective electric and geometric parameters. Indicative values according to [2.27] are described in clause 2.5.1.2. The resulting clearance distances shown in clause 2.5.2 assure a complete *personal safety*. The clearance distance a_{som} is a result of the individual line configuration. The minimum values D_{el} and D_{pp} can be alternatively determined from long-term satisfactory operation of lines; they are considered as sufficient for internal clearance distances (see Table 2.20). If they are intended to be used for external clearances, clause 2.5.2.6 should be taken into account.

Table 2.13: Usual coefficients of variation v_u and deviation factors K_z for calculation of withstand voltages

Overvoltage type	Coefficient of variation v_u	Standard deviation σ_u	Deviation factor K_z
Lightning impulse	0,03	0,03 $U_{50\%}$	$K_{z\_ff} = 0{,}961$
Switching surge	0,06	0,06 $U_{50\%}$	$K_{z\_sf} = 0{,}922$
Power frequency	0,03	0,03 $U_{50\%}$	$K_{z\_pf} = 0{,}910$

2.5.1.2 Calculation of electrical clearances

2.5.1.2.1 Required withstand voltages of air gaps

The procedures to determine the *required withstand voltage* described here are based on the data of EN 50 341-1, Annex E [2.27], and refer to [2.1, 2.29, 2.31, 2.30]. The capability of an air gap to withstand power frequency or impulse voltages of a given shape can be described with statistical concepts; for a given insulation and for impulse voltages of a given shape and a given altitude of the line, a certain probability of flashover can be associated to each value of the voltage; such probability is described through the parameters $U_{50\%}$, σ_u and N_x. Reference [2.31] recommends the use of a modified *Weibull distribution.* This distribution is determined such that its parameters correspond to the values of a Gaussian distribution at probabilities of 50 % and 16 % of being exceeded and is truncated at $U_{50\%} - 3\,\sigma_u$.

The *required withstand voltage* of an air gap is determined by considering an x % probability of being exceeded taking the critical voltage $U_{50\%}$ into account, so that:

$$U_{rw} = U_x = U_{50\%} - N_x \sigma_u \quad , \tag{2.32}$$

where $U_{50\%}$ is the 50 % *withstand voltage of the air gap*, σ_u the standard deviation and N_x the number of standard deviations, which correspond to the interval between the probabilities 50 % and x %, respectively.

For transient stresses (fast-front and slow-front overvoltages), the *required withstand voltage* should be the 90 % withstand voltage of the air gap. It is determined as a function of the 50 % withstand voltage by the following relation:

$$U_{rw} = U_{90\%} = U_{50\%} - 1{,}3\,\sigma_u \quad . \tag{2.33}$$

As far as the power frequency voltage is concerned, the required withstand voltage U_{rw} is considered as a deterministic parameter:

$$U_{rw} = U_{100\%} = U_{50\%} - 3\,\sigma_u \quad . \tag{2.34}$$

The required design withstand voltage can be determined by employing the *deviation factor* K_z and the coefficient of variation v_u through:

$$U_{rw} = (1 - v_u \cdot N)\, U_{50\%} = K_z U_{50\%} \quad , \tag{2.35}$$

where v_u designates the coefficient of variation. The resulting deviation factors K_z are given in Table 2.13.

In general, the type of air gap affects its *dielectric withstand strength.* The 50 % withstand voltage $U_{50\%}$ of an air gap of any arrangement can be equated as a function of the voltage of the rod-to-plane ($U_{50\%rp}$) air gap through:

$$U_{50\%} = K_g \cdot U_{50\%rp} \quad , \tag{2.36}$$

where K_g designates the *gap factor.* For every type of voltage stress, the respective gap factor can be related to the *gap factor for switching overvoltage* as follows:

Table 2.14: Gap factors for clearances in air

Type of gap	Slow-front overvoltage $K_{g\_sf} = K_g$	Fast-front overvoltage K_{g_ff}	Power frequency voltage K_{g_pf}
Rod-to-plane	1,00	1,00	1,00
Conductor-to-obstacle	1,30	1,08	1,16
Conductor-to-plane	1,15	1,04	1,09
Conductor-to-tower window	1,25	1,07	1,14
Conductor-to-tower	1,45	1,12	1,22
Conductor-to-guys	1,40	1,10	1,2
Conductor-to-conductor	1,60	1,16	1,26

Note: The gap factors for fast-front and power frequency voltages are derived from the factors for slow-front overvoltages.

- Slow-front overvoltages
$$K_{g\_sf} = K_g \quad ; \tag{2.37}$$
- Fast-front voltages
$$K_{g\_ff} = 0{,}74 + 0{,}26\, K_g \quad ; \tag{2.38}$$
- Power frequency voltages
$$K_{g\_pf} = 1{,}35\, K_g - 0{,}35\, K_g^2 \quad . \tag{2.39}$$

The required design withstand voltage results from (2.30) and (2.35) as:

$$U_{rw} = K_z\, K_g\, U_{50\%rp} \quad . \tag{2.40}$$

The values of air gap factors, applicable to slow-front overvoltages, depend on the air gap arrangement. Four types of arrangements are considered according to [2.27]:

- Conductor-to-obstacle (external clearances);
- Conductor-to-conductor in tower window, that is an I-string or V-string in the tower window (internal clearance);
- Conductor-to-tower, from freely swinging insulator string or from V-string to a crossarm or tower body (internal clearance);
- Conductor-to-conductor (internal clearance).

In Table 2.14, examples of *air gap factors* are shown according to [2.27], [2.29] and [2.31]. Other values obtained by experience or tests can be used. Other typical values for air gap factors can be obtained from [2.18].

Standard [2.31] contains formulae which describe the reaction of rod-to-plane air gaps against overvoltages; the *50 % withstand voltage* $U_{50\%rp}$ of rod-to-plane air gaps is used as reference for the *clearance distance d*. Therefore, the relation between the withstand voltage of an air gap and the clearance distance d can be expressed as:

$$U_{rw} = K_z \cdot K_g \cdot f(d) \quad . \tag{2.41}$$

The withstand voltage of any self-restoring insulation regarding slow-front overvoltages with front time 250 μs and time to half value 2500 μs is significantly lower than the corresponding voltage for fast-front overvoltages of the same polarity. Practically, the withstand voltage of a rod-to-plane air gap up to 25 m distance, for positive polarity and the standardized slow-front wave shape, can be determined by:

$$U_{50\%rp\_sf} = 1080 \ln(0{,}46\, d + 1) \quad , \tag{2.42}$$

where d is the clearance distance in m and $U_{50\%rp\_sf}$ represents the peak value of the impulse overvoltage in kV.

For standard *lightning impulses* with a front time of 1,2 μs and time to half value of 50 μs, and for rod-to-plane air gaps up to 10 m distance, the critical voltage of positive polarity is determined by:

$$U_{50\%rp\_ff} = 530\, d \quad , \tag{2.43}$$

Table 2.15: Altitude factor K_a as a function of the withstand voltage for insulation coordination according to [2.27]

Altitude (m)	Altitude factor K_a				
	up to 200 kV	from 201 kV to 400 kV	from 401 kV to 700 kV	from 701 kV to 1100 kV	above 1100 kV
0	1,000	1,000	1,000	1,000	1,000
100	0,994	0,995	0,997	0,998	0,999
300	0,982	0,985	0,990	0,993	0,996
500	0,970	0,975	0,982	0,987	0,992
1000	0,938	0,946	0,959	0,970	0,978
1500	0,904	0,915	0,934	0,948	0,960
2000	0,870	0,883	0,906	0,923	0,938
2500	0,834	0,849	0,875	0,896	0,913
3000	0,798	0,815	0,844	0,867	0,885

where d is the clearance distance in m and $U_{50\%\text{rp\_ff}}$ represents the peak value of the impulse overvoltage in kV.
The 50 % withstand voltage $U_{50\%\text{rp}}$ of a rod-to-plane air gap for power frequency voltage is determined by:

$$U_{50\%\text{rp\_pf}} = 750\sqrt{2}\,\ln\left(1 + 0{,}55\,d^{1{,}2}\right) \quad , \tag{2.44}$$

where d is the clearance distance in m and $U_{50\%\text{rp\_pf}}$ means the peak value of the voltage in kV. The critical disruptive voltage depends on the air density and, therefore, on the altitude of the area above the sea level, as explained in clause 2.4.5.3. Such dependence is considered through the altitude factor K_a according to equation (2.45) and Table 2.15:

$$U_{rw} = K_a \cdot K_z \cdot K_g \cdot U_{50\%\text{rp}} \quad . \tag{2.45}$$

2.5.1.2.2 Voltages to be considered

Fast-front overvoltages caused by lightning should be taken into account for the calculation of clearance distances in electric systems of ranges I and II; i. e. according to [2.31] for all nominal voltages.
Slow-front overvoltages caused by switching operations should be considered for the calculation of clearance distances in electric systems of range II, i. e. for nominal voltages equal or higher than 300 kV. The representative overvoltages to be taken into account are given in Table 2.16 according to clause 2.4.5.

Fast-front overvoltages

For the *determination of the air gap distance* regarding fast-front overvoltages, consideration should be given to the representative voltage that hits a certain point of the transmission line and spreads over a few supports. For determining phase-to-ground clearance distance, a voltage equal to 90 % of the lightning withstand voltage $U_{90\%\text{ff\_ins}}$ of the insulator set should be taken into account. This voltage depends on the flashover distance d_{ins} of the insulators sets and on the type of air gap.
For phase-to-phase clearances, the representative overvoltage $1{,}20\,U_{90\%\text{ff\_ins}}$ should be considered. According to [2.27], it applies:

$$U_{rp} = U_{90\%\text{ff\_ins}} = K_{z\_ff} \cdot K_{g\_ff\_ins} \cdot 530 \cdot d_{ins} \quad , \tag{2.46}$$

where K_{z_ff} is the deviation factor ($K_{z\_ff} = 0{,}961$), $K_{g\_ff\_ins}$ the lightning impulse air gap factor of the insulator set and d_{ins} the flashover distance of the insulator set.

Table 2.16: Representative voltages U_{rp} (external insulation)

Type of stress	Phase-to-earth	Phase-to-phase
Lightning	$U_{90\%ff\_is}$	$1{,}2 \cdot U_{90\%ff\_is}$
Switching	$K_{cs} \cdot U_{2\%\_sf}$	$1{,}4 \cdot K_{cs} \cdot U_{2\%\_sf}$
Power frequency	$(\sqrt{2}/\sqrt{3})U_s$	$\sqrt{2} \cdot U_s$
DC voltage	$1{,}05\sqrt{3/2} \cdot U_{DC}$	$2 \cdot 1{,}05\sqrt{3/2} \cdot U_{DC}$

Slow-front overvoltages

For insulation coordination of overhead lines regarding slow-front overvoltages, a simplified statistical method can be used. It is assumed in this case, that the distributions of both the overvoltages and the insulation withstand voltages can be defined by one point of the respective statistical distributions.

The overvoltage distribution is represented by the statistical overvoltage $U_{2\%\_sf}$, which corresponds to 2 % probability of being exceeded. The insulation withstand voltage is represented by the statistical withstand voltage, which corresponds to 90 % probability of withstanding. The representative overvoltage U_{rp} is determined through the multiplication of the statistical overvoltage by a *statistical coordination factor* K_{cs}. It results therefrom:

- Phase conductor to earth:
$$U_{rp} = K_{cs} \cdot U_{2\%\_sf} \quad \text{and} \tag{2.47}$$
- Phase-to-phase:
$$U_{rp} = K_{cs} \cdot U_{p2\%\_sf} = 1{,}4 \cdot K_{cs} \cdot U_{2\%\_sf} \quad . \tag{2.48}$$

The statistical coordination factor K_{cs} is related to the risk of failure. To determine the electrical clearance distances, K_{cs} can be set as equal to 1,05, corresponding to a flashover risk of around 0,001.

Power frequency voltages

For the purpose of insulation design and coordination, the representative permanent voltages should be considered as constant, being taken as equal to the peak value of the *highest power frequency voltage.*

- Phase-to-earth:
$$U_{rp} = (\sqrt{2}/\sqrt{3})U_s \quad \text{and} \tag{2.49}$$
- Phase-to-phase:
$$U_{rp} = \sqrt{2} \cdot U_s \quad , \tag{2.50}$$
where U_s means the highest system voltage.

Table 2.16 summarizes the representative voltage stresses to be considered.

DC voltages

The *insulation in direct current (DC) lines*, generally named as high voltage direct current (HVDC) systems, is stressed by lightning overvoltages, overvoltages induced by faults and the operating voltage. Slow-front overvoltages reach only moderate magnitudes of not more than 1,7 p.u. as a consequence of the attenuation in the converter stations, and are, therefore, not significant for line design. Fast-front overvoltages, as a consequence of lightning strokes, attain the same values as in AC systems.

Regarding the stresses at operating voltages, a DC line performs like an AC line with the peak value of the power frequency voltage. Therefore, it applies $U_{sAC} = \sqrt{3/2} \cdot U_{DC}$ where U_{sAC} is the highest phase-to-phase power frequency voltage of the comparable AC line and U_{DC} is the highest operating voltage of the DC line. For design, a voltage increased by 5 % compared with the nominal voltage should be adopted.

Table 2.17: Clearances D_{el} and D_{pp} corresponding to fast-front withstand voltages, of conductor-to-obstacle and conductor-to-conductor air gaps in altitudes up to 1000 m above sea-level

Lightning surge withstand voltage (kV)	D_{el_ff} (m)	D_{pp_ff} (m)
400	0,77	0,85
600	1,14	1,26
800	1,50	1,68
1000	1,88	2,08
1200	2,23	2,50
1400	2,61	2,92
1600	2,98	3,33
1800	3,35	3,75
2000	3,72	4,17
2050	3,82	4,27
2100	3,91	4,38
2150	4,00	4,48

Table 2.18: Clearances D_{el} and D_{pp} corresponding to slow-front overvoltages, of conductor-to-obstacle and conductor-to-conductor air gaps, in altitudes up to 1000 m above sea-level

Switching surge withstand voltage (kV)	D_{el_sf} (m)	D_{pp_sf} (m)
400	0,88	1,02
600	1,44	1,67
800	2,07	2,45
1000	2,84	3,41
1200	3,71	4,57
1400	4,77	5,97
1600	6,02	7,66
1800	7,50	9,70

2.5.1.2.3 Summary of formulae for electrical clearances

For each kind of voltage stress, the coordination withstand voltage of the air gap shall be equal or higher than the representative overvoltage. As a result, the following relationships can be deduced from equation (2.45), considering equations (2.42) to (2.44) and Table 2.16, for determining the *required electrical clearances* under the three mentioned conditions.

Fast-front overvoltages

$$D_{el\_ff} = U_{90\%ff\_ins}/(530 \cdot K_a \cdot K_{z\_ff} \cdot K_{g\_ff}) \tag{2.51}$$

and

$$D_{pp\_ff} = 1{,}2U_{90\%ff\_ins}/(530 \cdot K_a \cdot K_{z\_ff} \cdot K_{g\_ff}) \quad . \tag{2.52}$$

In Table 2.17, the values for D_{el_ff} and D_{pp_ff} are provided depending on the representative overvoltages for conductor-to-obstacle and conductor-to-conductor air gaps, in altitudes up to 1000 m above sea level.

Slow-front overvoltages

$$D_{el\_sf} = 2{,}17\left[\exp\frac{K_{cs}U_{2\%\_sf}}{1080 \cdot K_a \cdot K_{z\_sf} \cdot K_{g\_sf}} - 1\right] \tag{2.53}$$

and

$$D_{pp\_sf} = 2{,}17\left[\exp\frac{1{,}4\,K_{cs}U_{2\%\_sf}}{1080 \cdot K_a \cdot K_{z\_sf} \cdot K_{g\_sf}} - 1\right] \quad . \tag{2.54}$$

In Table 2.18, the values for D_{el_sf} and D_{pp_sf} are provided depending on the representative overvoltages, for conductor-to-obstacle and conductor-to-conductor air gaps, in altitudes up to 1000 m above sea level.

Table 2.19: Minimum clearances in air dependent on the highest voltage of equipment

Highest voltage of equipment U_s (kV)	D_{pf_pe} (m)	D_{pf_pp} (m)
52	0,11	0,17
72,5	0,15	0,23
82,5	0,16	0,26
100	0,19	0,30
123	0,23	0,37
145	0,27	0,42
170	0,31	0,49
245	0,43	0,69
300	0,51	0,83
420	0,70	1,17
525	0,86	1,47
765	1,28	2,30

Table 2.20: Empirical data for minimum clearance distances D_{el} and D_{pp}

Highest voltage of equipment U_s (kV)	D_{el} (m)	D_{pp} (m)
52	0,60	0,70
72,5	0,70	0,80
82,5	0,75	0,85
100	0,90	1,05
123	1,00	1,15
145	1,20	1,40
170	1,30	1,50
245	1,70	2,00
300	2,10	2,40
420	2,80	3,20
525	3,50	4,00
765	4,90	5,60

Power frequency voltages

$$D_{pf\_pe} = 1{,}64 \left[\exp \frac{U_s}{750\sqrt{3} \cdot K_a \cdot K_{z\_pf} \cdot K_{g\_pf}} - 1 \right]^{0{,}833} \tag{2.55}$$

and

$$D_{pf\_pp} = 1{,}64 \left[\exp \frac{U_s}{750 \cdot K_a \cdot K_{z\_pf} \cdot K_{g\_pf}} - 1 \right]^{0{,}833} . \tag{2.56}$$

In Table 2.19, the values for D_{pf_pe} and D_{pf_pp} are supplied being applicable to conductor-to-tower and conductor-to-conductor air gaps. They refer to insulation coordination considerations. Other requirements, such as for live-line work, may necessitate longer clearances.

Direct voltages

According to [2.32], the required *clearances in HVDC lines* can be obtained from equation (2.51) and (2.52), where the fast-front overvoltage has to be considered. The clearances required with respect to the operating voltage result from (2.55) and (2.56), whereby U_s has to be replaced by $1{,}22\,U_{DC}$.

2.5.1.3 Empirical data for clearances

Overhead transmission lines have been operated in all regions of the world, from which *empirical data for the clearances* D_{el} and D_{pp} can be obtained. In Table 2.20, such values are given as standardized in EN 50 341-1 [2.27]. If the clearances D_{el} of Table 2.20 are used to determine clearances necessary between conductors and obstacles in crossings, the following additional requirement should be complied with: The minimum clearance should be higher than 1,1 times the longest air gap a_{som} along the insulator sets. Under this assumption, it will be guaranteed that disruptive discharges, if any, occur along the insulator sets or within the line and never to crossed obstacles or persons under an overhead line. In practical terms, it is not known so far that any flashover ever occurred to obstacles or persons when these requirements had been fulfilled.

2.5.2 Internal and external clearances

2.5.2.1 Introduction

In case of overhead lines, internal and external clearances are considered. The *internal clearances* refer either to conductor-to-conductor or conductor-to-tower air gaps in the line. The *external clearances* are used for determining safety clearances between live conductors and objects under or in the vicinity of the overhead line. The internal clearances are specified solely for the purpose of designing for an acceptable ability to withstand overvoltages.

According to standards [2.29] and [2.31], the overvoltages, in connection with a limited number of flashovers, through the critical clearances, for instance conductor-to-tower, can lead to an economic design of a power network.

The purpose of the external clearances is to avoid any hazard of flashovers to the general public, to persons carrying out activities in the vicinity of the overhead power lines and to persons maintaining the power network. The external clearances are set so that flashovers have very high probability of occurring inside the overhead line. For *live-line work*, special rules are applied, which take care of special conditions applying in this situation.

The clearances relate to overhead transmission lines which use bare conductors. Lines which use a solid insulating layer around the phase conductors can be designed with clearances lower than the ones established in clause 2.5.1.

It is also accepted that for producing economic designs of a power network, the designer has to consider a foreseeable range of climatic conditions, such as wind velocities and ice load. If *exceptional meteorological events* occur, it is acceptable that the clearances established in clause 2.5.1 will not be complied with. An event can be considered as an exception if it is expected to occur once in more than 50 years. In these exceptional conditions, the safety of persons is paramount and should be the governing rule.

Vertical and horizontal clearances can be distinguished in order to determine the shortest distance between live parts and the object under consideration. If not specified as vertical or horizontal, the clearances should be taken as the shortest ones between live parts and the object under consideration.

2.5.2.2 Design principles

Disregarding live-line work, the following rules are applied for determining both internal and external clearances:

- There is a *basic electrical clearance* D_{el}, which, if obeyed as an external clearance, prevents flashovers between live parts and external objects at earth potential under normal system operation. Normal operation comprises switching operations, lightning surges and overvoltages resulting from earth faults. For internal clearances, it is permitted to use lower values than D_{el}, because flashovers affect only the operation of the network. For external clearances, according to [2.27], D_{el} should be applied in any case.
- A basic clearance D_{pp} should be used in order to avoid phase-to-phase flashovers during lightning or switching overvoltages. Clearances lower than D_{pp} can be accepted at adverse weather conditions, as flashovers in this case would affect only the network reliability and not the safety of persons.
- An *additional clearance component* D_{add} is necessary to ground or crossed objects, being intended to ensure that no person or conductive object violates the electric distance even when they are undertaking work or leisure activities which can be foreseen as reasonably probable. In Figure 2.11, the relationships are shown between electrical and additional clearance.

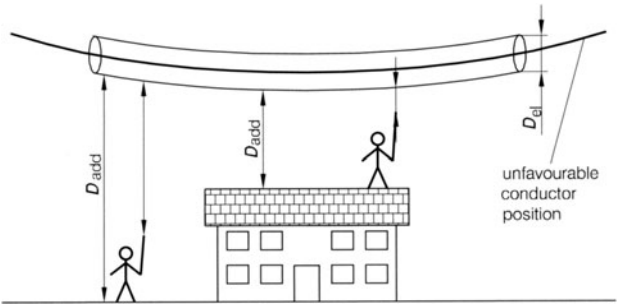

Figure 2.11: Components of clearances to crossed obstacles

- The *internal clearances* to earthed objects can be less than the lowest values of D_{el} and D_{pp} during infrequent events, such as those caused by the maximum swing of the conductors due to wind loading. In this case, there is a low probability of a coincidental transient voltage and such a coincidence would in any case result only in a supply interruption, presenting no danger to persons. It is, therefore, recommended in [2.33] that clearances lower than those required with respect to overvoltages can be accepted in 1 % of time duration of one year. Similarly, phase-to-phase clearances D_{pp} can be lower than the ones, required according to Tables 2.17, 2.18 and 2.20 under the occurrence of low probability events.
- The probability of flashover through the *lowest internal clearance* a_{som} should be always higher than that to any external object or person. Also with long insulator sets, the risk of flashover should always be through the internal distance a_{som} and not to any external object or person. In case of long insulator strings, an increase of the distances D_{el} to values more than $1{,}1 \cdot a_{som}$ can be expedient, according to [2.27].

The minimum distances required for live-line work can be determined according to [2.34].

2.5.2.3 Load cases for the calculation of clearances

2.5.2.3.1 Maximum conductor temperature at no-wind condition

Vertical clearances should be based on the *maximum design temperature* of the conductors and on their resulting position along the span and they should be designed sufficiently large. The maximum conductor temperature is a result of the line operation or can be considered as the highest permissible temperature for the conductor. In Table 2.21, the design temperatures according to EN 50 341-3 [2.35] are listed. According to international practice, maximum permanent conductor temperatures in the range of 75 to 90°C are used. Normal clearances are established for maximum permanent conductor temperature. If higher currents and temperatures are additionally taken into account for emergency conditions, clearances lower than D_{el} and D_{pp} can be accepted.

2.5.2.3.2 Ice load without wind

The *characteristic ice load* to be applied and the relevant temperature should be specified based on the experience gained in each region or at individual lines. Guidelines on ice loads to be applied are provided in clause 6.6.3.

A summary of ice load conditions to be considered for clearances in the individual European countries is given in Table 2.21. High ice loads are taken into account, specially in Northern European countries like Norway, Sweden and Finland. No ice load conditions are specified in Southern European countries; some standards refer to project specifications. The temperatures during icing periods are between -10 and 0°C.

Table 2.21: Conductor temperatures and ice loads to determine clearances in some European countries constituting CENELEC according to EN 50341-3[1)]

Country	Temperature °C	Ice load N/m	Source EN
Austria	40	$4 + 0,2 \cdot D^{2)}$	50341-3-1
Belgium	75	no ice load	50341-3-2
Switzerland	40	20	50341-3-3
Germany	Design temperature	$5 + 0,1 \cdot D^{2)}$; $10 + 0,2 \cdot D^{2)}$; $20 + 0,4 \cdot D^{2)}$; depending on line location	50341-3-4
Denmark	Design temperature	no ice load	50341-3-5
Spain	> 50	0 to 500 m no ice load 500 to 1000 m $1,8\sqrt{D}$ above 1000 m $3,6\sqrt{D}$	50341-3-6
Finland	70	0 to 50 m 10 50 to 100 m 25 100 to 200 m 50 above 200 m 75	50343-3-7
France	Design temperature	0 to 600 m – 20 mm radial[3)] above 600 m – project specification	50341-3-8
Great Britain	Design temperature	project specification	50341-3-9
Greece	50	no ice load	50341-3-10
Ireland	Design temperature	15 to 50 mm – radial[3)] depending on type of line	50341-3-11
Italy	up to 800 m 55 above 800 m 40	no ice load	50341-3-13
Netherlands	70/80	ice load with 50 years return period	50341-3-15
Norway	Design temperature	30 to 50 m, depending on height above sea-level and location	50341-3-16
Portugal	up to 100 kV 65 above 100 kV 75	up to 700 m no ice load above 700 m $11/40 \cdot (10 + D)^{2)}$	50341-3-17
Sweden	50	$9,2 + 0,51\ D^{2)}$	50341-3-18

[1)] not available for Luxembourg

[2)] D conductor diameter in mm

[3)] thickness of radial ice accretion, measured in mm, not in N/m

Besides a uniform ice load along the line section, some standards require to comply with minimum clearance when a *local ice load* acts just in one span, e. g. for crossings of traffic routes etc. EN 50341-3-4 [2.36], as an example, specifies 50 % of the uniform ice accretion in this case. Such an unbalanced ice load results in unequal longitudinal conductor tensile forces, causing longitudinal swings of the insulator sets and, therefore, higher sags may be created as compared with the conductor maximum temperature condition.

2.5.2.3.3 Wind load assumptions

Regarding *clearances at wind* load, three conditions should be taken into account:

- *Moderate wind load* having an average frequency of occurrence. According to [2.27], a wind load for a three years return period is suggested. Reference [2.33] recommends a wind speed which is not exceeded during at least 99 % of the time. The first assumption could lead to approximately twice the swing angle than the proposal according to [2.33]. In clause 2.5.2.4 further details will be given. According to [2.36], the dynamic wind pressure to be adopted reaches 80 % of the value which would be considered for a 50 year return period.
- *Extreme wind load* according to a design wind speed of e. g. 50 years. This wind load leads to the limit values of the conductor swing.
- *Wind action on ice covered conductors* may determine the electrical clearances under particular conditions. Then, the relevant conductor position can be calculated using the assumptions described in [2.33].

The *conductor temperature* depends on electric load, wind velocity, wind direction and ambient temperature. The more the wind velocity increases, the lower the increase of the conductor temperature will be compared with the ambient temperature. Such circumstances can be considered in the design of an overhead line, when the actual conductor position is calculated. According to [2.36], conductor swing is always calculated at +40°C temperature.

At medium wind load, internal clearances may be reduced compared with D_{el} and D_{pp}, because under these circumstances there is only a low probability that an overvoltage occurs and results in a disruptive discharge to persons or third party properties. The extent to which the clearances could be reduced is established in correspondence with the reliability level required for the line. According to [2.36], the values of D_{el} and D_{pp} of Tables 2.17, 2.18 and 2.20 may be multiplied by the factor 0,75.

Under extreme wind condition the internal clearances should withstand the highest phase-to-earth power frequency voltage in systems with directly-earthed-neutral and earth fault factors of 1,3 or below. Clearances according to Table 2.19 apply under this assumption. For higher earth fault factors, especially in systems with isolated and resonant-earthed-neutral, consideration of temporary overvoltage may be necessary.

The practice among several utilities in regions not subjected to ice loads, regarding association of wind velocity for *swing angle calculation*, temperatures and clearances for tower design or tower application is:

- Consideration of a no-wind condition at everyday stress (EDS) temperature and of clearances for *fast-front* or lightning *overvoltages*;
- Use of a moderate wind velocity equal to 50 to 60 % of the high-wind velocity for 50 year return period for the swing angle calculation and its combination with the clearance for the maximum *slow-front* or switching *overvoltages*;
- Use of the high-wind 50-year velocity for calculation of maximum swing angle and its combination with the clearance for *power frequency voltages.*

2.5.2.4 Insulator and conductor position under wind action

2.5.2.4.1 Definition of wind action

The available clearances between phase conductors or between phase conductors and earthed tower elements depend on the *conductor and insulator positions* which vary under the action of wind. The wind load causes swinging of the conductors and insulators, thus reducing the still air clearances. The wind action varies with time and location and can be described as randomly distributed using statistical approaches (see clause 6.3.2 and [2.1]). The *time-dependent conductor position* will be randomly distributed as well. Additionally, the swing angles depend on line parameters, such as ratio of wind to weight span, conductor type etc.

To determine the *distribution of conductor position* depending on the wind, it is necessary to consider the distribution of the wind velocity along the span and its variation with height above ground level. To assess the time distribution of the conductor position, a knowledge of the time distribution of wind velocity is necessary. Only the component of the wind acting perpendicularly to the conductor causes swinging of conductor and insulators. Wind statistics often comprise only wind values independently of the wind direction. To assess the probability of swing angles, it is necessary to take appropriate note of the wind direction.

According to IEC 60 826 [2.1] the probability of yearly extreme values of wind velocity may be described by the *Gumbel distribution* (see clause 6.9.4). According to this distribution the wind velocity V_τ corresponding to a given return period τ (measured in years) can be determined from

$$V_\tau = \overline{V} - \sigma_V[0,45 + \ln(-\ln(1-1/\tau)) \cdot \sqrt{6}/\pi] \quad . \tag{2.57}$$

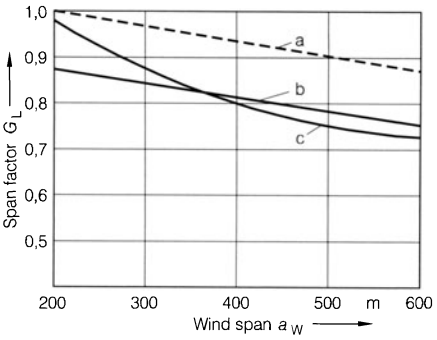

Figure 2.12: Span factor G_L according to IEC 60 826 (a), EN 50 341-1 (b) and EN 50 341-3-4 (c)

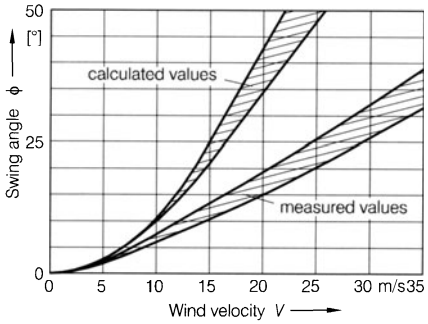

Figure 2.13: Calculated and measured swing angles as a function of instantaneous wind velocities

Equation (2.57) can be used to establish the wind velocity having a high probability of occurrence during one year, e. g. the wind velocity with a return period of two years, and to derive the yearly time distribution of the wind velocities based on this value. It may be assumed that the yearly time distribution of the wind velocities follows the *Weibull distribution*

$$P(V \leq V_\tau) = \left\{1 - \exp\left[-(V_\tau/V_\eta)^\beta\right]\right\} \cdot 100 \quad . \tag{2.58}$$

Equation (2.58) determines the percentage of time during which the wind velocity V will be below the value V_τ. The Weibull distribution (2.58) is described by the two parameters β and V_η. Data for the value β can be found in literature, ranging from 1,8 to 2,2. To assess the parameter V_η from extreme value statistics, $\beta = 2{,}0$ is recommended. The probability that a velocity V exceeds V_τ is then

$$P(V \geq V_\tau) = exp\left[-(V_\tau/V_\eta)^\beta\right] \cdot 100 \quad . \tag{2.59}$$

With standard practice for wind measurements in mind, it can be concluded that the wind velocity having a two years' return period will have a yearly time probability of occurrence of $P = 3{,}42 \cdot 10^{-4}$ (see [2.33]). Hence, V_η can be determined from (2.50) with $\beta = 2{,}0$:

$$V_\eta = V_{2a}/2{,}825 \quad . \tag{2.60}$$

According to the structure of the boundary air layer close to the ground surface, the wind velocities increase with the height above ground. To determine the wind velocity V_z at a height z above ground, the power law

$$V_z = V_R(z/z_R)^\alpha \tag{2.61}$$

is often accepted, where V_R is the reference wind velocity for the height z_R and α the roughness parameter depending on the terrain category. For the coefficients α see [2.1] or Table 6.13.

IEC 60 826 [2.1] contains figures describing the effect of span lengths above 200 m through the span factor G_L. The wind load on conductors is given by

$$Q_{WC} = G_L \cdot C_C \cdot \varrho/2 \cdot V_R^2 \cdot D \cdot a_W \quad . \tag{2.62}$$

In Figure 2.12, the span factor G_L is shown depending on the wind span according to IEC 60 826, EN 50 341-1 and EN 50 341-3-4. The drag factor C_C can be assumed to be 1,0 for standard conductors.

2.5.2.4.2 Calculation of swing angle

If the wind acted steadily along the line and constantly over a longer period of time, the *calculation of swing angle* would just be a simple matter. However, in reality the fluctuation of wind affects the swing angle considerably. The peak wind velocities will not cause swing angles statically equivalent to that calculated from the locally observed peak wind velocities.

Conductors possess a certain mass which has to be accelerated first and moved into a swung position before the wind forces will be transmitted to the support. Therefore, peak wind velocities of short duration will not affect neither the swing angles nor the forces acting on the towers. Only mean values of wind velocities averaged over a sufficiently long period of time affect the swing angle. This fact can be directly observed on overhead power lines. In heavy storms with distinctly discernible gusts, the conductors and insulators resist in a stable swung position without clearly reacting to the gusts. Accordingly, various investigations of swing angles indicate that the measured swing angles are smaller than those theoretically expected from the recorded instantaneous peak wind velocities adopting the basic relations between wind velocities, wind forces and swing angles. Figure 2.13 shows records from [2.37] in comparison with calculated data. This figure confirms that the relation between wind velocity and swing angle requires extensive considerations to become consistent. For bare stranded conductors a drag coefficient $C_C = 1{,}0$ is adequate [2.1]. To achieve sufficient agreement between calculations and measurements, the climatic data such as air density have to be duly considered.

The *swing angle* of an insulator set may be related to the wind velocity by:

$$\overline{\phi}_{ins} = \tan^{-1}\left[\frac{(\varrho/2)\cdot C_C \cdot V_R^2 \cdot G_L \cdot D \cdot a_W + Q_{Wins}/2}{W_C + W_{ins}/2}\right] \quad . \tag{2.63}$$

In this formula the following symbols are used:

ϱ	air density depending on temperature, humidity and altitude above sea level,
C_C	drag factor equal to 1,0 for stranded conductors,
V_R	reference wind velocity,
G_L	span factor taking into account the effect of span length,
D	conductor diameter,
a_W	wind span,
Q_{Wins}	wind load on insulator set,
W_C	effective conductor weight taking into account the differences in the level of conductor attachment points,
W_{ins}	dead weight of insulator set.

The effective conductor dead weight results from the weight span without considering the increase in tension due to wind action.

The *swing angle for a conductor* alone follows accordingly from

$$\overline{\phi}_C = \tan^{-1}\left[\frac{(\varrho/2)\cdot C_C \cdot V_R^2 \cdot G_L \cdot D \cdot a}{m_C g \cdot a}\right] \quad , \tag{2.64}$$

where a is the span length and m_C the conductor mass per unit length.

Evaluations of measurements demonstrate that the reference five- or ten-minute mean value should be used for the wind velocity V_R. Formulae (2.63) and (2.64) can then be used to calculate the mean value of the swing angle $\overline{\phi}$ for every given wind velocity. Using the five-minute mean wind velocity is a conservative assumption, as confirmed by observations [2.33]. It can be assumed that the actual swing angles for a given mean

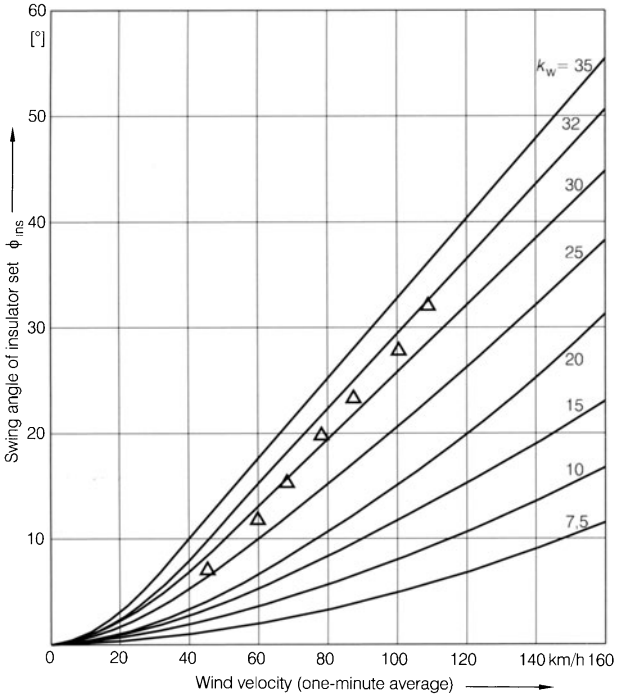

Figure 2.14: Swing angle of insulator sets as a function of wind velocity, according to [2.18]
△ obtained from measurements at horizontal twin and quadruple bundles according to [2.37];
k_w according to equation (2.66)

wind velocity follow a Normal distribution function with a mean value of $\overline{\phi}$ resulting from formulae (2.63) or (2.64), whereas the standard deviation is given by

$$\sigma_\phi = 2{,}25\left[1 - \exp(-V_R^2/230)\right] \quad \text{(in degrees)}. \tag{2.65}$$

For low wind velocities, the standard deviation σ_ϕ is 0° and for large values σ_ϕ will be 2,25°.

Most wind statistics refer only to the occurrence of absolute values without relating these wind velocities to wind directions. However, only winds acting perpendicularly to the line direction will cause maximum swing angles. Therefore, statistics on wind directions would be necessary as well, in order to establish realistic time probabilities for swing angles. As an approximation, it is proposed in [2.33] that the probability of the swing angle should be assumed as half of that of the corresponding wind velocity. This might be a fairly good assumption for swing angles of more than 2° [2.33].

2.5.2.4.3 Time distribution of swing angles

It is assumed that a Weibull function according to (2.59) represents the time distribution of the swing angles. The parameters are derived from the wind velocities having a return period of two years. The mean wind velocities under a given wind action can be reliably calculated with equation (2.63) for insulator sets and (2.64) for conductors using a mean wind speed averaged over five to ten minutes, where five minutes can be considered as a conservative value. This approach yields conservative values for the mean values of the swing angle. Formula (2.65) gives an estimate for the standard deviation of swing angles. Only wind directions perpendicular to the line cause the maximum swing angles.

2.5.2.4.4 Determination of swing angles by measurements

Several experiments have been carried out for studying the relationship between the swing angle of the insulator set and the observed wind velocities. A world-wide often used method for determining swing angle, as described in [2.18], is based on measurements carried out at Hornisgrinde on Black Forest, Germany, see [2.38] and [2.37]. In Figure 2.13, the results of swing angle measurements are shown. From such measurements, diagrams were prepared showing the relationship of the swing angles of the insulator sets with the wind velocity and the factor

$$k_{\mathrm{w}} = (D/m_{\mathrm{C}})/(a_{\mathrm{g}}/a_{\mathrm{W}}) \quad , \tag{2.66}$$

where D is the conductor diameter in mm, m_{C} the conductor mass per unit length in kg/m and $a_{\mathrm{g}}/a_{\mathrm{W}}$ the weight span to wind span ratio. In Figure 2.14 the swing angles are shown as a function of the wind speed, for various parameters k_{w}.

Diagrams of Figure 2.14 assume that wind velocities act always perpendicularly to the line direction. The measurements were performed in 300 m spans. In longer spans, the swing angles tend to be lower, while in shorter spans, the swing angles would be higher than the indicated values. However, according to [2.18], the impact on the swing angles is only low. The wind conditions and the time and spatial distribution at the measuring location were supposed to be similar to those regarding time and spatial distribution of real lines . Measurements on Hornisgrinde provided lower swing angles for bundle conductors than for single conductors with similar cross section. This difference cannot be recognized in Figure 2.14. So, for swing angles of bundle conductors, the approach seems conservative. The wind velocities refer to the one-minute average. An example in clause 2.5.2.8 explains the application of Figure 2.14.

2.5.2.4.5 Conductor and insulator position according to standards

According to [2.27] and [2.36], conductor swing angles are based on the wind action having medium frequency of occurrence corresponding to a three years' return period. In this case, the equations (2.63) and (2.64) can be used to determine the insulator and conductor swing angles, respectively.

2.5.2.5 Midspan clearances

The *midspan clearances* should be designed to avoid flashovers under overvoltage conditions, assuming medium-frequent wind actions, as well as under power frequency voltage combined with extreme wind action. If all the conductors were deflected with equal angles, then the same clearances as at the tower would result close to midspan position. As a result of [2.33], the most unfavourable conductor positions assuming swing angles can be calculated from

$$\phi_{\mathrm{C}} = \overline{\phi}_{\mathrm{C}} \pm 2\,\sigma_{\phi} \quad , \tag{2.67}$$

where $\overline{\phi}_{\mathrm{C}}$ is obtained from (2.64) and σ_{ϕ} from (2.65). The positions of the conductors should be separately examined for the two aforementioned conditions. The most unfavourable conductor relative positions occur when the swing angle for one conductor is set as $\phi_{\mathrm{C}} = \overline{\phi}_{\mathrm{C}} + 2\,\sigma_{\phi}$ or $\phi_{\mathrm{C}} = \overline{\phi}_{\mathrm{C}} - 2\,\sigma_{\phi}$.

In practice, several empirical procedures are used to calculate the necessary midspan clearances which proved their validity during long-term successful operation of lines designed based on these empirical procedures.

In case of equal cross sections, materials and conductor sags within a span, the following approach for evaluating *minimum clearances in midspan* can be used according to [2.36]. The swing angle ϕ_{C} is determined by (2.64).

Table 2.22: Values of the factor k_C as a function of swing angle ϕ and relative conductor positions (see Figure 2.15)

Range of swing angle degree ϕ_C	Relative position between conductors 2 and 1		
Grad	Range 1 $0° \leq \psi \leq 30°$	Range 2 $30° < \psi \leq 80°$	Range 3 $80° < \psi \leq 90°$
$\geq 65{,}1$	0,95	0,75	0,70
55,1 to 65,0	0,85	0,70	0,65
40,1 to 55,0	0,75	0,65	0,62
$\leq 40{,}0$	0,70	0,62	0,60

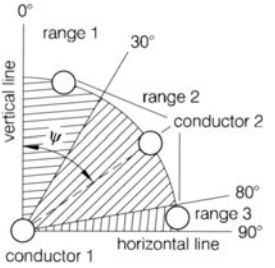

Figure 2.15: Determination of factor k_C depending on the relative position of conductor 2 to conductor 1

The minimum clearance c_{min} of the conductors at midspan in still air should be at least

$$c_{min} = k_C \sqrt{f_C + l_k} + 0{,}75 \cdot D_{pp} \quad \text{in m} \quad , \tag{2.68}$$

however, not less than k_C in m in case of phase-to-phase clearance. Between conductors and earth wires, it applies:

$$c_{min} = k_C \sqrt{f_C + l_k} + 0{,}75 \cdot D_{el} \quad \text{in m} \quad , \tag{2.69}$$

where:

f_C sag of the conductor at a temperature of 40°C, in m ;

l length of that part of the insulator set swinging orthogonally to the line direction, in m ;

k_C coefficient according to Table 2.22; the relative position of the conductors is explained in Figure 2.15;

D_{pp} minimum clearance (phase-to-phase), in m, which depends on the voltage according to Tables 2.16, 2.17 or 2.19;

D_{el} minimum clearance (phase-to-earth), in m, which depends on the voltage according to Tables 2.16, 2.17 or 2.19.

If circuits with different operating voltages run in parallel at the same structure, then the most unfavourable value for D_{pp} or D_{el} should be used.

Relationships similar to equations (2.68) and (2.69) are used in many countries: Austria, Belgium, Finland, Italy, Netherlands, Norway, Portugal, Spain, Sweden and Switzerland. There, the factor k_C varies between 0,45 and 0,95, sags at 10°C to maximum conductor temperature are inserted for f_C and instead of 0,75 D_{pp} values up to D_{pp} apply.

In case of conductors with different cross sections, materials or sags, the higher factor k_C from Table 2.22 should be used to determine the clearances; similarly, the biggest sag of both conductors, if they are different, should be used. In addition to the clearance for the conductors in still air, the clearances between *swung conductors* should also be investigated in this case. Then, the wind load should be assumed according to relevant loading assumptions. According to [2.36], it should be demonstrated, that whilst wind pressures differing by 40 % are acting on the individual conductors, a clearance not less than $0{,}75\,D_{pp}$ or $0{,}75\,D_{el}$, and D_{pf_pp} or D_{pf_pe}, respectively, should be maintained, where D_{pp} and D_{el} are obtained from Tables 2.17, 2.18 or 2.20, and D_{pf_pp} and D_{pf_pe} from Table 2.19.

The described determination of midspan clearances applies to conditions for standard line heights lower than 60 m. For taller towers, as applied in crossings, an extra clearance of 1 % of the span should be aimed at, as experience from Norway has shown [2.39].

Table 2.23: Minimum clearances within a span or at a tower

Load case	Mid-span		At tower	
	phase-to-phase	phase-to-earth wire	phase-to-phase	phase-to-earth
Maximum conductor temperature	D_{pp}	D_{el}	D_{pp}	D_{el}
Ice load	D_{pp}	D_{el}	D_{pp}	D_{el}
Wind load with medium frequency of occurrence	$k_1 \cdot D_{pp}$	$k_1 \cdot D_{el}$	$k_1 \cdot D_{pp}$	$k_1 \cdot D_{el}$
Local ice load	$k_1 \cdot D_{pp}$	$k_1 \cdot D_{el}$	$k_1 \cdot D_{pp}$	$k_1 \cdot D_{el}$
Extreme wind load	D_{pf_pp}	D_{pf_pe}	D_{pf_pp}	D_{pf_pe}

In case of crossings, the clearances should be checked for an additional loading case, which is defined by local ice load on one conductor in the relevant span, while the other conductors are unloaded. In this case, the clearances should be higher than $k_1 \cdot D_{pp}$ or $k_1 \cdot D_{el}$. The local ice load is assumed to be 50 % of the design ice load according to [2.36]. Other standards specify different limiting criteria in this case.

2.5.2.6 Minimum clearances within a span or at a tower

The *minimum clearances* according to EN 50 341-1 [2.27] and the associated conditions can be summarized, as presented in Table 2.23. Values between 0,7 and 1,0 seem acceptable for the factor k_1. As an example, a value $k_1 = 0{,}75$ has proved to be adequate for Germany. The existing clearances can be determined as recommended in clauses 2.5.2.4 and 2.5.2.5. The values for D_{el}, D_{pp} and D_{pf} are found in Tables 2.17 to 2.20.

2.5.2.7 Clearances to ground and obstacles

Due to the different history and safety principles, *clearances to ground*, to *buildings*, *traffic routes* etc. differ in a relatively wide range from country to country or even among utilities. When establishing the European standard EN 50 341-1 [2.27] a common basis was found for stipulation of clearances. Table 2.24 summarizes the most important data. For detailed information and conditions, the standard [2.27] and the accompanying National Normative Aspects [2.35] should be studied.
The aim of these clearances is to avoid that persons will approach to the conductors closer than the distance D_{el} also when carrying any objects (see also Figure 2.11). The following cases are distinguished:

- *Clearances to residential and other buildings*, when the line is above or adjacent to the buildings or near antennas or similar structures;
- *Clearances to* lines crossing *roads*, *railways* and *navigable waterways*;
- *Clearances* to lines crossing or parallel to *other power lines* or *overhead telecommunication lines*;
- *Clearances to recreational areas* with a power line above or in close vicinity.

Voltage-dependent values D_{el} shall be added to the values D_{add} of Table 2.24. Several standards specify special requirements on the line design in case of crossings, e. g. the use of multiple-string insulator sets. Details for European countries are given in EN 50 341-3 (National Normative Aspects) [2.35].

2.5.2.8 Examples

2.5.2.8.1 Electrical clearances for a 110 kV overhead line

The example shows the determination of electrical clearances for a 110 kV line equipped with one long rod insulator type L100 C325 or L210 C550 (according to IEC 60 433, see Table 9.4).

Table 2.24: Distances D_{add} to obstacles according to [2.27] in addition to D_{el}

Crossed obstacles	Maximum conductor temperature; ice load; average wind load	Local ice load
Ground in open country side		
– Normal ground profile, used by agriculture	5,0	(a)
– Steep slopes	2,0	(a)
Trees		
– Impossible to climb	0,0	(a)
– Possible to climb	1,5	(a)
Buildings with fire resistant roofs		
– Slope greater than 15°	2,0[1)]	2,0[1)]
– Slope less than 15°	4,0[2)]	4,0[2)]
Non-fire resistant roofs	10,0	10,0
Antennas, street lamps, flag poles and similar structures	2,0	2,0
Roads	6,0	6,0
Electric overhead contact lines	2,0	2,0
Ropeways	2,0	2,0
Towers of ropeways	4,0	4,0
Gauge of navigable waterways	2,0	2,0
Power lines and telecommunication lines	D_{pp}[3)]	D_{pp}[3)]
Recreational areas		
– General	7,0	7,0
– Swimming pools	8,0	8,0
– Permanently installed facilities	3,0	3,0

(a) Verification of clearances is not required for local ice loads .

[1)] Required minimum clearance distance 3 m

[2)] Required minimum clearance distance 5 m

[3)] Required minimum clearance distance 1 m

The line is located 500 m above sea level.

- Highest operating (power frequency) voltage: 123 kV.
- For voltages of range I, according to [2.29], it is not necessary to consider switching overvoltages.
- The 90 % withstand voltage for fast-front overvoltages $U_{90\%ff\_ins}$ is 325 kV phase-to-ground for insulator L100 C325 and 550 kV for insulator L210 C550.
- The altitude factor, according to Table 2.15, is $K_a = 0{,}975$ phase-to-earth and $K_a = 0{,}982$ phase-to-phase for fast-front overvoltages and 0,970 for power frequency voltages.
- The deviation factors K_z are: $K_{z\_ff} = 0{,}961$ for fast-front overvoltages and $K_{z\_pf} = 0{,}910$ for power frequency voltages (see Table 2.13).
- The four different air gap types result in the gap factors K_g shown in Table 2.14.

Electrical clearances for fast-front overvoltages are determined from equations (2.51) and (2.52):

$$\begin{aligned} D_{el} &= U_{90\%ff\_ins}/(530 \cdot K_a \cdot K_{z\_ff} \cdot K_{g\_ff}) = \\ &= 325/(530 \cdot 0{,}975 \cdot 0{,}961 \cdot 1{,}12) = 0{,}58 \text{ m} \end{aligned}$$

between conductors and tower (crossarm or tower body) and

$$\begin{aligned} D_{pp} &= 1{,}2 \cdot U_{90\%ff\_ins}/(530 \cdot K_a \cdot K_{z\_ff} \cdot K_{g\_ff}) = \\ &= 1{,}2 \cdot 325/(530 \cdot 0{,}982 \cdot 0{,}961 \cdot 1{,}16) = 0{,}69 \text{ m} \end{aligned}$$

between phase conductors.
The values D_{el} and D_{pp} for other air gap types are provided in Table 2.25.
For power frequency voltages, the electric distances are determined from (2.55):

$$D_{pf\_pe} = 1{,}64\left(\exp \frac{U_s}{750\sqrt{3} \cdot K_a \cdot K_{z\_pf} \cdot K_{g\_pf}} - 1\right)^{0.833} =$$

Table 2.25: Electrical clearances at a 110 kV overhead line, in m

	Phase-to-phase	Phase-to-earth wires	Phase-to-tower window	Phase-to-tower	Phase-to-obstacles
Fast-front overvoltage					
Insulators L 100 C 325	$D_{pp} = 0{,}67$	$D_{el} = 0{,}56$	$D_{el} = 0{,}60$	$D_{el} = 0{,}58$	$D_{el} = 0{,}60$
Insulators L 210 C 550	$D_{pp} = 1{,}14$	$D_{el} = 0{,}95$	$D_{el} = 1{,}03$	$D_{el} = 0{,}98$	$D_{el} = 1{,}02$
Power frequency voltage					
Both insulators types	$D_{pf} = 0{,}36$	$D_{pf} = 0{,}23$	$D_{pf} = 0{,}24$	$D_{pf} = 0{,}22$	$D_{pf} = 0{,}24$

$$= 1{,}64\left(\exp\frac{123}{750\sqrt{3}\cdot 0{,}970\cdot 0{,}910\cdot 1{,}22} - 1\right)^{0{,}833} = 0{,}22 \text{ m}$$

between conductor and tower body (or crossarm). The phase-to-phase distance follows from (2.56)

$$D_{pf\_pp} = 1{,}64\left(\exp\frac{U_s}{750\cdot K_a\cdot K_{z\_pf}\cdot K_{g\_pf}} - 1\right)^{0{,}833} =$$

$$= 1{,}64\left(\exp\frac{123}{750\cdot 0{,}970\cdot 0{,}910\cdot 1{,}26} - 1\right)^{0{,}833} = 0{,}36 \text{ m}.$$

When an insulator L210 C550 is installed, the withstand voltage $U_{90\%ff\_ins}$ is 550 kV and $K_a = 0{,}982$ applies also for fast-front overvoltages. Therefore, it results from (2.51) and (2.52), respectively:

$$D_{el} = 550/(530\cdot 0{,}982\cdot 0{,}961\cdot 1{,}12) = 0{,}98 \text{ m}$$

and

$$D_{pp} = 1{,}2\cdot 570/(530\cdot 0{,}982\cdot 0{,}961\cdot 1{,}16) = 1{,}18 \text{ m}.$$

The values for the clearances at power frequency voltage will be the same as for insulators L100 C325.

2.5.2.8.2 Electrical clearances for a 380 kV overhead line

The line is located at an altitude of 500 m above sea level and will be equipped with three long rod insulators L210 C550. The highest power frequency voltage is 420 kV. The lightning withstand voltage $U_{90\%ff\_ins}$ is 1780 kV. The statistical switching overvoltage $U_{2\%\_sf}$ is 1050 kV. The slow-front overvoltage to be considered is, according to (2.47) and (2.48), taking $K_{cs} = 1{,}05$ into account:

- Phase-to-earth $U_{rp} = 1{,}05\cdot 1050 = 1103$ kV;
- Phase-to-phase at voltages above 1100 kV $U_{rp} = 1{,}4\cdot 1{,}05\cdot 1050 = 1544$ kV.

The altitude factor K_a is determined from Table 2.15 for voltages higher than 1100 V, as $K_a = 0{,}992$ for overvoltages; in case of power frequency voltages $K_a = 0{,}975$ for phase-to-earth and $K_a = 0{,}982$ for phase-to-phase applies.

The deviation factors according to Table 2.13 are:

$K_{z\_ff} = 0{,}961$ for fast-front overvoltages,
$K_{z\_sf} = 0{,}922$ for slow-front overvoltages,
$K_{z\_pf} = 0{,}910$ for power frequency voltages.

The resulting clearances for fast-front overvoltages are determined from (2.51) and (2.52) as:
Phase-to-tower:

$$D_{el} = 1780/(530\cdot 0{,}992\cdot 0{,}961\cdot 1{,}12) = 3{,}15 \text{ m}$$

Phase-to-phase:

$$D_{pp} = 1{,}2\cdot 1780/(530\cdot 0{,}992\cdot 0{,}961\cdot 1{,}16) = 3{,}64 \text{ m} \quad .$$

For slow-front overvoltages, it results from (2.53) and (2.54):

Table 2.26: Electrical clearances in m for a 380 kV overhead line equipped with long rod insulators

Overvoltage type	Phase-to-phase	Phase-to-earth wires	Phase-to-tower window	Phase-to-tower body or crossarm	Phase-to-obstacles
Fast-front overvoltage	$D_{pp} = 3{,}64$	$D_{el} = 3{,}04$	$D_{el} = 3{,}29$	$D_{el} = 3{,}15$	$D_{el} = 3{,}26$
Slow-front overvoltage	$D_{pp} = 3{,}60$	$D_{el} = 2{,}19$	$D_{el} = 3{,}13$	$D_{el} = 2{,}52$	$D_{el} = 2{,}95$
Power frequency voltage	$D_{pf} = 1{,}14$	$D_{pf} = 0{,}60$	$D_{pf} = 0{,}66$	$D_{pf} = 0{,}61$	$D_{pf} = 0{,}61$

Table 2.27: Electrical clearances in m for a 500 kV overhead line equipped with cap-and-pin insulators

Overvoltage type	Phase-to-phase	Phase-to-earth wires	Phase-to-tower window	Phase-to-tower body or crossarm	Phase-to-obstacles
Fast-front overvoltage	$D_{pp} = 3{,}53$	$D_{el} = 2{,}94$	$D_{el} = 3{,}19$	$D_{el} = 3{,}05$	$D_{el} = 3{,}16$
Slow-front overvoltage	$D_{pp} = 4{,}30$	$D_{el} = 2{,}57$	$D_{el} = 3{,}73$	$D_{el} = 2{,}97$	$D_{el} = 3{,}50$
Power frequency voltage	$D_{pf} = 1{,}53$	$D_{pf} = 0{,}86$	$D_{pf} = 0{,}95$	$D_{pf} = 0{,}89$	$D_{pf} = 0{,}93$

Phase-to-tower:

$$D_{el} = 2{,}17\left(\exp\frac{1103}{1080 \cdot 0{,}992 \cdot 0{,}922 \cdot 1{,}45} - 1\right) = 2{,}52 \text{ m} \quad \text{and}$$

Phase-to-phase:

$$D_{pp} = 2{,}17\left(\exp\frac{1544}{1080 \cdot 0{,}992 \cdot 0{,}922 \cdot 1{,}6} - 1\right) = 3{,}60 \text{ m} \quad .$$

For power frequency operating voltages, (2.55) yields:

$$D_{el} = 1{,}64\left(\exp\frac{420}{750\sqrt{3} \cdot 0{,}975 \cdot 0{,}910 \cdot 1{,}22} - 1\right)^{0{,}833} = 0{,}61 \text{ m}$$

between phase conductors and tower structure.
The other electrical clearances shown in Table 2.26 have been determined similarly. It can be seen from the example that fast-front overvoltages prevail in the calculation of clearances, a consequence of the high value of the lightning withstand voltage $U_{90\%ff\_ins}$.

2.5.2.8.3 Electrical clearances for a 500 kV overhead line

The line is located at an altitude of 500 m above sea level and will be equipped with 22 cap and pin insulators U160BL. The highest power frequency voltage is 550 kV. The lightning withstand voltage $U_{90\%ff\_ins}$ is 1725 kV. The statistical switching voltage $U_{2\%sf}$ is 1175 kV. The slow-front overvoltages to be considered follow from (2.47) and (2.48) taking $K_{cs} = 1{,}05$ into account:

- Phase-to-earth $U_{rp} = K_{cs} \cdot U_{2\%sf} = 1{,}05 \cdot 1175 = 1234$ kV;
- Phase-to-phase at voltages above 1100 kV $U_{rp} = 1{,}4 \cdot 1{,}05 \cdot 1175 = 1727$ kV.

The altitude factor K_a is determined from Table 2.15 for voltages above 1100 kV, to be $K_a = 0{,}992$ for overvoltages; in case of power frequency voltages $K_a = 0{,}975$ for phase-to-ground and $K_a = 0{,}982$ for phase-to-phase apply.
The deviation factors according to Table 2.12 are:

$K_{z\_ff} = 0{,}961$ for fast-front overvoltages,
$K_{z\_sf} = 0{,}922$ for slow-front overvoltages,
$K_{z\_pf} = 0{,}910$ for power frequency voltages.

The resulting clearances for fast-front overvoltages are determined from (2.51) and (2.52) as:
Phase-to-tower:

$$D_{el} = 1725/(530 \cdot 0{,}992 \cdot 0{,}961 \cdot 1{,}12) = 3{,}05 \text{ m}$$

Phase-to-phase:

$$D_{pp} = 1{,}2 \cdot 1725/(530 \cdot 0{,}992 \cdot 0{,}961 \cdot 1{,}16) = 3{,}53 \text{ m} \quad .$$

For slow-front overvoltages, it results from (2.53) and (2.54), respectively:

Table 2.28: Technical data of a 380 kV overhead line

Conductor: 2 × 564-AL1/72-ST1A; diameter: 32,85 mm, mass; 2,11 kg/m		
Average conductor height above ground	20	m
Maximum span length	400	m
Wind span	500	m
Ratio wind span to weight span	1,3	–
Average of yearly maximum wind speeds	20	m/s
Coefficient of variation	0,14	–
Terrain category	B	–
Weight of the insulator set	300	kg
Wind exposed area of insulator set	1,5	m^2
Aerodynamic drag coefficient	1,2	–
Switching surge overvoltage	1050	kV

Phase-to-tower:

$$D_{el} = 2{,}17\left(\exp\frac{1234}{1080 \cdot 0{,}992 \cdot 0{,}922 \cdot 1{,}45} - 1\right) = 2{,}97 \text{ m} \quad \text{and}$$

Phase-to-phase:

$$D_{pp} = 2{,}17\left(\exp\frac{1727}{1080 \cdot 0{,}992 \cdot 0{,}922 \cdot 1{,}6} - 1\right) = 4{,}30 \text{ m} \quad .$$

For power frequency voltages it is obtained from (2.55) and (2.56):
Phase-to-tower

$$D_{pf\_pe} = 1{,}64\left(\exp\frac{550}{750\sqrt{3} \cdot 0{,}975 \cdot 0{,}910 \cdot 1{,}22} - 1\right)^{0{,}833} = 0{,}89 \text{ m}$$

Phase-to-phase

$$D_{pf\_pp} = 1{,}64\left(\exp\frac{550}{750 \cdot 0{,}982 \cdot 0{,}910 \cdot 1{,}26} - 1\right)^{0{,}833} = 1{,}53 \text{ m}$$

The other electrical clearances shown in Table 2.27 were determined similarly. Switching impulse determines the phase-to-phase, phase-to-tower window and phase-to-obstacle clearances, while lightning impulse prevails on phase-to-earth wire and phase-to-tower body clearances. The clearances for fast-front overvoltages as for the 380 kV example are nearly the same. Therefore, switching surges gain influence on the clearances.

2.5.2.8.4 Clearances to obstacles for line design, empirical approach

It is required to determine the minimum electrical clearances according to Table 2.24 for a 380 kV line, which crosses a fire resistant roof with a slope angle above 15°. The maximum air gap a_{som} in the crossing section of the line is assumed to be 4,50 m. with the data according to Tables 2.20 and 2.24, the following clearance results:

$$c_{min} = D_{el} + D_{add} = 2{,}0 + 2{,}80 = 4{,}80 \text{ m}.$$

However, as this clearance must be higher than $1{,}1 \cdot a_{som}$, a clearance of $1{,}1 \cdot 4{,}50 = 4{,}95$ m should be obeyed.
For a 110 kV line with $a_{som} = 2{,}0$ m it would result from Tables 2.20 and 2.24:

$$c_{min} = 2{,}0 + 1{,}00 = 3{,}00 \text{ m}$$

with the constraint $c_{min} \geq 1{,}1\, a_{som} = 2{,}20$ m. In this case, the value $c_{min} = 3{,}00$ m prevails.

Table 2.29: Return period of wind velocities

	Average of maximum yearly wind velocities: 20 m/s						
Return period (a)	2	5	10	20	50	150	500
$V_\tau/\overline{V}$ according to (2.57)	0,977	1,101	1,183	1,324	1,363	1,547	1,615
Velocity V_τ (m/s)	19,5	22,0	23,7	26,5	27,3	30,9	32,3

Table 2.30: Distribution of swing angles (example)

Return period	Wind velocity		Time percentage[1)]	Swing angle (20 m height, 5 min-average)		Standard deviation	Return period or time percentage[2)]
	Height			Span	Span		
	10 m 10 min m/s	20 m 5 min m/s	%	400 m Degree	200 m Degree	Degree	
50 a	27,3	32,0		47,6	48,3	2,25	100 a
25 a	25,7	30,1		44,1	44,8	2,20	50 a
10 a	23,7	27,8		39,6	40,3	2,15	20 a
5 a	22,0	25,8		35,5	36,1	2,12	5 a
3,5 a	21,1	24,8		33,3	34,0	2,10	7 a
2,0 a	19,5	22,9		29,3	29,9	2,00	4 a
250 d	18,2	21,4	99,9	26,1	26,7	1,90	0,05 %
100 d	16,9	19,8	99,75	22,8	23,3	1,80	0,125 %
50 d	15,9	18,7	99,5	20,5	21,0	1,70	0,25 %
25 d	14,8	17,4	99,0	17,9	18,4	1,60	0,5 %
5 d	13,7	16,1	98,0	15,5	15,9	1,50	1,0 %
2,5 d	12,9	15,1	95,0	13,7	14,0	1,35	2,5 %
30 h	10,5	12,3	90,0	9,2	9,4	1,05	5,0 %
12 h	8,8	10,3	80,0	6,5	6,6	0,80	10,0 %
0	0,2	0,25	0,1	~ 0	~ 0	0	100,0 %

[1)] During this time period of time the corresponding wind velocity is not exceeded

[2)] During this time period of time the corresponding can be exceeded.

2.5.2.8.5 Time distribution of swing angles

The *time distribution of swing angles* and the resulting tower top geometry will be established for a 380 kV suspension tower with the data summarized in Table 2.28.

Equation (2.57) yields the wind velocities corresponding to return periods from 2 to 500 years (Table 2.29). The parameter V_η of the Weibull distribution is then calculated from (2.60) based on the wind velocity having a return period of 2 years being 19,5 m/s.

$$V_\eta = 19{,}5/2{,}825 = 6{,}92 \text{ m/s}.$$

The wind velocities which will be exceeded with a given probability P per year can be determined from (2.59) with $\beta = 2{,}0$:

$$V = V_\eta \cdot \sqrt{-\ln(1-P)} \quad . \tag{2.70}$$

Table 2.30 contains the results.

The five-minute wind 20 m above ground is calculated from (2.61) and Figure 6.6

$$V_{5\text{min},20\text{m}} = V_{10\text{min},10\text{m}} \cdot (z/z_\text{R})^\alpha \cdot V_{5\text{min}}/V_{10\text{min}} = V_{10\text{min},10\text{m}} \cdot 1{,}12 \cdot 1{,}05 \quad . \tag{2.71}$$

The mean swing angles for insulators and conductors are obtained from equations (2.63) and (2.64), respectively. The factor G_L is taken from Figure 2.12 as 0,94 for 400 m and 1,0 for 200 m span. The air density ϱ is taken to be 1,225 kg/m^3. For the 50 year return period, swing angles of 47,6° for insulators and 41,8° for conductors result from (2.63) and (2.64), respectively, at a span of 400 m.

So far the procedure does not take into account the *angle of wind attack*. When assuming that the probability of occurrence of swing angles above approximately 2° is only half of that of the corresponding wind velocity, swing angles of 2,8° (insulators) and 2,3° (conductors) and above would then occur during 25 % of the year, while swing angles above 15,5° and 12,8° would occur only during 1 % of the year. During 75 % of the year, the swing angle will be below 2,3° (see Table 2.30).

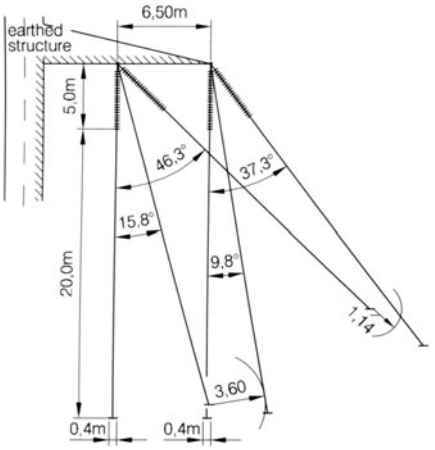

Figure 2.16: Midspan clearances

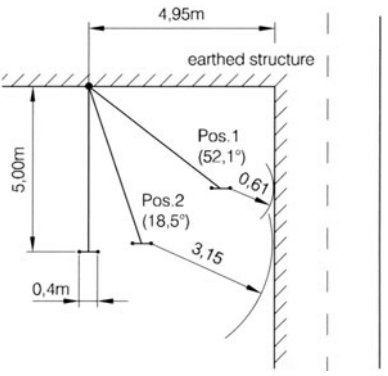

Figure 2.17: Phase-to-tower clearances for a statistic determination of swing angles

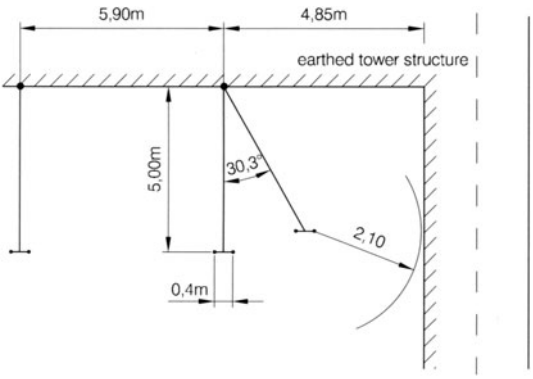

Figure 2.18: Phase-to-tower clearances when determining swing angle according to EN 50 341-3-4

2.5.2.8.6 Tower top geometry according to statistic considerations

For design of the tower top geometry, swing angles having a probability of occurrence of 1 % or more during a year should be combined with the clearance distance necessary to withstand switching or lightning surges. The swing angle under wind load according to the design return period should be correlated with the clearance necessary to withstand power frequency voltages. To take care of the scattering of swing angles under a given wind velocity, equation (2.65) is used. For $V_R = 32{,}0$ m/s a standard deviation of 2,25° results. The standard deviations are listed in Table 2.30. To determine an unfavourable conductor position, extreme swing angles of $\overline{\phi} \pm 2\,\sigma_\phi$ are assumed, which are $47{,}6 + 4{,}5 = 52{,}1°$ for insulators and $41{,}8 \pm 4{,}5 = 46{,}3°/37{,}3°$ for conductors. A standard deviation σ_ϕ of 1,5° results for the swing angles to be expected during 1 % of the year (15,5° and 12,8°, respectively). Then the swing angles to be considered under this condition are $15{,}5 + 3{,}0 = 18{,}5°$ (insulators) and $12{,}8 \pm 3{,}0 = 9{,}8°/15{,}8°$ (conductors).
According to Table 2.26, a phase-to-phase spacing of approximately 3,60 m is obtained for fast-front and slow-front overvoltages, while for power frequency voltage a phase-to-phase spacing of about 1,14 m would result. The investigated conditions are shown in Figure 2.16 for an insulator set 5 m long and a conductor sag of 20 m. It is demonstrated that the case of fast-front or slow-front overvoltages is predominant, the case of the extreme swing angle combined with the clearances for power frequency voltage does not prevail.
The clearances between conductors and earthed tower elements are shown in Figure 2.17. The minimum required phase conductor-to-earth or phase conductor-to-tower clearances are 3,15 m for overvoltages and 0,61 for power frequency voltages, as given in Table 2.26. For power fre-

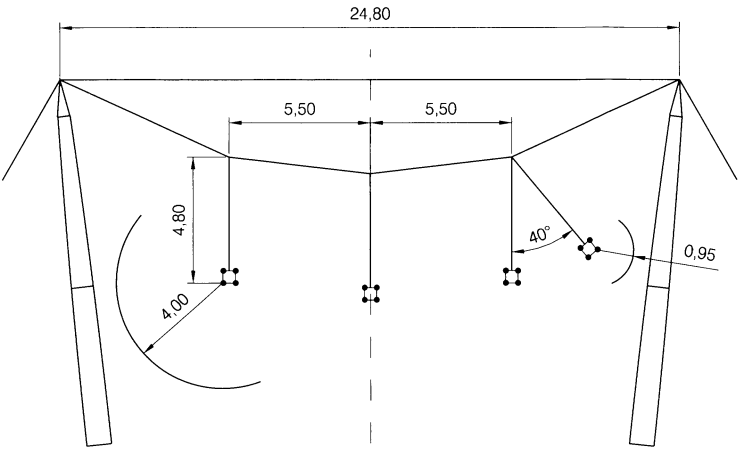

Figure 2.19: Tower top dimensions of a 500 kV compact crossarmless guyed tower (Brazil)

quency voltage, a clearance of 4,76 m results between tower body and conductor attachment point, and for fast-front overvoltages 4,95 m. The last data prevails here.

2.5.2.8.7 Tower top geometry according to European standards

For comparison, the *tower top geometry* according to [2.36] will be established as well. In midspan the required clearance is determined from (2.68):

$$c_{\min} = k_C \sqrt{f_C + l_k} + 0{,}40 + 0{,}75\, D_{pp} \quad .$$

The factor k_C depends on *conductor swing angle*. According to [2.36], it applies:

$$\phi_C = \tan^{-1}\left[\frac{q_C \cdot G_L \cdot D \cdot a}{m_C \cdot g \cdot a}\right] \quad ,$$

where $G_L = 0{,}45 + 60/400 = 0{,}60$ according to [2.36] for $a = 400$ m and $q_C = 0{,}58\, q_z = 0{,}58 \cdot 860 = 499$ N/m^2. Hence $\phi_C = 25{,}4°$. Therefore, it results from Table 2.22: $k_C = 0{,}60$.
The value D_{pp} should be taken from Table 2.20: $D_{pp} = 3{,}20$ m. It results, therefore, for the phase-to-phase clearance a value of 5,8 m instead of 6,5 m in case of statistical approach. The maximum clearance D_{pp} is here prevalent.
The swing angle of the insulator set follows from formula (2.63) as:

$$\begin{aligned}\phi_{ins} &= \tan^{-1}\left[\frac{0{,}58 \cdot 860 \cdot 0{,}6 \cdot 0{,}03285 \cdot 400 \cdot 2 + 1{,}2 \cdot 1{,}5 \cdot 0{,}58 \cdot 860/2}{2 \cdot 400/1{,}3 \cdot 2{,}11 \cdot 9{,}81 + 300 \cdot 9{,}81/2}\right] \\ &= \tan^{-1}(8314/14209) = 30{,}3°\end{aligned}$$

With such data, clearances of Figure 2.18 are obtained and they are somewhat lower than the ones calculated with the statistical approach.

2.5.2.8.8 Tower top geometry according to Brazilian practice

The tower top geometry will be determined for a 500 kV compact line as shown in Figure 2.19 according to Brazilian practice for such kind of lines: Phase conductors quadruple bundle 483-AL1/34-ST1A, diameter of subconductors 29,6 mm; weight 15,72 N/m; rated tensile strength 116,1 kN; everyday stress 20 %; subspan spacing 0,47 m; length of insulator string 4,80 m; span length 450 m.
Following Brazilian practice, the tower top geometry is verified for power frequency voltage and maximum swing angles. A swing angle of 40° is obtained for the 1-min wind velocity having a return period of 50 years using the approach described in clause 2.5.2.4.4. The required clearances can be taken from Table 2.27, the relevant data being $D_{pf\_pp} = 1{,}53$ m phase-to-phase and $D_{pf\_pe} = 0{,}95$ m phase-to-tower window. The sag at everyday condition is

$$f = (450^2 \cdot 15{,}72)/(8 \cdot 0{,}2 \cdot 116\,100) = 17{,}14 \text{ m} \; .$$

Studies carried out by Brazilian utilities have shown that asynchronous swinging of conductors does not exceed around 8° being in accordance with [2.40]. Assuming a swing angle of 40° for the middle phase and 32° for one of the outer phases, a clearance at midspan of

$$c = 5{,}50 - 0{,}46 - (4{,}8 + 17{,}14)(\sin 40° - \sin 32°) = 2{,}56 \text{ m}$$

results being more than the required 1,53 m. The required midspan clearance using equation (2.68) and $D_{\text{pp}} = 4{,}00$ m according to Table 2.20 would be

$$c_{\min} = 0{,}6\sqrt{17{,}14 + 4{,}80} + 0{,}75 \cdot 4{,}00 + 0{,}46 = 6{,}27 \text{ m} .$$

The main difference to Brazilian practice is the consideration of overvoltage clearances instead of power frequency clearances. The Brazilian practice has been developed for 500 kV compact lines, aimed at having a high surge impedance load. Its basic characteristic is the consideration of power frequency clearances together with maximum string angles. Operational performance of the 550 kV compact line is reported to be very satisfying.

2.6 References

2.1 IEC 60 826: Loading and strength of overhead transmission lines. Geneva, IEC, 1991

2.2 Cigré SC22 WG13: Management of existing overhead transmission lines. Paris, Cigré Brochure No. 175, 2001

2.3 Boos, K.-V. et al.: Experiences gained in the operation of multiple circuit high-voltage overhead lines of compact design. Cigré Report 22-12, 1986

2.4 Aluminium electrical conductor handbook. Washington. The Aluminium Association, 1982

2.5 Cigré: Electric and magnetic fields and health. Paris, Proceedings of the 1992 Session, 1992

2.6 Cigré SC36 WG36.06: Management of the EMF issue. Electra 168/1996), pp. 130 to 137

2.7 Dab, W. et al.: Magnetic fields and cancer: Recent studies on adults. Cigré Panel 1-03, 1994

2.8 International commission on non-ionizing radiation protection (ICNIRP): Guidelines for limiting exposure to time-varying electric, magnetic and electromagnetic fields. Health Physics 74 (1998), pp. 1 to 32

2.9 Pirotte, P.: Some facts about E and B fields at the power frequencies. Cigré proceedings of the 1992 session, Panel 2-01, 1992

2.10 International Radiation Protection Association (IRPA): Interim guidelines on limits of exposure to 50/60 Hz electric and magnetic fields. Health Physics 58 (1990), pp. 113 to 122

2.11 Directive 1999/519/EC: Council recommendation on the limitation of exposure of the general public to electromagnetic fields (0 Hz to 300 GHz). Brussels, EC, 1999

2.12 26.Verordnung zur Durchführung des Bundes-Immissionsschutzgesetzes (BImSchV), Verordnung über elektromagnetische Felder (26^{th} directive for application of immission protection law (BImSchG), directive on electromagnetic fields). Edition 1996

2.13 NRPB GS11: Guidance as to restricitons on exposure to time-varying electromagnetic fields and the 1988 Recommendations of the International Non-Ionizing Radiation Committee, 1989

2.14 Maddock, B. J.: Guidelines and standards to electric and magnetic fields at power frequencies. Cigré proceedings on the 1992 session, Panel 2-05, 1992

2.15 CIGRE SC22 WG22.14: Environmental concerns, procedures, impacts and mitigations. Paris, Cigré Brochure No. 147, 1999

2.16 Kießling, F.; Puschmann, R.; Schmieder, A.: Contact lines for electric railways. Erlangen. Publicis MD Verlag, 2001

2.17 Happoldt, H.; Oeding, D.: Elektrische Kraftwerke und Netze (Electric power stations and networks). Berlin, Heidelberg, New York. Springer-Verlag, 5th edition 1978

2.18 EPRI: Transmission line reference book 345 kV and above. Palo Alto, Electric Power Research Institute, 2nd edition 1987

2.19 Völcker, O.: Elektrische Randfeldstärken in Hochspannungsfreileitungen (Electric voltage gradients of high-voltage lines). Elektrizitätswirtschaft 64 (1965), pp. 59 to 62

2.20 Koronastörungen elektrischer Netze (Corona disturbances in electric networks). Mannheim, Forschungsgemeinschaft für Hochspannungs-Hochstromtechnik. Technical Report No. 2-31, 1976

2.21 Fink, D. G.; Beaty, H. W: Standard handbook for electrical engineers. New York, Mc Graw-Hill, 12th edition 1987

2.22 Allgemeine Verwaltungsvorschriften über genehmigungsbedürftige Anlagen nach §16 der Gewerbeordnung – GewO: Technische Anleitung zum Schutz gegen Lärm (Administrative directives on installations subject to approvals according to §16 of industry directive: Technical guidelines for noise protection). 1968

2.23 Chartier, V. L.; Stearns, R. D.: Formulae for predicting audible noise from overhead high-voltage AC and DC lines. IEEE Transactions on Power Apparatus and Systems, Vol. 100 (1981), 121 to 130

2.24 Sforzini, N.; Cortina, R.; Sacerdate, G.; Piazza, R.: Acustic noise caused by AC corona on conductors: Results of an experimental investigation in the anechoic chamber: IEEE Transactions on Power Apparatus and Systems, Vol. 94 (1974), 591 to 601

2.25 IEEE Task Force Report: Measurement of audible noise from transmission lines. IEEE Transactions on Power Apparatus and Systems, Vol. 100 (1981) No. 3, pp. 1442

2.26 Cigré SC22 WG22.06: Influence of line configurations on impacts of electrical origin. Paris, Cigré Brochure, will be published in 2002

2.27 EN 50 341-1: Overhead electrical lines exceeding AC 45 kV. Part 1: General requirements – Common specifications. Brussels, CENELEC, 2001

2.28 IEC 60 815: Guide for the selection of insulators in respect of polluted conditions. Geneva, IEC 1986

2.29 EN 60 071-1: Insulation coordination. Part 1: Definitions, principles and rules (IEC 60 071-1). Brussels, CENELEC, 1995

2.30 Cigré SC33: Guidelines for the evaluation of the dielectric strength of external insulation. Paris, Cigré Brochure No. 72, 1992

2.31 EN 60 071-2: Insulation coordination. Part 2: Application guide (IEC 60 071-2). Brussels, CENELEC, 1997

2.32 EPRI: HVDC Transmission line reference book. Palo Alto, Electric Power Research Institute, 1993

2.33 Cigré SC22 WG22.06: Tower top geometry. Paris, Cigré Brochure No. 48, 1995

2.34 IEC 61 472: Live working – Minimum approach distances – Method of calculation. Geneva, IEC, 1998

2.35 EN 50 341-3: Overhead electrical lines exceeding AC 45 kV. Part 3: National Normative Aspects (NNA). Brussels, CENELEC, 2001

2.36 EN 50 341-3-4: Overhead electrical lines exceeding AC 45 kV. Part 3-4: National Normative Aspects for Germany. Brussels, CENELEC, 2001

2.37 Leibfried, W.; Mors, H.: The mechanical behaviour of bundled and single conductors – New measurements at the Hornisgrinde testing station. Paris, Cigré Report No. 209, 1960

2.38 Mors, H.: Wind pressure on overhead transmission line conductors – Hornisgrinde testing station. Paris, Cigré Report No. 220, 1956

2.39 Ervik, N.; Horn, T.; Johnson, R.: Erection of and vibration protection of long fjord crossing in Norway. Paris, Cigré Report No. 23-03, 1968

2.40 EHV and UHV transmission lines: Electrical, structural and environmental concepts and evaluations. Washington D.C., US Department of Energy, No. DOE/ET/29236-2, 1982

3 Electric parameters

3.0 Symbols

Symbol	Signification
a	Line or conductor length
A	Conductor cross section
B	Susceptance
C_0	Zero-sequence capacitance
C_{0S}, C_{0D}	Zero-sequence capacitance, single- or double-circuit line, without earth wire
C_{0SE}, C_{0DE}	Zero-sequence capacitance, single- or double-circuit line, with earth wire
C_1	Positive-sequence capacitance
C_{1S}, C_{1D}	Positive-sequence capacitance of a single- or double-circuit line
d	Conductor diameter
D_{AB}, D_{AC}, D_{BC}	Phase-to-phase distances
D_{E1E2}	Distance between earth wires
D_M	Geometric mean distance
D_{M1}, D_{M2}	Auxiliary mean distance of each circuit of a double-circuit line
D_{ME}	Mean distance between conductors and earth-wire
f	Frequency
G	Conductance
h_E	Mean earth wire height above ground
h_M	Mean conductor height above ground
k_1	Quantity to determine the bundle conductor equivalent radius
L_1	Positive-sequence inductance
n_2	Number of subconductors per bundle
P_{nat}	Surge impedance load
P_W	Active power
P_{loss}	Line losses
r_0	Radius of bundle circle
r_B	Bundle conductor equivalent radius
r_E	Earth wire radius
r	Subconductor radius
R	Resistance, per unit values are designated by R'
R_{AC}	AC resistance
R_{DC}	DC resistance
R_E	Resistance of earth wire
s	Subconductor distance within a bundle
T	Temperature
U	Voltage
U_{pp}	Phase-to-phase voltage
X	Reactance
X_1	Positive-sequence reactance
X_0	Zero-sequence reactance
X_C	Capacitive reactance
Y_0	Zero-sequence admittance
Y_1	Positive-sequence admittance
Z	Impedance
Z_{0S}, Z_{0D}	Zero-sequence impedance of a single- or double-circuit line without earth wires
Z_{0S1E}, Z_{0D1E}	Zero-sequence impedance of a single- or double-circuit line with one earth wire
Z_{0S2E}, Z_{0D2E}	Zero-sequence impedance of a single- or double-circuit line with two earth wires

Symbol	Signification
Z_0	Zero-sequence impedance
Z_1	Positive-sequence impedance
Z_C	Surge impedance
Z_{CE}	Mutual impedance between phase conductors and earth wires
Z_{E1E2}	Mutual impedance between two earth wires
Z_{EE}	Self-impedance of earth wire
α	Temperature coefficient of resistance, attenuation constant
β	Phase constant
γ	Propagation constant
δ	Return depth of earth current
ΔU	Magnitude of the voltage drop
ε_0	Dielectric constant: $8{,}854 \cdot 10^{-12}$ F/m
θ	Phase angle
λ	Wave length
μ_0	Constant of magnetic field: $4 \cdot \pi \cdot 10^{-7}$ H/m
μ_E	Permeability of earth wires
μ_T	Permeability of phase conductors
ϱ	Resistivity
ϱ_E	Earth resistivity
φ	Phase angle
ω	Angular frequency

3.1 Introduction

The electric performance of a transmission line circuit is determined by its *electrical resistance*, *inductance* and *capacitance*. Such parameters depend at first on the conductor properties. However, when conductors with a certain physical configuration are strung in an overhead line, at variable phase-to-ground and phase-to-phase spacing along the line, the whole context of conductor internal properties and physical dimensions comprises the resulting *line parameters*. When considered in electric system studies, these parameters are usually treated in form of the so-called symmetrical components that are described as *positive-*, *negative-* and *zero-sequence impedances*.

In deriving the equations for inductance and capacitance of transposed transmission lines, balanced three-phase currents are assumed. When only zero-sequence current flows in a transmission line, for instance, the current in each phase is identical, if a phase-to-ground short-circuit occurs. The current returns through the ground, through earth wires or through both. Other secondary parameters, originated from the physical presence of an energized line and affecting the environment are also of importance, as it is the case of electrical and magnetic fields, inductive and capacitive coupling and their effect on persons or animals. These effects are treated in chapter 2. The transmission line representation in an electric system is treated as well, because of its frequent use in electrical studies.

In general, only the basic formulae for calculating the main line parameters will be presented. Those having interest in knowing more details can refer especially to [3.1] or to [3.2].

The line parameters and equivalent impedance circuits are broadly used in most of electric system calculations. Positive and zero-sequence impedances of overhead lines are part of *load flows*, losses, short-circuit and stability investigations. They are also required for setting *line protection* impedance and distance relays. The determination of series or shunt compensation requirements is closely dependent on line parameters, especially on series inductances and shunt capacitances.

While some new technologies aimed at improving line transmitting capabilities, such as so called high *surge impedance load lines*, try to increase the surge impedance load

of the lines, other technologies, such as *flexible alternating circuits transmission systems* (FACTS), are designed to control series inductive reactances or shunt capacitive reactances, so as to reach stable conditions under different loading requirements (see chapter 1). In all cases, the determination of line parameters is of paramount importance.

3.2 Resistance

The electrical resistance of an overhead line is one of the most influencing factors in designing an optimised line; the power and energy losses are a direct function of the *phase-conductor resistance*, so that their exact determination is important. Resistance is the property of an electric circuit or any body that may be used as part of an electric circuit, which determines the average rate at which electric energy is converted into heat as a function of the electric current.
A uniform cylindrical conductor of diameter d has a total resistance per unit length, in m, to direct current expressed by

$$R'_{\mathrm{DC}} = \varrho/A = \varrho \cdot 4/(\pi\, d^2) \quad , \tag{3.1}$$

where R'_{DC} is the resistance in Ω/m, ϱ the resistivity in $\Omega \cdot$ mm^2/m, A the conductor cross section in mm^2 and d conductor diameter in mm.
When used for conducting alternating currents, the effective *AC resistance* may be higher than the DC resistance defined above due to skin and spiral effects (see equation (7.16)).
The resistivity of standard annealed copper at 20°C is 0,01724 $\Omega \cdot$mm^2/m and its conductivity of 58 m/Ωmm^2 is designated as 100 % *IACS* (*International Annealed Copper Standard*) [3.2] and is used as a reference. Hard-drawn copper, with a tensile strength about 50 % greater than that of the annealed copper, has a conductivity of 56 m/Ωmm^2 corresponding to about 97 % IACS. Average hard-drawn aluminium has a conductivity of 35,38 m/$\Omega \cdot$mm^2 (61 % IACS) or a resistivity of 0,02826 $\Omega \cdot$mm^2/m. Knowing the resistance of a conductor at 20°C, one obtains the resistance at any temperature T, by

$$R'_{\mathrm{T\,DC}} = R'_{20\,\mathrm{DC}} \cdot [1 + \alpha\,(T - 20)] \quad , \tag{3.2}$$

where α is the temperature coefficient of resistance. Table 7.4 shows data for the most usual conductor materials. Additional data are given in in [3.2].
In the case of bundles with n_2 subconductors, the *equivalent resistance* is simply the resistance of one subconductor R'_{DC} divided by n_2: $R'_{\mathrm{tot}} = R'_{\mathrm{DC}}/n_2$, as the influence of the separation between subconductors is neglected.
When dealing with overhead line conductors, the resistance shall be considered at appropriate temperatures. Usually conductors of overhead lines are designed for 60 to 80°C as maximum conductor temperatures.
Temperature measurement of overhead conductors carried out in the field has shown that the real conductor temperature is generally lower than the values obtained theoretically. In view of that, for calculating Joule losses, it is more appropriate to take into account a lower conductor temperature, say 40 to 50°, in order to prevent an over-evaluation of the thermal losses in any economical consideration.

3.3 Positive-sequence impedance

3.3.1 Introduction

The *positive-sequence impedance* is the mostly used line parameter for normal operating conditions and calculations of AC circuits, such as voltage and current relationships,

Table 3.1: Conductor bundle equivalent radius

Number of conductors n_2	Radius of bundle circle r_0	Conductor bundle equivalent radius r_B	k_1	Example r_B $r_T = 16$ mm $s = 400$ mm
1	—	r	1	16
2	$s/2$	$\sqrt{rs}$	1	80
3	$s/\sqrt{3}$	$\sqrt[3]{rs^2}$	1	137
4	$s/\sqrt{2}$	$\sqrt[4]{rs^3 \cdot \sqrt{2}}$	1,12	195
5	$0,851\,s$	$\sqrt[5]{2,618\,rs^4}$	1,272	255
6	s	$\sqrt[6]{6\,rs^5}$	1,43	315
8	$1{,}307\,s$	$\sqrt[8]{52{,}12\,rs^7}$	1,76	438

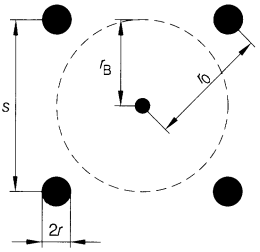

Figure 3.1: Determination of bundle conductor equivalent radius

power and energy losses, power flow etc. It is a vector quantity, that can be represented as a complex number either in rectangular format with real and imaginary components as

$$Z_1 = R_1 + \mathrm{j}\,X_1 \tag{3.3}$$

or in polar format

$$Z_1 = |Z_1|\,\angle\theta \quad , \tag{3.4}$$

where:

R_1	resistance as in (3.2),
X_1	positive-sequence reactance,
$\lvert Z_1\rvert = \sqrt{R_1^2 + X_1^2}$	module of Z_1 and
$\theta = \tan^{-1}(X_1/R_1)$	phase angle.

3.3.2 Inductance and inductive Reactance

The inductance relationships used in predicting the performance of overhead transmission lines often involve the effects of single and bundled conductors operating in series or in parallel. Configurations of groups of current-carrying elements of one circuit coordinated with similar circuits constituting other phases in three-phase systems are also treated in several cases. The *positive-sequence inductive reactance* of a fully transposed equivalent three-phase transmission line is given by:

$$X_1 = \omega L_1 = (\omega \mu_0 a/2\,\pi)\left(\ln \frac{D_M}{r_B} + \frac{1}{4\,n_2}\right) \quad , \tag{3.5}$$

hence $L_1 = (\mu_0 a/2\,\pi)\,(\ln D_M/r_B - 1/4n_2)$,
where

ω	angular frequency $= 2\,\pi \cdot f$,
L_1	positive-sequence inductance in H/m,
a	conductor length in m,
D_M	geometric mean distance,
μ_0	constant of magnetic field $= 4\,\pi \cdot 10^{-7}$ H/m,
r_B	*bundle conductor equivalent radius*

$$r_B = \sqrt[n_2]{n_2 \cdot r \cdot r_0^{n_2-1}} = r\,\sqrt[n_2]{(k_1 \cdot s/r)^{n_2-1}} \quad . \tag{3.6}$$

k_1	see Table 3.1, $k_1 = n_2^{1/(n_2-1)}/[2\,\sin(\pi/n_2)]$,
n_2	number of subconductors,

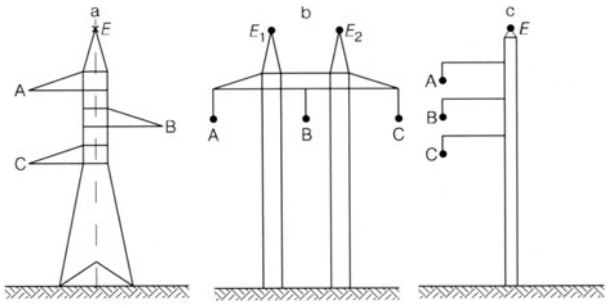

Figure 3.2: Phase conductor arrangement for single-circuit lines

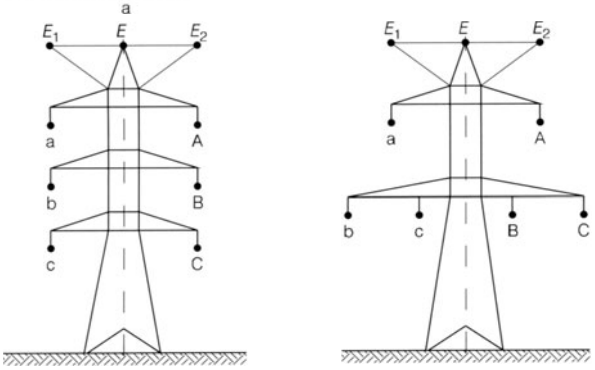

Figure 3.3: Phase conductor arrangement for double-circuit lines: a Vertical arrangement (symmetrical arrangement of phase conductors); b Danube arrangement (asymmetrical arrangement of phase conductors)

r subconductor radius,
s subconductor distance within the bundle and
r_0 radius of bundle circle $r_0 = s/[2 \sin(\pi/n_2)]$.

Table 3.1 contains values for r_0 and k_1. Figure 3.1 shows the relevant geometric quantities. In case of a single-circuit line (Figure 3.2), the *geometric mean distance* is:

$$D_M = \sqrt[3]{D_{AB} \cdot D_{AC} \cdot D_{BC}} \quad . \tag{3.7}$$

For double-circuit lines (Figure 3.3) equation (3.5) is transformed to

$$X_1 = \omega L_1 = \frac{\omega \mu_0 a}{2\pi} \left(\ln \frac{D_M D_{M2}}{r_B D_{M1}} + \frac{1}{4 n_2} \right) \quad , \tag{3.8}$$

where D_M follows from (3.7). If a symmetrical phase arrangement of the individual circuits is assumed, D_{M1} and D_{M2} are obtained from

$$D_{M1} = \sqrt[3]{D_{Aa} \cdot D_{Bb} \cdot D_{Cc}} \tag{3.9}$$

and

$$D_{M2} = \sqrt[3]{D_{Ab} \cdot D_{Ac} \cdot D_{Bc}} \quad . \tag{3.10}$$

In case of an asymmetrical arrangement D_{M2} is given by

$$D_{M2} = \sqrt[6]{D_{Ab} \cdot D_{Ac} \cdot D_{Bc} \cdot D_{Ba} \cdot D_{Ca} \cdot D_{Cb}} \quad . \tag{3.11}$$

For one kilometer of line and $f = 50$ Hz and single conductors it applies for the *reactance per unit length*

$$X_1' = 0{,}0628 \left(\ln \frac{D_M}{r} + \frac{1}{4} \right) \quad \Omega/\text{km} \tag{3.12}$$

Table 3.2: Electric parameters of typical overheadlines for 50 Hz

Rated phase-to-phase voltage kV	20[2]	110	220	380	500	750
	48-AL1/ 8-ST1A	184-AL1/ 30-ST1A	434-AL1/ 56-ST1A	562-AL1/ 49-ST1A	494-AL1/ 34-ST1A	653-AL1/ 45-ST1A
Number of subconductors	1	1	1	2	3	4
Subconductor diameter mm	9,6	19,0	28,8	32,2	29,9	34,4
Resistance R'_1 Ω/km[1]	0,666	0,176	0,075	0,029	0,022	0,012
Positive-sequence reactance X'_{L1} Ω/km	0,42	0,41	0,40	0,33	0,30	0,29
Operating capacitance C' μF/km	8,6	8,9	9,0	11,1	12,0	12,5
Capacitive reactance X_{C1} MΩ·km	0,37	0,36	0,35	0,29	0,26	0,25
Surge impedance Z_C Ω	395	385	375	310	280	270
Zero-sequence resistance R'_0 Ω/km [3]	0,81	0,42	0,30	0,24	0,23	0,22
Zero-sequence reactance X'_0 Ω/km[3]	1,60	1,00	0,98	0,84	0,80	0,78
Zero-sequence capacitance nF/km	4,95	6,10	6,40	8,65	9,12	9,36
Zero-sequence capacitive reactance X_{C0} MΩ·km	0,64	0,52	0,50	0,37	0,35	0,34
Ratio X'_0/X'_{L1}	3,81	2,44	2,45	2,55	2,67	2,69

1) at 50°C; 2) without earth wire; 3) one circuit with two earth wires

and in case of bundle conductors

$$X'_1 = 0{,}0628 \left(\ln \frac{D_M}{r_B} + \frac{1}{4\,n_2} \right) \quad \Omega/\text{km}. \tag{3.13}$$

In case of 60 Hz the factor 0,0628 will be replaced by 0,0754. For double-circuit lines D_M will be modified to $(D_M \cdot D_{M2}/D_{M1})$. Table 3.2 shows the positive-sequence reactance for typical line configurations. Fully transposed lines are considered, so that phase sequences ABC, BCA and CAB comprise each one a third of the total line length [3.3].

Example: For a 500 kV line, having self-supporting towers with flat conductor configuration as in Figure 3.2 b, triple bundle of ACSR conductors 494 mm²/34 mm² (494-AL1/34-ST1A), subconductor spacing $s = 400$ mm the inductance and positive-sequence impedance is required. Frequency $f = 50$ Hz, conductor diameter = 29,9 mm, conductor resistance $R = 0{,}0584$ Ω/km at 20°C, temperature coefficient of resistance $\alpha = 0{,}00403$ 1/K. Phase arrangement see Figure 3.4.
According to (3.2) the resistance at 50°C is

$$R_{50} = 0{,}0584 \cdot [1 + 0{,}00403(50 - 20)]/3 = 0{,}0218\ \Omega/\text{km}.$$

Geometric mean distance according to (3.7) is

$$D_M = \sqrt[3]{12{,}5 \cdot 12{,}5 \cdot 25} = 15{,}75\ \text{m}.$$

The radius of the bundle circle is given by:

$$r_0 = s/\,(2 \sin \pi/n_2) = 0{,}400/\,[2 \sin(\pi/3)] = 0{,}231\ \text{m}.$$

The bundle conductor equivalent radius results from (3.6):

$$r_B = \sqrt[3]{3 \cdot 0{,}014805 \cdot (0{,}231)^2} = 0{,}134\ \text{m}.$$

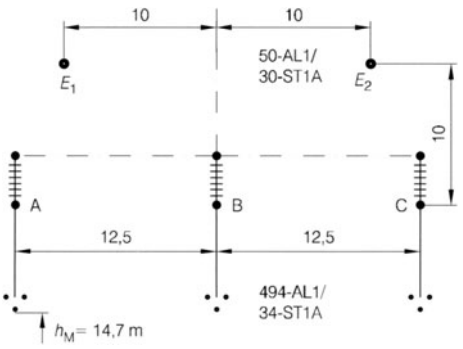

Figure 3.4: Tower top dimensions, 500 kV, example

As bundle conductors are concerned, inductance and inductive reactance are determined by (3.5) and (3.12), respectively, as:

$$L_1' = 4\pi \cdot 10^{-7}/(2\pi) \cdot (\ln 15{,}75/0{,}134 + 1/12)\,/1000 = 9{,}70 \cdot 10^{-4}\ \text{H/km}$$

and

$$X_1' = 0{,}0628\ \ln(15{,}75/0{,}134 + 1/12) = 0{,}3046\ \Omega/\text{km}.$$

For 60 Hz, X_1' is 0,3655 Ω/km.
The positive-sequence impedance follows from (3.3)

$$Z_1' = 0{,}0218 + \text{j}\,0{,}3046 = 0{,}3054\,\angle 85{,}9°\ \Omega/\text{km}.$$

3.4 Zero-sequence impedance

3.4.1 Introduction

Zero-sequence currents are identical in each phase conductor and not displaced by 120° as positive- and negative-sequence currents. The magnetic field due to zero-sequence currents is very different from that caused by either positive- or negative-sequence currents. The difference in magnetic field results in a zero-sequence reactance of a transmission line being in the range of 1,5 to 4 times the positive-sequence reactance. The zero-sequence currents flow only if a return path exists through which a completed circuit is provided. The impedance of the ground and ground wires is included in the zero-sequence impedance of the transmission line. The most common use of *zero-sequence impedance* is in the calculation of phase-to-ground short-circuit currents. Such current calculations are required for setting ground fault protection relays.

3.4.2 Simplified approach for the determination of zero-sequence impedances

The *zero-sequence impedance* of overhead line conductors involves the *self-impedances* and the *mutual impedances* of the ground return circuits.
Complex equations are required for a precise calculation of zero-sequence impedances, as they involve return circuits to ground, as treated in [3.2] and [3.4]. The calculation of zero-sequence impedances can be carried out with simplified approaches that provide a sufficient degree of accuracy for most practical applications. One of these approaches is presented in this clause.
The basic equations for the calculation of zero-sequence impedance were determined by Pollaczek [3.5] and Carson [3.6]. Considering that both the resistance and inductance of conductors, earth wires and ground return circuits are dependent on the frequency, simplified formulae have been developed for application in 50/60 Hz circuits.

The deduction of such formulae are beyond the scope of this book and can be studied in [3.1] and [3.3]. The simplified approach presented here after is applicable to single-circuit and double-circuit symmetrical lines, provided with no, one or two earth wires.

Single-circuit line without earth wires

The zero-sequence impedance is

$$Z'_{0S} = R'_0 + jX'_0 = \frac{R'_1}{n_2} + \frac{3}{4}\pi f\mu_0 + j f\mu_0 \left(3 \cdot \ln \frac{\delta}{\sqrt[3]{r_B D_M^2}} + \frac{\mu_T}{4 n_2}\right) \quad , \tag{3.14}$$

where

R'_1 conductor resistance per unit length at the design temperature in Ω/km, according to (3.1) or (3.2),
n_2 number of subconductors per bundle,
f frequency in Hz,
μ_0 constant of magnetic field $4\pi \cdot 10^{-4}$ H/km,
r_B bundle conductor equivalent radius according to (3.6); for single conductors $r_B = r$,
D_M geometric mean distance according to (3.7),
μ_T permeability of phase conductor, $\mu_T = 1,0$ for usually adopted phase conductors,
δ return depth of earth current (m),

$$\delta = 1{,}85/\sqrt{2\pi f\mu_0/\varrho_E} \tag{3.15}$$

with ϱ_E being the average earth resistivity in Ω·m.

Line with one earth wire (Figure 3.2 a and 3.2 c)

The impedance is determined from the impedance of a line without earth wire (see (3.14)) and the self- and *mutual impedances* of the earth wire

$$Z'_{0S1E} = Z'_{0S} - 3\,(Z'_{CE})^2/Z'_{EE} \quad . \tag{3.16}$$

The mutual impedance of the conductors to the earth wire is

$$Z'_{CE} = f\mu_0\pi/4 + j f\mu_0 \cdot \ln(\delta/D_{ME}) \quad , \tag{3.17}$$

where

$$D_{ME} = \sqrt[3]{D_{AE} \cdot D_{BE} \cdot D_{CE}} \tag{3.18}$$

is the mean distance between conductors and earth wire.
The *self-impedance* of the earth wire is

$$Z'_{EE} = R'_E + f\mu_0 \cdot \pi/4 + j f\mu_0\,(\ln \delta/r_E + \mu_E/4) \quad , \tag{3.19}$$

where

R'_E earth wire resistance in Ω/km;
μ_E is the relative magnetic permeability of the earth wire.
For copper and aluminium conductors or earth wires and ACSR conductors with a ratio of aluminium to steel section equal or higher than 6 the relative magnetic permeability can be taken as $\mu_T = \mu_E \cong 1$. For ACSR conductors or earth wires with one aluminium layer, μ_T or μ_E is taken between 5 and 10. For steel earth wires μ_T or μ_E can be taken as an average value of ≈ 25.
r_E earth wire radius in m.

Single-circuit line with two earth wires (Figure 3.2 b)

For any arrangement of the earth wires it follows

$$Z'_{0S2E} = Z'_{0S} - 3\,(Z'_{CE})^2/Z'_{E1E2} \quad . \tag{3.20}$$

The mutual impedance Z'_{CE} is given by (3.17), where D_{ME} can be taken from (3.18) in case of the symmetrical arrangement of earth wires. In case of asymmetrical arrangement it applies

$$D_{ME} = D_{M2E} = \sqrt[6]{D_{AE1} \cdot D_{BE1} \cdot D_{CE1} \cdot D_{AE2} \cdot D_{BE2} \cdot D_{CE2}} \quad . \tag{3.21}$$

The mutual impedance Z'_{E1E2} is given by

$$Z'_{E1E2} = R'_E/2 + f\mu_0\pi/4 + \mathrm{j}\, f\mu_0 \left[\ln\left(\delta/\sqrt{r_E D_{E1E2}}\right) + \mu_E/8\right] \quad , \tag{3.22}$$

where D_{E1E2} is the distance between the earth wires in m.
Table 3.2 contains the zero-sequence impedances of typical lines with one circuit and two earth wires.

Double-circuit line without earth wires

The zero-sequence impedance for two circuits is

$$Z'_{0D} = Z'_{0S} + 3\,Z'_{C1C2} \quad , \tag{3.23}$$

where Z'_{0S} is obtained from (3.14) and

$$Z'_{C1C2} = f\mu_0\pi/4 + \mathrm{j}\, f\mu_0 \ln\left(\delta/\sqrt{D_{M1} D_{M2}}\right) \quad , \tag{3.24}$$

with D_{M1} or D_{M2} determined from (3.9) and (3.10), respectively.

Double-circuit line with one earth wire (Figure 3.3 a or 3.3 b)

For this arrangement it applies:

$$Z'_{0D1E} = Z'_{0D} - 6\,(Z'_{CE})^2/Z'_{EE} \quad . \tag{3.25}$$

Considering the symmetrical arrangements Z'_{0D} can be taken from (3.23), Z'_{CE} from (3.17) and Z'_{EE} from (3.19).

Double-circuit line with two earth wires (Figure 3.3 a or 3.3 b)

For this arrangement it applies:

$$Z'_{0D2E} = Z'_{0D} - 6\,(Z'_{CE1E2})^2/(Z'_{E1E2}) \quad . \tag{3.26}$$

Because of the symmetry Z'_{0D} can be taken from (3.23), Z'_{0E} from (3.17), Z'_{E1E2} from (3.22) and Z'_{CE1E2} is according to

$$Z'_{CE1E2} = f\mu_0\pi/4 + \mathrm{j}\, f\mu_0 \ln(\delta/D_{M2E}) \quad , \tag{3.27}$$

where D_{M2E} is obtained from (3.21).

Example of calculation of zero-sequence impedance: The same line of example in section 3.3.2 will be used to determine the zero-sequence parameters. Further data are: average earth resistivity: 300 Ωm. Two earth wires 51-AL1/30-ST1A: diameter: 11,7 mm, electrical resistance at 20°C: 0,5644 Ω/km.
From (3.15) the return depth of earth current will be

$$\delta = 1,85 \Big/ \sqrt{2\pi \cdot 50 \cdot 4\pi \cdot 10^{-7}/300} = 1613 \text{ m}.$$

Equation (3.14) yields

$$\begin{aligned} Z'_{0S} &= 0,0218 + 3\pi/4 \cdot 50 \cdot 4\pi \cdot 10^{-4} + \text{j}\, 50 \cdot 4\pi \cdot 10^{-4} \\ &\quad \cdot \left[3 \ln \left(1613 \,/\, \sqrt[3]{0,134 \cdot 15,75^2}\right) + 1/(4 \cdot 3)\right] = \\ &= 0,0218 + 0,1480 + \text{j}\, 1,177 = 0,170 + \text{j}\, 1,177\ \Omega/\text{km} \quad . \end{aligned}$$

As the earth wires are symmetrical toward the phase conductors, the equivalent distance D_{ME} can be calculated easily by: $D_{ME} = \sqrt[3]{10,3 \cdot 14,14 \cdot 24,6} = 15,31$ m.
Equation (3.17) yields:

$$\begin{aligned} Z'_{CE} &= \pi/4 \cdot 50 \cdot 4 \cdot \pi \cdot 10^{-4} + \text{j}\, 50 \cdot 4\pi \cdot 10^{-4} \cdot \ln(1613/15,31) = \\ &= 0,0493 + \text{j}\, 0,2926\ \Omega/\text{km} \quad . \end{aligned}$$

Equation (3.22) yields

$$\begin{aligned} Z'_{E1E2} &= 0,5644/2 + \pi/4 \cdot 50 \cdot 4 \cdot \pi \cdot 10^{-4} + \text{j}\, 50 \cdot 4\pi \cdot 10^{-4} \cdot \\ &\quad \cdot \left[\ln \left(1613/\sqrt{0,00585 \cdot 20}\right) + 10/8\right] = \\ &= 0,2822 + 0,0493 + \text{j}\, 0,610 = 0,332 + \text{j}\, 0,610\ \Omega/\text{km} \quad . \end{aligned}$$

Finally the zero-sequence impedance is obtained from (3.20):

$$\begin{aligned} Z'_{02E} &= 0,170 + \text{j}\, 1,177 - \frac{3\,(0,0493 + \text{j}\, 0,2926)^2}{(0,332 + \text{j}\, 0,610)} \\ &= 0,170 + \text{j}\, 1,177 + 0,0621 - \text{j}\, 0,3754 = 0,232 + \text{j}\, 0,802\ \Omega/\text{km} \end{aligned}$$

or in polar format $Z'_{02E} = 0,835\ \angle 73,9°\ \Omega/\text{km}$.

3.5 Capacitance and capacitive reactance

3.5.1 General considerations

Capacitance is that property of a system of conductors and dielectrics which permits the storage of electrically separated charges when potential differences exist between the conductors. The capacitance is measured in Farads, where 1 F = 1 As/V. But due to the huge value of one Farad, the unit Microfarad, where 1 μF = 10^{-6} F, is more usual. The *capacitive reactance* is an inverse function of capacitance and frequency, or

$$X_C = 1/(2\pi f \cdot C) \quad . \tag{3.28}$$

X_C is measured in Ω or MΩ (10^6 Ω). The inverse of the capacitive reactance is called *capacitive susceptance* $B_C = 2\pi f \cdot C$, measured in S or μS (10^{-6} S).
The capacitance of the overhead lines is an important parameter, as it is responsible for accumulating and generating reactive power for system requirements. The conductors of an overhead line assume potentials in relation to each other and to the earth. The earth is considered in all cases as having the reference potential equal to zero. Electrical fields and capacitances are formed among conductors and earth (including the earth wires). The capacitances are distributed on the whole conductors along the line. For transposed lines the average total capacitances per phase are equal, so that usually the average conductor-to-ground height is taken into account for their calculation.

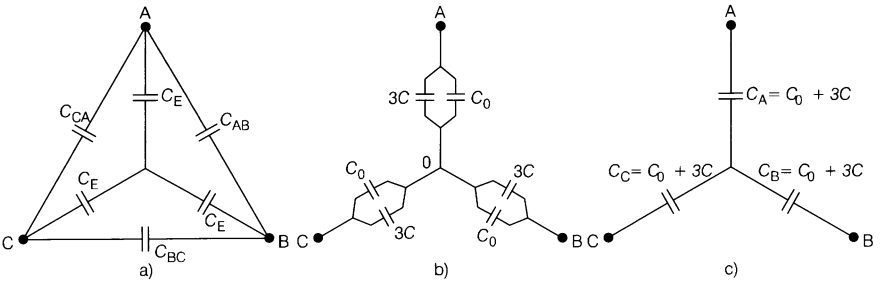

Figure 3.5: Capacitance in positive- and zero-sequence system. a) delta connection; b) transformation to star connection; c) schematic equivalent connection

Considering, therefore, $C_{AB} = C_{BC} = C_{AC} = C$ as the capacitances between phase conductors and $C_{A0} = C_{B0} = C_{C0} = C_0$ as the capacitances to ground or *zero-sequence capacitance*, it will result in the schematic representation of Figure 3.5.
The conversion of triangle to star connection permits going from Figure 3.5 a) to Figure 3.5 b) and another conversion leads to Figure 3.5 c), from which it can be deduced:

$$C_A = C_B = C_C = C_1 = C_0 + 3C \quad . \tag{3.29}$$

The total capacitance per phase is the so-called positive-sequence capacitance C_1, while the capacitance to ground is the zero-sequence capacitance C_0 and the capacitance between conductors is C. Mathematical approaches are deduced for calculating C_1, C_0 and C, so that equation (3.29) above allows to check the accuracy of the calculations.

3.5.2 Single-circuit lines

Single-circuit line without earth wire

The *zero-sequence capacitance per unit length* is according to [3.3]

$$C'_{0S} = \frac{2}{3}\pi\varepsilon_0 \Big/ \left[\ln\left(\frac{\sqrt{(2h_M)^2 + D_M^2}}{\sqrt[3]{r_B D_M^2}}\right)\right] \cong \frac{2}{3}\pi\varepsilon_0 \Big/ \ln\frac{2h_M}{\sqrt[3]{r_B D_M^2}} \quad , \tag{3.30}$$

where

ε_0 dielectric constant $8{,}854 \cdot 10^{-12}$ F/m,
h_M mean conductor height above ground

$$h_M = \sqrt[3]{h_A \cdot h_B \cdot h_C} \quad , \tag{3.31}$$

r_B bundle conductor equivalent radius according to (3.6),
D_M mean geometric phase-to-phase distance. Since $(D_M/2h_M)^2 \ll 1$ the approximation as in equation (3.30) can be made.

The capacitances between the conductors are

$$\begin{aligned} C'_S &= C'_{AB} = C'_{AC} = C'_{BC} = (C'_1 - C'_{0S})/3 = \\ &= 2\pi\varepsilon_0 \cdot [\ln(2h_M/D_M)] \Big/ \left[3\ln(D_M/r_B) \cdot \ln\left(2h_M/\sqrt[3]{r_B D_M^2}\right)\right] \end{aligned} \tag{3.32}$$

and the *positive-sequence capacitance*

$$C'_{1S} = 2\pi\varepsilon_0 \Big/ \ln\left(\frac{D_M}{r_B\sqrt{1 + (D_M/2h_M)^2}}\right) \cong 2\pi\varepsilon_0 / \ln(D_M/r_B) \quad . \tag{3.33}$$

Single-circuit line with one or two earth wires (Figure 3.2)

Earth wires affect only the *zero-sequence capacitance* while the positive-sequence capacitance can be taken from (3.33). With the approximation used in (3.30) the zero-sequence capacitance for a line with one earth wire is

$$C'_{0SE} = \frac{2}{3}\pi\varepsilon_0 \Big/ \left\{ \ln\left(2\,h_M / \sqrt[3]{r_B D_M^2}\right) - \left[\ln\frac{h_M + h_E}{D_{ME}}\right]^2 \Big/ \ln\frac{2\,h_E}{r_E} \right\} \quad , \tag{3.34}$$

where

h_M mean conductor height above ground according to (3.31) in m,
h_E mean earth wire height above ground in m,
D_{ME} mean geometric distance between conductors and earth wire(s) arranged symmetrically according to (3.18) in m,
r_E earth wire radius in m. In case of two earth wires at the same height and symmetrically arranged r_E will be replaced by $\sqrt{r_E \cdot D_{E1E2}}$, where D_{E1E2} is the distance between earth wires.

3.5.3 Double-circuit lines

Double-circuit line without earth wires

The zero-sequence capacitance per unit length is according to [3.3]

$$C'_{0D} = \frac{2}{3}\pi\varepsilon_0 \Big/ \ln\left(\frac{4\,h_M^2}{\sqrt[3]{r_B D_M^2}} \cdot \frac{\sqrt{1 + (D_{M2}/2\,h_M)^2}}{\sqrt[3]{D_{M1} \cdot D_{M2}^2}}\right) \quad , \tag{3.35}$$

where D_M is obtained from (3.7), D_{M2} from (3.10) or (3.11), D_{M1} from (3.9), h_M from (3.31) and r_B from (3.6).
The *positive-sequence capacitance* is

$$C'_{1D} = 2\,\pi\varepsilon_0 \Big/ \ln\left(\frac{D_M D_{M2}}{r_B D_{M1}\sqrt{1 + (D_M/2\,h_M)^2}}\right) \cong 2\,\pi\varepsilon_0 / \ln\frac{D_M D_{M2}}{r_B D_{M1}} \tag{3.36}$$

with the quantities as described above.

Double-circuit line with one or two earth wires (Figure 3.3 a or 3.3 b)

The zero-sequence capacitance for one or two earth wires can be obtained from

$$C'_{0DE} = \frac{2}{3}\pi\varepsilon_0 \Big/ \left\{ \ln\frac{4\,h_M^2}{\sqrt[3]{r_B D_M^2}} \frac{\sqrt{1 + (D_{M2}/2\,h_M)^2}}{\sqrt[3]{D_{M1} D_{M2}^2}} - \frac{2\ln[(h_M + h_E)/D_{ME}]}{\ln 2\,h_E/r_E} \right\} . \tag{3.37}$$

The quantities used in (3.37) have already been described above. In case of two earth wires arranged symmetrically at the same height in equation (3.37) r_E is replaced by $\sqrt{r_E D_{E1E2}}$. The positive-sequence capacitance C'_{1DE} can be taken from (3.36).

Example of calculation of positive- and zero-sequence capacitances: For the same line as used in examples 3.3.2 and 3.4.2, the capacitances and capacitive reactances will be determined. As it deals with a single-circuit line with two earth wires, formulae (3.33) and (3.34) will be applied. The average conductor height is determined from the conductor coordinates to be $h = 14{,}7$ m. The earth wire radius r_E is replaced by $\sqrt{r_E \cdot D_{E1E2}} = \sqrt{0{,}00585 \cdot 20} = 0{,}342$ m. Due to the symmetrical arrangement of conductors and earth wires D_{ME} is obtained from (3.18)

$$D_{ME} = \sqrt[3]{10{,}3 \cdot 14{,}14 \cdot 24{,}6} = 15{,}31 \text{ m} \quad .$$

The positive-sequence capacitance is received from (3.33)

$$C'_{1S} = 2\pi \cdot 8{,}854 \cdot 10^{-12} \cdot 10^3 \Big/ \ln \frac{15{,}75}{0{,}134\sqrt{1 + (15{,}75/2 \cdot 14{,}7)^2}} = 12{,}0 \cdot 10^{-3}\ \mu\text{F/km}.$$

The zero-sequence capacitance C'_0 is obtained from (3.34):

$$\begin{aligned} C'_{0SE} &= \frac{2}{3}\pi \cdot 8{,}854 \cdot 10^{-12} \cdot 10^3 \Big/ \\ &\quad \left[\ln \frac{2 \cdot 14{,}7}{\sqrt[3]{0{,}134 \cdot 15{,}75^2}} - \left(\ln \frac{14{,}7 + 24{,}7}{15{,}31}\right)^2 \Big/ \ln(2 \cdot 24{,}7/0{,}342)\right] = \\ &= 18{,}544 \cdot 10^{-9} / [2{,}213 - 0{,}8935/4{,}973] = 9{,}12 \cdot 10^{-3}\ \mu\text{F/km} \quad . \end{aligned}$$

Table 3.2 shows line parameters of typical lines determined using the formulae of clauses 3.2 to 3.5.

3.6 Admittance

When carrying out electric circuit calculations of transmission lines, it is generally preferable to use the *shunt admittance* to ground instead of the impedance to ground. Using the vector representation, the positive- and the zero-sequence unit shunt admittance, Y'_1 and Y'_0, can be equated as

$$Y'_1 = G'_1 + \mathrm{j}\, B'_1 \tag{3.38}$$

$$Y'_0 = G'_0 + \mathrm{j}\, B'_0 \quad . \tag{3.39}$$

In the formulae above, G'_1 and G'_0 are the real parts of the admittance, usually named as *conductances*, while B'_1 and B'_0 are the imaginary parts of the admittance, named as *susceptance*. For overhead lines, the real terms G'_0 and G'_1 are very small and can be neglected, meaning, therefore, $G_1 = G_0 \cong 0$. This means that the following approximate relations can be equated

$$Y'_1 = 1/X'_{C1} \quad \text{in S/km} \tag{3.40}$$

and

$$Y'_0 = 1/X'_{C0} \quad \text{in S/km.} \tag{3.41}$$

If X'_{C1} and X'_{C0} are given in the unit value of Ωkm, then Y'_1 and Y'_0, as respective inverses, will be given in S/km.
The capacitive susceptances, calculated as the inverse of (3.28), are respectively determined as
positive-sequence susceptance

$$B'_1 = 2\pi f C'_1 \quad \text{and} \tag{3.42}$$

zero-sequence susceptance

$$B'_0 = 2\pi f C'_0 \quad . \tag{3.43}$$

The admittance, as well as its components conductance and susceptance, are measured as an inverse unit of Ω, called Siemens (S), but the submultiple μS (10^{-6} S) is more usual.

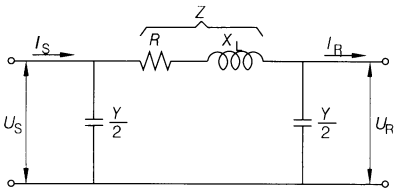

Figure 3.6: Representation of a line by a nominal Π-circuit.
U_S sending end voltage, U_R receiving end voltage, I_S sending end current, I_R receiving end current, $Y/2$ half of the admittance

Example: For the example of section 3.5.3 it is obtained, neglecting the real part in equation (3.38) and (3.39), for the positive-sequence unit admittance:

$$Y_1' = B_1' = 2\pi \cdot 50 \cdot 12{,}0 \cdot 10^{-9} = 3{,}77\ \mu\text{S/km}$$

and for the zero-sequence system:

$$Y_0' = B_0' = 2\pi \cdot 50 \cdot 9{,}12 \cdot 10^{-9} = 2{,}87\ \mu\text{S/km} \quad .$$

3.7 Electric representation of lines

3.7.1 Goals and basic conditions

In this clause formulae for *electric representation* of lines will be presented. These formulae can be used to calculate voltage, current and power factor at any point of a transmission line, provided the values of these variables are known at another point of the line. Usually those variables are known in one of the line ends and it is desired to calculate the values at the other line end. Loads are usually specified by their voltage, power and *power factor*, from which the current can be calculated for use in the equations. Other parameters, such as *surge impedance load* or *natural power*, voltage regulation and power losses can be indirectly determined.
Normally transmission lines are operated with balanced three-phase loads. Even if the conductors are not spaced equilaterally and may not be transposed, the resulting disymmetry is slight, and the phases are considered to be loaded equally by the currents.

3.7.2 Short- and medium-length lines

For carrying out electric calculations involving overhead lines, some simplification can be used depending on the line voltage and length. The main simplification consists in neglecting the capacitance of the line for low and medium voltages and *short lines*. In this case, the capacitances and the resulting admittance to ground would represent a relatively small contribution to the reactive power of the line and the relevant system. The equivalent circuit of a short line is represented by a series resistance and a series reactance only, which are concentrated or lumped parameters not uniformly distributed along the line. As the shunt admittance is neglected for short lines, it makes no difference, as far as measurements at the ends of the line are concerned, whether the parameters are lumped or uniformly distributed.
The shunt admittance, generally a pure susceptance, is included in the calculations for a *line of medium length*. In such a case, the line parameters resistance R, inductance L and capacitance C need not to be uniformly distributed along the line, but can be considered as concentrated or lumped parameters. The resulting errors are negligible, due to the relatively small value of the capacitance.
For this case, the representation of the lumped parameters is designated by the Greek letter Π. The values of the total resistance (Ω), inductive reactance (Ω) and shunt admittance (μS) are simply obtained by multiplying the unit values in Ω/km or μS/km, respectively, by the line length. Because of this simplified approach, such representation

is usually named as *nominal* Π-*circuit* of a line. The nominal Π-circuit, shown in Figure 3.6, is often used to represent medium-length lines.
In the circuit of Figure 3.6, the total shunt admittance is divided into two equal parts placed at the sending and receiving ends of the line. The total series resistance and reactance are put in the middle. The resulting parameters are calculated simply by multiplying the unit parameters by the line length, i. e. $R = R'_1 \cdot a$, $X_L = X'_1 \cdot a$, $Z' = Z'_1 \cdot a$ and $Y = Y' \cdot a$ and $Y/2 = Y' \cdot a/2$.
The voltage and current relationships used in electric calculations for medium-length lines under this approach are

$$U_S = (Z \cdot Y/2 + 1)\, U_R + Z \cdot I_R \quad \text{or} \quad U_S = (U_R \cdot Y/2 + I_R) \cdot Z + U_R \tag{3.44}$$

$$I_S = Y\,(1 + Z \cdot Y/4)\, U_R + (Z \cdot Y/2 + 1)\, I_R \quad . \tag{3.45}$$

Neglecting the capacitance for short lines, the above equations become the well-known simple relations

$$U_S = U_R + Z \cdot I_R \tag{3.46}$$

and

$$I_S = I_R \quad . \tag{3.47}$$

The magnitude of the *voltage drop* or voltage regulation (in %) is:

$$\Delta U\% = (|U_S| \,/\, |U_R| - 1) \cdot 100 \quad . \tag{3.48}$$

3.7.3 Long-length transmission lines

3.7.3.1 Representation by exponential functions

When dealing with *long lines*, for instance lines longer than 100 km, the consideration of the distributed parameters is necessary, if a higher degree of accuracy is required. According to [3.7] and [3.3], the exact mathematical model for a long line can be represented either as an exponential function or as a hyperbolic function. A summary of the method and its practical use will be presented in the following paragraphs.
Generally, in most practical applications, knowing voltage and current at the receiving end of the line (consumer side), it is required to calculate the voltage and current at the sending end of the line. In this case, U turns out into U_S, I into I_S and x into a.
According to [3.3] the following equations can be deduced

$$U = [(U_R + Z_C \cdot I_R)\, e^{\gamma x} + (U_R - Z_C \cdot I_R)\, e^{-\gamma x}]\,/2 \tag{3.49}$$

and

$$I = [(U_R/Z_C + I_R)\, e^{\gamma x} + (U_R/Z_C - I_R)\, e^{-\gamma x}]\,/2 \quad , \tag{3.50}$$

where

$$Z_C = \sqrt{L'/C'} = \left|\sqrt{X'_L \cdot X'_C}\right| \tag{3.51}$$

is the *surge impedance* of the line (see [3.7]) and

$$\gamma = \sqrt{L' \cdot C'} = \sqrt{X'_L/X'_C} = \alpha + j\,\beta \tag{3.52}$$

is called the *propagation constant.*
Both, Z_C and γ are complex quantities. The real part of the propagation constant γ is called the *attenuation constant* α and is measured in Nepers per unit length, while the imaginary part is called *phase constant* β and is measured in Radians per unit length.

The *wave length* λ is the distance along a line between two points of a wave which differs in phase by 360° or 2π. If β is the phase shift in radians per km, the wave length in km is

$$\lambda = 2\pi/\beta \quad . \tag{3.53}$$

At the frequencies of 50 Hz, the wave lengths is approximately 5 870 km and 4 895 km, respectively. The *velocity of wave propagation* in km/s is the product of the wave length in km and the frequency in Hz, $v = f \cdot \lambda$ in km/s.
In calculating the voltage U and the current I at any point of the line as a function of the voltage and current at the receiving end, the equations (3.49) and (3.50) are applicable as a function of the distance x to the receiving end.
With these quantities the equations (3.49) and (3.50) for voltage and current turn out into

$$U = \left[(U_R + Z_C I_R)e^{\alpha x}e^{j\beta x} + (U_R - Z_C I_R)e^{-\alpha x}e^{-j\beta x}\right]/2 \tag{3.54}$$

and

$$I = \left[(U_R/Z_C + I_R)\,e^{\alpha x}e^{j\beta x} + (U_R/Z_C - I_R)\,e^{-\alpha x}e^{-j\beta x}\right]/2 \quad . \tag{3.55}$$

A deep analysis, beyond the scope of these highlights, will prove that the first terms of the above equations are the incident voltage or current while the second terms are the reflected voltage or current. From (3.54) and (3.55) it can be concluded that a line terminated in its characteristic impedance Z_C has $U_R = I_R \cdot Z_C$ and, therefore, there is no reflected wave, as the second terms are equal to zero.
Such a line is called flat line or *infinite line*, the latter designation arising from the fact that a line of infinite length cannot have a reflected wave. Usually power lines are not terminated with their characteristic impedance, but communication lines are frequently so terminated in order to eliminate the reflected wave. Typical values of Z_C are given in Table 3.2 for single-circuit lines. The phase angle of Z_C is usually between 0 and $-15°$. Z_C is also called *surge impedance* in power lines. *Surge impedance load* (SIL) of a line is the power delivered by a line to a purely resistive load equal to its surge impedance

$$P_{nat} = U_{pp}^2/|Z_C| \text{ in MW} \quad , \tag{3.56}$$

where U_{pp} is the phase-to-phase voltage in kV and Z_C is given in Ω.

3.7.3.2 Representation by hyperbolic functions

Hyperbolic functions are mathematically easier to handle, so that its introduction permits relatively simple calculations. The incident and reflected waves of voltage and current of equations (3.54) and (3.55) can be rearranged and equated in terms of hyperbolic functions as

$$U_S = U_R \cosh(\gamma a) + I_R \cdot Z_C \sinh(\gamma a) \quad , \tag{3.57}$$

$$I_S = I_R \cosh(\gamma a) + U_R/Z_C \sinh(\gamma a) \quad , \tag{3.58}$$

where a is the line length. The equations can be solved in view of U_R and I_R

$$U_R = U_S \cosh(\gamma a) - I_S \cdot Z_C \sinh(\gamma a) \quad , \tag{3.59}$$

$$I_R = I_S \cosh(\gamma a) - U_S/Z_C \sinh(\gamma a) \quad . \tag{3.60}$$

Example: For the 500 kV line according to the example presented in clause 3.3.2 a line length of 300 km and a load of 1000 MW are assumed. The line parameters are

$$R'_1 = 0{,}0218\ \Omega/\text{km};\quad L'_1 = 9{,}70 \cdot 10^{-4}\ \text{H/km};\quad C'_1 = 12{,}0 \cdot 10^{-3}\ \mu\text{F/km}.$$

With $Z' = 0{,}3054\,\angle 85{,}9°\ \Omega/\text{km}$ and $Y' = 3{,}77\,\angle 90°\ \mu\text{S/km}$ it is obtained from (3.50) $\gamma = \sqrt{Z' \cdot Y'} = 1{,}073 \cdot 10^{-3}\,\angle 87{,}95°$ 1/km or $\alpha = 3{,}84 \cdot 10^{-5}$ 1/km and $\beta = 1{,}042 \cdot 10^{-3}$ 1/km.
For the total line it applies

$$\gamma \cdot a = 1{,}073 \cdot 10^{-3} \cdot 300\,\angle 87{,}95° = 0{,}322\,\angle 87{,}95° = 0{,}012 + \text{j}\,0{,}322 \quad .$$

The surge impedance follows from (3.51):

$$Z_\text{C} = \sqrt{0{,}3054\,\angle 85{,}9° / (3{,}77 \cdot 10^{-6})\,\angle 90°} = 284{,}6\,\angle -2{,}05° = 284{,}4 - \text{j}\,10{,}2\ \Omega \quad .$$

The line to earth voltage at the line end is

$$U_\text{R} = 500/\sqrt{3} = 288{,}7\,\angle 0°\ \text{kV}$$

and the corresponding current

$$I_\text{R} = 10^6/(500 \cdot \sqrt{3}) = 1154{,}7\,\angle 0°\ \text{A} \quad .$$

From (3.54) it is obtained with $x = 0$ for the incident voltage as U_R^+

$$\begin{aligned} U_\text{R}^+ &= [U_\text{R} + Z_\text{C} \cdot I_\text{R}]/2 = [288{,}7\,\angle 0° + 1{,}1547\,\angle 0° \cdot 284{,}6\,\angle -2{,}05°] \cdot 10^3/2 \\ &= (144{,}35 + 164{,}2 - \text{j}\,5{,}9) \cdot 10^3 = (308{,}6 - \text{j}\,5{,}9) \cdot 10^3 = 308{,}7\,\angle -1{,}09°\ \text{kV} \end{aligned}$$

and for the reflected component of the voltage as U_R^-

$$\begin{aligned} U_\text{R}^- &= [U_\text{R} - Z_\text{C} \cdot I_\text{R}]/2 = [288{,}7\,\angle 0° - 1{,}1547\,\angle 0° \cdot 284{,}6\,\angle -2{,}05°] \cdot 10^3/2 \\ &= (144{,}35 - 164{,}2 + \text{j}\,5{,}9) \cdot 10^3 = (-19{,}9 + \text{j}\,5{,}9) \cdot 10^3 = 20{,}7\,\angle 163{,}5°\ \text{kV}. \end{aligned}$$

At the sending end of the line it results with $x = 300$ km

$$\begin{aligned} U_\text{S}^+ &= [U_\text{R} + Z_\text{C} \cdot I_\text{R}]/2\, e^{\alpha \cdot 300} e^{\text{j}\beta\,300} = 308{,}7\,\angle -1{,}09° \cdot e^{0{,}012} e^{\text{j}\,0{,}322} = \\ &= 308{,}7\,\angle -1{,}09° \cdot 1{,}012\,\angle 17{,}83° = 312{,}4\,\angle 16{,}7\ \text{kV} \end{aligned}$$

and

$$\begin{aligned} U_\text{S}^- &= [U_\text{R} - Z_\text{C} \cdot I_\text{R}]/2\, e^{\alpha \cdot 300} e^{-\text{j}\beta\,300} = 20{,}7\,\angle 196{,}6° \cdot e^{-0{,}012} e^{\text{j}\,0{,}322} = \\ &= 20{,}7\,\angle 163{,}50° \cdot 0{,}988\,\angle -17{,}83° = 20{,}45\,\angle 145{,}7\ \text{kV}. \end{aligned}$$

The voltage $U_\text{S} = U_\text{S}^+ + U_\text{S}^-$ at the sending end to earth will be

$$\begin{aligned} U_\text{S} &= 312{,}4\,\angle 16{,}7° + 20{,}45\,\angle 145{,}7° = \\ &= 299{,}2 + \text{j}\,89{,}8 - 16{,}9 + \text{j}\,11{,}5 = 282{,}3 + \text{j}\,101{,}3 = 299{,}9\,\angle 19{,}7°\ \text{kV}. \end{aligned}$$

The line voltage at the sending line end is therefore $U_\text{S} = 299{,}9 \cdot \sqrt{3} = 519{,}5$ kV.
The wave length is obtained from (3.53) by $\lambda = 2\pi/\beta = 2\pi/1{,}042 \cdot 10^{-3} = 5861$ km and the propagation speed will be $50 \cdot 5861 = 293\,060$ km/s.

3.7.3.3 The equivalent Π-circuit of a long line

The *nominal* Π-*circuit* of Figure 3.6 doesn't represent a long transmission line exactly because it does not account for the parameters of the line being uniformly distributed. However, the format of the Π-circuit shown in Figure 3.6 is very convenient for electric calculations of voltages, currents and other related variables. In this aspect, it has been studied how a similar Π-circuit could be also defined for long lines, that is, taking into account the distributed line parameters.
The discrepancy between the nominal Π-representation and the real line behaviour becomes larger as the length of the line increases. It is possible, however, to find the *equivalent* Π-*circuit* of a long transmission line composed of lumped parameters so that

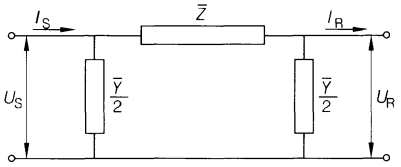

Figure 3.7: Equivalent Π-circuit of a long line

voltage and current relations at both ends are accurate. This means, in order to deduce an equivalent Π-circuit, the voltage and current in both, the sending and the receiving end, are calculated by the exact hyperbolic functions. Then, corrections are determined into the lumped parameters such to provide the same voltages and currents as in the exact method. An equivalent Π-circuit is, therefore, determined for the long line, with the following correction factors and resulting parameters, as shown in Figure 3.7.
The elements of the equivalent Π-circuit are

$$\overline{Z} = Z_C \sinh(\gamma a) = Z'/(\gamma a) \cdot \sinh(\gamma a) \quad , \tag{3.61}$$

$$\overline{Y}/2 = 1/Z_C \tanh(\gamma a/2) = Y'/(\gamma a) \cdot \tanh(\gamma a/2) \quad . \tag{3.62}$$

The relations between U_R and I_R as well as between U_S and I_S are given by the equations (3.44) and (3.45). The determination of U and I at every point of the line can be performed by equations (3.49) and (3.50). The hyperbolic functions according to (3.61) and (3.62) determine the equivalent Π-circuit elements.
The use of the *equivalent Π-circuit* permits to calculate voltage U_S and current I_S in the sending end, but no intermediate point is considered. The line is then represented by an equivalent series impedance in the middle and two legs with half of corrected admittance or capacitance. If any relation between voltage and current in an intermediate point is desired, another equivalent Π-circuit should be determined from this point until the receiving end. Powers and power factors are accordingly taken into account at both, the sending and the receiving end by the formulae relating these parameters with voltage and current in three-phase circuits.

Example for an equivalent Π-circuit of a long line: Voltage, current and power of the line calculated in the example carried out in clause 3.7.3.2 will be determined using an equivalent Π-circuit for the line and comparing with the nominal Π-circuit.
From preceding examples, the following parameters are known: $Z_C = 284{,}6\,\angle -2{,}05°\ \Omega$; $\gamma a = 0{,}012 + \mathrm{j}\,0{,}322$; voltage at the receiving end $U_R = 289\,\angle 0°$ kV; current $I_R = 1155\,\angle 0°$ A.
Equation (3.59) yields

$$U_S = 288{,}7\,\angle 0° \cdot \cosh(0{,}012 + \mathrm{j}\,0{,}322) + 1{,}1547 \cdot 284{,}6\,\angle -2{,}05° \cdot \sinh(0{,}012 + \mathrm{j}\,0{,}322) \quad .$$

Since $\cosh(\alpha + \mathrm{j}\,\beta) = \cosh\alpha \cdot \cos\beta + \mathrm{j}\,\sinh\alpha \cdot \sin\beta$ and $\sinh(\alpha + \mathrm{j}\,\beta) = \sinh\alpha \cdot \cos\beta + \mathrm{j}\,\cosh\alpha \cdot \sin\beta$ it is obtained $\cosh(0{,}012 + \mathrm{j}\,0{,}322) = 0{,}949 + \mathrm{j}\,0{,}0038 = 0{,}949\,\angle 0{,}23°$ and $\sinh(0{,}012 + \mathrm{j}\,0{,}322) = 0{,}011 + \mathrm{j}\,0{,}316 = 0{,}317\,\angle 87{,}9°$. Therefore,

$$\begin{aligned} U_S &= 288{,}7\,\angle 0° \cdot 0{,}949\,\angle 0{,}23° + 1{,}1547 \cdot 284{,}6\,\angle -2{,}05° \cdot 0{,}317\,\angle 87{,}9 = \\ &= 274\,\angle 0{,}23° + 104{,}2\,\angle 85{,}9° = 274 + \mathrm{j}\,1{,}1 + 7{,}5 + \mathrm{j}\,103{,}9 = \\ &= 281{,}5 + \mathrm{j}\,105{,}0 = 300{,}4\,\angle 20{,}45° \text{ kV}. \end{aligned}$$

From (3.58) it is calculated

$$\begin{aligned} I_S &= 1154{,}7\,\angle 0° \cdot 0{,}949\,\angle 0{,}23° + (288{,}7 \cdot 10^3\,\angle 0°)/(284{,}6\,\angle -2{,}05°) \cdot 0{,}317\,\angle 87{,}9° = \\ &= 1096\,\angle 0{,}23° + 322{,}1\,\angle 90{,}0° = 1096 + \mathrm{j}\ 4{,}4 + 0{,}0 + \mathrm{j}\,322{,}1 = \\ &= 1096 + \mathrm{j}\,326{,}5 = 1143\,\angle 16{,}6° \text{ A}. \end{aligned}$$

Line voltage at the sending end is

$$U_{pp} = 300{,}4 \cdot \sqrt{3} = 520{,}3 \text{ kV}.$$

Table 3.3: Comparison between nominal und equivalent Π-circuits; 500 kV line, 300 km long, conductors 3 × 494-AL1/34-ST1A

	Resistance R_1 (Ω)	Inductive reactance X_1 (Ω)	Impedance Z_1 (Ω)	Admittance $Y/2$ (μS)
nominal Π-circuit	6,54	91,4	91,6	565
equivalent Π-circuit	6,45	89,9	90,1	571

The power factor at the sending end is given by $\cos\varphi = \cos(20{,}45 - 16{,}6) = 0{,}998$; power required at the sending end will be

$$P_{WS} = \sqrt{3} \cdot 520{,}5 \cdot 1143 \cdot 0{,}998 = 1028 \text{ MW} \quad .$$

Therefore, the losses in the line are

$$P_{loss} = P_{WS} - P_{WR} = 28 \text{ MW} \quad .$$

In the following paragraphs the calculations with nominal and equivalent Π-circuits will be compared; considering $\sinh(\gamma a) = 0{,}317\,\angle 87{,}9°$ the equivalent impedance is obtained from (3.61)

$$\overline{Z} = 284{,}6\,\angle -2{,}05° \cdot 0{,}317\,\angle 87{,}9° = 90{,}15\,\angle 85{,}9° = 6{,}45 + \mathrm{j}\,89{,}9\ \Omega \quad .$$

Equation (3.62) yields

$$\begin{aligned} \overline{Y}/2 &= \frac{1}{Z_C}\tanh\frac{\gamma a}{2} = \frac{1}{Z_C}\frac{\cosh(\gamma a) - 1}{\sinh(\gamma a)} = \\ &= \frac{1}{284{,}6\,\angle -2{,}05°} \cdot \frac{0{,}949 + \mathrm{j}\,0{,}0038 - 1}{0{,}317\,\angle 87{,}9°} = \frac{0{,}0511\,\angle 175{,}8°}{284{,}6\,\angle -2{,}05° \cdot 0{,}317\,\angle 87{,}9°} = \\ &= 0{,}571 \cdot 10^{-3}\,\angle 89{,}9° \text{ S or } |\overline{Y}/2| = 571\ \mu\text{S} \quad . \end{aligned}$$

The series impedance of the nominal Π-circuit is obtained by just multiplying the unit series impedance Z' (Ω/km) by the line length

$$Z = Z' \cdot a = (0{,}0218 + \mathrm{j}\,0{,}3046) \cdot 300 = 6{,}54 + \mathrm{j}\,91{,}39\ \Omega = 91{,}6\,\angle 85{,}9°\ \Omega \quad .$$

The same is valid for the shunt admittance, so that the total admittance of the nominal Π-circuit is

$$Y = Y' \cdot a = 3{,}77 \cdot 300 = 1131\ \mu\text{S} \quad .$$

Each arm of the nominal Π-circuit will, therefore, be $Y/2 = 565\ \mu$S.
Table 3.3 provides a summary of the comparison between the nominal Π-circuit and the equivalent Π-circuit of the line.
The equivalent Π-circuit will provide the exact solution for the line, while the nominal Π-circuit will yield an approximate solution. It can be observed that the difference is not so large; in most cases the nominal Π-circuit is enough for solving most circuits involving lines, if a high degree of accuracy is not required. However, as the line length increases, the approach using the nominal Π-circuit will introduce bigger and bigger differences compared with the exact solution. Therefore, the use of the exact solution with the equivalent Π-circuit is recommended.

3.8 References

3.1 EPRI: Transmission line reference book: 345 kV and above. Palo Alto, Electric Power Research Institute, 2nd edition 1987

3.2 Fink, D. G.; Beaty, H. W.: Standard handbook for electrical engineers. New York, McGraw-Hill, 12th edition 1987

3.3 Happoldt, H.; Oeding,D.: Elektrische Kraftwerke und Netze (Electric power stations and networks). Berlin, Springer-Verlag, 5th edition 1978.3

3.4 Clarke, E.: Circuit analysis of AC power systems. New York, John Wiley & Sons 1943

3.5 Pollaczek, F.: Über das Feld einer unendlich langen, wechselstromdurchflossenen Einfachleitung (On the field of an infinitely long single line carrying AC currents). Elektr. Nachr.-Technik 3 (1926), pp. 339 to 359

3.6 Carson, J. R.: Wave propagation in overhead ground wires with ground return. Bell System Techn. Journal 1926, pp. 539

3.7 Stevenson, W.: Elements of power system analysis. New York, McGraw-Hill, 2nd edition 1987

4 Lightning protection

4.0 Symbols

Symbol	Signification
c	Earth wire factor
D	Lightning strike distance
h_E	Earth wire height
h_C	Phase conductor height
I	Lightning impulse current
k	Reduction factor
L	Inductance
L_M	Tower inductance
n_f	Number of flashovers
N_g	Number of flashes per km^2 and year
N_k	Keraunic level
S_I	Slope of lightning impulse current
U_c	Lightning overvoltage
U_M	Overvoltage at tower
U_{pf}	Power frequency voltage
Z_C	Line surge impedance
Z_M	Tower surge impedance
β_S	Shielding factor
θ	Protection angle
ϱ_E	Earth resistivity

4.1 Significance of lightning

Lightning discharges constitute the main cause of most non-programmed outages of electric systems. International statistics show that about 65 % of *line outages* originate from lightning strokes that hit the overhead transmission lines [4.1]. It is certainly possible to reduce the number of line outages to an acceptable level through a convenient protection scheme, with an adequate installation of earth wires and an appropriate earthing of the towers. The growing amount of power to be carried by transmission lines forces the electric systems to operate more and more at their limits, so that non-programmed line outages increase the *risk of instability.* At the same time, the increase of short-circuit currents contribute to increase such risks.

Every fault turns out into an *overvoltage surge*, that may last from a fraction of a second up to one second. Such surges, despite not felt by most of industrial equipment and facilities, are extremely harmful to weaker installations and devices, specially computers and other electronic apparatus. On the other hand, some industrial facilities, such as aluminium and steel mills as well as oil factories are often very sensitive to line outages, even if of short duration and subject to quick reclosing. The communities and users are, as a matter of fact, more and more sensible to electricity breakdowns, requiring from the utilities a continuous improvement of quality of supply. The reduction of *insulation flashovers* due to lightning strokes is, therefore, an important goal of the overhead transmission line design, especially those situated in regions of high keraunic levels [4.2].

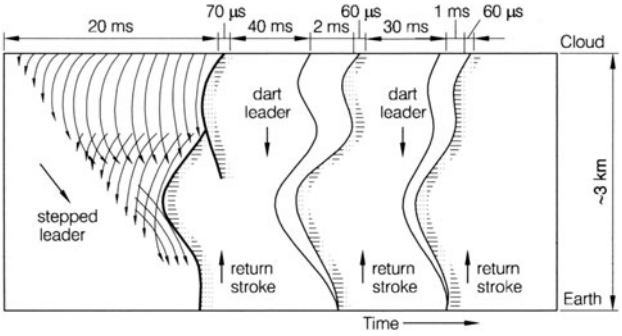

Figure 4.1: Mechanism of a lightning discharge to earth

4.2 Formation of lightning strokes

4.2.1 Mechanism of lightning discharge

The *lightning discharge* is initiated by a streamer from the cloud which progresses toward earth in a series of steps some tens of meters long. It is known as *stepped leader*. There is a time interval between the steps at the order of 40 to 100 μs. As this leader progresses, it splits in branches and the luminosity of the ionised way increases (see Figure 4.1). When the leader is upon reaching the earth, upward predischarges are developed usually from salient points: trees, structures, buildings, etc., toward the leader direction (see Figures 4.1 and 4.2).

At the moment in which one of these upward predischarges and the leader meet one another, a short circuit is established between the cloud and the ground, giving rise to a large current flow. This current is made up of charges at the soil surface that go up to the ionised channel formed by the leader, neutralising its charges. A highly luminous flash can be observed progressing from the earth to the cloud, the *return stroke*, at a speed of about one third of light speed.

A lightning discharge is usually constituted of several strokes flowing at the same ionised channel by the following process: when the current of the first return stroke ends up, there is an interval of about 40 ms until a second stroke appears, the cloud being still able to contain a certain amount of charge; this second stroke begins with a leader that, unlike the stepped leader, progresses continuously, being named *dart leader* and having a propagation speed about 100 times lower than the return stroke. Several successive strokes may occur according to the same mechanism; in general, a complete discharge lasts from 0,2 to 1 second and is made up of 3 to 4 partial discharges, in average.

4.2.2 Impulse behaviour of lightning discharges

The *stepped leader* is an ionised channel containing an excess of negative charges when it begins at the negative part of the cloud, and an excess of positive charges when it begins at the positive part of the cloud. It is considered that there exists a high concentration of charges of the same polarity at its edge. When the leader approaches the earth, the electrical field just below this concentration of charges increases significantly.

When the electrical field at ground level reaches the critical value, several positive upward strokes are developed toward the leader. One of the strokes, the nearest one or the one which progressed more quickly, gets in touch with the leader: an ionised channel is then established between the earth and the cloud, and a stroke occurs. If two or more upward strokes converge into the leader, a branched stroke occurs; the same happens when two branches of the leader give rise to an upward stroke.

The *electrical field* at ground level is a simultaneous function of the amount of charges

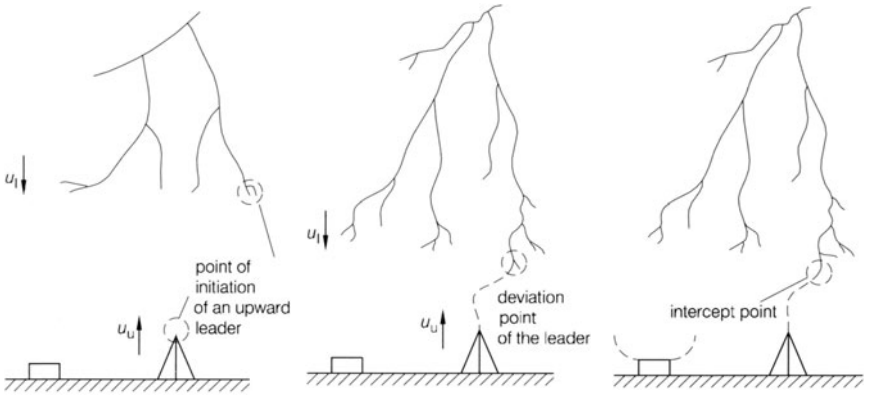

Figure 4.2: Segments of a lightning stroke path to an earthed structure

in the leader and of its separation towards the ground. So the distance to the ground after which the critical point is reached depends on the charge of the leader. The present models suppose that the first stroke neutralizes the leader charges, a constant relation existing between these charges and the discharge current. This relation is about 15 kA/Coulomb, according to measurements carried out at Monte San Salvatore, Switzerland [4.3]. A numerical relation is then established between the distance from the leader edge to the ground and the *stroke current* magnitude of the discharge when the critical electrical field is reached.
The following empirical formula has been proposed for calculation of the strike distance

$$D = 6{,}7 \cdot I^{0{,}8} \quad , \tag{4.1}$$

where D is the strike distance in m and I the stroke current in kA. It can, therefore, be concluded that the area of effectiveness of a *lightning arrester* will be greater and greater as the current magnitude increases, what is a favourable point. If, on the other hand, the current is low, the impact may occur even at the lightning arrester base. The lightning protection is then ineffective.

4.2.3 Electric characteristics of the discharges

The *lightning discharges* can be classified according to [4.4, 4.5, 4.6] and [4.7] in conformity with their polarity as:

- negative discharges (discharges from a negatively charged cloud);
- positive discharges (discharges from a positively charged cloud).

In regions with temperate climate 80 to 90 % of the discharges are negative. According to the direction of progress of the leader, the following classification is used:

- *downward discharges* where the leader develops from the cloud;
- *upward discharges* where the leader develops from the earth (see Figure 4.4).

In flat regions most discharges are downwards [4.4], while upward discharges hit more frequently sharp and elevated objects, such as telecommunication towers and transmission line towers situated on hilly tops. According to present knowledge, the discharge direction does not depend on the polarity of the cloud but on the formation of both electrodes: the cloud and the subject on earth potential.
The *negative discharges* are made up of a main stroke and several subsequent strokes, each one having several amplitudes and duration. The front time of the first partial stroke is about 10 μs. The front time of the secondary strokes is much lower, usually about 1 μs, but their wave tail is much more regular than that of the first stroke. The

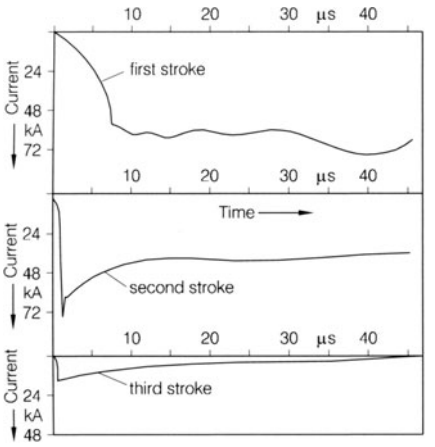

Figure 4.3: Oscillogram of current of a multiple lightning discharge according [4.8]

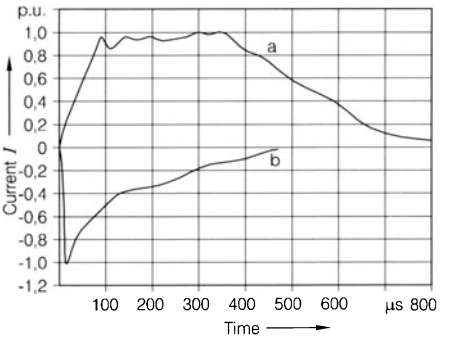

Figure 4.4: Typical current wave shapes of (a) positive and (b) negative lightning discharges

peak values of the subsequent strokes are generally lower than that of the main stroke (see Figure 4.3).
The *positive discharge* is made up of only one stroke, lasting from 0,1 to 0,2 seconds. The time of *wave front* is fairly long, varying between 20 and 50 μs, but the current amplitude may reach much larger values, even higher than 100 kA (see Figure 4.4).

4.3 Frequency and intensity of lightning strokes

4.3.1 Keraunic levels and earth flash density

The number of *line outages* is directly proportional to the number of strokes hitting the line. Of course, the higher the occurrence of thunderstorms in a region the higher the probability of lightning stroke incidence on a line crossing this region.
The frequency of incidence of lightning strokes at a certain locality has been along the years measured by the *keraunic level*, i. e. the average number of thunderstorm days per year in that locality as recorded by hearing of a thunder. Figure 4.5 shows keraunic levels on a worldwide map. This parameter, despite simple and depending on the hearing ability of weather observers, has proved valuable in the investigation and assessment of lightning performance of overhead transmission lines.
Regarding the validity of the keraunic levels, it is important to have a long period of observations because they are essentially statistical data so that a longer period of observations is significant in order to have a more reliable forecast for use in future projects.
Although keraunic levels give a good idea of the lightning activity at a certain region, however, because of their subjective and inaccurate nature, it is more advisable, under an engineering standpoint, to know the *flash density* defined as the number of flashes per km^2 and year along the line route.
The search of this parameter is unfortunately still rare in most countries, but some measuring systems have been developed for this purpose. One of the measuring devices, developed by Cigré, is known as "*counter of earth discharges*" and is based on the variation of the local electrical field produced by a lightning flash [4.9].
Using the results of such counters, several researchers have attempted to develop empirical formulae for correlating the number of flashes to ground N_g to the keraunic

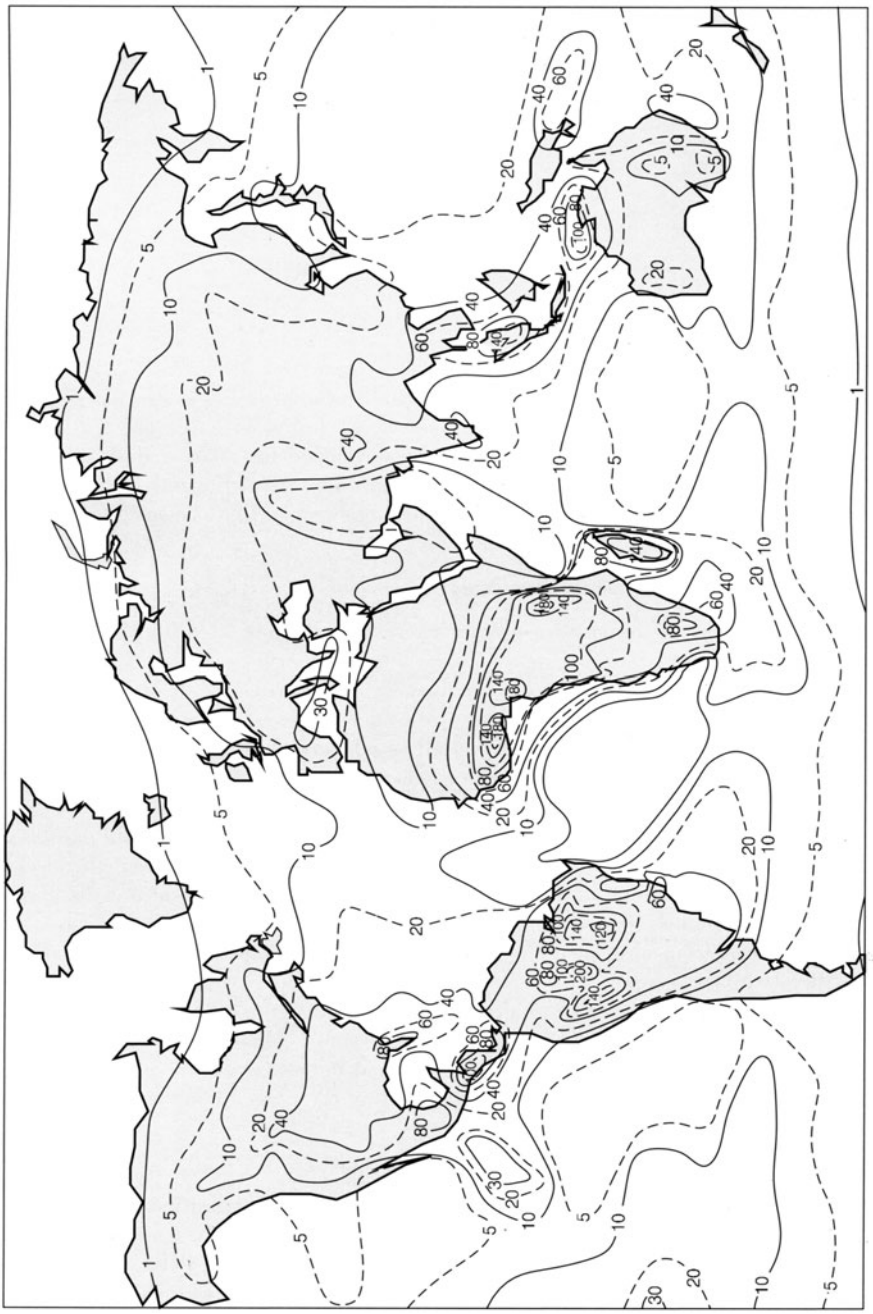

Figure 4.5: Keraunic levels on a worldwide basis

Table 4.1: Statistical measured data of lightning strokes

Curve	Source	Average value kA	Coefficient of variation %	Number of measurements	Measuring device	Measuring place
1	CEMIG Brazil	46	21	150	magnetic charts	tower top
2	ERIKSSON South Afrika	41	22	11	oszillo-graph	measuring mast
3	BERGER Swiss	30	42	101	oszillo-graph	measuring mast
4	POPOLANSKY Czech Republic	28	—	618	oszillo-graph	measuring mast
5	LEWIS USA	28	50	110	magnetic charts	tower top
6	SZPOR Poland	30	40	104	magnetic charts	Tower top
7	ANDERSON Rhodesia	40	19	140	magnetic charts	—

level N_k. Several empirical formulae have been developed for relating flash densities with keraunic levels. All provide similar results. Based on measurements held in South Africa, A.J. Eriksson [4.4] recommends the following formula, that is considered among electric utilities to be well acceptable:

$$N_g = 0{,}04 \cdot N_k^{1{,}25} \quad \text{flashes/(km}^2\,\text{year)}, \tag{4.2}$$

where N_k is number of thunderstorm days per year. According to [4.10], the following approach is valid:

$$N_g \sim 0{,}2 \cdot N_k \quad \text{flashes/(km}^2\,\text{year)}. \tag{4.3}$$

For a keraunic level of for instance, $N_k = 20$ to 40, formula (4.3) provides a ground density approximately twice as much as formula (4.2).

The *flash density to ground* is only an average indication valid for a region with a given keraunic level. There are other local factors favouring the incidence of lightning strokes, such as relief type, ionisation state of the atmosphere, etc. However, the mechanism determining the point of incidence of the stroke points of the lightning discharge seems to decide about this point only about a hundred meters above ground (see also 4.2.2). Local conditions are, therefore, supposed to have an important influence on the discharge at this moment.

The *lightning embracing exposure* of a transmission line depends on its height. For tower heights around 40 m, typical for 110 kV lines, the embracing exposure reaches about 150 m; for tower heights of 60 m around 250 m and for tower heights of 80 m around 350 m. The latter comprise tower heights for lines in the range of 362 to 785 kV.

4.3.2 Magnitude of lightning stroke currents

Under the standpoint of transmission line performance, the distribution of the *current magnitudes* and slope of the negative upward discharges should be known: WG-33.1 (Lightning) of Cigré [4.3] proposed that consideration should be given only to data obtained from structures not higher than 100 m. As for structures up to this height, the probability of occurring negative upward discharges doesn't exceed 10 %; this distribution is considered as the most representative for engineering studies, specially for lightning performance evaluation of transmission lines.

Under these premises, the average current of 35 kA is recommended as the mean value of lightning strokes; support of additional information from tropical and subtropical

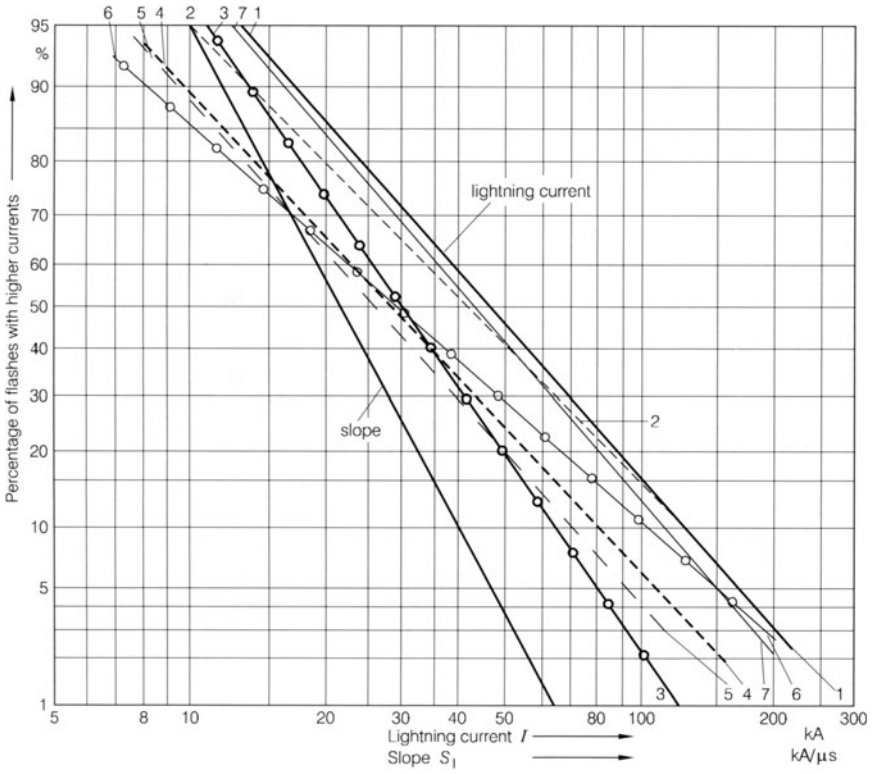

Figure 4.6: Distribution frequencies of lightning stroke currents and slopes (clarification in Table 4.1)

regions is not yet available at enough quantity. However, the average lightning current magnitude can vary from region to region and may depend on the altitude above sea-level as well. Figure 4.6 shows cumulative frequency distribution of lightning stroke currents obtained in some countries. Table 4.1 clarifies origin and statistical data of the measurements shown in Figure 4.6. The cumulative distribution contained in [4.10] corresponds to line 4.

Figure 4.6 shows cumulative distribution of *lightning stroke slopes* for negative single and multiple discharges. For a lightning current of 50 kA, the standard *front time* of 1,2 μs corresponds to a slope of about 40 kA/μs, which is exceeded by 10 % of all lightning strokes.

4.3.3 Direct and indirect lightning strokes

Lightning overvoltages occurring in a transmission line are related to the point of incidence of the lightning strokes and can, therefore, be classified as:

- *Induced overvoltages* that occur when the lightning strokes reach the ground near the line;
- Overvoltages due to *shielding failures* that occur when the lightning stroke reaches the phase conductors;
- Overvoltages caused by *back-flashovers* that occur when the lightning stroke reaches the shield wire or the tower.

Induced overvoltages rarely exceed 600 kV, being, therefore, negligible for transmission lines above 90 kV, whose insulation level is usually higher than 600 kV.
In case of a direct stroke reaching the conductor, the current I splits in two portions flowing toward both directions of the line. The peak value of the overvoltage U_c is given by:

$$U_c = 1/2 \cdot I \cdot Z_C \quad , \tag{4.4}$$

where Z_C is the *surge impedance* of the circuit (see clause 2.1.2). The overvoltage wave is similar to the stroke current, although it can be subsequently modified by the propagation, by corona effects and by reflections at the terminals.
A flashover along the insulator strings at the tower or to an adjacent conductor may occur or not, depending on the *insulation level* of the line. It is conventionally said that a flashover occurs if

$$U_c + U_{pf} \geq U_{50\%} \tag{4.5}$$

where U_c is the *lightning overvoltage*, U_{pf} the instantaneous value of power frequency voltage and $U_{50\%}$ is the critical *flashover voltage* of the insulator string with the same polarity as the impulse wave.
A convenient layout of earth wires will cause the lightning strokes to hit only the earth wires, the towers or the neighbouring ground, seldom the conductors.
The *back-flashovers* are a consequence of lightning strokes that reached the earth wire. When the stroke current is drained to the ground through the tower, an overvoltage is originated at the latter as a direct function of its earth surge impedance and an indirect function of the earthing resistance. If this overvoltage, combined with the instantaneous power frequency voltage of the phase conductors, exceeds the insulation level of the insulator strings, a *tower-to-conductor flashover* occurs. The tower earthing resistance or the surge impedance is, therefore, a parameter of paramount importance in the computation of the tower overvoltage, as expressed by the formula

$$U_M = (1 - k)(Z_M \cdot I + L_M \, dI/dt) \quad , \tag{4.6}$$

where U_M is the tower overvoltage (kV), Z_M the earth surge impedance of the tower as a function of the tower earthing resistance (Ω), L_M the *tower self-inductance*, I the stroke current (kA) and k the *coupling factor* between earth wires and conductors (see [4.5]).

4.4 Arrangement and efficiency of earth wires

4.4.1 Theoretical background

Whitehead [4.11] and others have provided significant contributions on the electromagnetic theory for totally shielding the conductors of an overhead line, both analytically and practically (see also [4.5]).
An effective shielding requires a strategic positioning of the earth wire so that the leaders of incident lightning strokes, whose currents exceed the critical current, reach always the earth wires or the ground, but not the conductors. In order to prove *earth wire efficiency*, a circle of diameter D, obtained from equation (4.1), is drawn around earth wire and conductor points. Besides, a parallel straight line is drawn at a distance $\beta_S \cdot D$ to ground surface (see Figures 4.7 and 4.8). The most favourable position of the earth wire is obtained when the circles around phase conductors and earth wires meet in the same point with the parallel straight line with the ground surface. (Figure 4.8). Then a complete *shielding protection* of the phase conductors is obtained because lightning strokes reach either the earth wires or the earth.

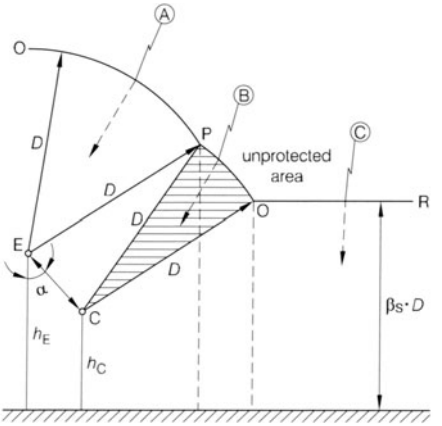

Figure 4.7: Electromagnetic model for shielding failures: incomplete shielding

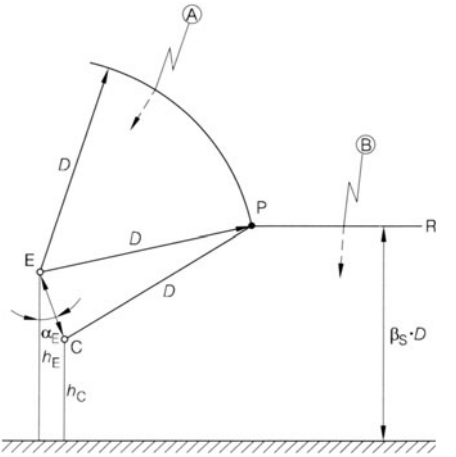

Figure 4.8: Electromagnetic model for shielding failures: effective shielding, no unprotected area

Figure 4.7 shows an example of an incomplete shielding, because flashes A and C make their final jumps to earth wire and earth, respectively, but flash B may jump only to the phase conductor. In Figure 4.8 no uncovered area exists and an effective shielding is reached.

The strike distance D is multiplied by a reduction factor β_S when it refers to ground. The coefficient β_S allows for the strong likelihood that the final strike distance to the horizontal ground plane, with its widespread attractive effects, will be significantly different from the strike distance to a wire suspended above the earth plane. The value of β_S recommended by EPRI [4.5] is 0,8 for lines of range I and 0,67 for lines of range II, according to IEC 60 071.

4.4.2 Effective shielding by earth wires

In regions with medium or high keraunic levels it is standard practice to equip transmission lines with *earth wires* to shield them against lightning discharges. In regions of low keraunic levels the use of earth wires can be precluded.

When designing an effective shielding of lines, effects caused by back-flashovers have to be considered as well. Therefore, an appropriate earthing of the towers is essential in addition to the arrangement of earth wires. Earthing with respect to lightning protection does not directly correspond to earthing for power frequency voltages.

For effective shielding both the strokes hitting directly the conductors and *back-flashovers* from towers to conductors have to be considered. The latter occur as a consequence of strokes into the earth wires or earthed towers causing the *tower potential* to be increased. This increase depends on the stroke current, surge earth resistance of the tower and eventual coupling between the earth wires and the phase conductors. In both cases a lightning flashover occurs when the lightning overvoltage exceeds the line insulation level.

The earth wires are installed with *shielding angles* that usually vary between 10 and 35°, depending on the importance of the line [4.12].

The first approaches developed for protecting the phase conductors against direct lightning strokes considered a maximum protection angle of 30° between the highest point of the shield wire attachment at the tower and the horizontally most external conductor

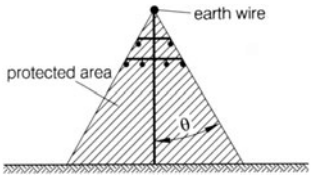

Figure 4.9: Protection area through an earth wire in a Danube Tower

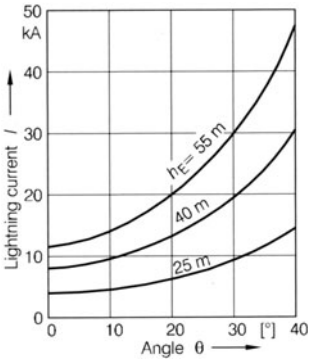

Figure 4.10: Highest current of lightning striking directly into phase conductor

(see Figure 4.9). Really the protection effect of the earth wires depends also on their height above ground and on the lightning current. Figure 4.10 according to [4.10] represents current peak values of lightning hitting phase conductors directly as a function of angle θ. As the *lightning current* increases, the protection effect will improve as well. Higher towers require lower shielding angles for attaining the same protection level.
For 55 m height above ground, only lightning currents lower than 30 kA, representing about 30 % of all currents, can hit directly the conductors. If a probability of 50 % for the lightning strokes is considered, then 7,5 to 15 discharges per year hit phase conductors in average. About half from those discharges, that means 4 to 8, cause flashovers through the insulation. The *impulse voltage peak* is determined through the surge impedance, considering also the current distribution at its point of incidence:

$$U_c = 1/2\, Z_C\, I \quad . \tag{4.7}$$

Figure 4.11 according to [4.10] represents the *shielding failure rate* measured by the number of flashovers per 100 km and year, for 25 and 55 m shield wire heights and 3,6 flashes per km^2 and year. The following comments are based on such values.
Additionally to the direct strokes in phase conductors, also the strokes to towers or earth wires can cause insulation failures due to *back-flashovers*, when the impulse overvoltage reaches a value above the *lightning withstand impulse* of the insulation.
Keraunic levels between 15 and 30 thunderstorm days per year are typical in Central Europe, while a maximum of 200 occurs in the equatorial region of South America, as it can be seen in Figure 4.5. For the above mentioned keraunic levels of Central Europe, a resulting flash density of 2 to 4 earth flashes per km^2 occurs for 60 m high towers of 380 kV overhead lines; the corresponding embracing exposure reaches about 250 m, while the number of flashes per 100 km and year is between 50 and 100.
For 500 kV overhead lines in North or South America with $Z_C = 300\ \Omega$ and lightning current of 30 kA, a voltage of 4500 kV is reached, what would result in insulator flashover. EHV lines of range II usually have shielding angles lower than 30°, mostly around 10°. For the latter protection angle only flashes below 15 kA can reach the conductors; such flashes have a probability of 15 % to occur, resulting in 50 % probability of shielding failures or in 4 to 8 flashes per year. Only flashes between 10 and 15 kA, or 1/3 of the total, can produce overvoltages that lead to insulation failures. The number of flashovers reaches, therefore, 1,5 to 2,5 per 100 km per year.
For 110 kV lines with 40 m high towers the embracing exposure reduces to 150 m and the number of flashes reaches 30 to 60 per 100 km and year. For 40 m high towers and 30° shielding angle, only flashes below 20 kA can hit phase conductors, or only 20 %

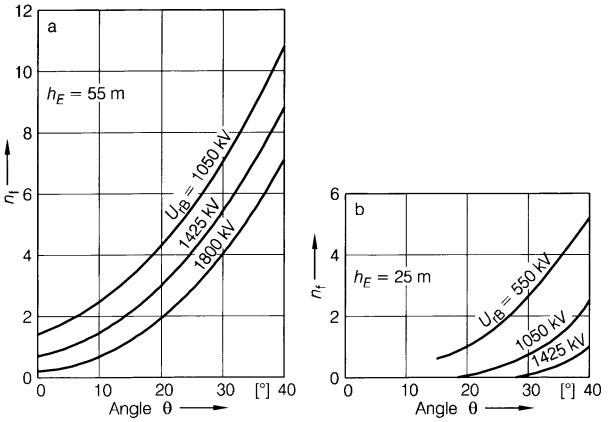

Figure 4.11: Shielding failures n_f as a function of shielding angle and lightning impulse voltage according to [4.10]
a earth wire height 55 m;
b earth wire height 25 m

of all flashes. Considering again a probability of 50 %, it results in 3 to 6 flashes per year. All flashes lead to *insulation flashovers* due to the low impulse withstand of the insulator string. Consideration should be given to 3 to 6 flashovers per 100 km and year. Because of the increase of the insulation level with the nominal voltage of the line, the risk of back-flashovers usually decreases with the voltage.

Statistics show that the number of flashovers from conductors to towers is about the same for all voltage levels. This apparently contradictory tendency is occasioned by the higher towers used in higher voltages, as for steeper lightning impulse events the higher surge impedance of the towers will be effective.

For a 110 kV line with an impulse withstand voltage of 550 kV, 10 Ω earth surge impedance and 15 % coupling factor of the phase conductors with the earth wire the critical lightning current attains $I \sim 550/(10 \cdot 0{,}85) \approx 65$ kA. If a *stroke* hit directly the tower then the lightning surge voltage strains the insulation. For 15 % of all strokes the current will be equal or higher than 65 kA. If a stroke hit the earth wire at midspan and a 50 % to 50 % distribution of the current on the neighbouring towers is considered then only lightning with currents above 130 kA would cause back-flashovers. Only 1 % of all strokes will reach or exceed this current. In Central Europe a current of 65 kA is achieved or exceeded by 4,5 to 9 lightning strokes per 100 km line and year, while 0,6 to 1,2 strokes per 100 km and year will reach 130 kA. Back-flashovers have to be expected when these lightning currents are reached or exceeded.

For 220 or 380 kV overhead lines with *basic insulation levels* of 1 050 or 1 425 kV, respectively, having higher towers and lower surge impedances, it results in critical current intensities of 100 or 110 kA for flashes reaching the towers. For equal lightning currents, a lower number of back-flashovers can be expected, therefore.

Statistics show that in Europe the number of lightning failures is practically independent on the voltage level for lines in the range of 110 to 380 kV, reaching between 1,1 to 1,6 flashovers per 100 km and year. Therefore, the estimates presented above lead to conservative values. Statistics available in South America show the following ranges for outages due to lightning strokes:

- 40 to 70 kV lines: up to 10 line *outages* per 100 km and year;
- 110 to 245 kV lines: 2 to 5 line outages per 100 km and year;
- 300 to 500 kV lines: 1 to 2 line outages per 100 km and year;
- 750 kV lines: 0,2 to 0,5 line outages per 100 km and year.

An interesting and valuable survey on the performance of EHV lines was carried out by Cigré Study Committee 33 [4.13]. This survey has been useful when designing new lines in the relevant regions.

4.4.3 Surge arresters

An alternative to the use of earth wires for protecting the conductors against the direct incidence of lightning strokes that has gained significance of late consists of using *surge arresters* in parallel to insulator strings. The need of using earth wires is, therefore, precluded and more economical towers can be designed. The technical advantages and economics of such solution should naturally be examined but in several cases surge arresters can be recommended if for other reasons lower towers are used [4.14]. Surge arresters have been already used in lines up to 145 kV for providing further protection against lightning strokes in especial regions. For EHV lines their use is still under consideration mostly for economical reasons.

4.4.4 Assessment of lightning performance of overhead lines

Lightning overvoltages usually govern the external insulation of overhead lines of the range I (up to 300 kV). They may govern even the insulation of lines with voltages of range II, for instance until 525 kV, if the keraunic levels and/or earth resistivities are high and the switching surges are limited by convenient means, such as the use of pre-insertion resistors or surge arresters.

Several analytical and simulation methods have been developed for the evaluation of overhead *line performance under lightning* overvoltages. The Monte Carlo's techniques consider that the process of lightning strokes reaching an overhead line comprises a series of events of a probabilistic nature [4.15]. Other methods employ analytical equations and calculate the critical voltages that are applied to the insulation. Therefore, the resulting back-flashover probabilities are determined. One of the most known software developed by IEEE, the FLASH program, has been one of more accurate approaches used of late [4.16]. This method takes into account the following sequence of calculation:

- Conversion of the keraunic levels of the region crossed by the line into flash densities or direct use of flash densities, if available;
- Determination of probability density of earthing surge impedances as a function of the assessed or measured probability distribution of the tower earthing resistance of the line;
- Consideration of the geometry of the basic or more frequently used tower configuration of the line, as well as the typical wave shape of the lightning stroke;
- Calculation of the two components of the lightning performance, namely the *shielding failure rate* and the *back-flashover failure* rate.

The standard *line performance index* is measured in number of line outages per 100 km and year. Basic directives and the respective tower earthing resistance are given in Table 4.2. The data are valid for keraunic levels of 30. The real number of line outages varies approximately proportional to the keraunic level, so that, having the keraunic level for a certain line, its performance can be roughly obtained from a simple proportion in relation to the data given in Table 4.2. Regarding the lightning performance of double-circuit transmission lines, special phase arrangements at the towers, e. g. disposing phases of one circuit at the inverse order in relation to the second circuit, may contribute to reduce the number of line outages [4.17].

4.5 Earthing in view of lightning protection

4.5.1 Significance of earthing for lightning protection

The *tower earthing resistance* and the relevant *surge impedance* of the earthing system of line structures is an extremely important parameter in the determination of lightning

Table 4.2: Guidelines for determination of lightning performance of overhead lines and relevant tower earthing resistances

Highest operating voltage kV	Lightning withstand voltage kV	Number of outages per 100 km and year	Tower earthing resistance Ω	Number of earth wires
123	550	5	15	1
245	950	3	20	1 or 2
420	1300	1,5	20	2
525	1550	1,0	25	2
765	2100	0,5	25	2

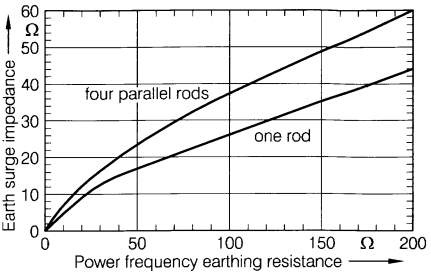

Figure 4.12: Relationship between earth surge impedance and power frequency resistance for determining lightning performance according to [4.4]

flashover rates due to back-flashovers. The *tower earthing resistance* is a varying statistical variable, the magnitude of which is governed not only by geography and geology of the soil but also by non linear conduction physics in the earth. It may swing over a two to one orders of magnitude or more owing to change in stroke current, and even with constant current it will change with time. A convenient tower earthing is, therefore, necessary in order to obtain a good protection against lightning (see also clause 5.3).

4.5.2 Surge impedance of earthing systems

The voltage increase of a tower following a *lightning stroke* is an important parameter for determining the back-flashover rate. Both the tower *surge impedance* (or its inductance) and earthing systems are involved in the calculation procedure. The surge impedance of the tower depends on its geometry and considers three basic geometry types, namely class 1: conical, class 2: cylindrical and class 3: towers with waist [4.5]. Measurements carried out have shown values of the tower *surge impedances* for the three classes between 10 to 30 Ω.

Earthing system measurements for power frequency voltages can be used as a basis for determining the lightning surge impedances as well as for the calculation of the lightning protection of the overhead lines. The conversion of power frequency resistance as measured by normal instruments, to *surge impedance* is performed for various types of electrodes according to values obtained by experience.

In any case, practical investigations carried out show that, at the most pessimistic case, the earthing surge impedance would reach the value of the power frequency resistance. Investigations carried out by EPRI show that earth surge impedance can vary between 0,25 and 1,0 time the power frequency resistance [4.18].

Earthing resistance decreases with increasing current, at least until the current dries out the soil. The proportional reduction is less for soils having low resistance than it is for soils of high resistance.

The relationship between earth surge impedance and power frequency resistance is shown in Figure 4.12 according to [4.4]. Other data can be found in [4.5]. Regarding

the behaviour of *horizontal earthing wires* (*counterpoise*) under strokes, it has been shown theoretically and by tests that the counterpoise has an initial transient surge impedance at the order of 150 Ω, which decays to its final value of resistance, the transition time being the time required for the first reflection to return, travelling with one third of the speed of the light (100 m/μs). For a given length of buried wire, the transient resistance will reduce to the steady-state resistance faster if the *counterpoise* is arranged as several, shorter radial strips than if it were laid as one long strip.
For lightning currents, the effective electrode length reaches around $0{,}2 \cdot \sqrt{I \cdot \varrho_E}$ for *deep electrodes* or $0{,}3 \cdot \sqrt{I \cdot \varrho_E}$ for *shallow electrodes*, corresponding to 24 or 36 m in case of peak lightning currents of 150 kA and a resistivity of 100 Ωm [4.19]. As a consequence deep electrodes are about 1,5 times more effective in normal soils than *shallow electrodes* of the same length, as far as the maximum electrode length is not exceeded. *Deep electrodes* are especially recommended when the conductivity of the soil near the surface is bad and improves at deeper soil layers. This point has often been confirmed by measurements of soil resistivity with the Wenner Method, as shown in clause 5.8.

4.6 References

4.1 Lewis, W. W.: The protection of transmission systems against lightning. New York, Dover Publications 1965

4.2 Electrical Transmission and Distribution Reference Book. Pennsylvania, Westinghouse, 4th edition 1964

4.3 Weck, K.-H.; Hileman, R.: Application of lightning parameters – lightning current shape and amplitude of multiple strokes. Cigré Report 33-78, 1978

4.4 Anderson, R. B.; Eriksson, A. J. et al.: Lightning and thunderstorm parameters. International conference on lightning and power systems. IEE 1984

4.5 EPRI: Transmission line reference book: 345 kV and above. Palo Alto. Electric Power Research Institute, 2nd edition 1987

4.6 Bewley, L. V.: Travelling waves on transmission systems. New York. Dover Publication, 2nd edition 1963

4.7 Zink, D. G.; Beaty, H. W: Standard handbook for electrical engineers. New York, Mc Graw-Hill, 12th edition 1987

4.8 Eriksson, A. J.: A modified electrogeometric model for shielding analysis. SAIEE Symposium on Lightning Performance of Lines. Pretoria, 1982

4.9 Prentice, S. A.: Frequency of lightning discharges. Lightning Vol. 1, edited by R.H.Golde. New York. Academic Press (1972), pp. 465 to 496

4.10 Hütte Energietechnik, Band 3: Netze (Power engineering, Volume 3,: Electric networks). Berlin, Heidelberg, New York. Springer Verlag 1987

4.11 Whitehead E. R.: Protection of transmission lines: Lightning – Vol. 2, edited by R.H. Golde. New York, Academic Press 1977

4.12 Dorsch, H.: Überspannungen und Isolationsbemessung bei Drehstrom-Hochspannungsanlagen (Overvoltages and insulation design for three-phase high-voltage installations). Erlangen, Siemens ZVW5-Verlag 1981

4.13 Whitehead E. R.: Cigré survey of the lightning performance of extra-high-voltage transmission lines. Electra 33 (1974), pp. 63 to 70

4.14 Stenstrøm, L. et al.: A compact 420 kV line utilising line surge arresters for areas with low isokeraunic levels. Cigré Report 22/33/36-08, 1998

4.15 Anderson, J. G.: Monte Carlo computer simulation of transmission line lightning performance. IEEE Transactions on Power Apparatus and Systems, Vol. 80 (1961), pp. 414 to 419

4.16 Anderson, R. B. et al.: A simplified method for estimating lightning performance of transmission lines. IEEE Transactions on Power Apparatus and Systems, Vol. 104 (1983), pp. 919 to 932

4.17 Sargent, M. A.; Darvenizia, M.: Lightning performance of double-circuit transmission lines. IEEE Transactions on Power Apparatus and Systems, Vol. 89 (1979), pp. 913 to 925

4.18 EPRI: Transmission line grounding. Project 1491-1. Palo Alto. Electric Power Research Institute 1982

4.19 BS-CP 1013: Code of practice: Earthing. London, BSI 1965

5 Earthing

5.0 Symbols

Symbol	Signification
a	Distance of probes
d	Diameter
$d_{1,2}$	Thickness of soil layer
e, f	Distance
D	Diameter of a ring-type electrode
E	Electrical field strength
F_{K}	Penetration factor
h	Depth of probe
i	Current density in soil
I	Short-term current, total current
I_0	Zero-sequence current
I_{A}	Current through earth resistance
I_C	Capacitive earth fault current
I_{E}	Earth current
I_{ES}	Earth wire current
I_{F}	Earth fault current
I_{im}	Peak value of lightning impulse current
I''_{k1}	Initial symmetrical short-circuit current
I''_{kEE}	Double earth fault current
I_{m}	Measured current
I_{RES}	Earth fault residual current
k	Reflection coefficient
K_{E}	Material-dependent value
l	Distance of probes
L	Length of an earthing electrode
M_0	Factor to determine the inflection point
N	Number of potential points
r	Radius of a hemispherical electrode
r_{e}	Radius of equivalent rod
r_{E}	Reduction factor of earth wires/of a line
R_{a}	Additional resistance
R_{E}	Earthing resistance
R_{T}	Earthing resistance of a tower
s	Distance of earthing rods
t	Depth of earthing strip installation
t_{F}	Duration of fault current
T_{i}	Initial temperature of a conductor
T_{f}	Permissible final temperature
U_{em}	Measured voltage
U_{im}	Lightning impulse withstand voltage of the insulation
U_{D}	Permissible touch voltage with additional resistance
U_{E}	Earthing voltage
U_{S}	Step voltage
U_{TP}	Permissible touch voltage without additional resistance
x	Distance
Z_∞	Iterative network impedance of a line
Z_{im}	Impulse earthing impedance of a tower
Z_{B}	Body resistance
Z_{CE}	Mutual impedance of conductors and earth wires
Z_{E}	Impedance to earth

Symbol	Description
Z_{EE}	Earth wire self-impedance
Z_S	Earth wire impedance of a span
α	Temperature coefficient of resistance
β	Reciprocal of temperature coefficient
ΔU_E	Earth potential rise
ϱ_E	Earth resistivity
$\overline{\varrho}_E$	Mean earth resistivity
φ	Surface potential
χ	Distance to probe/sphere

5.1 Purpose of earthing

The standard EN 50 341-1 [5.1] lists five requirements for earthing systems:

- Guaranteeing safety of persons when electric voltages occur during short circuits;
- Avoiding damage to third-party property and to other installations;
- Ensuring an acceptable performance;
- Complying design with the maximum short circuit earth current to be expected and
- A sufficient mechanical strength and corrosion resistance.

The first requirement is to be paid priority and includes animals, e. g. grazing cattle. Supports made of conductive material are earthed in principle through their foundations; however, in addition cost-effective earthing installations are sometimes necessary to achieve the required performance of the earthing system, e. g. for supports at sites with low earth resistivity.

With respect to the main purpose three types of earthing can be distinguished:

- *Operational earthing*,
- *Protection earthing* and
- *Lightning protection earthing.*

In case of systems above AC 1 kV the requirements on earthing depend on the system characteristics such as:

- Type of neutral point design: insulated, resonant earthing or low resistant neutral,
- Type of supports: supports with or without built-in disconnectors or transformer stations
- Material used for supports: steel, reinforced concrete or wood,
- Support sites: normal or particularly exposed sites in swimming areas, camping sites or play grounds.

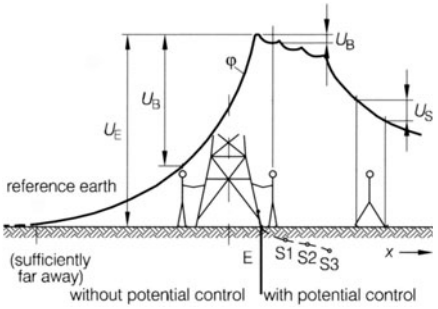

Figure 5.1: Example of ground surface potential and the voltages in case of a current-conducting earth electrode [5.2].
U_E earthing voltage; U_B touch voltage; U_S step voltage; φ surface potential; E earth electrode; S1, S2, S3 earth potential control electrodes (ring electrodes) connected to the earth electrode; x distance to the earth electrode E

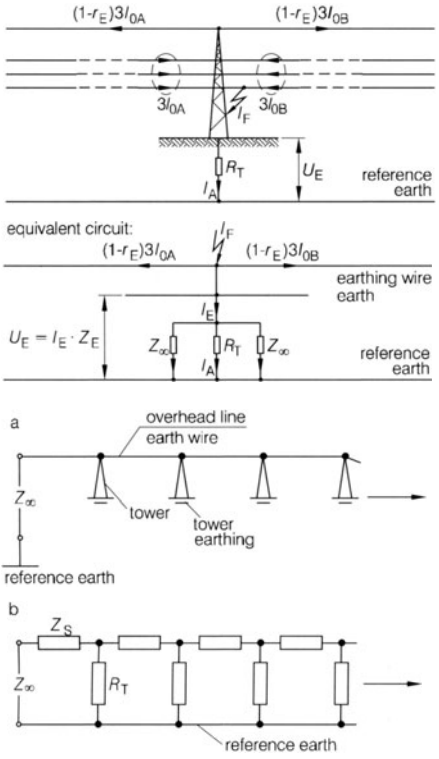

Figure 5.2: Earth fault currents, voltages and resistance in case of an earth fault at a tower. $I_F = 3 \cdot I_{0A} + 3 \cdot I_{0B}$; $Z_E = 1/(1/R_T + 2/Z_\infty)$; $I_E = r_E \cdot I_F$
$3 \cdot I_{0A}$ is the total zero-sequence current from system part A; $3 \cdot I_{0B}$ the total zero-sequence current from system part B; I_F earth fault current; I_E earth current (not measurable); I_A current flowing through the earth resistance of the tower having an earth fault; r_E reduction factor of the line; R_M tower resistance; Z_∞ impedance of the line; Z_E earthing impedance; U_E earthing voltage

Figure 5.3: Iterative network impedance of a line
a) arrangement of earth wires and towers
b) equivalent circuit diagram

5.2 Definitions and basic principles

Figure 5.1 can be used to explain terms frequently used in the context of earthing problems. The figure depicts the voltage potential on the ground surface in close proximity of a short circuited installation with or without potential control having an earthing rod, through which an earth fault current flows. In addition to the total earthing voltage the touch and step voltages can be recognised as partial potential differences. In practice these values may reach 50 % and 30 %, respectively, of the earthing voltage. Potential control measures can reduce them to values of less than 10 %. An example for the current distribution is shown in Figure 5.2 with consideration of voltages and resistance in case of an earth fault at a tower. The diagram of the equivalent circuit shows the impedance to earth Z_E as the result from paralleling the earth resistance R_T of the tower and the iterative network impedance Z_∞ of the line. From the figure the distribution of the fault current I_F on earth and earth wire can be seen. The latter current is affected by the earth wire reduction factor r_E resulting in a considerably lower earth potential when high-conductivity earth wires are adopted.
Figure 5.3 represents the recurrent network impedance of a line. The value of the recurrent network impedance is depicted in Figure 5.4 depending on the mean earth resistance R_T of the towers for varying types of earth wires and span lengths from 200 to 400 m. The graphs demonstrate that the iterative network impedance usually reaches a few ohms only.

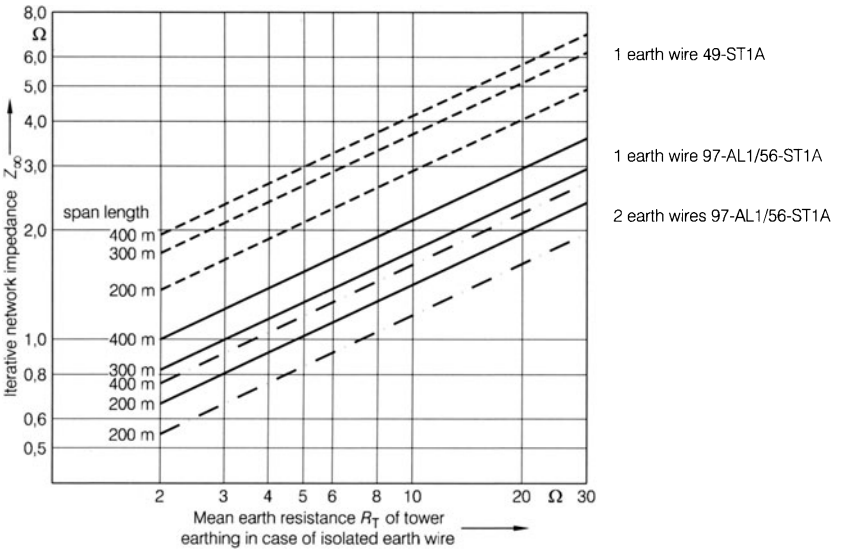

Figure 5.4: Iterative network impedance of lines depending on the mean earth resistance R_T of towers for varying span lengths and earth wires

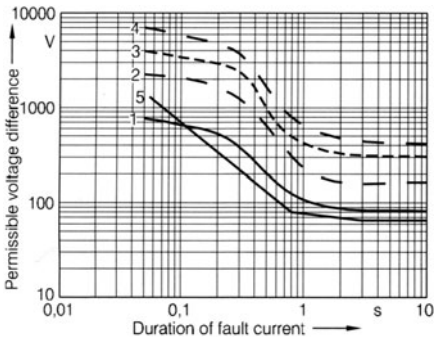

Figure 5.5: Permissible *touch voltage* depending on the insulation conditions at the location according to EN 50 341-1 [5.1].
1 without additional resistance such as play grounds, swimming pools, recreational areas where people may gather with bare feet; 2 with 1750 Ω resistance: parking places, public roads, where people wear shoes; 3 with 4000 Ω resistance: locations with high soil resistivity; 4 with 7000 Ω resistance: locations with very high soil resistivity; 5 permissible touch voltages according to [5.2]

5.3 Requirements

5.3.1 Standards

For transmission lines in Europe, EN 50 341-1 [5.1] establishes the basic requirements together with the corresponding National Normative Aspects (NNA) applicable to the associated countries, e. g. [5.3] for Germany, [5.4] for Austria and [5.5] for Switzerland. Outside Europe, among other relevant standards, that establish rules and limits regarding earthing and earthing potentials, the following can be mentioned:

- Guide for safety in alternating current substation design [5.6];
- Recommended guide for measuring ground resistance and potential gradients in the Earth [5.7].

5.3.2 Safety of persons

If an earth fault occurs, parts of a line installation are subjected to a voltage and a current may flow through the human body or through animals in case of touching, which can be hazardous. However, it is permitted to take into consideration site-depending

Table 5.1: Fault duration, permissible body current and touch voltage

Fault duration s	Body current mA	Human body impedance Ω	Touch voltage V
0,05	900	1090	735
0,10	750	1125	633
0,20	600	1175	528
0,50	200	1360	204
1,00	80	1780	107
2,00	60	2000	90
5,00	51	2130	81
10,00	50	2130	80

resistance, which reduce the body currents. The relationship between the acceptable intensity of short-circuit current and its duration is shown in IEC 60 479-1 [5.8]. Figure 5.5, therefore, shows graphs for permissible voltage differences without additional resistance and graphs for higher site resistance and foot wear. The data assume the correct functioning of protection devices which ensure that touch voltage acts during a short duration only.

The permissible values for *step voltages* would be higher than those for the touch voltages. Therefore, it can be assumed that, when complying with the requirements on touch voltages, any hazards due to step voltages will be excluded.

When determining the permissible touch voltages, it is assumed that

- the currents flow between one hand and both feet,
- the probability of the occurrence of the assumed human body impedance is 50 %,
- the probability of occurrence of ventricular fibrilation is lower than 5 % and
- no additional impedances are considered.

These assumptions lead to an optimum human safety due to the low probability of simultaneous earth faults and touching of a conductive component. Furthermore, they result in the values for the permissible touch voltages and the human body currents listed in Table 5.1 depending on the duration of current flow (according to [5.1], annex G.4). When determining the permissible touch voltages, only 75 % of the voltage-dependant body impedance were taken into account.

5.3.3 Thermal short-circuit strength

The dimensions of earth electrodes and earthing conductors shall be rated such that the permissible temperature of 300°C for copper and steel or of 200°C for aluminium will not be exceeded. The short-circuit loading of individual components of earthing systems can be determined according to the electric system, taking into account the subdivision of the current in the electrode system. For current duration lower than 5 s an adiabatic *temperature rise* can be assumed without heat transfer to the surrounding.

5.3.4 Mechanical strength and corrosion resistance

Mechanical strength and *corrosion resistance* determine the minimum dimensions of electrodes and earthing or bonding conductors. According to [5.1], the minimum cross section for earthing conductors is 16 mm^2 for copper, 35 mm^2 for aluminium and 50 mm^2 for steel. For horizontal earthing wires (counterpoises) it is a common practice in North and South America to adopt copper clad wires with a minimum diameter of 5,2 mm and minimum cross section of 21,2 mm^2. Electrodes having direct contact to earth shall withstand mechanical or biological attacks, oxidation, formation of an elec-

Table 5.2: Minimum dimensions of earth electrode materials according to EN 50341-1

Material	Type of earth electrode	Minimum size				
		Core			Coating/sheath	
		Diameter (mm)	Cross section (mm^2)	Thickness (mm)	Single value (μm)	Average values (μm)
Steel:	Strip		90	3	63	70
	Profile (incl. plates)		90	3	63	70
hot-dip galvanized	Pipe	25		2	47	55
	Round bar for earth rod	16			63	70
	Round bar for surface earth electrode	10				50
with lead sheath[1)]	Round wire for surface earth electrode	8			1000	
with extruded copper sheath	Round bar for earth rod	15[2)]			2000	
with electrolytic copper sheath	Round bar for earth rod	20			90	100
copper clad		5,2	21,2		156/200[3)]	
Copper:	Strip		50	2		
bare	Round wire for surface earth electrode		25[4)]			
	Stranded cable	1,8[5)]	25			
	Pipe	20		2		
tinned	Stranded cable	1,8[5)]	25		1	5
galvanized	Strip		50	2	20	40
with lead sheath[1)]	Stranded cable	1,8[5)]	25		1000	
	Round wire		25		1000	

1) Not suitable for direct embedding in concrete
2) Strip, rolled or cut with rounded edges
3) According to American practice ASTM B227, 30 and 40 % IACS, respectively
4) In conditions where experience shows that the risk of corrosion and mechanical damage is extremely low 16 mm^2 may be used
5) Diameter of single wire

trolytic couple and electrolysis. Thereof, the minimum requirements listed in Table 5.2 apply.

5.3.5 Currents to be considered

The currents to be considered for *earthing system rating* and for *touch voltage* depend on the earthing design criteria of the neutral point in the system and are given in Table 5.3 according to [5.3]. The minimum dimensions according to Table 5.2 shall be used. In case of touch voltages, the relevant current may be determined taking into account the earth wire *reduction factor*. This factor represents the ratio of the return current through earth to the sum of the zero-sequence currents of the AC circuit. It can be calculated for a balanced current distribution from the self- and mutual impedance of conductors and earth wires.

$$r_E = I_E/3\,I_0 = (1 - I_{ES}/3\,I_0) = 1 - Z_{CE}/Z_{EE} \tag{5.1}$$

where
I_{ES} is earth wire current;

Table 5.3: Currents to be considered according to [5.3]

Type of the neutral point	Thermal design of earth electrode	Thermal design of earthing connections	Verification of touch voltages
System with isolated neutral point	(1)	I''_{kEE} (2)	$r_E \cdot I_C$
Resonant earthed systems	(1)	I''_{kEE} (2)	$r_E \cdot I_{RES}$
Systems with low-resistant neutral earthing	I''_{k1}	I''_{k1}	$r_E \cdot I''_{k1}$
Resonant earthed systems and systems with temporarily low resistant neutral points	(1)	I''_{kEE}	$r_E \cdot I_{RES}$

(1) The minimum cross sections according to Table 5.2 are sufficient
(2) If the duration of a failure is lower than 1 s, the currents I_C or I_{RES}, respectively, may be used

Legend: I_C Calculated or measured capacitive earth fault current.
I_{RES} Earth fault residual current. If the precise value is not known, a value of 0,1 times I_C may be used for calculation.
I''_{kEE} Double earth fault current which may be assumed as 85 % of the three-phase initial short-circuit alternate current.
I''_{k1} Initial symmetrical short-circuit current in case of single-phase earth fault

Table 5.4: Reduction factors r_E for earth wires at 50 and 60 Hz

Type of earth wire	AL1/ST1A[1]					BZ II[2]		ST1A[3]	
cross section (mm^2)	304/49	264/34 243/39	184/30	97/56	44/32	50	70	50	70
AC resistance (Ω/km)	0,10	0,12	0,17	0,35	0,75	0,52	0,37	4,13	2,50
Reduction factor r	0,61	0,62	0,62	0,70	0,77	0,75	0,69	~1,00	0,97

[1] Earth wire type according to EN 50 182
[2] Earth wire made of copper alloy according to DIN 48 201 Part 2 or comparable standard
[3] Earth wire made of galvanized steel according to DIN 48 201 Part 3 or comparable standard

$3I_0$ sum of zero-sequence currents;
Z_{CE} mutual impedance of conductors and earth wires;
Z_{EE} self-impedance of earth wires.

The conductivity of earth wires and the distance between earth wires and conductors have the most important effect on the reduction factor, which varies between 0,2 and 1,0; Table 5.4 gives values for often used earth wires according to [5.9].

5.4 Earthing for personal safety purposes

Earthing of conductive components which are not part of the operation circuit to protect people and animals against excessive *touch voltages* is called *earthing for personal safety.* According to [5.1], supports made of conductive material such as steel or reinforced concrete are considered as earthed by their foundations. Supports made of non-conductive material, e. g. wood or plastic material, do not need earthing if there is no metallic connection between insulator supporting crossarms and earth.
As far as the requirements for earthing are concerned, the systems are distinguished by the type of *neutral point connection.* In case of systems with isolated neutral point or resonant earthed neutral, usually adopted only in systems up to 110 kV, earth faults could last for longer periods (more than several hours). In this case, the *touch voltage*

may not exceed 65 V. These requirements are complied with if the resulting earthing impedance Z_E from paralleling the support *earthing resistance* R_T to the adjacent supports via the earth wires complies with

$$Z_E \leq 130/I_{E\,rms} \quad , \tag{5.2}$$

where $I_{E\,rms} = r_E \cdot I_F$.
The earth fault current I_F has to be taken as

- the capacitive earth fault current I_C in case of systems with isolated neutral point,
- the residual earth fault current, which is between 5 and 15 % of I_C in case of resonant earthed systems (at maximum 10 % of I_C in case of missing data).

The reduction factor r_E depends on the type of earth wires, their number, material and cross section. Table 5.4 shows typical values between 0,6 and 0,99 for reduction factors; whereby values above 0,9 apply to steel earth wires and the lower values to higher conductive ACSR conductors. In case of several earth wires, values r_E close to zero can be achieved.
In case of a 110 kV resonant earthed system and 130 A residual current as the maximum limit for complying with the extinction limit, an earthing impedance of

$$Z_E \leq 130/(1{,}00 \cdot 130) = 1{,}00\,\Omega$$

results for a 50 mm^2 steel earth wire and less conductive cross sections. In case of a line with one earth wire 264-AL1/39-ST1A having a reduction factor $r_E = 0{,}62$, the impedance may rise to 1,55 Ω.
In systems with low-resistant neutral point and supports made of conductive material such as steel or reinforced concrete, an earth wire or ground conductor should be installed which is connected to the substation earthing installation.
The earthing current I_E can be determined from the single-phase fault current I_F being multiplied by the reduction factor r_E of the line. In case of lines with voltages of 110 kV and above, an additional expectation factor 0,7 can be considered because of the low probability of coincidence of all unfavourable conditions. If an automatic fault interruption within 0,5 s is guaranteed, as usual in case of low-resistant neutral earthing, the supports do not need to comply with particular limits for touch and earthing voltages. Only where no automatic disconnection within 0,5 s is carried out, the limits for the permissible touch voltages presented in Figure 5.5 apply. They drop from 200 V at 0,5 s fault duration to 85 V for a duration of 3 s. For supports near swimming pools, play grounds, sports fields or camping sites it should be ensured, as a function of neutral point type, that the touch voltage at the support and the voltage between two arbitrary points with a distance of 1,5 m in the support surrounding do not exceed the permissible limits according to Figure 5.5 if an earthing current flows. This can be achieved through

- a barrier made of non-conductive fences or planting bushes;
- application of a low-conducting surface, e. g. by means of gravel or asphalt;
- potential control, e. g. by means of grading earth electrodes.

In case of supports with disconnectors or transformers, it should be guaranteed that when an earth fault occurs the touch voltage is kept below 65 V. This requirement is complied with when the earthing voltage is lower than 250 V and a ring earth electrode is arranged around the support at a distance of about 1 m at a depth shallower than 0,5 m.
In Figure 5.6 according to [5.1] the steps are schematically shown to be taken with respect to safety earthing:

(1) For wood or other non-conductive poles or towers without any conducting parts to earth, earth faults are not possible in practice and there are no requirements for earthing.

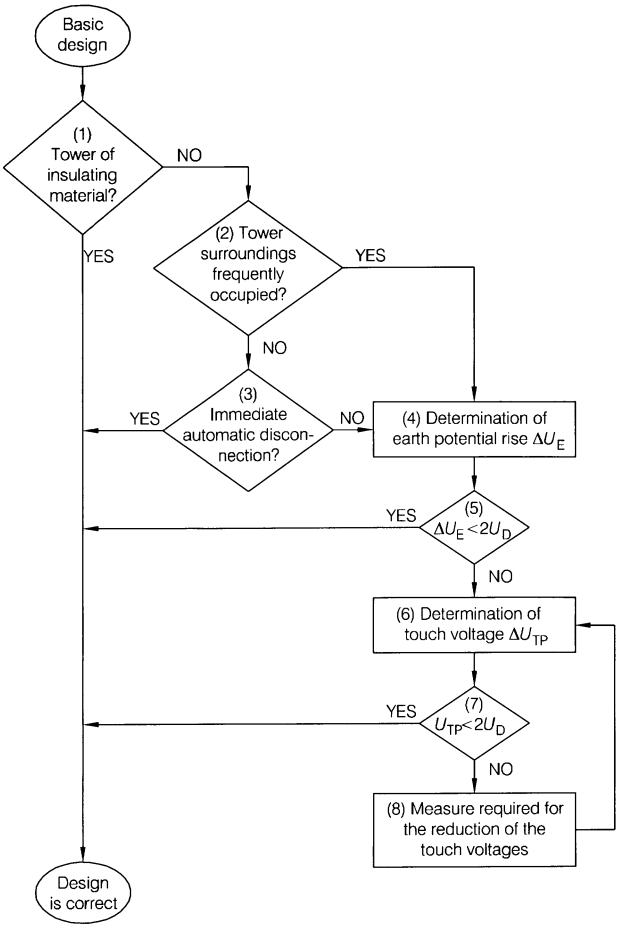

Figure 5.6: Design of earthing systems with regard to permissible touch voltage

(2) The criteria for safety should be carefully reviewed at tower sites freely accessible to people in the following cases:
   - If people are expected to be at such sites for a relatively long time (some hours per day) during some weeks;
   - If people may stay there for a short time but very frequently (many times a day) for example close to residential areas or play grounds;
   - If locations which are only occasionally occupied such as forests, open country sites etc. are not concerned.

(3) For towers at locations that are not freely accessible or where access by people will be rare, the touch voltages need not be considered in those cases where the line is provided with automatic disconnection for protection.
If it can be assumed that access by people will be rare, then the probability of this access and the incidence of a simultaneous automatically cleared fault can be considered negligible and thus the earthing design can be accepted as satisfactory.

(4) The earth potential rise ΔU_E is given by

$$\Delta U_E = Z_E \cdot r_E \cdot 3 \cdot I_0 \quad , \tag{5.3}$$

where
$3I_0$ is the zero-sequence current during earth fault;
Z_E is the impedance to earth. It can be taken from measurements or calculated

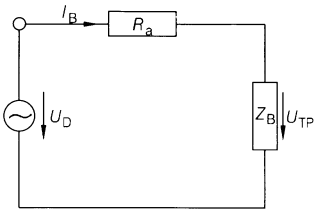

Figure 5.7: Equivalent circuit to determine the permissible touch voltage U_D

from

$$Z_E = 0,25\left(Z_S + \sqrt{Z_S \cdot (4\,R_T + Z_S)}\right) \quad , \tag{5.4}$$

where

Z_S is the earth wire impedance of a span;
R_T is the earthing resistance of a tower.

(5) If earth potential rise is lower than $2\,U_D$ related to appropriate circumstances 1, 2, 3 or 4, as defined in Figure 5.5, then the design can be considered as acceptable. The touch voltage under most of these circumstances is only a fraction of earth potential rise.

(6) The permissible touch voltage U_D depends on the resistance in addition to the body impedance. Figure 5.7 shows the equivalent circuit with pick up voltage U_D as the source voltage. U_{TP} is the permissible touch voltage without additional resistance according to Figure 5.5, graph 1, or Table 5.1.
Regarding the touch voltage along the body it applies

$$U_D = U_{TP} + R_a \cdot I_B = U_{TP}(1 + R_a/Z_B) \tag{5.5}$$

and vice versa

$$U_{TP} = U_D \,/\, (1 + R_a/Z_B) \quad . \tag{5.6}$$

The additional resistance R_a consists of the foot wear resistance and the resistance of the location against earth. Examples for R_a are explained in Figure 5.5.

(7) According to Figure 5.6, it has to be checked whether the touch voltage U_{TP} obtained from (5.6) is less than the permissible value according to Figure 5.5.

(8) If none of the conditions given above is satisfied, then measures to reduce the touch voltage shall be taken, until the requirements will be met. Such measures could be insulation of the location or improvement of earthing conditions.

5.5 Operational earthing

Operational earthing is necessary at specific points of the operational circuit to guarantee the correct operation of earth terminal of single-phase devices or neutral earthing, e. g. voltage transformers or the neutral of Y-connected transformers. In case of transmission lines, operational earthing may play a role only at poles with transformers or disconnectors. The cross section of the earthing conductors has to be designed according to the thermal loading (see clause 5.7).

5.6 Lightning protection earthing

The earthing resistance affects the back-flashover rate and, therefore, the line reliability. The reliability is a subject related to line performance and is dealt with in clause 4.4. In [5.3], it is required in view of avoiding back-flashovers that the impulse earthing impedance Z_{im} of a tower suffices the equation

$$Z_{im} \leq U_{im}/I_{im} \quad , \tag{5.7}$$

Table 5.5: Probability of short-circuit currents in overhead power lines

Short-circuit current up to	20 kA	30 kA	40 kA	50 kA	60 kA
Probability	80 %	90 %	95 %	98 %	99 %

Table 5.6: Characteristic data to determine the short-circuit capacity according to [5.1]

Material	Copper	Aluminium	Steel
Temperature coefficient of resistance α (1/K)	0,0039	0,0040	0,0045
Value β (reciprocal of coefficient α[1)]) in K	234,5	228,0	202,0
Constant K_E ($As^{1/2}mm^{-2}$)	226	148	78

[1)] according to [5.1], not exactly the reciprocal to α. The effect on the calculated results is low.

where

U_{im} is the lightning impulse withstand voltage of the insulation;
I_{im} is the peak value of the lightning impulse current;
Z_{im} is the impulse earthing impedance, dealt with in clause 4.5.2.

Table 5.5 shows probabilities of occurrence for short-circuit peak values in Central Europe. It can be seen that for 95 % of the short circuits the current does not exceed 40 kA.

5.7 Rating for short-term currents

For *short-term currents* lasting less than 5 s, the required cross section A can be obtained, according to IEC 60 724 [5.10] or [5.1]:

$$A = \frac{I}{K_E}\sqrt{t_F \Big/ \ln\frac{(\alpha T_f + 1)}{(\alpha T_i + 1)}} = \frac{I}{K_E}\sqrt{t_F \Big/ \ln\frac{T_f + \beta}{T_i + \beta}} \quad , \tag{5.8}$$

where

I is the short-term current in A;
K_E is a value depending on the material, see Table 5.6;
α is the temperature coefficient of resistance in 1/K, see Table 5.6;
β is the reciprocal of temperature coefficient in K, see Table 5.6;
t_F is the duration of the fault current in s;
T_i is the initial temperature when the current starts to flow in °C;
T_f is the permissible final temperature of the conductor in °C.

For materials frequently used as electrodes and earthing conductors, diagrams are given in Annex G to [5.1] with the current densities depending on the fault current duration t_F. These diagrams depict the permissible long-term current for earthing strips and conductors with circular cross section.

5.8 Soil resistivity and conductivity

The soil, like metallic conductors, presents a resistance and conductivity to the circulation of currents, depending on its physical and chemical properties. When a voltage is applied to a metallic conductor with uniform cross section and homogeneous material,

Table 5.7: Soil resistivities at 50 and 60 Hz

Type of soil	Earth resistivity (in Ω·m)
Sea water	1
Marshy soil	5 to 40
Loam, clay, humus	50 to 350
Sand	200 to 2500
Gravel	2000 to 3000
Lime stone	350
Weathered rock	up to 1000
Sand stone	2000 to 3000
Granite	~ 3000 to 50 000
Moraine	up to 30 000

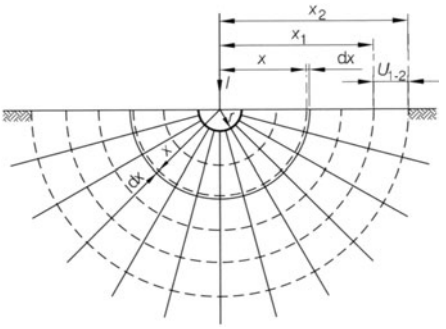

Figure 5.8: Hemispherical earthing electrode, radius of sphere r

the determination of its resistivity and resistance is a simple task. However, when dealing with conduction of currents through the earth, the analysis of the problem becomes very complex, due to the huge dimensions of the earth as compared to the metallic conductors and due to the great variety of its characteristics.

For example, experimental tests made with red clay soil indicated that with only 10 % moisture content, the resistivity was over 30 times that of the same soil having a moisture content of about 20 %. For values above 20 %, the resistivity is not affected too much, but below 20 % it increases rapidly with a decrease in moisture content.

Many studies have been published on *earth conductivity* depending on soil structure and dimensions, most of them seem too theoretical and require complicated mathematical developments. A mathematical model of high complexity is not worth-wile, if its application is dependent on parameters of dubious origin, such as apparent resistivity, thickness of layers, etc.

Today there is a trend to a practical simplification of earthing studies, as a result of the high degree of uncertainties involved in the determination of the relevant parameters and verification tests.

Resistivity of typical soils are indicated in Table 5.7.

5.9 Calculation of earthing resistance

5.9.1 Spherical electrode

A *spherical electrode* either buried completely in the ground or only with its lower hemisphere is the least difficult to be analysed (Figure 5.8). In the latter case, assuming uniform *soil resistivity*, a current I flowing from the hemisphere into the ground produces a current density i in the surrounding soil being

$$i = I_E/(2\pi\chi^2) \quad ; \tag{5.9}$$

where i is the current density, I_E the total current (A) and χ the distance from the centre of the sphere.

According to Ohm's Law, such a current produces in the soil an electrical field strength of

$$E(\chi) = i \cdot \varrho_E = I_E \cdot \varrho_E/(2\pi\chi^2) \quad , \tag{5.10}$$

where ϱ_E is the soil resistivity (Ω·m).

The voltage, as the line integral of the field strength from the surface of the hemisphere to any distance χ, is

$$U = \int_r^{\chi} E(x)\mathrm{d}x = \frac{I_\mathrm{E} \cdot \varrho_E}{2\pi} \int_r^{\chi} \frac{\mathrm{d}x}{x^2}$$

or

$$U = \frac{I_\mathrm{E} \cdot \varrho_\mathrm{E}}{2\pi} \left(\frac{1}{r} - \frac{1}{\chi}\right) \quad , \tag{5.11}$$

where r is the radius of the spherical electrode, see Figure 5.8.
The total voltage between the hemispherical electrode and a far distant point with $\chi \to \infty$ will then be

$$U_\infty = I_\mathrm{E}\varrho_\mathrm{E}/(2\pi r) \quad . \tag{5.12}$$

Thereof, the total *earthing resistance* becomes

$$R_\mathrm{E} = U/I = \varrho_\mathrm{E}/(2\pi \cdot r) \quad , \tag{5.13}$$

where the resistivity has been considered as constant in the whole considered part of subsoil.
As an example, a hemisphere with a radius of $r = 1$ m embedded in soil having the resistivity $\varrho_\mathrm{E} = 1000\ \Omega \cdot \mathrm{m}$ will have an earthing resistance of

$$R_\mathrm{E} = 1000/(2\pi \cdot 1) \approx 160\,\Omega \quad .$$

From equation (5.11) it can be concluded that most of the resistance is encountered in the close vicinity around the electrode. Thus 50 % of the total resistance is contained within one meter from the electrode ($\chi = 2r$) and 90 % is contained within nine meters beyond the electrode ($\chi = 10r$).

5.9.2 Earthing rods

The calculation of the earth resistance of simple *earthing rods* buried in homogeneous soil, despite not practically encountered, can be determined without complex mathematical developments. Table 5.8 shows formulae for calculation of earth resistance for some types of earth electrodes.
Figure 5.9 shows the earthing resistance of one ground rod of length L and diameter d for various earth resistivity in homogeneous soils.
The earthing resistance of rods can be obtained from

$$R_\mathrm{E} = \varrho_\mathrm{E}/(2\pi L) \cdot \ln(4L/d) \quad . \tag{5.14}$$

If the rods are moderately close to each other, the overall resistance will be higher than if the same number of rods were spaced apart. The increase in resistance depends on the number of rods involved.
Three rods with 19 mm diameter and 3 m length in parallel and spaced 3 m apart will have an approximately 15 % higher resistance than when being arranged with a wide distance apart. Four rods arranged in a square with 3 m long sides would have a resistance higher by 25 % (see Figure 5.10).
Two rods reach approximately 60 % of the resistance of one rod, three rods 40 % and four rods about 33 %.
Figure 5.11 shows the variation of resistance with rod length for various diameters. The curves have been drawn for a ground resistivity of 100 $\Omega \cdot$ m.
If the spacing between *parallel earthing rods* is wide compared with the length of the individual rods, the resistance will be reduced in proportion to the number of rods.

Table 5.8: Formulae to calculate the earthing resistance

Type of earth electrode	Schematic representation	Earthing resistance
Hemisphere diameter d	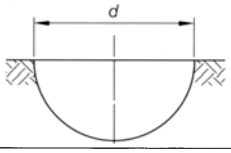	$R_E = \varrho_E/(\pi \cdot d)$
One earthing rod	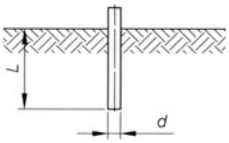	$R_E = \varrho_E/(2\pi L) \cdot \ln(4L/d)$
Several earthing rods	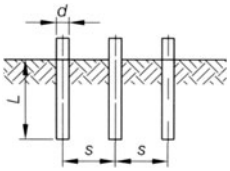	$R_E = \varrho_E/(2\pi L) \cdot \ln(2L/r_e)$ (r_e see (5.16) and (5.17))
Horizontally buried electrodes, circular cross section, independent of depth t	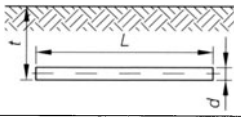	$R_E \sim \varrho_E/(2\pi L) \cdot \ln(2L/d)$
Horizontally buried electrodes, crosswise arranged, depth t	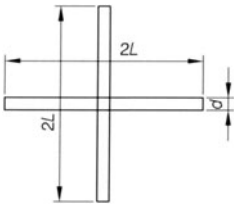	$R_E = \varrho_E/(2\pi L) \cdot \left(\ln\frac{4L}{d} + \ln\frac{2L}{t} + 2{,}91\right)$
Ring electrode, ring diameter D, independent of depth t	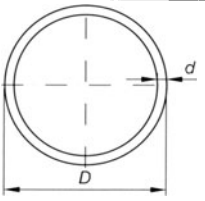	$R_E = \varrho_E/(\pi^2 D) \cdot \ln(2\pi D/d)$

If the rods are close together, each rod will be in the intensive electrical field of its neighbour. If the rods are very close together, then the overall resistance becomes

$$R_E = \varrho_E/(2\pi L) \cdot \ln(2L/r_e) \quad , \tag{5.15}$$

where r_e represents the radius of an equivalent rod.
For two, three or four ground driven rods in parallel and symmetrical configuration, the equivalent radii would be with two rods

$$r_e = \sqrt{d/2 \cdot s} \quad , \tag{5.16}$$

with three rods

$$r_e = \sqrt[3]{d/2 \cdot s^2} \tag{5.17}$$

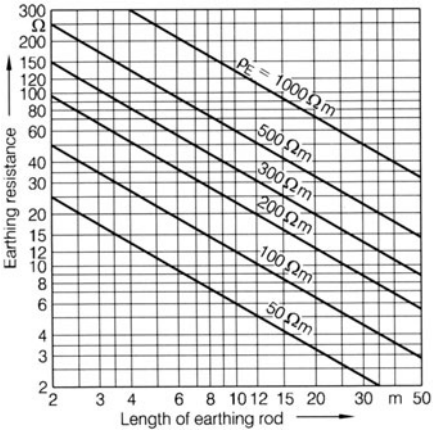

Figure 5.9: Earthing resistance of earthing rods

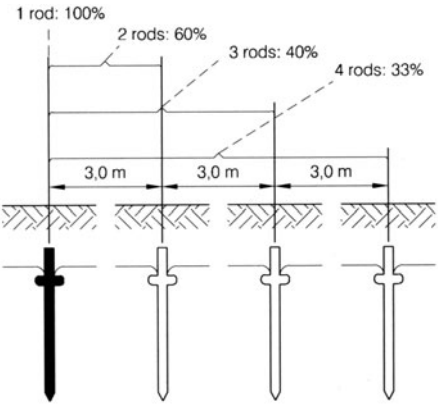

Figure 5.10: Earthing resistance of parallel rods in relation to a single rod

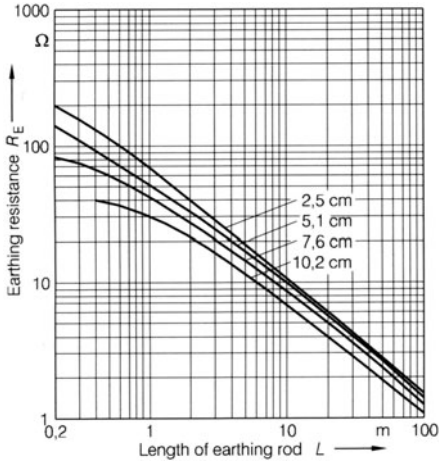

Figure 5.11: Earthing resistance R_E of an earthing rod depending on diameter and length, soil resistivity $\varrho_E = 100\ \Omega{\cdot}m$

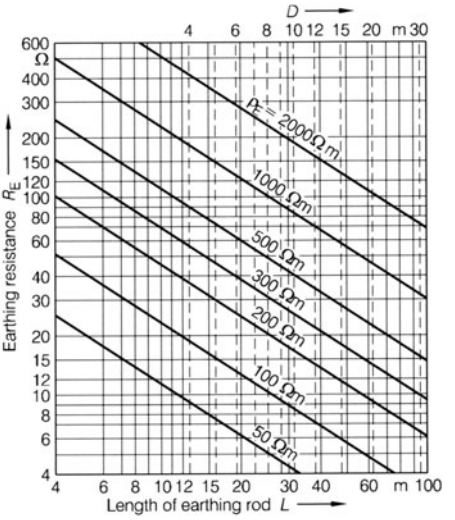

Figure 5.12: Earthing resistance R_E of electrodes arranged linearly or as horizontal ring in a homogeneous soil.
L length, D diameter of ring

and with four rods

$$r_e = \sqrt[4]{\sqrt{2} \cdot d/2 \cdot s^3} \quad , \tag{5.18}$$

where r_e is the equivalent radius (m), d the individual rod diameter (m) and s the separation between adjacent rods (m).

5.9.3 Horizontally arranged electrode wires (counterpoises)

Counterpoise wires arranged radial or as rings and rigidly connected with the tower are commonly used for earthing of supports. In [5.1], annex H, formulae are given for

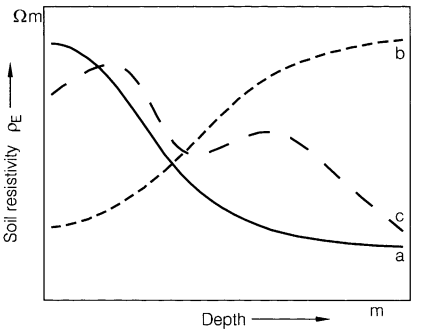

Figure 5.13: Examples for the qualitative variation of soil resistivity with depth

frequently used counterpoises. For *radial arranged electrodes* it applies

$$R_E = \varrho_E/(\pi L) \cdot \ln(2\,L/d) \quad , \tag{5.19}$$

for *ring electrodes*

$$R_E = \varrho_E/(\pi^2 D) \cdot \ln(2\,\pi D/d) \tag{5.20}$$

and for earthing meshes

$$R_E = \varrho_E/2\,D_A \quad , \tag{5.21}$$

where L is the length of the counterpoise, D the diameter of the ring electrode, d the diameter of the electrode in case of rods or stranded conductors or half of the width in case of stripes and D_A the diameter of a circle with the same area as the area of the earthing mesh.
Material and cross-sectional dimensions of the counterpoises are less important according to (5.19) to (5.21). Experience confirms as well, that a mechanically sufficient counterpoise complies with all the electric requirements. Therefore, copper-clad steel wires are frequently adopted today instead of copper wires, galvanized steel wires or stripes.

5.10 Measurements of soil resistivity

5.10.1 Basic principles

Knowledge of *soil resistivity* is an imperative condition to determine the earthing resistance correctly, the latter being proportional to the resistivity. According to [5.1], measurements should be carried out using a *four-point method*, e. g. the Wenner Method, to evaluate the soil resistivity for various depths.
If the *soil resistivity* were constant, it would suffice to measure the earth resistance of an earthing rod and the resistivity would be obtained from

$$\varrho_E = 2\,\pi \cdot R_E \cdot L/[\ln(4\,L/d)] \quad . \tag{5.22}$$

If ϱ_E were constant, a variation of the length L or the diameter d would accordingly change the resistance R_E. In most practical cases, the soil resistivity ϱ_E changes depending on the *stratification* of the soil, however. The values ϱ_E obtained by this procedure depend on geometric data of the electrode and may not be transferred to other electrodes. The soil resistivity measured on average is also called *apparent soil resistivity.* Figure 5.13 shows typical variations of soil resistivity with depth. When measuring soil resistivity, these facts have to be adequately considered.

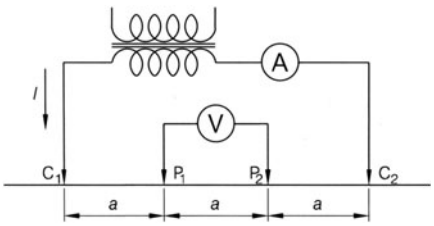

Figure 5.14: Principle diagram of an earthing tester

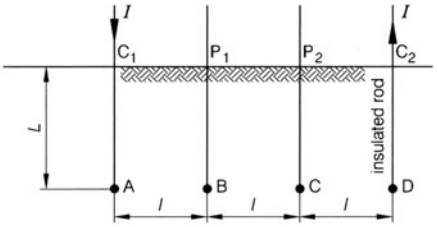

Figure 5.15: Current injection into the soil

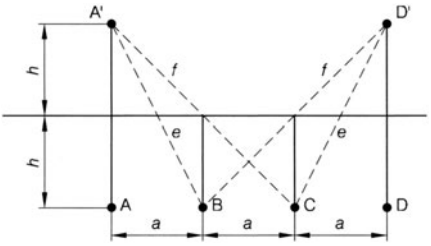

Figure 5.16: Evaluation of earthing measurements by means of reflection

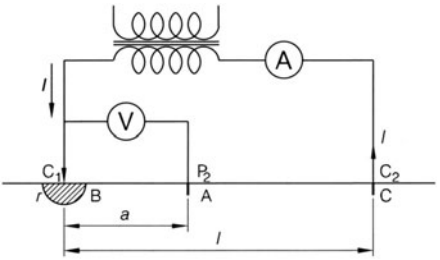

Figure 5.17: Three-point method to measure the resistivity ϱ_E

5.10.2 Measuring methods

The most frequently used method to determine the *soil resistivity* depending on the depth is the *four-point method*, also called *Wenner Method* [5.11], where an *earth megger* [5.12] is used (see Figures 5.14 to 5.16). The four rods are arranged with the same spacing a; five measurements with the spacing $a = 2$ m, 4, 8, 16 and 32 m are carried out. For each measurement a current I is injected between the probes C_1 and C_2 and the voltage between the points P_1 and P_2 is measured. With increasing spacing a, the measured soil resistivity applies for greater depths since the current flows through soil strata in greater depth. The probes C_1 and C_2 have to be cylindrical and short such that their resistance is low in relation to that of the soil. The voltage U occurring in a distance χ from the hemispherical electrode is

$$U = \varrho_E I_E/(4\pi\chi) \quad . \tag{5.23}$$

Since the subsoil performs like a hemisphere with respect to current expansion the mirror reflections according to Figure 5.16 can be applied with reflections of the probes A and D, which correspond to C_1 and C_2 of Figure 5.14, respectively, in the height h above the surface. The total voltages at the points B and C are due to the currents flowing through the rods A and D and their mirror images

$$U_B = \frac{\varrho_E I}{4\pi}\left(\frac{1}{e} + \frac{1}{a} - \frac{1}{f} - \frac{1}{2a}\right) = \frac{\varrho_E I}{4\pi}\left(\frac{1}{2a} + \frac{1}{e} - \frac{1}{f}\right) \tag{5.24}$$

and

$$U_C = \frac{\varrho_E I}{4\pi}\left(-\frac{1}{e} - \frac{1}{a} + \frac{1}{f} + \frac{1}{2a}\right) = \frac{\varrho_E I}{4\pi}\left(-\frac{1}{2a} - \frac{1}{e} + \frac{1}{f}\right) \quad . \tag{5.25}$$

The voltage difference between B and C is

$$U_{BC} = U_B - U_C = \frac{\varrho_E I}{4\pi}\left(\frac{1}{a} + \frac{2}{e} - \frac{2}{f}\right) = \frac{\varrho_E I}{4\pi a}\left(1 + \frac{2a}{e} - \frac{2a}{f}\right) \quad . \tag{5.26}$$

Therefore, it applies

$$R_E = \varrho_E/(4\pi a)\,(1 + 2a/e - 2a/f) \tag{5.27}$$

and

$$\varrho_E = 4\pi \cdot a\, R_E/\,(1 + 2a/e - 2a/f) \quad . \tag{5.28}$$

Using $e = \sqrt{4h^2 + a^2}$ and $f = \sqrt{4h^2 + 4a^2}$, it results

$$\varrho_E = 4\pi \cdot a\, R_E \,/\, \left(1 + 2a/\sqrt{4h^2 + a^2} - 2a/\sqrt{4h^2 + 4a^2}\right) \quad . \tag{5.29}$$

In practice, it is $h \ll a$. Therefore, h^2 may be neglected compared with a^2 in (5.29) and it is obtained

$$\varrho_E = 2\pi \cdot a \cdot R_E \quad . \tag{5.30}$$

The *soil resistivity* results from the probe distance a and the recorded resistance R_E.

5.11 Measurement of earthing resistance

The *earthing or footing resistance* of a tower can be measured using differing methods.

Fall-of-potential method with an earth megger

The earth megger is suited for measurements at earth electrodes or earthing systems of small or medium extent such as single rod earth electrodes, strip earth electrodes, earth electrodes of towers with attached or lifted off earth wires, high-voltage earthing systems and separation of low-voltage earthing systems. The frequency of the alternating voltage used should not exceed 150 Hz. The earth electrode tested, the probe and auxiliary electrodes should lie in a straight line as far apart as possible. The distance of the probe from the earth electrode tested should be at least 2,5 times the maximum extension of this electrode, but not less than 20 m. The distance between the probe and the auxiliary electrode should be at least 4 times the maximum extension of the electrode tested, but not less than 40 m (see [5.13]).

High-frequency earth tester

The *high-frequency earth tester* facilitates the measurement of the resistance to earth of a single tower without lifting off the earth wire. The frequency of the measuring current should be so high that the recurrent network impedance of the earth wire and the neighbouring towers becomes high, representing a practically negligible shunt circuit to the earthing system of a single overhead line tower (see [5.14]). From practical applications it could be realized that with this instrument less reliable results can be expected when compared with earth meggers.

Heavy-current injection method

The *heavy-current injection method* is used particularly for the measurement of the resistance to earth of large earthing systems but also if *transferred potentials*, i. e. through metallic pipes, are to be taken into account and, therefore, greater distances between the earthing system of the relevant tower and the remote earth electrode are necessary. By applying an alternating voltage with approximately the system frequency between the earthing system and a remote earth electrode, a test current I_m is injected into the earthing system, leading to a measurable potential rise of the earthing system. Earth wires and cable sheaths with earth electrode effect which are operationally connected

to the earthing system, should not be disconnected for the measurement. The modulus of the *impedance to earth* Z_E is given by:

$$Z_E = U_{em}/I_m \cdot r \quad , \tag{5.31}$$

where U_{em} is the measured voltage between the earthing system and a probe in the area of the reference earth, the remote earth in V; I_m is the measured test current in A; r is the reduction factor of earth wires, which may be determined by calculation (see clause 5.3.5) or measurements. For overhead lines without earth wires $r = 1$ applies. The distance between the tested earthing system and the remote earth electrode should be not less than 5 km, so far as possible. The test current should be selected at least so high that the measured voltages are greater than possible interference and disturbance voltages. This is generally ensured for test currents above 50 A. The internal resistance of the voltmeter should be at least 10 times the resistance to earth of the probe. With currents below 50 A, suitable measurement results can only be achieved in smaller installations.

An *earth tester* is used as measuring instrument, the principle of which is explained by Figure 5.17. The controllable measuring current is injected into the soil through the probes C_1 and C_2. The voltage is taken between the probes C_1 and P_2. This method is also called *three-point method.* If the electrode C_1 is assumed as a hemispherical electrode having the radius r, the potential U_{BB} occurs at its surface due to the current I

$$U_{BB} = \varrho_E \cdot I/2\pi r \quad . \tag{5.32}$$

The voltage between the probes at points B and C is

$$U_{BC} = \varrho_E I/[2\pi(l - r)] \quad , \tag{5.33}$$

where l is the distance between points B and C (see Figure 5.17). The voltage of the probe at point B against the remote earth, the *reference earth*, will then be

$$U_{B\infty} = U_{BB} - U_{BC} = \frac{\varrho_E \cdot I}{2\pi}\left(\frac{1}{r} - \frac{1}{l-r}\right) = \frac{\varrho_E \cdot I}{2\pi}\frac{l}{r(l-r)} \quad . \tag{5.34}$$

According to Figure 5.17, the voltage between points A and B is

$$U_{AB} = \varrho_E \cdot I/2\pi a \tag{5.35}$$

and the voltage between points A and C will be

$$U_{AC} = -\varrho_E \cdot I/[2\pi(l - a)] \quad . \tag{5.36}$$

Thereof, the voltage of the probe at point A to the remote earth results to be

$$U_{A\infty} = U_{AB} + U_{AC} = \frac{\varrho_E \cdot I}{2\pi}\left(\frac{1}{a} - \frac{1}{l-a}\right) \quad . \tag{5.37}$$

By combining equations it results, for the voltage between A and B, from equations (5.34) and (5.37)

$$U = U_{B\infty} - U_{A\infty} = \frac{\varrho_E \cdot I}{2\pi}\left(\frac{1}{r} - \frac{1}{l-r} - \frac{1}{a} + \frac{1}{l-a}\right) \quad . \tag{5.38}$$

Due to $U = R_E I$ then it applies

$$R_E = \frac{\varrho_E}{2\pi}\left(\frac{1}{r} - \frac{1}{l-r} - \frac{1}{a} + \frac{1}{l-a}\right) \quad . \tag{5.39}$$

Figure 5.18 depicts the qualitative dependency between *earthing resistance* R_E and the distance a. If the voltage probe P_2 is situated close to the current probe C_2 or close to probe C_1 which represents the electrode or earthing system to be tested, no useful

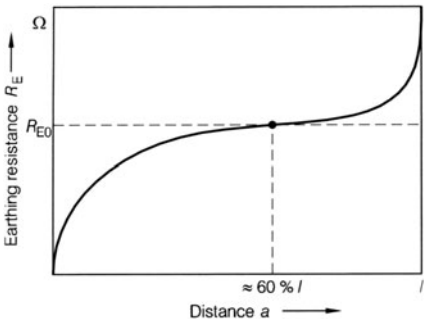

Figure 5.18: Variation of earthing resistance depending on the distance a between probes C_1 and P_2

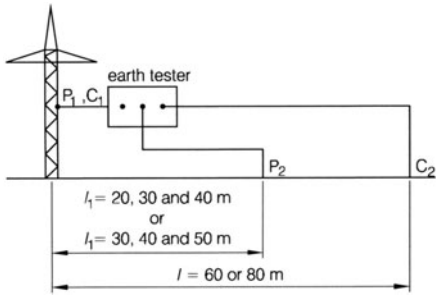

Figure 5.19: Location of potential probes P_1, P_2 and current probes C_1, C_2 to measure the earthing resistance of overhead lines

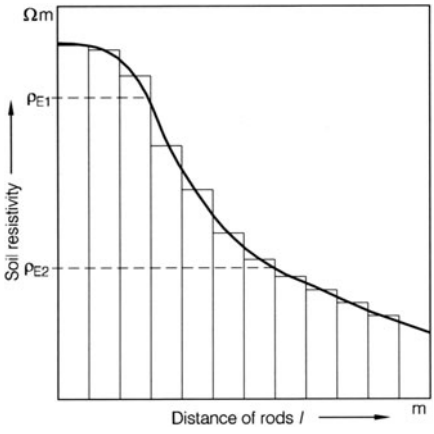

Figure 5.20: Soil resistivity depending on the distance of earthing rods

results are obtained. For medium-range values of a, R_E represents a parallel line to the abscissa; the resistance is independent of U and I and is equal to R_{E0}. The distance between C_1 and C_2 must be long enough, so that no interference exists between the probe C_2 and the system to be tested. The most favourable value for a is given by $0{,}62\,l$.

The consideration presented here for a hemispherical electrode applies also to other shapes of earthing electrodes provided the measurements are carried out with adequate distances a and l (Figure 5.17). For overhead lines, three measurements are carried out with the arrangement according to Figure 5.19, varying a from 30 to 50 m in 10 m steps, whereby $l = 60$ m is kept constant. Each of the three measurements should not deviate by more than 20 % from the mean value. If the differences are higher, the distance between probes C_1 and C_2 (Figure 5.17 or 5.19) should be increased to 80 m and an additional series of measurements should be carried out.

Example: The measurements carried out with a distance of $l = 60$ m yield the results given in Table 5.9 for towers A and B. The highest deviation $100 \cdot (R_{E\,max} - R_{E\,mean})/R_{E\,mean}$ is more than 20 % at tower B. Therefore, an additional measuring series should be carried out using $l = 80$ m.

Table 5.9: Measurement of earthing resistance R_E

	Distance a			Mean	Maximum
	30 m	40m	50 m	value	difference
Tower A	12,0 Ω	13,0 Ω	15,0 Ω	13,3 Ω	12,8 %
Tower B	7,5 Ω	10,5 Ω	12,0 Ω	10,1 Ω	25,7 %

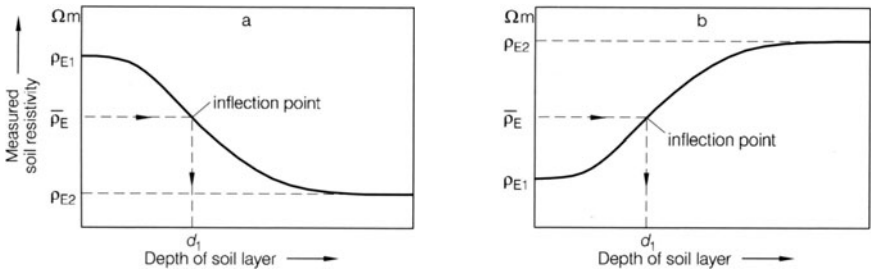

Figure 5.21: Replacing the measured soil resistivity by a two-layer soil structure with one layer having the depth d_1 and the resistivity ϱ_{E1} and the resistivity ϱ_{E2} in the underlying soil; a) soil resistivity decreasing with depth, b) soil resistivity increasing with depth

5.12 Earthing resistance in non-homogeneous soils

5.12.1 Soil resistivity in a two-layer soil structure

The readings of soil resistivity ϱ measured by varying probe distances a and l reflect really the *resistivity* of the soil layers *in non-homogeneous soils* as the depth increases vertically. The resulting diagrams suggest the existence of an infinite number of deeper and deeper layers, as per Figure 5.20.

However, the formulae presented for calculating the ground resistance (Table 5.8) use only one resistivity value as a homogeneous soil was considered. In these formulae, the mean resistivity or the apparent earth resistivity has to be used.

In view of this problem, several investigations have been carried out, trying to find out a mathematical model for the calculation of *earthing resistance in real soils*, i. e. considering more than one layer of soil resistivity. One of the methods with more widespread use consists in stratifying the soil in two resistivity layers, that would represent the effect of multiple layers in reality. The first layer reaches a depth d_1 and is characterized by a resistivity ϱ_{E1}, while the second layer has an infinite depth and a resistivity ϱ_{E2}. For the great majority of lines, it is possible to determine a two-layer soil structure that can represent typical soils for earthing purposes. In some cases, depending on the resistivity measurements, it might not be possible to define a *two-layer soil structure* and hence a *three-layer soil model* is considered.

According to [5.15], the formula for computing the earth resistivity as a function of the depth is

$$\varrho_E = \varrho_{E1} + 4\,\varrho_{E1} \sum_{n=1}^{\infty} \left(\frac{k^n}{\sqrt{1 + (2nd_1/a)^2}} - \frac{k^n}{\sqrt{4 + (2nd_1/a)^2}} \right) \quad , \tag{5.40}$$

where $k = (\varrho_{E2} - \varrho_{E1})/(\varrho_{E1} + \varrho_{E2})$ is called *reflection coefficient*. There, ϱ_{E1} is the resistivity of the first layer and ϱ_{E2} is the resistivity of the deeper layer of the soil. The reflection coefficient k will be positive if $\varrho_{E2} > \varrho_{E1}$ and negative if $\varrho_{E2} < \varrho_{E1}$. This identifies an increasing or decreasing curve of ϱ_E depth, which is reflected by the Figures 5.21 a and b. The values ϱ_{E1} and ϱ_{E2} represent the earth resistivity of the uppermost and lowermost soil strata. The depth d_1 of the first layer corresponds to the inflection

Table 5.10: Factor M_0 for calculating the average resistivity of a soil in a two-layer model

$\varrho_{E2}/\varrho_{E1}$	M_0	$\varrho_{E2}/\varrho_{E1}$	M_0	$\varrho_{E2}/\varrho_{E1}$	M_0
0,0010	0,6839	0,75	0,9480	15,50	1,418
0,0020	0,6864	0,80	0,9593	16,00	1,421
0,0025	0,6847	0,85	0,9701	16,50	1,423
0,0030	0,6850	0,90	0,9805	17,00	1,425
0,0040	0,6855	0,95	0,9904	17,50	1,427
0,0045	0,6858	1,00	1,0000	18,00	1,429
0,0050	0,6861	1,50	1,078	18,50	1,430
0,0060	0,6866	2,00	1,134	19,00	1,432
0,0070	0,6871	2,50	1,177	20,00	1,435
0,0080	0,6877	3,00	1,210	30,00	1,456
0,0090	0,6882	3,50	1,237	40,00	1,467
0,010	0,6887	4,00	1,260	50,00	1,474
0,015	0,6914	4,50	1,278	60,00	1,479
0,020	0,6940	5,00	1,294	70,00	1,482
0,030	0,6993	5,50	1,308	80,00	1,484
0,040	0,7044	6,00	1,320	90,00	1,486
0,050	0,7095	6,50	1,331	100,00	1,488
0,060	0,7145	7,00	1,340	110,00	1,489
0,070	0,7195	7,50	1,349	120,00	1,490
0,080	0,7243	8,00	1,356	130,00	1,491
0,090	0,7292	8,50	1,363	140,00	1,492
0,10	0,7339	9,00	1,369	150,00	1,493
0,15	0,7567	9,50	1,375	160,00	1,494
0,20	0,7781	10,00	1,380	180,00	1,495
0,25	0,7981	10,50	1,385	200,00	1,496
0,30	0,8170	11,00	1,390	240,00	1,497
0,35	0,8348	11,50	1,394	280,00	1,498
0,40	0,8517	12,00	1,398	350,00	1,499
0,45	0,8676	12,50	1,401	450,00	1,500
0,50	0,8827	13,00	1,404	640,00	1,501
0,55	0,8971	13,50	1,408	1000,00	1,501
0,60	0,9107	14,00	1,410	—	—
0,65	0,9237	14,50	1,413	—	—
0,70	0,9361	15,00	1,416	—	—

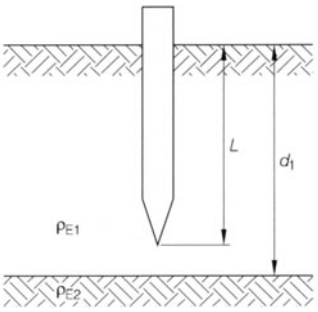

Figure 5.22: Earthing rod in a two-layer soil structure, where $L < d_1$.

point of the curve (see Figure 5.21) and can be calculated from the *mean resistivity* $\overline{\varrho}_E$ which is obtained from

$$\overline{\varrho}_E = M_0 \cdot \varrho_{1E} \quad . \tag{5.41}$$

From Table 5.10, the factor M_0 as a function of the inflection point is determined depending on $\varrho_{E2}/\varrho_{E1}$. Having $\overline{\varrho}_E$, the depth d_1 is determined from Figure 5.21.
An application example for a two-layer model is given in clause 5.12.5. Within the formulae given in Table 5.8, the *mean resistivity* $\overline{\varrho}_E$ according to (5.41) is to be used.

5.12.2 Computation of earthing resistance in a two-layer soil structure

The *computation of the earthing resistance* depends on the type of earth electrode and the depth of the first layer in relation to the length of the earthing rod. The formulae given in Table 5.8 represent a relatively simple method for computation of the earthing resistance. If the rod is driven only into the upper layer, as shown in Figure 5.22, the resistance of the rod is deduced from the following formula

$$R_E = \frac{\varrho_{E1}}{2\pi L}\left[\ln(4L/d - 1) + \sum_{n=1}^{\infty}\frac{k^n}{2}\ln\frac{nd_1/L + 1}{nd_1/L - 1}\right] \quad . \tag{5.42}$$

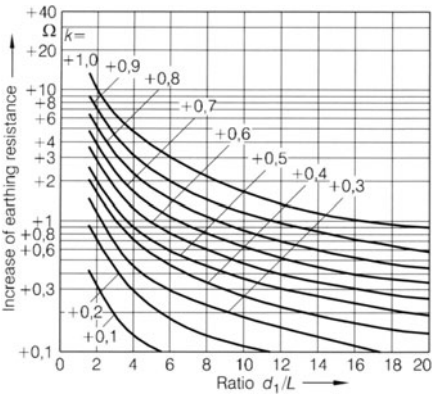

Figure 5.23: Correction of the earthing resistance of a driven rod computed by means of a one-layer soil structure, reflection coefficient positive, length of the earthing rod 3 m. $\varrho_{E1} = 100\ \Omega m$ $(L < d_1)$

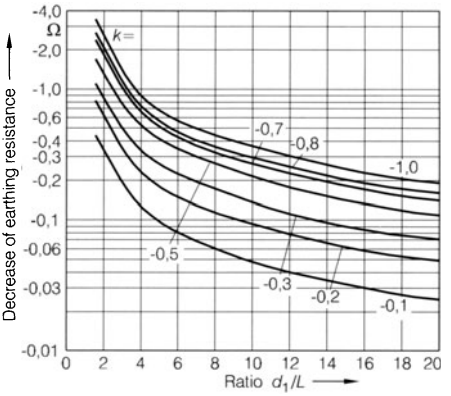

Figure 5.24: Correction of the earthing resistance of a driven rod computed by means of a one-layer soil structure, reflection coefficient negative, length of the earthing rod 3 m. $\varrho_{E1} = 100\ \Omega m$ $(L > d_1)$

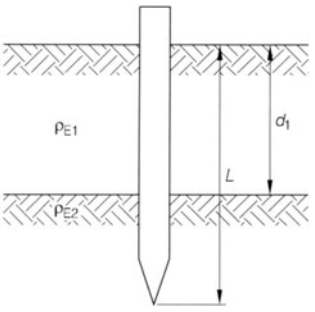

Figure 5.25: Earthing rod in a two-layer soil, where $L > d_1$.

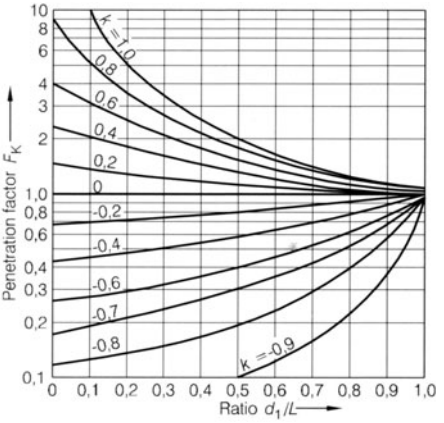

Figure 5.26: Penetration factor F_K for an earthing rod with $L > d_1$

The first term in this expression is the resistance of a rod having the length L driven into soil of resistivity ϱ_{E1}, and the second term represents the additional resistance due to the second layer. Figures 5.23 and 5.24 show respectively the increase or the decrease in resistance due to lower layers of higher or lower resistivity with different reflection coefficients k and the ratios d_1/L as parameters.
If, as shown in Figure 5.25, both layers are penetrated by the rod, then

$$R_E = F_K \cdot (R_{E1} + R_{Ea}) = \frac{\varrho_{E1}}{2\pi L} \frac{1+k}{1-k+2kd_1/L} \left[\ln \frac{2L}{d} + \sum_{n=1}^{\infty} k^n \ln \frac{nd_1/L+1}{(2n-2)d_1/L+1} \right], \quad (5.43)$$

where F_K is called *penetration factor* being equal to

$$F_K = \frac{1+k}{1-k+2k \cdot d_1/L} \quad . \quad (5.44)$$

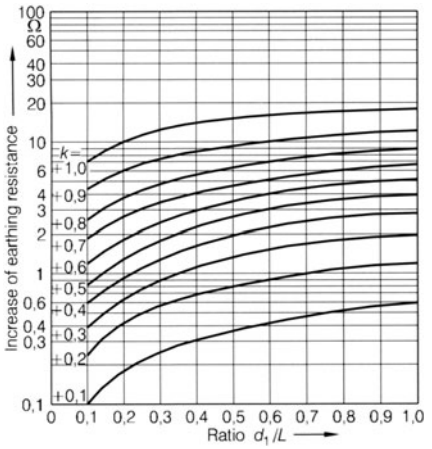

Figure 5.27: Correction of the earthing resistance of a driven rod computed by means of a one-layer soil structure, reflection coefficient positive, length of the earthing rod 3 m. $\varrho_{E1} = 100\ \Omega m$ $(L < d_1)$

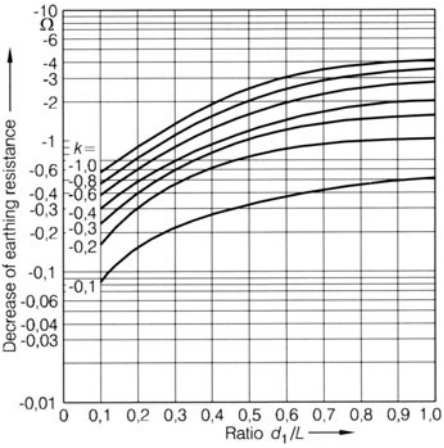

Figure 5.28: Correction of the earthing resistance of a driven rod computed by means of a one-layer soil structure, reflection coefficient negative, length of the earthing rod 3 m. $\varrho_{E1} = 100\ \Omega m$ $(L > d_1)$

R_{E1} is the resistance of the rod driven in uniform soil of resistivity ϱ_{E1}, R_{Ea} is the additional resistance due to the second layer. Figure 5.26 gives the penetration factor F_K as a function of d_1/L ratio with the reflection coefficient k as a parameter.
Figures 5.27 and 5.28 show the increase or decrease, respectively, of the resistance R_E for positive or negative values of k, respectively.

5.12.3 Computation of earthing resistance by means of the apparent resistivity

Another method often used for computing the *earthing resistance* consists in using the *apparent resistivity* [5.16]. This resistivity would represent the effect of all soil layers. Table 5.8 shows formulae for calculating the earthing resistance as a function of the apparent resistivity and of other parameters.
These formulae, however, don't yield good results for disymmetrical electrodes such as steel grillage and counterpoise wire systems of a tower.

5.12.4 Computation of earthing resistance of three-dimensional structures

In [5.17], a computer program was developed which calculates the potential in earth, the resistance and the favourable probe position in field resistance measurements for any *complex electrodes* in a two-layer earth structure. The theoretical study is carried out to the following sequence:

- Computation of earth potential due to a *point-type electrode.*
- Computation of earth potential for an *extended electrode* (practical case).
- Finally, determination of the resistance of extended electrodes based on the known expressions for the potential.

The *earthing resistance* of the electrode is then given by

$$R_E = \frac{1}{N \cdot I} \sum_{i=1}^{N} U_i \quad , \tag{5.45}$$

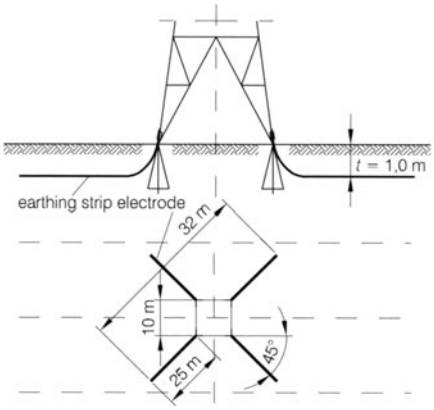

Figure 5.29: Tower with earthing system

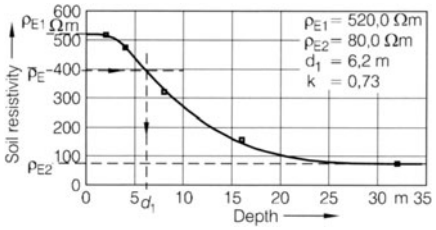

Figure 5.30: Measured values for soil resistivity

where N is the total number of points where the potential has been calculated, U_i are the potentials computed and I the current, for which the potentials are computed [5.17].

5.12.5 Example for computation of earthing resistance

The mean soil resistivity and the earthing resistance of a lattice tower, equipped with four radial *earthing strips* (counterpoise wires) of 25 m length and 5 mm diameter are to be computed. Figure 5.29 shows the arrangement.

The soil resistivity measured by means of the Wenner Method are depicted in Figure 5.30, connected by a curve. The soil resistivity $\varrho_{E1} = 520\ \Omega$m of the uppermost layer is represented by the intersection of the curve with the ordinate. The soil resistivity of the imaginary second layer ϱ_{E2} corresponds to the asymtote of the curve, being 80 Ωm. The depth of the first layer is obtained as follows:

- The ratio $\varrho_{E2}/\varrho_{E1}$ is $80/520 = 0{,}15$;
- From Table 5.10 it is obtained for $\varrho_{E2}/\varrho_{E1} = 0{,}15$: $M_0 = 0{,}757$;
- Then, mean soil resistivity, is $\overline{\varrho}_E = 520 \cdot 0{,}757 = 393\ \Omega$;
- For $\overline{\varrho}_E = 393\ \Omega$ $d_1 = 6{,}2$ m is obtained from Figure 5.30;
- The reflection coefficient is calculated as $k = (\varrho_{E2} - \varrho_{E1})/(\varrho_{E1} + \varrho_{E2}) = 0{,}73$.

To compute the earthing resistance, the formulae presented in Table 5.8 for crosswise-arranged earthing strips are used. The effective length L will be $25 + 10 \cdot \sqrt{2}/2 = 32$ m. Therefore, the earthing resistance follows from Table 5.8 to be

$$R_E = \frac{\varrho_E}{8\pi \cdot L}\left(\ln\frac{4L}{d} + \ln\frac{2L}{t} + 2{,}91\right) = \frac{393}{8\pi \cdot 32}\left(\ln\frac{4 \cdot 32}{0{,}005} + \ln\frac{2 \cdot 32}{1} + 2{,}91\right) =$$
$$= 8{,}41\ \Omega \quad .$$

Measurements resulted in 11,4 Ω for this example. The agreement with computation using the formulae from Table 5.8 is satisfactory for this relatively complex arrangement.

5.13 Practical rules for installation of earthing systems

5.13.1 Radial and ring-type earthing counterpoises

Radial and ring-type earthing counterpoises are frequently placed on the bottom of a trench or within the foundation base in depths between 0,5 and 1,0 m, where a frost-proof depth should be duly aimed at. The backfill is compacted to a low extent only, whereby gravel and stones should not contact the earthing counterpoises because of

their high resistance. If the encountered soil could corrosively attack the metallic earth electrode, it should be replaced by more suitable backfill. Earthing electrodes made of rectangular strips should be installed end up.

5.13.2 Vertically or obliquely driven earthing rods

The *earthing electrodes* driven in by mechanic force should be arranged at distances wider than the rod length. Damage should be avoided when driving.

5.13.3 Bonding between earthing electrodes

The *bonds for* establishing an *earth electrode* network must have at least the same electric conductivity, mechanical and thermal strength as the electrode itself. They should be corrosion-resistant and may not give rise to *contact corrosion.* They may not be damaged during the driving process. The joints, if any, must be protected against contact with electrolytes in their vicinity.

5.13.4 Earthing connections

The *earthing connections* should be as short as possible and protected against mechanical damage, especially when buried in the soil. At the surface, they should always be accessible. Earthing connections may be installed in concrete, as well. Special care should be taken at the transitions of bare earthing conductor from air to soil or concrete, because of the increased corrosion hazard.
The connections between *earthing conductors* should have a sufficient conductibility to avoid inadmissible temperatures also in case of faults. They should be protected against corrosion, in particular against contact corrosion if different metals are connected. In this case, protection against contact with an electrolyte is necessary. The connections may not get loose by its own and may not be disconnected without tools. These requirements apply also for connections between earthing conductors and earthing electrodes.

5.14 References

5.1 EN 50 341-1: Overhead electrical lines exceeding AC 45 kV. Part 1: General requirements – common specifications. Brussels, CENELEC 2001

5.2 DIN VDE 0141: Earthing of power installation above 1 kV. Berlin, DKE, 1989

5.3 EN 50 341-3-4: Overhead electrical lines exceeding AC 45 kV. Part 3-4: Set of index of National Normative Aspects for Germany. Brussels, CENELEC, 2001´

5.4 EN 50 341-3-1: Overhead electrical lines exceeding AC 45 kV. Part 3-1: National Normative Aspects for Austria. Brussels, CENELEC, 2001

5.5 EN 50 341-3-3: Overhead electrical lines exceeding AC 45 kV. Part 3-3: National Normative Aspects for Switzerland. Brussels, CENELEC, 2001

5.6 IEEE Standard 80-1986: Guide for safety in alternating current substation design. New York, IEEE 1986

5.7 IEEE Standard 81-1983: Recommended guide for measuring ground resistance and potential gradients in the Earth. New York, IEEE, 1983

5.8 IEC/TR2 60 479-1: Effects of current on human beings and live stock. Part 1: General aspects. Geneva, IEC, 1995

5.9 DIN VDE 0228, Part 2: Remedies in case of interference of telecommunication insulations by power installations. Berlin, DKE, 1987

5.10 IEC 60 724: Short-circuit temperature limits of electric cables with rated voltages of 1 kV (U_m = 1,2 kV) and 3 kV (U_m = 3,6 kV). Geneva, IEC, 2000

5.11 Wenner, F.: A method of measuring earth resistivity. Scientific papers of the Bureau of Standards 258 (1917), pp. 469 to 478

5.12 Digital earth tester MEGGER DET/3R & DET5/3D – User Guide, AVO-International, Kent CT179EN, England

5.13 Kinyon, A. L.: Earth resistivity measurements for grounding grids. IEEE Transactions on Power Apparatus and Systems. Vol. 80 (1961), pp. 795 to 800

5.14 Ufermann, J.; Jahn, K.: Hochfrequenz-Erdungsmessgerät. (High-frequency earthing tester). BBC-Nachrichten 49 (1967), pp. 132 to 135

5.15 Tagg, G. F.: Earth resistivity. London. George Newnes Ltd, 1964.

5.16 Darveniza, M. et al.: Modelling for lightning performance calculations. IEEE Transactions on Power Apparatus and Systems, Vol. 98 (1979), pp. 1900 to 1908

5.17 Dalawibi, F.; Mukhedkar, D.: Optimum design of substation grounding in a two-layer earth structure. IEEE Transactions on Power Apparatus and Systems, Vol. 94 (1975), pp. 252 to 271

6 Requirements on loading and strength

6.0 Symbols

Symbol	Signification
a	Span length
$\overline{a}$	Mean span length
a_g	Weight span
a_w	Wind span
A	Area exposed to wind
A_{ins}	Area exposed to wind at an insulator
A_T	Area exposed to wind at a tower
A_{TQ}	Area exposed to wind at a crossarm
C_I	Drag factor for ice covered conductor
C_{IH}	High probability drag factor
C_{IL}	Low probability drag factor
C_x	Drag factor, C_C for conductors, C_T for towers, C_{ins} for insulators
C_1, C_2	Parameters of the Gumbel distribution
D_I	Equivalent conductor diameter with ice accretion
d	Conductor diameter without ice
e	Exclusion limit
$f_{R,Q}$	Probability density function of strength or loading
F_N	Normal distribution function
$F_{R,Q}$	Cumulative distribution function of strength or loading
g	Gravitational acceleration
g_I	Ice load per unit length
$\overline{g}_I$	Ice load per unit length, mean value
g_{IH}	High probability reference ice load
g_{IL}	Low probability reference ice load
g_{IR}	Reference ice load
G_C	Combined wind factor for conductors
G_{IK}	Characteristic ice load
G_{ins}	Combined wind factor for insulators
G_L	Span factor for conductors
G_T	Combined wind factor for towers
G_q	Gust wind response factor
G_x	Structural resonance factor
H	Altitude above sea level
k	Factor for wind loads
k_g	Wind velocity gust factor
k_j	Factor related to the terrain category of the meteorological station
k_T	Terrain factor related to the area exposed to wind
K_d, K_n, K_z , $K_{\sigma I}$	Factors related to the determination of the reference ice load g_{IR}
L	General term for variable loading or strength
m	Mean value of a statistical distribution
m_C	Conductor mass per unit length
n	Number of variables or of observations in a statistical distribution
N	Number of components subjected to maximum load intensity, number of years
p_1, p_2, p_3	Parameters of distribution functions
P_S	Reliability, probability of survival
P_{SS}	Reliability, probability of survival of the system
P_f	Unreliability, probability of failure
q	Dynamic wind pressure
q_0	Reference dynamic wind pressure

Symbol	Signification
$q_{C,T}$	Dynamic wind pressure on conductors and towers
q_z	Dynamic wind pressure at the height z
Q_T	Load having a return period of T_r years, design load
Q	Load effect
Q_W	Wind load
$\overline{Q}_W$	Wind load mean value
$Q_{W\,ins}$	Wind load on insulators
Q_{WC}	Wind load on conductor
Q_{WI}	Wind load on ice covered conductor
Q_{WK}	Characteristic wind load
Q_{Wm}	Recorded wind load on conductors
Q_{Wth}	Calculated wind load on conductors
Q_{WT}	Wind load on support
Q_{WTQ}	Wind load on crossarm
R	Strength
$\overline{R}$	Mean value of strength
R_c	Characteristic strength
R_e	Strength with an exclusion probability of e
t_{RI}	Radial ice thickness
T	Temperature, absolute temperature
T_r	Return period
u	Variable of a cumulative distribution function
u_e, u_T	Variables of normal distribution
U	Use factor
$\overline{U}$	Mean use factor
$\overline{U}_g, \overline{U}_w$	Mean use factor for weight span, wind span
v, v_x	Coefficient of variation
$v_{R,Q}$	Coefficient of variation of strength or load
v_V	Coefficient of variation of wind velocity
V	Wind velocity
$\overline{V}$	Wind velocity, mean value of wind velocity
V_I	Wind velocity associated with icing
V_{IH}	High probability reference wind velocity associated with icing
V_{IL}	Low probability reference wind velocity associated with icing
V_{IT}	Wind velocity with return period T_r associated with ice load
V_R	Reference wind velocity
V_T	Wind velocity with return period T_r
V_x	Wind velocity at terrain category x
V_z	Wind velocity at height z, reference wind velocity
w_{CI}	Wind effect on ice covered conductors per unit length
x	General variable
$\overline{x}$	Mean value of a variable
x_T	Variable with return period T_r
X	Generalized function
z	Variable, height above ground
z_0	Roughness length
z_C	Average conductor height above ground
α	Roughness exponent
α_I	Factor used for ice load definition
γ_I	Partial factor for ice load
γ_M	Material partial factor
γ_U	Use factor coefficient
δ_I	Ice density
ϑ	Angle between wind direction and the perpendicular to conductor
θ	Supplement to the line angle
ξ	General variable
ϱ	Air density
ϱ_0	Air density at +15°C and sea-level, assumed as 1,285 kg/m^3

Symbol	Signification
ϱ_{I}	Specific weight force of ice
σ	Standard deviation
σ_{I}	Standard deviation of ice load g_{I}
σ_{M}	Standard deviation of use factor
σ_{Q}	Standard deviation of load Q
σ_{U}	Standard deviation of use factor
σ_{V}	Standard deviation of wind velocity V
ϕ_{N}, ϕ_{C}	Strength coefficient
ϕ	Angle between wind direction and crossarm axis
χ	Solidity ratio of a tower panel
$\Psi_{\mathrm{I,W}}$	Combination factor for ice and wind

6.1 Mechanical design of the overhead line system

6.1.1 Components and elements of an overhead line

Recent methods of *overhead line design* consider an overhead line as a system constituted by individual components [6.1, 6.2, 6.3]. The system design permits to coordinate the mechanical strength of these components taking care of the fact that a failure of any component may lead to the loss of the complete transmission capacity. As shown in Figure 6.1, the overhead line system is divided into four *components*: *supports*, *foundations*, *conductors* and *interfaces*. There, the supports may be suspension, angle, strain or dead-end towers.

Each component is divided into elements. In case of supports, these elements are steel, wood or concrete parts, bolts as well as guys and their fittings. Foundations consist of concrete bodies, piles, steel grillages or structures made up of concrete and steel piles. Conductors are not subdivided into elements. The elements of interfaces are insulators and hardware.

6.1.2 Reliability

The *reliability* of a system expresses the probability that this system will survive a given period, e. g. one year, without experiencing a failure. The reliability $P_{\mathrm{S}i}$, therefore, is related to the unreliability or *probability of failure* $P_{\mathrm{f}i}$ according to

$$P_{\mathrm{S}i} = 1 - P_{\mathrm{f}i} \quad . \tag{6.1}$$

In case of a system made up of several components, the reliability is equal to the product of the reliabilities of the components:

$$P_{\mathrm{SS}} = P_{\mathrm{S1}} \cdot P_{\mathrm{S2}} \ldots P_{\mathrm{Sn}} = \prod_{i=1}^{n} P_{\mathrm{S}i} \quad . \tag{6.2}$$

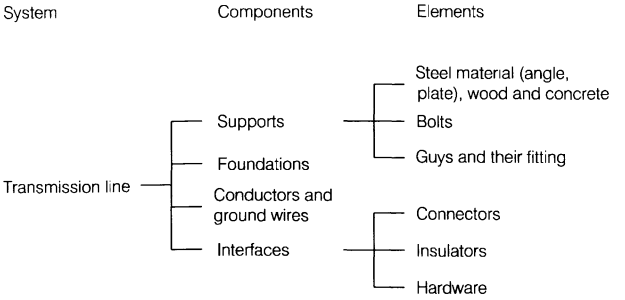

Figure 6.1: Components and elements of an overhead line

If the probability of failure of all components is less than 10^{-2} and the least reliable component has an unreliability approximately one order of magnitude higher than those of the other components, the reliability of the system P_{SS} can be approximated by that of the least reliable component, because of

$$P_{SS} = \prod_{i=1}^{n} (1 - P_{fi}) \sim 1 - \prod_{i=1}^{n} P_{fi} = 1 - \max P_{fi} = \min P_{Si} \quad . \tag{6.3}$$

This situation occurs naturally in many transmission lines. For example, in areas without ice, limitations of the everyday conductor stress to obviate vibration problems may limit the maximum tension under wind. This in turn increases very substantially the probability of survival of conductors, as compared to supports. Also, the insulators and hardware show a higher reliability than the supports. The reliability of a transmission line can be estimated using the following procedure:

- For each type of climatically produced load, at first the probability density function of loads f_Q is established. This function is adjusted to reflect the maximum loading intensity that might occur within the area crossed by the line. All available information on loads then will be considered by this function.
- The same procedure is applied to establish a probability density function of the strength f_R of the transmission line system. That may be complicated in general, however, it is simplified if an overhead line is designed such that one component has a considerably lower strength than all the others. In this case, the strength of the overhead line can be represented by the strength of the weakest component. It should be mentioned that both, the load and strength probability density functions, need to refer to the same critical action, e. g. the compression force of the highest strained member and its buckling strength.
  For a better practical evidence, it is preferable to use the *cumulative distribution function of strength* F_R instead of the *probability density function* f_R. The cumulative distribution function of strength F_R is given by

$$F_R(x) = \int_0^x f_R(\xi)\, d\xi \quad . \tag{6.4}$$

The probability density functions of loads and strengths can be used to estimate the overhead line reliability, as well as to design a line for a given reliability.

6.1.3 Calculation of reliability

Load effects Q and strengths R of transmission lines are random variables, each being described by its specific distribution function. Through technical studies [6.1, 6.3], it has been recognized that ice and wind variables may be represented by an extreme value distribution function , for instance the *Gumbel distribution*, the probability density function of which is given by equation (6.105) and their cumulative distribution function by equation (6.106). The cumulative distribution function (6.106) defines the probability that a given value x will not be exceeded.
The strengths can be represented by the Gaussian *normal distribution* with the probability density function according to (6.88) and the cumulative distribution function according to (6.89). In many cases, the strength distribution of components is characterized by a lower threshold. In such cases, the *logarithmic normal distribution* represents the strength characteristics more adequately. Its probability density function is described by (6.98) and its cumulative distribution function by (6.99). In clause 6.9, the parameters of the functions mentioned are explained.
When statistical parameters of loads and strengths and their statistical distribution functions are known, it is possible to calculate or estimate the yearly reliability or probability of survival P_S through analytic models or approximate methods. In the

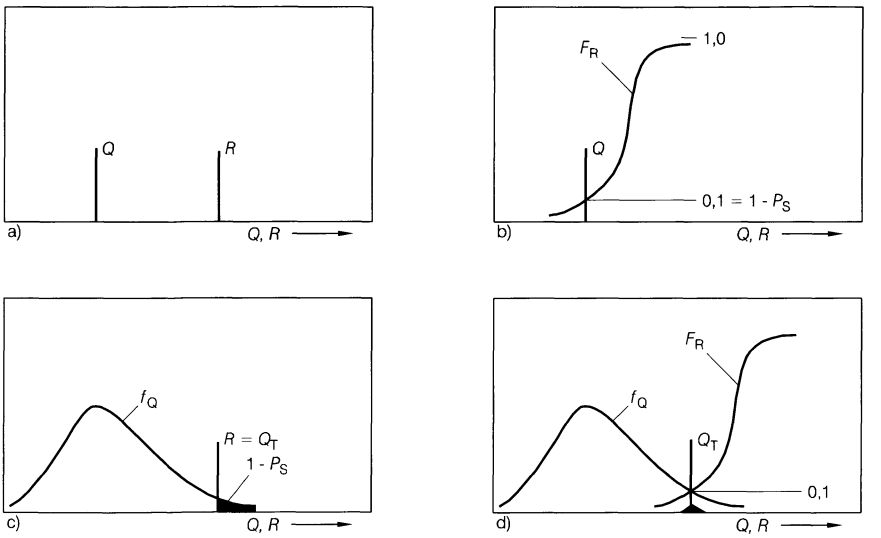

Figure 6.2: Relations between load effects and strengths
a) load effect and strength constant
b) load effect constant, strength statistically distributed
c) load effect statistically distributed, strength constant
d) load effect and strength statistically distributed

following relations, F_Q and F_R are defined as the cumulative distribution functions (CDF) of Q and R, while f_Q and f_R are the probability density functions (PDF) of the same variables, e. g. the load of a leg member and its strength. The yearly reliability is obtained from

$$P_S = P_S\left((R - Q) > 0\right) = 1 - \int_0^\infty f_Q(\xi) F_R(\xi)\, d\xi \quad . \tag{6.5}$$

Equation (6.5) can be solved numerically in each case by computer programs, if the functions f_Q and F_R are known. When only the average and standard deviation of Q and R variables are known, the reliability P_S can be obtained from (6.5), nevertheless. In this case, it is assumed that the loads follow the *Gumbel distribution* and the strengths the Gaussian normal distribution, whereby both distributions are defined by their mean value and standard deviation. Other procedures for estimating the reliability can be obtained from [6.2].
The reliability depends on the *load effect* parameters Q and the *strength* parameters R. Four cases can be considered as shown in Figure 6.2:

Case 1
The load effect Q and strength R are assumed to be constant values. If the strength R is higher than the load effect Q, the reliability will always be 1 or 100 % (Figure 6.2 a).

Case 2
The load effect Q is assumed as constant (deterministic) and the strength R is a statistically distributed variable. If the constant load is equal to the *design strength* R having an *exclusion limit* e, then the yearly reliability P_S is equal to $1 - F_R(e)$. If $e = 10$ %, then the reliability is 0,9. The reliability expresses the probability, that the load effect Q is less than the strength R (Figure 6.2 b).

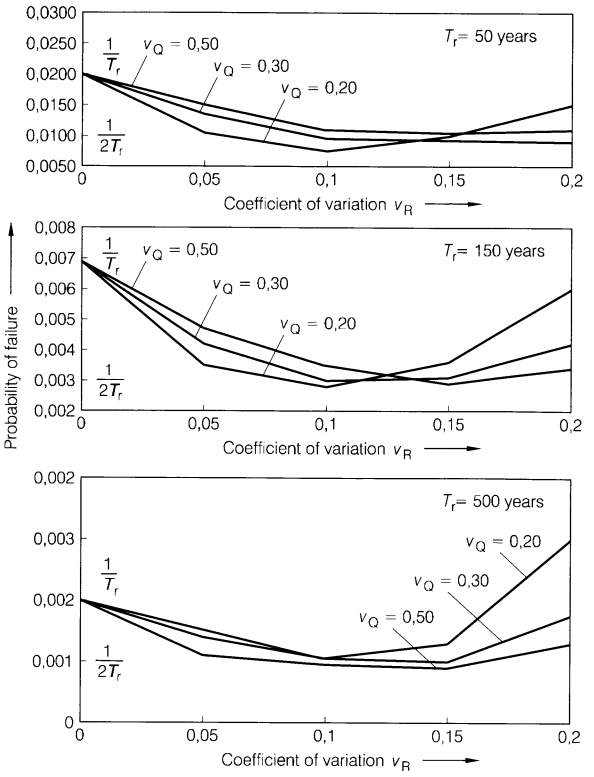

Figure 6.3: Probabilities of failure for differing coefficients of variation. For the load effects Q, the Gumbel distribution is assumed, and the Normal distribution for the strengths R.

Case 3

The load effect Q is a statistical distributed variable and the strength R is constant (deterministic). Since strength R is constant and equal to the design load Q_T, the yearly reliability depends only on the *return period* T_r and not on the coefficient of variation of load effects Q. The yearly reliability is $1 - 1/T_r$ (Figure 6.2 c).

Case 4

Load effect Q and strength R are statistically distributed variables (Figure 6.2 d). This is obviously the most general case and typical for transmission lines. The load effect Q with a return period T_r matches with the strength $\overline{R}(1 - u_e \cdot v_R)$. The yearly reliability depends on the parameters of the loads and the strengths.

According to [6.2], a major break-through in the application of probability methods for the design of overhead lines was achieved when a relation between load, and strength was established, leading to an almost constant probability of failure. This relation is

$$Q_T = (10\ \%)R \text{ or } Q_T = R_{e=10\%} \quad . \tag{6.6}$$

The load effect with a return period T_r is equal to the strength, which is characterized by an exclusion limit of 10 % or met with 90 % probability. Calculations of failure probabilities covering the most common combinations of load effects Q and strengths R for overhead lines are presented in Figure 6.3 for the return periods of load effects of 50, 150 and 500 years. There, the range of coefficients of variation of load effects Q scatters between 0,20 and 0,50 and that of the strengths R of the weakest component between 0 and 0,2.

From Figure 6.3, it can be seen that, for a constant strength, the yearly probability of failure is $1/T_r$. This probability of failure is reduced within the interesting range

Table 6.1: Yearly reliability for differing assumptions for loads and strengths

Case	Load			Strength			Reliability P_S
	Mean value	Coefficient of variation	Design value	Mean value	Coefficient of variation	Design strength	
1	Q	0	Q	R	0	$R > Q$	1,0
2	Q	0	Q	$\overline{R}$	v_R	$\overline{R}(1 - u_e v_R)$	$1 - \int_0^Q f_R \, dL =$ $1 - F_R(u_e) = 0{,}90$ (for $u_e = 1{,}28$)
3	$\overline{Q}$	v_Q	Q_T	R	0	R	$1 - \int_{Q_T}^{+\infty} f_Q \, dL$ $= 1 - 1/T_r$
4	$\overline{Q}$	v_Q	Q_T	$\overline{R}$	v_R	$\overline{R}(1 - u_e v_R)$	$1 - \int_0^{+\infty} f_Q F_R \, dL$ $\approx 1 - 1/(2T_r)$

of *coefficients of strength variation* up to 0,1 to the value $1/(2T_r)$ independent of the coefficients of variation of loads. Computations using other distribution functions lead to practically equal results. In Table 6.1, the formulae for the yearly reliability applying for the four considered cases are summarized.

Concerning the application to overhead lines, equation (6.6) offers more advantages. First, the loads are described by the return period: an approach very common in building design for *weather-related loads*. Second, the analysis of strength data shows that the *characteristic strength* is always above the 10 % exclusion limit. Therefore, the reliability calculated using equation (6.6) can be considered as a lower boundary of real values and leads to designs on the conservative side. Third, when using exclusion limits lower than 10 % in equation (6.6), for example of 2 %, the reliability P_S would be overestimated in cases where the characteristic strength would have a higher exclusion limit than 2 %, for example 10 %.

For the design of overhead lines, *return periods* of the climatic loads between 50 and 1000 years are used in general. From Figure 6.3, it can be seen that the yearly failure probability is between $1/T_r$ and $1/(2T_r)$ if the characteristic strength with 10 % exclusion limit is that equal to the load with the specified return period. Then, the yearly reliability will be

$$P_{S1} = 1 - P_{f1} \quad . \tag{6.7}$$

From this basic consideration, the probability of failure P_{fN} and the probability of survival P_{SN} for a *life cycle* of a line comprising N years can be determined by

$$P_{SN} = P_{S1}^N = [1 - P_{f1}]^N \quad . \tag{6.8}$$

The *probability of failure* P_{fN} during this life cycle period results from

$$P_{fN} = 1 - P_{SN} \quad . \tag{6.9}$$

Table 6.2 gives values for the probabilities of survival and of failure for return periods of climatic loads in 50, 150, 500 or 1000 years and life cycles of a line between 50 and 100 years. The design for loads with 50 year return period as limit loads results in theoretical failure probabilities between 39 and 87 %. Even for a design for loads with a return period of 1000 years, the *failure probabilities* reach between 2 and 10 % related to the life cycle of the line. According to relevant standards, in addition to the limit

Table 6.2: Relations between probability of occurrence of loads and reliabilities of overhead lines

Return period T_r of design loads (years)		50	150	500	1000
Lowest yearly reliability	P_{S1}	0,98 to 0,99	0,993 to 0,997	0,998 to 0,999	0,999 to 0,9995
Yearly probability of failure	P_{f1}	0,02 to 0,01	0,0067 to 0,0033	0,002 to 0,001	0,001 to 0,0005
Reliability during					
50 years	P_{S50}	0,36 to 0,61	0,71 to 0,86	0,90 to 0,95	0,95 to 0,98
100 years	P_{S100}	0,13 to 0,37	0,50 to 0,74	0,82 to 0,90	0,90 to 0,95
Theoretical failure probability during					
50 years	P_{f50}	0,64 to 0,39	0,29 to 0,14	0,10 to 0,05	0,05 to 0,02
100 years	P_{f100}	0,87 to 0,63	0,50 to 0,26	0,18 to 0,10	0,10 to 0,05

loads, partial factors on the load side and *partial factors* on the material side have to be considered when designing lines. Using this approach, the actual frequencies of failures are reduced by one to two orders of magnitude, compared with the data given in Table 6.2. When designing according to climatic limit loads, the failure probability will be lower than the probability of occurrence of the extreme loads, as the maximum load does not always meet a support with a low strength because of the statistical distribution of the support strength. The estimations presented in Table 6.2 assume that all of the supports affected in a loading event are stressed up to their theoretical maximum load. This again is a conservative assumption. The *reliability* of overhead lines can be theoretically described only with a wide band width because of the explained conditions. For comparisons of different loading assumptions or different designs, the presented considerations are helpful, however.

6.1.4 Strength coordination and selection of reliability

Treating an overhead line as a system requires the *coordination of strengths* of all components which set up the overhead line. The statistical distributions of strengths of the individual line components differ; the components react differently on loadings. In case of components arranged in series, a failure would occur if the acting load exceeded the strength at least in one of the components.
A coordination of strength of the line components can be achieved using the following criteria:

- The lowest reliability should be assigned to a component, the failure of which would only introduce the least secondary load effects, statically as well as dynamically, on other components, in order to minimize the probability of a *propagation of failure* or *of cascading.*
- The strengths of the individual components should be selected and tuned to the others, such that time and efforts for repair after a failure would be as low as possible.
- The component with the lowest reliability should ideally show only a small difference between damage and complete breakdown, as well as a scattering of the strength as low as possible. If the strength of a component with the lowest reliability scattered to a wide extent, a deliberated coordination of strengths would only be possible with a low confidence and with high investments.
- A low-cost component in series with a high-cost component should be designed at least as strong and reliable as the major component, if the consequences of failure were as severe as the failure of that major component. An exception of

Table 6.3: Proposal for the coordination of strengths

	Major component	Coordination within the major components
Component with lowest strength	Suspension support	support, foundations, hardware
Should not possess the lowest strength with 90 % probability	Angle support Section support Dead-end support	support, foundations, hardware
	Conductors	conductors, hardware

this criterion is given when a component or element is purposely designed to act as a load limiting device. In such a case, the strength should be well tuned with the component it is supposed to protect.

Using the criteria mentioned above, it can be concluded for suspension supports, strain supports, conductors, foundations and interfaces that:

- The conductors should not be the weakest component because they do not comply with the first three criteria.
- The hardware cannot be selected as the weakest component because of the last criterion.
- The strain supports are not suited because of the first two criteria.
- The foundations do not meet the second and the third criterion and, therefore, should not be the component with the lowest reliability.

As logical consequence of the considerations above, the suspension supports should constitute the component with the lowest strength. If a line designed according to this rule experienced climatic loads exceeding by far the design loads, the suspension supports would fail first. The damage would be limited to one or a few suspension supports. New structures could be erected on intact foundations within a relatively short period. A failure cascade would be avoided by a corresponding design of the line.

In Table 6.3 a typical coordination of strengths in an overhead line is shown. According to this table, the suspension supports form the components with the lowest strength. The presented coordination of strength can be used for most lines. Within each major component, the element mentioned first should have the lowest strength with 90 % confidence. From review of existing lines in practice, it can be concluded that their design corresponds to this coordination with few exceptions.

In some special situations, for example in case of specific load conditions, another sequence of strengths may be required. The suspension structures for crossings over *shipping lanes* could be designed such that they withstand breaking of conductors. In such a case, no failure of the supports would occur even if the conductor broke due to external effects, for example due to vessels with exceedingly high structures. In areas where avalanches occur, the erection of towers is difficult. Also in this case, towers could be designed such that they would withstand one-sided conductor tensile forces and would not fail if the conductors broke.

For the practical realization of the strength coordination, two methods are possible according to [6.4]:

- The component with the lowest target reliability is designed with limit loads, considering the necessary partial factors given in [6.4]. The component having the next higher *target reliability* should be designed with the same design values of actions, however, combined with an exclusion limit with a percentage factor 5 to 10 lower than that of the weakest component.
- The partial factors for material properties are established such that the target strength coordination between two components will be achieved with a high level of confidence (approximately 80 to 90 %).

Due to the random distribution of strengths, it is theoretically not possible to guar-

antee the target reliability and strength coordination with 100 % probability. Details concerning the coordination of strengths are given in [6.2] and [6.3].

Overhead lines can be designed for different reliability levels or classes depending on the individual requirements, e. g. concerning the function of the line in an extended system or due to special requirements given in standards. Standard EN 50 341-1 [6.4] distinguishes three levels of reliability to which return periods of *climatic loads* of 50, 150 or 500 years are associated. For all lines, at least the reliability level corresponding to a return period of 50 years should be achieved. The reliability level can be selected by comparison of design loads with those of existing lines, which have shown a satisfying operational record during a long period of time, or through technical and *economic optimization* [6.5]. If standards do not contain special stipulations for certain applications, the following guidelines can be used for selecting the reliability level:

- The reliability level 1 with loads according to 50 years return period is selected for lines in distribution and transmission systems with voltages up to 150 kV.
- The reliability level 2 with loads according to 150 years return period is used for transmission lines with voltages of 230 kV and above, if the lines constitute the principal or only source of supply to a particular electric load.
- The reliability level 3 with loads according to 500 years return period should be selected for lines in interconnecting grids, for connection of power plants and for supply of large important consumers. Also close to residential areas, at crossings with important traffic routes and in the vicinity of large substations, the reliability level 3 could be used for design.

The application of reliability levels may be set differently in individual standards or by individual *line owners*, also depending on the structure of the grid and the consequences of a line failure. In this case, also other than climatic loading assumptions have to be considered. As an example, the loading assumptions for overhead lines in Germany are based on climatic loads with a return period of 50 years. However, they are multiplied by partial factors on the load and material side resulting in total limit strengths which comply with the requirements for 500 years return period of the considered climatic event.

In general, it is difficult to determine the *absolute reliability* of a line. The defined reliability levels, therefore, should be assessed in relation to each other. The difference between the reliability level 1 with 50 years return period and the reliability level 3 with 500 years return period results in reduction of the yearly failure probability by one order of magnitude. Related to the life cycle of a line with 50 or 100 years, however, the difference between the failure frequency associated to these two reliability levels is less than one order of magnitude (see Table 6.2).

6.1.5 Effect of maximum load intensity on a high number of components

When the *maximum intensity* of a load event Q_T affects a high number of components or elements, failure will be triggered by the weakest link or component. This effect needs to be considered when establishing the strength distribution or the required strength of components or elements. In this case, the characteristic parameters of N components loaded in series apply to the distribution of the strengths. The *exclusion limit* e_N of N components or elements in series can be calculated from the exclusion limit e_1 of one single component or single element of the series, as follows:

$$1 - e_N = [1 - e_1]^N \text{ or } e_N = 1 - [1 - e_1]^N \quad . \tag{6.10}$$

When an exclusion limit e_N is envisaged for the combined components or elements, then the exclusion limit of each individual component or each individual element can

be determined from

$$e_1 = 1 - (1 - e_N)^{1/N} \quad . \tag{6.11}$$

For $N = 10$ and $e_N = 0{,}1$, $e_1 = 0{,}0105$ is obtained from (6.11). The relation between the mean value of the strengths $\overline{R}$ and the exclusion limit of the corresponding *characteristic strength* R_c is

$$R_c = \overline{R}(1 - u_e \cdot v_R) \tag{6.12}$$

where $\overline{R}$ is the mean strength, v_R the coefficient of variation of the strengths and u_e the number of standard deviations within the Gaussian distribution, associated to the exclusion limit. The variable u_e is obtained from

$$F_R(u_e) = e \quad . \tag{6.13}$$

When determining the required strength, the number of components subjected to the same load is considered by the strength coefficient ϕ_N according to

$$\phi_N = (1 - u_{e1} v_R)/(1 - u_{eN} v_R) \quad . \tag{6.14}$$

As an example, ϕ_N should be calculated for $N = 10$ and $v_R = 0{,}20$. If $e_N = 0{,}1$, then $e_1 = 1 - (1 - 0{,}1)^{1/10} = 0{,}0105$ is obtained from (6.11). From tables of standardized normal distribution [6.6] it can be obtained $u_{eN} = 1{,}28$ for $F_R = 0{,}1$ and $u_{e1} = 2{,}31$ for $F_R = 0{,}0105$. With these data the strength coefficient ϕ_N can be determined from (6.14) to be $\phi_N = (1 - 2{,}31 \cdot 0{,}2)/(1 - 1{,}28 \cdot 0{,}2) = 0{,}72$. The significance of this result is important. When the maximum load intensity of an event acts on ten components, the strength of which is represented by a normal distribution function characterized by a coefficient of variation of $v_R = 0{,}2$, the reliability will be considerably lower than in case of load action only on one component. In order to obtain the same reliability in both cases, a nominal strength has to be chosen for the ten components such that, if multiplied by the strength factor $\phi_N = 0{,}72$, it will be able to withstand the corresponding design action. For $v_R = 0{,}05$, a corresponding factor of 0,94 would result. These considerations apply also to insulator strings. If the load acts simultaneously on 80 insulators, the strength distribution of which shows a coefficient of variation of 0,05, then $e_1 = 0{,}00131$ is obtained from (6.11) and $u_{e1} = 3{,}00$ from the Gaussian distribution. Then, a factor of ϕ_N equal 0,91 results from (6.14), while to ten units a value of 0,94 would apply. However, if $v_R = 0{,}15$, then ϕ_N would be 0,68 for 80 units and $\phi_N = 0{,}81$ for ten components, respectively. This example underlines the significant effect of the number N of involved units, when the strength dispersion is high.
Also the type of the distribution function is of significance. Therefore, the consideration will be repeated assuming a log-normal distribution. The *strength factor* ϕ_N is defined by

$$\phi_N = R_{e1}/R_{eN} \quad , \tag{6.15}$$

where R_{e1} is the relative strength of each individual component of N components in series and R_{eN} the target strength of all components in series, which are loaded by the limit load. According to the example above, R_{e1} is associated with the exclusion limit of 0,0105 and R_{eN} with that of the target exclusion limit of 0,1. To determine the values of the *logarithmic normal distribution*, the standardized *Gaussian distribution* can be used:

$$F_R(u) = e \quad , \tag{6.16}$$

where u is obtained from

$$u = [\ln(R - p_1) - p_3]/p_2 \quad . \tag{6.17}$$

Table 6.4: Strength factor ϕ_N for N components in series or in parallel subjected to maximum load effect based on normal or log-normal distribution (values in parenthesis)

	Coefficient of variation of strength						
N	0,05	0,075	0,10	0,15	0,20	0,25	0,30
1	1,00	1,00	1,00	1,00	1,00	1,00	1,00
2	0,98	0,98 (0,97)	0,97 (0,97)	0,94 (0,95)	0,91 (0,93)	0,87 (0,92)	0,84 (0,90)
5	0,96	0,94 (0,94)	0,92 (0,93)	0,85 (0,89)	0,80 (0,86)	0,72 (0,83)	0,64 (0,80)
10	0,94 (0,95)	0,92 (0,93)	0,89 (0,90)	0,81 (0,86)	0,72 (0,82)	0,62 (0,77)	0,51 (0,73)
20	0,93 (0,94)	0,90 (0,91)	0,85 (0,88)	0,77 (0,83)	0,66 (0,77)	0,53 (0,73)	0,38 (0,68)
40	0,92 (0,93)	0,87 (0,89)	0,83 (0,86)	0,72 (0,80)	0,59 (0,74)	0,44 (0,69)	0,26 (0,64)
60	0,91 (0,92)	0,86 (0,88)	0,81 (0,85)	0,70 (0,78)	0,56 (0,72)	0,40 (0,67)	0,20 (0,62)
60	0,91 (0,92)	0,86 (0,88)	0,80 (0,84)	0,68 (0,77)	0,53 (0,71)	0,36 (0,65)	0,16 (0,60)
160	0,90 (0,91)	0,85 (0,87)	0,79 (0,83)	0,67 (0,76)	0,52 (0,69)	0,34 (0,62)	0,13 (0,57)

In (6.17), the term p_1 can be taken as zero and the parameters p_2 and p_3 result from (6.103) and (6.104), with $p_1 = 0$ and $\sigma/m = v_R$, to be

$$p_2^2 = \ln(v_R^2 + 1) \tag{6.18}$$

and

$$p_3 = \ln \overline{R} - 1/2 \cdot \ln(v_R^2 + 1) \quad . \tag{6.19}$$

There, $\overline{R}$ is the mean strength of the individual components or elements and v_R their coefficient of variation.
For the example above with $v_R = 0{,}2$, $\overline{R} = 1$ and $N = 10$, it applies $p_2^2 = \ln(0{,}2^2 + 1) = 0{,}0392$; $p_2 = 0{,}198$ and $p_3 = -1/2 \ln(0{,}2^2 + 1) = -0{,}0196$. From the standardized Gaussian distribution $u_{eN} = -1{,}28$ results for $e_1 = 0{,}1$ and $u_{e1} = -2{,}31$ for $e = 0{,}0105$. From (6.17) the relations

$$\ln R_{eN} = u_{eN} p_2 + p_3 \tag{6.20}$$

and

$$\ln R_{e1} = u_{e1} p_2 + p_3 \tag{6.21}$$

can be obtained with $p_1 = 0$. Therefore, it follows: $\ln R_{eN} = -0{,}28 \cdot 0{,}198 - 0{,}0196 = -0{,}273$ and $R_{eN} = 0{,}761$ as well as $\ln R_{e1} = -2{,}31 \cdot 0{,}198 - 0{,}0196 = -0{,}477$ and $R_{e1} = \exp(-0{,}477) = 0{,}621$. Therefore, from (6.15) $\phi_N = 0{,}621/0{,}761 = 0{,}82$ is obtained instead of 0,72 from the Gaussian distribution.
Table 6.4 depicts strength factors ϕ_N, depending on the number of N components or elements simultaneously exposed in series or in parallel to a critical load for both assumptions of a *normal* or *log-normal distribution*. In a similar way, strength factors can be determined for other distributions. Especially in case of high numbers of components or elements, the type of distribution plays an important role. Since these considerations refer to the lower tail of the distribution, the log-normal distribution seems more adequate than the normal distribution, because there is a defined threshold for the minimum strength of components or elements.

6.1.6 Use factor and its effect on the design

Assuming Q is the load resulting from a climatic action applied to the maximum span length a_{max}, then the load on a support with the span length a_i can be expressed as $Q \cdot a_i/a_{max}$, a linear system provided. In case of wind loads and large differences between a_i and a_{max}, a non-linearity can occur due to differing gust response effects. However, this effect will be neglected here and the relation between load and span

Table 6.5: Statistical parameters $\overline{U}$ and σ_U for wind span length (1)

Terrain and constraints	A1		B1, A2		B2, C1		C2	
	$\overline{U}$	σ_U	$\overline{U}$	σ_U	$\overline{U}$	σ_U	$\overline{U}$	σ_U
Number of suspension support types								
1	0,95	0,05	0,85	0,10	0,75	0,15	0,55	0,20
2	$\approx 1,0$	0,00	0,95	0,05	0,85	0,10	0,65	0,15
3	$\approx 1,0$	0,00	$\approx 1,0$	0,00	0,95	0,05	0,75	0,10

length assumed to be linear. The ratio a_i to a_{max} represents a randomly distributed variable and is called *use factor* U. The use factor U has an upper limit of 1,0 and a lower limit of approximately 0,4. From analysis of lines designed according to the limit load approach, it has been found that the use factor U can be simulated by a *Beta distribution function.* In [6.3] a description of the Beta function can be found. Three parameters affect the use factor to an essential extent:

- The number of types and height alternatives of suspension supports which are used for a specific line,
- The type of terrain and
- The constraints for selection of tower sites, e. g. due to availability or non-availability of land.

If each support was designed exactly for the conditions applicable for each tower site, then the use factor would be 1,0 in general. If on the other hand, one suspension type only was used, then an average use factor between 0,6 and 0,75 would result in a hilly terrain. The statistical characteristics of the use factor, namely the mean value $\overline{U}$ and standard deviation σ_U, can be derived with relatively good accuracy from the number of suspension tower types, the terrain and the constraints concerning the number of available tower sites. The mean use factors can be determined from the mean span length of a tensioning section and the design wind and weight span, since the mean span length $\overline{a}$ is equal to the mean *wind span length* and also to the *mean weight span length.* Therefore, it applies

$$\overline{U}_w = \overline{a}/a_w \tag{6.22}$$

and

$$\overline{U}_g = \overline{a}/a_g \quad , \tag{6.23}$$

where a_w is the design wind span and a_g the design weight span. In Tables 6.5 and 6.6, typical use factor mean values $\overline{U}$ and the associated standard deviations σ_U for the wind and weight span lengths, respectively, are presented. The constraints refer thereby to deviations from a tower site selection as economic as possible because the need of taking care of real estate properties, roads, land for buildings or other overhead power lines. The values given in Tables 6.5 and 6.6 could be used for design, if no specific data were available. If the use factors characterized by the mean value and the standard deviation were known already when designing the supports, this could be considered by the use factor coefficient γ_U. According to

$$Q_{TU} = Q_T \cdot \gamma_U \tag{6.24}$$

the load having a return period T_r will be multiplied by the factor γ_U, where γ_U is called the *use factor coefficient.* For the calculation of this coefficient, several methods are known, which are explained in [6.2] and [6.3]. In this calculation, among other effects, the number of supports plays a role which will be simultaneously affected by a climatic load event. Based on these considerations, the recommendations for the coefficient γ_U

Table 6.6: Statistical parameters $\overline{U}$ and σ_U for weight span length

Terrain and constraints	A1		B1, A2		B2, C1		C2	
	$\overline{U}$	σ_U	$\overline{U}$	σ_U	$\overline{U}$	σ_U	$\overline{U}$	σ_U
Number of suspension support types								
1	0,85	0,05	0,75	0,10	0,65	0,15	0,50	0,20
2	0,95	0,03	0,85	0,05	0,75	0,10	0,60	0,15
3	$\approx 1,0$	0,00	$\approx 1,0$	0,00	0,85	0,05	0,70	0,10

(1) In Tables 6.5 and 6.6 a letter expresses the terrain type:
A flat terrain
B rolling, hilly terrain
C mountaneous terrain

and a figure characterizes constraints concerning the selection of tower sites:
1 no special constraint,
2 constraints for selection of tower sites.

Table 6.7: Use factor coefficient γ_U depending on use factor $\overline{U}$ and coefficient of variation v_R of strength

			Coefficient of variation of strength v_R				
$\overline{U}$	σ_U	N	0,05	0,10	0,15	0,20	(1)
0,95	0,05	1	0,97	0,96	0,96	0,96	
		10	0,97	0,97	0,96	0,97	0,95
		100	0,98	0,97	0,97	0,97	
0,85	0,10	1	0,92	0,90	0,88	0,87	
		10	0,94	0,92	0,89	0,88	0,90
		100	0,96	0,94	0,90	0,92	
0,80	0,15	1	0,92	0,89	0,86	0,84	
		10	0,94	0,91	0,88	0,87	0,88
		100	0,96	0,94	0,90	0,88	
0,75	0,20	1	0,83	0,81	0,79	0,78	
		10	0,87	0,83	0,80	0,78	0,83
		100	0,88	0,84	0,81	0,78	

(1) recommended use factor coefficient for the design

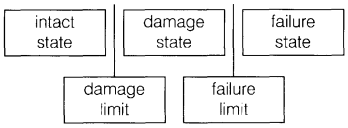

Figure 6.4: Functional states within the overhead line system and their limits

given in Table 6.7 have been derived. If supports were to be used in several lines with variable use factors, the coefficient γ_U should be taken as 0,95 or 1,00 for support design. The design will then be on the conservative side.

6.2 Strengths of line components and elements

6.2.1 Strength limits

The components and elements of overhead lines perform differently concerning their limits of strength. In case of *brittle components* and buckling events, the failure or loss of strength is sudden and usually corresponds to instability, rupture or complete separation. In other components, the loss of strength is a progressive mechanism. For example, a *grillage foundation* subjected to uplift does not fail suddenly: The uplift increases steadily until the foundation will be completely lifted finally.
Two limits have been defined to describe the strength behaviour of components and elements: the damage and the failure limit. The *damage limit* of a component corresponds to its elastic limit while the *failure limit* corresponds to the complete collapse or to rupture of a component or element. If the damage limit of a component is exceeded, the transmission system will be in a *damaged state* while, if the failure limit of a com-

Table 6.8: Data for the statistical parameter u_e depending on the exclusion limit

Exclusion limit e	~ 10 %	2 % to 5 %	< 2 %
u_e	1,28	1,6	2,1
Frequency of rejects	frequent	sometimes	rare

ponent is exceeded, the system will be in a *failure state.* A graphical interpretation of this is shown in Figure 6.4 according to [6.3]. In case of components without a definite elastic or yield limit, such as foundations, a suitably selected characteristic value can be chosen on the stress-strain or load-displacement curve.
Damage and failure limits are related to the *function of the transmission line*: I. e. to its capacity to transfer power. In a damaged state, the line function could be impaired but would be possible, at least partially, while in a failure state the power transmission capability would be completely lost.
For some components, the deformation of an element reduces the strength of another element to which the former is connected. In such a case, the damage limit has to be defined in relation to the strength of the second element. For example, movement of support foundation reduces the strength of the supported tower. Therefore, damage and failure limits of foundations are to be established in relation to the behaviour of the tower.
The definitions of the damage and failure state presented above are in accordance with IEC 60 826. Contrary to this, EN 50 341-1 [6.4] defines the damage limit as *serviceability limit state* beyond which the specified service criteria for the structure or a structural element are no longer met. The failure limit is defined as *ultimate limit state* beyond which the breakdown of the component occurs due to exceedingly high deformation, by loss of stability, by overturning, by breakage or buckling. Since these definitions do not correspond to the function of an overhead line system, they will not be used here.

6.2.2 Rating of individual components and elements

The *rating* of individual components or elements is based on the *characteristic strength* R_c, which is defined by a given exclusion limit. The characteristic strength can be obtained from a mean value $\overline{R}$ and the coefficient of variation v_R by

$$R_c = \overline{R}(1 - u_e \cdot v_R) \quad . \tag{6.25}$$

The factor u_e depends on the selected exclusion limit. According to [6.1], the strength corresponding to an exclusion limit of 10 % is correlated to the load presenting the selected return period. The strength corresponding to the *exclusion limit* of 10 % can be determined from

$$(10\ \%)\,\overline{R} = \phi_c R_c \quad , \tag{6.26}$$

where R_c is the strength with a known exclusion limit e and ϕ_c results from

$$\phi_c = (1 - 1{,}28\, v_R)/(1 - u_e v_R) \quad . \tag{6.27}$$

For the Gaussian distribution, the values u_e can be taken from Table 6.8. A conservative design of a component is achieved with $\phi_c = 1$.
According to DIN EN 50 341-1 [6.4], the design value of a component is obtained from the characteristic material property R_c by

$$R = R_c/\gamma_M \quad , \tag{6.28}$$

where γ_M represents the *partial factor* for the material property depending on the type of loading and the material. Table 6.9 shows partial factors according to [6.4]. The

Table 6.9: Partial factors for materials γ_M according to EN 50 341-1

Component	Type of stress	Type of loading	γ_M
Conductors	tension	limit load	1,25
Insulators	tension, bending	limit load	2,00
Fittings	all types of loading	minimum failing load	1,90
Lattice towers			
– members	tension, compression	limit load	1,10
	buckling, bearing	limit load	1,10
– bolted connections	shearing, bearing	limit load	1,25
– welded connections	shearing	limit load	1,25
Poles			
made of steel	tension, compression, bending, buckling	limit load	1,10
concrete	compression	limit load	1,50
reinforcement	tension	limit load	1,15
Guyed towers, anchors	tension	limit load	1,60
Foundations	uplift loading	limit load	national requirements

characteristic strength of the individual components such as conductors, insulators, interfaces, lattice steel towers etc. have to be taken from manufacturer's information or to be calculated from the *physical material properties* or determined by standardized or non-standardized methods in an individual case. The relevant chapters of this book contain the corresponding information.

6.2.3 Damage and failure limits

From testing of components of transmission lines, statistical parameters have been obtained. It is expensive, time consuming and not practical in most cases to establish the characteristic data of components for each individual project. Therefore, coefficients of variation for important components are given in [6.3]. For other components, the *characteristic material properties* are contained in the corresponding standards which can be directly used for design calculations. The ultimate strength of supports and foundations has to be determined through calculation or tests. General data are given in [6.3]. Table 6.10 shows *damage* and *failure limits* for components to be used in the design process.

6.3 Wind loads

6.3.1 Wind measurements

Wind measurements are carried out and evaluated world-wide by meteorological observation stations. Thereby, the guidelines of the World Meteorological Organisation (WMO) [6.7] are used, especially in order to compare collected data with long-time series of standardized measurements. The *observation stations* should be arranged in an open terrain where the wind will not be affected by obstacles or buildings. Such a terrain is designated as terrain B according to [6.1] and [6.2] and as terrain II according to [6.4]. The height above ground is standardized with 10 m. When using other measuring heights, the results have to be adjusted accordingly. For the evaluation, the mean values over a ten minute or one hour period are used. Also the gusts with three to five seconds duration and the wind direction are recorded. In case of continuous measurements, it is usual to carry out an evaluation over a ten minute period every hour. For application of wind data for designing overhead lines, it is assumed that the

Table 6.10: Damage and failure limits of components according to [6.3]

Component	Loading	Damage limit	Failure limit
Members of lattice steel towers	tension, compression	yield strength —	breaking strength buckling
Poles made of			
– steel	bending moments	1 % non-elastic deformation at the tower top	collapse by local buckling or bending
– concrete	bending moments	crack openings or 0,5 % non-elastic deformation at the tower top	collapse of the pole
Separate foundations	uplift	1° rotation of the support	excessive uplift of 50 to 100 mm
	compression	reduction of 5 % in support strength	excessive settlement of 50 to 100 mm
Compact foundations	overturning moments	1° rotation of the support	excessive rotation of 5°and more
Conductors	tension	appr. 75 % of characteristic strength or rated tensile strength (RTS)	ultimate tensile strength
Insulators	tension	appr. 70 % of rated strength	rupture
Interface fittings	tension	permanent deformation	rupture

yearly maximum values of wind velocities have been available for at least twenty years and evaluated statistically.
In meteorology and in general public, scaling of *wind force according to Beaufort Scale* is often adopted where the wind effects are associated with corresponding wind velocities. In Table 6.11 the Beaufort scale is represented.

6.3.2 Determination of meteorological reference wind velocities

6.3.2.1 Evaluation of wind measurements

The magnitude and frequency of *wind velocities* can be described by statistical distributions. The *Gumbel distribution* (6.106) can be used for the yearly maximum values of the wind velocities. The Gumbel distribution represents the probability $F(x)$ that a variable will be below the value x, a mean value $\overline{x}$ and the standard deviation σ provided. According to [6.1], the Gumbel distribution is applied to the yearly maximum values of the wind velocities. Other civil engineering standards assume that the wind pressure and not the wind velocity follows the Gumbel distribution. This applies to the Eurocodes [6.8] and is based on theoretical studies, e. g. [6.9].
Using (6.112), the Gumbel distribution will be

$$F(x) = \exp\left\{-\exp\left[-\frac{C_1}{\sigma}\left(x - \overline{x} + \frac{C_2}{C_1}\cdot\sigma\right)\right]\right\} \tag{6.29}$$

and if the number of observations n is large, then

$$F(x) = \exp\left\{-\exp\left[-1{,}28\ (x - \overline{x} + 0{,}45\,\sigma)\,/\sigma\right]\right\} \quad . \tag{6.30}$$

The probability that during one year a value will be higher than the value x is equal $1 - F(x)$. As a simplification, the return period T_r of the value x is given by

$$T_\mathrm{r} = 1/(1 - F(x)) \quad . \tag{6.31}$$

Therefore, it results from (6.29) and (6.31):

$$x_\mathrm{T} = \overline{x} - \frac{C_1\sigma}{C_1} - \frac{\sigma}{C_1}\left\{\ln[-\ln(1 - 1/T_\mathrm{r})]\right\} \quad . \tag{6.32}$$

Table 6.11: Beaufort wind velocity scale

Beaufort Force Number	Term	Indications		Wind velocity in m/s
		on land	on sea	
0	calm	smoke rise vertically	sea like mirror	0 to 0,2
1	light air	smoke drifts slowly downwind	ripples with appearance of scales: no foam crests	0,3 to 1,5
2	light breeze	leaves rustle	small wavelets; crests of glassy appearance, not breaking	1,6 to 3,3
3	gentle breeze	leaves are in motion	large wavelets; crests begin to break; scattered whitecaps	3,4 to 5,4
4	moderate breeze	small branches on trees move	small waves, becoming longer; numerous whitecaps	5,5 to 7,9
5	fresh breeze	small trees sway	moderate waves, taking longer form; many whitecaps; some spray	8,0 to 10,7
6	strong breeze	large branches sway	larger waves forming; whitecaps everywhere; more spray	10,8 to 13,8
7	near gale	whole trees in motion	sea heaps up; white foam from breaking waves begins to be blown in streaks	13,9 to 17,1
8	gale	twigs and small branches break off trees	moderately high waves of greater length; edges of crests begin to break into spindrift; foam is blown in well-marked streaks	17,2 to 20,7
9	strong gale	large branches break off trees; slight structural damage	high waves; sea begins to roll; dense streaks of foam; spray may reduce visibility	20,8 to 24,4
10	storm	trees broken; minor structural damage	very high waves with overhanging crests; sea takes white appearance as foam is blown in very dense streaks; rolling is heavy and visibility is reduced	24,5 to 28,4
11	violent storm	widespread damage	exceptionally high waves; sea covered with white foam patches; visibility further reduced	28,5 to 32,6
12	hurricane	violent movement of trees and much destruction	air filled with foam; sea completely white with driving spray; visibility greatly reduced	32,7 to 36,9
13	hurricane	—	—	36,9 to 41,1
14	hurricane	—	—	41,2 to 45,8
15	hurricane	—	—	45,9 to 50,8
16	hurricane	—	—	50,9 to 55,6
17	hurricane	—	—	above 55,6

Table 6.12: Ratio $x_T/\overline{x}$ for the Gumbel distribution function, T return period, n number of years with observation, v_x coefficient of variation

		Return period T (years)											
		50				150				500			
v_x	n	10	20	50	∞	10	20	50	∞	10	20	50	∞
0,05		1,18	1,16	1,14	1,13	1,24	1,21	1,19	1,17	1,30	1,27	1,24	1,22
0,10		1,36	1,32	1,29	1,26	1,48	1,42	1,38	1,36	1,60	1,54	1,49	1,44
0,12		1,43	1,38	1,35	1,31	1,57	1,51	1,46	1,41	1,72	1,64	1,59	1,53
0,16		1,57	1,51	1,46	1,41	1,76	1,68	1,61	1,55	1,96	1,86	1,78	1,70
0,20		1,72	1,64	1,58	1,52	1,95	1,84	1,77	1,69	2,20	2,07	1,98	1,88
0,30		2,08	1,95	1,87	1,78	2,43	2,27	2,15	2,04	2,81	2,61	2,46	2,32
0,40		2,43	2,27	2,16	2,04	2,90	2,69	2,54	2,36	3,41	3,14	2,95	2,76
0,50		2,79	2,59	2,44	2,30	3,38	3,11	2,92	2,73	4,01	3,68	3,44	3,20
0,60		3,15	2,91	2,73	2,56	3,85	3,53	3,30	3,07	4,61	4,21	3,93	3,64

Equation (6.32) gives the value x of a variable, e. g. the wind velocity, which has a return period T_r. In addition to the parameters C_1 and C_2, the value x depends on the mean value $\overline{x}$ and standard deviation σ of the observation series. For $n \to \infty$, it is obtained

$$x_T = \overline{x} - 0,45\,\sigma - \sigma/1,28\ \{\ln[-\ln(1 - 1/T_r)]\} \quad . \tag{6.33}$$

Eventually, the ratio of the wanted value x_T to the mean value $\overline{x}$ can be calculated from

$$x_T/\overline{x} = 1 - v_x/C_1\ \{C_2 + \ln[-\ln(1 - 1/T_r)]\} \quad , \tag{6.34}$$

where $v_x = \sigma/\overline{x}$ is the *coefficient of variation*. Table 6.12 represents the values $x_T/\overline{x}$ for return periods of 50, 150 and 500 years, depending on the number of observations n and coefficients of variation v_x. When the variable x is replaced by the wind velocity V, the relations for wind actions are obtained.
The wind load Q_W is proportional to the square of the wind velocity V

$$Q_W = kV^2 \quad . \tag{6.35}$$

This relation applies to each value of the wind velocity, for example to its mean value $\overline{V}$. The factor k depends on various parameters like conductor diameter, drag coefficient, gust response factors etc. From the statistical distribution of the wind velocities, equation (6.35) yields a distribution of the wind loads which can be used together with the distribution of the support strengths for assessment of the reliability, in case of wind loading. According to [6.3], the relation between the standard deviations of both distributions is

$$\sigma_Q/\overline{Q}_W \sim 2\,\sigma_V/\overline{V} \tag{6.36}$$

or

$$v_Q = 2\,v_V \quad , \tag{6.37}$$

where $\overline{Q}_W$ is the mean value of the wind loads, σ_Q its standard deviation and v_Q its coefficient of variation. To compute the reliability of lines in case of wind loads, the mean value of the loads can be assumed as proportional to the square of the mean value of the wind velocities. For the coefficient of variation of the loads, twice the value of the coefficient of variation of the wind velocities should be used. If a wind velocity with 50 years return period and a coefficient of variation $v_V = 0,20$ is assumed, then $v_Q = 0,40$ applies to coefficients of variation of the loads and, assuming $v_R = 0,05$, the yearly failure probability is obtained from Figure 6.3 to be $P_f = 0,015$. If, instead of $v_Q = 0,40$, the incorrect assumption $v_Q = v_V = 0,20$ had been used, the wrong result $P_f = 0,010$ would have been obtained.

Table 6.13: Terrain categories according to IEC 60826 and EN 50341-1 and associated parameters

Terrain category according to IEC 60826	EN 50341-1	Characteristics of the terrain	k_j	k_T	z_0 (m)	α
A	I	Rough open sea, lakes with at least 5 km fetch upwind and smooth flat country without obstacles	0,92	0,17	0,01	0,12
B	II	Farmland with boundary hedges, occasional small farm structures, houses or trees	1,00	0,19	0,05	0,16
C	III	Suburban or industrial areas, permanent forest	1,77	0,22	0,30	0,22
D	IV	Urban areas in which at least 15 % of the surface is covered with buildings with mean heights above 15 m	1,49	0,24	1,00	0,28

6.3.2.2 Effect of the terrain roughness

The *terrain roughness* has an effect on the wind velocities for design and on the gust response factors. The greater the roughness, the more turbulent and slower the wind flow will be.

According to [6.1] and [6.4], four *terrain categories* are considered, as indicated in Table 6.13. For the practical design of overhead lines, only the terrain categories A and B are important. In suburban areas (terrain category C) or urban areas (terrain category D), the reliability of overhead lines should be higher than in open terrain. Therefore, a design according to terrain category B is recommended for lines to be erected in these terrain categories as well.

Usually, *meteorological stations*, except those along the coast or in urban areas, are placed in areas of terrain category B. Then, the *meteorological wind velocity* will be $V_{B,10min}$. Alternatively, the meteorological wind velocity may be recorded in a height of 10 m over an averaging period of T_r differing from 10 min. Then, according to IEC 60826, the ten minute mean value can be obtained from

$$V_{x,10\,\mathrm{min}} = V_{x,t}/(V_{x,t}/V_{x,10\,\mathrm{min}}) \quad , \tag{6.38}$$

where the ratio $V_{x,t}/V_{x,10\,\mathrm{min}}$ is depicted in Figure 6.5. For measurements in the *terrain category* x different from B, the reference wind velocity $V_{B,10min}$ in terrain category B is given by the relation

$$V_{\mathrm{B},10\,\mathrm{min}} = V_{x,10\,\mathrm{min}} \cdot k_j \tag{6.39}$$

according to IEC 60826, where k_j can be taken from Table 6.13. If the wind velocity 10 m above ground in the terrain category B is known, the corresponding meteorological wind velocity for a terrain type x at the same height can be calculated from

$$V_{x\mathrm{R}} = V_{\mathrm{B}}/k_j \quad , \tag{6.40}$$

where the parameter k_j takes care of the differing terrain categories.

If the measurement height z differs from 10 m, the variation of wind velocity with the height z can be derived from the *power law* according to EN 50341-1

$$V_{x10\,\mathrm{m}} = V_{xz}/(z/10)^{\alpha} \tag{6.41}$$

or according to the *logarithmic law*

$$V_{x10\,\mathrm{m}} = V_{xz} \cdot \ln(10/z_0)/\ln(z/z_0) \quad . \tag{6.42}$$

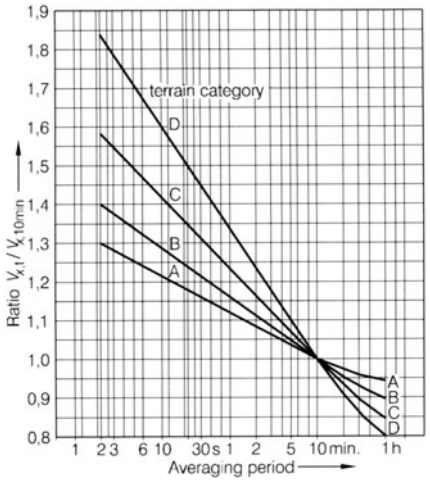

Figure 6.5: Relationship between meteorological wind velocities $V_{x,t}$ in 10 m height above ground to the 10-min-average $V_{x,10\,\mathrm{min}}$ depending on the averaging period t and the terrain category x

The parameters α and z_0 used in these equations can be taken from Table 6.13, depending on the *terrain category.*
The wind velocity in a terrain category x can be calculated from the logarithmic relation according to

$$V_{x\mathrm{R}} = [k_{\mathrm{T}} \ln(10/z_0)] \cdot V_{\mathrm{II}} \quad . \tag{6.43}$$

The expression $k_{\mathrm{T}} \ln(10/z_0)$ is typical for each type of terrain. Comparing equations (6.40) and (6.43), it could be concluded $1/k_{\mathrm{j}} = [k_{\mathrm{T}} \ln(10/z_0)]$. However, there are differences which are due to differing definitions of the terrain categories.

6.3.2.3 Variation of reference wind velocity with height

In clause 6.3.2.2, the wind velocity depending on the type of terrain 10 m above ground is determined. For other heights z, the power law

$$V_{x\,z} = V_{x\mathrm{R}} \cdot (z/10)^{\alpha} \tag{6.44}$$

or the logarithmic law

$$V_{x\,z} = k_{\mathrm{T}} V_{\mathrm{B}} \ln(z/z_0) \tag{6.45}$$

according to EN 50 341-1 can be used, where the parameters α, k_{T} and z_0 follow from Table 6.13, depending on the terrain category.

6.3.3 Wind action on line components and elements

The value of the force $Q_{\mathrm{W}x}$ due to wind blowing horizontally and perpendicularly to any element of a line is given by

$$Q_{\mathrm{W}x} = q_z \cdot G_{\mathrm{q}} \cdot G_{\mathrm{x}} \cdot C_{\mathrm{x}} \cdot A \quad , \tag{6.46}$$

where q_z is the *dynamic wind pressure* at the height z, G_{q} the *gust response factor* and G_{x} the *structural resonance factor* for the structural element being considered, C_{x} the *drag factor* depending on the shape of the element being considered and A the area of the element projected on a plane perpendicular to the wind direction. However, the parameters of equation (6.46) are defined differently in relevant standards.

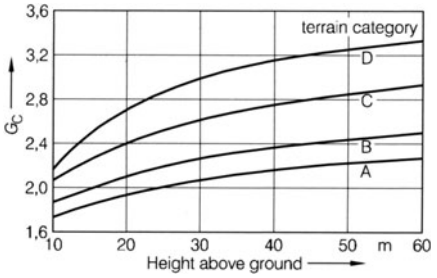

Figure 6.6: Combined wind factor G_C for conductors according to [6.1]

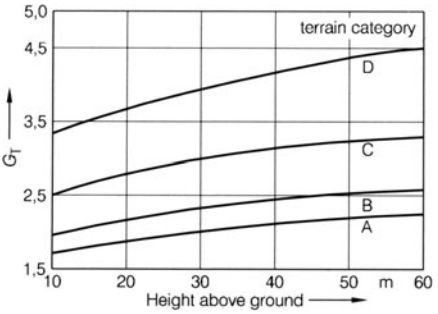

Figure 6.7: Combined wind factor for supports G_T according to [6.1]

The dynamic wind pressure q_z at the height z above ground is determined by

$$q_z = 1/2\,\varrho V_z^2 \quad , \tag{6.47}$$

where ϱ is the air density and V_z the reference wind velocity in m/s. The *air density* depends on the temperature and the altitude of the line above sea-level and can be obtained from

$$\varrho = \varrho_0(288/T)\exp(-0{,}00012 \cdot H) \quad , \tag{6.48}$$

where ϱ_0 is the density at +15°C on sea level, taking 1,225 kg/m^3 as reference, T the absolute temperature and H the altitude above sea-level in m. For the altitude of 1000 m and +5°C (T = 278 K), a density of 1,126 kg/m^3 results thereof. A value frequently used in standards is 1,25 kg/m^3.
According to [6.4], the gust response factor is obtained from

$$G_q = k_g^2 = (1 + 2{,}28/\ln(z/z_0))^2 \quad , \tag{6.49}$$

where z is the height above ground.
According to [6.10], the expression $q_z \cdot G_q \cdot G_x$ in equation (6.46) is combined to a total dynamic wind pressure q_z, which increases linearly with the height:

$$q_z = q_0 + 30 \cdot (z/10) \quad , \tag{6.50}$$

where q_0 is the basic wind pressure depending on the wind zone, where the line is to be built (see clause 6.6.2.3).
According to [6.1], the dynamic wind pressure is calculated based on the wind velocity $V_{R,10m}$ at a height of 10 m above ground using equation (6.47). The variation with height, the gust response factor and the structural resonance factor are considered by the combined wind factors G_C (conductors) and G_T (supports). Combined wind factors G_C and G_T are different, while this does not apply to the gust response factor G_q, according to (6.49), following from [6.4]. Figures 6.6 and 6.7 represent combined wind factors G_C for conductors and G_T for towers according to [6.1].
In case of wind loads on conductors, the *resonance factor* G_x depends on span length and is called *span factor* G_L. In Figure 6.8, the span factors G_L according to IEC 60 826, EN 50 341-1 and EN 50 341-3-4 are represented. It can be seen that there are considerable differences between IEC 60 826 [6.1] and the other sources mentioned.
Wind loads on insulators are computed using equation (6.46) as well, whereby the same gust response factors are used as in case of supports. The drag factor C_x can be assumed to be 1,2 for this case. Drag factors for the individual line elements are dealt with in clause 6.6.2.

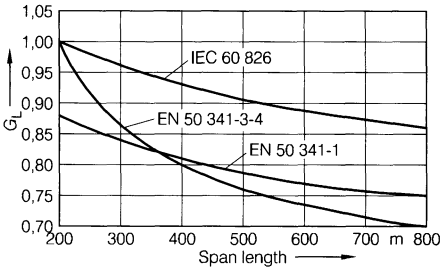

Figure 6.8: Span factor G_L for conductors

6.4 Ice loads

6.4.1 Atmospheric icing

Atmospheric icing is a general term for a number of processes where water in various forms freezes in the atmosphere and sticks to objects exposed to the air. In case of overhead lines, there are two types of icing, which are named according to the main processes as *precipitation icing* and *incloud icing.*

A third process, where water vapour is transformed directly into ice and forms *hoar-frost*, does not lead to significant loadings and is not considered further. Ice accretion due to precipitation icing may occur in different forms, namely glaze due to freezing rain, *wet snow accretion* and *dry snow accretion.*

The regional and local topography affects the ice accretion. Coastal mountains along the windward side of the continents act to force moist air upwards, leading to a cooling of the air with condensation of water vapour and droplet growth with the consequence of *incloud icing.* The most severe incloud icing occurs above the condensation level and the freezing level on openly exposed heights, where mountain valleys force the moist air through passes and thus both lift the air and strengthen the wind. On the leeward side of the mountains, however, the descent of air mass results in internal heating of the air and evaporation of droplets thus protecting overhead power lines routed there against high ice accretion.

Precipitation icing may occur at any altitude. However, in general, the probability of precipitation icing is greater in the bottom of valleys in general than in the middle of valley sides, because of higher occurrence of cold air. Since the air flow has an important effect, the ice accretion on overhead lines, which are routed transversely to a valley, is often higher than on other lines running along the valley. In case of lines mentioned first, an additional hazard is given because of the wind action having a higher probability of occurrence, simultaneously with *ice accretion* on the conductors.

Glaze due to freezing rain

When rain droplets or drizzle fall into a layer with cold air at a temperature below freezing point, the drops become supercooled. They are still in the liquid (water) phase and do not freeze before they hit the ground or an object. The resulting accretion is a clear and solid ice, called *glaze*, often with icicles. This accretion is hard and strong and, therefore, difficult to remove. The density is 800 to 900 kg/m^3, depending on the content of air bubbles in the ice. Freezing rain occurs mostly on wide planes or basins, where relatively thick layers of cold air accumulate during periods of cold weather. When a low pressure system with a warm front and rain penetrates the air, the cold and heavier air may remain near the ground and thus favour the formation of glaze during temperature inversion. Such a situation may persist until the upper wind may manage to mix the cold surface layer of the air with the warmer air aloft. A similar

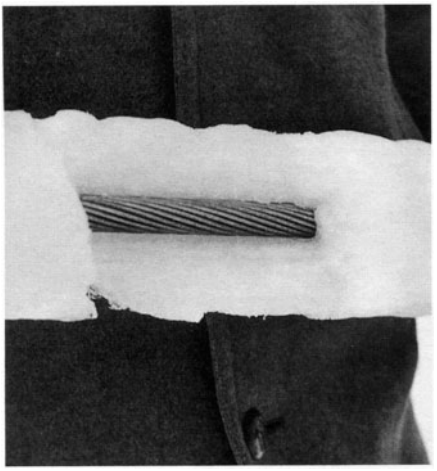

Figure 6.9: Ice accretion caused by freezing rain

Figure 6.10: Ice accretion caused by incloud icing

situation may occur in the overlapping zones of cold air and warm air systems. The warmer air combined often with precipitation is lifted over the colder air, forming a frontal zone where precipitation is enhanced. Such a weather system was observed in Canada at the beginning of 1998 [6.11, 6.12] and resulted in massive and widespread damage to overhead lines. Often, there are only moderate winds during freezing rain events. Then, the amount of accumulated ice depends on the rate and duration of precipitation. Figure 6.9 depicts ice accretion due to freezing rain.

Wet snow

If snow flakes fall through warmer layers in the atmosphere, they start to melt when passing the zero degree zone. The *wet snow* flakes will contain a mixture of ice and water until they eventually melt totally into rain drops if the warm layer is thick enough. As long as they are only partly melted, they are sticky and may adhere to objects in the air flow, e. g. the conductors of overhead lines. The density may vary widely between 100 and 800 kg/m^3, but mostly between 400 and 700 kg/m^3. The density and intensity of wet snow deposits depend on precipitation rate, wind velocity and temperature. If the temperature drops below zero degree after the accretion, the ice will freeze into a hard and dense layer with strong adhesion to the objects. *Wet snow* events resulted in severe damage to overhead lines in the past [6.13].

Soft and hard rime due to incloud icing

Incloud icing is a process where supercooled droplets in a cloud or fog freeze immediately on objects in the air flow, for instance on overhead transmission lines in mountains above the cloud base. The resulting ice accretion is called *soft rime* according to the density which is typically 200 to 600 kg/m^3 [6.3]. Under similar conditions, *hard rime* is formed with a density between 700 and 900 kg/m^3. At temperatures below -10°C, the water content of the air becomes smaller and less icing occurs. Under extreme conditions, high ice loads have also been observed at high winds and temperatures below -20°C. In Figure 6.10 a conductor is shown with ice formed in an incloud icing process. In Table 6.14 the *properties of ice accretion* are summarized. In Figure 6.11 typical ranges are explained for the formation of the individual types of ice, depending on air temperature and wind velocity.

Table 6.14: Physical properties of ice on conductors

Type of ice	Density kg/m^3	Adhesion	Colour	Shape	Cohesion
Glaze	700 to 900	strong	transparent	cylindrical icicles	strong
Wet snow	400 to 700	medium	white	cylindrical	medium to strong
Hard rime	700 to 900	strong	opaque to transparent	eccentric pennants into wind	very strong
Soft rime	200 to 600	medium	white	eccentric pennants into wind	low to medium

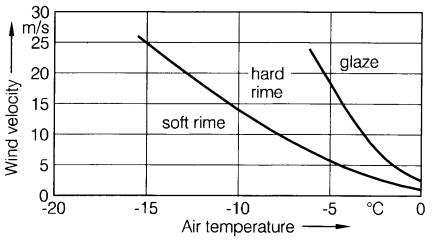

Figure 6.11: Typical formation of ice accretion

Table 6.15: Statistical parameters of ice loads

Number of observations	Mean value	Standard deviation
only $g_{I\,max}$	$0{,}45\, g_{I\,max}$	$0{,}225\, g_{I\,max}$
10 to 20	$\overline{g}_I$	$0{,}5\,\overline{g}_I \leq \sigma_I \leq \overline{g}_I$
≥ 20	$\overline{g}_I$	$\sigma_I \leq \overline{g}_I$

6.4.2 Ice observations and measurements

Since ice loads are not measured in general by meteorological stations, information on ice accretion needs to be recorded directly on overhead line conductors or at correspondingly designed observation devices. If data needed for line design are not available, it is recommended to carry out a program for collecting field data. Field ice data can be obtained through the following activities [6.14]:

- Direct *measurements of icing thickness* or *weight of ice* samples, taken from observation installations or line conductors. Ice samples fallen on the ground from conductors can be used, if consideration is given to the shape of initial accretion on conductors;
- Measurements by devices that *simulate ice accretion* on conductors. Some devices currently used in a few countries consist of simple tube or cable assemblies installed near ground level for ease of observations.
- *Estimation of icing* using conductor tension or vertical component of weight at the insulator attachment point;
- Estimation of icing based on measurements of the conductor tension and sag.

Ice loading data are important not only to establish load criteria for design of supports but can also be useful in the planning stages of transmission networks and route selection of a specific line. So far other ice load information is not available, measurements lasting for at least ten years of field observation are necessary to establish a reliable data base. The observation of extreme ice loads on existing overhead lines provides important information. In [6.15], guidelines are given for evaluation of such ice observations.

Meteorological models can be used as well to obtain basic information on ice loadings to be expected. The bases for such meteorological models are formed by the temperature, humidity, precipitation rate and wind direction to be expected. In [6.14], icing models are described and guidelines for the selection of observation stations, measuring devices and the evaluation of measurements are given. In some Central European countries, ice *observation stations* had been installed. However, because of the rare frequency of substantial ice loads, useful results were not always obtained.

6.4.3 Determination of reference ice loads

6.4.3.1 Basic relations

Ice load is a random variable, usually expressed either as a load g_I per unit length of conductor, in N/m, or as a uniform radial thickness t_{RI}, in mm, around the conductors and ground wires. The equation

$$g_I = 9{,}81 \cdot 10^{-3} \cdot \delta_I \cdot \pi\, t_{RI}(d + t_{RI}/1000) \tag{6.51}$$

expresses the relation between the *ice weight per unit length* g_I and the *radial ice thickness* t_{RI}, where g_I is the ice weight per unit length in N/m, δ_I the ice density in kg/m^3, t_{RI} the radial ice thickness in mm and d the conductor diameter in m. With the assumption $\delta_I = 900$ kg/m^3 and t_{RI} and d in mm, it is obtained

$$g_I = 0{,}0277\, t_{RI}(d + t_{RI}) \quad \text{(N/m)}. \tag{6.52}$$

Ice loads should ideally be deduced from measurements taken at conductors and locations representative of the line route.

6.4.3.2 Evaluation of ice load information

The evaluation of ice load information depends on the available type of data and number of years with observations:

- If records of yearly maximum ice loads during a period of at least ten years are available, the mean value $\overline{g}_I$ is derived from the records of the *yearly maximum ice load*. The corresponding standard deviation σ_I is calculated or estimated according to the procedure given in Table 6.15. There, $\overline{g}_I$ means the mean value of the yearly extreme ice loads g_{Ii} and σ_I is the calculated or estimated standard deviation.
- If only the maximum value $g_{I\,max}$ of ice loads observed during a certain number of years is available and no statistical data can be evaluated, $\overline{g}_I$ may be assumed as $0{,}45 \cdot g_{I\,max}$ and the standard deviation σ_I being $0{,}5\,\overline{g}_I$.
- A *meteorological analysis* model is used to calculate values for yearly maximum ice loads during a certain number of years. Reliable data will be obtained if a period of 20 years or more is studied. So far as possible, reference to observations at lines should be made.
- Conclusions on ice loads can be made from observations in the terrain and damage to trees and vegetation in areas where high ice loads have to be expected.

As a result of the evaluation, the mean value $\overline{g}_I$ of the yearly maximum ice observations and the corresponding standard deviation σ_I are obtained.

6.4.3.3 Reference ice load

The *reference design ice load* g_{IR} depends on the required reliability of the line and on the following parameters:

$\overline{g}_I$ mean value of the yearly maximum ice loads;
σ_I standard deviation of the yearly maximum ice loads;
n number of years with observations;
d conductor diameter;
z_C average conductor height above ground.

The reference design ice load g_{IR} can be expressed by

$$g_{IR} = K_{\sigma I} \cdot K_n \cdot K_d \cdot K_z \cdot \overline{g}_I \quad . \tag{6.53}$$

The data $K_{\sigma I}$ and K_n can be computed from the *Gumbel distribution*. The product $K_{\sigma I} \cdot K_n$ corresponds to the ratio $x/\overline{x}$, according to Table 6.12. The factor K_d takes

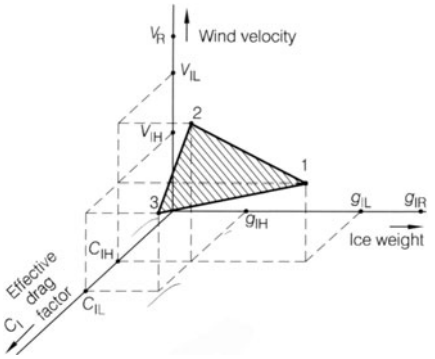

Figure 6.12: Schematic presentation of parameter combinations in case of simultaneous action of wind and ice

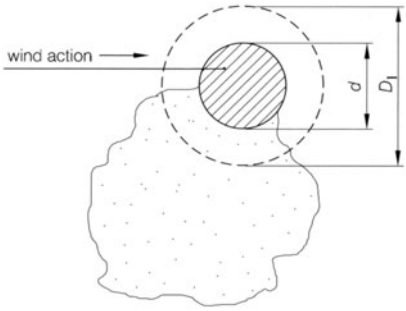

Figure 6.13: Conductor with equivalent cylindrical ice formation. D_I resulting equivalent diameter of ice accretion, d conductor diameter

care of the conductor diameter, the factor K_z of the conductor height above ground. According to [6.3], they can be approximated by the following formulae:
For *incloud icing*:

$$K_d \sim 0{,}15\, d/30 + 0{,}85 \quad ; \quad K_z = 1{,}0 \quad , \tag{6.54}$$

For *precipitation icing*:

$$K_d \sim 0{,}35\, d/30 + 0{,}65 \quad ; \quad K_z \sim 0{,}075\, z_C/10 + 0{,}925 \quad . \tag{6.55}$$

The temperature to be assumed in icing conditions should be $-5°C$ for both main types of icing. Lower temperatures can be assumed for line design where climatic conditions can vary rapidly and where a severe drop in temperature during or immediately after an ice storm can be expected.

6.4.3.4 Loading of supports and load cases

The loads to be withstood by the supports are equal to the loads transmitted to the supports by the conductors. They are composed of the vertical loads and the conductor tensile forces increased by the effect of ice accretion. In general, three conditions may be distinguished which cover most of possible load cases:

- *Uniform ice formation* on all conductors, maximum weight condition;
- Non-uniform ice formation resulting in a longitudinal and transverse bending condition with respect to the support;
- *Non-uniform ice formation* resulting in a torsional loading, because the individual conductors in the adjacent spans are loaded differently.

It can be assumed that non-uniform ice formations occur less frequently than uniform ice formations. To take adequate care of the expected ice accretions, standards provide loading assumptions which should result in supports strong enough to withstand the loads created by ice accretion. In clause 6.6.3 these aspects will be dealt with.

6.5 Combined wind and ice loads

6.5.1 Probability of occurrence and combination of parameters

The *action of wind on ice covered conductors* involves at least three variables:

- The wind velocity that occurs in presence of icing;

Table 6.16: Combination of wind and ice loads

Load case	Ice weight	Wind velocity	Effective drag coefficient	Ice density
Condition 1	g_{IL} [1)]	V_{IH}	C_{IH}	δ_{I1}
Condition 2	g_{IH}	V_{IL}	C_{IH}	δ_{I1}
Condition 3	g_{IH}	V_{IH}	C_{IL}	δ_{I2}

[1)] The index L indicates a low frequency of occurrence, i. e. high values; the index H stands for a high frequency of occurrence, i. e. low values

Table 6.17: Drag factor for conductors with ice accretion and ice densities

		Wet snow	Soft rime	Hard rime	Glaze ice
Drag factor C_{IH}		1,0	1,2	1,1	1,0
Density δ_{I1} (kg/m^3)	IEC 60 826	600	600	900	900
	EN 50 341-1	500	300	700	900
Drag factor C_{IL}		1,4	1,7	1,5	1,4
Density δ_{I2} (kg/m^3)		400	400	700	900

- The ice weight and
- The shape of ice formation with the corresponding drag factor.

These combined effects result directly in both, transversal and vertical loads and indirectly in increase of longitudinal loads. Since detailed statistical data and observations on ice weight, ice shape and coincident wind action are not commonly available, it is proposed to combine these variables in such a way, that the resulting load combination will have the same return periods T_r as those adopted for each reliability level. As a simplified approach, a low probability value, indicated by the index L, of one variable is combined with high probability values, indicated by the index H, for the other two variables, as presented in Table 6.16 [6.3] and Figure 6.12. Practically speaking, the maximum value of one variable will be combined with average values of the yearly maximum observations of the other variables to define a loading condition. A low ice density is, therefore, combined with a low value of the drag factor, which has a high probability of occurrence.

Ice loads with a low probability of occurrence should, thereby, correspond to the values determined in clause 6.4.3. For wind loads, only those data need to be considered which have to be expected during icing periods, but not data which correspond to the yearly maximum wind velocities. As indicated in Table 6.16, a loading condition is defined for each combination. Condition 3 mentioned there will only prevail if high values of the effective *drag factor* occur. This condition needs to be considered only in special cases.

6.5.2 Determination of design parameters

6.5.2.1 Ice load

Where no statistics are available on the *simultaneous occurrence of wind and ice loads*, the ice load having a low probability of occurrence should be taken as the reference ice load. As a mean value of the yearly maximum ice loads, 0,45 times the ice load with a 50 years return period is assumed (see Table 6.15) and the corresponding temperature will be −5°C.

6.5.2.2 Wind load

In [6.3], there are detailed explanations on the determination of wind loads occurring simultaneously with ice load, depending on the different types of ice. If statistics are available on the wind velocities, which were observed during the presence of ice load, these statistics can be evaluated with the relations presented in clause 6.3.2.1. Where

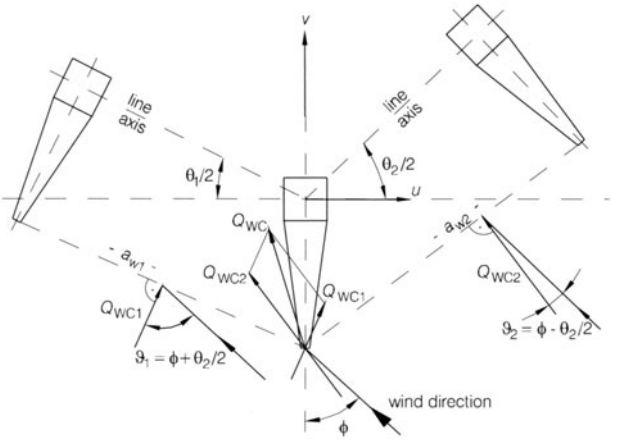

Figure 6.14: Wind action on conductors

such data are not available, the *reference wind velocity* having a low probability of occurrence can be related to the wind velocity occurring without ice accretion, according to

$$V_{IL} = (0{,}60 \text{ to } 0{,}85) \cdot V_T \quad . \tag{6.56}$$

The wind velocity having a high probability of occurrence is determined similarly by

$$V_{IH} = (0{,}40 \text{ to } 0{,}50) \cdot V_{50} \quad , \tag{6.57}$$

where V_{50} is the wind velocity having a 50 years return period. If no other data are given, it is recommended to use the upper limits in the relations (6.56) and (6.57) to provide a conservative design.

6.5.2.3 Effective drag factors and ice densities

In Table 6.17, the effective drag factors and the related *ice densities* are presented for the types of ice accretion discussed in this clause, according to the information given in [6.1] and [6.3]. The drag factors, thereby, apply to a cylindrical ice shape with a weight equivalent to that assumed (see Figure 6.13).

6.5.3 Wind action on the ice covered conductor

The *wind load on an ice covered conductor* acting rectangularly to the span and on the supports at both ends of the span having a span length a_w, is obtained from equation

$$Q_{WI} = 1/4\, \varrho \cdot V_I^2 \cdot C_I \cdot G_q \cdot G_L \cdot D_I \cdot a_w \cdot \cos^2 \vartheta \tag{6.58}$$

(see Figure 6.14). There, ϱ is the air density, V_I the wind velocity during ice accretion according to Table 6.16, C_I the relevant effective *drag factor* according to Table 6.16, corresponding to the condition considered, G_q the gust response factor according to (6.49), G_L the span factor according to Figure 6.8, D_I the diameter of the equivalent cylindrical ice formation, a_w the span length and ϑ the angle of wind attack related to the plumb line to the conductor (see Figure 6.14). The equivalent *conductor diameter with ice accretion* is calculated from

$$D_I = \sqrt{d^2 + 4\, g_I/(9{,}81 \cdot \pi \delta_I)} \quad . \tag{6.59}$$

There, d is the conductor diameter without ice accretion, g_I the ice weight per unit length according to Table 6.16 and δ_I the ice density according to Table 6.17.
The wind action on conductors with ice accretion increases the conductor tensile force and results in the maximum loading of the conductors. If a tensioning section consists of several spans supported by suspension insulators, the equivalent span length can be used for the calculation of the conductor tensile stresses (see clause 14.5). If the line tensioning section is long, the maximum wind load will act not simultaneously on the total tensioning section. Then, the wind load used to calculate the conductor tensile forces (6.58) can be reduced by multiplication with the factor 0,6. However, such a reduction of wind load for design of supports should be considered with care, since strain supports may also be used for tensioning sections with a few spans only in actual line projects.

6.6 Climatic loads according to relevant standards

6.6.1 Standards for overhead power lines

Standards for overhead power lines have existed in many industrialized countries for many years. Examples are DIN VDE 0210 [6.16] for Germany, ÖVE-L11 [6.17] for Austria, LeV [6.18] for Switzerland and NBR 5422 [6.19] for Brazil.
The International Electrotechnical Commission (IEC) deals with overhead lines standards for world-wide application. IEC 60 826 [6.1] applies to the evaluation of climatic loads and rating of line strength. This publication, still referred to as a Technical Report, was under revision in 2002. Since there is an overlapping with the regional standardization in Europe, this new IEC standard will not be mandatory for Europe. However, it serves as the basis for the standardization in Europe and for countries, which do not run standardization of overhead power lines on their own. International bids frequently refer to it in project specifications.
In Europe, the standard EN 50 341-1 [6.4] was established as a *regional overhead electrical line standard* and published in 2002. This standard consists of a main body with general requirements and common specifications, as well as of National Normative Aspects for the individual CENELEC member countries [6.20], e. g. EN 50 341-3-1 [6.21] will be applicable in Austria, EN 50341-3-3 [6.22] in Switzerland and EN 50 341-3-4 [6.10] in Germany. From Table 6.20, the parts of EN 50 341-3 valid for the individual countries can be taken. Still existing national standards have to be withdrawn until January 1st, 2004.
The standards IEC 60 826 and EN 50 341-1 describe procedures for the determination of climatic loads based on measurements, e. g. wind velocities and ice loads, but no fixed values for the line design. Such precise figures obtained from the evaluation of measurements in the respective application area and from operational experience are given in the National Normative Aspects for countries which are CENELEC members [6.10] or in project specifications. Tables 6.20, 6.23 and 6.24 provide an overview on wind loads, ice loads and combined wind and ice loads applied in European countries. Standards of countries outside Europe are often based on IEC 60 826.

6.6.2 Wind loads

6.6.2.1 Wind load model according to IEC 60 826

The *IEC 60 826 wind load model* is based on measurements of wind velocities. The ten minute mean wind velocity recorded 10 m above ground in an open terrain, which is designated as category B in IEC 60 826 and corresponds to terrain category II according

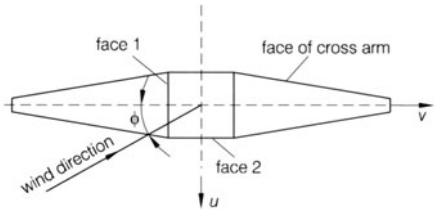

Figure 6.15: Wind action on supports

Tabelle 6.18: Reference wind pressure in N/m² according to IEC 60 826

Zone	Terrain category			
	A	B	C	D
$1/k_j$	1,08	1,00	0,85	0,67
1	422	362	261	162
2	544	467	337	209
3	731	627	453	281

to EN 50 341-1, serve as reference. The evaluation of wind velocities recorded at sites with characteristics different from terrain category B is presented in clause 6.3.2.2.
Data for *wind velocities in Europe* can be found in ENV 1991-2-4 [6.8]. The *reference wind pressure* for the relevant terrain category results from

$$q_0 = 0{,}6125\,(V_B/k_j)^2 \quad , \tag{6.60}$$

where k_j takes care of the terrain category, according to Table 6.14 and V_B is the reference wind velocity for terrain category B.
According to the IEC 60 826 wind load model, the *wind loads on conductors* are determined from (see Figure 6.14):

$$Q_{WC} = q_0 \cdot G_C \cdot G_L \cdot C_C \cdot d \cdot a_w \cos^2 \vartheta \quad . \tag{6.61}$$

The *drag factor* C_C can be assumed to be 1,0. The combined wind factor G_C considers the variation of wind load with height and the gust wind velocity; the span factor G_L takes care of the variation of effective wind pressure with the wind span. In Figures 6.6 and 6.8, the parameters G_C and G_L, respectively, are shown. For a 400 m span length, a factor G_L equal 0,94 results from IEC 60 826, being considerably higher than according to EN 50 341-1, where this factor is approximately 0,84. The angle ϑ refers to the angle between the wind direction and the perpendicular to the conductor.
The *wind load on supports* is computed from equation

$$Q_{WT} = q_0 \cdot G_T(1 + 0{,}2\sin^2 2\phi)(C_{T1}A_{T1} \cdot \cos^2 \phi + C_{T2} \cdot A_{T2} \cdot \sin^2 \phi) \quad . \tag{6.62}$$

The combined wind factor G_T is shown in Figure 6.7, ϕ is the angle of wind incidence relative to the crossarm axis, as explained in Figure 6.15.
A_{T1} and A_{T2} refer to the area of transverse and longitudinal tower faces filled with profiles, and C_{T1} and C_{T2} designate the associated drag factors. Such drag factors are given in Figure 6.16 for towers made of angle sections or of tubes, depending on the solidity ratio.
The *wind on insulators* is obtained from

$$Q_{Wins} = q_0 \cdot C_{ins} \cdot G_{ins} \cdot A_{ins} \quad , \tag{6.63}$$

where the drag factor C_{ins} is 1,2 and the combined wind factor G_{ins} is equal to G_T.

Example: In EN 50 341-3-4 [6.10], three zones are defined for wind actions on transmission lines. The associated wind velocities 10 m above ground with a return period of 50 years, for terrain category B, averaged over ten minutes are:

Zone 1: $V_{B\,10min} = 24{,}3$ m/s;
Zone 2: $V_{B\,10min} = 27{,}6$ m/s;
Zone 3: $V_{B\,10min} = 32{,}0$ m/s.

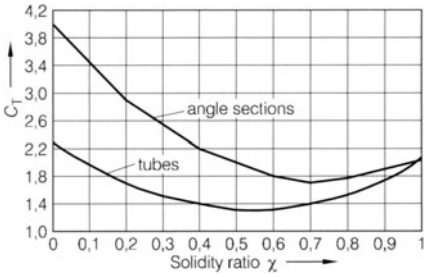

Figure 6.16: Drag factor C_T for structures made of angle sections or tubes

With these wind velocities the reference wind pressures q_0 result from equation (6.60) as presented in Table 6.18 for lines in terrain categories A, B, C or D.
The design wind pressures q_z are obtained from $q_z = q_0 \cdot G_{C,T}$ for conductors and towers, where G_C and G_T are taken from Figures (6.6) and (6.7), respectively. For $z = 30$ m and terrain category B the parameters G_C and G_T are 2,25 and 2,30 resulting in $q_{zC} = 2{,}25 \cdot 362 = 815\ \mathrm{N/m^2}$ and $q_{zT} = 2{,}30 \cdot 362 = 833\ \mathrm{N/m^2}$.
The resulting design wind pressures for conductors and towers are depicted in Figure 6.17 for wind zone 1 depending on the height above ground. For wind loads in zone 2, the wind pressures are higher by the ratio $(27{,}6\ /\ 24{,}3)^2$, that means approximately 1,3 times higher than the values shown in Figure 6.17. For wind zone 3 the ratio is $(32/24{,}3)^2 = 1{,}73$. The stability of the towers has to be verified for a wind action perpendicularly to the line axis and under an angle of 45°.
The ratio of wind loads on 1 m^2 effective tower area to 1 m^2 effective conductor area can be used for a comparison of wind models, in view of their effects on towers and conductors. For a drag factor $C_T = 2{,}8$, a span length of 400 m and a corresponding span factor $G_L = 0{,}94$, this ratio results to be $Q_{WT}/Q_{WC} = 2{,}8 \cdot 833/(0{,}94 \cdot 815) = 3{,}05$ in case of terrain category B, 30 m above ground. For terrain category C, it results $Q_{WT}/Q_{WC} = 2{,}8 \cdot 3{,}0 \cdot 261/(0{,}94 \cdot 2{,}6 \cdot 261) = 3{,}44$ and $Q_{WT}/Q_{WC} = 2{,}8 \cdot 3{,}90 \cdot 162/(0{,}94 \cdot 2{,}90 \cdot 162) = 4{,}01$ for terrain category D.

6.6.2.2 Wind model according to the European standard EN 50 341-1

For determination of wind actions, EN 50 341-1 [6.4] specifies a *General Approach* and an *Empirical Approach*. In case of the General Approach, the wind actions are deduced from recorded wind data. This approach is detailed hereafter. In case of the Empirical Approach, the determination of wind and ice loads and their combinations is specified in the National Normative Aspects and assumed as well validated by experience and long-term operation of overhead lines.
Clause 4.2 of EN 50 341-1 [6.4] describes a wind load model which enables establishing wind loads for overhead line components and elements based on wind velocities. As in case of IEC 60 826, the ten minute mean wind velocity in open terrain 10 m above ground forms the basis for this model. The variation with height is given by:

$$V_z = k_T \cdot V_R \cdot \ln(z/z_0) \quad , \tag{6.64}$$

where k_T is a parameter depending on the type of terrain (see Table 6.13), z the height above ground, z_0 the roughness length according to Table 6.13 and V_R the reference wind velocity for terrain category II, 10 m above ground, expressed as the ten minute mean value.
The wind pressure in a height z above ground follows from

$$q_z = 1/2\, \varrho\, V_z^2 \tag{6.65}$$

with $\varrho = 1{,}225\ \mathrm{kg/m^3}$.
The *wind load on conductors* can be computed from (see Figure 6.14)

$$Q_{WC} = q_z \cdot G_q \cdot G_L \cdot C_C \cdot d \cdot a_w \cdot \cos^2 \vartheta \quad , \tag{6.66}$$

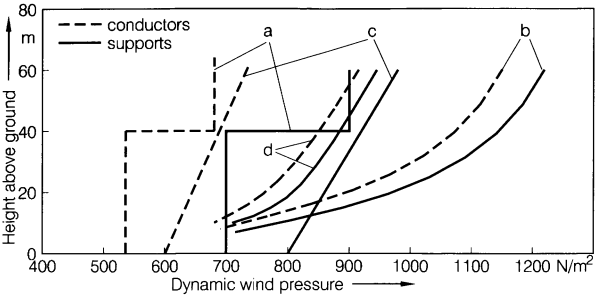

Figure 6.17: Comparison of design wind pressures depending on height above ground for
a) DIN VDE 0210/12.85;
b) EN 50 341-1;
c) EN 50 341-3-4;
d) IEC 60 826

where
G_q is the *gust response factor* determined by

$$G_q = [1 + 2{,}28/(\ln z/z_0)]^2 \quad , \tag{6.67}$$

G_L is the span factor, equal to:

$$G_L = 1{,}30 - 0{,}082 \ln a_w \tag{6.68}$$

applicable to the terrain category II (Table 6.13).
C_C is the drag factor which can be set 1,0 for conductors, ϑ is the angle of incidence as defined in Figure 6.14.
The *wind load on lattice towers* is obtained from

$$Q_{WT} = q_z \cdot G_q \cdot G_x(1 + 0{,}2 \sin^2 2\,\phi)(C_{T1}\, A_{T1} \cos^2 \phi + C_{T2}\, A_{T2} \sin^2 \phi)\,, \tag{6.69}$$

where G_q is the gust response factor according to equation (6.67), G_x a structural resonance factor which is assumed to be 1,05 for overhead line structures. To C_{T1}, C_{MT}, A_{T1}, A_{T2} and ϕ, the same definitions apply as explained in the context of equation (6.62). Figure 6.16 applies to drag factors C_T. The wind model according to EN 50 341-1 uses the same gust response factors for wind on conductors as for wind on supports, meaning that also for wind load on conductors a peak gust with only 2 s duration is used. This assumption contradicts all known observations and experience.

Example: Standard EN 50 341-1 does not contain data for wind velocities but refers to National Normative Aspects in EN 50 341-3. As an example, the same data are evaluated as in clause 6.6.2.1, however, limited to wind zones 1 and 2 and terrain categories II, III and IV, which correspond to categories B, C and D of IEC 60 826. The reference wind velocity results from (6.64) with $k_T = 0{,}19$, 0,22 and 0,24 for the categories II, III and IV, respectively, and $z_0 = 0{,}05$, 0,30 and 1,0 m. For category II $V_{10\,m} = 0{,}19 \cdot 24{,}3 \ln(10/0{,}05) \approx 24{,}3$ and $V_{50\,m} = 0{,}19 \cdot 24{,}3 \ln(50/0,05) = 31{,}9$ m are obtained. The gust response factor results from (6.67) to be $G_q = [1 + 2{,}28/(\ln 10/0{,}05)]^2 = 2{,}05$ for 10 m above ground and $G_q = [1 + 2{,}28/(\ln 50/0{,}05)]^2 = 1{,}77$ for 50 m above ground. The corresponding wind pressures on supports are $q_{10\,m} = 1{,}225/2 \cdot 1{,}05 \cdot 2{,}05 \cdot (24{,}3)^2 = 779$ N/m^2 10 m above ground and $q_{50\,m} = 1{,}225/2 \cdot 1{,}05 \cdot 1{,}77 \cdot (31{,}9)^2 = 1158$ N/m^2 50 m above ground. The wind pressures on conductors are obtained similarly, without the factor 1,05. Therefore, $q_{10\,C} = 742$ N/m^2 and $q_{50\,C} = 1103$ N/m^2.
Figure 6.17 depicts the design wind pressures for supports and conductors having a return period of 50 years. In addition to the reliability level according to a 50 years return period, EN 50 341-1 mentions two other *reliability levels for wind load design.* For level 2, referring to a return period of 150 years, the wind loads resulting from level 1 have to be multiplied by the factor 1,2, and for level 3, related to a return period of loads of 500 years, by the factor 1,4.
In Table 6.19, the wind loads for the terrain categories II to IV and the relation of the corresponding aerodynamic wind pressures for assumptions according to terrain category II, are presented. For terrain category III, the relation varies from 0,79 to 0,87 depending on the height

Table 6.19: Wind loads for the terrain categories II to IV according to EN 50 341-1

Terrain	Height	Reference wind velocity		Gust factor	Wind pressure on supports		Wind pressure on conductors		Relation to terrain category II
		Zone 1	Zone 2		Zone 1	Zone 2	Zone 1	Zone 2	
	z	V_{z1}	V_{z2}	G_q	q_{T1}	q_{T2}	q_{C1}	q_{C2}	q_x/q_{II}
	m	m/s	m/s	—	N/m^2	N/m^2	N/m^2	N/m^2	—
II	10	24,3	27,6	2,05	779	1 005	742	957	1,00
	50	31,8	36,2	1,77	1 158	1 489	1 103	1 423	1,00
III	10	18,7	21,3	2,72	612	794	583	756	0,79
	50	27,4	31,1	2,09	1 009	1 300	961	1 238	0,87
IV	10	13,4	15,2	3,96	457	588	436	560	0,59
	50	22,8	25,9	2,51	839	1 083	799	1 031	0,72

above ground, for terrain category IV between 0,59 and 0,72. With respect to the increased reliability requirements in the terrain categories III and IV, a design of the supports for wind loads lower than those adopted in an open terrain, does not seem to be justified.
To compare the wind action on supports and conductors, the wind load on 1 m^2 area of supports and conductors exposed to wind is calculated: $Q_{WT} = C_T \cdot 1{,}05 \cdot q_Z$ and $Q_{WC} = C_C \cdot G_L \cdot q_Z$. Assuming $C_T = 2{,}8$, $C_C = 1{,}0$ and $G_L = 1{,}30 - 0{,}082 \ln 400 = 0{,}81$ for 400 m wind span, it is obtained $Q_{WT}/Q_{WC} = 2{,}8 \cdot 1{,}05\, q_Z/(1{,}0 \cdot 0{,}81 \cdot q_Z) = 3{,}63$.

6.6.2.3 Wind models according to EN 50 341-3

The *National Normative Aspects* of European standard on overhead lines EN 50 341-3 [6.20] specify *wind models* and *data* valid for CENELEC member countries. Table 6.20 gives an overview on these specifications. For details, the mentioned parts of EN 50 341-3 should be studied. The given data assume a drag factor of $C_T = 2{,}8$ for structures and $C_C = 1{,}0$ for conductors to provide a basis for comparison. In many countries, several different geographically defined wind zones exist. There is no country where the General Approach of EN 50 341-1 is applied without modifications. The majority of specifications uses the Empirical Approach.
The German National Normative Aspects EN 50 341-3-4 [6.10] are an example for the Empirical Approach. The wind model is based on the wind data for Germany as specified in the Eurocode 1 [6.8] for wind loads and detailed in other German standards dealing with wind load assumptions, e. g. DIN 4131: *Antenna structures* made of steel [6.23]. The geographical classification of wind zones according to the associated wind velocities were taken from standard DIN 4131. The provisions made in EN 50 341-3-4 are detailed in the following as an example for the Empirical Approach.
The *basic wind pressure* increases linearly with the height z according to

$$\begin{aligned} &\text{– Zone 1: } q_z = \ 800 + 30\,(z/10) \text{ N/m;} \\ &\text{– Zone 2: } q_z = 1050 + 30\,(z/10) \text{ N/m;} \\ &\text{– Zone 3: } q_z = 1300 + 30\,(z/10) \text{ N/m.} \end{aligned} \tag{6.70}$$

Hereafter, the wind load for zone 1 is dealt with because of its significance for overhead power lines. Figure 6.17 depicts the variation with height of wind loads for supports and conductors in wind zone 1. To enable comparison with the design values according to IEC 60 826 and EN 50 341-1, the wind data have been multiplied by a partial factor of 1,35 as stipulated in [6.10].
The standard specifies the relevant components of wind loads on conductors in direction of the crossarm axis and perpendicularly to that axis. The general equations are (see Figure 6.14):

$$Q_{WCv} = \frac{q_z \cdot C_C \cdot G_L \cdot d}{2} \left[a_{w1} \cdot \cos^2\left(\phi + \frac{\theta_1}{2}\right) \cos\frac{\theta_1}{2} \right.$$

$$+ a_{w2} \cdot \cos^2\left(\phi - \frac{\theta_2}{2}\right) \cos\frac{\theta_2}{2}\Bigg] \tag{6.71}$$

and

$$Q_{WCu} = \frac{q_z \cdot C_C \cdot G_L \cdot d}{2}\Bigg[a_{w1} \cdot \cos^2\left(\phi + \frac{\theta_1}{2}\right) \sin\frac{\theta_1}{2} - a_{w2} \cdot \cos^2\left(\phi - \frac{\theta_2}{2}\right) \sin\frac{\theta_2}{2}\Bigg] \quad . \tag{6.72}$$

The definitions of the angles ϕ and θ can be taken from Figure 6.14. To a suspension tower in a straight line, it applies $\theta_1 = \theta_2 = 0$ and $(a_{w1} + a_{w2})/2 = a_w$.
The span factor is defined by $G_L = 0{,}45 + 60/a_w$ and considers a component of 0,75, which takes care of the lower effective gust wind velocity on conductors compared with wind action on towers (see clause 6.6.2.4).
Therefore, it is obtained for the case of a suspension tower in straight line:

$$Q_{WCv} = q_z \cdot C_C \cdot d \cdot a_w \cos^2\phi \cdot (0{,}45 + 60/a_w) \quad . \tag{6.73}$$

The wind loads on towers are presented using the same format; the quantities have the same significance as in equation (6.62) and have been explained in Figure 6.15.
Parallel to crossarm axis:

$$Q_{WTv} = q_z(1 + 0{,}2\ \sin^2 2\phi)(A_{T1} \cdot C_{T1} \cdot \cos^2\phi + A_{T2} \cdot C_{T2} \sin^2\phi) \cdot \cos\phi\,; \tag{6.74}$$

Perpendicular to crossarm axis:

$$Q_{WTu} = q_z(1 + 0{,}2\ \sin^2 2\phi)(A_{T1} \cdot C_{T1} \cdot \cos^2\phi + A_{T2} \cdot C_{T2} \sin^2\phi) \cdot \sin\phi\,. \tag{6.75}$$

From the general equations (6.74) and (6.75), it results for wind action in direction of the crossarm axis, i. e. $\phi = 0°$:

$$Q_{WTv} = q_z \cdot A_{T1} \cdot C_{T1}\,; \quad Q_{WTu} = 0 \tag{6.76}$$

and for wind action under 45°, i. e. $\phi = 45°$,

$$\left.\begin{aligned} Q_{WTv} &= q_z \cdot 0{,}424\,(A_{T1}C_{T1} + A_{T2}C_{T2}) \\ Q_{WTu} &= q_z \cdot 0{,}424\,(A_{T1}C_{T1} + A_{T2}C_{T2}) \end{aligned}\right\} \quad . \tag{6.77}$$

Also for wind on crossarms, EN 50 341-3-4 contains specific stipulations which are:

$$\left.\begin{aligned} Q_{WTQv} &= 0{,}4 \cdot q_z \cdot A_{TQ} \cdot C_{TQ} \cdot \cos^2\phi \\ Q_{WTQu} &= q_z \cdot A_{TQ} \cdot C_{TQ} \cdot \sin^2\phi \end{aligned}\right\} \quad . \tag{6.78}$$

Thereof, for wind action in direction of the crossarm axis, it is obtained:

$$Q_{WTQv} = 0{,}4 \cdot q_z \cdot A_{TQ} \cdot C_{TQ}\,; \quad Q_{WTu} = 0 \tag{6.79}$$

and for wind action under $\phi = 45°$,

$$\left.\begin{aligned} Q_{WTQv} &= 0{,}4 \cdot q_z \cdot A_{TQ} \cdot C_{TQ} \cdot 0{,}50 \\ Q_{WTu} &= q_z \cdot A_{TQ} \cdot C_{TQ} \cdot 0{,}50 \end{aligned}\right\} \quad . \tag{6.80}$$

The ratio of wind on supports to wind on conductors related to an area of 1 m^2 can be computed as a characteristic value: $Q'_{WTv}/Q'_{WLv} = q_z \cdot 2{,}8 \cdot A/(q_z \cdot C_C \cdot d \cdot a_w(0{,}45 + 60/a_w))$. With $A = d \cdot a_w = 1$ m^2, $C_C = 1$ and $a_w = 400$ m a value of 4,67 results.
Wind velocities and wind pressures according to European standard EN 50 341-3 are listed in Table 6.20.

Table 6.20: Wind pressures in N/m^2 or wind velocity in m/s according to EN 50341-3 (National Normative Aspects)

Country	Height (m)	Structures N/m^2	Conductors N/m^2	Source
Austria	—	700	520	EN 50341-3-1
Belgium			Span length > 100 m	EN 50341-3-2
	up to 25	750	375	
	25 to 50	800	400	
	50 to 75	850	425	
	75 to 100	900	450	
Switzerland	0 to 30	640[1)]	500	EN 50341-3-3
	30 to 80	740[1)]	650	
	above 80	1030[1)]	850	
	[1)] for drag factor $C_T = 2{,}8$			
Germany				EN 50341-3-4
	Three wind zones, defined geographically, $q = q_0 + 30\,(z/10)$[2)]			
Zone 1	10	830	620	
$q_0 = 800$ N/m^2	40	920	690	
Zone 2	10	1080	810	
$q_0 = 1050$ N/m^2	40	1170	880	
Zone 3	10	1330	1000	
$q_0 = 1300$ N/m^2	40	1410	1060	
	[2)] z = height above ground			
Denmark	Two wind zones defined by reference wind velocities (50 years return period)			EN 50341-3-5
Zone 1: 24,0 m/s				
Zone 2: 27,1 m/s				
Spain		~ 700[1)]	~ 500[2)]	EN 50341-3-6
	[1)] for drag factor $C_T = 2{,}8$			
	[2)] conductor diameter more than 16 mm			
Finland	Two wind zones defined by reference wind speeds (50 years return period)			EN 50341-3-7
Zone 1 (inland): 21,0 m/s				
Zone 2 (shore): 25,0 m/s				
France	inland	715[1)]	480	EN 50341-3-8
	sea side, northern part	950[1)]	640	
	[1)] for drag factor $C_T = 2{,}8$			
Great Britain	Reference wind velocities according to map: 20 m/s to 31 m/s, application of General Approach according to EN 50341-1			EN 50341-3-9
Greece		765	460	EN 50341-3-10
Ireland	Reference wind load: Terrain A: 732 N/m^2; B: 627 N/m^2; C: 453 N/m^2; D: 282 N/m^2; Gust factors according to IEC 60826			EN 50341-3-11
Italy	Wind velocity 130 km/h			EN 50341-3-13
		835[1)]	706	
	[1)] for drag factor $C_T = 2{,}8$			
Netherlands	Dynamic wind pressures including gust factors are			EN 50341-3-15
Zone 1	10	1060		
	40	1540		
Zone 2	10	880		
	40	1350		
Zone 3	10	730		
	40	1150		
Norway	Reference wind speed to be chosen according to Norwegian wind standard			EN 50341-3-16

Table 6.20: continued

Portugal	Two regional wind zones			EN 50 341-3-17
Zone A	10	550	330	
	40	960	576	
Zone B	10	660	396	
	40	1150	690	
Sweden	below 10	800	400	EN 50 341-3-18
	above 10	$800 + 6(z - 10)$	$400 + 3(z - 10)$	

Table 6.21: Comparison of wind load models by means of the bending moments at base of a 400 kV double-circuit suspension tower

	IEC 60 826 Level 1		EN 50 341-1 Level 1		EN 50 341-3-4 Zone 1	
Reference wind pressure N/m^2	690		780		830	
	kNm	%	kNm	%	kNm	%
Wind perpendicular to the line (a)	7557[1)]	100	8867	100	8597[1)]	100
– Conductor	5510	73	5804	66	5467	64
– Other elements	2047	27	3062	34	3129	36
Wind under 45° (b)	6928	100	9439[1)]	100	8133	100
– Conductor	2756	40	2977	32	2771	34
– Other elements	4172	60	6462	68	5362	66
Ratio (a) to (b)	1,09		0,94		1,06	
Ratio of prevalent loading to that for EN 50 341-3-4	88 %		110 %		100 %	

[1)] prevalent loading condition

6.6.2.4 Comparison of wind load models with measurements

The consequences of the *wind load models* studied will be demonstrated with an example of a 400 kV double-circuit suspension tower. Its conductors are

- earth wire 1 × 264-AL1/34-ST1A $d = 22{,}4$ mm,
- phase conductors 6 × 4 × 264-AL1/34-ST1A $d = 22{,}4$ mm.

The wind span is 400 m. Figure 6.17 depicts the wind pressures on conductors and towers. The wind load models are compared by means of the moments acting at the tower base and presented in Table 6.21, resulting from the load cases "wind action perpendicular to the line" and "wind action under 45°".

In case of wind action perpendicularly to the line, two thirds of the total moment result from wind action on conductors in the given example, with the exception of the model according to IEC 60 826, where approximately 75 % of the total wind action result from wind loads on conductors and only 25 % from wind on tower structures. According to the available experience, the wind load acting on conductors resulting from this model is too high as compared with wind load on towers.

In case of wind action under 45°, the proportion of the wind load on conductors varies to a greater extent. The highest proportion results from assumptions according to IEC 60 826 and reaches 40 %, while according to EN 50 341-1 this proportion would be 32 % only. Wind load on towers and the other elements varies between 60 and 68 % in case of wind action under 45°. When the load case "wind action under 45°" prevails, the wind load on towers is of great significance.

The effect of the wind acting perpendicularly to the line in relation to the wind action under 45° can be assessed by the ratios of the sum of moments acting perpendicularly to the line and in line direction. While in case of the EN 50 341-1 wind load model, the wind action under 45° predominates as expressed by a factor of 0,94, the wind model according to IEC 60 826 leads to considerably higher loading for wind action perpendicularly to the line. The corresponding ratio is calculated to be 1,09. The data refer to the tower studied; for taller towers, the influence of wind load on tower will

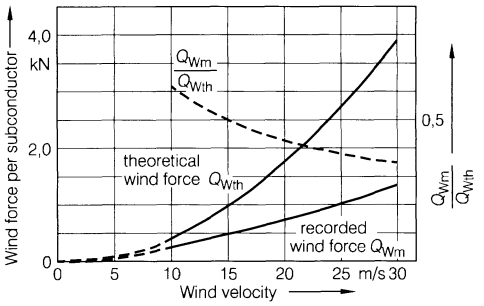

Figure 6.18: Theoretical and recorded values for wind forces acting on a subconductor dependent on the instantaneous wind velocity (2-sec-gust) according to [6.24] and its ratio

Table 6.22: Wind load on lattice steel towers and conductors

Source	Q_{WT}/Q_{WC}
IEC 60 826	
Terrain B	3,05
C	3,44
D	4,01
EN 50 341-1	3,63
EN 50 341-3-4	4,70
Hornisgrinde	~ 6,50

increase and, therefore, also the significance of the load case "wind under 45°". From experience, it can be concluded that in the wind model proposed by EN 50 341-3-4, the relation between wind perpendicularly to the line and wind acting under 45° simulates satisfactorily the reality.

For comparing globally the three wind models, the loading resulting due to EN 50 341-3-4 is assumed as 100 %. Then, EN 50 341-1 gives a loading of 110 % and IEC 60 826 of 88 %, as it can be seen in Table 6.21.

Figure 6.17 depicts the studied wind models with respect to wind pressures on towers and conductors. In case of wind load on towers, the stipulations at a height of 10 m are relatively close to each other, being between 690 and 780 N/m^2. However, for a height of 60 m, the band width is from 900 N/m^2 according to DIN VDE 0210/12.85 up to 1210 N/m^2 according to EN 50 341-1, showing a difference of approximately 35 %. The assumptions according to EN 50 341-3-4, being 980 N/m^2, can be found close to IEC 60 826 and DIN VDE 0210/12.85. Lines designed according to DIN VDE 0210 have shown a long-lasting positive operational performance. The increase of the wind loads with height according to EN 50 341-3-4 is confirmed by the assumptions according to IEC 60 826. The increase of the wind load with height according to EN 50 341-1 is substantially different from the other models and yields 25 % higher wind loads as compared with EN 50 341-3-4 at a height of 60 m.

The ratio between wind pressures on towers and conductors differs to a large extent between the individual wind models. In case of EN 50 341-1 and IEC 60 826, there is only a difference of approximately 5 % concerning this ratio, whereas the difference in cases of DIN VDE 0210/12.85 and EN 50 341-3-4 is 25 %. The ratio between loads on conductors and structures can be assessed by the quotient Q_{WT}/Q_{WC} related to 1 m^2 of structural components and 1 m^2 conductor surface as given in Table 6.22. There, the results from Hornisgrinde measurements [6.24] are also given. Compared to these data, IEC 60 826 and EN 50 341-1 result in considerably lower ratios, indicating that the wind action on conductors is overestimated when compared to wind action on towers.

Figure 6.18 depicts the results of *wind load measurements on subconductors of bundles* carried out at the wind test station at the Hornisgrinde in Germany between 1955 and 1960 [6.24]. There, the calculated wind load according to

$$Q_{W\,th} = 1{,}25/2 \cdot V_{max}^2 \cdot d \cdot a \tag{6.81}$$

and the measured wind load $Q_{W\,m}$ are presented.

The ratio $Q_{W\,m}/Q_{W\,th}$ is approximately 0,4 at 20 m/s and 0,35 at 30 m/s wind velocity (see Figure 6.18). This ratio decreases with increasing wind velocities. If the dynamic

wind pressure on towers $q_T = 1{,}25/2 \cdot V_{max}^2$ is assumed as a reference, then the wind pressure for wind action on conductors can be expressed by $q_C = k \cdot q_T$.
According to the results obtained from the test station Hornisgrinde, values between 0,35 and 0,44 apply to the factor k. If on the safe side $k = 0{,}5$ and the span factor G_L is assumed to be $(1{,}30 - 0{,}082 \cdot \ln a_w)$ according to EN 50 341-1, then the wind load on conductors is obtained from (6.61):

$$Q_{WC} = 0{,}5\, q_z \cdot d \cdot C_C \cdot a_w\, (1{,}30 - 0{,}082 \cdot \ln a_w) \cos^2 \phi \quad . \tag{6.82}$$

Due to $0{,}5\, q_z \approx (\sqrt{0{,}5} \cdot V_z)^2$, the wind pressure $0{,}5\, q_z$ corresponds to 0,71 times the wind velocity V_z of a 2 sec wind gust. In case of open terrain, this corresponds to the ten minute mean value of the wind velocity. Therefore, the observations at the test station *Hornisgrinde* [6.24] demonstrated that the wind loads on conductors are governed from the ten minute mean values of the wind velocities. Studies carried out in Canada and by the Cigré Working Group 06 came to the same result [6.25]. Therefore, Working Group 06 of Cigré Study Committee 22 proposed, that wind loads on conductors should be calculated for ten minute mean values or, conservatively, for 5 minutes mean values.
These studies give reasons for the statement that the wind model according to EN 50 341-3-4 can be considered as conservative so far the *wind loads on conductors* are concerned. The assumptions according to IEC 60 826 and EN 50 341-1 are outside the range of experience. In case of EN 50 341-1, this can be traced back to the fact that the same gust response factors are considered for the determination of the wind load on conductors as for the wind load on the towers.

6.6.3 Ice loads

6.6.3.1 Ice load model according to IEC 60 826

IEC 60 826 describes the yearly maximum *ice loads* by means of the Gumbel distribution (see clause 6.9.4). The evaluation of available information on ice loads can be carried out according to clause 6.4.3.2 and results in the reference ice load g_{IR} obtained from equation (6.53), forming the basis for line design.
Concerning the loading of supports in case of ice accretion, four conditions are stipulated:

- **Uniform ice formation on all conductors:** All conductors and earth wires are loaded by the reference ice load g_{IR}, thus resulting in a total vertical loading per unit length of $m_C \cdot g + g_{IR}$, where m_C is the conductor mass per unit length and g the gravitational acceleration.
- **Non-uniform ice formation on one phase conductor or one earth wire:** Non-uniform ice accretion on a conductor in adjacent spans results in a longitudinal load at the support. Such loading may be created either by a *non-uniform ice accretion* as a consequence of the line exposure or due to *ice shedding*. According to IEC 60 826, it is assumed in this case that all the conductors are loaded by an ice load according to $0{,}7 \cdot g_{IR}$ and one phase conductor or earth wire with a reduced ice load of $0{,}28 \cdot g_{IR}$. The conductor with reduced ice load has to be selected such that the individually most unfavourable loading results. This type of loading is considered as a torsional loading condition.
- ***Non-uniform ice formation* on all conductors in adjacent spans:** In this case, it is assumed that all conductors in one span or in one tensioning section adjacent to the tower studied are loaded by an ice load according to $0{,}28 \cdot g_{IR}$, while the conductors in the span at the other side of the support are loaded by $0{,}7 \cdot g_{IR}$. This condition is considered as longitudinal bending.
- ***Non-uniform ice formation* on one circuit of a double- or multi-circuit line:** In this case, it is assumed that all conductors of one circuit are loaded by ice

Table 6.23: Ice load assumptions for some European countries according to EN 50 341-3

Country	Ice load	Example N/m d = 30 mm	Source
Austria	Nominal ice load $4 + 0{,}2\,d$[1] N/m	10	EN 50 341-3-1
	Exceptional ice load $\leq$ 110 kV 25 N/m	35	
	$>$ 110 and $\leq$ 220 kV 40 N/m	40	
	$>$ 220 and $\leq$ 380 kV 50 N/m	50	
Belgium	Only for altitudes above 400 m, ice thickness 20 mm, density 600 kg/m^2	19	EN 50 341-3-2
Switzerland	At least 20 N/m	20	EN 50 341-3-3
Germany	Ice load depends on line location:		EN 50 341-3-4
	Zone 1: $5 + 0{,}1\,d$/ N/m	8	
	Zone 2: $10 + 0{,}2\,d$ N/m or	16	
	Zone 3: $20 + 0{,}4\,d$ N/m	32	
Denmark	$12 + 0{,}9\,d$ N/m	39	EN 50 341-3-5
Spain	Altitude 0 to 500 m no ice load		EN 50 341-3-6
	Altitude 500 to 1 000 m $1{,}8\sqrt{d}$ N/m	9,9	
	Altitude 1 000 to 1 500 m $3{,}6\sqrt{d}$ N/m	19,7	
	Altitude above 1 500 m $5{,}4\sqrt{d}$ N/m	29,6	
Finland	Altitude 0 to 50 m 10 N/m	10	EN 50 341-3-7
	Altitude 50 to 100 m 25 N/m	25	
	Altitude 100 to 200 m 50 N/m	50	
	Altitude above 200 m 75 N/m	75	
France	Altitude 0 to 600 m, thickness 20 mm, densitiy 600 kg/m^3 above 600 m: See project specifications	19	EN 50 341-3-8
Great Britain	Thickness $t = (2/3 + 4/d)[r_0 + (H \cdot 200)/25]$		EN 50 341-3-9
	r_0 basic thickness according to	40*	
	location, H altitude in m,	60	
	density 500 kg/m^3, $50 < r_0 < 80$ mm	64	
	* at 200 m height		
Greece	Thickness 6,35 or 12,7 mm, as specified by project specification density 900 kg/m^3	6,5 15,3	EN 50 341-3-10
Ireland	Ice thickness 40 mm, density 900 kg/m^3	79	EN 50 341-11
Italy	Ice thickness 12 mm, density 920 kg/m^3	19	EN 50 341-3-13
Netherlands	Region A: $5{,}0\sqrt{d}$ N/m	27,4	EN 50 341-3-15
	Region B: $1{,}8\sqrt{d}$ N/m	9,9	
Norway	20 to 50 N/m depending on altitude and region	20 to 50	EN 50 341-3-16
Portugal	Altitude 0 to 700 m: No ice load, above 700 m: 11/40 (10+d) N/m	11	EN 50 341-3-17
Sweden[2]	$\sqrt{(9{,}2 + 0{,}51\,d + m_C g)^2 + w_{CI}^2} - m_C g$ N/m	33	EN 50 341-3-18

[1] d is the conductor or subconductor diameter

[2] w_{CI} is the wind load on ice-covered conductor in N/m

loads according to $0{,}28 \cdot g_{IR}$, while the conductors of all other circuits are loaded by $0{,}7 \cdot g_{IR}$. This combination is considered as transverse bending.

Loading conditions with non-uniform ice accretion may only prevail for the line design in case of high ice loads.

6.6.3.2 Ice load model according to EN 50 341-1

Following EN 50 341-1, the characteristic ice load g_{IR} of lines with *ice accretion* is assumed according to the local conditions. For determination of these values, the standard refers to National Normative Aspects (EN 50 341-3). Four load cases are defined, which practically correspond to those defined in IEC 60 826 with slightly different reduction factors. Therefore, this loading model is not considered in detail here.

6.6.3.3 Ice load model according to EN 50 341-3

Standard EN 50 341-3 specifies the *ice loads* for countries which constitute CENELEC. In Table 6.23, the specifications are summarized. As it can be seen, the specifications vary with the region and the altitude above sea-level. In some countries, fixed data independent of the conductor diameter are stipulated, while in other countries the ice data depend on this parameter. In Northern Europe, higher ice loads are specified than in Central Europe and Southern Europe. When comparing the data, different partial factors need to be considered. Table 6.23 lists data obtained for a conductor diameter of 30 mm.

As an example, some details concerning EN 50 341-3-4 [6.10] are given. There, three zones are distinguished:

Ice load zone 1 $g_{\mathrm{IR}} = 5 + 0{,}1\,d$ N/m,
Ice load zone 2 $g_{\mathrm{IR}} = 10 + 0{,}2\,d$ N/m,
Ice load zone 3 $g_{\mathrm{IR}} = 20 + 0{,}4\,d$ N/m,

where d is the conductor or subconductor diameter in mm.

In *ice load zone* 1, there are areas, where due to the climatic conditions, confirmed by long-term experience only low ice loads occur, which did not result in damage of existing overhead lines.

In zone 2, there are areas, where due to the climatic conditions, confirmed by long-term experience, high ice loads have to be expected which, among other things, resulted in damage of existing overhead lines.

In zone 3, there are areas, where, as induced from long-term experience very high ice loads have to be expected, due to the climatic conditions and the geographical situation. In such cases considerable damage of existing overhead lines has so far occurred.

The classification of the terrain of an overhead line or parts thereof into one of the three zones defined above, needs to be decided by the operator or erecting company of the line. An evaluation of ice loads experienced on lines in Germany is given in [6.13], concluding that, in extended parts of Southern Germany, ice loads of 40 N/m and in Northern Germany ice loads of 25 N/m can be expected as maximum values. Together with the partial factors for loads and materials, the assumptions for ice loads in zones 1 and 2 cover these maximum ice load observations.

Ice accretion has to be assumed for insulators, radar markers and air traffic warning spheres as well, however, not for structures.

EN 50 341-3-4 defines two load cases for ice effect without wind:

- Reduction of the conductor tensile force of one conductor. According to the function of the support and the length of the insulator set, the conductor tensile force is reduced by 25 to 65 %. This reduction creates a *torsional loading of the tower body* as the most significant result.
- All conductor tensile forces on one side of the structure are reduced between 15 and 20 %. This results in a *longitudinal bending of the support* considered.

These cases are considered as *exceptional loading*, whereby the partial factor for loads is assumed to be 1,0. These loadings are considerably higher than those resulting from the ice load models according to IEC 60 826 and EN 50 341-1. They frequently govern the rating of the bracings of lattice steel towers.

6.6.4 Combined wind and ice action

6.6.4.1 Model according to IEC 60 826

In IEC 60 826, *combined wind and ice action* is considered only regarding to conductors. The procedure to determine design loads corresponds to the steps described in clause 6.5.1.

The combination of wind drag factors and ice densities having a long return period with ice and wind of high probability of occurrence does not result in critical loads. Therefore, only two load cases are considered:

- Ice loads with a return period T_r combined with an average value of yearly maximum wind loads on conductors and
- Ice loads according to the average of yearly maximum values combined with the wind load during icing periods with a return period T_r.

The reference ice load g_{IR}, as dealt with in clause 6.6.3.1, is assumed as the one having a return period T_r. Only those wind velocities need to be considered which may occur during the icing period.

According to these assumptions, the ice load with low probability of occurrence is assumed to be g_{IR} and that with a high probability of occurrence is $0{,}4 \cdot g_{IR}$. The corresponding temperature is $-5°C$.

The wind loads with low probability of occurrence may be assumed to be 0,6 to 0,85 times the reference wind velocity V_R, according to clause 6.6.2.1. The wind velocity with a high probability of occurrence can be taken as 0,4 to 0,5 times the reference wind velocity V_R. The drag factors and ice densities follow from Table 6.17. The *wind action on ice covered conductors* may then be computed as presented in clause 6.5.3.

6.6.4.2 Model according to EN 50 341-1

The basic assumptions for the determination of loads for combined wind and ice action are the same as in case of IEC 60 826, whereby the provisions concerning the numerical data are practically the same (see [6.4]). Regarding load cases, EN 50 341-1 refers to National Normative Aspects. The data for the ice densities differ from the assumptions according to IEC 60 826 and are given in Table 6.17. The dynamic wind pressures can be obtained using the equations given in clause 6.6.2.2, whereby the equivalent diameter D_I of a conductor with ice accretion follows from equation (6.59). The actions on supports result from equation (6.58).

In EN 50 341-1 [6.4], a simplified method is used to determine the loads for combined wind and ice action, taking into account two main combinations:

- An extreme ice load equal to the design value of the ice load, $\gamma_I \cdot G_{IK}$, combined with a moderate wind load $\Psi_W \cdot Q_{WK}$. The moderate wind speed associated with ice loads can be taken as 0,55 to 0,65 times the extreme 50 year wind speed depending on the type of ice. Accordingly, a representative value of the combination factor for wind action Ψ_W equal to 0,4 is suggested.
- A high wind speed combined with a moderate ice load $\Psi_I \cdot G_{IK}$. The high wind speed associated with ice load can be based on a wind speed corresponding to 0,70 to 0,85 times the extreme wind speed used for design, depending on the type of ice. A combination factor for ice action Ψ_I equal to 0,35 generally applies.

Table 6.17 gives indicative values for the density of various ice types for a range of values of the drag factors.

6.6.4.3 Combined wind and ice action according to EN 50 341-3

In EN 50 341-3 [6.20], detailed loading assumptions for combined wind and ice actions are given, which are summarized in Table 6.24. The majority follows the first option of EN 50 341-1, combining design ice load with a moderate wind load, the combination factor Ψ being 0,30 to 0,64. The specific ice weight is assumed between 6000 and 9200 N/m^3. The equivalent diameter of a cylindrical ice formation D_I is

$$D_I = \sqrt{d^2 + 4\, g_I/(\pi \cdot \varrho_I)} \quad , \tag{6.83}$$

where d is the conductor diameter in m, g_I the ice load and ϱ_I the ice density in N/m^3.

Table 6.24: Specifications for combined wind and ice load according to EN 50 341-3

Country	Ice load	Wind load	Source
Austria		No wind load on ice covered conductors	EN 50 341-3-1
Belgium	See Table 6.23	25 % of nominal wind pressure	EN 50 341-3-2
Switzerland		No wind load on ice covered conductors	EN 50 341-3-3
Germany	See Table 6.23	50 % of wind pressure without ice	EN 50 341-3-4
Denmark	See Table 6.23	40 % of wind pressure without ice	EN 50 341-3-5
Spain		No wind load on ice covered conductors	EN 50 341-3-6
Finland	See Table 6.23	40 % of wind pressure without ice	EN 50 341-3-7
France	See Table 6.23	Wind pressure 180 N/m^2	EN 50 341-3-8
Great Britain	Ice thickness see Table 6.23	64 % of wind pressure without ice	EN 50341-3-9
Greece	Ice thickness 6,35 or 12,7 mm	Wind pressure 190 N/m^2	EN 50341-3-10
Ireland	Ice thickness 25 mm	Wind pressure 490 N/m^2	EN 50 341-3-11
Italy	Ice thickness 12 mm	Wind velocity 65 km/h	EN 50 341-3-13
Netherlands	See Table 6.23	30 to 45 % of wind pressure without ice, depending on type of support and limit state	EN 50 341-3-15
Norway	a) Ice load according to Table 6.23 b) 35 % of ice load acc. to Table 6.23	40 % of wind pressure without ice ~70 % of wind pressure without ice	EN 50 341-3-16
Portugal	See Table 6.23	40 % of wind pressure without ice	EN 50 341-3-17
Sweden	$9{,}2 + 0{,}51\,d$ N/m	Height 0 to 25 m: 500 N/m^2 above 25 m: $500 + 6(h - 25)$ N/m^2	EN 50 341-3-18

As an example according to EN 50 341-3-4, the ice load is combined with 50 % of the wind load, as defined for the individual wind load zones. The reduced wind load applies to conductors, towers and the equipment. The specific ice weight ϱ_I is assumed to be 7500 N/m^3, the aerodynamic drag factor being 1,0. The equivalent diameter of the conductor with ice accretion D_I, in m, then results from

$$D_\mathrm{I} = \sqrt{d^2 + 0{,}00017\, g_\mathrm{I}} \quad . \tag{6.84}$$

Concerning the load cases, the wind actions have to be considered in direction of the crossarm axis, in the perpendicular direction to the crossarm axis and under 45° to these axes. Since these assumptions are considered as normal load cases, higher loadings result in each case than in the case of a uniform ice accretion on all conductors without wind action.

6.7 Loads at construction, operation and maintenance

6.7.1 Introduction

A failure of a tower element during *construction* or *maintenance* could lead to injuries of people. Such work, therefore, has to be planned and carried out such that a loading is avoided which would necessitate an expensive strengthening of the supports. When preparing construction and maintenance procedures, the specifications for *labour safety* need to be duly obeyed. Therefore, already when designing supports, likely loads due to such procedures should be considered.

6.7.2 Requirements according to IEC 60 826

According to IEC 60 826, the supports should be designed such that their elements withstand at least twice the loads which can occur during lifting of components using fixing points at the supports. In case of a well controlled procedure, a design for 1,5 times the expected loads suffices.

With respect to the forces occurring during the stringing procedures, it is recommended that the tensile forces for those conductors instantaneously not moving be assumed with 1,5 times their actual values and with twice the value for moving conductors. During the *conductor stringing procedure*, the vertical components at the support originating from a temporary anchoring of the conductors to the ground create additional loadings. The same applies to loads which result from variations of conductor tensile forces.

Longitudinal loads can occur at the supports which are temporarily used as end points of the conductor stringing operation. These temporary dead-end supports should withstand the *longitudinal loads*, as defined above.

If supports are temporarily secured by slack or pretensioned anchors, these increase the vertical load at their fixing points. Therefore, it is necessary to check the supports with respect to the additional loads exerted by the anchors.

During stringing operations, additional longitudinal loads may occur at the suspension support. According to IEC 60 826, these longitudinal loads can be considered by assuming a value which is produced by the product of the difference in height of the vertices in the adjacent spans and the conductor weight per unit length. However, this load is relatively low in most cases and can be neglected if provisions for the *line security* have been made (see clause 6.8).

Members, where linesmen may stand on during *construction* and *maintenance* should be able to carry a vertical load of 1,5 kN acting in their middle. The members should be able to carry this load in addition to the strain occurring during erection or maintenance.

6.7.3 Requirements according to EN 50 341-1 and EN 50 341-3

Only detailed requirements for loads caused by the construction or maintenance people can be found in EN 50 341-1. For this purpose, a load of 1,0 kN has to be assumed together with a partial factor of 1,5.

If walkways or working platforms are installed, these have to be designed for the maximum load to be expected. In addition, all members having an inclination lower than 60° against the horizontal and, therefore, being considered as mountable, have to be designed for a characteristic load of 1,0 kN acting vertically in the middle of the member. Other loads do not need to be taken into account in this case. Stirrups and stepbolts need to be designed as well for a characteristic load of 1,0 kN acting at the most unfavourable position.

Detailed provisions for *loads due to construction procedures* are specified in EN 50 341-3-4. They supplement the specifications given in EN 50 341-1.

Special *walkways* for climbing and access to working positions are necessary at towers. Such walkways should be arranged on at least two diagonally opposite leg members and may consist of a ladder, a *stepbolt* or a *stirrup arrangement.*

Crossarms should be equipped with a walkway and a *handrail*, unless they are designed such that the structural members can be used for climbing and structural members can be held on continuously.

Steel poles and *reinforced concrete poles* do not require any walkways for climbing and access to working positions if climbing devices separated from the poles are used, such as ladders or elevating platforms.

6.8 Failure containment and other special loads

6.8.1 Introduction

The objective of *security measures* is to minimize the probability of *cascading failures* which might otherwise extend well beyond the failed line section, whatever the reason and extent of the initial failure might be. There are several possibilities and options for corresponding provisions.

6.8.2 Provisions according to IEC 60 826

According to IEC 60 826, at each *attachment point* of an earth wire or a phase conductor, a *residual static load* should be assumed resulting from the release of the tension of one phase conductor or earthwire in the adjacent span. The residual static load corresponds to the conductor tension at the sagging temperature without any wind and ice loads. In case of suspension towers, allowance may be made for the relaxation of the load resulting from swing of the insulator sets in line direction. The value of this residual static load may be reduced by special devices, such as slipping clamps, in which case the minimum security requirements could be adjusted accordingly.
Furthermore, IEC 60 826 recommends to consider *longitudinal loads* at each conductor attachment point. To determine these residual loads, an additional load according to the conductor dead weight can be assumed in the adjacent spans. As an alternative, a difference of the conductor tensile force according to 50 % of the forces under sagging conditions, is proposed. With respect to line security, additional measures are recommended, such as:

- Increase of the residual static load by a factor of 1,5 at any point for lines which require a higher security.
- Assumption of torsional loads simultaneously at several conductor attachment points of a support, in case of double- or multi-circuit lines.
- Calculation of the *residual static load* for conditions, which cause a higher load than that occurring under everyday condition, e. g. assuming some wind or ice loads. This assumption is advisable for angle structures and lines subjected to severe climatic conditions.
- Insertion of *section supports within the line*, for example at every tenth tower, in case of important lines in areas with high ice accretion. Towers adopted for this purpose should be designed for the reduction or even loss of all conductor tensile forces from one side.

6.8.3 Provisions according to EN 50 341-1

In EN 50 341-1, the *security loads* are assumed according to the following conditions:

- With respect to *torsional loading* of the supports a relevant *residual static load* should be applied at any earth wire or phase conductor attachment point resulting from the release of the tensile force of a phase conductor or subconductor or of an earth wire in an adjacent span. It can be adequate to assume this residual static load simultaneously at several conductor attachment points. Loads and conductor tensile stresses may be calculated at the normal ambient reference temperature without any wind or ice load.
- With respect to *longitudinal loading*, reduced conductor tensile forces are assumed simultaneously at all conductor attachment points. The loads can be determined as a one-sided reduction of the conductor tensile forces, as described above, or as unbalanced load exerted by the tensile force of a conductor, when a fictitious

overload equal to the dead weight of conductors is assumed in all spans in the opposite line direction.

- *Security loads* resulting from the cases stated above for suspension supports may be determined, taking into account the relaxation of the loading resulting from any swing of the insulator sets and the elastic deflection or rotation of the support. The calculation may normally be carried out for the *equivalent span length* of the tensioning section. Alternatively, the security load can be obtained by multiplying the conductor tensile force with a reduction factor. However, there are no numerical values for these reduction factors given in EN 50 341-1.

EN 50 341-1 explains in general terms the loadings due to *short circuits,avalanches, creeping snow* and *earthquakes.* Concerning specific values or procedures to determine these loadings, reference is made to EN 50 341-3. Such loadings are essential only in few cases. Therefore, no details are given here.

6.9 Statistical distributions

6.9.1 Introduction

This clause presents statistical functions that are of interest for determination of loadings and reliabilities of overhead lines. In principle, these functions describe loads of meteorological origin, as well as strengths of components [6.26]. Within these functions, the following parameters are generally used:

Mean value m of observations x_i:

$$m = \frac{1}{n} \sum_{i=1}^{n} x_i \quad , \tag{6.85}$$

where n is the number of the observed values x_i.

Standard deviation σ of observations x_i:

$$\sigma = \frac{1}{n} \sqrt{\sum_{i=1}^{n} (x_i - m)^2} = \frac{1}{n} \sqrt{\sum_{i=1}^{n} x_i^2 - m^2} \quad . \tag{6.86}$$

Coefficient of variation v:

$$v = \sigma / m \quad . \tag{6.87}$$

6.9.2 *Normal distribution* (Gaussian distribution)

General format:

Probability density function:

$$f(x) = \frac{1}{\sigma \sqrt{2\,\pi}} \exp \left[-\frac{1}{2} \left(\frac{x - m}{\sigma} \right)^2 \right] \quad , \; \sigma > 0 \quad , \tag{6.88}$$

Cumulative distribution function:

$$F_{\mathrm{N}}(x) = \frac{1}{\sigma \sqrt{2\,\pi}} \int_{-\infty}^{x} \exp \left[-\frac{1}{2} \left(\frac{\xi - m}{\sigma} \right)^2 \right] \mathrm{d}\xi \quad . \tag{6.89}$$

Standardized format:

Variable change for standardized format

$$u = \frac{x - m}{\sigma} \quad , \tag{6.90}$$

Table 6.25: Number of standard deviations u correspoding to return periods T_r and exclusion limits e

T_r Years	Frequency $F_N(u_T)$	Standard deviation u_T from (6.92)	from (6.94)
50	0,98	2,054	2,040
150	0,9833	2,476	2,463
500	0,998	2,878	2,873
e %	$F_N(u_e)$	u_e	u_e
2	0,02	−2,054	−2,040
5	0,05	−1,645	−1,633
10	0,10	−1,282	−1,276

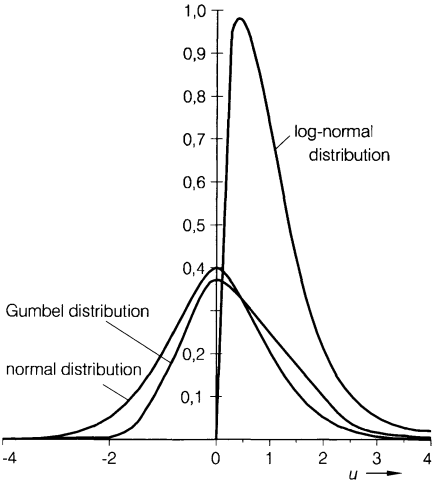

Figure 6.19: Probability density function of Gumbel, normal und log-normal distribution

Probability density function:

$$f(u) = \frac{1}{\sqrt{2\pi}} \exp\left[-\frac{u^2}{2}\right] \quad , \tag{6.91}$$

Cumulative distribution function:

$$F_N(u) = \frac{1}{\sqrt{2\pi}} \int_{-\infty}^{u} \exp\left[-\frac{\xi^2}{2}\right] \mathrm{d}\xi \quad . \tag{6.92}$$

There is no closed analytical presentation for the cumulative distribution. Tables available in the literature, e. g. in [6.6], or approximations can be used to determine the values. According to [6.27], the following approximation applies

$$F_N(u) \sim 0{,}6931 \exp\left[-((9u - 8)/14)^2\right] \tag{6.93}$$

for $-4 < u < 0$. The reciprocal equation is

$$u \sim \frac{1}{9}\left[8 - 14\sqrt{\ln(0{,}6931/F_N(u))}\right] \tag{6.94}$$

for $F_N(u)$ lower than 0,5. For $0{,}5 < F_N(u) \leq 1{,}0$ the relation $F_N(u) = 1 - F_N(u)$ can be used to determine u. Using equations (6.93) or (6.94) involves an error lower than 1 %. The relations with the return period T_r in years and the exclusion limit e in % are

$$F_N(u_T) = 1 - 1/T_r \text{ and } F_N(u_e) = e/100 \quad . \tag{6.95}$$

Table 6.25 shows relations between T_r and e, respectively, and u.
The relation of the variables $x(T_r)$ or $x(e)$ having a return period T_r or an exclusion limit e to the mean value m and the standard deviation σ or the coefficient of variation v are

$$x(T_r) = m + u_T\sigma = m(1 + u_T v) \tag{6.96}$$

and

$$x(e) = m + u_e\sigma = m(1 + u_e v) \quad . \tag{6.97}$$

Figure 6.19 depicts the standardized Gaussian normal distribution.

6.9.3 Log-normal distribution

General format:
The *logarithmic normal distribution* is defined as a distribution where the expression $\ln(x - p_1)$ follows a normal distribution.
Probability density function:

$$f(x) = \frac{1}{p_2(x-p_1)\sqrt{2\pi}} \exp\left[-\frac{1}{2}\left(\frac{\ln(x-p_1)-p_3}{p_2}\right)^2\right] \quad , \tag{6.98}$$

where $x > p_1$; $p_2 > 0$; $p_3 > 0$. The log-normal distribution is defined by three parameters. The parameter p_1 represents the lower threshold of the distribution.
Cumulative distribution function:

$$F(x) = \frac{1}{p_2\sqrt{2\pi}} \int_{p_1}^{x} \frac{1}{\xi - p_1} \exp\left[-\frac{1}{2}\left(\frac{\ln(\xi-p_1)-p_3}{p_2}\right)^2\right] \mathrm{d}\xi \quad . \tag{6.99}$$

Standardized format:
Variable change for standardized format

$$u = [\ln(x - p_1) - p_3]/p_2 \quad . \tag{6.100}$$

With this variable change, the relations (6.91) and (6.92) can be used for the probability density function and the cumulative distribution function, respectively, of the logarithmic normal distribution. With respect to the return period T_r and the exclusion limit e, the same numerical values for $u(T_r)$ and $u(e)$ as in case of the normal distribution are valid. The relations with the variables $x(T_r)$ and $x(e)$ having a given return period T_r or a given exclusion limit e to the mean value m and the standard deviation σ are

$$x(T_r) = p_1 + \exp(p_3 + u(T_r)p_2) \tag{6.101}$$

and

$$x(e) = p_1 + \exp(p_3 + u(e)p_2) \quad . \tag{6.102}$$

The parameters p_2 and p_3 are obtained from

$$p_2 = \sqrt{\ln[1 + \sigma^2/(m - p_1)^2]} \tag{6.103}$$

and

$$p_3 = \ln\left[(m - p_1)^2/\sqrt{(m - p_1)^2 + \sigma^2}\right] \quad . \tag{6.104}$$

The parameter p_2 is the mean value of the variable $\ln(x - p_2)$, the parameter p_3 its standard deviation. Figure 6.19 depicts the standardized probability density function of the logarithmic normal distribution with $p_1 = 0$.

6.9.4 Gumbel distribution

Gumbel distribution is named also *extreme value distribution – type I* and is dealt with in detail in [6.28].
General format:
Probability density function:

$$f(x) = (1/p_2)\exp[-(x - p_1)/p_2 - \exp(-(x - p_1)/p_2)] \quad , \; p_2 > 0 \tag{6.105}$$

Cumulative distribution function:

$$F(x) = \exp[-\exp(-(x - p_1)/p_2)] \quad . \tag{6.106}$$

Table 6.26: Parameter C_1 and C_2 of the Gumbel distribution

n	C_1	C_2	C_2/C_1
10	0,94963	0,49521	0,52148
15	1,02057	0,51284	0,50250
20	1,06282	0,52355	0,49260
25	1,09145	0,53086	0,48639
30	1,11237	0,53622	0,48250
35	1,12847	0,54034	0,47882
40	1,14131	0,54362	0,47631
45	1,15184	0,54630	0,47428
50	1,16066	0,54854	0,47261
∞	1,28255	0,57722	0,45005

Standardized format:
Variable change for standardized format

$$u = (x - p_1)/p_2 \quad , \tag{6.107}$$

Probability density function:

$$f(u) = \exp[-u - \exp(-u)] \quad , \tag{6.108}$$

Cumulative distribution function:

$$F(u) = \exp[-\exp(-u)] \quad . \tag{6.109}$$

The relations with the return period T_r and the exclusion limit e are

$$x(T_r) = p_1 - p_2 \ln[-\ln(1 - 1/T_r)] \tag{6.110}$$

and

$$x(e) = p_1 - p_2 \ln[-\ln(e/100)] \quad . \tag{6.111}$$

The parameters p_1 and p_2 follow from

$$p_2 = \sigma/C_1 \text{ and } p_1 = m - C_2 \cdot p_2 = m - (C_2/C_1)\ \sigma \quad . \tag{6.112}$$

The parameters C_1 and C_2 depend on the number of values considered in a measurement series, e. g. the number of years with annual maximum values. For n observations, n values z_i can be calculated from

$$z_i = \ln[-\ln(i/(n+1))] \quad , \ 1 \le i \le n \quad . \tag{6.113}$$

Thereof, it is obtained

$$C_2 = \overline{z} = \frac{1}{n} \sum_{i=1}^{n} z_i \tag{6.114}$$

and

$$C_1 = \sigma_z = \sqrt{\frac{1}{n} \sum_{i=1}^{n} z_i^2 - \overline{z}^2} \quad . \tag{6.115}$$

For an infinite number of observations ($n \to \infty$), it can be obtained

$$C_1 = \pi/\sqrt{6} = 1{,}28255 \text{ and } C_2 = 0{,}57721 \text{ (Euler constant)} \quad .$$

Table 6.26 gives parameters C_1, C_2 and their relation C_2/C_1, depending on the number n of observations. Figure 6.19 shows the standardized Gumbel distribution.

6.10 References

6.1 IEC 60826: Technical Report: Loading and strength of overhead transmission lines. Geneva, IEC, 1991.

6.2 CIGRE SC22 WG 22-06: Review of IEC 60826 "Loading and strength of overhead power lines". Paris, Cigré Brochure No. 109, 1996

6.3 Cigré SC22 WG 22-06: Probabilistic design of transmission lines. Paris, Cigré Brochure No. 178, 2001

6.4 EN 50341-1: Overhead electrical lines exceeding AC 45 kV. Part 1: General requirements – Common specifications. Brussels, CENELEC, 2001

6.5 Ghannoum, E.: A rational approach to structural design of transmission lines. IEEE Transactions on Power Apparatus Systems, Vol. 100 (1983), pp. 3057 to 3071

6.6 Hütte: Die Grundlagen der Ingenieurwissenschaften (Handbook of Engineering sciences). Berlin. Springer Verlag, 29th edition 1989

6.7 WMO-Manual on the GOS (Global observation system): WMO-No. 544, 1981

6.8 Eurocode 1: EN V 1991-2-4: Actions on structures – Wind loads. 1995

6.9 Cook, N. J.: Towards better estimation of extreme wind. Journal Wind Engineering, Industry Aerodynamics 9 (1982), pp. 295 to 323

6.10 EN 50341-3-4: Overhead electrical lines exceeding AC 45 kV. Part 3: National Normative Aspects for Germany. Brussels, CENELEC, 2001

6.11 Ghannoum, E.: Ice storm in Quebec. Electra No. 177 (1998), pp. 8 to 9

6.12 Bell, N. et al.: Increasing the reliability of transmission lines rebuilt after the January 1998 ice storm. Cigré Report 22-106, 2000

6.13 Kießling, F.; Ruhnau, J.: Ice loads and their effects on reliability and design of overhead lines. IWAIS 93, 6th international workshop on atmospheric icing on structures, Budapest 1993

6.14 IEC 61774TR: Meteorological data for assessing climatic loads, Technical Report. Geneva, IEC, 1998

6.15 Cigré SC22 WG 22-06: Guidelines for observation and measurement of ice loading on overhead power line conductors. Paris, Cigré Brochure No. 179, 2001

6.16 DIN VDE 0210: Planning and design of overhead power lines with rated voltages above 1 kV. Berlin, DKE, 1985

6.17 ÖVE-L11: Construction of overhead power lines of more than 1 kV. Edition 7.1969

6.18 Swiss law on power lines: Ordinance of March 30, 1994 on electrical power lines. Bern, Swiss Government 1994

6.19 NBR-5422: Projeto de linhas aereas de transmissao de energia electrica. (Overhead power lines for transmission of electric energy). Brazilian Standard, 1985

6.20 EN 50341-3: Overhead electrical lines exceeding AC 45 kV. Part 3: National Normative Aspects. Brussels, CENELEC, 2001

6.21 EN 50341-3-1: Overhead electrical lines exceeding AC 45 kV. Part 3-1: National Normative Aspects for Austria. Brussels, CENELEC, 2001

6.22 EN 50341-3-3: Overhead electrical lines exceeding AC 45 kV. Part 3-3: National Normative Aspects for Switzerland. Brussels, CENELEC, 2001

6.23 DIN 4131: Antenna structures made of steel. Berlin, DKE, 1991

6.24 Leibfried, W.; Mors, H.: The mechanical behaviour of bundled and single conductors – New measurements at the Hornisgrinde testing station. Paris, Cigré Report No. 209, 1960

6.25 Cigré SC22 WG 22-06: Tower top geometry. Paris. Cigré-Brochure No. 48, 1995

6.26 Siegel, A; Morgan, C. J.: Statistics and data analysis. New York, John Wiley & Sons. 2nd edition, 1996

6.27 Ordaz, M.: A simple approximation of the Gaussian distribution. Structural Safety 9 (1991), pp. 315 to 318

6.28 Gumbel, E. J.: Statistics of extremes. New York. Columbia University Press, 1958

7 Selection of conductors

7.0 Symbols

Symbol	Signification
A	Cross-sectional area
A_{Al}	Aluminium cross-sectional area
A_{Fe}	Steel cross-sectional area
A_{tot}	Total conductor cross-sectional area
c	Specific heat
c_{Al}	Specific heat of aluminium
c_{Fe}	Specific heat of steel
C_i'	Capacitance per unit length
D	Conductor diameter
D_{I}	Conductor diameter with ice
D_{M}	Mean conductor distance
$D_{\mathrm{M1}}, D_{\mathrm{M2}}$	Mean conductor distance of double circuit lines
e	Creep elongation
$e_{1\mathrm{h}}$	Creep elongation after one hour
E	Modulus of elasticity
E_{Al}	Modulus of elasticity of aluminium
E_{Fe}	Modulus of elasticity of steel
E_{DC}	Specific erection investments of a double circuit line
E_{P}	Specific investments for energy generation
E_0, E_1, E_2	Factors used to determine installation investment
f	Frequency
F_{C}	Conductor tensile force
g_{I}	Ice load per unit length
h_{al}	Altitude above sea-level
h_{M}	Mean conductor height above ground
h_{s}	Solar angle
I	Effective current
k_{a}	Absorption coefficient
k_{e}	Coefficient of emission of a black body
k_{s}	Stefan-Boltzmann constant
K_{L}	Specific costs of energy losses
K_{a}	Specific annual transmission costs
K_{SC}	Fixed specific annual costs of one circuit
K_{P}	Specific costs of power losses
K_{Tr}	Specific transmission costs
m_{C}	Conductor mass per unit length
m_1	Cross-sectional ratio of conductor envelope to core (aluminium to steel)
n	Exponent of the creep elongation
n_2	Number of subconductors in a bundle
N_{c}	Energy loss by convection
N_{J}	Joule heat
N_{M}	Magnetic losses
N_{S}	Energy input by solar radiation
N_{R}	Energy loss by radiation
N_{Sh}	Standard solar radiation
Nu	Nußelt number
p_1	Factor for fixed annual costs
p_2	Power demand factor
p_3	Specific energy costs
P_{L}	Power losses

Symbol	Signification
P_{max}	Maximum transmitted power
r	Conductor radius
R_{20}	DC resistance at 20°C
R'	Resistance per unit length
$R'_{T\,AC}$	AC resistance per unit length
$R'_{T\,DC}$	DC resistance per unit length
R_T	DC resistance at temperature T
Re	Reynolds number
RTS	Conductor rated tensile stress
s	Subconductor spacing
t	Time
t_m	Annual utilization period
t_L	Annual utilization period of power losses
T	Temperature, absolute temperature
T_{am}	Ambient temperature (absolute)
T_h	Temperature of the external atmosphere (absolute)
U	Transmission voltage
U_N	Nominal transmission voltage
V	Wind velocity
w	Wind load per unit length
w_I	Wind load per unit length with ice
x	Parameter for skin and spiral effects
α	Temperature coefficient of resistance
α_{Al}	Temperature coefficient of resistance of aluminium
α_{Fe}	Temperature coefficient of resistance of steel
γ	Specific mass, density
γ_{Al}	Specific mass of aluminium
γ_{Fe}	Specific mass of steel
δ	Angle for consideration of the geographic orientation
ε_t	Coefficient of thermal expansion
$\varepsilon_{t\,Al}$	Coefficient of thermal expansion of aluminium
$\varepsilon_{t\,Fe}$	Coefficient of thermal expansion of steel
η	Dynamic viscosity of air
κ	Specific conductivity
κ_{20}	Specific conductivity at 20°C
λ	Thermal conductivity of air
μ_0	Permeability in vacuum
μ_r	Relative permeability of material
ϱ	Resistivity
ϱ_{Al}	Resistivity of aluminium
ϱ_{Fe}	Resistivity of steel
σ	Tensile stress
σ_{Al}	Tensile stress of aluminium
σ_B	Ultimate tensile strength
σ_{Fe}	Tensile stress of steel
$\sigma_{1\%Fe}$	Tensile stress of steel wires corresponding to 1 % elongation
φ	Latitude, power load angle
ψ	Angle of line direction to the north-south axis

7.1 Conductor types and design

7.1.1 Introduction

Overhead power lines are aimed at reasonable and reliable *transmission of electric energy* between two points. The conductors carry the electric energy and are, therefore, the most important components of an overhead power line. The expenditures necessary to purchase and install them correspond to something between 30 and 50 % of the

Table 7.1: Standards for overhead line conductors and individual wires

	IEC standards	European standards	German standards	ASTM standards
Standards for conductors				
Aluminium	IEC 61 089	EN 50 182	DIN 48 201 Part 5	ASTM-B231
Aluminium alloy	IEC 61 089	EN 50 182	DIN 48 201 Part 6	ASTM-B399
Copper	–	–	DIN 48 201 Part 1	ASTM-B8
Copper alloy	–	–	DIN 48 201 Part 2	–
Steel	–	EN 50 189	DIN 48 201 Part 3	ASTM-A363
Aluminium-clad steel	IEC 61 089	EN 50 182	DIN 48 201 Part 8	ASTM-B416
ACSR	IEC 61 089	EN 50 182	DIN 48 204	ASTM-B232
AACSR	IEC 61 089	EN 50 182	DIN 48 206	ASTM-B711
ACSR/AC	–	EN 50 182	–	ASTM-B341
AACSR/AC	–	EN 50 182	–	–
Formed wire conductors	IEC 62 219	–	–	–
Standards for wires				
Aluminium	IEC 60 889	EN 60 889	DIN 48 200 Part 5	ASTM-B230
Aluminium alloy	IEC 60 104	EN 50 183	DIN 48 200 Part 6	ASTM-B398
Copper	–	–	DIN 48 200 Part 1	ASTM-B1
Copper alloy	–	–	DIN 48 200 Part 2	ASTM-B105
Aluminium-clad steel	IEC 61 232	EN 61 232	DIN 48 200 Part 8	ASTM-B415
Steel	IEC 60 888	EN 50 189	DIN 48 200 Part 3	ASTM-A475

Table 7.2: Recommended minimum conductor cross sections in mm^2

Conductor made of	Nominal voltage above 1 kV	up to 1 kV
ACSR according to EN 50 182	34-AL1/6-ST1A	24-AL1/4-ST1A
Aluminium according to EN 50 182	48-AL1	24-AL1
AACSR according to EN 50 182	34-AL3/6-ST1A	24-AL3/4-ST1A
Aluminium alloy according to EN 50 182	34-AL3	24-AL3
Copper according to DIN 48 201 Part 1	25-E-Cu	10-E-Cu
Copper alloy according to DIN 48 201 Part 2	25-Bz	10-BzI
Aluminium-clad steel according to EN 50 182	24-A20SA	24-A20SA

total *investment for an overhead line*. Many different *types of conductors* have been used since overhead lines were first installed. In many industrialized countries there are *standards for conductors*, and also international ones from IEC [7.1] and CENELEC [7.2]. US American standards like [7.3, 7.4] and [7.5] are of widespread use as well. The EN standards replaced the national standards valid up to now in European countries; e. g. in Germany the conductor standards of the DIN 48 200 series (Table 7.1). From the standards, the best-suited conductor can be selected for a specific application. Besides that, special overhead conductors can also be manufactured, whenever deemed necessary.

According to [7.6], *conductors* are bare or covered, insulated or earthed cables strung between the supports of an overhead line, irrespective of whether they are alive or not. *Bundle conductors* are arrangements of two or more *subconductors* used instead of a *single conductor* and usually kept at an approximately constant spacing on their entire length. According to [7.7], conductors are wires or combinations of wires not insulated and suitable for carrying an electric current. Conductors can be wires, stranded conductors or cables made of electrically conductive materials, but also, in accordance with the definition given in [7.6], non-metallic *optical fibre cables* for telecommunication purposes. Wires will not play any role for overhead lines in the future. Recommended *conductor minimum cross sections* are given in Table 7.2, in accordance with [7.8].

Conductors are made either of one material – *single material conductors* – or of two materials – *composite conductors*. Single-material conductors can be formed by mono-

Table 7.3: Examples of conductor designations

Type of conductor	EN 50 182	IEC 61 089	International designation
Aluminium	93-AL1	93-A1-19	AAC
Aluminium alloy	93-AL3	93-A3-19	AAAC
Steel	93-ST1A	93-S1A-19	—
Aluminium-clad steel	93-A20SA	–	ACS
Aluminium/steel	243-AL1/39-ST1A	243-A1/S1A-26/7	ACSR
Aluminium alloy/steel	243-AL3/39-ST1A	243-A3/S1A-26/7	AACSR
Aluminium/aluminium clad-steel	243-AL3/39-A20SA	–	ACSR/ACS
Aluminium/aluminium alloy	243-AL1/39-AL3	–	ACAR

metallic or metal-clad steel wires. Composite conductors include combinations of monometallic and metal-clad steel wires. Aluminium and aluminium alloys, copper and copper alloys are applied as base materials, as well as steel. The conductors are manufactured with at least one or more successive layer with changing *layer direction*, arranged helically around a core wire. The direction of layer is designed as right-hand or left-hand. With *right-hand layer*, the wires conform to the direction of the central part of the letter Z when the conductor is held vertically. With *left-hand layer*, the wires conform to the central part of the letter S when the conductor is held vertically. The outermost layer is preferably right-hand. The standards listed in Table 7.1 contain conductors often used for overhead power lines. Beside the compositions and conductor structures mentioned there, other designs can be found in national standards. Not-standardized special *conductor types*, in particular types with integrated optical fibres, are adopted as well.

7.1.2 Conductor designation

The designation of *standardized wires and conductors* can be found in the relevant standards as shown in Table 7.1. According to EN 50 182 [7.2], *hard-drawn aluminium* is indicated as AL1 and *aluminium alloys* are indicated as ALx, where x varies from 2 to 7 (EN 50 183 [7.9]) and refers to standardized alloys usually applied. *Steel wires* are identified as STyz, the letter y representing the mechanical strength according to the six different classes standardized by EN 50 189 [7.10]. The letter z stands for the *type of zinc coating*, classes A to E being standardized by EN 50 189.
Aluminium-clad steel wires are identified as yzSA, where y designates the steel strength (y = A or B) and z the conductivity [7.11]. The figure stands for the percentage of conductivity in relation to copper *IACS* (International Annealed Copper Standard [7.21], see also clause 7.1.4.5). There are four types of conductivity being 20 SA, 27 SA, 30 SA and 40 SA.
The conductors are identified by a code number which corresponds to the cross-sectional area in square millimetres and a code for the material. For composite conductors, the data are separated for the envelope and the conductor core. Table 7.3 presents examples for conductor identifications according to the European standard EN 50 182, in comparison with the previous Central European identification and North American practice. In North America, UK and France, the conductors have distinguished by names of flowers, birds or animals like Crocus 228 for 185-AL1/43-ST66, Finch for 565-AL1/72-ST1A and Lynx for 183-AL1/43-ST1A.

7.1.3 Progress in technical development

The *technical development of conductors* for overhead power lines is described in [7.9, 7.13] and [7.14]. Copper conductors were used in the initial period of energy transmis-

sion via overhead lines around 1880. They were designed considering the mechanical rather than the conductive and electric behaviour of materials, thus the high conductivity of copper was not utilized to full extent. Therefore, the employed cross sections were larger than necessary in view of the required conductivity. Due to the high weight of copper, spans were short, which in turn increased the total investment. At the end of the 19th century, copper was replaced gradually by aluminium for transmission and distribution lines. The first overhead power lines adopting aluminium were built in California in 1895 and in Germany in 1900. The first overhead power line using a seven strand aluminium conductor was erected in Connecticut in 1899 and had been in operation for more than 50 years. After these early applications, the use of aluminium conductors increased continuously, being the practically exclusive material for overhead conductors nowadays. Around the year 2000, aluminium has been used for overhead lines for more than 100 years. Regarding *conductivity*, aluminium is second in the rank of non-precious metals, behind copper. The ratio of conductivity to weight is twice as that applicable to copper, and the ratio of mechanical strength to weight is approximately 30 % higher.

Since the introduction of aluminium in 1900, a higher ratio of mechanical strength to weight of the conductors had been considered advantageous, as compared with pure aluminium. Therefore, a *composite conductor* made of aluminium and steel was introduced in 1907. This conductor combined the low weight and higher current capacity of aluminium with the higher mechanical strength of a zinc coated *steel core*. The advantages achieved by the so-called *aluminium conductor steel-reinforced* (ACSR) were soon acknowledged; they have been used in Germany since 1920 and captured the market within 10 years, by 1930. The good conductivity of the conductors, together with their favourable ratio of mechanical strength to weight, and their easy handling were the reasons why they were almost exclusively applied in overhead power line projects during the first half of the 20thth century.

After some experiments carried out in Switzerland in 1921, a new *aluminium magnesium alloy*, designated as *Aldrey* in Germany and *Almelec* in France, was introduced during the 1930's. Mono-metallic conductors were developed with this material, which achieved the same mechanical and electric characteristics as aluminium-steel conductors, reduced the weight and also improved the corrosion performance. These all aluminium alloy conductors (AAAC) and the composite conductors (AACSR), which combine this material with steel cores, represented alternatives to the aluminium-steel conductors. However, the acceptance of this conductor type, as it sometimes happens to any new product, was not the same in all industrialized countries. In France, this type of conductor has already been used almost exclusively for many years. In other countries, its use was restricted to special applications, because of unexpected problems caused by conductor vibrations.

During the past years, however, there has been a worldwide trend towards the selection of AAAC conductors, preferably to the aluminium-steel conductors, or even towards the use of composite conductors made of aluminium alloy and steel.

In most recent years, some *innovative conductor designs* have appeared in the market which comply with the changing requirements of the electricity industry [7.15]. New alloys have been developed, which show a better thermal stability and electric conductivity. Innovative designs improved the vibration endurance capability, besides other special characteristics.

The *selection* or development *of conductors for transmission* and distribution *lines* has become a demanding task from both the technical and the economic point of view. Selection of the best-suited conductor type and dimension for a certain line requires a detailed knowledge of the characteristics of commercially available types of conductors. The following items should be taken into account for an optimum selection:

Table 7.4: Physical characteristics of main conductor materials

Material	Standard	Density	Specific conductivity	Specific heat	Temperature coefficient of resistance variation	Coefficient of thermal expansion	Resistivity	Conductivity
		γ kg/dm^3	x_{20} m/Ωmm^2	c Ws/gK	α_{20} 1/K	ε_t 10^{-6}/K	ϱ_{20} Ωmm^2/m	IACS %
AL1	EN 60 889	2,703	35,38	0,897	0,00403	23,0	0,02826	61
AL2	EN 50 183	2,703	30,45	0,909	0,0036	23,0	0,03284	53
AL3	EN 50 183	2,703	30,74	0,909	0,0036	23,0	0,03253	53
AL4	EN 50 183	2,703	30,40	0,909	0,0036	23,0	0,03289	52
AL5	EN 50 183	2,703	31,06	0,909	0,0036	23,0	0,03220	54
AL6	EN 50 183	2,703	31,75	0,909	0,0036	23,0	0,03150	55
AL7	EN 50 183	2,703	32,79	0,909	0,0036	23,0	0,03050	57
TAL	—	2,703	34,80	0,963	0,00403	23,0	0,02873	60
ST1A	EN 50 189	7,78	5,21	0,481	0,0045	11,5	0,1919	9
ST2B	EN 50 189	7,78	5,21	0,481	0,0045	11,5	0,1919	9
ST3D	EN 50 189	7,78	5,21	0,481	0,0045	11,5	0,1919	9
ST4A	EN 50 189	7,78	5,21	0,481	0,0045	11,5	0,1919	9
ST5E	EN 50 189	7,78	5,21	0,481	0,0045	11,5	0,1919	9
ST6C	EN 50 189	7,78	5,21	0,481	0,0045	11,5	0,1919	9
20SA	EN 61 232	6,59	11,80	0,518	0,0036	13,0	0,08475	20
27SA	EN 61 232	5,91	15,66	0,544	0,0036	13,4	0,06385	27
30SA	EN 61 232	5,61	17,40	0,559	0,0038	13,8	0,05747	30
40SA	EN 61 232	4,64	23,20	0,619	0,0040	15,5	0,04310	40
Cu [1)]	—	8,89	58,0	0,394	0,0039	17,0	0,01724	100
E-Cu	DIN 48 200 Part 1	8,89	56,0	0,394	0,0039	17,0	0,01786	97
BzI	DIN 48 200 Part 2	8,89	48,00	0,377	0,0038	17,0	0,02083	83
BzII	DIN 48 200 Part 2	8,89	36,00	0,377	0,0038	17,0	0,02773	62
BzIII	DIN 48 200 Part 2	8,89	18,00	0,377	0,0038	17,0	0,05556	31

[1)] Annealed copper

- *Electric conductivity* and *thermal behaviour*,
- *Thermal load limits*,
- *Economy of transmission*,
- *Mechanical strength of conductor*,
- Mechanical load and *stress-strain curves*,
- *Creep characteristics* and the resulting *sag increase* as well as
- *Behaviour under vibrations* and *fatigue strength.*

7.1.4 Materials

7.1.4.1 Aluminium

Hard-drawn aluminium is the most frequently used material for overhead lines. It shall consist of 99,5 % Al. Its 35,38 S conductivity amounts to 61 % of copper conductivity, and is described as 61 % *IACS* by the respective standard IEC 60 889 [7.16].

Aluminium and its alloys belong to a group of non-precious metals that shows low *corrosion resistance* even in less aggressive atmospheres. However, aluminium in contact with air builds up a thick oxide layer that protects the metal against corrosion and presents effective protection even under more aggressive environmental conditions, for instance, near the sea. In Table 7.4, the *physical characteristics* of conductor materials are presented. Its relatively low mechanical strength forms a disadvantageous character-

Table 7.5: Mechanical strength characteristics of the most important conductor materials

Material	Standard	Modulus of elasticity E kN/mm^2	Tensile stress at 1 % elongation N/mm^2	Tensile stress before stranding N/mm^2	Elongation %
AL1	EN 60 889	60	—	160 to 200	—[1)]
AL2	EN 50 183	60	—	315 to 325	3,0
AL3	EN 50 183	60	—	295	3,5
AL4	EN 50 183	60	—	315 to 325	3,0
AL5	EN 50 183	60	—	295	3,5
AL6	EN 50 183	60	—	304 to 314	3,5
AL7	EN 50 183	60	—	255 to 300	3,0
TAL	—	60	—	160 to 190	—
ST1A	EN 50 189	207	1 100 to 1 170	1 300 to 1 400	3,0 to 4,0
ST2B	EN 50 189	207	1 000 to 1 100	1 200 to 1 300	4,0
ST3D	EN 50 189	207	1 100 to 1 120	1 400 to 1 500	4,0
ST4A	EN 50 189	207	1 225 to 1 275	1 620 to 1 670	3,0 to 4,0
ST5E	EN 50 189	207	1 370 to 1 420	1 620 to 1 670	3,0 to 4,0
ST6C	EN 50 189	207	1 340 to 1 450	1 600 to 1 700	2,0 to 2,5
A20SA	EN 61 232	162	1 000 to 1 200	1 070 to 1 340	—
B20SA	EN 61 232	155	1 100	1 320	–
27SA	EN 61 232	140	800	1 080	—
30SA	EN 61 232	132	650	880	—
40SA	EN 61 232	109	500	680	—
E-Cu	DIN 48 200 Part 1	130	—	422	—
BzI	DIN 48 200 Part 2	130	—	520	—
BzII	DIN 48 200 Part 2	130	—	618	—
BzIII	DIN 48 200 Part 2	130	—	706	—

[1)] not standardized

istic of conductive aluminium. It ranges from 160 to 200 N/mm^2; therefore, aluminium alloys or aluminium-steel composite conductors are preferably chosen for transmission lines. After being stranded, the characteristics shown in [7.16] and Table 7.5 may be reduced by 5 %. Wires produced in the *casting/rolling process*, also known as *Properzi blanks*, are almost exclusively used in the production of aluminium wires [7.17].

7.1.4.2 Aluminium-magnesium-silicon alloys

Six types of *aluminium-magnesium-silicon alloys* are given in [7.9], which can be distinguished by their conductivity and mechanical strength. They are designated as AL2 to AL7. Their conductivity is between 30,4 and 32,8 m/Ωmm^2, that is between 86 and 93 % of the conductivity of aluminium resulting in 52,5 and 57,5 % *IACS*. The *mechanical strength* is between 255 and 325 N/mm^2, which amounts to about as much as 1,6 times the corresponding aluminium value. These *mechanical strengths* should be obtained also after *stranding the conductors*. The essential data are given in Tables 7.4 and 7.5. ALx alloys are standardized in EN 1715-2 [7.18]. For the production of aluminium alloy strands, blank material resulting from the *casting/rolling process* [7.19] is used and then drawn to the final diameter. Blank material prepared by the *extruding process* is expensive and seldom used for overhead conductor strands.

In the USA, the aluminium alloy named 6201-T81 is most commonly used for overhead line conductors. Its rated strength is around 310 N/mm^2, similar to that of AL6 listed in Table 7.5.

7.1.4.3 Steel wires

Zinc-coated steel wires are used for aluminium-steel composite conductors and also for steel earth wires. In [7.10], six types of steel wires are mentioned: ST1A, ST2B, ST3D, ST4A, ST5E and ST6C. The numbers indicate the mechanical strength and the last capital letter the type of *zinc coating*. The requirements of zinc coating depend on the wire diameter and are as follows: between 150 and 290 g/m^2 for classes A, C and E; between 370 and 580 g/m^2 for class B and between 365 and 825 g/m^2 for class D. Standard EN 10 244-2 [7.20] describes the testing of *zinc coating*.
The *tensile strength of steel wires* is between 1200 and 1800 N/mm^2, depending on the steel class and the wire diameter, which is standardized between 1,25 and 4,75 mm. Tables 7.4 and 7.5 contain the most important characteristics of steel wires. In case of testing of wire samples taken from stranded conductors, their acceptable tensile strength may be 5 % lower than specified in Table 7.5.

7.1.4.4 Aluminium-clad steel wires

Aluminium-clad steel wires are produced by sintering aluminium on a steel wire and, afterwards, drawing them to the final strand diameter. This process results in a combination of high mechanical strength of steel and, increased conductivity and good resistance against corrosion of aluminium [7.21]. In [7.11], five types of aluminium-clad steel wires are standardized with the codes A20SA, B20SA, 27SA, 30SA and 40SA. The letter A or B refers to the steel strength. The numbers indicate the conductivity in percent *IACS* and correspond to an aluminium portion of 25, 37, 42 and 62 %, respectively, of the total cross section of individual wires or to a mean thickness of aluminium layers with 13,4, 20,5, 24,5 or 38,4 % of wire radii. The mechanical strengths depend substantially on the thickness of the aluminium layer (see Table 7.5). The strength data of A20SA wires correspond approximately to those of steel wires ST1A.

7.1.4.5 Copper and copper alloys

Conductive *copper* (E-Cu) and *copper wrought alloys* with *magnesium (bronze)* are seldom used for overhead lines, however, they are still found in old lines and in railway electric power supply installations, where high mechanical strength and high conductivity are required. Nevertheless, the resistivity of annealed copper is used as a comparative basis for the resistivity of other materials. The International Annealed Copper standard is expressed in terms of mass resistivity as 0,5328 $\Omega \cdot g/m^2$, or the resistance of a uniform round wire 1 m long weighing 1 g at 20°C. An equivalent expression is 0,017241 $\Omega \cdot mm^2/m$. The equivalent conductivity is 58 $S \cdot m/mm^2$ defined as 100% IACS. Addition of magnesium significantly increases the mechanical strength of copper wires, but greatly reduces the conductivity, as can be seen in Table 7.4. Since the application of copper conductors is limited, no international standard has been prepared so far.

7.1.4.6 Thermal resistant aluminium alloys

Hard-drawn aluminium recrystallizes at temperatures above 100°C and looses its mechanical strength (Figure 7.1). This applies to aluminium-magnesium-silicon alloys as well. Thus, their permissible permanent temperature is limited to 80°C [7.6]. Higher temperatures are also linked with higher permanent unelastic elongation, which leads to an irreversible increment of sag. To allow operation at higher temperatures and to enable the transmission of higher currents, some *zirconium* is added to the aluminium. This component increases the *recrystallization temperature* to a value around 200°C, keeping the other characteristics approximately the same. In Figure 7.2, the residual strength of aluminium and *Thermal-resistant Aluminium* (TAL) at 200°C is shown as a

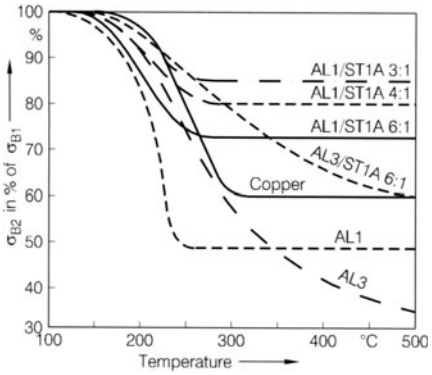

Figure 7.1: Strength of conductor materials depending on the temperature
σ_{B1} tensile strength before temperature rise
σ_{B2} tensile strength after temperature rise

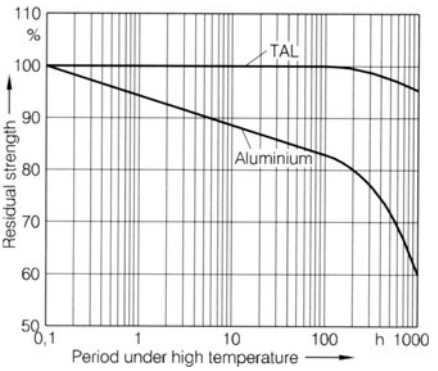

Figure 7.2: Strength of aluminium and TAL at 200°C

function of the heating period. After the first 100 hours only an insignificant decrease of the mechanical strength is observed for TAL. The electric conductivity of TAL is 60 % IACS instead of 61 % for aluminium (see Table 7.4). The mechanical strength is as with aluminium. Conductors made of AlZr alloys [7.22] can be operated at temperatures of 150°C, whereby correspondingly large sags can result, however.

7.1.5 Wire testing

7.1.5.1 Introduction

EN 60 888, EN 60 889, EN 50 183, EN 50 189 and EN 61 235 describe testing of various types of *metallic wires* used for overhead line conductors. *Sample tests* should be carried out at every 10 % of the wire lengths prepared for stranding. When a sample does not comply with any of the requirements, the client has a right to reject the whole lot the sample was taken from. The manufacturer is then allowed to test every single reel or every single coil of blank material and to present those wires for acceptance which have accomplished the requirements. However, in any case, the client will take samples with strands from already stranded conductor. At these samples, the tensile strength may be up to 5 % lower than that required for the wires before stranding.

7.1.5.2 Dimensions and surfaces

The *wire diameters* are given in millimetres and are accurate to two decimal places. For AL1 to AL7, permissible deviations given by the standards are: ±0,03 mm for diameters up to 3,00 mm and ±1 % for larger diameters.
The *wire surface* must be smooth, free from fissures, cavities, inclusions as well as from impurities like, for instance, copper particles. The same applies to the surface of zinc coated steel wires.

7.1.5.3 Testing the tensile strength

Every wire sample is submitted to a *tensile strength test* according to EN 10 002-1 [7.23] or [7.24]. The tensile strength measured may not fall below the required values. When carrying out the tensile test, the *breaking strain* is recorded related to a measuring length of 250 mm. In case of steel and aluminium-clad steel strands, the *tensile load*

corresponding to a *1 % elongation* related to a measuring length of 250 mm is recorded as well.

7.1.5.4 Wrapping and twisting test

Every sample is submitted to a *wrapping test* in accordance with ISO 7802 [7.25]. Eight wrappings of the aluminium wire are wound around a mandrel with the same diameter as the wire and, then, six turns are wound off and wound up again around the mandrel. The wire may not break. For ALx wires, standard EN 50 183 requires only winding up of the wires tested.
For zinc coated steel, the *mandrel diameter* depends on the classification of material. Here, winding up of only eight turns is enough. A *twisting test* is also required for steel and aluminium-clad steel wires where a wire as long as 100 times its diameter is twisted around itself and, depending on the steel class and on the wire diameter, should withstand without rupture 10 to 18 rotations in case of steel wires, or 20 such rotations in case of aluminium-clad steel wires.

7.1.5.5 Testing zinc mass, cladding thickness and uniformity

The *zinc mass* of galvanized steel wires can be tested using the volume or the mass method according to EN 10 244-2 [7.20], whereby the zinc coating is detached by application of hydrochloric acid. The uniformity is tested by applying the *zinc dip test* by dipping in a copper sulphate solution. The required minimum number of dips depends on the thickness of the zinc coating and is specified in [7.10].
The *cladding thickness* and *cladding uniformity* of aluminium-clad steel wires is determined either applying the *magnetic penetration* or by direct measurement on the *photomicrograph* of a sample embedded in cast resin.

7.1.5.6 Testing resistivity

The *resistivity* is measured at temperatures between 10 and 30°C in accordance with IEC 60 468 [7.26]. The measured resistance R_T is adjusted to the reference temperature of 20°C as follows:

$$R_{20} = R_T/(1 + \alpha(T - 20)) \quad , \tag{7.1}$$

where

T	temperature during measurement,
R_T, R_{20}	resistance at temperature T and 20°C, respectively, and
α	temperature coefficient of resistance (see Table 7.4).

The resistivity can be evaluated from the measured diameter of the wire and the measuring length.

7.1.6 Conductors made of wires with the same material

7.1.6.1 All aluminium conductors

Standards include all aluminium conductors *(AAC)*as in [7.2], where information is given about many types used in European countries. In Table 7.6, composition and mechanical strength are given as an example for conductors specified in EN 50 182, together with the *current carrying capacity* (ampacity), which ranges from 110 to 1540 A. The current carrying capacity applies to 35°C ambient temperature and 0,6 m/s wind velocity.
Due to the relative small ratio of mechanical strength to weight as well as the high susceptibility to vibrations, AL1 conductors are nowadays used mainly in distribution

Table 7.6: Technical data for conductors made of aluminium (AL1 or AAC)

Designation	Cross-sectional area	Number of strands	Diameter		Rated breaking strength	DC resistance	Current carrying capacity (ampacity)
			Strand	Conductor			
	mm^2		mm	mm	kN	Ω/km	A
16-AL1	15,9	7	1,70	5,10	3,02	1,7986	110
24-AL1	24,2	7	2,10	6,30	4,36	1,1787	145
34-AL1	34,4	7	2,50	7,50	6,01	0,8317	180
49-AL1	49,5	7	3,00	9,00	8,41	0,5776	225
48-AL1	48,3	19	1,80	9,00	8,94	0,5944	225
66-AL1	65,8	19	2,10	10,5	11,85	0,4367	270
93-AL1	93,3	19	2,50	12,5	16,32	0,3081	340
117-AL1	117,0	19	2,80	14,0	19,89	0,2456	390
147-AL1	147,1	37	2,25	15,8	26,48	0,1960	466
182-AL1	181,6	37	2,50	17,5	31,78	0,1588	520
243-AL1	242,5	61	2,25	20,3	43,66	0,1193	625
299-AL1	299,4	61	2,50	22,5	52,40	0,0966	710
400-AL1	400,1	61	2,89	26,0	68,02	0,0723	855
500-AL1	499,8	61	3,23	29,1	82,47	0,0579	990
626-AL1	626,2	91	2,96	32,6	106,45	0,0464	1140
802-AL1	802,1	91	3,35	36,9	132,34	0,0362	1340
1000-AL1	999,7	91	3,73	41,1	159,95	0,0291	1540

Table 7.7: Technical data for conductors made of aluminium alloy (AL3 or AAAC)

Designation	Cross-sectional area	Number of strands	Diameter		Rated breaking strength	DC resistance	Current carrying capacity (ampacity)
			Strand	Conductor			
	mm^2		mm	mm	kN	Ω/km	A
16-AL3	15,9	7	1,70	5,10	4,69	2,0701	105
24-AL3	24,2	7	2,10	6,30	7,15	1,3566	135
34-AL3	34,4	7	2,50	7,50	10,14	0,9572	170
49-AL3	49,5	7	3,00	9,00	14,60	0,6647	210
48-AL3	48,3	19	1,80	9,00	14,26	0,6841	210
66-AL3	65,8	19	2,10	10,5	19,41	0,5026	255
93-AL3	93,3	19	2,50	12,5	27,51	0,3546	320
117-AL3	117,0	19	2,80	14,0	34,51	0,2827	365
147-AL3	147,1	37	2,25	15,8	43,40	0,2256	425
182-AL3	181,6	37	2,50	17,5	53,58	0,1827	490
243-AL3	242,5	61	2,25	20,3	71,55	0,1373	585
299-AL3	299,4	61	2,50	22,5	88,33	0,1112	670
400-AL3	400,1	61	2,89	26,0	118,04	0,0832	810
500-AL3	499,8	61	3,23	29,1	147,45	0,0666	930
626-AL3	626,2	91	2,96	32,6	184,73	0,0534	1075
802-AL3	802,1	91	3,35	36,9	236,62	0,0417	1255
1000-AL3	999,7	91	3,73	41,1	294,91	0,0340	1450

networks and substations, where high conductivity is required and the span lengths are relatively short. Their high resistance against corrosion qualifies these conductors also for lines in coastal regions. In USA, all aluminium conductors (AAC) are standardized in ASTM B231 [7.3].

7.1.6.2 All aluminium alloy conductors

All aluminium alloy conductors are standardized in [7.2] with the designation ALx. As an example, AL3 conductors as per EN 50 182, Table F.18, are provided in Table 7.7. Depending on the diameter of the individual strands, the rated breaking strength for

Table 7.8: Technical data for conductors made of aluminium-clad steel (A20SA)

Designation	Cross-sectional area	Number of strands	Diameter		Rated breaking strength	DC resistance[1)]	Current carrying capacity (ampacity)
			Strand	Conductor			
	mm^2		mm	mm	kN	Ω/km	A
24-A20SA	24,2	7	2,10	6,30	32,49	3,5364	65
34-A20SA	34,4	7	2,50	7,50	46,04	2,4953	80
49-A20SA	49,5	7	3,00	9,00	66,30	1,7328	115
66-A20SA	65,8	19	2,10	10,5	88,18	1,3102	135
93-A20SA	93,3	19	2,50	12,5	124,98	0,9245	170
117-A20SA	117,0	19	2,80	14,0	156,77	0,7370	195
147-A20SA	147,1	37	2,25	15,8	197,13	0,5881	225
182-A20SA	181,6	37	2,50	17,5	243,38	0,4764	255
243-A20SA	242,5	61	2,25	20,3	325,00	0,3579	310
299-A20SA	299,4	61	2,50	22,5	401,24	0,2899	355

[1)] Aluminium and steel cross sections considered

the same conductor design is 55 to 84 % higher than that of AL1 conductors, while the steady-state current carrying capacity amounts to 95 % of the AL1 data.
The ALx conductors share a large application in the international market due to their high mechanical strength and their high conductivity when compared with composite conductors of the same diameter, for example in France, where this alloy is called *Almelec*. In [7.2], this material is referred to as AL4. The higher *coefficient of thermal expansion* is disadvantageous compared to AL1/STyz conductors, as is their low weight with respect to aeolian vibrations. In the USA, aluminium alloy conductors (AAAC) are mainly manufactured according to ASTM B399 [7.4].

7.1.6.3 Aluminium-clad steel conductors

As an example, Table 7.8 contains technical data for *aluminium-clad steel conductors* (A20SA) which are standardized according to EN 50 182, Table F21. The rated breaking strength is approximately 7,5 times higher than of AL1 conductors having the same dimension. Such conductors are specially adequate as earth wires [7.27], as well as for span lengths of 2 000 m and above, however using special designs which have larger cross sections and a higher number of strands [7.28]. In the USA, aluminium-clad steel conductors (ACS) are standardized according to ASTM B416 [7.29]

7.1.6.4 Copper, copper alloy and steel conductors

Copper, copper alloy and steel conductors are applied today only in cases where high resistance to corrosion is needed (copper and *bronze*), for earth wires or in cases where unusually high loads are expected in overhead lines. Here, steel conductors may represent an alternative solution. There are no European standards for such conductors. German standard DIN 48 201, Part 1 deals with copper, DIN 48 201, Part 2 with bronze and DIN 48 201, Part 3 with zinc coated steel conductors. Copper magnesium alloys are used for bronze conductors.

7.1.7 Composite conductors

7.1.7.1 Configuration and design

Composite conductors are made up of wires produced from different types of metals. They are usually formed by a steel core and a one- or multiple-layer envelope of aluminium (AL1) or aluminium alloy (ALx). These conductors are also designated

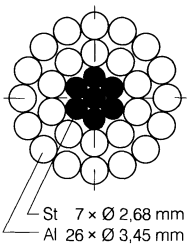

Figure 7.3: Cross section of a composite conductor 243-AL1/39-ST1A according to EN 50 182, previously ACSR 240/40

as *ACSR* (aluminium conductor steel reinforced) or *AACSR*. However, there are also designs in which steel and aluminium wires are mixed in individual layers of the conductors. Furthermore, there are also conductors with a core made of aluminium-clad steel wires (yzSA) or of ALx (AAAC) wires which are known as AL1/yzSA, ALx/yzSA or AL1/ALx, respectively. They are also named as ACSR/ACS or ACAR, respectively. In Figure 7.3, the cross section is shown of a 243-AL1/39-ST1A composite conductor previously designated as ACSR 240/40 in Germany, having a seven-wire steel core and 26-wire aluminium envelope.

Composite conductors provide some advantages which contribute to their widespread use. The composition allows a high *conductivity* by adequate selection of the section of conductive envelope, combined with high mechanical strength of a steel, aluminium-clad steel or ALx core. The high strength enables to reduce the sags and achieve long span lengths. Thus, ALx/STyz (AACSR) and ALx/yzSA (AACSR/ACS) conductors have proved to be adequate for overhead lines across wide rivers or valleys. The strength may be adapted to every application by means of variations in the components of the core or in its mechanical strength. ALx (aluminium alloy) used as conductive material increases the breaking strength in comparison with AL1, without causing a significant decrease of the total conductor conductivity.

The multiple-layer aluminium envelope of composite conductors protects the zinc-coated steel wires permanently against corrosion, when the steel cores are greased. In Central Europe, the practice of greasing is followed. However, especially in regions of hot climate, the grease could melt and drop from the conductor thus producing corona discharges. Therefore, attention should be paid to a sufficiently high *drop point* of the grease (above 80°C) and a high *viscosity*. Standard prEN 50 326 [7.30] applies to *grease*. Composite conductors with a core made of aluminium-clad steel wires [7.21] combine a high conductivity with an excellent resistance against corrosion and, therefore, no greasing is needed.

Composite conductors have shown a superior *long-term performance* under *aeolian vibration* due to wind excitation. Under permanent tensile load, aluminium is continuously elongated, a phenomenon called *creep*. In composite conductors, steel creeps to a much lower extent than aluminium [7.31]. With passing period of time, the tensile stress of aluminium wires decreases while that of steel wires increases. This results in a higher resistance against *alternating bending stresses* caused by aeolian vibrations. This *load displacement* cannot take place in mono-metallic or AL1/ALx conductors. That is the reason why these conductors are highly susceptible to fatigue problems [7.32].

Every composition, especially every cross-sectional ratio of conductive material to core is conceivable for composite conductors; however, with passing time, certain ratios have become popular. Internationally, there is a lot of standardized dimensions. In Europe, the various national standards for conductors were replaced by EN 50 182. Table 7.9 contains information on AL1/ST1A conductors according to EN 50 182, Table F.19. The *standardized cross-sectional ratios* of aluminium and aluminium alloy, respectively, to steel are 1,4, 1,7, 4,3, 6,0, 7,7, 11,3, 14,5 or 23,1. Today, phase conductors are used

Table 7.9: Characteristic data of ACSR conductors – configuration AL1/ST1A as per EN 50 182, Table F.19

Designation	Former code	Cross section	Number of strands		Conductor diam.	Mass per unit length	Rated strength	DC resistance	Current carrying capacity
	ACSR	total							
		mm^2	Al	St	mm	kg/km	kN	Ω/km	A
15-AL1/3-ST1A	16/2,5	17,8	6	1	5,40	61,6	5,80	1,8769	105
24-AL1/4-ST1A	25/4	27,8	6	1	6,75	96,3	8,95	1,2012	140
34-AL1/6-ST1A	35/6	40,1	6	1	8,10	138,7	12,37	0,8342	170
44-AL1/32-ST1A	44/32	75,6	14	7	11,2	369,3	44,24	0,6574	200
48-AL1/8-ST1A	50/8	56,3	6	1	9,60	194,8	16,81	0,5939	210
51-AL1/30-ST1A	50/30	81,0	12	7	11,7	374,7	42,98	0,5644	230
70-AL1/11-ST1A	70/12	81,3	26	7	11,7	282,2	26,27	0,4132	290
94-AL1/15-ST1A	95/15	109,7	26	7	13,6	380,6	35,93	0,3060	350
97-AL1/56-ST1A	95/55	152,8	12	7	16,0	706,8	77,85	0,2992	370
106-AL1/76-ST1A	105/75	181,2	14	19	17,5	885,3	105,82	0,2742	400
122-AL1/20-ST1A	120/20	141,4	26	7	15,5	491,0	44,50	0,2376	410
122-AL1/71-ST1A	120/70	193,4	12	7	18,0	894,5	97,92	0,2364	415
128-AL1/30-ST1A	125/30	157,8	30	7	16,3	587,0	56,41	0,2260	425
149-AL1/24-ST1A	150/25	173,1	26	7	17,1	600,8	53,67	0,1940	470
172-AL1/40-ST1A	170/40	211,8	30	7	18,9	788,2	74,89	0,1683	520
184-AL1/30-ST1A	185/30	213,6	26	7	19,0	741,0	65,27	0,1571	535
209-AL1/34-ST1A	210/35	243,2	26	7	20,3	844,1	73,36	0,1381	590
212-AL1/49-ST1A	210/50	261,5	30	7	21,0	973,1	92,46	0,1363	620
231-AL1/30-ST1A	230/30	260,8	24	7	21,0	870,9	72,13	0,1250	630
243-AL1/39-ST1A	240/40	282,5	26	7	21,8	980,1	85,12	0,1188	645
264-AL1/34-ST1A	265/35	297,7	24	7	22,4	994,4	81,04	0,1095	680
304-AL1/49-ST1A	300/50	353,7	26	7	24,4	1227,3	105,09	0,0949	740
305-AL1/39-ST1A	305/40	344,1	54	7	24,1	1151,2	96,80	0,0949	740
339-AL1/30-ST1A	340/30	369,1	48	7	25,0	1171,2	91,71	0,0852	790
382-AL1/49-ST1A	380/50	431,2	54	7	27,0	1442,5	121,30	0,0758	840
389-AL1/34-ST1A	385/35	420,1	48	7	26,7	1333,6	102,56	0,0749	850
434-AL1/56-ST1A	435/55	490,6	54	7	28,8	1641,3	133,59	0,0666	900
449-AL1/39-ST1A	450/40	488,2	48	7	28,7	1549,1	119,05	0,0644	920
490-AL1/64-ST1A	490/65	553,8	54	7	30,6	1852,9	150,61	0,0590	960
494-AL1/34-ST1A	495/35	528,4	45	7	29,9	1632,6	117,96	0,0584	985
511-AL1/45-ST1A	510/45	585,8	48	7	30,7	1765,3	133,31	0,0566	995
550-AL1/71-ST1A	550/70	620,9	54	7	32,4	2077,2	166,32	0,0526	1020
562-AL1/49-ST1A	560/50	611,2	48	7	32,2	1939,5	146,28	0,0515	1040
571-AL1/39-ST1A	570/40	610,6	45	7	32,3	1887,1	136,40	0,0506	1050
653-AL1/45-ST1A	650/45	698,8	45	7	34,4	2159,9	156,18	0,0442	1120
679-AL1/86-ST1A	680/85	764,5	54	19	36,0	2549,7	206,56	0,0426	1150
1046-AL1/45-ST1A	1045/45	1090,9	72	7	43,0	3248,2	218,92	0,0277	1580

having cross-sectional ratios between 6,0 and 14,5 for the majority of lines; lower ratios are used for earth wires, larger ratios in substations. The respective number of wires varies between 6 and 72 for the envelope and between 1 and 19 for the core. For special applications, conductors with more than 100 wires are applied. In these cases, the *stranding* is performed in several consecutive runs. The number of reels available at the stranding machines determines the maximum number of wires of the outermost layer and the number of runs to manufacture the conductor (see clause 7.1.7.3). In the USA, composite conductors are standardized according to ASTM B232 [7.33]

7.1.7.2 Characteristic data

In many practical calculations, composite conductors can be treated as mono-metallic conductors, therefore, a virtual *modulus of elasticity*, a virtual tensile stress, a specific heat, a resulting resistance, a temperature coefficient of resistance and a resulting ther-

Table 7.10: Mechanical and electrical values of standard conductors

Conductor material, Standard	Cross-sectional ratio	Number of strands	Coefficient of thermal expansion ε_t $\cdot 10^{-6}$/K	Temperature coefficient of resistance α 1/K	Specific conductivity κ m/Ωmm^2	Specific resistivity ϱ Ωmm^2/m	Specific heat c Ws/(kg·K)
AL1 (AAC) EN 50 182		7 to 91	23,0	0,00403	35,4	0,0283	897
AL3 (AAAC) EN 50 182		7 to 91	23,0	0,00360	30,7	0,0326	909
Copper DIN 48 201 Part 1		7 to 61	17,0	0,00394	56,0	0,0179	394
Bronze DIN 48 201 Part 2		7 to 61	17,0	0,00377	BzI 48,0 BzII 36,0 BzIII 18,0	0,0208 0,0278 0,0556	377
Steel DIN 48 201 Part 3		7 to 19	11,5	0,00450	5,2	0,1916	481
A20SA EN 50 182		7 to 61	13,0	0,00360	11,8	0,0848	518
AL1/ST1A (ACSR) and AL3/ST1A (AACSR) according to EN 50 182	1,4	14/7	15,0				605
		14/19	15,0				618
	1,7	12/7	15,3	0,00403 (AL1)	35,4 (AL1)	0,0283[1] (AL1)	623
	4,3	30/7	17,8				717
	6,0	6/1	19,2				750
		26/7	18,9	0,00360 (AL3)	30,7 (AL3)	0,0326[1] (AL3)	
		24/7	19,6				
	7,7	54/7	19,3				772
		54/19	19,4				
	11,3	48/7	20,5				803
	14,5	45/7	20,9				820
	23,1	72/7	21,7				845

[1] envelope only

mal expansion coefficient can be used in the calculations. The modulus of elasticity is approximately given by

$$E = \frac{E_{Al} \cdot m_1 + E_{Fe}}{m_1 + 1} \quad , \tag{7.2}$$

where m_1 is the *cross-sectional ratio* of conductor envelope to core (aluminium to steel), E_{Al} the modulus of elasticity of aluminium and E_{Fe} the modulus of elasticity of steel. The values given in Table 7.11, which are based on [7.2] and [7.6], differ slightly from the result obtained from (7.2), because the *stranding effects* were taken into account. The *coefficient of thermal expansion* ε_t is

$$\varepsilon_t = \frac{\varepsilon_{tAl} \cdot E_{Al} \cdot m_1 + \varepsilon_{tFe} \cdot E_{Fe}}{m_1 \cdot E_{Al} + E_{Fe}} \quad , \tag{7.3}$$

where ε_{tAl} is the coefficient of thermal expansion of aluminium and ε_{tFe} the coefficient of thermal expansion of steel. Table 7.11 contains the standard values.
The *specific mass* γ or density can be calculated by

$$\gamma = \frac{\gamma_{Al} \cdot m_1 + \gamma_{Fe}}{m_1 + 1} \quad , \tag{7.4}$$

where γ_{Al} is the specific mass of aluminium and γ_{Fe} the specific mass of steel.

Table 7.11: Modulus of elasticity, everyday and long-term stress according to EN 50 341-3-4 for standardized conductors

Conductor material, Standard	Cross-sectional ratio	Number of strands	Modulus of elasticity E kN/mm^2	Everyday stress N/mm^2	Long-term stress N/mm^2
AL1 EN 50 182	1,0	7	60	30	120
		19, 37	57		
		61, 91	55		
AL3 (ACSR) EN 50 182	1,0	7	60	44	240
		19, 37	57		
		61, 91	55		
Copper DIN 48 201 Part 1	1,0	7	113	85	300
		19, 37	105		
		61	100		
Bronze DIN 48 201 Part 2	1,0	7	113	BzI 100	400
		19, 37	105	BzII 100	500
		61	100	BzIII 100	620
Steel DIN 48 201 Part 3	1,0	7	180	ST I	320
				ST II 120	560
		19	175	ST III 130	900
				ST IV 150	1100
A20SA EN 50 182	1,0	7,37	159	137	

				AL1/ ST1A	AL3/ ST1A	AL1/ ST1A	AL3/ ST1A
AL1/ST1A (ACSR) and AL3/ST1A (AACSR) according to EN 50 182	1,4	14/7	110	90	104	401	464
		14/19	110				
	1,7	12/7	107	84	102	368	435
	4,3	30/7	82	57	69	240	328
	6,0	6/1	81	56	67	208	300
		26/7	77				
		24/7	74				
	7,7	54/7	70	52	63	189	284
		54/19	68				
	11,3	48/7	62	44	53	165	265
	14,5	45/7	61	40	50	152	255
	23,1	72/7	60	35	—	130	—

The *specific heat* is obtained from

$$c = \frac{c_{\mathrm{Al}}\gamma_{\mathrm{Al}} \cdot m_1 + c_{\mathrm{Fe}}\gamma_{\mathrm{Fe}}}{\gamma_{\mathrm{Al}} \cdot m_1 + \gamma_{\mathrm{Fe}}} \quad , \tag{7.5}$$

where c_{Al} is the specific heat of aluminium and c_{Fe} the specific heat of steel.
The *resistivity* is given by

$$\varrho = \frac{\varrho_{\mathrm{Al}}\varrho_{\mathrm{Fe}}(m_1 + 1)}{\varrho_{\mathrm{Al}} + \varrho_{\mathrm{Fe}} \cdot m_1} \quad , \tag{7.6}$$

where ϱ_{Al} is the resistivity of aluminium and ϱ_{Fe} the resistivity of steel.
The *tensile stress* σ, defined as the quotient of the conductor tensile force F_{C} by the total cross-sectional area A_{tot}, is not a real physical quantity of composite conductors, since the actual stresses occurring in aluminium and steel wires differ from that quotient. The stresses in the aluminium envelope, assuming the same elongation for all the aluminium wires, can be calculated as follows:

$$\sigma_{\mathrm{Al}} = \sigma \cdot \frac{m_1 + 1}{m_1 + E_{\mathrm{Fe}}/E_{\mathrm{Al}}} \quad , \tag{7.7}$$

where $\sigma = F_C/A_{tot}$ is the tensile stress related to the area of the total conductor.
For the steel core, the tensile stress is given by

$$\sigma_{Fe} = \sigma \cdot \frac{1 + m_1}{1 + m_1(E_{Al}/E_{Fe})} \quad . \tag{7.8}$$

The results given by (7.7) and (7.8) are theoretical values which assume a homogeneous distribution of the proportional tensile load on all wires of the same material. Due to the differing stranding of each layer, significant differences may occur between *tensile stresses in individual wires* [7.34].
Nevertheless, (7.7) and (7.8) give an estimate of the stresses in each individual wire. Depending on the proportion of both materials – aluminium and steel – in composite conductors of different design, their stresses can differ, despite the same *total tensile stress*. Corresponding data can be obtained for other materials, if aluminium is replaced by the envelope material and steel by the material of the core, respectively.
For a 304-AL1/49-ST1A conductor with a cross-sectional ratio of 6,0 and the overall tensile stress of 60 N/mm^2, a tensile stress of 45,8 N/mm^2 results for the aluminium wires and 144,8 N/mm^2 for the steel wires. For a 562-AL1/49-ST1A conductor with a cross-sectional ratio of 11,3 and an overall tensile stress of 60 N/mm^2, a tensile stress of 51,0 N/mm^2 results for the aluminium wires and 161,1 N/mm^2 for the steel wires. It can be seen that, the larger the aluminium proportion, the higher the aluminium and steel stresses will be for the same overall tensile stress.
The calculated distribution of the total force does not take into account the different temperature behaviour. To a decreasing temperature, the aluminium reacts with a higher participation in the total force, due to the different coefficients of thermal expansion; if the temperature increases, the effect is the opposite.
The *rated tensile strength (RTS)* of composite conductors is determined in accordance with EN 50 182, section 5.9. For ALx/STyz and ALx/yzSA conductors, it is equal to the minimum tensile strength of aluminium wires before the stranding process, multiplied by their rated cross section plus the tensile stress of steel or aluminium-clad steel wires corresponding to 1 % elongation in a 250 mm gauge length before stranding, multiplied by their rated cross section

$$RTS = \sigma_{B\,Al} \cdot A_{Al} + \sigma_{1\ \%\,Fe} \cdot A_{Fe} \quad . \tag{7.9}$$

The requirements on RTS of conductors are considered to be accomplished by a test when failing of individual wires occurs only after 95 % of that rated strength have been reached.

7.1.7.3 Production

The machines used for *stranding of conductors* must accomplish different requirements depending on the materials of the wires to be stranded and the conductors to be produced. Twisting of steel, aluminium-clad steel or aluminium alloy wires should be avoided. Therefore, stranding machines provided with *untwisting equipment* are used. The reel supports turn in the opposite direction to that of the stranding process; they keep the relative position of their axles in the space, thus reducing the twisting of the individual wires. Contrary to that, aluminium wires can be stranded using machines with reels fixedly arranged in the cage which cause the individual wires to twist around themselves during the stranding process.
During a run, one to three layers of wires can be stranded with 6, 12 and 18 wires per lay or by 12, 18 and 24 wires, respectively, depending on the design and the capacity of the stranding machines. The *lay ratio* of a conductor is the ratio of the lay length to the external diameter of the corresponding lay of wires in the stranded conductor. The

lay ratios are in between 14 and 20 in case of steel wires and in between 10 and 16 in case of aluminium and aluminium alloy wires. The lay ratio should decrease from the core to the outermost layer or at least remain constant.
The consecutive layers are stranded in opposite *lay directions*, the external layer being stranded preferably right-hand. For composite conductors, the core and the envelope are stranded separately. All steel wires should lie naturally in their position in the stranded core, and when the core is cut the wire ends should remain in position or be readily replaced by hand and then remain approximately in position. To comply with this requirements, the individual *steel wires* are *preformed* prior to the stranding process.
To improve the resistance against corrosion, zinc coated steel wires are usually greased. There are *soap-containing* or *soap-free greases* which are mainly distinguished by their drop point; when the temperature exceeds the drop point, the grease gets liquid and lost. The *drop point of the grease* has to be adjusted to the maximum *operating temperature of the conductor*. For soap-free greases, the drop point is below 100°C. The standard EN 50 326 [7.30] specifies details for conductor greasing. In EN 50 182 [7.2], Annex B, four cases of grease application are specified:

- Case 1: only steel core is greased.
- Case 2: all the conductor is greased, except the outer layer.
- Case 3: all the conductor is greased, including the outer layer.
- Case 4: all the conductor is greased, except the outer surface of the wires in the outer layer.

Case 1 should be used for conductors with galvanized steel wires in the core as a minimum requirement [7.2]. Experience and tests show that the zinc coating will not be corroded even during long-term exposure to corrosive atmosphere, especially in case of several ALx layers. On the other hand, severe corrosion is reported in case of non-greased galvanized steel cores, even when the exposure has been for a short period of time only. Greasing of the outer layer is not recommended, since corona could occur and the performance of clamps would be affected.

7.1.7.4 Joints

Joints in aluminium and aluminium alloy blanks may be made prior to final drawing without restrictions [7.9, 7.16]. One joint may also be made in the finished wire provided

- The mass of the coil is at least 500 kg;
- There is not more than one joint in such coil;
- Not more than 10 % of coils in a lot contain a joint and
- When requested by the purchaser, the manufacturer can provide evidence that the joints do not have a tensile strength below 130 N/mm^2.

Joints in steel wires are allowed in the base hot rolled rod and semi-finished wire by electric butt or flash welding process, before or after heat treatment and prior to final drawing (see [7.10]). The following should be considered:

- After drawing to the final diameter, joints should have a minimum tensile strength not less than 80 % of a wire without joint.
- The finished wire with a joint is not required to pass the ductility wrapping test.
- No joints should be made in the coated steel wires at final diameter.
- No joint should be made after heat treatment in wires destined to be used in conductors containing only one steel wire.

Joints in aluminium-clad steel wires may only be made in the blanks prior to drawing. The finished wire with a joint sould have a strength of 80 % of the wire without a joint. Several tests may not be passed by welded wires.
In [7.2], several additional requirements are provided on the use of jointed wires for conductors:

- For conductors with one steel wire only, there may be no joint made after heat treatment.
- No joints at all may be made in finished zinc-coated or aluminium-clad steel wires.
- Not more than one jointed aluminium wire may be used per length of conductor.
- During stranding, aluminium wires may not be welded for the purpose of achieving the required conductor length.

However, joints are permitted in aluminium wires unavoidably broken during stranding.

- The number of joints may not exceed a certain number as per [7.2].
- Their minimum distance is 15 m between joints in the same or in any other wire.
- The welding method should be approved by the purchaser.
- The joints should be dressed smoothly.
- The joints should withstand a stress not less than 75 N/mm^2.
- Some purchasers do not allow wires of the outer layer to be welded.
- The identification of joints should be agreed upon when placing the contract.
- Wires of conductors containing optical fibres should not be welded.

7.1.7.5 Shipment

For *shipping the conductors*, they are wound on reels in accordance with [7.2], where either *fitted lengths* adjusted to the lengths of the tensioning sections or fixed lengths corresponding to the capacity of the reels are supplied. Both, type of shipment and size of reels should be agreed upon together with the order. The diameter of the reel barrel should be 30 times the conductor diameter or 60 times the steel core diameter, whichever is the larger.

Occasionally, conductors on wooden reels shipped in containers [7.35] showed dark discoloration, which was attributed to condensation water within the containers or could also be traced back to damp wooden reels. In the mentioned publication, some recommendations to prevent such discoloration are provided. The discoloration does not represent any damage of the conductors. Duly not impregnated wood may be used for wooden reels, because salts used for impregnation cause a chemical reaction with aluminium, damaging their surface.

The use of steel reels is generally much more acceptable for EHV lines, because they can be reused and cause no damage to the conductors.

7.1.8 Conductor testing

7.1.8.1 Classification of tests

Type and sample tests are specified for overhead conductors. *Type tests* are intended to verify the main characteristics of the conductor which depend mainly on its design. These tests are normally performed only once for a given conductor design.

Sample tests are intended to guarantee the quality of conductors and compliance with the requirements of relevant standards or client's specifications. In Table 7.12, an overview is given on the tests according to [7.2]. Before stranding the conductor, the blank material and in particular the wires should be submitted to tests described in clause 7.1.5. Such tests are carried out at the wires of stranded conductors to comply with the requirements of the relevant specifications. Single wire tests are not discussed further within this clause.

7.1.8.2 Extent of sample tests

In accordance with EN 50 182, *sample tests* are foreseen for 10 % of the total number of reels belonging to a lot being shipped, whereby the extent of the tests may be agreed upon between the purchaser and the manufacturer.

Table 7.12: Type and sample tests for conductors according to [7.2]

	Type test	Sample test		Type test	Sample test
Aluminium wires			**Conductor**		
- diameter	×	×	- surface condition	×	×
- tensile strength	×	×	- diameter	×	×
- elongation	×	×	- inertness	×	×
- resistivity	×	×	- lay ratio and direction of lay	×	×
- wrapping test	×	×	- number and type of wires	×	×
- welding	×	–	- mass per unit length	×	×
Zinc-coated steel wires			- stress-strain curve	(1)	–
- diameter	×	×	- tensile breaking strength	(1)	–
- tensile strength	×	×	- stringing test	(1)	–
- stress at 1 % elongation	×	×	- creep test (2)	(1)	–
- elongation or torsion test	×	×	**Grease**		
- wrapping test	×	×	- mass per unit length	×	×
- mass of zinc	×	×	- drop point	×	×
- zinc dip test	×	×			
- adhesion of zinc coating	×	×			
Aluminium-clad steel wires					
- diameter	×	×			
- tensile strength	×	×			
- stress at 1 % elongation	×	×			
- elongation	×	×			
- torsion test	×	×			
- cladding thickness and uniformity	×	×			
- resistivity	×	×			

(1) according to agreement between manufacturer and purchaser

(2) according to IEC 61 395

7.1.8.3 Surface condition, dimensions, inertness and mass

As required for wires, the conductor surfaces should be free from imperfections observed with the unaided eye as, for example, nicks, indentations or scores. The dimensions should accomplish the standard indications or the requirements of the order for diameters, lay lengths and number of wires. The inertness of the form is related to the steel core, where, after cutting, the wires should remain in a cross section (see clause 7.1.7.3). The *conductor mass* without grease should not deviate more than 2 % from the rated value.

7.1.8.4 Stress-strain diagram

Stress-strain diagrams for conductors inform on the behaviour of a conductor under load. Annex C of [7.2] gives explanations on the stress-strain test method. The test sample length between the end terminations should be at least 400 times the conductor diameter but not less than 10 m. A shorter length may be agreed between purchaser and manufacturer. The gauge length should be a minimum of 100 times the conductor diameter. Great care should be taken in the preparation of the test samples. Relative displacements as small as 1 mm between steel core and aluminium layers of the conductor cause significant changes in the recorded stress-strain diagram. Therefore, no relative displacement should occur between the steel core and the envelope during the test procedure. At both ends of the sample length, end fittings such as compression clamps, epoxy-type or solder-type terminations approved by the purchaser should be used for the test. The application of the end fitting should not induce any slack in the wires which might affect the stress-strain diagram of the conductor.

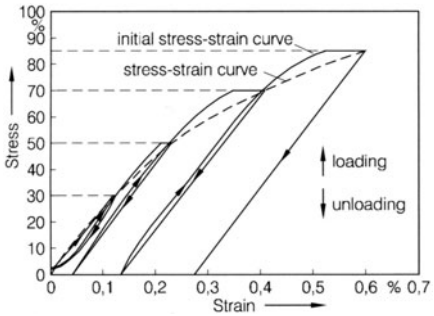

Figure 7.4: Evaluation of a stress-strain curve

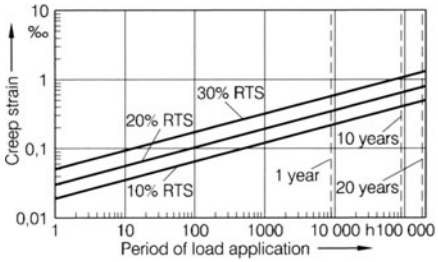

Figure 7.5: Creep curve, conductor 483-AL1/63-ST1A (Cardinal)

The *test loads* should be applied on the conductor by the following steps:

- Initial load of 5 % of the *rated tensile strength* (RTS) to straighten the conductor and set the strain gauges to zero.
- For non-continuous stress-strain data recordings, the strain readings should be taken at intervals of 2,5 % RTS, rounded to the nearest kN during both loading and unloading procedure.
- Load with 30 % RTS and holding the load for 0,5 h. Readings should be taken after 5, 10, 15 and 30 min during the holding period. Then the load is released to the initial load.
- Reload to 50 % RTS and holding for 1 h. Readings should be taken after 5, 10, 15, 30, 45 and 60 min during the holding period. Then the load is released to the initial load.
- Reload to 70 % RTS and holding for 1 h. Readings should be taken after 5, 10, 15, 30, 45 and 60 min during the holding period. Then the load is released to the initial load.
- Reload to 85 % RTS and holding for 1 h. Readings should be taken after 5, 10, 15, 30, 45 and 60 min during the holding period. Then the load is released to the initial load.
- After the fourth application of load, the conductor is loaded again by increasing the tensile force steadily until the actual breaking strength is reached. Simultaneous readings of tensile force and elongation should be taken up to 85 % of RTS at least at the same time intervals as for the previous loading cycles.

The rate of load application should be uniform during testing. The time required to reach 30 % RTS should not be less than 1 min or more than 2 min. The same rate of loading should thereafter be maintained throughout the tests.

The initial stress-strain diagram is obtained by drawing a smoothed line through the strain point after 0,5 h at 30 % RTS and the strain points after 1 h at 50, 70 and 85 % RTS. The curve should be adjusted to pass through the zero point. The initial stress-strain diagram is represented by the broken line in Figure 7.4. The characteristic final stress-strain diagram may be determined from the unloading part (from 50, 70 or 85 % RTS) of the graph, as agreed upon between the manufacturer and the client. In Figure 7.4, an example is shown for a stress-strain diagram.

7.1.8.5 Tensile breaking strength

The *tensile breaking strength* is determined at a sample with a minimum length of 400 times the conductor diameter, but at least 10 m in accordance with [7.2]. The breaking load is reached when one or more wires are fractured. If the fracture occurs within a

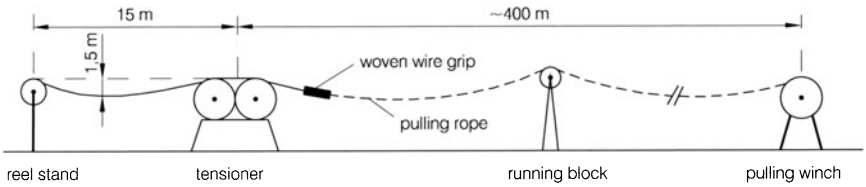

Figure 7.6: Arrangement for testing the tension stringing ability of conductors

distance of 50 mm from the dead-end termination, and before 95 % of the *rated tensile strength* is achieved, it can be attributed to the influence of the end terminations and the test may be repeated. The test is considered to be successful when the fracture occurs for a load equal to or above 95 % of the rated tensile strength (RTS).

7.1.8.6 Test of creep behaviour

Conductor creep is described according to [7.36] by the equation

$$e = e_{1\mathrm{h}} \cdot t^n \quad , \tag{7.10}$$

where

t is the time in hours and

$e_{1\mathrm{h}}, n$ are parameters which depend on conductor type and load condition.

These values are measured by means of the tests described in [7.36], which is performed on a sample which is at least as long as 100 times the conductor diameter, clamped in a test device, which keeps the load constant during the test, with an accuracy of ±1 % or ±120 N. To measure the *creep elongation*, some marks are made on the conductor and their displacement is recorded during the test in relation to an unloaded structure or bars arranged in parallel to the conductor. The measuring intervals are selected in a logarithmic scale. The results of the tests are then represented in a double logarithmic scale corresponding to the equation

$$\log e = \log e_{1\mathrm{h}} + n \cdot \log t \quad . \tag{7.11}$$

With this scale, the creep elongation in the ideal case forms a straight line. So, $e_{1\mathrm{h}}$ is the intersection with the ordinate for $t = 1$ h and n the slope of the straight line.
In Figure 7.5, a *creep diagram* is shown, forming a mean straight line through the measuring points in a double logarithmic scale. The creep elongation can then be extrapolated until 100 000 h (approximately 10 a). Indicative data for $e_{1\mathrm{h}}$ and n can be found in [7.31] and clause 16.8.5.3.

7.1.8.7 Testing the tension stringing ability of conductors

This test is intended to simulate the tensile load existing during tension stringing and to verify, in particular, the absence of *bird caging*. The test arrangement according to [7.2] is shown in Figure 7.6. The reel should be installed on an unwinding reel stand equipped with an adjustable disk brake which is not under automatic control from the tensioner. The *tensioner* is arranged in a distance of approximately 15 m from the reel stand. The diameter of the tensioner should be as low as just permissible for stringing of the conductor to be tested, i. e. it should be approximately 30 times the conductor diameter (see clause 16.8.3.6). The conductor *pulling winch* should be installed approximately 400 m apart from the tensioner, and the conductor should be pulled by means of a pulling rope. A running block should be installed at mid-distance between the pulling winch and the tensioner at an adequate height so that the conductor does not touch

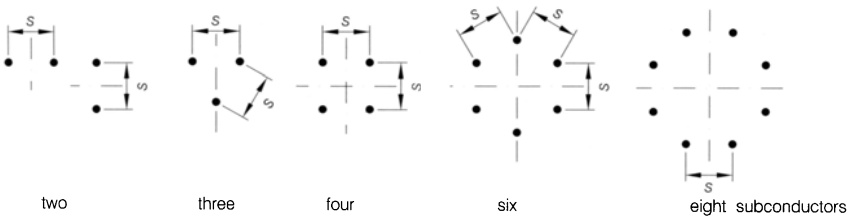

Figure 7.7: Configuration of twin, triple, quadruple, five, six and eight bundle conductors, subconductor spacing 400 to 600 mm

the ground during unwinding. During the test, the conductor is unwound by means of the pulling winch and braked by the tensioner.
During unwinding, the sag between the reel stand and the tensioner should be adjusted to approximately 1,5 m. The tensile force at the output of the tensioner should be maintained at 20 % of the RTS of the conductor tested and the unwinding speed be approximately 1 m/s.
During the unwinding of the conductor length, observation should be made if any individual outer layer wire is raised above its normal position by more than one wire diameter; if this occurred, the conductor should be deemed unacceptable.

7.1.9 Bundle conductors

In accordance with [7.7], *bundle conductors* are a set of individual conductors connected in parallel and disposed in a uniform geometrical configuration, that constitute one phase conductor of an AC line or one pole of a DC line.
With the inauguration of the 220 kV transmission voltage in 1929, *corona phenomena* occurred, which were then solved by larger conductor diameters obtained by non-conventional designs, as, for example, *hollow copper conductors* (Figure 7.9). As an alternative to that, the use of two or more subconductors instead of a single one was introduced. In 1930, Markt and Mengele got a patent for that alternative [7.37]. They first described in detail the advantages, such as lower *surface voltage gradient* and increase of the *transmission capacity* [7.38]. Power transmission at 420 kV and above is not feasible without the use of bundle conductors.
Bundle conductors are very sporadically applied for 110 kV voltage transmission where high *current carrying capacity* is required. For 220 kV, bundle conductors are usually an alternative to single conductors with larger diameters. For 400 kV, twin, triple or quadruple bundle conductors are applied. For 500 kV lines, both triple and quadruple bundle conductors have been extensively used worldwide. For 800 kV, quadruple and six bundle conductors have been applied [7.39]; for transmissions with higher voltage levels, even more subconductors are required. The new 1000 kV lines in Japan are provided with bundles of eight subconductors [7.40, 7.41].
Subconductors are installed in Europe with a usual spacing of 400 mm and in North America with 18 inches (457 mm) as well as wider spacing. They are protected against clashing due to short-circuit or wind by means of *bundle spacers* arranged at predetermined distances (see clause 10.2.5). Bundle spacers with integrated damping elements are used to reduce amplitudes due to *aeolian vibrations* and *subspan oscillation*. Larger subconductor diameters require the use of higher subconductor spacing, to more than 18 times of the subconductor diameter to counteract the subspan oscillations [7.42].
Twin bundle conductors are arranged either horizontally or vertically (Figure 7.7). A horizontal arrangement facilitates the guiding of the conductors at angle strain towers and enables an effective *protection against aeolian vibrations* by means of dampers at

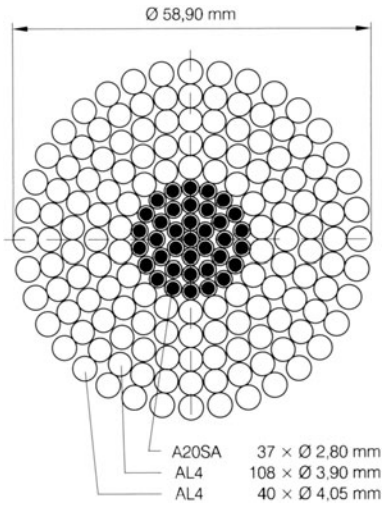

Figure 7.8: Cross section of the conductor for the 400 kV Bosphorus crossing (Turkey)

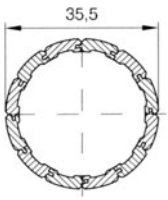

Figure 7.9: Hollow copper conductor

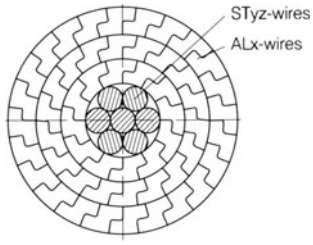

Figure 7.10: Conductor made of z-shaped formed wires according to [7.44]

the span ends. The vertical arrangement is less sensitive against *sagging errors* and differing creep of the subconductors; the lower subconductor is then a little bit less submitted to tension than the upper one.
A twin bundle 243-AL1/39-ST1A has approximately the same cross-sectional area as a single conductor 490-AL1/64-ST1A. Both can be operated at 220 kV. The current carrying capacity amounts to 1290 A for the bundle in accordance with Table 7.9; for the single conductor the value is 960 A, that is 75 % of the former one. The *surge impedance* of the bundle reaches 300 Ω; in case of the single conductor, it amounts to 360 Ω, i. e. its *surge impedance load* amounts to only 83 %. The *surface gradient* of the single conductor reaches 16,0 kV/cm for a triangular circuit configuration; for the bundle, that value amounts to 15,6 kV/cm; the *audible noise* level for the single conductor is about 50 dB(A) and for the bundle it is about 40 dB(A) close to ground surface in the right-of-way centre. This comparison shows the advantages of bundle conductors, being even more significant at higher voltage levels.
The dimensions of the bundle subconductors influence the electric characteristics, specially the surge impedance, the surge impedance load, the conductor surface gradient, and thus, the *corona performance*. The increase of the surge impedance load implies an increase of the *transmission capacity* of long lines. In [7.43], a 500 kV line is cited, whose subconductor spacing in the bundle is variable and can amount up to a maximum of 1,7 m. Thereby, the surge impedance load increases up to 130 % of the value with 450 mm subconductor spacing.

7.1.10 Special conductor designs

7.1.10.1 Non-standardized conductors made of round wires

Beside the usual standard conductor designs, many other *special conductors* are applied. Long spans require conductors with higher rated tensile strength [7.45]. For this application, conductors with high steel content and a correspondingly large cross section offer an interesting alternative. In the 220 kV line over the river Elbe, 310-AL3/110-ST1A

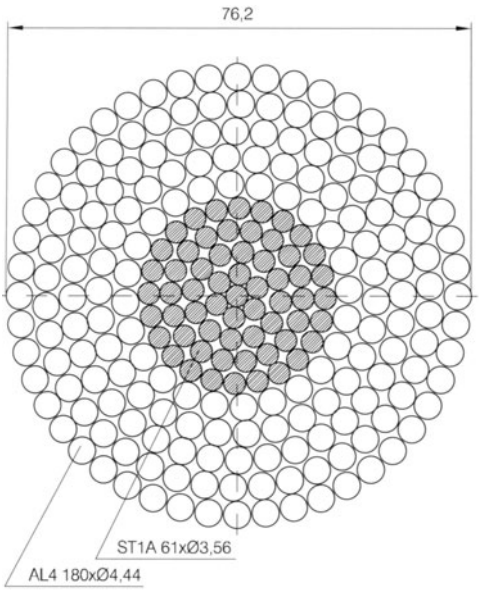

Figure 7.11: Cross section of 2787-AL4/607-ST1A conductor used as single conductor for a 500 kV line across the Mission Ridge in British Columbia, Canada (BC Hydro, Vancouver)

conductors were used with a cross-sectional ratio equal to 3:1 and a diameter of 29 mm. In order to reach the required power transmission by means of one single conductor and to keep the conductor surface gradient as low as possible, the 400 kV overhead line over the Bosphorus has been equipped with a 1805-AL4/228-A20SA composite conductor having an aluminium-clad steel core [7.28] (Figure 7.8) and a cross-sectional ratio of 7,9:1. A rated strength of 850 kN was achieved by using an AL4 alloy with 320 N/mm^2 tensile strength.

A 6,80 km long section of BC Hydro's 500 kV Peace River line was equipped with a single conductor having a 76,2 mm diameter instead of a quadruple bundle consisting of 24,1 mm diameter subconductors. This section crosses the Mission Ridge mountains at elevations between 1200 m and 1900 m and is prone to severe icing. The longest span is 1 100 m. In Figure 7.11, the conductor cross section is shown. It is made up of 61 steel strands having each 3,56 mm diameter and 180 aluminium alloy strands having 4,4 mm diameter. The alloy cross section is 2 787 mm^2, that of steel 607 mm^2. Therefore, the conductor could be named 2787-AL4/607-ST1A. Its rated tensile strength is 1 463 kN. The conductors were not tension-stringed but the conductor reels were pulled along the ground to place the conductors on wood lagging.

7.1.10.2 Conductors for increased operation temperature

Annealing of hard-drawn aluminium wires limits the permissible temperature of conventional conductors. Thus, *conductors for higher operational temperatures* were developed with annealed low-tensile aluminium wires, which present a slightly higher conductivity of 63 % IACS in comparison with that of 61 % IACS shown by hard-drawn aluminium in conventional conductors. In this case, the aluminium wires do not carry any mechanical stress; the mechanic function is guaranteed by the steel core alone. Such conductors can operate at temperatures up to 150°C and are suited to reinforce existing lines if larger sags and high Joule losses can be accepted.

A similar function is performed by conductors with aluminium alloy wires of high thermal capacity (TAL), which can be operated with temperatures up to 150°C. Compared with a conductor that shows the same design as 243-AL1/39-ST1A, the current carrying

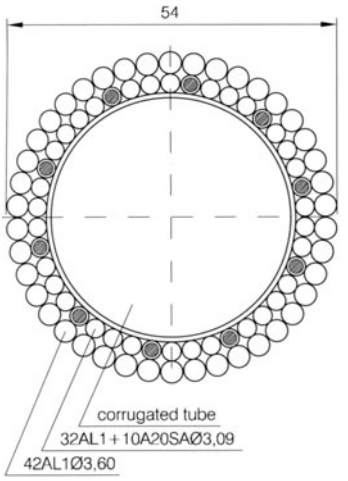

Figure 7.12: Hollow AL1/A20SA conductor used as single conductor for a 4000 kV line in Austria (Lumpi GmbH, Linz)

capacity increases from 650 to 1 015 A, that is by about 60 %. The sags also increase in correspondence with the higher temperatures; therefore, together with the replacement of the existing conductors, adjustment of tower heights might also be necessary to take full advantage of the higher transmission capacity. Prices for such conductors exceed those for AL1/ST1A conductors by about 50 %.
To keep sags within certain limits, conductors with *INVAR steel wires* were developed, whose coefficient of thermal expansion is low. The sag can thus be kept almost constant, even under elevated temperatures. These conductors, however, imply very large costs, in addition to high losses at high temperatures. When using such conductors, attention should be paid to the design of clamps and joints, as they will be submitted to the same high temperatures as the conductors and should withstand them. Construction of a new line, with optimum conductor cross sections, on the same right-of-way, should be the most economic solution long-sighted.

7.1.10.3 Conductors with enlarged diameters

Conductors with enlarged diameters were developed for transmission at 220 kV or higher voltage level, to reduce the conductor surface gradient, without having to accept the large conductor weights and unnecessary large cross sections of conventional conductor designs. Therefore, the first 220 kV lines were equipped with one-layer hollow copper conductors, which consisted of formed wires provided with featherkey and keyway (Figure 7.9).
The diameter of aluminium-steel composite conductors can be increased by using wires with large diameters in one or more internal layers, which result in a small *fill ratio*. Due to their difficult and expensive production as well as to problems with fittings to terminate and suspend these conductors, they are seldom applied today.
Uprating of an existing 220 kV double circuit line in Austria to 400 kV operation required new conductors that limit the audible noise emission to acceptable levels because the line runs close to residential areas. The geometric clearances and the structural strength did not permit to use twin bundle 635-AL1/117-A20SA conductors as usual for 400 kV transmission. Therefore, a hollow single conductor 667-AL1/75-A20SA was developed having 54 mm in diameter. In Figure 7.12, the cross section of that conductor is shown. Two layers are stranded around a flexible corrugated aluminium tube. The inner layer consists of 32 AL1 and 10 A20SA strands having 3,09 mm diameter each. The outer layer is made up of 42 AL1 strands with 3,60 mm diameter. The rated tensile

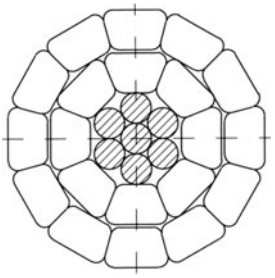

Figure 7.13: Conductor made of trapezoidal aluminium wires and INVAR steel core

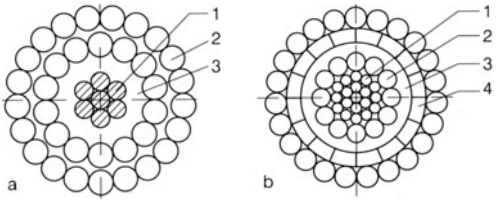

Figure 7.14: Self-damping conductors: a) German design, b) US-American design. 1 steel cores with long lay lengths; 2 aluminium layer with long lay lengths; 3 void space; 4 layer with self-supporting formed wires

strength is 203 kN, the weight 2,89 kg/m. The current carrying capacity amounts to 1 400 A.

7.1.10.4 Conductors with smooth surfaces

The use of *formed wires* instead of round wires results in compact *conductors with smooth surfaces* and less void spaces, which means a high fill ratio and a smaller diameter for the same cross-sectional area. This type of conductor is characterized by a lower *wind force* and supposedly lower trend to *galloping*. This was the reason why such conductors were used for the 380 kV line crossing over the river Schelde in Belgium [7.46]. It can be seen from [7.15], that formed wires can be produced with various shapes, such as *z-shaped cross sections* (Figure 7.10) or *trapezoidal cross sections* (Figure 7.13) and from all materials used for conventional conductors as well. With such wires, aluminium-steel conductors with any cross-sectional ratio can be designed. Figure 7.13 shows an example. The aerodynamic drag factor is between 0,46 and 0,8 for conductor diameters between 20 and 40 mm.
Conductors made of formed wires are applied where low wind forces together with a cross-sectional area as high as possible is required [7.15]. For such conductors, a standard is under approval procedure at IEC and CENELEC [7.44].

7.1.10.5 Compacted conductors

Compacted conductors are manufactured by stranding at first the conductor with layers of round wires as a conventional ALx/STyz or pure ALx conductor and finally compacting them through rollers or dies to a cross section with smooth, circular surface. This procedure forms the wires of the outer layers to trapezoidal cross sections and reduces the conductor diameter by 8 to 11 %. The surface becomes smooth and reduces the wind forces and the local peaks of voltage gradients. Additional layers of round wires or formed wires may be stranded over a compacted core. The production of compacted conductors is restricted to relatively small cross sections.

7.1.10.6 Self-damping conductors

Aeolian vibrations of conductors may cause damage at high-voltage overhead lines. Therefore, in Switzerland and Germany, *self-damping conductors* were developed in the 1930's, which consisted of an *aluminium hollow conductor* made of circular or profile wires with an internally movable steel core (Figure 7.14). In the 1930's, conductors

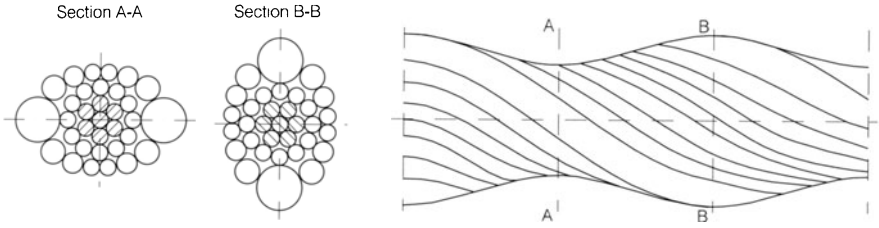

Figure 7.15: Vibration resistant oval conductors

with similar designs, but applying profile wires in the outer layers appeared in the USA. There, these conductors have been frequently applied [7.47]. Conditioned by the construction of the conductor, the *self-damping* should be large enough as not to lead to dangerous conductor vibration even in case of high tensile loads of the conductor in regions which favour vibrations. However, the conductor damping characteristics cannot prevent the occurrence of galloping. Further development of such conductor types was suspended in Europe due to their noise emission.

7.1.10.7 Vibration resistant conductors

By occasion of the above mentioned studies made in Germany, which aimed at developing conductors as vibration-inert as possible, designs were investigated having non-circular cross sections. The peculiar profile creates air turbulence so that the *laminar flow of the wind* around the conductor is altered and, as a consequence, a significant reduction of the *vibration amplitude* is achieved. Problems concerning fittings, however, prohibited practical application of such *vibration-resistant conductors* [7.48]. Efforts made to solve problems of conductor vibration and conductor galloping led in the USA to the development of vibration resistant conductors. This type of conductor is formed by left-hand stranding of two single conductors (*T2 conductors*). The resulting cross section has the form of a rotating "eight". In Germany, this type of T2 conductor was successfully used as a remedy against aerodynamically caused audible noise emissions on conventional conductors. Due to the conductor shape, no uniform wind flow happens, similarly to Maass' experience [7.48]. The utilization of the conventional fittings for the T2 conductors privileged their application. In the beginning of the 1980's, that type of conductor was used in many thousands kilometres of lines [7.49], specially in the USA. *Oval conductors* are formed by wires of different diameters stranded with each other (see Figure 7.15) [7.50].

7.1.10.8 Low noise conductors

In densely populated Japanese areas, noise pollution caused by the wind acting on conductors but not by corona, plays an important role under certain topographic conditions. The noise level could be reduced by means of special conductor configurations. These *low noise conductors* include several *formed wires* in their outer layer (Figure 7.16). Here, the benefit of disturbing the laminar flow described by Maass [7.48] as a conclusion of his experience has been utilized again. In comparison with a conventional conductor having the same cross-sectional area, the noise level can be reduced by up to 15 dB(A) [7.40, 7.51].

Table 7.13: Permissible conductor temperatures under short-circuit condition

Type of conductor	Material	EN 60 865-1, Table 6	EN 50 341-3-4	International practice
Mono-metallic conductor	E-Cu	200°C	170°C	300°C
	AL1	200°C	130°C	200°C
	ALx	200°C	160°C	200°C
	A20SA	—	200°C	400°C
	STyz	300°C	200°C	400°C
Composite conductor	AL1/STyz	200°C	160°C	200°C
	ALx/STyz	200°C	160°C	200°C

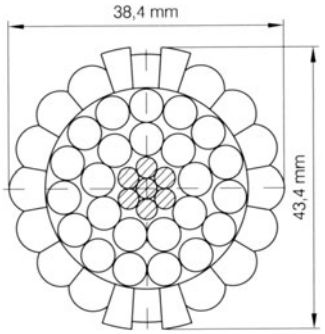

Figure 7.16: Low-noise ALx/STyz conductor for a 1000 kV line in Japan

7.1.10.9 Conductors with treated surfaces

Conductors with treated surfaces show favourable characteristics in view of *current carrying capacity* when compared with conventional ones. Blacking of the conductors increases their ampacity. By coating the outer layers with a black polyurethane paint, a worth mentioning increase of the *emission coefficient* to the value of 0,8 is achieved, as well as an increased *thermal radiation* in accordance with *Stefan-Boltzmann's radiation law* (see equation (7.23)) [7.52]. Replacement of the existing conductors by the blacked ones results in an increase of the thermal transmission capacity with no need to reinforce the towers.

Clean metallic conductors may give rise to objections coming from landscape protector, who may complain about the visual impact caused by new conductors. Therefore, some utilities have decided to apply a coloured coating on the conductors. In Austria, for example, they have used a green camouflage for conductors of a 380 kV transmission line. Thus, the conductors became nearly invisible against the background landscape [7.52]. From the ornithological point of view, however, this camouflage is disadvantageous because of the increased danger which the less visible conductors create for approaching birds.

In Australia, reduction of the brightness of new conductors was accomplished by a *dull finish*. The outer layer of the conductor was treated by blazing with a special fine sand, so that a surface roughness between 0,8 and 1,6 μm was obtained.

7.2 Design with regard to current loading

7.2.1 Introduction and requirements

According to EN 50 341-1 [7.53], every overhead line should be able to withstand with an acceptable reliability the electric load due to both *operating current* and *short-circuit current*. Due to conductor electrical resistance, the operating current and the short-circuit current lead to conductor heating, which would cause a reduction of the mechanical strength if the temperature exceeded a limit value. Figure 7.1 according to [7.19], shows the tensile strength for conductors made of aluminium, aluminium alloy, copper as well as AL1/ST1A and AL3/ST1A as a function of the temperature. In conformity with [7.8], conductor materials and cross sections should be chosen so as not to reach any inadmissible temperatures.

Neither [7.2] nor [7.53] give any information about the *permissible* steady-state and

short-term *temperatures*. They merely refer to national standards and project specifications. According to [7.6], the permissible temperatures for AL1/ST1A, AL3/ST1A, AL1 and AL3 conductors and for copper conductors, under steady-state load, are 80 and 70°C, respectively. In Table 7.13, the permissible temperatures under short-circuit condition are shown according to [7.6]. Other standards indicate higher permissible temperatures (see clause 8.3.1).

The standards mentioned before do not give any indication about the *ambient conditions*, which could be used for the assessment of standard *current carrying capacity* values. Ambient temperatures of 35 to 40°C and *wind velocities* of 0,6 to 1,0 m/s are often used as basis for the evaluation of the current carrying capacity.

As given by equation (2.9), the electrical resistance results in energy losses, which influence significantly the transmission costs. The conductor design is to keep the maximum *permissible conductor temperatures* below certain limits, and restrict the expected *transmission losses*. Consequently, conductor design is carried out with the target to minimize the *transmission costs*. This is an optimization task, since the losses are reduced and the investment rises as the cross-sectional area increases [7.54].

The *magnetic field* depends on the current as well, but differently from the electrical field it has no influence on the selection of the conductors and will, thus, not be dealt with here. In clause 2.3.2, information is given on magnetic fields.

7.2.2 Principles for determination of conductor temperature

The determination of the *conductor temperature* is based on the *heat balance at the conductor*, which is influenced in accordance with [7.55], by:

- *Joule heat* N_J, due to the current,
- *Solar radiation* N_S,
- *Magnetic losses* N_M,
- *Energy loss by convection* N_c and
- *Energy loss by radiation* N_R.

From these values, the heat balance can be established by

$$m_C \cdot c \cdot \mathrm{d}T/\mathrm{d}t = N_J + N_S + N_M - N_R - N_c \quad , \tag{7.12}$$

where m_C is the conductor mass per unit length, c the specific heat, T the conductor temperature and $\mathrm{d}t$ the derivative in terms of time.

Two cases are of substantial practical interest:

- The *adiabatic process*. Because of the magnitude of the term N_J compared with the other components in equation (7.12), under short-circuit conditions the latter can be disregarded. This case is essentially important for rating of earth wires. Therefore, it is dealt with in Chapter 8. In this case, equation (7.12) can be expressed as
$$m_C \cdot c \cdot \mathrm{d}T/\mathrm{d}t = N_J \quad . \tag{7.13}$$
- The steady-state condition. The conductor temperature T is constant; so, in (7.12) $\mathrm{d}T/\mathrm{d}t$ will be zero resulting in
$$N_J + N_S + N_M = N_R + N_c \quad . \tag{7.14}$$

The energy delivered to the conductor by Joule heat, magnetic losses due to AC current and solar radiation is equal to the energy lost by radiation and convection. This condition determines the steady-state operating current and, thus, represents an important value for line operation. The evaluation of conductor temperature in the most general unsteady state is dealt with in [7.56].

7.2.3 Design with regard to current carrying capacity

The literature includes some approaches for the evaluation of the *current carrying capacity*, also called *ampacity*, given by equation (7.14), for a predetermined conductor temperature and given ambient conditions. Some approaches will be mentioned here. In [7.55], a summary of used approaches is given, which also served as basis for the equations contained in [7.57]. Detailed studies of the subject are described in [7.58], which formed the basis for the current carrying capacities indicated in EN 50 182. An account of the measurements on overhead line conductors is presented in [7.59], whereby the tolerances between calculated and measured values are quoted by ± 3 K. The components N_J and N_M, which are a function of the current, can be expressed as follows

$$N_J + N_M = R'_{T\,AC} \cdot I^2 \quad , \tag{7.15}$$

where I is the effective current in the conductor, in Amperes and $R'_{T\,AC}$ the AC resistance at the temperature T in Ω/m.
The AC resistance increases, in comparison with the DC resistance, as a result of *skin and spiral effects*. Skin effect occurs due to the higher inductance of the internal layers of wires, because the internal flux density is larger. As the voltage drop in all wires is the same, a larger portion of the current flows through the outer conductor layers causing an increase of the effective resistance. The AC resistance $R'_{T\,AC}$ is calculated from

$$R'_{T\,AC} \approx R'_{T\,DC} \cdot (1 + x^4/3) \quad \text{for} \quad x \leq 1 \tag{7.16}$$

and

$$R'_{T\,AC} \approx R'_{T\,DC} \cdot (0{,}25 + x + 3/64) \quad \text{for} \quad x \geq 1 \tag{7.17}$$

with x being a parameter taking care of skin and spiral effects:

$$x = 0{,}5 \cdot r \cdot \sqrt{\pi \cdot f \cdot \kappa \cdot \mu_0 \cdot \mu_r} \quad , \tag{7.18}$$

where r is the conductor radius in mm, f the frequency in Hz, κ the conductivity in m/Ω· mm², μ_0 the vacuum permeability ($1{,}256 \cdot 10^{-6}$ H/m) and μ_r the relative permeability of the material (equal to 1 for non-magnetic materials). The spiral effect significantly influences composite conductors with odd numbers of layers, in particular when there is only one aluminium layer. Reference is made to [7.60]. Data for typical values of AC resistance are found in [7.57].
The *AC resistance* $R'_{T\,AC}$ depends on the conductor temperature T according to

$$R'_{T\,DC} = R'_{20}\,[1 + \alpha(T - 20)] \quad , \tag{7.19}$$

where R'_{20} is the DC resistance at 20°C in Ω/m and α the temperature coefficient of resistance in K^{-1}. Values for α are given in Table 7.4.
In accordance with [7.58], *solar radiation* is given by

$$N_S = D \cdot k_a \cdot N_{Sh} \cdot \sin\delta \quad \text{in W/m} \quad , \tag{7.20}$$

where k_a is the absorption coefficient (see Table 7.14), $\delta = \arccos[\cos h_s \cdot \cos(180° - \psi)]$. The solar angle h_s is defined by

$$h_s = 113{,}5° - \varphi \quad \text{for} \quad \varphi \geq 23{,}5°, \tag{7.21}$$

where φ is the latitude and ψ the angle of line direction with the north-south axis.
In (7.20), D is the conductor diameter, k_a the absorption coefficient and N_{Sh} the *standard solar radiation*, which assumes values between 850 and 1 350 W/m² depending on

Table 7.14: Total coefficient of emission k_e and absorption k_a for overhead conductors at low temperatures

Surface condition	Material	
	Copper	Aluminium, aluminium alloy
Half polished	0,15	0,08
Dull bright	0,24	0,23
Oxidized	0,5	0,35
Oxidized and Slightly dirty	0,6	0,5
Heavily oxidized	0,75	0,7
Heavily oxidized and dirty	0,88 to 0,93	0,88 to 0,93

Table 7.15: Material constants of air

Temperature T °C	Specific mass γ kg/m^3	Thermal conductivity λ W/Km	Dynamic viscosity η Ns/m^2
0	1,29	0,0243	0,175
10	1,25	0,0250	0,180
20	1,20	0,0257	0,184
30	1,17	0,0265	0,189
40	1,13	0,0272	0,194
50	1,09	0,0280	0,199
60	1,06	0,0287	0,203
70	1,03	0,0294	0,208
80	1,00	0,0301	0,213
90	0,97	0,0309	0,217
100	0,95	0,0316	0,222

the sun position and the air pollution. A typical value for Central Europe is 900 W/m^2. The value of 0,5 can be taken for the absorption coefficient k_a for most practical conductor types.
In accordance with [7.57], the following relation is valid for the total solar radiation

$$N_S = D \cdot k_a \cdot N_{Sh} \quad . \tag{7.22}$$

The *energy loss by radiation* is given by the following equation, in accordance with [7.58]

$$N_R = k_s \cdot k_e \cdot D \cdot \pi \left[0{,}75 \cdot \left(T^4 - T_{am}^4\right) + 0{,}25 \cdot \left(T^4 - T_h^4\right)\right] \quad \text{in W/m}, \tag{7.23}$$

where T is the absolute temperature of the conductor, T_{am} the absolute ambient temperature, T_h the absolute temperature of the external atmosphere (equal to 217° K), k_s the *Stefan-Boltzmann constant* equal to $5{,}67 \cdot 10^{-8}$ W/(m^{2}K^4) and k_e the emission coefficient (see Table 7.14). A value of 0,6 may usually be used for k_e.
In [7.57] it is not distinguished between ambient air conditions and the external atmosphere. The following equation is taken for the radiation loss

$$N_R = k_s \cdot k_e \cdot D \cdot \pi \left(T^4 - T_{am}^4\right) \quad . \tag{7.24}$$

Energy loss by convection can be calculated from

$$N_c = \pi \cdot \lambda \cdot Nu \cdot (T - T_{am}) \quad \text{in W/m}, \tag{7.25}$$

where λ is the thermal conductivity of air in W/(K·m) and Nu the Nußelt number.
The *Nußelt number* Nu depends on *Reynolds number* Re and according to [7.58], two regions are distinguished:

$$\begin{aligned} Nu &= 0{,}32 + 0{,}43 \cdot Re^{0{,}52} \quad \text{for} \quad 0{,}1 \leq Re \leq 10^3 \quad \text{and} \\ Nu &= 0{,}24 \cdot Re^{0{,}6} \quad \text{for} \quad 10^3 < Re \leq 5 \cdot 10^4 \quad . \end{aligned} \tag{7.26}$$

According to [7.57], the following equation applies

$$Nu = 0{,}65\, Re^{0{,}2} + 0{,}23\, Re^{0{,}61} \quad . \tag{7.27}$$

The differences between the Nußelt numbers resulting from both approaches amount to 5 % for $Re = 100$, 6 % for $Re = 1\,000$ and 3 % for $Re = 10\,000$. Thus, both alternatives result in acceptable results for the current carrying capacity. The equations are valid for the case of forced convection due to wind flow. For the exceptional case of free convection without wind, see [7.58].

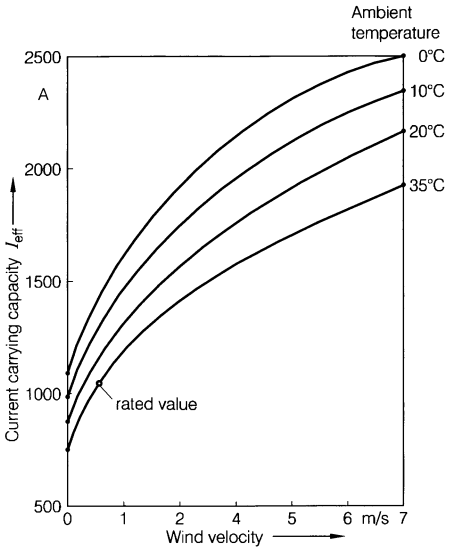

Figure 7.17: Current carrying capacity of a 564-AL1/72-ST1A conductor as function of wind velocity and ambient temperature; conductor temperature 80°C

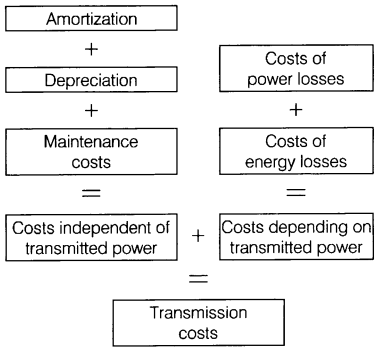

Figure 7.18: Transmission costs and their components

The Reynolds number Re is given by

$$Re = V \cdot D \cdot \gamma/\eta \quad , \tag{7.28}$$

where V is the wind velocity in m/s, γ the *specific mass of air* in kg/m^3, and η the *dynamic viscosity* in N·s/m^2. These values are dependent on temperature and air pressure. At sea-level the data given in Table 7.15 apply. For practical calculations the characteristics of air should be evaluated for the mean temperature $(T - T_{am})/2$. The influence of the altitude on the current carrying capacity can be determined by [7.55]. The dependency of the specific air mass γ on ambient temperature T_{am} and altitude h_{al} is given by

$$\gamma = \gamma_0 \cdot (288/T_{am}) \exp(-0,0001\, h_{al}) \quad , \tag{7.29}$$

where γ_0 is 1,225 kg/m^3 at 15°C and sea level and T_{am} is the absolute ambient temperature.
According to [7.57], the Reynolds number Re can be obtained from

$$Re = 1,644 \cdot 10^9 \cdot V \cdot D \cdot [T_{am} + 0,5(T - T_{am})]^{-1,78} \quad . \tag{7.30}$$

The current carrying capacity is calculated by equation (7.15), solving this equation with respect to the required current:

$$I = \sqrt{(N_R + N_c - N_S)/R'_{T\,AC}} \quad . \tag{7.31}$$

Figure 7.17 represents an example of application of (7.31), showing the current carrying capacity as a function of the ambient temperature and the wind velocity for a 564-AL1/72-ST1A conductor. The current carrying capacity is often quoted for an ambient temperature of 35°C, a conductor temperature of 80°C, a solar radiation of 900 W/m^2 and a wind velocity equal to 0,6 m/s. The corresponding current carrying capacities

are shown in Tables 7.6 and 7.9. These data can be considered as conservative. A wind velocity of 1,0 m/s could be used as well with a low probability of being fallen below. In [7.57], values are given for ambient temperatures of 20°C and a wind velocity of 1,0 m/s. A value of 1040 A results with the above mentioned conditions for the conductor 564-AL1/72-ST1A, whereas a value of about 1460 A is mentioned in [7.57], Table A.6. This example explains clearly the effect of ambient temperature and wind on the *current carrying capacity.* (See also [7.61]).
The described deterministic approach usually leads to conservative values for the current carrying capacity, since conditions having a low probability of occurrence are assumed as acting simultaneously. Measurements of conductor temperatures have systematically shown lower temperatures than the ones determined by the deterministic approach. Therefore, statistical approaches have been introduced for determining conductor temperatures in the steady-state condition. These approaches lead to higher current ratings for given design temperatures with low and, therefore acceptable probability of being exceeded [7.62].

7.2.4 Design with regard to short-circuit current

The *design of conductors with regard to short-circuit currents* is mainly important for earth wires due to the significantly smaller cross sections. Therefore, it is dealt with in Chapter 8. The equations described there can also be applied to phase conductors, where required [7.63].

7.2.5 Design based on economic considerations

Conductor design based on economic considerations with regard to minimum *transmission costs* is an essential aspect for conductor selection. The transmission costs, usually expressed as the amount of money needed to transport 1 kWh over a distance of 100 km [7.27, 7.64] consist of costs independent of the transmitted power or energy and costs dependent on the transmitted energy. *Amortization, depreciation* and *maintenance* are within the first category (Figure 7.18). The second category of costs is due to power and energy losses. *Power loss costs* result from the need to provide the network with sufficient power to compensate these losses; they do not depend on the line's *annual utilization period. Energy loss costs* are determined by the electric transmission operation and, therefore, depend both on the power as well as on the annual utilization period of the line (Figure 7.18).
Power-dependent transmission cost components result from the expenditures due to depreciation, interest rates, taxes and maintenance for the line and are applied in proportion to the investment for installation. Fixed specific annual costs calculated per circuit of a double circuit line amount to

$$K_{\mathrm{SC}} \approx 0{,}5 \cdot p_1 \cdot E_{\mathrm{DC}} \qquad \text{in EUR/(km} \cdot \text{year)}, \tag{7.32}$$

where E_{DC} means the investment of a double circuit line in EUR/km and an actual value of 0,15 1/year can be taken for the investment demand factor p_1. The *power losses* of a three-phase circuit result from (2.9)

$$P_{\mathrm{L}} = 3 \cdot I^2 \cdot R'_{\mathrm{T\,AC}} \cdot 10^{-3} \qquad \text{in kW/km}, \tag{7.33}$$

where I is the current in A and $R'_{\mathrm{T\,AC}}$ the AC resistance per unit length of a line, in Ω/km, at the temperature T.
The resistance depends basically on conductor material and temperature T and, therefore, indirectly, on the transmitted current (see (3.2) and (7.16)). With adequate accuracy, a resistance value can be applied which corresponds to conductor temperatures

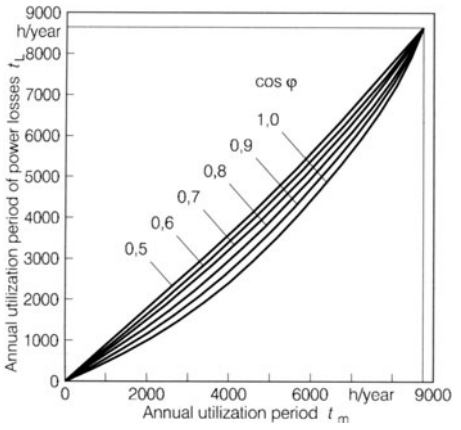

Figure 7.19: Utilization period of power losses as a function of the annual utilization period according to [7.64]

between 10 and 20°C, as conductor average annual temperatures. The power loss increases with the square of the current.
Costs for power losses depend on the investments for the production of electric power. Annual fixed expenditures due to depreciation, interests, taxes and insurance are taken into account by the demand factor p_2 for power plant investments. Investments per kW depend on the type of power generation; today, they are between 1000 and 3000 EUR/kW. The annual specific costs of power losses are given by

$$K_P \approx p_2 \cdot E_P \cdot P_L \qquad \text{in EUR/(km} \cdot \text{year)}, \tag{7.34}$$

where E_P represents the specific investments for energy generation in EUR/kW and p_2 can also be set to 0,15 having the unit 1/year.
The *costs of annual energy losses* are determined by the integral of the power loss during the operation period within one year. Transmission power flow depends on the type of transmission. Power plant outcoming lines carry a practically constant power flow over the year, while the power transmitted by lines supplying consumers may fluctuate heavily, depending on the type of consumers, and on the duration of high power peaks. The *annual utilization period* t_m is defined by the quotient of the total energy transported during one year and the *maximum transmitted power* P_{max}. Due to the quadratic dependence on the current, the operational losses are not proportional to the product between the maximum power and the annual utilization period t_m. A number of loss hours t_L has rather to be assigned to the annual utilization period (see Figure 7.19 according to [7.64]) and is expressed in h/year.
The costs of energy losses K_L can be obtained by

$$K_L \approx p_3 \cdot P_L \cdot t_L \qquad \text{in EUR/(km} \cdot \text{year)}, \tag{7.35}$$

where p_3 is the cost for the electric energy in EUR/kWh.
The costs p_3 depend on the type of energy generation and are between 0,02 and 0,12 EUR/kWh.
The *specific transmission costs* related to transport 1 kWh over a 100 km long line result from

$$K_{Tr} = \frac{100 \cdot 100 \cdot (K_{SC} + K_P + K_L)}{\sqrt{3} \cdot U \cdot I \cdot t_m \cdot \cos\varphi} \qquad \text{in Cent/(kWh} \cdot \text{100 km)}, \tag{7.36}$$

where U is the transmission voltage and $\cos\varphi$ the power factor.
As an example, the specific transmission costs are shown in Figure 7.20 for a 110 kV line using 231-AL1/30-ST1A (ACSR 230/30) and 434-AL1/56-ST1A (ACSR 435/55)

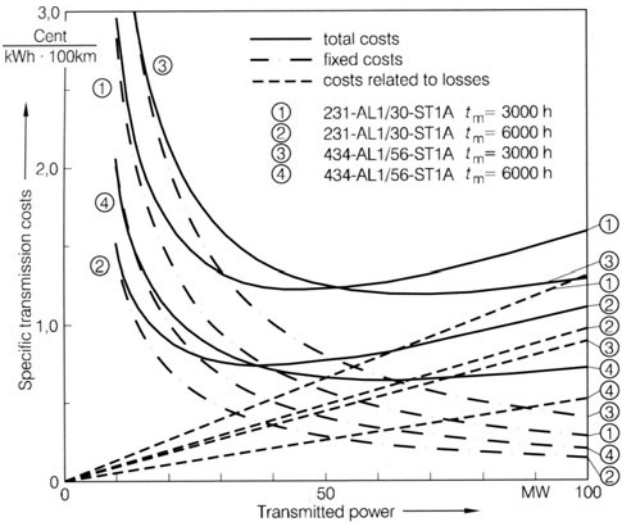

Figure 7.20: Specific transmission costs for conductors 231-AL1/30-ST1A and 434-AL1/56 ST1A depending on the transmitted power, transmission voltage 110 kV

conductors. The cost component due to the fixed costs decreases with the transmitted power and the annual utilization period, while the loss component increases also specifically. Therefore, the specific transmission costs exhibit minimum values. At 3000 h annual utilization period, the 231-AL1/30-ST1A conductor yields lower costs up to approximately 50 MW; however, at $t_m = 6000$ h, costs decrease only up to 40 MW transmitted power. These results are valid for an energy price of 0,05 EUR/kWh and a power price of 2000 EUR/kW. The difference between specific transmission costs for both conductors increases when the transmitted power rises. Therefore, the larger cross section becomes much more economic with higher power.

Economic selection of conductors with regard to transmission costs becomes continuously more important with both increasing loads and energy prices. The design engineer should take this dependence into account.

In accordance with equation (1.6), clause 1.10, the installation investment for an overhead line with two circuits depends linearly on the conductor cross-sectional area

$$E_{DC} = E_0 + E_1 \cdot U_N + E_2 \cdot A_{Al} \qquad \text{in kEUR/km}, \tag{7.37}$$

with $E_0 = 60$ kEUR/km, $E_1 = 0{,}4$ kEUR/(kV·km), $E_2 = 0{,}4\ \sqrt[4]{n_2}$ kEUR/(mm²·km). The expenditures for indemnities depend on the conductor type to a limited extent only, because of the differing swing angles and, therefore, differing widths of the right-of-way. However, its influence on the optimization is not important and can be neglected. The fixed costs for a line circuit result from (7.32), the power-dependent costs and the energy-dependent costs from (7.34) and (7.35), respectively.

When equation (7.33) is transformed into

$$P_L = \overline{R} \cdot I^2 / A_{Al} \qquad \text{in kW/km} \tag{7.38}$$

with $\overline{R} = 3 \cdot 10^{-3} \cdot 28{,}36$ kW/(W · A)·mm² · V/(A·mm) = 0,0849 mm²·kW/(A²·km) for aluminium, the *specific annual transmission costs* K_a result from

$$K_a = 0{,}5\, p_1\, (E_0 + E_1 \cdot U_N + E_2 \cdot A_{Al}) + (p_2 E_P + p_3 \cdot t_L)\, \overline{R} I^2 / A_{Al} \quad . \tag{7.39}$$

The *optimum conductor cross-sectional area* is obtained from the derivation $\partial K_a / \partial A_{AL} = 0$ or

$$0{,}5\, p_1 \cdot E_2 - (p_2 \cdot E_P + p_3 \cdot t_L)\, \overline{R} \cdot I^2 / A_{Al}^2 = 0 \tag{7.40}$$

to be

$$A_{\mathrm{Al}} = I\sqrt{\frac{(p_2 \cdot E_{\mathrm{P}} + p_3 \cdot t_{\mathrm{L}}) \cdot \overline{R}}{0{,}5\, p_1 \cdot E_2}} \qquad \text{in mm}^2. \tag{7.41}$$

In practice, the determination of the optimum conductor cross-sectional area is difficult, because the whole set of parameters is seldom known. Current I, as well as the factors E_{P}, p_3, t_{L} and the capital cost factors p_1 and p_2 can change unpredictably in the course of the long-term operation of transmission line.

Example: An apparent power of 50 MVA is to be transmitted with a utilization duration of 6 000 h by a 110 kV single-conductor circuit. The cost-related factors are $E_{\mathrm{P}} = 2\,000$ EUR/kW, $p_3 = 0{,}05$ EUR/kWh and $t_{\mathrm{L}} \sim 4\,800$ h as given in Figure 7.20
The current is equal to $I = 50 \cdot 10^6/\sqrt{3} \cdot 110 \cdot 10^3 = 262$ A. From (7.41), the optimum cross-sectional area is obtained:

$$A_{\mathrm{Al}} = 262\sqrt{\frac{(0{,}15 \cdot 2000 + 0{,}05 \cdot 4\,800)\, 0{,}0849}{0{,}5 \cdot 0{,}15 \cdot 400}} = 324 \text{ mm}^2.$$

A conductor with a 325 mm^2 aluminium cross section, for example 339-AL1/30-ST1A (ACSR 340/30) according to EN 50 182, Table F.19, would constitute the optimum for this application.

7.2.6 Line capacity as a function of the weather conditions

Power utilities commonly use fixed values of overhead line *current carrying capacity*, under consideration of the maximum permissible conductor temperature and conservative weather conditions such as an ambient temperature of 35°C and a wind speed of only 1,0 m/s. According to studies [7.65], such conservative ambient conditions are very rare; e. g. in Central Europe, temperatures of about 30°C usually happen with wind speeds between 1,0 and 2,0 m/s. Worldwide statistics show that the time probability of wind velocity to exceed 1,0 m/s is above 98 %. Also, 35°C happens to occur on a few days a year. In winter, the temperatures do not exceed 20°C. Occurrence of maximum sun intensity is also no frequent, therefore, adjustment of the allowable load conditions on a seasonal basis is possible, without increasing the probability of occurrence of unsafe situations. The permissible conductor temperature of older transmission lines should be assessed individually, since their clearances are sometimes not adequate for conductor temperatures as high as 60 or 80°C. The clearances to ground or to crossed objects limit the permissible temperatures. Furthermore, the sags could have increased due to conductor creep, thus limiting the conductor permissible temperature further, if creep compensation was not taken into account when the line was constructed. Concerning the thermal current carrying capacity, overhead lines are not always fully utilized; this would be completely uneconomic, mainly due to the high losses occurring under permanent operation at the thermal limit.
However, some network operation conditions may exist, for which the utilization of the *maximum* possible *overhead line capacity* would be desirable, without the risk of line disconnection due to its thermal capacity being exceeded. In [7.66], some usually adopted procedures are given to enable a better *utilization of the lines*. Under normal operation of the network, instantaneous measurements of the conductor temperature can help only to the extent as they enable an alarm indication for the network control of critical lines. Thereby, an optimization of the *network loading balance* is usually not possible.
Therefore, methods were developed, which permit prognostics of the line current carrying capacity as a function of the weather conditions up to 24 h ahead. Weather forecasts for 12 to 24 hours enable the optimization of power plant usage, guarantee the stability and also enable the planning of line interruption for maintenance services. Forecasts

for 1 to 12 hours can be useful for the optimization of highly loaded network sections and for avoiding the use of expensive peak-load power plants. At last, forecasts for one hour can be useful to control a disturbed condition.
An example of load forecast is described in [7.67]. The ambient temperature and the load carrying capacity are continuously forecast during periods of 1 to 24 hours; wind velocity and solar radiation are taken as conservative values. Information from the national weather services can be used. The forecast transmission capacities are used to enable

- *Planning* and optimum *utilization of resources*;
- *Postponing of investments*;
- Planning of *maintenance and repair services*;
- Probabilistic planning of transmission lines and
- Operation under *disturbed conditions.*

The *line capacity* increases by 25 to 30 % when actual weather conditions are taken into account. Risks of insufficient safety clearances are very low. Clause 7.2.1 and Papers [7.68, 7.69, 7.70, 7.71] give further information regarding the utilization of real, instantaneous line load carrying capacity for the operation of the network. Such procedures, however, can serve as a remedy only in exceptional situations: the corresponding losses would be uneconomical and harmful to the environment, if the lines had to be operated continuously on their capacity limits. Together with the systems to control load flows such as *flexible AC transmission systems (FACTS)*, the continuous forecast of carrying capacities will gain more importance. Statistical approaches have also been developed combining the relevant parameters in order to permit higher line loads [7.62, 7.66].

7.3 Design with regard to stresses caused by voltages

7.3.1 Introduction and requirements

In accordance with EN 50 341-1 [7.53], every overhead line should be capable to withstand the stresses caused by electric voltages with a reasonable reliability. *Design regarding voltage stresses*, in particular the *power frequency voltage*, plays an important role in the selection of conductors. The electric voltage produces an *electrical field* around the overhead line. The highest *field strength* occurs on the surface of the conductors and can lead to *corona phenomena*, which are accompanied by *corona noise* and *corona losses*, due to the related emission of electromagnetic waves. The electrical field on an overhead line could affect human beings and animals and, thus, may not exceed certain precaution values.
The electrical field at ground level depends to a low extent on the conductor configuration. The smaller the conductor surface gradient, the higher the field strength at ground level, when the remaining parameters such as voltage, conductor configuration and height above ground are kept the same. Usually, the electrical field at ground level is not taken into account for the selection of the conductors, but could be relevant for planning of the line installation. The electric parameters: inductance, capacitance, surge impedance and, thus, the surge impedance load depend on the selected conductors (see clauses 3.3, 3.5 and 3.7.3).

7.3.2 Design with respect to the electric parameters

The formulae for the calculation of *electric parameters* like inductive and capacitive reactance, impedance, surge impedance and surge impedance load have already been introduced in Chapter 3. The reactances gain the largest influence on the parameters which depend on the geometric conductor data such as: subconductor radius, number and spacing of the subconductors, spacing between the conductors and to ground. By

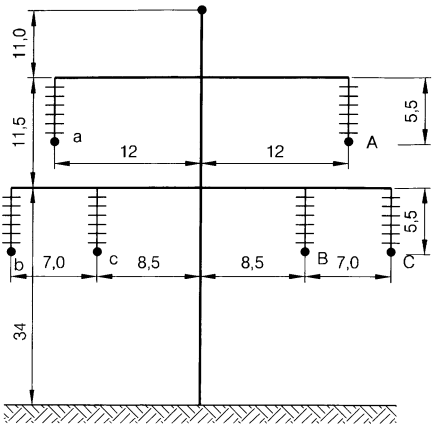

Figure 7.21: Typical dimensions of a suspension tower of a 400 kV line used as basis for studying the impact of design parameter variations on electric characteristics

Table 7.16: Electric parameters of a 400 kV double circuit line

Conductor data	Subconductor radius mm	Equivalent bundle conductor radius m	Inductive reactance Ω/km	Resistance at 50°C Ω/km	Positive sequence capacitance μF/km	Capacitive reactance MΩ·km	Surge impedance Ω	Surge impedance load [2] MW
1×1805-AL4/228-A20SA	29,5	0,030	0,384	0,0193	9,4	0,339	360	445
2×565-AL1/72-ST1A	16,5	0,081	0,314	0,0280	11,3	0,282	300	535
3×434-AL1/56-ST1A	14,4	0,132	0,280	0,0243	12,6	0,253	260	615
4×264-AL1/34-ST1A	11,2	0,178	0,260	0,0300	13,5	0,237	250	640
4×264-AL1/[1] 34-ST1A	11,2	0,355	0,217	0,0300	16,2	0,197	210	765

[1] Subconductor spacing within the bundle 1,0 m [2] at 400 kV

the example given in Figure 7.21 for a 400 kV line, the impacts of the use of single conductors, twin, triple or quadruple bundle conductors can be compared. The values obtained for D_M, D_{M1}, D_{M2} and h_M (see clause 3.3.2) are 10,0, 24,0, 22,8 and 19,9 m, respectively. The subconductor spacing in the bundle was assumed as 0,4 m. The results are summarized in Table 7.16. The *inductive* and the *capacitive reactance* as well as the *surge impedance* value decrease with higher number of subconductors. The ohmic resistance does not play a role here. The *surge impedance load* increases together with the number of subconductors and reaches the value of 640 MW for a quadruple bundle. An *increase of the surge impedance load* is of interest for the *stability of long lines* and, thus, viability was examined in order to accomplish such an increase. Larger subconductor spacing within the bundle achieves that objective, as shown in Table 7.16 for the quadruple bundle conductor with 1,0 m subconductor spacing. The surge impedance load increases to 765 MW, that is by 20 %. Practical applications exist in South America [7.43]. This configuration, however, is connected with higher conductor surface gradients and corona effects; therefore, it can not be recommended for densely populated regions.

7.3.3 Design with respect to conductor surface gradients and corona effects

Dimensions and configuration of the conductors affect the *conductor surface gradient* and the resulting *corona phenomena*. Clause 2.3.3 explains the underlying principles. The conductors should be selected such that the requirements of *radio interference* and *audible noise* emission are accomplished. A limit equal to 17 kV_{rms}/cm can be mentioned as a guideline for the conductor surface gradient.
Equation (2.12) is valid for the *mean surface gradient* of one conductor. The capacitance C_i' per unit length is, in general, different for every phase conductor of a three-phase circuit. Publication [2.8] describes methods for the computation of the capacitance; computer programming is available, too. However, for the practical design of a line it is enough to use the *circuit mean capacitance*, whose evaluation will be explained by some examples.
For the example given in clause 7.3.2, the *positive sequence capacitance* shown in Table 7.16 is determined, as well as the *mean surface gradients* obtained by equations (2.12) and (2.17), respectively. The single conductor as used over the Bosphorus in Turkey [7.28] shows the minimum conductor surface gradient. If the subconductor spacing were increased to 1,0 m, this would lead to a conductor surface gradient of more than 17 kV_{rms}/cm for a quadruple bundle conductor 264-AL1/34-ST1A, being disadvantageous with regard to corona behaviour.
Conductor voltage gradients calculated by computer and carried out for the individual phases of a quadruple bundle conductor produced the following values: 12,6 kV_{rms}/cm for phase conductor A, 15,4 kV_{rms}/cm for conductor B and 16,0 kV_{rms}/cm for conductor C. Applying equations (2.22) and (2.24) along with the data given by Figure 7.21 and the mean value of the conductor surface gradients, a noise level of about 37 dB(A) was obtained at ground level in the middle of the right-of-way; taking the different phase conductor data into account, a value of 41 dB(A) resulted. The basic principles given in Chapters 2 and 3 can be used for the rating of the *electric parameters* of the conductors.

7.3.4 Corona losses

Corona discharges are linked with loss of energy; this, in turn, is highly dependable on the weather. Under foul weather conditions the losses increase severely. *Corona losses* are important, mainly for transmission lines above 300 kV rated voltage. Publication [7.39] contains methods for their evaluation. Under fair weather conditions they amount to 2 kW/km; under rainy conditions they rise to 5 kW/km and under frosty weather up to 100 kW/km. The total of losses to be considered depends on the climate conditions in the region where the line will be constructed, that is, on the number of rainy or frosty days a year. Corona losses are usually not significant in comparison with the total energy losses. They do not play any role concerning the selection of conductors; however, they are considered when predicting line in-service losses, in view of the guaranteed power to be supplied. It should be noted that maximum corona losses do not occur simultaneously with maximum Joule losses because foul weather conditions are associated with improved cooling conditions for the conductors.

7.4 Mechanical design of conductors

7.4.1 Introduction and requirements

The *mechanical design of conductors* for overhead lines involves the selection of conductors with sufficient mechanical strength, as well as the determination of data for

Table 7.17: Limits for everyday and long-term stresses according to EN 50 341-3-4 [7.6]

Conductor type	Cross-sectional ratio	Limits for everyday stress N/mm²		Limits for long-term stress N/mm²		Rated tensile strength N/mm²	
Standards		AL1/ ST1A	AL3/ ST1A	AL1/ ST1A	AL3/ ST1A	AL1/ ST1A	AL3/ ST1A
AL1/ST1A	1,4:1	90	104	401	464	585	649
and	1,7:1	84	102	368	435	509	592
AL3/ST1A	4,3:1	57	69	240	328	354	455
according to	6,0:1	56	67	208	300	301	413
EN 50 182	7,7:1	52	63	189	284	272	392
	11,3:1	44	53	165	265	239	364
	14,5:1	40	—	152	—	223	—
	23,1:1	35	—	130	—	200	—
AL1 according to EN 50 182		30		120		160	
AL2 according to EN 50 182		44		240		295	
Copper according to EN 48 201, Part 1		85		300		400	
Bronze II according to EN 48 201, Part 2		100		500		580	
Bronze III according to EN 48 201, Part 3		130		900		1245	
A20SA according to EN 50 182		137		1112		1340	

sagging, so that no mechanical overloading occurs during construction or operation of the lines. The mechanical strength is the determining characteristic for overhead lines in case of extraordinary span lengths [7.28, 7.72] where high tensile loads are involved. The *conductor design* and dimensions should be selected so that the values of mechanical stresses are kept within permissible limits. Dimensions and tensile loads of conductors also influence the investments for a line.

According to [7.1] and [7.53], annex A, the mechanical resistance of the conductors should be chosen in relation to the mechanical resistance of the supports and foundations such that the conductors achieve the highest reliability. In [7.6], detailed information is given about the requirements of mechanical strength related to the *long-term stress* as a limiting value. Requirements are stipulated in [7.6] regarding stresses under everyday conditions, *the everyday stress (EDS).*

7.4.2 Stresses under extreme load conditions

Ice and wind loads cause *extreme conductor stresses* and led also to *conductor failures* in the past [7.73]. The conductor design, the *rated tensile strength* and sagging condition should guarantee sufficient reliability under the prospective highest load conditions. The conductor tensile forces corresponding to the ultimate loads may not surpass the *conductor rated tensile strength* for all types of conductors [7.53] divided by the *material partial factor* 1,25.

According to [7.6], the conductor tensile stress occurring under most unfavourable conditions such as

- Temperature −20°C or less without ice and wind forces,
- Temperature −5°C with the ultimate ice load,
- Temperature −5°C with simultaneous action of ice and wind loads corresponding

to the conditions assumed for the line area as well as
- Temperature +5°C and maximum wind load,

multiplied by a partial factor of 1,30, should not exceed the value of the long-term tensile stress. The *long-term stresses* are given by Table 7.17, reaching values from 70 to 75 % of the rated tensile strengths. The long-term stress is defined as that stress sustained by the conductor over a period of one year without any failure.

7.4.3 Stresses under everyday conditions

To protect conductors against fatigue failures caused by *alternating bending stresses* due to aeolian vibration and also to assure their fatigue resistance, the *everyday stress (EDS)* criterion was introduced and corresponding guideline values were established ([11.35], [7.74]). In [7.6], such guideline values are stipulated which should not be surpassed to care for *conductor reliability* under everyday conditions. When selecting the everyday stress according to these stipulations, there will be only a minor *failure probability* for composite conductors made of aluminium and steel. This applies also to homogeneous conductors made of copper, of steel, of copper-wrought alloys or of aluminium-clad steel assuming favourable environmental conditions and a proper design of suspension arrangements. In case of lines susceptible to vibration, possible damage can be effectively counteracted by providing *vibration protection fittings.*

Conductors with a small steel portion, homogeneous conductors made of aluminium or aluminium alloy and reinforced conductors made of aluminium alloy and steel are more susceptible to fatigue problems as are conductors with diameters larger than 25 mm as well as conductors in spans longer than 500 m.

If an increased *vibration susceptibility* is assumed or has been observed, the design of the suspension set and of the *damping devices* should be properly selected to guarantee an effective protection of the conductors.

More recently, the subject of *safe tensile stresses* was considered again. In [11.39], *limits for conductor tensile stress* without damping are given; in [11.40], limits for conductors with damping devices are indicated. These proposals are discussed in detail in clause 11.2.7. It is still open whether practical consequences concerning line design will arise therefrom.

The everyday stress often determines the stringing conditions, in particular for voltages of 110 kV and above. For the 231-AL1/30-ST1A (ACSR 230/30) conductor, which is often applied to 110 kV lines in Central Europe, an everyday stress of 52,0 N/mm^2 is specified in EN 50 341-3-4 [7.6]. The ultimate resistance is obtained by RTS/γ_M. With RTS is 276 N/mm^2 and $\gamma_M = 1{,}25$ according to [7.5], the maximum stress should be less than 221 N/mm^2. For 500 m span length, the tensile stress of 221 N/mm^2 would be achieved for an ice load of about 35,0 N/m. For the 565-AL1/72-ST1A (ACSR 564/72) conductor, the everyday stress is assumed to be 52,0 N/mm^2, as well. This conductor would reach its limit stress (see Figure 7.22) for a 500 m span length only when submitted to 88,0 N/m ice load. From these examples, the importance of the everyday tensile stress can be realized for conductor sagging and for reliabilities under extreme load conditions.

Example for mechanical conductor design: The sagging condition should be selected for a 500 m long span, equipped with a 231-AL1/30-ST1A (ACSR 230/30) conductor. The load is assumed according to [7.6] for wind zone 3 and ice zone 1, 2, and 3. The conductor mass is 0,877 kg/m, the diameter 21,0 m and the cross section 260,8 mm^2 (see Table 7.9).

The everyday stress is limited to 52,0 N/mm^2, the maximum stress is 276/1,25 ~ 221 N/mm^2 at the suspensions or dead ends. The partial factor on conductor stress is assumed as 1,35.

Ice load (see clause 6.6.3.3) $g_{I,1} = 5{,}0 + 0{,}1 \cdot 21 = 7{,}1$ N/m; $g_{I,2} = 14{,}2$ N/m; $g_{I,3} = 28{,}2$ N/m,

Wind load (see equation (6.73)) $w = 0{,}021 \cdot 1{,}0 \cdot (0{,}45 + 60/500)\,(1\,300 + 3 \cdot 50) = 17{,}36$ N/m,

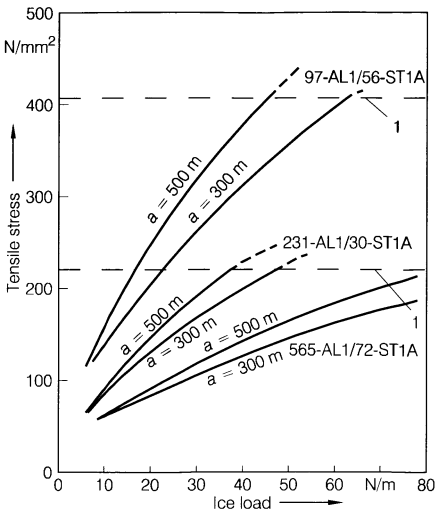

Figure 7.22: Tensile stress as a function of ice load and span length for 97-AL1/56-ST1A, 231-AL1/90-ST1A and 565-AL1/72-ST1A conductors. a span length, 1 rated tensile stress divided by partial factor 1,25

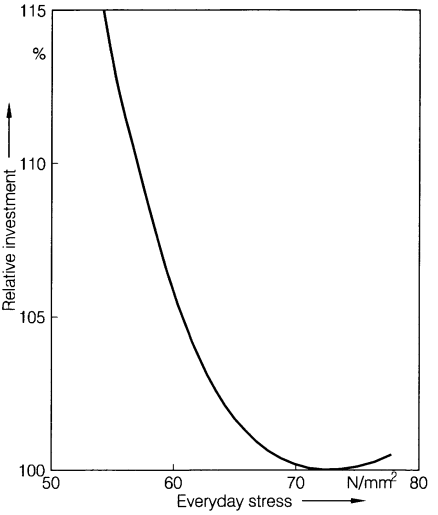

Figure 7.23: Relative investments for installation of river Elbe crossing as a function of the everyday stress [7.72]

Table 7.18: Mechanical conductor design (example), wind and ice load, 231-AL1/30-ST1A

Case	Ice	Wind	Everyday stress	Tensile stress	Stress at support	Partial factor included
	N/m	N/m	N/mm²	N/mm²	N/mm²	N/mm²
1	7,1	16,80	52*	128,6	130,5	176
2	14,2	22,07	48	159,3	162,2	219*
3	28,4	29,09	35	158,0	164,4	222*

* prevalent condition

Specific weight force of ice: 7 500 N/m^3.
Diameter with ice (see equation (6.84)) $D_{I,1} = \sqrt{d^2 + 0{,}00017\, g_I} = 0{,}0406$ m, $D_{I,2} = 0{,}0534$ m; $D_{I,3} = 0{,}0724$ m;
Wind on conductor with ice $w_{I,1} = 0{,}0406 \cdot 1{,}0 \cdot (0{,}45 + 60/500)\,(1300 + 3 \cdot 50)/2 = 16{,}78$ N/m; $w_{I,2} = 22{,}07$ N/m; $w_{I,3} = 29{,}90$ N/m.
The tensile stress is calculated using equation (14.37) for the thress cases considered; the stress at the conductor supports follows from (14.24). The results are summarized in Table 7.18. As can be seen from the table, the limit for everyday stress is prevalent in case 1, while the limit for maximum stress govern the cases 2 and 3.

7.4.4 Impact of the conductor tensile load on line investment

The sag decreases linearly with increasing tensile stress of the conductor, resulting in a reduction of the *tower heights*, of the materials needed for the suspension towers as well as of the loading of their foundations. However, the decrease of the sags causes an increase of the loads on angle, strain or dead-end towers due to higher tensile loads of the conductors, thus increasing the forces applied to the tower members and foundations. The *investment for an overhead line* essentially depends on tower dimensions and on the load to which the towers are submitted. Due to various opposite effects, it is viable

to search for the *optimum conductor tensile stress* regarding the investment for a certain line. This optimum value depends on components such as the ratio between suspension, dead-end or strain towers, as well as the span lengths and the external loads. The variation of the investment due to variations in the everyday tensile stress was examined for a 220 kV line equipped with 383-AL1/49-ST1A (ACSR 380/50) twin bundle, starting with a value of 52 N/mm^2 everyday tensile stress. An increase of the everyday tensile stress by 20 % yielded a 4 % investment decrease, if the *portion of strain towers* was 10 %; if this portion were 20 %, the investments would remain practically the same. If a higher percentage of strain towers were considered, the investments would probably increase. In Figure 7.23, the investment for the 380 kV line across the river Elbe [7.72] in Germany is shown as a function of the everyday tensile stress. An everyday tensile stress around 70 N/mm^2 proved to be an optimum.

7.4.5 Conductor creep

Due consideration of *conductor creep* is required for the conductor sagging or for the determination of the clearance between conductors. The clearance may not fall below the required values. Installation of conductors with lower initial sags than the planned final ones meets this requirements (see clauses 7.1.8.6 and 16.7.4.3). In this case, the tensile stresses of the conductors, used as a basis for the design of the towers, should not be surpassed.

7.4.6 Recommendations for selection of conductor tensile stresses

Selection of conductor tensile stresses is an important step during the design process of an overhead line. Experience gained from lines has shown [7.32, 7.75] that the everyday tensile stress of lines situated in regions which are less subject to aeolian vibrations forms a sound basis for the determination of the *conductor sagging conditions* when using aluminium-steel reinforced conductors with cross-sectional ratios ranging from 4,3:1 to 11,3:1. For aluminium and aluminium alloy mono-metallic conductors the experience is less positive. Therefore, taking into account the everyday tensile stresses or the safe tensile stress as well as the limits imposed by extreme loads due to ice or wind, it is also advisable to select the conductor tensile stress with respect to investments as low as possible. Then, the line should be investigated with respect to the aeolian vibrations it may suffer, using the information and methods explained in Chapter 11. As a result of these studies, the suspension fittings can be selected and, if necessary, damping devices could be used.

7.5 References

7.1 IEC 61089: Round wire concentric-lay electrical stranded conductors. Geneva, IEC, 1991

7.2 EN 50182: Conductors for overhead lines – Round wire concentric-lay stranded conductors. Brussels, CENELEC, 2001

7.3 ASTM B231M: Concentric-lay-stranded 1350 aluminium conductors. New York, ASTM, 1995

7.4 ASTM B399: Concentric-lay-stranded 6201-T81 aluminium alloy conductors. New York, ASTM, 1995

7.5 ASTM B524: Concentric-lay-stranded aluminium conductors, aluminium alloy reinforced. New York, ASTM, 1999

7.6 EN 50341-3-4: Overhead electrical lines exceeding AC 45 kV. Part 3-4: National Normative Aspects for Germany. Brussels, CENELEC, 2001

7.7 IEC 60 050-466: International electrotechnical vocabulary – Chapter 466: Overhead lines. Geneva, IEC, 1995

7.8 DIN VDE 0210: Planning and design of overhead power lines with rated voltages above 1 kV. Berlin, VDE-Verlag, 1985

7.9 EN 50 183: Conductors for overhead lines – Aluminium-magnesium-silicon alloy wires. Brussels, CENELEC, 2000

7.10 EN 50 189: Conductors for overhead lines – Zinc-coated steel wires. Brussels, CENELEC, 2000

7.11 EN 61 232: Conductors for overhead lines – Aluminium-clad steel wires for electrical purposes. Brussels, CENELEC, 1995

7.12 International Annealed Copper Standards ((open))

7.13 Nefzger, J.: Vorsicht Hochspannung (Attention: High voltage!). Schwabach, Richard Bergner, 1973

7.14 Thrash, F. R.: Transmission conductors – A review of the design and selection criteria. Carrolton, Southwire, Technical support resources, 1999

7.15 Gaudry, M. at al.: Increasing the ampacity of overhead lines using homogeneous compact conductors. Cigré Report 22-201, 1998

7.16 EN 60 889: Hard-drawn aluminium wires for overhead line conductors. Brussels, CENELEC, 1997

7.17 Aluminium electrical conductor handbook. Waldorf, The Aluminium Association, 3rd edition 1989

7.18 EN 1715-2: Aluminium and aluminium alloys – Drawing stock – Part 2: Specific requirements for electrical applications. Brussels, CEN, 1998

7.19 Behrens, W.; Nefzger, J.; Philipps, W.: Aluminiumfreileitung (Overhead power lines using aluminium conductors). Düsseldorf. Aluminium-Verlag, 8th edition 1965

7.20 EN 10 244-2: Steel wire and wire products – Non-ferric metallic coatings on steel wires, Part 2: Zinc or zinc alloy coatings. Brussels, CEN 1995

7.21 Fink, D. G.; Beaty, H. W: Standard handbook for electrical engineers. New York, Mc Graw-Hill, 12th edition 1987

7.22 Oogi, I.; et al.: Conductors for overhead transmission lines in Japan. Sendai, Cigré SC 22 Colloquium, Sendai Meeting, 1997

7.23 EN 10 002-1: Metallic materials – Tensile testing – Part 1: Method of testing at ambient temperature. Brussels, CEN, 2001

7.24 ASTM E8 MM: Standard test methods for tension testing of metallic materials. New York, ASTM, 2000

7.25 ISO 7802: Metallic materials – Wire – Wrapping test. Geneva, ISO, 1983

7.26 IEC 60 468: Method of measurement of resistivity of metallic materials. Geneva, IEC, 1974

7.27 Köhler, W.: Die Wirtschaftlichkeit von Alumoweld beim Einsatz in Freileitungen (Economics of aluminium-clad steel used for overhead lines). Elektrizitätswirtschaft 74 (1975), pp. 691 to 695

7.28 Fenz, J. et al.: 380 kV overhead transmission line over the Bosphorus. Siemens Power Engineering 6 (1984), pp. 208 to 212. Siemens A19100-E433-A871-X-7600

7.29 ASTM B416: Concentric-lay-stranded aluminium-clad steel conductors. New York, ASTM, 1998

7.30 EN 50326: Conductors for overhead lines Characteristics of greases. Brussels, CENELEC, 2001

7.31 Cigré SC22 WG22-04: A practical method of conductor creep determination. Electra 24 (1974), pp. 105 to 137

7.32 Kießling, F.; Nefzger, P.: Zur Wahl der Zugspannung für die Leiter einer Hochspannungsfreileitung (Selection of tensile stress for overhead power line conductors). Elektrizitätswirtschaft 80 (1981), pp. 648 to 691

7.33 ASTM B232: Aluminium conductors, concentric-lay-stranded conductors, coated steel reinforced (ACSR). New York, ASTM, 1995

7.34 Papailiou, K. O.: Die Seilbiegung mit einer durch die innere Reibung, die Zugkraft und die Seilkrümmung veränderlichen Biegesteifigkeit (Conductor bending considering the variable bending stiffness depending on the internal friction, the tensile force and the conductor curvature). Doctorate thesis, ETH Zürich No. 11057, 1995

7.35 Winkler, D.: Oberflächenveränderungen beim Transport von Aluminiumseilen in Containern (Changing of surface quality at transport of aluminium conductors in containers). Elektrizitätswirtschaft 100 (2001)5, pp. 52 to 55

7.36 EN 61395: Overhead electrical conductors – Creep test procedure for stranded conductors (IEC 61395). Brussels, CENELEC, 1998

7.37 Markt, G.; Mengele, B.: Elektrische Leitung mit Bündelleitern (Overhead electrical lines with bundle conductors). Austrian patent 121 704 (1930)

7.38 Timascheff, A.: Ursprung und Entwicklung der Bündelleiter (Origin and development of bundle conductors). Elektrotechnik und Maschinenbau 93 (1976), pp. 213 to 218

7.39 EPRI: Transmission line reference book: Transmission lines with 345 kV and above. Palo Alto, Electric Power Research Institute, 1978

7.40 TEPCO: 1000 kV transmission lines. Tokyo, Tokyo Electric Power Company 1996

7.41 Yamagishi, H.; Murooka, M.; Urushibara, H.: Mechanical test results of full scale 1000 kV transmission towers. Cigré Report 22-301, 1990

7.42 Rowbottom, M. D.; Aldham-Huges, R. R.: Subspan oscillations: A review of the existing knowledge. Cigré Report 22-09, 1972

7.43 Regis, O. et al.: Expanded bundle technique: The application of HSIL concept to increase the capacity of overhead lines. Cigré Report 22-207, 1998

7.44 IEC 62219: Formed wire concentric-lay overhead electrical stranded conductors. Geneva, IEC, 2000

7.45 Ervik, M. et al.: Erection of and vibration protection on long fjord crossings in Norway. Cigré Report 23-03, 1968

7.46 Riez, M.: Crossing of the Schelde by an overhead 380 kV line. Brussels, Tractionel, 1975

7.47 McCulloch, A. R.; Pue-Gilchrist, A. C.; Kirkpatrick, L. A.: Ten years of progress with self-damping conductors. IEEE Trans. on Power Apparatus and Systems Vol. PAS-99, No. 3 (1980), pp. 998 ff

7.48 Maass, H.: Beobachtungen über das Auftreten und Versuche zur Bekämpfung der mechanischen Freileitungsschwingungen (Observation on occurrence and tests on control of mechanical vibrations on overhead line conductors). Elektrotechnik und Maschinenbau 52 (1934)13

7.49 Douglass, D. A.; Roche, J. B.: T2 wind motion resistant conductor. IEEE Transaction on Power Apparatus and Systems, Vol. 103, No. 10 (1985), pp. 2879

7.50 Hesterlee, J. M. et al.: Bare overhead transmission and distribution conductors. Carrolton, Southwire, www.southwire.com, 2000

7.51 Tsujimoto, K. et al.: Development of an ACSR conductor with extremely suppressed aeolian noise and audible noise level. Hitachi Cable Review (1988), pp. 33 ff

7.52 Lugschitz, H.; Egger, H.: Experience with a 380 kV camouflage line. Cigré Report 22/33/36-04, 1998

7.53 EN 50 341-1: Overhead electrical lines exceeding AC 45 kV. Part 1: General requirements – Common specifications. Brussels, CENELEC, 2001

7.54 Nolasco, J. F.: Design and construction features of the first 500 kV transmission line with guyed towers in Brazil. Sienna, Cigré SC 22 Symposium, 1979

7.55 Cigré SC22 WG22-12: The thermal behaviour of overhead conductors. Section 1 and 2: Mathematical model for evaluation of conductor temperature in the steady state and the application thereof. Electra 144 (1992), pp. 107 to 125

7.56 Cigré SC22 WG22-12: The thermal behaviour of overhead conductors. Section 3: Mathematical model for evaluation of conductor temperature in the unsteady state. Electra 174 (1997), 59 to 69

7.57 IEC 61 597: Overhead line electrical conductors – Calculation methods for stranded bare conductors. Geneva, IEC, 1995

7.58 Webs, A.: Dauerstrombelastbarkeit von nach DIN 48 201 gefertigten Freileitungsseilen aus Kupfer, Aluminium und Aldrey (Current carrying capacity of overhead line conductors made of copper, aluminium and aluminium alloy according to DIN 48 201). Elektrizitätswirtschaft 61 (1962), pp. 861 to 872

7.59 Palic, M.; Plehn, M.: Temperaturmessungen an Freileitungsseilen bei wechselnder Strombelastung (Temperature measurements at overhead line conductors during varying current load). Elektrizitätswirtschaft 89 (1990), pp. 493 to 497

7.60 Aluminium electrical conductor handbook. Washington. The Aluminium Association, 1982

7.61 Current temperature characteristics of aluminium conductors. Pittsburgh, Alcoa Conductor Products Company, 1965

7.62 Cigré SC22 WG22-12: Probabilistic determination of conductor current ratings. Electra 164 (1996), pp. 103 to 117

7.63 Overload and fault current limitations of bare aluminium conductors. Pittsburgh, Alcoa Conductor Products Company, 1965

7.64 Schneider; Schnaus: Elektrische Energiewirtschaft (Electric power economics). Berlin, Springer-Verlag, 1936

7.65 Kießling, F. et al.: Contact lines for electrical railways. Munich and Erlangen, Publicis Cooperate Publishing, 2001

7.66 Cigré SC 22 WG22-12: Real-time monitoring. Electra 197 (2001), pp. 35 to 37

7.67 Cebolka, W. J. et al.: PG and E's ATLAS (Ambient temperature line ampacity system). Transmission line dynamic thermal rating system. Cigré Report 22-102, 1992

7.68 Seppa, T. O. et al.: Application of real-time thermal ratings for optimizing transmission line investment and operating decisions. Cigré Report 22-301, 2000

7.69 Douglass, D. A. et al.: IEEE's approach for increasing transmission line ratings in North America. Cigré Report 22-302, 2000

7.70 CIGRE SC22 WG22-12: Description of state of the art of methods to determine thermal rating of lines in real-time and their application in optimizing power flow. Cigré Report 22-304, 2000

7.71 Vognild, L. H.; Fikke, S. M.: Utilizing meteorological data for peak load reference temperature and ambient temperature for conductor ratings in system planning and operation. Cigré Report 22-103, 1992

7.72 Ann, W.; Kießling, F.; Schnakenberg, D.: Die Leiter der 380-kV-Elbekreuzung der Nordwestdeutsche Kraftwerke AG und ihre Verlegung (The conductors of 380 kV river Elbe crossing of Nordwestdeutsche Kraftwerke AG and their stringing). Elektrizitätswirtschaft 78 (1979), pp. 245 to 256

7.73 Kießling, Ruhnau, J.: Ice loads on overhead power lines in Germany and their impact on reliability and design. Budapest, IWAIS Conference 1993

7.74 Möcks, L.: Everyday stress und die mechanische Sicherheit der Freileitungsseile (Everyday stress and mechanical reliability of overhead line conductors). Elektrizitätswirtschaft 64 (1965), pp. 67 to 75

7.75 Cigré SC22 WG22-04: Recommendations for the evaluation of the lifetime of overhead line conductors. Electra 63 (1979), pp. 103 to 145

8 Earth wire selection

8.0 Symbols

Symbol	Signification
A	Conductor cross section
A_1	Cross section of well-conducting material
A_2	Cross section contributing to heat storage
c	Specific heat
c_{Al}	Specific heat of aluminium
c_{tot}	Specific heat of total conductor
f	Frequency
H	Conductor tensile force
I	Current
I_{th}	Thermal equivalent current
I''_{k}	Initial alternating short-circuit current
m	Direct current factor
m_{C}	Mass per unit length
$m_{\mathrm{C}} \cdot g$	Weight per unit length
n	Alternating current factor
N_{j}	Joule losses
R	Electrical resistance
t	Time
t_{K}	Short-circuit duration
T	Temperature
T_1	Initial temperature
T_2	Final temperature
α	Temperature coefficient of resistance
α_{Al}	Temperature coefficient of resistance of aluminium
α_{tot}	Temperature coefficient of resistance of total conductor
γ	Specific mass
γ_{Al}	Specific mass of aluminium
γ_{tot}	Specific mass of total conductor
κ_{S}	Impulse factor
ϱ	Resistivity
ϱ_{Al}	Resistivity of aluminium
ϱ_{tot}	Resistivity of total conductor

8.1 Types of earth wires

Most overhead transmission lines having voltages of 110 kV and above are provided with *earth wires* (or ground wires). In this context, the term earth wire is used for all types of conductors on earth potential according to EN 50 341-1, although all earth wire designs consist of a multitude of individual strands. The main purpose of the earth wires is the protection of the conductors against the *direct incidence of lightning strokes*, that can cause line outages (see Chapter 4). However, lightning strokes, even when reaching the earth wires, may cause a voltage rise at the towers high enough to cause a *back-flashover* from the tower to the conductor along the insulator set. Thus, in order to minimize the occurrence of flashovers along the insulator sets, beside using earth wires, it is necessary to reduce the voltage increase on the towers; this can be obtained through an appropriate earthing of the towers either by counterpoise wires, by deep rods or other means (see Chapter 5).
The earth wires provide also a return path for phase-to-ground short-circuit currents.

They should, therefore, be appropriately specified so as to conduct the predicted short-circuit currents of the system. They reduce also the electrical interference of the line on parallel lines. Moreover, the use of earth wires contributes to alleviate the earthing mat of substations as the portion of current that circulates in the earth wire, at the first line spans near the substation, will reduce the current flowing through the earthing mat. The size of and investments for this mat can be correspondingly reduced.

In the past, *earth wires having low conductivity*, such as steel strands or AL1/STyz (ACSR) conductors with low aluminium content, were mostly employed and are still used in several countries. However today, most utilities, especially in Europe, have changed to the use of larger AL1/STyz (ACSR) conductors or other high-conductive cables, because of the high level of short-circuit currents presented by electric systems. Another practice commonly employed by several utilities consists in designing highly conductive earth wires near the terminal substations, at the first 5 to 10 km, changing to steel strands in the remaining parts of the line, when the short-circuit currents drop to lower values, compatible with the rating of steel conductors.

More recently, the use of earth wires has been extended to other purposes, such as for transmitting small amounts of energy at lower voltages [8.1] or for carrying telecommunication signals on integrated glass fibres. Such earth wires are named *optical ground wires* (OPGW). Thus, the earth wires are losing their condition of dead or inactive conductors to become more useful and efficient live components.

8.2 Electric and thermal design

8.2.1 Requirements

In steady-state conditions the earth wires or optical ground wires, usually earthed at every tower, are only submitted to small circulating currents due to *electromagnetic induction* or *electrostatic influence*, causing negligible power and energy losses.

Some utilities adopt the practice of insulating the earth wires through a low-voltage insulator and only earthing them at some points, in order to reduce the losses by interference. Anyway, the normal operating conditions do not govern the *earth wire selection* under the point of view of electric currents as they are only low and any reasonable cross section will have a conductivity high enough to stand such currents.

The selection of the earth wire for an overhead line is, therefore, determined by the phase-to-earth *short-circuit currents* that will circulate in such conductors in transient conditions.

Under occurrence of a phase to earth short circuit, a significant portion of the current will flow through the earth wire, especially at the first spans close to the terminal substations where the short-circuit currents are of higher intensity.

Circulating through the earth wire, the short-circuit current will heat it, until the protection relays trip the line out. The heating of the earth wire during the short circuit follows an *adiabatic process* as, due to its short duration, there will be no *heat exchange* with the environment. Earth wire cross sections are selected such that no undesirable temperature increase is reached. The maximum *permissible temperatures* depend basically on the *earth wire material* and properties.

8.2.2 Earth wire design under short-circuit conditions

The design of earth wires under short-circuit conditions can be carried out according to [8.2] and EN 60 865-1 [8.3]. The heat produced by the short-circuit current through the *Joule law* will be fully employed in increasing conductor temperature until a balance

is reached without heat dissipation by convection or radiation. From (7.13), it results:

$$A_2 \cdot c \cdot \gamma \cdot \mathrm{d}T/\mathrm{d}t = N_j \quad . \tag{8.1}$$

Through use of (7.13) and (7.16), it is obtained:

$$\mathrm{d}T/\mathrm{d}t = I^2 \cdot [R(1 + \alpha(T - 20)]/(A_2 \cdot \gamma \cdot c) \quad , \tag{8.2}$$

where I represents the current, R the earth wire resistance, A_2 the earth wire cross section contributing to the heat storage, γ the conductor unit mass and c the specific heat of the conductor. Considering for a unit length of conductor $R' = \varrho'/A_1$, where ϱ is the resistivity of the well-conducting conductor part and A_1 its cross section, it results from (8.2):

$$\int_{T_1}^{T_2} \frac{\mathrm{d}T}{1 + \alpha(T - 20)} = \int_0^{t_\mathrm{K}} \frac{I^2 \varrho}{A_1 A_2 \cdot \gamma \cdot c} \, \mathrm{d}t \tag{8.3}$$

and after integration:

$$\frac{1}{\alpha} \ln \frac{1 + \alpha(T_2 - 20)}{1 + \alpha(T_1 - 20)} = \frac{I^2 \varrho \cdot t_\mathrm{K}}{A_1 A_2 \cdot \gamma \cdot c} \quad , \tag{8.4}$$

where t_K is the *short-circuit duration* and T_1 and T_2 are the *initial* and *final temperatures*. The *final earth wire temperature* for a *thermally equivalent short-circuit current* is then obtained from (8.4):

$$T_2 = 20 + \left\{ [1 + \alpha(T_1 - 20)] \exp \frac{I_\mathrm{th}^2 \cdot \varrho \cdot \alpha \cdot t_\mathrm{K}}{A_1 A_2 \cdot \gamma \cdot c} - 1 \right\} / \alpha \quad . \tag{8.5}$$

Through an inversion of equation (8.5), the short-circuit current equivalent to a final temperature T_2 is determined by:

$$I_\mathrm{th} = \sqrt{\frac{\gamma \cdot c}{\varrho \cdot \alpha} \ln \frac{1 + \alpha(T_2 - 20)}{1 + \alpha(T_1 - 20)}} \cdot \sqrt{\frac{A_1 \cdot A_2}{t_\mathrm{K}}} \quad . \tag{8.6}$$

When dealing with ACSR conductors, there are several assumptions regarding the parameters of equation (8.6), according to [8.2], namely:

Assumption A
The earth wire is considered as a homogeneous aluminium conductor and only the conducting component is taken into account neglecting the steel portion. The following data are applicable then:

$$A_1 = A_2 = A_\mathrm{Al};\ \alpha_\mathrm{Al};\ \varrho_\mathrm{Al};\ \gamma_\mathrm{Al} \text{ and } c_\mathrm{Al}.$$

In case of *steel earth wires*, the index Al for aluminium can be replaced by the index Fe for steel.

Assumption B
By this assumption, the mass and the conductivity of the steel portion is also considered. It is then applicable:

$$A_1 = A_2 = A_\mathrm{Al} + A_\mathrm{Fe};\ \alpha_\mathrm{tot};\ \varrho_\mathrm{tot};\ \gamma_\mathrm{tot} \text{ and } c_\mathrm{tot}.$$

Table 8.1: Permissible short-circuit current of conductor 264-AL1/34-ST1A, duration 1 s

Input data and results		Assumption A	B	C
Cross section A_1	mm^2	263,7	297,8	263,7
Cross section A_2	mm^2	263,7	297,8	297,8
Specific heat c	Ws/(kg·K)	897	772	772
Specific mass γ	kg/(m· mm^2)	0,002703	0,00328	0,00328
Temperature coefficient of resistance α	1/K	0,00403	0,00403	0,00403
Resistivity ϱ	$\Omega mm^2/m$	0,0283	0,0326	0,0283
Initial temperature T_1	°C	40	40	40
Final temperature T_2	°C	160	160	160
Nominal frequency f	Hz	50	50	50
Factor κ_S	—	1,8	1,8	1,8
Factor m	—	0,0448	0,0448	0,0448
I_{th}	kA	23,4	25,2	25,4
I''_k	kA	22,9	24,6	24,8

Assumption C

The *conductivity of the steel* is not considered, however, its mass is taken into account. It is then applicable:

$$A_1 = A_{Al};\ A_2 = A_{Al} + A_{Fe};\ \alpha_{Al};\ \varrho_{Al};\ \gamma_{tot} \text{ and } c_{tot}.$$

According to [8.3], the following relation exists between the thermally equivalent short-circuit current I_{th} and the *initial alternating short-circuit current* I''_k:

$$I_{th} = I''_k \cdot \sqrt{m+n} \quad . \tag{8.7}$$

The factor m takes into account the direct current component while n considers the alternating current component in the heating process. IEC 60 865-1 provides diagrams for determining m and n. In usual cases, n can be set to 1. The factor m is calculated from:

$$m = \frac{\exp[4 \cdot f \cdot t_K \cdot \ln(\kappa_S - 1)] - 1}{2 \cdot f \cdot t_K \cdot \ln(\kappa_S - 1)} \quad . \tag{8.8}$$

In (8.8), the meaning of parameters is:

κ_S factor which takes into consideration the initial short-circuit current. Usually, κ_S is equal to 1,8 for overhead line systems;

t_K short-circuit duration;

f nominal frequency of alternating current component.

As shown in the following example, the DC component has usually only a slight influence and, in view of the uncertainties in the other parameters, can be neglected, therefore. Then, it results: $I_{th} = I''_k$.

Example: Determine the permissible short-circuit current of the conductor 264-AL1/34-ST1A for a duration of 1 s. Assumptions A, B and C should be considered. Table 8.1 contains the input data. For assumption B it is obtained

$$I_{th} = \sqrt{\frac{0{,}00328 \cdot 772}{0{,}0326 \cdot 0{,}00403} \ln\left(\frac{1 + 0{,}00403(160-20)}{1 + 0{,}00403(40-20)}\right)} \cdot \sqrt{\frac{297{,}8 \cdot 297{,}8}{1{,}0}} = 25{,}2 \text{ kA}\,.$$

With

$$m = \frac{\exp[(4 \cdot 50 \cdot 1\ \ln(1{,}8-1))] - 1}{2 \cdot 50 \cdot 1 \cdot \ln(1{,}8-1)} = 0{,}0448$$

the initial short-circuit current will be

$$I_k'' = \frac{25{,}2}{\sqrt{0{,}0448 + 1}} = 24{,}7 \approx 25 \text{ kA}.$$

The results are shown in Table 8.1. The permissible short-circuit current is approximately 25 kA. The example demonstrates that the effect of the DC component is low and can be neglected in most cases.

8.2.3 Temperature limits of earth wires in case of short circuits

The *highest permissible temperature* of a conductor under short-circuit conditions is established so that it retains all its conducting properties after the clearing of the maximum expected short circuit load. In clause 7.2.1, the recommended maximum temperatures are discussed for conductors and earth wires during a short circuit according to [8.3] and [8.4]. They are presented in Table 7.13. When establishing the maximum temperatures for specific cases, it should be prevented that clearances to phase conductors decrease below acceptable limits. In case of OPGW, the same temperature limits, as used for other earth wires having the same structure, are accepted by the relevant standards. Suppliers of OPGW usually specify short circuit performance limits indicated in $I^2 \cdot t$, where I is the short-circuit current in kA and t its duration in s. Maximum permissible temperatures for OPGW are usually established by manufacturers in the range of 180° to 220 °C.

8.2.4 Fault clearing and reclosing operations

In high voltage systems, relay *protection systems* of different types take care of fast recognizing short circuits so that the fault currents are interrupted through opening the relevant circuit breakers.

Normally, a switching period of 0,1 s is established for the first protection zone, including relay and circuit breaker time. If a relay or circuit breaker fails, a time of 0,4 to 0,5 s is usually taken into account for the back-up or remote protection to switch off the relevant circuit breakers.

Transmission systems above 110 kV are generally provided with *automatic reclosing* equipment, which is designed to put the line in operation again instantaneously after a fault had occurred, in case of lightning outages, too.

When automatic *reclosing scheme* of lines is used, the first reclosing operation usually is carried out after the fault clearing and is, therefore, successful in most cases. The line returns to service and the fault current time remains below 0,1 s. However, if the fault is not transient and remains, the protection scheme switches the line off again. The total fault current time reaches then between 0,2 and 0,3 s. The second and third reclosing operations, when used, are manual and usually start at around 60 and 300 s after the line failed, respectively.

These time intervals are not long enough for providing some cooling effect for the conductor temperature. Therefore, cooling cannot be considered in conductor heating calculations. The process is in itself very complex and utilities prefer to use simplified approaches.

Instead of separately considering different heating and cooling periods during reclosing operation, it can be recommended in earth wire rating, for reasons of simplification, to determine an equivalent time for the duration of short circuits as a function of the relaying periods adopted for the different voltage levels.

For voltages up to 300 kV (Range I according to [8.5]) an equivalent period of 0,5 to 1,0 s and for voltages above 300 kV (Range II according to [8.5]) 0,2 to 0,6 s are recommended. Such periods consider operation intervals between fault clearing and reclosing, switching time and a potentially stuck circuit breaker.

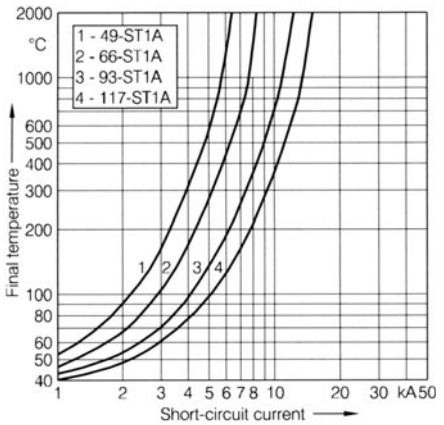

Figure 8.1: Final temperature for steel conductors 49-, 66-, 93-and 117-ST1A; initial temperature 40°C, short-circuit duration 0,5 s

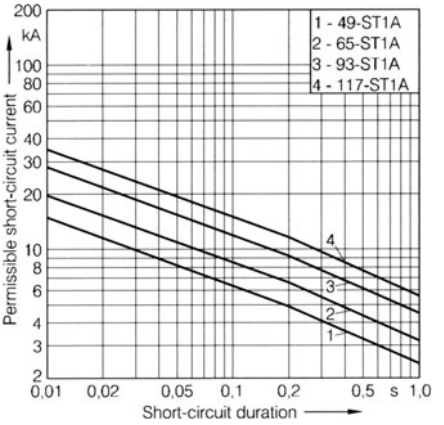

Figure 8.2: Permissible short-circuit current as a function of short-circuit duration for steel conductors 49-, 65-, 70- and 117-ST1A according to [8.6]; initial temperature 40°C, final temperature 200°C

Table 8.2: Technical data and admissible short-circuit currents (in kA) of some earth wires ST1A, and A20SA (final temperature 200°C) and AL1/ST1A (final temperature 160°C)

Shield wire type	Cross-sectional area A_2 (mm^2)	Specific heat c (Ws/kgK)	Resistivity ρ ($\Omega mm^2/m$)	Specific mass γ ($kg/m\,mm^2$)	Short-circuit duration 0,2 s	0,5 s	1,0 s
49-ST1A	49,5	481	0,192	0,00778	4,9	3,3	2,4
66-ST1A	65,8	481	0,192	0,00778	6,6	4,4	3,2
93-ST1A	93,3	481	0,192	0,00778	9,2	6,2	4,5
117-ST1A	117,0	481	0,192	0,00778	11,6	7,8	5,6
49-A20SA	49,5	518	0,0848	0,0066	7,0	4,7	3,4
66-A20SA	65,8	518	0,0848	0,0066	9,1	6,1	4,4
93-A20SA	93,3	518	0,0848	0,0066	13,0	8,7	6,3
117-A20SA	117,0	518	0,0848	0,0066	16,4	11,0	7,9
44-AL1/32-ST1A	75,7	605	0,0450	0,00488	11,2	7,5	5,5
97-AL1/56-ST1A	152,8	623	0,0457	0,00463	23,3	15,6	11,3
122-AL1/71-ST1A	193,8	623	0,0457	0,00463	29,5	19,8	14,3
264-AL1/34-ST1A	297,8	772	0,0326	0,00328	51,2	34,3	27,9

8.2.5 Examples of earth wire current carrying capacity in case of short circuits

The *short-circuit current carrying capacity* of earth wires is given in Table 8.2 using assumption B described in clause 8.2.2. This table supplies the main technical data and permissible short-circuit currents for duration of 0,2, 0,5 and 1,0 s. The *temperature coefficient of resistance* was taken as $\alpha = 0{,}0045$ for steel strands ST1A, 0,0036 for conductors A20SA and 0,00403 for AL1/ST1A (ACSR) conductors. The impulse factor κ_S was taken as 1,8. In Figure 8.1, the final temperature is shown as a function of the short-circuit current for conductors 49-ST1A, 66-ST1A, 93-ST1A and 117-ST1A, with an effective duration of 0,5 s. In Figure 8.2, the short-circuit current is shown as a function of short-circuit duration for the same conductors, considering a final temperature of 200°C. The corresponding values for 300°C and 400°C can be obtained by multiplying the values of Table 8.2 by the factors 1,20 and 1,33, respectively. The

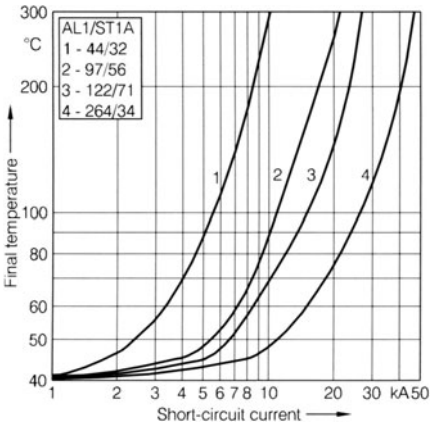

Figure 8.3: Final temperature for conductors AL1/ST1A - 44/32, 97/56, 122/71 and 264/34 according to EN 50 182 [8.7], Table F19, initial temperature 40°C, short-circuit duration 0,5 s

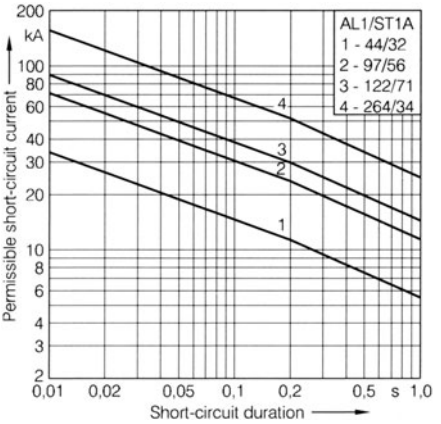

Figure 8.4: Short-circuit current as a function of short-circuit duration for conductors AL1/ST1A - 44/32, 97/56, 122/71 and 264/34 according to EN 50 182, Table F19, initial temperature 40°C, final temperature 160°C

Table 8.3: Technical data of some OPGW (see Figure 8.7)

		OPGW	
	97-AL1/ 48-A20SA	167-AL3/ 43-A20SA	68-A20SA
Rated tensile strength (kN)	82	103	81
Modulus of elasticity (kN/mm^2)	96	79	162
Expansion coefficient ($10^{-6}/K$)	17,4	18,8	13,0
Conductor diameter (mm)	16,0	19,2	12,1
Tube diameter (mm)	3,2	3,0	5,5
Wire diameter (mm)	3,2	2,5/3,0	3,3
Everyday stress (N/mm)	85	78,0	137
Long-term stress (N/mm)	400	340	1110
OPGW with stainless steel tube			
Number of fibres	16	36	36
Mass (kg/km)	615	788	505
Short-circuit capacity $I^2 \cdot t\left([\mathrm{kA}]^2 \cdot s\right)$	112	425	38
DC resistance (Ω/km)	0,265	0,182	0,88

same relations are valid for A20SA conductors.
In Figure 8.3, the final temperatures are presented for AL1/ST1A conductors 44/32, 97/56, 122/71 and 264/34 and a short-circuit duration of 0,5 s; Figure 8.4 contains the permissible short-circuit current as a function of short-circuit duration for the referred conductors, when the final conductor temperature reaches 160°C. The corresponding values for 200°C and 300°C can be obtained through multiplying the values extracted from Figure 8.4 by 1,12 and 1,35, respectively.
For conductors with optical fibres (OPGW), the manufacturers supply the highest temperature and the short-circuit capacity with the unit $(\mathrm{kA})^2 \cdot t$ (see Table 8.3).

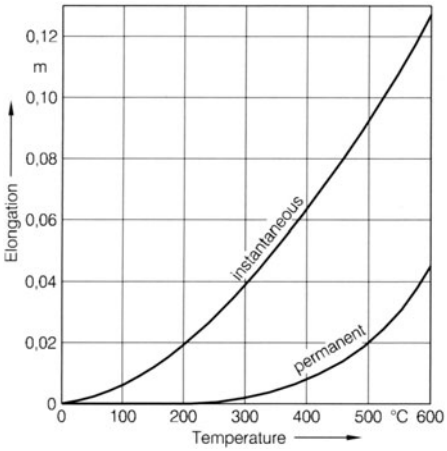

Figure 8.5: Instantaneous and permanent elongation of STyz or ALx/STyx conductors, span length 400 m, everyday stress 10 %

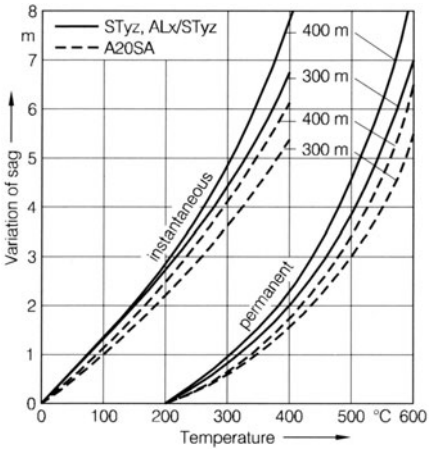

Figure 8.6: Variation of sag of STyz; ALx/STyz and A20SA conductors, depending on the conductor temperature after occurrence of a short-circuit

8.3 Mechanical design

8.3.1 Loss of mechanical strength during heating process

The excessive heating of the earth wire during a short circuit can cause a permanent elongation, loss of strength or rupture.

A permanent elongation of the earth wire will cause a reduction of the separation between the earth wires and the phase conductors, threatening the security of the line. Conductor failing on the other hand, either immediate or resulting from earth wire loss of strength, can cause a permanent outage of the line as well as damage to towers and other line components.

Concerning galvanized steel earth wires, the short-circuit currents can cause damage to the galvanization reducing, therefore, life time of the earth wire. The consequences of such phenomena depend on specific conditions. The nominal strength of stranded steel conductors decreases above 200°C and, therefore, such conductors are not recommended to be designed for operation above 200°C.

However, considering the low probability of maximum fault currents and the only minor deterioration to the steel conductors at 200°C, the limit of 200°C is considered by some utilities as too conservative resulting, therefore, in over-rated earth wire sizes. Such companies assume a maximum acceptable temperature of 300°C, including cumulative heating of the conductor, when the line is reclosed under short-circuit conditions. It can be observed that, after 300°C, the steel conductors may be already subject to slight variations in the zinc coatings, resulting in corrosion. So it is not recommended to accept higher temperatures than 300°C for steel conductors. It should furthermore be emphasised that the zinc coating of the steel conductors starts to melt at temperatures above 420°C.

However, the data in Table 7.13 of [8.3] are more conservative and limit the steel conductor temperature to a maximum of 200°C.

For conductors ALx/STyz (ACSR conductors), a maximum temperature of 200°C is specified in [8.4]. However, according to [8.3], only 160°C are acceptable.

Some experiments were carried out to determine the influence of temperatures above 200°C on loss of conductor strength and on the resultant instantaneous or permanent

rise of sags assumed by the conductor after the heating process.
In Figure 8.5, the variation of permanent and maximum instantaneous elongation of a conductor is presented as a function of temperature for a 400 m span and an EDS of 10 % of rated tensile strength.
Considering the variation of tensile loads due to the elongation, practical experiments determined the relevant variations on permanent and instantaneous sags for several spans, as a function of maximum temperatures reached by the conductors after the short circuit, as presented in Figure 8.6.
Steel conductors, for instance, when reaching 200°C at a span of 400 m present an *instantaneous sag* increase of 2,7 m, which can be accepted as the conductor returns to the original condition after the cooling process.
For a temperature of 300°C, there is an instantaneous sag increase of 4,5 m and a permanent variation of 1,0 m. For a temperature of 400°C, the instantaneous sag variation is about 7,5 m and the *permanent sag* increase is about 2,2 m. While a temperature of 300°C is considered as acceptable by some utilities, a temperature of 400°C is only accepted in exceptional cases, e. g. for old lines designed for lower short-circuit ratings in the past.

8.3.2 Establishing tensile stresses and forces

The tensile stresses and sags of earth wires or aerial cables with optical fibres and the relevant stringing conditions need to be established so that the separation between earth wires and conductors at mid span is wider than their separation at the towers. It should be demonstrated that long-term vibrations having large amplitudes do not occur as to cause unacceptable reduction of earth wire or OPGW life time. Thus, attention should be given to proper vibration protection (see Chapter 11). It is usual to set the earth wire or OPGW sag as 90 to 95 % of the conductor sag at average yearly temperature (everyday condition), for instance 10°C in Europe, and then to take care that earth wire sag never exceeds the conductor sag. The resulting tensile stresses are then adopted for individual spans or towers, keeping in mind the maximum acceptable longitudinal loads (see clause 7.4 and [8.4]).

8.4 Steps for selection of conventional earth wires

In Table 8.2 examples are shown of earth wires frequently used by utilities, together with the respective short circuit data. The selection of earth wires comprises the following steps:

- Determination of short-circuit currents at least for a period of 10 years ahead;
- Computation of *short-circuit current distribution* among earth wires and earth when the fault location is varied along the line, considering the most pessimistic conditions inside the considered time horizon.
- Selection of one or two earth wire sizes for the line, depending on the type of lines, single or double circuit, on the voltage level and on the tower configuration. The optimum position of the earth wires for a good shielding against direct lightning strokes should also be taken into account (see Chapter 4). The arrangement and size of the earth wires should be conveniently designed. A strain tower is the best point to change earth wire sizes.
- Selection of the *everyday stress* for the earth wires for an adequate sag matching with the conductors and considering eventual *vibration protection* needs (see [8.4]).
- Determination of measures and devices for vibration protection, as described in Chapter 11, considering the type of conductors.

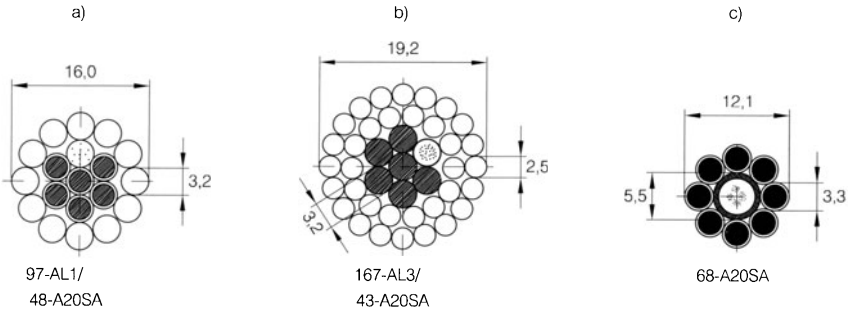

Figure 8.7: Examples of OPGW designs
a) Structure as conductor 97-AL1/56-ST1 - steel tubes arranged in the second layer
b) Design type with two AL3 layers
c) Design type with a central tube

8.5 Earth wires comprising optical fibres (OPGW)

8.5.1 Generalities and design

During decades, the earth wires of overhead transmission lines were aimed only at protecting the line conductors against lightning strokes and, as a consequence, to reduce the number of line outages. In addition, they reduced the interference on neighbouring installations. Another important function began, when overhead lines were equipped with earth wires constituting specific circuits for transmitting telecommunication signals. Such utilization has become widespread with the advent of fibre optic cables (OPGW), that provide a means of compact and interference-free signal transmission for use on electric power lines. So, the earth wires assumed additionally an active function in the overhead transmission.

Power networks connect population centres and, therefore, can provide alternative telecommunication routes, not only for electric utilities but also for other companies and cable TV networks. An extra capacity could be used for business ventures and other commercial applications. The immunity of fibre optic cables to electromagnetic interference is a major advantage for their use in power transmission systems. Paper [8.8] contains the essential basis for OPGW. The standards [8.9, 8.10, 8.11] and [8.12] give basic requirements for optical fibre cables. Along the time, three basic systems of aerial cables with optical elements have been developed:

- **Self-supporting optical ground wires (OPGW).** A *self-supporting optical ground wire* is a stranded metallic conductor incorporating optical fibres. It is best suited to be installed on new overhead power lines or when there is a need to replace existing earth wires. The basic characteristics of OPGW manufactured nowadays include designs with more than 100 fibres. In Figure 8.7 examples of OPGW are shown having up to 36 fibres.
  The glass fibres are usually protected by tubes of stainless steel; maximum fibre number is fit to the tube diameter. The glass fibres must be decoupled from the mechanical and electrical impact that may appear on the earth wire; so the fibres are installed and protected by a thixotropic gel filling before laser welding of tubes. In case of OPGW types, where the tube replaces a strand different from the core strand, the glass fibres contain an additional longitudinal reserve through the helix of the tube. The steel tube is usually not considered in the mechanical design of the OPGW. The loss in mechanical strength of the conductor can be tolerated when replacing only one steel strand through a tube (Figures 8.7 a, b).

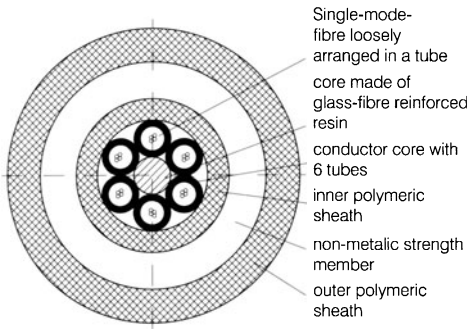

Figure 8.8: Example of an ADSS cable type

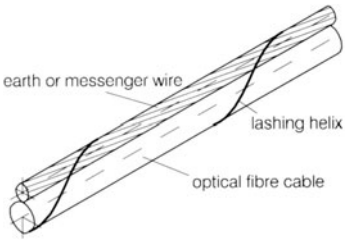

Figure 8.9: Optical cables attached to the earth wire

However, when more steel strands are replaced by stainless steel tubes with glass fibres, the resulting cross section reduction of the steel core should be specially taken into account.

If aluminium strands in the outer layer are replaced by aluminium alloy strands to compensate the strength lost by insertion of tubes instead of steel strands, then the more pronounced strength reduction by melting of some of these strands through lightning stroke effects should be considered.

- **All dielectric self-supporting cables (ADSS).** The *dielectric self-supporting cable* consists of multiple-mode or single-mode fibres arranged in tubes, stranded around a dielectric central strand, reinforced by glass fibres. The core is protected by an inner sheath, by aramid yarns and a polyethylene jacket that are flame retardant and humidity protected. Around the polyethylene jacket a layer of tensile-proof aramid fibres is arranged which are protected against mechanical damage by a polyethylene sheath. These cables reach sufficient tensile strength to allow for large unsupported spans between attachment points. They are physically separated from, and operated independently of the power line. In Figure 8.8, the structure of a dielectric cable is shown. Paper [8.13] contains details about the design and use of such types of optical cables, while [8.14] describes the fittings and their testing.

  ADSS cables are more subjected to vibrations than conventional conductors; in the case of ice loads, their sag is considerably high and with additional wind, there is a danger of touching phase conductors. As their installation on tower usually causes problems, power utilities seldom employ such cables.
- **Optical fibre cables attached to earth or messenger wires.** *Attached cables* are all-dielectric optical cables attached to the earth wire or phase conductors. Such cables rely on the conductor or earth wire as their support and do not require, therefore, high mechanical strengths. In Figure 8.9, an optical cable attached to a messenger wire is shown.

  The attached cables are not protected against thermal damages produced by lightning strokes. Failures can only be repaired by loosening and installation of new intermediate cable sections requiring joints.

In [8.15] an interesting experience in the UK is described about maintenance strategies of optical cables installed in high-voltage overhead lines.

Table 8.4: Tests at conductors with optical fibres (OPGW) and accessories

Type tests	Sample tests
Conductors with optical fibres	
Tests of optical fibres and individual strands	
– Attenuation as a function of wave length, variation in case of bending and temperature change	– Visual inspection – Optical attenuation – Strand tests as with conventional conductors
– Chromatic dispersion	
– Modal radius	
– Band width measurement	
Test on complete conductors with optical fibres	
– Stress-strain curve	
– Behaviour under longitudinal load (behaviour of optical fibres)	– Visual check on existence of flaws and ripples – Measurement of dimensions
– Stringing conditions	– DC resistance
– Conductor galloping	– Coil or drum conditions
– Aeolian vibrations	– Packing
– Creep test	– Shipment descriptions
– Thermal cycle test	
– Water absorption test	
– Short circuit test	
– Impulse voltage withstand test	
Accessories	
– Tensile load	– Visual surface check
– Aeolian vibrations	– Measurement of dimensions
– Conductor galloping	– Zinc coating
– Short circuit test	– Mechanical strength
– Vertical load, bending angle at suspension points	– Tests at accessories according to IEC 61 284 [8.16]
– Unbalanced loads	
– Test at accessories according to IEC 61 284 [8.16]	

8.5.2 Installation conditions

Conductors with optical fibres (OPGW) are subjected to the same requirements regarding everyday stress (EDS) and ice loads as conventional conductors. The conditions of average and maximum tensile forces, and the recommendation on everyday stress (EDS) to be adopted, are specially important in correspondence with the conductor type, as given in [8.4], Table 9.2.1/DE1.1, and recommendations for the parameter $H/m_c g$ according to clause 11.2.7. The design of suitable protection against vibrations is of prominent importance. Vibration protection devices are required for most OPGW and should be selected according to the guidelines presented in Chapter 11. Particular care is necessary in the stringing works of optical cables (see clause 16.8.4.9).

8.5.3 Accessories

The special functions of OPGW require also corresponding special accessories for their attachment at suspension and strain supports. The fittings should prevent damage or deformation, that can harm the function of the optical fibres. Damping fittings, in particular, should take care of the optical fibres. In [8.14], [8.17] and [8.18], fittings for OPGW are extensively described. In Chapter 10, examples are shown with armor rods for suspension supports and dead end supports, as well as examples of vibration dampers.

8.5.4 Tests

OPGW and their accessories are tested according to relevant standards and recommendations of international organisations.

- **Tests on optical cables.** The optical fibres of OPGW are tested according to IEC 60 793-1-4 [8.19]. The *optical attenuation* is checked at the wave length of 1550 nm in a testing loop, that consists of at least one continuous fibre per tube. Then, the mechanical integrity of the metallic tubes and the density against water absorption are tested. *Manufacturing ovalities* should be limited to narrow tolerances previously provided by the manufacturer and are not allowed to expand to unacceptable values during stringing operations.
  The complete conductors are tested according to [8.20], and the metallic strands assume the same testing methodology as strands for conventional conductors. In Table 8.4 type and routine tests applicable to optical cables are summarized.
- **Tests on accessories of optical cables.** The following accessories should be submitted to tests: suspension and dead-end fittings, suspension clamps, vibration dampers, galloping dampers, warning spheres, connectors for jumper loops, earthing connectors and branch-off clamps. They should fulfil all requirements applicable to conventional conductors and are not allowed to impair their function. Regarding testing, the relevant standards [8.20], [8.19] and [8.16], as well as publications [8.14], [8.18] and [8.21] are applied. Table 8.4 contains type and sample tests to be conducted with accessories for optical cables.

8.6 References

8.1 D'Ajuz, A. et al.: Energized overhead ground wires – OHGW: The pioneer Brazilian application. IVth SEPODE, Foz do Iguaçu, 1994

8.2 Cigré SC22 WG22-12: The thermal behaviour of overhead conductors. Section 4: Mathematical model for calculation of conductor temperature in the adiabatic state. Electra 185, (1999), pp. 75 to 87

8.3 EN 60 865-1: Short-circuit currents – Calculation of effects. Part 1: Definitions and calculation methods (IEC 60865-1). Brussels, CENELEC, 1994

8.4 EN 50 341-3-4: Overhead electrical lines exceeding AC 45 kV. Part 3-4: National Normative Aspects for Germany. Brussels, CENELEC, 2001

8.5 EN 60 071-1: Insulation coordination. Part 1: Definitions, principles and rules (IEC 60071-1). Brussels, CENELEC, 1995

8.6 DIN 48 201, Part 3: Steel stranded conductors. Berlin, DKE, 1994

8.7 EN 50 182: Conductors for overhead lines – Round wire concentric-lay stranded conductors. Brussels, CENELEC, 2000

8.8 Mahlke, G.; Gössing, P.: Aerial cables with optical fibres. Munich – Erlangen, Publicis Corperate Publishing, 5th edition 1998

8.9 IEC 60 794: Optical fibre cables. Part 1-1: Generic specifications; General. Geneva, IEC, 2001

8.10 IEC 60 794-1-2: Optical fibre cables. Part 1-2: Generic specification – Basic optical cable test procedures. Genova, IEC, 1999

8.11 IEC 60 794-2: Optical fibre cables. Part 2: Product specifications, Geneva, IEC, 1989

8.12 IEC 60 794-3: Optical fibre cables. Part 3: Sectional specifications on outdoor cables. Geneva, IEC 1998

8.13 ASTM E8: Standard for All-Dielectric Self-Supporting (ADSS) optic cable for use on overhead utility lines. New York, ASTM, 1997

8.14 Cigré SC22, WG22-11: Guide to fittings for optical cables on transmission lines. Part 2B: Testing procedures, all-dielectric self-supporting cable fittings and optical attached cable fittings. Electra 191 (2000), pp. 63 to 75

8.15 Cigré SC35 WG35-04: Preventive and corrective maintenance for optical cables on overhead power lines. Paris, Cigré Brochure 133, 2000

8.16 EN 61 284: Overhead lines – Requirements and tests for fittings (IEC 61284). Brussels, CENELEC, 1998

8.17 Cigré SC22 WG22-11: Guide to fittings for optical cables on transmission lines. Part 1: Selection and use. Electra 176 (1998), pp. 55 to 65

8.18 Cigré SC22 WG22-11: Guide to fittings for optical cables on transmission lines. Part 2A: Testing procedures for optical ground wire fittings and optical phase conductor fittings. Electra 188 (2000), pp. 43 to 53

8.19 IEC 60 794-1-4: Optical fibre cables. Part 1: Generic specifications – Section 4: Measuring methods for transmission and optical characteristics. Geneva, IEC, 1995

8.20 IEC 60 794-4-1: Optical fibre cables. Part 4-1: Aerial optical cables for high-voltage power lines. Geneva, IEC, 1999

8.21 Ghannoum, E. et al.: Design, testing and validation of optical ground wires and hardware for use in Hydro-Quebec's 5000 km of telecommunication network. Cigré Report 22-301, 1996

9 Insulators

9.0 Symbols

Symbols	Signification
a_g	Weight span
a_{eq}	Equivalent span
a_W	Wind span
C_c	Aerodynamic drag factor
d_1	Diameter of ball-and-socket connection
d	Maximum diameter of insulator body
D	Conductor diameter without ice
D_I	Conductor diameter with ice accretion
E	Modulus of elasticity
E_d	Electric strength
E_1, E_2	Number of samples to be tested
g	Acceleration of gravity
g_I	Weight of ice accretion per unit length
g_{res}	Resulting conductor load per unit length
K	Correction factor for air humidity and density
L	Nominal length of the insulator
m_C	Conductor mass per unit length
$m_C g$	Conductor weight per unit length
n_2	Number of subconductors
N	Total number of units in a lot
P	Nominal height of a cap-and-pin insulator
q	Wind pressure
q_0	Reference wind pressure
Q_C	Conductor tensile force
Q_G	Weight force
Q_{is}	Load of insulator
Q_W	Wind load
Q_{WI}	Wind load on conductor with ice accretion
T_1, T_2	Conductor temperature
U_{cw}	Insulation coordination withstand voltage
U_{rp}	Representative overvoltage
U_{rw}	Required withstand voltage
U_s	Highest voltage of equipment
w	Wind force per unit length
z	Height above ground
γ_M	Material partial factor
δ_{1M}	Dissipation angle
ε_r	Relative permitivity
ϱ_a	Density of ceramic raw material
σ_{ft}	Flexural strength, unglazed
σ_{fg}	Flexural strength, glazed
σ_1, σ_2	Conductor tensile stress

9.1 Introduction

The *insulators* are overhead line components installed between live conductors and earthed parts of the structures, being simultaneously subjected to mechanical and electric stresses. The *insulation performance* needs, therefore, to be designed for the most adverse *operating conditions* resulting from climatic impacts, such as ambient temper-

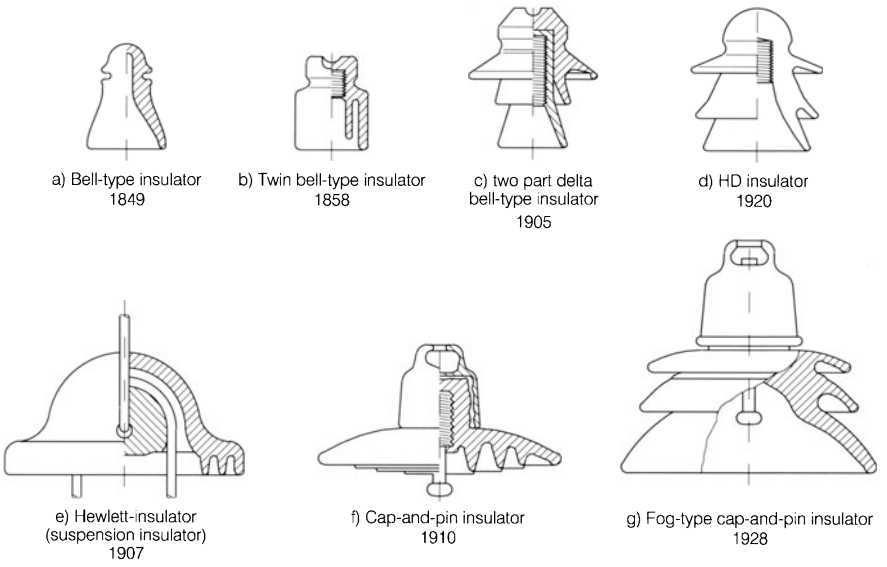

Figure 9.1: Line post and cap-and-pin insulators

atures, humidity, dew, fog, rain, as well as *pollution* by deposits of dusts, salts, firing residuals and industrial gases. The *mechanical resistance* should be so high that every incident load is carried with enough operational security. *Disruptive strength* and *electrical arc resistance* should be large enough to withstand the *resulting stresses*. Definitions can be found in IEC 60 050-471 [9.1]

To accomplish such tasks, several *insulator shapes* have been developed and some have disappeared from the market in the last 100 years since transmission of electric energy had started; the currently existing *insulator designs* result therefrom.

Porcelain as the first insulator *material* developed has been used until today, though with improved composition design. Toughened *glass* and *plastic* of different types and recipes appeared along the time as insulator raw materials, too. International standards of insulators reflect the high quality available today, but do not exclude new raw materials and further development to new insulator types and designs.

According to IEC 60 383-1 [9.2], overhead line insulators are classified in two types, type A and type B, respectively. Type A insulators are characterized by the fact, that the length of the shortest *puncture path* through the insulating body is at least half of the *flashover path* on the insulator surface. This applies to long rod insulators, for instance. Such insulators are considered as *puncture-proof*. Insulators for which the length of the shortest puncture path through the body is less than the half of the flashover path are classified as type B insulators, for instance cap-and-pin insulators and line post insulators. They are considered as not puncture-proof. According to present technology, puncture-proof *solid-core insulators* cannot be manufactured from glass.

9.2 Ceramic insulators

9.2.1 Insulator types and their application

Since the creation of the first units of porcelain bell-type insulators by Werner von Siemens in 1849 (Figure 9.1 a), the ceramic insulators have been developed to accomplish all operational requirements to be complied with by high-quality components.

Table 9.1: Cap-and-pin insulators according to IEC 60 305 with ball-and-socket connection

Designation	Electro-mechanical or mechanical failing load	Maximum nominal diameter of the insulator body d	Nominal height P	Minimum nominal creepage path	Standardized connection acc. to IEC 120
	kN	mm	mm	mm	d_1
U 40 B	40	175	110	190	11
U 40 BP	40	210	110	295	11
U 70 BS	70	255	127	295	16
U 70 BL	70	255	146	295	16
U 70 BLP	70	280	146	440	16
U 100 BS	100	255	127	295	16
U 100 BL	100	255	146	295	16
U 100 BLP	100	280	146	440	16
U 120 B	120	255	146	295	16
U 120 BP	120	280	146	440	16
U 160 BS	160	280	146	315	20
U 160 BSP	160	330	146	440	20
U 160 BL	160	280	170	340	20
U 160 BLP	160	330	170	525	20
U 210 B	210	300	170	370	20
U 210 BP	210	330	170	525	20
U 300 B	300	330	195	390	24
U 300 BP	300	400	195	590	24
U 400 B	400	380	205	525	28
U 530 B	530	380	240	600	32

The bell-type insulator from 1858 shown in Figure 9.1 b was originally used for the insulation of telephone lines. That *shape* was basically kept, when the line post insulator of the HD type *(high-voltage delta insulator)* for overhead lines was created and further developed into the HW type *(high-voltage wide shed insulator)*. The existing techniques at that time required *cap-and-pin insulators* (Figure 9.1 f) for higher voltage levels to be produced in separate parts and cemented together then. The development of *pin-type insulators* with higher puncture and flashover voltages came to an end in 1920 when the HD types shown in Figure 9.1 d were achieved. They have been still used up to 69 kV in some parts of the world.

Another insulating principle had to be studied due to the increasing transmission voltage levels. So, at the beginning of the 20th century the *suspension insulator* appeared. By means of similar units joined together like chain elements, the insulation level required for the respective operation conditions could be accomplished. The *Hewlett insulator* shown in Figure 9.1 e was one of the earliest types of *string insulators*, whose bodies were embraced by cable loops and are, thus, loaded by compression only. Both the low dielectric puncture strength and the risk of damage of the cable loops due to vibrations and arcs were disadvantageous aspects. The Hewlett insulators were replaced by the *cap-and-pin insulators* (Figure 9.1 f) which have been used worldwide since then.

In Central European countries, the cap-and-pin insulators were produced and used, at first, in various designs to comply with different electric and mechanical load conditions. The many existing designs for the attachment of the *pin* to the porcelain body indicate the degree of difficulties production and operation were faced with, a situation not different from that in other countries. While there it was aimed at further development of cap-and-pin insulators (Figure 9.2) through improvement of the production techniques, more economic materials as well as moulding and cementing processes, in Central Europe new alternative insulation systems were being researched.

By 1919, the *Motor insulator* appeared in Switzerland, a double shed *solid-core insula-*

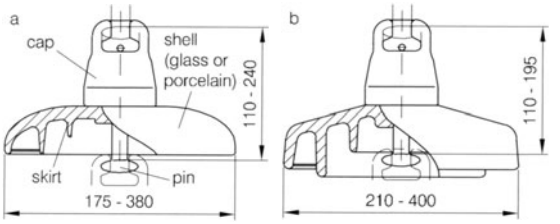

Figure 9.2: Cap-and-pin insulator according to IEC 60 305: a) standard type, b) anti-pollution type (P)

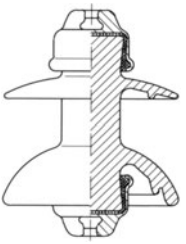

Figure 9.3: Double shed solid-core insulator

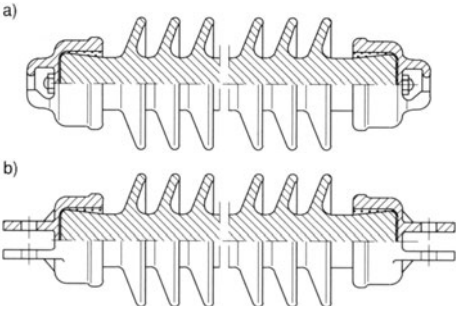

Figure 9.4: Long rod insulators: a) with socket caps; b) with clevis caps

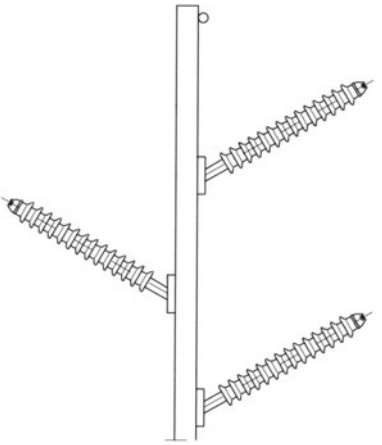

Figure 9.5: Typical application of insulating crossarms (delta configuration)

tor (Figure 9.3). A novelty was the fact that the porcelain was loaded by tensile stress, although its tensile strength reached only one tenth of the resistance to compression. This design set high tensile strengths and a reliable production as premises. Due to the relation between the length of the flashover path in the air and the puncture path in the insulating medium, this type of insulator is not susceptible to puncture.

The *long rod insulator* according to Figure 9.4 represents a further development of the double shed solid-core insulator. Its simple and clear structure, the advantageous electric characteristics under high pollution and its high reliability have led the long rod insulator to a privileged rank in several European countries. Due to the possibility of easy modifications, several special versions were designed to accomplish different tasks. So, the same basic cross section of the body may encompass diverse shed diameters, *shed shapes* and shed distances. EN 60 433 [9.3] standardizes long rod insulators with *ball-and-socket* and *clevis-and-tongue type caps*. The most frequently used insulator types are shown in Figures 9.2 and 9.4. Their data can be seen in Tables 9.1 to 9.3.

Advances in technologies of insulating materials enable to replace support crossarms by insulators. *Insulating crossarms* with long rod insulators can be mounted directly at the tower body. The conductor is attached to the insulator head. Their advantages can be mentioned as being a reduced overall dimension and height of the supports. Rights-of-way and crossed areas can be noticeably reduced. Emergency structures or other temporarily used line designs are preferably equipped with such type of structural elements. In some countries, they are applied to voltages up to U_s = 145 kV as an

Table 9.2: Characteristics of long rod insulators with clevis and socket caps according to IEC 60433

Designation	Standardized lightning impulse withstand voltage kV	Power withstand voltage wet kV	Specified minimum failing load kN	Maximum nominal diameter d of the insulator body mm	Minimum creepage path mm
L 40 B/C 170	170	70	40	160	576
L 60 B/C 170	170	70	60	160	576
L 100 B/C 170	170	70	100	180	576
L 100 B/C 250	250	95	100	180	832
L 100 B/C 325	325	140	100	180	1160
L 100 B/C 450	450	185	100	180	1968
L 100 B/C 550	550	230	100	180	1968
L 120 B/C 325	325	140	120	200	1160
L 120 B/C 450	450	185	120	200	1968
L 120 B/C 550	550	230	120	200	1968
L 120 B/C 650	650	275	120	200	2320
L 160 B/C 325	325	140	160	210	1160
L 160 B/C 450	450	185	160	210	1968
L 160 B/C 550	550	230	160	210	1968
L 160 B/C 650	650	275	160	210	2320
L 210 B/C 325	325	140	210	220	1160
L 210 B/C 450	450	185	210	220	1968
L 210 B/C 550	550	230	210	220	1968
L 210 B/C 650	650	275	210	220	2320
L 250 B/C 550	550	230	250	230	1968
L 250 B/C 650	650	275	250	230	2320
L 300 B/C 550	550	230	300	240	1968
L 300 B/C 650	650	275	300	240	2320
L 330 B/C 550	550	230	330	250	1968
L 330 B/C 650	650	275	330	250	2320
L 360 B/C 550	550	230	360	250	1968
L 360 B/C 650	650	275	360	250	2320
L 400 B/C 550	550	230	400	260	1968
L 400 B/C 650	650	275	400	260	2320
L 530 B/C 550	550	230	530	270	1968
L 530 B/C 650	650	275	530	270	2320

alternative to conventional line designs. In Figure 9.5, a 110 kV line with insulating crossarms is shown. For this application, line post insulators are used, the characteristics of which can be found in IEC 60720 [9.4].

The use of insulators in cantilever applications combines structural with electric characteristics; such solutions, with no metallic elements between phases, need low phase spacing thus resulting in compact supports being an important and desirable condition in new lines where high capacities are required. Papers [9.5] and [9.6] describe several compact lines with insulators used as insulated crossarms. Insulated crossarms are favourable for uprating lines as described in [9.7] for conversion of a 66 kV line into 220 kV in Spain.

Cap-and-pin insulators are standardized regarding ultimate strength, diameter, spacing and creepage distance according to [9.8]. Their couplings are standardized by IEC 60120 (ball-and-socket couplings) [9.9] and IEC 60471 (clevis-and-tongue couplings) [9.10]. Locking devices are specified in IEC 60372 [9.11].

Table 9.3: Dimensions of connections of long rod insulators with clevis and socket according to IEC 60 433

Designation	Connection B [1]		Connection C [2]	
	Maximum nominal length L mm	Standardized dimension of connection (bolt diameter according to IEC 60 120)	Maximum nominal length L mm	Standardized dimension of connection (bolt diameter according to IEC 60 471)
L 40 B/C 170	380	11	400	13L
L 60 B/C 170	400	11	420	13L
L 100 B/C 170	450	16	475	19L (16L) [3]
L 100 B/C 250	580	16	605	19L (16L) [3]
L 100 B/C 325	870	16	900	19L (16L) [3]
L 100 B/C 450	1085	16	1120	19L (16L) [3]
L 100 B/C 550	1240	16	1270	19L (16L) [3]
L 120 B/C 325	870	16	905	19L (16L) [3]
L 120 B/C 450	1085	16	1120	19L (16L) [3]
L 120 B/C 550	1240	16	1275	19L (16L) [3]
L 120 B/C 650	1430	16	1465	19L (16L) [3]
L 160 B/C 325	885	20	920	19L
L 160 B/C 450	1100	20	1135	19L
L 160 B/C 550	1255	20	1290	19L
L 160 B/C 650	1445	20	1465	19L
L 210 B/C 325	905	20	940	22L
L 210 B/C 450	1120	20	1155	22L
L 210 B/C 550	1275	20	1310	22L
L 210 B/C 650	1465	20	1500	22L
L 250 B/C 550	1305	24	1335	22L
L 250 B/C 650	1500	24	1530	22L
L 300 B/C 550	1330	24	1365	25L
L 300 B/C 650	1520	24	1560	25L
L 330 B/C 550	1360	28	1400	28L
L 330 B/C 650	1550	28	1595	28L
L 360 B/C 550	1360	28	1410	28L
L 360 B/C 650	1550	28	1600	28L
L 400 B/C 550	1400	28	1460	28L
L 400 B/C 650	1600	28	1660	28L
L 530 B/C 550	1450	32	1520	32L
L 530 B/C 650	1650	32	1720	32L

[1] ball-and-socket connection, [2] clevis-and-tongue connection, [3] size not preferred

9.2.2 Raw materials

Today, insulators made of *ceramic raw materials* are produced from quartz porcelain C-110, aluminium oxide porcelain C-120 or C-130 according to IEC 60 672-1 [9.12] or *steatite* of the C-220 type. A report on the long-term experience with long rod insulators can be found in [9.13]. Insulators produced today consist mainly of C-120 and C-130, the latter being high-strength aluminium oxide porcelain.

Properties of porcelain are controlled by the proportion of different minerals in the mixture (Figure 9.6). The quality of the product, especially the uniformity of its properties, depends mainly on uniform and as far as possible constant composition of the mixture. Group C-100 are *siliceous and aluminous porcelains* based on alkaline aluminium silica and produced from kaolin, feldspar and quartz. All group C-100 porcelains have the same electric properties, especially a high electric strength to puncture, but differ in their mechanical strength (Table 9.4). The ceramic materials of group C-200 (steatites and forsterites) are based on magnesium silicate and characterized by a high *compression resistance* and low dielectric losses; they are often used for insulation of

Table 9.4: Characteristics of ceramic materials according to IEC 60672-3

		Group	C-100			C-200	
		Type	110	120	130	220	221
Characteristics	Symbol	Units					
Density of raw material [1]	ρ_a	g/cm^3	2,2	2,3	2,5	2,6	2,7
Flexural strength, unglazed	σ_{ft}	MPa	50	90	140	120	140
Flexural strength, glazed	σ_{fg}	MPa	60	110	160	–	–
Modulus of elasticity [1]	E	GPa	60	n. d.[2]	100	80	110
Electric strength [1]	E_d	kV/mm	20	20	20	15	20
Relative permitivity 48 to 62 Hz	ε_r		6 to 7	6 to 7	6 to 7,5	6	6
Dissipation factor at 20°C, 1 MHz	$\tan\delta_{1M}$	$\cdot 10^{-3}$	12	12	15	3	1,2

Explanations: Type 110: siliceous porcelain, plastic-processed; Type 120: aluminous porcelain; Type 130: aluminous porcelain, high-strength; Type 220: normal steatite; Type 221: low-loss steatite
[1] minimum values, [2] not defined

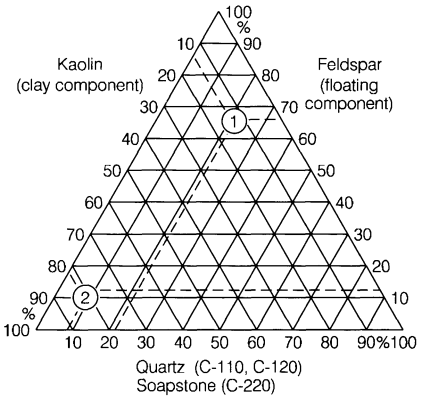

Figure 9.6: Triangle of condition for hard porcelain and steatite. 1 C-110 and C-120; 2 C-220

HF-transmitting stations. Soapstone is used instead of *quartz* in case of steatites, thus determining the properties of the final product (Figure 9.6). Basic properties of different raw materials are established in international standards IEC 60672-3 [9.14].
The mechanical properties of the raw materials *hard porcelain* and steatites can be remarkably affected by both the addition of oxides and the employed glazes. *Glaze* aims at the reduction of *dirt accumulation* by means of smoothing the insulator surface, and increases simultaneously the strength of the insulator by *prestressing*.
Individual technical data of electric insulator raw materials depend on the temperature and the frequency of the electric voltage. The *fatigue strength* of ceramic raw materials, unlike metals, is very close to their static strength. The reduction of their specific strength as the cross section of the insulating body increases is a characteristic of ceramic materials. In fact, there are standard *test specimens* (for instance according to IEC 60672-2 [9.15]); however, the ultimate strength values obtained cannot be assumed for larger cross sections directly. The strength of porcelain as a function of the insulator diameter is set down in the graphs of Figure 9.7. Those diagrams can vary depending on the differing production procedures and knowledge of individual manufacturers.

9.2.3 Production

Long rod insulators
The highly simplified and schematic representation of Figure 9.8 shows the different

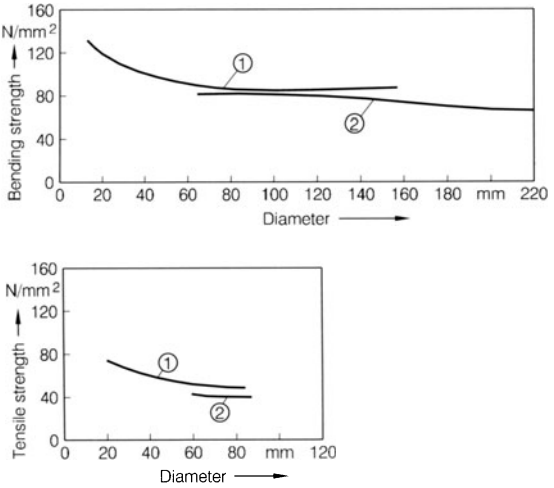

Figure 9.7: Bending and tensile strength of cylindrical rods depending on the diameter.
1 rods without sheds; 2 rods with sheds

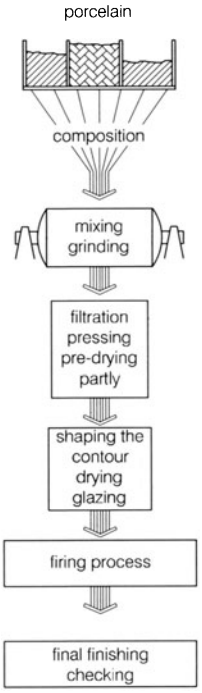

Figure 9.8: Production stages of porcelain insulators

stages of the production of hard porcelain starting from the storage of raw materials until final inspection. Selected *ingredients of high purity* and homogeneous properties are weighed, mixed to formula specifications and subjected to a grinding process. *Vacuum extrusion presses* form the plastic *filter cake* into cylindrical blanks adjusted with diameters to the long rod type to be produced. After being cut to length, they are subjected to a closely controlled *drying process* to condition them for the following shaping steps. *Vertical lathes* are used to machine the blank to the desired contour for the raw product. After another drying stage the unfinished insulator already possesses a high strength due to the clay bond and is ready for the application of the glazing by an *immersion process*. The subsequent *firing stage* creates new types of crystals out of the conglomerate of various minerals forming the porcelain and the hard ceramic structure. The control of firing process gains high significance when producing porcelain insulators. Too strongly or too lowly fired porcelain is capable of sucking and, therefore, does not comply with the requirement of a high density. Modern furnaces with automatic control of the firing temperature and energy recuperation from the exhaust gases enable a constant quality of firing and have proved to be economic and environmentally friendly.

Cap-and-pin insulators

The material of porcelain cap-and-pin insulators is processed as in case of long rod insulators. The cakes are uniformly kneaded, extruded by a pugmill and cut into pieces of proper length. After preforming, the pieces are put into moulds and formed into the shape wanted by pressing. Then, they are finished and dried. After drying, the glaze is applied. The prepared units are fired in tunnel kilns at a temperature of 1 300°C. The control of the firing process guarantees a constantly high quality.

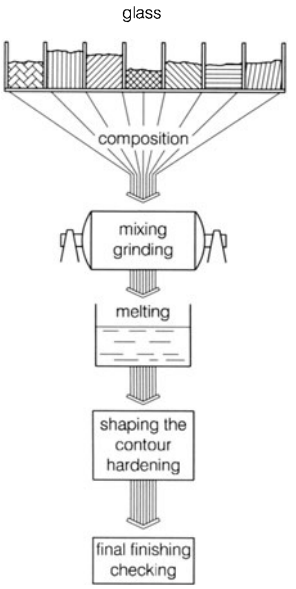

Figure 9.9: Production of glass cap-and-pin insulators

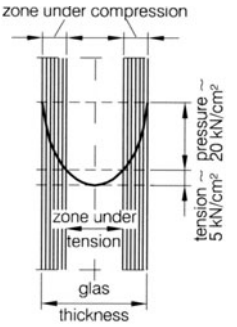

Figure 9.10: Stress distribution for hardened glass insulators

Assemblies

All overhead line insulators are equipped with *fittings* before delivery. Fastening of metallic caps on long rod insulators is carried out today mostly through pouring of the space between fitting and ceramic cone with a *lead antimony alloy* or *Portland cement*; *sulphur cement* is used only seldom. In regions where the insulator caps can reach temperatures above 80°C, Portland cement or lead antimony alloy with a melting temperature of 400 to 450°C should be used. Before completion with clevis or socket caps, the additional insulator length required for the firing stage is separated from the ceramic blank and internal *quality checks* are carried out, e. g. the *ultrasonic test*. Portland or sulphur cement is employed for *connecting the fittings* of cap-and-pin insulators.

9.3 Glass insulators

9.3.1 Raw materials and production

Cap-and-pin *toughened glass* insulators have been developed as an alternative to porcelain insulators for overhead lines. The insulating body is made of molten silica oxide and other mineral salts.

The glass dielectric part is obtained through melting the raw materials by a continuous process which guarantees homogeneity of the chemical composition of the insulating unit. The production starts with the mixing and grinding of raw materials followed by the addition of a portion of recycled glass (Figure 9.9). The next step is the melting; its purity is responsible for a uniform quality of the final product. In a sequence, the fluid glass mass corresponding to the insulator type is taken out of the furnace so that the insulating body can be produced in rotating moulds. Undesired internal stresses are prevented through controlled cooling after shaping the insulator body. The blank is submitted to an intermediate cooling followed by heating to a temperature of about

600° C, while its surface is tempered by compression air. Without any structural changes – merely by means of diverse cooling speeds of the glass zones of the insulator bodies – compressive stresses close to the surface as well as tensile stresses in the inner parts are formed so that the glass parts are *prestressed* [9.16] (Figure 9.10). This process results in an essential increase of the strength values. The differences in stresses result in the characteristic splitting behaviour whenever sudden impacts reach the stressed zone. A final *temperature shock* through immersion in cold water tests this effect during production of the unfinished bodies and selects faulty ones. After the cooling process, the glass bodies are submitted to a detailed visual test to search for inclusions and, whenever desired, a second temperature shock treatment can be applied in order to minimize premature failures.

Glass cap-and-pin insulators are then finished at a fully automatic production line by means of completion cementing between the socket or clevis caps and the pins or tongues to the glass bodies. The *caps* are made of galvanized *malleable cast iron*, the pins or tongues are made of galvanized heat treatable steel. The highly automated production of the glass cap-and-pin insulators has proved to be commercially profitable. When it is deemed necessary for DC applications or in polluted areas, the pin is protected against corrosion by pressing around with a *zinc alloy sleeve* to form a *sacrificial electrode.*

After completion of the production process including hardening of the cementing and a mechanical routine test, the insulators are stored for some weeks, since the heterogeneous distribution of the stresses within the insulator bodies leads to noticeable *self breaking* during the subsequent weeks. However, the fragments within the cap, due to their increased volume, keep the cemented pin within the cap with a force of about 90 % of its original value, which would practically prevent separation of the insulator strings whenever damage occurred during operation.

9.3.2 Insulator types and application

Cap-and-pin insulator minimum failing loads, cross sections, rated spacing and creepage path characteristics follow the standards given in [9.8]. The ball-and-socket or clevis-and-tongue connections are standardized by IEC 60 120 [9.9] and IEC 60 471 [9.10], respectively.

Glass cap-and-pin insulators with ball-and-socket connection are found to be under the most marketable types both in narrow and wide spacing. Cap-and-pin insulators for use in heavily polluted regions are manufactured with larger creepage paths achieved by means of modification of the skirts on the bottom side of the insulator. Insulators with larger creepage paths are also standardized in [9.8]. IEC 60 815 [9.17] refers to the selection of insulators depending on the degree of pollution at the line construction site.

In *polluted areas*, a simple *adjustment of the creepage distance* by increasing the number of insulators within a string or by selecting shells with increased creepage distance is possible in an economic manner. Cap-and-pin insulators proved to be advantageous for use in V-type insulator sets which permit a smaller right-of-way because of the absence of swinging transversally to the conductor direction. Due to the fact that mechanical integrity is usually maintained in case of cap- and-pin-type glass insulator strings even when loosing individual shells, e. g. by effects of arcing or *vandalism*, conductor bus bars of substations are frequently equipped with single cap-and-pin glass insulator sets. The higher weight of cap-and-pin glass insulator sets compared with long rod insulator sets is a disadvantage.

In areas of high pollution levels, corrosion at the pins occurs resulting in reduction of the cross section caused by *leakage currents.*

According to experience, the self-destroying of insulator shells comes to a stop in case of modern cap-and-pin glass insulators after the first year being in service. Statistic long-

term studies carried out within a network led to an annual *failure rate* of approximately $4 \cdot 10^{-5}$ without recognizable external actions.

9.4 Composite insulators

9.4.1 Raw materials, design and production

For many years, *plastic* or *synthetic resins* of diverse compositions have been used, besides ceramic and glass, for the insulation of electric installations. Insulating materials such as aromatic and aliphatic epoxid reactive resins, *teflon* (PTFE – polytetrafluoroethylene) as well as silicone rubbers are used. Besides the usual insulating characteristics necessary in case of overhead applications, high *resistance against ultraviolet radiation* is required for the plastic or synthetic resins. As long as they do not fulfil that latter requirement, aromatic epoxy resins are only applied indoors.

Insulators made of homogeneous plastic or synthetic resins are applied at voltages up to $U_s = 36$ kV. These insulators are made of cycloalyphatic resins. They are characterized by a wide degree of freedom with respect to their moulding, a good accuracy to size and the possibility of joint casting of fastening elements. They also have low weight. However, their low leakage current strength is disadvantageous. Research to improve the composition of raw materials is continuously under way.

Insulation for higher voltages is also highly stressed from the mechanical standpoint, thus requiring composite insulators with *glass fibre reinforced cores (GFC)* of cast resin to be used. In order to obtain the necessary creepage path, sheds of diverse materials such as resin-epoxy, polytetrafluoroethylene (PTFE), ethylene-propylene rubber (EPR) or *silicone rubber* are arranged around the cores [9.18, 9.19].

Composite insulators can be formed by individual sheds fixed on a core rod with or without an intermediate layer or alternatively by a cover of sheds applied on the core rod in one or several production steps. The composition of materials used and the production process vary from manufacturer to manufacturer. Figure 9.11 presents a section of a composite insulator. It is possible to manufacture a continuous GFC rod of *glass fibre material resistant to brittle failure (electric grade corrosion resistant glass, ECR)* and hydrolysis-resistant cast resin with practically any diameter. The length required for any insulator type can be obtained by cutting. The final step is the application of compression aluminium or steel fittings, which is cost-effective from the technical standpoint, because of the need of a stress distribution in the GFC rod as uniform as possible during operation. Cone- and wedge-type fittings are seldom used today due to the risk of slipping, thus jeopardizing the sensitive sealing between the fittings and the GFC rod. The possibility of heating the fittings caused by power arcs should be taken into account whenever considering their structural design. Adequately designed *arcing protection fittings* should be used to prevent every kind of damage to insulator fittings.

For production of a large number of units, e. g. of 110 kV insulators, the use of more expensive *cast moulds* can be justified, in which the GFC rod is introduced, silicone is applied under pressure and overheating is applied to harden it. For production of few units, this mould can also be applied for elements arranged in a series for the single sheds and a variable length. The production process enables the fabrication of composite long rod insulators up to 6 m long. Where the use of single-part moulds would be too expensive, separate sheds made of *high-temperature cross-linked silicone* are produced by a *high pressure injection moulding process.* These sheds are then slid on the *GFC rod* previously coated with a seamless silicone layer and vulcanized. The chemical connection between the GFC rod, the silicone coating and the sheds eliminates any physical interface. Attention should be paid to the permanent sealing of the sensitive interface area between the fittings, the GFC rod and its correlated coating in order to

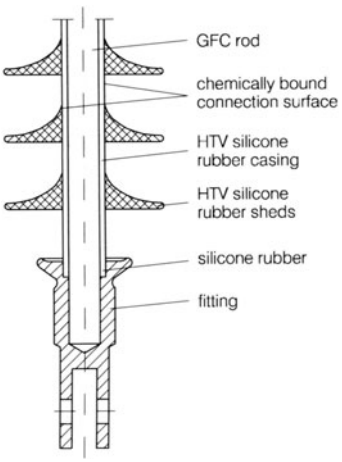

Figure 9.11: Section through a plastic composite insulator
(RODURFLEX made by CeramTec AG)

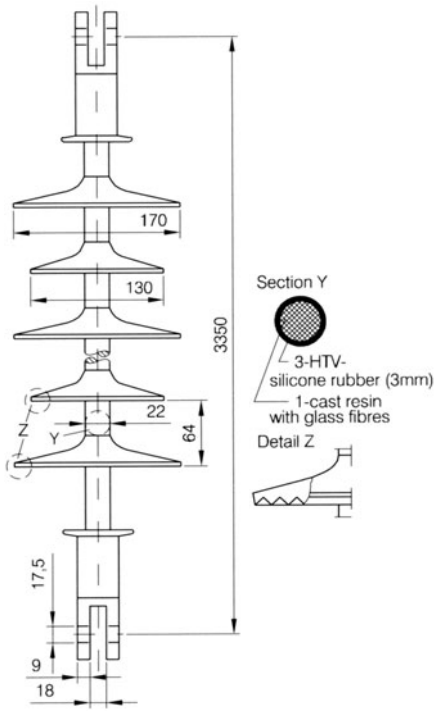

Figure 9.12: Composite insulator made of GFC and silicone rubber
(RODURFLEX made by CeramTec AG)

avoid the intrusion of *humidity* and the associated *risk of brittle failure*. Figure 9.12 shows a composite insulator. Paper [9.19] gives a detailed bibliography on the subject.

9.4.2 Types of composite insulators and their application

Although composite insulators have been in use since the middle of the sixties, standardization and description of characteristics exist just for the medium-voltage range [9.20]. Mechanical loads established as well as connection types are found in [9.21]. Materials and designs for non-standardized insulators can be selected according to [9.22], so that they can withstand environmental and atmospheric impacts. Their properties and adequacy to practical use should be proved. In view of that, the responsibility for the technical and economic selection of the adequate type of composite insulators from a range of different models depends on the line designer or the purchaser in charge of the relevant project.

Composite insulators present several advantages, such as *low weight*, high mechanical strength, considerable *reduction of required creepage distance* through a hydrophobic surface [9.23], durability especially under critical pollution conditions, high resistance against vandalism and optimum ability to comply with project requirements by means of their modular fabrication system; in view of such outstanding characteristics, composite insulators have been more and more accepted by users. Due to their insulating capacity, composite insulators have been often used to replace conventional insulators in critical areas. Composite insulators can be manufactured as a unit piece to replace existing long insulator sets, thus reducing the total length of the insulator set and mak-

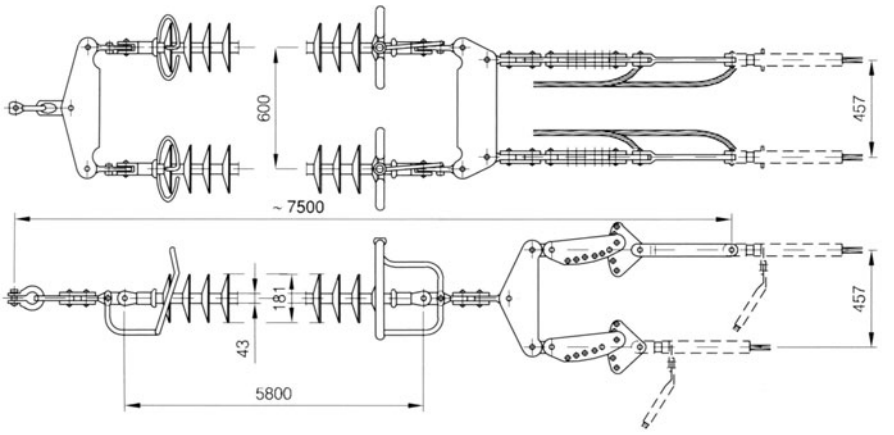

Figure 9.13: Dead-end insulator set with GFC composite insulators for a 500 kV line (CeramTec AG)

ing them especially appropriate for *uprating of lines*, without the need to modify tower dimensions or rights-of-way whenever higher system voltages are adopted [9.24].
The advantage presented by composite insulators with respect to their weight is prevalent at the 500 kV voltage level and higher. Figure 9.13 shows a dead-end insulator set for a 500 kV line with two composite insulators in parallel. When compared with conventional insulators at this voltage level, composite insulator sets are preferable due to their lower needs of material, installation and maintenance. For adverse weather conditions, for lines along the sea coast and for DC transmission lines [9.25], the good performance of composite insulators with silicone rubber sets is determinant under critical pollution conditions. Paper [9.26] reports on worldwide experience on use of composite long rod insulators.
Due to its low weight and its high flexibility, the GFC insulator is used as *phase-to-phase spacer* at medium-voltage compact and high-voltage lines to protect them against phase-to-phase flashovers during galloping.

9.5 Comparison of insulator types

In the preceding clauses it has been shown that three basic alternatives of raw materials and two insulator design principles are employed for high-voltage overhead line insulators worldwide at present. Besides the classic porcelain and glass insulator, composite insulators made of plastics or synthetic resins have been introduced in the market. Cap-and-pin insulators are made of porcelain and glass as they used to be, whereas long rod insulators are constituted either of porcelain or of composite materials.
According to estimates presented in [9.27], the worldwide insulator market is shared to approximately 50 % by overhead power line insulators. About 75 % out of that portion are manufactured as glass and porcelain cap-and-pin insulators. The remaining 25 % are split into a larger portion of long rod composite insulators and a smaller portion of porcelain long rod insulators.
As an important technical difference to the long rod insulator, the *insulating length* of the cap-and-pin insulator, either of porcelain or glass, is shorter between the metallic cap and the pin; thus, the insulation level of the insulator string is to be obtained by means of a corresponding number of insulating paths in series connection. The electric stress expressed in kV/cm in the insulating material is high, too. The large

portion constituted by non-insulating metallic fittings and cement increases the *weight of the string* and is disadvantageous for installation and maintenance at higher voltage levels. Cap-and-pin insulators are not conceived to be puncture-proof. For glass cap-and-pin insulators, failure identification caused by electric puncture is possible due to a simple visual indication of *broken sheds*, while porcelain cap-and-pin insulators require periodical time-consuming measurements under live-line conditions to identify electrically failed caps that are mechanically no longer reliable.

Porcelain long rod insulators differ from composite insulators in as much as they consist of thermally stable material not affected by the environment. High-quality porcelain, as presently produced, is resistant to tensile load; however, it presents a limited capacity to support dynamic impact loads or bending strains, which implies more attention to multiple-string configurations as far as the performance after a failure of one string is concerned.

The weakest point of the long rod composite insulator is due to the vulnerability of the silicone layer above the GFC rod, which should effectively protect against moisture penetration to prevent reduction and eventually loss of the mechanical strength of the insulator.

A *comparison of insulator types* (porcelain or glass) can be made by their advantages and disadvantages:

Cap-and-pin insulators:

Advantages:

- High mechanical capability even with shells damaged,
- Simple and most favourable engineering design of each unit,
- High impact and bending capability of the insulator strings.

Disadvantages:

- High electric stressing of the insulating material,
- Risk of electric puncture (porcelain units),
- Susceptibility to corrosion of the numerous fittings,
- Higher weight of insulator sets, higher maintenance costs.

Porcelain long rod insulators:

Advantages:

- Puncture-proof,
- High electric and mechanical reliability,
- Very low maintenance requirements, no need for live-line maintenance,
- Lower weight than cap-and-pin insulator sets.

Disadvantages:

- Production is more expensive,
- Low mechanical impact strength,
- Design of insulator sets regarding dynamic load,
- Technology less frequently adopted outside Europe and Middle East.

Composite long rod insulators:

Advantages:

- Low weight,
- Hydrophobic insulator surface,
- Creepage path, insulator length and load capacity can be adapted easily to the project requirements.

Disadvantages:

- Mechanically sensitive silicone surface of the GFC rod,
- High technical production efforts, silicone materials are expensive,
- Higher sensitivity to ageing.

Cigré gathered data on the operating performance of the various insulator types throughout the past years. Users had been questioned about their practice and expe-

rience and reported basic data. From the statistics, a comparison of the performances was prepared and presented in [9.27]. A fictitious 400 kV overhead line with 10 000 insulating sets was studied. After that, prospective *mean times between failure* (MTBF) were evaluated for

- porcelain cap-and-pin insulators 10 hours,
- glass cap-and-pin insulators 6 days,
- composite insulators 2,5 weeks,
- porcelain long rod insulators 18 years.

9.6 Tests on insulator units

9.6.1 Basic information

With respect to the various *insulator testing procedures*,overhead insulators are classified as follows:

- Pin-type insulators,
- Line post insulators,
- String insulators, classified into
  - Cap-and-pin insulators and
  - Long rod insulators.

Because of their frequent application in high-voltage overhead lines, *string insulators* will be treated with special attention in the following clauses.

Insulators for high-voltage overhead lines are characterized by mechanical and electric data. The values presented in Tables 9.1 to 9.3 constitute the basis for the selection of a certain type of insulator for a given application. During the development of new insulators, not all of the characteristics can be theoretically determined. Therefore, they are more usually evaluated through electric or mechanical *tests.*

The existing standards usually classify the tests into *type tests*, *sample tests* and *routine tests* depending on the parameters influencing the individual characteristics and also with the instant at which the tests are performed. Annex P of EN 50 341-1 [9.28] gives an informative overview on all the *stipulated* and the *optional tests* .

According to the definitions given by EN 60 383-1 [9.2], which can be similarly found in all standard test or acceptance procedures, type tests determine all the data that are dependent on the structural design of both the insulator and the fittings. A sample test is performed in order to check the insulator characteristics which may be subject to alterations due to manufacturing process and quality of the materials. Routine tests to be applied to each insulator should detect all the individual production deficiencies as well as sort out the defective units.

A *quality management system* in accordance with standardized requirements can be agreed upon to enable quality verification during the production. EN ISO 9002 is suggested as a guideline for a quality management system for insulators. The test on insulator units are summarized in Table 9.5.

9.6.2 Tests on ceramic and glass insulators

9.6.2.1 Type tests

Type tests are performed on a small number of insulators and only once for a new engineering design or a new production process; they will be repeated only in case those characteristics or any other rated values are modified. Individual insulators made of ceramic can be tested according to EN 60 383-1 [9.2]. The *number of units* and the *acceptance criteria* for the electric, mechanical as well as any other rated characteristics

Table 9.5: Tests on overhead line insulators

	String insulator units		Line post insulators
	Long rod	Cap-and-pin	
Standard type tests			
Verification of dimensions	x	x	x
Wet power frequency withstand voltage test	x	x	x
Dry lightning impulse withstand voltage test	x	x	x
Thermal mechanical performance test	x	x	–
Mechanical or electro-mechanical failing load test	x	x	x
Optional type tests			
Impulse withstand puncture test	–	x	–
Zinc sleeve test	–	x	–
Residual strength test	–	x	–
Sample tests			
Verification of dimensions	x	x	x
Verification of locking system and displacements	x	x	–
Temperature cycle test	x	x	x
Mechanical or electro-mechanical failing load test	x	x	x
Thermal shock test (toughened glass insulators only)	–	x	x
Puncture voltage withstand test	–	x	–
Porosity test (porcelain insulators only)	x	x	x
Galvanizing test	x	x	x
Optional sample tests			
RIV test	–	x	–
Impulse voltage puncture test	–	x	–
Zince sleeve test	–	x	–
Routine tests			
Visual inspection	x	x	x
Mechanical test	x	x	x
Electric test	–	x [1])	–
Optional routine tests			
Ultrasonic examination	x	–	–

[1]) Applicable only to insulators of ceramic materials (see EN 60 383-1)

can be found in that standard reference, in case they have not been agreed upon in a different way between purchaser and manufacturer.

Type tests refer to:

- Verification of the dimensions;
- *Wet power frequency withstand voltage test*, 50 or 60 Hz;
- *Dry fast-front withstand voltage test*, 1,2/50 μs;
- *Thermal mechanical performance test (heat cycle test)* (not for line post insulators);
- *Test of mechanical failing.*

The knowledge on the withstand voltage of the insulator units is an essential condition for the design of the insulator string according to the necessary insulation level specified by *insulation coordination* [9.29, 9.30] (see clause 2.4.5).

Electric tests include the study of 50 or 60 Hz withstand voltages as well as *fast-front overvoltages* (front time 1,2 μs, time to half crest value 50 μs). Some national standards require additional *interference voltage tests* at some hundred kilohertz.

Clean, dry insulators are used to measure the flashover and the withstand voltages for lightning impulses. The power frequency withstand voltage test is performed with a wet insulator. The standards give the requirements on quantity of water, its conductivity, angle of rain fall and the temperature (IEC 60 060-1) [9.31].

In order to obtain comparable data, the respective measured values are related to *standardized atmospheric conditions* [9.2, 9.31]. The operating voltage itself is not con-

sidered as a characteristic value.
The following optional type tests can be agreed upon for individual cap-and-pin insulators:

- *Radio interference voltage test*;
- *Impulse voltage puncture test;*
- *Test of residual strength*;
- Test of the zinc sleeves

and, for line post insulators besides the radio interference test, both a *pollution test* and a *power arcing test* can be included. The standardized guidelines for these optional type tests can be taken from [9.28]. Residual strength of string insulator units is tested in accordance with the former IEC 60 797 [9.32], puncture tests are carried out as specified by IEC 61 211 [9.33].
All results should be recorded through certificates issued by the manufacturer or by another qualified entity. Their validity is unlimited for the case of electric tests and amounts to ten years in case of mechanical tests. They are considered valid within their respective limits as long as the subsequent sample tests do not yield any essential differences to the results obtained by the type tests.

9.6.2.2 Sample tests

Sample tests are by far the most interesting for the users to check the quality of the finished batches. The tests as specified in [9.2] are performed with samples selected randomly from each lot to be supplied and should be in accordance with the respective standards. The *number of samples* depends on the number of units to be accepted and is divided into two portions, called E1 and E2, for the various tests. In case of only one individual sample not passing during the tests, the process is to be repeated with twice the original quantity. In case two or more samples failed during the sample tests or in case only one single sample failed during the repetition of the process, the total number of units in a lot has to be rejected.
The scope of sample tests is as follows:

- Verification of dimensions;
- Check of dimensional deviations (axial, radial or angular deviations);
- Verification of the *locking system* (only for ball-and-socket connections);
- Temperature cycle test (only for ceramic materials);
- Test of mechanical failing load;
- *Thermal shock test* (only for cap-and-pin insulators made of toughened glass);
- Puncture voltage withstand test (only for type B insulators);
- *Porosity test* (only for ceramic materials);
- *Test of the galvanization* of the steel elements.

Other optional sample tests are known only for cap-and-pin insulators, that is the radio interference test and the test of the sacrificial zinc sleeves.
Type B (for type A and B insulators see clause 9.1) ceramic insulators are submitted to a combined electric and mechanical load test instead of the pure mechanical failing load test, when the electric puncture is used to indicate a mechanical failure in the body. The *puncture voltage* depends on the temperature (Figure 9.14) both for ceramics as well as for glass.

Test of mechanical failing load
From the previous list, it can be seen that most of the sample tests, except for the puncture voltage withstand test connected with the insulator design, are mainly mechanical tests. These tests do not refer anymore to routine test load and minimum failing load, but to the *mechanical failing load*, due to the adaptation of the test standards for sta-

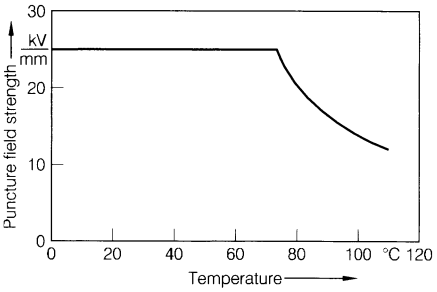

Figure 9.14: Influence of temperature on the puncture field strength of porcelain insulators

Tabelle 9.6: Quantities for sample tests according to EN 60 383-1

Quantity to be accepted (N)	Extent of samples E1	E2
$N \leq 300$	acc. to agreement	
$300 < N \leq 2000$	4	3
$2000 < N \leq 5000$	8	4
$5000 < N \leq 10000$	12	6

tistically verified *acceptance criteria.* Tests can be carried out as specified in IEC 60 575 [9.34]. All specimens pertaining to the quantity E1 mentioned before are then loaded up to their failing limit in order to obtain the average value and the dispersion of the failing loads. A sample is said to have passed if the average value of the failing loads is greater than or equal to the value of an established failing load plus an additional incremental value. This additional load is defined in [9.2] as the product of standard deviation and a coefficient for the statistical analysis in accordance with each test type and testing level. In case the sample test is not successful, a repetition test may be performed, which should also be statistically supported. To avoid misinterpretation, it is suggested to study the detailed example presented in Annex B of standard IEC 60 383-1 [9.2].

Temperature cycle test

The *temperature cycle test* for long rod insulators is defined as three 15 min heating and cooling cycles, each one followed by a tensile load amounting to 80 % of the specified failing load. This test can be considered as dispensed for modern densely fired insulators. Failures would be expected only in case of long insulator units or insulators with larger cross sections; in accordance with the standards, less stringent procedures can actually be agreed upon for such insulators.

Thermal shock test

In case of toughened glass insulators, the conditions for *thermal shock testing* are different from the procedure mentioned before. Microscopic inclusions of the fluid mass, not visually detectable, may play an important role especially when the coating of the furnace is just new or presents an advanced ageing process. In such cases, a statistically relevant increase of the *insulator failures* may be expected.

Puncture voltage withstand test

The *puncture voltage withstand test* is foreseen exclusively for puncture-susceptible ceramic type B insulators (for definitions see clause 9.1 and for glass cap-and-pin insulators. The single insulator unit is immersed in an insulating fluid having defined characteristics [9.2] and will be subjected to voltage application. However, punctures have never been observed throughout the author's long-term practice.

Porosity test

The *porosity test* was introduced in the past when ceramic products could not always be fired to a completely dense texture. Nowadays, with the aluminium oxide ceram-

ics, intrusion of a colouring component into the ceramic fragments can very rarely be detected.

Galvanization test

Fittings shall be tested with respect to uniformity and density of galvanization. The *magnetic testing* is standardized as a non-destructive and fast procedure delivering sufficiently precise results under observation of boundary conditions determined by ISO 2178. As a minimum value for casting and forging parts, an average *weight per unit area* of 600 g/m^2 (thickness approximately 85 μm) for all units and a value of 500 g/m^2 (approximately 70 μm) for each single specimen [9.2] applies. In case only one sample would not pass, a repeated testing may be carried out. In case the average value of each single specimen is satisfactory, but not the average value of all the specimens together, a decisive test needs to be carried out by means of a *gravimetric method* (EN ISO 1400). In critical cases, the uniformity of the zinc coating may be verified by immersion in a *copper sulphate solution* and brushing off in accordance with EN 60 672-2 [9.15]; however, an agreement between customer and manufacturer has to be made when placing the order. The repair of eventual *failures at the zinc coating*is allowed to some extent, but is not recommended. It should be performed only at uninstalled fittings. The results of the sample tests should be *certified* by the manufacturer for each lot supplied. In case other requirements of certification are asked for, they should be indicated in the purchaser's *project specification.*

9.6.2.3 Routine tests

The requirements of *routine tests* are stipulated in [9.2] as well. They are performed by the manufacturer at each single unit of the lot to be supplied and comprise for long rod and cap-and-pin glass insulators the following:

- Visual inspection for *glaze defects* at ceramic insulators or superficial defects at glass insulators,
- Mechanical test with 80 % of failing load applied for 1 minute at long rod insulators or 50 % of failing load for 3 seconds at glass cap-and-pin insulators,
- *Ultrasonic testing* of long rod insulators (optional).
- For ceramic type B insulators, a puncture voltage withstand test according to [9.2] has to be carried out.

In case of requirements for further routine tests due to the operational conditions, their details should be settled in the design specifications or be agreed upon together with the order.

The ultrasonic test is applied to check the serviceability of second hand insulators. Inclusions, cavities, density of firing and fissures in the porcelain of long rod insulators can be detected by ultrasonic testing with *impulse reflection analysis.* Ultrasound at a frequency of 1 to 5 MHz, that is to say, at porcelain with 1,1 to 5,3 mm wave length, is irradiated into the specimen. There, the absorption is measured by observation of the decaying *multiple echoes* or the *velocity of the sound wave*, that is the travel time between the transmitting impulse and the echoes from the rear surface. Efficient densely fired porcelain can be recognized by the power of the echoes or by the sound velocity. Separation of material, for example, cavities, porosity, cracks and similarities are clearly detectable when at least one echo from the rear surface can be identified and also when the defects reach one square millimetre measured perpendicularly to the direction of the radiation into the porcelain. Long rod insulators can be tested both transversally and longitudinally to the insulator longitudinal axis. The *angular ultrasonic test head* allows oblique radiation so that tests can be performed to verify occurrence of cracks or *disc-type fractures* inside the insulator cap at insulators provided with fittings. By

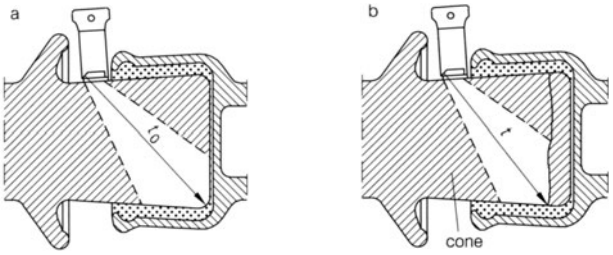

Figure 9.15: Testing of disc-type cracks in the cone within the cap with an ultrasonic angular test head
a) cone without defects
b) cone with crack

ultrasonic testing of insulators after the mechanical routine tests, it can be assured that no damage has been caused at the fitting cone of the insulator due to testing (Figure 9.15).

Line post insulators are relatively seldom applied at overhead power lines. They are tested in conformity with IEC 60 168 [9.35, 9.36] and will not be further discussed hereafter.

All the tests presented in clause 9.6.2 for ceramic cap-and-pin insulators apply also for cap-and-pin insulators of toughened glass according to [9.28]. A thermal shock test is added here as a sample test, whereas the electric test prescribed for the porcelain cap-and-pin insulator is not applied.

9.6.3 Tests on composite insulators

9.6.3.1 Basic information

Since it is not dealt with standardized designs, the characteristics and the suitability for the relevant application of composite insulators should be specifically proved in accordance with [9.22]. Composite insulators are type A insulators. Their testing is performed with single insulator units in conformity with the recommendations of IEC 61 109 [9.37].

9.6.3.2 Test of the structural design and type test

Differently from ceramic or glass insulators, an extensive *design test* is required by IEC 61 109 [9.37] prior to type testing. The design test is performed just once and serves to verify the adequacy of design, materials and manufacturing process. It is valid for a whole group of composite insulators, whose characteristics coincide within certain limits. To assure a satisfying life time under normal operating loads the influence of time upon both electric and mechanical characteristics as well as upon the insulators as a whole is considered. The following process is foreseen to test the structural design:

Test of the bonding surfaces and of load application by the fittings

- AC voltage test, dry;
- Dynamic impact tensile load release test;
- Thermo-mechanical test;
- *Immersion test*;
- *Impulse voltage withstand test*;
- Second AC voltage test, dry.

Test of the load-time characteristic of the rod

- Determination of the mean failing load of the rod equipped with fittings;
- Determination of the slope of the load-time characteristic of the insulator.

Test of the shed sheath with respect to leakage current traces and erosion under salt fog

The test lasts 1000 hours with a voltage of 1 kV per 34,6 mm creepage path under salt fog condition with a concentration of 10 kg NaCl per m^3.

Test of the rod material

- Test of porosity by colouring agents;
- *Water diffusion test*;
- Testing of bending strength and toughness.

Bending strength and toughness to impact load of *plastic materials* are established at the specimens with a size of 10 × 15 × 120 mm. A class of certain composite insulator types can only be qualified after all the test specimens have been successfully performed with the structural design test.

Test of pollution performance

Standardized procedures for testing composite insulators under *influence of pollution layers* do not exist at present due to the particular hydrophobic characteristics of the silicone surfaces.

Type test

The *type tests* serve to prove the rated characteristics which depend on the shape and dimensions of the composite insulator. The corresponding electric type tests are performed including the arcing protection fittings, if they are part of the insulator type. The type test consists of:

- Fast-front overvoltage withstand test, dry;
- AC voltage test, wet;
- Slow-front overvoltage withstand test, wet;
- Mechanical load-time test.

During the latter test, the specimen bodies are submitted to a tensile load of 70 % of the specified mechanical failing load for 96 hours, followed by another load amounting to 100 % and lasting one minute. Neither breaking of rods, nor pulling-off or breaking of the fittings may occur at the test specimens.

9.6.3.3 Sample and routine tests

Sample tests are performed with composite insulators in the same way as with other insulator types, using test quantities divided into two portions. After checking the dimensions of every unit a portion serves for the verification of the *specified mechanical load (SML)* and another portion of units serves to test the zinc coating and the function of fittings. Failure of one insulator or of a metallic component implies the repetition of the test series with an increased number of units in accordance with [9.37].

During the *routine tests* every insulator of a certain lot is tested with respect to:

- Identification: Type, manufacturing year, specified mechanical load;
- Visual test: Defects on the surface, colour, conformity with drawings;
- Mechanical routine tests: Tensile load with routine test load (at least 50 % of SML) for at least ten seconds.

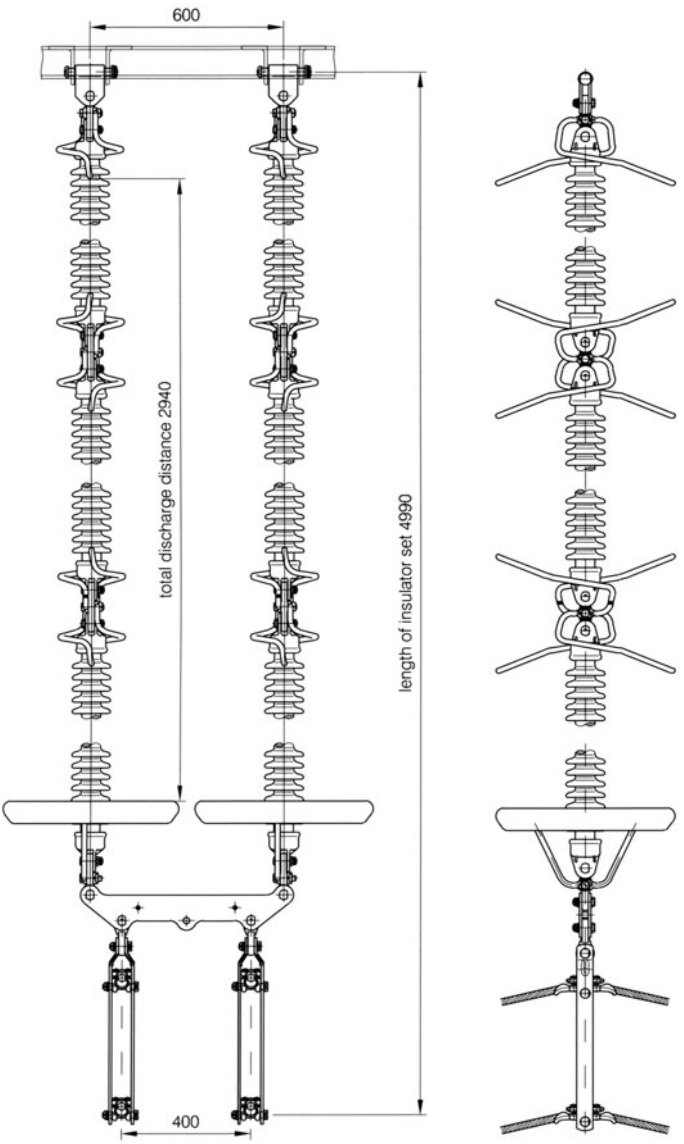

Figure 9.16: 420 kV double suspension insulator set for quadruple bundle (RWE Net AG, Germany)

9.7 Design of insulator sets

9.7.1 Suspension insulator sets

Suspension insulator sets can consist of one or more *insulator strings* composed of suspension insulators. *Multiple insulator sets* are applied where required by the operational loads as well as in other cases when a higher security is desired, e. g. at crossings. *Double insulator sets* are commonly used, in particular in densely populated areas. Their assembly as a double suspension set composed of long rod insulators is shown for a 420 kV highest operating voltage in Figure 9.16. In Figure 9.17 a single insulator set made of glass cap-and-pin insulators is presented as used for 550 kV lines in Brazil.

Double suspension sets can be arranged longitudinally or transversally to the direction

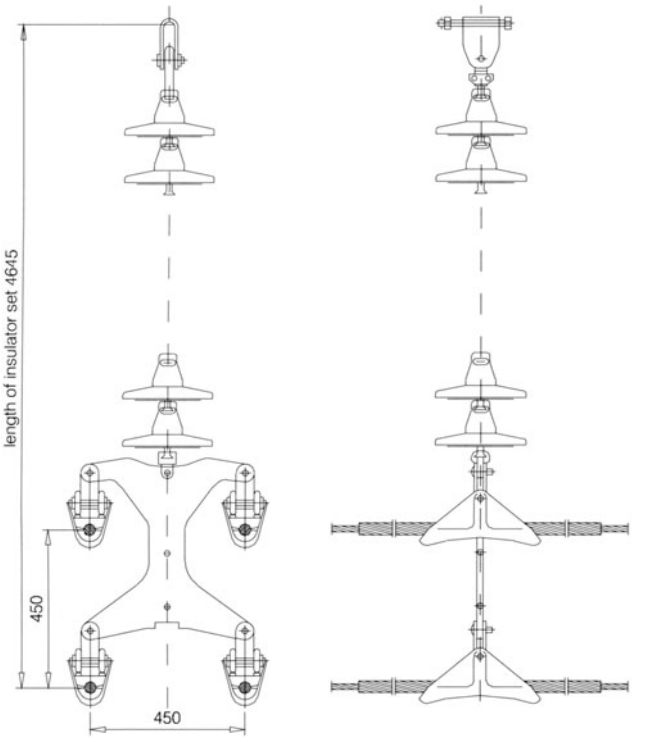

Figure 9.17: Single insulator set for a 550 kV line in Brazil

of the line. Insulators of double sets mounted longitudinally are less endangered by electric arcs than insulators of multiple sets that are transversally arranged, since the *magnetic field* caused by the short-circuit current circulating in the crossarm and the tower body pushes the arc outwards from the tower body [9.38]. Besides that, when the string swings due to the wind force, it is not distorted to a parallelogram, so that the components cannot clash. The insulator sets are less visible when arranged in line direction. On the other side, transversally arranged double insulator sets result in lower dynamic stresses to the remaining sound string in case of failure of the other one. Due to the accomplished advantages, double insulator sets are preferably arranged in line direction particularly when frequently loaded by high wind.

The individual insulator strings should be attached directly to the crossarms. The U-bolts, shackles or hinges used to attach the strings result in a universal mobility. In case of long rod insulators with clevis-type caps, the connection pins should be installed in line direction, because in this case the risk of a defective string to touch the intact one is low [9.39].

To protect the insulators from power arcs with temperatures ranging up to 12 000 K, the insulator strings can be equipped at both ends with *protective arcing fittings*, starting sometimes at voltages of 36 kV [9.38]. Long rod insulator strings composed of several units need additional *intermediate arcing protection fittings.*

The arcing protection fittings should form a ring around the insulator, to attract the *power arc base* as fast as possible in order to guide it to a defined *final burning position*, as well as to feed the power arc base from only one side and to allow for sufficient mechanical strength. The final burning position has to be formed and arranged such that the irradiated heat does not damage the insulators. The arcing protection horns should be installed at suspension sets such that the final burning positions are directed outwards from the tower.

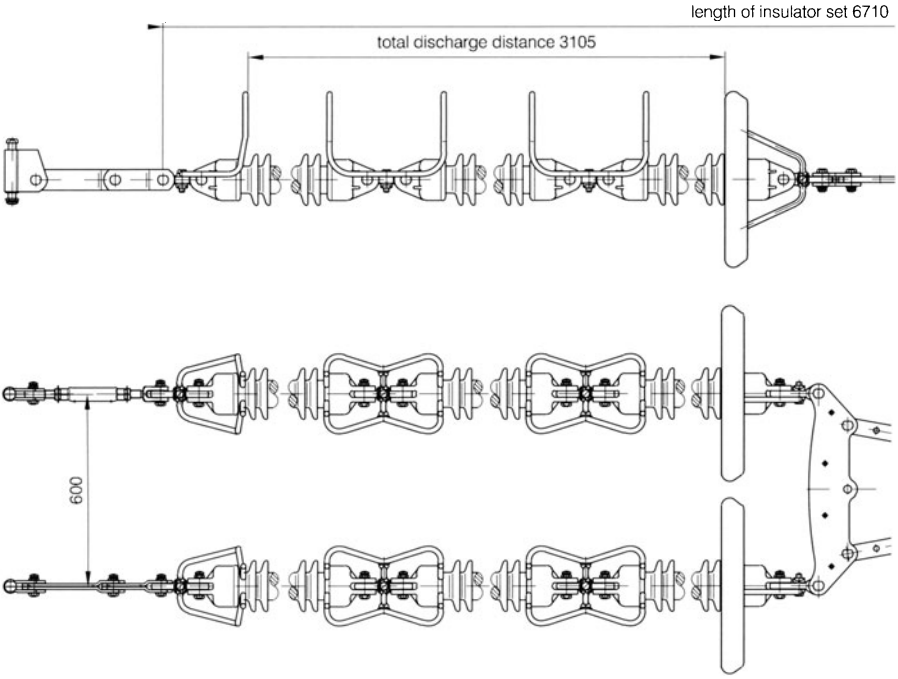

Figure 9.18: 420 kV double tension insulator set for quadruple bundle (RWE Net AG, Germany)

Cigré Study Committee 22 carried out an investigation on the use of protective devices for insulator sets [9.40]. According to this investigation, a majority of AC, HV and EHV lines is equipped with horns, rackets or rings. Some utilities in Europe and Japan use protective devices systematically, especially for insulator sets composed of long rod or composite insulators. The main purpose is to protect insulators and conductors from power arcs. In this case, protective devices are adopted irrespective of the voltage. Other utilities use protective devices depending on the voltage level, the main target being minimizing radio interference and improving the voltage distribution.

Utilities which do not equip their lines do so, because the keraunic level is low, the pollution is not severe and the duration of short circuits is too short or the power not high enough to cause failures. Moreover, they allege that protective fittings will reduce the effective clearances to structures, thus increasing the flashover probabilities.

The design of protective devices is based on the power arc ratings and radio interference criteria resulting in large differences between the various designs. Therefore, there are not generally applicable design criteria.

At transmission voltages higher than 220 kV, the arcing protection fittings should also take care of *electrical field control* at the live end of the insulator set to avoid undue *corona effects*. Efficient arcing protection fittings should, therefore, be selected with rather large surface radii to suit the transmission voltage levels. *C-shaped rings* fulfil this requirement [9.41]. *Bundle rings* with two partial electrodes reduce the voltage gradients. Besides that, the power arc base can move faster to the final burning position [9.38]. Raising the upper subconductor level by a correspondingly designed yoke as close as possible to the lower most insulator skirt equalized the electrical field and reduces the voltage gradient, thus precluding the use of protective fittings.

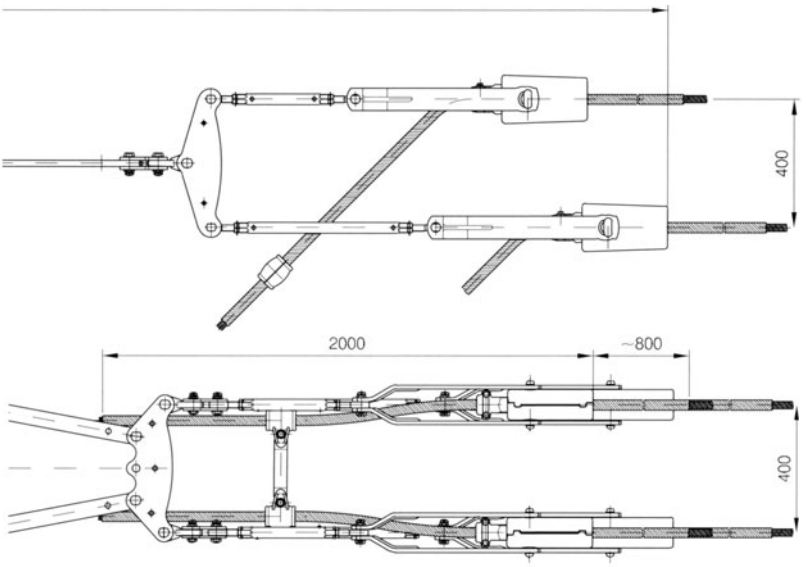

9.7.2 Tension insulator sets

To attach the conductors to angle, strain, section or dead-end supports, multiple insulator sets are used, whose insulator strings should be directly connected to the crossarm by means of *hinges* or *shackles*. The arrangement of a *double insulator set* for 420 kV rated voltage is shown in Figure 9.18. Figure 9.19 presents a quadruple tension insulator set for 550 kV in Brazil.

The information presented in the context of suspension insulator sets concerning *load transfer* after failure of an individual string applies as well for tension insulator sets. If long rod insulators with clevis-type caps are used they will be coupled by a universal joint (Figure 9.18). The dimension of the yoke plate in direction of the insulator set axis should be so large as to reduce impact loads after failing of an individual string. In case of triangular yoke plates, the height should be larger than the width.

A connection between conductor bundle and insulator set by *one pivot* only is advisable for bundle conductors since the failure of one insulator string will not alter the geometry of the bundle. On the other hand, a *trapezoidal yoke plate* leads to shorter design lengths of insulator sets and might be advantageous with regard to the load transfer. If the design and configuration of the yoke plates alone is not enough to limit the dynamic stresses on the long rod insulators, additional weights or *deformation elements* can be used [9.39, 9.41]. Protection fittings should be attached to the insulator strings so that the arcing burning positions are arranged upwards, since thermal effects push the power arc into that direction.

9.8 Requirements for insulator sets

9.8.1 Electric requirements for AC lines

According to their function, insulator sets need to be designed taking into consideration their *electric* and *mechanical strength requirements*. The insulators and the insulator

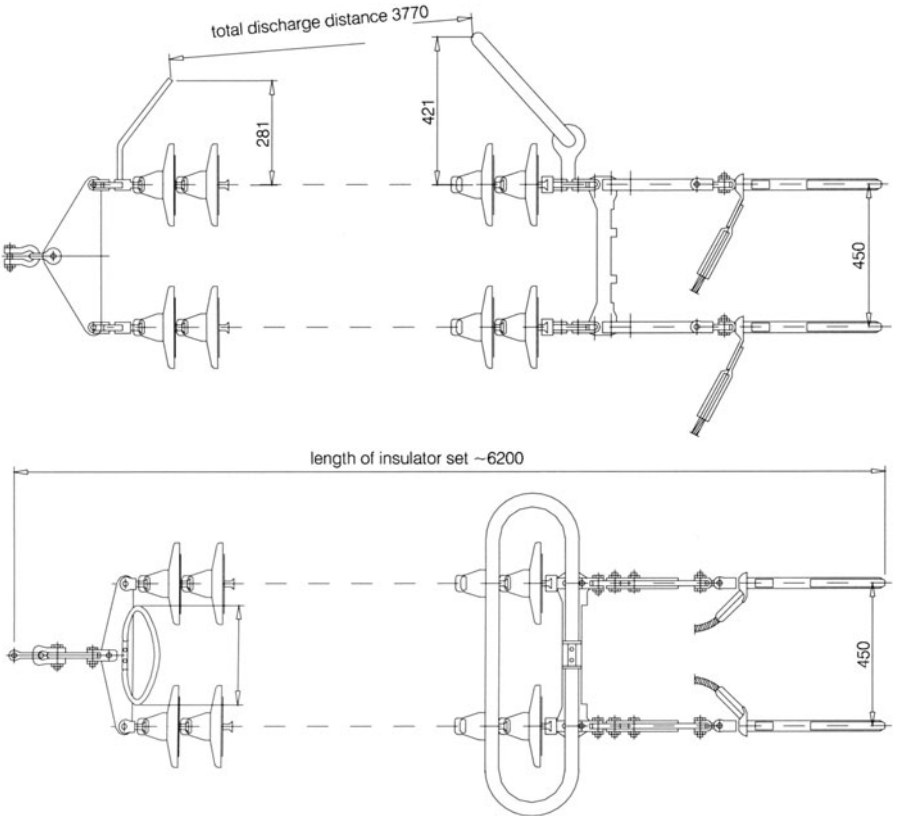

Figure 9.19: Quadruple tension insulator set for a 550 kV line in Brazil

strings should be designed in accordance with EN 50 341-1 [9.28] such that the required withstand voltages are achieved. In Table 9.7, these requirements are summarized depending on the voltage range and the insulator type.
The required withstand voltage levels are determined by an *insulation coordination study* for the overhead transmission system if such values cannot be assumed from existing installations. This process consists of the determination of the required withstand voltage U_{rw} which corresponds to the insulation level. Basic rules and guidelines are given and explained in details by IEC 60 071-1 [9.29] and IEC 60 071-2 [9.30], respectively. The procedure involves three steps as follows:

Determination of representative overvoltages
Power frequency voltages and insulation stressing overvoltages are determined through *network analysis* taking into account their amplitude, wave form and duration. The required total creepage distance is determined also by the pollution level encountered along the line. Thus the required length of the insulator sets as well as the necessary profile and type of individual units need to be selected with respect to the pollution level. Where insulator sets swing under wind action, the *air gaps* should be determined under moderate and extreme wind conditions as well.
Representative overvoltages U_{rp} include:

- Steady-state *operating power frequency voltages* identical to the highest system voltages under normal conditions;

Table 9.7: Electric requirements on insulator sets according to EN 50 341-1

Stipulated requirements	Highest system voltage 45 to 245 kV		Highest system voltage > 245 kV	
	Cap-and-pin insulators	Long rod and composite insulators	Cap-and-pin insulators	Long rod and composite insulators
Power frequency withstand voltage, wet	×	×	—	—
Fast-front withstand voltage, dry	×	×	×	×
Slow-front withstand voltage, wet	—	—	×	×
RIV test [1)]	×	×	×	×
Pollution [1)] performance test	×	×	×	×
Power arc test [1)]	×	×	×	×

[1)] Optional tests to be agreed upon

- *Temporary overvoltages* due to earth faults, switching operations, load rejection or non-linearities of relatively long duration (1 minute);
- *Slow-front overvoltages* due to earth faults, switching operations or far distant lightning strokes. The overvoltage stresses are characterized by the standardized 250/2500 μs *switching shape impulse* and a representative amplitude;
- *Fast-front overvoltages* through direct lightning strokes on the conductor or back flashovers. The voltage stress is characterized here by the standard 1,2/50 μs *lightning impulse shape* and a representative amplitude.

In IEC 60 071-2, clause 2 and EN 50 341-1 [9.28], Annex E, recommendations for the determination of representative overvoltages are presented (see clause 2.4.5).

Determination of the insulation coordination withstand voltage

The definition of the *insulation coordination withstand voltage* U_{cw} is based on the determination of the lowest insulating withstand voltage value. Recommendations are given in IEC 60 071-2, clause 3 [9.30]. The effects of power frequency voltages and of overvoltages stressing the insulation are taken into consideration as well.

The rated phase-to-earth voltage defines the required minimum length for an insulator set in case of systems with low resistant neutral earthing or earth fault factors $\leq 1{,}3$. Temporary overvoltages need to be considered when the earth fault factors are higher or in case of isolated-neutral or resonant-compensated systems. In case of pollution, the insulator profile should be accordingly selected so that the polluted insulators can withstand the highest operating power frequency voltage with a reasonably low *flashover probability.*

Slow-front overvoltage is one of the parameters that affect the insulating distances in systems above 245 kV. The insulator fittings may become crucial in some cases when determining the air gaps of insulator sets (see clause 2.5.1.2). The *coordination withstand voltage* or the corresponding basic surge insulation level (BSIL) can be determined either *deterministically* or *statistically* in accordance with [9.30].

In case of fast-front overvoltages, the coordination withstand voltage or insulation level BSIL can be assumed as being at least equal to the overvoltage value that may occur due to a lightning stroke at the site and migrating over a few adjacent supports only.

Determination of the required withstand voltage

The *required withstand voltage* U_{rw} is evaluated through the division of the coordination withstand voltage U_{cw} or insulation level BSIL by an *altitude factor* which depends

again on the magnitude of the coordination withstand voltage. This altitude factor is given by EN 50 341-1 [9.28], Annex E.2.1.4, Table E.4.
Taking into consideration that standards for insulators establish the dimensions of the insulator units without reference to the highest voltage for equipment or the maximum system voltage, the insulation coordination process for overhead insulators may stop here. Selection of a *design voltage* is not required.

Radio interference strength (RIV)
Radio interference voltage (RIV) and the corona extinction voltage are also essential for rating the insulator strings. The *radio interference levels* generated by any type of overhead line insulators under test conditions should be in conformity with the total radio interference level specified for the transmission line installation; the visible *corona extinction voltage* should be stipulated before carrying out tests. Radio interference can be generated within a large frequency band and originates from discharges or from flashovers at heavily loaded insulator components or from defective contact points, for example, at ball-and-socket connections of cap-and-pin insulator strings under low tensile load. Strings of *long rod insulators* show a better performance with respect to *radio interference* when compared with cap-and-pin insulators. CISPR 18-2 [9.42] explains how the *limit values* can be obtained to ensure good radio and television reception. Papers [9.43] and [9.44] contain details on RIV levels and testing.

Pollution
Insulator strings should also satisfy certain requirements of performance under pollution. Four *levels of pollution* are qualitatively defined in Table 9.8 obtained from [9.30] including a description of corresponding environments, from which an assessment of the existing pollution effects to be expected on an individual line can be performed. If experience from existing transmission lines is not available, IEC 60 815 provides information for a quantitative evaluation of local pollution levels through measuring procedures. IEC 60 815 [9.17] gives guidelines for the design and the selection of insulators to be applied in polluted areas; IEC 60 507 [9.45] indicates the corresponding test procedures. Experience about insulator performance under pollution can be found in [9.46].

9.8.2 Particularities for DC lines

Insulation in DC lines – generally named as *HVDC systems* (High Voltage Direct Current) – is stressed by lightning overvoltages, fault-induced overvoltages and operating voltages. The first two types of voltage stresses are applied primarily to design the *insulator string length* and *arcing distance*, while the latter affects the selection of the creepage distance, consideration being given to pollution conditions of the line route. Fault induced overvoltages in DC systems are usually appreciably lower than switching surges in AC lines, as a consequence of the attenuation in the converter station.
Temporary overvoltages or slow-front overvoltages are usually not significant in HVDC systems. Such overvoltages, of a transient nature, are almost exclusively caused by surges induced on a healthy pole by an earth fault on the other pole of a bipolar line. This type of surge reaches usually a moderate magnitude of not more than 1,7 p.u., what is appreciably less than a typical AC switching surge.
Most of *fast-front overvoltages*, are caused by *lightning*. DC line behaviour is similar to that of AC lines, but the insulator string length that is adequate for operating voltage normally ensures a sufficient lightning performance of the line.
Therefore, as a consequence of lower insulation requirements on the string length due to fast-front and slow-front overvoltages, the insulator capability to withstand operating

Table 9.8: Pollution levels and recommended minimum nominal specific creepage distance according to IEC 60 071-2 and IEC 60 815

Polution level	Examples of typical environments	Minimum nominal specific creepage distance mm/kV AC[1)]	DC[2)]
I Light	– Areas without industries and with low density of houses equipped with heating plants – Areas with low density of industries or houses but subjected to frequent winds and/or rainfall – Agricultural areas [3)] – Mountainous areas All these areas shall be situated at least 10 to 20 km from the sea and shall not be exposed to winds directly from the sea [4)]	16,0	30,0
II Medium	– Areas with industries not producing particularly polluting smoke and/or with average density of houses equipped with heating plants – Areas with high density of houses and/or industries but subjected to frequent winds and/or rainfall – Areas exposed to wind from the sea but not too close to the coast (at least several kilometres distant [4)])	20,0	40,0
III Heavy	– Areas with high density of industries and suburbs of large cities with high density of heating plants producing pollution – Areas close to the sea or in any case exposed to relatively strong winds from the sea [4)]	25,0	50,0
IV Very heavy	– Areas generally of moderate extent, subjected to conductive dusts and to industrial smoke producing particularly thick conductive deposits – Areas generally of moderate extent, very close to the coast exposed to sea-spray or to very strong polluting winds from the sea – Desert areas, characterized by no rain for long periods, exposed to strong winds carrying sand and salt, and subjected to regular condensation	31,0	70,0

Note 1: This table may only be used for glass and porcelain insulators. It does not consider special environmental conditions like snow and ice with high pollution, heavy rainfall, desert areas etc.

Note 2: In very lightly polluted areas, specific nominal distances lower than 16 mm/kV can be used depending on service experience. 12 mm/kV seems to be a lower limit. For Central European conditions such a specific creepage distance cannot be recommended.

Note 3: In the case of exceptional pollution severity, a specific nominal creepage distance of 31 mm/kV may not be adequate. Depending on service and/or on laboratory test results, a higher value of specific creepage distance can be used, but in some instances the practicability of washing or greasing may have to be considered.

1) Ratio of the leakage distance measured between phase and earth over the rms phase-to-phase value of the highest voltage for the equipment.

2) Ratio of the leakage distance between pole and earth over the voltage between pole and earth, value according to international practice, not standardized in IEC 60 071-2 or IEC 60 815.

3) Use of fertilizers by spraying, or the burning of crop residues can lead to a higher pollution level due to dispersal by wind.

4) Distances from sea coast depend on the topography of the coastal area and on the extreme wind conditions.

voltages will be the governing factor for the design under all pollution levels. The rate of *contaminant deposition* on HVDC lines is several times greater than that occurring on AC lines [9.47, 9.48]. Therefore, the pollution level, which is reached after cycles of contaminant deposition and of washing by rain, is significantly larger for DC insulators than for AC insulators (even 10 to 100 times larger). Consequently, it is advantageous to use insulators with long creepage distances, to keep insulator strings as short as possible. In Table 9.8, recommended specific creepage distances are shown for DC lines different *pollution levels.*

Regarding insulator types, due to the high degree of pollution protection required, *anti-fog cap-and-pin insulators* having a ratio between creepage distance and spacing (height) in the range of 2,8 to 3,2 have been found to be well suited in HVDC lines as well as *composite insulators* with water-repellent features. *Self-cleaning properties* of the insulators are important in case of DC lines. The leakage current density will be highest near the pin of a cap-and-pin insulator and causes effective drying. The surface voltage gradient may become very high there, although the NaCl deposit is high. To avoid insulator failing, a *zinc sleeve* can be placed around the pin as a sacrificial electrode. Definitions, test methods and acceptance criteria are specified in EN 61 325 [9.49].

The non-linear *deposit distribution* along the insulator string is caused by the forces acting on the particles in the air surrounding the string. There are forces due to wind, gravitation and electric forces on charged or uncharged particles in a non-uniform electrical field. Therefore, under the influence of an uni-directional electrical field, both charged and uncharged particles in the air surrounding a DC string are set into motion and attracted specially at the energized and earthed end of the string where the electrical field strength is highest. The random deposit distribution causes a non-linear *voltage distribution* along the string, which, to a certain extent, reduces the discharge voltage.

To reduce the insulator pollution and to improve deposit distribution along the string, *potential grading rings* can be mounted at the top and bottom end of the insulator string. The electrostatic field around the insulators will then change such that the gradient voltage will be highest on the surface of the ring itself. Consequently, the particles will move to that ring instead of the insulator.

The reduction in insulator pollution by use of *collector rings* is greater at positive than at negative polarity. Also, the influence of potential grading rings is stronger on pollution at the undersurface of the insulating elements than at their upper surface.

Application of coatings, such as *silicone grease*, on the insulator is another means for reducing the effect of pollutant accumulation on the flashover voltage. Grease coatings 0,5 to 2,0 mm thick have been applied with good results. The application of *GFC insulators* with sheds made of silicone rubber (see clause 9.4) has proved to be advantageous in pollution-prone sections of HVDC lines.

The *DC nominal voltage* refers to positive or negative pole voltage, that is comparable to peak value of AC phase-to-earth voltage, and the leakage distance requirements are similar in both cases, as it can be seen in IEC 60 815 [9.17]. However it should be recognized that DC lines are more prone to accumulate pollutants than AC lines. As a guideline in light polluted regions, a figure of 30 mm/kV can in principle be adopted for the preliminary insulator string design of a DC line. A maximum pole voltage 5 % higher than the rated DC voltage should be considered in the insulation design.

9.8.3 Audible noise (AN) performance

Design specifications may require the insulator strings to accomplish performance with respect to audible noise (AN) although it is known that only from a 400 kV voltage level upwards corona noise is important and that corona effects are crucial only under

foul weather conditions. Aeolian noise caused by laminar winds through the insulator skirts can only seldom be observed at glass cap-and-pin insulators. This special form of noise cannot be predetermined by tests and is not specifically addressed here.

9.8.4 Mechanical design

In principle, the rated mechanical failing load of the insulator selected needs to be higher than the value obtained by multiplying the maximum occurring mechanical load by a partial factor. The mechanical load of multiple insulator sets is obtained by distributing the load on the individual insulator strings.

For tension insulator sets, the maximum load should be obtained from the conductor tensile load occurring under one of the following conditions:

- Temperature −20°C without ice load or
- Temperature −5°C with ice load or
- Temperature −5°C with ice and wind load or
- Temperature +5°C with wind load.

For suspension insulator sets and line post insulators, the maximum load has to be considered, which results from the most unfavourable combination of conductor weight, ice load, wind action and the horizontal conductor tensile forces as stipulated in standards or project specifications. Line post insulators should not be used for angle, strain or dead-end supports.

The *design load* of an insulator set is the total load resulting from the multiplication of each of the permanent and variable loads and conductor tensile forces by partial factors on the load side or from the ultimate load. The partial factor is 1,35 according to [9.22] as an example. Additionally, a *partial factor for material* has to be considered for the mechanical design of the insulator set. In EN 50 341-1, this factor is specified as 2,0 independently of the insulator type. Deviating higher factors can be stipulated in national standards or project specifications.

For *multiple insulator sets* consisting of n strings, the maximum permissible load may at maximum be n-times as much as the permissible load of a single insulator set. A *distribution of the total load* stressing a multiple insulator set as uniform as possible on the individual insulator strings should be aimed at in this case.

The design of the insulator set should ensure that in case of *failure of one insulator string*

- An as far as possible uniform distribution of the total load along the remaining sound insulator strings is assured;
- The partial factors for material corresponding to the insulators under tensile load may be reduced appreciably;
- The dynamic forces and moments should be counteracted in order to avoid the failing of the remaining strings by the occurring load transfer. Otherwise, the aim of adopting multiple strings would not be achieved, that is, to support the conductors even after the failure of an insulator or of an individual string. This can, for instance, be guaranteed by an adequate design of the yoke plates. The mechanical design of the associated fittings is treated in clause 10.4.3.

9.9 Operational performance of insulator strings

9.9.1 Introduction

Overhead line insulators are stressed by both the applied electric voltage and the mechanical loads. The *insulating capacity* of the insulators is specially influenced by pollution which, together with humidity, can lead to conducting superficial layers. The in-service performance of the insulators depends also on their *arrangement* either in

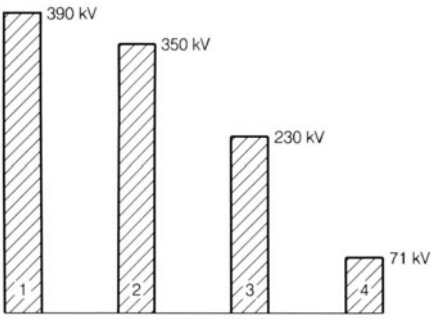

Figure 9.20: Voltage stress of a 123 kV long rod insulator.
1 power frequency flashover voltage, dry;
2 power frequency flashover voltage, wet;
3 power frequency withstand voltage wet, according to IEC 60071-1;
4 phase-to-earth voltage for $U_s = 123$ kV

suspension or in dead-end position and on the *self-cleaning processes* caused by rain or wind. Operational reliability and security are determined mainly by the electric stress on polluted insulators.

9.9.2 Voltage stresses

Overhead line insulators experience different electric stresses. The phase-to-earth voltage is permanently applied between the conductor and the earth, corresponding to $(1/\sqrt{3})$ times the phase-to-phase rated power frequency voltage. Lightning strokes cause overvoltages for some microseconds. Switching operations cause overvoltages in the time range of milliseconds. In case of an earth fault in resonant earthed systems, the phase-to-phase voltage can act between the conductor and the earth along the insulator for approximately 10 seconds.
In Figure 9.20, the power frequency flashover voltage, dry, the power frequency flashover voltage, wet, the power frequency withstand voltage, wet, and the phase-to-earth voltage of a 110 kV insulation are compared.
In case of *pollution layers* showing high conductivity, insulators can be subject to flashover already at operational phase-to-earth voltage. Thus, the actual power frequency flashover voltage will only be approximately 20 % of the power frequency flashover voltage of the clean, dry insulator. Therefore, both the wet and the dry *power frequency flashover voltages* of the clean insulator do not have much importance in practice. The influence of the pollution layer should always be taken into account when the stresses due to operational voltages are assessed.
Every insulator presents two metallic fittings which, together with the insulator body as the *dielectric*, possess a capacitance. The *partial capacitance* of the individual insulator units and the individual shells as well as the capacitances to earthed parts and to conductors influence the *voltage distribution along the insulator.*
In Figure 9.21, the voltage distribution is shown along a cap-and-pin insulator string and along a long rod insulator. These distributions are similar. Along one third of the insulation on the live end, the decrease in voltage is about 55 %, while the remaining voltage is distributed along the other two thirds. The voltage drop at the live end is influenced by the conductor configuration. In addition, *potential control rings* and the arrangement of subconductors help to reduce the voltage stresses on the insulator string to such an extent that a smooth voltage drop is obtained.
The leakage current through the insulator capacitances is low. Under practical operation, pollution causes a *conducting pollution layer* resulting in a *surface current* much higher than the *capacitive current.* During operation, the voltage distribution along the insulator string is practically determined by the *ohmic surface resistance.* In Figure 9.22, the voltage distribution is presented along a ten-unit insulator string, under both low and high humidity levels. It can be seen that the voltage decreases uniformly

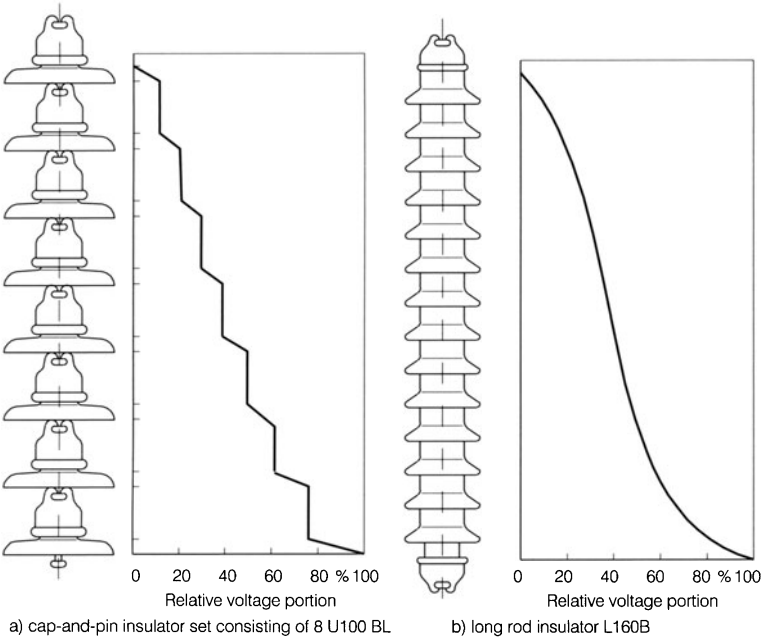

Figure 9.21: Voltage drop along a cap-and-pin insulator set and a long rod insulator

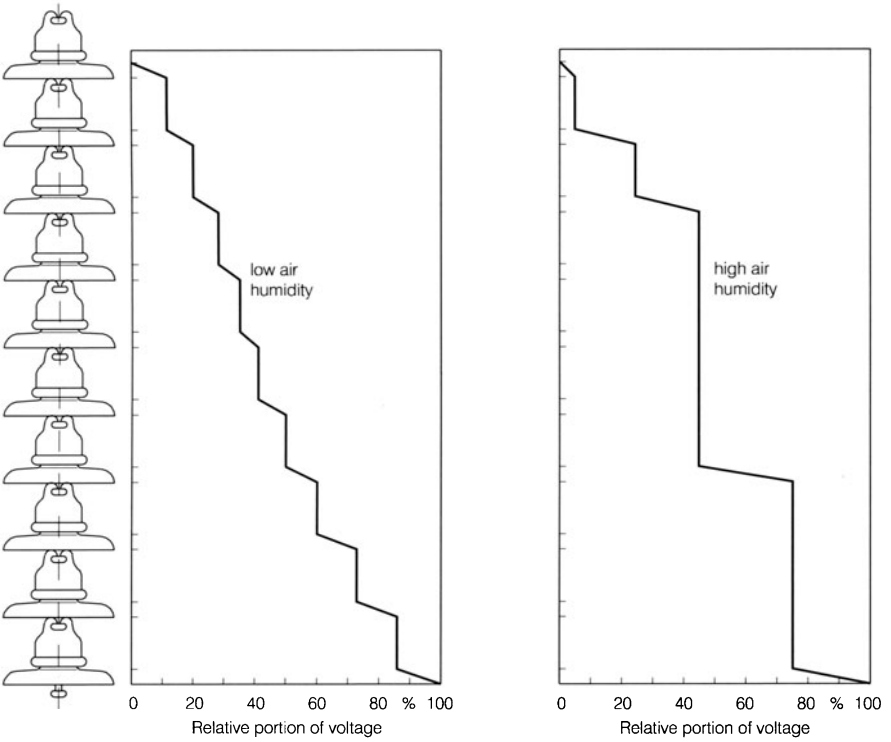

Figure 9.22: Voltage drop along an insulator string for differing air humidity

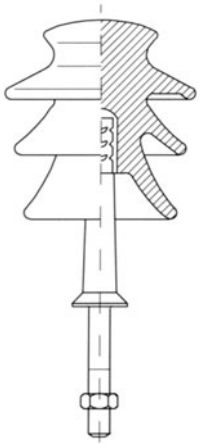

Figure 9.23: Non-puncture-proof line post insulator according to DIN 48 004

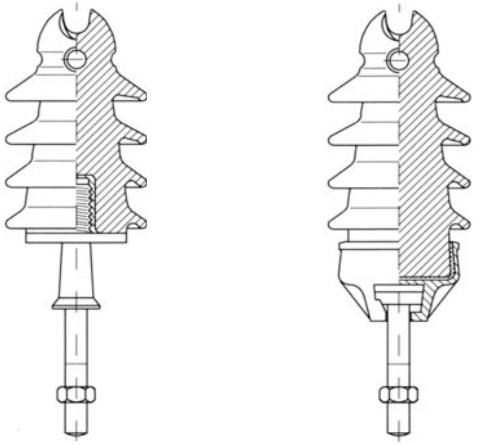

Figure 9.24: Puncture-proof line post insulator

due to low conductivity under low humidity conditions. On the right side of the figure, larger differences of the conductivities cause the voltage to decrease only over some insulator units. Due to the high conductivity of the pollution layer, the remaining insulators do not contribute to the insulating capacity of the string. This is also the reason for the sharp decrease of the flashover voltage under pollution.

As a consequence of the decrease in voltage along individual insulator caps due to pollution, the affected units can experience puncture and, therefore, damage of the relevant units. To a lower extent, long rod insulators can also present a non-uniform voltage distribution under pollution. Since they are puncture-proof, they are less endangered under such conditions.

The non-uniform voltage drop can result in *compensating discharges* that are accompanied by *high-frequency interference* and undesired *RI-noise levels*. If the surface current is not limited by the resistance of the remaining insulating path, those partial discharges can develop into a *complete flashover* with a power arc.

9.9.3 Behaviour of individual insulator types

Non-puncture-proof types (Figure 9.23) as well as puncture-proof types of line post insulators (Figure 9.24) are used. Flashovers due to lightning strokes on medium-voltage networks can cause damage to non-puncture-proof insulators which is not directly visible, but may lead to failures later on. Thus, puncture-proof insulators should be rather used for operational reasons. The rigid fastening of the conductors to the line post insulators does not allow the compensation of the unbalanced loads that occur as a consequence of differing ice accretion on the conductors. These loads lead to relatively high loads on the insulators. The *bending resistance* of the insulators and their supports is usually limited; thus, the use of line post insulators is restricted to low loads.

Large birds may alight on the crossarms of medium-voltage overhead lines, in a dangerous proximity to the live line in case of pin-type insulators. As a result, flashovers could be caused with lethal consequences for birds as reported in some cases. Suspension insulators prevent such occurrences. Even the relative short insulator length corresponding to the low operating voltage allows the compensation of the unbalanced loads, thus decreasing the loads on the supports. Large birds are then better protected. Suspension insulators require longer poles than line post insulators and are deflected

under wind, so that the right-of-way might be wider.

Networks operating at 90 kV or higher voltages use exclusively suspension insulators for the straight line sections. In Central Europe, the long rod insulator is preferred, while either the porcelain or the glass cap-and-pin insulators are favoured outside that region. The assessment of the various aspects of performance of those insulator types is not unanimous. This is caused by different operational requirements of the networks, so that also in areas having the same climate differing experience is gained. Meaningful comparisons can only be obtained when both types of insulators are installed in parallel on an overhead line section. But this is a rare case.

From an operational point of view, the *performance of the insulators under pollution* is their most important feature. Pollution leads to a non-uniform voltage distribution along the insulators as explained in clause 9.9.2. This can result in flashovers or damage to the individual cap-and-pin insulators. The complete insulator path is always effective in case of puncture-proof long rod insulators; therefore, shed damage due to pollution cannot occur. Power arcs originated, for instance, from atmospheric overvoltages can cause the cap-and-pin insulators to puncture. Toughened glass cap-and-pin insulators always possess internal stresses or microscopic impurities from the melting process, which may lead to a sudden loss of the shed during operation. The *creepage currents* flowing on the surface erode it, thus building up a potential reason for the destruction of sheds [9.50]. As a consequence, much more cap-and-pin insulators than long rod insulators fail [9.51]. That is the reason why in regions where the cap-and-pin insulators are used in radial networks, which do not allow the disconnection of a line, methods were developed for the cap-and-pin insulators to be substituted under live-line conditions [9.52]. This expensive maintenance is not necessary when long rod insulators are applied. In Central Europe, the *labour safety legislation* does not permit this maintenance technology.

The *surface currents* on polluted insulators represent only an active power loss of about 1 thousandth of the total loss, which is mainly formed by ohmic losses. The losses due to surface currents can thus be neglected.

Long rod insulator surfaces are less structured and can thus be cleaned by both rain or wind. In many cases where this *cleaning effect* is definitely needed, long rod insulators are preferably applied. They can also be cleaned by water jet as well as by other methods.

Regarding pollution, insulators have a different performance depending on the arrangement in suspension or in dead-end position. Insulators in dead-end positions are more effectively cleaned. Therefore, according to practice of some utilities, the required creepage path can be reduced by 10 % compared with insulators in suspension position.

Corona discharges on the insulator surfaces and sparking discharges at low-conductive interconnections of the insulators cause high-frequency interference. Since the magnitude of these interference depends on the number of the interconnections between the insulators, the larger the number of individual cap-and-pin insulators, the more extended the interference will be. Long rod insulator strings have few individual elements, thus limiting the possibility of *cascade arcing.*

Even after the failure of a toughened glass cap-and-pin insulator body, its mechanical strength is maintained, although to some reduced extent. This decreases the risk of failure of the total insulator string caused by flashovers or vandalism to be feared in some areas. In any case, long rod insulators are much more difficult to damage than the shells of cap-and-pin insulators. Any cap-and-pin insulator string is not unlimitedly failure-proof at all. According to statistics, approximately the same relative quantity of long rod insulator strings is completely destroyed by all kinds of reasons as cap-and-pin insulator strings by power arcs.

9.9.4 Behaviour under pollution layers

9.9.4.1 Formation of pollution layers

The air in all regions of the world contains solid or dissolved substances that can precipitate on the insulators. Coastal *saline pollution*, diverse kinds of *dust* in industrial areas as, for example from cement mills, steel mills or from power plants, desert sand, all of them can have components which are highly conductive when moistened. In agricultural areas, fertilizers can be carried by the wind and precipitate on the insulators. All these solid or fluid precipitation can build up *pollution layers* on the insulator which become conductive under moist conditions, thus reducing the insulating capability. Insulator behaviour in the presence of such pollution layers has a decisive significance from the standpoint of reliable operation. For this reason, the evaluation of the expected pollution stresses is important for every transmission line, just as the selection of a corresponding insulation. An extensive literature exists on the subject of *pollution performance*. Paper [9.53] should be mentioned here.
Diverse factors influence the formation of the pollution layers and the flashovers they give rise to. They are as follows:

- Type and quantity of solid, liquid or gaseous materials in the air, together with forces which affect the movement of such materials or particles,
- Insulator shapes and conditions that determine the adhesion of the materials or particles on the insulator surfaces as well as the possibility of *self-cleaning* by wind or rain,
- Moistening of the pollution layers through light rain or dew.

Pollution layers on insulators have no damaging effect as long as they remain dry and thus practically non-conductive. Light rain or humidity, which causes the layer to be conductive and does not wash the particles out, strongly reduces the insulating capability, and causes a steady and heavy increase of the surface current on the insulator. At the spots with the largest current densities, the water is partially vaporized. *Partial arcs*, are formed at the drying spots and extinguish again in general. With the decrease of the resistance of the remaining humid pollution layer, the current increases again. Flashover occurs on some individual insulators, later developing to a flashover of the complete insulator set.

9.9.4.2 Simulation of pollution layers

Growing problems involving the behaviour of insulators under pollution gave rise to studies which began in the 1930's, concerned with laboratory analysis of the behaviour of insulators affected by pollution. These studies resulted in test procedures in the 1950's, with standardized artificial pollution layers for the assessment of the insulator behaviour. A certain test procedure was developed in Germany, which consists of applying *kieselgur* or *brine* to form a *solid pollution layer*. The *surface conductivity* of a completely moist square part of that layer was applied as a quantity characterizing the degree of pollution for which diverse types of insulators were comparatively tested. It aims at determination of the conductivity for which, at operation voltage, a selected insulator experiences flashover, or determination of the conductivity which a given insulation can withstand.
International investigations used other methods as, for example, salty water spraying on insulators which formed a *liquid pollution layer*. The *salt concentration* for which the insulator still supports a certain voltage (withstand voltage) or has a 50 % probability of flashover (critical voltage), is the characteristic value for the evaluation of the insulator resistance to pollution layers. The salt concentration under which the insulator supports a given voltage is called *withstand salinity*.

Table 9.9: Withstand levels of pollution layers corresponding to the four pollution levels according to IEC 60 815

Pollution level	Solid pollution layer		Liquid pollution layer
	Withstand layer conductivity in μS	Withstand salt deposite in mg/cm^2 (NaCl)	Withstand salinity in kg/m^3
I Light	15 to 20	0,03 to 0,06	5 to 14
II Medium	24 to 35	0,10 to 0,20	14 to 40
III Heavy	36	0,30 to 0,60	40 to 112
IV Very heavy	—	—	> 160

Both test procedures with solid or liquid pollution layers are used today to evaluate the withstand voltage characteristics of overhead line insulators made of ceramics or glass in accordance with IEC 60 507 [9.45]. Up to now, composite insulators have no standardized test procedures for pollution performance because of the hydrophobic behaviour of their surfaces.

9.9.4.3 Pollution levels

Based on findings from laboratory studies on the insulator behaviour under pollution and by means of comparison of results obtained from lines, four *pollution levels* were defined, ranging from light to very heavy pollution; suggestions for the *minimum creepage distances* were also given, referred to phase-to-phase voltages in case of AC applications (Table 9.8). These specific *pollution levels* were associated to characteristic values taken from the laboratory studies as conductivity of the layer in case of solid pollution layers and as withstand salinity for the liquid pollution layers. In Table 9.9 this correlation is shown.

In accordance with [9.17] (Table 9.8), areas with *light pollution* level are those without industries and without houses. They are mainly agricultural areas, which are regularly subject to rainfall and wind. They should not be directly at the seaside.

Medium pollution is given in areas described as those with industries not producing particularly polluting smoke or those areas with an average density of houses. Frequent rainfall and wind are assumed as occurring.

Heavy pollution appears in areas with high industrial density, in the surroundings of large cities and close to the sea coast.

Very heavy pollution can exist in the immediate neighbourhood of the sea, where insulators can be subject to seawater-spray and in desert areas characterized by no rain for long periods, exposing insulators to strong winds carrying salt and sand, and subject to regular moistening by dew.

In some areas nearly no or *very light pollution* occurs. Areas in mountains and forests remote from industries with enough rain are within this category. There, a specific creepage distance less than that for level I can be applied if validated by experience (see Table 9.8).

In Table 9.9, the correlation of a specified *pollution level* is shown with withstand level obtained from insulator tests using artificial pollution layers.

9.9.4.4 Assessment of pollution levels by means of local measurements

Local pollution of insulators can be assessed by in-situ measurements. IEC 60 815 [9.17] mentions five procedures. They require, on one side, long-term observation and, in some cases, also expensive measuring devices, and, on the other side, still some difficulties exist to correlate the results with the expected stresses caused by the pollution layer. Often, measurement results are not available for regions where overhead lines are to be

constructed or there is no sufficient period of time to perform them. For this reason, the suggested procedures have not reached practical significance, when the correlation of a certain pollution level to a determined future overhead line route is needed. Therefore, they are just mentioned here, without any details about the procedures and the evaluation processes:

- *Measurement of the volume conductivity* for the pollutant, collected by means of collecting gauges;
- Determination of *equivalent salt deposit density* on the insulator surface (ESDD method);
- *Measurement* of the total number *of flashovers* on insulator strings of various lengths;
- *Measurement of the surface conductance* of test insulators;
- *Measurement of the leakage current* of insulators subject to service voltage.

9.9.4.5 Measures to maintain insulation capacity

Although the possibility of pollution layers affecting the insulation behaviour is usually taken into account during design and selection of the insulators, it may happen that the insulation capability cannot be achieved unless *insulation maintenance measures* are taken to prevent occurrence of flashovers. Because of that, several methods have been developed, especially for switch-gear installations, which care for the increase of the resistance against pollution layers or for the restoring the insulating capability.

These measures can be carried out either regularly or after deposition of critical pollution layers. The method described in [9.54] has proved to be efficient for the indication of such critical levels.

If it is known that the critical pollution condition is restricted to a determined period over the day, for example, in the early morning due to dew, the reduction of the operational voltage by 20 % of its rated value proves to be efficient [9.54]. This method has been occasionally applied for installations close to the sea coast. Loose or lightly adhesive pollution layers can be removed by *spraying the insulators* under live-line condition. Water conductivity should be low here. Special nozzles should be used [9.54] and minimum distances must be observed. If applied under live conditions, there is the risk of flashovers because of possible increase of water conductivity caused by salt deposits on the insulators, which could expose the personnel to danger. The *insulator washing* should then be repeated in determined time intervals, obtained from the experience with this method [9.55] and [9.56]. Preferably, the washing should be applied when the line is switched off, so that the maximum efficiency of washing is achieved. In this case, the water conductivity is not a problem.

Hand cleaning cannot be avoided when the pollution layers are extremely hard and strongly adhering to the insulators. Special scrubbing devices or steel wool is used to remove the solidly adhesive layers. Application of thin layers of *silicone-based grease* prevents the formation of a continuous water film on the insulator surface. This improves the insulator behaviour. The silicone layer is about 1 mm thick and applied by airless-spraying devices. It enables protection for approximately two years in areas with heavy pollution conditions. After that period, the layer should be mechanically removed and reapplied. The effectiveness consists, in a simplified explanation, of enclosing with silicone oil the solid pollutant particles existing on the silicone layer. It is thus avoided that a continuous conductive pollution layer is formed.

Flashover across a pollution layer develops from initial local arcs, when the insulating capability of the remaining path is no more sufficient. This occurs when moisture leads to a conducting pollution layer. Outside Europe, *insulators* are coated in some cases with a *semi-conductive glaze* [9.57]. This enables the flow of a certain current value

that warms up the insulator surface, dries out the pollution layer and thus eliminates its conductivity. That semi-conductive glaze also smoothens the voltage distribution over the insulator string so that individual insulators are not stressed more heavily and cannot flashover prematurely.

9.10 Testing of insulator sets

9.10.1 Basic information and assumptions

Testing of insulator sets concerns the electric characteristics. Therefore, requirements on the performance under power frequency voltage as well as lightning and switching surge voltages are verified by testing. Insulation coordination as discussed in clause 9.8.1 results in these requirements. The standard levels can be taken from [9.29, 9.30]. The design of insulation has to guarantee the required data corresponding to the selected insulation level. Tests on complete insulator sets can be carried out to verify these characteristics. However, such tests are optional and not mandatory, as mentioned in IEC 60 383-2 [9.58], applicable for testing of insulator sets made of ceramic or glass insulators. The verification of the rated electric characteristics of composite insulators follows IEC 61 109 [9.37], which is applicable only to individual insulator units (see clause 9.6.3).
The insulators should be clean and dry before high-voltage tests. They should be stored at test laboratory ambient temperature for a sufficiently long period so that temperature equalizing is reached before starting the tests, thus preventing condensation on the insulator surfaces. If not otherwise agreed upon, the relative humidity may not exceed 85 % during the tests. The time interval between consecutive tests should be sufficiently long to reduce the influence of previous flashover or withstand voltage tests to a minimum.

9.10.2 Standard atmospheric conditions

When the atmospheric conditions during testing deviate from the *standard reference atmosphere* indicated by IEC 60 060-1 [9.31], the test results should be corrected. The correction factor called *relative insulation strength* (RIS), can be obtained from air density and humidity, as described in clause 2.4.5.3. In case of tests under rain, only the factor for air density correction should be applied. The following is then valid for the power frequency withstand and surge withstand voltage values:

$$\text{Applied test voltage} = \text{specified withstand voltage} \cdot \text{RIS}$$

and for flashover voltages

$$\text{recorded flashover voltage} = \text{measured flashover voltage}/\text{RIS} \quad .$$

9.10.3 Artificial rain

The standard test procedure under *artificial rain* is standardized in [9.31], which also gives the characteristic values of the artificial rain. Rain direction should be agreed upon before testing the insulators in horizontal or inclined position.

9.10.4 Testing arrangements

Differing test results can be obtained for flashover and withstand voltages of insulators from the electric test procedures, depending on whether the insulator sets undergo tests in accordance with standard specifications or in a certain assembly arrangement

which simulates most closely the real operating conditions. For example, the specimen to be tested may be mounted at a metallic structure that simulates the in-service arrangement on a tower. Assembly details should be agreed between the purchaser and the manufacturer, together with the purchase order.
If previously agreed upon, non-standardized tests can be performed with arrangements simulating real operating conditions. In such cases, the resulting characteristic values can admittedly deviate from the standard values obtained under standard test conditions.
Finally, there are two different *standard assembly arrangements* for electric tests, depending on whether switching surge tests are necessary or not. A detailed description is found in [9.58], Chapter 12; its repetition would be superfluous here.

9.10.5 Power frequency voltage test

The *power frequency voltage test* is made under rain conditions and is foreseen only for insulator sets up to 245 kV in accordance with [9.21]. The test circuit and the test procedure are given in [9.31]. The power frequency withstand voltage applied is the specified value after its correction due to the existing air density at the moment of the tests. It is applied for 1 minute and no flashover or puncture may occur. The flashover voltage can be determined, only as additional information or even as the result of previous agreement, by means of increasing the applied 75 % value of the withstand voltage by steps of 2 % per second up to the point when flashover occurs. The *flashover voltage* is determined then as the arithmetic mean of the last five consecutive readings.

9.10.6 Fast-front and slow-front overvoltage tests

The *fast-front withstand voltage test* dry, simulating lightning surges, is required for every voltage level, while the *slow-front withstand voltage test*, wet, simulating switching surges, is a standardized requirement for insulator sets only for highest voltages of equipment above 245 kV [9.28]. The usual procedure to determine withstand voltages consists of calculating the 50 % flashover voltage value which is obtained from the *up and down procedures* indicated by [9.31]. Either a standard $1,2/50$ μs lightning surge or a $250/2500$ μs switching surge is applied, with both positive and negative polarities. No damage may occur to the insulators, although slight traces on the surfaces or crumbling of cementing material may be allowed. In some cases, the application of 15 surges or impulses is deemed necessary for the withstand voltage test.

9.10.7 Power arc behaviour

Testing of power arc behaviour can be performed in accordance with IEC 61 467 [9.59], where the purchaser and manufacturer have agreed upon to carry out such tests.

9.10.8 Radio interference strength test

Generally, radio interference levels caused by corona at high voltage overhead lines are important only at voltages of 245 kV and above. In fact, only the corona effects caused by the conductors are considered to be prevalent, while corona caused by the insulator sets are only taken into account in certain special cases. Because of that, the *radio interference strength test* according to [9.28] is considered an optional test, to be agreed upon between purchaser and manufacturer so far as type tests of insulator sets are concerned. If it is the case, the test should be carried out according to IEC Report 60 437 [9.60].

CISPR 18-2 [9.42] gives the methods by which *limit values of radio interference* can be assessed to ensure good radio and television reception; the design of overhead lines and corresponding fittings that take care of the restriction of the different kinds of radio interference to acceptable levels are described in CISPR 18-3 [9.61].

9.10.9 Corona onset or extinction voltage test

Since *corona* on overhead transmission lines is caused mainly by conductors, the corona component produced by insulator sets is not dominant. Information about this matter can be found in [9.28], clause 5.5.2.
When purchaser and manufacturer decided to verify the minimum perceptible *corona onset* as well as *extinction voltage* by a type test on an insulator set, the required value should be indicated by the purchaser. As a guideline, the extinction voltage should be at least $1{,}05\ U_s/\sqrt{3}$. The tests should be performed in accordance with IEC 60 437. Type tests are usually performed on a complete insulator set.

9.11 Example for insulator selection

Long rod and glass cap-and-pin insulators for suspension and dead-end insulator sets should be selected for an overhead line with the following parameters: U_s = 420 kV, quadruple bundle conductor 264-AL1/34-ST1A (ACSR 265/35), diameter d = 22,4 mm, cross section 297,8 mm^2, weight span 600 m and wind span 450 m. Different insulator sets should be designed for each alternative, one for light and another for heavy pollution, in accordance with IEC 60 815. The conductors are strung with 50 N/mm^2 tensile stress at +10°C. Wind load zone 1 and ice load zone 1, in accordance with [9.22], are considered for the installation site. Conductor height z is 30 m above ground.

Mechanical design
The mechanical design of insulator sets is carried out following EN 50 341-3-4 [9.22]. The procedure is similar for other standards just with differing figures. In regions where ice accretion occurs, the highest load on suspension strings is often given under simultaneous action of wind and ice corresponding for example to load case D, according to EN 50 341-3-4 [9.22] section 4.3.10/DE.1.2, or for unbalanced conductor forces according to load case J. The load is calculated for the first condition from the weight force Q_G acting vertically and the wind load Q_W acting horizontally

$$Q_{is} = \sqrt{Q_G^2 + Q_W^2} \quad .$$

The weight force Q_G is given by conductor and ice weight

$$Q_G = n_2 \cdot a_g \cdot (m_C \cdot g + g_I) \quad ,$$

where m_C = 0,994 kg/m, $g_I = 5 + 0{,}1 \cdot D = 5 + 0{,}1 \cdot 22{,}4 = 7{,}24$ N/m according to [9.22], section 4.3.3/DE.1, $n_2 = 4$ and a_g = 600 m, resulting to

$$Q_G = 4 \cdot 600 \cdot (0{,}994 \cdot 9{,}81 + 7{,}24) = 40{,}8 \text{ kN}.$$

The wind load Q_{WI} on the conductor covered with ice is given by

$$Q_{WI} = 0{,}5 \cdot C_c \cdot q \cdot a_W \cdot D_I \cdot (0{,}45 + 60/a_W) \cdot n_2 \quad ,$$

where the dynamic wind pressure $q = q_0 + 3z = 800 + 3 \cdot 30 = 890$ N/m^2 at 30 m height above ground according to [9.22], section 4.3.2/DE.1; C_C = 1,0; a_W = 450 m and $D_I = \sqrt{D^2 + 0{,}00017 \cdot g_I} = 0{,}0416$ m according to [9.22], section 4.3.4/DE.1

$$Q_{WI} = 0{,}5 \cdot 1{,}0 \cdot 890 \cdot 450 \cdot 0{,}0416(0{,}45 + 60/450) \cdot 4 = 19{,}5 \text{ kN}.$$

The resulting load of the insulator string is

$$Q_{\text{is}} = \sqrt{40{,}8^2 + 19{,}5^2} = 45{,}2 \text{ kN}.$$

For load case D, a partial factor equal to 1,35 applies in accordance with [9.22], section 4.3.11/DE.2. The design load is thus equal to $1,35 \cdot 45,2 = 61,0$ kN.
For load case J, the loads on the insulator set are calculated from the weight force Q_{G} and a longitudinal load corresponding to 25 % of the conductor horizontal tensile force Q_{C} at $-5°\text{C}$ with the ice load

$$Q_{\text{is}} = \sqrt{Q_{\text{G}}^2 + (0{,}25 \cdot Q_{\text{C}})^2} \quad .$$

The horizontal tensile force Q_{C} results from the action of ice on the conductor at -5°C. The load per unit length is $m_{\text{C}}g + g_{\text{I}} = 9,75 + 7,24 = 16,99$ N/m. From equation (14.41), the tensile stress $\sigma_2 = 84,60$ N/mm^2 is obtained. The horizontal force of the quadruple bundle is $Q = 4 \cdot 84,6 \cdot 297,8 = 100,8$ kN in this case. The insulator load results to

$$Q_{\text{is}} = \sqrt{40,8^2 + (0,25 \cdot 100,8)^2} = 48,0 \text{ kN}.$$

The partial factor to be considered here is equal to 1,0, resulting in a design load of 48,0 kN for the suspension set under this condition. Therefore, the suspension set has to be designed for a limit load of 61,0 kN.
The partial factor γ_{M} for material is equal to 2,3, according to EN 50 341-3-4, Table 10.7/DE.1, so that a rated nominal load equal to $61,0 \cdot 2,3 = 140,3$ kN is needed. L 160 long rod insulators or U 160 cap-and-pin insulators are required in accordance with IEC 60 433 and IEC 60 305, respectively. For suspension supports, a single insulator set is sufficient, from the point of view of external load.
The maximum load for the dead-end insulator sets occurs under the simultaneous action of wind and ice. There, the resulting load per unit length is given by

$$g_{\text{res}} = \sqrt{(m_{\text{C}}g + g_{\text{I}})^2 + w^2} \quad ,$$

with $m_{\text{C}} \cdot g = 9,75$ N/m and $g_{\text{I}} = 7,24$ N/m as explained above and $w \sim Q_{\text{W}}/(4 \cdot a_{\text{W}}) = 10,83$ N/m it is obtained $g_{\text{res}} = \sqrt{(9,75 + 7,24)^2 + 10,83^2} = 20,15$ N/m.
The conductor state change equation (14.41) yields $\sigma_2 = 97,5$ N/mm^2 with consideration of $a_{\text{eq}} = 400$ m, $\sigma_1 = 50$ N/mm^2, $m_1 g = 9,75$ N/m, $m_2 g = 20,15$ N/m, $T_1 = 10°\text{C}$ and $T_2 = -5°\text{C}$ and the conductor data of 264-AL1/34-ST1A. The conductor horizontal force of the quadruple bundle is then $Q_{\text{C}} = 4 \cdot 97,5 \cdot 297,8 = 116,1$ kN.
Insulator sets in dead-end position are designed for the maximum conductor horizontal force resulting from one of the specified load cases to be considered. Also here, load case D as per [9.22], section 4.3.10/DE.1.2 is prevalent, with a conductor horizontal force of 116,1 kN for the quadruple bundle as calculated above, and the partial factor required as 1,35. The ultimate load of the insulator set will then be $1,35 \cdot 116,1 \sim 157$ kN. The partial factor for the insulators amounts to 2,3, resulting in a total rated load of 361 kN. Requirements in standards for crossings, as per [9.22], section 5.4.5/DE.1.2, stipulate that double strings are installed. Either L 210 long rod insulators, in accordance with IEC 60 433, or U 210 glass cap-and-pin insulators, in accordance with IEC 60 305 meet this requirement.

Electric design

The electric data governing the selection of insulators are given by IEC 60 071-1. The value of 950 kV is required for the switching withstand voltage and 1425 kV is required for the lightning withstand voltage. Furthermore, according to Table 9.8, 16 mm/kV is

Table 9.10: Example of insulator selection

Pollution level		light	heavy	light	heavy
Rated voltage	kV	420	420	420	420
Specific creepage distance	mm/kV	16	25	16	25
Required creepage distance	mm	6720	10 500	6720	10 500
		Single suspension set		Double dead-end set	
		Long rod insulators			
Type		L 160 C 650	LG 75/32S/1465	L 210 C 650	LG 85/32S/1515
Creepage distance/ insulator	mm	2320	3850	2320	3850
Length/insulator	mm	1465	1465	1500	1515
Required number		3	3	3	3
Intermediate		2	2	2	2
fitting length	mm	130	130	130	130
Total length [1)]	mm	4655	4655	4760	4805
Existing creepage distance	mm	6960	11 550	6960	11 550
		Cap-and-pin insulators			
Type		U 160 BS	U 160 BS	U 160 BSP	U 210 B	U 210 B	U 210 BP
Creepage distance/ insulator	mm	315	315	440	370	370	525
Length/insulator	mm	146	146	146	170	170	170
Required number		22	34	24	19	29	20
Total length [1)]	mm	3212	4964	3500	3230	4930	3400
Existing creepage distance	mm	6930	10 710	10 560	7030	10 730	10 500

[1)] Without fittings at the conductor side

the recommended value to be achieved for the minimum creepage distance referred to the phase-to-phase voltage for light pollution level, as well as 25 mm/kV for heavy pollution level. So, under light pollution conditions, a total creepage distance of 6720 mm results for an operating voltage of 420 kV, while a value of 10 500 mm results under heavy pollution (Table 9.10).

A suspension string composed of three L 160 C 650 long rod insulators achieves a creepage path of $3 \times 2320 = 6960$ mm, and accomplishes the requirements for light pollution. For suspension sets under heavy pollution, three non-standardized LG 75/32S/1465 long rod insulators are recommended, which have a creepage distance of 3850 mm each and a 11 550 mm total creepage distance complying with the requirements.

For suspension sets composed of glass cap-and-pin insulators, U 160 BS units can be used with 315 mm creepage distance each, thus resulting in 22 cap-and-pin units for light pollution conditions (see Table 9.10). Heavy pollution would require 34 units, which is the reason why an alternative insulator set formed by 24 cap-and-pin units type U 160 BSP with 440 mm creepage distance each is recommended instead.

For light pollution, dead-end insulator sets can be composed of L 210 C 650 long rod insulators with three units in a string leading to 6960 mm creepage distance (Table 9.10). For heavy pollution, non-standardized LG 85/32S/1515 insulators are recommended, resulting in approximately the same length of the complete set as under light pollution.

Dead-end insulator sets for light pollution can be composed of 19 U 210 B glass insulators with 370 mm creepage distance each. A total of 29 such units is required under heavy pollution. Alternatively, 20 units of U 210 BP insulators with 525 mm creepage distance per unit provide the required creepage path. By utilizing U 210 BP insulators, the set reaches the same length under heavy pollution, as with U 210 B insulators under light pollution conditions (Table 9.10). This is advantageous with regard to tower

dimensions.
The lightning withstand voltage of the long rod insulator set is equal to $3 \times 650 = 1950$ kV; the one of the cap-and-pin insulator strings amounts to at least 1620 kV (dead-end insulator set with 19 U 210 B units), according to information from the manufacturer. Thereby, the lightning withstand voltage requirements are met. The required creepage distance governs the number of insulators to be used. If U 210 BP insulators were applied for light pollution, 13 units would be sufficient to keep the required creepage distance, but the lightning withstand voltage would be only 1260 kV, not achieving the required value. Such an insulator set would not be suitable.

9.12 References

9.1 IEC-60 050-471: International electrotechnical vocabulary. Part 471: Chapter 471: Insulators. Geneva, IEC, 1984

9.2 EN 60 383-1: Insulators for overhead lines with nominal voltage above 1 kV. Part 1: Ceramic or glass insulators units for AC systems – Definitions, test methods and acceptance criteria. Brussels, CENELEC, 1993

9.3 EN 60 433: Insulators for overhead lines with a nominal voltage above 1 kV. Ceramic insulators for AC systems – Characteristics of insulator units of the long rod type. Brussels, CENELEC, 1998

9.4 IEC 60 720: Characteristics of line post insulators. Geneva, IEC, 1981

9.5 Paris, L. et al.: Application of composite insulators for overhead lines. Cigré Symposium Leningrad, Report 400-04, 1991

9.6 Experience from HV and EHV compact lines. Cigré Symposium Leningrad, Report 200-07, 1991

9.7 Cottereau, D. et al.: Utility retrofits towers to increase system voltage. Transmission & Distribution, March 2002, pp. 28 to 34

9.8 IEC 60 305: Insulators for overhead lines with a nominal voltage above 1 kV. Ceramic or glass insulator units for AC systems – Characteristics of insulator units of the cap-and-pin type. Brussels, CENELEC, 1996

9.9 IEC 60 120: Dimensions of ball and socket couplings of string insulator units. Geneva, IEC, 1987

9.10 IEC 60 471: Dimensions of clevis and tongue couplings of string insulator units. Geneva, IEC, 1987

9.11 IEC 60 372: Locking devices for ball-and-socket couplings of string insulator units. Geneva, IEC, 1984

9.12 IEC 60 672-1: Ceramic and glass insulating materials. Part 1: Definitions and classification. Geneva, IEC, 1995

9.13 Frese, H.-J.; Pohlmann, H.: Betriebserfahrungen und Untersuchungen an Langstabisolatoren (Experience and investigations on long rod insulators). Elektrizitätswirtschaft 98 (1999), pp. 38 to 43

9.14 IEC 60 672-3: Ceramic and glass insulating materials. Part 3: Specifications for individual materials. Geneva, IEC, 1997

9.15 IEC 60 672-2: Ceramic and glass insulating materials. Part 2: Methods of test. Geneva, IEC, 1999

9.16 Toughened glass suspension insulators. Paris: Edited by Ceraver 1982

9.17 IEC/TR 60 815: Guide for the selection of insulators in respect of polluted conditions. Geneva, IEC, 1986

9.18 Kunststoff-Langstabisolatoren, System Rodurflex. Selb: Edited by Hoechst Ceram Tec AG 1986

9.19 Dietz, H. et al.: Latest developments and experience with composite long rod insulators. Cigré Report 15-09, 1986

9.20 EN 61 466-2: Composite string insulator units for overhead electrical lines with a nominal voltage greater than 1 kV. Part 2: Dimensions and electric data. Brussels, CENELEC, 1998

9.21 EN 61 466-1: Composite string insulator units for overhead electrical lines with a nominal voltage greater than 1 kV. Part 1: Standardized strength classes and end fittings. Brussels, CENELEC, 1997

9.22 EN 50 341-3-4: Overhead electrical lines exceeding AC 45 kV. Part 3-4: National Normative Aspects for Germany. Brussels, CENELEC, 2001

9.23 Kindersberger, J.; Kuhl, M.: Effect of hydrophobicity on insulator performance. 6th ISH, Paper 12.01, New Orleans, August 1989

9.24 Sailer, H.; Ruhnau, J.: Entwicklung und Einsatz einer 380-kV-Isolationshängekette in asymmetrischer V-Anordnung (Development and use of a 380 kV assymmetric V-suspension insulator set). Elektrizitätswirtschaft, 94 (1995), pp. 1344 to 1350

9.25 Cigré SC22 WG22-03: Service performance of composite insulators on HVDC lines. Electra 161 (1995), pp. 53 to 57

9.26 Cigré SC22 WG22-03: World-wide service experience with HV composite insulators. Electra 191 (2000), pp. 27 to 43

9.27 Johansson, T. et al.: A comparative study for transmission insulators. Insulator news & market report; Vol.5; (1997) No.2, ISSN 1198-7332

9.28 EN 50 341-1: Overhead electrical lines exceeding AC 45 kV. Part 1: General requirements – common rules. Brussels, CENELEC, 2001

9.29 IEC 60 071-1: Insulation coordination. Part 1: Definitions, principles and rules. Geneva, IEC, 1993

9.30 IEC 60 071-2: Insulation coordination. Part 2: Guideline for application. Geneva, IEC, 1996

9.31 IEC 60 060-1: High-voltage testing technique. Part 1: General requirements and testing conditions. Geneva, IEC, 1989 + Corrigendum 1990

9.32 IEC 60 797: Residual strength of string insulator units of glass or ceramic material for overhead lines after mechanical damage of the dielectric. Geneva, IEC, 1984 (withdrawn)

9.33 IEC/TR 61 211: Insulators of ceramic material or glass for overhead lines with a nominal voltage greater than 1 000 V. Puncture testing. Geneva, IEC, 1994

9.34 IEC/TR 60 575: Thermal-mechanical performance test and mechanical performance test on string insulator units. Geneva, IEC, 1977

9.35 IEC 60 168: Tests on indoor and outdoor post insulators of ceramic material or glass for systems with nominal voltages greater than 1 000 V. Geneva, IEC, 1994

9.36 IEC 60 168A1: Tests on indoor and outdoor post insulators of ceramic material or glass for systems with nominal voltages greater than 1 000 V. Amendment 1. Geneva, IEC, 1997

9.37 IEC 61 109: Composite insulators for AC overhead lines with a nominal voltage above 1 000 V – Definitions, test methods and acceptance criteria. Geneva, IEC, 1992

9.38 Möcks, L.: Lichtbogenschutzarmaturen für Isolierstrecken in Freileitungen und Schaltanlagen (Arcing protection fittings for overhead lines and substations). ETZ-Report 16. Berlin: VDE-Verlag 1982

9.39 Bauer, E. et al.: Dynamic process during load transposition in multiple sets with long rod type insulators. Cigré Report 22-03, 1982

9.40 Cigré SC22 WG22.03: Protective devices for insulator sets (HV and EHV transmission overhead lines). Electra 136(1991), pp. 22 to 29

9.41 Ann, W. et al.: Isolatoren und Armaturen für die neue 380-kV-Elbekreuzung der Nordwestdeutsche Kraftwerke AG (Insulators and fittings for the new 380 kV crossing over the river Elbe of Nordwestdeutsche Kraftwerke AG). Elektrizitätswirtschaft 77 (1978), pp. 653 to 660

9.42 CISPR 18-2: Radio interference characteristics of overhead power lines and high-voltage equipment. Part 2: Methods of measurement and procedure for determining limits. 1986

9.43 EN 61 284: Overhead lines – Requirements and tests for fittings (IEC 61 284). Brussels, CENELEC, 1997

9.44 BS 137: Specification of insulators of ceramic material or glass for overhead lines with a nominal voltage greater than 1 000 V. Part 2: Requirements. London, BSI, 1973

9.45 IEC 60 507: Artificial pollution test on high-voltage insulators to be used on AC systems. Geneva, IEC, 1991

9.46 Cigré SC33 WG33-13: Polluted insulators: A review of current knowledge. Paris, Cigré Brochure 158, 2000

9.47 Fink, D. G.; Beaty, H. W.: Standard handbook for electrical engineers. New York. McGraw Hill, 12th edition 1987

9.48 EPRI: HVDC Transmission line reference book. Palo Alto. Electric Power Research Institute, 1993

9.49 EN 61 325: Insulators for overhead lines with a nominal voltage above 1 000 V – Ceramic or glass insulator units for DC systems – Definitions, test methods and acceptance criteria (IEC 61 325). Brussels, CENELEC, 1995

9.50 Macey, R. E.: The performance of high-voltage outdoor insulation in contaminated environment. Transaction South African Institute of Electrical Engineers (1981), pp. 80 to 92

9.51 Cigré SC22 WG22-03: Study and conclusions from the results of the inquiry on insulators: Information on damage. Electra 78 (1983), pp. 13 to 33

9.52 Ciskos, B.: Service continuity of 750 kV transmission lines ensured by suitable structure and working under voltage. Cigré Report 22-10, 1984

9.53 Verma, M. P.: Isolierverhalten von Hochspannungs-Langstabisolatoren verschiedener Bauform unter natürlichen Fremdschichtbedingungen (Insulating performance of high-voltage long rod insulators with differing design under natural pollution conditions.) ETZ-A 92 (1971), pp. 407 to 413

9.54 Auxel, H.: Erfassung kritischer Fremdschichtbedingungen in Hochspannungsanlagen (Detection of critical pollution conditions in high-voltage installations). Elektrizitätswirtschaft 84 (1985), pp. 84 to 90

9.55 EN 50 186-1: Live-line washing systems for power installations with nominal voltages above 1 kV – Common requirements. Brussels, CENELEC, 1999

9.56 EN 50 186-2: Live-line washing systems for power installations with nominal voltages above 1 kV – National Annexes. Brussels, CENELEC, 1999

9.57 Lambeth, P. J.: The use of semi-conducting glaze insulators. Electra 86 (1983), pp. 89 to 103

9.58 IEC 60 383-2: Insulators for overhead lines with a nominal voltage above 1 000 V. Part 2: Insulator strings and insulator sets for AC systems. Definitions, test methods and acceptance criteria. Geneva, IEC, 1993

9.59 IEC 61 467: Insulators for overhead lines with nominal voltages above 1 000 V. AC power arc tests on insulator sets. Geneva, IEC, 1997

9.60 EN 60 437: Radio interference test on high-voltage insulators (IEC 60 437). Brussels, CENELEC, 1997

9.61 CISPR 18-3: Radio interference characteristics of overhead power lines and high-voltage equipment. Part 3: Code of practice for minimizing the penetration of radio interference. 1986

10 Overhead line fittings

10.1 Definitions

According to [10.1, 10.2], *overhead line fittings* serve for the mechanical attachment, for the electric connection and for the protection of conductors and insulators. In relevant standards, fittings are frequently designated as accessories which may consist of elements or assemblies.
According to [10.3], *fittings for conductors* serve to terminate, suspend or join the conductors and are directly connected to the conductors. *Suspension* and *dead-end clamps*, *connectors*, *branch-off clamps*, *vibration protection fittings* as well as *bundle spacers* are within this category. According to their function, they may form an assembly consisting of several elements, e. g. suspension and dead-end clamps including the required connecting links.
Fittings for insulator sets and other attachments serve to connect the tension or suspension components with the attachment points at the supports. In case of insulator sets, components to connect insulators are also within this category; the insulators, however, are excluded. These fittings comprise all components arranged between the assembly of the dead-end or suspension clamps and the first detachable element at the support, e. g. the jointing pin or the U-bolt. *Yoke plates*,indexyoke plate *corona protection fittings* and *grading rings* are also included.

10.2 Fittings for conductors

10.2.1 Conductor attachment at suspension insulator sets

To attach conductors to *suspension insulator sets*, different types of fittings are adopted. Within the suspension clamp and in its vicinity, the conductor is subjected to mechanical stresses higher than in the free span [10.4]. As shown in Figure 10.1, static tensile stress σ_t due to conductor tensile forces and dead weight are superimposed by static bending stresses σ_b due to the conductor curvature, static compression stresses σ_D resulting from conductor clamping and *alternating* bending stresses σ_{bW} due to conductor vibration.
To keep the dynamic strain of the conductor low in the range of the suspension clamps, the body of the clamps should be light-weighted and pivoted to be able to follow asymmetrical modes of conductor vibrations as far as possible unhindered. The *articulated suspension clamp* according to Figure 10.2 is the most frequently used type of suspension clamp. A clamp body suspended articulately at a pair of straps supports the conductor, which is fixed by means of the clamp cover [10.5]. Radius and length of the groove have to be designed such that also in case of large conductor downstrain

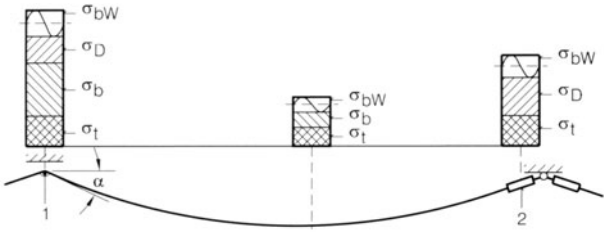

Figure 10.1: Mechanical stress within a conductor. σ_t static tensile stress; σ_b static bending stress; σ_D static compression stress; σ_{bW} alternating bending stress; 1 suspension clamp; 2 dead-end clamp

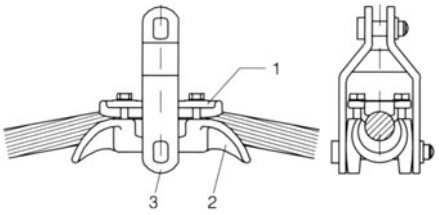

Figure 10.2: Articulated suspension clamp. 1 clamp cover; 2 clamp body; 3 suspension straps

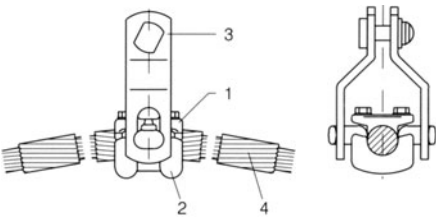

Figure 10.3: Armor rod suspension (ARS) (Richard Bergner GmbH). 1 clamp cover; 2 clamp body; 3 suspension straps; 4 armor rods

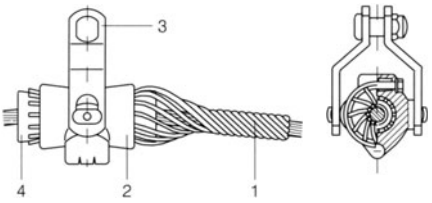

Figure 10.4: Armor grip suspension (AGS) (Richard Bergner GmbH). 1 armor rods; 2 clamp body; 3 suspension straps; 4 rubber-elastic lining

angles the conductor will not be bent sharply at the end of the body. The pivot of the articulation should be arranged approximately at the same level as the conductor axis to keep the alternating bending strain low when the clamp is swivelling. In [10.5], the mechanical design of suspension clamps is studied in detail.

The *armor rod suspension (ARS)* (Figure 10.3) and the *armor grip suspension (AGS)* (Figure 10.4) are characterized by a set of helically formed circular rods [10.5] wound around the conductor. These rods distribute the forces exerted from the clamps on a longer conductor section of up to 2,5 m depending on the conductor cross section. The bending stiffness of the armor rods is approximately equal to that of the suspended conductor and achieves a sufficiently large curvature radius keeping low the static bending strains. The short and light-weight clamp bodies possess a small moment of inertia and, therefore, can follow the conductor movements in case of asymmetrical vibration modes. Thereby, the alternating bending stresses at the conductor remain low. Additionally, the armor grip suspension has got a rubber-elastic lining, which is enclosed by helically formed rods like a basket. Around this basket, the articulated suspension clamp is arranged and fixes the conductor in longitudinal direction. The rubber-elastic lining reduces the radial compression on the conductor. This design results in a comfortable and vibration-resistant but more expensive suspension fitting, which is in particular adopted where more reasonable fittings do not sufficiently protect the conductors. The armor grip suspension is used worldwide, especially to suspend OPGW and dielectric *aerial cables*. The transmission capability of optical fibres would be substantially disturbed by locally concentrated compression forces as exerted by conventional suspension clamps; therefore, the armor grip suspension is in particular suited to all types of optical cables. The length of the armor rods should be selected such that the required dampers can be arranged on the armor rods. The report [10.6] outlines selection and use of *fittings for optical cables*.

Operational experience has demonstrated that earth wires and aerial cables could be prone to *oscillating movements* in direction of the conductors. These movements cannot be damped or suppressed by conventional remedies; they cause an increased abrasion within the universal joint of the armor grip suspension. As tests have shown, the longitudinal conductor movements will be limited if the universal joint is replaced by a simple hinge.

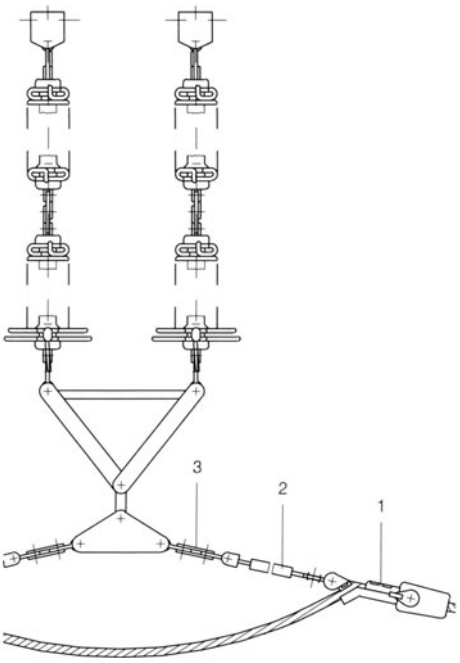

Figure 10.5: Suspended dead-end arrangement for 245 kV twin bundle conductors. 1 dead-end clamp; 2 turn buckle; 3 triangular yoke plate

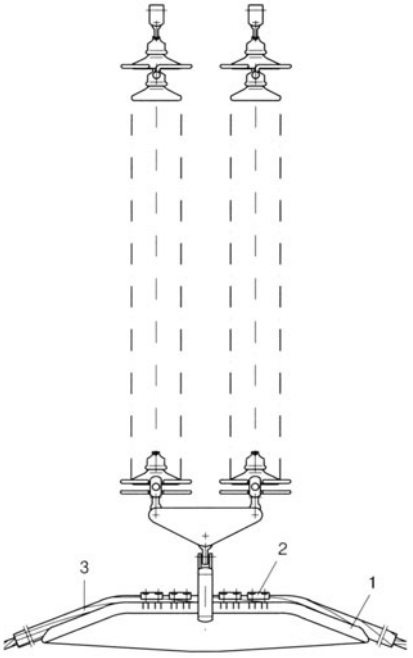

Figure 10.6: Suspension insulator set of the 400 kV Bosphorus crossing (Turkey) using a saddle-type clamp. 1 clamp body; 2 clamp cover; 3 armor rods

In case of long spans such as in *river crossings*, the strains to the conductor at the suspension attachments are additionally increased due to the large downstrain angle. By using a *suspended dead-end arrangement* (Figure 10.5) attaching the conductors by means of dead-end clamps, no static bending stress will occur at the conductor suspension [10.4]. If *wedge-type clamps* cannot be used because of the conductor make-up and the conductor should pass uncut from strain tower to strain tower across the suspension towers, extremely long suspension clamps will be necessary. These designs are also called *saddle-type clamps* [10.7]. Due to the high conductor downstrain angles occurring at long spans, up to two meters long suspension bodies can be required. Such clamps are custom-made designs tailored to the individual application. Shape of the body and radius of groove have to be thorougly adjusted to the conductor dead weight such that the shear force in the conductor does not exceed permissible limits and the conductor structure will not get loose. It is as well understood that the clamps must comply with all the other project requirements (Figure 10.6).

Release suspension clamps are adopted occasionally to protect not sufficiently torsion-proof suspension towers. The clamps release the conductor at an insulator inclination of approximately 45° which might be caused by unbalanced conductor forces in the adjacent spans caused for instance by differing ice loads. *Sliding suspension clamps* [10.8] enable the conductor to slide through the clamp above a stipulated difference in conductor tensile forces between adjacent spans. In many European countries, release and sliding clamps are not anymore used due to their not sufficiently reliable functioning.

To avoid line cascading caused by extraordinary high longitudinal tensile forces, specific designs for fittings have been developed being summarized under the term *load control devices (LCD)*. Paper [10.8] reports in detail on design and application of these devices.

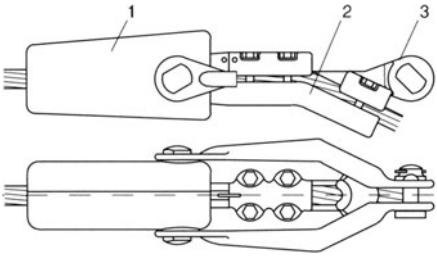

Figure 10.7: Wedge-type dead-end clamp. 1 clamp body; 2 clamp wedge; 3 terminal strap

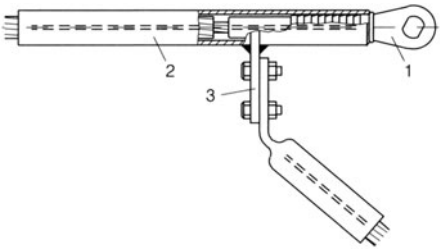

Figure 10.8: Compression-type dead-end clamp. 1 clamp body with sleeve for steel core; 2 outer sleeve; 3 lug for jumper loop

10.2.2 Conductor attachments at dead-end terminations

Conductors can be terminated by *dead-end clamps* or by *preformed dead-ends*. Attachments of conductors at tension insulator sets must be able to carry the conductor tensile force occurring at the individual line or support. The requirements on the mechanical performance depend on the type of clamp, on the relevant standards or on the project specification.

The application of preformed dead-ends is limited to conductor types with small dimensions. They are preferably used for *metal-reinforced aerial cables* with integrated optical fibres. Compression-type or wedge-type clamps are predominantly adopted for phase conductors of high- and medium-voltage lines. *Wedge-type clamps* do not require special tools for installation and are relatively simply to be fitted. A correction of conductor sag can be achieved by shifting the clamp. Wedge-type clamps are in particular suited to single-material conductors and to compound conductors with more than one aluminium or aluminium alloy layer and, therefore, low steel content. They consist of a wedge system tailored and fixed to the conductor and of a one- or two-piece clamp body with pins to which the terminal straps of the insulator set are attached (Figure 10.7). According to the design principle of the wedge-type clamp, the wedge system slides within the wedge body when the conductor tensile force increases. As a consequence, there is a progressive rise of the transverse force on the conductor. This rise is needed to increase the terminating force accordingly. In case of compound conductors, the steel core participates adequately and sufficiently at the total terminating force due to frictional interlocking with the aluminium layers arranged above. The greasing of the steel core may impair the extent of interlocking [10.9].

Compression dead-end clamps are suited to terminate all standard types of conductors available in the market. They are designed to achieve ultimate terminating forces up to the rated tensile strength (RTS) of the conductors. Shifting of the clamp after installation is not anymore possible. Special tools, namely a hydraulic press and corresponding dies, are required for installation of compression dead-end clamps. They are designed with one metal sleeve for single material conductors and with two sleeves for composite conductors (Figure 10.8).

In case of compound conductors, at first the steel sleeve is crimped onto the steel core on a corresponding length after cutting back the aluminium strands. Afterwards, the outer sleeve made of aluminium alloy is crimped on one end with steel terminal of the clamp and on the other end with the entire conductor consisting of aluminium and steel layers. The manufacturer's instructions should be followed when installing compression clamps. The length, thickness and material of the sleeve, as well as the position and number of crimps, affect the ultimate terminating force to a great extent. As an example, the conductors of the 400 kV Bosphorus crossing, 1805-AL3/228-A20SA (Figure 10.6),

Figure 10.9: Termination of an optical aerial cable (OPGW) by means of preformed dead-end rods

formerly addressed as AACSR/AC 1805/228, were terminated by compression dead-end clamps [10.7]. Their ultimate terminating force was 850 kN.

Preformed dead-end rods distribute the radial compression forces required for the friction locking on a longer section than dead-end clamps and, therefore, are in particular suitable for terminating metal-reinforced cables with optical fibres (OPGW) and dielectric cables with optical fibres and other aerial cables.

Preformed dead-end rods comply with all the requirements on conductor terminations. They can be simply installed bare hand without tools and are widely used worldwide. They consist of several helically-formed circular metal rods, the inner diameter being somewhat smaller than the outer diameter of the conductor to be terminated. The tensile forces are transferred onto the conductor through the helices by means of friction generated by radial pressure. Length and shape of the preformed dead-end rods keep the radial pressures at a low level and thus avoid any damage of the conductor (Figure 10.9). The inner surface of the preformed dead-end rods is sand-covered to increase the ultimate terminating forces.

10.2.3 Turn buckles

Turn buckles are arranged in dead-end insulator sets to compensate tolerances in lengths of elements in parallel or of subconductors in bundles. In DIN 48 334 [10.10] they have been standardized according to their characteristic forces. Due to the notch sensitivity of the threaded spindle, special requirements apply for the partial factors according to [10.2]. Turn buckles may not be loaded by bending.

10.2.4 Connectors

Connectors are fittings jointing one or more phase conductors or earthwires to each other or producing a conductor branch-off. *Tension-proof* and *non-tension-proof connectors* can be discerned.

Regarding thermal rating, the same principles apply as in case of other line accessories. For mid-span joints, the voltage drop and the electrical resistance along the connector may not exceed that of an equivalent conductor length. The features of the connectors are verified according to [10.3].

The same requirements apply for tension-loaded conductor joints as for dead-end clamps. When constructing new overhead power lines, compression-type connectors are predominantly adopted today, the design, function and installation of which are equal to those of compression dead-end clamps.

In particular, for medium-voltage lines *preformed splices* are used made of preformed rods having the same function as preformed dead-end rods. For conductor cross sections used in medium-voltage lines, the minimum failing load of preformed splices attains the same values as obtained with compression joints.

Protective patch rods or *repair patch rods* are frequently adopted to restore the electric and mechanical function after a damage or strand failures at conductors, earthwires or aerial cables . These patch rods can be installed without special tools. They are supplied with adapted lengths, whereby the manufacturer's instructions declare to what extent of damage they may be suited as remedy for repair. As a rule, repair patch rods are used where the proportion of failed strands in the outer conductor layer does not exceed

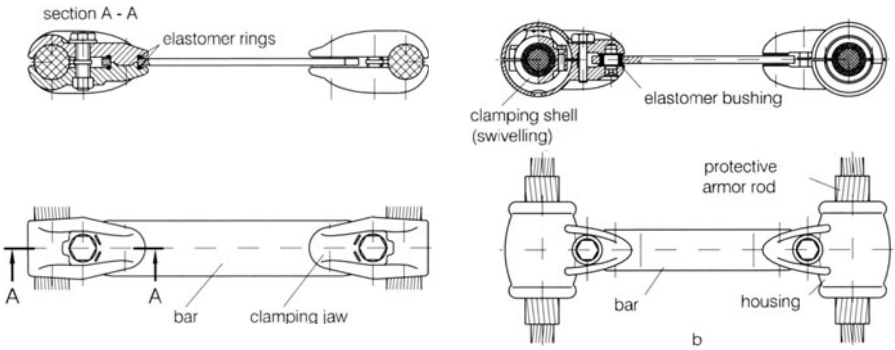

Figure 10.10: Subconductor spacers without damping: a low-noise design; b design with swivelling clamp (Richard Bergner GmbH)

25 %. The application of a tension-proof connector patch rod will be necessary in case of a more severe damage.

Connectors applied in *jumper loops* or conductor branch-offs are not loaded by tensile forces and have only to comply with the electric requirements. Such connectors may be used to joint conductors having different diameters or materials. In jumper loops, the conductors overlap on a length of several meters and are connected electrically and mechanically by three or four parallel groove clamps. In case of bundle conductors, rigid spacers with directly fixed current resistant clamps are adopted. This arrangement is advantageous because sufficient reserve of conductor length is available for resetting of dead-end clamps where necessary.

Contacting of metals having different electro-chemical potentials may not result in *galvanic contact corrosion* in the presence of humidity. Combinations of aluminium and copper are in particular endangered. In this case, a sheet of *Al/Cu bimetal* must be fitted to the contact area. An Al/Cu clamp is substantially more reliable since the contact areas have been durably sealed against humidity during production.

10.2.5 Spacers for bundle conductors

Bundle conductors, consisting of two, three, four or more subconductors, are adopted for transmission lines with rated voltages of 220 kV and above. Occasionally, also 110 or 150 kV lines designed for a high bulk power transmission are equipped with bundle conductors. The *spacers* keep the subconductors within a span and in jumper loops at designed spacing to avoid damage caused by clashing, twisting or entwining. The number of spacers and their spacing should be adjusted to the span length and the damping requirements, if any. Twisting or entwining of subconductors will be less probable and the retaining moment will be enhanced if the subspan length starting with for example 15 m at the supports increases in steps of 5 m up to 70 m in midspan.

According to their function, it is discerned between *rigid spacers*, keeping the subconductors at a constant distance at the location of installation, *flexible spacers*, permitting small relative displacements of the subconductors at the location of installation, and *spacer dampers*, which reduce the vibration level by energy dissipation in rubber-elastic elements, thus avoiding fatigue damage of conductors.

Spacers should ensure the designed subconductor spacing at the location of installation in all operational conditions, also during wind or ice action. In case of a short circuit, they have to withstand high dynamic loads and to limit the damage of subconductors without being themselves permanently deformed. Hinges and insulating elements

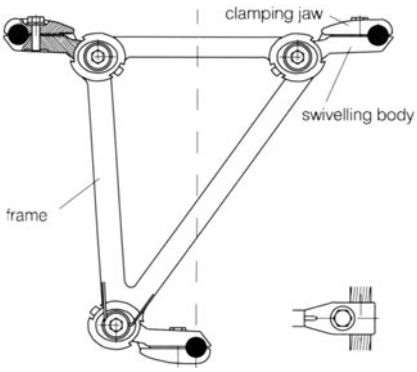

Figure 10.11: Spacer damper for triple bundles (Richard Bergner GmbH)

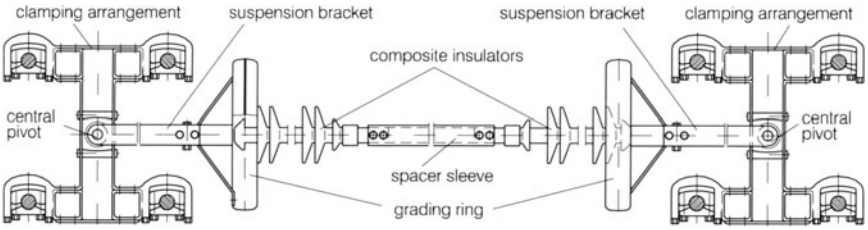

Figure 10.12: Phase spacer for quadruple bundles (Richard Bergner GmbH)

cannot conduct currents between subconductors in normal operation. The distancing element of a spacer, therefore, does not suit as a fixing point for earthing devices in case of maintenance. The corresponding design should ensure that no inadmissible discharges or radio interference occur and audible noise is avoided.
Since spacers are mostly installed from *bundle conductor line cars*, a design with elements which cannot be lost during installation is expedient. Installation gauges provide the linemen with the precise subconductor spacing and take care of a rectangular arrangement. Therefore, the use of such gauges is advantageous. Figure 10.10 shows spacers without damping features as used today. Requirements as well as test and acceptance criteria are stipulated in [10.11].
Phase spacers are adopted in spans of lines where *conductor galloping* occurs frequently due to topographical or climatic peculiarities. The conductor movement during galloping, having a low frequency and being accompanied by considerably large amplitudes, can result in flashovers or clashing between phase conductors or to earth wires. This can give rise to massive mechanical or thermal conductor damage as well as to interruptions of the power supply. The selective arrangement of several phase spacers within a span cannot avoid conductor galloping at all but reduces the probability of flashovers or clashing considerably. Figure 10.12 shows a phase spacer. Standards on design and testing of phase spacers do not exist.

10.2.6 Vibration dampers for single conductors

Chapter 11 deals with vibrations occurring at overhead line conductors. These vibrations result in alternating bending stresses, which are added to the existing static stresses (Figure 10.1). These fatigue stresses have maxima at suspension and dead-end attachments as well as at mass discontinuities and may lead to failures of individual strands and eventually to failure of all aluminium layers of a composite conductor.
Vibration dampers offer effective protection against vortex-induced vibrations. With

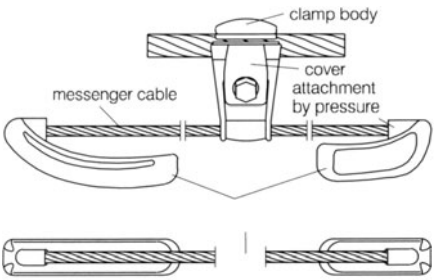

Figure 10.13: Stockbridge-type vibration damper (Richard Bergner GmbH)

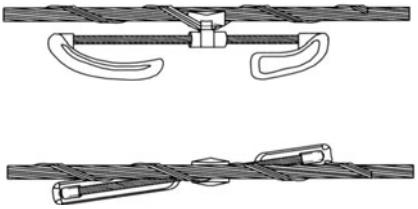

Figure 10.14: Damper for aerial cables with optical fibres (Richard Bergner GmbH)

respect to their mechanical features, they need to be thoroughly tuned to line and conductor parameters; their location has to be selected such that neither the conductor nor the messenger cable of the damper will be overstressed. In particular, the relatively low investments necessary for dampers are always justified in case of cost-effective *aerial cables with optical fibres*. Most utilities use *dampers* of the *Stockbridge-type* (Figure 10.13), [10.12] as a standard for controlling vibration in case of single conductors. Stockbridge-type dampers function according to the principle of a damped spring/mass oscillator and dissipate a main portion of the wind input energy into the conductor. Therefore, the conductor stresses remain on a safe level. Due to the wide range of frequencies in which the conductors are able to vibrate, it is required that dampers function over a broad frequency band width (see clause 11.2.7). This requirement can be met by an appropriate design of the damper masses and an adjusted length of the messenger cable. A theoretical optimization of the system consisting of conductor and damper became achievable by application of the *energy balance principle* (EBP) [10.13], which is based on the balance of energies imparted by wind action and dissipated by conductors and dampers. Information on the conductor self-damping is needed to apply the energy balance principle. Requirements on and testing of Stockbridge-type dampers are stipulated by the standard EN 61 897 [10.14].

10.2.7 Spacer dampers for bundle conductors

Spacers for bundle conductors can be designed such that, in addition to comply with the characteristics required in clause 10.2.5, they suppress vortex-induced conductor vibrations. Figure 10.11 shows such a spacer damper for a triple bundle. Usually, the spacer consists of a rigid frame, at the corners of which the connection with the conductors is provided by means of hinges with clamps. The hinges are lined with rubber-elastic cushions made of silicon or ethylene-propylene rubber (EPDM), thus providing a remarkable damping capacity. They enable the clamp to follow the conductor movements and dissipate energy to an amplitude-depending extent. The amount of damping power of one hinge can correspond roughly to that of 100 m of conductor. The oscillating movement of the subconductors is reduced by the dissipation of energy. Number and location of *spacer dampers* should be optimized and verified by a study for each individual application. The optimum distribution of spacer dampers along the span varies depending on span length, wind velocity regime and local topography. Spacers should meet the requirements of EN 61 854 [10.11].

10.3 Fittings for insulator sets

According to the definition given in [10.2], *fittings for insulator sets* comprise

- *Fittings to attach the insulator set*(s) to the support, e. g. U-bolts or bolts of hinges;
- *Fittings to join the insulators* of one string, e. g. *ball and socket* or *clevis and tongue connections*, *yoke plates* for multi-string insulator sets;
- *Fittings for grading* of electrical fields and *arcing protection*, e. g. *coordinating spark gaps*, *arcing horns* and rings, as well as *grading fittings* .

Ball and socket connections are used for connecting long rod and cap-and-pin insulators, clevis and tongue connections for long rod and composite insulators. The dimensions of ball and socket connections are standardized by IEC 60 120 [10.15], for clevis and tongue connections by IEC 60 471 [10.16]. Connections between balls and sockets are secured against unintentional loosening by elastic V- or W-type split pins. Standardized dimensions can be found in [10.17].

Arcing protection fittings should safe-guard insulators sensitive to abrupt temperature changes which might occur due to power arcs. The magnetic field produced by the arc is utilized to stabilize and guide the arc. In case of multiple insulator strings, the merging of partial arcs to an integral arc is aimed at, so that the arc burns apart from the insulators until being extinguished.

The technical system parameters such as nominal voltage and short-circuit current together with its interruption period decide on the selection of arcing protection devices as well as on the arrangement of the individual insulator strings in parallel or perpendicularly to the conductors in case of multiple insulator sets.

Grading fittings primarily homogenize the electrical field along the insulator string in particular at cap-and-pin insulator sets. Most of the arcing protection devices take care of potential grading simultaneously. Separate *grading rings*, therefore, are only necessary in case of arrangement and design of insulator sets for special applications, which need shielding of individual elements to keep the insulator set totally free of partial discharges. Such grading fittings do not function as arcing protection fittings.

10.4 Rating and tests

10.4.1 General

According to EN 50 341-1 [10.1], *fittings for overhead power lines* have to be designed, manufactured and installed such that they comply with all requirements resulting from operation, maintenance and impacts on the environment. With respect to their mechanical and electric characteristics, they have to be designed according to [10.1, 10.3]. Thus, the design parameters of the line based on stipulations in standards will be met. Their structural design should ensure that damage of the conductors will be avoided and it will be guaranteed that no individual elements get loose during operation. A design life time may be agreed upon between purchaser and supplier.

10.4.2 Electric requirements

All fittings should comply with the general *electric requirements* stipulated for a specific line. All current-connecting fittings such as clamps and conductor connectors, may not reach a higher temperature than the conductor itself under the impact of the maximum permissible design current. Therefore, these fittings may not possess a higher resistance and a smaller heat energy dissipating surface than a piece of conductor having the same length. The *voltage drop* along current-carrying fittings may not exceed that of an equivalent conductor section. When exposed to the expected *short-circuit loading*,

Table 10.1: Corona test voltages and radio interference noise limits (according to [10.18])

Highest system voltage U_S	Stringent requirements		Standard requirements	
	Test voltage	Noise limit [1)]	Test voltage	Noise limit [1)]
kV	kV	dB	kV	dB
123	95	30	75	34
145	110	30	88	34
245	185	35	150	40
420	320	40	260	46

[1)] dB above 1 μV across 300 Ω at 1 MHz

current-carrying fittings may not attain a temperature which would lead to annealing or damage of galvanization of steel and cast iron elements. Arcing protection fittings should conduct the specified fault current during the associated failure period without adverse effects on safety of persons during maintenance activities. A current density of 70 A/mm^2 can be tolerated for tension-loaded fittings and a density of 80 A/mm^2 in case of non-tension-loaded ones.

To verify the electric long-term performance of current-carrying connections, *heat cycle tests* have been stipulated and described as a type test according to clause 13 of [10.3].

When tested, the *radio interference level* of line accessories – spacers and clamps included – should comply with the total interference level specified for the individual installation. To reduce the electrical field strength at live ends of insulator sets, *grading rings*, if any, or similar devices can be utilized. A *corona extinction voltage* just perceivable by the non-equipped eye should be stipulated by the project specification, if any.

Information on *corona effects*, radio interference included, is provided by clause 14 of [10.3]. To avoid corona effects and the correlated electric and acoustic interference, the surface radii of fittings have to be designed with respect to the effective highest voltage. Required corona extinction voltages and acceptable radio interference levels are provided by project specifications. In [10.18], recommended values are given corresponding to a test voltage of $U_{\text{test}} = 1,05\ U_S/\sqrt{3}$, where U_S is the highest system voltage. A test voltage of 260 kV results for $U_S = 420$ kV.

Regarding limits for radio noise, two levels are distinguished: very stringent and standard requirements. In Table 10.1, the data for frequency used voltages are listed.

Design and material selection for fittings directly connected with the conductors should minimize magnetic losses, caused by eddy currents and magnetic reversals, thus not leading to an inadmissible heating of the conductor. To reduce *eddy currents* and the heating resulting thereof, clamps should be manufactured from diamagnetic or paramagnetic materials.

Test procedures and acceptance criteria for magnetic losses should comply with [10.3] or the individual specifications for the supply batch. The complete suspension or dead-end insulator sets are eventually submitted to type tests, as per subclause 9.10. Then, individual elements of such sets should also remain intact after the test was passed successfully.

10.4.3 Mechanical requirements

The permissible mechanical load of a component is determined using a material partial factor which depends on the purpose of use and the relevant standards. As an example, the Normative National Aspects for Germany [10.2] stipulate an empirical approach to specify numerical data for actions and partial factors instead of a statistically based approach also permissible according to [10.1]. A rational calibration of design criteria

has been achieved due to long-lasting and successful design and construction of high-voltage lines.

Tensile-loaded conductor and earth wire fittings have to be designed such that the mechanical requirements are complied with. *Dead-end clamps* and tension-proof conductor joints should sustain the conductor with at least 85 % of its rated tensile strength (RTS). *Suspension clamps* should be designed with respect to the acting wind and/or ice loads with sufficient reliability. According to [10.2], they have to be designed based on 1,35 times the conductor tensile force. Also in case of differences in the conductor tensile forces of adjacent spans, the suspension clamps have to sustain reliably the conductor load, so far they should not deliberately permit slipping of conductor due to the corresponding design. The sustaining force should be specified depending on the climatic conditions, the type of conductor and the type of clamps. A minimum slipping resistance in the range of 20 to 25 % of conductor RTS has been used worldwide.

Protective fittings would only be loaded mechanically if linemen used them as a place to stand on. Then they should withstand a concentrated force of 1,5 kN without being deformed plastically.

Fittings for conductors should withstand the short-wave and long-wave conductor oscillations during the projected service life. Fittings prone to abrasion or articulation have to be designed and manufactured such that a high *resistance to abrasion* will be guaranteed.

Materials and structural design of *fittings for insulator sets* have been specified in relevant standards, e. g. [10.2, 10.3]. They will be loaded electrically only in case of short circuits and may not attain a temperature which would result in an inadmissible reduction of mechanical strength. They have to carry the acting external forces with a sufficient safety margin.

Some additional stipulations need to be considered when designing *multiple insulator sets*. The loads should be distributed as equally as possible among the individual strings [10.1, 10.2]. The fittings need to be designed accordingly. After failure of an insulator string, the loads should be carried out by the residual strings to an equal extent. The material partial factors may be reduced compared with the requirements on the sound set [10.2]. The failing of an insulator string causes dynamic impact loads on the insulators and fittings which could result in secondary failures. An adequate design of insulator sets and fittings can avoid such consequences [10.19, 10.20].

The mechanical requirements and partial factors are stipulated in relevant standards, e. g. EN 50 341-1 [10.1], clause 11.6 and EN 50 341-3-4 [10.2], or in project specifications. A partial factor of at least $\gamma_M = 1{,}6$ has to be applied to the minimum mechanical failing loads specified in [10.3] for all types of fittings.

10.4.4 Corrosion protection

So far the individual elements of line fittings are not resistant to atmospheric corrosion by its own, they have to be protected against corrosion as can be experienced during transport, storing and operation. *Hot-dip galvanizing* according to [10.21, 10.22] is most suitable to all iron-based materials, stainless and acid-resistant alloys excepted. The purchaser, however, may stipulate other equivalent methods in his project specification. All male threads have to be rolled before galvanizing, female threads may be cut before or after the galvanizing procedure; in the latter case, they have to be oiled or greased. Contact corrosion at connections between fittings or conductors made of different materials should be prevented by an appropriate selection of fittings and/or materials.

10.4.5 Selection of material

The manufacturer of overhead line fittings ensures the stipulated characteristics and requirements on performance of the fittings by selecting suitable materials. The effects of low temperatures have to be taken into consideration, if any. It is recommended to use ISO standards for materials so far as available.
The adopted metallic materials may not be sensitive to *grain boundary* or *stress cracking corrosion.* Materials for compression fittings should withstand to cold forming; compressed steel elements should possess a sufficient *notched impact strength* even after compression.
Aluminium alloys for clamps and armor rods, hot-dip galvanized steel or malleable cast iron for connectors and spacers, stainless steel for bolts and annealed steel for balls represent frequently used materials.
Non-metallic material should show a good resistance against ageing, ozone, ultra-violet radiation and air pollution over the complete range of operating temperatures. They may not cause corrosion at other materials in contact with them. *Polyethylene* is frequently used, as well as *silicone-rubber* or *ethylene-propylene rubber*(EPDM), predominantly for damping purposes.

10.4.6 Tests

For *testing* of fitting quality during production, a quality assurance management program may be agreed upon between purchaser and manufacturer taking care of the requirements stipulated in relevant standards. Detailed information on the application of *quality assurance* can be found in the ISO standards of the 9000 series [10.23, 10.24, 10.25].
Whether and to what extent testing of fittings needs to be carried out depends on the type of fitting and the standards to be applied. An overview on testing stipulated or to be agreed upon between purchaser and manufacturer is listed in Table 10.2. The relevant standards distinguish between

- Type tests,
- Sample tests and
- Routine tests.

Type tests are provided for verifying the design characteristics and will usually be carried out once and repeated only if structural design or material of a fitting has changed. The extent of required tests can be taken from Table 10.2. Beyond this extent, additional tests can be agreed upon, e. g. corrosion, ageing, short-circuit or power arc tests, the requirements of which have to be defined before commissioning a contract. Fatigue tests are most important as they enable to verify the quality of elastomer regarding life time. The results of type tests should be recorded to give evidence of the compliance with the requirements on the structural design.
Sample tests are provided for checking the material and production quality. The purchaser is entitled, thereby, to select randomly a certain number of specimens, whereby the plan of taking specimens follows ISO 2859-1 [10.26] and -2 [10.27] (testing by attributes) or ISO 3951 (testing by variables) [10.28]. The type of testing and detailed procedures have to be agreed upon between purchaser and manufacturer in advance. If specimens pass the sample test, the batch concerned is considered as accepted.
Routine tests are provided for verifying specific requirements and for supervision of the production of fittings with an increased probability of defects. Mainly, these parts are tensile-loaded in operation. The extent of these tests is presented in Table 10.2 and needs in each case an agreement between purchaser and manufacturer. For testing procedures of fittings for optical cables see [10.29] and [10.30]. Routine tests are carried out at each individual fitting and, therefore, may not result in damage of the fitting.

Table 10.2: Tests on fittings according to [10.5]

	Type of test	Visual examination	Verification of dimensions and material	Hot-dip galvanizing	Non-destructive testing	Damage and failure load test	Slip test	Clamp bolt tightning test	Tensile test	Test of attachment point	Magnetic loss test	Heat cycle test	Corona and RIV test
Insulator and	T	x	x	x [3]	x [3]	x	–	–	–	x	–	–	x [3),6]
earth wire	S	x [2]	x	x	x [3]	x	–	–	–	x [3]	–	–	–
fittings	R	x [3]	x [3]	–	x [3]	x [3),4]	–	–	–	–	–	–	–
Suspension	T	x	x	x [3]	x [3]	x	x	x	–	–	x [3]	–	x [3),6]
clamps	S	x [2]	x	x	x [3]	x	x	x [2]	–	–	–	–	–
	R	x [3]	x [3]	–	x [3]	x [3),4]	–	–	–	–	–	–	–
Tension-proof	T	x	x	x [3]	x [3]	x	–	x	x	x	x [3]	x [5]	x [3]
joints and	S	x [2]	x	x	x [3]	x [3]	–	x [2]	x	x [3]	–	–	–
clamps	R	x [3]	x [3]	–	x [3]	–	–	–	–	x [3),4]	–	–	–
Partial	T	x	x	x [3]	x [3]	–	–	–	x	–	–	x [5]	x [3]
tension-proof	S	x [2]	x	x	x [3]	–	–	–	–	–	–	–	–
fittings	R	x [3]	x [3]	–	–	–	–	–	–	–	–	–	–
Repair sleeves	T	x	x	x [3]	–	–	–	–	x	–	–	–	x [3]
	S	x [2]	x	–	–	–	–	–	x	–	–	–	–
	R	x [3]	x [3]	–	–	–	–	–	–	–	–	–	–
Insulator	T	x	x	x [3]	x [3]	x [3]	–	–	–	–	–	–	x [3),6]
protective	S	x [2]	x	x	x [3]	x [3]	–	–	–	–	–	–	–
fittings	R	x [3]	x [3]	–	x [3]	x [3]	–	–	–	–	–	–	–

T type tests; S sample tests; R routine tests

[2] Inspection by attributes only

[3] By agreement between purchaser and supplier

[4] Only as regards damage load test

[5] Only for current-carrying joints

[6] Only in connection with complete insulator set

That is why *non-destructive test methods* are preferred. All fittings not complying with the requirements must be rejected.

10.5 References

10.1 EN 50 341-1: Overhead electrical lines exceeding AC 45 kV. Part 1: General Requirements – Common specifications. Brussels, CENELEC, 2001

10.2 EN 50 341-3-4: Overhead electrical lines exceeding AC 45 kV. Part 3-4: National Normative Aspects for Germany. Brussels, CENELEC, 2001

10.3 EN 61 284: Overhead lines – Requirements and tests for fittings (IEC 61284). Brussels, CENELEC, 1997

10.4 Ann, W. et al.: Insulators and fittings of the new 380 kV river Elbe crossing of Nordwestdeutsche Kraftwerke AG. Schwabach, JHW-RIBE Information No. 15e, 1978

10.5 Biedenbach, G. et al.: Die Tragklemme der Hochspannungs-Freileitung (Suspension clamps for high-voltage overhead lines). etz-Report 31, Berlin-Offenbach, VDE-Verlag GmbH, 1998

10.6 Cigré SC22 WG22-11: Guide to fittings for optical cables on transmission lines. Part 1: Selection and use. Electra 176 (1998), pp. 55 to 66

10.7 Giray, M.; Kießling, F.: Selection and rating of conductors, insulators and fittings for a 380 kV transmission line across the Bosphorus. Translation from Elektrizitätswirtschaft 83 (1984), pp. 893to 903, Siemens Energy A19100-C433-A871-X-7600

10.8 Cigré SC22 WG22-06: Load control devices on overhead transmission lines. Paris, Cigré Brochure 174, 2000

10.9 Möcks, L.: Das Verhalten des Leiterseiles unter dem Einfluss der Armaturen (Behaviour of conductors under the impact of fittings). Elektrizitätswirtschaft 68 (1969), pp. 336 to 341

10.10 DIN 48 334: Turnbuckles for overhead power lines. Berlin, DIN, 1977

10.11 EN 61 854: Overhead lines – Requirements and tests for spacers (IEC 61 854). Brussels, CENELEC, 1998

10.12 Möcks, L.: Damping of high-voltage overhead line conductor vibrations. etz-Report 15, Berlin-Offenbach, VDE-Verlag GmbH 1981

10.13 Cigré SC22 WG22-01: Report on aeolian vibration. Electra 124 (1989), pp. 41 to 77

10.14 EN 61 897 (VDE 0212 Teil 3): Overhead lines – Requirements and tests for Stockbridge-type aeolian vibration dampers (IEC 61 897). Brussels, CENELEC, 1998

10.15 IEC 60 120: Dimensions of ball-and-socket coupling of string insulator units. Geneva, IEC, 1987

10.16 IEC 60 471: Dimensions of clevis and tongue couplings of string insulator units. Geneva, IEC, 1987

10.17 IEC 60 372-1: Locking devices for ball and socket couplings of string

10.18 BS 137: Specification for insulators of ceramic material or glass for overhead lines with a nominal voltage greater than 1000 V. Part 2: Requirements. London, BSI, 1973

10.19 Bauer, E. et al.: Dynamic process during load transposition in multiple sets with long-rod-type insulators. Cigré Report 22-03, 1982

10.20 Hagedorn, P.; Idelberger, H.; Möcks, L.: Dynamische Vorgänge bei Lastumlagerungen in Abspannketten von Freileitungen (Dynamic phenomena occurring during load transposition in dead-end insulator sets of overhead lines). etz archive Volume 2, Report 4. Berlin-Offenbach, VDE-Verlag GmbH, 1980

10.21 EN ISO 1461: Hot-dip galvanized coatings on iron and steel articles. Specifications and test methods (ISO 1461). Brussels, CEN, 1999

10.22 EN ISO 14 713: Protection against corrosion in iron and steel. Zinc and aluminium coatings – Guidelines (ISO 14 713). Brussels, CEN, 1999

10.23 EN ISO 9001: Quality systems. Model for quality assurance and design, development, production, installation and servicing (ISO 9001). Brussels, CEN, 1994

10.24 EN ISO 9002: Quality systems. Model for quality assurance and production, installation and servicing (ISO 9002). Brussels, CEN, 1994

10.25 EN ISO 9003: Quality systems. Model for quality assurance and final inspection and tests (ISO 9003). Brussels, CEN, 1994

10.26 ISO 2859-1: Sampling procedures for inspection by attributes – Part 1: Sampling schemes indexed by acceptance, quality limit (AQL) for lot-by-lot inspection. Geneva, ISO, 1991

10.27 ISO 2859-2: Sampling procedures for inspection by attributes – Part 2: Sampling plans indexed by limiting quality (LQ) for isolated lot inspection. Geneva, ISO, 1985

10.28 ISO 3951: Sampling procedures and charts for inspection by variables for percent nonconforming. Geneva, ISO, 1989

10.29 Cigré SC22 WG22-11: Guide to fittings for optical cables on transmission lines. Part 2A: Testing procedures. Optical ground wire fittings and optical phase conductor fittings. Electra 188 (2000), pp. 42 to 53

10.30 Cigré SC22 WG22-11: Guide to fittings for optical cables on transmission lines. Part 2B: Testing procedures. All-dielectric self-supporting cable fittings and optical attached cable fittings. Electra 191 (2000), pp. 62 to 75

11 Conductor vibrations

11.0 Symbols

Symbol	Signification
a	Span length
A_d	Cross section of a strand
$\hat{A}_\mathrm{f}$	Conductor free-span vibration amplitude
c	Travelling wave velocity
c_s	Travelling wave velocity of conductor with bending stiffness
C	Parameter of conductor self-damping
C_1, C_2, C_3, C_4	Constants
d	Strand diameter
D	Conductor diameter
e	Distance of a strand between neutral axis and surface
E	Modulus of elasticity
EI	Conductor bending stiffness
f	Frequency
f_s	Frequency of conductor with bending stiffness
f_W	Wind excitation frequency
g	Acceleration due to gravity
H	Horizontal conductor tensile force
H_B	Conductor minimum failing load
I	Moment of inertia
$I_{\mathrm{pd}i}$	Polar moment of inertia of a strand in the layer i
j	Number of stress classes
K	Solution function
k	Number of vibration modes, harmonic coefficient
m_C	Conductor mass per unit length
n	Number of strands
n_i	Number of vibration cycles recorded in one year
N	Number of layers, number of cycles to failure
N_i	Number of cycles to failure at stress level i
p, q, r	Exponents of conductor self-damping
P_D	Damper power, power loss of a damper
P_S	Conductor damping power, power loss of vibrating conductor
P_W	Conductor energy imparted by wind
q	Function of time
q_D	Conductor damping function
q_W	Wind power input function
Q_A	Uplift and downward wind force
Q_L	Aerodynamic drag force
r	Root of characteristic equation
R_i	Radius of helix of the layer i
S_r	Strouhal number
t	Variable of time
t_l	Life period of a conductor
$\hat{v}_\mathrm{K}$	Velocity of damper clamps
V_W	Wind velocity transverse to conductor
w	Conductor transverse displacement
w_b	Bending amplitude at distance x_b from the clamp
x	Variable of coordinate
x_b	Distance between clamp and position of amplitude measurement
z	Exponent
Z	Damper impedance (complex)

Symbol	Signification
α	Real natural value of characteristic equation
α_1	Factor equal $\sqrt{H/EI}$
β	Imaginary natural value of characteristic equation
ε	Strain of strand, bending strain
λ	Wave length
λ_s	Wave length of conductor with bending stiffness
μ	Dimensionless parameter
σ	Stress of strand
σ_{bF}	Dynamic limit stress
φ	Phase shifting angle, conductor swing angle
ψ	Free-span vibration angle
ω	Angular frequency

11.1 Overview and types of vibration

As an unprotected structure, each power transmission line is exposed to the natural wind which produces a series of mechanic-dynamic phenomena within the power line. *Wind-induced vibrations* occur with different features and attain particular significance. The wind flow induces aerodynamic forces on a conductor causing hazardous vibrations that impair the reliability and *lifetime* of a power line. Special attention should be paid to all types of *conductor vibrations* when designing a power line to keep adverse drawbacks at a minimum. Three main groups may be distinguished, so far as vibration excitation, vibration modes and frequencies are concerned [11.1].

Aeolian vibrations

The wind forces acting transversely on the conductor cause alternating excitations in the vertical direction resulting in *aeolian vibrations*, also called *Kármán vibrations*. They are characterized by relatively short wave lengths and frequencies between 5 and 100 Hz. The vibration amplitudes may reach the magnitude of the conductor diameter at the antinode. Kármán vibrations belong to the *vortex-induced vibrations* and are classified as high-frequency [11.2, 11.3]. Aeolian vibrations occur at winds having a laminar structure, generally with wind velocities up to 5 m/s in rough terrain and up to 10 m/s in flat terrain.

Subspan oscillations

Subspan oscillations occur only at bundle conductors with subconductors arranged one after the other in wind direction. The leeward conductor is aerodynamically excited by the inhomogeneous wind field behind the windward conductor; this is addressed as an instability due to aerodynamic coupling. The frequency of subspan oscillation is between 1 and 5 Hz, the wave length being equal or twice the subspan length. The wind velocities causing subspan oscillations are between 4 and 18 m/s and may result in differing oscillation modes. The oscillation amplitude depends on the oscillation mode and may reach half of the subconductor spacing causing conductor clashing, therefore. Subspan oscillations are considered as *flow-induced vibrations* and are classified as low-frequency [11.4].

Conductor galloping

Galloping oscillations occur at single conductors and, particularly, at bundle conductors. The amplitudes may reach the conductor sag, potentially leading to clashing of conductors or to flashovers. Some special cases excluded, conductor galloping is always combined with ice accretion on the conductors, causing a disymmetrical and, therefore, aerodynamically unstable profile. A non-stationary aerodynamic transverse force acts

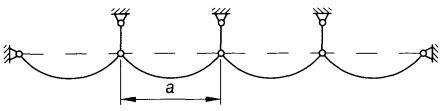

Figure 11.1: Schematic representation of a line with four spans

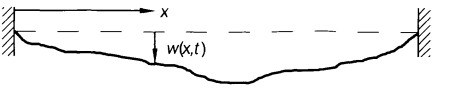

Figure 11.2: String rigidly fixed at both ends

in direction of the oscillation motion and excites the oscillating conductor further. In case of bundle conductors, the transversal oscillation is superimposed by a torsional oscillation, which leads to the angle of wind flow attack necessary for the energy input. The exciting wind velocities are between 6 and 25 m/s and, as a rule, result in the first oscillation mode, where a span is oscillating as half wave, or to higher natural modes, where at least one oscillation mode is present in a span. The oscillation frequency is low, being less than 1 Hz. Conductor galloping is considered as a *flow-induced vibration* with motion-induced excitation; it is classified as low-frequency [11.5].

11.2 Aeolian vibrations

11.2.1 Basic physical aspects, mathematic-mechanic model of a line

For a long period of time, *aeolian vibrations*(*Kármán-vibrations*) have been the subject of intensive studies and numerous publications [11.6] to [11.8]. Only some basic aspects can be treated here. For detailed information, reference should be made to the quoted publications.

The mechanic model [11.6] is related to a span with the length a. Thereby, the coupling of adjacent spans by the insulator sets (Figure 11.1) is neglected and the conductor sag is considered to be low compared with the span length [11.9]. Then, the conductor is strung between two attachment points mathematically replaced by a string with small *bending stiffness* (Figure 11.2). This model can be described by the partial differential equation [11.8] and [11.10].

$$EI\frac{\partial^4 w}{\partial x^4} - H\frac{\partial^2 w}{\partial x^2} + m_C\frac{\partial^2 w}{\partial t^2} = q_W(x,t) + q_D(w,\dot{w},t) \quad . \tag{11.1}$$

The term $q_W(x,t)$ represents the force due to wind flow and the term $q_D(w,\dot{w},t)$ the damping force due to *conductor self-damping*. For further considerations, it suffices to consider the free oscillations only. Therefore, the right side in (11.1) can be set to zero. The remaining differential equation can be separated by the expression

$$w(x,t) = w(x) \cdot \sin(\omega \cdot t) \quad , \tag{11.2}$$

where $\sin(\omega \cdot t)$ is a solution of the time equation

$$\ddot{q}(t) + \omega^2 q(t) = 0 \quad . \tag{11.3}$$

Inserting (11.2) into (11.3) the spatial equation is obtained:

$$EI \cdot (w'')''(x) - H \cdot w''(x) - \omega^2 \cdot w(x) = 0 \quad . \quad . \tag{11.4}$$

There, ω is the angular frequency of the considered vibration mode.

For the further considerations, the time-related component of the complete solution is without significance; therefore, only the spatial equation (11.4) needs to be studied. By using the set of solutions

$$w(x) = K \cdot e^{rx} \tag{11.5}$$

inserted into (11.4), the characteristic equation

$$r^4 - (H/EI)\, r^2 - m_C\omega^2/EI = 0 \tag{11.6}$$

is obtained, the solutions of which are

$$\begin{aligned} r_{1,2,3,4} &= \pm\sqrt{\frac{H}{2\cdot EI} \pm \sqrt{\frac{m_C\omega^2}{EI} + \left(\frac{H}{2\cdot EI}\right)^2}} \\ &= \pm\sqrt{\frac{H}{2\cdot EI}} \cdot \sqrt{1 \pm \sqrt{1 + \frac{4\,EI\, m_C\omega^2}{H^2}}} \quad . \end{aligned} \tag{11.7}$$

Since $(1 + 4\,EI \cdot m_C \cdot \omega^2/H^2) > 1$, two real roots exist:

$$r_{1,2} = \pm\alpha \tag{11.8}$$

and two imaginary ones:

$$r_{3,4} = \pm \mathrm{j}\,\beta \tag{11.9}$$

with the natural values

$$\alpha = \sqrt{H/2\,EI}\,\sqrt{\sqrt{1+\mu}+1} \quad \text{and} \tag{11.10}$$

$$\beta = \sqrt{H/2\,EI}\,\sqrt{\sqrt{1+\mu}-1} \quad . \tag{11.11}$$

There, the dimensionless parameter

$$\mu = 4\,EI m_C\omega^2/H^2 \quad . \tag{11.12}$$

has been used. The corresponding integration constants can be obtained from the boundary conditions, finally finding the *location-dependent displacement* $w(x)$.

$$w(x) = C_1 \cosh\alpha x + C_2 \sinh\alpha x + C_3 \cos\beta x + C_4 \sin\beta x \quad . \tag{11.13}$$

A numerical study, taking into account the conductors usually used for overhead power lines together with the corresponding tensile forces and vibration frequencies, demonstrated that μ is small compared with 1. Therefore, the approximations

$$\alpha = \sqrt{H/EI} \quad \text{and} \tag{11.14}$$

$$\beta = \omega\sqrt{m_C/H} \tag{11.15}$$

can be accepted. Taking into account $\mu \leq 1$ and $\alpha \geq \beta$, it is obtained from (11.13) and (11.2)

$$w(x) = \hat{A}_f \sin(\beta x) \tag{11.16}$$

as an approximation for the location-dependent displacement, where $\hat{A}_f$ is the *free-span amplitude*. Assuming, that the *conductor bending stiffness* is negligible, the approximate solution of the frequency equation is, independently of the boundary conditions,

$$\sin\beta a = 0 \quad . \tag{11.17}$$

Equation (11.17) is solved by

$$\beta = k\pi/a \quad , \tag{11.18}$$

with k being natural numbers $k = 1, 2, 3 \ldots$. Equations (11.18) and (11.11) deliver the *natural frequencies*, taking into account the *bending stiffness*:

$$f_S = \frac{k}{2a}\sqrt{\frac{H}{m_C}}\sqrt{1+\frac{(k\pi a)^2 \cdot EI}{H}} \quad , \tag{11.19}$$

or, when the stiffness EI is neglected,

$$f = (k/2a) \cdot \sqrt{H/m_C} \quad . \tag{11.20}$$

Equation (11.20) corresponds to the well-known expression for the *natural frequencies* of a string rigidly fixed at both ends and, in practice, is adopted for overhead line conductors as well. The expression under the square root in (11.20) represents the *travelling wave velocity* c when neglecting the bending stiffness

$$c = \sqrt{H/m_C} \quad . \tag{11.21}$$

When taking into account the bending stiffness, the travelling wave velocity is obtained from

$$c_S = \sqrt{\frac{H}{m_C}}\sqrt{1+\frac{(k\pi a)^2 EI}{H}} \quad . \tag{11.22}$$

The relation between the order number k, also called *harmonic coefficient*, the *span length* a and the wave length λ is

$$k/2a = 1/\lambda \quad . \tag{11.23}$$

The wave length of a conductor with *bending stiffness* is obtained from (11.23) and (11.19):

$$\lambda_S = \sqrt{\frac{H}{2m_C f_S^2} + \sqrt{\left(\frac{H}{2m_C f_S^2}\right)^2 + 4\pi^2\left(\frac{EI}{m_C f_S^2}\right)}} \quad , \tag{11.24}$$

and without bending stiffness

$$\lambda = (1/f)\sqrt{H/m_C} \quad . \tag{11.25}$$

11.2.2 Conductor free-span amplitude

To determine the conductor stress, the *free-span vibration amplitude* is needed. To find this quantity, equation (11.1) could be used. However, its solution provides some difficulties, since the equation contains terms for wind input energy and conductor damping, which cannot be equated mathematically in a simple manner. Therefore, vibration amplitudes are approximately determined using the *energy balance principle* (EBP) [11.3, 11.9, 11.11]. Using this approach, a stationary vibration condition is assumed for the conductor together with the *free-span amplitude* $\hat{A}_f$. The vibration modes are assumed as standing harmonic waves, where the exciting frequency complies with the Strouhal relation [11.12]

$$f_W = S_r V_W / D \quad , \tag{11.26}$$

where f_W is the *wind excitation frequency*, S_r the *Strouhal number* (between 0,18 and 0,22), V_W the wind velocity and D the conductor diameter.
In a stationary vibration condition, the mean power P_W fed into the system by the wind balances the mean damping power P_S due to the self-damping of the conductor and the mean power loss P_D of dampers [11.13]. These power components depend non-linearly

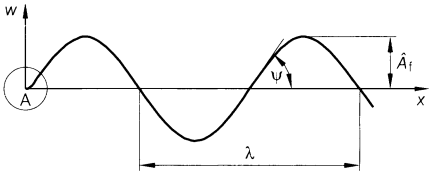

Figure 11.3: Standing wave, conductor rigidly fixed at the left boundary

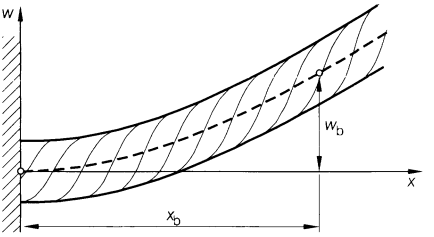

Figure 11.4: Detail A of Figure 11.3, bending amplitude w_b in a distance x_b from the rigidly fixed conductor end

on the free-span amplitude $\hat{A}_f$ and the excitation or vibration frequency f. In this case, the energy balance is equated as

$$P_W(\hat{A}_f, f) = P_D(\hat{A}_f, f) + P_S(\hat{A}_f, f) \quad . \tag{11.27}$$

To determine the free-span amplitude, terms for the quantities P_W, P_D and P_S are required. The expression

$$P_W = f_W^3 D^4 a \cdot g(\hat{A}_f/D) \tag{11.28}$$

has proved to be adequate for representing the *wind input power* related to a span with the length a [11.3]. The function is usually determined by measurements in wind tunnels [11.14, 11.15]. The polynom

$$g(\hat{A}_f/D) = 2,6 \left(\frac{\hat{A}_f}{D}\right) + 81,2 \left(\frac{\hat{A}_f}{D}\right)^2 - 76,5 \left(\frac{\hat{A}_f}{D}\right)^3 \tag{11.29}$$

can be used as an approximation for $g(\hat{A}_f/D)$. For the *effective power* of a *Stockbridge-type damper*, the relation

$$P_D = 1/2\, \hat{v}_K^2 \,\mathrm{Re}[Z] \tag{11.30}$$

applies according to [11.16], where $\hat{v}_K$ is the velocity amplitude of the damper clamps and $\mathrm{Re}[Z]$ the real part of the complex, frequency-dependent impedance Z of the damper. The damper impedance characterizes each type of damper and cannot be expressed in a mathematical format. It is determined by measurements for each type of vibration damper type [11.17]. Figure 11.14 depicts the module of the impedance $|Z|$ and the phase shift φ. The real component $\mathrm{Re}[Z]$ will be $|Z| \cdot \cos\varphi$ in this case.
The dissipated power of a vibrating conductor is measured in a laboratory or can be obtained from [11.3]

$$P_S = C f_W^p \hat{A}_f^q H_B \cdot a/H^r \quad , \tag{11.31}$$

where $\hat{A}_f$ is the free-span vibration amplitude, H the conductor tensile force and H_B the conductor minimum failing load. The quantities of the damping constant C and the exponents p, q, r are usually determined from measurements at a vibrating conductor [11.18, 11.19]. The evaluation of numerous measurement [11.3] results led to the following quantities for the damping parameter C and the exponents p, q and r:

$$C = 6,5 \cdot 10^{-11} \text{ to } 1,5 \cdot 10^{-5},\ p = 3,8 \text{ to } 6,0,\ q = 1,9 \text{ to } 2,6,\ r = 2,0 \text{ to } 2,8.$$

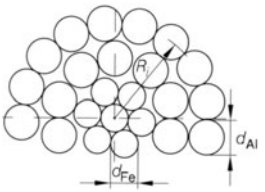

Figure 11.5: Geometric data to determine the bending stiffness of a conductor

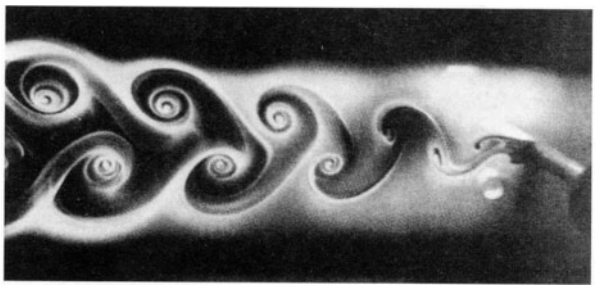

Figure 11.6: Kármán vortex pattern [11.22, 11.23]

11.2.3 Conductor strains and stresses

The *vibration intensity* of a conductor is defined by the *free-span vibration angle* ψ which results from the free-span amplitude, the vibration frequency and the wave length (Figure 11.3). Using the approximation (11.15), it applies

$$\psi = 2\pi \hat{A}_f / \lambda \quad . \tag{11.32}$$

The *bending strain* of the conductor strands can be taken as a bench mark for their stressing. The relation between the bending strain of a strand ε in the outer layer and the curvature of the conductor is according to [11.20]

$$\varepsilon(x) = e \cdot w''(x) \quad , \tag{11.33}$$

where e is the distance between neutral axis and surface of a strand.
For a rigidly clamped conductor, the bending strain is obtained using $\omega = 2\pi f_W$ for the resonance condition at the clamping position

$$\varepsilon(0) = e\hat{A}_f \omega \sqrt{m_C/EI} = e\psi\sqrt{H/EI} \quad . \tag{11.34}$$

The conductor bending strain can alternatively be expressed by the *bending amplitude* w_b [11.21]. For this purpose, the displacement of the conductor is calculated at a distance x_b from the clamping position (Figure 11.4). The corresponding bending strain at the clamping position results from

$$\varepsilon(0) = \frac{(d \cdot w_b \cdot \alpha_1)/4}{x_b - [1 - \exp(-\alpha_1 x_b)]/\alpha_1} \quad , \tag{11.35}$$

where d is the diameter of the strand in the outer layer and $\alpha_1 = \sqrt{H/EI}$ with H conductor tensile force and EI the bending stiffness according to equation (11.37) or (11.38).
The correlation between the strain and the stress in a *strand* is according to [11.18]

$$\sigma = \varepsilon E_{Al} \quad , \tag{11.36}$$

where E_{Al} is the *modulus of elasticity.*

11.2.4 Bending stiffness of a conductor

Due to the conditions between the individual wires and the layers of a stranded conductor, the *bending stiffness* can only be determined between its upper and lower limit. The minimum value results with the assumption that the strands can move without

any friction relative to each other. For this case, the *minimum bending stiffness* of a composite conductor is

$$(EI)_{\min} = \left(n_{\mathrm{Fe}} E_{\mathrm{Fe}} \pi d_{\mathrm{Fe}}^2 + n_{\mathrm{Al}} E_{\mathrm{Al}} \pi d_{\mathrm{Al}}^2\right) / 64 \quad , \tag{11.37}$$

where n_{Fe} is the number of steel strands, n_{Al} the number of aluminium strands, E_{Fe} and E_{Al} the modulus of elasticity of steel and aluminium strands, respectively, d_{Fe} and d_{Al} the diameter of steel and aluminium strands, respectively. The assumption of completely non-displaceable strands yields the *maximal bending stiffness* of a composite conductor

$$(EI)_{\max} = \frac{1}{2} \sum_{i=1}^{i=N} (I_{\mathrm{pd}i} + R_i^2 A_{\mathrm{d}i}) n_i E_i \quad , \tag{11.38}$$

where N is the number of layers counting the core wire as the 1st layer, R_i the average radius of the helix of the layer i and $I_{\mathrm{pd}i}$ the polar moment of inertia of a strand in the layer i:

$$I_{\mathrm{pd}i} = d_i^4 \cdot \pi / 32,$$

(see Figure 11.5), $A_{\mathrm{d}i}$ the cross section of a strand in the layer i, n_i the number of strands of the layer i and E_i the modulus of elasticity of the layer i.
If the tensile-loaded conductor is bent, the layers will move relatively to each other, depending on the conductor curvature and the friction between the layers. The *conductor structure* is partly destroyed and the *effective bending stiffness* will be in between both limits [11.24].

11.2.5 Origin of vibrations

Already at the beginning of electric power transmission by overhead lines, wind excited *conductor vibrations* were observed, e. g. the singing of an overhead telephone wire. The origins for these vibrations formed the subject of many studies and were described in detail and extensively in the literature [11.25]. Air pressure variations are caused by vortex shedding behind the conductor in the air flow, inducing a periodic force to the conductor rectangularly to the air flow direction. If the *frequency of vortex shedding* coincides with a natural frequency of conductor just to an approximate extent, a resonance condition will be given. This physical phenomenon is the same as the behaviour of rigid subjects in flowing fluids as studied by Kármán [11.22], where according to [11.23] the *Kármán vortex street* can be observed (Figure 11.6). Prior to Kármán, Strouhal concluded the relation (11.26) according to [11.12] between air flow velocity, the diameter of the cylindric body in the air flow and the shedding frequency of the vortices when studying the behaviour of moving wires in still air. In principle, the dimensionless *Strouhal number* depends on the *Reynolds number* (see clause 7.2.3). It is only for Reynolds numbers between 500 and 20 000, that well structured vortex shedding occurs at conductors and excites vibrations. For this range, the Strouhal number can be assumed to be constant and equal to 0,185. From (11.26) it results that vibrations with frequencies between 3,1 and 61,7 Hz will occur for a 30 mm conductor diameter at wind velocities between 0,5 to 10 m/s.
The process of excitation is more complex in case of a vibrating conductor than the shedding of Kármán vortices at a cylinder not in motion. There is a feed back between the elastic structure and the air flow. If the excitation frequency is close to the natural frequency of the vibrating conductor, the motion will be amplified. When approaching a range of resonance, the frequency of vortex shedding will be synchronized with the conductor frequency and the vibration frequency will not change even if the velocity of air flow varies. As a consequence, the vortex shedding will be controlled by the *vibrating*

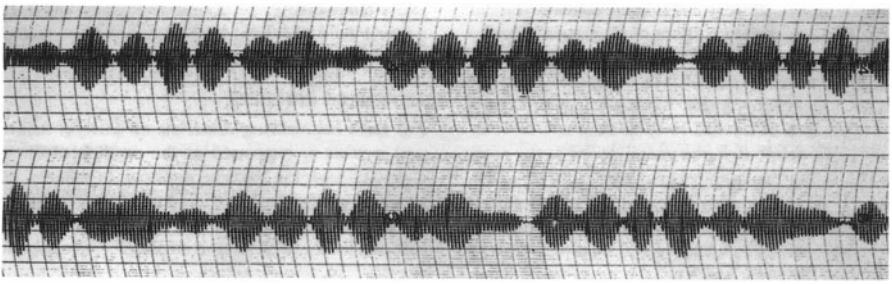

Figure 11.7: Beat pattern of aeolian vibrations of conductor in a 275 m long span observed at its ends [11.23]

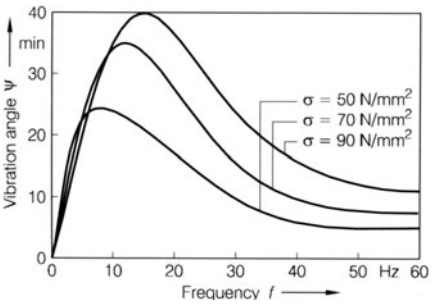

Figure 11.8: Vibration angle of a conductor 565-AL1/72-ST1A (ACSR 564/72) depending on conductor tensile stress and frequency [11.26]

process. This explains as well why the resonance condition is not basically affected by varying wind velocities.

Being a slender structure in longitudinal direction, the conductor shows a very dense spectrum of natural frequencies, such that the exciting frequency of vortex shedding will always meet a matching conductor natural frequency. Therefore, resonance is possible in a relatively wide range of frequencies with the result that conductors will vibrate always when favourable air flow conditions exist.

Measurements at conductors confirmed their permanent and continuous readiness for vibrations and demonstrated a close coincidence between vibration frequency and *vortex shedding frequency* determined from (11.26). In this context, it is important that only the component of the velocity is considered, which acts perpendicularly to the conductor. In addition, measurements have shown that within the frequency spectrum only some specific frequencies will be excited to bigger amplitudes, whereby several frequencies occur simultaneously and result in *beat patterns* (Figure 11.7). This phenomenon is given reason by varying wind velocities along a span [11.23].

11.2.6 Consequences of vibrations

For assessing the alternating bending stress and possible damage resulting thereof, not only the amplitude but also the *frequency of occurrence* is significant. Figure 11.8 depicts the effect of vibration frequency and conductor tensile stress, determined using the *energy balance principle.* With increasing tensile stress, the vibration intensity grows and simultaneously the band width of frequencies is broadened where hazardous alternating bending stresses may occur. Intensive conductor vibrations occur particularly in case of quasi-laminar air flow conditions. Turbulent air flows, as occurring in rolling terrain and terrain with abundant vegetation, do not cause a controlled vortex shedding. The less disturbed a laminar air flow affects the conductor, the more intensive the vibration will be. This condition applies in particular for conductors at great heights

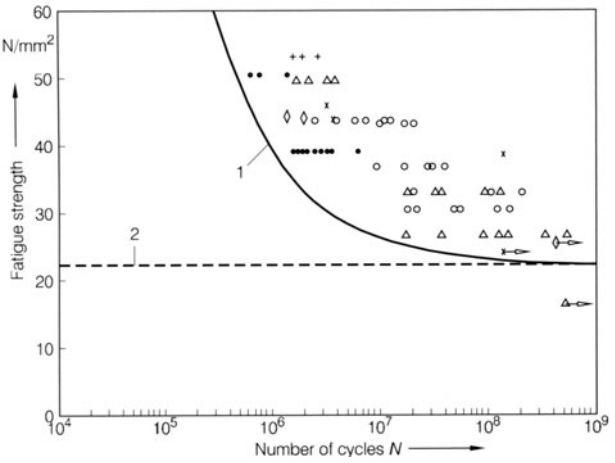

Figure 11.9: Results from fatigue tests at AL1/STxy (ASCR) conductors with different suspension clamps [11.23] (endurance capability diagram)

△	ACSR 54 × 3,08 / 7 × 3,08	Condor according to ASTM B232-78;
⊕	ACSR 45 × 3,38 / 7 × 2,25	Tern according to ASTM B232-78;
×	ACSR 45 × 3,70 / 7 × 2,47	Rail according to ASTM B232-78;
•	ACSR 26 × 3,14 / 7 × 2,44	Ibis according to ASTM B232-78;
◇	ACSR 30 × 2,92 / 7 × 2,92	Lark according to ASTM B232-78;
○	ACSR 30 × 2,92 / 7 × 2,92	Lark according to ASTM B232-78;
→	no wire failure;	

1 upper limit in the fatigue diagram; 2 line of endurance capability

above ground. The occurrence of vibrations depends on numerous parameters, besides the topography, on locally given wind conditions and the wind distribution along a span. Therefore, not all lines will be affected by vibrations to a harmful extent.

Flat terrain favours vibrations, while rolling terrain, mountainous and alpine terrain conditions impair the laminar air flow to an increasing extent. The *surface roughness* of the terrain affects the vibrations to the same extent as the terrain category. In a rolling terrain, a highly laminar air flow may exist, too, if the surface is smooth, e. g. due to ice or snow. Water surfaces, sandy soil in desert areas and flat grass areas proved to be vibration-favourable as well. On the other hand, stretches of boulders, rocks, trees or urban buildings reduce the probability of laminar air flows to an increasing extent. Experience confirms that vibration failures occur always in cases where terrain and ground surface favour laminar air flows. The worldwide intensive investigations have permitted to identify the differing influencing parameters. However, the vibration intensity to be expected on a certain line cannot be forecast definitively with quantitative figures.

The type of conductor considerably affects the *vibration intensity*, as well as duration of vibration. Conductors with a low weight, compared with their diameter, reach much faster a stationary vibration condition than heavy conductors. This is the reason why in particular single material conductors made of aluminium (AL1) or aluminium alloy (ALx) have to be classified as being endangered by vibrations to an increased extent.

Besides the vibration intensity, the *endurance capability* of the material affects the occurrence and extent of vibration failures, together with the design of the conductor suspension. The total of stresses on the conductor and, therefore, on the individual strands is remarkably higher in the vicinity of the *suspension clamps* than in the free span or close to the *tension clamps* (see clause 10.2.1). Type and design of suspension arrangements, therefore, will govern on the endurance capability of a conductor together with some other parameters. According to experience, vibration failures occur at the

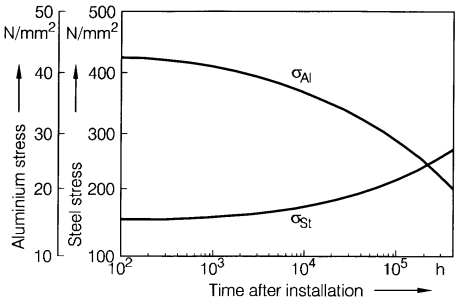

Figure 11.10: Tensile stress at aluminium and steel of conductor 565-AL1/72-ST1A (ACSR 564/72) depending on the time after installation

conductor suspension first [11.27, 11.28]. Remedies and protection methods have to start at the suspension points, with the target to keep the stress as low as possible there. Even, when during a period of approximately one hour only per day, intensive vibrations occur, 10^7 to 10^8 vibration cycles will be reached during one year.

The reliability against *vibration failure* is a problem of endurance. From testing materials, it is known that metals show fatigue. They fail in case of alternating stresses far below the static strength or the yield stress.

The *endurance capability diagram* (Figure 11.9) shows the amplitudes of the alternating bending strength against the number of cycles for various conductors. A high number of tests is necessary to establish such a diagram.

Conductors used for transmission lines represent relatively complex structures with respect to their endurance strength behaviour. Alternating bending stresses in the individual strands are superimposed to the initial tensile and bending stresses due to the static curvature of the conductor at the suspension points. Within the conductors, the individual strands cross each other and a variation in the curvature results in a displacement of the strands, causing friction and *friction corrosion*, so-called *fretting*. The fretting marks form regularly the starting points of fatigue failures [11.29]. At the clamps, a complex stress condition is formed due to the additional transmission of transversal forces. Fatigue tests at conductors without taking care of the fittings yield, therefore, only an indication of the fatigue strength. They do not permit a reliable conclusion on the performance of the combination between conductor and clamp. The effect of corrosive media cannot be neglected under unfavourable environmental conditions.

Results from extensive fatigue tests at AL1/ST1A conductors are summarized in [11.23]. There a value of approximately 22 N/mm^2 is mentioned as fatigue strength for $5 \cdot 10^8$ cycles. In Figure 11.9, some results from these tests are shown. The tensile stress of 22 N/mm^2 corresponds to an *alternating bending strain* of approximately 300 μm/m for typical conductors assuming $EI_{\min}$ according to (11.37) for the bending stress. To be on the safe side, it is common international practice to permit a limit of 150 μm/m for the bending strain when rating and deciding on vibration damping systems. This value corresponds to half of the fatigue strength [11.11, 11.30, 11.31].

During operation, the conductors elongate permanently under the action of the mechanical stress, they creep. In case of composite conductors, tensile force components are transposed from the aluminium to the steel (Figure 11.10), [11.26, 11.32, 11.33, 11.34]. This *load transfer* represents an important feature of *composite conductors* which add to their favourable fatigue performance, because the range of acceptable alternating bending stresses rises with decreasing stress in the aluminium. In case of *single material conductors*, such a transfer cannot occur. Such conductors will, therefore, show a more unfavourable fatigue behaviour, the same initial tensile stresses in the aluminium wires assumed.

Table 11.1: Recommended everyday stress as percentage of the rated tensile stress (RTS) to protect conductors without dampers against aeolian vibrations

Conductor type	Cigré 1960 [11.38]	EN 50 341-3-4	Cigré 2000 [11.39]
AL1/ST1A (ACSR)			Terrain C
4,3:1	18	18,5	13
6,0:1	18	18,5	14
7,7:1	18	19,0	15
11,3:1	18	18,4	16
Aluminium AAC	17	18,8	20,8
AlMgSi AAAC	18	15,0	11,3
Steel			
– rigid clamps	11	—	—
– flexible clamps	13	—	—

For the design of the suspension attachments, the fatigue strength of the conductor is important. Suspension clamps without any damping effects have proved their qualification for transmission lines in less vibration-prone areas. However, for vibration-prone lines, improved designs are necessary. The use of protective rods, clamps with long supporting sections, armor rod suspensions or other special designs (see section 10.2.1) improve the conditions at the suspension points in the mentioned sequence ([11.35] to [11.37]). These fittings reduce the stresses within the conductor, but they do not act as dampers.

11.2.7 Consequences for line design

With respect to aeolian vibrations, relatively heavy composite conductors are preferred. Light-weight single conductors made of aluminium or aluminium alloy are more intensively prone to long-lasting vibrations under the same conditions. The same applies to AL1/ALx (ACAR) conductors. Their use in vibration-prone areas requires, therefore, a particularly thorough selection of damping arrangements. Especially the higher tensile strength of aluminium alloy cannot be utilized in all cases compared to aluminium without running into increased vibration hazards.

For a long period of time, the selection of the *conductor stress* has been given high priority with respect to the aeolian vibrations. A corresponding selection of the conductor tensile stress under *everyday conditions (everyday stress)* with approximately 20 % of the conductor tensile strength should exclude vibration hazards from conductors.

In [11.38], recommendations for the selection of conductor stresses in view of protection against failures resulting from aeolian vibrations are given as established by the so-called EDF-Panel of the Study Committee "Overhead Lines" at Cigré before 1960. These recommendations establish an everyday stress as percentage of the rated tensile strength (RTS). In Table 11.1, these recommendations are shown. However, they did not prove their qualification, especially in case of aluminium and aluminium alloy conductors and resulted in strand failures. This is also true for unprotected composite conductors with a cross-sectional ratio higher than 7,7:1 and in rare cases also for ACSR conductors with damping devices [11.40].

A high tensile stress reduces the conductor self-damping and increases the vibration intensity (see Figure 11.8). Vice versa, a low conductor stress results also in a lower vibration intensity, but consequently in larger sags, taller towers and in higher investments. Therefore, in [11.39] and [11.40], the question on a *vibration-safe conductor stress* for undamped and damped conductors has been considered again. A *safe design tension* (SDT) is aimed at, below which no vibration fatigue is to be expected. The

Table 11.2: Limits for the parameter $H/m_C g$ for protection against vibration damage

Terrain category	Terrain characteristics	$H/m_C g$ m
A	Open, flat, no trees, no obstructions, with snow cover or near/across large bodies of water; flat desert	1 000
B	Open, flat, no trees, no obstructions, no snow; e. g. farmland without any obstructions	1 125
C	Open, flat, or undulating with very few obstacles, e. g. open grass or farmland with few trees, hedgerows and other barriers; prairie, tundra	1 225
D	Built-up with some trees and buildings; e. g. residential suburbs; small towns; woodlands and shrubs; small fields with bushes, trees and hedges	1 425

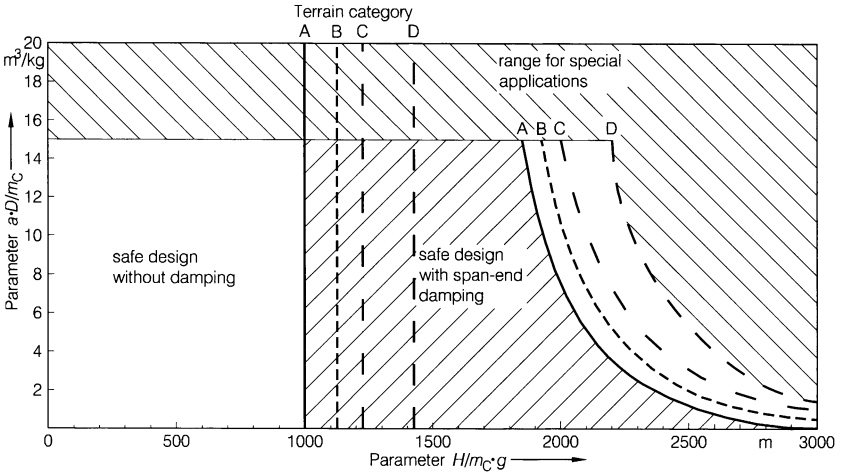

Figure 11.11: Recommendations for the selection of the everyday stress with and without damping according to [11.40]

considerations led to two parameters: $H/m_C g$, known as *catenary parameter* in the sag calculation (see clause 14.2), and $a \cdot D/m_C$, where a is the span length, D the conductor diameter, H the conductor tensile force and m_C the conductor mass per unit length. The parameter $H/m_C g$ has got the unit m, the parameter $a \cdot D/m_C$ the unit m^3/kg. Vibration protection for lines without dampers will be assessed only by the parameter $H/m_C g$, for which limits have been established using the *energy balance principle* (see clause 11.2.2 and [11.11]), which take into account the level of *vibration intensity* depending on terrain categories. The limits are also based on experience from overhead line practice. The results are given in Table 11.2; they apply for conductors made of aluminium AL1 (AAC) and aluminium alloy ALx (AAAC), bi-metallic aluminium conductors AL1/ALx (ACAR), as well as aluminium conductors steel reinforced ALx/STyx (ACSR). The limit according to Table 11.2 for terrain category C corresponds to an everyday stress of approximately 42 N/mm^2 in case of ALx/STyz conductors with the cross-sectional ratio of 6:1 and to 40 N/mm^2 in case of a cross-sectional ratio of 7,7:1, that are 14 % and 15 %, respectively, of the rated tensile stress. In case of aluminium and aluminium alloy conductors, the same data for permissible safe conductor stresses result, because of the same mass per unit length. These consequences are not plausible. While in case of aluminium an increase of the safe limit compared to EN 50 341-3-4 results (33 N/mm^2 instead of 30 N/mm^2), for aluminium alloy a reduction

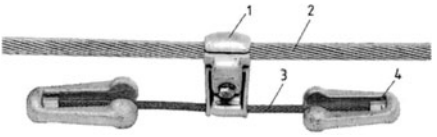

Figure 11.12: Vibration damper – type Stockbridge: 1 damper clamp; 2 conductor; 3 messenger cable; 4 damper weight (Richard Bergner GmbH)

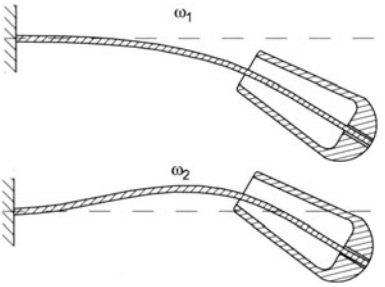

Figure 11.13: First and second vibration mode of a damper, type Stockbridge [11.16]

from 44 N/mm^2 to 33 N/mm^2 is given. The values for ALx/STyz and ALx conductors are considerably below the data used for example in Germany with positive experience for lines without damping systems in operation during many years. Orientation at the recommendations of Table 11.2, last column, would result, therefore, in uneconomic lines and will not be very relevant in practice, therefore.

The recommendations according to [11.40] for a *safe design tension* of single conductors with damping installations do not depend only on the parameter $H/m_C g$ but also on the parameter aD/m_C. For the terrain categories defined in Table 11.2, the recommendations according to [11.40] are presented in Figure 11.11. The limits were established based on the *energy balance principle* and, according to [11.40], confirmed by practical experience, so far information has been available. Within the range for special applications, vibration studies and special damping installations are necessary. Contrary to the EDS method [11.38] which was based on statistical evaluations, the SDT procedure is scientifically backed.

The *conductor tensile stresses* should be selected considering the requirements resulting from the safe design tension and the reliability aspects concerning extreme ice and wind loads [11.26, 11.41]. In case of lines with long spans, such as crossings over rivers, e. g. the river Elbe crossing [11.41], the effect of the conductor tensile stresses on the investment is considerably high. This aspect requires a separate study, because the optimum tensile stress depends to a large extent on the given conditions, such as maximum loads, ratio between number of suspension and strain towers etc. [11.26]. A satisfactory reliability of the conductors against *fatigue* can then be achieved by suitable selection of clamps and fittings tuned to the type of conductor.

In vibration-prone areas, however, a sufficient *fatigue strength* of the conductors cannot be achieved by selection of standard fittings only as experience has proved. Additional devices are necessary for dissipating energy from the vibrating conductor. The individual damping units have been considerably improved during the last years and combined to effective damping systems [11.16]. Now, proved components and designs are available, such as *dampers of the Stockbridge-type,festoon-type dampers* or *spacer dampers* for bundle conductors. They enable to counteract reliably vibration problems at lines, as measurements in laboratories and experience in practice have demonstrated [11.23]. For many utilities, therefore, dampers are standard components of a transmission line. The practically approved possibility to control successfully conductor vibrations by dampers explains as well why nowadays not much effort is spent to investigate the fatigue behaviour of conductors with clamps in arrangements as used in practice. The additional investments for high-quality fittings and suitable damping systems do not

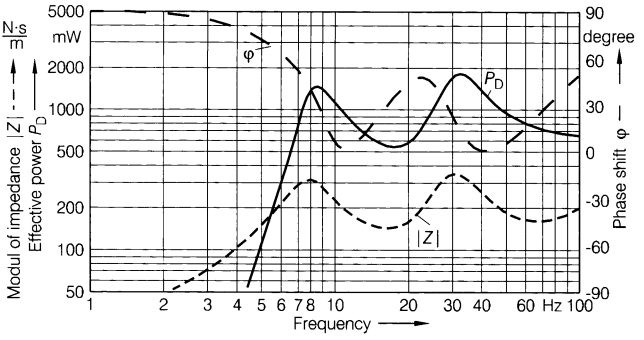

Figure 11.14: Effective power, mode of the impedance and phase shift of a damper, type Stockbridge [11.16]

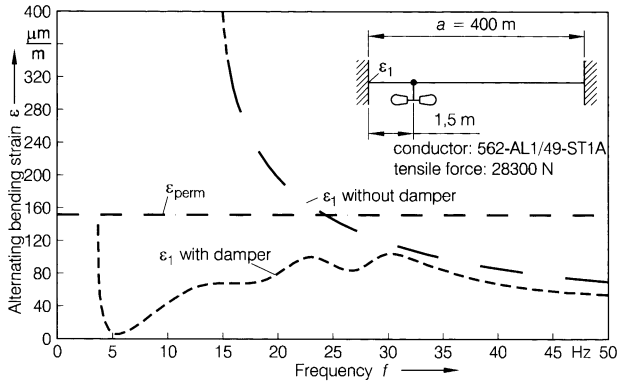

Figure 11.15: Alternating bending strain at a conductor with or without damper [11.16]

weigh much compared with the other investments for line installation.

The Stockbridge-type damper (Figure 11.12) consists of a clamp body supporting an elastic steel messenger cable and two masses fixed at the ends of the messenger cable and forming thus a vibration damping system. This system can be simulated as a damped spring/mass oscillator with sinus-type foot excitation as an approximation [11.16]. This damper has got two degrees of freedom and, therefore, two vibration modes (see Figure 11.13) and two resonance frequencies in case of symmetric design. A disymmetric design of damper weights and messenger cable length can double the number of degrees of freedom supported by utilization of the *torsional vibration mode*. The dynamic characteristic of a damper can be completely described by its complex impedance. The *mechanical impedance* Z is the vibration force divided by the vibration velocity [11.11, 11.16]. The *impedance* Z and the *effective power* P_D depend on the frequency and can be measured directly and reproducibly by means of an exciter. Figure 11.14 shows the *effective power* and the module of the impedance of a standard damper depending on the vibration frequency.

Regarding Stockbridge dampers, different designs for the *damper weights* have been developed. The mechanical function of the weight is only determined by the position of its gravitation centre and its moment of inertia. The form of the weight is determined by the manufacturer with respect to the manufacturing process.

The characteristics of the dampers, their number per span and the locations have to be selected with respect to the individual application. *Vibration studies* serve this purpose. Conductor damping aims at reducing the *bending strain* within the conductor to an extent that critical values do not occur either in the proximity of the suspension clamps or close to the damper clamps. Figure 11.15 shows the graph of the *bending strain* at the conductor support, depending on the vibration frequency with or without damper,

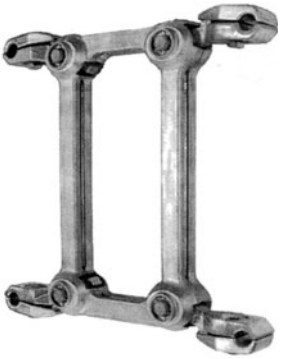

Figure 11.16: Spacer damper for quadruple bundle (Richard Bergner GmbH)

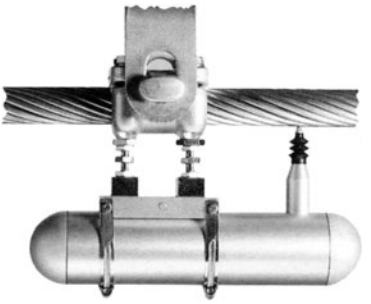

Figure 11.17: Vibration recorder rigidly fixed at the suspension clamp (Richard Bergner GmbH)

as a result of a vibration study. Subject of the vibration study is also the determination of the optimum *damper location*, where the permissible bending strain in the conductor will not be exceeded. A location in a distance of 0,5 to 2,0 m in front of the suspension clamp can be taken as a guideline. When determining the most favourable location, the dynamic characteristic of the used damper is of decisive significance. If dampers with other characteristics were used than those considered in the study, the location would have to be checked again.

Based on developments in Norway and France, *festoon dampers* and bridle cables, called "Bretelles" in France, are adopted as protective remedies. In this case, a conductor section of the same type as the conductor to be protected is fixed on both sides of the suspension clamp [11.23]. The function of these devices has been studied experimentally and theoretically to a lower extent. Their effectiveness remains an open question. Stockbridge-type dampers should be preferred to this damping arrangement.

Spacers can be designed such that, in addition to the required spacing of the subconductors, they also provide effective damping against aeolian vibration. In Figure 11.16, such a *spacer damper* is shown for a *quadruple bundle*. The spacer couples the movement of the subconductors and presents a point of disturbance which detunes the vibration system. The rubber spring elements arranged in the pivots of the spacing frame possess a damping capability which is in the magnitude of the self-damping of 100 m conductor length. With this feature, the formation of vibrations is disturbed and the system dissipates energy. The degree of elasticity and the damping of the spring elements, as well as the location of the spacers within the span, are decisive for the effectiveness of spacer dampers [11.42] to [11.45]. In case of lines equipped with conductor bundles, a complete study of the damping system as a whole, comprising conductors, spacer dampers and vibration dampers, is recommended. The performance of spacer dampers is discussed in [11.46] and [11.47].

11.2.8 Verification of vibration intensity and effectiveness of damping measures

Vibration intensity and *effectiveness of damping measures* can be verified by measurements or calculation. For measurement, two methods are available and both have proved their qualification in practice. First, there is the possibility of a contactless measurement of the vibration intensity at a live line. A mobile *vibration test stand* consists of three main components: Mobile vibration measuring device, anemometer and com-

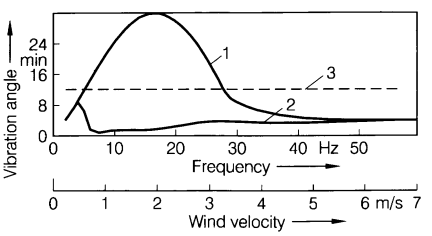

Figure 11.18: Free-span vibration angle of a conductor 264-AL1/34-ST1A, span length 300 m, tensile force 13,3 kN. 1 free-span vibration angle without damper; 2 free-span vibration angle with damper; 3 limit

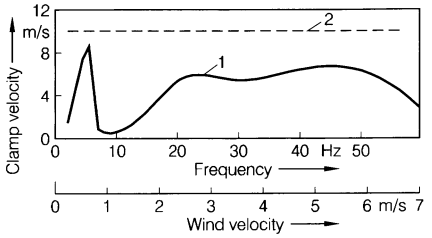

Figure 11.19: Clamp velocity with damper, data as in Figure 11.18. 1 clamp velocity; 2 limit

puter to store and analyse the data. The vibration measuring device is installed in a distance between 30 and 150 m to the conductor section to be analysed. No preparations are necessary at the conductor. Anemometer and computer are installed in a minibus, ensuring a swift change of the measuring locations and also apt for analysis of a line section by sample testing in a relatively short period of time. In addition to the vibration intensity, the installation records the basic frequency of the span, the frequencies of the natural vibration modes and the frequencies of the subconductors in case of bundle conductors. The equipment is designed for short-period measurements.

In case of doubts on the operational reliability of the line, *long-term measurements* should be carried out which are described hereafter. Here, a *vibration recorder* is fixed rigidly at the suspension clamp (Figure 11.17). The recorder is equipped with a sensor which measures the conductor displacement relatively to the clamp in a distance of approximately 89 mm in front of the last contact point between conductor and clamp. This displacement, also called *bending amplitude*, represents the magnitude of the dynamic stress of the conductor. The recorder usually measures the vibration movement every 15 minutes during a period of 10 s, evaluates the vibration pattern according to frequency and amplitude and stores the values in a 16 by 16 matrix. After an operational period of approximately four months, the recorder is dismantled from the line, the matrix is read out and the result is evaluated according to the aspect of lifetime of conductors. This procedure permits to assess the failure probability of the conductor.

Both measuring methods are suited to determine the vibration intensity of a line and consequently to review the damping measures. When using the recorder, no damper may be installed in front of the recorder to the middle of the span. Measurements carried out according to both methods should be accompanied by experts, in view of the operation of the devices, as well as in view of the evaluation of the results.

The *calculation of the vibration intensity* and the review of damping measures is based on the model of a span with rigid clamping of the conductor at both ends. The *energy balance principle* is used as the calculation model, whereby all necessary input data are based on measurements. The result is presented as the free-span vibration angle dependent on the frequency, as shown in Figure 11.8.

This procedure is explained by means of an example. A conductor 264-AL1/34-ST1A is installed in a span with 300 m length and with a tensile force of 3 270 N; a Stockbridge-type damper is installed approximately one meter in front of the pivot of the suspension clamp. In Figure 11.18, the result of the study is presented graphically. Graph 1 shows the free-span vibration angle without damper and graph 2 the free-span vibration angle with damper. The broken line marks the maximum permissible free-span vibration angle with respect to the endurance capability of the conductor. Comparison of graphs 1 and

Table 11.3: Vibration measurements presented in an amplitude-frequency-matrix

Frequency	Amplitude (μm)							Total
(Hz)	00/125	125/251	251/376	376/502	502/627	627/753	above 753	cycles
2	113	7	0	0	0	0	0	120
5	634	31	2	0	0	0	0	667
10	1889	735	209	44	5	0	0	2882
15	3085	2211	871	184	20	0	0	6371
20	3381	2308	1029	294	45	3	0	7060
25	2698	1076	189	14	0	0	0	3977
30	828	183	9	0	0	0	0	1020
34	140	8	0	0	0	0	0	148
40	8	0	0	0	0	0	0	8
45	1	0	0	0	0	0	0	1
50	0	0	0	0	0	0	0	0
59	0	0	0	0	0	0	0	0
83	0	0	0	0	0	0	0	0
100	0	0	0	0	0	0	0	0
143	0	0	0	0	0	0	0	0
200	0	0	0	0	0	0	0	0
Total cycles	12777	6559	2309	536	70	3	0	22254

2 with 3 demonstrates that in the given case one damper within the span is sufficient to protect the conductor against vibration failures. In Figure 11.19, graph 1 can be recognized as the velocity of the clamp as a function of the frequency, while graph 2 shows the maximum permissible velocity of the clamp. The velocity of the damper clamp is equivalent to the stress of the messenger wire. The maximum permissible velocity of the damping clamp is obtained from fatigue tests at dampers.

11.2.9 Evaluation of vibration measurements

Line owners require sometimes as part of guarantee to carry out measurements of vibrations and of the efficiency of the damping system at the line during commissioning. Such tests may last for a period of three months to about one year after the line construction has been completed. Such measurements can be evaluated following the procedure described hereafter.

Paper [11.48] prepared by Cigré SC22 Working Group 11 deals with *vibration field measurements* and their evaluation. Various kinds of instruments are in use, e. g. digital and analogic devices. Depending on the objective of the measurement, a different instrument could be chosen. For instance, for the validation of vibration theories, it may be desirable to obtain the signal of the vibration activity in which case an analogic device is preferable. For endurance investigations or assessment of maximum stresses, digital devices which perform data reduction are desirable.

The instrument installed at a conductor and the attachment bracket should be as light and compact as possible to limit the effect on the conductor behaviour. An amplitude range of approximately 2 mm peak to peak is sufficient. The instrumentation should be able to measure frequencies up to 200 Hz. Instruments using digital sampling techniques should be capable of accurately taking at least 10 samples per vibration cycle, e. g. at a vibration frequency of 200 Hz the sampling frequency should be at least 2000 Hz.

One full measuring sequence consists of a measuring period and a paused period. The measuring period should be preferably 10 seconds for a minimum of four times per hour, 24 hours a day, for a minimum of three months. To confirm the continuous operation of the instrument, it should have the capability of recording the total number of measurements taken during the total measurement duration. The storage of data should be done in an *amplitude-frequency-matrix*, according to [11.49], containing at

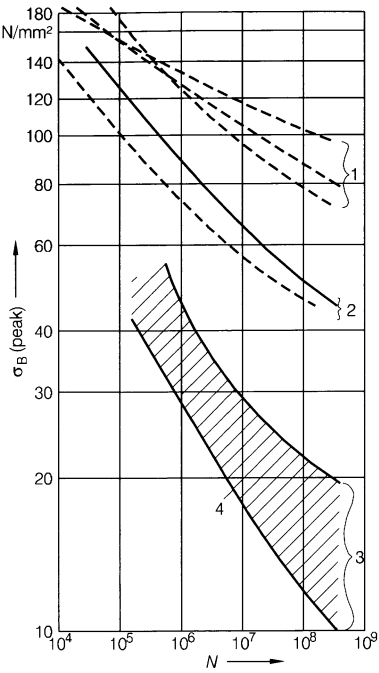

Figure 11.20: S–N–curves and Cigré safe border line. 1 aluminium-alloy wire; 2 aluminium wire; 3 stranded conductors; 4 safe border line; σ_b alternating bending stress (peak); N number of cycles up to failure of 1 to 3 wires

least 10 by 10 elements. Due to standardized hardware, a 16 by 16 matrix is often used. In Table 11.3, a typical amplitude-frequency-matrix is shown.

As fatigue limits are normally expressed in terms of stress or strain, the first step of the evaluation is to convert the measured bending amplitude w_b to bending stress σ_b. The conversion can be achieved by using the *Poffenberger-Swart formula* (11.35) (see also [11.21]) and relation (11.36) to obtain the bending stress.

The Poffenberger-Swart formula, although based on simple assumptions, gives in most cases good agreement with experimental results. More details can be found in reference [11.23]. In the case of suspension clamps, incorporating an elastomeric insert, it is recommended that the conversion formula be determined by vibration tests in the laboratory. However, for practical reasons, is it sufficient to use equation (11.35). Where armor rods are used forming a cage around the clamp, the sensor should be located outside the cage area for easier installation. The dimension x_b is measured from the centre line of the suspension to the point of measurement.

The *fatigue limits* are established in *S-N-curves* which describe the fatigue stress S depending on the number N of cycles up to failure. The failure criterion being the breakage of three strands. Tests show a wide scatter of cycles for different conductor and clamp combinations and also between individual tests carried out at the same combination. In [11.50], fatigue tests are discussed.

The Cigré *safe border line* is a S–N–curve derived from various laboratory fatigue measurements. It represents the conservative lower limit of the permissible number of cycles at various stress levels. It is applicable for commonly used aluminium, aluminium-alloy and multi-layer ACSR conductors and all types of clamps (Figure 11.20).

The safe border line is represented by the following equation:

$$\sigma_{bF} = C \cdot N^z \quad , \tag{11.39}$$

where σ_{bF} is the dynamic limit stress in N/mm^2, N the number of cycles until failure, $C = 450$ and $z = -0,2$ for $N \leq 2 \cdot 10^7$ and $C = 263$ and $z = -0,17$ for $N \geq 2 \cdot 10^7$.

Table 11.4: Conductor data 525/Al1/68-ST1A (ACSR 525/68, Curlew)

Cross-sectional area	mm^2	573
Minimum bending stiffness	$N{\cdot}mm^2$	$36,5 \cdot 10^6$
Stress at 20°C	N/mm^2	60
Stress amplitude factor at $x_b = 89$ mm	N/mm^2	31,6

The safe border line is shown in Figure 11.20). For further test results, reference is made to [11.51].
Endurance limits are defined as the bending amplitude or bending stress which, for a given clamp–conductor combination, can be endured indefinitely. Reference [11.23] is a valuable reference with regard to acceptable limits for ACSR conductors. The *endurance limit* for single-layer ACSR conductors is estimated to be 22,5 N/mm^2. Corresponding ranges of values of peak to peak bending amplitude, 0,5 to 1,0 mm are also given.
When a conductor is subjected to dynamic mechanical stress, it may show damage or even fail after a certain number of stress cycles. This phenomenon is called *fatigue*.
Some rules have been developed to estimate how long a structure may survive when it is submitted to complex stress-amplitude spectra [11.52]. The application of *Minor's rule* to conductors [11.31] permits to assess the *minimum lifetime* during which no damage should occur to the conductor. It is calculated and expressed in years and is an indication of the life expectancy of the conductor. The calculations are based on a safe border line and measured or simulated as stress cycles expected during the lifetime of the conductor. Since conservative assumptions are made, the calculated lifetime is on the safe side in most cases.
Another commonly used method is to compare the maximum stress or strain obtained by the measurement or simulation with the *endurance limits* explained above. The risk of damage is considered to be negligible, if these endurance limits are not exceeded.
Aeolian vibration and subspan oscillation measurements were carried out at the 500 kV Rincón-Garabe line interconnecting Brazil and Argentina [11.53].

Example: As an example, the recorded data as shown in Table 11.3 will be evaluated. The conductor data are shown in Table 11.4. The measurements were carried out for 10 s every 15 min. Therefore, four measurements per hour lasting 40 s are available. Since the measuring lasted in total 3024 h, the total measuring period is $3024 \cdot 40 = 120960$ s = 33,6 h. For extrapolating to a whole year, the data given in Table 11.3 are multiplied by $8760/33,6 \sim 261$.

The conversion of the measured bending amplitude is carried out using the data given in Table 11.4. The results are presented in Table 11.5. According to the Minor's rule, the estimated minimum life period t_l is

$$t_l = 1/\sum_{i=1}^{j} (n_i/N_i) \quad , \tag{11.40}$$

where n_i is the number of cycles recorded during one year, N_i the number of cycles to failure and j the number of stress classes. For the example, the sum $\sum n_i/N_i$ is 0,0092 and the calculated lifetime $t_l = 1/0,0092 = 110$ years.

11.3 Subspan oscillations

11.3.1 Origin and consequences

Subspan oscillations can occur only in bundle conductors and are observed frequently at twin bundles with horizontally arranged subconductors. Due to aerodynamic coupling of the subconductors situated one behind the other in the air flow, antiphase

Table 11.5: Accumulated cycles per year and cycles to failure

Class	Amplitude 1/100 mm	Stress σ_b N/mm^2	Number of cycles to failure N_i	Cycles n_i per year	n_i/N_i	%
1	125	2,1	$2\,174\,546 \cdot 10^6$	$3{,}331 \cdot 10^6$	0,0000	0,0
2	251	5,9	$4\,813 \cdot 10^6$	$1{,}710 \cdot 10^6$	0,0004	3,9
3	376	9,9	$237 \cdot 10^6$	$0{,}602 \cdot 10^6$	0,0025	27,6
4	502	13,9	$33 \cdot 10^6$	$0{,}140 \cdot 10^6$	0,0043	46,6
5	627	17,8	$10 \cdot 10^6$	$0{,}018 \cdot 10^6$	0,0018	19,6
6	753	21,8	$4 \cdot 10^6$	$0{,}001 \cdot 10^6$	0,0002	2,3

oscillations occur at the subconductors at wind velocities between 4 and 18 m/s with frequencies between 1 and 5 Hz (basic frequency and first harmonic). The susceptibility to oscillations is increased by a twisting of the bundle along the horizontal axis by 5 to 15° due to inexact adjustment of the subconductors or due to differing conductor creep. The amplitudes of the oscillations may become so large that the subconductors touch each other. Vertical subspan oscillation of the subconductors with ice accretion were observed at 400 kV quadruple bundle lines, lasting for several hours. Oscillations of that type stress conductors and spacers extremely. The high bending stress of the conductors in the vicinity of the spacers can lead to fatigue problems also in case of a relatively low number of cycles.

11.3.2 Remedy measures

Due to the fact that subspan oscillation occurs predominantly at subconductors arranged horizontally in the wind flow one behind the other, a bundle arrangement which avoids this pre-condition, e. g. a vertical twin bundle, should be preferred with respect to subspan oscillation. In addition, the spacing of the subconductors in relation to the subconductor diameter gains important influence on the aerodynamic coupling. Tests in wind tunnels demonstrated that values for this ratio of more than 18 in case of twin or triple bundles and more than 20 in case of quadruple bundles reduce the susceptibility to oscillation of the subconductors essentially [11.45]. Furthermore, it is recommended as a remedy to arrange the spacers in distances of not more than 40 m and with unequal subspan lengths. Spacer dampers do not completely suppress the subspan oscillations. This applies particularly in case of ice accretion, since the exciting energy is extraordinary high in this case.

11.4 Galloping

11.4.1 Origin and consequences

Conductor galloping occurs at single conductors as well as at bundle conductors mostly when they are ice covered. Galloping has its origin in a modified aerodynamic characteristic of the conductor, as compared with its originally approximately cylindric shape. The conductor experiences a considerable uplift due to the disymmetric shape which varies, rhythmically combined with an axial twisting and, therefore, causes a periodical oscillation (Figure 11.21). For detailed explanations of the galloping phenomenon, it is referred to the relevant literature, e. g. [11.23, 11.54]. A large number of studies is devoted to the occurrence and consequences of galloping. Since galloping is a relatively rare event, measurements turn out to be difficult and are successful only if a long observation period is used [11.5, 11.23, 11.56]. From observations, which should be reported in a standard format [11.57], it can be concluded that the conductors move on elliptical curves, the long axis of which can be inclined against the vertical (Figure 11.22 b)

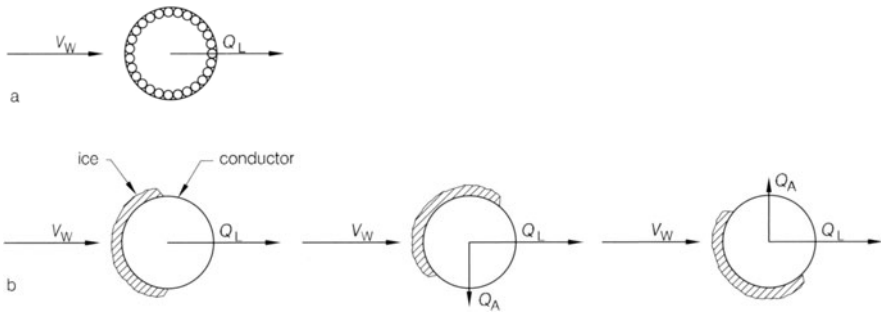

Figure 11.21: Forces acting at the conductor under wind [11.23]: a) without ice accretion, b) with differing ice formation; V_W wind force; Q_A uplift or downward force ; Q_L aerodynamic drag force

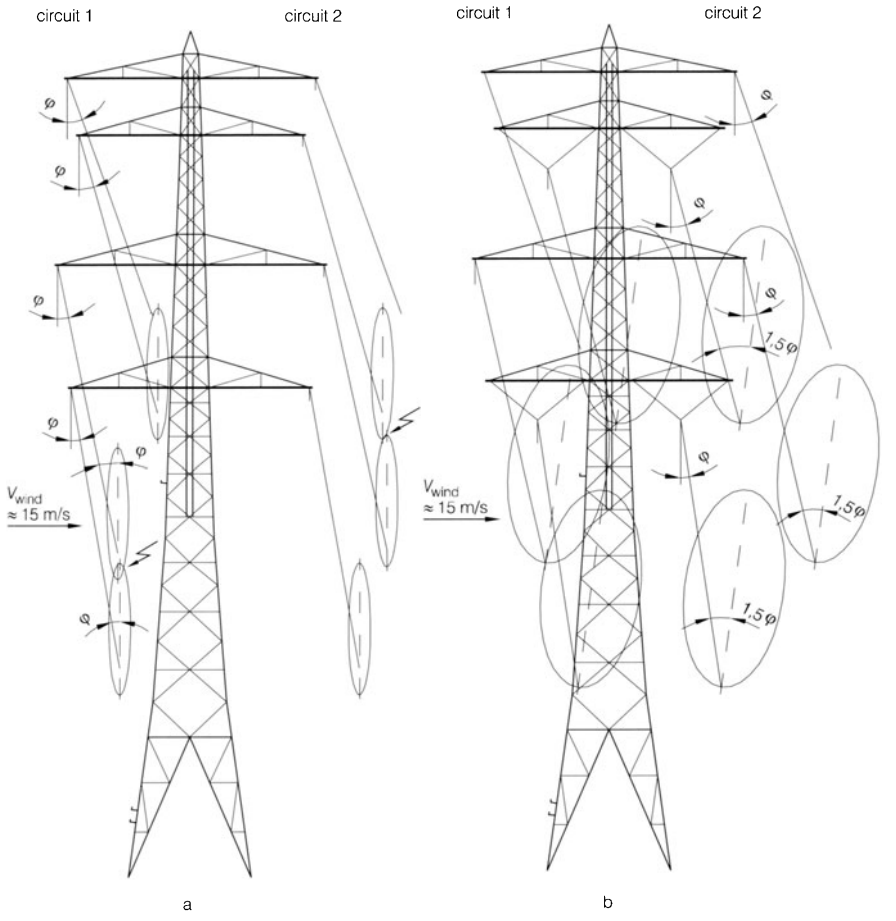

Figure 11.22: Elliptic curves of galloping conductors, example according to [11.55], φ conductor swing angle; a) long axis vertical, ratio long axis/short axis 6:1; b) long axis inclined by $0{,}5 \cdot \varphi$ degrees against the vertical, ratio long axis/short axis 2:1

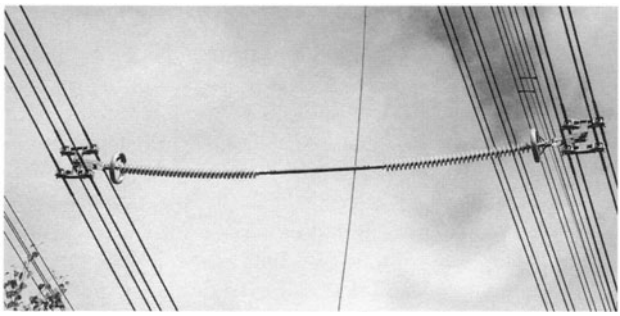

Figure 11.23: Phase spacer of a 380 kV line (Richard Bergner GmbH)

[11.55]. The ratio between the lengths of long and short axis is between 6:1 and 2:1. In case of galloping, flashovers or even touching between the phase conductors can occur, leading to short circuits. *Short circuits* combined with high arcing currents, as a rule, lead to local conductor damage but could also result in melting of the complete conductor. In case of long-lasting galloping, mechanical overloadings of the components of insulator sets and towers may occur; damage of fittings and towers due to galloping was frequently observed. Thus, galloping leads to damage of the overhead line, causes severe operational disturbances and may lead to impair the public safety because of violating the required minimum clearances to ground or obstacles [11.54] to [11.59].

11.4.2 Remedy measures

Remedies against galloping have been discussed for many years and also tested. However, an overall and totally satisfying solution has not yet been found. The remedies can be classified as measures to avoid galloping and measures to mitigate its consequences. Regarding the remedies to suppress the galloping excitation, a distinction between single and bundle conductors is to be made. For single conductors, *pendulums* to shift the torsional natural frequency of the conductors and dampers designed as spring mass systems are used. These remedies were successful in some cases; they were not able to suppress galloping at all; however, they lead to a remarkable reduction of the amplitudes [11.60, 11.61]. In case of bundle conductors, pendulums and spring mass systems arranged between the spacers were adopted as well [11.61, 11.62]. Arrangements of this type have the disadvantage that an additional mass is added to the system, resulting in an increase of the conductor tensile force. Attempts were made to decrease the susceptibility to galloping of bundles by means of spacers which enable the individual subconductors to rotate freely [11.63]. If the subconductor can rotate freely within the spacer clamp during an ice accretion process, the ice accretion along the conductor circumference will be more uniform and cause an aerodynamically more stable profile. Tests were carried out also to waive spacers at all. The frequency of occurrence of galloping was reduced in this case [11.63, 11.64]. However, the subconductors may clash very heavily under wind action, resulting in deformation of the conductor outer layer and causing electric discharges. During short circuits, the subconductors may clash, and moving back into their standard position is not always guaranteed due to the operational current (kissing conductors).

For bundles, as well as for single conductors, *phase spacers* between the individual phases of a circuit were developed and adopted [11.65]. According to the present knowledge, phase spacers represent a successful remedy to limit the movements of the conductors. To keep their weight low, the insulating part of the phase spacers is formed by composite insulators today, which react flexibly to compression if they are long. In case of a phase distance of more than 5 m, the conductors will get closer in case of

galloping. The oscillation motion, however, is remarkably affected when the conductors are swinging back, since the *phase spacers* behave rigidly in case of a tension load. The number of phase spacers in one span, their location and the protection of the conductors at the spacer attachment points have to be selected carefully, in order to avoid vibration damage at the conductors due to the increased conductor tensile forces under normal operation conditions. According to the experience gained up to now, at least three phase spacers should be installed in one span. Tests demonstrated, that the probability of flashovers or touching of the conductors decreases with an increasing number of spacers. Figure 11.23 shows a phase spacer of a 380 kV line.
The consequences of galloping can be minimized by an adjusted design of the towers. A horizontal arrangement of the conductors is preferable with respect to galloping, as compared with a vertical or triangular arrangement. The maximum amplitudes due to galloping depend mainly on the conductor sag within the span. Amplitudes up to 12 m were observed. In principle, it is possible to select the distances of the conductors at the towers such that galloping will not lead to flashovers. However, this means a remarkable enlarging of the tower top in case of operating voltages below 400 kV and, therefore, would lead to increased investments. In case of double circuit lines, it was frequently observed that galloping had unfavourable consequences only for one circuit due to the main wind direction (see Figure 11.22 b). In this case, it is recommended to de-energize the particularly endangered circuit, if possible, to avoid conductor damage due to flashovers [11.56].
Since 1985, a task force, now part of the Cigré SC22, takes care of the versatile problems of conductor galloping. This task force presented in [11.5] extensive observations, studies and remedy measures and described the updated state of the art.

11.5 Short-circuit oscillations

11.5.1 Origin and consequences

Short-circuit currents generate electro-magnetic forces within the conductors exciting *short-circuit oscillations*. Depending on the direction of the current flowing in the short-circuit condition, the phases of an AC circuit are attracted or pushed-off. Since the short-circuit periods are short (less than 1 s), the short-circuit forces in an overhead line will remain low because of the large phase distances and of the low natural frequency (less than 0,3 Hz) of the sagged conductors; the phase conductors are excited to free oscillations with only relatively low amplitudes. Practically, the stresses resulting thereof can be neglected.
The conditions change in principle if the phase conductors are designed as bundle conductors. The *short-circuit force* within the subconductors achieves considerably high values due to the small distance between the adjacent subconductors and, as a rule, leads to clashing of the subconductors. In this case, the strands of the outer layer may be permanently deformed. Therefore, they get loose on the conductor core and wind flow as well as magnetic forces between the strands result in vibrations which cause annoying noises. In case of clashing of the subconductors, an alternating bending stress of high amplitude occurs within the conductor, thus considerably accelerating its fatigue.

11.5.2 Remedy measures

A short-circuit-resistant design should be adopted for the spacers, i. e. they may not be deformed permanently under short-circuit forces or destroyed at all. In particular, the subconductor spacing may not be decreased permanently, since the electric characteristics of the line would be unfavourably affected. Only very short subconductor lengths

in the range between 5 and 10 m could avoid clashing of the conductors also in case of high currents. Such a solution can only be applied in substations but not in lines due to technical and economical reasons. Whether the subconductors will clash in a short-circuit condition does not only depend on the fault current but also on the period of time during such a current acts. Short switching-off periods can avoid clashing of the conductors also in case of high currents [11.66].

11.6 References

11.1 Hadulla, T.: Wirbelerregte Schwingungen in Freileitungsbündeln (Vortex-induced vibrations in overhead line bundle conductors). Doctorate thesis D17, University Darmstadt 2000

11.2 Meier-Windhorst, A.: Flatterschwingungen von Zylindern im gleichmäßigen Flüssigkeitsstrom (Flutter vibrations of cylinders in a laminar hydraulic fluid flow). Hydraulic Institute of Technische Hochschule München. Oldenbourg Verlag 1939, pp. 3 to 29

11.3 Cigré SC22 WG22-11: Modelling of aeolian vibration of single conductors: Assessment of the technology. Electra 181 (1998), pp. 53 to 69

11.4 Rowbottom, M. D.; Aldan-Hughes, R. R.: Subspan oscillation: A review of existing knowledge. Cigré Report 22-04, 1972

11.5 Cigré SC22 WG22-11: Review of galloping control methods. Electra 191 (2000), pp. 45 to 62

11.6 Möcks, L.: Die Beanspruchung und Lebensdauer von Leiterseilen unter dem Einfluss winderregter Schwingungen (Loading and service life of transmission cables subjected to wind-induced vibrations). Elektrizitätswirtschaft 86 (1987), pp. 920 to 925

11.7 Nefzger, J.: Störungen durch mechanische Leiterschwingungen und Mittel zu deren Behebung (Disturbances by mechanical conductor vibrations and remedies). Cigré Report 126, 1933

11.8 Hagedorn, P.: Leiterseilschwingungen in Theorie und Praxis: Ein Überblick (Conductor vibrations in theory and practice: An overview). etz-Report 26, Berlin. VDE-Verlag GmbH 1990

11.9 Schäfer, B.: Zur Entstehung und Unterdrückung winderregter Schwingungen an Freileitungen (On the excitation and suppression of wind-induced vibrations on overhead lines). Doctorate thesis D17, University Darmstadt, 1980

11.10 Hagedorn, P.: On the computation of damped wind-excited vibrations of overhead transmission lines. Journal of Sound and Vibration 83(1982), pp. 253 to 271

11.11 Cigré SC22 WG22-01: Report on aeolian vibration. Electra 124 (1989), pp. 40 to 77

11.12 Strouhal, V.: Über eine besondere Art der Tonerregung (On a special type of sound excitation). Annalen Physik und Chemie, Band V, (1878), pp. 216 to 251

11.13 Cigré SC22 WG11: Guide on conductor self-damping measurements. Electra 62 (1979), pp. 79 to 90

11.14 Diana, G.; Falco, M.: On the forces transmitted to a vibrating cylinder by a blowing fluid. Meccanica 6, (1971), pp. 9 to 22

11.15 Rawlins, C.B.: Model of power imparted by turbulent wind to vibrating conductor. Massena, NY, Alcoa Laboratories. Technical Report No. 93-83-3, 1983

11.16 Möcks, L.: Damping of high-voltage overhead line conductor vibrations. ETZ Report 15e, Berlin. VDE-Verlag GmbH, 1984

11.17 Schmidt, J. T. et al.: Laboratory measurements of the power dissipation characteristics of aeolian vibrations dampers. IEEE, Transaction on Power Delivery, Vol. 12 (1997), pp. 1614 to 1621

11.18 Krispin, H.-J.; Möcks, L.; Schmidt, J.: Neue Ergebnisse zur Messung der mechanischen Eigendämpfung von Freileitungsseilen und Luftkabeln (New findings on measurements of mechanical self-damping of overhead line conductors and aerial cables). Elektrizitätswirtschaft, 93 (1994), pp. 1414 to 1418

11.19 Cigré SC22 WG11TF-1: Conductor self-damping. Cigré WG11 22-94 (WG11), 1994

11.20 Hütte, des Ingenieurs Taschenbuch, Band I: Theoretische Grundlagen (Hütte, the Engineer's Handbook. Vol. I: Theoretical basics).Berlin, Verlag Wilhelm Ernst & Sohn, 28th edition 1955

11.21 Poffenberger, J. C.; Swart, R. L.: Differential displacement and dynamic conductor strain. IEEE Transactions on Power Apparatus and Systems, Vol. 84 (1965), pp. 281 to 289

11.22 von Kármán, T.: Über den Mechanismus des Widerstandes, den ein Körper in einer Flüssigkeit erfährt (On the mechanism of the resistance experienced by a body in a fluid). Reports of Royal Scientific Academy in Göttingen (1911), pp. 509 to 517

11.23 EPRI: Transmission line reference book: Wind-induced conductor motion. Palo Alto. Electric Power Research Institute, 1979

11.24 Papailiou, K. O.: On the bending stiffness of transmission line conductors. IEEE Transaction on Power Delivery, Vol. 12 (1997), pp. 1576 to 1588

11.25 Maas, H.: Zur Beseitigung der mechanischen Freileitungsschwingungen (On the suppression of mechanical overhead line vibrations). Forschung auf dem Gebiet des Ingenieurwesens 1933, Vol. 5

11.26 Kießling, F.; Nefzger, P.: Zur Wahl der Zugspannung für die Leiter einer Hochspannungsleitung (On the selection of tensile stress for conductors of overhead lines). Elektrizitätswirtschaft 80 (1981), pp. 684 to 691

11.27 Möcks, L.: Das Verhalten des Leiterseiles unter dem Einfluss der Armaturen (On the performance of conductors affected by fittings). Elektrizitätswirtschaft 68 (1969), pp. 336 to 341

11.28 Bückner, W. et al.: Stresses in transmission line conductors near the suspension clamp. Cigré Report 23-07, 1968

11.29 Möcks, L.: Schwingungsschäden in Leiterseilen (Vibration damage on conductors). Bulletin-SEV 61 (1970), pp. 223 to 227

11.30 Philipps, W. et al.: The endurance capability of single and bundle transmission line conductors and its evaluation. Cigré Report 22-05, 1972

11.31 Cigré SC22 WG22-04: Recommendations for the evaluation of the life time of overhead line conductors. Electra 63 (1979), pp. 103 to 145

11.32 Cigré SC22 WG22-05: A practical method of conductor creep determination. Electra 24 (1974), pp. 105 to 137

11.33 Bohner, R.; Möcks, L.: Die Spannungsverteilung im Verbundseil (Stress distribution in compound conductors). Elektrizitätswirtschaft 64 (1965), pp. 230 to 235

11.34 Papailiou, K. O.: Die Seilbiegung mit einer durch die innere Reibung, die Zugkraft und die Seilkrümmung veränderlichen Biegesteifigkeit(Conductor bending considering the variable bending stiffness depending on the internal friction, the tensile force and the conductor curvature). Doctorate thesis, ETH Zürich No. 11057, 1995

11.35 Giray, M.; Kießling, F.: 380 kV overhead transmission line over the Bosphorus. Siemens AG, A19100 E433-A871-x-7600 (1984)

11.36 Möcks, L.: Spiralarmaturen für Freileitungen (Armor rods for overhead lines). RIBE Mitteilungen 5, Schwabach. Richard Bergner 1963

11.37 Ann, W.; Kießling, F.; Möcks, L.: Isolatoren und Armaturen für die neue 380-kV-Elbekreuzung der Nordwestdeutsche Kraftwerke AG (Insulators and fittings of the new 380 kV river Elbe crossing of the Nordwestdeutsche Kraftwerke AG, Elektrizitätswirtschaft 77 (1978), pp. 653 to 660

11.38 Zetterholm, O. D.: Bare conductor and mechanical calculation of overhead conductors. Cigré Report 223, 1960

11.39 Cigré SC22 WG22-11: Safe design tension with respect to aeolian vibrations, Part 1: Single unprotected conductors. Electra 186 (1999), pp. 53 to 67

11.40 Cigré SC22 WG22-11: Safe design tension with respect to aeolian vibrations, Part 2: Single damped conductors. Electra 198 (2001), pp. 28 to 43

11.41 Ann, W.; Kießling, F.; Schnakenberg, D.: Die Leiter der 380-kV-Elbekreuzung der Nordwestdeutsche Kraftwerke AG und ihre Verlegung (The conductors of the new 380 kV river Elbe crossing of the Nordwestdeutsche Kraftwerke AG). Elektrizitätswirtschaft 78 (1979), pp. 254 to 256

11.42 Diana, G. et al.: Field measurement and field data processing on conductor vibration (comparison between experimental and analytical results). Cigré Report 22-11, 1982

11.43 Hearnshaw, D.: Spacer damper performance, a function of in-span positioning. IEEE Paper T74 061-8, 1974

11.44 Hearnshaw, D.: Optimization of system performance for spacer dampers. IEEE Paper A75 496-0, 1975

11.45 Hearnshaw, D.: Aeolian vibration on bundled conductors. IEEE Paper Canadian conference on communications and power. 1976

11.46 Hagedorn, P.; Kraus, M.: On the performance of spacer dampers in bundled conductors. EUREL Publication ETEP Vol. 3 (1992), pp. 305 to 311

11.47 Ranke, K.; Krispin, H.-J.: Efficiency of spacer dampers. Evaluation of measurements of the bending amplitude at suspension and spacer clamps due to aeolian vibrations. Cigré SC22 WG11 Report WG11(90)53, 1990

11.48 Cigré SC22 WG22-11: Guide to vibration measurements on overhead lines. Electra 163 (1995), pp. 125 to 137

11.49 IEEE Committee Report: Standardization of conductor vibration measurements. IEEE Transactions on Power Apparatus and Systems, Vol. 85, No. 1, 1966, pp. 10 to 20

11.50 Cigré SC 22, WG04: Guide for endurance tests of conductors inside of clamps. Electra 100(1985), pp. 77 to 86

11.51 Cigré SC22 WG04: Endurance capability of conductors. Final Report. Paris, Cigré, 1988

11.52 Miner, M. A.: Cumulative damage in fatigue. Proc. ASME, J. Appl. Mech., 1945, pp 159

11.53 da Silva, J. B. G. F. et al.: First interconnection Brazil-Argentina. Design of the AC 500/525 kV 50/60 Hz line Rincón-Garab-Itá. Foz do Iguaçu, IX South American Cigré Regional Meeting, 2001

11.54 Hagedorn, P., Meier-Dörnberg, K.-E.: Tanzschwingungen in Freileitungen und ihre Unterdrückung: Beschreibung eines laufenden Versuchs (Galloping of overhead lines and their suppression. Description of a running test). ETZ-Report 21. Berlin. VDE-Verlag 1986

11.55 Leppers, P. H.: Galopperen van geleiders in hoogspanningslijnen en de door de NV PLEM toegepaste maatregelen om storingen te voorkomen. NV Provinciale Limburgse Elektriciteits-Maatschapij (NV PLEM)

11.56 Jürdens, C.; Möcks, L.; Müller, K.-H.: Seilmessstation, ein Beitrag zur Lösung des Seiltanzproblems (Conductor testing station, a contribution to solving the conductor galloping problem). Elektrizitätswirtschaft 82 (1983), pp. 706 to 711

11.57 Cigré SC22 WG11: Field observations of overhead line galloping: Galloping reporting forms. Electra 162 (1995), pp. 97 to 113

11.58 Brand, R. et al.: Network disturbances and damages of conductors caused by galloping. Cigré Report 112-06, 1981

11.59 Richardson, A. S.: Some effects of conductor twisting on galloping. IEEE Transactions on Power Apparatus and Systems, Vol. 99 (1980), pp. 811 to 822

11.60 Akiyama, T. et al.: Development of galloping control devices and its operation records in Japan. Cigré Report 22-07, 1986

11.61 Havard, D. G.; Pohlman, J. C.: Control of galloping conductors by detuning. Cigré Report 22-05, 1980

11.62 Havard, D. G. et al.: The economic benefits of controls for conductor galloping. Cigré Report 22-02, 1982

11.63 Brand, R. et al.: Suppression of galloping for medium-size bundle conductors by spacer removal or similar means. Cigré Report 22-09, 1978

11.64 Leppers, P. H. et al.: Galloping suppression tests on overhead lines. Cigré Report 22-03, 1986

11.65 Langmacker, D. et al.: Separators in high-voltage overhead lines to prevent disturbances of electric power transmission. Cigré Report 22-08, 1986

11.66 Möcks, L.: Berechnung der elektromagnetischen Kurzschlussstromkräfte an den Feldabstandhaltern im Bündelleiter einer Hochspannungs-Freileitung (Calculation of electromagnetic short-circuit forces at the spacers of bundle conductors of a high-voltage line). VDI Series 21, No. 21, Offenbach, VDI-Verlag 2001

12 Supports

12.0 Symbols

Symbols	Signification
a	System length of lattice truss
a_e	Complementary span length
a_g	Weight span
a_W	Wind span
A	Cross-sectional area
A_c	Cross-sectional area of concrete
A_d	Cross-sectional area of bracings
A_{eff}	Effective cross-sectional area
A_G	Cross-sectional area of a single chord
A_{net}	Net cross-sectional area
A_s	Tensile cross section of a bolt
A_t	Minimum net area from the centre of borehole to the edge of angle under axial torsion
A_T	Area enclosed by the centre line of the cross-sectional contour
A_v	Shearing cross section, cross-sectional area of a strut, minimum net area in shear along a line of transmitted force
b	Leg width, side width, width of tower body
b_1	Total width of tower at the base of shortest leg extension
b_1, b_2	Leg width of an angle
b_A, b_B	Width of faces A or B of a lattice tower
b_{eff}	Effective leg width of an angle
b_i	Width of faces the base of leg extension i, system width
b_m	Width of faces at the base of longest leg extension
b_n	System width of lowest panel n
b_o	Width of lattice tower at top of panel
b_s	Distance between jumper loop and tower
b_{sW}	Displacement of the end points of the jumper loop under wind
b_T	Distance between the attachment points at suspension tower
b_u	Width of lattice tower at base of panel
b_V	Distance between the non-symmetrically acting vertical force P_V and the axis of tower body
b_w	Distance between the conductor attachments at angle tower
c	Coefficient for calculation of warping resistance
c_{min}	Clearance of conductor at midspan
$c_{min\,pe}$	Minimum clearance between phase conductor and earth wire
$c_{min\,pp}$	Minimum clearance between phase conductors at midspan
C_c	Limit of proportionality
C_C	Drag factor for conductor
C_x	Drag factor for towers
d	Length of bracings, conductor diameter without ice, bolt diameter
d_0	Hole diameter
d_b	Bolt shank diameter
d_{Di}	Distance between the compression force of a bracing member and the reference point of moment
d_I	Conductor diameter with ice
d_{Zi}	Distance between the tension force of a bracing member and the reference point of moment
D	Bracing member force of a lattice framework
D_1	Bracing member force of the shortest leg extension
D_A, D_B	Force of bracings in face A or B

Symbols	Signification
D_{Di}	Compression force of bracings in panel i
D_{el}	Minimum phase-to-earth clearance dependent on voltage
D_H	Horizontal component of the bracing member force D
D_i	Bracing member force of leg extension i
D_m	Bracing member force of the longest leg extension
D_o	Bracing member force in case of equal leg extension
D_{pp}	Minimum phase-to-phase clearance dependent on voltage
D_V	Vertical component of the bracing member force D
D_{Zi}	Tensile force of bracings in panel i
e	Distance between the centroidal axes
e_0	Bow imperfection
e_1	End distance from centre of hole to adjacent end
e_2	Edge distance from centre of hole to adjacent edge
e_s	Substitute imperfection for slip
e_x, e_y	Coordinates of the centre of gravity
E	Modulus of elasticity, Young's modulus
E_d	Total design value of the effects of actions
f_0	Vertical position of the points connecting the ends of the jumper loop
f_C	Sag of conductor at +40°C in m, sag in the longest span
f_{cd}	Design value of concrete compression strength
f_{ck}	Characteristic strength of concrete under compression
f_{cr}	Critical stress
f_d	Deflection
f_e	Sag of the complementary span
$\mathbf{f}_i$	Vector of axial forces of element i in local coordinate system
f_{i1}, f_{i2}	Longitudinal forces of element i in local coordinate system
f_s	Sag of jumper loop
f_{tot}	Total deflection of a tower or a pole
f_u	Ultimate tensile strength
f_{ub}	Ultimate tensile strength for bolts
f_y	Yield strength
f_{yd}	Design value of yield strength
$\mathbf{F}$	Node forces vector of the total system in global coordinate system
$\overline{F}$	Vertical force
$\mathbf{F}_a$	Vector of known node forces
$\mathbf{F}_b$	Vector of unknown node forces
$F_{b,Rd}$	Bearing resistance
F_d	Design value of an action
$\mathbf{F}_i$	Vector of forces of element i in global coordinate system
F_K	Characteristic value of an action
F_T	Action having a return period of T years
F_{vRd}	Shear resistance
g	Gravity constant
g_o	Peak factor
G_q	Gust factor
G_x	Structural response factor
G_{xC}	Gust and span length reaction factor of conductors
G_K	Dead weight of conductor, insulator and supports
h	Distance between point of application of the load and the reference point of moment
h_0	Distance between the centre of gravity of the corner members
h_1	Height of shortest leg extension
h_i	Distance between the panel i and the point of application, height of leg extension i, distance between the joint i and the position of the displacement, lever arm
h_m	Height of longest leg extension
h_o	Distance between top of panel and the reference point of moment
h_u	Distance between base of panel and the reference point of moment

Symbols	Signification
i	Number of panels, elements, etc., radius of gyration
i_{M}	Polar radius of gyration around the centre of gravity
i_{p}	Polar radius of gyration around the shearing centre
i_{uu}	Radius of gyration related to the principal axis (in case of equal angle section related to axis of symmetry)
i_{vv}	Radius of gyration related to the weak principal axis
i_{yy}	Radius of gyration related to axis rectangularly to the longer angle leg
i_{zz}	Radius of gyration related to axis parallel to the longer angle leg
I, I_u, I_v	Moment of inertia
I_{eff}	Effective moment of inertia of a laced member
I_{T}	Torsional moment of inertia
I_{u}	Moment of inertia around the principal axis (in case of equal angle section related to axis of symmetry)
I_ω	Warping constant around the shearing centre
j	Number of elements
k_{l}	Reduction factor for electrical clearances
k_{C}	Factor dependent on the swing angle of conductor
$\mathbf{k}_i$	Element stiffness matrix of element i in local coordinate system
k_{I}	Factor for the calculation of the moment of inertia of regular polygons
k_{T}	Factor for the calculation of the torsional moment of inertia of regular polygons
k_y, k_z	Coefficient for the calculation of the moment factor β_{M}
K	Factor for the calculation of the hypothetical force in redundant member
$\mathbf{K}$	Total stiffness matrix
K_1	Factor
$\mathbf{K}_{\mathrm{aa}}$, $\mathbf{K}_{\mathrm{ab}}$, $\mathbf{K}_{\mathrm{bb}}$	Submatrices of the total stiffness matrix
$\mathbf{K}_i$	Element stiffness matrix of the element i in global coordinate system
K_x, K_y	Transversal forces due to bending of leg member
K_σ	Buckling coefficient of plates
l	Distance between the bracing member force and the reference point of moment, member length, length of a laced member
l_1	Buckling length of a single chord
$l_{\mathrm{B}}, l_{\mathrm{D}}, l_{\mathrm{E}}$, $l_{\mathrm{I}}, l_{\mathrm{H}}, l_{\mathrm{g}}$	Dimension of a guyed tower
l_{d}	Length of bracings
l_{k}	Length of the swinging part of an insulator set
L	System length, member length
L_1, L_2	Buckling length, length of span
L_{M}	Height of tower, pole length
L_v	Permissible member length in case of bending around the axis v
L_y	Permissible member length in case of bending around the axis y
m	Constant, for single bracings 2, for cross bracings 4; number of profiles of compound members
m_{C}	Conductor mass per unit length
$m_{\mathrm{C}}g$	Conductor dead weight per unit length
$\overline{M}$	Vertical moment
M^{I}	Moment in first order theory
M^{II}	Moment in second order theory
M_{c}	Moment due to concrete stress
M_{d}	Design value of bending moment
M_{P}	Moment due to steel stress
M_{S}	Bending moment of a laced member
M_{T}	Torsional moment
M_{Td}	Design value of torsional moment
$M_{y\mathrm{d}}$, $M_{z\mathrm{d}}$	Design value of the moment around axis y, z
M_x, M_y, M_z	Moments around the axis x, y, z
$M(x)$	Bending moment due to external load

Symbols	Signification
$\overline{M}(x)$	Bending moment due to virtual load
n	Number of subconductors
N	Axial force
N_{cr}	Ideal elastic buckling force, axial force at smallest bifurcation load
N_{d}	Design value of axial force
N_{D}	Bracing member force of a laced member
N_{G}	Force of a single chord of a compound member
N_{hyp}	Hypothetical force in redundant member
N_{Rd}	Design value of axial force resistance
$N(x)$	Axial force due to external load
$\overline{N}(x)$	Axial force due to virtual load
O_i	Force in upper chord of panel i
p_1	Distance between the centre of holes
P	External concentrated load
P_{A}, P_{B}	Horizontal acting forces in face A or B
P_{V}	External vertical force
P_x, P_y, P_z	Components of concentrated loads P in x-, y-, z-direction
q	Dynamic wind pressure
q_0	Reference wind pressure
q_z	Dynamic wind pressure at height z above ground
Q	Shear force
Q_{o}	Background response part
Q_{CK}	Conductor tensile force dependent on temperature, wind and ice load
Q_{WM}	Wind load on tower
Q_{IK}	Ice load on conductor
Q_{K}	Characteristic value of an action
Q_{PK}	Loads from construction and maintenance
Q_{WC}	Wind load on conductor
Q_{Wins}	Wind load on insulator
Q_{WK}	Characteristic value of wind load
RTS	Rated tensile strength
R_{d}	Structural design resistance
R_{x}	Resonant response part
R_{K}	Characteristic value of structural resistance
s_1	Distance between batten plates
s_{k}	Buckling length
s_y	Distance between the angle legs
S	Leg member force, member force
$\overline{S}$	Member force due to vertial load
S_{d}	Axial force of the supporting member in case of cross bracings
S_{g}	Force of guy wire
S_{E}	Leg member force
S_{H}	Horizontal component of leg member force
S_{L}	Horizontal force perpendicular to the crossarm axis
S_{V}	Shear stiffness of a laced member, vertical component of leg member force
S_x, S_y	Leg member force due to external load P_x, P_y
t	Distance between the force S_{L} and the tower axis; thickness of angle leg; thickness of plates
$\mathbf{T}_i$	Transformation matrix
T_{s}	Shear
T_{t}	Return period
u	Coordinate
u_1	Edge distance from centre of gravity
$\mathbf{u}_i$	Vector of longitudinal node displacement of element i in local coordinate system
u_{i1}, u_{i2}	Longitudinal node displacements of element i in local coordinate system
$\mathbf{U}$	Node displacement vector of total system in global coordinate system
$\mathbf{U}_{\mathrm{a}}$	Vector of unknown node displacements

Symbols	Signification
$\mathbf{U}_\mathrm{b}$	Vector of known node displacements
U_i	Lower chord force of a crossarm in panel i
$\mathbf{U}_i$	Node displacement vector of element i in global coordinate system
U_{i1x}, U_{i2x}, U_{i1y}, U_{i2y}	Node displacements of element i in global coordinate system
U_A, U_B	Horizontal force in face A or B of a lattice tower
U_M	Distance between centre of gravity and shear centre
U_S	Highest system voltage of a line
v	Distance between the spire of crossarm and reference point of moment
V_1	Edge distance from centre of gravity
V_s	Traverse force of a batten plate
w	Width of angle leg, wind load on conductor per unit length
W_C	Conductor weight
W_eff	Effective cross section modulus
W_el	Elastic cross section modulus
W_ins	Dead weight of insulator set
W_T	Torsional cross section modulus
W_y, W_z	Cross section modulus related to axes y, z
y	Distance of the edge from the centroidal axis
y_M	Distance between centre of gravity and shearing centre
z	Height of attachment, height above ground
z_max	Maximum edge distance from centre of gravity of section
α	Imperfection factor, angle between the crossarm axis and the perpendicular to the line centre axis, leg slope, factor for concrete compression strength
α_b	Coefficient of bearing resistance
α_s	Tilting angle of a joint
α_v	Coefficient of shearing resistance
β	Angle line deflection
β_M	Moment coefficient
$\beta_{\mathrm{M}y}$, $\beta_{\mathrm{M}z}$	Moment coefficients related to the axes y, z
β_WN	Nominal strength of concrete
β_{yy}	Buckling length factor related to the axis parallel to one leg
γ_cr	Partial factor for resistance of concrete
γ_C	Partial factor for conductor tensile forces
γ_F	Partial factor for actions
γ_G	Partial factor for permanent action
γ_I	Partial factor for ice action
γ_M	Partial factor for material property
γ_P	Partial factor for construction and maintanance loads
γ_s	Partial factor for resistance of reinforcing steel
γ_W	Partial factor for wind action
Δ	Increase of latitude of tower
Δ_A, Δ_B	Increase of latitude of face A or B of a lattice tower
Δ_AF, Δ_BF	Increase of latitude of face A or B of a lattice tower within the foundation
Δ_s	Bolt slippage
ΔA	Sum of all borehole areas
Δt	Increase of latitude of the crossarm lower chords
ε_c	Concrete strain
ε_cu	Ultimate concrete strain
ε_c2	Concrete strain of 0,2 %
ε_p	Steel strain
κ	Buckling reduction factor
κ_min	Minimum buckling reduction factor
κ_y, κ_z	Buckling reduction factor related to the axes y, z
λ	Slenderness ratio
$\overline{\lambda}$	Non-dimensional slenderness ratio

Symbols	Signification
λ_1	Slenderness ratio of a submember of a compound member
λ_a	Reference slenderness ratio
$\overline{\lambda}_{eff}$	Effective slenderness ratio
$\overline{\lambda}_p$	Non-dimensional slenderness ratio of plates
λ_{vi}	Equivalent slenderness ratio
λ_y, λ_z	Slenderness ratio related to axes y, z
μ_y, μ_z	Coefficient for the calculation of the moment factor β_M
ϱ	Reduction factor for the calculation of effective cross section properties
ϱ_1, ϱ_2	Reduction factor for the calculation of effective angle leg width
σ_b	Bending stress
σ_c	Concrete stress in concrete poles
σ_d	Design value of normal stress
σ_{CR}	Conductor tensile stress without wind
σ_P	Steel stress in concrete poles
σ_{Rd}	Design value of resistance of normal stress
σ_{vd}	Design value of the yield condition
σ_{CW}	Conductor tensile stress under wind
τ_d	Design value of shear stress
ϕ	Coefficient for calculation of the buckling reduction factor
ϕ_C	Swing angle
ϕ_{CR}	Swing angle without wind action in case of angle suspension supports
ϕ_{CW}	Swing angle under wind at an angle suspension support
ψ	Combination factor

12.1 Support types and their applications

12.1.1 Definitions

Towers or *poles* of overhead power lines are parts of the *supports* and consist of *tower or pole body*, *earth wire peaks* and *crossarms*. The transmission voltage, the number of circuits, the height of the supports and other aspects determine the support design and materials, whereby *steel*, *reinforced concrete* or wood are used. The supports dominate the aesthetic impact of an overhead line, govern the operational reliability and determine the necessary investment to a certain extent. They need to withstand reliably the conductor forces and external loads.

Poles made *of reinforced concrete*,*solid-wall steel* and *wood* as well as *lattice steel towers* and *portal structures* are summarized as *self-supporting structures*. Additional guy wires guarantee the stability of *guyed structures*.

The type of conductor attachment through the insulators at the supports depends on the task of the support within the transmission system. At *suspension supports*, the conductors are fixed to *suspension insulator sets* or to line post insulators in case of low- and medium-voltage lines. Line post insulators are only to a low extent able to transfer forces in line direction. Suspension insulator sets swing rectangularly to the conductor direction being prevalent for the tower top geometry. At *angle-strain* and *dead-end supports*, the conductors are attached by means of tension insulator sets which transfer the total conductor tensile force to the support.

12.1.2 Tasks of supports in an overhead line

12.1.2.1 Suspension supports

Suspension supports carry the conductors in a straight line. During normal operation, they do not transfer conductor tensile forces to the supports and, therefore, can be designed relatively light-weight. Since they represent the most favourable conductor supports, so far investment is concerned, line sections as long as possible equipped with

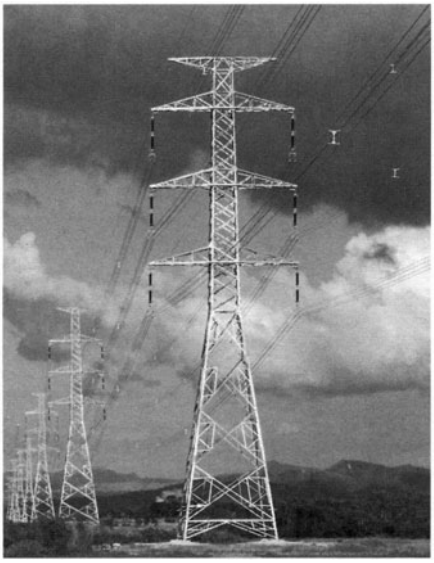

Figure 12.1: Suspension tower of a 220 kV line with suspension insulator sets

Figure 12.2: Suspension pole of a 33 kV line with line post insulators

suspension supports are aimed at. In Figure 12.1, the suspension support of a 220 kV line is shown, in Figure 12.2 the suspension pole of a 33 kV line.

12.1.2.2 Angle suspension supports

Angle suspension supports serve as suspension supports for the conductors where the line changes direction at line angle deflections. In this case, the suspension insulator sets assume an inclined position even without wind action. Angle suspension supports are used for line deflections between 0 and 20° and attain more significance for lines with one or two circuits and voltages up to 110 kV. In case of higher voltages, an unfavourable tower top geometry results; therefore, their economic advantage as compared with angle supports should be studied for each project. The conductor attachment to angle suspension structures is technically disadvantageous.

12.1.2.3 Angle supports

Angle supports carry the resulting conductor tensile forces where the line changes direction at line angle deflections. Contrarily to angle suspension supports, they are equipped with tension insulator sets. Angle supports are loaded in the same manner as angle-strain supports. In the spans adjacent to such supports, considerable differences in the conductor tensile force can occur, e. g. due to non-uniform ice accretion; however, this support type is not designed for a corresponding load case, contrarily to angle-strain supports. Due to this reason, angle supports are rarely used in areas which are prone to heavy icing, e. g. in Central and Northern Europe.

12.1.2.4 Strain and angle-strain supports

Strain and *angle-strain supports* carry the conductor tensile forces in line direction or in the resultant direction, respectively, and serve additionally as *rigid points* in the line. They are designed for conductor tensile forces differing in both line directions and

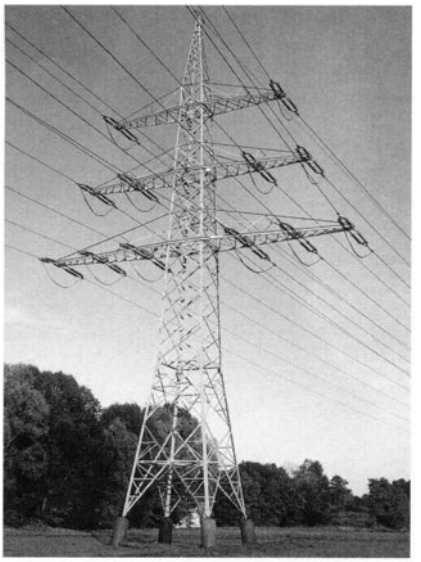

Figure 12.3: Strain support of a 110 kV line with tension insulator sets

secure the line against cascading failures. In Central Europe, it is common practice to use angle-strain towers at practically each angle point of the line. This eases the conductor installation as well. In case of long, straight line sections, strain supports should be arranged in distances between 5 to 10 km to provide rigid points in the line, thus limiting *cascading failures* which might start at suspension supports. In Figure 12.3, a strain support of a 110 kV line is shown.

12.1.2.5 Dead-end supports

Dead-end supports carry the total conductor tensile forces in line direction on one side. Frequently, dead-end supports are additionally loaded by the conductors leading to the substation portals which act often under a large angle to the horizontal and with conductor tensile forces caused by the short distances to the portal. These load conditions may lead to unfavourable loads of individual members of lattice steel towers and need to be considered during design. Dead-end supports of double circuit lines with only one circuit installed experience a high torsional load.

12.1.2.6 Special supports

In transmission lines, a support may be used for several functions of individual support types, e. g. in case of branch-off supports where two circuits may pass through and one or two other circuits are terminated. Such a *branch support* assumes the task of an angle or angle-strain support concerning the circuits passing through. The terminated circuits load the support as in case of a dead-end support. The load cases need to be combined to cover the most unfavourable load conditions taking care of the function of such a support.

12.1.3 Support design and application

12.1.3.1 Selection of support design

Numerous designs of supports are used in overhead transmission lines, such as *self-supporting steel towers*, *guyed steel towers*, either of the conventional type or cross rope suspension [12.1], *self-supporting steel poles*, flexible and semi-flexible steel towers [12.2]

and poles, *wood poles*, wood H-frames and *concrete poles* or concrete structures. The *selection* of the most appropriate *support design* for a certain overhead transmission line is a sensitive issue, depending on several parameters of paramount importance:

- An optimum *utilization* of the *rights-of-way*, considering that the obtainability of land for new lines is becoming increasingly difficult and costly. Thus, for a better use of land, the design of compact lines or of multiple-circuit lines is more and more attractive and economic.
- The *reduction of environmental impacts* of lines has also turned out to be a key factor, especially regarding the impact of electrical and magnetic fields, the visual impact and the impact of location.
- One of the line designer's primary interest is ensuring that the transmission line is capable of transferring the necessary power at a reasonable price.
- The prospected life time of the line is of high interest as well, because this point will have a prevalent role in the selection of the support type for a new line.
- Location and importance of the line.
- The terrain and its access decides on the span lengths and support sites. Heavy concrete poles cannot be used in a terrain not accessible to heavy trucks.
- Number of circuits to be installed on common structures.
- The mechanical load of the conductors and climatic loads to be withstood.
- The height of structures necessary to cross obstacles.
- The land use under a new line and in its vicinity.
- The possibilities to acquire the right-of-way and support sites as well as the compensations to be paid.
- The keraunic level and the arrangement of earth wires.
- The availability of support designs.
- The methods to be used for line construction and maintenance.
- Last but not least the investment necessary to construct a new line.

The impact of these aspects varies from line to line and from region to region. Optimizing the support design for an individual line can prove to be economic particularly for long lines.

12.1.3.2 Self-supporting lattice steel towers

Self-supporting lattice steel towers are the most traditional types used in overhead power lines. They are predominantly adopted where the requirements due to local conditions and the environment call for narrow tower locations and right-of-way (Figure 12.4). Lines exceeding AC 150 kV are frequently equipped with this support type. Their configuration can be adjusted to accommodate several circuits and all types of *conductor configurations*; the lattice steel design is economic also in case of tall towers (Figure 12.5).

Weights and lengths of tower elements to be transported are lower compared with concrete or solid-wall steel poles.

If necessary, upgrading of existing towers can be carried out relatively simply. The exchange of crossarms is possible. *Increasing of existing tower heights* can be achieved by inserting additional tower body sections. Damage occurring during operation can be repaired by simple means as well. The installation of additional components such as telecommunication antenna and associated platforms is possible if the structural stability permits that. Towers not anymore necessary can be scrapped and recycled.

Steel without a protected surface offers only a low resistance against the impact of climate and environment. Today, all lattice steel towers are hot-dip galvanized for *corrosion protection* and receive often an additional protective coating resulting in a long life cycle.

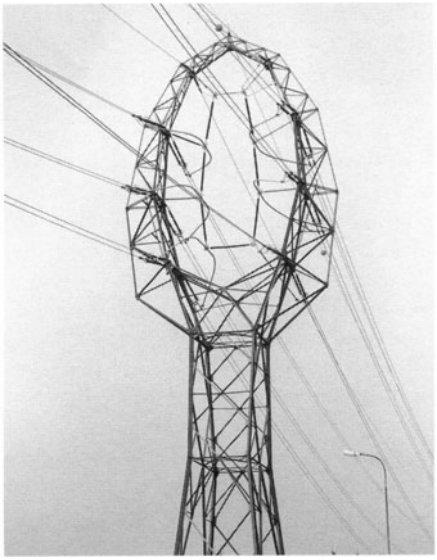

Figure 12.4: 380 kV tower adjusted to local requirements, EOS, Lausanne, Switzerland

Figure 12.5: Suspension tower of 500 kV Suez crossing, Egypt

Lines fitted with self-supporting lattice steel towers need a high amount of steel to be manufactured, transported and erected. Therefore, other designs replaced them, particularly in long single-circuit extra-high-voltage lines in less densely populated areas and in agricultural or non-cultivated terrain.

12.1.3.3 Self-supporting steel poles

Self-supporting steel poles are frequently used in congested urban or suburban areas where rights-of-way availability is limited and short spans are possible only. Their use, in such cases, plays a valuable alternative to underground cables. They provide also the possibility of being used as compact structures including the employment of *insulating crossarms* made, for instance, of composite insulators. Regarding aesthetics, steel poles comply with the desire to use visually pleasing structures, often required in urban areas or other sites where aesthetics may play a role in the support selection.

Suspension poles made of H-beam sections can be adopted for medium-voltage lines. Since they do not require much effort in the production, their costs per weight unit are relatively low, although they have a relatively high dead weight. H-beam sections show different resistance related to their principal cross-sectional axes and a low *torsional stiffness* only.

Seamless tubular steel poles with section by section differing diameters or with continuously conical shape are produced by rolling or drawing. It is possible to adjust their cross-sectional dimensions to the bending moment. Since expensive equipment is necessary for manufacturing, this type of poles is adopted in countries where local manufacturers offer them.

Conical steel poles with six, eight or more sides are made of steel plates by bending and welding, thus enabling to produce poles with relatively high resistance and sufficient torsional stiffness as well. Shape and cross section can be adjusted to the load. Conical steel poles are also used for high-voltage lines. In Figure 12.6, a solid-wall suspension pole of a 110 kV double circuit line is shown. Also 400 kV lines have been constructed

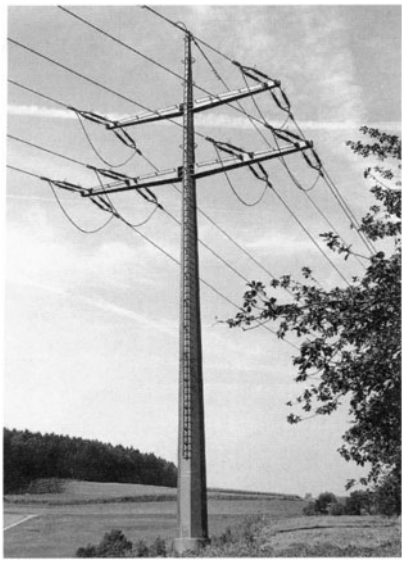

Figure 12.6: One-piece, conical solid-wall steel pole of a 110 kV line (Pfleiderer AG)

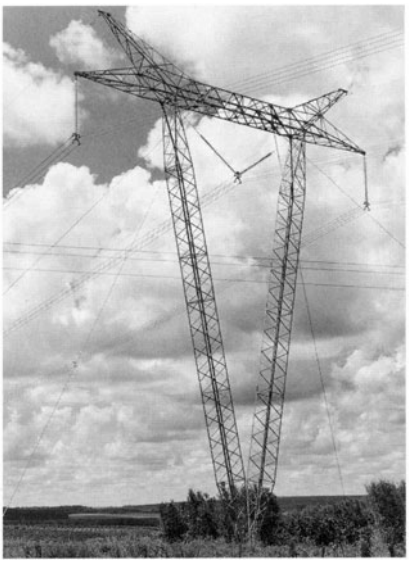

Figure 12.7: Guyed V-tower (Brazil)

world-wide using steel poles, for example in the United States and in the Netherlands [12.3]. Lines equipped with such poles need considerably higher investments for 110 kV and higher transmission voltages because of the considerably higher efforts for the foundations among other things compared with wide-spread lattice steel tower design especially in case of unfavourable subsoil.

12.1.3.4 Steel-reinforced concrete poles

Steel-reinforced concrete poles have been used in different designs for overhead power lines during many years and are used wide-spread as *spun concrete poles* for low- and medium-voltage installations nowadays. Also for 110 and 132 kV double circuit lines, this design has been adopted more recently. The possibility to achieve the strength necessary for angle and angle-strain poles with spun concrete was a precondition for this application. *Vibrated concrete poles* are used for lines where the installation of a plant for spun concrete poles cannot be economically justified and, on the other hand, the transportation of spun concrete poles would be too expensive [12.4, 12.5].

When designed and manufactured properly, concrete poles will have a long *service life* without any efforts for maintenance. In particular, recoating of poles will not be necessary contrarily to steel structures. Concrete poles possess an unreduced serviceability also after having been 50 years in service, as demonstrated by examples.

Concrete poles are characterized by a favourable visual impact being of special interest close to residential areas. They are reasonable and competitive concerning costs due to the essentially lower requirement of steel. This is of special interest for projects in countries where steel needs to be imported but cement and concrete aggregates are available.

The high weight presents a major disadvantage for concrete poles, thus increasing the efforts for transportation and erection. The high weight restricts the application to less tall pole heights in most cases. Correspondingly powerful tools are necessary for *erection* which cannot be used in every type of terrain. When being unduly transported, cracks

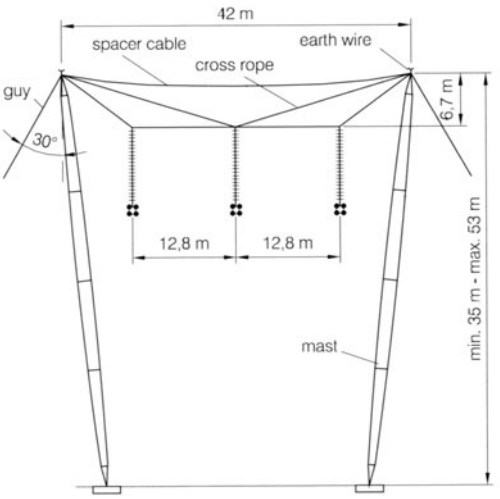

Figure 12.8: General layout of chainette tower (Hydro Quebec, Canada)

can occur and the pole would not be anymore serviceable. Due to the high weight, only a transportation over short distances should be considered. In addition to production, the possibilities of transportation limit the lengths of poles to be realized. In mountainous regions, the use of concrete poles is often precluded due to the difficulty to transport the poles to the location sites (see [12.6]).

12.1.3.5 Wood poles

The use of *wood poles* for overhead power lines is common in countries where wood is available in good quality and large quantities. For example, 110 and 220 kV lines have been constructed using timber structures in North and South America and in Australia.

12.1.3.6 Guyed supports

Guyed supports have been introduced early in the thirties in the shape of H- or portal types. Guyed V- (and rarely guyed Y-) types came later, but little by little have been used as a substitute for self-supporting structures for long single-circuit lines, especially in flat or easily accessible terrain, for economical and aesthetic reasons. In agricultural areas, which are predominantly flat, guyed supports should be provided with protection of the anchors against impact of machines prone to damage them. In Figure 12.7, a guyed V-tower is shown.

12.1.3.7 Crossarmless supports

The advent of *crossarmless towers*, where the crossarm was replaced by ropes, reduced still further the weight of steel necessary for the design of single-circuit lines. Such tower types made it easier to obtain compact lines with increased surge impedance load. Crossarmless towers were first adopted for 735 kV single-circuit lines in Canada [12.7]. In Figure 12.8, their general layout is shown. These tower types need relatively wide areas for tower sites. Their use is limited to more or less uncultivated terrain, therefore.

12.2 Tower top geometry

12.2.1 Requirements

Transmission line supports require a design with sufficiently safe clearances between the conductors within a span, as well as between earth and live components at the supports under all climatic and electric effects likely to occur. The attachment height of the conductors depends on the required clearance to ground or to crossed objects. The required clearance is mainly determined by the relevant line voltage. The *attachment height* itself does not directly affect the dimensions of the tower top. The clearance required between the conductors depends mainly on the sag and, therefore, on the span length, while the clearances to earthed parts on the support is determined by the type and arrangement of insulators, the electric stresses acting on the line and the wind action on conductors and insulators. Conductors and insulators swing under wind. Therefore, the positions of the conductors and insulators depend on the wind action, which plays an important role when designing the *tower top geometry*. The occurrence probability of a certain clearance can be described by statistical distributions.
The required minimum electrical clearances depend on the environmental conditions, the type of air gap and the voltage stress:

- Power frequency voltages,
- Slow-front overvoltages and
- Fast-front overvoltages.

Details on voltages and overvoltages are dealt with in clause 2.5.1.2.2.

12.2.2 Electrical clearances according to relevant standards

The distances between the conductor attachments are selected such that in normal system operation *flashovers* between live and earthed components of an overhead line will be unlikely. Normal system operation includes *switching operations*, *lightning strokes* and *overvoltages* due to system failures. According to EN 50 341-1 [12.8], it is distinguished between the *minimum air clearance* D_{el}, which is required to avoid a disturbing discharge between conductors and earth potential, and the minimum air clearance D_{pp}, which is required to avoid a discharge between live conductors. The minimum clearances to be adopted are described in clause 2.5.1.2.3. The clearances between conductors in midspan and the clearance of swung conductors to earthed components need to be studied as well.

12.2.3 Clearance between conductors

12.2.3.1 Equal cross sections, alike materials and equal sags of conductors

As defined in EN 50 341-1 [12.8], clearances between conductors are *internal clearances*. Thereby it is accepted that the economic design of a power network will have a limited number of flashovers across some internal clearances. In still air, the electrical clearances D_{el} between phase conductors and earth wires and D_{pp} between phase conductors need to be complied with. Due to the low probability of simultaneous occurrence of overvoltages whilst the conductors are moved by wind load, the mentioned electrical clearances D_{el} and D_{pp} may be reduced by multiplying them by a factor k_1. Factors k_1 are defined in the Normative National Aspects (NNA) established by the members of CENELEC. There, k_1 is between 0,75 and 1,00.
The *minimum clearance* between phase conductors at midspan should be

$$c_{\min pp} = k_C \sqrt{f_C + l_k} + k_1 \cdot D_{pp} \tag{12.1}$$

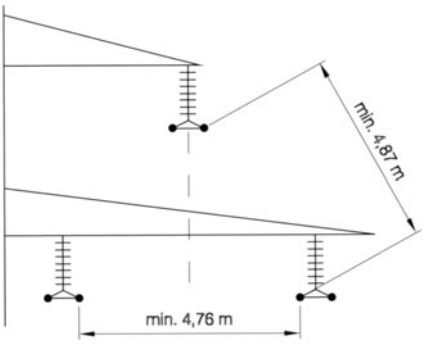

Figure 12.9: Minimum clearances between conductors of a 220 kV line (example)

and between a phase conductor and an earth wire

$$c_{\min\,\mathrm{pe}} = k_\mathrm{C}\sqrt{f_\mathrm{C} + l_\mathrm{k}} + k_1 \cdot D_\mathrm{el} \quad , \tag{12.2}$$

where

k_C factor depending on the relative position of the conductors and the swing angle ϕ_C of the conductor under wind action;
f_C sag of the conductor at +40°C, in m;
l_k length of the insulator set swinging rectangularly to the line axis, in m; $l_\mathrm{k} = 0$ applies in case of line post insulators and tension insulator sets;
D_pp minimum phase to phase clearance depending on the voltage, in m;
D_el minimum phase to earth clearance depending on the voltage, in m.

The relations (12.1) and (12.2) can be found in several National Normative Aspects of the European standard EN 50 341-3 [12.9]. There, the factor k_C varies between 0,5 and 0,7 for horizontal arrangement of the conductors and between 0,6 and 1,0 for vertical position of the two conductors. In Table 2.21 and Figure 2.15 the data according to the German NNA EN 50 341-3-4 [12.10] are presented. These data apply as well for Austria, Belgium and Switzerland. As a further example, the practice from Brazil should be mentioned [12.11]. The minimum clearance should be at least

$$c_\mathrm{min} = 0{,}37\sqrt{f_\mathrm{C}} + 0{,}0076\,U_\mathrm{S} \text{ in m} \quad , \tag{12.3}$$

where f_C is the sag in the longest span and U_S the highest system voltage in kV.
The following example is based on the approach as given in [12.10]. There, the factor k_1 is 0,75 and k_C is obtained from Table 2.21.
The clearance c_min may not be less than k_C, in m. In case of parallel circuits with differing operational voltages on the same supports, the higher values for D_pp and D_el, respectively, are used.
The *conductor swing angle* ϕ_C results from

$$\phi_\mathrm{C} = \tan^{-1}\left[w/\left(m_\mathrm{C} \cdot g\right)\right] = \tan^{-1}\left[q_z \cdot d \cdot G_\mathrm{xC} \cdot C_\mathrm{C}/\left(m_\mathrm{C} \cdot g\right)\right] \quad . \tag{12.4}$$

According to EN 50 341-3-4, the wind load having a return period of three years amounting to 58 % of the maximum dynamic wind pressure is used in equation (12.4). The sag f_C is assumed at a conductor temperature of +40°C without wind action. The sag f_C in equations (12.1) and (12.2) depends on the span length. The maximum span between two supports, for which a tower family is designed, is designated as *phase span length*, therefore. The length l_k of the swinging part of the insulator set is assumed to be zero in case of tension insulator sets and line post insulators. Equations (12.1) and (12.2) apply to commonly encountered conditions and span lengths; they do not include any provisions for *galloping* and should not be used for spans longer than 1000 m; for

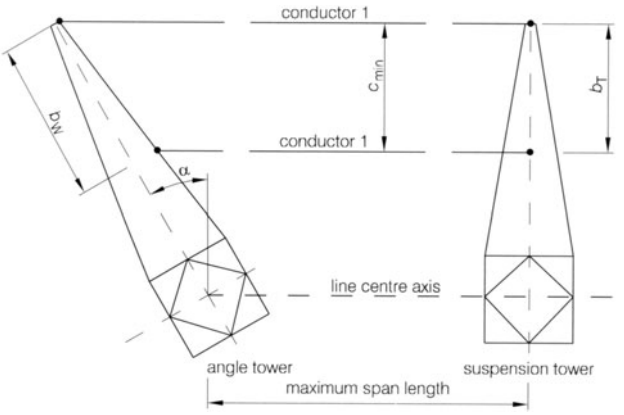

Figure 12.10: Determination of clearances at an angle support

such spans, a clearance between the conductors equal to 1 % of the span length has proved its adequacy [12.12]. Furthermore, it is recommended for such cases to study in detail the swinging of the conductors under the action of differing wind loads on the individual conductors (see clause 12.2.3.2).

Example: Danube configuration of the conductors at a tower (Figure 12.9)

Twin bundle conductor 264-AL1/34-ST1A (Table 7.9) arranged horizontally	
Subconductor diameter	$d = 22{,}4$ mm
Conductor mass	$m_C = 0{,}994$ kg/m
Drag factor	$C_C = 1{,}0$
Nominal voltage	220 kV, ($U_S = 245$ kV)
Minimum clearance according to Table 2.20	$D_{pp} = 2{,}0$ m
Span length	$a = 500$ m
Span length reaction factor	$G_{xC} = 0{,}45 + 60/500$
Sag at 500 m and +40°C	$f_C = 25{,}60$ m
Length of the insulator set	$l_k = 4{,}0$ m
Reference wind pressure (wind zone 1)	$q_0 = 800$ N/m^2
Conductor at the lower crossarm:	
height of attachment	$z = 34{,}0$ m
dynamic wind pressure	$q_z = 0{,}58\,(q_0 + 3 \cdot z) = 523$ N/m^2
swing angle	$\phi_C = \tan^{-1}[(q_z \cdot d \cdot G_{xC} \cdot C_C)/(m_C \cdot g)] = 34{,}4°$
Conductor at the upper crossarm:	
height of attachment	$z = 40{,}0$ m
dynamic wind pressure	$q_z = 0{,}58\,(q_0 + 3 \cdot z) = 533$ N/m^2
swing angle	$\phi_C = \tan^{-1}[(q_z \cdot d \cdot G_{xC} \cdot C_C)/(m_C \cdot g)] = 34{,}9°$

Based on these swing angles, $k_C = 0{,}60$ follows from Table 2.22 for conductors in a horizontal plane and $k_C = 0{,}62$ for conductors at differing crossarms.
According to (12.1), the minimum horizontal clearance is

$$c_{min} = 0{,}60 \cdot \sqrt{25{,}6 + 4{,}0} + 0{,}75 \cdot 2{,}0 = 4{,}76 \text{ m}$$

and the minimum clearance to the third conductor is

$$c_{min} = 0{,}62 \cdot \sqrt{25{,}6 + 4{,}0} + 0{,}75 \cdot 2{,}0 = 4{,}87 \text{ m} \quad .$$

In the spans with angle supports, the angle position needs to be considered when determining the minimum clearances. In Figure 12.10, an example is shown for span between an angle support with a suspension support. The distance of the attachments at the angle tower results to be

$$b_w = (2\,c_{min} - b_T)/[(1 - \Delta t/2 \cdot \tan\alpha)\cos\alpha] \quad , \tag{12.5}$$

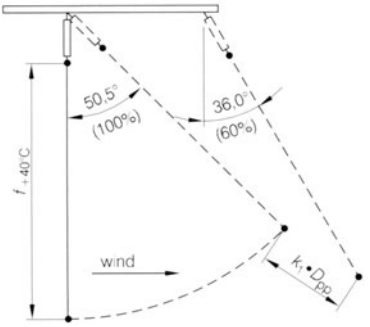

Figure 12.11: Swinging of two conductors at wind loads reduced by 40 % on one of the two conductors

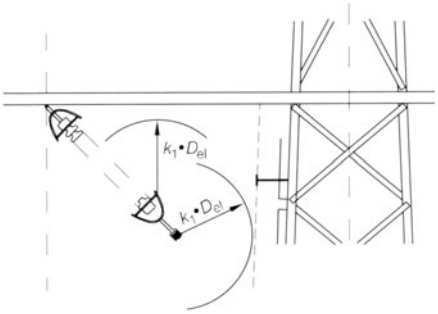

Figure 12.12: Swinging of a 110 kV single-suspension insulator set

where b_T is the distance of the attachment points at the suspension supports, c_{min} is the clearance in midspan and Δt the increase of width of the crossarm lower face.

12.2.3.2 Conductors with different cross sections, materials or sags

In case of conductors with different cross sections, materials or sags, the factor k_C corresponding to the higher swing angle ϕ_C is used for calculating the clearances according to (12.1) and (12.2), as well as the higher sags in case of differing sags.
In addition to the *clearances between the conductors* in still air, the clearances between swung conductors should be studied. It can be recommended that under the action of dynamic wind pressures differing up to 40 % for the individual conductors, the clearances should be at least $k_1 \cdot D_{el}$ or $k_1 \cdot D_{pp}$, respectively. Due to the low probability of simultaneous occurrence of overvoltages and extreme wind loads, a return period of three years for the wind is recommended for computing the swung conductor position. The wind load acts perpendicularly to the conductor. According to EN 50 341-1, it applies to the wind load

$$Q_{WC} = n \cdot q_z \cdot G_{xC} \cdot C_C \cdot d \cdot a_W \quad \text{in kN} \quad , \tag{12.6}$$

where

n number of subconductors
q_z the dynamic wind pressure on the conductors for the reference height z,
G_{xC} gust and span length reaction factor depending on the span length and the dynamic behaviour of the conductors, also called *span length coefficient.*
According to [12.8], the factor G_{xC} can be obtained from
$G_{xC} = 1{,}30 - 0{,}082 . \ln a_W$ for the most important terrain category II.
According to [12.10], it can be assumed:
$G_{xC} = 0{,}75$ for span lengths up to 200 m,
$G_{xC} = 0{,}45 + 60/a_W$ for span lengths longer than 200 m,
C_C drag factor for conductors,
d conductor diameter in m,
a_W wind span equal to $(L_1 + L_2)/2$ in m.

Based on this wind load, the *conductor swing angle* can be calculated according to (12.4). The sag at 40°C conductor temperature should be used. In Figure 12.11, swinging of the conductor 264-AL1/34-ST1A is shown according to the above mentioned example. For a dynamic wind pressure reduced by 40 %, a conductor swing angle of

36° follows for 200 m span length. The closest distances of two conductors may not always occur at the maximum wind action on one of the conductors, but at lower wind pressures. Therefore, the whole range of swing angles from zero to the maximum needs to be studied.

12.2.4 Clearances at supports

The conductor next to the tower body needs to be arranged such that the required minimum clearances between live components and earthed support parts are obeyed also under wind action. In many cases, the fittings such as yoke plates of double insulator sets or protection fittings prevail on the minimum *clearances at supports* since they approach closer to the tower body than the conductors in a swung condition. The minimum clearances occur between the live parts and the angle leg of the bracing arranged outside the tower body or the stepbolts. The *swing angle of the insulator set* under wind action is

$$\phi_{\mathrm{C}} = \tan^{-1}\left[(Q_{\mathrm{WC}} + 0{,}5 \cdot Q_{\mathrm{Wins}}) \,/\, (W_{\mathrm{C}} + 0{,}5 \cdot W_{\mathrm{ins}})\right] \quad , \tag{12.7}$$

where Q_{WC} is the wind load on the conductor, Q_{Wins} the wind load on the insulator, W_{C} the conductor weight for the shortest weight span and W_{ins} the weight of the insulator set.

The lowest *weight span* takes care of the difference in heights between neighbouring supports. The fittings of double insulator sets arranged perpendicularly to line direction may touch each other or even get stuck when large swing angles occur. When arranging the double insulator sets in line direction, the individual insulator strings do not interfere with each other in case of swinging under wind action.

The clearance between the swung insulator set and the crossarm needs to be checked as well. In Figure 12.12, the swinging of a 110 kV suspension insulator set is shown with the clearances to the tower body and to the lower face of the crossarm. If the clearance to the lower face is not sufficient, the hinge of the insulator set can be lowered by means of a *dropper*. Hinged droppers reduce the torsional load on the crossarm resulting from forces in line direction. Extensions of the insulator length by means of links between the hinge bracket and the attachment eye can also be used to increase the clearance.

In case of *angle suspension supports*, the insulator sets attain a swung position also without wind action due to the conductor tensile forces. The *swing angle* without wind action at an angle suspension support is

$$\phi_{\mathrm{CR}} = \tan^{-1}\left[(2 \cdot n \cdot A \cdot \sigma_{\mathrm{CR}} \cdot \sin\beta/2) \,/\, (a_{\mathrm{g}} \cdot n \cdot m_{\mathrm{C}}g + 0{,}5 \cdot W_{\mathrm{ins}})\right] \quad , \tag{12.8}$$

where A is the conductor cross section, σ_{CR} the conductor tensile force, n the number of subconductors, β the angle of line deflection, a_{g} the weight span, $m_{\mathrm{C}}g$ the conductor dead weight per unit length and W_{ins} the dead weight of the insulator set. Without wind action, minimum clearances D_{el} have to be complied with.

The *swing angle* under wind action is determined considering the conductor tensile force at a temperature of +5°C.

$$\phi_{\mathrm{CW}} = \tan^{-1} \frac{Q_{\mathrm{WC}} + 2 \cdot A \cdot n \cdot \sigma_{\mathrm{CW}} \cdot \sin\beta/2 + 0{,}5 \cdot Q_{\mathrm{Wins}}}{a_{\mathrm{g}} \cdot n \cdot m_{\mathrm{C}}g + 0{,}5 \cdot W_{\mathrm{ins}}} \quad , \tag{12.9}$$

where Q_{WC} is the wind load on the conductor according to (12.6), Q_{Wins} the wind load on the insulator, A the conductor cross section, n the number of subconductors, σ_{CW} the conductor tensile force under wind action at +5°C; regarding other parameters see under (12.8).

At angle and dead-end supports, the movement of the *jumper loops* is composed of a transfer of the points connecting conductor and jumper loop and the movement of the

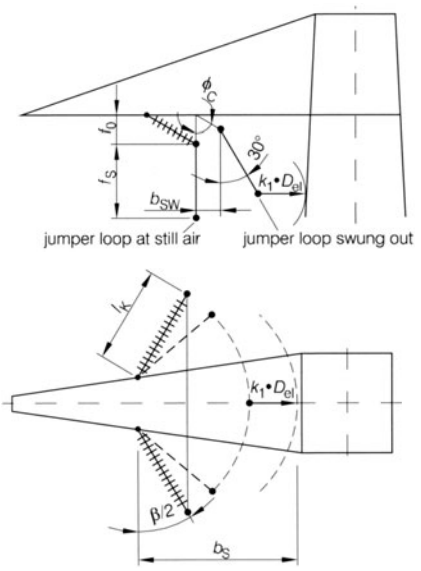

Figure 12.13: Swinging of jumper loops at an angle support

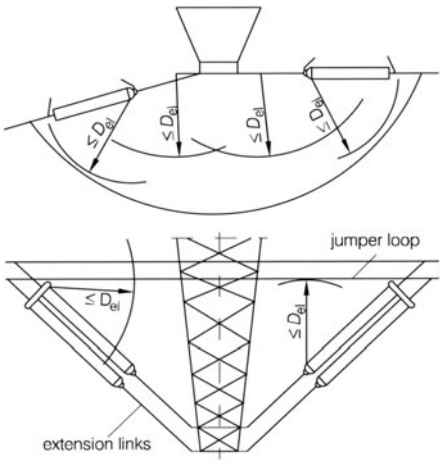

Figure 12.14: Clearance of a double dead-end insulator set to lower crossarm chords and jumper loop

jumper loop itself (Figure 12.13). The position of the innermost conductor attachment to the crossarm needs to be selected such that the required clearance to the tower body is complied with. The increase of latitude of the tower body and the dimensions of the bracings arranged outside the tower body or the length of stepbolts need to be considered as well. The clearance to the closest element of the tower body should be at least

$$b_s = l_k \cdot \sin\beta/2 + f_0 \cdot \sin\phi_C + f_s \cdot \sin 30° + k_1 \cdot D_{el} \quad , \tag{12.10}$$

where l_k is the length of the insulator set; regarding β see (12.8). The value f_0 represents the distance between the lower face of the crossarm and the connections between the conductors and the jumper loop, ϕ_C is the swing angle of the conductor under wind and f_s the sag of the jumper loop.
If applicable, the subconductor distance of a bundle conductor has to be considered as well. The distance f_0 can be determined from the sag f_e in the *complementary span* a_e which considers the difference of conductor attachment heights at adjacent towers:

$$f_0 = 4 \cdot f_e \cdot l_k \cdot (a_e - l_k)/a_e^2 \quad . \tag{12.11}$$

Long spans excepted, it is sufficient to assume a conductor downstrain angle of 10° and $f_0 = l_k \cdot \sin 10°$. The end points of the jumper loop are displaced due to the swinging of the conductor under wind load in direction to the tower body by (see Figure 12.13)

$$b_{sW} = f_0 \cdot \sin\phi_C \quad , \tag{12.12}$$

where ϕ_C is determined according to (12.4) and b_{sW} the displacement of jumper loop ends under wind action.
Jumper loops have a certain stiffness due to their short length and their attachment to the tension clamps, therefore, a swing angle of 30° has proved to be sufficient independently of the conductor type and wind load.

If the distance b_s is high for big line deflections, it can be more economic to adopt an *auxiliary insulator set* to provide for the clearance between the jumper loop and the tower body and to keep the crossarm dimensions shorter. Such auxiliary insulator sets can be designed as V-shaped sets or inclined single insulator strings. *Additional weights* arranged at the jumper loops serve the same purpose. In case of big line deflections, it to be considered has additionally that the clearances between the earthed fittings of the tension insulator set and the jumper loop in still air, as well as in the swung condition will be sufficiently large (Figure 12.14). If necessary, *extension links* can be used to reach the required clearances.

12.3 Basic design requirements

12.3.1 Introduction

EN 50 341-1 [12.8] defines the *basic requirements for design* of overhead electrical lines as follows.

- It shall perform its purpose under a defined set of conditions, with acceptable levels of reliability and in an economic manner. This refers to aspects of *reliability requirements.*
- It shall not be liable to a progressive collapse (*cascading*) if a failure is triggered in a defined component. This refers to aspects of *security requirements.*
- It shall not be liable to cause human injuries or loss of life during construction and maintenance. This refers to aspects of *safety requirements.*

To comply with these basic requirements, all components of an overhead line should be selected, designed and installed such that they perform reliably under the climatic impacts to be regularly expected, under the maximum operating voltage, under the effect of the electric load current and under a short-circuit load. Impacts of atmospheric and switching overvoltages should be taken into consideration.
Regarding the *support design*, the *actions on the supports* are combined to load cases such that *reliability,security* and *safety* performance will be accomplished. Uncertainties due to scattering of actions, imperfections of the supports and variation of material properties need to be considered to achieve a probability of occurrence low enough to be accepted regarding reliability and security.
The loads acting on the supports under normal operation depend on the structural design and on the use and location of the supports within the overhead line. This circumstance is taken into account when designing the supports because a grading of their strength results in a reduction of *investments* without jeopardizing the reliability. When designing supports the actions due to differences in the conductor tensile force because of non-uniform icing and to a local damage are considered. Due to economic reasons, not all supports will be designed such strong that they would withstand all the most unfavourable loads. But at outstanding locations within the right-of-way, supports are arranged being designed for these special conditions. Therefore, *cascading failures* will be limited to a short line section only. Due to these considerations, different support types are used in one line (see clause 12.1.2).

12.3.2 Static design

The supports are designed such that sufficient *ultimate strength* and *serviceability* under the given requirements are guaranteed. Calculations are carried out using suitable *design models* which describe the static performance correctly. These design models are based on approved design theories and practices, which are verified by tests as well. Such models for analysis and design are established in relevant standards, too. The

modelling as a three-dimensional lattice framework with hinged members for *lattice steel towers* and the *equivalent-member method* for buckling according to Eurocode 3 [12.13] should be mentioned as suitable design models.

The *serviceability* might be restricted or not anymore ensured if the support experienced large deformations. These may affect the aesthetics, however, the deformations of the conductor attachment reduce also the *electrical clearances*. The serviceability is ensured if the deformations of the supports do not impair the function of the overhead line (see clause 12.5.14). Calculation of deformations is carried out to verify the serviceability.

A sufficient strength ensures that damage of the support due to exceedingly high deformations, loss of stability, overturning or collapse is not likely. If the strength limits of the individual elements are not exceeded, sufficient strength of the whole structure is verified. Those limits are determined by the design values for internal forces and moments or for stresses. A limit for strength, as an example, is the plastic deformation of the material which is described by the design value f_{yd} of the *yield strength*. The strength limit is also called *structural design resistance*. The actions on the supports result in internal forces and moments as well as in stresses which are called *effects of actions*. A sufficient strength of an element is verified if the effect of action does not exceed the structural resistance.

The *static design* of supports is subdivided into several steps. In the first step, the actions are determined for the load cases to be considered. They depend on the type and arrangement of conductors, the type and application of support and the support geometry. In the second step, the effects of actions, which are the internal forces and moments in the individual elements are computed for the stipulated load cases. In each case, the maximum forces and moments are selected since only these data influence the rating. In the third step, the rating of the elements is carried out. For each individual element, the prevalent load is determined, the material and cross sections being selected such that their design resistance is sufficient to withstand the effects of actions. When the global dimensions and the material of the selected design are known, the dead weight of the structure and the area exposed to wind can be calculated. Due to the influence of the dead weight and the wind action on the support structure itself, the final design depends on these parameters as well. The static design of a transmission line support is, therefore, an iterative process, in principle.

12.3.3 Design values and verification methods

It is the target of the design to verify that *damage* or *failure limits* will not be exceeded under all relevant *design conditions*.

The method of *partial factors* forms the basis for the design and construction of transmission line supports. Partial factors for actions and for resistance take care of uncertainties in the actions, in geometric data and in the static model simulation. Partial factors may also be selected with respect to a desired *coordination of strength* and can depend, therefore, on the type of support and its function within the line. The functional conditions within the overhead line system are explained in clause 6.2.1; clause 6.1.4 contains information on coordination of strengths. If the design values for actions, material properties and geometrical data are used suitably in the design models, damage or failure states within overhead lines are unlikely.

The *design value* F_d *of* an *action* is expressed in general by

$$F_d = \gamma_F F_K \quad or \quad F_d = F_T \quad , \tag{12.13}$$

where F_K is the characteristic value of the action, γ_F the partial factor for this action and F_T the action having a return period of T_r years. Partial factors for actions are based on theoretical considerations, experience and calibration by retrospective analysis

Table 12.1: Standard load cases according to EN 50 431-1 [12.8]

Load case	Conditions
1a	Extreme wind load
1b	Wind load at a minimum temperature
2a	Uniform ice loads on all spans
2b	Uniform ice loads, transversal bending
2c	Unbalanced ice loads, longitudinal bending
2d	Unbalanced ice loads, torsional bending
3	Combined wind and ice load
4	Construction and maintenance loads
5a	Security loads, torsional loads
5b	Security loads, longitudinal loads

of existing designs. Values are given for example in EN 50 341-1 [12.8] and the associated National Normative Aspects, e. g. EN 50 341-3-4 [12.10].
The *design value* R_d *of* a *structural resistance* is defined by

$$R_d = R_K/\gamma_M \quad . \tag{12.14}$$

The partial factor for the material property γ_M takes care of the unfavourable variations from the characteristic value R_K, of inaccuracy in the applied conversion factors and uncertainties in geometric properties and resistance models. Therefore, it applies to the verification of the failure limit or an excessive deformation of a component, an element or a connecting joint:

$$E_d \leq R_d \quad , \tag{12.15}$$

where E_d is the total design value of the effect of actions and R_d the corresponding *structural design resistance*, associating all structural properties with the respective design values.
The *total effect of actions* results from the combination of the actions according to the load case considered. Thereby, the actions are defined by their characteristic values and multiplied by partial factors or by ultimate design loads:

$$E_d = f\left\{\gamma_G\ G_K; \sum_{i=1}^{n} \gamma_i\ Q_{iK}\right\} \quad . \tag{12.16}$$

The individual components of actions are defined by the load cases to be considered.

12.4 Load cases and partial factors

12.4.1 Combination of loads

Differing external loads acting simultaneously on the supports of overhead lines are combined to *load cases* in an adequate manner. These combinations of actions need to comply with the requirements concerning *reliability*, *security* and *safety*. The load cases should take care of all loading conditions to be expected during construction and during the whole life period of an overhead line such that damage will be unlikely. For the design of elements, all actions of a load case are assumed as acting simultaneously, and that load case will be selected which results in the highest load of the element in question. In many standards for overhead lines, e. g. [12.10] and [12.14], it is distinguished between *normal* and *exceptional loads*, whereby differing stability requirements or differing permissible stresses apply. The classification of those specific loads may occur to

Table 12.2: Load cases according to EN 50341-3-4 [12.10]

Load case	Conditions
A	Wind load in direction of crossarms, conductors without ice loads
B	Wind load in line direction, conductors without ice loads
C	Wind load under 45°, conductors without ice loads
D	Reduced wind load in direction of crossarms, conductors with ice loads
E	Reduced wind load in line direction, conductors with ice loads
F	Reduced wind load under 45°, conductors with ice loads
G	Conductor tensile forces at -20°C, unbalanced ice loads, conductors particularly with ice loads
H	Conductor tensile forces at -20°C or -5°C with ice load, conductors with ice loads. Differing conductor tensile forces. This case does only apply for strain towers.
I	Construction and maintenance loads, conductors without ice loads
J	Torsional load, one conductor tensile forces reduced, conductors with ice loads
K	Longitudinal bending, all conductor tensile forces reduced, conductors with ice loads
L	Load after failing of one insulator string, conductors with ice loads

be chosen arbitrarily in a specific case. In general, all cases occurring during the normal operation of an overhead line are considered as normal load. Wind load is, therefore, an example for a normal load. Loads or load combinations having a low probability of occurrence are considered as exceptional loads, e. g. a non-uniform ice accretion of the spans or ice shedding. In EN 50341-1 five *standard load cases* are specified. They affect the individual elements in a different manner, whereby it cannot be predicted in advance which load cases will be prevalent for the individual elements of a support. The load cases according to EN 50341-1 [12.8] are summarized in Table 12.1.

Load cases for design of supports and foundations are defined in each overhead line standard or project specification. As an example for useful definitions, the load cases according to EN 50341-3-4 [12.10] are described hereafter.

In view of the design, the load cases are subdivided taking care of the variation of weight spans and line deflections corresponding to the application of each individual support type. As an example, for an *angle support* designed for line deflections between 0 and 20°, all load cases should be established for these two angles to cover all prevalent stresses of individual elements. To compute tensile forces in elements and uplift of the foundations, the lowest values of the permanent loads need to be used if these actions reduce the effects of other actions. Here, the shortest weight span needs to be assumed for the dead loads of conductors.

12.4.2 Extreme wind load

In case of *extreme wind load*, permanent loads, wind load in all relevant directions on the conductor, the support, on insulators, accessories and on the equipment as well as the conductor tensile forces increased by wind action are assumed as acting simultaneously. The wind action perpendicularly to the line or under an angle of 45° (diagonal wind) will be prevalent for the majority of suspension supports. Other wind directions may gain relevance depending on the conductor arrangement and line angles. The applicable temperature affects the conductor tensile force and depends on the climatic conditions of the geographical area considered. In Table 12.2, the corresponding load cases are listed according to EN 50341-3-4 [12.10] as an example.

Load case A assumes permanent loads, *wind in direction of the crossarm axis* on conductors, tower and equipment as well as conductor tensile forces at a temperature of +5°C as acting simultaneously. This load case, in particular, will be prevalent for the

leg members and bracings in the face in parallel to the crossarm axis for suspension, angle suspension and tall angle towers.
Load case B assumes permanent loads, *wind load rectangularly to the crossarm axis* on conductors, tower and equipment as well as the associated conductor tensile force at a temperature of +5°C as acting simultaneously. This load case yields the highest forces in the faces parallel to the wind direction in case of tall lattice towers.
Load case C assumes permanent loads, wind load on conductors, tower and equipment under an angle of 45° towards the crossarm axis and conductor tensile forces at a temperature of +5°C as acting simultaneously. The diagonal wind action yields frequently the highest loads of leg members and their foundations in case of suspension and angle suspension towers and, in some cases, for angle towers and angle-strain towers as well.

12.4.3 Wind load at minimum temperature

This load case assumes permanent loads, a reduced wind load compared with load case 1a (Table 12.1), and conductor tensile forces at minimum temperature as acting simultaneously. This load case may be important where conductor forces act against the gravitation at the support. They are called *uplift forces.*
Load case G according to [12.10] is applicable only where uplift forces occur; two load combinations need to be studied. In the first case, the permanent loads and conductor tensile forces act at a temperature of -20°C. Thereby, the lowest conductor sags occur resulting in the maximum uplift forces. This load case will be prevalent if uplift forces act in both adjacent spans. In the second case, the permanent loads act and ice loads are assumed in one span.

12.4.4 Uniform and unbalanced ice loads without wind

Extreme ice load

In case of *extreme ice load*, permanent loads, ice loads and conductor tensile forces increased due to the ice load at a corresponding temperature act simultaneously. Several conditions can be distinguished with respect to ice load. A uniform ice load may be assumed at the conductors and earth wires in all spans of a line section either with the same magnitude at all conductors (load case 2a) or with differing values at individual conductors resulting then in a bending of the supports perpendicularly to the line direction (load case 2b). In case of non-uniform ice accretion at conductors and earth wires, differences in the conductor tensile forces are created which load the support in line direction (load case 2c) and may result in torsional moments (load case 2d). The ice accretion on supports themselves is significant only in countries with extremely high ice loads, e. g. in northern Scandinavia.
Load case J according to [12.10] assumes a *torsional load* taking care of differing ice accretion in the adjacent spans, of ice shedding and of differing conductor tensile forces after a line failure and corresponds to load case 2d of [12.8]. The permanent loads and ice loads on conductors at a temperature of -5°C are assumed as acting simultaneously, while the horizontal tensile force of one or several conductors is reduced depending on the design of the conductors. The tensile force of conductors is assumed as one-sided reduced. Details can be obtained from [12.10].
The amount of *reduction of the conductor tensile force* depends on the support type and design. In case of suspension and angle suspension supports, the horizontal tensile force of one conductor is reduced to one side by 50 % in case of single conductors, in case of bundle conductors with lengths of insulator sets up to 2,5 m by 35 %, in case of bundle conductors with lengths of insulator sets above 2,5 m by 25 %. In case of earth wires, the reduction is assumed to be 65 %. In [12.15], conditions concerning ice

accretion or reduction of conductor tensile forces are explained which would lead to these loads.
In case of angle, strain, dead-end and angle dead-end towers, the horizontal tensile force of one single or bundle conductor is assumed to be reduced to one side by 100 %.
This load case affects in particular the crossarm lower chords of suspension and angle towers and is frequently prevalent for the design of bracings of lattice tower bodies.
In load case K according to [12.10] which corresponds to the load case 2c, permanent loads and ice loads on all conductors at a temperature of -5°C act simultaneously with conductor tensile forces being reduced at all conductors on one side of the support. For suspension and angle suspension supports, the horizontal tensile forces of all conductors are reduced by 20 % for line post insulators and suspension insulator sets with lengths up to 2,5 m, by 15 % for suspension insulator set lengths above 2,5 m. For earth wires, the conductor tensile forces are reduced by 40 %. For strain and angle-strain towers, the horizontal tensile force is reduced on one side by 40 %. Load case K affects in particular the design of strain supports with only one circuit installed so far the rating of bracings of lattice steel supports structures is concerned.

12.4.5 Combined wind and ice load

In case of *combined wind and ice load* (load case 3 of Table 12.1) permanent loads, ice loads, wind loads on supports, equipment and ice covered conductors as well as the conductor tensile forces increased by wind and ice load act simultaneously. Extreme wind and ice loads occur simultaneously only in rare cases. As a rule, a load combination will be selected where the extreme ice load and a moderate wind load corresponding to 40 to 70 % of the 50 years wind load will be combined.
Load case D according to [12.10] combines permanent loads, ice loads, wind load in direction of the crossarm axis on conductors with ice load, on the support and equipment together with the associated conductor tensile force under ice accretion and wind action. The dynamic wind pressure is reduced by 50 %, as compared with the load cases A to C. Since the wind action on the ice covered conductors represents an additional load, the conductor tensile forces are increased. This load case results in the maximum load for leg members of angle and angle-strain towers with line deflections above approximately 40° and for dead-end towers. The extent to which this load case will be prevalent for suspension supports depends on the magnitude of the ice load, the dimensions of the conductors and on the support design [12.15].
Load cases E and F correspond to load case D, however, with wind acting rectangularly and under 45°, respectively, to the crossarm axis.

12.4.6 Construction and maintenance loads

During construction and maintenance, loads may result for example from climbing members, from temporary anchors or by attachment of tools or from stringing of conductor. These loads should be duly considered when designing the supports.
In [12.16], a series of such loads is discussed. During *tower erection*, forces due to the arrangement of *derricks* have to be considered as well as resulting from anchors. Supports are anchored temporarily during *stringing operations*, whereby loads occur which could exceed those loads acting permanently. Especially, increased conductor tensile forces may occur during stringing operations because of impacts, joints getting stuck in running blocks or similar events. Increased loads may occur at temporary terminations of the conductor stringing operation. When maintaining the line, towers are climbed resulting in an additional load on lattice framework members. The lowering of conductors using snatch blocks arranged at the crossarms may also result in increased loads to which the supports should withstand.

The supports should provide adequate resistance to all the *loads* probably occurring *from construction* and *maintenance procedures*. Construction and maintenance procedures should be paid special attention since failing of an element would probably lead to injuries of linemen. Supports designed for ice load conditions are, as a rule, strong enough to withstand the commonly occurring construction and maintenance loads. Some elements of supports in areas without ice loads may, however, experience their maximum load during construction or maintenance.
For simulating loads during *construction and maintenance*, permanent loads and construction loads as well as conductor tensile forces at +5°C are assumed as acting simultaneously in load case I of [12.10]. A temporarily higher load by *over tensioning the conductors* is considered by increased conductor tensile forces, if applicable. Construction and maintenance load cases affect especially the design of crossarms. In case of lattice steel structures, the loads are assumed as acting at the most unfavourable nodes of the lower chord of a crossarm face. For other designs, they are assumed at the attachment points of a conductor. This load case may also be prevalent for long members in the tower body used for climbing because these members need to be rated for bending due to the construction and maintenance loads.

12.4.7 Security loads

Line components may fail due to an insufficient quality or due to sabotage and may cause, as a consequence, additional loads to the other components of a line. The target of the design will then be the *containment of damage* and, especially, the *prevention of cascades*. Especially, the failure of an angle support may lead to *cascading* and is, therefore, hazardous.
The extent of a damage will be contained by adequate load assumptions and corresponding line design. The arrangement of strain supports in long line sections protects the line against cascading because these special supports are designed to withstand longitudinal conductor forces. As an example, according to [12.16] the conductors on one side of the relevant support are assumed to be loaded with a fictitious additional load equal to the conductor dead weight.
In [12.8], torsional and longitudinal loads are specified. Details should be stipulated in standards or project specifications. Load case H according to [12.10] is planned to provide rigid points in a line and applies to {emphstrain and *angle-strain towers*. To ensure the stability of the strain towers for unbalanced longitudinal conductor loads a conductor force is assumed as acting at the most unfavourable position and two thirds of the one-sided conductor forces of all the other conductors act in the same direction.
Load case L of [12.10] simulates the load which would occur after a *failure of a string of a multiple insulator set*, and affects mainly the design of crossarms. Permanent loads, ice loads and associated conductor tensile forces at -5°C act simultaneously in this load case, whereby the failing of one insulator string is considered additionally.

12.4.8 Partial factors for actions on supports

Permanent and variable actions are combined according to the load cases considered. The design values are obtained by multiplying the characteristic values of the action with *partial factors*. EN 50 341-1 distinguishes between the *General Approach* and *Empirical Approach* for design. In the General Approach, the partial factors are applied on the actions, like ice and wind load. In the Empirical Approach, partial factors are applied on the effects of the actions. For example, the reactions of conductors to temperature changes, as well as to wind and ice actions are calculated with characteristic values; then the design values are determined by multiplying the conductor tensile forces

Table 12.3: Partial factors for actions, ultimate limit states

Action	Symbol	EN 50 341-1[1]			EN 50 341-1[2]	EN 50 341-3-4
Permanent action						
– unfavourable	γ_G	1,0	1,0	1,0	1,1 (1,0)[3]	1,35 (1,0)[3]
– favourable	γ_G	1,0	1,0	1,0	1,0	1,0
Variable action						
– wind load	γ_W	1,0	1,2	1,4	1,3 (1,0)	1,35 (1,0)
– ice load	γ_I	1,0	1,25	1,5	1,3 (1,0)	1,35 (1,0)
– conductor forces	γ_C	–	–	–	1,3 (1,0)	1,35 (1,0)
Accidental action						
– torsional load	γ_A	1,0	1,0	1,0	1,0	1,0
– longitudinal load	γ_A	1,0	1,0	1,0	1,0	1,0
Construction and maintenance load	γ_P	1,5	1,5	1,5	1,5	1,5

[1] General Approach; [2] Empirical Approach; [3] in case of an accidental action

by partial factors. The *design value* E_d results from the combination of characteristic values of simultaneous actions multiplied by the corresponding partial factors:

$$E_d = \sum (\gamma_G G_K + \gamma_W Q_{WK} + \gamma_I Q_{IK} + \gamma_P Q_{PK} + \gamma_C Q_{CK}) \quad .$$

There, G_K is the dead weight of the conductors, insulator sets and supports, Q_{WK} the wind load, Q_{IK} the ice load on the conductor, Q_{PK} the load due to construction and maintenance, Q_{CK} the conductor tensile force depending on temperature, wind and ice load, γ_G the partial factor for the dead weight, γ_W the partial factor for the wind load, γ_I the partial factor for ice load, γ_P the partial factor for loads due to construction and maintenance and γ_C the partial factor for the conductor tensile forces.
EN 50 341-1 distinguishes between permanent, variable and accidental actions as well as construction and maintenance loads. The relevant partial factors are given in Table 12.3. National requirements may be defined in the National Normative Aspects. As an example, the partial factors according to EN 50 341-3-4 are presented in Table 12.3.
In case of the General Approach, the partial factors of wind and ice loads were specified in [12.8] dependent on the reliability level or the design values of the wind and ice load are determined directly for the selected reliability level.
When calculating the effect of action on the conductor, the partial factors are applied to the characteristic value of the action, i. e. directly on wind and ice load acting on the conductor. The computed value of the conductor tension is then the design value.

12.4.9 Partial factors for materials

In Table 12.4 the partial factors according to EN 50 341-1 for material are presented used for towers and poles. The material design values are obtained by dividing the characteristical values of the material strength by the partial factor.

12.5 Lattice steel towers

12.5.1 Structural design

12.5.1.1 Structural design of members

Lattice steel towers are made of individual members fabricated in the workshop, then shipped to the construction site and assembled and erected there using bolts.
Hot-rolled angle sections according to EN 10 056-1 [12.17] or other specifications are predominantly used for *members of lattice steel towers* [12.18]. The joints can be designed simply and often without additional plates or other structural elements. Angle

Table 12.4: Material partial factor for structural material according to EN 50 341-1

Material	Type of strain	Material partial factor γ_M
Concrete and reinforced concrete	compressive concrete strength	1,50
	compressive concrete strength for prefabricated parts	1,40
	reinforcing steel, yield strength or $\sigma_{0,2}$	1,15
Steel	resistance of sections and stability (yield strength)	1,10
	resistance of bolted and welded connections (ultimate tensile strength)	1,25
	members with boreholes in tension (ultimate tensile strength)	1,25
Timber	resistance of sections	1,50
	resistance of bolted connections	1,25

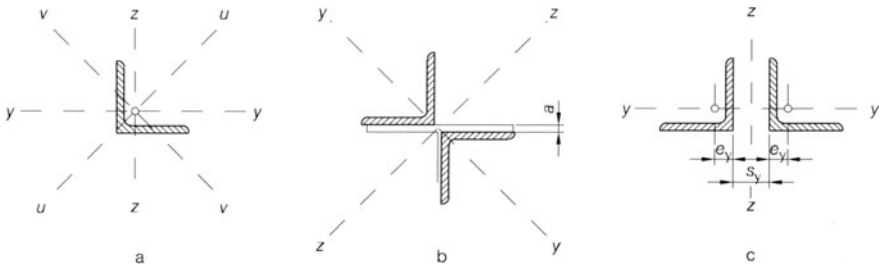

Figure 12.15: Commonly adopted member sections. a: angle section; b: cruciform section; c: back-to-back angle section

sections can be economically processed by program-controlled machinery available today. The profiles can be bundled in a space-saving manner for transport.

Single angle sections are the most economic design; they are manufactured up to a size of 250 × 28 mm with a total cross section of 133 cm^2 (Figure 12.15 a). Using the steel grade S355, a strength of approximately 4 200 kN results with these angle sections being sufficient also for the majority of strain towers of double circuit 400 and 550 kV lines. For towers of multi-circuit lines and, particularly for very tall towers, member designs with a higher strength may be necessary. In this case, *cruciform sections* made up of two, three or four angle sections are used for the leg members according to Figure 12.15 b. Where this arrangement does not suffice, special members can be welded from plates or box-type members can be adopted. Examples for such designs are described in [12.19].

Hot-rolled angle sections are predominantly used for the bracings as well. Due to static reasons, it could be favourable to use non-equal angle sections. For bracings, cold-formed sections are used sometimes where the angle between the two legs of the section can be designed with 60° instead of 90°, thus achieving an increased minimum *radius of gyration* as compared with standard angle sections. Joints between leg members and bracings with bigger dimensions often necessitate gusset plates with an adjusted dimension. In these cases, *back-to-back angle sections* according to Figure 12.15 c offer advantages because the joints possess two shear planes resulting in a considerably shorter total length of the joint. Reference [12.19] contains typical examples for the design of bracings.

Single angle sections proved their qualification for the upper chords of crossarms and, alternatively, if single angle sections are not sufficient, back-to-back angle sections according to Figure 12.15 c can be adopted for this application.

According to EN 50 341-3-4 [12.10] and other standards, the *minimum thickness of the elements* may not fall below 4 mm; bolts with diameters below 12 mm are not permissi-

Table 12.5: Dimensions of joints and edge distances of jointing components in mm according to EN 50 341-3-4

Dimension of bolt		M12	M16	M20	M24	M27	M30
Maximum diameter of borehole							
Hexagon bolts		14	18	22	26	29	32
Rivets		13	17	21	25	28	31
Minimum width of angle leg		35	50	60	70	75	80
Minimum edge distance in direction of the force	(a)	20	25	30	40	45	50
	(b)	25	35	40	50	55	65

a connection of bracings and redundants; b connections of leg members and upper crossarm chords

ble. A minimum width of the angle sections of 35 mm results from these specifications; the angle section L35 × 4 is, therefore, the *smallest cross section* used for overhead line towers. Many utilities, however, specify larger minimum dimensions, e. g. L40 × 4 or L40 × 5.

12.5.1.2 Connections

While formerly rivets were used for lattice steel towers, *bolted* connections predominate by far today. This connection element is adequate for hot-dip galvanization. The individual members and bolts can be galvanized separately and bolted together afterwards. A tolerance between 1 and 2 mm is provided between the diameter of the bolt and the diameter of the hole. Members are frequently connected with one bolt only, in particular all *redundant members* in lattice frameworks and *bracings* of less heavily loaded towers. Due to this design, the bracings or redundant members can be directly connected to the leg members without any *gusset plates*. Not more than six bolts should be arranged in a line for all types of connections thus ensuring the utilization of total strength of the individual bolts. Where this type of connection did not suffice, connections with two shear planes or the arrangement of bolts in two parallel lines should be adopted.
The width of angle sections determines as well the largest diameter of bolts or rivets to be used. Regarding *arrangement of boreholes*, EN 50 341-1 refers to ENV 1993-1-1. Arrangement of holes should prevent corrosion and local buckling and facilitate the installation of bolts. The end distance e_1 from the centre of a borehole to the adjacent end of the member, measured in direction of force (Figure 12.53), should be not less than 1,2 d_0, where d_0 is the hole diameter. The *edge distance* e_2 from the centre of a borehole to the adjacent edge of the member, measured perpendicularly to the direction of force, should normally be not less than 1,5 d_0. Complying this specification, the edge distances e_2 perpendicularly to the direction of force should be at least 1,2 times the borehole diameter, the *distances between centres of boreholes* should at least be 2,5 times the borehole diameter. The edge distance may be reduced to not less than 1,2 d_0 provided that the design bearing resistance is reduced accordingly (see clause 12.5.11). To prevent corrosion, the maximum end or edge distance should not exceed 40 mm $+4\,t$, where t is the thickness of the thinner of the connected parts. The minimum spacing p_1 between centres of bolts in direction of force should be not less than 2,2 d_0 and their maximum should not exceed the lesser of 1,4 times t or 200 mm.
Table 12.5, according to EN 50 341-3-4, represents the correlation between diameter of holes and width of angle sections. There, the edge distances are as well shown which measure from the centre of the holes. The values indicated in Table 12.5 by (b) should be complied with for tensile-loaded elements of crossarms and for joints of leg members. The smaller values apply to all other connections, e. g. for the connections of bracings. When designing towers, the *eccentricity* of connections in the nodes should be kept as low as possible. This eccentricity needs not to be especially considered in the analysis

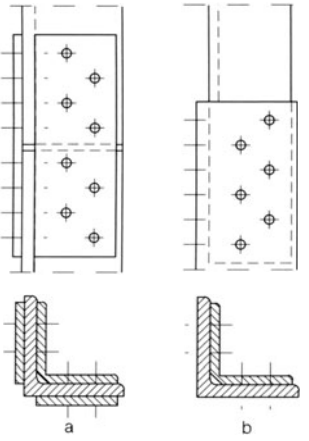

Figure 12.16: Design of leg member joints: a double butt joint; b lap joint

in case of bracings connected by one angle leg only.
For leg members either *butt joints* according to Figure 12.16 a or *lap joints* according to Figure 12.16 b are used. Butt joints can be designed with two shear planes and are preferred in case of towers for higher strengths to facilitate the erection. Lap joints save material, however, are not frequently used anymore because of the more costly erection process.
All nuts should be secured against getting loose. Frequently, *spring washers* are used for this purpose. Alternatively, the nuts can be punched on three points spaced at 120°, being protected with anti-corrosive dyes.

12.5.1.3 Walkways

Lattice steel towers need to be climbed by experienced staff during construction and maintenance. Therefore, accordingly designed *walkways* are necessary. For this purpose, *stepbolts* or*stirrup arrangements* are often installed at two diagonally opposite leg members. Alternatively, *ladders* in the faces or within the body can be installed.
Walkways should be installed on self-supporting steel structures, starting at a height of 3 m above ground level and progressing until the top of the structure. Stepbolts are made of galvanized steel and should be arranged on two legs for each tower and be spaced between 300 to 400 mm on centres. These bolts should be at least 16 mm in diameter, 125 mm long, furnished with a button head and two hex nuts and locknuts. Stepbolts should be installed from the main crossarm to the earth wire peaks as well.
In case of guyed structures, walkways are usually precluded if the mast trusses are sufficient to provide a good path for climbing.
At tubular or polygonal steel poles, as well as concrete poles, support bolts for climbing ladders are installed starting from a distance of 3 m above the ground level. This practice aims at avoiding or at least discouraging persons to climb the structures just for curiosity, vandalism or other purposes. The ladders can be permanently installed for use by maintenance crews or are fixed temporarily at the occasion of services. Details are given in [12.10] and [12.20].
Stepbolts and stirrups are rated for a concentrated load of 1 kN acting at the most unfavourable position according to EN 50 341-1, whereby a partial factor of $\gamma_p = 1{,}5$ is assumed.

12.5.1.4 Production

Manufacturing of holes for bolts or rivets is an essential step in the *production of lattice steel towers.* The holes can either be drilled or punched or subpunched and reamed. Punching full-size is a fast, economical way to get precise hole size, but the material thickness being punched is limited. Different limits are given in project specifications. The thickness should not be greater than 20 mm for mild steel, e. g. S235, or 16 mm for high-strength steel, e. g. S355. An alternative specification limits the material thickness to the nominal diameter of the bolt plus 3 mm. According to EN 50 341-3-4, punching of full-size holes is permitted for a material thickness not greater than 12 mm. Permanent supervision should ensure that sharp punches and suiting dies are used for the manufacturing. A slightly conical form of holes that naturally results from punching operation is acceptable. Since the punching process leads to hardening of the hole edge with the consequence of flaws occurring later, members of crossarms permanently loaded in tension may not be punched. If the material thickness is greater than the limits above mentioned, the holes should either be drilled or subpunched and reamed. The die for all subpunched holes should be at least 1,5 mm smaller than the nominal diameter of the bolt.
The quality of the welding seams should be adequately controlled. The structural steels specified in EN 50 341-1 for the manufacturing of overhead line towers are suited for welding without any limitations.

12.5.1.5 Corrosion protection

Practically all lattice steel towers are hot-dip galvanized nowadays in view of *corrosion protection.* Hot-dip galvanization according to international standard EN ISO 1461 [12.21] ensures a durable and long-lasting corrosion protection. This standard specifies the requirements and test methods of hot-dip galvanization. A *protective* layer of iron-zinc alloy is formed on the steel during *hot-dip galvanizing* and above that a layer made of pure zinc is constituted. The iron-zinc crystals occur to be dull-grey while pure zinc shows brilliant flower ornaments. To what extent the individual layers occur at the surface, depends mainly on the content of silicon within the steel. Silicon is used as a desoxidation agent during steel production. With a silicon content between 0,03 to 0,12 % and above 0,3 %, thick zinc layers are formed while at a silicon content between 0,12 and 0,3 % these layers will not exceed 100 μm. While for steel grade S235 the silicon content will stay below 0,3 %, it rises in case of steel grade S355 up to 0,5 %. Therefore, frequently iron-zinc crystals are formed up to the surface of S355, resulting in a dull-grey appearance of the galvanized steel grade S355. On the contrary, the zinc surface on steel grade S235 has a brilliant-flowery structure.
For members made of S355 with large cross sections, thick zinc layers may be formed which are undesired since they show a less firm adhesion. In addition to a corresponding uniformity, enough *adhesion strength* is required for the *zinc layer.* At present, no ISO standard exists for testing of adhesion. But the adhesion can be tested with the *hammer test* according to Nieth [12.22] standardized in DIN 50 978 [12.23]. For testing the uniformity of the zinc layers, the *Preece test* [12.24] was used formerly in general. For this test, a specimen is dipped in a copper-sulphur solution. No adherent copper layer is permitted to be formed during this process. The result of this test, however, depends on the conditions of the execution and is, therefore, not anymore standardized. Zinc is weathered with time whereby the annual loss of zinc occurs to be between 2 and 10 μm. Therefore, it should be assumed that after approximately 10 to 15 years the zinc layer will be weathered to such an extent that an alternative corrosion protection will be necessary. The weathering period of zinc layers might be even shorter in corrosive atmospheres. Therefore, operators of overhead lines apply the *Duplex system* more and

Table 12.6: Characteristic values of yield strength and ultimate tensile strength for structural steel

Steel grade	Yield strength f_y N/mm^2	Ultimate tensile strength f_u N/mm^2
S235	235	360
S355	355	510

Table 12.7: Characteristic values of yield strength and ultimate tensile strength for bolt materials

Bolt grade	Yield strength f_y N/mm^2	Ultimate tensile strength f_u N/mm^2
4.6	240	400
5.6	300	500
8.8	640	800
10.9	900	1000

more, whereby a paint coating is applied directly after the hot-dip galvanizing of steel parts [12.8]. Together with the hot-dip galvanization, the coating achieves synergetic effects [12.25] resulting in a more than doubled life cycle as achieved by one corrosion protection method alone. The thickness of the coating should be approximately 70 μm. A number of differing systems is used for paint coating which are under continuous development also with respect to the protection of environment.

12.5.2 Materials

12.5.2.1 Materials for angle sections and plates

The materials used for angle sections need not only be sufficiently strong but also tough since impact and alternating loads as well as vibrations may occur in addition to the static loading. A superior *capacity to deformation* reduces local stress peaks, thus avoiding cracks. Fully killed steel complies with these conditions. By adding silicon, aluminium, calcium or titan, the oxygen solved in the liquid steel is bound within the melt, it is desoxidized and the steel solidifies without bubbles. This procedure results in homogeneous steel well suited for welding not prone to brittle fracture. The steel grades S235J0 or S235J2G3/G4 as well as S355J0 and S355J2G3/G4 according to EN 10 025 [12.26] belong to these types of steels. After the rolling process, the products made of S235J0 and S355J0 are not further processed. Products made of S235J2G3/G4 and S355J2G3/G4 are heated and cooled down slowly. This procedure is called *normalizing*. By this process, brittle zones are removed and a fine grain structure is obtained.
The materials used in the fabrication of transmission line supports should comply with the requirements of ENV 1993-1-1, chapter 3, annexes B and D, or with equivalent standards. For structural steel, these requirements are complied with if the material corresponds to EN 10 025 [12.26]. Steel to be galvanized should meet the requirements concerning the maximum silicon (Si) and phosphorus (P) contents of EN ISO 1461, subclause C.1.4 [12.21] to avoid dull, dark grey and excessively thick coating which may result in an increased risk of *coating damage*. All the steel grades according to EN 10 025 are suitable for welding.
In general, angle sections made of S235J0 and S355J2G3/G4 are available in the market. Nominal values for the *yield point* and the *ultimate tensile strength* are used as characteristic values for the design. These data are given in Table 12.6 for steel grades S235 and S355. They apply to a thickness not more than 40 mm.

12.5.2.2 Material for bolts

In general, only the strength qualities 4.6, 5.6, 8.8 and 10.9 according to EN ISO 898-1 [12.27] or equivalent material may be used as *material for bolts*. When analysing towers, the strength of bolts is verified by assuming a constant stress across their cross sections.

The local peaks of stresses occurring at the bolts and close to the holes may not be specifically considered in case of a sufficient ductile material since after exceeding the yield point, large deformations can be endured until failure. For overhead line towers, connections with one or two shear planes stressed on shearing and bearing are adopted *(shear/bearing connections)*. The deformation occurring during the shearing process is determined predominantly by the element with the lower yield point in addition to the tolerance of the boreholes. Thereby, bolts may show a bending deformation and a shearing off-set while the boreholes in sections and plates will get oval and are deformed to a longitudinal shape. The deformation potential of low-tensile bolts of grades 4.6 and 5.6 is higher than that of high-tensile bolts of grades 8.8 and 10.9. The less strong element has to ensure a sufficient deformation potential. Deformations of bolts as well as of profiles occur in the failure condition at connections using low-tensile bolts of grades 4.6 and 5.6. When using bolts of grades 8.8 and 10.9, the bolt strength is higher than that of the angle sections, resulting in permanent deformations of the angle section.

The *coordination of strength* between bolt and elements to be connected should be carried out such that no failure of the bolt might occur since such a failure would result in a complete separation of the connected elements. Some tower manufacturers use bolts of the grades 5.8 and 6.8 as well. However, EN ISO 898-1 [12.27] requires only minor ductility described by the *elongation at breaking* and low data for the toughness [12.28] of these grades. The minimum elongation at breaking, required for bolts made of grade 6.8, reaches only 40 % of the values for bolts made of grade 5.6. There are no requirements on the *sharpy-V-notch energy* according to the standard. Bolts made of grades 5.8 and 6.8 will not show sufficient ductility, resulting in connections without sufficient possibilities for deformation especially in angle sections made of grade S355. If the bolt strength is lower than that of the angle sections, the bolt will fail without a noticeable deformation before the connected elements are deformed adjacent to the borehole. If the strength is approximately equal to that of the angle section, a local exhausting of the deformation potential cannot be excluded. Special attention should be paid to this problem in areas with low ambient temperatures. Bolts of grades 5.8 and 6.8 have only a low ductility leading to *brittle fracture* under high impact load. Therefore, they are not permitted to be used in Central Europe for overhead line towers. The characteristic values of yield strength and ultimate tensile strength of bolts as used for design are presented in Table 12.7.

12.5.3 Analysis of member forces

Lattice steel towers can be considered as three-dimensional hyper-static truss systems. The individual members are mainly loaded by axial tensile and compression forces. The *member forces* can be calculated at the three-dimensional system or at the equivalent plane system. By utilizing the conditions of symmetry for designs with rectangular tower bodies and crossarms, the three-dimensional static system may be reduced to a statically determined plane system. Some *design computer programs* are based on the application of conventional design methods for plane trusses.

Other tower configurations are not suitable to be analysed by using equivalent plane systems due to the missing symmetrical conditions. *Y-shaped towers* or *portal designs* used frequently for single-circuit lines fall into this category. Computer programs available today enable to analyse lattice steel towers based on a three-dimensional truss system with acceptable efforts [12.29]. For the analysis of the *three-dimensional system*, the *deformation method* is frequently used because of the favourable possibility of systematic processing. For frame or truss structures, the deformation method is identical to the *finite element method*. Thus, lattice steel towers can be analysed in principle

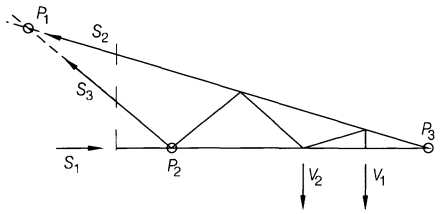

Figure 12.17: Calculation of member forces

with any finite element program. However, the manhours for the data input can be considerably high. A Y-type tower possesses approximately 400 nodes and 600 members, the geometry and the correlations of which need to be described. In addition, all loads acting on the structure need to be defined as loads acting at the nodes. The hazard of input errors is increased by such a high number of data and requires thorough checks. To enable calculation with acceptable effort, specific computer programs for lattice steel towers are required which limit the input data considerably.

12.5.4 Calculation of the member forces at a plane system

12.5.4.1 Basic procedure

To analyse lattice steel towers with acceptable effort reliably by hand, methods were developed which consider lattice steel towers as statically determined plane truss faces. The result of the analysis leads to a reliable rating of the towers in case of a symmetric design; this procedure for analysis is used, therefore, in the overhead line design today as well. The acting loads can be distributed in directions of the individual tower faces. However, additional assumptions are required in case of torsional load around the vertical tower axis.

The centroidal axes of the individual members in one face constitute the static system. The member forces can be calculated by sectioning the truss appropriately. A cut is made through the truss structure such that three members not ending to the same node are separated and the truss system is divided into two parts (Figure 12.17). For each part, the equilibrium conditions need to be complied with. Since in a plane system three equilibrium conditions are available, these are sufficient to determine the three unknown member forces. The equilibrium conditions are established most-effectively for the moments around points where two of the member forces intersect. Then, each equilibrium equation contains only one unknown member force. For example, to calculate the member force S_1 (Figure 12.17), the equilibrium of moments is established around the point P_1. The forces S_2 and S_3 intersecting in this point do not contribute to the equilibrium of moments and the unknown force S_1 can be directly computed.

12.5.4.2 Forces in the leg members

By sectioning the truss, the *leg member force* S can be obtained from the equilibrium of moments around point 1 (Figure 12.18)

$$\sum P \cdot h = 2 \cdot S \cdot e \cdot \sqrt{1 + \Delta^2/4}, \quad S = \left(\sum P \cdot h\right) \Big/ \left(2e \cdot \sqrt{1 + \Delta^2/4}\right), \quad (12.17)$$

where e is the distance of the centroidal axes and Δ the increase of latitude of the tower body per unit length.

In case of symmetrical double warrens according to Figure 12.19, it can be assumed that both leg member forces are equal but act in opposite directions. The equilibrium of moments around the crossing point 1 results again in equation (12.17).

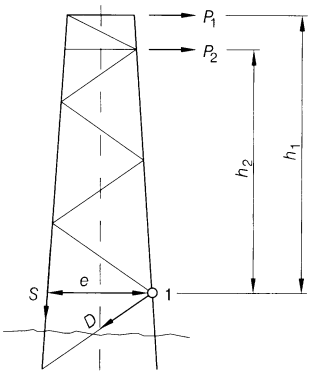

Figure 12.18: Determination of leg member force (simple warren bracings)

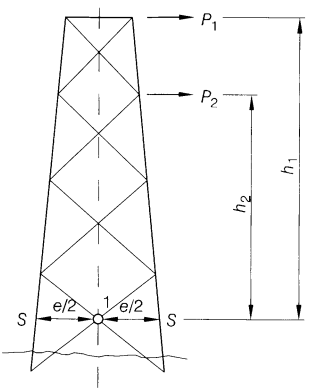

Figure 12.19: Determination of leg member force (double warrens)

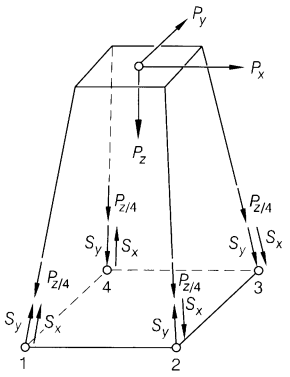

Figure 12.20: Determination of maximum leg member forces

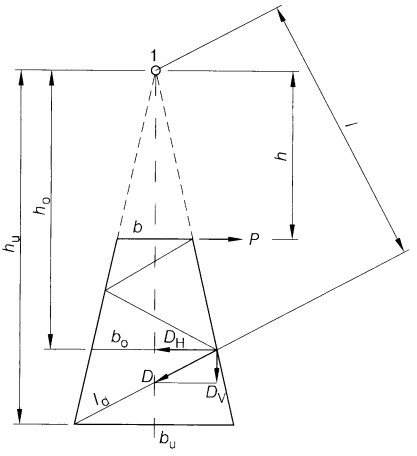

Figure 12.21: Determination of forces in bracings

For any kind of tower load, the leg member forces are constituted from the individual components P_x and P_y acting parallel to the individual tower faces. The vertical load P_z is distributed equally on the four leg members. The maximum force results, therefore, for the leg members 1 or 3 (Figure 12.20) to be

$$S = \mp S_x \mp S_y - P_z/4 \quad , \tag{12.18}$$

where the upper signs applies to compression, the lower signs to tension (Figure 12.20).

12.5.4.3 Forces in bracings, loaded by horizontal forces

The load P is distributed on two tower faces. The moment around point 1 (Figure 12.21) yields

$$D = P \cdot h/(2 \cdot l) \quad . \tag{12.19}$$

The member force obtained by this procedure can act as a tensile or a compression force since the external load may act in both directions. In case of double warrens, the member forces are half of the value obtained from (12.19).

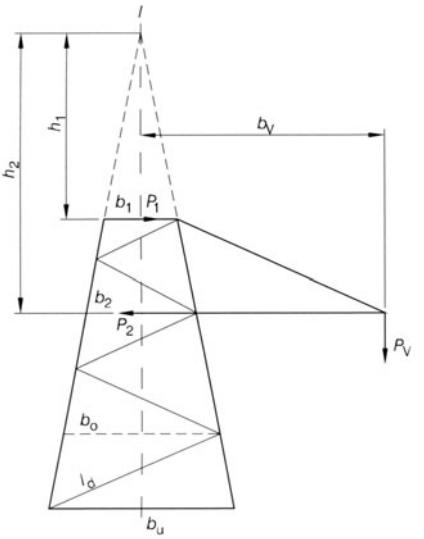

Figure 12.22: Determination of member forces in case of asymmetric vertical loads

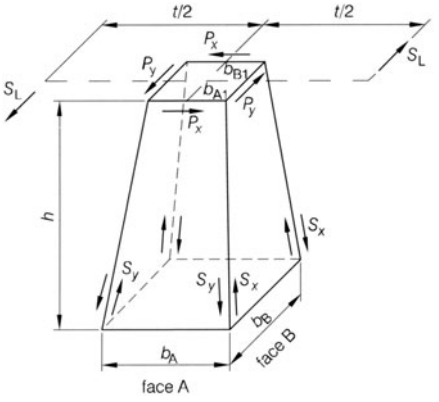

Figure 12.23: Determination of member forces in case of a torsional moment

Since the determination of the values h and l can be troublesome, the following transformations might be favourable (Figure 12.21):

$$P \cdot h = 2\,(D_{\mathrm{H}} h_{\mathrm{o}} + D_{\mathrm{V}} b_{\mathrm{o}}/2) \quad ,$$

where $D_{\mathrm{H}} = D \cdot (b_{\mathrm{o}} + b_{\mathrm{u}})/(2\,l_{\mathrm{d}})$, $D_{\mathrm{V}} = D \cdot (h_{\mathrm{u}} - h_{\mathrm{o}})/l_{\mathrm{d}}$. Since $h/b = h_{\mathrm{o}}/b_{\mathrm{o}} = h_{\mathrm{u}}/b_{\mathrm{u}}$, $h = h_{\mathrm{o}} \cdot b/b_{\mathrm{o}}$, $h_{\mathrm{u}} = h_{\mathrm{o}} \cdot b_{\mathrm{u}}/b_{\mathrm{o}}$ it is obtained $D = P \cdot b \cdot l_{\mathrm{d}}/(2\,b_{\mathrm{o}} \cdot b_{\mathrm{u}})$ and in general

$$D = l_{\mathrm{d}}/\,(2\,b_{\mathrm{o}} \cdot b_{\mathrm{u}}) \cdot \sum P \cdot b \quad . \tag{12.20}$$

12.5.4.4 Forces in bracings, loaded by asymmetrical vertical forces

The load created by asymmetrically acting vertical forces yields analogously to (12.20) (Figure 12.22)

$$D = \Delta \cdot l_{\mathrm{d}}/\,(2\,b_{\mathrm{o}} \cdot b_{\mathrm{u}}) \cdot \sum P_{\mathrm{V}} \cdot b_{\mathrm{V}} \quad , \tag{12.21}$$

where Δ designates the increase of latitude of the considered tower face per unit length. This equation applies only to bracings below the level of the acting force P_{V}.

12.5.4.5 Forces in bracings, loaded by torsional moments

The loading of the tower body by *torsional moments* is a hyperstatic problem [12.30]. However, simplifying assumptions for the distribution of the torsional moment on the individual tower faces may be assumed according to, e. g. EN 50 341-3-4, if at all crossarm levels and at changes of slope of leg members, horizontal bracings are provided and the ratio of the width of faces is not more than 1:1,5 and the shape of the tower is prismatic or corresponds to a truncated pyramid.
The load of the tower face by a torsional moment M_{T} should not result in leg member forces, i. e. the leg member forces S_x and S_y resulting from the forces P_{x} and P_{y} should be equal and act in the opposite direction (Figure 12.23), therefore:

$$P_x \cdot h/b_{\mathrm{A}} = P_y \cdot h/b_{\mathrm{B}} \quad ; \quad P_x/P_y = b_{\mathrm{A}}/b_{\mathrm{B}} = b_{\mathrm{A1}}/b_{\mathrm{B1}} \quad .$$

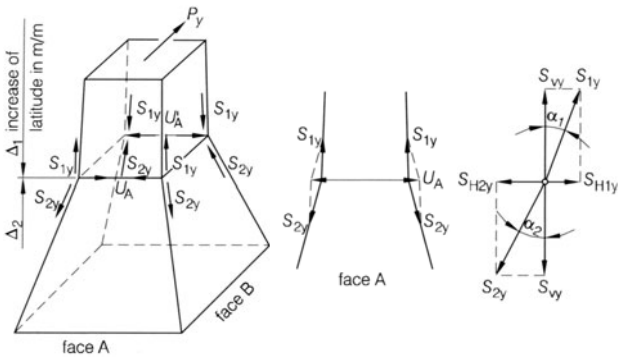

Figure 12.24: Determination of member forces at change of latitude increase of a tower body

The torsional moment is obtained from:

$$M_T = S_L \cdot t = P_x \cdot b_{B1} + P_y \cdot b_{A1} = P_y \cdot (b_{A1}/b_{B1}) \cdot b_{B1} + P_y \cdot b_{A1} = 2\,P_y \cdot b_{A1} \quad .$$

From these relations, it follows for P_x and P_y

$$P_x = M_T/(2\,b_{B1}) \quad ; \quad P_y = M_T/(2\,b_{A1}) \quad . \tag{12.22}$$

By inserting P_x as external load in (12.20), the forces in the bracings of tower face A are obtained as

$$D_A = M_T \cdot (b_{A1}/b_{B1}) \cdot l_d/\,(2\,b_{Ao} \cdot b_{Au}) \quad . \tag{12.23}$$

To bracings in the tower face B, it applies analogously

$$D_B = M_T \cdot (b_{B1}/b_{A1}) \cdot l_d/\,(2\,b_{Bo} \cdot b_{Bu}) \quad . \tag{12.24}$$

12.5.4.6 Total forces in bracings

Equations (12.20), (12.21) and (12.23), applying to forces in the bracing due to horizontal load, asymmetrical vertical load and torsional moments, can be combined to obtain the *total bracing force*

$$D_A = \left(\sum P \cdot b + \Delta \cdot \sum P_V \cdot b_V + \sum M_T \cdot \frac{b_A}{b_B}\right) \cdot \frac{l_d}{m \cdot b_{Ao} \cdot b_{Au}} \quad . \tag{12.25}$$

For a single bracing, m will be 2, in case of double warrens, m will be 4. For D_B in face B, the values b_A and b_B have to be changed and b_{Ao}, b_{Au} are replaced by b_{Bo}, b_{Bu}.

12.5.4.7 Forces in horizontal members at tower waist

Lattice steel towers are frequently designed with a wide spread lower part with respect to the foundation forces and because of aesthetical reasons (Figure 12.24). The horizontal forces produced by the change of leg member inclination have to be withstood by a horizontal bracing. When loaded by the force P_y, no force will occur in the horizontal member at the waist of face B. In face A, the horizontal force U_A will be

$$\begin{aligned} S_{H2y} &= S_{Vy} \cdot \tan\alpha_2 = S_{Vy}\Delta_{2A}/2 \approx S_y \cdot \Delta_{2A}/2 \quad , \\ S_{H1y} &= S_{Vy} \cdot \tan\alpha_1 = S_{Vy}\Delta_{1A}/2 \approx S_y \cdot \Delta_{1A}/2 \quad , \\ U_A &= S_{H2y} - S_{H1y} = S_y(\Delta_{2A} - \Delta_{1A})/2 \quad . \end{aligned} \tag{12.26}$$

Accordingly it applies for face B

$$U_B = S_x(\Delta_{2B} - \Delta_{1B})/2 \quad .$$

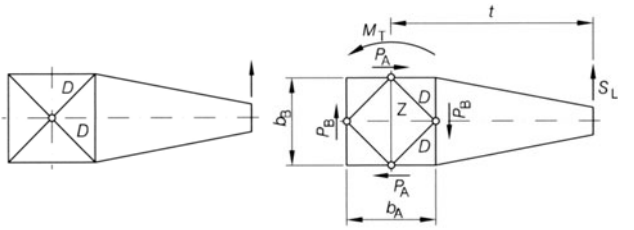

Figure 12.25: Determination of member forces in a horizontal plan bracing

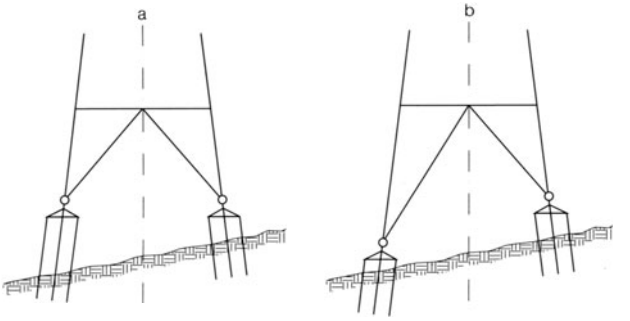

Figure 12.26: Compensation of terrain height differences in case of separate foundations: a extensions of foundation muffs; b arrangement of leg extensions

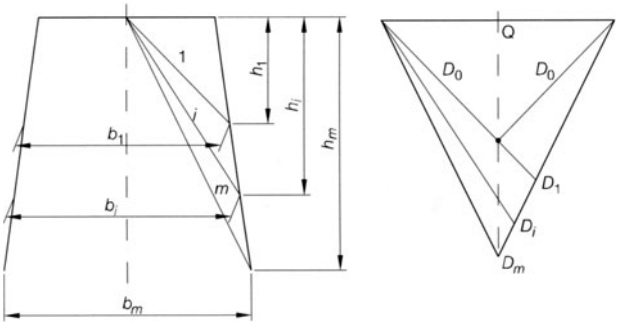

Figure 12.27: Analysis of member forces of leg extension: Q shear force, D_1 bracing member force of shortest leg extension, D_i bracing member force of leg extension i, D_m bracing member force of longest leg extension

12.5.4.8 Forces in horizontal bracings within the tower body

Horizontal bracings arranged at the level of the lower crossarm chords in the tower body distribute the torsional moments resulting from the crossarms to the four faces of a tower body (Figure 12.25). The members D transfer a portion of the torsional moment to the faces B, such that the force $P_B = S_L \cdot t/2b_A$ will act there. Therefore, it is obtained

$$D = S_L \cdot \sqrt{b_A^2 + b_B^2} \cdot (t - b_A)/(4b_A \cdot b_B) \quad . \tag{12.27}$$

The member Z is not loaded by torsional moments.

12.5.4.9 Forces in leg extensions

The foundation muff should be arranged as close as possible below the connection of the lower bracing member to the corner leg to keep low the bending of the unsupported leg members resulting from the horizontal components of the bracing forces.
The extension of foundation muffs according to Figure 12.26a requires a strong concrete reinforcement, especially in case of high differences in the ground surface. To avoid these expensive reinforcement, the connection of the lowermost bracing is arranged at the same height above ground for each individual tower leg (Figure 12.26b) resulting

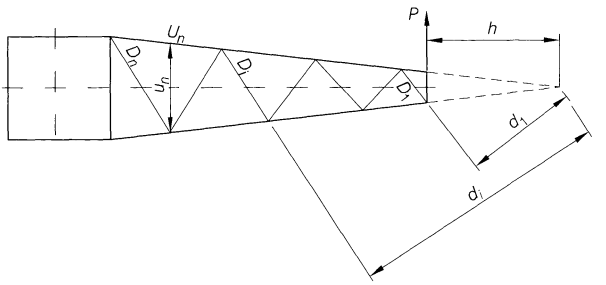

Figure 12.28: Analysis of member forces in a horizontal crossarm face

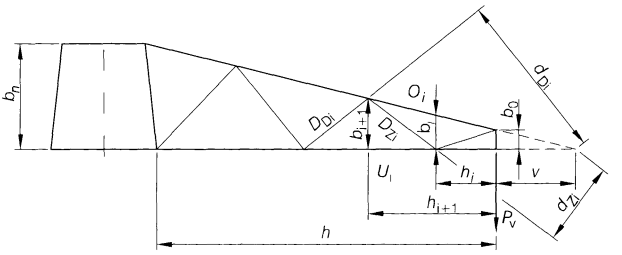

Figure 12.29: Analysis of member forces in a vertical crossarm face

in differently long leg extensions. These differing leg extensions need to be considered when calculating the lower parts of the tower body, because the member forces and the buckling length of the members change. Since the design is not symmetrical, the distribution of the loads on leg members and bracings changes as well. A precise rating requires a three-dimensional study. To limit the effort for calculation and design, *leg extensions* are provided with steps of 0,25 or 0,50 m and the design is based on the most unfavourable combination of leg extensions (Figure 12.27). As an approximation, the determination of forces can be carried out according to Figure 12.27 from which the relation

$$D_i = 2D_0 \frac{b_1}{b_i + h_i \cdot b_m/h_m} \cdot \frac{\sqrt{b_i^2 + (2\,h_i)^2}}{\sqrt{b_1^2 + (2\,h_1)^2}} \tag{12.28}$$

can be derived. The member force D_0 is taken from the basic tower analysis. The maximum forces in the leg extensions result from the combination with the longest leg extension in each case.

12.5.4.10 Forces in crossarm members

Similar to tower bodies, the *crossarms* are composed of plane truss structures; however, there is only a simple symmetry to the crossarm longitudinal axis. The member forces in the horizontal crossarm face (Figure 12.28) are computed as in case of a tower body face. Equations (12.17), (12.20) and (12.21) apply to the forces in the chords and bracings, whereby the number 2 in the denominator is dropped.
The member forces in a vertical crossarm face are computed by appropriate sectioning, whereby the leverarms are measured from a to-scale drawing of the static system or are computed (Figure 12.29).
The force in panel i of the lower chord results, considering the relations according to Figure 12.29, from

$$U_i = -P_v \cdot h_{i+1}/(2\,b_{i+1}) \quad . \tag{12.29}$$

There, P_v is the total vertical load which is distributed to two faces.

The system height b_{i+1} can be computed from

$$b_{i+1} = [(b_n - b_0) \cdot h_{i+1}]/(h + b_n \cdot \Delta/2) + b_0 \quad . \tag{12.30}$$

There, Δ means the increase of latitude of the tower body. In case of several vertical loads acting at different attachments, the lever arms h_{i+1} are accordingly applied. The force in the upper chord of panel i is obtained from

$$O_i = P_v \cdot \frac{h_i}{2\,b_i}\sqrt{1 + \left(\frac{b_n - b_0}{h + b_n \cdot \Delta/2}\right)^2} \quad . \tag{12.31}$$

The bracing members inclined towards the crossarm peak are loaded by tensile forces according to

$$D_{Zi} = P_v \cdot \frac{v}{2\,d_{Zi}} = \frac{P_v \cdot v}{2\,b_{i+1}} \cdot \frac{\sqrt{b_{i+1}^2 + (h_{i+1} - h_i)^2}}{v + h_i} \quad , \tag{12.32}$$

where $v = (h + b_n \cdot \Delta/2) \cdot b_0/(b_n - b_0)$.
The bracing members inclined towards the tower body experience compression forces according to

$$D_{Di} = -P_v \cdot \frac{v}{2\,d_{Di}} = \frac{-P_v \cdot v}{2\,b_i} \cdot \frac{\sqrt{b_i^2 + (h_{i+1} - h_i)^2}}{v + h_{i+1}} \quad . \tag{12.33}$$

To determine the forces of the lower chords, the values determined from horizontal and vertical loads have to be summed up with due consideration of their direction of action.

12.5.5 Analysis of member forces at a three-dimensional system

12.5.5.1 Basic approach of the finite element method

The *finite element method* represents an approach enabling systematic computation of any type of three-dimensional, statically determined or hyperstatic truss structures. The complete structure is divided into elements, the mechanical behaviour of which is known. The theory of member truss structures, which forms the basis for the matrix methods of the member static [12.31, 12.32], is used to analyse lattice towers. The element stiffness matrix describes the correlation between displacements of nodes and forces acting at the nodes of each individual element. By formulating the *equilibrium conditions* between internal and external forces at the nodes with due consideration of the kinematic compatibility of the *deformation of nodes* and *elements*, a system of linear equations is obtained describing the relations between the unknown deformations of the nodes, the *deformation quantities* and the forces at the nodes. This system of linear equations forms the basis of the *displacement method of analysis*. The matrix of coefficients of this system of equations is called the *total stiffness matrix*. The deformations of nodes are obtained by solving this system of linear equations. The member forces can then be determined from the displacements using the *stress-strain relation*. For analysis of towers small displacements and a linear elastic behaviour of the material are assumed. The calculation yields the deformation state of the structure as well.
As far as the programming is concerned, the displacement method of analysis is identical to the *finite element method* with respect to the system. The results are precise, the theory of linear static analysis provided. The method has been systematically developed to such an extent that all types of truss structures can be analysed. Many computer programs for framework systems are available for practical application. At the beginning of a specific calculation, data need to be prepared describing the studied framework in detail and completely. These data are:

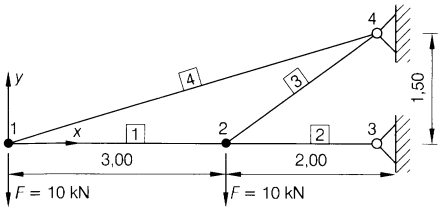

Figure 12.30: Structure in the global coordinate system

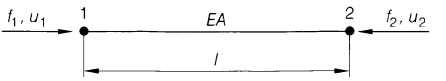

Figure 12.31: Finite truss structure element in the local coordinate system

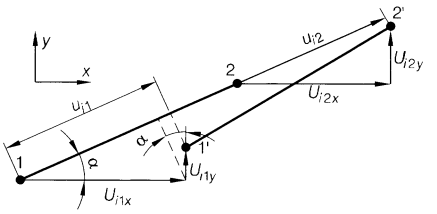

Figure 12.32: Displacement of element in the global coordinate system

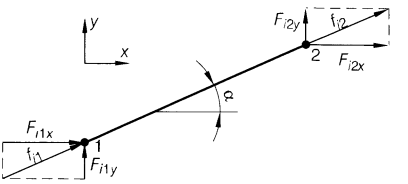

Figure 12.33: Element forces in the global coordinate system

- The number of members;
- The position of the nodes in an x-, y-, z-coordinate system;
- Information on the two nodes connected for each member;
- The external forces with the corresponding node of attack, their magnitude and direction, as well as the supporting conditions of nodes and direction of the forces.

In this context, a member is addressed as a finite element of the truss structure, where the word finite, i. e. limited, is to be understood contrarily to infinitesimally small. The method will be explained at the example of a simple plane truss structure (Figure 12.30). For this truss structure, the axial forces (member forces) are to be calculated under the action of external loads. A compression or tension loaded member with pivoted connections at its end forms one element. Its mechanical behaviour is described by the relation between the forces f_1, f_2 and the displacements u_1, u_2 at the member ends (Figure 12.31). The displacements of the element ends and the member forces in direction of the member axis are designated with small characters and are related to the local coordinate system of an element.

A global coordinate system is defined where the displacements and forces are designated by capital letters. The forces are related to the displacements in the local coordinate system as follows:

$$\begin{bmatrix} f_{i1} \\ f_{i2} \end{bmatrix} = \frac{EA}{l} \begin{bmatrix} 1 & -1 \\ -1 & 1 \end{bmatrix} \begin{bmatrix} u_{i1} \\ u_{i2} \end{bmatrix} \tag{12.34}$$

or abbreviated

$$\mathbf{f}_i = \mathbf{k}_i \mathbf{u}_i \quad . \tag{12.35}$$

The matrix $\mathbf{k}_i$ is the *element stiffness matrix* of the element i in the *local coordinate system*, E is the modulus of elasticity and A the cross-sectional area. Matrices are designated with bolt-typed letters.

The local element coordinates possess differing positions in the global coordinate system. The position of an element in the overall structure is obtained by a transformation

of the equation (12.35) into the *global coordinate system.* This procedure yields the element stiffness matrix related to the global coordinate system. From Figure 12.32 it is concluded:

$$u_{i1} = U_{i1x} \cdot \cos\alpha + U_{i1y} \cdot \sin\alpha \tag{12.36}$$

$$u_{i2} = U_{i2x} \cdot \cos\alpha + U_{i2y} \cdot \sin\alpha \quad . \tag{12.37}$$

The indices 1 and 2 are related to the two ends of the member i.
Equations (12.36) and (12.37) can be represented by means of matrices:

$$\mathbf{u}_i = \mathbf{T}_i \mathbf{U}_i \quad , \tag{12.38}$$

where $\mathbf{T}_i = \begin{bmatrix} \cos\alpha & \sin\alpha & 0 & 0 \\ 0 & 0 & \cos\alpha & \sin\alpha \end{bmatrix}$.

The matrix $\mathbf{T}_i$ transfers displacements from the global coordinate system into the local one. As per definition, a truss member carries forces only in its longitudinal direction. The forces f_{i1} and f_{i2} can be related to the global coordinates x and y (Figure 12.33):

$$F_{i1x} = f_{i1} \cdot \cos\alpha \quad ; \quad F_{i1y} = f_{i1} \cdot \sin\alpha \tag{12.39}$$

$$F_{i2x} = f_{i2} \cdot \cos\alpha \quad ; \quad F_{i2y} = f_{i2} \cdot \sin\alpha \quad . \tag{12.40}$$

These equations can be written in the matrix format:

$$\mathbf{F}_i = \mathbf{T}_i^{\mathrm{T}} \mathbf{f}_i \quad . \tag{12.41}$$

The *transformation matrix* $\mathbf{T}_i^{\mathrm{T}}$ represents the transposed of the matrix $\mathbf{T}_i$ as defined by equation (12.38). If (12.35) is inserted into (12.41), it is obtained

$$\mathbf{F}_i = \mathbf{T}_i^{\mathrm{T}} \mathbf{k}_i \mathbf{u}_i \quad . \tag{12.42}$$

With (12.38) it results:

$$\mathbf{F}_i = \mathbf{T}_i^{\mathrm{T}} \mathbf{k}_i \mathbf{T}_i \mathbf{U}_i \quad . \tag{12.43}$$

This equation is simplified using the abbreviation

$$\mathbf{K}_i = \mathbf{T}_i^{\mathrm{T}} \mathbf{k}_i \mathbf{T}_i \tag{12.44}$$

to be

$$\mathbf{F}_i = \mathbf{K}_i \mathbf{U}_i \tag{12.45}$$

and establishes the relation between the forces and displacements in the global coordinate system. The matrix $\mathbf{K}_i$ is the *element stiffness matrix* in the global coordinate system. The relations are equally structured for each element within the truss; however, the elements of the matrix $\mathbf{K}_i$ are dependent on the mechanical and geometric characteristics of each element.
In case of the example described by Figure 12.30, four elements form the complete structure which is described by equation (12.45). The position of each element is determined by its angle α and by the nodes connected by the element. The mechanical characteristics are described by the elongation stiffness EA/l. The relations between forces and displacements for the overall structure can be expressed by the format of (12.45); the number of node forces and displacements is increased then. The matrices are connected by a matrix equation with the format

$$\mathbf{F} = \mathbf{K}\mathbf{U} \quad . \tag{12.46}$$

$\mathbf{U}$ is the node displacement vector of the overall structure in the global coordinate system. The matrix $\mathbf{K}$ is the *total stiffness matrix* of the structure. It is obtained

by applying the direct stiffness method [12.32, 12.33]. For this purpose, the stiffness matrices of the individual elements i are added:

$$\mathbf{K} = \sum_i \mathbf{K}_i \quad . \tag{12.47}$$

Then, each element matrix $\mathbf{K}_i$ is transformed into matrix $\mathbf{K}^{(i)}$ which has got the same order as the stiffness matrix $\mathbf{K}$. It contains values differing from zero only at such positions which correspond to a degree of freedom of the relevant element. Thus, it applies for the element 3 of the example

$$\mathbf{K}^{(3)} = \begin{array}{c} \begin{matrix} U_{1x} & U_{1y} & U_{2x} & U_{2y} & U_{3x} & U_{3y} & U_{4x} & U_{4y} \leftarrow \text{ degrees of freedom} \end{matrix} \\ \begin{bmatrix} 0 & 0 & 0 & 0 & 0 & 0 & 0 & 0 \\ 0 & 0 & 0 & 0 & 0 & 0 & 0 & 0 \\ 0 & 0 & K_3^{11} & K_3^{12} & 0 & 0 & K_3^{13} & K_3^{14} \\ 0 & 0 & K_3^{21} & K_3^{22} & 0 & 0 & K_3^{23} & K_3^{24} \\ 0 & 0 & 0 & 0 & 0 & 0 & 0 & 0 \\ 0 & 0 & 0 & 0 & 0 & 0 & 0 & 0 \\ 0 & 0 & K_3^{31} & K_3^{32} & 0 & 0 & K_3^{33} & K_3^{34} \\ 0 & 0 & K_3^{41} & K_3^{42} & 0 & 0 & K_3^{43} & K_3^{44} \end{bmatrix} \end{array} \begin{matrix} U_{1x} \\ U_{1y} \\ U_{2x} \\ U_{2y} \\ U_{3x} \\ U_{3y} \\ U_{4x} \\ U_{4y} \end{matrix} \quad .$$

Applying the above mentioned procedure on the overall structure, the stiffness matrix is obtained:

$$\mathbf{K} = \begin{array}{c} \begin{matrix} U_{1x} & U_{1y} & U_{2x} & U_{2y} & U_{3x} & U_{3y} & U_{4x} & U_{4y} \end{matrix} \\ \begin{bmatrix} \overline{K}_1^{11} & \overline{K}_1^{12} & K_1^{13} & K_1^{14} & 0 & 0 & K_4^{13} & K_4^{14} \\ \overline{K}_1^{21} & \overline{K}_1^{22} & K_1^{23} & K_1^{24} & 0 & 0 & K_4^{23} & K_4^{24} \\ K_1^{31} & K_1^{32} & \overline{K}_1^{33} & \overline{K}_1^{34} & K_2^{13} & K_1^{14} & K_3^{13} & K_3^{14} \\ K_1^{41} & K_1^{42} & \overline{K}_1^{43} & \overline{K}_1^{44} & K_2^{23} & K_1^{14} & K_3^{23} & K_3^{24} \\ 0 & 0 & K_2^{31} & K_2^{32} & K_2^{33} & K_1^{14} & 0 & 0 \\ 0 & 0 & K_2^{41} & K_2^{42} & K_2^{43} & K_1^{14} & 0 & 0 \\ K_4^{31} & K_4^{32} & K_3^{31} & K_3^{32} & 0 & 0 & \overline{K}_3^{33} & \overline{K}_3^{34} \\ K_4^{41} & K_4^{42} & K_3^{41} & K_3^{42} & 0 & 0 & \overline{K}_3^{43} & \overline{K}_3^{44} \end{bmatrix} \end{array} \begin{matrix} U_{1x} \\ U_{1y} \\ U_{2x} \\ U_{2y} \\ U_{3x} \\ U_{3y} \\ U_{4x} \\ U_{4y} \end{matrix} \quad ,$$

where $\overline{K}_1^{11} = K_1^{11} + K_4^{11}$; $\overline{K}_1^{21} = K_1^{21} + K_4^{21}$; $\overline{K}_1^{12} = K_1^{12} + K_4^{12}$; $\overline{K}_1^{22} = K_1^{22} + K_4^{22}$; $\overline{K}_1^{33} = K_1^{33} + K_2^{11} + K_3^{11}$; $\overline{K}_1^{43} = K_1^{43} + K_2^{21} + K_3^{21}$; $\overline{K}_1^{34} = K_1^{34} + K_2^{12} + K_3^{12}$; $\overline{K}_1^{44} = K_1^{44} + K_2^{22} + K_3^{22}$; $\overline{K}_3^{33} = K_3^{33} + K_4^{33}$; $\overline{K}_3^{34} = K_3^{34} + K_4^{34}$; $\overline{K}_3^{43} = K_3^{43} + K_4^{44}$; $\overline{K}_3^{44} = K_3^{44} + K_4^{44}$.

The *node forces* within the column matrix $\mathbf{F}$ of equation (12.46) can be separated into two groups. The unknown forces form the first group and the acting external forces the other one. Similarly, the *node displacements* are divided into two groups. One consists of the unknown node displacements and the other of the displacements given by the support conditions. For a given displacement, the corresponding node force will be unknown; in case of a known force, the corresponding displacement will be unknown. From Figure 12.30 it is obtained for the matrices $\mathbf{F}$ and $\mathbf{U}$

$$\mathbf{F} = \begin{bmatrix} 0 \\ -F \\ 0 \\ -F \\ \hline F_{3x} \\ F_{3y} \\ F_{4x} \\ F_{4y} \end{bmatrix} \quad ; \quad \mathbf{U} = \begin{bmatrix} U_{1x} \\ U_{1y} \\ U_{2x} \\ U_{2y} \\ \hline 0 \\ 0 \\ 0 \\ 0 \end{bmatrix} \quad .$$

There, the node forces F_{3x}, F_{3y}, F_{4x}, F_{4y} are the unknown *support reactions* and the displacements U_{1x}, U_{1y}, U_{2x}, U_{2y} the unknown node displacements. All other quantities are known. Known displacements need not to be zero in any case. From a given displacement of a support member, forces can result in hyperstatic systems, e. g. by foundation settlements.
The lines and columns of the equation system $\mathbf{F} = \mathbf{KU}$ are rearranged such that the format

$$\left[\begin{array}{c} \mathbf{F}_a \\ \hline \mathbf{F}_b \end{array}\right] = \left[\begin{array}{c|c} \mathbf{K}_{aa} & \mathbf{K}_{ab} \\ \hline \mathbf{K}_{ba} & \mathbf{K}_{bb} \end{array}\right] \left[\begin{array}{c} \mathbf{U}_a \\ \hline \mathbf{U}_b \end{array}\right] \tag{12.48}$$

is obtained, where $\mathbf{F}_a$ is the vector of the known forces and $\mathbf{F}_b$ the vector of the unknown forces. The matrix $\mathbf{K}$ has a symmetric structure which is composed from the sub-matrices $\mathbf{K}_{aa}$, $\mathbf{K}_{ab}$ and $\mathbf{K}_{bb}$ in the manner described. There, $\mathbf{K}_{ba} = \mathbf{K}_{ab}^{T}$ because of the symmetry. The equations can be solved with respect to the unknown vectors. From the first line of the matrix, it is obtained

$$\mathbf{F}_a = \mathbf{K}_{aa}\mathbf{U}_a + \mathbf{K}_{ab}\mathbf{U}_b \quad . \tag{12.49}$$

The solution with respect to the unknown *node displacements* results in

$$\mathbf{U}_a = \mathbf{K}_{aa}^{-1}\left(\mathbf{F}_a - \mathbf{K}_{ab}\mathbf{U}_b\right) \quad . \tag{12.50}$$

In case of rigid supports ($\mathbf{U}_b = 0$), it is obtained:

$$\mathbf{U}_a = \mathbf{K}_{aa}^{-1}\mathbf{F}_a \quad . \tag{12.51}$$

A corresponding system of linear equations may contain several hundreds of unknown variables in case of large static systems with many elements and nodes such as a lattice tower. The solution will then only be possible with adequate computer programs.
After calculating the displacements $\mathbf{U}_a$ from equation (12.51), the unknown force quantities $\mathbf{F}_b$ can be determined from the second line of the matrix in (12.48)

$$\mathbf{F}_b = \mathbf{K}_{ab}^{T}\mathbf{U}_a + \mathbf{K}_{bb}\mathbf{U}_b \quad . \tag{12.52}$$

The element stiffness matrices $\mathbf{k}_i$ are multiplied by the element displacements to compute the member forces:

$$\mathbf{f}_i = \mathbf{k}_i\mathbf{u}_i \quad . \tag{12.53}$$

The local displacements $\mathbf{u}_i$ can then be expressed according to equation (12.38) by the global vector $\mathbf{U}_i$ and the member force for the element i is obtained from

$$\mathbf{f}_i = \mathbf{k}_i\mathbf{T}_i\mathbf{U}_i \quad .$$

The same sequence of calculations applies to all tasks to be achieved:

(a) Establishing geometry, materials and section properties, numbering nodes and members;
(b) Establishing the element stiffness matrices;
(c) Transformation to the global coordinate system;
(d) Forming the stiffness matrix of the overall system;
(e) Insertion of load and supporting conditions;
(f) Solving the system of equations or (12.50) or (12.51);
(g) Calculation of the member forces using equation (12.53);
(h) Calculation of the support reactions using equation (12.52).

Example: The steps of calculation will be demonstrated by means of a simple example (Figure 12.30).

Table of nodes:

Nodes	x	y
1	0,00	0,00
2	3,00	0,00
3	5,00	0,00
4	5,00	1,50

Relations between nodes and elements:

Element	Nodes l	Nodes r	l_i [m]	$\cos\alpha$	$\sin\alpha$	Cross section A_i (cm^2)
1	1	2	3,00	1,0000	0,0000	9,40
2	2	3	2,00	1,0000	0,0000	9,40
3	2	4	2,50	0,8000	0,6000	4,08
4	1	4	5,22	0,9578	0,2873	3,08

Material: steel $E = 210\,000\ \mathrm{N/mm^2}$

The vector of the external loads is obtained by the external forces acting at nodes 1 and 2

$$\mathbf{F}_a = \begin{bmatrix} 0 \\ -10\ \mathrm{kN} \\ 0 \\ -10\ \mathrm{kN} \end{bmatrix} .$$

Furthermore, the displacements of nodes at the supports are known. Rigid supports are assumed in this case.

$$\mathbf{U}_b = \begin{bmatrix} 0 \\ 0 \\ 0 \\ 0 \end{bmatrix} .$$

The element stiffness matrices in the global system are computed according to equation (12.44). For this purpose the element stiffness matrices in the local system and the transformation matrices are needed. At first, the element stiffness matrices are established:

$$\mathbf{k}_i = \frac{E \cdot A_i}{l_i} \begin{bmatrix} 1 & -1 \\ -1 & 1 \end{bmatrix} ;$$

$$\mathbf{k}_1 = \begin{bmatrix} 658{,}00 & -658{,}00 \\ -658{,}00 & 658{,}00 \end{bmatrix} \cdot \frac{\mathrm{kN}}{\mathrm{cm}} ; \qquad \mathbf{k}_2 = \begin{bmatrix} 987{,}00 & -987{,}00 \\ -987{,}00 & 987{,}00 \end{bmatrix} \cdot \frac{\mathrm{kN}}{\mathrm{cm}} ;$$

$$\mathbf{k}_3 = \begin{bmatrix} 342{,}72 & -342{,}72 \\ -342{,}72 & 342{,}72 \end{bmatrix} \cdot \frac{\mathrm{kN}}{\mathrm{cm}} ; \qquad \mathbf{k}_4 = \begin{bmatrix} 123{,}90 & -123{,}90 \\ -123{,}90 & 123{,}90 \end{bmatrix} \cdot \frac{\mathrm{kN}}{\mathrm{cm}} .$$

To the transformation matrices it applies:

$$\mathbf{T}_i = \begin{bmatrix} \cos\alpha_i & \sin\alpha_i & 0 & 0 \\ 0 & & \cos\alpha_i & \sin\alpha_i \end{bmatrix} \quad \text{and}$$

$$\mathbf{T}_1 = \begin{bmatrix} 1{,}00 & 0{,}00 & 0{,}00 & 0{,}00 \\ 0{,}00 & 0{,}00 & 1{,}00 & 0{,}00 \end{bmatrix} ; \quad \mathbf{T}_2 = \begin{bmatrix} 1{,}00 & 0{,}00 & 0{,}00 & 0{,}00 \\ 0{,}00 & 0{,}00 & 1{,}00 & 0{,}00 \end{bmatrix} ;$$

$$\mathbf{T}_3 = \begin{bmatrix} 0{,}80 & 0{,}60 & 0{,}00 & 0{,}00 \\ 0{,}00 & 0{,}00 & 0{,}80 & 0{,}60 \end{bmatrix} ; \quad \mathbf{T}_4 = \begin{bmatrix} 0{,}96 & 0{,}29 & 0{,}00 & 0{,}00 \\ 0{,}00 & 0{,}00 & 0{,}96 & 0{,}29 \end{bmatrix} .$$

On this basis, the stiffness matrices are obtained according to equation (12.44)

$$\mathbf{K}_i = \mathbf{T}_i^{\mathrm{T}} \mathbf{k}_i \mathbf{T}_i$$

$$\mathbf{K}_1 = \begin{bmatrix} 658{,}0 & 0{,}0 & -658{,}0 & 0{,}0 \\ 0{,}0 & 0{,}0 & 0{,}0 & 0{,}0 \\ -658{,}0 & 0{,}0 & 658{,}0 & 0{,}0 \\ 0{,}0 & 0{,}0 & 0{,}0 & 0{,}0 \end{bmatrix} \cdot \frac{\mathrm{kN}}{\mathrm{cm}} ;$$

$$\mathbf{K}_2 = \begin{bmatrix} 987{,}0 & 0{,}0 & -987{,}0 & 0{,}0 \\ 0{,}0 & 0{,}0 & 0{,}0 & 0{,}0 \\ -987{,}0 & 0{,}0 & 987{,}0 & 0{,}0 \\ 0{,}0 & 0{,}0 & 0{,}0 & 0{,}0 \end{bmatrix} \cdot \frac{\mathrm{kN}}{\mathrm{cm}} ;$$

$$\mathbf{K}_3 = \begin{bmatrix} 219{,}3 & 164{,}5 & -219{,}3 & -164{,}5 \\ 164{,}5 & 123{,}4 & -164{,}5 & -123{,}4 \\ -219{,}3 & -164{,}5 & 219{,}3 & 164{,}5 \\ -164{,}5 & -123{,}4 & 164{,}5 & 123{,}4 \end{bmatrix} \cdot \frac{\text{kN}}{\text{cm}};$$

$$\mathbf{K}_4 = \begin{bmatrix} 113{,}7 & 34{,}1 & -113{,}7 & -34{,}1 \\ 34{,}1 & 10{,}2 & -34{,}1 & -10{,}2 \\ -113{,}7 & -34{,}1 & 113{,}7 & 34{,}1 \\ -34{,}1 & -10{,}2 & 34{,}1 & 10{,}2 \end{bmatrix} \cdot \frac{\text{kN}}{\text{cm}}.$$

The system has eight degrees of freedom. The total stiffness matrix **K** is an 8 by 8 matrix. It is established according to the direct stiffness method from the element matrices $\mathbf{K}_i^e$. The node–element relation can be used for this purpose. On this basis, a correlation matrix **C** will be established for each element. The elements of the matrix **C** are 1 if the deformation at the member end coincides with the deformation of the node and will be zero otherwise.

$$\mathbf{C}_1 = \begin{bmatrix} 1 & 0 & 0 & 0 & 0 & 0 & 0 & 0 \\ 0 & 1 & 0 & 0 & 0 & 0 & 0 & 0 \\ 0 & 0 & 1 & 0 & 0 & 0 & 0 & 0 \\ 0 & 0 & 0 & 1 & 0 & 0 & 0 & 0 \end{bmatrix}; \quad \mathbf{C}_2 = \begin{bmatrix} 0 & 0 & 1 & 0 & 0 & 0 & 0 & 0 \\ 0 & 0 & 0 & 1 & 0 & 0 & 0 & 0 \\ 0 & 0 & 0 & 0 & 1 & 0 & 0 & 0 \\ 0 & 0 & 0 & 0 & 0 & 1 & 0 & 0 \end{bmatrix};$$

$$\mathbf{C}_3 = \begin{bmatrix} 0 & 0 & 1 & 0 & 0 & 0 & 0 & 0 \\ 0 & 0 & 0 & 1 & 0 & 0 & 0 & 0 \\ 0 & 0 & 0 & 0 & 0 & 0 & 1 & 0 \\ 0 & 0 & 0 & 0 & 0 & 0 & 0 & 1 \end{bmatrix}; \quad \mathbf{C}_4 = \begin{bmatrix} 1 & 0 & 0 & 0 & 0 & 0 & 0 & 0 \\ 0 & 1 & 0 & 0 & 0 & 0 & 0 & 0 \\ 0 & 0 & 0 & 0 & 0 & 0 & 1 & 0 \\ 0 & 0 & 0 & 0 & 0 & 0 & 0 & 1 \end{bmatrix}.$$

With $\mathbf{K}_i^e = \mathbf{C}_i^T \mathbf{K}_i \mathbf{C}_i$ it is obtained:

$$\mathbf{K}_1^e = \begin{bmatrix} 658{,}0 & 0{,}00 & -658{,}0 & 0{,}00 & 0{,}00 & 0{,}00 & 0{,}00 & 0{,}00 \\ 0{,}00 & 0{,}00 & 0{,}00 & 0{,}00 & 0{,}00 & 0{,}00 & 0{,}00 & 0{,}00 \\ -658{,}0 & 0{,}00 & 658{,}0 & 0{,}00 & 0{,}00 & 0{,}00 & 0{,}00 & 0{,}00 \\ 0{,}00 & 0{,}00 & 0{,}00 & 0{,}00 & 0{,}00 & 0{,}00 & 0{,}00 & 0{,}00 \\ 0{,}00 & 0{,}00 & 0{,}00 & 0{,}00 & 0{,}00 & 0{,}00 & 0{,}00 & 0{,}00 \\ 0{,}00 & 0{,}00 & 0{,}00 & 0{,}00 & 0{,}00 & 0{,}00 & 0{,}00 & 0{,}00 \\ 0{,}00 & 0{,}00 & 0{,}00 & 0{,}00 & 0{,}00 & 0{,}00 & 0{,}00 & 0{,}00 \\ 0{,}00 & 0{,}00 & 0{,}00 & 0{,}00 & 0{,}00 & 0{,}00 & 0{,}00 & 0{,}00 \end{bmatrix} \cdot \frac{\text{kN}}{\text{cm}};$$

$$\mathbf{K}_2^e = \begin{bmatrix} 0{,}00 & 0{,}00 & 0{,}00 & 0{,}00 & 0{,}00 & 0{,}00 & 0{,}00 & 0{,}00 \\ 0{,}00 & 0{,}00 & 0{,}00 & 0{,}00 & 0{,}00 & 0{,}00 & 0{,}00 & 0{,}00 \\ 0{,}00 & 0{,}00 & 987{,}0 & 0{,}00 & -987{,}0 & 0{,}00 & 0{,}00 & 0{,}00 \\ 0{,}00 & 0{,}00 & 0{,}00 & 0{,}00 & 0{,}00 & 0{,}00 & 0{,}00 & 0{,}00 \\ 0{,}00 & 0{,}00 & -987{,}0 & 0{,}00 & 987{,}0 & 0{,}00 & 0{,}00 & 0{,}00 \\ 0{,}00 & 0{,}00 & 0{,}00 & 0{,}00 & 0{,}00 & 0{,}00 & 0{,}00 & 0{,}00 \\ 0{,}00 & 0{,}00 & 0{,}00 & 0{,}00 & 0{,}00 & 0{,}00 & 0{,}00 & 0{,}00 \\ 0{,}00 & 0{,}00 & 0{,}00 & 0{,}00 & 0{,}00 & 0{,}00 & 0{,}00 & 0{,}00 \end{bmatrix} \cdot \frac{\text{kN}}{\text{cm}};$$

$$\mathbf{K}_3^e = \begin{bmatrix} 0{,}00 & 0{,}00 & 0{,}00 & 0{,}00 & 0{,}00 & 0{,}00 & 0{,}00 & 0{,}00 \\ 0{,}00 & 0{,}00 & 0{,}00 & 0{,}00 & 0{,}00 & 0{,}00 & 0{,}00 & 0{,}00 \\ 0{,}00 & 0{,}00 & 219{,}3 & 164{,}5 & 0{,}00 & 0{,}00 & -219{,}3 & -164{,}5 \\ 0{,}00 & 0{,}00 & 164{,}5 & 123{,}4 & 0{,}00 & 0{,}00 & -164{,}5 & -123{,}4 \\ 0{,}00 & 0{,}00 & 0{,}00 & 0{,}00 & 0{,}00 & 0{,}00 & 0{,}00 & 0{,}00 \\ 0{,}00 & 0{,}00 & 0{,}00 & 0{,}00 & 0{,}00 & 0{,}00 & 0{,}00 & 0{,}00 \\ 0{,}00 & 0{,}00 & -219{,}3 & -164{,}5 & 0{,}00 & 0{,}00 & 219{,}3 & 164{,}5 \\ 0{,}00 & 0{,}00 & -164{,}5 & -123{,}4 & 0{,}00 & 0{,}00 & 164{,}5 & 123{,}4 \end{bmatrix} \frac{\text{kN}}{\text{cm}};$$

$$\mathbf{K}_4^e = \begin{bmatrix} 113{,}7 & 34{,}1 & 0{,}00 & 0{,}00 & 0{,}00 & 0{,}00 & -113{,}7 & -34{,}1 \\ 34{,}1 & 10{,}2 & 0{,}00 & 0{,}00 & 0{,}00 & 0{,}00 & -34{,}1 & -10{,}2 \\ 0{,}00 & 0{,}00 & 0{,}00 & 0{,}00 & 0{,}00 & 0{,}00 & 0{,}00 & 0{,}00 \\ 0{,}00 & 0{,}00 & 0{,}00 & 0{,}00 & 0{,}00 & 0{,}00 & 0{,}00 & 0{,}00 \\ 0{,}00 & 0{,}00 & 0{,}00 & 0{,}00 & 0{,}00 & 0{,}00 & 0{,}00 & 0{,}00 \\ 0{,}00 & 0{,}00 & 0{,}00 & 0{,}00 & 0{,}00 & 0{,}00 & 0{,}00 & 0{,}00 \\ -113{,}7 & -34{,}1 & 0{,}00 & 0{,}00 & 0{,}00 & 0{,}00 & 113{,}7 & 34{,}1 \\ -34{,}1 & -10{,}2 & 0{,}00 & 0{,}00 & 0{,}00 & 0{,}00 & 34{,}1 & 10{,}2 \end{bmatrix} \cdot \frac{\text{kN}}{\text{cm}}.$$

The total stiffness matrix $\mathbf{K}$ is obtained from equation (12.47).

$$\mathbf{K} = \sum_i \mathbf{K}_i^e$$

$$\mathbf{K} = \begin{bmatrix} 771{,}7 & 34{,}1 & -658{,}0 & 0{,}0 & 0{,}0 & 0{,}0 & -113{,}7 & -34{,}1 \\ 34{,}1 & 10{,}2 & 0{,}0 & 0{,}0 & 0{,}0 & 0{,}0 & -34{,}1 & -10{,}2 \\ -658{,}0 & 0{,}0 & 1864{,}3 & 164{,}5 & -987{,}0 & 0{,}0 & -219{,}3 & -164{,}5 \\ 0{,}0 & 0{,}0 & 164{,}5 & 123{,}4 & 0{,}0 & 0{,}0 & -164{,}5 & -123{,}4 \\ 0{,}0 & 0{,}0 & -987{,}0 & 0{,}0 & 987{,}0 & 0{,}0 & 0{,}0 & 0{,}0 \\ 0{,}0 & 0{,}0 & 0{,}0 & 0{,}0 & 0{,}0 & 0{,}0 & 0{,}0 & 0{,}0 \\ -113{,}67 & -34{,}1 & -219{,}3 & -164{,}5 & 0{,}0 & 0{,}0 & 333{,}0 & 198{,}6 \\ -34{,}10 & -10{,}2 & -164{,}5 & -123{,}4 & 0{,}0 & 0{,}0 & 198{,}6 & 133{,}6 \end{bmatrix} \cdot \frac{\text{kN}}{\text{cm}} .$$

The degrees of freedom 1 to 4 establish the unknown node displacements. From the total stiffness matrix, the sub-matrices $\mathbf{K}_{aa}$ and $\mathbf{K}_{ab}$ are obtained.

$$\mathbf{K}_{aa} = \begin{bmatrix} 771{,}7 & 34{,}1 & -658{,}0 & 0{,}0 \\ 34{,}1 & 10{,}2 & 0{,}0 & 0{,}0 \\ -658{,}0 & 0{,}0 & 1864{,}3 & 164{,}5 \\ 0{,}0 & 0{,}0 & 164{,}5 & 123{,}4 \end{bmatrix} \cdot \frac{\text{kN}}{\text{cm}} ;$$

$$\mathbf{K}_{ab} = \begin{bmatrix} 0{,}0 & 0{,}0 & -113{,}7 & -34{,}1 \\ 0{,}0 & 0{,}0 & -34{,}1 & -10{,}2 \\ -987{,}0 & 0{,}0 & -219{,}3 & -164{,}5 \\ 0{,}0 & 0{,}0 & -164{,}5 & -123{,}4 \end{bmatrix} \cdot \frac{\text{kN}}{\text{cm}} .$$

From equation (12.51), the node deformations $\mathbf{U}_a$ are obtained and from equation (12.52) the unknown support reaction forces $\mathbf{F}_b$:

$$\mathbf{U}_a = \mathbf{K}_{aa}^{-1}\mathbf{F}_a = \begin{bmatrix} 0{,}98 \\ -13{,}04 \\ 0{,}47 \\ -1{,}44 \end{bmatrix} \cdot \text{mm} ; \qquad \mathbf{F}_b = \mathbf{K}_{ab}^{T}\mathbf{U}_a = \begin{bmatrix} -46{,}7 \\ 0{,}0 \\ 46{,}7 \\ 20{,}0 \end{bmatrix} \cdot \text{kN} .$$

To calculate the member forces from (12.53), the deformation vector is needed. The total deformation vector will be:

$$\mathbf{U}_g = \begin{bmatrix} 0{,}98 \\ -13{,}04 \\ 0{,}47 \\ -1{,}44 \\ 0{,}00 \\ 0{,}00 \\ 0{,}00 \\ 0{,}00 \end{bmatrix} \cdot \text{mm} .$$

For the element displacements in the global system, it applies:

$$\mathbf{U}_1 = \begin{bmatrix} U_1 \\ U_2 \\ U_3 \\ U_4 \end{bmatrix} = \begin{bmatrix} 0{,}98 \\ -13{,}04 \\ 0{,}47 \\ -1{,}44 \end{bmatrix} \cdot \text{mm} ; \qquad \mathbf{U}_2 = \begin{bmatrix} U_3 \\ U_4 \\ 0 \\ 0 \end{bmatrix} = \begin{bmatrix} 0{,}47 \\ -1{,}44 \\ 0{,}00 \\ 0{,}00 \end{bmatrix} \cdot \text{mm} ;$$

$$\mathbf{U}_3 = \begin{bmatrix} U_3 \\ U_4 \\ 0 \\ 0 \end{bmatrix} = \begin{bmatrix} 0{,}47 \\ -1{,}44 \\ 0{,}00 \\ 0{,}00 \end{bmatrix} \cdot \text{mm} ; \qquad \mathbf{U}_4 = \begin{bmatrix} U_1 \\ U_2 \\ 0 \\ 0 \end{bmatrix} = \begin{bmatrix} 0{,}98 \\ -13{,}04 \\ 0{,}00 \\ 0{,}00 \end{bmatrix} \cdot \text{mm} .$$

The wanted axial member forces are obtained from equation (12.53) using the above quantities

$\mathbf{f}_i = \mathbf{K}_i\mathbf{T}_i\mathbf{U}_i$ and

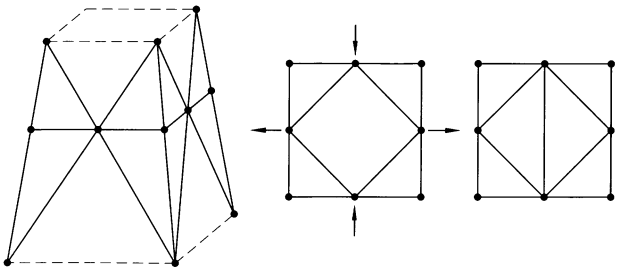

Figure 12.34: Bracings with pivots at connection with members of tower faces

$$\mathbf{f}_1 = \begin{bmatrix} 33{,}33 \\ -33{,}33 \end{bmatrix} \cdot \mathrm{kN}; \quad \mathbf{f}_2 = \begin{bmatrix} 46{,}67 \\ -46{,}67 \end{bmatrix} \cdot \mathrm{kN};$$

$$\mathbf{f}_3 = \begin{bmatrix} -16{,}67 \\ 16{,}67 \end{bmatrix} \cdot \mathrm{kN}; \quad \mathbf{f}_4 = \begin{bmatrix} -34{,}80 \\ 34{,}80 \end{bmatrix} \cdot \mathrm{kN}.$$

The example demonstrates that the numerical effort is high even in case of the simple structure. It does not make much sense to calculate such a structure using the finite element method since conventional approaches lead much faster to the target. The example, however, explains the procedure.

The size of the *stiffness matrix* $\mathbf{K}_{aa}$ in equation (12.52) has a prevalent impact on the calculation effort. The stiffness matrices are symmetrical, positive definite and assume a band-type structure in case of large systems. The inversion of the matrix $\mathbf{K}_{aa}$ is combined with much effort if it is of large order. In general, the inverse of band matrices will be completely occupied requiring many calculation operations for their inversion. Then, it might be more effective to use the *elimination procedure* according to Gauss or the Cholesky method for solving the equation $\mathbf{K}_{aa}\mathbf{U}_a = \mathbf{F}_a$. The Cholesky method is in particular suited for solving equation systems with several load vectors (several load cases). Details can be followed up in the references [12.32, 12.33].

12.5.5.2 Application to three-dimensional truss structure systems

The finite element method is an outstanding tool for analysing large truss systems such as lattice steel towers. While applications of the *three-dimensional system* represented exceptions in the past and were limited to special cases [12.34], application of the finite element method is standard practice now. This is due to the possibilities of data processing available nowadays and to the requirements of the European and international overhead line standards and open market.

The use of the *finite element method* leads to exact results within the frame of linear static. However, the computation effort is considerably high such that it is indispensable for an economic execution of the calculation to adopt programs specifically designed for lattice towers in order to limit the input effort to an acceptable extent. The geometry should be defined by a few input data only, forming the basis for generation of nodes and member relations by the computer program. The node loads corresponding to the considered load cases are determined by the computer program itself. The rating of the member cross sections and connections depends on the standards to be applied and is carried out by the computer program as well.

The selection of the *model of the overhead line structure* forms an important aspect for the analysis. Lattice towers can be modelled as pure truss structure or as a framework. In case of the *truss* with hinged connections, all members will be modelled as hinged truss members. Such a model can only be formed if the kinematic stability of the truss structure is guaranteed. Every existing instability leads to a singular total stiffness matrix; then, the equation system can not be solved anymore.

Instabilities occur at such nodes where members are jointed being all situated in the same plane. This is true of the crossing points of bracings and the connections with the leg members in case of staggered bracings. Figure 12.34 shows a truss structure with double warrens, where the bracings are connected by hinges at crossing points. This system will be unstable in view of the truss theory, because the centre nodes can be moved rectangularly to the plane of the face. To generate stability, it would be not sufficient just to supplement the truss structure by a horizontal bracing consisting of four members which connect the centre nodes of the bracings. The four triangles generated would be stable, however, they could rotate around the leg member like a rigid body. In this case, two nodes of the crossing points would move in direction to the tower body axis and the others to the opposite. The system can be deformed without any constraint. The system would assume stability only if two opposite nodes were connected additionally.

However, the instability described is a theoretical one only, because in reality the bracings and the horizontal members in the faces pass through at the crossing point without losing their bending stiffness. This bending stiffness transfers the three-dimensional truss structure into a general framework system.

Modelling of a lattice steel tower as a pure truss structure proofs to be difficult in practice, since in case of a three-dimensional system, instability can frequently occur. Therefore, it needs to be consequently obeyed that the three-dimensional truss consists of triangles only which form rigid panels being unable to carry out rigid body movements.

Therefore, lattice steel towers are modelled mostly as *framework systems* consisting of *bending-resistant beams* modelling the leg and truss members forming the bracings. A hinge is assumed at the bend of leg members and horizontal bracings are arranged there to withstand the *forces* due to *leg member bends.* If the leg member profiles vary in sections with constant increase of latitude then leaps of the centroidal axes occur at the limits of the body sections. These eccentricities can be neglected if the centroidal axes are averaged along the range having the same increase of latitude. This pragmatic approach yields to sufficiently precise stresses in the members.

Double warrens can be modelled as truss elements if connections of their crossing points are waived. Thereby, the problem of the apparent instability is practically circumvented. *Redundant* and *horizontal members* are neglected in most cases when forming the model structure. They serve to stabilize the main members against buckling and are arranged accordingly without being considered in the static model.

The magnitude of the occurring bending moments in the members needs to be considered when modelling the system. For rating, it can be treated as a truss structure where predominantly axial member forces occur, despite the modelling as a framework. The occurring bending moments may be considered as secondary moments which are negligibly small. High bending moments draw the attention to a violation of the truss structure modelling, with the result that external loads are withstood by bending. In these cases, the truss structure should be accordingly adjusted or the bending moments need to be considered when verifying the cross sections. This could lead to big cross sections of individual members and might be uneconomic.

12.5.6 Comparison of computations at plane and three-dimensional systems

Lattice steel towers can be analysed using an approximate method considering the structure as composed of plane trusses or the three-dimensional system using the *displacement method.* The approximate method had been developed in view of an analysis by conventional processing by hand. The member forces are derived only on the condi-

tions of equilibrium. Thereby, a recursive calculation of the member forces is possible. The calculation starts at the tower peak, whereby the proportional dead weights and wind forces can be immediately determined and the member considered can be rated directly with its final dimension. The calculation of towers designed with different body extensions is possible in a simple manner since at the beginning of an extension, the loads resulting from the tower sections above are unambiguously defined.

This will not be possible when using the displacement method. The structure is totally described by its nodes and connecting elements and needs to be analysed taking care of the external actions, the wind and dead loads of the structure included. Therefore, in a first step profiles with a minimum dimension are assumed for which the wind and dead load can be calculated in a second step. The rating of the members for the forces obtained results in changes of angle sections obtained in the preceding step. The iterative calculation of the total structure is to be continued until no changes of profiles occur anymore. The numerical effort for the calculation using the displacement method is essentially higher than in case of the calculation using the conventional approximate procedures not only because of basic procedures but also because of the overall iteration.

The displacement method can be used for all types of towers. Certain types of towers are not suited to the calculation using the approximate procedures because of their design, especially when symmetry is missing. The world-wide frequently used Y-type towers or portal structures fall within this category. Data for adjusting the position of the individual leg member stubs with respect to the inclination of the unloaded tower to take care of the expected deformations can be stipulated without additional calculations. When the structure has been established for the computer, additional studies such as analysis of its dynamics and of effects of *foundation settlement* can be carried out. Constraints are given just by the performance of the computer program system used. In mining areas with setting terrain in particular, the foundation settlements can be of interest. This strain cannot be analysed using calculations based on a plane static-determined system. The transposition of loads due to the failure of a member or a foundation can be studied as well.

There is a close coincidence between both methods of calculation, especially for the lateral load of the towers without torsional effects. In case of a torsional load, there are deviations especially close to the points where the loads act and in parts of the towers with horizontal bracings.

Smaller differences of the member forces may be due to different modelling of the static systems. In case of the conventional approximate procedure, the total structure is analysed as a truss system. In case of the calculation using the displacement method, the leg members are assumed as bending-stiff beams and the bracings as members of a truss structure. Within this hyperstatic system, forces due to constraints are created because of the member deformations. Therefore, the results are different as well. While in case of the conventional approximate procedure dead weights and wind loads are determined for each tower panel as acting in the gravitational centre of the panel, the loads act at the nodes in case of the displacement method. The differences are relatively small in case of leg members, those points excepted where the loads from the crossarms are introduced.

Horizontal bracings are arranged at the crossarm connections and at positions where the increase of latitude of the tower faces changes. This horizontal bracings take care of the distribution of the introduced forces on the individual tower faces. However, a hyperstatic system is created there, especially, where horizontal members are arranged above or below double warrens. The constraint forces created by the deformations result in member forces which are different from those obtained by the conventional procedure, where it is assumed that the vertical loads are withstood just by the leg members. This hypothesis is not true for hyperstatic systems. This effect will be recognized in particular

Table 12.8: Reduction factor ϱ for angles depending on the relative plate slenderness $\overline{\lambda}_p$

Hot-rolled angles		Cold-formed angles	
$\overline{\lambda}_p$	ϱ	$\overline{\lambda}_p$	ϱ
$\leq 0{,}91$	1,0	$\leq 0{,}809$	1,0
0,91 to 1,213	$2 - \overline{\lambda}_p/0{,}91$	0,809 to 1,213	$(5 - \overline{\lambda}_p/0{,}404)/3$
$> 1{,}213$	$0{,}98/\overline{\lambda}_p^2$	$> 1{,}213$	$0{,}98/\overline{\lambda}_p^2$

at application of the vertical loads from the crossarm upper chord to the tower body and at bends in the tower faces. In this part of a tower, the bracing forces obtained from both methods differ to a considerable degree.

Torsional load cases result in differing bracing forces. In case of suspension towers with square bodies, the bracing forces will be higher in the faces in parallel to the line direction when using the conventional approximate procedure than in the other faces. They are composed from the conductor tensile force in longitudinal direction and the reactions to torsional moments. The forces perpendicular to the line are assumed to withstand the other half of the torsional moment only. The calculation using the displacement method results in higher forces in the bracings of the faces perpendicular to the line direction.

Using the *conventional approximate procedure* for loads in parallel to one tower face, the bracings in the faces rectangular to the direction of the load are assumed as not contributing to the load reaction. According to the displacement method, the expansion of tensile-loaded leg members and setting of the compression-loaded leg members produce forces within these bracings as well. These member forces, however, are mostly lower than those resulting from the external loads. In case of double warrens, the virtual buckling length is changed because both bracings will be compression-loaded due to the setting of the leg members and the supporting effect of the connection at their crossing point is no longer effective. As explained in clause 12.5.8.2, the resistance is lower in this case, therefore.

Leg extensions with differing lengths of the individual legs affect the distribution of the forces within the leg members. This effect is not considered when using a conventional procedure. The supporting conditions and stiffness in case of differently long leg extensions create an asymmetry in the static model, resulting in a differing distribution of the forces. These differences of member forces, however, do not lead to a more economic rating by one or the other method. Steel lattice towers need to be analysed for a large number of load cases. Although from both methods different distributions of the forces may result for individual load cases such difference will be compensated considering the results of the load cases at all. Their effect on the rating will be limited, therefore.

12.5.7 General format of verification of members and connections

The *rating of lattice steel towers* according to EN 50 341-1 [12.8] follows the European standard ENV 1993-1-1 (Eurocode 3) [12.13] for steel structures. The design is based on the *limit state approach.* The member forces are determined from the design values of actions using the *elastic global analysis.* These design values are obtained from the characteristic values by multiplication with partial factors γ_F. The maximum member forces form the basis for the rating of the members.

The total *design value* E_d of a tower element caused by the design load is compared with the *structural design resistance* R_d. The stability of an element is verified if the design value is not greater than structural resistance:

$$E_d \leq R_d \quad . \tag{12.54}$$

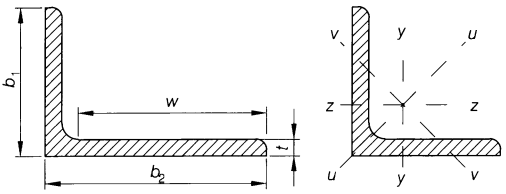

Figure 12.35: Dimensions and cross-sectional axes

The *structural design resistance* R_d is calculated from the characteristic values of the resistance R_K divided by the partial factors γ_M:

$$R_d = R_K/\gamma_M \quad . \tag{12.55}$$

12.5.8 Design of compression members

12.5.8.1 Effective cross section properties for compression members

For verification of *stability of compression-loaded members*, the *effective cross section* is considered. When exceeding certain ratios between the leg width b and the thickness t, the effect of local buckling on the instability needs to be considered by reducing the available cross-sectional area. The effective cross-sectional area A_{eff} is computed from the effective leg width b_{eff} which depends on the relative plate slenderness $\overline{\lambda}_p$, assuming a uniform stress distribution on the angle leg. The *relative plate slenderness* is

$$\overline{\lambda}_p = 0{,}0537\, b \,/\, \left(t \cdot \sqrt{235/f_y}\right) = 0{,}0035 \cdot (b/t) \cdot \sqrt{f_y} \quad , \tag{12.56}$$

where b is the nominal leg width, t the thickness and f_y the yield strength.
The effective leg width is obtained from

$$b_{eff} = \varrho \cdot b \quad . \tag{12.57}$$

The reduction factor ϱ is determined depending on the relative plate slenderness $\overline{\lambda}_p$ for hot-rolled angles according to Table 12.8. The cross-sectional area of hot-rolled angles is reduced if the ratios b/t is above 17,0 for mild steel S235 or above 13,8 in case of high-tensile steel S355.
The *effective cross-sectional area* of any angle (Figure 12.35) can be calculated according to [12.35] from:

$$A_{eff} = A - t\,[b_1\,(1 - \varrho_1) + b_2\,(1 - \varrho_2)] \quad , \tag{12.58}$$

where ϱ_1 and ϱ_2 are determined for each leg by Table 12.8 using $\overline{\lambda}_p$ from (12.56).

12.5.8.2 Flexural buckling of axially compressed members

Members of lattice towers may be considered as straight and axially compressed, whereby the eccentricity of the load action may not be considered in case of leg members, as well as in case of bracings consisting of one angle section which is frequently connected by one leg only. Then, the design value of the compression force N_d divided by the design value of the *flexural buckling resistance* N_{Rd} should satisfy the condition

$$N_d/N_{Rd} \leq 1 \quad . \tag{12.59}$$

There, N_d is the *design value of the compression force* for the member considered. The design buckling resistance N_{Rd} is defined by

$$N_{Rd} = \kappa \cdot A_{eff} \cdot f_y/\gamma_M \quad , \tag{12.60}$$

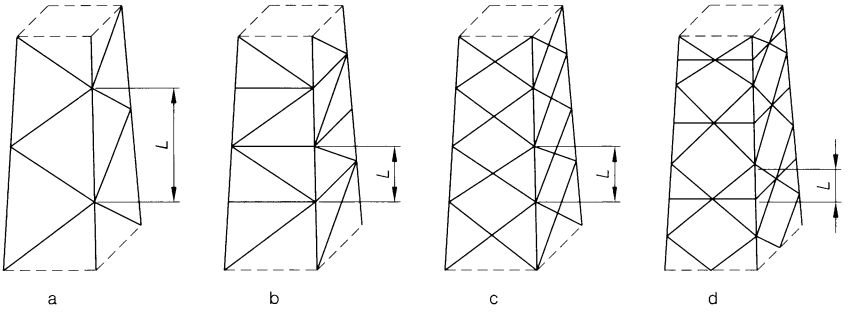

Figure 12.36: Symmetric bracing types

where κ is the reduction factor, A_{eff} the effective cross-sectional area, f_y the yield strength of the material and γ_M the partial factor of resistance, being at least 1,1 according to EN 50 341-1 [12.8].

In case of compression load, the members fail due to instability, whereby the resistance does not only depend on the material values but also on the geometric dimensions of the members. Therefore, the reduction factor κ depends on the slenderness λ, on the material data E and f_y and on the type of *buckling curve* used.

The *European buckling curves* [12.36] were created as a result of comprehensive research. The buckling curves consider geometric imperfections due to precurvature and structural imperfections due to profile-depending residual stresses. Using the reference slenderness ratio λ_a, the buckling curves are defined independently of the yield strength:

$$\lambda_a = \pi \sqrt{E/f_y} \quad . \tag{12.61}$$

The slenderness λ of the considered member is related to λ_a and results in the *non-dimensional slenderness* $\overline{\lambda}$, taking care of the effective cross-sectional area:

$$\overline{\lambda} = (\lambda/\lambda_a)\sqrt{A_{\text{eff}}/A} = (\lambda/\pi) \cdot \sqrt{(f_y \cdot A_{\text{eff}})/(E \cdot A)} \quad . \tag{12.62}$$

The buckling curves can be equated as follows:

$$\kappa = 1/\left(\phi + \sqrt{\phi^2 - \overline{\lambda}^2}\right) \quad , \tag{12.63}$$

where

$$\phi = 0{,}5\left[1 + \alpha(\overline{\lambda} - 0{,}2) + \overline{\lambda}^2\right] \quad . \tag{12.64}$$

The *imperfection factor* α depends on the type of buckling curve and, therefore, on the classification of the cross section. For the design of compressed members, two alternatives can be adopted according to EN 50 341-1:

- Design without load tests;
- Design verified by testing of full-scale structures.

In some countries, like Germany, only the first approach is permitted and should be followed also if load tests are carried out [12.10]. Both design procedures are distinguished by the selection of the buckling curve for angle sections and their differing assessment of load eccentricity and conditions of connections. If the design is done by calculation only, the *buckling curve c* applies to angle sections with an imperfection factor α equal to 0,49.

The verification of buckling stability is based on the *member slenderness*

$$\lambda = s_k/i \quad . \tag{12.65}$$

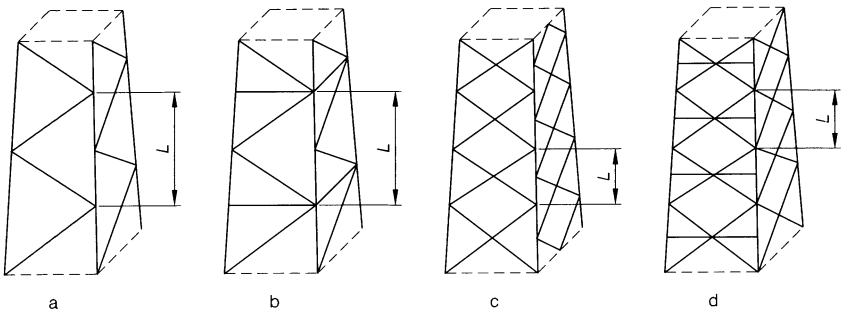

Figure 12.37: Staggered bracings for leg members

The relevant radius of gyration i is determined according to the buckling direction, taking care of the gross cross section. Slenderness ratios and *buckling lengths* depend on the type of bracing; for leg members and chords, several cases are distinguished. For leg members and chords with symmetric bracings according to Figure 12.36 where the nodes are supported within two faces, the buckling length is equal to the distance of the nodes. Then, the *slenderness ratio* is

$$\lambda = L/i_{vv} \quad , \tag{12.66}$$

where L is the *system length* of the leg member or chord and i_{vv} the smallest radius of gyration of the profile (Figure 12.35).
If the buckling is constrained to a certain direction by intermediate redundant members or staggered bracings, the radius of gyration is used in relation to the axis rectangularly to the direction of buckling. In case of *staggered bracings* (Figure 12.37), the slenderness ratios of leg members made of equal-leg angles are:

$$\begin{aligned} &\text{With intermediate bracing acc. to Figure 12.37 b, d: } \lambda &&= 1{,}0 \cdot L/i_{yy}\,; \\ &\text{With staggered bracings acc. to Figure 12.37 a, c: } \lambda &&= 1{,}2 \cdot L/i_{yy}\,. \end{aligned} \tag{12.67}$$

Leg members supported alternately in two faces according to Figure 12.37 a and c have been subject of *stability investigations.* The three-dimensional problem of stability (Figure 12.37) was studied by several authors [12.37, 12.38, 12.39]. The results of their studies are summarized in Table 12.9. In [12.37], a leg member was studied considering a varying axial force from panel to panel and a differing number of panels. Paper [12.38] deals with the problem of a differing number of panels, however, with a constant longitudinal force. In [12.39], the problem was studied for a differing number of panels with constant axial force, however, considering the drilling of the cross section. The results obtained in [12.39] are presented in Table 12.9 without taking care of the drilling. The *slenderness ratio* λ is related to the axis yy parallel to one leg by means of the buckling length factor β_{yy}

$$\lambda = \beta_{yy} \cdot L/i_{yy} \quad . \tag{12.68}$$

The results presented in [12.37] demonstrate that the *buckling length factor* β_{yy} depends on the distribution of the axial force; the higher the increase per panel, the lower the buckling length factor is. The most unfavourable case occurs if the same axial force acts in all panels. With increasing number of panels, the buckling length factor increases as well. The most unfavourable value is reached already at six panels in case of a constant axial force. The increase of the axial force of the leg members of lattice steel towers is less than 10 % from panel to panel above the tower waist, as a rule. Below the tower waist, the axial force can decrease further down as well. A buckling length factor $\beta_{yy} = 1{,}20$

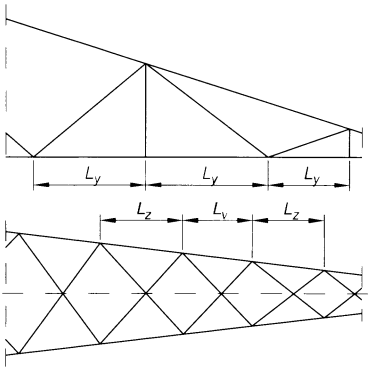

Figure 12.38: Buckling length of a crossarm lower chord

Table 12.9: Buckling length factor for legs with staggered bracings

	Number of panels	Increase of axial force	Buckling length factor β_{yy}
Girkmann [12.37]	2	10%	0,98
		0%	1,00
	5	20%	1,00
		10%	1,08
		0%	1,19
Bleich [12.38]	2	0%	1,00
	5		1,19
	∞		1,20
Djubek [12.39]	3	0%	1,19
	5		1,20
	∞		1,20

Table 12.10: Buckling length factor for bracing patterns according to Figure 12.37 a and c

	Buckling length factor β_{yy}
DIN VDE 0210 [12.14]	1,00
DIN 4114 [12.40]	1,10
ASCE Manual 52 [12.20]	1,20
BS [12.41]	1,20
ECCS [12.42]	1,20
Literatur [12.37, 12.38, 12.39]	1,20

yields results on the safe side. In the literature, different buckling length factors can be found for alternately supported members in two faces. In Table 12.10, the buckling length factors are summarized as presented in standards or references. According to [12.14], it is assumed that buckling occurs rectangularly to the supporting face within the system length L. For the calculation, the radius of gyration i_{yy} is used resulting in a buckling length factor $\beta_{yy} = 1{,}0$. The evidence of this calculation assumption has been proved by tests. These values coincide with the data determined in [12.37] for two panels, corresponding to a bracing according to Figure 12.37 b. The buckling length factor according to the former DIN 4114 [12.40] is adequate if the leg member force decreases downwards by at least 10 % per panel. This value coincides well with the result obtained according to [12.37] for five panels with a corresponding distribution of axial force. In case of a constant axial force in all panels, the factor $\beta_{yy} = 1{,}20$ can be found in the literature. Using this factor, conservative results are obtained because the leg member compression forces and the effective buckling lengths of lattice steel towers decrease in upward direction. This result has been considered in ASCE [12.20], BS [12.41] and ECCS [12.42].

As a rule, the *chords of crossarms* are alternately supported by bracings, whereby the buckling is tied to a certain direction. Figure 12.38 shows the cases to be studied. Between two consecutive nodes, the profile buckles around its weakest cross-sectional axis. Then, the minimum radius of gyration is assumed for the calculation of the slenderness ratio. The radius of gyration related to the axis in parallel to one leg is used for buckling rectangularly to the horizontal or vertical crossarm face.

Commonly used *bracing arrangements* for tower bodies and crossarm faces are presented in Figure 12.39. In case of single warren, the buckling length corresponds to the system length of the member (Figure 12.39 a). In case of single warren with redundant truss (Figure 12.39 b), the buckling out of the truss plane has to be considered as well.

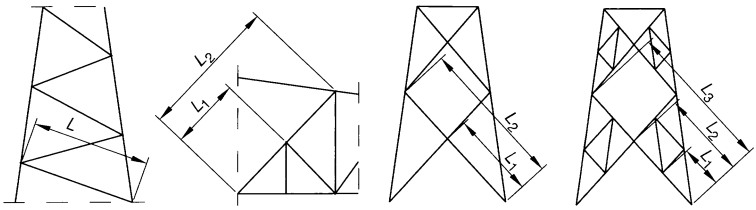

Figure 12.39: Commonly adopted diagonal bracings. a: single warren; b: single warren with redundant members; c: double warren; d: double warren with redundant members

The crossing point can be assumed as fixed in case of double warren (Figure 12.39 c) if both members pass uncut and are connected by at least one bolt. The constraint of deformation rectangularly to the plane of bracings depends on the ratio of the forces $|S_d/N_d|$ of the double warren, where S_d is the force in the supporting member and N_d the force in the compression member. S_d can be a tensile or compression force. If a sufficiently high tensile force S_d acts in the supporting member, then the compression member is stabilized.

$$\text{If} \quad |S_d/N_d| \geq 2/3, \quad \text{then it applies} \quad \lambda = L_1/i_{vv} \quad . \tag{12.69}$$

The stabilizing effect decreases if the tensile force is getting lower. Then, buckling out of the truss plane needs to be studied as well.

$$\text{If} \quad |S_d/N_d| < 2/3, \quad \text{then it applies} \quad \lambda = (L_1/i_{yy})\sqrt{2 - 1{,}5\,|S_d/N_d|} \quad . \tag{12.70}$$

If equal compression forces $S_d = N_d$ act in both members, then the buckling length corresponds to the system length L_2. The members deviate rectangularly to the truss plane. If the compression forces are different, the member loaded to a lower extent stabilizes the member with the higher compression force. Then, it applies to the slenderness ratio

$$\lambda = (L_1/i_{yy})\sqrt{2 + 2\,|S_d/N_d|} \quad \text{with} \quad \lambda \leq L_2/i_{yy} \quad . \tag{12.71}$$

Buckling lengths for other bracings are given in [12.36] and in EN 50 341-1 [12.8].
In case of *design validated by tower tests*, the *buckling curve b* according to ENV 1993-1-1 [12.13] is adopted with an imperfection factor $\alpha = 0{,}34$. To calculate the *member resistance*, the dimensionless effective slenderness $\overline{\lambda}_{eff}$ is introduced, depending on:

- The type of member;
- The cross-sectional axis for which the resistance is determined;
- The connection type;
- The bracing type and
- The member continuity.

To take care of these effects, six buckling cases are introduced for angle sections.

$$\begin{aligned}
&\text{Case 1:} && \overline{\lambda}_{eff} = \exp(1{,}747 \cdot \overline{\lambda} - 1{,}98) && \text{for} \quad 0{,}2 \leq \overline{\lambda} \leq 1{,}035 \\
& && \overline{\lambda}_{eff} = 1{,}091 \cdot \overline{\lambda} - 0{,}287 && \text{for} \quad \overline{\lambda} > 1{,}035, \\
&\text{Case 2:} && \overline{\lambda}_{eff} = \exp(1{,}747 \cdot 1{,}2 \cdot \overline{\lambda} - 1{,}98) && \text{for} \quad 0{,}2 \leq 1{,}2 \cdot \overline{\lambda} \leq 1{,}035 \\
& && \overline{\lambda}_{eff} = 1{,}091 \cdot 1{,}2 \cdot \overline{\lambda} - 0{,}287 && \text{for} \quad 1{,}2 \cdot \overline{\lambda} > 1{,}035, \\
&\text{Case 3:} && \overline{\lambda}_{eff} = 0{,}02 + 0{,}88\,\overline{\lambda}, \\
&\text{Case 4:} && \overline{\lambda}_{eff} = 0{,}30 + 0{,}68\,\overline{\lambda}, \\
&\text{Case 5:} && \overline{\lambda}_{eff} = 0{,}52 + 0{,}68\,\overline{\lambda}, \\
&\text{Case 6:} && \overline{\lambda}_{eff} = 0{,}16 + 0{,}94\,\overline{\lambda} \quad .
\end{aligned} \tag{12.72}$$

Table 12.11: Buckling cases according to EN 50341-1 [12.8]

Function	Buckling axis	Slenderness condition $\overline{\lambda}$	Load eccentricity condition	Member continuity condition	Number of bolts at non-continuous end	Number of case
Bracing member	*vv*	$< \sqrt{2}$	1 end	–	–	3
		$< \sqrt{2}$	2 ends	–	–	4
		$> \sqrt{2}$	–	2 ends	–	1
		$> \sqrt{2}$	–	1 end	2 bolts	4
		$> \sqrt{2}$	–	1 end	1 bolt	1
		$> \sqrt{2}$	–	0 end	2 bolts	4
		$> \sqrt{2}$	–	0 end	1 bolt	1
	yy or *zz*	$< \sqrt{2}$	1 end	–	–	4
		$< \sqrt{2}$	2 ends	–	–	5
		$> \sqrt{2}$	–	2 ends	–	1
		$> \sqrt{2}$	–	1 end	2 bolts	4
		$> \sqrt{2}$	–	1 end	1 bolt	1
		$> \sqrt{2}$	–	0 end	2 bolts	5
		$> \sqrt{2}$	–	0 end	1 bolt	6
Leg member	*vv*	all values of $\overline{\lambda}$	Figure 12.36			1
	yy or *zz*		Figure 12.37 b, d			1
			Figure 12.37 a, c (staggered)			2

There, $\overline{\lambda}$ is calculated according to equation (12.62). The appropriate *buckling case* can be selected from Table 12.11. Two cases are considered for leg members and bracings connected with both legs. The first case refers to an axially loaded member, continuously running through a number of panels with supports not staggered as in Figure 12.36. Equation (12.72), case 1, refers to $\overline{\lambda}_{\text{eff}}$. The second case refers to an axially loaded member, however, with staggered supports according to Figure 12.37 a and c. Equation (12.72) case 2, applies to $\overline{\lambda}_{\text{eff}}$.

The ends of bracing members of lattice steel towers are connected at one angle leg only. This connection produces an eccentric load on the member which reduces its resistance. If the member is connected by more than one bolt or by welding, a restraint is given which yields a higher resistance. With increasing slenderness ratio, the effect of the eccentricity decreases and the beneficial effect of the restraint increases. For calculation purposes it should be assumed that these effects cancel out each other at a non-dimensional slenderness ratio $\overline{\lambda} = \sqrt{2}$. In case of slenderness ratios $\overline{\lambda} < \sqrt{2}$, the effect of the eccentricity predominates. In case of slenderness ratios $\overline{\lambda} > \sqrt{2}$, the effect of constraints at the ends predominates, enabling to utilize the favourable effect of connections carried out by welding or by more than one bolt.

The buckling verification according to ASCE 52 [12.20] is wide-spread internationally, whereby eccentricities and restraints of the connections are considered as well. Effective slenderness ratios are calculated depending on the task of the member, its slenderness ratio and the type of end connection.

A *centric load* is given if the member is connected with both legs or continues uncut at a crossing point. An *eccentric load* is given if the member is connected by one leg only. Then, it is assumed that above a slenderness ratio of 120 the effect of the restraint cancels out the effect of the eccentricity. A restraint can be assumed if the member is welded or connected by more than one bolt.

The resistance can be calculated based on the slenderness ratio λ_{eff} (see Table 12.12). Elastic and unelastic buckling is distinguished depending on the slenderness ratio. *Elastic buckling* occurs above the *limit of proportionality* C_{c}, unelastic buckling below this limit. C_{c} represents a characteristic slenderness ratio

$$C_{\text{c}} = \pi \cdot \sqrt{2 \cdot E / f_{\text{y}}} \quad , \tag{12.73}$$

Table 12.12: Effective slenderness ratio according to ASCE 52

Type of member	Slenderness	Slenderness condition	Support condition
Leg member	$\lambda_{\text{eff}} = \lambda$	$0 \leq \lambda \leq 150$	bolted in both faces at connections
Bracing member	$\lambda_{\text{eff}} = \lambda$	$0 \leq \lambda \leq 120$	concentric load at both ends
	$\lambda_{\text{eff}} = 30 + 0{,}75 \cdot \lambda$	$0 \leq \lambda \leq 120$	concentric load at one end and normal framing eccentricity at the other end
	$\lambda_{\text{eff}} = 60 + 0{,}50 \cdot \lambda$	$0 \leq \lambda \leq 120$	normal framing eccentricities at both ends
	$\lambda_{\text{eff}} = \lambda$	$120 \leq \lambda \leq 200$	unrestrained against rotation at both ends
	$\lambda_{\text{eff}} = 28{,}6 + 0{,}762 \cdot \lambda$	$120 \leq \lambda \leq 225$	partially restrained against rotation at one end
	$\lambda_{\text{eff}} = 46{,}2 + 0{,}615 \cdot \lambda$	$120 \leq \lambda \leq 250$	partially restrained against rotation at both ends
Redundant member	$\lambda_{\text{eff}} = \lambda$	$0 \leq \lambda \leq 120$	concentric load at both ends
	$\lambda_{\text{eff}} = \lambda$	$120 \leq \lambda \leq 250$	unrestrained against rotation at both ends
	$\lambda_{\text{eff}} = 28{,}6 + 0{,}762 \cdot \lambda$	$120 \leq \lambda \leq 290$	partially restrained against rotation at one end
	$\lambda_{\text{eff}} = 46{,}2 + 0{,}615 \cdot \lambda$	$120 \leq \lambda \leq 330$	partially restrained against rotation at both ends

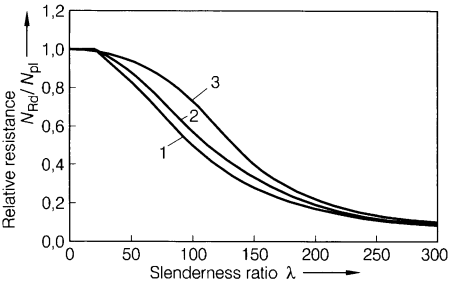

Figure 12.40: Resistance in case of flexural buckling of angle sections made of S235 according to: 1 EN 50341-1, buckling curve c; 2 EN 50341-1, buckling curve b; 3 ASCE manual 52 [12.20]

where E is the modulus of elasticity (210000 N/mm^2) and f_y the yield strength of the material. C_c is 133 for steel S235 and 108 for steel S355.
Then, the resistance is:

$$\begin{aligned} N_{\text{Rd}} &= A \cdot \left[1 - 1/2\,(\lambda/C_c)^2\right] \cdot f_y \quad \text{for} \quad \lambda \leq C_c \quad , \\ N_{\text{Rd}} &= A \cdot \pi^2 \cdot E/\lambda^2 \qquad\qquad\quad \text{for} \quad \lambda > C_c \quad . \end{aligned} \tag{12.74}$$

To take care of *local buckling* in case of slender members, the yield strength f_y is replaced by the critical stress f_{cr} in equations (12.73) and (12.74), which is determined depending on the ratio of the leg angle width to the angle thickness. The leg width w is measured from the beginning of the radius (Figure 12.35).

$$\begin{aligned} \frac{209{,}6}{\sqrt{f_y}} \leq \frac{w}{t} \leq \frac{377{,}3}{\sqrt{f_y}} \quad & f_{cr} = \left[1{,}677 - 0{,}677 \cdot \frac{b}{209{,}6 \cdot t} \cdot \sqrt{f_y}\right] \cdot f_y \\ \frac{377{,}3}{\sqrt{f_y}} < \frac{w}{t} \quad & f_{cr} = \frac{0{,}0332 \cdot \pi^2 \cdot E}{(w/t)^2} \end{aligned} \tag{12.75}$$

Figure 12.40 shows the resistance for a leg member depending on the slenderness ratio λ for the three methods of verification discussed here. The resistance N_{Rd} is presented in relation to the axial force N_{pl} according to the full-plastic state.

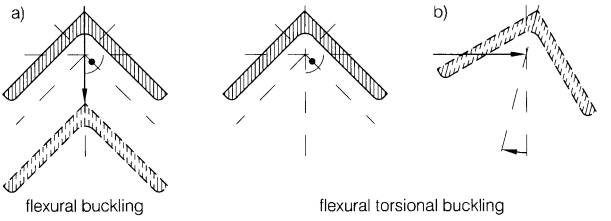

Figure 12.41: Deformation behaviour of an equal-leg angle section at a) flexural buckling and b) flexural torsional buckling

12.5.8.3 Flexural torsional buckling of centrally compressed members

As a rule, thin-walled angles with open cross sections are used for lattice steel towers. The stability behaviour of these members depends on the shape of the cross section, being completely irregular, single-, double- or centrally-symmetric. Depending on the position of the gravitational centre, the shearing centre and the point of load action *flexural buckling*, *flexural torsional buckling* or *torsional buckling* can occur. Flexural torsional buckling or torsional buckling will be the more likely to be prevalent the lower the slenderness ratio of the member is. Low slenderness ratios occur in particular at leg members or crossarm lower chords and more rarely at bracings or redundant members. The cross sections of profiles used for leg members are single- or double-symmetric. For lower chords of crossarms, single-symmetric sections are used.

Equal-leg angles are single-symmetric cross sections, the gravitational centre of which does not coincide with the shearing centre. The members are assumed as centrally compressed such that the gravitational centre is the load point. A member can fail either by flexural buckling in direction of one of the symmetry axes or by flexural torsional buckling. Figure 12.41 shows instability of an equal-leg angle. In case of flexural buckling, the cross section moves rectangularly to the cross-sectional axis (Figure 12.41 a). This axis shows the minimum radius of gyration.

In case of *flexural torsional buckling*, the cross section moves rectangularly to one of the cross-sectional axis – in case of equal-leg angles rectangularly to the axis of symmetry (Figure 12.41 b) – while it is drilled simultaneously along its longitudinal axis. Failing by flexural torsional buckling will be prevalent in case of equal-leg angles with low slenderness ratios. Channel sections fail either by flexural buckling in direction of the symmetry axis or by flexural torsional buckling where the cross section moves rectangularly to the symmetry axis and is drilled around its longitudinal axis simultaneously.

Cruciform angles are double-symmetric cross sections where the centre of load, the *shearing centre* and the gravitational centre coincide. This cross section fails either by flexural buckling rectangularly to the weaker axis or by torsional buckling. In the latter case, the cross section is drilled without a lateral movement.

The resistance against flexural torsional and torsional buckling is determined by equation (12.60) as in case of flexural buckling considering, however, an *equivalent slenderness ratio* λ_{vi} for calculation of the buckling reduction factor κ. The non-dimensional slenderness is defined as (see equation (12.62))

$$\overline{\lambda} = (\lambda_{vi}/\lambda_a)\sqrt{A_{eff}/A} \quad . \tag{12.76}$$

In case of a single-symmetric cross section where the y-axis forms the symmetry axis, the *equivalent slenderness ratio* is

$$\lambda_{vi} = \frac{s_k}{i_{yy}}\sqrt{\frac{c^2 + i_M^2}{2\,c^2}\left(1 + \sqrt{1 - \frac{4\,c^2(i_p^2 + 0{,}093\,(\beta^2/\beta_0^2 - 1)\,y_M^2}{(c^2 + i_M^2)^2}}\right)} \quad . \tag{12.77}$$

The factors β and β_0 take care of the degree of restraint for bending and warping. The values depend on the design of the structure. For truss structures, $\beta = 1{,}0$ can be as-

sumed. The values β_0 for *warping* can be taken between 0,5 for a rigid warping restraint and 1,0 for unrestricted support against warping. Since the complete *unrestricted support against warping* is not present due to the design of the nodes, an approximation on the safe side is obtained by $\beta_0 = 1{,}0$. The effect of the warping is anyway not essential for tower members, where cross sections with only low warping resistance are adopted. In case of lattice towers, it is assumed that the members are supported at their ends by hinges without any constraint for warping. The difference between the system length of the member and the distance between the connections at both member ends is negligibly small. Considering these simplifications, it is obtained for single-symmetric cross sections having the u-axis as symmetry axis:

$$\lambda_{\mathrm{vi}} = \frac{s_{\mathrm{k}}}{i_{uu}} \sqrt{\frac{c^2 + i_{\mathrm{M}}^2}{2\,c^2} \left(1 + \sqrt{1 - \frac{4\,c^2 i_{\mathrm{p}}^2}{(c^2 + i_{\mathrm{M}}^2)^2}}\right)} \tag{12.78}$$

$$\text{where } c = \sqrt{\left(I_\omega + 0{,}039 \cdot s_{\mathrm{k}}^2 \cdot I_{\mathrm{T}}\right) / I_u} \quad , \tag{12.79}$$

In these formulae there are

s_{k} the buckling length of the leg member or chord;
i_{uu} the radius of gyration around the symmetry axis;
u_{M} distance between centre of gravity and shearing centre;
$i_{\mathrm{p}} = \sqrt{i_{vv}^2 + i_{uu}^2}$ polar radius of gyration around the gravitational centre;
$i_{\mathrm{M}} = \sqrt{i_{\mathrm{p}}^2 + u_{\mathrm{M}}^2}$ polar radius of gyration related to the shearing centre;
I_u moment of inertia related to the symmetry axis;
I_ω warping constant related to the shearing centre;
I_{T} torsional moment of inertia.

The *equivalent slenderness ratio* can be calculated from equation (12.78) for angle sections as well as for U-type channel sections. Results well coinciding with those from equation (12.78) are obtained for equal-leg angles by an approximation according to [12.43]:

$$\lambda_{\mathrm{vi}} = \frac{5{,}06 \cdot b/t}{\sqrt{1 + 3{,}53\,(b/s_{\mathrm{k}})^2}} \quad , \tag{12.80}$$

where s_{k} is the buckling length of the leg member or the chord, b the leg width of the section and t the thickness of the angle.
According to EN 50 341-1 [12.8], the equivalent slenderness ratio for equal-leg angles can be calculated as an approximation from

$$\lambda_{vi} = 5\,b/t \quad . \tag{12.81}$$

This approximation, however, leads to unfavourable results in case of low slenderness ratios. The approximation (12.80) yields more reliably results.
Figure 12.42 shows the limits for the relation $\lambda_{vi}/\lambda_{vv}$ of centrally compressed equal-leg angles for varying ratios of width to thickness. Flexural torsional buckling prevails above the relevant curves and flexural below. It can be seen that the ratio b/t has an essential influence on the stability performance. With *thin angle sections*, flexural torsional buckling is possible also at slenderness ratios which commonly occur at leg members.
Torsional buckling occurs in case of *double-symmetrical cross sections* only if the polar radius of gyration i_{p} is greater than the value c according to equation (12.79). The equivalent slenderness ratio is calculated for such cross sections from:

$$\lambda_{vi} = (s_{\mathrm{k}} \cdot i_{\mathrm{p}})/(i_y \cdot c) \quad . \tag{12.82}$$

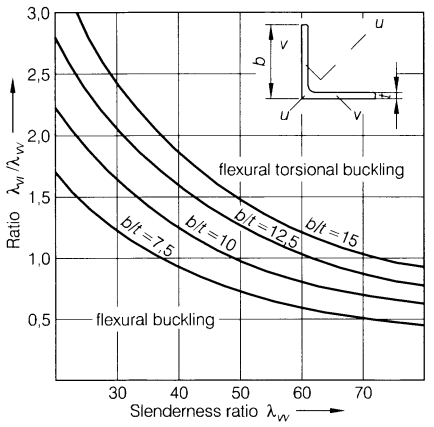

Figure 12.42: Limits of ratio $\lambda_{vi}/\lambda_{vv}$ for discerning flexural and flexural torsional buckling in case of centrally compressed equal-leg angle sections with varying relations of width b to thickness t

Table 12.13: Moment coefficients β_M according to ENV 1993-1-1 [12.13]

Moments at member ends	Moments due to transverse loading
M_1 ψM_1 $-1 \le \psi \le 1$ $\beta_M = 1{,}8 - 0{,}7\,\psi$	M_Q $\beta_M = 1{,}4$

12.5.8.4 Bending and axial compression forces

Bending around both principal axes combined with *axial compression forces* represents the most general loading of a member. Bending is caused either by an eccentrically acting compression force as designed or by transverse external loads. The verification of members is carried out according to ENV 1993-1-1 [12.13], whereby the cross-sectional modulus related to the principal axes y and z are considered. It should be verified that

$$\frac{N_d}{\kappa_{min} A f_y/\gamma_M} + \frac{k_y M_{yd}}{W_y f_y/\gamma_M} + \frac{k_z M_{zd}}{W_z f_y/\gamma_M} \le 1 \quad , \tag{12.83}$$

where
$$\begin{aligned} k_y &= 1 - \mu_y N_d/(\kappa_y \cdot A \cdot f_y)\,, && \text{however, } k_y \le 1{,}5\,, \\ \mu_y &= \overline{\lambda}_y(2\beta_{My} - 4)\,, && \text{however, } \mu_y \le 0{,}9\,, \\ k_z &= 1 - \mu_z N_d/(\kappa_z \cdot A \cdot f_y)\,, && \text{however, } k_z \le 1{,}5\,, \\ \mu_z &= \overline{\lambda}_z(2\beta_{Mz} - 4)\,, && \text{however, } \mu_z \le 0{,}9\,. \end{aligned}$$

The value κ_{min} is the lower of κ_y and κ_z. The reduction factors κ_y and κ_z are determined from equation (12.63) for the y- and z-axis. The moment coefficients β_{My} and β_{Mz} can be taken from Table 12.13 depending on the diagram of bending moments. For angle sections, the cross-sectional moduli and other parameters related to the principal axes u and v (see Figure 12.35) have to be used. For other types of loads, the moment coefficients are given in ENV 1993-1-1 [12.13].

12.5.9 Design of compound members

12.5.9.1 Member connected by batten plates

Members connected by batten plates are used for high-loaded leg members and bracings. They consist at least of two individual angle sections which are connected by batten

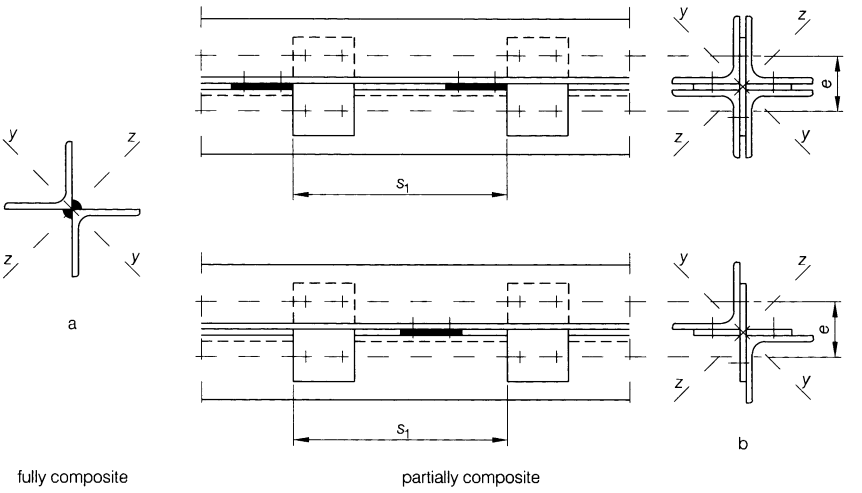

Figure 12.43: Cruciform compound members: a continuously welded, b with batten plates

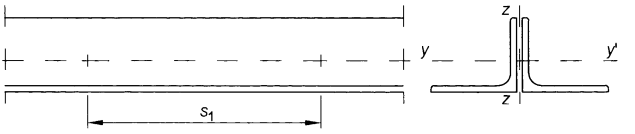

Figure 12.44: Members composed of back-to-back angle sections

plates. Frequently, *cruciform angle sections* according to Figure 12.43 are used for leg members of towers for high loads. If they are continuously welded they can be treated as a single fully-compound member. *Back-to-back angle sections* (Figure 12.44) are used for diagonal bracings. *Batten plates* should at least be arranged at one third of the total buckling length. Each batten plate is connected to the submembers by means of bolts or an equivalent welded seam. For *cruciform angle sections*, at least two bolts are necessary at each submember at each batten plate. The slenderness ratio y_1 of the submember should comply with

$$\lambda_1 = s_1/i_{vv} \leq 50 \quad , \tag{12.84}$$

where s_1 is the distance between the batten plates (see Figure 12.44) and i_{vv} the minimum radius of gyration of a submember.

Compression-loaded compound members which consist of m submembers and have a material principal axis may be calculated against buckling transversely to these material axis as a single compression member. As far as buckling transversely to that *principal axis* is concerned, the compound member can be treated as a single-compression member with an equivalent slenderness of

$$\lambda_{vi} = \sqrt{\lambda_z^2 + (m/2)\lambda_1^2} \quad , \tag{12.85}$$

where m is the number of submembers, λ_z the slenderness ratio of the compound member and λ_1 the slenderness ratio of one submember.

The submembers of the design shown in Figures 12.43 and 12.44 have only a low distance. Connections by bolts or by welding to transfer the longitudinal shear forces between the submembers are designed for a transverse force V_s equal to 2,5 % of the longitudinal force acting in the compound member. For batten plates and *flat steel packing plates*, it is sufficient to verify that their connections can transfer a shear force

$$T_s = V_s \cdot s_1/e \quad , \tag{12.86}$$

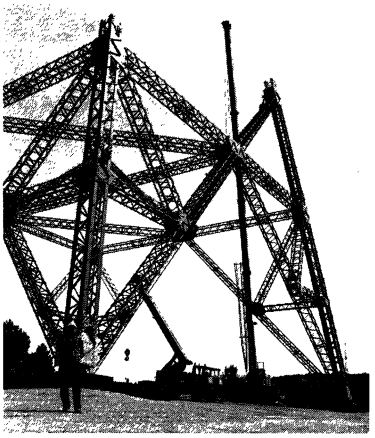

Figure 12.45: Lower section of a 400 kV crossing suspension tower, Bosphorus, Turkey

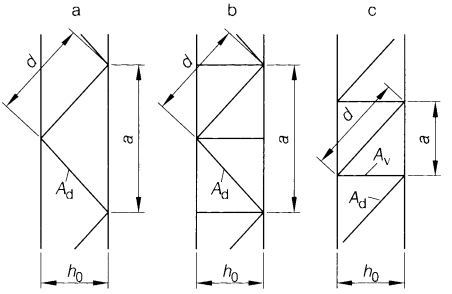

Figure 12.46: Parameters to determine the shear stiffness of compression-loaded members: a single warren; b single warren with horizontal member; c bracing with diagonal and horizontal members

resulting from the transverse force V_S. There, s_1 is the distance between the batten plates and e the distance of the centroidal axes of the submembers. When designing the connections of the batten plates, also the moment is considered which is created by the eccentric action of the shear force T_S. The batten plates of compression-loaded cruciform angle sections can be staggered rectangular or in parallel.

12.5.9.2 Laced box-type members

Laced box-type members are needed for tall, highly-loaded towers. The suspension towers of long-span *overhead line crossings* ([12.12, 12.44, 12.45], Figure 12.45) fall into this category. The member forces to be withstood reach up to 13 000 kN in case of leg members and up to 1000 kN in case of bracings [12.44].

The laced box-type members consist of four submembers arranged in parallel which are laced in the four side faces by a regular single warren bracing. They are loaded by a centrally acting compression force N_d, which results from the static analysis of the structure. For this analysis, the laced member may be considered as a single member. The section properties of the complete member are used for the analysis based on the finite element method, as an example. The stresses in the submembers are calculated according to the *second order theory* considering a sinus-type deformation with a deflection of $e_0 = l/500$. To the bending moment in the middle of the member, it applies

$$M_S = N_d \cdot e_0 / [1 - (N_d/N_{cr}) - (N_d/S_V)] \quad , \tag{12.87}$$

where

$N_{cr} = \pi^2 E I_{eff}/l^2$	virtual buckling load of the laced member,
$I_{eff} = A_G \cdot h_0^2$	effective moment of inertia of the laced member,
A_G	cross-sectional area of one corner member,
h_0	distance of the centre of gravitation of corner members,
l	length of the total member,
E	modulus of elasticity and
S_V	shear stiffness of the bracing.

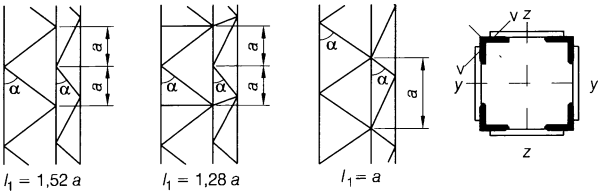

Figure 12.47: Buckling lengths of laced corner members

The *shear stiffness* S_V is determined depending on the type of bracing according to Figure 12.46. It applies to the cases according to Figures 12.46 a and b

$$S_V = EA_d \cdot a \cdot h_0^2/d^3 \quad , \tag{12.88}$$

and to the case according to Figure 12.46 c

$$S_V = 2\,EA_d \cdot a \cdot h_0^2 \,/\, \left\{d^3 \left[1 + \left(\Lambda_d h_0^3/(\Lambda_v d^3)\right)\right]\right\} \quad . \tag{12.89}$$

These assumptions for the shear stiffness are based on rigid connections of the bracings to the corner members. *Resilience* in the connections may reduce the strength and, therefore, should be considered when verifying the stability. *Slipping of the connections* can be considered by increasing the virtual geometric imperfection e_0. As an approximation, the additional deformation can be taken as

$$e_s = (\Delta_s \cdot d \cdot l) \,/\, \left(2\,h_0 \sqrt{h_0^2 + d^2}\right) \tag{12.90}$$

where Δ_s is the slipping, l the total length of the laced compound member; h_0 and d, see Figure 12.46.
Then, $e_0 + e_s$ instead of e_0 is assumed as the set of the precurvature.
The maximum member force in the corner members results in the middle of the compound member to be

$$N_G = N_d/4 + M_S/(2\,h_0) \quad . \tag{12.91}$$

Each individual corner member is verified for a hinged connection at both ends as well as for a slenderness $\lambda_1 = l_1/i_{vv}$ and the axial force N_G as a single member. The buckling length l_1 has to be selected from Figure 12.47 depending on the type of bracing. The shear force determines the member forces of the bracing. The maximum shear force occurs at the end of the main member to be $V_S = \pi\ M_S/l$. Therefore, the axial force in the bracings results to be

$$N_D = V_S \cdot d/(2\,h_0) \quad . \tag{12.92}$$

The bracings are designed for this force in view of an axially-loaded compression with the buckling length d. The verification of the connections between bracings and corner members is necessary as well.

Example: Verification of a laced compound member (Figure 12.48)

Compression force	N_d	= 12 800 kN
Modulus of elasticity	E	= 210 000 N/mm^2
Length of total member	l	= 13,5 m
Imperfection	e_0	= 1 350/500 = 2,7 cm
Distance between the centre of gravity	h_0	= 100 cm
System length of lattice truss	a	= 200 cm
Length of bracings	d	= $\sqrt{2} \cdot a$ = 141,4 cm
Cross-sectional area of corner member	A_G	= 2 · 83,5 = 167 cm^2
Cross-sectional area of bracings	A_d	= 9,40 cm^2

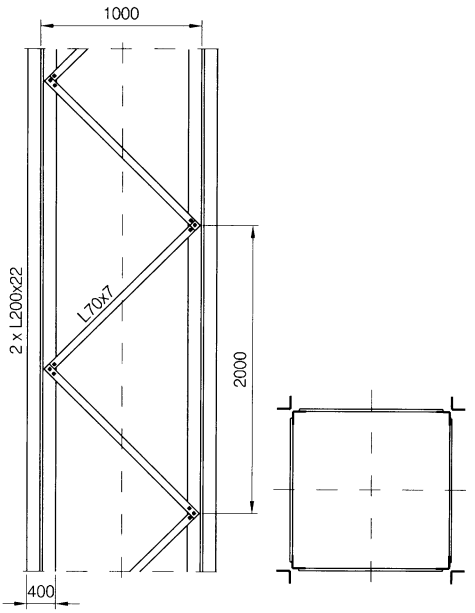

Figure 12.48: Design of a compound member

Effective moment of inertia	$I_{\text{eff}} = 167 \cdot 100^2 = 1{,}67 \cdot 10^6$ cm^4
Ideal elastic buckling load	$N_{\text{cr}} = \pi^2 \cdot 21\,000 \cdot 1{,}67 \cdot 10^6 / 1\,350^2 = 190 \cdot 10^3$ kN
Shear stiffness	$S_{\text{V}} = 21\,000 \cdot 9{,}40 \cdot 200 \cdot 100^2 / 141{,}4^3 = 140 \cdot 10^3$ kN
Bending moment	$M_{\text{S}} = 12\,800 \cdot 2{,}7/[1 - (12\,800/190 \cdot 10^3) - (2\,800/140 \cdot 10^3)] = 411$ kNm
Axial force of corner member	$N_{\text{G}} = 12\,800/4 + 41\,100/(2 \cdot 100) = 3\,406$ kN
Shear force	$V_{\text{S}} = \pi \cdot 411/13{,}5 = 95{,}6$ kN
Axial force of bracing member	$N_{\text{D}} = 95{,}6 \cdot 141{,}4/(2 \cdot 100) = 67{,}6$ kN
Resistance of corner member	
Minimum radius of gyration	$i_y = \sqrt{2 \cdot 1\,276/167} = 3{,}91$ cm
Buckling length	$l_1 = 1{,}52 \cdot 100 = 152$ cm
Slenderness ratio	$\lambda = 152/3{,}91 = 38{,}87$
	$\lambda_{\text{a}} = \pi \cdot \sqrt{210\,000/355} = 76{,}4$
	$\overline{\lambda} = 38{,}87/76{,}4 = 0{,}5088$
Buckling curve c	$\alpha = 0{,}49$
	$\phi = 0{,}5(1 + 0{,}49(0{,}5088 - 0{,}2) + 0{,}5088^2) = 0{,}7051$
Buckling reduction factor	$\kappa = 1/(0{,}7051 + \sqrt{0{,}7051^2 - 0{,}5088^2}) = 0{,}8375$
Resistance	$N_{\text{Rd}} = 0{,}8375 \cdot 167 \cdot 35{,}5/1{,}1 = 4\,524$ kN
	$N_{\text{G}}/N_{\text{Rd}} = 3\,406/4\,514 = 0{,}755 < 1{,}0$
Resistance of bracing member	
Minimum radius of gyration	$i_u = 1{,}37$ cm
Buckling length	$l_1 = d = 141{,}4$ cm
Slenderness ratio	$\lambda = 141{,}4/1{,}37 = 103$
	$\lambda_{\text{a}} = \pi \cdot \sqrt{210\,000/355} = 76{,}4$
	$\overline{\lambda} = 103/76{,}4 = 1{,}348$
Buckling curve c	$\alpha = 0{,}49$
	$\phi = 0{,}5(1 + 0{,}49(1{,}348 - 0{,}2) + 1{,}348^2) = 1{,}6901$
Buckling reduction factor	$\kappa = 1/(1{,}6901 + \sqrt{1{,}6901^2 - 1{,}348^2}) = 0{,}3691$
Resistance	$N_{\text{Rd}} = 0{,}3691 \cdot 9{,}40 \cdot 35{,}5/1{,}1 = 111{,}97$ kN
	$N_{\text{D}}/N_{\text{Rd}} = 67{,}6/111{,}97 = 0{,}601 < 1{,}0$

12.5.10 Design of tensile-loaded members

12.5.10.1 Members axially loaded in tension

For *truss members loaded in tension*, it needs to be verified that the design value N_d is less than the resistance N_{Rd} or:

$$N_d/N_{Rd} \leq 1 \quad . \tag{12.93}$$

The connection part of the angle section determines the resistance N_{Rd}. According to EN 50 341-1, the *tensile resistance* at the connection is not based on the yield strength f_y but on the ultimate strength f_u of the material:

$$N_{Rd} = 0{,}9\, A_{net} f_u/\gamma_M \quad , \tag{12.94}$$

where A_{net} is the net cross-sectional area, f_u the tensile strength of the material and γ_M the partial factor of material ($\gamma_M = 1{,}25$ according to EN 50 341-1).
Related to the gross cross-sectional area A, the resistance is $N_{Rd} = A \cdot f_y/\gamma_M$, where f_y is the yield strength and $\gamma_M = 1{,}1$. The lower of both values is prevalent for the rating. The verification based on the net cross section is, therefore, prevalent if

$$\frac{A}{A_{net}} > \begin{cases} 1{,}21 & \text{for S235 and} \\ 1{,}14 & \text{for S355.} \end{cases} \tag{12.95}$$

Otherwise, the verification is carried out considering gross cross-sectional area and the yield strength. However, this verification can only be prevalent if the compression force acting in the member is considerably below the tensile force.
In case of angle sections connected at both legs such as joints of leg members and chords, the boreholes in both legs are substracted from the gross cross-sectional area. The connections are designed with the bolts in one line in case of angle sections with legs up to 110 mm wide, whereby the bolts arranged in the two legs may be staggered to each other. Two rows of staggered bolts can be arranged in one leg of angle sections with at least 110 mm wide legs. In wider legs, the arrangement of bolts in two lines in parallel is possible in both legs, depending also on the bolt diameter.
For angle sections connected with both legs, the *net cross-sectional area* is the lowest value which is obtained along differing sectional lines

$$A_{net} = A - \Delta A \quad , \tag{12.96}$$

where A_{net} is the net cross-sectional area, A the gross area along the section studied and ΔA the sum of the area of all boreholes in the studied section. The net cross-sectional area is the gross area of the member less the sum of the area of all boreholes in the regarded section perpendicular to the axis of the angle. If the boreholes are staggered it needs to be checked whether the net cross-sectional area along any diagonal or zigzag line leads to a lower value (Figure 12.49). In this case, the net cross-sectional area is determined by deducting from the gross area in the sum of borehole sections in the diagonal or zigzag line and adding $s^2 t/(4p)$ for each gauge space, where t is the thickness of the angle leg, s the longitudinal centre-to-centre pitch of two consecutive boreholes and p the transverse centre-to-centre pitch between the bolt gauge lines. The spacing p is measured perpendicular to the axis of the member.
If applicable, the reduction of the leg member cross section by boreholes for connection of diagonal bracings needs to be considered (Figure 12.50) in addition to verify the resistance to tensile forces.
If an angle is connected at one leg only by one bolt, the tensile resistance is obtained from (Figure 12.51 a):

$$N_{Rd} = A_{net} \cdot f_u/\gamma_M = (b_1 - d_0) \cdot t \cdot f_u/\gamma_M \quad . \tag{12.97}$$

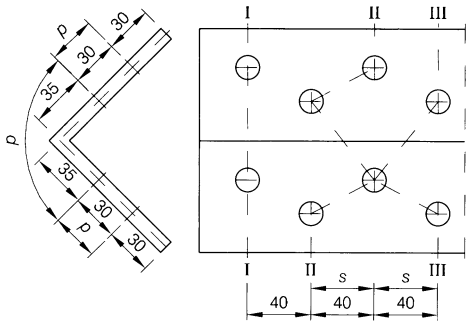

Figure 12.49: Staggered boreholes

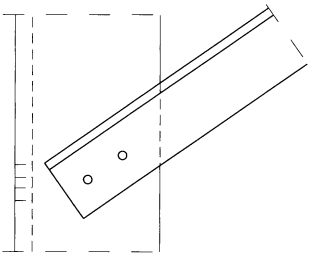

Figure 12.50: Connection of a bracing to a leg member

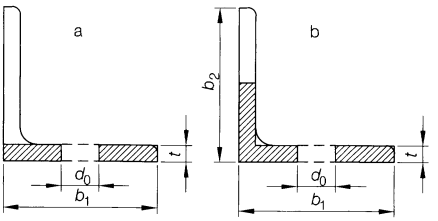

Figure 12.51: Net cross sections in case of tension-loaded angle section connected by one leg: a connection with one bolt; b connection with several bolts

If an angle is connected at one leg with two or more bolts then the tensile resistance is obtained from (Figure 12.51 b):

$$N_{\mathrm{Rd}} = A_{\mathrm{net}} \cdot f_{\mathrm{u}}/\gamma_{\mathrm{M}} = (b_1 - d_0 + b_2/2) \cdot t \cdot f_{\mathrm{u}}/\gamma_{\mathrm{M}} \quad . \tag{12.98}$$

According to standard ASCE 52 [12.20], the tensile resistance is based on the yield strength f_{y} of the material. The tensile resistance of centrally loaded members bolted in both angle legs is

$$N_{\mathrm{Rd}} = A_{\mathrm{net}} \cdot f_{\mathrm{y}} \quad , \tag{12.99}$$

where A_{net} is the net cross-sectional area of the angle being calculated as above mentioned. If an angle is connected at one leg only, the tensile resistance is

$$N_{\mathrm{Rd}} = 0,9 \cdot A_{\mathrm{net}} \cdot f_{\mathrm{y}} \quad . \tag{12.100}$$

If the legs are unequal and the angle is connected at the shorter leg, the unconnected leg is considered with the same size as the connected leg. The net cross-sectional area A_{net} is the cross-sectional area less the borehole section perpendicularly to the angle axis. If the gauge line of the bolts on the connected leg is outside the centroidal axis of the angle, the connection is checked for rupture (Figure 12.52). The rupture resistance is obtained from

$$N_{\mathrm{Rd}} = 0,6 \cdot A_{\mathrm{v}} \cdot f_{\mathrm{u}} + A_{\mathrm{t}} \cdot f_{\mathrm{y}} \quad , \tag{12.101}$$

where f_{y} is the yield strength and f_{u} the tensile strength of the material, A_{v} the minimum net area in shear along a line of the transmitted force and A_{t} the minimum net area from the centre of the borehole to the edge of the angle perpendicular to the line of action of the tensile force.

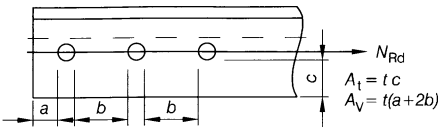

Figure 12.52: Rupture resistance

Example: (Figure 12.49)
Angle section: L100×8 S235
Cross-sectional area: $A = 1\,550$ mm^2
Borehole diameter: $d_0 = 17$ mm
Net cross-sectional area:
Section I $A_{\text{netI}} = 1\,550 - 2 \cdot 17 \cdot 8 = 1\,278$ mm^2
Section II $A_{\text{netII}} = 1\,550 - 4 \cdot 17 \cdot 8 + 2 \cdot 40^2 \cdot 8/(4 \cdot 30) + 40^2 \cdot 8/(4 \cdot (35 + 35)) = 1\,265$ mm^2
Section III $A_{\text{netIII}} = 1\,550 - 3 \cdot 17 \cdot 8 + 40^2 \cdot 8/(4 \cdot 30) + 40^2 \cdot 8/(4 \cdot (35 + 35)) = 1\,294$ mm^2

12.5.10.2 Axial tensile force and bending

If a member is loaded by an axial tensile force N_d and bending moments M_{yd} and M_{zd}, then the cross section without any reduction for boreholes is verified if the following condition is complied with:

$$\frac{N_d}{A\, f_y/\gamma_M} + \frac{M_{yd}}{W_y\, f_y/\gamma_M} + \frac{M_{zd}}{W_z\, f_y/\gamma_M} \leq 1 \quad , \tag{12.102}$$

where A is the cross-sectional area, W the cross section modulus, f_y the yield strength of the material and γ_M the partial factor for material ($\gamma_M = 1{,}1$ according to EN 50 341-1). When a bending moment around one principal axis only or no tensile forces act, the verification can be carried out using the same approach.

12.5.11 Design of connections

For overhead line towers, predominantly *shearing-bearing connections* are used and more rarely *prestressed shearing-bearing connections*, slipping resisting prestressed connections or *welded connections*. The specifications made in EN 50 341-1 [12.8] apply together with ENV 1993-1-1 [12.13] to these connections. Connections by bolts are designed such that the force to be transferred acts rectangularly to the bolt axis and the bolt is loaded by *shearing* in the contact plane of the elements to be jointed. Sections may have several *shear planes*. Therefore, they are addressed as single-shear, double-shear or triple-shear connection. It is necessary to verify that the *shear force* F_d in each shear plane and each connecting element does not exceed the *shear resistance* $F_{v\,Rd}$:

$$F_d / F_{v\,Rd} \leq 1 \quad . \tag{12.103}$$

Thereby, it is distinguished between connections where the shear plane passes through the unthreaded portion of the shank and those where it passes through the threaded portion. If the shear plane passes through the unthreaded portion, the shearing cross section corresponds to the cross section of the shank. If the shear plane passes through the threaded portion, the *tensile cross section* is used. Therefore, the shear resistance per shear plane is:

$$F_{v\,Rd} = \alpha_v \cdot A_v \cdot f_{ub}/\gamma_M \quad . \tag{12.104}$$

If the shear plane passes through the unthreaded portion of the bolt, it applies:

$A_v = \pi \cdot d_b^2/4$	cross section of the shank,
f_{ub}	*tensile strength* of the bolt,
α_v	factor equal to 0,6 for all bolt grades according to EN 50 341-1,
γ_M	partial factor of material equal to 1,25 according to EN 50 341-1.

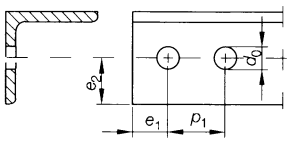

Figure 12.53: Position of boreholes for connections in an angle member

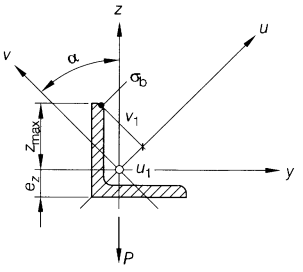

Figure 12.54: Design of an angle loaded by a bending moment

Table 12.14: Permissible member length in m for bending by a force 1,0 kN acting on the middle of the member

Section	S235		S355	
	L_v	L_y	L_v	L_y
35 × 4	0,57	0,69	0,85	1,04
35 × 5	0,68	0,85	1,02	1,27
40 × 4	0,75	0,91	1,12	1,37
40 × 5	0,90	1,12	1,35	1,68
45 × 4	0,95	1,15	1,43	1,73
45 × 5	1,16	1,43	1,74	2,14
50 × 4	1,19	1,45	1,78	2,17
50 × 5	1,46	1,79	2,19	2,69
50 × 6	1,69	2,11	2,54	3,17
55 × 4	1,45	1,75	2,17	2,62
55 × 5	1,77	2,17	2,67	3,25
55 × 6	2,10	2,57	3,15	3,86
60 × 5	2,13	2,61	3,19	3,91
60 × 6	2,52	3,11	3,77	4,65

The shear resistance may be summed up even if some of the shear planes of a multi-shearing connection pass through the unthreaded portion and the others through the threaded portion.

The forces are introduced into the bolt shank by pressing on the bearing area. The acting bearing force F_d of a connecting element may not exceed the *bearing resistance* of the borehole face:

$$F_d / F_{b\,Rd} \leq 1 \quad . \tag{12.105}$$

The bearing resistance is:

$$F_{b\,Rd} = \alpha_b \cdot d_b \cdot t \cdot f_u / \gamma_M \quad , \tag{12.106}$$

where f_u is the tensile strength of the material, d_b the bolt diameter, γ_M the partial factor of material (equal to 1,25 according to EN 50 341-1) and α_b a factor, which is determined according to EN 50 341-1 from the following conditions, where the smallest value will be prevalent (Figure 12.53):

$$\alpha_b = 1{,}20 \cdot e_1/d_0 \quad ; \tag{12.107}$$

$$\alpha_b = 1{,}85 \cdot (e_1/d_0 - 0{,}5) \quad ; \tag{12.108}$$

$$\alpha_b = 0{,}96 \cdot (p_1/d_0 - 0{,}5) \quad ; \tag{12.109}$$

$$\alpha_b = 2{,}30 \cdot (e_2/d_0 - 0{,}5) \quad . \tag{12.110}$$

Therein, e_1 is the end distance from the centre of hole to the adjacent end in direction of the force, e_2 the edge distance from the centre of hole to the adjacent edge rectangularly to the direction of force, p_1 the distance between borehole centres and d_0 the borehole diameter.

Specifications of the permissible end, edge and hole distances are given in clause 12.5.1.2.

For the verification in compliance with EN 50 341-1 and ENV 1993-1-1, the edge distance e_2 is normally 1,5 d_0, but may be reduced to not less than 1,2 d_0 provided the design bearing resistance is reduced accordingly. If e_2 is reduced to 1,2 d_0, then the bearing resistance $F_{b\,Rd}$ should be reduced to two third of the value given in (12.106).

For intermediate values $1,2d_0 < e_2 \leq 1,5d_0$, the value $F_{b\,Rd}$ may be determined by linear interpolation. EN 50 341-3-4 permits edge distances $e_2 = 1,2d_0$ without reduction of the design bearing resistance $F_{b\,Rd}$.

12.5.12 Design for bending due to transverse loads

All members which can be climbed during erection or maintenance are bent and should be designed accordingly. Following EN 50 341-1, members of lattice steel towers which are inclined with an angle not more than 30° to the horizontal should withstand a load of 1,0 kN acting vertically at the member centre. Other loads need not to be considered simultaneously. When calculating the design value of the *construction load*, a partial factor $\gamma_P = 1{,}5$ is considered. Similar requirements are stipulated in other standards, e. g. [12.16].
In case of angle sections, the construction load acts mostly in parallel to one of the legs while the member is bent around its principal axes (Figure 12.54). For a beam supported at both ends by hinges, the bending stress is obtained from

$$\sigma_b = 1/4\,\gamma_P \cdot P \cdot L_v\,(v_1/I_u \sin\alpha + u_1/I_v \cos\alpha) \quad . \tag{12.111}$$

If bending is restricted to an axis in parallel to one leg (Figure 12.54), it applies

$$\sigma_b = \gamma_P \cdot P \cdot L_y \cdot z_{max}/(4\,I_y) \quad . \tag{12.112}$$

The maximum length for which a section may be used when loaded by a given vertical load, is calculated based on the tensile yield stress. It is obtained

$$L_{v\,max} = 4\,f_y/\,[\gamma_M\gamma_P \cdot P\,(v_1/I_u \sin\alpha + u_1/I_v \cos\alpha)] \tag{12.113}$$

or

$$L_{y\,max} = 4\,f_y \cdot I_y/\,(\gamma_M\gamma_P \cdot P \cdot z_{max}) \quad . \tag{12.114}$$

The maximum permissible lengths are in Table 12.14 given for frequently used profiles made of S235 or S355.

12.5.13 Design of redundant members

Redundant members stabilize leg members and main bracings by reducing their buckling length. The redundant or secondary members are not loaded directly by the external forces if the analysis is carried out assuming a model consisting of planes according to 12.5.4. By an analysis using a three-dimensional model, such members may experience forces due to restraint and deformation of the structure if the system is hyperstatic. To guarantee the stabilizing effect for the supported member, the secondary members are designed with hypothetical forces N_{hyp} which are assumed as acting at each node where a secondary member is attached. However, these forces do not act simultaneously at all nodes but only one force is assumed as acting in the most unfavourable position. The hypothetical forces need not to be added to the member forces resulting from the external load. Where a secondary member is loaded as a result of the global analysis, this load is used for the design only if the force is higher than the *hypothetical force*. The hypothetical force is stipulated in EN 50 341-1 by:

$$N_{hyp} = K \cdot N_d/100 \quad , \tag{12.115}$$

where $K = 1/60\,(\lambda{+}32)$ with $1 \leq K \leq 2$, and λ is the slenderness ratio of the supported member and N_d the design value of the supported member.
The factor K depends on the slenderness ratio of the supported member. For slenderness ratios $\lambda \leq 28$, K is 1,0 and the design value of the secondary member is 1 % of the

compression force N_d in the member. For slenderness ratios $\lambda \geq 88$, K is 2,0 and the design value of the secondary member reaches 2 % of the force in the member. Other standards specify different hypothetical forces. The ASCE Manual 52 [12.20] assumes 0,5 to 2,5 % of the supported member force for the design of the secondary member.

12.5.14 Deformation

Lattice steel towers constitute stiff constructions which, nevertheless, will be deformed under a load. The occurring *bending deformation* may be visible at towers permanently loaded by horizontal conductor forces such as angle and dead-end towers. To reduce the visibility of the deformation, it is standard practice to erect these towers with an inclination against the anticipated direction of load such that the tower will be vertical after stringing of conductors. From the aesthetical point of view, a horizontal position of the lowest crossarm after stringing the conductors should be favoured. To determine the *necessary inclination* of the stubs, when installing the foundations, the displacements or overturning angles need to be well known.

Furthermore, the *deformation* under maximum loads may not reach an extent which would limit the *serviceability* of the overhead line. The serviceability of the towers themselves will not be restricted by the deformation. However, the effect of the deformation on the conductor position may be crucial. In particular, the horizontal deflection of an angle tower affects the sag substantially and can lead to a situation where the required electrical clearance is not anymore obeyed. An increase of the deflection under the acting of maximum loads should, therefore, be limited to 0,5 m compared with the deflection under everyday condition [12.46].

The deformations are computed based on the *characteristic values of the load.*. Practically speaking, the partial factor for actions γ_F is assumed as 1,0. The calculation of the deformation for the necessary inclination when erecting angle and dead-end towers is carried out for the everyday condition. Typically standards, e. g. EN 50 341-3-4, define the everyday condition as 10°C ambient temperature without wind action.

For lattice steel towers, the deformation caused by the *bolt slippage* may contribute essentially to the total deformation. Elastic deformations may be determined using the *principle of virtual work*. For this purpose, a virtual force $\overline{F} = \overline{1}$ is assumed as acting in the direction and at the position of the deflection to be determined. The virtual internal forces and moments are calculated for this force. If the inclination is wanted, a virtual moment $\overline{M} = \overline{1}$ is assumed. The deflection wanted is obtained by superposition of the real and the virtual internal forces and moments:

$$\overline{1}\,\delta = \int \frac{N(x)\overline{N}(x)}{EA(x)}\,\mathrm{d}x + \int \frac{M(x)\overline{M}(x)}{EI(x)}\,\mathrm{d}x \quad , \tag{12.116}$$

where $N(x)$ is the axial force due to the external load, $\overline{N}(x)$ the axial force due to the virtual load, $A(x)$ is the cross-sectional area, $M(x)$ the bending moment due to the external load, $\overline{M}(x)$ the bending moment due to the virtual load, $I(x)$ the moment of inertia and E the modulus of elasticity.

The members of lattice steel towers are substantially loaded by axial forces. Moments may be neglected. Then, it is obtained for this case from equation (12.116)

$$\overline{1}\,\delta = \sum_{i=1}^{n} l_i S_i \overline{S}_i/(EA_i) \quad , \tag{12.117}$$

where, for the member i, S_i is the member force due to the external load, $\overline{S}_i$ the member force due to the virtual load, l_i the member length, A_i the cross-sectional area and E the modulus of elasticity.

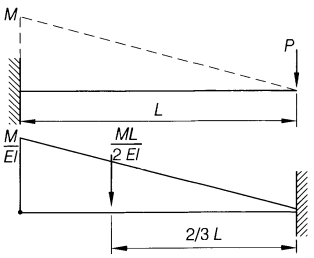

Figure 12.55: Determination of deflection at virtual beam

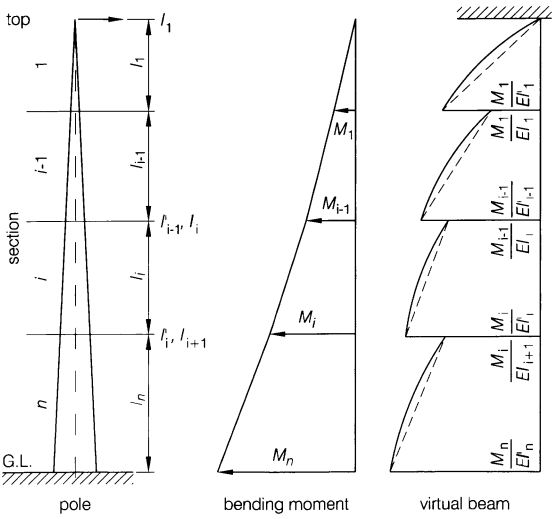

Figure 12.56: Determination of deflection at the peak of a lattice steel pole

The application of equation (12.117) yields precise values for the *elastic deflection condition* in case of linear global analysis; however, it is combined with a considerable calculation effort because of the high number of members. As an approximation, the deflection of a lattice steel tower can be calculated based on the analogy of the deformation of a bent beam with the moment of a beam loaded by a linearly increasing load $M/EI(x)$. The analogy will yield a correct result if the boundary conditions of the deformation and the area of moments corresponds. Figure 12.55 illustrates the approach by means of a virtual beam. The approach is favourable, especially when studying by hand the bending deformation of structures having a variable bending stiffness.
At the free end of the beam, the deflection and the bending angle are not restrained; therefore, also moments and transverse force at the virtual system may not be restrained there, being different from zero. In case of a beam with a fixed support at one end, this leads to exchanged boundary conditions. The bending moment increases linearly from the free end of the beam to the value $M = P \cdot l$ at the support. This bending moment is divided by the bending stiffness of the beam EI and is assumed as the load per unit length of the *virtual beam* which is supported at the top. If the bending stiffness of the beam is constant, the virtual moment at the support resulting from the triangularly distributed load will be:

$$1\overline{M} = \frac{M \cdot L}{2\,EI} \cdot \frac{2}{3} L = \frac{P \cdot L^3}{3\,EI} \quad . \tag{12.118}$$

The virtual moment under the load P is equal to the bending deflection. Therefore $f = P \cdot L^3 / (3\,EI)$ is the bending deflection of a beam rigidly supported at one end with a concentrated load at its top. The bending stiffness of lattice steel towers, however, will not be constant but changes from section to section due to variation in the leg member cross section and, within the individual sections, because of the changing width.
For the moment of inertia, it applies

$$I = 4\,A\,(b(x)/2 - e)^2 \quad ,$$

where A is the cross section of the leg member, $b(x)$ the external width of the tower body at the coordinate x and e the distance between the tower edge and the centroidal axis of the leg member.

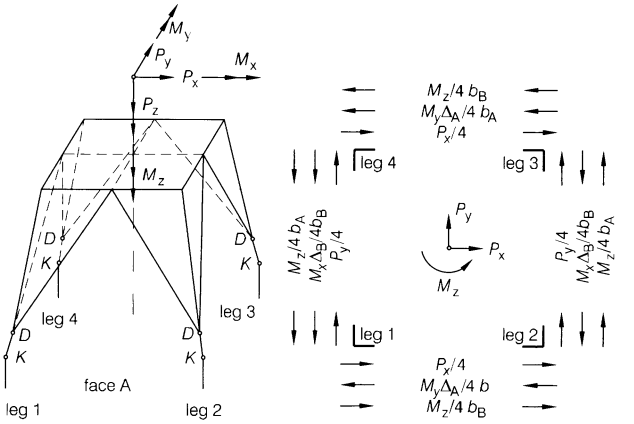

Figure 12.57: Horizontal forces at connection D of bracings

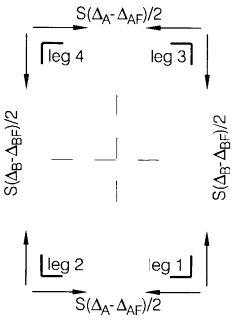

Figure 12.58: Horizontal forces at leg member bend K

If the width of the tower increases linearly with x, the moment of inertia increases squarely. As an approximation, it is permissible to assume a linear distribution of the virtual load along one tower section when determining the bending deflection. Then, the moment of the virtual load will assume the shape of a hyperbola. Using the designations of Figure 12.56, the *bending deformation at tower top* will be

$$f_{\mathrm{d}} = \sum_{i=1}^{n} \frac{l_i}{2E} \left[\left(\frac{2\,M_i}{I_i'} + \frac{M_{i-1}}{I_i} \right) \frac{l_i}{3} + \left(\frac{M_i}{I_i'} + \frac{M_{i-1}}{I_i} \right) \sum_{j=1}^{i-1} l_j \right] \quad . \tag{12.119}$$

The relation (12.119) does neither take care of the elasticity of the bracing diagonals nor of the slippage in the leg member joints. Comparative calculations [12.47] have shown that the portion of elasticity of the bracings will be 12 to 15 % of the total deflection [12.48]. This portion can be considered approximately by reducing the bending stiffness by a factor of 0,9.

The *bolt slippage* within the leg member joints leads to tilting at each joint by the angle $\alpha_{\mathrm{s}} = \Delta_{\mathrm{s}}/b$, where Δ_{s} is the bolt slippage and b the width of the tower.

For the bolt slippage, a value of 4 mm per joint can be assumed. The *total deflection* is obtained by summing up the elastic deflection and the tilting of the sections due to the bolt slippage

$$f_{\mathrm{tot}} = f_{\mathrm{d}} + (\tan \alpha_{\mathrm{s}}) \sum_{i=1}^{n} h_i \quad , \tag{12.120}$$

where f_{d} is the elastic deflection, α_{s} the tilting angle of a joint and h_i the distance between the joint i and the position of the deflection.

12.5.15 Calculation of foundation loads

For *compact foundations* according to clause 13.4.3.1, the moments and transverse forces acting in the foundation base are necessary for each load case. These data can be determined from the external forces by well known relations (see example clause 12.5.18).

In case of *separated foundations* according to clause 13.4.4.1, however, the forces in the direction of the leg members and the corresponding transverse forces are necessary for

each tower leg. Transverse forces, which load the foundations, occur at the connections of the bracings D and, when the leg members are bent within the foundation, at the bend K as well (Figure 12.57). It can be assumed that the moments M_x, M_y and M_z and the forces P_x, P_y and P_z at the level of the diagonal connections are known. Then the *vertical components of the leg member forces* are obtained from

$$S = \pm M_x/(2\,b_\mathrm{B}) \pm M_y/(2\,b_\mathrm{A}) - P_z/4 \quad . \tag{12.121}$$

The force will act in direction of the leg member

$$S_\mathrm{E} = S \cdot \sqrt{1 + (\Delta_\mathrm{A}/2)^2 + (\Delta_\mathrm{B}/2)^2} \quad , \tag{12.122}$$

where Δ_A and Δ_B are the increase of latitude in the faces A and B, respectively. As an approximation, it can be assumed $S_\mathrm{E} \approx S$. The *forces at the connections of the bracings* are (Figure 12.57)

$$D_x = P_x/4 - M_y/(2\,b_\mathrm{A}) \cdot \Delta_\mathrm{A}/2 \pm M_z/(4\,b_\mathrm{B}) \tag{12.123}$$

and

$$D_y = P_y/4 - M_x/(2\,b_\mathrm{B}) \cdot \Delta_\mathrm{B}/2 \pm M_z/(4\,b_\mathrm{A}) \quad . \tag{12.124}$$

If the leg member is bent at the foundation top level, additional transverse forces will occur there:

$$K_x = \pm S/2 \cdot (\Delta_\mathrm{A} - \Delta_\mathrm{AF}) \quad , \tag{12.125}$$

$$K_y = \pm S/2 \cdot (\Delta_\mathrm{B} - \Delta_\mathrm{BF}) \quad . \tag{12.126}$$

The values Δ_AF and Δ_BF represent the increase of latitude of the faces within the foundation. In most cases, Δ_AF and Δ_BF are either equal to Δ_A and Δ_B, respectively (leg members without bend), or equal zero (vertical arrangement of leg members, e. g. in case of augered foundations). Figure 12.58 shows the forces at the leg member bend assuming that a leg member tensile force acts. If a compression force acts in a leg member, the horizontal forces will act in the opposite direction.

12.5.16 Application of computer programs for calculation of lattice steel towers

During design of lattice steel towers, many steps of calculation are carried out in the same manner for which computer programs can be utilized efficaciously. Starting around 1960, the approved computer programs for static calculation of lattice steel towers were used in Germany [12.49] and have been steadily developed since then [12.50]. The first programs were based on conventional design procedures. Meanwhile programs based on the finite element method are used for three-dimensional analysis [12.29].
The capacity of computers can be utilized the full extent only if:

- The program flow and the correctness of the results can be validated by means of comparative calculations with low effort. The data necessary for checks should be part of the output.
- All input data, important values and all other parameters necessary for the further processing can be followed up by the outprint.
- The results are presented such that they can be understood without extensive training by each overhead line expert being civil engineer for static or transmission line engineer.

Modern computer programs for lattice towers employ a graphical interactive user interface which visualizes the design process. During the design work, it is possible to check the tower configuration and to carry out modifications, if necessary. The programs are structured into modules which ease supplementing new types of bracings, alternative angle sections, materials, new standards for calculation and rating. The programs make use of extensive databases with world-wide available steel sections, bolts, materials and type of bracings.

The geometry of the lattice tower needs to be provided for the determination of the member forces. To ease the input process, it is necessary that the tower geometry can be described by a few parameters only. By graphical presentation on the screen, simple and quick modifications of the tower geometry are possible. Programs should use a parametric structure which enables to modify parameters such as tower height, crossarm dimensions, increase of latitude of the tower body or the width at the tower base without much effort. Tower body and crossarm are divided into sections which are characterized by the same dimensions of leg members or chords. These sections are divided into panels. Each individual panel is described by its height and type of bracing. The types of bracings are characterized by parametric patterns and can be graphically inserted into the tower model. This leads to a quick and error-free generation of tower models. Members to which the same design specifications apply are automatically grouped together. Maximum permissible slenderness ratios and minimum dimensions can be stipulated for a preselection of profiles.

The analysis and design of towers can be divided into three steps. The first step is the determination of the external loads resulting from tower use, the conductoring and standards to be considered. Then, the member forces are calculated as resulting from the external load for the individual load cases taking into account the geometry and, in particular, the maximum internal load for each member is selected. Finally, the rating of each individual member follows.

The external loads are determined by the corresponding program modules based on the load cases to be considered for the individual tower types such as suspension, angle suspension, angle-strain and dead-end towers. Also the loads for complex branch-off and special towers, e. g. with cruciform crossarms can be handled by these programs. The possible applications to a certain tower tpye are subdivided into stages which are characterized by the type and arrangement of the conductors. An input information on conductors, tower type, wind and weight span length, line angle, position of the crossarms, the arrangement and type of the individual conductors, the type and data for the crossarms is required for the calculation of the external loads. If a tower is planned to serve several purposes, e. g. the purpose of an angle-strain and a dead-end support, then this can be considered by different development steps. The dead weight and the wind load acting on the tower are calculated considering the dimensions and dead weight of sections used for the individual members. The aerodynamic wind pressure can be described as a function of the height above ground. The load cases are composed based on the relevant standards or project specifications. The rules for determining the actions and combining them to load cases can be defined and stored in the program system. The adjustment to any load conditions and standard is, therefore, possible in a simple manner. The member forces are calculated on the assumption of plane trusses or following the finite element method based on a three-dimensional system.

When calculating the member forces using conventional procedures, separate program modules are used for tower bodies and crossarms, because of their geometrically different structure. The external loads are grouped together and assumed as acting on the tower body or crossarm. Each load group is defined by the forces P_x, P_y and P_z and the moments around the three axes M_x, M_y and M_z and acts at the relevant tower

height. The calculation results in compression and tensile member forces for each load case, from which the maxima are selected for each member.
Using the finite element method, the tower as a whole is considered as a three-dimensional system. Its static model is automatically produced by generation of the nodes and their connections by elements. The external loads are defined as loads acting at the nodes. The calculation as well results in compression and tensile member forces and deformations for all load cases.
For obtaining an economic tower design, an optimization is carried out in compliance with the design stipulations after having determined the member forces. For example, the design procedures according to ASCE [12.20], ECCS [12.42], DIN 18 800 [12.51, 12.52], EC 3 [12.13] and EN 50 341-1 [12.8] with the corresponding National Normative Aspects, e. g. EN 50 341-3-4 [12.10], can be carried out. A statically appropriate section is selected for the maximum tensile and compression forces considering buckling length, resistance and design details. The selected section provides the most economic solution together with the joints. A database containing available and especially custom-designed angle sections and other profiles is available for solving this task, where the profiles with differing grades of materials are grouped according to economic aspects. The database also contains all necessary static data for sections. The optimization comprises material, cross section and type of profile and its joints.
Calculation and rating of a lattice steel tower is an iterative process. At first, only the external loads exerted by the conductors are known for which a first set of member dimensions can be determined. The member forces, however, are also affected by the wind load acting on the tower structure and tower dead weight. In a second step of iterations, these data can be obtained for the cross sections selected in the preceding step. The iterative process is continued until no change of profiles will occur anymore.
An unlimited number of body extensions can be analysed after the basic type of the tower has been designed. The analysis scheme is the same as in case of the basic type. Leg extensions can also be connected to each tower basic type and each body extension. Each leg extension is analysed and rated for the most unfavourable combination of different extension lengths.
All input data and results are documented in a report organized such that it can be checked easily. The report contains as well all data necessary for the planning of the line. This is in particular true of the loads of the foundations, of compact foundations as well as of separate footings. The results comprise also the tower dead weight, a summary of the angle sections and connecting material used and the surface to be coated. Data needed for further processing are stored in a database to which other programs have access.
Tower outline drawings serve as a basis for establishing the production drawings for lattice steel towers. All necessary input data resulting from the design process are stored, thus enabling plotting of the outline drawings. Additionally, information on the arrangement of details, on scale and on drawing format are necessary. In detail, the tower body, crossarms, body extensions, leg extensions as well as horizontal bracings and three-dimensional redundant members are presented. The drawings can be passed to any CAD and CAM programs for further processing.

12.5.17 Upgrading the support strength

As a consequence of the development of electric systems with changing transmission tasks, *uprating of existing supports* for modified conductoring or *upgrading* in view of improved load assumptions might be necessary. Therefore, the *strength of leg and bracing members* is to be enhanced. No special effort is necessary to reinforce the bracings since an exchange of members with others having the required higher strength

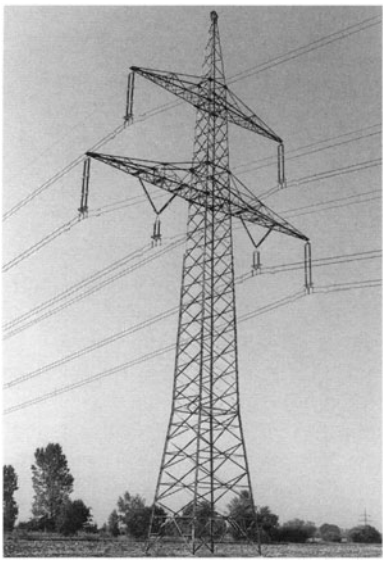

Figure 12.59: 380 kV suspension tower with reinforced leg member

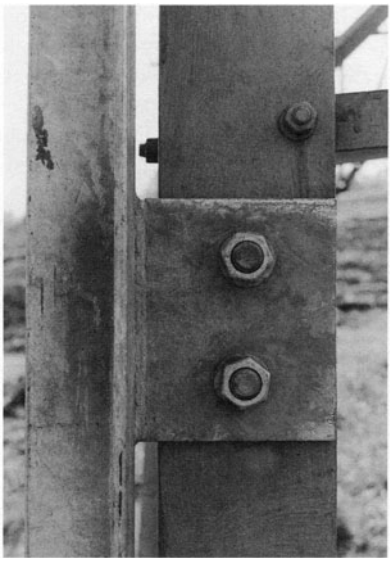

Figure 12.60: Connection of the supplemented profile

capacity is easily possible. An increase of the leg member strength can be achieved if the buckling length can be reduced by inserting additional redundant members. However, this is only possible if it suffices to increase the compression strength. A reduction of the buckling length is only effective if *flexural buckling* is prevalent. In case of *flexural torsional buckling*, the reduction of the buckling length has only a minor effect on the strength. If both the compression and tensile strength at the joints do not suffice, the installation of redundant members will not achieve the required increase of strength.

The exchange of individual leg member sections is possible only in case of suspension supports with low height. In case of tall suspension towers or supports permanently loaded by conductor tensile forces such as angle-strain towers, an *increase of the leg member strength* can be achieved by batten plates bolted with the existing leg member and supplementing angle sections to cruciform sections by an additional angle.

If the leg members should be redesigned with respect to stability, plates arranged between the nodes of leg members can solve the problem. A strengthening within the range of the nodes and across the joints is not necessary if the net cross section multiplied by the yield stress is higher than the maximum force. The connections need to be designed for a shear force equal to 2,5 % of the leg member compression force (see clause 12.5.9.1). The distance between the bolts is designed such that local buckling and opening of the plates between the bolts will be excluded and should not exceed six times the borehole diameter.

If the cross-sectional strength of the existing leg members is exhausted, a *reinforcement just by plates* does not solve the problem. The plates would have to be arranged across the nodes and joints, thus requiring that all bolts at the connections of the bracings and joints are opened resulting in an excessive installation effort.

Examples for line uprating and upgrading are presented in [12.53]. Leg members can be supplemented to *cruciform sections*. The size of the supplemented profile is selected according to static requirements. In most cases, an angle is sufficient with a smaller cross section than that of the existing leg member. In Figure 12.59 a 380 kV suspension tower is shown, where the existing L120 × 12 leg member profiles have been reinforced

by additional L70 × 7 angle sections below the lower crossarm. The profiles are joined by batten plates arranged at least at one third of the buckling length. The thickness of the batten plates depends on the design of the existing joints and is selected such that the supplemented angle section passes the joints without any constraint. The distance between the joint material and the *supplemented angle section* should be wide enough to compensate potential tolerances due to the production and assembling. However, the distances should not be too wide since the thickness of the batten plates affects the total weight of the necessary reinforcement material to a large extent.

It is preferable to weld the batten plate at the circumference with fillet seams to the supplemented sections in the workshop and adjust them to the leg members of the existing towers at site (Figure 12.60). An integrated load carrying by both sections will be guaranteed only if their relative movement is kept to a minimum. This requirement is not complied with by a shearing-bearing connection with black bolts for the jointing between the existing leg member and the supplemented sections. Therefore, *fitted bolts* or *slip-resistant connections* should be selected. Connection by welding should not be adopted because of the costly execution and the infringement of the galvanized material. A slip-resistant, prestressed bolted connection with high-strength bolts requires a preparation of the surface which could be carried out with significant difficulties only at the galvanized structure. Good experience has been gained by the use of fitted bolts. The boreholes are produced with drilling machines fixed to the leg members by strong magnets adopting core drills. By a precise installation, the permissible borehole tolerances can be met and reaming of the boreholes can be waived.

Paper [12.54] describes supplementing of existing leg members to *cruciform sections*. The plates between existing and supplemented leg member sections were fixed to existing bracing connections. No new boreholes were necessary in this case. The bolts of the bracing connections were removed, the batten plate was inserted and new, longer bolts were installed. Bolts with the grade 8.8 or 10.9 were used to ensure the load transfer to the added angle sections.

Addition of an angle section moves the centroidal axis of the leg members outwards. For common calculation it is assumed that the leg member force is equally distributed on the *composite section*, e. g. the axial load within the leg member is distributed in relation to the cross-sectional areas. However, the existing leg member will not be unloaded when the additional section is installed because the support is loaded by permanent loads, wind loads and conductor tensile forces depending on the type of supports. This initial condition leads to a higher proportionate axial force in the existing leg member and a lower one in the supplemented section. Eventually, the supplemented profile will not carry a proportionate load. To take care of this load features, an assumption on the installation condition should be made.

The increased foundation loads need to be transferred to the foundations as well. The supplemented angles are embedded into the *foundations* such that their proportion of the force will be completely transferred to the foundation. In some cases it might be necessary to supplement the reinforcement as well. Then, the foundation muffs are removed and concreted anew after installing the supplemented leg members. According to [12.54], a concrete core drill procedure can be applied as well. By means of hydraulically driven core drill devices, boreholes with 180 mm diameter and a depth of 1,20 m are drilled beneath the existing leg member and the core is broken out. After installing the leg member stub in the borehole, the hole is filled up with grout concrete.

12.5.18 Example: Static calculation of a 110 kV suspension support

Analysis of a suspension tower for two circuits 110 kV arranged in Danube configuration according to EN 50341-1 and EN 50341-3-4 (Figure 12.61).

Conductors: 1 earth wire 97-AL1/56-ST1A (Al/St 95/55), 6 conductors 231-AL1/30-ST1A (Al/St 230/30),
Preliminary installation: one circuit on one side of the tower body and one earth wire.
Span lengths: wind span 380 m, maximum weight span $1{,}5 \cdot 380 = 570$ m, minimum weight span $0{,}5 \cdot 380 = 190$ m.

Conductor data		97-AL1/56-ST1A	231-AL1/30-ST1A
Total cross section	mm^2	152,8	260,8
Diameter	mm	16,0	21,0
Weight	kg/m	0,714	0,874
Ice load (ice load zone 1)	N/m	6,60	7,10
Weight with ice load	N/m	13,60	15,67
Conductor stress	N/mm^2	123,0	85,0
Conductor tensile force	kN	18,79	22,17
Insulators (double suspension sets):			
Weight	N		800
Weight with ice load	N		1000
Wind load	N		250

Maximum tower body extension T 37,0

Suspension heights: Earth wire 45,80 m
Phase conductor upper crossarm 40,80 m
Phase conductor lower crossarm 37,00 m

In the example, wind and ice load zone 1 according to [12.10] are considered.
Vertical loads:
Conductor and insulator weights:

Earth wire:	without ice load $m_C g = 9{,}81 \cdot 0{,}714 = 7{,}004$ N/m with ice load $m_{CI} g = 7{,}004 + 6{,}6 = 13{,}604$ N/m	
Vertical load	max	min
Without ice load	$570 \cdot 7{,}004 = 3{,}99$ kN	$190 \cdot 7{,}004 = 1{,}33$ kN
With ice load	$570 \cdot 13{,}604 = 7{,}75$ kN	$190 \cdot 13{,}604 = 2{,}58$ kN
Phase conductor:	without ice load $m_C g = 9{,}81 \cdot 0{,}874 = 8{,}574$ N/m with ice load $m_{CI} g = 8{,}574 + 7{,}10 = 15{,}674$ N/m	
Vertical load	max	min
Without ice load	$570 \cdot 8{,}574 = 4{,}89$ kN	$190 \cdot 8{,}574 = 1{,}63$ kN
Insulation	$= 0{,}80$ kN	$= 0{,}80$ kN
	$= 5{,}69$ kN	$= 2{,}43$ kN
With ice load	$570 \cdot 15{,}674 = 8{,}93$ kN	$190 \cdot 15{,}674 = 2{,}98$ kN
Insulation	$= 1{,}00$ kN	$= 1{,}00$ kN
	$= 9{,}93$ kN	$= 3{,}98$ kN

Tower dead weights: earth wire peak: 1,30 kN; crossarm 1: 3,50 kN; crossarm 2: 5,20 kN; tower section 1: 4,00 kN; tower section 2: 5,70 kN; tower section 3: 8,20 kN; tower section 4: 9,50 kN; tower in total: 37,40 kN.
Horizontal loads:
Wind load on conductors:
Earth wire: $z = 45{,}80$ m; $q_z = 800 + 3 \cdot 45{,}80 = 937{,}4$ N/m^2
Wind load rectangularly to line ($\phi = 0°$):

$$Q_{WC\perp} = 937{,}4 \cdot 1{,}0 \cdot 0{,}016 \cdot 380\,(0{,}45 + 60/380) = 3{,}46 \text{ kN}$$

Diagonal wind ($\phi = 45°$):

$$Q_{WCE} = 937{,}4 \cdot 1{,}0 \cdot 0{,}016 \cdot \cos^2 45° \cdot 380\,(0{,}45 + 60/380) = 1{,}73 \text{ kN}$$

Wind load on the ice-covered earth wire: $d_I = \sqrt{16^2 + 6{,}6 \cdot 4/(0{,}0075 \cdot \pi)} = 37{,}10$ mm.
Wind load rectangularly to the line ($\phi = 0°$):

$$Q_{WC\perp} = 0{,}5 \cdot 937{,}4 \cdot 1{,}0 \cdot 0{,}0371 \cdot 380\,(0{,}45 + 60/380) = 4{,}02 \text{ kN}.$$

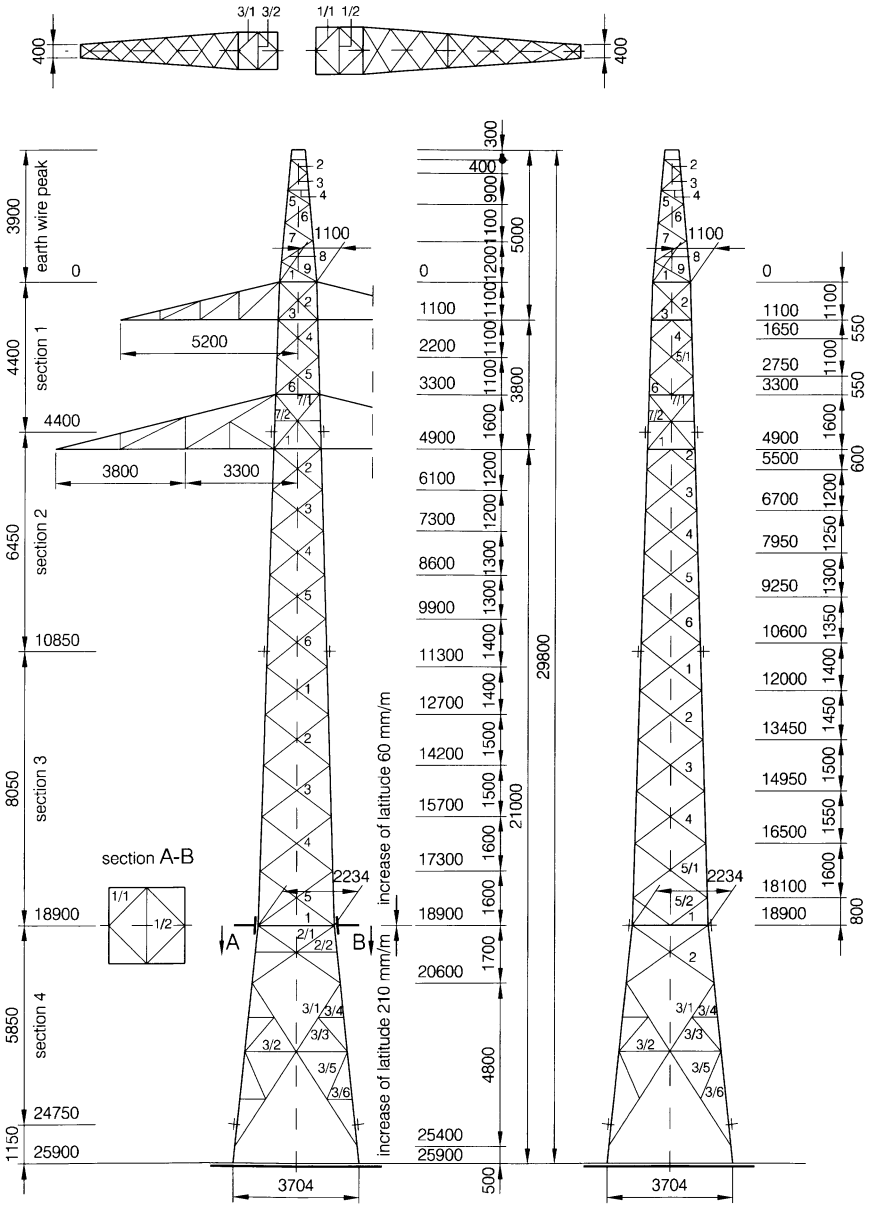

Figure 12.61: Suspension tower for a 110 kV line

Diagonal wind ($\phi = 45°$):

$$Q_{\mathrm{WCE}} = 0{,}5 \cdot 937{,}4 \cdot 1{,}0 \cdot 0{,}0371 \cdot \cos^2 45° \cdot 231 = 2{,}01 \text{ kN}.$$

Phase conductors upper crossarm: $z = 40{,}80$ m; $q_z = 800 + 3 \cdot 40{,}80 = 922{,}4$ N/m^2.
Wind load rectangularly to the line ($\phi = 0°$):

$$Q_{\mathrm{WC}\perp} = 922{,}4 \cdot 1{,}0 \cdot 0{,}021 \cdot 380\,(0{,}45 + 60/380) = 4{,}47 \text{ kN}.$$

Diagonal wind ($\phi = 45°$):

$$Q_{\mathrm{WCE}} = 922{,}4 \cdot 1{,}0 \cdot 0{,}021 \cdot \cos^2 45° \cdot 231 = 2{,}24 \text{ kN}.$$

Wind on ice-covered phase conductors: $d_{\mathrm{I}} = \sqrt{21^2 + 7{,}1 \cdot 4/(0{,}0075 \cdot \pi)} = 40{,}58$ mm.
Wind rectangularly to the line($\phi = 0°$):

$$Q_{\mathrm{WC}\perp} = 0{,}5 \cdot 922{,}4 \cdot 1{,}0 \cdot 0{,}04058 \cdot 231 = 4{,}32 \text{ kN}.$$

Quartering wind ($\phi = 45°$):

$$Q_{\mathrm{WCE}} = 0{,}5 \cdot 922{,}4 \cdot 1{,}0 \cdot 0{,}04058 \cdot \cos^2 45° \cdot 231 = 2{,}16 \text{ kN}.$$

Phase conductor lower crossarm: $z = 37{,}0$ m; $q_z = 800 + 3 \cdot 37 = 911$ N/m^2.
Wind rectangularly to the line($\phi = 0°$):

$$Q_{\mathrm{WC}\perp} = 911 \cdot 1{,}0 \cdot 0{,}021 \cdot 380\,(0{,}45 + 60/380) = 4{,}42 \text{ kN}.$$

Diagonal wind ($\phi = 45°$):

$$Q_{\mathrm{WCE}} = 911 \cdot 1{,}0 \cdot 0{,}021 \cdot \cos^2 45° \cdot 231 = 2{,}21 \text{ kN}.$$

Wind on phase conductors with ice rectangularly to the line ($\phi = 0°$):

$$Q_{\mathrm{WC}\perp} = 0{,}5 \cdot 911 \cdot 1{,}0 \cdot 0{,}04058 \cdot 231 = 4{,}27 \text{ kN}.$$

Diagonal wind on phase conductors with ice ($\phi = 45°$):

$$Q_{\mathrm{WCE}} = 0{,}5 \cdot 911 \cdot 1{,}0 \cdot 0{,}04058 \cdot \cos^2 45° \cdot 231 = 2{,}13 \text{ kN}.$$

Wind on tower:
earth wire peak: $A_{\mathrm{w}\perp} \approx A_{\mathrm{w}\parallel} = 2 \cdot 3{,}9 \cdot 0{,}05 + 6{,}1 \cdot 0{,}035 = 0{,}60$ m^2;

$z = 42{,}4$ m; $q_z = 800 + 3 \cdot 42{,}4 = 927$ N/m^2;

$$Q_{\mathrm{WM}\perp} = Q_{\mathrm{WM}\parallel} = 0{,}60 \cdot 2{,}8 \cdot 927 = 1{,}56 \text{ kN};\ Q_{\mathrm{WME}} = 1{,}2 \cdot 0{,}707 \cdot Q_{\mathrm{WM}\perp} = 1{,}32 \text{ kN}.$$

tower section 1: $A_{\mathrm{w}\perp} \approx A_{\mathrm{w}\perp} = 2 \cdot 4{,}9 \cdot 0{,}06 + 2 \cdot 4{,}9 \cdot 0{,}035 + 2 \cdot 0{,}7 \cdot 0{,}040 + 2 \cdot 2{,}1 \cdot 0{,}045 + 2 \cdot 2{,}3 \cdot 0{,}05 + 1{,}9 \cdot 0{,}06 = 1{,}51$ m^2;

$z = 37{,}7$ m; $q_z = 800 + 3 \cdot 37{,}7 = 913$ N/m^2;

$\phi = 0°$: $Q_{\mathrm{WM}\perp} = 1{,}51 \cdot 2{,}8 \cdot 913 = 3{,}86$ kN; $Q_{\mathrm{WM}\parallel} = 0$.
$\phi = 90°$: $Q_{\mathrm{WM}\perp} = 0$; $Q_{\mathrm{WM}\parallel} = 3{,}86$ kN.
$\phi = 45°$: $Q_{\mathrm{WM}\perp} = 1{,}2 \cdot 3{,}86 \cdot 0{,}707 = 3{,}27$ kN; $Q_{\mathrm{WM}\parallel} = 1{,}2 \cdot 3{,}86 \cdot 0{,}707 = 3{,}27$ kN.

tower section 2: $A_{\mathrm{w}\perp} \approx A_{\mathrm{w}\perp} = 2 \cdot 6{,}4 \cdot 0{,}075 + 2 \cdot 9{,}5 \cdot 0{,}04 + 1{,}4 \cdot 0{,}06 = 1{,}80$ m^2;

$z = 31{,}3$ m; $q_z = 800 + 3 \cdot 31{,}3 = 894$ N/m^2;

$\phi = 0°$: $Q_{\mathrm{WM}\perp} = 1{,}80 \cdot 2{,}8 \cdot 894 = 4{,}51$ kN; $Q_{\mathrm{WM}\parallel} = 0$.
$\phi = 90°$: $Q_{\mathrm{WM}\perp} = 0$; $Q_{\mathrm{WM}\parallel} = 4{,}51$ kN.
$\phi = 45°$: $Q_{\mathrm{WM}\perp} = Q_{\mathrm{WM}\parallel} = 1{,}2 \cdot 4{,}51 \cdot 0{,}707 = 3{,}83$ kN.

tower section 3: $A_{\mathrm{w}\perp} \approx A_{\mathrm{w}\perp} = 2 \cdot 7{,}6 \cdot 0{,}1 + 2 \cdot 12{,}6 \cdot 0{,}04 + 2{,}2 \cdot 0{,}06 = 2{,}66$ m^2;

$z = 26{,}6$ m; $q_z = 800 + 3 \cdot 26{,}6 = 880$ N/m^2;

$\phi = 0°$: $Q_{WM\perp} = 2{,}66 \cdot 2{,}8 \cdot 880 = 6{,}55$ kN; $Q_{WM\parallel} = 0$.
$\phi = 90°$: $Q_{WM\perp} = 0$; $Q_{WM\parallel} = 6{,}55$ kN.
$\phi = 45°$: $Q_{WM\perp} = Q_{WM\parallel} = 1{,}2 \cdot 6{,}55 \cdot 0{,}707 = 5{,}56$ kN.

tower section 4: $A_{w\perp} \approx A_{w\perp} = 2 \cdot 6{,}5 \cdot 0{,}11 + 2 \cdot 4{,}1 \cdot 0{,}05 + 2 \cdot 5{,}7 \cdot 0{,}06 + 2 \cdot 1{,}5 \cdot 0{,}055 + 2 \cdot 1{,}5 \cdot 0{,}04 + 2 \cdot 2{,}8 \cdot 0{,}035 = 2{,}99$ m^2;

$z = 23{,}1$ m; $q_z = 800 + 3 \cdot 23{,}1 = 869$ N/m^2;

$\phi = 0°$: $Q_{WM\perp} = 2{,}99 \cdot 2{,}8 \cdot 869 = 7{,}28$ kN; $Q_{WM\parallel} = 0$.
$\phi = 90°$: $Q_{WM\perp} = 0$; $Q_{WM\parallel} = 7{,}28$ kN.
$\phi = 45°$: $Q_{WM\perp} = Q_{WM\parallel} = 1{,}2 \cdot 7{,}28 \cdot 0{,}707 = 6{,}17$ kN.

crossarm 1: $A_{w\parallel} = 4{,}7 \cdot 0{,}06 + 4{,}8 \cdot 0{,}05 + 6{,}0 \cdot 0{,}035 = 0{,}73$ m^2;

$z = 41{,}2$ m; $q_z = 800 + 3 \cdot 41{,}2 = 924$ N/m^2;

$\phi = 0°$: $Q_{WM\perp} = 2 \cdot 0{,}4 \cdot 924 \cdot 0{,}73 \cdot 2{,}8 \cdot \cos^2 0° = 1{,}51$ kN; $Q_{WM\parallel} = 0$.
$\phi = 90°$: $Q_{WM\perp} = 0$; $Q_{WM\parallel} = 2 \cdot 924 \cdot 0{,}73 \cdot 2{,}8 \cdot \sin^2 90° = 3{,}78$ kN.
$\phi = 45°$: $Q_{WM\perp} = 1{,}51 \cdot \cos^2 45° = 0{,}76$ kN; $Q_{WM\parallel} = 3{,}78 \cdot \sin^2 45° = 1{,}89$ kN.

crossarm 2: $A_{w\parallel} = 6{,}5 \cdot 0{,}065 + 6{,}7 \cdot 0{,}05 + 9{,}1 \cdot 0{,}035 = 1{,}08$ m^2;

$z = 37{,}5$ m; $q_z = 800 + 3 \cdot 37{,}5 = 913$ N/m^2;

$\phi = 0°$: $Q_{WM\perp} = 2 \cdot 0{,}4 \cdot 913 \cdot 1{,}08 \cdot 2{,}8 = 2{,}21$ kN; $Q_{WM\parallel} = 0$.
$\phi = 90°$: $Q_{WM\perp} = 0$; $Q_{WM\parallel} = 2 \cdot 913 \cdot 1{,}08 \cdot 2{,}8 = 5{,}52$ kN.
$\phi = 45°$: $Q_{WM\perp} = 2{,}21 \cdot 0{,}5 = 1{,}11$ kN; $Q_{WM\parallel} = 5{,}52 \cdot 0{,}5 = 2{,}76$ kN.

Differences in conductor tensile forces:
Load case J:
Earth wire: $S_L = 0{,}65 \cdot 152{,}8 \cdot 123{,}0 = 12{,}22$ kN; phase conductors: $S_L = 0{,}5 \cdot 260{,}8 \cdot 85{,}0 = 11{,}08$ kN.
Load case K
Earth wire: $S_L = 0{,}4 \cdot 152{,}8 \cdot 123{,}0 = 7{,}52$ kN; phase conductors: $S_L = 0{,}2 \cdot 260{,}8 \cdot 85{,}0 = 4{,}43$ kN.

Load cases

The individual loads are combined to load cases according to clause 12.4. Figure 12.62 shows the characteristic values and Figure 12.63 the design values of the loads for the individual load cases. If only one circuit is installed, the loads on just one tower side act (Figure 12.64). The design values were calculated considering the partial factors according to EN 50341-3-4 (see clause 12.4.8).

Design of a crossarm

As an example, the upper crossarm of the 110 kV tower is verified. Figure 12.65 shows the dimensions of the crossarm.
The load cases to be considered are represented in Figure 12.66. The dead weight of 3,5 kN will be distributed equally on the attachment points of the bracings in the vertical crossarm face. The load cases D, L and I might be prevalent. For load case L, the vertical load will be carried only by one face of the vertical truss after failing of one insulator string. This condition is covered by load case J. In load case I, the construction load 1,5 kN is assumed as acting alternatively at the nodes of the vertical truss.
The force in the upper chord results from (12.31) for the load case L, whereby the force of 9,93 kN is carried by one lower chord only:

$$O = [9{,}93 \cdot 4{,}62 + 0{,}9/2\,(4{,}62 + 3{,}47 + 2{,}32 + 1{,}17)]\,1{,}023/1{,}069 = 48{,}9 \text{ kN} \quad .$$

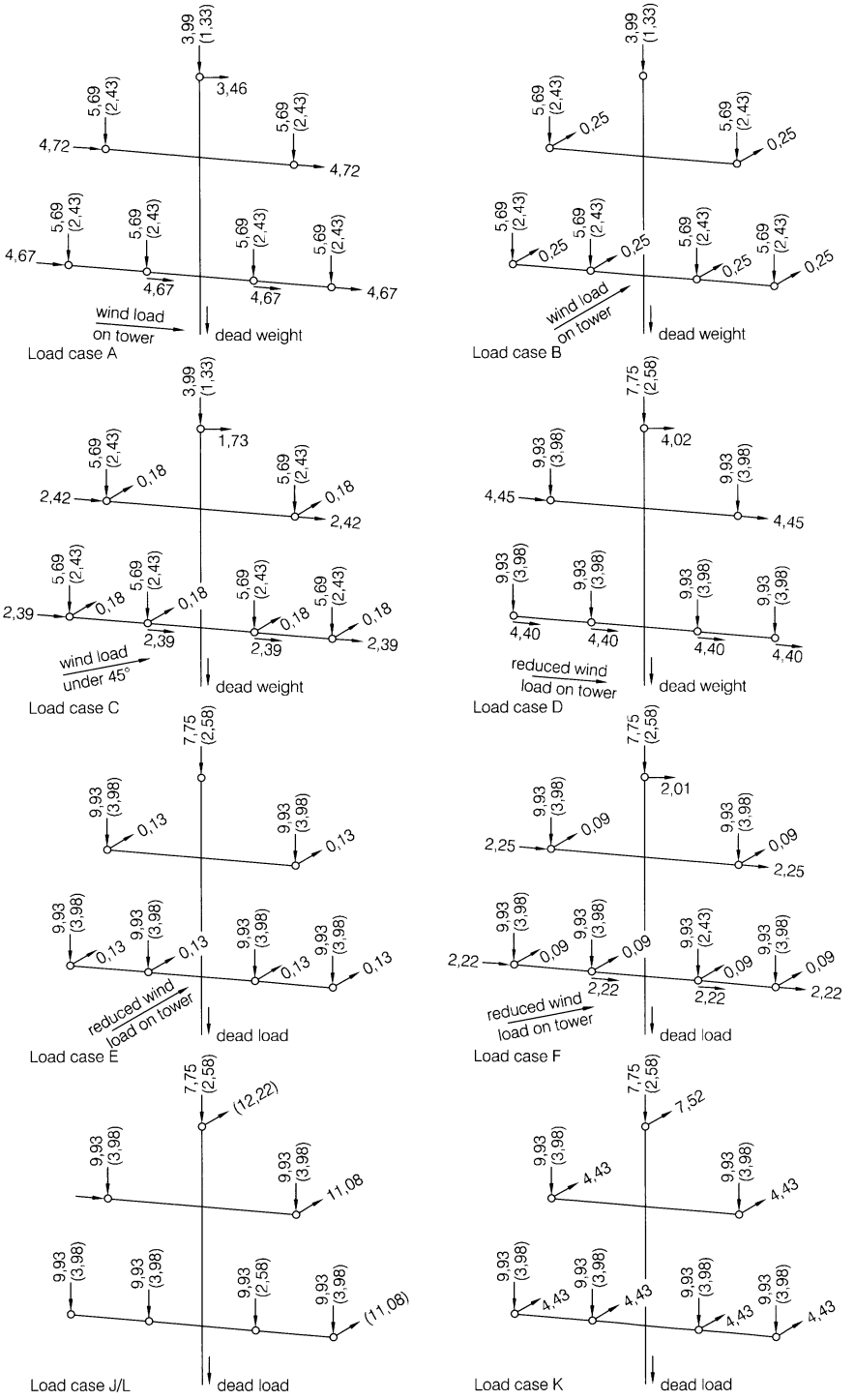

Figure 12.62: Characteristic values of forces for the considered load cases (according to EN 50 341-3-4)

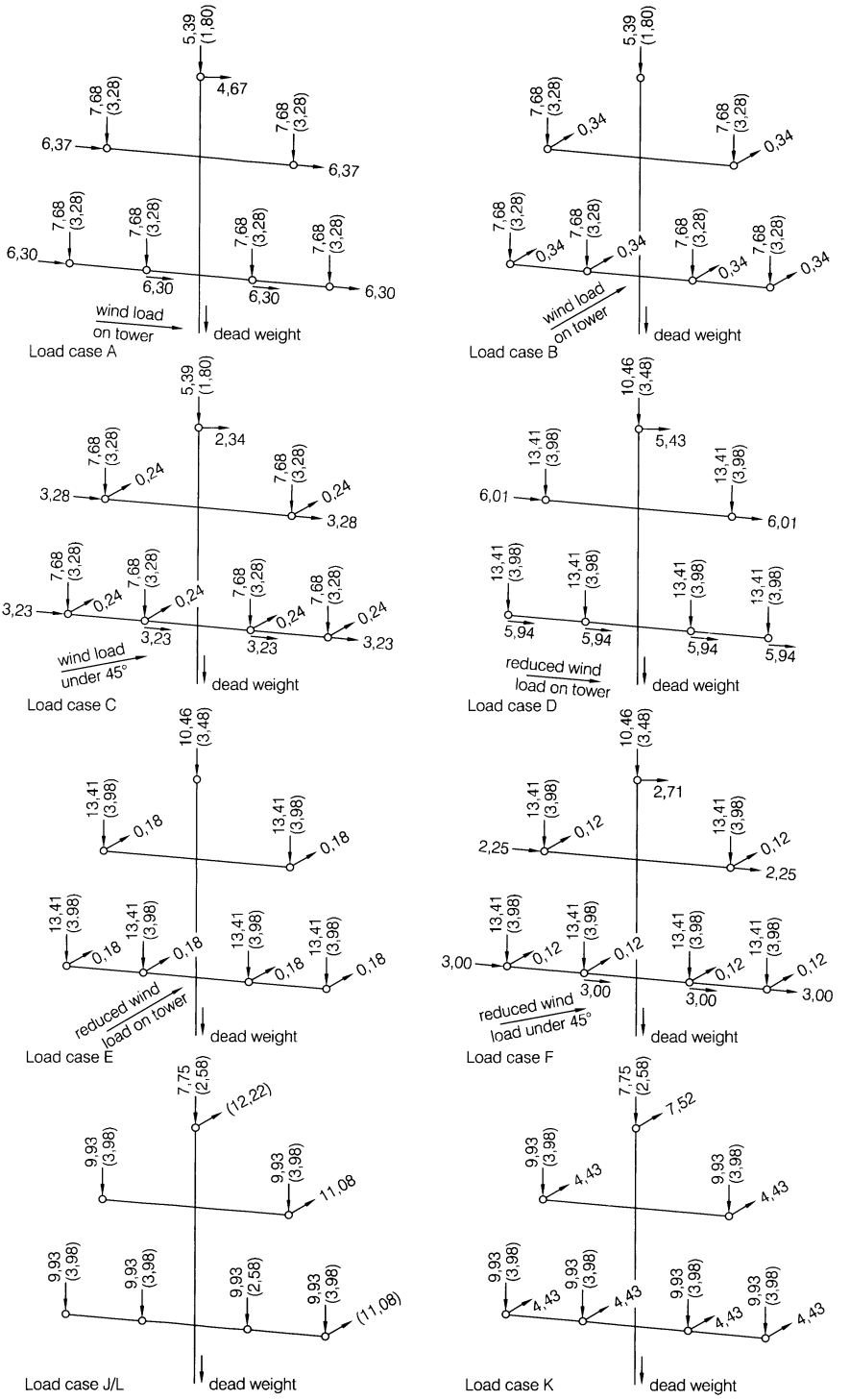

Figure 12.63: Design values of forces according to the considered load cases; two circuits installed

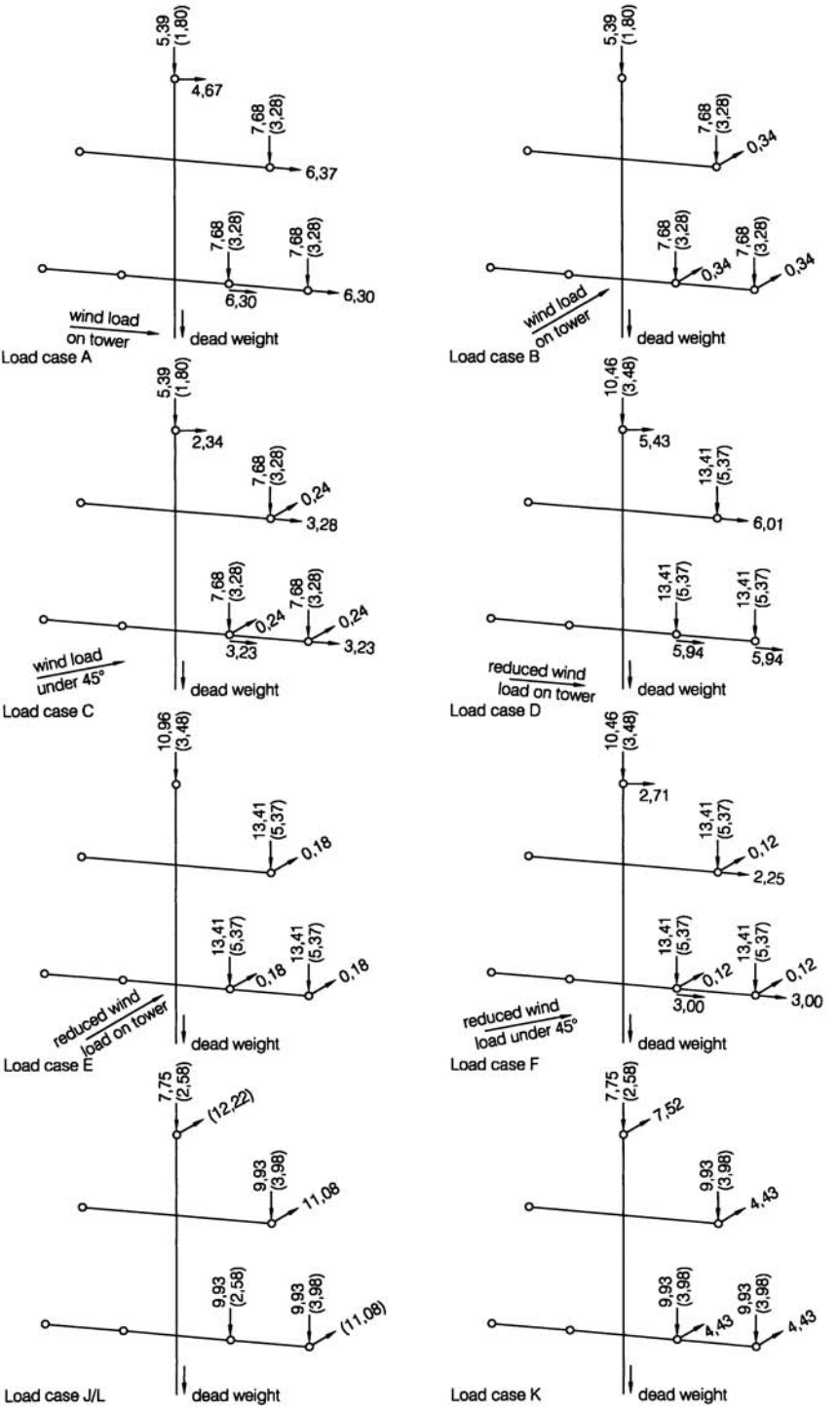

Figure 12.64: Design values of forces according to the considered load cases; one circuit installed only

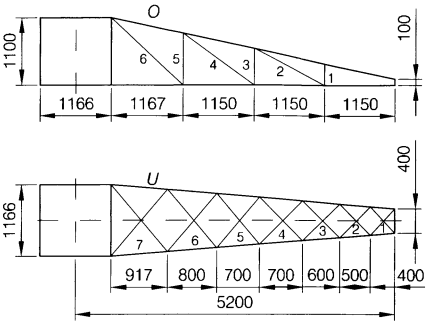

Figure 12.65: Dimensions of upper crossarm

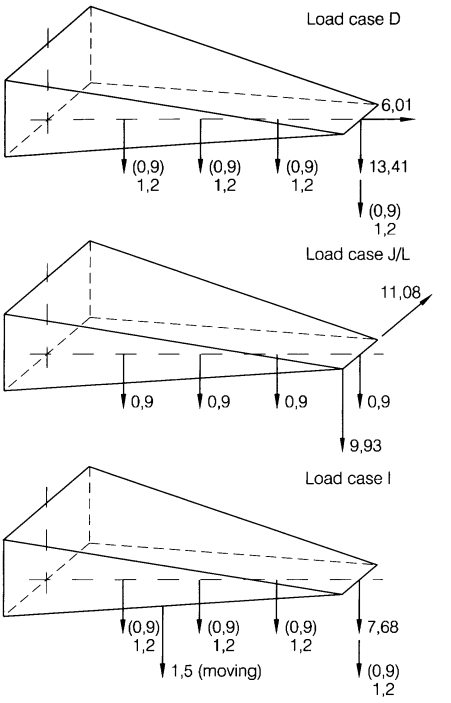

Figure 12.66: Load cases for upper crossarm (the forces shown represent design values)

The geometric data used in (12.31) result from Figure 12.65 considering the centroidal axis of the profile to be:

$$h_i = 4{,}617 \text{ m}; \quad b_i = b_n = 1{,}1 - 0{,}0169 - 0{,}014 = 1{,}069 \text{ m},$$
$$b_0 = 0{,}1 - 0{,}0169 - 0{,}014 = 0{,}069 \text{ m},$$
$$\Delta/2 = 0{,}03 \text{ m/m}.$$

The compression and tensile force of the lower chord result from (12.17) and (12.29), respectively, using $b = 1{,}051$ m and $h = 4{,}13$ related to the crossing point of the bracings within the panel adjacent to the tower body to be:
Compression force

$$U_D = -(11{,}08 \cdot 4{,}13)/1{,}051 - [9{,}93 \cdot 4{,}62 + (4{,}62 + 3{,}47 + 2{,}32 + 1{,}17)0{,}9/2]/1{,}069$$
$$= -91{,}3 \text{ kN}$$

and tensile force

$$U_Z = (11{,}08 \cdot 4{,}13)/1{,}051 - 0{,}9\,(4{,}62 + 3{,}47 + 2{,}32 + 1{,}17)/(2 \cdot 1{,}069) = 38{,}7 \text{ kN}.$$

Since only one face carries the load, it applies to double warren in the horizontal crossarm face according to (12.20)

$$D_i = l_{di} \cdot P \cdot b/(2\, b_{oi} \cdot b_{ui}) \quad .$$

The load case J is prevalent. The product $P \cdot b$ results to be

$$P \cdot b = 11{,}08 \cdot (0{,}4 - 2\,e) = 11{,}08 \cdot (0{,}4 - 2 \cdot 0{,}0169) = 11{,}08 \cdot 0{,}366 = 4{,}06 \text{ kNm}.$$

All dimensions are related to the centroidal axes of the static system. The distance of the centroidal axes of lower chords needs to be evaluated from the overall dimensions. Table 12.15 contains the geometric data and the forces calculated, thereof.

Table 12.15: Calculated member design forces of the diagonals in the crossarm horizontal face

Diagonal	b_{ui} m	b_{oi} m	h_i m	l_{di} m	D_i kN
1	0,366	0,432	0,400	0,565	±7,25
2	0,432	0,515	0,500	0,688	±6,28
3	0,515	0,615	0,600	0,824	±5,28
4	0,615	0,731	0,700	0,971	±4,38
5	0,731	0,847	0,700	1,055	±3,46
6	0,847	0,980	0,800	1,214	±2,97
7	0,980	1,132	0,917	1,390	±2,55

Table 12.16: Calculated design member forces of the members in the crossarm vertical face

Member	①	②	③	LC[1] L $\sum S_v \cdot v/2$	LC[1] I $\sum S_v \cdot v/2$	Member force V_i LC[1] L kN	LC[1] I kN
1	0,32	0,32	1,47	3,322	1,901	−2,26	−1,29
2	0,564	1,281	1,47	3,983	4,508	6,15	6,96
3	0,564	0,564	2,62	3,983	4,508	−1,52	−1,72
4	0,811	1,407	2,62	5,162	7,805	3,42	5,17
5	0,811	0,811	3,77	5,162	7,805	−1,37	−2,07
6	1,069	1,607	3,77	6,859	11,792	2,74	4,70

Column ① b_i and b_{i+1}, respectively,
Column ② $\sqrt{b_i^2 + (h_{i+1} - h_i)^2}$ and $\sqrt{b_{i+1}^2 + (h_{i+1} - h_i)^2}$, respectively,
Column ③ $v + h_i$ and $v + h_{i+1}$, respectively.
[1] LC = load case

The member forces in the vertical face result from (12.32) and (12.33). There, load case L or I may be governing. In Table 12.16 the calculation is demonstrated. The value v is obtained from

$$v = (4{,}617 + 1{,}069 \cdot 0{,}03)/(1{,}069 - 0{,}069) \cdot 0{,}069 = 0{,}32 \text{ m}.$$

With the member forces, the rating of angles can be carried out. The buckling length for the bracings in the horizontal crossarm face can be obtained from

$$s_K = l_{di} \cdot b_{oi}/(b_{oi} + b_{ui}) \quad .$$

For example, it is obtained for the member D_3:

$$s_K = 0{,}824 \cdot 0{,}615/(0{,}515 + 0{,}615) = 0{,}45 \text{ m}.$$

In Tables 12.17 and 12.18, the results are presented. The resistance of the members and connections are not exceeded. For all angle sections, the steel grade S235 with $f_y = 235$ N/mm^2 and $f_u = 360$ N/mm^2 is used. All bolts are provided with grade 5.6. The compression strength is determined using equation (12.60) for flexural buckling. Flexural torsional buckling is not governing here. The upper chord is jointed with three bolts arranged in one angle leg. The net cross-sectional area for the upper chord is determined using equation (12.98). The members in the horizontal crossarm face and the vertical faces are connected by one bolt only. The net cross-sectional area is computed according to equation (12.97). In case of shearing, it is assumed that the shear planes pass through the unthreaded bolt shank. The factor $\alpha_b = 1{,}61$ is considered for the bearing resistance according to equations (12.106) and (12.110). For verification of bending due to construction load, the buckling length of the diagonal members in the horizontal face is governing. The requirements are complied with if the permissible bending length l_{max} given in Table 12.14 is not exceeded.
As an example, the rating of bracing V_5 in the vertical face is detailed here.

Effective cross section (12.56): $\overline{\lambda}_p = 0{,}0035\sqrt{235} \cdot 35/5 = 0{,}38$
According to Table 12.8: $\overline{\lambda}_p < 0{,}91, \varrho = 1{,}0;\ A_{eff} = A = 267$ mm^2

Table 12.17: Rating of members and connections of crossarm

Member	Angle section	Joints	Cross section		Buckling length	Radius of gyration	Slenderness ratio	Buckling coefficient	Permissible length in case of bending
			A mm^2	A_{net} mm^2	m	cm	λ	κ	m
O	L50 × 5	3 M 12	480	310	—	—	—	—	—
U	L60 × 6	3 M 16	691	438	0,92	1,17	79	0,639	—
D_1	L35 × 4	1 M 12	267	88	0,31	0,68	46	0,851	0,57
D_2	L35 × 4	1 M 12	267	88	0,37	0,68	54	0,798	0,57
D_3	L35 × 4	1 M 12	267	88	0,45	0,68	66	0,722	0,57
D_4	L35 × 4	1 M 12	267	88	0,53	0,68	78	0,643	0,57
D_5	L40 × 4	1 M 12	308	108	0,57	0,78	73	0,676	0,75
D_6	L40 × 4	1 M 12	308	108	0,65	0,78	83	0,608	0,75
D_7	L45 × 4	1 M 12	349	128	0,75	0,88	85	0,595	0,95
V_1	L35 × 4	1 M 12	267	88	0,32	0,68	47	0,842	—
V_2	L35 × 4	1 M 12	267	88	—	—	—	—	—
V_3	L35 × 4	1 M 12	267	88	0,56	0,68	82	0,614	—
V_4	L35 × 4	1 M 12	267	88	—	—	—	—	—
V_5	L35 × 4	1 M 12	267	88	0,81	0,68	119	0,402	—
V_6	L35 × 4	1 M 12	267	88	—	—	—	—	—

Table 12.18: Rating of members and connections of crossarm

Member	Loading		Resistance			
	Tension kN	Compression kN	Compression kN	Tension kN	Shearing kN	Bearing kN
O	48,90	—	—	80,35	81,43	83,46
U	38,70	91,30	94,30	113,61	144,76	133,54
D_1	7,25	7,25	48,55	22,81	27,14	22,26
D_2	6,28	6,28	45,49	22,81	27,14	22,26
D_3	5,28	5,28	41,17	22,81	27,14	22,26
D_4	4,38	4,38	36,70	22,81	27,14	22,26
D_5	3,46	3,46	44,47	27,99	27,14	22,26
D_6	2,97	2,97	39,98	27,99	27,14	22,26
D_7	2,55	2,55	44,38	33,18	27,14	22,26
V_1	—	2,26	48,05	22,81	27,14	22,26
V_2	6,96	—	—	22,81	27,14	22,26
V_3	—	1,72	35,03	22,81	27,14	22,26
V_4	5,17	—	—	22,81	27,14	22,26
V_5	4,06	2,07	22,96	22,81	27,14	22,26
V_6	4,70	—	—	22,81	27,14	22,26

Buckling resistance

Slenderness ratio (12.65): $\lambda = 81/0{,}68 = 119{,}12$

Non-dimensional slenderness (12.62): $\overline{\lambda} = 119{,}12/\pi \cdot \sqrt{235/210\,000} = 1{,}268$

Buckling reduction factor

According to (12.64): $\phi = 0{,}5[1 + 0{,}49(1{,}268 - 0{,}2) + 1{,}268^2] = 1{,}566$

According to (12.63): $\kappa = 1/\left(1{,}566 + \sqrt{1{,}566^2 - 1{,}268^2}\right) = 0{,}402$

Resistance according to (12.60): $N_{\mathrm{Rd}} = 0{,}402 \cdot 267 \cdot 235/1{,}1 = 22{,}96$ kN

Tension resistance:

According to EN 50 341-3-4, the design tension resistance of angle calculated according to (12.97) needs to be reduced by 10 %

$$N_{\mathrm{Rd}} = 0{,}9(35 - 13)4 \cdot 360/1{,}25 = 22{,}81 \text{ kN}$$

Shear resistance (12.104): $F_{\mathrm{v\,Rd}} = 0{,}6 \cdot 12^2 \cdot \pi/4 \cdot 500/1{,}25 = 27{,}14$ kN

Bearing resistance:

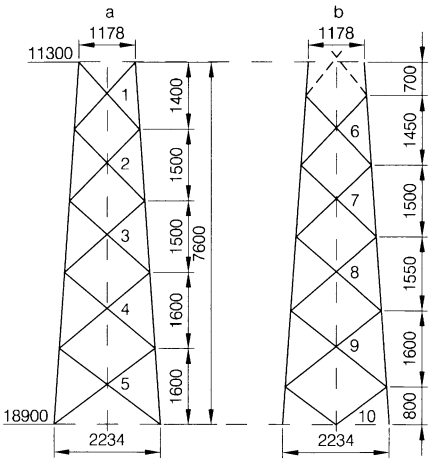

Figure 12.67: Dimensions of section 3:
a face rectangularly to line;
b face in parallel to line

The bearing resistance coefficient α_b is calculated according to (12.107), (12.108) and (12.110) considering the selected end distance in direction of the force $e_1 = 1{,}5\,d_0$ and the edge distance rectangularly to the direction of force $e_2 = 1{,}2\,d_0$ as specified in EN 50341-3-4 [12.10].

$$\alpha_b = 1{,}20 \cdot 1{,}5 \qquad = 1{,}80$$

$$\alpha_b = 1{,}85 \cdot (1{,}5 - 0{,}5) = 1{,}85$$

$$\alpha_b = 2{,}30 \cdot (1{,}2 - 0{,}5) = 1{,}61$$

The minimum value $\alpha_b = 1{,}61$ is governing.
Bearing resistance: $F_{b\,Rd} = 1{,}61 \cdot 12 \cdot 4 \cdot 360/1{,}25 = 22{,}26$ kN

Design of a tower section

As an example, the tower section 3 is designed. In Figure 12.67, the dimensions of this section are shown.

Leg members
Vertical forces:

Without ice load
all circuits installed $S_{V\,max} = 1{,}35 \cdot 27{,}9 + 5{,}39 + 6 \cdot 7{,}68 = 89{,}14$ kN,
$S_{V\,min} = 27{,}9 + 1{,}33 + 6 \cdot 2{,}43 = 43{,}81$ kN.
only one circuit installed $S_{V\,max} = 1{,}35 \cdot 27{,}9 + 5{,}39 + 3 \cdot 7{,}68 = 66{,}10$ kN,
$S_{V\,min} = 27{,}9 + 1{,}33 + 3 \cdot 3{,}28 = 39{,}07$ kN.

With ice load
all circuits installed $S_{V\,max} = 1{,}35 \cdot 27{,}9 + 10{,}46 + 6 \cdot 13{,}41 = 128{,}59$ kN,
$S_{V\,min} = 27{,}9 + 2{,}58 + 6 \cdot 3{,}98 = 54{,}36$ kN,
only one circuit installed $S_{V\,max} = 1{,}35 \cdot 27{,}9 + 10{,}46 + 3 \cdot 13{,}41 = 88{,}36$ kN,
$S_{V\,min} = 27{,}9 + 2{,}58 + 3 \cdot 5{,}37 = 46{,}59$ kN,

Leg member forces
The calculation of the moments is presented in Table 12.19. The leg member forces result from (12.18).

Load case A
$$S_E = \pm\frac{937{,}52}{2 \cdot 2{,}13} - \frac{1}{4}\left\{\begin{array}{c} 43{,}81 \\ 89{,}14 \end{array}\right\} = \begin{array}{r} 209{,}12\ \text{kN} \\ -247{,}37\ \text{kN} \end{array}$$

Load case C:
$$S_E = \pm\frac{549{,}09}{2 \cdot 2{,}13} \pm \frac{313{,}98}{2 \cdot 2{,}179} - \frac{1}{4}\left\{\begin{array}{c} 43{,}81 \\ 89{,}14 \end{array}\right\} = \begin{array}{r} 157{,}13\ \text{kN} \\ -223{,}23\ \text{kN} \end{array}$$

Load case D:
$$S_E = \pm\frac{780{,}19}{2 \cdot 2{,}13} \pm \frac{1}{4}\left\{\begin{array}{c} 54{,}36 \\ 128{,}59 \end{array}\right\} = \begin{array}{r} 169{,}55\ \text{kN} \\ -215{,}29\ \text{kN} \end{array}$$

Table 12.19: Leg member, section 3, calculation of moments

Designation	Height	Lever arm		Load case A		Load case C			
		Face A	Face B	rectangularly		rectangularly		in parallel	
				Force	Moment	Force	Moment	Force	Moment
	m	m	m	kN	kNm	kN	kNm	kN	kNm
Earth wires	−3,90	22,00	22,80	4,67	102,76	2,34	51,38	0	0,00
Earth wire peak	−1,95	20,05	20,85	2,11	42,23	1,28	35,73	1,78	37,15
Conductors 1	1,10	17,00	17,80	12,74	216,65	6,53	111,08	0,49	8,65
Crossarm 1	1,10	17,00	17,80	2,04	34,65	1,03	12,44	2,55	45,41
Section 1	2,45	15,65	16,45	5,21	81,55	4,41	69,09	4,41	72,62
Conductors 2	4,90	13,20	14,00	25,22	332,88	12,91	170,36	0,92	13,61
Crossarm 2	4,90	13,20	14,00	2,98	39,38	1,50	19,78	3,73	52,16
Section 2	8,10	10,00	10,80	6,09	60,89	5,17	51,71	5,17	55,84
Section 3	15,00	3,00	3,80	8,84	26,53	7,51	22,52	7,51	28,39
Total moment					937,52		549,09		313,98

Designation	Load case D		Load case F				Load case A one circuit		Load case D one circuit	
	rectangularly		rectangularly		in parallel		rectangularly		rectangularly	
	Force	Moment	Force	Moment	Force	Moment	Force	Moment	Force	Moment
	kN	kNm	kN	kNm	kN	kNm	kN	kNm	kN	kNm
Earth wires	5,43	119,39	5,45	59,70	0	0,00	4,67	102,76	5,43	119,39
Earth wire peak	1,05	21,11	0,89	17,86	0,89	18,58	2,11	42,23	1,05	21,11
Conductors 1	12,02	204,26	6,08	103,28	0,24	4,32	6,37	108,32	6,01	102,13
Crossarm 1	1,03	17,44	0,51	8,72	1,28	22,83	2,04	34,66	1,03	17,44
Section 1	2,61	40,77	2,21	34,78	2,21	36,42	5,21	81,55	2,61	40,77
Conductors 2	23,76	313,63	8,88	158,25	0,49	7,32	12,61	166,44	11,88	156,82
Crossarm 2	1,50	19,78	11,99	9,98	1,86	26,08	2,98	39,38	1,50	19,78
Section 2	3,05	30,51	2,59	25,92	2,59	28,00	6,09	60,89	3,05	30,51
Section 3	4,43	13,28	3,75	11,26	3,75	14,26	8,84	26,53	4,43	13,84
Total moment		780,19		429,61		157,29		662,76		521,25

Load case F:
$$S_E = \pm\frac{429{,}16}{2 \cdot 2{,}13} \pm \frac{157{,}29}{2 \cdot 2{,}179} - \frac{1}{4}\left\{\begin{array}{r} 54{,}36 \\ 128{,}59 \end{array}\right\} = \begin{array}{r} 123{,}35 \text{ kN} \\ -169{,}07 \text{ kN} \end{array}$$

Load case A, only one circuit installed:
$$S_E = \pm\frac{662{,}76 + 7{,}68\,(5{,}2 + 3{,}3 + 7{,}1)}{2 \cdot 2{,}13} - \frac{1}{4}\left\{\begin{array}{r} 39{,}07 \\ 66{,}10 \end{array}\right\} = \begin{array}{r} 173{,}93 \text{ kN} \\ -200{,}23 \text{ kN} \end{array}$$

Load case D, only one circuit installed:
$$S_E = \pm\frac{521{,}25 + 13{,}41\,(5{,}2 + 3{,}3 + 7{,}1)}{2 \cdot 2{,}13} - \frac{1}{4}\left\{\begin{array}{r} 46{,}59 \\ 88{,}36 \end{array}\right\} = \begin{array}{r} 159{,}82 \text{ kN} \\ -193{,}56 \text{ kN} \end{array}$$

Load case A is prevalent. Design value of the leg member compression and tensile force:

$$S_E = \left\{\begin{array}{r} 209{,}12 \text{ kN} \\ -242{,}37 \text{ kN} \end{array}\right\}$$

The forces in the bracings result from (12.25), where it is assumed

$$\sum P \cdot b + \Delta \cdot \sum S_V \cdot b_V + \sum M_T \cdot b_A / b_b = M_D \quad .$$

The load case J, one circuit installed only, torsion at lower crossarm, results in the maximum forces.

$$b_{Ao} = b_{Bo} = 1{,}723 - (11{,}3 - 4{,}9) \cdot 0{,}06 = 1{,}339 \text{ m}.$$

Bracings D_1 to D_5 (face rectangularly to the line)

$$M_D = 0{,}06\,[9{,}93 \cdot (5{,}2 + 3{,}3 + 7{,}1)] + 11{,}08 \cdot 7{,}1 = 88{,}00 \text{ kNm}.$$

Table 12.20: Forces of diagonals in section 3

Diagonal	b_{ui} m	b_{oi} m	h_i m	l_{di} m	D_i kN
D_1	1,723	1,807	1,40	2,253	15,92
D_2	1,807	1,897	1,50	2,383	15,29
D_3	1,897	1,987	1,50	2,454	14,32
D_4	1,987	2,083	1,60	2,589	13,76
D_5	2,083	2,179	1,60	2,665	12,92
D_6	1,765	1,852	1,45	2,318	16,58
D_7	1,852	1,942	1,50	2,418	15,72
D_8	1,942	2,035	1,55	2,522	14,92
D_9	2,035	2,131	1,60	2,627	14,16
D_{10}	2,131	(2,229)	(1,637)	(2,726)	13,41

Table 12.21: Rating of members and connections of tower section 3

Member	Angle section	Joint	Cross-sectional area A mm^2	Cross-sectional area A_{net} mm^2	Buckling length m	Radius of gyration cm	Slenderness ratio λ	Buckling reduction factor κ
Leg member	L100×8	6 M 16[1)]	1550	1278	1,60[2)]	3,06	63[3)]	0,743
Face A								
D_1	L40×4	1 M 12	308	108	1,04	0,78	133	0,342
D_2	L40×4	1 M 12	308	108	1,10	0,78	141	0,314
D_3	L40×4	1 M 12	308	108	1,13	0,78	145	0,301
D_4	L40×4	1 M 12	308	108	1,19	0,78	153	0,277
D_5	L40×4	1 M 12	308	108	1,23	0,78	158	0,263
Face B								
D_6	L40×4	1 M 12	308	108	1,07	0,78	137	0,328
D_7	L40×4	1 M 12	308	108	1,11	0,78	142	0,310
D_8	L40×4	1 M 12	308	108	1,16	0,78	149	0,289
D_9	L40×4	1 M 12	308	108	1,21	0,78	155	0,270
D_{10}	L40×4	1 M 12	308	108	1,20	0,78	154	0,274

[1)] double covered [2)] buckling length l_y [3)] flexural torsional buckling

Table 12.22: Rating of members and connections of tower section 3

Member	Loading		Resistance			
	Tension kN	Compression kN	Compression kN	Tension kN	Shearing kN	Bearing kN
Leg member	205,29	242,37	245,92	331,26	579,06	356,11
Face A						
D_1	15,92	15,92	22,50	27,99	27,14	22,26
D_2	15,29	15,29	20,66	27,99	27,14	22,26
D_3	14,32	14,32	19,81	27,99	27,14	22,26
D_4	13,76	13,76	18,25	27,99	27,14	22,26
D_5	12,92	12,92	17,30	27,99	27,14	22,26
Face B						
D_6	16,58	16,58	21,56	27,99	27,14	22,26
D_7	15,72	15,72	20,37	27,99	27,14	22,26
D_8	14,92	14,92	19,01	27,99	27,14	22,26
D_9	14,16	14,16	17,77	27,99	27,14	22,26
D_{10}	13,41	13,41	18,01	27,99	27,14	22,26

Table 12.23: Determination of moments for foundation loads

Designation	Height	Lever arm	Load case A		Load case C			
			rectangularly		rectangularly		in parallel	
			Force	Moment	Force	Moment	Force	Moment
	m	m	kN	kNm	kN	kNm	kN	kNm
Earth wires	−3,90	29,80	3,46	103,11	1,73	51,55	0,00	0,00
Earth wire peak	−1,95	27,85	1,56	43,45	1,32	36,76	1,32	36,76
Conductors 1	1,10	24,80	9,44	234,11	4,84	120,03	0,36	8,93
Crossarm 1	1,10	24,80	1,51	37,45	0,76	18,85	1,89	46,87
Section 1	2,45	23,45	3,86	90,52	3,27	76,68	3,27	76,68
Conductors 2	4,90	21,00	18,68	392,28	9,56	200,76	0,72	15,12
Crossarm 2	4,90	21,00	2,21	46,41	1,11	23,31	2,76	57,96
Section 2	8,10	17,80	4,51	80,28	3,83	68,17	3,83	68,17
Section 3	15,00	10,90	6,55	71,40	5,56	60,60	5,56	60,60
Section 4	22,40	3,50	7,28	25,48	6,17	21,60	6,17	21,60
In total			59,06	1124,47	38,15	678,32	25,88	392,70

Bracings D_6 to D_{10} (face in parallel to the line). Load case J, torsion at lower crossarm,

$$M_D = 11{,}08 \cdot 1{,}339 + 11{,}08 \cdot 7{,}1 = 93{,}50 \text{ kNm}.$$

In Table 12.20, the calculation of the forces is presented. The rating is carried out as presented in Tables 12.21 and 12.22. The strengths of the members and their connections comply with acting forces. As an example, the rating of the leg member is detailed here.

Effective cross section (12.56): $\overline{\lambda}_p = 0{,}0035\sqrt{235} \cdot 100/8 = 0{,}67$
According to Table 12.8: $\overline{\lambda}_p < 0{,}91, \varrho = 1{,}0; A_{\text{eff}} = A = 1\,550 \text{ mm}^2$
Buckling resistance
Slenderness ratio, flexural buckling: $\lambda = 160/3{,}06 = 53$
torsional flexural buckling: $\lambda_{ci} = 5 \cdot 100/8 = 63$
The maximum value is governing.
Non-dimensional slenderness (12.62): $\overline{\lambda} = 63/\pi\sqrt{235/210\,000} = 0{,}671$

Buckling reduction factor
According to (12.64): $\phi = 0{,}5[1 + 0{,}49(0{,}671 - 0{,}2) + 0{,}671^2] = 0{,}841$
According to (12.63): $\kappa = 1/\left(0{,}841 + \sqrt{0{,}841^2 - 0{,}671^2}\right) = 0{,}743$
Resistance according to (12.60): $N_{\text{Rd}} = 0{,}743 \cdot 1\,550 \cdot 235/1{,}1 = 245{,}92 \text{ kN}$

Tension resistance:
Net cross section: $A_{\text{net}} = 1\,550 - 2 \cdot 17 \cdot 8 = 1\,278 \text{ mm}^2$
According to EN 50341-3-4, the tension resistance of angle according to (12.94) follows from:

$$N_{\text{Rd}} = 0{,}9 \cdot 1\,278 \cdot 360/1{,}25 = 331{,}26 \text{ kN}.$$

Shear resistance of the connection with six bolts and two shear planes results in

$$F_{\text{v Rd}} = 0{,}6 \cdot 2 \cdot 0{,}6 \cdot 16^2 \cdot \pi/4 \cdot 500/1{,}25 = 579{,}06 \text{ kN}.$$

Bearing resistance:
The bearing resistance coefficient α_b is calculated considering the edge, end and borehole distances $e_1 = 1{,}5\,d_0$, $e_2 = 1{,}2\,d_0$ and $p_1 = 2{,}5\,d_0$. The minimum value results from (12.110) $\alpha_b = 1{,}61$. The bearing resistance for the leg member is calculated according to (12.107) for six bolts

$$F_{\text{b Rd}} = 6 \cdot 1{,}61 \cdot 16 \cdot 8 \cdot 360/1{,}25 = 356{,}1 \text{ kN}.$$

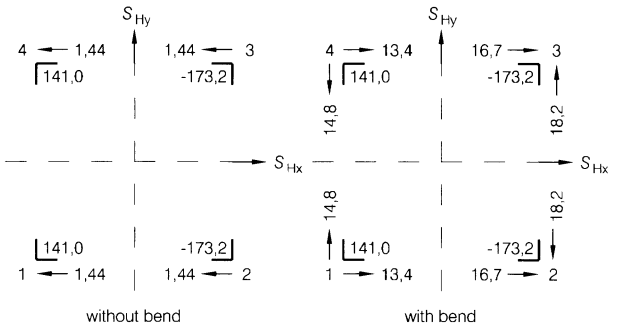

Figure 12.68: Foundation loads

Foundation loads

The calculation of foundation loads is represented for load cases A and C in Table 12.23. Load case A is governing.

$$S_{\mathrm{V\,max}} = 37{,}4 + 3{,}99 + 6 \cdot 5{,}69 = 75{,}53 \text{ kN},$$
$$S_{\mathrm{V\,min}} = 37{,}4 + 1{,}33 + 6 \cdot 2{,}43 = 53{,}31 \text{ kN}.$$

System width $b = 3{,}704 - 2 \cdot 0{,}0298 = 3{,}644$ m (angle section L110×8),

$$S_{\max} = \pm\frac{1124{,}47}{2 \cdot 3{,}644} - \frac{1}{4} \cdot \left\{ \begin{array}{c} 53{,}31 \\ 75{,}53 \end{array} \right\} = \begin{array}{r} 141{,}0 \text{ kN}. \\ -173{,}2 \text{ kN}. \end{array}$$

The external horizontal load is $S_{\mathrm{Hx}} = 56{,}06$ kN. The residual horizontal force at the connection of the bracing is (see (12.123)

$$D_{\mathrm{Hx}} = 59{,}06/4 - 1124{,}47 \cdot 0{,}21/(2 \cdot 2 \cdot 3{,}644) = 14{,}8 - 16{,}2 = -1{,}44 \text{ kN}.$$

If the leg members are bent, the forces $K_{\mathrm{x}} = S \cdot \Delta/2 = S \cdot 0{,}21/2$ (Figure 12.58 and equation (12.124)) will result.
The total transverse forces result as sum of the forces at the diagonal connection and the deviation forces. The external horizontal loads $S_{\mathrm{H}x}$ and $S_{\mathrm{H}y}$, respectively, result from the sum of forces P_x and P_y in the x and in the y direction (Figure 12.68).

12.5.19 Example: Calculation guy wire and mast loads in a guyed-V tower

The loads in the guy wires and masts should be calculated for guyed-V tower used for a 500 kV line in Brazil. The principal dimensions of the tower are shown in Figure 12.69. The length of a mast is 34,9, that of a guy wire 40,5 m. The loads are determined for high wind loads and for unbalanced longitudinal loads at an outer phase. For the 1st order theory analysis, the structure is assumed as not deformed and the equilibrium method is employed.

Analysis for high wind loads

Considering the static system and the load application, a basic assumption can be made: The loads are equally distributed on the guy wires 1 and 2 and the tensile force in guy wires 3 and 4 is relieved.
The design loads are:

- Vertical load of conductors and insulators: $G_{\mathrm{Cd}} = 40$ kN
- Tower weight $G_{\mathrm{Td}} = 50$ kN
- Wind load on crossarm $Q_{\mathrm{WCAd}} = 5$ kN
- Wind load on conductors and insulators: $Q_{\mathrm{WCd}} = 58$ kN
- Wind load on the masts $q_{\mathrm{WT}} = 0{,}60$ kN/m

The length of guy wires and masts are (see Figure 12.69):

$$l_{\mathrm{g}} = \sqrt{(l_{\mathrm{D}} - l_{\mathrm{E}})^2 + l_{\mathrm{I}}^2 + l_{\mathrm{H}}^2} = \sqrt{(22{,}0 - 8{,}0)^2 + 17{,}0^2 + 34{,}0^2} = 40{,}5 \text{ m}$$

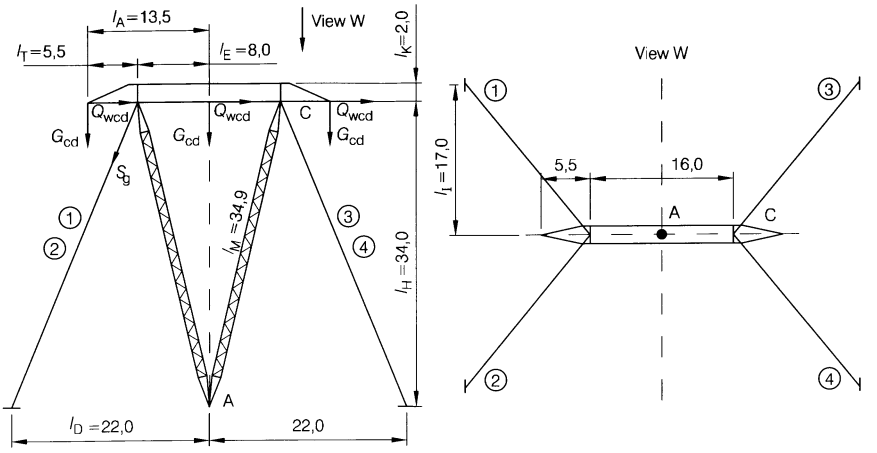

Figure 12.69: Outline of a 500 kV guyed-V tower

$$l_M = \sqrt{l_E^2 + l_H^2} = 34{,}9 \text{ m}$$

Overturning moment around base A is

$$M_A = 3 \cdot Q_{WC} \cdot l_H + Q_{WCAd}\,(l_H + l_K/2) + 2 \cdot q_{WT} \cdot l_H^2/2 =$$
$$= 3 \cdot 58 \cdot 34 + 5{,}0\,(34 + 2/2) + 2 \cdot 0{,}60 \cdot 34^2/2 = 6785 \text{ kN} \cdot \text{m}$$

The masts are pivoted on foundation A and the guy wires counteract the bending moment $M_A = 6785$ kNm. Both guy wires 1 and 2 receive equal portion of loads, therefore

$$2 \cdot S_g \cdot l_H \cdot (l_D/l_g) = M_A \text{ or } S_g = M_A \cdot l_g/(2 \cdot l_H/ \cdot l_D) \quad ;$$
$$= 6785 \cdot 40{,}5\,(2 \cdot 22{,}0 \cdot 34{,}0) = 184 \text{ kN}$$

The required strength of the guy wire is obtained assuming a material partial factor $\gamma_M = 1{,}5$

$$\text{RTS} \geq \gamma_M \cdot S_g = 1{,}5 \cdot 184 = 276 \text{ kN}$$

The windward mast is that loaded highest by compression. The following components contribute to the load:

- The vertical conductor loads $S_{gV1} = 3/2 \cdot G_{cd} = 3 \cdot 40/2 = 60$ kN
- The vertical component for guy wire forces $S_{gV2} = 2 \cdot S_g \cdot l_H/l_g = 2 \cdot 184 \cdot 34/40,5 = 308$ kN
- The tower weight $S_{gV3} = G_{Td}/2 = 50/2 = 25$ kN

The total vertical reaction is $S_{gV} = 60 + 308 + 25 = 393$ kN. The compression force of the mast will be $S_{Md} = S_{gV} \cdot l_M/l_H = 393 \cdot 34{,}9/34 = 403$ kN.

Analysis for an unbalanced longitudinal load

The guy wire and mast force are to be determined for a single longitudinal torque load $S_L = 55$ kN at one of the outer phases (Figure 12.69). Guy wire 2 will go slack and the longitudinal component S_{gH} of the force in guy wire 1 by equilibrium of moments about a vertical axis through point C will be:

$$S_{gH} = S_L \cdot (2\,l_E + l_T)/2\,l_E = 55 \cdot (2 \cdot 8{,}0 + 5{,}5)/2 \cdot 8{,}0 = 74{,}0 \text{ kN}.$$

The guy wire tension is

$$S_g = S_{gH} \cdot l_g/l_l = 74{,}0 \cdot 40{,}5/17{,}0 = 177 \text{ kN}.$$

The required strength of the guy wire is

$$\text{RTS} \geq \gamma_M \cdot S_g = 1{,}5 \cdot 177 = 264 \text{ kN}.$$

There, the RTS is less than that in case of wind action. A 19 mm extra-high tensile steel strnd conductor with a RTS of 311 kN or an aluminium clad steel conductor 243-A20SA having a RTS of 325 kN (see Table 7.8) could be used.

12.6 Steel poles

12.6.1 Structural design

Solid-wall *steel poles* with various designs are used for low-voltage, medium-voltage and high-voltage lines. *Polygonal conical poles* have 8-, 12- or 16-sided shapes whereby the plates are bent and finally welded in longitudinal direction. The material grades S235 and S355 are mainly used for these poles. The lengths of the poles or their sections is limited to approximately 15 m by the weights for transportation and the possibilities of galvanization. The required joints of taller pole lengths can be designed as *slip joints* or *flange joints* with prestressed high-tensile bolts.

Slip joints can be adopted without specific connection elements and without a verification by calculation if the following conditions are complied with [12.8]:

- When modelling the tower body in view of global static analysis of resistance, only the nominal cross section of the inserted part is considered in the range of the joint.
- The nominal *slipping length* is at least 1,5 times the maximum average diameter measured across the corners of the outer section.
- Assembling is carried out on site. With respect to the tolerances of material thickness due to galvanization and of polygonal cross-sectional dimensions, the final slipping length of the connection should be more than 1,35 times the maximum average diameter, measured across the corners of the female section.
- The force for fitting both parts should exceed the maximum design compression force, the partial factor being included, at the level of the joint.
- If necessary, brackets should be arranged on both ends of the slip joint at the pole body, thus enabling an appropriate fitting using hydraulic jacks or pulling equipment on site.
- The increase of pole width should be not less than 10 mm/m.
- The thickness of the wall should be not more than to 16 mm.

The poles can be fitted together on the construction site in a horizontal or vertical position, whereby a fitting and marking of the pole parts in the manufacturing plant has proved to be advantageous.

Bolted flange joints are necessary for poles used for high loads, for which prestressed high-strength bolts of the strength grade 8.8 or 10.9 are used. The flange joints can be arranged outside or inside the pole shaft. In case of an inside arrangement, the dimensions of the pole must be sufficiently wide to enable arrangement of cut-outs and ladders in the pole.

Poles can be connected to the foundations by embedding directly the pole body or by means of a flange and *anchor bolts*. Embedding in concrete is less costly. If the foundation is designed as a *sleeve foundation*, a significant part of the pole length is not used effectively for supporting the conductors. Poles can be more easily adjusted when a foundation with anchor bolts is used. Poles can be equipped with single or double flanges depending on the static requirements. The use of bolts, nuts and washers facilitates the plumbing adjustment.

When cut-outs are necessary for doors and the like, the pole resistance is verified based on the effectively available section properties. If necessary, the pole faces need to be strengthened around the openings. In order to avoid precipitation of humidity within the pole, its shaft as well as hollow crossarms should be ventilated using a design which avoids penetration of rain water.

The *crossarms* can be designed using open sections (U-type channels or H-beams) which are bolted to the pole shaft by means of a flange. For longer crossarms, hollow conical shapes with four- to eight-sided cross sections are used. Brackets are welded to the pole shaft for the connection of the crossarms. An example is shown in Figure 12.70.

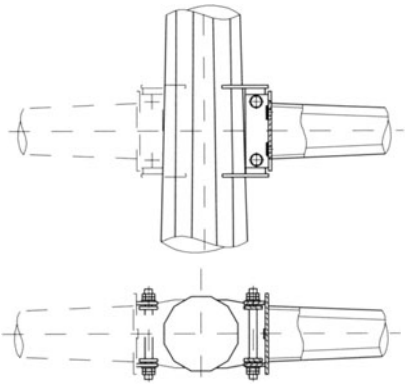

Figure 12.70: Connection of crossarms

Either staggered *stepbolts* are welded or ladders are arranged permanently or when required for climbing of the poles. Rails are arranged on the crossarms for hanging on the safety equipment.
All solid-wall steel poles should be hot-dip galvanized. A design of connections appropriate for galvanizing should be used. The poles should be coated by using green, grey or black paint with a corresponding layer thickness for improvement of the corrosion protection and for visual adjusting to the environment. Thick layer coating systems have proved their qualification for galvanized steel components and reach a lifetime of 20 years without recoating (see also clause 12.5.1.5).

12.6.2 Analysis of loads

Solid-wall steel poles can be considered as predominantly loaded statically as is the case of lattice steel towers. The internal forces and moments are computed by a global elastic analysis. A linear-elastic stress-strain relation is assumed for the materials. The internal forces and moments need to be determined using the *second order theory* at the deformed pole because of the relatively high elasticity under the horizontal load. Some standards, such as EN 50 341-3-4, accept an analysis according to the first order theory for poles with a certain length, e. g. 40 m between the top of foundation and the top of the upper crossarm, whereby the internal moments have to be increased. According to EN 50 341-3-4, the following applies:

- Suspension poles, angle suspension and angle poles: $M^{\mathrm{II}} = 1{,}05\, M^{\mathrm{I}}$,
- Strain poles, angle-strain poles and dead-end poles: $M^{\mathrm{II}} = 1{,}03\, M^{\mathrm{I}}$.

The analysis using the second order theory represents the state of the art and should be used for determining the internal forces and moment as well as the deformations. The internal moment results according to the second order theory from

$$M^{\mathrm{II}} = \sum_{i=1}^{n_1} S_{\mathrm{V}i} \cdot f_{\mathrm{d}i} + \sum_{i=1}^{n_2} S_{\mathrm{H}i} \cdot h_i \quad , \tag{12.127}$$

where $S_{\mathrm{V}i}$, $S_{\mathrm{H}i}$ are vertical and horizontal forces, respectively, $f_{\mathrm{d}i}$ is the horizontal deformation relatively to the pole axis at the point of attack of the force $S_{\mathrm{V}i}$ and h_i the lever arm of the force $S_{\mathrm{H}i}$ with respect to the studied section. The wind action on the pole is considered for the determination of the internal forces and moments. The wind load may be assumed section by section or approximately for the pole as a whole. The wind load for conical poles is according to [12.8]

$$Q_{\mathrm{WM}} = q_{\mathrm{z}} \cdot G_{\mathrm{q}} \cdot G_{\mathrm{x}} \cdot C_{\mathrm{x}} \cdot L_{\mathrm{M}} \left(d_1 + d_2\right)/2 \quad , \tag{12.128}$$

Table 12.24: Coefficients for moments of regular polygons

Number of sides	6	8	12	16
$k_{I(y)}$	2,71	6,16	21,39	51,22
$k_{I(z)}$	2,50	6,16	21,39	51,22
k_T	2,60	4,83	11,20	20,11

where d_1, d_2 is pole diameter at the top and basis, respectively, and L_M the length of the pole. The aerodynamic drag factor C_x is 0,7 for circular cross sections, and 1,0 for cross sections with six or more sides. The gust factor G_q can be obtained from equation (6.49) and the *structural response factor* G_x from

$$G_x = (1/G_q) \cdot \left(1 + 2\,g_o \sqrt{Q_o^2 + R_x^2} / \ln(z/z_0)\right) \quad , \tag{12.129}$$

where the peak factor g_o, the background response part Q_o and the resonant response part R_x can be obtained from ENV 1991-2-4, clause B.2 [12.55]. In addition, z is the height above ground and z_0 the ground roughness parameter (see Table 6.13).
According to [12.10], the product $q_z \cdot G_q$ is replaced by the wind pressure q and G_{rmx} is set to be 1,1. Therefore, equation (12.128) is transformed to

$$Q_{WM} = 1,1 \cdot q \cdot C_x \cdot L_M \cdot (d_1 + d_2)\,/2 \quad . \tag{12.130}$$

The wind load may be assumed as acting at half of the pole height.
The calculation of the internal moment according to (12.127), taking care of (12.128) and (12.130), if relevant, is an iterative process since the wind load and the deflection f_{di} depend on the selected cross section. The *deflection of a pole* with continuously constant cross section, for example an H-beam section, can be determined from

$$f_d = (S_H/3 + Q_{WM}/8) \cdot L_M^3/(EI) \quad . \tag{12.131}$$

In case of a varying moment of inertia $I(x)$, an analytic calculation according to

$$f_d = 1/E \int_0^{L_M} M(x) \cdot x/I(x) \cdot \mathrm{d}x \tag{12.132}$$

is recommended where the coordinate x starts at the position of the deflection.
However, the deflection can be calculated according to the *equivalent beam method* as described in clause 12.5.14 in case of stepped or conical poles. In particular, the axial compression force can affect the rating of guyed poles in addition to the bending moment. Design of steel poles is especially dealt with in [12.56].

12.6.3 Rating

The following partial factors γ_M have to be used according to EN 50 341-1 to determine the *resistance*:

- Resistance of cross sections $\gamma_{M1} = 1,10$,
- Resistance of the residual cross section at boreholes $\gamma_{M2} = 1,25$.

The verification is carried out by means of stresses, whereby the load σ_d may not exceed the resistance strength σ_{Rd}:

$$\sigma_d/\sigma_{Rd} \leq 1 \quad ,$$

where the resistance stress is $\sigma_{Rd} = f_y/\gamma_M$.

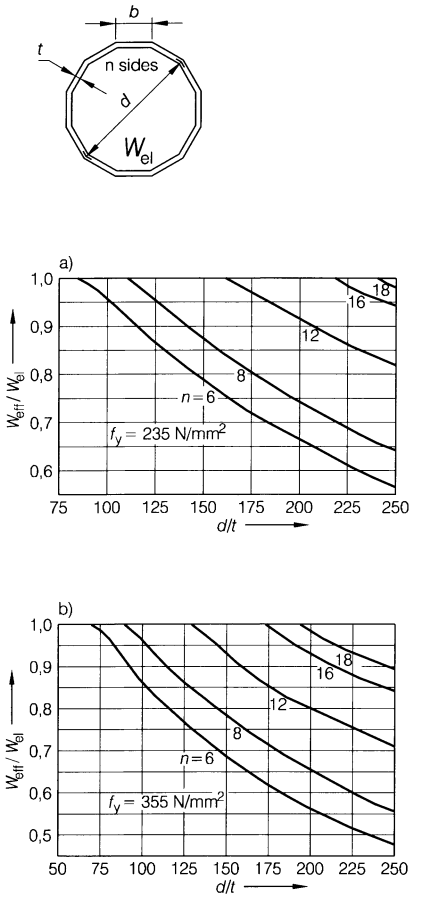

Figure 12.71: Relation of the effective cross-sectional modulus W_{eff} to the elastic cross-sectional modulus for polygonal cross sections; a) S235; b) S355

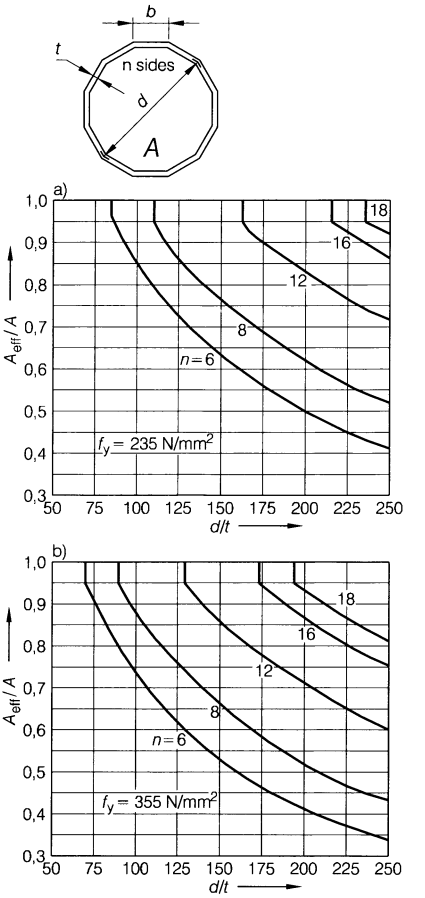

Figure 12.72: Relation of the effective cross-sectional area A_{eff} to the total area for polygonal cross sections; a) S235; b) S355

The walls of solid-wall steel poles will buckle locally under compression or bending compression load if the wall thickness t is sufficiently low, as compared with the other cross-sectional dimensions. Reliability against buckling is guaranteed if the following limits are obeyed. Circular cross sections are not endangered by buckling if

$$\frac{d}{t} \leq \begin{cases} 176 & \text{for steel grade S235;} \\ 117 & \text{for steel grade S355,} \end{cases}$$

where d is the pole diameter and t the thickness of walls. For polygonal cross sections with 6 to 24 sides local buckling will not be hazardous if

$$\frac{b}{t} \leq \begin{cases} 42 & \text{for steel grade S235;} \\ 34 & \text{for steel grade S355,} \end{cases}$$

where b is the width of a side and t the thickness of walls. The verification of thickness is carried out with the existing cross sections if a hazard of buckling does not exist. In case of cross sections endangered by buckling, the resistance against load by moments

or compression needs to be determined considering the local buckling. The verification is carried out using the effective section properties A_{eff} and W_{eff}.
The stress σ_{d} of circular cross sections is obtained from

$$\sigma_{\text{d}} = (N_{\text{d}}/A + M_{\text{d}}/W_{\text{el}})\,/\varrho \quad , \tag{12.133}$$

where $\varrho = 1{,}0$ for cross sections without a hazard of buckling and

$$\varrho = 0{,}7 + [53/(d/t)] \cdot (235/f_{\text{y}}) = 0{,}7 + 12455/\,[f_{\text{y}} \cdot (d/t)] \quad . \tag{12.134}$$

for cross sections endangered by buckling.
The stress for polygonal cross sections without a hazard of buckling is obtained from

$$\sigma_{\text{d}} = N_{\text{d}}/A + M_{\text{d}}/W_{\text{el}} \quad . \tag{12.135}$$

There, N_{d} is the design value of the axial force, A the cross-sectional area, M_{d} the design value of the bending moment and W_{el} the elastic cross-sectional modulus.
The *elastic cross-sectional modulus* is

$$W_{\text{el}} = I/y \quad , \tag{12.136}$$

where y is the distance of the edge from the centroidal axis and I the moment of inertia.
The moment of inertia I can be obtained for regular polygonal cross section from

$$I_{y,z} = k_{\text{I}(y,z)} \cdot b^3 \cdot t \quad , \tag{12.137}$$

where b is the average width of the sides and t the thickness. The factor k_{I} can be obtained from Table 12.24.
For polygonal cross sections which are endangered by buckling, the stress is determined considering the effective cross-sectional values:

$$\sigma_{\text{d}} = N_{\text{d}}/A_{\text{eff}} + M_{\text{d}}/W_{\text{eff}} \quad , \tag{12.138}$$

where A_{eff} is the effective cross-sectional area under uniform compression and W_{eff} the effective modulus of the cross section if it is loaded by a moment around the considered axis. The effective cross-sectional values A_{eff} and W_{eff} can be determined from the nomograms in Figures 12.71 and 12.72.
The design value for the shear stress due to the *torsional load* is calculated from

$$\tau_{\text{d}} = M_{\text{Td}}/(2\,A_{\text{T}} \cdot t) \quad , \tag{12.139}$$

where A_{T} is the area enclosed by the centre line of the cross-sectional contour. To a circular cross section it applies $A_{\text{T}} = d^2 \cdot \pi/4$, and to polygonal cross sections $A_{\text{T}} = k_{\text{T}} \cdot b^2$ where k_{T} is obtained from Table 12.24. If shear and axial stresses act simultaneously, the equivalent stress is obtained from

$$\sigma_{\text{vd}} = \sqrt{\sigma_{\text{d}}^2 + 3\,\tau_{\text{d}}^2} \quad . \tag{12.140}$$

In addition to the *verification of stability*, the deformation at the pole top resulting from the loads needs to be determined in order to guarantee the serviceability of the poles. As stipulated by EN 50 341-3-4, the deformation may be calculated using the first order theory without considering movements of the foundation, whereby the following limits apply for the deformation of the pole:

- Suspension and angle suspension poles: 4% of the pole length loaded according to load cases A or D (clause 12.4) using the partial factor $\gamma_{\text{F}} = 1{,}0$.
- Angle, strain and dead-end poles: 2,5% of the pole length loaded according to load case D (clause 12.4) using a partial factor $\gamma_{\text{F}} = 1{,}0$.

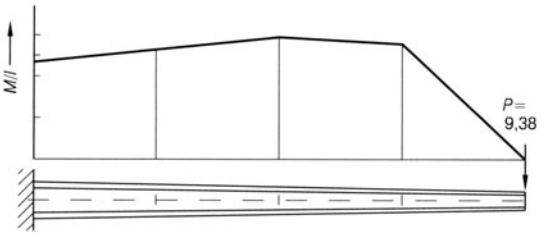

width over flats (mm)	450	387,5	325	262,5	200
length of side (mm)	184	159	133	107	81
moment of inertia(10^8 mm^4)	1,92	1,24	0,72	0,37	0,16
first order theory bending moment (kN·m)	138,6	101,4	65,4	31,8	0
M/I (N/mm^3)	0,723	0,818	0,908	0,859	0
second order theory bending moment (kN·m)	142,8	105,4	69,4	35,8	4,01
M/I (N/mm^3)	0,744	0,850	0,964	0,968	0,250

Figure 12.73: Determination of deformation of a tubular steel pole

Limiting the deformation should guarantee the *serviceability* of poles since the deformation affects the conductor position, particularly in case of angle and angle-strain poles and, as a consequence, affects the clearances as well. The serviceability criterion can be prevalent for the rating in case of tall slender poles. The deformation needs to be determined considering all significant impacts. In addition to the elastic deformation of the poles, the *slippage* of slip joint needs to be considered. In [12.57], a bending of 0,4° per joint is assumed. In [12.46], measurements of the deformation at solid-wall steel poles are reported. Independently of the load, a bend of 0,3 to 0,4° per joint should be taken into consideration. The deformation under load affects the position of the conductors to a substantial extent. It would increase with pole length if the deformation were only limited in relatively to that length. With respect to the serviceability, the deformation under maximum load compared with the deformation under everyday condition should be limited in absolute values. To take care of this aspect, EN 50 341-3-4 stipulates, that independently of the pole length, the deflection of the top of angle, angle-strain or dead-end poles under maximum load may not increase by more than 0,5 m, as compared with the situation under everyday conditions. The everyday condition can be defined by a temperature of 10°C without wind load or similarly depending on the geographical area of application.

12.6.4 Example for design of a conical solid-wall steel pole

Eight-sided steel pole, length 13,0 m, 3 conductors 122-AL1/20-ST1A (ACSR 120/20), d = 15,5 mm, m_C = 0,494 kg/m, wind span 200 m, weight span 250 m, weight of insulator 200 N, wind load: q_0 = 800 N/m^2.
Governing case: wind load on conductors with ice (γ_F = 1,35), basis EN 50 341-1 and EN 50 341-3-4.

Ice load $m_{CI}g = 5 + 0{,}1 \cdot 15{,}5 = 6{,}55$ N/m,

Diameter with ice $d_I = \sqrt{15{,}5^2 + (6{,}55 \cdot 4)/(0{,}0075 \cdot \pi)} = 36{,}8$ mm.

Wind load on conductors: $Q_{WC} = 1{,}35 \cdot 3 \cdot 200 \cdot 0{,}0368 \cdot 0{,}75\,(800 + 3 \cdot 13{,}0)/2 = 9{,}38$ kN,
Vertical load: $S_V = 1{,}35 \cdot 3 \cdot 250\,(6{,}55 + 9{,}81 \cdot 0{,}494) + 1{,}35 \cdot 3 \cdot 200 = 12{,}35$ kN.
Selected: Dimension at the basis 450 mm, at the top 200 mm, material S235;
Wind load on pole: $Q_{WM} = 1{,}35 \cdot 1{,}1\,(0{,}2 + 0{,}45)/2 \cdot 13{,}0 \cdot (800 + 3 \cdot 6{,}5)/2 = 2{,}57$ kN.

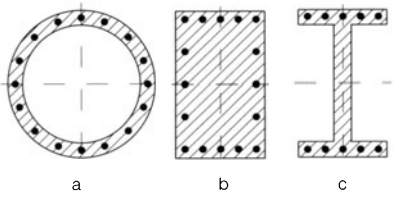

Figure 12.74: Cross sections of concrete poles: a circular cross section; b rectangular cross section; c double-T-cross section

Moment at the top of foundation with a supplement of 5 % for considering the moment due to the vertical load

$$M_{\mathrm{d}} = 1{,}05\,(9{,}38 \cdot 13{,}0 + 2{,}57 \cdot 6{,}5) = 145{,}6 \text{ kNm} \quad .$$

Design value of the resistance ($\gamma_{\mathrm{M}} = 1,1$) $\sigma_{\mathrm{Rd}} = 235/1{,}1 = 213{,}6$ N/mm^2.
Required moment of inertia

$$I_{\mathrm{req}} = (145{,}6 \cdot 450 \cdot 10^6)/(213{,}6 \cdot 2) = 1{,}53 \cdot 10^8 \text{ mm}^4 \quad .$$

Selected: $t = 5$ mm, $b = 1/2\,(450 - 5) \cdot 2 \cdot \tan 22{,}5° = 184$ mm,

$$I = 6{,}16 \cdot 184^3 \cdot 5 = 1{,}92 \cdot 10^8 \text{ mm}^4 \text{ according to (12.137)} \quad .$$

The relation b/t is 36,8 at the foundation base. Therefore, a reduction of the section properties regarding of buckling is not necessary.
Alternatively, the deformation and iterative approach to the bending moment according to the second order theory as per (12.119) are carried out. The pole is divided into four sections, determination of data see Figure 12.73.
The deformation according to the first order theory is, therefore:

$$\begin{aligned} f_{\mathrm{d}}^{\mathrm{I}} &= [(2 \cdot 0{,}859 \cdot 3250)/3 + (2 \cdot 0{,}908 + 0{,}859)\,3250/3 + (0{,}908 + 0{,}859)3250 \\ &\quad + (2 \cdot 0{,}818 + 0{,}908)\,3250/3 + (0{,}818 + 0{,}908)\,6500 + (2 \cdot 0{,}723 + 0{,}818)\,3250/3 \\ &\quad + (0{,}723 + 0{,}818)\,9750] \cdot 3250/(2 \cdot 210\,000) \\ &= (1861 + 2898 + 5643 + 2756 + 11\,219 + 2452 + 15\,024) \cdot 0{,}007738 = 325 \text{ mm}. \end{aligned}$$

From the deformation and the vertical load, an additional moment $\Delta M = 12{,}35 \cdot 0{,}325 = 4{,}01$ kNm results. This moment is added to the moment resulting from the first order theory and the deformation is calculated again according to (12.119)

$$\begin{aligned} f_{\mathrm{d}} &= [(2 \cdot 0{,}968 + 0{,}250)\,3250/3 + (2 \cdot 0{,}964 + 0{,}968)\,3250/3 + (0{,}964 + 0{,}968)\,3250 \\ &\quad + (2 \cdot 0{,}850 + 0{,}964)\,3250/3 + (0{,}850 + 0{,}964)\,6500 + (2 \cdot 0{,}744 + 0{,}850)\,3250/3 \\ &\quad + (0{,}744 + 0{,}850)\,9750] \cdot 0{,}007738 \\ &= (2368 + 3137 + 6279 + 2886 + 11\,791 + 2533 + 15\,542) \cdot 0{,}007738 = 345 \text{ mm}. \end{aligned}$$

The deformation according to the second order theory results from

$$f_{\mathrm{d}}^{\mathrm{II}} = 325/(2 - 345/325) = 346 \text{ mm}.$$

The bending moment according to the second order theory will be, therefore,

$$M_{\mathrm{d}}^{\mathrm{II}} = 9{,}38 \cdot 13 + 2{,}57 \cdot 6{,}5 + 12{,}35 \cdot 0{,}346 = 142{,}9 \text{ kNm}.$$

Finally, the stress obtained from

$$\sigma_{\mathrm{d}} = 12\,350/(5 \cdot 8 \cdot 184) + 1{,}429 \cdot 10^8 \cdot 225/(1{,}92 \cdot 10^8) = 169{,}1 \text{ N/mm}^2.$$

The deformation of the tower top under the load of the second order theory corresponds to 2,7 % of the pole length and complies, therefore, with the permissible deformation under serviceability conditions.

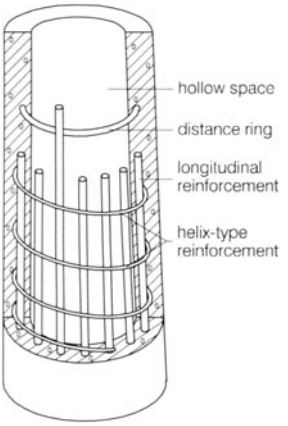

Figure 12.75: Design of a spun concrete pole

Figure 12.76: Production of vibrated concrete poles

12.7 Steel-reinforced concrete poles

12.7.1 Selection of cross sections

Three types of *concrete cross sections* have been used for single poles or multiple-pole structures, as schematically shown in Figure 12.74 and described as follows:

- Poles with tubular hollow cross sections, varying conically from the pole top until to pole base. They have the same resistance for loads applied in any direction provided a symmetrically arranged reinforcement;
- Poles with rectangular cross sections, also with sections increasing from the top to the base of the pole; they are heavier than hollow concrete poles, however, can be manufactured using simple equipment on site;
- Poles with H-cross sections, also called double-T- or I-section, which can increase uniformly from the top to the base. Such kind of poles have a higher resistance perpendicularly to the narrower side than to other directions. They can be more economic for medium loads than the other types.

The possibility of fabricating concrete poles near to the installation site is an additional advantage, which often has transferred concrete poles into an attractive solution.

12.7.2 Spun concrete poles

Spun concrete poles possess a ring-type circular cross section with a continuous hollow space inside. Their outer shape is conical with an increasing diameter from top to the base by at least 15 mm/m. Spinning is carried out in two-piece horizontal moulds which are rotated around their longitudinal axis. The spinning process achieves *concrete strengths* up to 100 N/mm^2 corresponding to the concrete class C 100/115. The dense concrete texture being formed protects the reinforcement against corrosion and avoids cracks. Spun concrete poles, therefore, are endangered by corrosion to a low extent only if correctly manufactured and erected.

Spun concrete poles can be fitted with *slack reinforcement* by using common reinforcement steel or with *prestressed reinforcement*. Prestressing is adopted to the reinforcement already before the spinning process. After hardening of concrete and reaching the necessary strength, the tensile force of the steel reinforcement is transferred to the concrete cross section generating compressive prestresses there. These compressive stresses need to be exceeded in case of bending before the concrete would be loaded by tensile

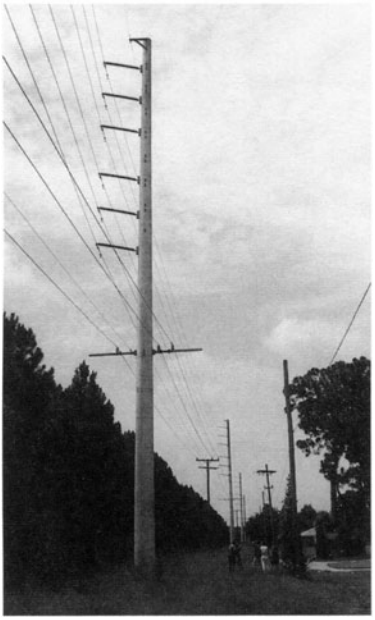

Figure 12.77: Double circuit 132 kV line in the USA, design with spun concrete poles (Newmark Ltd, Birmingham, Alabama, USA, affiliate of Pfleiderer AG, Neumarkt, Germany)

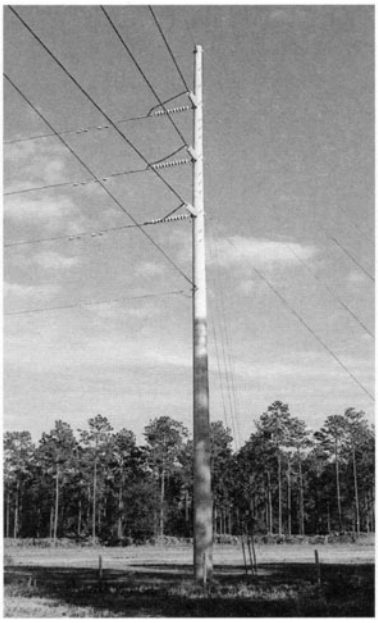

Figure 12.78: Angle-strain pole of a 132 kV line with guy wire for each conductor (Newmark Ltd, Birmingham, Alabama, USA, affiliate of Pfleiderer AG, Neumarkt, Germany)

stresses, thus avoiding transverse cracks, otherwise possible to occur in case of high loads. Figure 12.75 shows the design of a spun concrete pole. For spun poles, crossarms made of concrete are preferred as well. Cantilevers made of steel and line post insulators form alternatives used to an increasing extent, especially in North America. A production of concrete crossarms by spinning is not possible because of their shape. Therefore, crossarms are produced in the plant on vibrating boards resulting in concrete strengths up to 55 N/mm^2 corresponding to the concrete class C 55/67.

Spun concrete poles are used to an increasing extent in North America, too [12.58]. In Figure 12.77, a suspension pole is shown, as often used there. The conductors are attached to composite line post insulators which are fixed directly to the pole shaft. Angle poles are mostly guyed with one separate guy wire for each conductor (Figure 12.78). This design reduces the horizontal loads enabling the use of relatively slim poles. The poles are embedded directly into up to 8 m deep boreholes. The space around the pole in the borehole is filled up with backfill bound together by adding cement.

In addition to the working bending moment for which the poles need to be designed, a cracking moment is stipulated. No cracks may occur below this moment when the poles are tested. On site, a loading could occur which resulted in transverse cracks, e. g. when hurricanes hit the poles and cause exceeding of concrete tensile strength, and, as a consequence, transverse cracks. However, the prestressing closes the cracks after release of the loads and the poles remain fully serviceable.

This design constitutes an economic solution providing optimum reliability and security. In particular, damage is considerably reduced in hurricane prone areas compared with other designs.

12.7.3 Vibrated concrete poles

Vibrated concrete poles with a solid or double-T-cross section are produced on vibrating boards as are crossarms for spun concrete poles. Due to the high weight resulting from this design, the pole length is limited, however. This type of pole and its production is used for individual projects where the installation of a plant for spun concrete poles would be too expensive. Figure 12.76 shows a production line for vibrated concrete poles in Nigeria. The reinforcement is installed in moulds with rectangular cross section, the concrete is poured in and compacted by external vibrators. With respect to the varying qualities of aggregates and cement, only the concrete class C 30/37 should be selected, when rating concrete poles to be produced on site. Pole lengths up to approximately 12 m can be obtained with this concrete class (see [12.4]).

12.7.4 Structural design

As a consequence from experience gained in particular in Central Europe, the following aspects should be duly considered for the *structural design of spun concrete poles*:

- To avoid adverse longitudinal cracks, a strong enough *helical reinforcement* is necessary and serves to distribute tensile stresses occurring at the surface to the whole cross section. The helical reinforcement, therefore, should consist of ribbed concrete steel, independently of the static requirements. As a recommendation, helical reinforcement with a rod diameter of 5 mm and a pitch of 60 mm or a rod diameter of 4 mm and a pitch of 50 mm should be used.
- The wall thickness of the spun concrete poles should be at least 50 mm.
- The clearance between parallel reinforcement bars needs to be half of the bar diameter; however, it should be at least as large as the maximum aggregate particle size.
- The concrete covering should be at least 15 mm above the helical reinforcement or 20 mm above prestressed reinforcement.

The embedding of the pole shaft within the foundation needs to be verified separately. Such a verification is not necessary for pole lengths less than 20 m, *characteristic tensile forces* less than 20 kN and embedding depths of at least 1,7 m.

12.7.5 Production

Production of vibrated concrete poles requires a precise compliance with the concrete class and, therefore, a continuous supervision of aggregates and water-cement ratio which should be approximately 0,5 as is usual in case of high-strength concrete. At least, 320 kg cement should be used per cubic meter concrete. The mould should be sufficiently stiff and supported on a rigid base to guarantee straight poles. The reinforcement is installed in the mould by means of spacers. Also the correct position of the helical or stirrup reinforcement is important. The concrete is compacted by external vibrators which are applied at distances of 1,5 to 2 m. They excite the mould to vibrations with a frequency of approximately 15 000 Hz, whereby the concrete is densely compacted and air inclusions can escape. With a similar method, the crossarms for all concrete poles are produced. Openings, boreholes and inserts for bolts can be applied during production. The poles can be taken out of the mould approximately one day after concreting and reach the strength necessary for transportation to the line site after a storing period of approximately 10 days. During the hardening period, the concrete should be kept humid, particularly in hot climate.

Some details of *production of spun concrete poles* are presented in [12.6] and [12.59]. To achieve a sufficiently dense concrete, at least 440 kg cement should be provided per cubic meter concrete. The content of cement in the hardened concrete is reduced

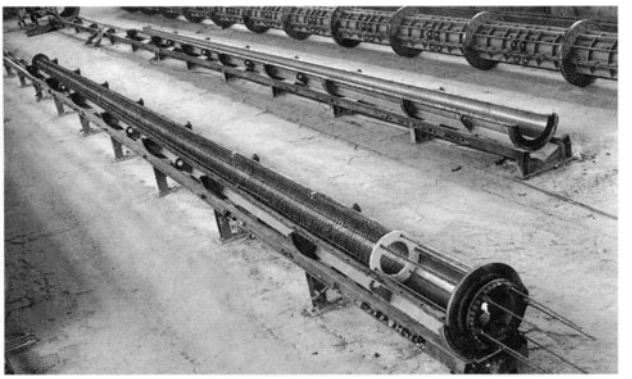

Figure 12.79: Production of a spun concrete pole (Pfleiderer AG, Neumarkt, Germany)

by approximately 10 %, since the finest particles are directed to the rotation axis. The *maximum particle size* should not exceed 16 mm and, therefore, remain within the dimension of the required minimum concrete covering. The *water-cement ratio* is reduced to values below 0,4 during the spinning process, a desirable effect in principle. Spun concrete poles are produced in two-piece moulds split along their longitudinal axes. At first, the preformed helical reinforcement is installed in the mould and afterwards the slack or prestressed longitudinal reinforcement is guided through the helical reinforcement. For prestressing, a head is applied on each individual bar. After the installation of inserts and other elements, the concrete is poured in and the upper part of the mould is applied and bolted. Then, the reinforcement is prestressed to approximately 1000 N/mm^2.
The revolutions during the spinning process (Figure 12.79) are adjusted to the pole diameter. Centrifugal accelerations between 10 and 30 times the earth gravity are aimed at. The spinning process is finished after 8 to 15 minutes depending on the pole diameter. Then, the mould with the pole can be stored within a heated chamber. The moulds should be closed on both ends during the storing period to keep the moisture inside. The concrete temperature should not exceed 55°C. The poles should remain in the steel mould for approximately 24 hours. Then, the poles will reach 80 % of their designed resistance as long as they are in the mould. *Heat treatment* with elevated temperatures is not recommended because of the hazard of longitudinal cracks. A correct structural design and a thorough production form preconditions for a *long lifetime* without damage.

12.7.6 Rating

The external loads for the *rating of concrete poles* result from the relevant standards, e. g. EN 50 341-1 or EN 50 341-3-4, or from project specifications. For low- and medium-voltage lines, it is sufficient to determine the necessary working or characteristic load of a pole as a horizontal force acting at the pole top, however, without wind load on the pole itself. Utilities' practice, in general, considers all external loads acting on the poles by converting them into an equivalent force at the tower top. The *characteristic load* acts horizontally and is assumed in general at a distance of 0,25 below the pole top. The characteristic load is defined as that force resulting in the same moment at the pole base as the external loads together and is equal to

$$S_{\mathrm{H}} = 1/L_{\mathrm{M}} \sum_{i=1}^{n} S_{\mathrm{H}i} \cdot h_i \quad , \tag{12.141}$$

where h_i is the lever arm of the force $S_{\mathrm{H}i}$ related to the base at ground surface and L_{M} the pole length. With this data, the required pole can be selected from manufacturer's

Table 12.25: prEN 1992-1 [12.61]: Concrete for steel-reinforced concrete poles

Designation	Characteristic cylinder strength f_{ck} N/mm^2	Characteristic cube strength $f_{ck\,cube}$ N/mm^2	Design strength value $f_{cd} = 0,85 \cdot f_{ck}/\gamma_{cr}$ Standard concrete	Prefabricated concrete
C 30/37	30	37	17,0	18,2
C 35/45	35	45	19,8	21,3
C 40/50	40	50	22,7	24,3
C 45/55	45	55	25,5	27,3
C 50/60	50	60	28,3	30,4
C 55/67	55	67	31,2	33,4
C 60/75	60	75	34,0	36,4
C 70/85	70	85	39,7	42,5
C 80/95	80	95	45,3	48,6
C 90/105	90	105	51,0	54,6
C 100/115	100	115	56,7	60,7

catalogues, either with prestressed or slack reinforcement.

The rating of the cross sections is carried out based on the relevant standards. The moments are determined from the characteristic load and the wind load or from the acting individual forces using the *second order theory*. For *concrete poles produced in a plant*, the European standard prEN 12 843 [12.60] can be applied to design and rating in combination with prEN 1992-1 [12.61]. The guide [12.6] is often used internationally for designing concrete poles.

According to prEN 12 843 and prEN 13 369 [12.59], the concrete classes C 30/37 to C 55/67 are stipulated for steel-reinforced concrete poles and, for prestressed spun concrete poles the classes C35/45 to C 55/67 (Table 12.25). Higher concrete classes may be adopted if authorized by national standards. In practice, *concrete classes* C 70/85 to C 100/115 are preferably used to produce prestressed spun concrete poles. For this concrete class, the German Institute for Civil Engineering Technology (Deutsches Institut für Bautechnik) released an authorized general permission. Poles using concrete C 100/115 can be designed with a dead weight reduced by up to 25 % reaching the same overall strength.

The following cases should be distinguished for determining the most unfavourable actions:

- Case 1: permanent actions,
- Case 2: variable actions,
- Case 3: accidental actions,
- Case 4: other actions, e. g. transport and construction loads.

In addition to the vertical loads, the conductor tensile forces at the annual mean temperature, e. g. of +10°C in Central Europe, are considered as *permanent loads*. Wind loads need not to be dealt with as permanent loads.

Variable actions result from the individual load cases as required by the applicable standard, e. g. EN 50341-1 [12.8] for Europe and EN 50 341-3-4 [12.10] for Germany. *Accidental actions* result from the relevant load cases as specified by the above mentioned relevant standards. The *transport and construction loads* account for the corresponding actions on the poles. For determining the design loads in cases 2 to 4, the characteristic values of actions are multiplied by the *partial factors* γ_F according to the applicable standard (Table 12.26). The *resistance of concrete* is computed with the stress-strain diagram according to Figure 12.80. The design value of the concrete compression strength is $f_{cd} = \alpha \cdot f_{ck}/\gamma_{cr}$. According to prEN 1992-1, clause 11.3.5, the factor α is 0,85 for light-weight structures. The characteristic cylinder strength f_{ck}

Table 12.26: Partial factors according to prEN 1992-1, EN 50341-1 and EN 50341-3-4

Case	Description		Value and source
	Partial factor for actions		
1	Permanent actions, vertical loads		
	acting favourably	γ_F	1,0 (EN 50341-1; EN 50341-3-4)
	acting unfavourably	γ_F	1,0 (EN 50341-1); 1,35 (EN 50341-3-4)
	conductor tensile force	γ_F	1,0 (EN 50341-1); 1,35 (EN 50341-3-4)
2	Variable actions		
	wind loads	γ_F	1,0 to 1,4 (EN 50341-1); 1,35 (EN 50341-3-4)
	ice loads	γ_F	1,0 to 1,5 (EN 50341-1); 1,35 (EN 50341-3-4)
	conductor tensile force	γ_F	1,0 to 1,5 (EN 50341-1); 1,35 (EN 50341-3-4)
3	Exceptional actions	γ_F	1,0 (EN 50341-1); 1,0 (EN 50341-3-4)
4	Transport and construction	γ_F	1,1 (EN 12843)
	Partial factors for material		
5	Concrete		
	normal load	γ_{cr} [1)]	1,50 (prEN 1992-1)
	accidental load	γ_{cr} [1)]	1,20 (prEN 1992-1)
	precast concrete	γ_{cr} [1)]	1,40 (EN 50341-3-4, Table 4.3.11/DE.3)
6	Reinforcing steel		
	normal load	γ_S	1,15 (prEN 1992-1)
	accidental load	γ_S	1,00 (prEN 1992-1)

[1)] The partial factor is related to $0,85 \cdot f_{ck}$ according to prEN 1992-1, clause 11.3.5

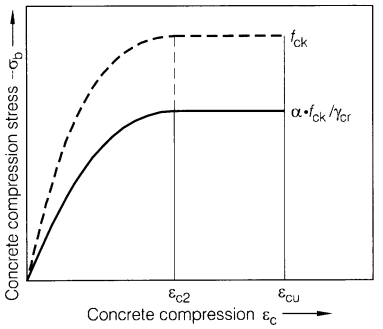

Figure 12.80: Stress-strain diagram for concrete in compression to determine the resistance for internal forces and moments at the limit state of strengths (parabola-rectangle diagram)

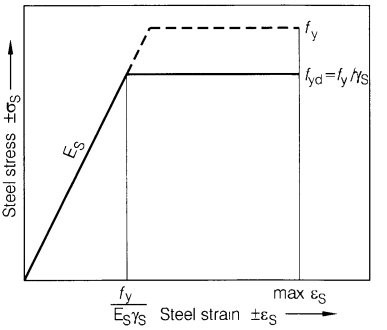

Figure 12.81: Stress-strain diagram for reinforcing steel for determining the resistance for internal forces and moments and the deformations at the limit state of strengths

corresponds to the nominal cylinder strength of the concrete class. In general, a partial factor $\gamma_{cr} = 1{,}50$ applies for concrete [12.61]. According to EN 50341-3-4, Table 4.3.11/DE.3, $\gamma_{cr} = 1{,}40$ is accepted for prefabricated concrete parts. The design values for compression stress are given in Table 12.25 assuming $\gamma_{cr} = 1{,}50$ and 1,40.

The stress-strain curve presented in Figure 12.81 is used for reinforcing steel and prestressed steel. According to prEN 1992-1, the modulus of elasticity for analysis is $E_S = 200\,000$ N/mm^2. The steel strain can be utilized up to a value of max $\varepsilon_S = 2$ %.

The *design torsional moment* M_T in N·mm may be determined from:

$$M_T = 0{,}42 \cdot f_{ck\,cube}^{2/3} \cdot W_T/\gamma_{cr} \quad \text{for spun concrete} \tag{12.142}$$

and from

$$M_T = 0{,}3 \cdot f_{ck\,cube}^{2/3} \cdot W_T/\gamma_{cr} \quad \text{for vibrated concrete,} \tag{12.143}$$

where $f_{ck\,cube}$ is the characteristic cube strength of the concrete in N/mm^2 and W_T the *torsional section modulus* of the concrete cross section in mm^3. When using high-strength concrete, only the characteristic strength of C 55/67 should be assumed for $f_{ck\,cube}$ independently of the actual concrete strength.
The internal forces and moments for the *limit states* of the strength are determined by assuming γ_F times the characteristic load and taking care of *pole deformation* (second order theory). Thereby, an unintentional inclination of the unloaded pole of 5 mm/m is assumed. The inclination takes as well care of curvatures due to unequal heating.
The effects of pole deformation need not to be considered if the additional moment due to deformation and inclination is less than 5 % at the top of foundation or less than 10 % for the most unfavourable section. For verification, an assessment on the safe side is sufficient. This condition is fulfilled by most of the overhead power line poles.
Prestressed poles have to be designed such that tensile stresses do not occur neither in case of permanent loads (case 1) nor under action of 40 % of the maximum loads according to case 2 without any partial factors.
The maximum *width of cracks* under normal load is limited to 0,3 mm in case of reinforced concrete according to EN 50 341-1. The verification of constraint of crack widths is carried out according to prEN 1992-1 [12.61].
All actions are assumed with their characteristic values without partial factors for verification of the *serviceability*. The deformation of the pole top is limited to 0,025 L_M, where L_M is the total pole length (see EN 50 341-1 [12.8]).

12.7.7 Example for design of a spun concrete pole

12.7.7.1 Basic data

A prestressed spun concrete suspension pole should be designed for a double circuit 110 kV line equipped with:
1 OPGW, cross section A_c = 141 mm^2; diameter d = 21,5 mm; mass m_c = 0,77 kg/m; σ_I = 126 N/mm^2 at 14,30 N/m ice load.
2 x 3 conductors 243-AL1/39-ST1A, cross section A_c = 232,5 mm^2; diameter d = 21,8 mm; mass m_c = 0,98 kg/m; σ_I = 101 N/mm^2 at 14,36 N/m ice load.
Wind span 300 m, maximum weight span 400 m
Wind load according to EN 50 341-3-4 [12.10], zone 1; ice load according to zone 2.
Dimensions of poles see Figure 12.82, total length 37,2 m, joint at 20,0 m from top, increase of diameter 18 mm/m, weight of pole 280 kN, concrete quality C 80/95, steel S1570/1770.

12.7.7.2 Calculation of loads

Wind load without ice:
OPGW: height z = 35 m; $q_z = 800 + 3 \cdot 35 = 905$ N/m^2
Wind load (equation (6.73)): $Q_{WC} = 905 \cdot 1{,}0 \cdot 0{,}0215 \cdot 300(0{,}45 + 60/300) = 3{,}79$ kN
Conductors average height z = 25 m, q_z = 875 N/m^2
Wind load: $Q_{WC} = 875 \cdot 1{,}0 \cdot 0{,}0218 \cdot 300(0{,}45 + 60/300) = 3{,}72$ kN
Insulators: $Q_{W\,ins} \sim 0{,}35$ kN
Pole: Top of pole (equation (6.76)): $Q'_{W\,pole} = 905 \cdot 0{,}7 \cdot 0{,}408 = 258$ N/m; Bottom of pole: $Q'_{W\,pole} = 800 \cdot 0{,}7 \cdot 1{,}038 = 581$ N/m; total pole: $Q_{W\,pole} = (258 + 581)/2 \cdot 35{,}0 = 14{,}7$ kN
Vertical loads:
OPGW: $W_C = 400 \cdot 9{,}81 \cdot 0{,}77 = 3{,}40$ kN
Conductors: $W_C = 400 \cdot 9{,}81 \cdot 0{,}98 = 3{,}85$ kN
Insulators: $W_{ins} \sim 1{,}0$ kN
Total vertical loads:
OPGW $G_K \sim 3{,}5$ kN

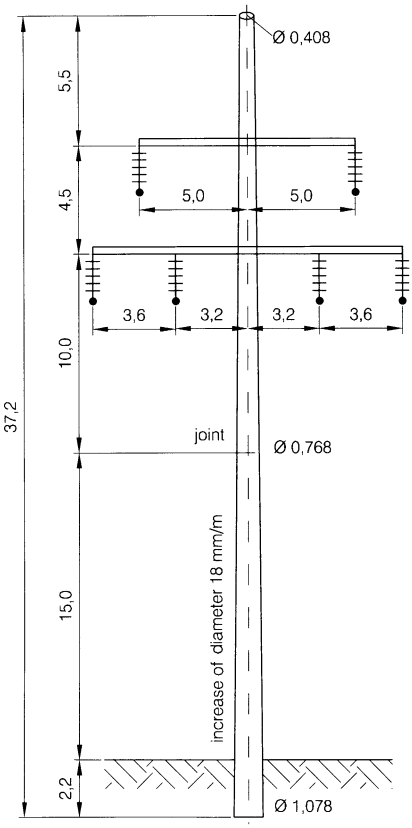

Figure 12.82: Dimensions of a suspension pole for a 110 kV double circuit line (example)

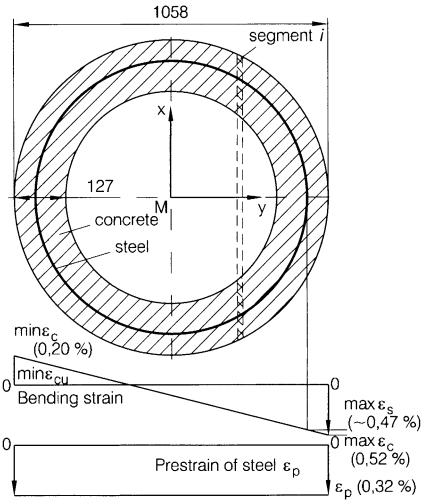

Figure 12.83: Cross section for verification of bending

Crossarm 1 $G_K = 2(3{,}9 + 1{,}0) + 40 \sim 50$ kN
Crossarm 2 $G_K = 4(3{,}9 + 1{,}0) + 60 \sim 78$ kN
Pole $G = 180$ kN

Wind loads with ice:
OPGW: Diameter with ice (equation (6.84)), ice load $g_I = 14{,}30$ N/m
$D_I = \sqrt{d^2 + 0{,}00017\, g_I} = \sqrt{0{,}0215^2 + 0{,}00017 \cdot 14{,}30} = 0{,}0538$ m
$Q_{WCI} = 0{,}5 \cdot 905 \cdot 1{,}0 \cdot 0{,}0538 \cdot 300/0{,}45 + 60/300) = 4{,}75$ kN

Conductors: Ice load 14,36 N/m; $D_I = \sqrt{0{,}0218^2 + 0{,}00017 \cdot 14{,}36} = 0{,}054$ m
$Q_{WCI} = 0{,}5 \cdot 875 \cdot 1{,}0 \cdot 0{,}054 \cdot 300(0{,}45 + 60/300) = 4{,}61$ kN

Insulators: $Q_{WinsI} \sim 0{,}35$ kN

Pole: $Q_{WpI} = 0{,}5\, Q_{Wp} = 7{,}35$ kN

Vertical loads:
OPGW: $W_{CI} = 400 \cdot (9{,}81 \cdot 0{,}77 + 14{,}3) = 8{,}74$ kN
Conductors: $W_{CI} = 400 \cdot (9{,}81 \cdot 0{,}98 + 14{,}36) = 9{,}59$ kN
Insulators: $W_{insI} \sim 1{,}5$ kN

Total vertical loads:
OPGW $G_K \sim 8{,}75$ kN
Crossarm 1 $G_K = 2(9{,}59 + 1{,}5) + 40 \sim 62$ kN
Crossarm 2 $G_K = 4(9{,}59 + 1{,}5) + 60 \sim 105$ kN
Pole $G_K = 180$ kN

Torsional loads:

Table 12.27: Calculation of bending moment according to the 2nd order theory

Desig-nation	Lever arm	Deflec-tion	Wind without ice				Wind with ice			
			$Q_W \cdot \gamma_W$	M_Q	$G_K \cdot \gamma_K$	M_G	$Q_W \cdot \gamma_W$	M_Q	$G_K \cdot \gamma_K$	M_G
	m	m	kN	kN·m	kN	kNm	kN	kN·m	kN	kNm
OPGW	35,0	3,0	5,12	179	4,6	14	6,41	224	11,8	35
Crossarm 1	27,5	2,2	10,05	276	67,5	149	13,39	368	83,7	184
Crossarm 2	23,0	1,7	20,10	462	105,3	179	26,78	616	141,8	241
Pole	17,5	0,6	19,85	347	243,0	146	9,92	147	243,0	146
Total	–	–	–	**1 265**	–	**488**	–	**1 382**	–	**606**

Table 12.28: Data for verification concrete cross section

Concrete class		B 80/95
Steel quality		S1570/1770
External pole diameter	mm	1 038
Thickness of wall	mm	127
Concrete cover	mm	48
Total cross section of prestressed steel	mm^2	3 800
Axial force without prestressing	kN	481
Concrete design stress $f_{cd} = 0,85 \cdot 80/1,4$	N/mm^2	48,6
Exponent of parabola (see Figure 12.80)		1,70
Concrete compression strain ε_{cs} (see Figure 12.80)	%	0,22
Concrete compression strain ε_{cu} (see Figure 12.80)	%	0,24
Modulus of elasticity of concrete	N/mm^2	44 000
Yield stress of steel	N/mm^2	1 365
Yield strain of steel	%	0,70
Modulus of elasticity of steel	N/mm^2	195 000
Prestrain ε_p (see Figure 12.83)	%	0,322
Prestress of steel	N/mm^2	628
Maximum tensile strain concrete	%	0,52
Maximum tensile strain steel	%	0,50
Maximum compression strain concrete	%	0,20
Prestressing force of steel $628 \cdot 3\,800$	kN	2 368
Cross section concrete	cm^2	3 635
Moment of inertia concrete	cm^4	$3,84 \cdot 10^6$
Diameter of steel ring	mm	940
Moment of inertia steel	cm^4	$42,0 \cdot 10^3$

Crossarm 1: $M_T = 0,5 \cdot 282,5 \cdot 101 \cdot 5,0 \sim 71,3$ kN·m
Crossarm 2: $M_T = 0,5 \cdot 282,5 \cdot 101 \cdot 6,8 \sim 97,0$ kN·m
The resistance of the pole will be verified for the cross section at the ground surface. The bending moment is determined according to the 2nd order theory using equation (12.127). The deflection at the points of the load actions are the result of an iteration process as described in clause 12.6.2. Here, they are assumed as a result of a calculation carried out by a computer program.
The resulting moment will be

$$M^{II} = \sum Q_W \gamma_W \cdot h + \sum G_K \cdot \gamma_K \cdot f \quad .$$

The calculation is shown in Table 12.27. Partial factors $\gamma_W = \gamma_K = 1,35$ are considered.
Total bending moment for wind without ice is 1 753 kNm, for wind with ice 1 988 kNm. The moments do not differ so much; therefore, the same deflections can be used to take care of the effects due to the 2nd order theory.

12.7.7.3 Verification of cross sections

In Figure 12.83 the cross section is shown of the concrete pole at the ground surface. In Table 12.28 the data are given. The concrete class is C 80/95, the quality of prestressing steel is S1570/1770. The bending resistance of the cross section is determined assuming that the steel strain does not exceed 0,5 %. The cross section is divided into 20 segments. In Table 12.29 the

Table 12.29: Calculation of design resistance

Segment No.	Concrete area	Lever arm	Steel area	Strain concrete	Strain steel	Stress steel	Concrete compression	Force steel	Force concrete	Moment steel	Moment concrete
	A_c cm^2	y mm	A_p cm^2	ε_c %	ε_s %	σ_p N/mm^2	σ_c N/mm^2	N_p kN	N_c kN	M_p kN·m	M_c kN·m
1	117,4	493	1,9	0,520	0,842	1 365	0,00	259,4	0,0	127,9	0,0
2	279,0	441	1,9	0,482	0,804	1 365	0,00	259,4	0,0	114,4	0,0
3	354,0	389	1,9	0,445	0,767	1 365	0,00	259,4	0,0	101,0	0,0
4	207,9	337	1,9	0,407	0,729	1 365	0,00	259,4	0,0	87,5	0,0
5	172,7	285	1,9	0,369	0,691	1 348	0,00	256,2	0,0	73,1	0,0
6	155,1	234	1,9	0,332	0,654	1 275	0,00	242,2	0,0	56,6	0,0
7	144,5	182	1,9	0,294	0,616	1 202	0,00	228,3	0,0	41,5	0,0
8	138,0	130	1,9	0,257	0,579	1 128	0,00	214,4	0,0	27,8	0,0
9	134,1	78	1,9	0,219	0,541	1 055	0,00	200,4	0,0	15,6	0,0
10	132,3	26	1,9	0,181	0,503	981	0,00	186,5	0,0	4,8	0,0
11	132,3	-26	1,9	0,144	0,466	908	0,00	172,5	0,0	-4,5	0,0
12	134,1	-78	1,9	0,106	0,428	835	0,00	158,6	0,0	-12,3	0,0
13	138,0	-130	1,9	0,068	0,390	761	0,00	144,7	0,0	-18,8	0,0
14	144,5	-182	1,9	0,031	0,353	688	0,00	130,7	0,0	-23,7	0,0
15	155,1	-234	1,9	-0,007	0,315	615	-2,61	116,8	-40,5	-27,3	9,6
16	172,7	-285	1,9	-0,044	0,278	541	-15,88	102,8	-274,3	-29,4	78,3
17	207,9	-337	1,9	-0,082	0,240	468	-27,24	88,9	-566,2	-30,0	191,0
18	354,0	-389	1,9	-0,120	0,202	394	-36,52	74,9	-1 292,7	-29,2	503,2
19	279,0	-441	1,9	-0,157	0,165	321	-43,50	61,0	-1 213,9	-26,9	535,5
20	117,4	-493	1,9	-0,195	0,127	248	-47,78	47,1	-561,0	-23,2	276,6
$\sum$	3 669,9	–	38	–	–	–	–	3 463,5	-3 948,5	425,0	1 594,0
								$\sum$N =	**-485,0**	$\sum$M =	**2 019,0**

calculation is demonstrated. The strain due to bending is linearly distributed as shown in Figure 12.83. The total strain of the steel is the sum of the bending strain and the prestressing strain of 0,322 %. From the bending strain, the stresses in concrete and steel can be obtained assuming a parabola function for concrete (Figure 12.80) and a bilinar function for steel (Figure 12.81). The concrete contributes to the bending resistance only where the section is under compression, i. e. where the bending strain ε_c is negative.
The partial axial force for each segment is

$$N_c = A_c \cdot \sigma_c \quad \text{for concrete}$$

and

$$N_p = A_p \cdot \sigma \quad \text{for steel.}$$

Finally, the partial moment for each segment is obtained from

$$M_c = N_c \cdot y \quad \text{for concrete}$$

and

$$M_p = N_p \cdot y \quad \text{for steel.}$$

As can be seen from Table 12.29, the bending resistance due to steel is 425 kNm and that of concrete amounts to 1 594 kNm resulting in a total of 2 019 kN·m, being more than the ultimate loading of 1 988 kN·m.

The torsional resistance is verified at crossarms 1 and 2. At crossarm 1, the pole diameter is $d_a = 0,408 + 5,5 \cdot 0,018 = 0,507$ m. Assuming a thickness of 80 mm, the inner diameter is 0,347 m. The torsional section modulus is $W_T = (d_a^4 - d_i^4) \cdot \pi/(16\, d_a) = 20,0 \cdot 10^6$ mm^3.
Equation (12.142) yields with $f_{ck\,cube} = 67$ N/mm^2 (maximum according to C 55/67) and $\gamma_{cr} = 1,4$

$$M_{Td1} = 0,42 \cdot 67^{2/3} \cdot 20,0 \cdot 10^6/1,4 = 99,0 \cdot 10^6 \text{ N} \cdot \text{ mm} = 99,0 \text{ kNm}.$$

At crossarm 2, the pole diameter is $d_a = 0,408 + 10 \cdot 0,018 = 0,588$ m. Here, it is $W_T = (588^4 - 428^4) \cdot \pi/(16 \cdot 588) = 28,71 \cdot 10^6$ mm^3 and

$$M_{Td2} = 0,42 \cdot 67^{2/3} \cdot 28,71 \cdot 10^6/1,4 = 142,1 \cdot 10^6 \text{ N} \cdot \text{ mm} = 142,1 \text{ kNm}.$$

The design moments are higher than the loading.

12.8 Wood poles

12.8.1 Application and design

Wood poles are used extensively where they are readily available. Medium and lower-voltages lines can be built economically with such poles fitted with either steel or wood crossarms. Wood H-frames composed of two poles tied together at the top with wood or steel crossarms have been successfully used up to 345 kV. To take full advantage of the transverse strength, such poles can be braced internally in at least a portion of their height with wood or metal crosses.
In Europe, five standards apply to poles made of hard and soft wood. Such standards contain specifications and requirements for the classification of wood poles according to visual and mechanical testing procedures [12.62], determination of characteristic data [12.63, 12.64], procedures for establishing protective treatments [12.65] and preferred dimensions [12.66].
Economically viable solutions adopting wood poles are possible if the wood can be supplied at a reasonable price, the poles are simple to produce, last long enough and sufficiently long spans can be obtained by the pole heights. Economic designs can be achieved for of overhead power lines with low operating voltages and span lengths up to approximately 50 m. The poles can be used as single or double poles. However, longer spans should be aimed at with respect to the investment necessary for the insulation of lines with higher nominal voltages. Span lengths up to 250 m can be achieved by *wooden portal-type structures* where the conductors are arranged in a horizontal plane. Still longer spans require heights of structures which cannot be achieved by one-piece wood poles. The arrangement of joints, however, leads to a more expensive production.
Predominantly, conifer wood is used characterized by a straight, slender growing. In Europe, especially pines and spruce conifer as well as larch are used according to availability. Other types of wood can be used as well, whereby straight growth and good condition of the stem without holes and cracks are important. EN 12 510 [12.62] contains requirements for the visual classification of strength and specifications for preferred types of wood to produce poles. In Australia, South America and other countries, eucalyptus and pine trees have been used successfully. Some preferred species are paniculata, citri odora, terenticornis and alba rostata.
The wood poles are specified as a function of the rated force at the top and of the top and base dimensions.
The rated force at the top should not be exceeded by the characteristic loads which may correspond, for instance, to a transverse wind having the probability of 2 % of being exceeded. A high partial factor (usually in the range 5 to 10) is considered towards the rupture of the pole.

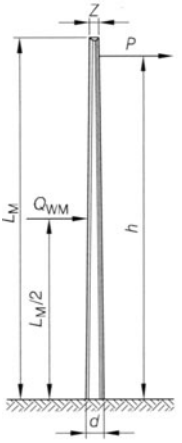

Figure 12.84: Calculation of a wood pole

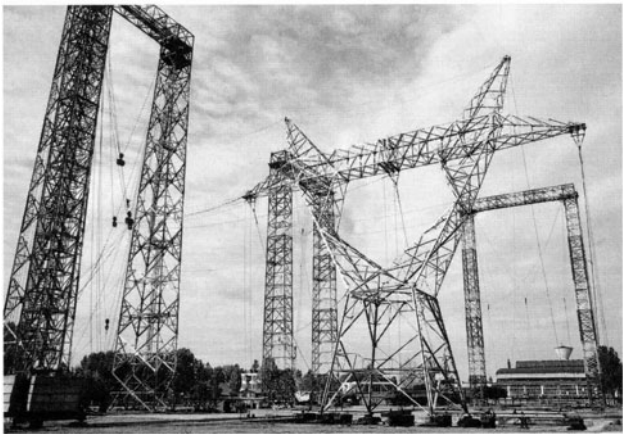

Figure 12.85: Station for testing overhead line towers

The reason for high partial factors is tied to the *organic decomposition* of the wood, which is accelerated within the pole section close to the soil surface, where the bending moment resulting from loads applied to the pole is the biggest. The external fibres of the pole section at the earth level are loaded with the highest stress and is counteracted with the wood resistance modulus. So the selection of a wood pole refers that section. Wood poles can consist of a single pole or of two poles connected to double poles, A-shaped poles or portals depending on the required resistance. *Double poles* consist of two individual poles which are arranged one beside the other and connected by bolting or doweling. *A-shaped poles* are formed by two individual poles inclined to each other and bolted or connected by dowels at the top and connected by a transverse bar approximately at half of the total height. Portal structures consist of two wood poles and a horizontal crossarm.

12.8.2 Rating

In most cases, a verification of the stresses can be waived for wood poles. It is sufficient to determine the *characteristic force* from the stipulated actions. The required pole can be selected from the catalogues of the manufacturers or according to EN 12 479 [12.66]. The moment due to the external actions including the wind load on the pole is determined at ground surface and, therefrom, the stress. According to Figure 12.84 it applies:

$$M = P \cdot h + Q_{\mathrm{WM}} \cdot L_{\mathrm{M}}/2 \quad , \tag{12.144}$$

where P is the effective characteristic load and W_{M} the wind load on pole.
The stress in the section at ground level is

$$\sigma = N/A + M/W \quad , \tag{12.145}$$

where $W = \pi \cdot d^3/32$ and $A = \pi \cdot d^2/4$. N is the axial force due to external vertical loads and the pole dead weight. The actions have to be multiplied by the relevant partial factors, for example according to EN 50 341-1. The *resistance* of the pole may not be exceeded. ENV 1995-1-1 [12.67] specifies the resistance concerning tensile, compression and bending load. A partial factor $\gamma_{\mathrm{M1}} = 1{,}50$ is considered to calculate the design

value of the resistance. On the load side, partial factors between 4 and 10 are applied, relating the characteristic load to the resistance.
The *deformation* of wood poles can be obtained from

$$f_d = (P/3 + Q_{WM}/8) \cdot h^3/(EI) \quad , \tag{12.146}$$

where the modulus of elasticity E can be assumed to be 10 000 N/mm^2, I is the moment of inertia at the ground surface being $I = d^4 \cdot \pi/64$ with d being the pole diameter.
With respect to the resilience of the upper soil layers, the length h in (12.146) and the diameter d should be related to a cross section approximately 0,5 m below the ground surface level. According to EN 50 341-1, it is recommended to limit the deformation to a maximum of 10 % of the pole length under the relevant external load.
Three times the section modulus of a single pole can be considered for the verification of the resistance of double poles which are sufficiently connected to each other and the load acts in the plane represented by both pole axes. In case of load in another direction, only twice the section modulus of a single pole may be considered.
The strength of *A-type poles* depends on the compression stability of the struts. The compression force is obtained approximately from

$$S_D = 2 \cdot P \cdot h/b \quad , \tag{12.147}$$

where b is the distance of the central axes of both struts at ground surface level. The verification of stability for one strut can be demonstrated according to ENV 1995-1-1 considering the corresponding buckling curve.

12.8.3 Treatment of wood poles

Wood decay is due to a fungus which requires air, moisture, warmth and food for its subsistence. The wood of the pole constitutes its food. The conditions most favourable to the growth of the fungus are found at the ground line. The preservatives should have toxic and antiseptic properties which make the wood either poisonous or unfit for the fungus.
A way used everywhere to improve the wood qualities, as far as resistance to weathering is concerned, is the *chemical preservative treatment* with creosote or pentachlorophenol. The main methods for applying the preservatives to the poles are:

- The open-tank method, which consists in boiling the butts of the poles in a tank of creosote oil, after which the oil is allowed to cool or the poles are transferred to a cold tank of oil.
- The pressure treatment, in which the poles lie on a trunk and are run into a steel cylinder and subjected to a steam treatment for a period of several hours at a temperature which will not damage the wood cells. The pressure is then removed and a vacuum is applied.

Beside the preservative treatment, it is recommended that the base section and a length up to a depth of about 0,6 m below the ground line receives an additional protection, such as plastic band-aids or special painting coating. The objective of a pole treatment and additional protective measures of the coatings is to make it fit for a minimum life of 30 years.

12.9 Loading and failing tests

12.9.1 Introduction

Tests on supports may be performed for various reasons. In a traditional *proof test*, the test is set up to verify the design conditions, that is, only static loads are applied,

the support has level, fixed foundations, and the restraints at the load points are the same as in the design model. If a proof test is ordered, it should be done on a full size prototype structure before that support, or another tower of similar design for the same overhead line, is fabricated in quantity. This kind of test will verify the adequacy of the members and their connections to withstand the static design loads specified for that structure as an individual entity under controlled conditions. Proof tests provide information on support behaviour under load, fit-up verification, action of the structure in deflected positions, adequacy of connections, and other benefits. The test cannot completely confirm, how the tower will react in the transmission line where the loads may be dynamic, the foundations may be less than ideal, and where there is some restraint from intact wires at the load points.

The following guidelines are based on performing a proof test using a test installation that has facilities to anchor a single tower to a fixed base, to load and monitor pulling lines in the vertical, transverse, and longitudinal directions, and to measure deflections. ASCE Manual 52 [12.20] and IEC 60 652 [12.68] provide details on support testing. IEC 60 652 is under revision and will be published in 2002.

Loading tests supplement the calculations and should validate that the static calculations are correct and any shortcomings potentially given in the structure be recognized. In case of *failure tests*, the loads are increased until the failure of the structure. This procedure enables to determine the actual magnitude of the *support resistance* and its strength reserves, if any. Testing stations are similarly designed (see Figure 12.85). The specified loads are exerted on the tested structures by means of ropes. To enable a horizontal loading, auxiliary portal frames are necessary.

With respect to loading tests, IEC 60 652 distinguishes between design tests and acceptance tests. *Design tests* are carried out at prototypes of the supports at full scale. The load is increased either up to the design load (ultimate failure limit) or until the failing of the structure. *Acceptance tests* are carried out either before or during production of a serial batch of structures, whereby the quality of production and materials used should be verified. The structure may be taken from the serial production on a random basis. Acceptance tests are carried out up to the design load. A structure neither damaged nor failed may be used within the line after being successfully tested.

12.9.2 Foundations for support under test

Tests should be made with the support on rigid foundations. The design engineer and the test facility engineer should establish allowable setting tolerances. Positioning of the foundations should be checked to ensure that accurate alignment prevents any abnormal stresses in the support or tower members.

12.9.3 Material for the tower under test

For a test, the structure needs to be made of material that is representative of the material that will be used in the production of towers. Mill test reports or coupon tests should be available for all important members in the tower comprising at least the members designed for tension loading only and compression members with a slenderness ratio less than 120. Proper interpretation of the data obtained from testing is required for establishing the true capacity of individual members. There is concern about using members in a test tower which have yield points considerably higher than the minimum guaranteed values used as the basis for design. The actual yield points of tension members and of compression members with slenderness ratio values less than 120 are critical in determining the member capacity. All other members of test tower should conform to standard material specifications, but their actual yield points are not as crucial to their *load-carrying capabilities.*

12.9.4 Fabrication of the prototype tower under test

Fabrication of the prototype tower should be done in the same manner as for the towers in the production run. A tower that is specified to be galvanized for the transmission line needs not be galvanized for the test, but the purchaser has the option of specifying that the test tower must be galvanized.

12.9.5 Strain measurements

Stress determination methods, primarily *strain gauging*, may be used to monitor the loads in individual members during testing. Comparison of the measured unit stress to the predicted unit stress is useful in validating the proof test and refining analysis methods. Care must be exercised when instrumenting with *strain gauges*, both as to location and number, to assure valid correlation with design stress levels. In most cases, only the total loads are measured through load cells installed near the load application points or panels.

12.9.6 Assembly and erection

The *tower assembly method* of the tested structure should be specified by the purchaser. If tight bolting of subassemblies is not permitted by the construction specifications, the test tower should be assembled and erected with all bolts finger tight only, and tightening to final torque should be done after all tower members are in place. Pick-up points that have been designed in the tower can be used during erection as part of the test procedure. The erected tower should conform with the special requirements of the purchaser's instructions; many purchasers specify minimum torque for bolt tightening, and that the vertical axis should not be out of plumb by more than around 3 % of height. or 0,5 m at maximum. In Figure 12.85 a tower in a test station is shown.

12.9.7 Test loads

The loads to be applied to the test support should reflect the load cases specified for design and should include all overload capacity partial factors. The testing specifications describe the procedure for testing to *destruction.* Wind-on-tower loads may be applied as concentrated loads on the tower at selected panel points. These loads should be applied at panel points where stressed members intersect so that the loads can be resisted by the main structural system of the tower.

Carrying out of a load test is described by a *testing specification.* Its essential contents concern information on the design loads which are specified for each individual load case of the structure. In addition, information is contained on the position of the load actions, the measuring points of deflection and members which should be equipped with strain gauges. The loads are usually applied either manually by hydraulic jacks and block and tackles or by motor-driven winches and are measured by load cells installed close to the application points to eliminate the losses in the application systems. Based on the testing specification, the testing entity establishes a *testing program.* Essential details of the testing program concern the explanation and schematic presentation of the test arrangement, the position of dynamometers, of deflection measurement points and strain gauges as well as details on the loads for each individual load case tested and each step of load.

The directions and point of actions of loads are specified for each individual load case together with the forces. The forces should as far as possible correspond to those which may occur during operation. Wind loads need to be simulated as concentrated actions, the arrangement of which should result in the same moments as the design wind load.

12.9.8 Load application

Ropes should be attached to the load points on the test tower simulating the in-service *load application* as close as possible. The attachment hardware of the test should have the same degrees of freedom as in-service hardware. V-type insulator strings should be loaded at the point were the insulator sets intersect. If the insulator for the tower in the line are V-type sets that will not support compression, it is recommended that articulated bars or wire rope slings are used to simulate the insulators. If compression or cantilever insulators are planned for the towers, members that simulate those conditions should be used in the test.

As a structure deflects under load, ropes may change their direction of pull. Adjustments should be made in the applied loads or the test rigging be offset accordingly, so that the vertical, transverse and longitudinal vectors at the deflected load points correspond the loads specified in the tower loading schedule.

12.9.9 Load procedure

The number and sequence of load cases tested should be specified by testing specification and the testing program, both approved by the purchaser. It is recommended that those load cases having the least influence on the results of successive tests be tested first. The sequence should simplify the operations necessary to carry out the *load procedure* and the test program.

Loads are normally incremented to 50, 75, 90, 95 and 100 % of the maximum specified loads. After each *load increment* is applied, there should be a hold to allow time for reading deflections and to permit engineers observing the test to check for signs of structural distress. The 100 % load for each load case should be held at least for one minute and for five minutes at maximum.

In case of design tests, the difference between the required and the measured load at an individual load action point should not exceed 5 %, and 10 % in case of acceptance tests. Loads should be removed completely between testing of individual load cases except for non critical cases where, the loads may be adjusted as required for the next load case. Unloading of the tower should be controlled to avoid overstressing any members.

12.9.10 Load measurement

All applied loads should be measured as close to the point of attachment to the support as possible. Loads should be measured through a suitable arrangement of strain devices or by predetermined dead weights. The effects of pulley friction should be minimized. *Load measurement* by monitoring the load in a single part of a multipart block and tackle arrangement should be avoided. Strain devices should be used in accordance with manufacturer's recommendations and calibrated prior to and after the conclusion of testing.

12.9.11 Deflections

Support deflections under load should be measured and recorded except as waived by the purchaser. Points to be monitored should be selected to verify the deflections predicted by the design analysis. Deflection reading should be made before and after loading at all intermediate holds during testing. All deflections should be referenced to common base reading such as the initial plumb position taken before any test loads are applied.

12.9.12 Acceptance and failures

A load test is considered as passed if the structure withstood the design loads for one minute without failure of an element or an assembly. Then, *acceptance* of the structures can be declared by the purchaser. If a premature *structural failure* occurred, the cause of the failure mechanism and the corrective measures to be taken should be determined in conjunction with the engineer responsible for the test. Failed members and members affected by consequential damage should be replaced. The load case which caused the failure should be repeated. Load cases previously completed need not be repeated.
After the structure has successfully withstood all load cases, the tower should be dismantled and all members inspected. The following should not be considered as a failure:

- Residual bowing of members designed for tension only.
- Ovalization of no more than half of the holes in a connection.
- Slight permanent deformation of no more than half of the bolts in a connection.

12.9.13 Destruction test

In some cases, the tower under test after passing successfully all load combinations may be loaded until rupture, as part of an agreement between purchaser and manufacturer. This is called *destruction test* and the load combination for taking the tower to ruptures is selected according to technical reasons. Generally, the load combination is taken as the one that prevails in the design of most components. Loads are incremented in steps of 5 %. The purpose of destruction tests could be to determine the surplus capacity of the structure and the economic adequacy of the design.

12.9.14 Disposition of test tower

The test specifications should state what use, if any, may be made of the test tower after the test is completed. An undamaged tower is usually accepted for use in the line after all components are visually inspected and found to be structurally sound and within design tolerances. If a test exceeding the accepted loads had been performed, caution should be exercised in accepting the parts that appear to be undamaged since they might have been overstressed.

12.9.15 Test report

The testing organisation should furnish the number of copies required by the testing specifications of a *test report* that should include:

- The designation and description of the support tested.
- The name of utility or line owner that will use the tower.
- The name of person or organisation that specified the loading, electrical clearances, technical requirements and general arrangement of the tower.
- The names of engineers responsible for design of structure and execution of the test.
- The manufacturer's name.
- A brief description and the location of the *test station.*
- The name and affiliations of the test witnesses.
- The dates of each test load case.
- Design and detail drawings of the tested tower including any changes made during the testing program.
- *Testing specification.*
- Testing program.
- A rigging diagram with details of the points of attachment to the tower.
- Calibration records of the load-measuring devices.

- A loading diagram for each load case tested.
- A list of deflections for each load case tested.
- In case of failure: photographs of the failure, loads at the time of failure, a brief description of failure, the remedial actions taken, the physical dimensions of the failed members, test coupon reports of failed members.
- Photographs of the overall testing arrangement and rigging.
- Air temperature, wind speed and direction, any precipitation and other pertinent meteorological data.
- Mill test reports as submitted due to the requirements of material together with additional information specified by the purchaser

12.10 References

12.1 Boldin, Y. A. et al.: Guyed circuit-type suspension tower of polymer long-rod insulators for 1 150 kV transmission lines. Cigré Report 100-02, Symposium Leningrad, 1991

12.2 Boni, F. et al.: ENEL's achievements and prospects in the area of compact 380 kV overhead lines. Cigré Report 100-10, Symposium Leningrad, 1991

12.3 Steel poles in the US for 400 kV lines ((open))

12.4 Fenz, J.; Kortmann, S.: Freileitungen für Nigeria (Overhead power lines for Nigeria. Siemens Power Engineering 2 (1980), pp. 223 to 226

12.5 Schmidt, G.: Stahlbetonmastfertigung im Ausland (Production of concrete steel poles in foreign countries). BBC-Nachr. 59 (1977), pp. 62 to 65

12.6 ASCE 1052: Guide for the design and use of concrete poles. New York, ASCE, 1987

12.7 Souchereau, N. et al.: Validation of a chainette tower for a 735 kV line. Cigré Report 22-04, 1978

12.8 EN 50 341-1: Overhead electrical lines exceeding AC 45 kV. Part 1: General requirements – Common specifications. Brussels, CENELEC, 2001

12.9 EN 50 341-3: Overhead electrical lines exceeding AC 45 kV. Part 3: National Normative Aspects (NNA). Brussels, CENELEC, 2001

12.10 EN 50 341-3-4: Overhead electrical lines exceeding AC 45 kV. Part 3-4: National Normative Aspects (NNA) for Germany. Brussels, CENELEC 2001

12.11 NBR 5422: Design of overhead transmission lines – Procedures. Rio de Janeiro, March 1985

12.12 Kießling, F.; Sperl, H. D.: The new 380 kV river Elbe crossing of the Nordwestdeutsche Kraftwerke AG. Siemens Power Engineering 1 (1979), pp. 75 to 79

12.13 ENV 1993-1-1: Eurocode 3: Design of steel structures; Part 1-1: General rules and rules for buildings. Brussels, CEN, 1992

12.14 DIN VDE 0210: Planning and design of overhead power lines with rated voltages above 1 kV. Berlin, DKE, 1985

12.15 Kießling, F.; Ranke, K.: Beanspruchung von Freileitungen durch extreme Wind- und Eislasten (Loading of overhead lines by extreme wind and ice load). Elektrizitätswirtschaft 79 (1980), pp. 683 to 692

12.16 IEC/TR 60 826: Loading and strength of overhead transmission lines. Geneva, IEC, 1991

12.17 EN 10 056: Structural steel equal and unequal leg angles.

Part 1: Dimensions. Brussels, CEN, 1998;

Part 2: Tolerances on shape and dimensions. Brussels, CEN, 1994

12.18 Mors, H.: Gittermaste für Hochspannungsleitungen (Lattice steel towers for high-voltage overhead lines). Leaflet steel 389. Düsseldorf. Beratungsstelle für Stahlverwertung 1966

12.19 Kießling, F. et al.: Die Maste der neuen 380-kV-Hochspannungsfreileitung über die Elbe (The towers of the new 3880 kV high-voltage crossing over the rive Elbe). Stahlbau 48 (1979), pp. 321 to 326, 360 to 366

12.20 ASCE Manual 52: Guide for design of steel transmission towers. New York, ASCE, 1988

12.21 EN ISO 1461: Hot-dipped galvanized coatings on iron and steel articles. Specifications and test methods (ISO 1461). Brussels, CEN, 1999

12.22 Nieth, F.: Die Haftfestigkeit feuerverzinkter Überzüge (The adhesion of galvanized zinc coating). Bänder, Bleche & Rohre. 14 (1973), pp. 95 to 102

12.23 DIN 50 978: Testing of metallic coatings. Adherence of hot-dip zinc coatings. Berlin, DIN, 1985

12.24 Horstmann, D.: Untersuchung über die Prüfung verzinkter Drähte nach W. H. Preece (Investigation on testing galvanized wires according to W. H. Preece). Stahl und Eisen 80 (1960), pp. 931 to 935

12.25 van Oeteren, K.-A.: Feuerverzinken und Beschichten = Duplex-System (Galvanization and coating by paint constitutes the Duplex system). Merkblatt Stahl 329. Düsseldorf: Beratungsstelle für Stahlverwertung, 1981

12.26 EN 10 025: Hot-rolled products of non alloy structural steels. Technical delivery conditions. Brussels, CEN, 1994

12.27 EN ISO 898-1: Mechanical properties of fasteners made of carbon steel and alloy steel. Part 1: Bolts, screws and studs. Brussels, CEN, 1999

12.28 Dünkel, V.: Verformungsfähigkeit und Tragfähigkeit von Verbindungsmitteln für den Stahlbau/Mastbau – Gebrauchstauglichkeit von Schrauben der Festigkeitsklasse 5.6 und 6.8 nach ISO 898-1 (Ductility and strength of fasteners for steel structures and steel towers – serviceability of bolts of strength classes 5.6 and 6.8 according to ISO 898-1). Bochum und Parey. Schrauben und Draht Union GmbH & Co KG

12.29 Schmidt, B.: Die Berechnung von Freileitungsmasten nach der Methode der finiten Elemente (Calculation of overhead towers using the finite element method). Elektrizitätswirtschaft 84 (1985), pp. 846 to 851

12.30 Bufler, H.; Kießling, F.: Digitale Berechnung torsionsbeanspruchter Gittermaste von Freileitungen (Calculation of torsion-loaded lattice steel towers of overhead lines). Elektrizitätswirtschaft 64 (1965), pp. 711 to 718

12.31 Hahn, H. G.: Methode der finiten Elemente in der Festigkeitslehre (Method of finite elements in strength analysis). Wiesbaden. Akademische Verlagsgesellschaft, 2nd edition, 1982

12.32 Lawo, M., Thierauf, G.: Matrizenmethoden der Statik und Dynamik (Matrix methods of statics and dynamic). Braunschweig, Wiesbaden: Vieweg Verlag, 1980

12.33 Bathe, K.-J.: Finite element procedures in Engineering analysis. London, Prentice-Hall, 1982

12.34 Fenz, J.; Koch, E.: Die Maste der 380-kV-Leitung KKE Lingen-Station Hanekenfähr, berechnet nach der Methode der finiten Elemente (The towers of the 380 kV line KKE Lingen to substation Hanekenfähr, designed on the finite element method). Elektrizitätswirtschaft 86 (1987), pp. 926 to 930

12.35 Gemperlein, W. et al.: Der moderne Tragsicherheitsnachweis von Freileitungsmasten (Modern strength verification of overhead line towers). Elektrizitätswirtschaft 96 (1997), pp. 1359 to 1362

12.36 Petersen, C.: Statik und Stabilität der Baukonstruktionen (Statics and stability of building structures). Braunschweig, Wiesbaden, Vieweg Verlag, 1980

12.37 Girkmann, K.: Die Knickfestigkeit von Raumtragwerken mit ebenen Knoten (The buckling stability of three-dimensional truss structures with plane nodes). Z. d. VDI 72 (1928), pp. 588 to 590

12.38 Bleich, H.: Das Ausknicken der Eckstiele von Gittermasten (Buckling of leg members of lattice towers). Bauingenieur 17 (1936), pp. 557 to 558

12.39 Djubek, J.: Die Stabilität eines dünnwandigen abwechselnd in zwei Ebenen gestützten Stabes (Stability of a thin-walled member alternately supported in two planes). Stahlbau 29 (1960), pp. 218 to 220

12.40 DIN 4114-1: Steel structures; stability (buckling, overturning, bulging), method of calculation, regulations. Berlin, DIN, 1952

12.41 BSI DD 133: Code of practice for strength assessment of members of lattice towers and masts. London, BSI, 1986

12.42 ECCS Code No. 39: Recommendations for angles in lattice transmission towers. Brussels, ECCS, 1985

12.43 Beer, H.: Statische und konstruktive Gesichtspunkte im Stahlleichtbau (Static and structural aspects of light-weight steel structures). Stahlbau-Rundschau, Zeitschrift des österreichischen Stahlbauvereins (1964), pp. 31 to 48

12.44 Fuchs, A.: Freileitungsmaste mit außergewöhnlichen Dimensionen für die Kreuzung des Suez-Kanals (Overhead line towers with extraordinary dimensions for the crossing of Suez Channel). Elektrizitätswirtschaft 98 (1999), pp. 36 to 41

12.45 Schramm, H. et al.: Freileitung der Superlative verbindet Europa und Asien (Overhead line of the superlative connects Europe and Asia). Elektrizitätswirtschaft 99 (2000), pp. 13 to 20

12.46 Gohm, H.; Kießling, F.; Mahr, V.: Verformungen von Stahlvollwandmasten mit Steckstößen beim Einsatz in Hochspannungsfreileitungen (Deformation of steel poles with slipped joints used for high-voltage transmission lines). Elektrizitätswirtschaft 97 (1998) 23, pp. 27 to 31

12.47 Bauer, K.-H.; Schmidt, B.: Ein Verfahren zur näherungsweisen Ermittlung des Verformungszustandes von Freileitungsmasten (An approach to approximate determination of the deformation condition of overhead line towers). Elektrizitätswirtschaft 88(1989) 23, pp. 1605 to 1611

12.48 Peterson, C.: Stahlbau (Steel structrures). Braunschweig, Wiesbaden. Vieweg Verlag, 3rd edition 1993

12.49 Fenz, J. et al.: Digitale Berechnung der Tragwerke von Hochspannungsfreileitungen (Digital computation of overhead power lines supports). Elektrizitätswirtschaft 61 (1962), pp. 866 to 871

12.50 Fenz, J,: 20 Jahre Einsatz von Digitalrechnern für die mechanische Bemessung von Freileitungen (Twenty years of computer application for the mechanical design of overhead lines). Elektrizitätswirtschaft 81 (1982), pp. 189 to 197

12.51 DIN 18 00-1: DIN 18 800–Part 1: Structural steelwork. Design and construction. Berlin, DIN, 1990

12.52 DIN 18 00-2: DIN 18 800–Part 2: Structural steelwork. Safety against buckling of linear members and frames. Berlin, DIN, 1990

12.53 Kießling, F. et al.: Upgrading high-voltage lines to increase their capacity and mitigate environmental impacts. Cigré Report 22-208, 1998

12.54 Beck, H.; Bentzen, P.; Knauer, F.: Verstärkungsmaßnahmen an einer 110-kV-Doppelleitung (Upgrading of a 110 kV double circuit line). Elektrizitätswirtschaft 97 (1998), pp. 40 to 42

12.55 Eurocode 1. ENV 1991-2-4: Actions on structurs. Wind loads. Brussels, CEN, 1995

12.56 ASCE Manual 72: Design of steel transmission pole structures. New York, ASCE, 2nd edition 1990

12.57 Stahlmaste in Vollwandbauweise (Solid-wall steel poles). Studiengesellschaft Stahlanwendung e. V., Projekt 152. Universität-Gesamthochschule Essen, Fachbereich Bauwesen, 1992

12.58 Sherman, D.: Why concrete poles? Missouri Valley electric association conference. Kansas City 1991

12.59 prEN 13 369: Common values for precast concrete products. Brussels, CEN, 2002

12.60 prEN 12 843: Precast concrete masts and poles. Brussels, CEN, Draft 1999

12.61 prEN 1992-1 (Final draft): Eurocode 2: Design of concrete structures; Part 1: General rules and rules for buildings. Brussels, CEN, 2001

12.62 EN 12 510: Wood poles for overhead lines – Strength grading criteria. Brussels, CEN, Draft 1996

12.63 EN 12 511: Wood poles for overhead lines – Determination of characteristic values. Brussels, CEN, 1996

12.64 EN 12 509: Wood poles for overhead lines – Test methods, determination of modulus of elasticity, bending strength, density and moisture content. Brussels, CEN 1996

12.65 EN 12 465: Wood poles for overhead lines – Durability requirements. Brussels, CEN, 1996

12.66 EN 12 479: Wood poles for overhead lines – Sizes – Methods of measurement and permissible deviations. Brussels, CEN, Draft 2001

12.67 ENV 1995-1-1: Eurocode 5: Design of timber structures; Part 1-1: General rules and rules for buildings. Brussels, CEN, Draft 1993

12.68 IEC 60 652: Loading tests on overhead line towers. Geneva, IEC, Draft 2000

13 Foundations

13.0 Symbols

Symbol	Signification
A	Cross-sectional area
A_s	Cross-sectional area in case of tensile load
b, b_x, b_y	Foundation width
b_1, b_2	Foundation width with rectangular subface
B_E	Tower width at ground level
c	Auxiliary value
c'	Cohesion
c_u	Undrained shear strength
C_L	Clear distance of foundation testing equipment
d	Diameter of foundation shaft
d	Pile diameter
d_s	Anchor rod diameter
D	Diameter of a pole at ground level
e	Eccentricity
e_p	Mechanical earth resistivity
e_p	Passive earth pressure
e_x, e_y	Eccentricity of total load in the foundation subface
E	Modulus of elasticity
E_d	Design value of the foundation load
E_K	Characteristic value of the foundation load
E_s	Compressibility modulus
f_{cK}	Characteristic concrete strength
f_s	Local skin friction
f_{ub}	Tensile strength
f_w	Mechanical earth resistivity according to Blum
$F_{b,d}$	Design resistance of an anchor
$F_{t,Rd}$	Design value of the resistance of an anchor
$F_{t,Sd}$	Design tensile force of an anchor
G	Sum from foundation dead load and earth weight vertically above foundation subface
G_B	Dead weight of concrete body
G_E	Dead weight of earth body
h	Equivalent height of load action
h'	Free pole length
h_v	Grouting length of an anchor
H	Horizontal load
I	Moment of inertia
k_p	Coefficient of passive earth pressure
K_s	Subgrade modulus
L	Pile length
M, M_x, M_y	Bending moment
n	Ratio of height of step to width of projection of a stepped concrete foundation
n_{10}, n_{30}	Number of blows for a penetration of 10 and 30 cm, respectively
N	Resultant total vertical load
P_r	Resultant horizontal force acting horizontally at pole peak
P_x, P_y, P_z	Horizontal forces in x, y, z direction
P_x^D, P_y^D	Horizontal forces resulting from bracings
P_x^K, P_y^K	Horizontal forces at leg member bend
q_s	Pile point compression
Q_g	Ultimate tensile strength of a pile

Symbols	Signification
R_c	Crushing strength
R_d	Design resistance
$R_{d\,comp}$	Design compression resistance
$R_{d\,lat}$	Lateral design resistance
$R_{d\,sf}$	Design resistance of foundation subface
R_f	Ratio of local skin friction to pile point compression
R_{perm}	Permissible loading
R_t	Tensile strength
s	Settlement
$S_{d\,up}$	Vertical component of the ultimate uplift force
$S_{K\,up}$	Vertical component of the characteristic uplift force
S_i	Equivalent skin friction
S_Z	Vertical component of uplift force
t	Depth of foundation subface, penetration depth in good-bearing soil
t_0	Auxiliary value for insertion depth according to Blum
t_E	Insertion length
t_s	Height of lowermost step of a stepped foundation
T	Depth of earth frustum
W	Section modulus
x_m	Location of the maximum moment in good-bearing soil
Y	Deflection of a pile
z	Thickness of non-bearing soil layer
perm σ_t	Permissible bearing pressure at depth t
β, β_0	Earth frustum angle
γ	Specific dead weight
γ'	Specific dead weight with buoyancy
γ_B	Specific dead weight of concrete
γ_{cr}	Partial factor for concrete strength
γ_F	Partial factor for action
γ_M	Partial factor for resistance
δ	Angle of skin friction
Δ_A	Reject of the shuttering compared to the 2^{nd} step
κ	Factor
μ	Poisson's coefficient
σ	Soil pressure
$\sigma_{1,5}$	Permissible bearing pressure at a depth of $1,5$ m
σ_d	Design value of stress
$\sigma_{R,d}$	Design value of limit stress
σ_{ult}	Ultimate bearing pressure
φ	Angle of internal friction

13.1 Requirements and preconditions

Foundations of supports are designed to transfer the foundation loads resulting from the structures according to the individual load cases into the subsoil with sufficient reliability, while inadmissible movements of the foundation body may not occur. Standards such as chapter 8 of EN 50 431-1 [13.1] stipulate the rules for selection, analysis, structural design and verification of foundations.

Tower dimensions and forces acting on the foundations as established by support analysis form the basis for the *foundation design.* Support sites and terrain formation are known from surveying documents. Since the subsoil conditions at the support sites affect the selection and design of foundations to a great extent, they need to be studied by *soil investigation.*

Table 13.1: Commonly encountered soils according to EN 50341-1 [13.1], Annex M

	Soil type	Mode of formation	Description	Technical features and aptitude as foundation course
1	Lateral moraine, gravelly	sandy-gravelly deposit of glacial origin, deposited at the edge of glacier	sandy-gravelly material, with a wide range of particle sizes; very heterogeneous	medium to high compaction, low compressibility, pervious; very good foundation layer
2	Glacial till (unsorted)	unsorted glacial deposit from clay to gravel, usually in dense state; usually covers molassic layers or bedrock	gravelly material in a silty-clayey matrix, with wide range of particle sizes	high compaction, low compressibility, imperious; good foundation layer
3	Glacial drift, sorted by rivers	sandy-gravelly layer from morainic aluvium	sandy-gravelly material, without boulders, and clay, with little silt	mean compaction, mean to high compressibility, pervious; good foundation layer
4	Glacial clay	very fine grained material from morainic aluvium and deposited in lakes	varied clays with layers of silt and fine sands; possible presence of peat and mud	low compaction, medium to high plasticity, compressible, impervious; poor foundation soil
5	Alluvial soil	deposits in flood plains and estuaries	alternately silty-sandy and gravelly deposits; possible presence of peat and mud	variable compaction and permeability, inhomogeneous soil; poor to good foundation soil
6	Boulders	boulders heap at the toe of a cliff	detached angular rock fragments of varying sizes	low compaction, high permeability; acceptable for foundations, although unstable
7	Overconsolidated soils	sedimentary soils subjected to greater overburden than at present	clays, sands, silts	generally acceptable for foundations
8	Soft rock (weathered to unweathered)	sedimentary soils etc. subjected to greater overburden pressure than overconsolidated soils	mud-stone (incl. marl), sandstone, chalk	weathered rocks should be evaluated from case to case; otherwise generally good for foundings

13.2 Types of subsoils

13.2.1 Classification of soil

The subsoil encountered is assigned to the individual types of soils during soil investigation and the *soil characteristics* necessary for selection and design of foundations are determined. Table 13.1 contains commonly encountered soils.

The subsoil forming the *Earth's crust* is classified geotechnologically into *undisturbed loose soils*, *rock (solid soil)* and *filled-up ground*. Loose soil is a natural pile stock of mineral particles. It can be separated into its particle sizes by mechanical tools without application of force. It is self-evident that there are transition ranges where a classification either to loose soils or to solid soils might be difficult because of the stronger permanent cohesion forces between the individual soil particles. The classification assumed here is commonly used in civil engineering. However, it will not be adopted everywhere. For example, in the geological science the term *rock* comprises all material forming the Earth's crust without considering the mutual cohesion of the mineral particles. Within the agricultural science, again the term *soil* is applied only to that part of the Earth's crust which is able to produce vegetation.

Table 13.2: Classification of non-cohesive soil according to particle size

	Designation	Symbol	Particle sizes in mm
Range of coarse particles	Boulders	Y	above 200
	Stones	X	between 63 and 200
Range of sieve particles	Gravel particles	G	between 2 and 63
	coarse gravel	gG	between 20 and 63
	medium gravel	mG	between 6,3 and 20
	fine gravel	fG	between 2,0 and 6,3
	Sand particles	S	between 0,06 and 2,0
	coarse sand	gS	between 0,6 and 2,0
	medium sand	mS	between 0,2 and 0,6
	fine sand	fS	between 0,06 and 0,2

Table 13.3: Classification of cohesive soil according to particle size

	Designation	Symbol	Particle size in mm
Range of fine particles	Silt	U	between 0,002 and 0,06
	coarse silt	gU	between 0,02 and 0,06
	medium silt	mU	between 0,006 and 0,02
	fine silt	fU	between 0,002 and 0,006
	Clay	T	below 0,002

13.2.2 Undisturbed natural soil

Undisturbed, natural soil is the result of a decayed Earth-historical process. It can be formed by chemical or physical weathering and decomposition of rocks but may also be of organic origin. If the residues of rock weathering remained at the place of their formation, they are called *residual soil*, otherwise *transferred soil*. Residual soils are firm and stable in general. Transferred soils, in particular formed during a glacial period, can be loose and soft up to a great depth. If *organic components* are found in between, the soils are sensitive to settlements. More difficulties to install foundations exist in particular in case of transferred soils.

However, in geotechnology the soils are not classified according to their formation but as inorganic and organic soils. In case of *inorganic soils*, two main groups are distinguished: *Non-cohesive soils* and *cohesive soils*. Pure soil types consist of one range of particle sizes only. Most natural soils are mixtures of differing particle sizes. These composed soils have to be classified according to their main component; main component is thereby that type of soil which shapes the determining characteristics.

Non-cohesive soils

Soils with particle sizes above 0,06 mm are classified as a *non-cohesive soil*. In particular, incoherent piles of sand, gravel, stones and rocks are within this category. According to DIN 4022 [13.2], as an often used standard, this type of soil is further subdivided according to the particle size (Table 13.2).

Cohesive soils

The *cohesive soils* consist of particle sizes below 0,06 mm. The individual particles cannot be told apart by the unequipped eye. Cohesive soils are subdivided according to the particle size into *silt* and *clay* (Table 13.3).

Soils with mixed particle sizes

Most soils are mixtures of non-cohesive and cohesive portions. *Mixed particle size soils* are classified as non-cohesive if the proportion of weight of particles below 0,06 mm

is less than 15 % and the non-cohesive parts determine the characteristics of the soil. Otherwise, the soil is addressed as cohesive soil with non-cohesive additions.

Organic soils

Organic soils contain residues of more or less decomposed plants and animal organisms. There are purely organic soils such as *peat*. Frequently, soils are encountered with clayey or silty characteristics and an essential organic portion. These soils are called *mud*. The organic components are finely distributed in most cases. However, there can be shells of mussels and visible residuals of partly decomposed plants. The colour varies between light and grey-black. These soils often contain gases like CO_2 and H_2S, the latter being recognized by its odour. Since the compressibility of these soils is high, they are not suitable to transfer loads. Due to the determining effects of organic components on the foundation selection, non-cohesive soils with organic components of more than 3 % portion of weight and cohesive soils with organic components having more than 5 % portion of weight are classified as organic soils. They are addressed for example as *humusy sand*, *peaty sand*, *organic silt* or *organic clay*.

13.2.3 Rock

All *solid soils* are addressed by the term *rock*. The rock represents the hard parts of the Earth's crust. The degree of weathering is important (see clause 13.3.4.2) for the load bearing capacity of rocks. Rocks can be classified according to DIN 4022 [13.2]. Regarding the history of their formation, rocks are divided into *solidification rocks*, *sedimentation rocks* and *metamorphoses rocks*. Solidification rocks are of magma origin (depth and eruption rocks), sediment rocks were formed by sedimentation and metamorphoses rocks by mechanical or thermal transformation.

13.2.4 Filled-up soil

Filled-up soil can be formed by artificial filling or floating. The material for planned, engineered filling is selected thoroughly in order to attain a satisfying compaction. Foundations can be accommodated in well-compacted fillings. Uncompacted fillings and especially rubbish damps settle so much that installation of foundations will not be possible there.

13.3 Subsoil investigation

13.3.1 Purpose of subsoil investigation

The supports of an overhead line are distributed over long distances where alternating and widely differing soil conditions are frequently encountered at the individual support sites. By *subsoil investigation*, the necessary information is gathered for selecting a well-suited foundation type and determining the dimensions of the individual foundation bodies. Subsoil investigation forms the basis for the global analysis of the foundations. A subsoil investigation should, therefore, be carried out at each individual support site and comprise all soil layers affecting the foundation resistance.

According to IEC 61 773 [13.3], the depth of soil investigation should be not less than the foundation depth in case of uplift and should be adequately augmented in case of compression foundations. The recommended depth in this case is the greatest of 1,1 times the foundation depth or the maximum horizontal dimension plus the foundation depth. The depth of the soil investigation needs not to reach deeper than 3,0 m below the foundation base. A similar specification can be found in DIN 1054 [13.4]. For rock sites, IEC 61 773 recommends cores to be sampled to a minimum depth of 3,0 m.

Due to economic reasons and because of lack in time, soil investigations need not to be carried out at all individual support sites in a constant terrain. Then, final decisions on the type and dimensions of the foundations have to be made when installing the foundation. In this case, foundations are designed for two or three subsoil conditions, e. g. for normal, weak and very good soil, with or without consideration of ground water, if any. The decision on the foundation type to be used will be made during excavation.

However, soil investigations are absolutely necessary when it is obvious that *non-bearing soil layers* such as peat, mud, silt or quick sand are encountered where it is necessary to determine the depth at which well-bearing soil is found. Soil investigations are also necessary in filled-ups, dams and areas of land slides.

A thorough *inspection of the right-of-way* and the individual support sites should be made to decide on the type of soil investigation. Information on the soil to be expected can be obtained from the ground water condition, from water course, vegetation of trees and plants, from other existing structures and settlements being observed there, if any. Details can be recognized at sand or gravel pits as well as excavations. Information obtained from authorities or local people may help as well. Additional information can be obtained from *geological maps.*

In case of soil investigations, it is distinguished between methods which serve to *collect soil samples* and *supplementing probings* to investigate other characteristics such as *density of soil strata* or skin friction values.

13.3.2 Methods for obtaining soil samples

13.3.2.1 Type of samples

The methods for obtaining soil samples can be classified as established in DIN 4021 [13.5], as an example. Other standards dealing with this subjects are BS 5930 [13.6] and ASTM D 1452 [13.7]. In DIN 4021, five quality classes of the gathered samples are distinguished:

- Quality class 1:
  Unaffected samples with respect to granulated composition, moisture content, density, coefficient of permeability, modulus of stiffness, shear strength.
- Quality class 2:
  Unaffected samples with respect to granulated composition, moisture content, density, coefficient of permeability.
- Quality class 3:
  Unaffected samples with respect to granulated composition, moisture content.
- Quality class 4:
  Unaffected samples with respect to granulated composition.
- Quality class 5:
  Incomplete samples, only sequence of strata to be determined.

For overhead lines, it is normally sufficient to obtain *soil samples disturbed* from their natural stratification since for determining the soil characteristics, geotechnical characteristics established by laboratory tests are not necessary. The disturbed samples serve to determine the *sequence of soil strata*, their boundaries, the characteristics of the stratum, the *composition of particles*, the consistence, the *watertable* and organic components. For this purpose, soil samples of class 4 or 5 are sufficient.

13.3.2.2 Trial pits

Trial pits can be carried out without special tools, however, they are time-consuming and costly. Pits as narrow as possible are excavated step by step deeper in a longitudinal

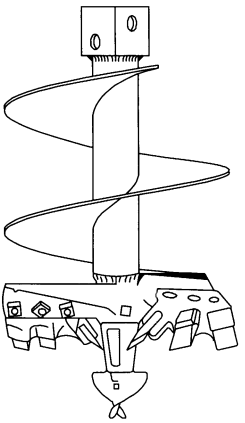

Figure 13.1: Auger-type drill for heavy soils

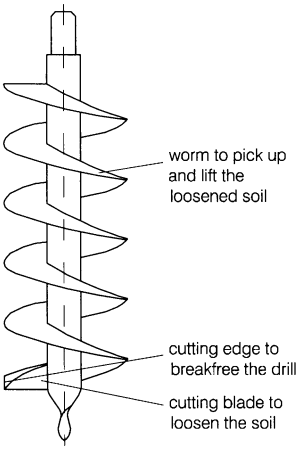

Figure 13.2: Worm for boring in all kind of soil, excepted sand and gravel with ground water

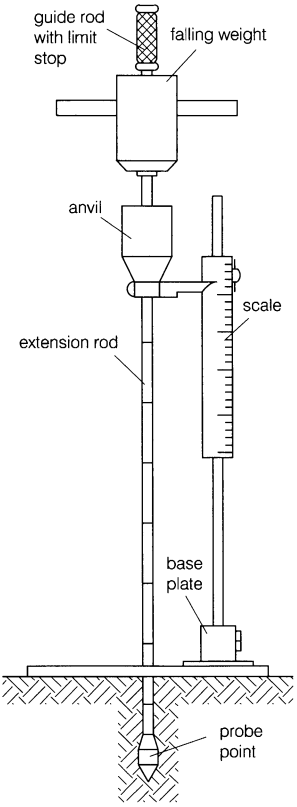

Figure 13.3: Light-duty probe according to DIN 4094

direction where the individual type of soils of the upper layers down to the watertable can be studied.

13.3.2.3 Exploratory borings

In well-standing soils, *borings* with diameters between 300 to 500 mm and without any casing deliver suitable results concerning the identification of the soil, the water content and the watertable, the *stability* and the *density of soil strata.* Borings up to 7 m depth can be carried out with the tools used for overhead lines. Auger-type drills are used for this purpose (Figure 13.1). The depth is sufficient if pad-and-chimney or auger-bored foundations will be used. The boring diameters mentioned need high-performance boring tools as used for augered foundations as well. Specially designed low-duty boring tools are available for exploratory borings enabling boring diameters between 100 and 150 mm. For lifting the soil, *worm-type drills* are used (Figure 13.2), which are suited to explore less stable and ground water conducting soils. Boring depths up to 12 m can be achieved without undue efforts. The soil samples lifted from the boreholes are more or less mixed. The *soil profile* can be recognized from the soil adhering to the individual pitches of the worm.

The *ground-water level* will be stable only after a certain period of time, e. g. after several hours in case of cohesive soils. The borehole, therefore, should remain open

Table 13.4: Data of driven probes according to DIN 4094

Device		Hammer weight	Height
Light-duty probe	(DPL)	10 kg	0,50 m
Medium-heavy-duty	(DPM)	30 kg	0,20 m
probes	(DPM-A)	30 kg	0,50 m
Heavy-duty probe	(DPH)	50 kg	0,50 m

over a sufficient long period. Borings adopting casings need to be carried out in ground water saturated soils. The soil is lifted by special tools, e. g. split spoon samplers. In case of rocky subsoil, *core drillings* can be envisaged.

13.3.2.4 Soil investigation by drilling probes

To gather low quantities of samples, *drilling probes* are used which are equipped with a *longitudinal groove*. The grooved probe consists of a probe linkage with a 1 m long longitudinal groove at its point. After driving, soil samples are pressed into the groove by rotating the probe. The soil samples are lifted by pulling the linkage out of the borehole. Sandy soils under ground water cannot be explored with this method since the sand is washed out. For this purpose, a probe with a sampler at its point is used to encase the soil sample to be lifted. Drilling probes deliver continuous soil profiles in not too hard soil for which pile foundations are in particular suitable. The stability of the soil which is essential for adoption of augered foundations can be assessed by the soil samples recovered, whereby adequate experience is necessary.

13.3.3 Probes

13.3.3.1 Types of probes

Driven and *compression probes* are distinguished depending on the method of application. The resistance occurring during penetration into the soil is recorded in both cases. Soil samples are not recovered. Probings complement the soil profile obtained from borings since the majority of boring methods do not permit any quantitative findings on the *density of stratification*. The probes permit to distinguish in particular loose and hard zones and to assess the *uniformity of subsoil*.

13.3.3.2 Driven probes

Dimensions of the probes as well as advice for their application can be found in DIN 4094 [13.8]. In case of driven probes as shown in Figure 13.3, a rod with a conus-type point is driven into the soil under standardized conditions, whereby the *number of blows* is recorded as necessary for a penetration by 0,1 m (n_{10}). From this quantity, it is concluded to the compactness and *consistence* of the tested stratum. It is distinguished between the *light-duty*, *medium-duty* and *heavy-duty driven probe* (Table 13.4) depending on the weight of the hammer. The light-duty driven probe is suited for less firm soils up to a depth of 6 m. The heavy-duty driven probe is suited for investigation of subsoil in greater depth and in coarse, firm soil.
Results of probing depend on a great number of parameters with differing influence (see DIN 4094 [13.8]). A correct assessment of the probing results would only be possible if the type of soil was known from an exploratory boring. The *resistance of penetration* of the driven probe alone does not permit to determine reliably the type of soil. Conclusions on the compactness are only possible in case of non-cohesive soil. According to [13.8] and [13.9], the correlation between number of blows and compactness given in Table 13.5 can be assumed for non-cohesive soils.

Table 13.5: Guiding data for the relation between number of blows and compactness

Type of soil, compactness	Number of blows n_{10} Light probe	Heavy probe
Sand		
medium dense	≥ 15	≥ 5
dense	≥ 30	≥ 10
Sand-gravel mixture		
medium dense	≥ 15	≥ 5
dense	—[1)]	≥ 18

1) light-duty probe not suited

Table 13.6: Standard penetration test (SPT) in non-cohesive and cohesive soil

Non-cohesive soil Number of blows n_{30}	Compactness	Cohesive soil Number of blows n_{30}	Consistence
0 to 4	very losse	0 to 2	very soft
4 to 10	loose	2 to 4	soft
10 to 30	medium-dense	4 to 8	medium
30 to 50	dense	8 to 15	stiff
> 50	very dense	15 to 30	very stiff
		> 30	hard

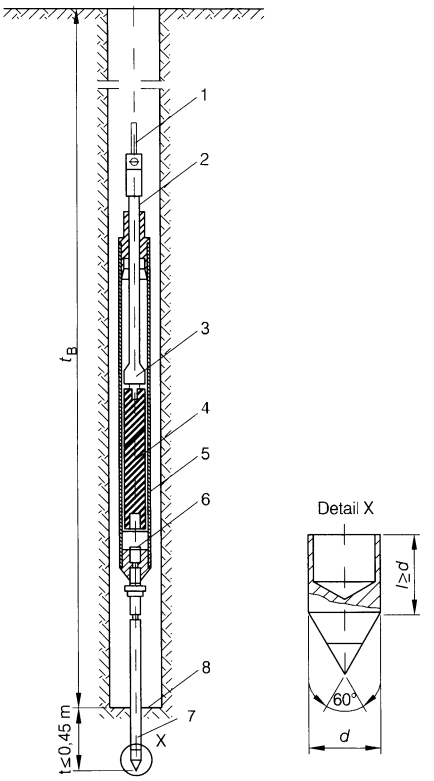

Figure 13.4: Standard penetration test (SPT). 1 cable; 2 stuffing box; 3 automatic release mechanism; 4 pushrod; 5 protective mantel; 6 anvil; 7 penetrometer; 8 bottom of borehole; t depth of investigation; t_B borehole depth

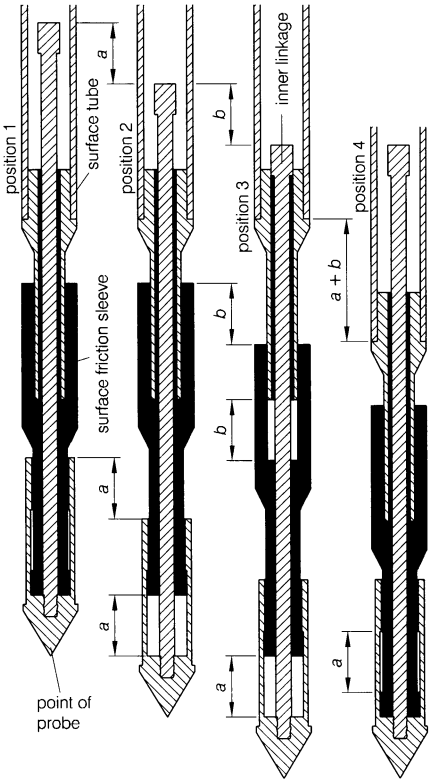

Figure 13.5: Working positions of Gouda probe to measure the point pressure and the local skin friction (manufacturer: Goudasche Maschinenfabriek, Gouda, Netherlands)

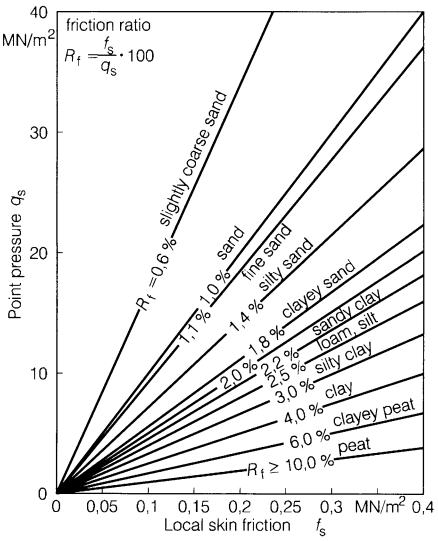

Figure 13.6: Relation between point pressure and local skin friction (friction ratios) in typical soils according to [13.13]

Table 13.7: Correlation between point pressure and compactness in uniform fine- and medium grain sand

Point pressure q_s (MN/m²)	Compactness
< 2,5	very loose
2,5 to 7,5	loose
7,5 to 15,0	medium dense
15,0 to 25,0	dense
> 25,0	very dense

13.3.3.3 Standard penetration test

The *standard penetration test* (SPT) was developed in the USA [13.10] and is now used world-wide. In Figure 13.4 the testing device is shown. At first, a borehole is produced and equipped with a casing. Into this borehole, a tube sampler with 35 mm female diameter is pressed downwards and finally driven 0,15 m into the soil by means of a 63,2 kg weight from a height of 0,76 m. Along the following 0,30 m depth of penetration, the corresponding number of blows is recorded (n_{30}). The soil samples pressed into the tube sampler during driving can be recovered then. The standard penetration test is carried out where information on the soil profile is desired. Compared with the driven probes standardized in DIN 4094, the soil will not be completely displaced by the point of the probe. Therefore, the penetration resistance is composed of the punching of the soil and the friction along the cylinder. Depending on the number of blows, the correlation presented in Table 13.6 according to [13.11] is proposed for assessing the compactness of non-cohesive soils and the consistence of cohesive soils.

13.3.3.4 Van-type probes

Dimensions and application of *van-type probes* are standardized in DIN 4096 [13.12]. Van-type probes are used in water saturated cohesive soils of soft to stiff consistence to determine the shearing strength and serve to recognize gliding zones and gliding planes. It is not possible to divide the shear strength recorded into its skin friction and cohesion components. Experience on the application of results obtained by van-type probes to design overhead power line foundations do not exist to a sufficient extent.

13.3.3.5 Compression probes

For overhead line technology, the *Gouda probe* is frequently used which was developed for fine-grain sandy soil without stones or coarse gravel in the Netherlands. Its point

consists of a device to record the *point pressure* and the *skin friction*, a tube for pressing the point and a linkage arranged in the tube to operate the probe point and the sleeve for recording the skin friction. In Figure 13.5 the function of the Gouda probe is demonstrated. In position 1 the probe is pressed via the sleeve tube into the starting position and the total resistance encountered is recorded. By pressing the probe point by the length a using the inner linkage (position 2), the point pressure is determined and by exerting additional compression on the inner linkage, the point is extended by the length b (position 3) and the sum of point pressure and local skin friction is determined. After that, the probe is advanced into the new starting position 0,20 m deeper by exerting pressure on the outer sleeve of the probe. This sequence is repeated in 0,20 m steps until the desired depth or the maximum permissible compression is attained. The probes are equipped with mechanical or electronic measuring devices.
Studies [13.13] carried out in the Netherlands lead to the conclusion that for a given type of soil the ratio R_f between local skin friction f_s and point pressure q_s is approximately constant and typical for the kind of soil encountered. Values R_f equal to 6,0 % correspond to peat, of 2,5 to 6,0 % to cohesive soil, of 2,5 to 1,0 % to mixed particle soil and less than 1,0 % to non-cohesive soil as can be seen from Figure 13.6. In case of earth-humid uniform sand, the correlations between point pressure and compactness presented in Table 13.7 apply according to [13.9].
The watertable cannot be monitored by compression probes. The skin friction values obtained from compression probing can be used directly for the design of pile lengths due to the similarity of the models.
For design of horizontally loaded piles, the development of the *horizontal subgrade modulus* along the depth is necessary which depends on the type of soil, the compactness and also on the dimensions of the loaded area. According to [13.14], the subgrade modulus can be obtained from $K_s = 1{,}4 \cdot E_s/d$ where E_s is the *modulus of compressibility* and d the pile diameter. The modulus of compressibility can be assessed from the point pressure q_s according to $E_s = (1{,}5 \text{ to } 3) \cdot q_s$ as mentioned in [13.9]. The values obtained from this procedure should be calibrated with the guideline data given in Tables 13.11 and 13.15.

13.3.4 Evaluation of soil investigation

13.3.4.1 Classification and description of soil types

The *classification of* the *soil* according to standards and its condition is essential with respect to the technically correct and economically viable design of foundations. The procedures for *classification and description of the soil types* are given in DIN 4022 [13.2], as an example. In this standard, it is distinguished between visual and manual procedures for the identification.
The *visual identification* comprises the particle size and colour. It applies to the *particle size ranges*:

Range of gravel:	smaller than hen's eggs, larger than match heads;
Coarse gravel:	smaller than hen's eggs, larger than hazelnuts;
Medium gravel:	smaller than hazelnuts, larger than peas;
Fine gravel:	smaller than peas, larger than match heads;
Range of sand:	smaller than match heads, down to the limit of visibility;
Coarse sand:	smaller than match heads, larger than grit;
Medium sand:	equal to grit;
Fine sand:	smaller than grit, still visible by the unequipped eye.

The *colour of soil* is caused by additions. Light colours indicate humus-free soils, red colours are due to iron oxide. Dark colours arise due to organic components. The colour is the darker, the more organic components are contained.

A *manual soil identification* is used in case of *cohesive soil* where individual particles cannot be anymore distinguished by the eye. By means of hand and finger tests, information on the fine and coarse particle content can be obtained. It can be distinguished between silt and clay; plasticity and consistence can be determined.

Dry strength

The results obtained from *dry strength testing* provide information on the plasticity of a soil and thus on its classification as silt or clay.

To establish the dry strength, a soil sample is dried in air, in the sun or in an oven. Its resistance to being crumbled or powdered between the fingers is a measure of the soil dry strength, which is governed by the type and percentage of fines. Thus, it permits the soil to be classified as follows:

- Soil has no dry strength, if it disintegrates without being touched or at the slightest touch.
- Soil has low dry strength, if it disintegrates under light to moderate finger pressure.
- Soil has medium dry strength, if it disintegrates only under substantial finger pressure into pieces which still show cohesion.
- Soil has high dry strength, if the soil can no longer be disintegrated by finger pressure but can only be broken between the hand.

Pure gravel or sand does not have any dry strength. Silt, silt-fine sand and silt-gravel mixtures show a low dry strength. Mixtures between gravel and clay, sand and clay as well as silt and clay show a medium dry strength. Clay, clay-silt and clay-sand mixtures as well as clay-silt-sand and gravel mixtures possess a high dry strength.

Dilatancy

The behaviour of a soil when shaking indicates whether and to what extent *silt* is present.

To establish the *dilatancy*, a pat of soil moistened to be soft is shaken from hand to hand. Dilatancy is shown by the appearance of a shiny film of water on the surface of the pat. When the pat is squeezed or pressed with the fingers, the surface dulls as the pat stiffens and finally crumbles. With further shaking, the crumbs once again become a cohesive mass on which the test can be repeated.

Considering the time taken for water to appear and disappear during shaking and pressing, the soil can be classified as follows:

- High dilatancy, if the process described occurs very quickly;
- Low dilatancy, if the shiny film of water forms and changes very slowly;
- Showing no reaction, if the sample does not respond to the dilatancy test.

Very fine sand, silty fine sand, fine sandy silt, coarse silt and rock powder show a quick reaction. Clayey silt and sandy-clayey silt react slowly, silty clays and pure clays do not show any reactions.

Plasticity

To establish the *plasticity* (toughness), a soil sample prepared to be soft but not sticky is rolled on a smooth surface or on the palm of the hand to produce threads about 3 mm in diameter, moulded together, and rolled again until it has dried sufficiently and finally crumbles when rolled out. From this point onwards, the sample can no longer be rolled out, but only moulded until it crumbles, this property being taken as a basis for classifying soil as follows:

- Low plasticity, if lumps showing cohesion can no longer be moulded from the threads;

- Medium plasticity, if the lump formed cannot be moulded because it crumbles under light finger pressure;
- High plasticity, if the lump formed from the threads can be moulded without crumbling, even under stronger finger pressure.

Heavily sandy clays and weakly clayey silts are distinguished by a low plasticity, silt-clay mixtures as well as weakly sandy clays by a medium plasticity and clay and little silty clays by high plasticity.

Sand content of soils

To check a soil for the *content of sand*, silt and clay, a small soil sample is rubbed between the fingers, if necessary under water. The proportion of the sand fraction can be determined from the degree to which the material feels gritty. In cases of doubt, the test may be carried out by grinding the soil between the teeth, the presence of sand being felt due to its grittiness.

A clayey soil feels soapy and sticks to the fingers and cannot be removed without washing, even when in the dry state, whereas silty soils feel smooth to the touch. The dry soil particles that stick to the fingers can be easily blown away or removed by clapping the hands.

Clay and silt content of soils

To check a soil for the *content of clay or silt*, a sample in its naturally moist state is cut with a knife. A shiny cut surface indicates the presence of clay, while a dull sample surface is characteristic of silt or of clayey-sandy silt of low plasticity. For a rapid assessment, the sample surface may be scored with a fingernail or smoothed.

Organic soil and peat

The odour of a soil gives an indication of whether it is of inorganic or organic nature. Fresh, moist *organic soils* generally have a mouldy odour which can be intensified by heating a moist sample.

Putrefying, rotten organic components in soil can be recognized by the typical hydrogen sulfide odour which can be intensified by pouring dilute hydrochloric acid on the sample. This odour is produced particularly by mud and fresh slightly decomposed peat. Dry inorganic clays have an earthy odour after being moistened.

Consistence

The consistence of a cohesive soil can be determined in a field test, thus permitting the following classification:

- A soil is to be classed as pasty if it exudes between fingers when squeezed in the hand.
- A soil is to be classed as soft if it can be moulded by light finger pressure.
- A soil is to be classed as stiff if it cannot be moulded by fingers but rolled in the hand to 3 mm thick threads without breaking or crumbling.
- A soil is to be classed as semi-solid if it crumbles and breaks when rolled to 3 mm thick threads but is still sufficiently moist to be moulded to a lump again.
- A soil is to be classed as firm if it has dried out and is mostly light coloured. It can no longer be moulded but crumbles under pressure.

13.3.4.2 Classification of rock

For the classification of rock material, there are, in contrast to soil, no simple distinguishing features that can be observed on site. Details on the classification on the basis of its mineral composition and formation history are given in DIN 4022, Part 1 [13.2]. Regarding the formation history, rock is classed as:

Table 13.8: Assessment of rock weathering condition by inspection of excavated material

	Shape of the rock	Weathering of the surface	Strength of the rock	Strength of the surface	Degree of disintegration in water
W0	Regular rock material with at least two approx. parallel surfaces	fresh sound, no oxidation, no change of colour	only divisible by hitting powerfully with hammer	cannot be fissured using steel nail or tip of knife	no disintegration in water, no disintegration is visible
W1	Irregular rock material, surfaces often not parallel	discoulered, little oxidation, little loss of strength, hard	fissures crack using hammer	can hardly be fissured using steel nail or tip of knife	no disnitegration in water, no disintegration is visible
W2	Rock material has sharp edges and some parts of surface have broken off	weakened, oxidated and partially disintegrated and decomposed	visual cracks, divisable with hammer	rather difficult to fissure using steel nail or tip of knife	no disintegration in water, no disintegration is visible
W3	Rock material with only a few sharp edges and large parts of surface broken off	rock material mostly visible, heavily decomposed and weathered	breakes easily, only fragments can be obtained	can easily be fissured using steel nail or tip of knife	only surfaces disintegrate in water
W4	Rock material has a round form, no sharp edges	rock material decomposed into small particles due to weathering	falls apart into little pieces at light stroke of hammer	little parts can be rubbed off easily with finger	decomposition into parts
W5	No solid parts obtainable	no rock material left due to weathering	can be crushed easily by hand	falls apart when being rubbed	total disintegration, no solid parts left,paste-like substance

- *Igneuos rock* such as andesite, basalt, diabase, diosite, granite, quartz.
- *Sedimentary rock* such as chalk, claystone, dolomite, gypsum, limestone, marlstone, sandstone.
- *Metamorphisic rock* such as gneiss, marble, micaceous shist.

The characteristics used to class rock such as granulation, grain size, clay mineral content, bulk density, grain bond and hardness, stability in water can only be determined from core drilling which is not often carried out when investigating sites for overhead line supports. For design and implementation of foundations, the weathering condition is more important.

Proposals for assessment and classification of the *degree of rock weathering* are given in [13.15]. The range between loose and solid rock is divided into six groups W0 to W5 depending on the degree of weathering. Based on visual characteristics of the rock stratum, the degree of weathering, the strength of the rock and the formation of grains it is distinguished by

– W0 mountain fresh, – W1 weathering started, – W2 moderately weathered,
– W3 strongly weathered, – W4 completely weathered, – W5 formation of soil.

Rock-type foundations can be adopted in case of the weathering conditions W0 to W2. Without costly soil investigations by core drilling and investigation of the rock characteristic in the laboratory, the weathering condition of the excavated material is addressed according to Table 13.8 and the condition of compactness according to Table 13.9 by simple measures. By these measures a classification to one of the weathering conditions is possible.

Table 13.9: Assessment of rock compactness

	Layer thickness, average distance m	Clefting distance, mean values m	Degree of disintegration of rock on fields	Zones of weathering	Structure of zones
W0	0,60 to 2,00	0,60 to 2,00	disintegration only when blasted	not visible	very closed, closely linked together
W1	0,20 to 0,60	0,20 to 0,60	disintegration only with hydraulic hammer, use of compressor, hardly possible	several narrow zones	partially closed and linked together
W2	0,06 to 0,20	0,06 to 0,20	can easily be disintegrated with compressor or mechanically	several broad zones	usually open, partially still linked together
W3	0,02 to 0,06	0,02 to 0,06	not easy to disintegrate manually	many zones and areas	open and not linked together
W4	0,006 to 0,02	< 0,02	easy to disintegrate manually, using shovel	hardly anymore zones	wide open
W5	< 0,006	—	loose material, e. g. sand, clay, easy to dig with shovel	no zones	not visible due to weathering

13.3.4.3 Concrete-aggressive water and soils

Water and soils may attack concrete if free acids, sulphides, sulphates, magnesium salt, ammonium salt or grease and oil are contained. *Concrete-aggressive ground water* is recognized by a dark colour, rotten odour and emerging gas bubbles. In case of suspicions on concrete aggressiveness of the ground water or of the soil, samples should be taken. In DIN 4030 [13.16], instructions are given for collecting and examining samples. The samples are tested in the laboratory and the degree of aggressiveness is determined. It is distinguished between lowly, heavily and very heavily aggressive. The *degree of aggressiveness of water and soil* is assessed according to the limit data given in Table 13.10. For the degree of aggressiveness, the maximum value is prevalent also if it is recorded only once. Depending on the existing degree of aggressiveness, special requirements on the concrete quality (see clause 16.3.7.3) are requested according to ENV 1992-1 [13.17] or specific measures to protect the concrete should be taken.

13.3.4.4 Borehole log

The results of the soil investigation can be evaluated according to DIN 4022 [13.2] and presented in *borehole logs*. The *results of probings* can be recorded according to DIN 4094 [13.8]. The borehole logs form the basis for determining the *soil characteristics*. A format for the borehole log and its filling in are standardized in DIN 4022 (Figure 13.7). When carrying out the soil investigations, the columns 1 to 3 are filled in. In column 1 the depth of the currently encountered stratum is recorded. In column 2 the type of soil is filled in under item a) using the designations according to DIN 4022, Table 6. In case of mixed-type soils, that type of soil is mentioned first which determines the characteristics of the soil, for example gravel, sandy; silt, sandy or clay, silty. Additional components such as wood or parts of bricks, filled-up soils etc. should be added.
In column 2 c), the *condition of the recovered samples* with standardized characteristics

DIN 4022 Part 1

Appendix B

Specimen form for a borehole log (field log)

The note in the margin on page 1 prohibiting reproduction of any part of the standard does not apply to the following specimen form.

Borehole log (field log)

for drilling not involving continuous sample recovery

Sheet No. 1
Report No.:
Ref.: 433-100667

Name of project: 110 kV line North station

Borehole / **Trial pit** No. Tower/Sheet 1 No. 3

Date: 29.10.99

1	2				3	4	5	6
End of borehole at...m depth	a) Designation of soil type and secondary constituents b) Notes[1] c) Condition of sample / d) Condition of soil/rock according to depth / e) Colour f) Usual designation / g) Geological designation[1] / h) [1] Group / i) Lime content				Notes (special sample, water conditions, drilling tools, core loss, miscellaneous)	Samples recovered		
						Type	No.	Depth (bottom sample face), in m
0,10	a) humus, fine sandy b) c) / d) easy to drill / e) brown f) Top soil / g) Top soil / h) / i)				rotary drilling, auger-type drill, 300 mm diameter, dry			
0,50	a) coarse sand, little clayey b) c) round edges, loose / d) easy to drill / e) brown/grey f) sand / g) ___ / h) ___ / i) ___				dry			
1,50	a) fine sand b) c) round edges / d) normal to drill / e) light brown f) sand / g) ___ / h) ___ / i) ___				dry, borehole is enlarged			
3,00	a) clay, fine sandy b) c) semi-hard / d) normal to drill / e) brown/grey f) loamy soil / g) ___ / h) ___ / i) ___							
4,00	a) coarse sand, very clayey b) c) rounded, dense / d) difficult to cut / e) grey f) sand stone / g) ___ / h) ___ / i) ___				Water table reached not to drill deeper because of sandstone			

[1] This section shall be completed by the geologist.

Figure 13.7: Borehole log according to DIN 4022, Part 1

Table 13.10: Limits for assessment of aggressiveness of water and soil

Type of investigation	Level of aggressiveness		
	Lowly aggressive pH value 6,5 to 5,5	Heavily aggressive pH value 5,5 to 4,5	Very heavily aggressive pH value below 4,5
Water			
Lime soluting carbonic acid (CO_2) in mg/l determined by the marble test according to Heyer	15 to 40	40 to 100	above 100
Ammonia (NH_4^+) in mg/l	15 to 30	30 to 60	above 60
Magnesium (Mg^{2+}) in mg/l	300 to 1 000	1 000 to 3 000	above 3 000
Sulphate (SO_4^{2-}) in mg/l	200 to 600	600 to 3 000	above 3 000
Soil			
Sulphate (SO_4^{2-}) in mg/kg of air-dry soil	2 000 to 3 000	3 000 to 5 000	above 12 000

should be mentioned:

- *Non-cohesive soil*: sharp edges, round edges, like plates, dry, earth humid;
- *Cohesive soils*: consistence: pasty, soft, stiff, semi-hard, hard;
- *Organic soils*: with much wood, flaky, like a sponge, decomposed, non-decomposed;
- *Filled-up soils*: compacted, non-compacted.

Under column 2 d), information on the drilling process is given which is important for the assessment of the load-bearing capacity and stability of the soil. The following terms should be used: Easy or difficult to drill, high or low penetration resistance, drill deviates laterally, sloughing of drill, hindrances to drilling available.

Under column 2 e), the colour of the soil is mentioned, e. g. grey, brown, bluey, rusty-speckled, yellowly-grey.

In column 2 f), the locally used name is filled in to ease the identification of soil: *Quick sand* is fine sand which flows under water action. *Mud* is a silty, lime-containing clay with residuals of plants. *Loam* is a clay soil with a proportion of silt and fine sand between 30 and 70 %. Because of the content on iron hydroxide, it is mostly yellow to brown coloured. Depending on the mass proportions of clay and sand, it is addressed as sandy loam or loamy sand. *Marl* is a clay with 25 to 30 % of lime. Marl is hard in its natural stratification. However, it falls apart quickly at air. *Looze* is a designation for organic soil with clayey and fine-sandy additions, especially on river beds. Looze stands for a fine sandy, silty soil cemented by chalk. Its colour is yellow to light brown. *Foul mud* is a sediment of predominantly organic substances below water. It is brown to black, greasy and of bad odour.

In column 3, the drilling tool used and all other observations are filled in, which are of significance for the decision on the foundation, e. g. borehole collapse, borehole is enlarged from z m depth, borehole stands firmly, deeper drilling not possible. The water table observed during drilling and the permanent water table observed after some hours should be mentioned there. The columns 4, 5 and 6 are only necessary when soil samples are recovered.

13.3.4.5 Graphical representation

In order to get an overview on the soil conditions along the total line, a graphical presentation of borehole logs might be suited, whereby the symbols and colours as specified in DIN 4023 [13.18] can be used for the individual soil types.

13.4 Design and calculation of foundations

13.4.1 Type of foundation and load

The *type of foundation* for an overhead line support depends on the type of the support, on the magnitude and type of load, on the soil conditions and on the possibilities for *installing the foundation.* Since a close interdependence exists between the design of supports and foundations, the possibilities for design and installation of foundations should be considered already when designing the supports.
The decision on the foundation type is based on its *limit resistance.* The limit resistance is the load, beyond which the foundation cannot anymore carry out its function and fails. It is a specific characteristic of each foundation type. Methods to determine the limit resistance or the *ultimate strength* will be given for foundation types frequently used for overhead power lines in the following. These methods are based on geotechnical theories or empirical formulae validated through tests and long-term experience.
The *geotechnical design of foundation* aims at the load transfer to the subsoil and the determination of the limit resistance or at the dimensions required to achieve the limit resistance. E. g., determination of pile lengths is part of the geotechnical design. The requirements and basis of geotechnical design follow from the state of the art, which can be found in the literature and in standards, especially in Europe in EN 50 341-1 [13.1] and the associated National Normative Aspects EN 50 341-3 [13.19], e. g. EN 50 341-3-4 [13.20] for Germany. Also the experience from tests and previously constructed lines can be used for the geotechnical design of foundations. An overview is given in [13.21].
The geotechnical design of foundations can be based on characteristic or design loads, which, as defined in EN 50 341-1, correspond to ultimate loads. Regarding detailed design and stipulation of partial factors, EN 50 341-1 refers to the National Normative Aspects established for the individual countries [13.19].
According to [13.20] valid for Germany, to mention an example, verification of foundations is based on characteristic loads. Since European standards using the partial factor approach based on ultimate loads and resistance do not exist so far, the stability of foundations is verified by proofing that

$$E_{\mathrm{K}} \leq R_{\mathrm{perm}} \quad , \tag{13.1}$$

where R_{perm} is obtained either by dividing the foundation resistance R_{d} by a partial factor γ_{M} or by evaluating R_{perm} directly from permissible resistance parameters. Determination of uplift capacity is an example for the option mentioned first, the evaluation of compression capacity an example for the second approach.
The *characteristic foundation loads* result from the support analysis using characteristic external loads. Since the support analysis is carried out with design or ultimate loads, a separate analysis is required. If the support analysis has been carried out with design loads only, the characteristic values E_{K} of foundation loads may be approximately derived from the design values E_{d} of foundation loads by

$$E_{\mathrm{K}} = E_{\mathrm{d}}/1,35 \quad . \tag{13.2}$$

An alternative approach of verification of foundation stability is presented here, where the geotechnical design is carried out on split partial factors. This approach is the same as adopted for design of supports and for the structural design of foundation and has the advantage of consistence of geotechnical and structural foundation design.
It is required to prove that

$$E_{\mathrm{d}} \leq R_{\mathrm{d}}/\gamma_{\mathrm{M}} \quad , \tag{13.3}$$

where the partial factors γ_{M} may be different from those used in the conventional approach. These factors can be established such that the coordination between strength

Table 13.11: Geotechnical characteristics of some frequently encountered soils according to EN 50341-1, Annex M

Soil	Specific weight force naturally humid γ kN/m^3	under buoyancy γ' kN/m^3	Angle of internal friction φ Degree	Cohesion c' kN/m^2	Undrained shear strength c_u kN/m^2	Subgrade modulus K_s MN/m^3
Marl, compact	20 ± 2	11 ± 2	25 ± 5	30 ± 5	60 ± 20	> 200
Marl, altered	19 ± 2	11 ± 2	20 ± 5	10 ± 5	30 ± 10	50 ± 10
Gravel, graded	19 ± 2	10 ± 2	38 ± 5	—	—	150 ± 10
Sand, loose	18 ± 2	10 ± 2	30 ± 5			60 ± 10
semi-dense	19 ± 2	11 ± 2	32 ± 5	—	—	80 ± 10
dense	20 ± 2	12 ± 2	35 ± 5			100 ± 10
Sandy silt	18 ± 2	10 ± 2	25 ± 5	10 ± 5	30 ± 10	60 ± 10
Clayey silt	19 ± 2	11 ± 2	20 ± 5	20 ± 10	40 ± 10	50 ± 10
Loam, silt, malleable	17 ± 2	7 ± 2	20 ± 5	—	20 ± 10	35 ± 5
Clay, soft	17 ± 2	7 ± 2	12 ± 5			25 ± 5
semi-stiff	19 ± 2	9 ± 2	15 ± 5	25 ± 5	60 ± 10	30 ± 5
stiff	20 ± 2	10 ± 2	20 ± 5			40 ± 5
Clay till	20 ± 2	10 ± 2	30 ± 5	12 ± 7	400 ± 350	—
Clay with organic addition	15 ± 2	5 ± 2	15 ± 5	—	—	—
Peat, marsh	12 ± 2	2 ± 2	—	—	—	—
Backfill, embankment, medium compaction	19 ± 2	10 ± 2	25 ± 5	—	15 ± 5	20 ± 5

of supports and foundations is achieved as required by [13.1], the strength of foundation being higher than that of the supported structures. The partial factors γ_M can be stipulated as required for the type of foundation, also in a project specification.
The *structural design of foundation* is related to the internal strength of the foundation body. The load of the foundation is determined from the design values of the supports. In case of concrete foundations, the analysis, the determination of the internal forces and moments and the structural design can be carried out according to ENV 1992-1 [13.17]. The concrete used for foundation should have a minimum compressive strength according to C20/25. The structural design of steel components of the foundations can be carried out according to ENV 1993-1-1 [13.22]. The partial factors for actions are contained in the design values; for the determination of the resistance, the partial factors for materials can be taken from the relevant standard or project specification.

13.4.2 Soil characteristics

If soil investigation did not yield other values, the soil characteristics according to Tables 13.11, 13.12, 13.13 and 13.14 can be used for design of foundations. A sufficient *compaction of the backfill* is assumed when adopting this values.
In Tables 13.13 and 13.14 taken from EN 50341-3-4 [13.20], *soil characteristics* are given for different soil types for use when designing foundations. The soil types determined during soil investigation should be correlated to the *soil types* given in Tables 13.12, 13.13, and 13.14. As a precondition, the rules mentioned in clause 13.3.4.4 should be duly considered when filling in the borehole log.
For the individual soil types, the specific weight, the *internal friction angle*, the *permissible bearing pressure* under characteristic and ultimate loads and the *earth frustum angle* are given in tables 13.13 and 13.14. The density of a soil type is needed for the verification of stability and the determination of the soil pressure below a foundation.

Table 13.12: Mechanical properties of some commonly encountered rocks according to EN 50 341-1, Annex M

Rock designation	Crushing strength R_c MN/m^2	Tensile strength R_t MN/m^2	Modulus of elasticity E MN/m^2
Granite, gneiss, basalt	100 to 200	4 to 10	20 000 to 70 000
Clay, shale	15 to 100	0 to 10	7 000 to 50 000
Limestone, compact	50 to 100	5 to 7	30 000 to 60 000
Limestone, soft	10 to 20	1 to 3	4 000 to 20 000
Marl, not altered	10 to 20	1 to 2	200 to 1 000
Sandstone	10 to 100	1 to 6	10 000 to 40 000
Molasse	2 to 10	0,2 to 1	1 500 to 5 000
Gypsum	3 to 10	0,3 to 1	2 000 to 5 000

– Poisson's coefficient μ is commonly between 0,25 and 0,35.
– The angle of internal friction φ is commonly between 35 and 45° and strongly depends upon degree and direction of fissures.

The specific weight of the soil affects also the *permissible* and *ultimate bearing pressure* given in Table 13.13, column 5, for 1,5 m depth ($\sigma_{1,5}$). If the embedment depth t is more than 1,5 m at all sides of the foundation body, the permissible and ultimate bearing pressure (σ_t) may be increased by a value which results from the surcharge of the soil associated with the additional depth multiplied by the factor κ to be

$$\sigma_t = \sigma_{1,5} + (t - 1{,}5) \cdot \gamma \cdot \kappa \tag{13.4}$$

for the permissible bearing pressure and

$$\sigma_t = \sigma_{1,5} + 1{,}6 \cdot (t - 1{,}5) \cdot \gamma \cdot \kappa \tag{13.5}$$

for the ultimate condition.
If *ground water* is found, the specific weight reduced by the *buoyancy* according to column 3, Table 13.13 can be used, only. In this case, the most unfavourable water table should be considered.
The *earth frustum angle* β_0 according to Table 13.14 columns 2 to 4 is used for the *verification of stability* in case of uplift-loaded auger-bored, concrete stepped block and pad and chimney foundations. Column 5 applies to monoblock foundations loaded predominantly by bending moments. Not only the dead weight of the foundation and the load of the soil resting vertically above the foundation base is considered but in addition a body of earth extending over the foundation subface. The volume of this earth frustum is determined by means of the angle β_0 depending on the foundation dimensions .
The dead weight of monoblock foundations may be increased by the dead weight of an earth frustum with the angle β according to Table 13.14 column 5. This approach leads to a conservative foundation resistance as confirmed by full-scale tests.

13.4.3 Compact foundations

13.4.3.1 Definition

In case of *compact foundations*, the tower or pole body is embedded in a monolitic foundation body loaded substantially by bending moments, in addition to horizontally and vertically acting forces. The transfer of the structural loads to the subsoil is achieved by bearing pressures in the foundation subsoil or by lateral earth resistance depending on the type of compact foundation. Compact foundations are carried out for any type of overhead line structures, in particular also for towers with extraordinarily high loads, e. g. bending moments of 200 000 kNm and more.

Table 13.13: Soil characteristics for design of foundation according to EN 50341-3-4

1	2	3	4	5		6
Type of soil	Specific weight force naturally humid (values for design)	with buoyancy	Angle of internal friction	Bearing pressure at a depth of 1,5 m permissible	ultimate[1)]	Coefficient
	γ kN/m^3	γ' kN/m^3	φ Degree	$\sigma_{1,5}$ kN/m^2	$\sigma_{1,5}$ kN/m^2	κ —
Non-cohesive soil						
1 Sand, loose	17	9	30	200	320	3,5
2 Sand, semi-loose	18	10	32,5	300	480	4
3 Sand, dense	19	11	35	400	640	5
4 Gravel, bolder, uniform	17	9	35	400	640	5
5 Gravel, sand, graded	18	10	35	400	640	5
6 Boulder, stones, macadam, graded	18	10	35	400	640	6
Cohesive soils						
7 pasty	16	8	0	0	0	1
8 soft (easy to knead), purely cohesive	18	9	15	40	65	2
9 soft, with non-cohesive additions	19	10	17,5	40	65	2,5
10 firm (difficult to knead), purely cohesive	18	9	17,5	100	160	2,5
11 firm, with non-cohesive additions	19	10	22,5	100	160	3
12 stiff, purely cohesive	18	10	22,5	200	320	3
13 stiff, with non-cohesive additions	19	11	25	200	320	3,5
14 hard, purely cohesive	18	—	27,5	400	640	3,5
15 hard, with non-cohesive additions	19	—	30	400	640	4
Organic soils and soils with organic additions	5 to 16	0 to 7	15			1
Rock						
-with considerable fissures or unfavourable stratifaction	20			up to 1000[2)]	1600[2)]	
-in sound, non-decomposed condition with minor fissures or favourable stratification	25			up to 3000[2)]	4800[2)]	
Made up ground and fill						
uncompacted embankment	12 to 16	6 to 10	10 to 25	30 to 100	48 to 160	2
compacted embankment	Classification according to type of soil, density of stratification and consistence, respectively					

[1)] data established by the authors; [2)] independent of depth

13.4.3.2 Monoblock foundations

Monoblock foundations are made up of concrete either as a prismatic body with vertical faces or as stepped body with one or several steps. The bearing pressure in the subface as well as the lateral earth resistance contribute to the limit strength of this foundation type. Today, monoblock foundations are predominantly carried out for medium-voltage lines equipped with concrete poles, solid-wall steel poles or lattice steel towers with small width. In case of wide-spread lattice steel towers, the concrete volume would be extremely high and, therefore, this type of foundation would be uneconomic. In this case, concrete slab foundations offer an interesting alternative.

Table 13.14: Angle of earth frustum according to EN 50341-3-4 for design of foundation

1	2	3	4	5
Type of soil	Auger-bored foundation	Stepped concrete foundation concreted to undisturbed soil β_0	planking	Monoblock foundation β
Non-cohesive soil				
1 Sand, loose	—	18 to 21	16 to 18	5 to 10
2 Sand, semi-loose	38 to 49	20 to 23	18 to 20	5 to 10
3 Sand, dense	41 to 53	22 to 25	20 to 22	8 to 10
4 Gravel, bolder, uniform	41 to 53	22 to 25	20 to 22	8 to 12
5 Gravel, sand, graded	41 to 53	22 to 25	20 to 22	8 to 12
6 Boulder, stones, macadam, graded	—	22 to 25	20 to 22	8 to 12
Cohesive soils				
7 pasty	—	—	—	—
8 soft (easy to knead), purely cohesive	—	9 to 11	6 to 8	4
9 soft, with non-cohesive additions	—	11 to 13	8 to 10	4
10 firm (difficult to kneed), purely cohesive	21 to 27	11 to 15	8 to 11	6
11 firm, with non-cohesive additions	26 to 34	13 to 17	10 to 13	6
12 stiff, purely cohesive	26 to 34	15 to 23	11 to 19	8
13 stiff, with non-cohesive additions	29 to 38	17 to 26	13 to 21	8
14 hard, purely cohesive	32 to 42	23 to 28	19 to 23	10
15 hard, with non-cohesive additions	35 to 46	26 to 28	21 to 23	10
Made up ground and fill				
Uncompacted embankment			6 to 13	4 to 10
Compacted embankment	Classification according to type of soil, density of stratification and consistence, respectively			

13.4.3.3 Monoblock foundations without base enlargement

When designing *monoblock foundations without base enlargements*, the lateral resistance of soil may be taken into account according to the compaction and the soil characteristics, if it is ensured that the soil will be neither permanently nor temporarily removed as long as the external loads are applied. The lateral earth resistance may be considered by the dead load of an earth frustum, the faces of which start at the lower edges of the foundation subface and are inclined at an angle β according to Table 13.14 outwards from the vertical.

The geotechnical design of monoblock foundations refers to inclination and to the verification of stability. The design can be carried out based on characteristic loads as specified e. g. in EN 50341-3-4 or on ultimate loads, the second alternative representing the more general approach.

Using the first approach, it should be verified that the foundation body will not be inclined by more than 1 % under the action of characteristic loads.

If the resistance due to the lateral earth pressure $R_{\mathrm{d\,lat}}$ exceeds the resisting moment $R_{\mathrm{d\,sf}}$ in subface, it is sufficient to verify that

$$E_{\mathrm{K}} \leq (R_{\mathrm{d\,lat}} + R_{\mathrm{d\,sf}}) \quad . \tag{13.6}$$

With decreasing contribution of lateral resistance, it should be proved that

$$E_{\mathrm{K}} \leq (R_{\mathrm{d\,lat}} + R_{\mathrm{d\,sf}})\,/\gamma_{\mathrm{M}} \quad , \tag{13.7}$$

where, according to EN 50 341-3-4,

$$\gamma_M = 1,5 - 0,5\,(R_{d\,lat}/R_{d\,sf}) \tag{13.8}$$

and $\gamma_M \geq 1,0$.
In addition, the bearing pressure in the subface as well as in the lateral faces may not exceed the permissible bearing pressures as given in Table 13.13.
Following the second approach, the inclination of the foundation body should not exceed 1,5 % under the action of ultimate loads. If the resistance due to the lateral earth pressure exceeds that due to the subface, it should be verified that

$$E_d \leq (R_{d\,lat} + R_{d\,sf}) \tag{13.9}$$

with decreasing contribution of lateral resistance, it should be proved that

$$E_d \leq (R_{d\,lat} + R_{d\,sf})\,/\gamma_M \quad , \tag{13.10}$$

where

$$\gamma_M = \gamma_{M\,max} - (\gamma_{M\,max} - 1,0)\,(R_{d\,lat}/R_{d\,sf}) \quad . \tag{13.11}$$

The material partial factor $\gamma_{M\,max}$ should be at least 1,2 and γ_M not less than 1,0. The bearing pressure in the subface as well as in the lateral faces may not exceed the ultimate bearing pressure as given in Table 13.13, in international and national standards or in project specifications.

Rating under consideration of the lateral soil resistance
In case of prismatic foundation bodies, the height of which is greater than its width, the load is predominantly transferred by a lateral embedment. The design will be conservative if the contribution of the subface is neglected. Assuming the pivoting axis of the foundation body at two thirds of its depth and a parabolic distribution of the bearing pressure between the foundation body and the soil, the *maximum bearing pressure* occurs at the foundation lower edge and is

$$\sigma_e = 12 \cdot M \cdot (h + 2/3 \cdot t)/(h \cdot b \cdot t^2) \quad , \tag{13.12}$$

where the significance of h, b and t can be taken from Figure 13.8. The virtual height of attack h results from the characteristic or ultimate moment M and the sum of the transverse loads H according to $h = M/H$.
The permissible or ultimative moment is obtained from

$$M_{perm(ult)} = \sigma_{perm(ult)} \cdot t^2 \cdot b \cdot h/\,[\gamma_M \cdot 12\,(h + 2/3 \cdot t)] \quad , \tag{13.13}$$

where
$\gamma_M = 1,0$ for characteristic values and
$\gamma_M = 1,2$ for ultimate values, at least.
More sophisticated models are described in [13.23] and [13.24].

Example: Monoblock foundation: Width 1,5 m, depth 2,0 m, permissible bearing pressure 200 kN/m^2, ultimate bearing pressure 320 kN/m^2, design bearing pressure 320/1,20 = 267 kN/m^2, characteristic moment M_K = 80 kNm and transverse force H_K = 10 kN, ultimate moment M_d = 108 kNm, ultimate force H_d = 13,5 kN, virtual height of attack $h = 80/10 = 8,0$ m.
Bearing pressure: $\sigma = 12 \cdot 80 \cdot (8,0 + 2/3 \cdot 2,0)/(8,0 \cdot 1,5 \cdot 2,0^2) = 187$ kN/m^2 < 200 kN/m^2.
Ultimate pressure: $\sigma = 12 \cdot 108 \cdot (8,0 + 2/3 \cdot 2,0)/(8,0 \cdot 1,5 \cdot 2,0^2) = 253$ kN/m^2 < 267 kN/m^2.
Permissible moment: $M_{perm} = 200 \cdot 2,0^2 \cdot 1,5 \cdot 8,0/[12 \cdot (8,0 + 2/3 \cdot 2,0)] = 85,71$ kNm.
$M_{ult} = 320 \cdot 2,0^2 \cdot 1,5 \cdot 8,0/[1,2 \cdot 12 \cdot (8,0 + 2/3 \cdot 2,0)] = 114,3$ kNm.

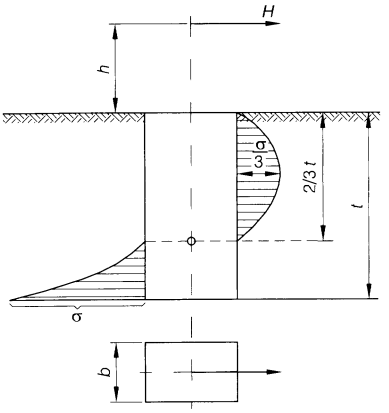

Figure 13.8: Monoblock foundation with parabolic distribution of earth pressure

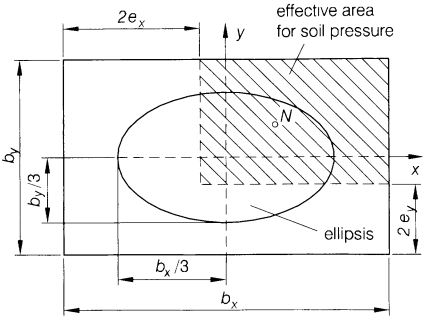

Figure 13.9: Permissible range within the rectangular subface for the positions e_x and e_y of force N resulting from the soil pressures in the subface

13.4.3.4 Monoblock foundation with base enlargement

Monoblock foundations with base enlargement are selected in case of subsoil conditions, where the vertical faces of the foundation block cannot be concreted against the natural soil, e. g. in case of less stable soils or high watertable. When high external loads act, monoblock foundations with base enlargements are selected because of economic reasons.

With this foundation type, the load is predominantly transferred through the foundation subface. The vertical faces of the foundation block add to the foundation resistance to a lower extent only, since the lateral embedment is not very effective because of the backfill of soil. The effect of the lateral embedment is considered by a soil body, the limiting faces of which start at all sides at the lower edges of the foundation base and are inclined at an *earth frustum angle* β outwards from the vertical according to Table 13.14, column 5. The magnitude of the earth frustum angle β depends on the soil type, on the density of non-cohesive soils and on the consistence of cohesive soils. The earth frustum angle β may only be considered when the backfill is well compacted and the soil will be neither permanently nor temporarily removed as long as the external load is acting.

When loaded by the characteristic or ultimate moments M_x and M_y, the force N resulting from the *bearing pressures* in the subface must act within an ellipsis according to Figure 13.9 to achieve a *stability against overturning* expressed by the partial factor γ_M. For rectangular subfaces according to Figure 13.9, this condition is met if

$$\gamma_M \leq 1/\left(2 \cdot \sqrt{(e_x/b_x)^2 + (e_y/b_y)^2}\right) \quad , \tag{13.14}$$

where $e_x = M_y/N$ and $e_y = M_x/N$. The partial factor γ_M should be at least 1,5 when the proof is carried out based on characteristic loads and at least 1,2 for ultimate loads. The verification of the bearing pressure can be carried out assuming a constant pressure distributed on a rectangular area equal to $(b_x - 2/e_x)$ times $(b_y - 2/e_y)$ (see Figure 13.9). Then, the sum N of the virtually acting loads should be

$$N \leq \sigma_{\text{perm(ult)}} \cdot (b_x - 2\,|e_x|) \cdot (b_y - 2\,|e_y|)\,/\gamma_M \quad , \tag{13.15}$$

where σ_{perm} or σ_{ult} can be obtained from Table 13.13 and equation (13.4) (see clause 13.4.2). The partial factor γ_M is 1,0 for characteristic loads and 1,2 for ultimate loads.

13.4.3.5 Slab foundations

Slab foundations accommodate the leg members in a foundation body consisting of a steel-reinforced concrete slab. The loads are transferred to the soil by pressures in the foundation subface. The lateral embedment is low only and should be neglected when verifying the stability. Therefore, only a relative low depth of the foundation subface is sufficient. The minimum foundation depth results from the requirements of a frost-proof position of the foundation subface in countries, where temperatures below freezing point occur, from a sufficient embedment length of the leg members within the slab and the load-bearing capacity of the subsoil. Slab foundations are selected at tower sites with a high watertable and relatively good-bearing subsoil.

Also in case of small tower widths and high leg member forces, slab concrete foundations can be necessary because separated pad and chimney foundations would not reach a sufficient distance from each other due to the necessary dimensions. Slab foundations are preferred for very high leg member forces because of the resulting large dimensions of separate foundations.

The *proof of stability* is carried out as described in clause 13.4.3.4. More information can be found in [13.25]. The steel-reinforced concrete cross section may be rated according to ENV 1992-1 [13.17] or other relevant standards, where the loads resulting from the individual load cases and the dead load of the foundation body as well as the load resulting from the soil above the foundation are considered, taking into account the effect of buoyancy, if any. A proof of stability using ultimate loads and split partial factors on the load and resistance is preferable, since this proof is consistent with the verification of structural strength.

The design internal forces and moments of the steel-reinforced concrete slab can be determined according to differing models. The plate can be described by a grillage with beams connecting the four leg members. This design model, however, results in an unfavourable distribution of the reinforcement because its main portion is arranged within the beams necessitating a stirrup reinforcement to take care of shearing.

A model more frequently used nowadays considers the leg members as supports when analysing concrete slabs. The slab is treated as loaded by the dead weight of concrete and soil above the foundation as well as the bearing pressures. These components form a system of equilibrium with the leg member forces under the assumption of ultimate loads. The internal design forces and moments in slab structure are calculated using the finite element method or another approximate procedure as described in [13.26]. A more uniform distribution of the reinforcement across the slab is obtained compared with the grillage model. A stirrup reinforcement is not necessary. A sufficient resistance in view of the *punching* in the vicinity of the leg members has to be verified for the compression forces as well as for uplift forces.

The thickness of the slab results either from the design in view of bending or from the verification of punching. The design moments in the slab depend substantially on the distribution of the pressure in the subsoil which is usually determined according to one of the following three methods:

- The conventional procedure assuming an equivalent bearing pressure distribution,
- The subgrade modulus procedure or
- The compressibility modulus procedure.

The application of the subgrade modulus or compressibility modulus procedure requires an extensive numerical effort and, therefore, the application of corresponding computer programs while the conventional procedure can be applied by hand as well.

In case of the *conventional procedure*, the deformation behaviour of the slab and of the subsoil are not considered and a linear distribution of the *bearing pressure* in the foundation subsoil results. The *subgrade modulus* and *compressibility modulus procedures*

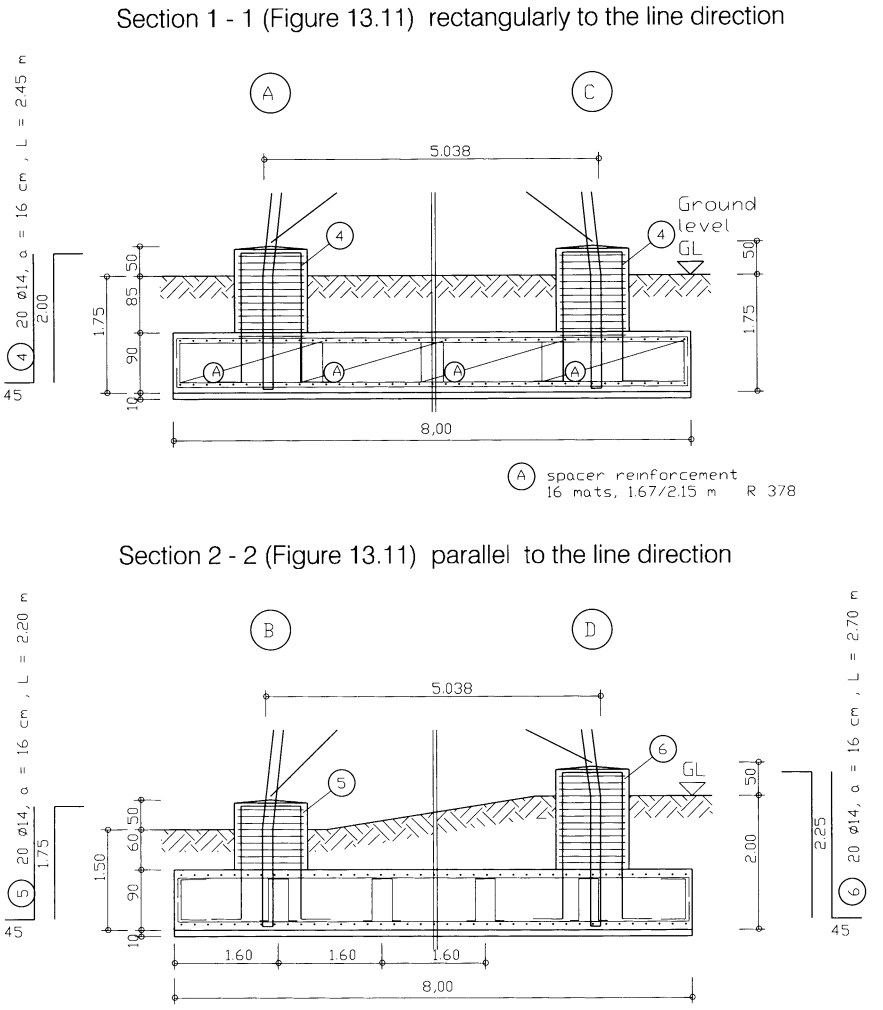

Figure 13.10: Slab foundation, dimensions and reinforcement, sections

assume a deformation-dependent distribution of the bearing pressure. The assumption that the settlement s is proportional to the bearing pressure forms the basis of the subgrade modulus procedure: $s = \sigma/K_s$. The subgrade modulus K_s is determined based on values obtained from experience or by calculation of the settlement. It is not a characteristic value of the soil, however, depends on the type of soil, the dimensions of the foundation slab and the thickness of the compressive soil layers. The calculation following the subgrade modulus procedure is frequently carried out using the finite element method, whereby the subgrade reaction can be substituted by a bed of uniformly distributed coil springs with a spring constant K_s.

The *compressibility modulus procedure* is adopted very rarely in overhead transmission line engineering. It assumes that the settlement of the subsoil and the deformation of the slab coincide. It can be adopted for any type of soil stratification. In case of cohesive soils, a constant compressibility modulus can be assumed, however, in case of non-cohesive soils this is a rough approximation only. Reference [13.27] provides more information on the determination of bearing pressure distribution in the subface.

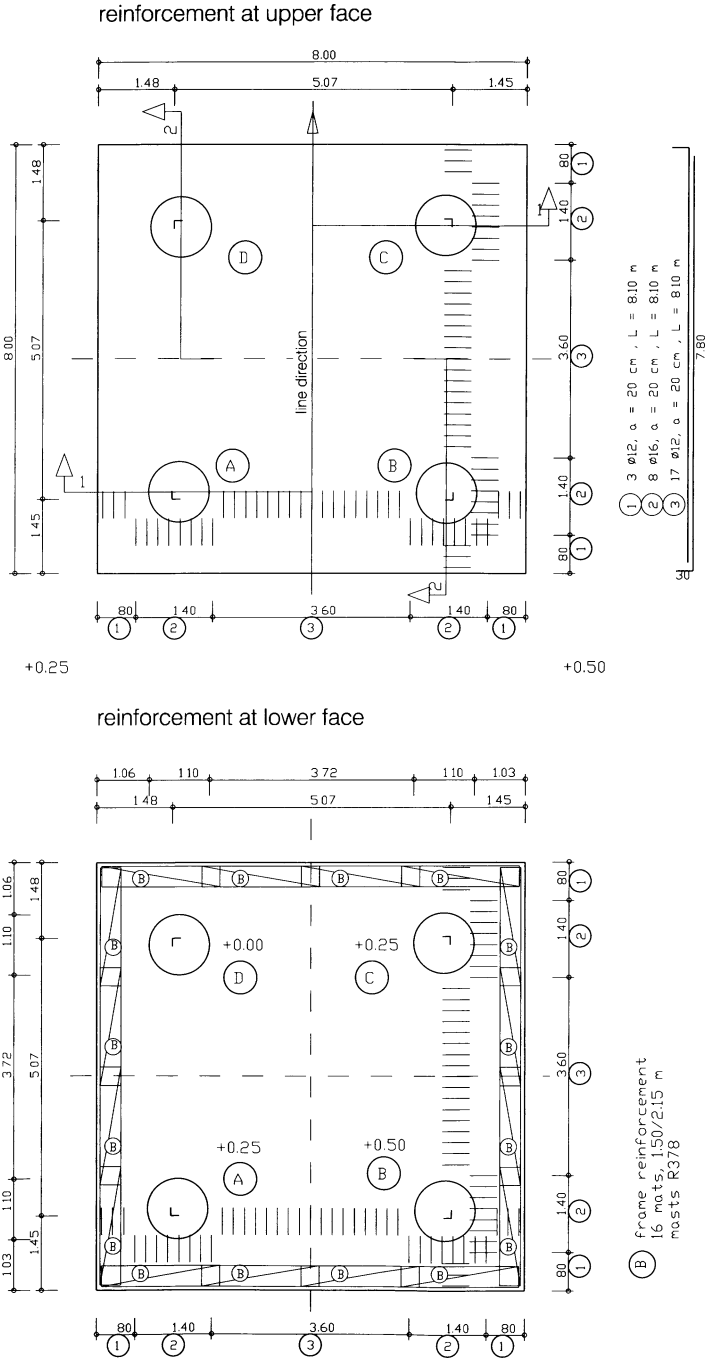

Figure 13.11: Slab foundation, reinforcement, plan view

Optimization of the slab dimensions, design of the reinforcement and establishment of the corresponding documents can be carried out by computer programs. Figure 13.10 depicts partial views of a reinforcement plan of a slab foundation. The procedures to be carried out for geotechnical verification is described by the following example.

Example: A slab foundation has to be designed for a 110 kV dead end tower.
Loads at the level of lowermost bracing connection:
Load case wind action on ice covered conductors, angle between crossarm axis and axis of line direction 90°, ultimate design loads

– Perpendicularly to crossarm axis	$M_x = 5\,775$ kNm,	$P_y = 217$ kN.
– In direction to crossarm axis	$M_y = 1\,072$ kNm,	$P_x = 62$ kN.
– Tower dead weight:		$P_z = 200$ kN.

Load case wind action on ice-covered conductors, angle between crossarm axis and axis of line direction 50°

– In direction to crossarm axis	$M_x = 2\,215$ kNm,	$P_y = 83$ kN.
– Perpendicularly to crossarm axis	$M_y = 6\,641$ kNm,	$P_x = 271$ kN.
– Tower and equipment dead weight:		$P_z = 250$ kN.

Tower width at ground level B_E:	5,038 m.
Increase of width of the lowermost tower section:	220 mm/m.

Type of soil according to soil investigation: Clay, sandy, semi-hard, no ground water.
Earth covering of the slab: At least 0,60 m.
Leg extensions: A : +0,25 m, B : +0,50, C : +0,25, D : ±0.
Since the moments rectangular and in parallel to the line do not differ that much, a square slab is used. The soil characteristics can be obtained from Table 13.13 for a semi-hard cohesive soil with non-cohesive additions:
Specific weight of soil $\gamma = 19$ kN/m^2, permissible bearing pressure 200 kN/m^2, ultimate bearing pressure 320 kN/m^2 at 1,5 m depth, specific weight of the reinforced concrete $\gamma_B = 24$ kN/m^2.
Average depth 1,75 m.
Using the dimensions according to Figure 13.10, the dead weight of the concrete results to be:

Slab $8{,}00 \cdot 8{,}00 \cdot 0{,}90 \cdot 24$	=	1 382 kN
Foundation muffs $4 \cdot 1{,}10^2 \cdot \pi/4 \cdot (0{,}85 + 0{,}30) \cdot 24$	=	105 kN
Weight of soil considering avarage soil covering:		
$(8{,}00 \cdot 8{,}00 \cdot 0{,}85 - 4 \cdot 1{,}10^2 \cdot \pi/4 \cdot 0{,}85) \cdot 19$	=	972 kN
Tower and equipment dead weight		250 kN
Total weight		2 709 kN

Verification under ultimate loads

$$M_{xd} = 2\,215 + 83(1{,}35 + 0{,}9) = 2\,402 \text{ kNm},$$
$$M_{yd} = 6\,641 + 271(1{,}35 + 0{,}9) = 7\,251 \text{ kNm}.$$

Hence, it is obtained

$$e_x = 2\,402/2\,709 = 0{,}89 \text{ m}; \; e_y = 7\,521/2\,709 = 2{,}68 \text{ m}.$$

The partial factor γ_M follows from (13.14)

$$\gamma_{Md} = 1/\left(2 \cdot \sqrt{(0{,}89/8{,}0)^2 + (2{,}68/8{,}0)^2}\right) = 1{,}42 > 1{,}20.$$

Since γ_M is greater than 1,20, the required minimum stability is verified.
The ultimate vertical resistance results from equation (13.15)

$$N_d = (320 + 1{,}6 \cdot 0{,}25 \cdot 3{,}5 \cdot 19) \cdot (8{,}0 - 2 \cdot 0{,}89)(8{,}0 - 2 \cdot 2{,}68)/1{,}2 = 4\,743 \text{ kN},$$

which is greater than $1{,}35 \cdot 2\,709 = 3\,657$ kN.
Verification using the conventional approach based on characteristic loads. The characteristic loads are

$$M_{xK} = M_{xd}/1{,}35 = 2\,402/1{,}35 = 1\,779 \text{ kNm},$$
$$M_{yK} = M_{yd}/1{,}35 = 7\,251/1{,}35 = 5\,371 \text{ kNm}.$$

Therefore,

$$e_x = 1\,779/2\,709 = 0{,}66 \text{ m}; \; e_y = 5\,371/2\,709 = 1{,}98 \text{ m}.$$

Table 13.15: Guideline data for the subgrade modulus according to [13.28]

Type of soil	MN/m^3
Light-weight peat	5 to 10
Heavy-weight peat and fine sand	10 to 15
Fill-ups of humus, sand, gravel	10 to 20
Loam, wet	20 to 30
Loam, humid	40 to 50
Loam, dry	60 to 80
Loam, dry, hard	100
Sand, loam and few boulders	60 to 80
Sand, loam and many boulders	80 to 100
Fine gravel with much fine sand	70 to 90
Medium gravel with fine sand	90 to 110
Medium gravel with much coarse sand	110 to 130
Coarse gravel with coarse sand	110 to 130
Coarse gravel with little coarse sand	130 to 160
Coarse gravel with little coarse sand, Densely stratified	130 to 200

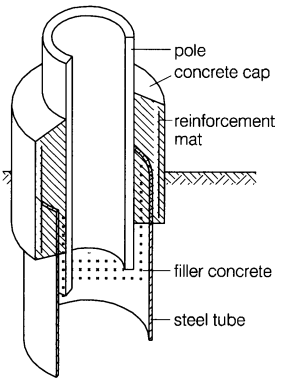

Figure 13.12: Pole inserted in a steel tube

The partial factor γ_M follows from (13.14)

$$\gamma_{MK} = 1/\left(2 \cdot \sqrt{(0{,}66/8{,}0)^2 + (1{,}98/8{,}0)^2}\right) = 1{,}92 > 1{,}50.$$

Since γ_{MK} is greater than 1,50, the stability of the slab is verified.
The permissible vertical load is obtained from (13.15)

$$N_K = (200 + 0{,}25 \cdot 0{,}35 \cdot 19)/(8{,}0 - 2 \cdot 0{,}66)(8{,}0 - 2 \cdot 1{,}98) = 5\,846 \text{ kN} > 2\,709 \text{ kN} \quad .$$

The dimensions of the slab complies with the requirements concerning the geotechnical design of the foundation.

13.4.3.6 Single grillage foundation

Single grillage foundation for supports may be suited in areas where concrete is expensive. Also in case of difficulties concerning procurement or transport of ready-mixed concrete, single grillage foundations present a favourable alternative.
The foundation slab consists of individual sleepers, either made of impregnated hard wood or of steel sections. In Central Europe, there is experience from 50 years of application of this foundation type, however, generally valid findings on the durability of sleepers and structural components buried in soil cannot be concluded.
The geotechnical design is carried out as in case of concrete slab foundations. The foundation subface as a whole can be applied in design calculations if the intermediate space between the sleepers is not more than one third of the sleeper width. The rules for steel or wood structures apply to the rating of the grillage. Members of the supports embedded in earth and inclined by more than 15° from the vertical should be assumed as additionally loaded by the soil resting upon the member. The additional load to be assumed should at least correspond to the load of a prismatic earth body formed by three times the member width and with vertical side faces.

13.4.3.7 Single pile foundations

Single pile foundations are adopted for medium-voltage lines in case of soil conditions not permitting the installation of a monoblock foundation or where economically viable. Subsoils with high watertable or non-bearing layers under the surface are within this category. To transfer the load to the deeper good bearing layers, *piles* are necessary. Piles with tube-type cross section into which the pole can be inserted are frequently

used (Figure 13.12). *Spun concrete poles* and steel poles with compact cross section are more suited for this foundation type than lattice steel towers.
The horizontal load effects on the pole are transferred by lateral embedment of the pile, the vertical loads by skin friction and point pressure. The rating of single pile foundation assumes elastic behaviour of the subsoil and pile up to the failure conditions of the soil. Elastic behaviour may be assumed up to a maximum of the horizontal displacement of 30 mm or, depending on the pile diameter d, up to $0{,}03 \cdot d$. The smaller value will be prevalent. The pile should be considered as being in failure condition, when these horizontal displacements are exceeded.

Continuous elastic support
For pile rating using the theory of a beam-bedded on an *elastic foundation*, the magnitude and variation of the *subgrade modulus* is necessary (see clause 13.3.3.5) for the soil profile in question. The subgrade modulus, however, cannot be determined such precisely from soil investigations commonly adopted for overhead contact lines with reasonable effort such that reliable results will be obtained. Therefore, design should be based on subgrade moduli from publications (Tables 13.11 and 13.15) and on proposals for its variation with depth according to literature [13.29, 13.30]. For cohesive soil, a constant subgrade modulus along the depth is assumed, while in case of non-cohesive soil an increase of subgrade modulus with depth is proposed. The pile will be rated for the calculated internal design loads and moments. Under the assumption of a skin friction angle $\delta = 0$, it needs to be verified that the existing bearing pressures are lower than the earth resistance.
At first, the *coefficient of passive earth pressure* k_p according to [13.31, 13.32] is calculated based on soil characteristics according to soil investigation or Table 13.13. For a horizontal terrain surface and an approximately vertical pile, the coefficient of passive earth pressure is

$$k_\mathrm{p} = \tan^2(45 + \varphi/2) \quad , \tag{13.16}$$

where φ is the *internal friction angle*, e. g. according to Table 13.13.
The formula for the calculation of the coefficient of passive earth pressure is given in [13.31, 13.32] for inclined terrain and a raked pile. The coefficient of passive earth pressure determined using the soil characteristics include partial factors already [13.33]. By their compilation an effective reliability against *soil fracture* with an order of 2,0 results. The earth resistance is obtained by

$$\mathrm{perm}\, e_\mathrm{p} = k_\mathrm{p} \cdot \gamma \cdot t \quad , \tag{13.17}$$

where γ is the specific weight of the soil and t the depth.
A *displacement of the pile point* of 20 to 30 mm can be tolerated with respect to the pole deformation. The displacement of the pile head is essentially higher under the condition of soil fracture.

Approach based on failure condition according to Blum
The calculation on the basis of the failure condition originates from a procedure developed by Blum [13.34] to *analyse piers* for ships. The foundation pile needs to experience plastic displacements within the soil before stabilizing moments are created. The earth resistance is assumed as linearly increasing with depth. The reliability of this approach was approved empirically by tests and by long-term experience. One main objection against finds fault with the assumed condition of a residual plastic displacement of the pile. *Blum's calculation approach* and the associated formuli will be presented by means of the following example.

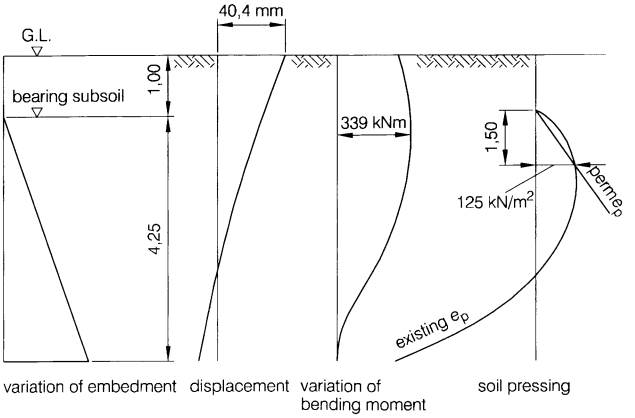

Figure 13.13: Data for analysis of a single-pile foundation following the method of elastic embedment

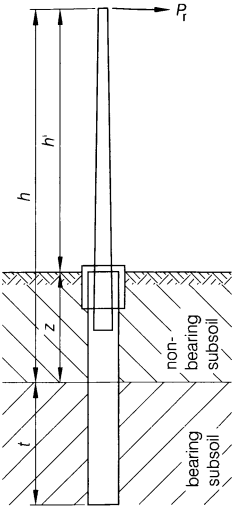

Figure 13.14: Data for analysis of a single-pile foundation following Blum's approach

Example: A single pile foundation will be analysed according to the two methods described above: Pole for a medium-voltage single circuit line, ultimate design force at the pole top $P_{rd} = 28{,}4$ kN, free length $h' = 10{,}0$ m, embedment length $t_E = 2{,}0$ m, diameter at bottom $D = 574$ mm, dead weight of the pole 33 kN, the crossarm and conductors included.
The mentioned design load acts at the top. Additionally, a wind load of 2,3 kN on the pole shaft in a height of 4,6 m above ground level will be considered. The design load at the top is increased due to wind on the pole to $P_{rd} = 28{,}4 + 2{,}3 \cdot 4{,}6/10 = 29{,}5$ kN.
Soil: Up to a depth of 1,00 m peat, from 1,00 m depth sand, ground-water level 3,0 m below surface. The layer of peat is assumed as non-bearing ($z = 1{,}0$ m).
The soil characteristics of the sand are: Specific weight with buoyancy $\gamma' = 10$ kN/m^3 and $\gamma = 17$ kN/m^3 without buoyancy; angle of internal friction $\varphi = 30°$; $K_s = 40$ MN/m^3 in a depth of 6 m; variation of the subgrade modulus: Linearly increasing starting at a depth of 1 m up to 6 m depth.
Since the sand is loosely stratified, a lower subgrade modulus is used than given in Table 13.15.
A helically-welded tube with a diameter $d = 762$ mm is selected for the pile. Its wall thickness is 8 mm, its cross section $A = 190$ cm^2, its moment of inertia $I = 134\,683$ cm^4; its cross-sectional modulus $W = 3535$ cm^3.
The result of the calculation according to the method of the elastic embedment is presented in Figure 13.13 [13.35].
Using the above mentioned soil characteristics under buoyancy and the data according to Figure 13.14, the coefficient of passive earth pressure introduced by Blum will be

$$f_w = \gamma' \cdot \tan^2(45° + \varphi/2) = 10 \cdot \tan^2(45° + 30°/2) = 30 \text{ kN/m}^3 \quad . \tag{13.18}$$

The position x_m of the maximum bending moments measured from the upper level of the bearing soil layer results from

$$x_m^3 + 3 \cdot d \cdot x_m^2 = 6 \cdot P_{rd}/f_w \quad , \tag{13.19}$$

$$x_m^3 + 3 \cdot 0{,}762 \cdot x_m^2 = 6 \cdot (28{,}4 + 2{,}3)/30 = 6{,}14 \quad ,$$

to be $x_m = 1{,}30$ m.

The maximum moment will be

$$\begin{aligned} M_{\max} &= P_{\mathrm{rd}} \cdot (h + z + x_{\mathrm{m}}) - f_{\mathrm{w}} \left(d \cdot x_{\mathrm{m}}^3/6 + x_{\mathrm{m}}^4/24\right) = \\ &= 29{,}5\,(10 + 1{,}00 + 1{,}30) - 30\,(0{,}762 \cdot 1{,}30^3/6 + 1{,}30^4/24) = \\ &= 362{,}9 - 11{,}9 = 351 \text{ kNm}. \end{aligned} \tag{13.20}$$

The steel stress of the pile will be

$$\sigma_{\mathrm{d}} = (1{,}35 \cdot 33/190 + 35\,100/3535) = 12{,}27 \text{ kN/cm}^2 \leq \sigma_{\mathrm{R,d}} = 23{,}5/1{,}1 = 21{,}4 \text{ kN/cm}^2.$$

According to [13.1], the resistance of steel grade S235 is $f_y = 23{,}5$ kN/cm^2. The partial factors are assumed according to [13.20] $\gamma_{\mathrm{F}} = 1{,}35$ and $\gamma_{\mathrm{M}} = 1{,}1$ for steel components for normal load conditions.
According to Blum, the embedment depth in the bearing soil t is obtained from $t = 1{,}2 \cdot t_0$, where t_0 can be calculated by solving the equation

$$t_0^3 \cdot (t_0 + 4\,d) \,/\, (t_0 + h) = 4 \cdot x_{\mathrm{m}}^2 (x_{\mathrm{m}} + 3\,d) \quad . \tag{13.21}$$

Equation (13.21) can be solved numerically. From $t_0^3 \cdot (t_0 + 4 \cdot 0{,}762) \,/\, (t_0 + 11{,}0) = 4 \cdot 6{,}14 = 24{,}56$ it is obtained $t_0 = 3{,}76$ m and $t = 1{,}2 \cdot 3{,}76 = 4{,}51$ m.
The embedment depth will be rounded to be $t = 4{,}50$ m. Therefore, a pile length L of $4{,}50 + 1{,}00 = 5{,}50$ m results.
The displacement Y of the pile at the ground level is

$$\begin{aligned} Y &= \frac{P_{\mathrm{rd}}}{E \cdot I} \left[\frac{(h + 0{,}65 \cdot t)^3}{3} - \frac{(h + 0{,}65 \cdot t)^2}{2} \cdot h' + \frac{h'^3}{6} \right] \\ &= \frac{29{,}5}{21\,000 \cdot 134\,683} \left[\frac{(1\,100 + 0{,}65 \cdot 450)^3}{3} - \frac{(1\,100 + 0{,}65 \cdot 450)^2}{2} \cdot 1\,000 + \frac{1\,000^3}{6} \right] \\ &= 1{,}01 \text{ cm} \quad . \end{aligned} \tag{13.22}$$

The maximum bending moments coincide quite well for both methods of analysis. The displacement of the pile, however, differs considerably. Substantially higher pile displacements result from the method of elastic embedment as compared to Blum's empirically developed formulae which have been validated by experiments of other authors. The available bearing pressure according to Figure 13.13 would exceed the permissible values in the upper range of the pile; this can be tolerated, however.

13.4.3.8 Foundation of self-supporting timber poles

Self-supporting timber poles can be embedded directly into soils with sufficient bearing capacity so far the load permits to do so. According to EN 50341-1, the depth should be at least one sixth of the pole length and not less than 1,6 m. The excavation should be filled with gravel and stones which should be carefully compacted to ensure the lateral resistance of the embedment. In case of less bearing soil, a ring of stones or sleepers arranged rectangular to the direction of the load should be provided.
To avoid rottenness in the soil, timber poles are connected to *footings* made of reinforced concrete. The timber pole ends above the ground level out of the range of splashing water and is clipped to the footing. Figure 13.15 shows an example of a footing made of concrete. Insertion of timber poles into concrete sheaths is not advisable due to the high hazard of rottenness.

13.4.4 Separate foundations

13.4.4.1 Definition

It is the characteristic of *separate foundations* that each leg member of lattice steel towers is anchored into an individual footing, and each of the foundations is loaded by vertically acting forces in addition to horizontal ones. Uplift loads are counteracted by

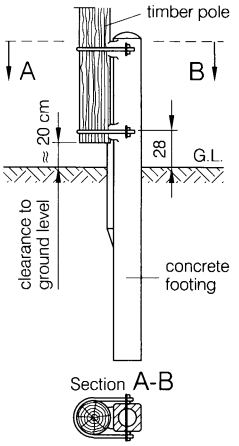

Figure 13.15: Timber pole with concrete footing

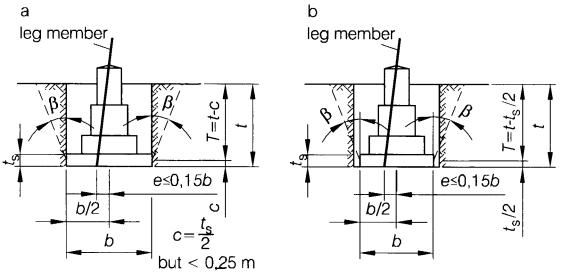

Figure 13.16: Concrete block foundation according to EN 50 341-3-4: a foundation type A – concreted to earth; b foundation type S – concreted to planking

the dead weight of the foundation body and an available *dead load of the soil*, if any, and/or through shearing in the subsoil. Separate foundations are used for *wide-spread lattice steel towers* whereby uplift forces up to 5 000 kN need to be transferred to the subsoil in case of standard lines.

This type of foundation is technically sound and economic in case of loads occurring typically at lines with nominal voltages of 110 kV and above. A sufficiently wide distance between the leg members is necessary for construction of the foundations in question, as well as with respect to their load-carrying function. The tower width should be at least 3,5 m for the application of separate footings. Depending on the soil conditions, the loads, the available tools, the accessibility to the tower sites and economic aspects, the suitable type of separate footings can be selected for each individual tower type.

13.4.4.2 Stepped block foundations

As far as installation and performance under load are concerned, *stepped block foundations* can be classified as (see e. g. EN 50 341-3-4 [13.20]):

Foundation type A (Figure 13.16 a): The lowermost step is concreted to the undisturbed subsoil. The planking of the excavation pit reaches down to the upper surface of the lower step. This type of foundation needs firmly-standing, cohesive, dry soil. Since one or two days are necessary to adjust the tower stubs, the lower part of the excavation is endangered by collapsing until the concrete will be placed.

Foundation type S (Figure13.16 b): The lowermost step is concreted to the planking. The *planking of the excavation* ends at the foundation subface and is used as formwork for the lower step. The foundation type S can be adopted in not firmly-standing and wet soils.

Geotechnical design

Differing approaches for designing *stepped block foundations* are followed in individual countries as can be seen from [13.19]. However, they are mainly distinguished by the parameters adopted and the reliability level required. The standard EN 50 341-3-4 [13.20] should be used here as an example for a geotechnical design standard. The bearing pressure under compression needs to be verified under consideration of a dead weight

of the foundation and the soil resting vertically upon the foundation base.
Shear forces occur in an area limited by the perimeter of the lower step and the ground level and determine substantially the resistance of a foundation loaded by uplift. Since generally valid information on the magnitude of the shear forces cannot be provided, a procedure was developed which substitutes the shear forces by the weight of a soil body limited by the *earth frustum angle* β [13.36]. This angle does not represent the limits of the earth body which will be lifted when pulling out the foundation. The magnitude of earth frustum angles β depends on the installation method of the foundation, its dimensions and the type of subsoil and is calculated according to [13.20] from

$$\beta = \beta_0 \sqrt{b/T} \quad , \tag{13.23}$$

where b is the width of the foundation and T the depth of the earth frustum body (Figure 13.16). In Table 13.14, the angles of earth frustum β_0 are given for representative types of subsoils correlated to the installation procedure and the type of soil. The values apply to foundation widths between 1,5 to 5,0 m. The foundation width b is the length of one side in case of quadratic lowermost blocks or the diameter in case of circular blocks. In case of a rectangular subface, the equivalent width is determined from the length of the sides b_1 and b_2 according to

$$b = \sqrt{b_1 \cdot b_2} \quad . \tag{13.24}$$

This applies as long as $b_1/b_2 \leq 1{,}4$ and b_1 is the width of the longer side. The lower value β_0 of the range presented in Table 13.14 applies to a foundation width of 5,0 m and the upper β_0 value to 1,5 m foundation width. Intermediate values may be linearly interpolated.
The depth of the earth frustum depends on the foundation construction method. In case of foundation types A and S, the point of attack of the earth frustum angle is situated above the foundation subface and the depth T of the earth frustum body is defined in Figure 13.16 for these cases. If the ratio b/T exceeds the value 1, then $\beta = \beta_0$ is to be used for the analysis. The earth frustum angle is limited to values less than 35°.
The described calculation method applies to stepped block foundations with a ratio of width b to depth T of more than 0,60.
When verifying the *stability* using characteristic loads, the bearing pressure may not exceed permissible limits. Examples for permissible bearing pressures are given in Table 13.13. Were ultimate design loads are given, it is required to prove that

$$E_\mathrm{d} \leq R_{\mathrm{d\,comp}}/\gamma_\mathrm{MC} \quad , \tag{13.25}$$

where the design compression resistance is

$$R_{\mathrm{d\,comp}} = \sigma_\mathrm{ult} \cdot A \tag{13.26}$$

with σ_ult ultimate bearing pressure according to Table 13.13 and A subface area of the foundation. The partial factor γ_MC should be taken as 1,2 at least.
A uniform distribution of the pressure in the subface is assumed. The *dead weight of soil* resting vertically upon the foundation base needs to be considered as acting permanently. The influence of the horizontal loads on the bearing pressure may be neglected, compared with the prevalent effect of the vertical loads. The horizontal load may, however, increase the bearing pressure considerably with bent stubs or high loads, e. g. for dead-end towers. The stability against uplift is verified by

$$E_{\mathrm{K,(d)}} = R_{\mathrm{d\,up}}/\gamma_{\mathrm{M\,up}} \quad . \tag{13.27}$$

When characteristic loads E_K are given, the partial factor $\gamma_{\mathrm{M\,up}}$ should ensure the stability under ultimate conditions and consider the uncertainties on the resistance

side. As an example, the partial factor is 1,5 according to EN 50 341-3-4 [13.20]. The partial factor should be chosen such that the foundation resistance is higher than that of the tower because of coordination of strengths.
When the proof is carried out for ultimate loads, the partial factor $\gamma_{\mathrm{M\,up}}$ should be at least 1,2 to care for the correlation of strength between supports and foundations.
In addition to the stipulated uplift stability, it should be verified that

- for foundation type A: $G/S_{\mathrm{K\,up}} \geq 0{,}67$ or $G/S_{\mathrm{d\,up}} \geq 0,50$;
- for foundation type S: $G/S_{\mathrm{K\,up}} \geq 0{,}80$ or $G/S_{\mathrm{d\,up}} \geq 0,60$ are met.

There, G is the sum of the dead weight of foundation and the soil resting vertically upon the foundation subface; $S_{\mathrm{K\,up}}$ is the vertical component of the characteristic uplift force and $S_{\mathrm{d\,up}}$ the vertical component of the ultimate uplift force acting on the foundation.
The *resistance* of foundations *loaded by uplift* is substantially affected by the density and consistence of the surrounding subsoil. Intensive artificial compaction of the subsoil by vibrating compaction or similar procedures can be considered accordingly. According to EN 50 341-3-4 [13.20], the intersection of the leg member axis and the foundation subface may deviate from the centre of the foundation base only by the dimension e defined in Figure 13.16.

Structural design

When certain conditions are complied with, *reinforcement of stepped block foundations* can be waived. However, if the load of the foundation requires a reinforcement, the internal forces and moments may be determined according to ENV 1992-1 [13.17] form the foundation loads and the rating is carried out according to this standard as well. The concrete employed should at least comply with the strength class C20/25. On the other hand, concrete of a higher strength class should be avoided as far as possible to ease the installation process.
The selected dimensions of the foundations should also take care of the required space for working. Requirements concerning this aspect are given in relevant standards, e. g. DIN 4124 [13.37]. The *working space* is assumed as the clearance between the formwork of the foundation body and the inner edge of beams for the excavation planking. The working space should be 0,35 m at the closest position and at least 0,5 m in case of rectangular foundation blocks and circular foundation blocks up to 1,50 m diameter. For 0,1 m thick beams of the excavation shuttering, a minimum projection of the lower block of 0,45 m results and, as a consequence, a minimum foundation width of 2,0 m in case of a foundation shaft with 1,10 m diameter.
The *height of blocks* made of non-reinforced concrete is determined by the ratio n of the height of steps to the width of the projection being at least 1,4 according to the long-term practice in Germany. In case of transition from a circular foundation block to a quadratic lowermost block, the diameter d should be replaced by the equivalent width $b = d/1{,}13$ of a quadratic subface when checking the mentioned criteria.
The projecting foundation block is stressed by bending when an uplift load acts. In case of a rectangular concrete block, the maximum bending moment and stress will occur at the lower edge of the second concrete block, counted from the bottom, if a monolithic concrete structure is assumed. In case of a circular design of that block, it may be assumed that the maximum bending stress will occur in a cross section at a distance according to $d/2,26$ from the block centre, where d is the diameter of the circular concrete block. The ratio $n \geq 1{,}4$ should be obeyed for all steps of the foundation. Foundations where projections result in $n < 1{,}4$ need to be reinforced and specifically verified.
With bent leg member stubs, the individual blocks can be symmetrically arranged one above the other. In case of a continuous, unbent stub, the first block is arranged centrally above the foundation subface and the following blocks are staggered according

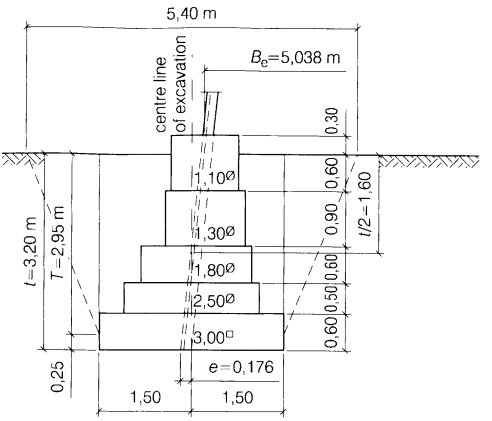

Figure 13.17: Concrete block foundation (example)

to the inclination of the leg member. The centre of the foundation subface may only deviate from the virtual penetration of the leg member through the foundation subface by the dimension e given in Figure 13.16. This requirement needs also to be considered when pegging out the foundation excavation.

Example: A separated concrete block foundation (Figure 13.17) has to be designed for the 110 kV dead-end tower treated in clause 13.4.3.5. The data are: Leg member uplift force 888 kN (ultimate design load), load case wind action on conductors with ice; leg member compression force 1 012 kN (ultimate design load); the equivalent characteristic loads are 658 kN and 750 kN, respectively; leg member angle section L180 × 16; tower width at the ground level: 5,038 m; increase of width of the lowermost tower section: 220 mm/m.
Subsoil according to soil investigation: Clay, sandy, semi-hard. The soil encountered permits to install a block foundation type A concreted to the undisturbed soil. The soil characteristics for the design are taken from Tables 13.13 and 13.14 for semi-hard cohesive soil with non-cohesive additions. The following values result for foundation type A: Specific weight of the soil $\gamma = 19$ kN/m^3; permissible bearing pressure up to 1,5 m depth 200 kN/m^2; ultimate bearing pressure 320 kN/m^2; factor $\kappa = 3{,}5$; earth frustum angle $\beta_0 = 17°$ for 5,0 m foundation width, earth frustum angle $\beta_0 = 26°$ for 1,5 m foundation width and specific weight of the non-reinforced concrete $\gamma_B = 22$ kN/m^3.
Since $b/T = 3{,}00/2{,}95 = 1{,}02 > 1{,}0$, the earth frustum angle is equal to β_0 (see above under subclause 13.4.4.2, geotechnical design). The angle of adequate earth frustum will be for the 3,00 m wide foundation $\beta = 17 + (26 - 17) \cdot (5{,}00 - 3{,}00)/(5{,}00 - 1{,}50) = 22{,}14°$.
Width of the earth frustum at ground level $3{,}00 + 2 \cdot 2{,}95 \tan 22{,}14° = 5{,}40$ m.
Volume of the soil body with an earth frustum angle β: $V_{EF} = 1/3 \cdot 2{,}95 \cdot (5{,}4^2 + 5{,}4 \cdot 3{,}0 + 3{,}0^2) - 8{,}9 = 53{,}45 - 8{,}9 = 44{,}55$ m^3
Weight of the soil body $G_{EF} = 44{,}55 \cdot 19 = 846$ kN
Volume of the soil body vertically upon the foundation subface:
$V_E = (3{,}20 - 0{,}60) \cdot 3{,}00^2 - (0{,}570 + 1{,}195 + 1{,}527 + 2{,}454) = 17{,}654$ m^3
Weight of the soil body $G_E = 17{,}654 \cdot 19 = 335$ kN
Volume of the concrete body 11,463 m^3
Dead weight of the concrete body $G_B = 11{,}463 \cdot 22 = 252$ kN
Ratio of the projection of the lower step $0{,}60/[(3{,}00 - 2{,}50/1{,}13) - 0{,}5] = 1{,}52 > 1{,}40$
Design based on characteristic loads:
Verification of resistance in case of load by compression:
Maximum bearing pressure: $\sigma = (750 + 252 + 335)/(3{,}0 \cdot 3{,}0) = 149$ kN/m^2
The permissible bearing pressure in a depth of 3,20 m results from (13.4):
perm $\sigma = 200 + (3{,}20 - 1{,}50) \cdot 19 \cdot 3{,}5 = 313$ kN/m^2
Proof: $\sigma = 149$ kN/m^2 < perm $\sigma = 313$ kN/m^2
Proof of stability under uplift:
Uplift load: $E_K = 658$ kN

Resistance results from weight of concrete and earth frustum: $R_K = 252 + 846 = 1098$ kN
Proof: $R_K/E_K \geq 1{,}5$: $1098/658 = 1{,}67 > 1{,}5$
Additional conditions: $G/S_{K\,up} = (252 + 335)/658 = 0{,}89 > 0{,}67$

Design based on design ultimate loads:
Verification of resistance in case of load by compression:
Partial factor for weight of concrete and soil $\gamma = 1{,}35$
Compression load: $E_d = 1012 + 1{,}35 \cdot (252 + 335) = 1804$ kN
The ultimate bearing pressure in a depth of 3,20 m results from (13.5):
ult $\sigma = 320 + 1{,}60 \cdot (3{,}20 - 1{,}50) \cdot 19 \cdot 3{,}5 = 500$ kN/m^2
Partial factor of resistance $\gamma = 1{,}2$
Resistance: $R_d = 500(3{,}0 \cdot 3{,}0)/1{,}2 = 3750$ kN
Proof: $E_d/R_d \leq 1{,}0$: $1804/3750 = 0{,}48 < 1{,}0$
Proof of stability under uplift:
Uplift load: $E_d = 888$ kN
Partial factor of resistance $\gamma_M = 1{,}2$
Resistance results from weight of concrete and earth frustum: $R_d = (252 + 846)/1,2 = 915$ kN
Proof: $E_d/R_d \leq 1{,}0; 888/915 = 0{,}97 < 1{,}0$
Additional conditions: $G/S_{d\,up} = (252 + 335)/888 = 0{,}66 > 0{,}50$

It is expedient to adjust the individual steps of the foundation to the inclination of the leg member. Therefore, the individual blocks will be designed with wider projections in the outward direction than inwards, the second block excepted. The projection to the tower centre has to be selected such that the formworks can be arranged one above the other. An expedient design of the block foundation is achieved, if the middle of the excavation intersects the axis of the leg member at half of the foundation depth. This arrangement assumed, the eccentricity of the leg member penetration point relative to the centre of the excavation will be

$$e = 220/2 \cdot 1{,}60 = 176 \text{ mm} < \max e = 0{,}15 \cdot 3000 = 450 \text{ mm} \quad .$$

The distance between the edge of the lower steps of the foundation is: $5{,}038 + 2 \cdot 0{,}176 - 3{,}00 = 2{,}39$ m. The projection of the earth frustum is $2{,}95 \cdot \tan 22{,}14° = 1{,}20$ m. Due to $2 \cdot 1{,}20$ m $\sim$ 2,39 m, the earth frustums of two footings just meet at the ground level. The distance of the footing is sufficient, therefore.

13.4.4.3 Auger-bored and excavated foundations

The excavation of *auger-bored foundations* is carried out by a dry-drilling process. An auger is commonly used as the drilling tool. To achieve the required resistance, the augered foundation is expanded at its base using an *under-cutting tool.* This excavation method assumes soils able to be augered, load-bearing and dry, having substantially cohesive characteristics. Bigger stones form obstacles for augering. Decomposed brittle layers of rock might be penetrated under certain circumstances whilst compact rock cannot anymore be excavated with this procedure. Augered foundations are drilled vertically to counteract the hazard of collapsing of holes. Due to the bend between the axis of the drilling and the axis of the leg member, horizontally acting radial forces are created in addition to the residual transverse forces from the tower loads. These horizontal forces are transferred to the subsoil by the lateral embedment of the foundation body. The bending moments loading the concrete cross section require a corresponding reinforcement. With respect to the construction of the foundation, short tower stubs are used which do not reach to the foundation subface. Therefore, also the longitudinal forces need to be transferred through the reinforcement.
Excavated foundations are only distinguished by the excavation procedure from augered foundations since excavation is carried out by means of a grab and soil planking is as well not used.

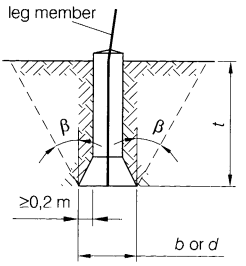

Figure 13.18: Auger-bored or excavated foundation, foundation type B

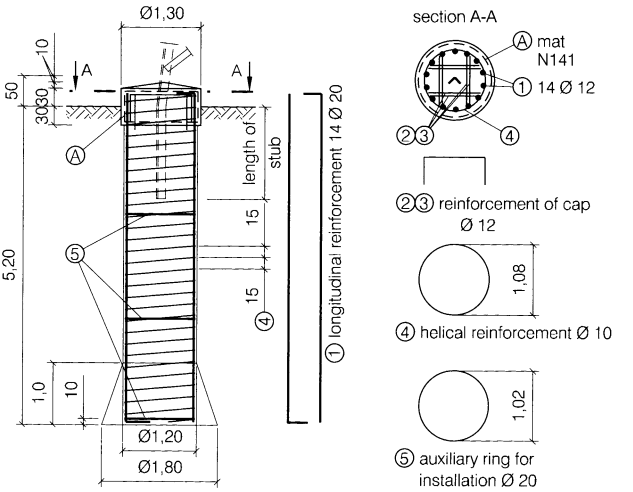

Figure 13.19: Reinforcement of an auger-bored foundation

Geotechnical design

The *geotechnical design* of auger-bored or excavated foundations can be carried out using the *earth frustum* procedure as in case of block foundations.

At first the soil encountered at the site is assigned to the corresponding type of soil according to Table 13.14 and the earth frustum angle β_0 for the foundation type B is determined (Figure 13.18). The β_0 values apply to foundation widths between 1,20 and 2,10 m. Within the ranges mentioned for the individual types of soil, a lower value β_0 applies to a large foundation width of approximately 2,1 m and the upper value β_0 to a low foundation width of 1,20 m. Values in between may be interpolated linearly. According to [13.20], the *earth frustum angle* starts at the foundation subface and is determined from

$$\beta = \beta_0 \cdot \sqrt{b/t} \quad . \tag{13.28}$$

The *ultimate compression resistance* can be obtained by assuming the ultimate bearing pressure as equally distributed within the foundation subface.

$$R_{\mathrm{d\,comp}} = \sigma_{\mathrm{ult}} \cdot d^2 \cdot \pi/4, \tag{13.29}$$

where σ_{ult} can be taken from table 13.13 and equation (13.5).

When characteristic loads are used for verifying the foundation, the bearing pressure in the foundation subface may not exceed the permissible bearing pressures according to Table 13.13 and equation (13.4).

The dead load of the foundation body as well as the dead load of the soil resting vertically upon the foundation subface may be neglected when calculating the bearing pressure because the dead load of foundation and soil body are counteracted by the skin friction and only the leg member compression force will be transferred to the subface.

The verification for uplift loads can be carried out using the *earth frustum method* to determine the uplift resistance. Whereby, additionally to the load of the foundation body, the dead load of the soil body defined by an earth frustum angle β starting at the edge of the foundation subface may be taken into consideration (see Figure 13.18).

Equation (13.28) for the determination of the *earth frustum angle* β is validated for foundations with dimensions complying with the following conditions (see [13.20]):

- Depth of foundation between 1,8 and 7,0 m;
- Diameter of concrete shaft between 0,7 and 1,5 m;
- Width of foundation between 1,2 and 2,1 m;
- Projection of the foundation subface $\geq 0{,}2$ m;
- Ratio of foundation width to foundation depth $0{,}25 \leq b/t \leq 0{,}7$.

With regard to installation, the ratio of the *projection of foundation subface* to the height of foundation base should be approximately 0,5 in case of cohesive soil and approximately 0,33 in case of non-cohesive soil.
When *ultimate design loads* are given, it is required to prove that

$$E_{\mathrm{d}} / \left(R_{\mathrm{d\,up}}/\gamma_{\mathrm{M}}\right) \leq 1{,}0 \quad , \tag{13.30}$$

where γ_{M} should be at least 1,2 to take care of coordination of strength between towers and foundations. Partial factors γ_{M} between 1,35 and 2,00 are applied when *characteristic uplift loads* are given. Then

$$R_{\mathrm{d\,up}}/E_{\mathrm{K}} \geq \gamma_{\mathrm{M}} \tag{13.31}$$

according to EN 50 341-3-4, the partial factor is 1,5 to mention a specific example.

Example: An auger-bored foundation has to be designed for the 110 kV dead-end tower treated under clause 13.4.3.5. The dimensions of the foundation are assumed according to Figure 13.19.
From the static analysis of the tower, it results: Horizontal ultimate design force of the bracings $P_{\mathrm{x}}^{\mathrm{D}} = 7{,}75$ kN, $P_{\mathrm{y}}^{\mathrm{D}} = 3{,}08$ kN and radial force due to bending of the leg member $P_{\mathrm{x}}^{\mathrm{k}} = P_{\mathrm{y}}^{\mathrm{k}} = 96{,}5$ kN. The corresponding characteristic values are: $P_{\mathrm{x}}^{\mathrm{D}} = 5{,}74$ kN; $P_{\mathrm{y}}^{\mathrm{D}} = 2{,}28$ kN and $P_{\mathrm{x}}^{\mathrm{k}} = P_{\mathrm{y}}^{\mathrm{k}} = 71{,}48$ kN.
The soil characteristics result from Tables 13.13 and 13.14 for semi-hard cohesive soil with non-cohesive additions: Specific weight of the soil $\gamma = 19$ kN/m^3, earth frustum angle $\beta_0 = 29°$ for $d = 2{,}10$ m; $\beta_0 = 38°$ for $d = 1{,}20$ m, angle of internal friction $\varphi = 25°$, specific weight of reinforced concrete $\gamma_{\mathrm{B}} = 24$ kN/m^3.
Since $b/t = 1{,}80/5{,}20 = 0{,}35$, the condition $0{,}25 \leq b/t \leq 0{,}70$ is met.
The earth frustum angle β_0 results for $b/t = 1{,}0$ and $d = 1{,}80$ m to be
$\beta_0 = 29 + (38 - 29) \cdot (2{,}10 - 1{,}80)/(2{,}10 - 1{,}20) = 32°$.
Therefore, it is obtained $\beta = 32 \cdot \sqrt{0{,}35} = 18{,}83°$.
Diameter of the soil body at ground level: $d_{\mathrm{a}} = 1{,}80 + 2 \cdot 5{,}20 \cdot \tan 18{,}83° = 5{,}35$ m.
The distance of the leg members at ground level is 5,038 m. That means, the inverted truncated cones of earth intersect by $5{,}35 - 5{,}038 = 0{,}31$ m. The reduction of the reactive force is such insignificant that it will not be considered, also with respect to the fictitious assumption of the earth frustum shape.
Volume of soil frustum considering the angle β: $V_{\mathrm{E}} = 5{,}2/3 \cdot (1{,}8^2 + 1{,}8 \cdot 5{,}35 + 5{,}35^2) \cdot 0{,}785 - 6{,}599 = 56{,}458 - 6{,}599 = 49{,}9$ m^3.
Weight of earth frustum: $G_{\mathrm{E}} = 49{,}9 \cdot 19 = 947$ kN
Volume of concrete body 7,041 m^3; volume of concrete body below ground level 6,599 m^3
Weight of concrete body: $G_{\mathrm{B}} = 7{,}041 \cdot 24 = 169$ kN
Volume of soil body resting vertically upon the foundation subface $5{,}20 \cdot 1{,}8^2 \cdot \pi/4 - 6{,}599 = 6{,}627$ m^3; weight of soil body $6{,}627 \cdot 19 = 126$ kN

Design based on characteristic loads:
Proof of stability under compression loads:
Maximum bearing pressure:
Action of leg member compression force together with the concrete and soil frustum weight:
$\sigma = (750 + 169 + 126)/(1{,}8^2 \cdot 0{,}785) = 411$ kN/m^2
Action of the leg member compression force only: $\sigma = 750/(1{,}8^2 \cdot 0{,}785) = 295$ kN/m^2
The permissible bearing pressure under characteristic loads amounts to:
perm $\sigma = 200 + (5{,}20 - 1{,}50) \cdot 19 \cdot 3{,}50 = 446{,}05$ kN/m^2 according to (13.4)
Under both assumptions, the bearing pressure does not exceed the permissible value of 446 kN/m^2.

Proof of stability under uplift:
Uplift load: $E_K = 658$ kN
Resistance results from weight of concrete and earth frustum: $R_K = 169 + 947 = 1116$ kN
Proof: $R_K/E_K \geq 1{,}5: \quad 1116/658 = 1{,}7 > 1{,}5$

Design based on design ultimate loads:
Verification of resistance in case of load by compression:
Partial factor for weight of concrete and soil $\gamma = 1{,}35$
Compression load: $E_d = 1012 + 1{,}35 \cdot (169 + 126) = 1440$ kN
The ultimate bearing pressure in a depth of 5,20 m results from (13.5):
ult $\sigma = 320 + 1{,}60 \cdot (5{,}20 - 1{,}50) \cdot 19 \cdot 3{,}50 = 714$ kN/m^2
Partial factor of resistance $\gamma = 1{,}2$
Resistance: $R_d = (714 \cdot 1{,}8^2 \cdot \pi/4)/1{,}2 = 1514$ kN
Proof: $E_d/R_d \leq 1{,}0: 1440/1514 = 0{,}95 < 1{,}0$
Proof of stability under uplift:
Uplift load: $E_d = 888$ kN
Partial factor of resistance $\gamma_M = 1{,}2$
Resistance results from weight of concrete and earth frustum: $R_d = (169 + 947)/1{,}2 = 930$ kN
Proof: $E_d/R_d \leq 1{,}0: 888/930 = 0{,}96 < 1{,}0$

The bending moments required for the design of the reinforcement are determined mostly using the approach described in clause 13.4.3.7 under ultimate condition or with the procedure of the elastic embedment. As shown there, the maximum calculated moments differ to a low extent only.
The bracings are connected to the leg members 0,5 m above the ground level. The leg member is bent at the ground level. The total resulting ultimate horizontal force will be

$$P_{rd} = \sqrt{(P_x^D + P_x^K)^2 + (P_y^D + P_y^K)^2} = \sqrt{(7{,}75 + 96{,}5)^2 + (3{,}08 + 96{,}5)^2} = 144 \text{ kN} \quad .$$

The soil resistant coefficient is obtained for the available subsoil

$$f_w = \gamma \cdot \tan^2(45 + \varphi/2) = 19 \cdot \tan^2(45 + 25/2) = 46{,}8 \text{ kN/m}^3 \quad .$$

The position of the maximum moment results from (13.19)

$$x_m^3 + 3 \cdot 1{,}2 \cdot x_m^2 = 6 \cdot 144/46{,}8 = 18{,}46 \quad \text{to be} \quad x_m = 1{,}85 \text{ m},$$

where the foundation shaft diameter is $d = 1{,}20$ m.
The bending moments resulting from the forces P_x and P_y at the position x_m are:

$$\begin{aligned} M_y &= P_x^D \cdot (h + x_m) + P_x^K \cdot x_m = 7{,}75 \cdot (0{,}5 + 1{,}85) + 96{,}5 \cdot 1{,}85 = 196{,}7 \text{ kNm} \quad , \\ M_x &= P_y^D \cdot (h + x_m) + P_y^K \cdot x_m = 3{,}08 \cdot (0{,}5 + 1{,}85) + 96{,}5 \cdot 1{,}85 = 185{,}8 \text{ kNm} \quad . \end{aligned}$$

Therefore, the resulting moment will be:

$$M = \sqrt{M_x^2 + M_y^2} = \sqrt{196{,}7^2 + 185{,}8^2} = 270{,}6 \text{ kNm} \quad .$$

The bending moment for the rating results from (13.20) to be

$$M_{max} = 270{,}6 - 46{,}8 \cdot \left(1{,}20 \cdot 1{,}85^3/6 + 1{,}85^4/24\right) = 188{,}5 \text{ kN} \quad .$$

According to general agreed practice, the tolerances of installation are considered by an eccentricity of $e = 0{,}05 \cdot d$. The moment resulting from the eccentricity under uplift load will be

$$S_z \cdot e = 888 \cdot 0{,}05 \cdot 1{,}20 = 53{,}3 \text{ kNm} \quad .$$

The shaft, therefore, has to be rated for an ultimate bending moment $M = 188{,}5 + 53{,}3 = 241{,}8$ kNm. These calculated internal forces and moments are ultimate values. The design of the reinforced concrete cross sections is carried out according to ENV 1992-1 [13.17].

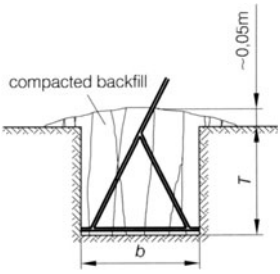

Figure 13.20: Grillage foundation

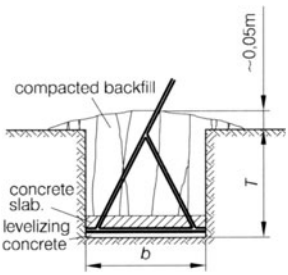

Figure 13.21: Grillage foundation with concrete slab

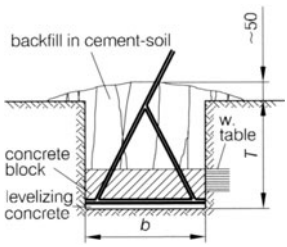

Figure 13.22: Grillage foundation with concrete block

13.4.4.4 Separate grillage foundations

Description and applications

Grillage foundations are shallow foundations, with a depth varying between 2,0 and 4,0 m, made entirely of galvanized steel sections, forming a pyramid either triangular or square with a grillage bolted to the bottom end. The steel pyramid transfers the horizontal shear load down to the grillage base by truss action. In Figure 13.20, a standard design is shown consisting of steel only. Sometimes, the grillage is enclosed by concrete slab (Figure 13.21) or a concrete block (Figure 13.22). The latter designs are adopted to enable the use of the same steel components at tower sites with soil of lower bearing capacity.

Geotechnical design

The resistance of grillage foundations against compression may be verified either for characteristic or for ultimate loads. When proving the stability using characteristic loads, the bearing pressure related to the gross area of the grillage subface may not exceed half of the permissible bearing pressures σ_{perm} according to Table 13.13, column 5. The bearing pressure related to the net subface area may not exceed the values σ_{perm}. When ultimate loads are given, it is required to prove that equation (13.25) is complied with. There, γ_{MC} is 1,2 or more depending on the standard or project specification to be adopted. The design resistance can be obtained from equation (13.26) where A is the net area of grillage and σ_{ult} can be obtained from Table 13.13 or from experience.

The maximum clear spacing between steel members that form the grillage base should be not less than 150 mm nor more than 200 mm. The surface of any such member bearing directly on soil should have a minimum lateral dimension of 50 mm.

The verification of stability under uplift is carried using equation (13.27) based on characteristic or limit design loads. There, the partial factor $\gamma_{\mathrm{M\,up}}$ should be higher than in case of concrete blocks, since the resistance is provided by earth resistance only, which varies to a great extent. Values of $\gamma_{\mathrm{M\,up}}$ between 1,5 and 1,8 are used for characteristic loads and 1,3 to 1,5 for limit loads.

The ultimate uplift resistance of the grillage foundations can be calculated by the addition of the weight of the foundation and the weight of soil enclosed in a frustum of an inverted pyramid whose faces make an angle β with the vertical, where β can be taken from experience or from Table 13.14, column 4. Other data according to national standards, utility or contractor experience and tests can be adopted as well. The weight of the soil should be taken from Table 13.13, where optimum compaction of backfill is assumed, or from local experience.

These values depend naturally on the soil characteristics and the main design objective is to prevent big displacements when the grillage is subjected to uplift forces. The

compacted backfill soil is then one main security factor against uplift. It is important to control the humidity of the backfill soil during compaction. Grillages cannot be applied in swampy soils prone to cause corrosion and in sites subjected to erosion prone to cause instability.

A practical example for the application of grillage foundations is illustrated in Figures 13.20 to 13.22. For the three cases, the same structural steel parts are used:

- The grillage foundation shown in Figure 13.20 is used at sites with permissible bearing pressure of 340 kN/m^2 and more. The net area of the grillage is sufficient to keep the pressure under that limit. The frustum angle is 20° or more and the specific weight force of the well compacted backfill is at least 14 kN/m^2. There is not watertable.
- The grillage foundation with a concrete slab at the bottom shown in Figure 13.21 is used at sites with permissible bearing pressures between 200 and 340 kN/m^2. The gross area of the grillage is not enough to withstand the loads without exceeding the specified soil pressure. Therefore, it is necessary to build a concrete slab with a larger area in order to increase the bearing surface and also provide additional resistance against uplift. The frustum angle is 16° and the specific weight force of the compacted backfill is 12 kN/m^3. There is no watertable.
- The grillage foundation with a concrete block shown in Figure 13.22 is used at sites with a permissible bearing pressure less than 200 kN/m^2. The grillage and slab alone is not sufficient to withstand the loads. The frustum angle is 10° and there is a maximum watertable up to the mid-depth of the excavation. The height of the concrete block may vary from a minimum of 0,5 m until a height equal to the mid-depth of the excavation, so that in any case the top of the concrete block stands above the water level.

13.4.4.5 Pile foundations

Pile foundations are adopted for technological and economic reasons in subsoils with high ground-water level. Stepped concrete foundations cannot be adopted at such soil conditions because of the costly watertable lowering within the excavation and the resulting foundation dimensions due to the buoyancy below the water table. Pile foundations are also expedient when bearing soil layers are only encountered in greater depth and an exchange of non-bearing or settlement-sensitive soil is not economic. Driven and drilled piles are distinguished according to the construction method.

Driven piles

In EN 12 699 [13.38], general principles for design of concrete, steel and timber driven piles are established. The application of *driven piles* needs subsoils suited for driving and having sufficient thickness such that the uplift and compression loads of the leg member can be transferred to the subsoil. Heavily compacted layers, cohesive soils, especially clay of stiff and hard consistence and subsoils with big stones exert a high resistance against pile driving, often completely prohibiting this technology.

Pile types are selected on the possibility to drive the pile, the driving characteristic of the pile and the specific requirements imposed from transmission lines such as transfer of uplift loads, mobility of the construction machinery, low quantities of material and a relatively simple construction. From the manifold of known pile types [13.39] only a few are suited to overhead power lines and are used to an extent worth to be mentioned here.

Bare steel piles

Bare steel piles are used as *hollow tube-type piles*, consisting of single sheet-wall piling sections welded together, or open *hot-rolled sections* (Figure 13.23). Type and shape of

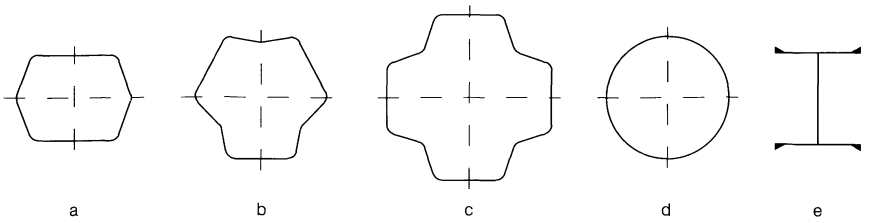

Figure 13.23: Cross section of driven bare steel piles: a, b, c driven pile composed from single sheet piling wall sections; d tube-type pile, helically-welded tube; e hot-rolled steel pile (used for sheet piling walls)

piles are selected as suited to the dimensions of the leg member stubs, the resistance requirements and the ability of driving piles into the subsoil. If the leg member is embedded in a hollow profile by encasing in concrete, *steel cleats* are being used for anchoring. In case of hot-rolled sections, a reinforced concrete muff is provided which, however, is more expensive. Hollow tube-type sections are well-suited for transferring bending moments especially in case of soft subsoil layers due to their high section modulus. Their larger perimeter results in a larger friction surface between pile and soil compared with hot-rolled sections. Open hot-rolled sections can be driven with lower effort since they cut into the soil. However, depending on the type of soil, the soil in between the flanges is compacted to such an extent that the soil will move deeper together with the pile. This plug of soil can assume the size of the pile contour area. It is also formed inside hollow piles and seals the tube. The resistance against driving, therefore, increases considerably since the soil needs to be displaced. Thereby, the soil is compacted and the skin friction increases more intensively than in case of open hot-rolled sections. Steel piles can be extended easily, whereby the joints are produced by welding or by means of gliding-resistant, prestressed bolted connections [13.40]. Driving depths up to 40 m can be reached for overhead lines [13.41].

Grouted steel piles

The skin friction of *grouted steel piles* is considerably increased by a *mortar layer* between steel pile and soil [13.42]. The pile point projects over the pile contour (Figure 13.24), as to form a hollow space between the pile and the displaced soil. Cement mortar is pressed during the driving process into this hollow space using a hose which ends closely above the pile point. The grouting pressure is controlled such that the upper level of the cement mortar is kept at the terrain level. After reaching the planned driving depth, the pressure is increased to achieve a close interlocking with the soil. Grouted steel piles can be extended by means of welded joints similarly to bare steel piles.

Cast-in-situ driven concrete piles

For constructing *driven in-situ concrete piles*, a thick-wall steel tube with a diameter between 0,4 and 0,5 m and a loosely inserted pile point [13.43] are driven in the soil. The tube is used as a casing for the concrete. The point projects laterally somewhat above the wall of the tube. The projection is selected wider in case of silt and clay soils than in case of non-cohesive soils. A seal between the tube and the point hinders the ground water to ingress into the tube. After driving, the steel reinforcement is installed into the tube and then the tube is filled up with concrete. During lifting of the tube, the concrete is compacted by a vibrator and, thereby, pressed to the surrounding soil. A rough pile surface is formed providing correspondingly high *skin friction*. The installation process can be observed within the tube at any stage since water ingress is avoided. Conclusions on the pile resistance to be expected can be made from the

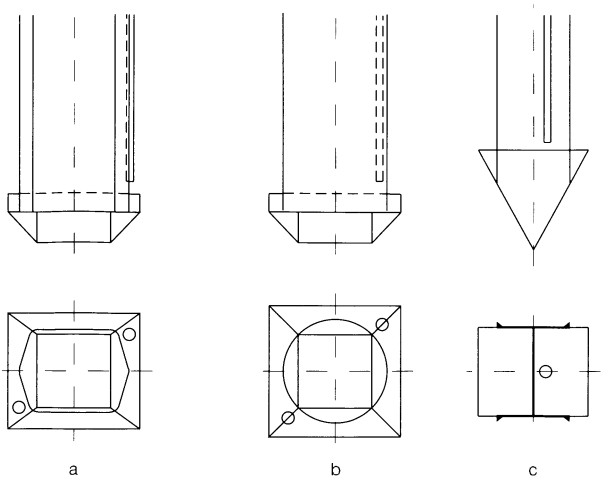

Figure 13.24: Design of pile points of grouted driven steel piles: a pile composed of sheet-wall piling sections; b tube-type pile; c H-beam section (MV piling system)

energy exerted for pile driving as well as from resistance during tube lifting. Due to the difficult construction process, cast-in-situ driven concrete piles are rarely used for overhead lines nowadays.

Precast concrete piles

Precast concrete piles are adopted for overhead lines with cross-sectional dimensions up to 0,35 × 0,35 m and with lengths up to 20 m. They are produced with slack or prestressed reinforcement. Their high weight does not favour the use at tower sites difficult to access. An extension of the piles can be achieved by specific coupling arrangements [13.44]. Requirements are given in prEN 12 794 [13.45].

Drilled piles

Design, calculation and installation of *drilled piles* can be carried out according to EN 1536 [13.46] or DIN 4014 [13.47], as an example. Drilled piles can be installed with or without casing. For an installation without casing, similar restrictions exist concerning the subsoil as in case of auger-bored and excavated foundations. When using a casing, the drilled piles can be adopted also in unstable and ground water-prone soils. Drilled piles can be also installed in soils difficult to loosen as well as in soft rock. An expansion of the pile point is possible depending on the drilling method. Such a point expansion should only be planned in firm, stable soil layers.

Hammer drilling and *rotating drilling* are distinguished depending on the function of the drilling tools. Hammer drilling drives the casing tube by a casing machine and the soil is excavated by means of a circular grab. Rotating drilling machines possess a rotation drive for the drilling tool and the casing arranged moveably and height adjustable at a rig. The soil is excavated by means of worm drills, buckets or other tools adjusted to the individual drilling process.

Drilled piles require relatively heavy machinery which frequently cannot be moved to the individual sites of an overhead line. Therefore, their application is limited to special cases, e. g. close to buildings where hammer driving cannot be permitted.

Geotechnical design

Separate pile foundations are designed such that the loads from the structure are transferred to the soil by the piles alone. High horizontal load components can be counteracted by a bending resistant design of the piles in addition to an oblique arrangement of

raked piles or *piles in groups*. Piles for separate foundations should be predominantly loaded in the direction of their longitudinal axes. *Geotechnical design* refers then to rating with regard to uplift and compression forces and lateral loadings.

Within a separate pile foundation, piles should be used for the same static function, for example transfer of uplift or compression forces, which by their arrangement, their material properties and their construction provide approximately the same performance in respect of uplift or settlement.

If a load distributed over an extended area, for example due to fill, acts upon a soft soil layer above good bearing subsoil in the vicinity of a pile foundation, horizontal movements of soft soil can occur. The piles will then be additionally loaded by bending.

The *external pile loads* result from the ultimate design load or characteristic load of the structures. When rating the piles, the effect of buoyancy and other effects which might reduce the stability need to be considered. However, the releasing effect of *buoyancy* may not be taken into account for piles loaded by compression.

Piles for transmission line supports should be constructed with a minimum length of 6,0 m and be embedded at least 3,0 m into good-bearing soil unless their stability is demonstrated by proof tests.

Parallel and raked piles should have sufficient spacing between their axes, such that neither during construction nor after loading adverse reactions can occur on adjacent piles. This requirement is met if the distance of the pile axes at the pile points reaches at least three times the maximum cross-sectional dimension of the pile.

The *resistance of a pile* depends on the structure and characteristics of the subsoil, on the ground water condition, on the length of embedment in bearing soil layers, on the shape of the pile and its cross-sectional or circumferential area, on the material of the pile, on the nature of the pile surface, on the design of the pile point, on the arrangement of the piles and on the distance of piles as well as on the construction procedure. Additionally, the thickness and strength of overburden soil layers are significant. Moreover, the effects of aging, of negative skin friction and of superimposed lateral loading might be of interest. The resistance of driven piles, the *skin friction* of which provides an substantial portion of their total capacity, may even increase over longer periods after driving especially in fine-sandy, silty and clayey soils.

A compression-loaded pile may be stressed additionally by negative skin friction if the upper layers of the soil settle. The effect of negative skin friction on the pile and on the foundation can be reduced by suitable design of piles and by choice of adequate spacing between piles. The releasing effect may not be taken into consideration for uplift loaded piles.

The analysis of the *ultimate tensile resistance* of piles may be carried out based on the skin friction per unit area and the resistance of the pile point. The values of skin friction can be deduced for the soil condition given and the selected type of pile, as based on experience and tests carried out with the particular types of soils and piles or evaluated from soil investigation. In case of soil layers with varying skin friction, the ultimate resistance may be determined separately for each individual layer and the ultimate tensile load may then be calculated by summation of the individual values, whereby the thickness of the layers and the sequence of layers as well as the watertable should be adequately considered. The resistance of *pile groups* may be determined by summation of the resistance of the individual piles.

Since for piles a wide variation of skin friction values has to be expected, the partial factors have to be adjusted accordingly. They are higher compared with those data used for stepped block or auger-bored foundations. Moreover, the required partial factors should consider whether the uplift resistance is checked by tests or not.

The design based on *ultimate design resistance* should include a partial factor $\gamma_M = 1,5$ when the uplift resistance is calculated theoretically on this basis of the skin friction,

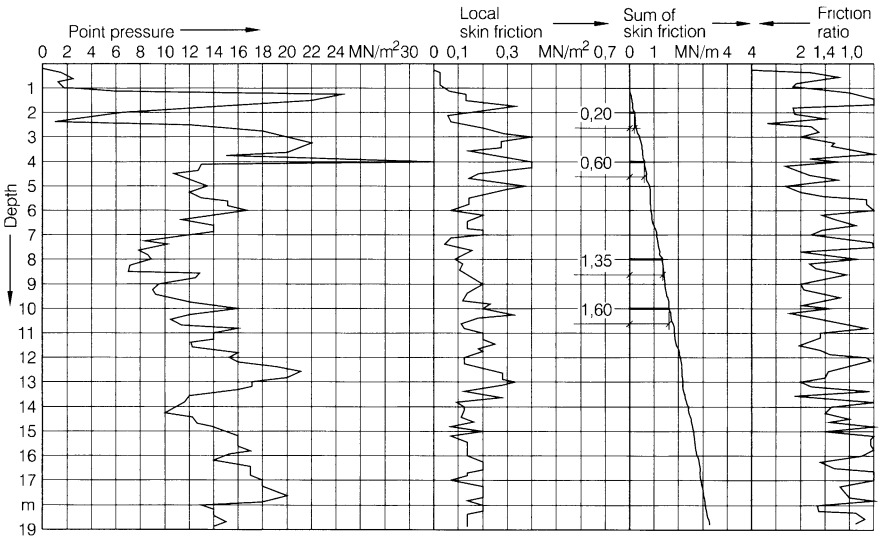

Figure 13.25: Result of compression probing

and a factor $\gamma_M = 1,2$ when the uplift resistance is approved by tests.
The design based on characteristic loads should include a partial factor $\gamma_M = 2,0$ when the uplift is determined theoretically, and a factor $\gamma_M = 1,5$ when approved by tests. This specification corresponds to the stipulations made by EN 50 341-3-4, to mention an example.
When determining the resistance of compression-loaded piles, at least those values of skin friction adopted for uplift-loaded piles in addition to the resistance of the pile point may be taken into consideration. The partial factors may be assumed as in case of uplift loaded piles. In addition to the skin friction, the point pressure counteracts the compression load.
The permissible point pressure depends also on the pile settlement. Data can be obtained from soil investigation using a compression probe (see clause 13.3.3.5 and Figure 13.22). Further details can be found in [13.48] and [13.47].
The buckling stability of *free-standing piles* should be analysed considering the buckling length and the restraining conditions. Piles embedded in soil are not prone to buckling, even not in very soft layers.

Design of pile lengths

The soil investigation recorded in *borehole* or *probe logs* form the basis for *design of pile lengths*. Probings do not suffice alone since their results could be wrongly interpreted without knowledge of the type of subsoil.
The pile lengths cannot be directly determined from the resistance to penetration of driven probes into the particular soil type. Instead, the density of the individual soil layer (see clause 13.3.3.2) has to be determined from the results of the probing. Based on this results, the *skin friction* can be determined based on research tests carried out previously and on experience. On the other hand, the required lengths of piles can be directly determined from the results of *compression probings* (see clause 13.3.3.5).
A procedure to calculate the pile length from the results of compression probings is given in [13.13]. At first, the local skin friction is determined from the testing results according to clause 13.3.3.5. Then, the friction force related to the perimeter of the

Table 13.16: Reduction factor for determining the length of uplift loaded piles in fine sand

Type of pile	Reduction factor
H-beam section, grouted	0,8[1)]
	1,0[2)]
Hollow pile, bare without pile point	0,35
H-beam section, bare	0,35
Concrete pile with point	0,6
Concrete pile without point	0,30

1) specific weight of grout mortar 1,8

2) specific weight of grout mortar 2,0

Table 13.17: Data of skin friction for bare hollow steel piles

Type of soil	Skin friction in MN/m^2
Sand, very dense	0,037
Sand, dense	0,022
Sand, medium dense to dense	0,020
Sand, medium dense	0,019
Sand, medium dense to loose	0,017
Sand, loose	0,014
Sand, very loose	0,008
Silt, stiff	0,022
Silt, soft to stiff	0,017
Silt, soft	0,011
Silt, very soft	0,009
Clay	0,022
Peat	0
Mud	0

probe is summed up from the ground level down to the particular depth (see Figure 13.25). It was concluded from tests on piles that after several loading and unloading cycles the transferred friction force is distributed along the pile such that in the upper and lower quarter of the pile the total friction forces expected from the probing will be transferred at full extent and in both of the middle quarters only to 30 %. Reduction factors are used to take care of the differing *skin friction* values. These reduction factors depend on the pile type and are presented in Table 13.16 for fine sand.

Skin friction data for bare steel piles

In [13.49] it is reported that, as a result obtained from uplift tests, the hot-rolled H-beam sections PSp 300 (Figure 13.23 e) transfer on average only 64 % of the uplift limit load of an equally long box-type pile LP 20 (Figure 13.23 a). In case of the box-type pile LP 20, the total perimeter of 1,40 m can be assumed as load-carrying. Equal skin friction values assumed, a load-carrying perimeter of $0{,}64 \cdot 1{,}40 = 0{,}90$ m results for the PSp 300 pile. The perimeter of the PSp 300 pile, however, is 1,34 m and its development is 1,90 m. Therefore, when quoting skin friction values, reference to a specific profile and its load-carrying perimeter is necessary. Related to the perimeter of an H-beam section, only two thirds of the skin friction values of a hollow pile can be assumed as contributing to load bearing.

In [13.49] skin friction data for the profile types PSp 300 are quoted which were transformed to skin friction data in MN/m^2 for bare hollow piles as presented in Table 13.17. These *limit skin friction data* correspond to the resistance reached by the piles. The values presented in Table 13.17 are average values. Considerable deviations might be possible which would lead to a wide scatter of the uplift resistance. Therefore, it is recommended to test each individual bare steel pile under uplift load.

Skin friction data of grouted steel piles

The concrete grout forming a cover around the pile results in a rough surface, and, therefore, in considerable increased skin friction data. The *skin friction data of grouted steel piles* presented in Figure 13.26 have been determined from uplift tests carried out at 45 test piles, according to [13.50].

Example: Pile foundation for a 110 kV dead-end tower

The 110 kV dead-end tower of the example according to clause 13.4.3.5 should be erected with driven grouted hollow steel piles.

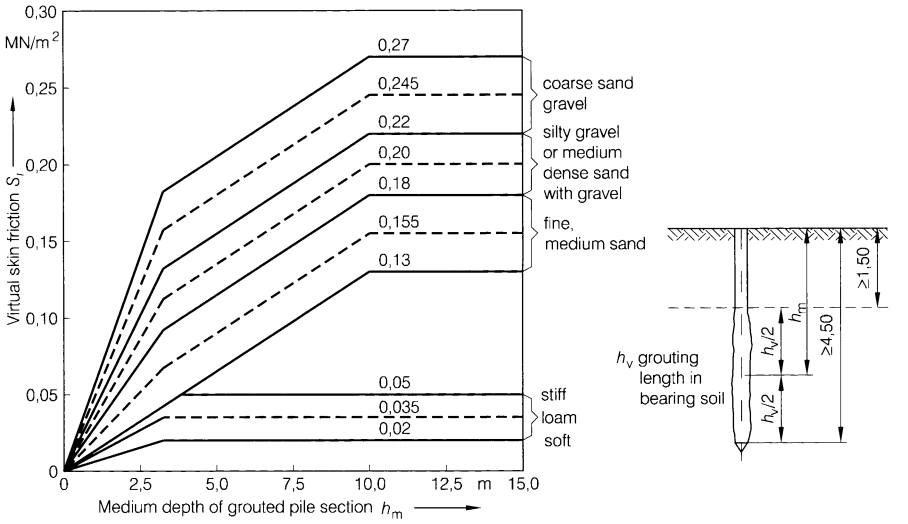

Figure 13.26: Skin friction data of grouted steel piles for calculation of the ultimate resistance

Leg member uplift design load: 888 kN, load case: Wind action on ice covered conductors; leg member compression design load: 1 012 kN; horizontal design loads of the diagonals: $P_x^D = 7{,}75$ kN, $P_y^D = 3{,}08$ kN; characteristic loads: uplift 658 kN; compression 750 kN; $P_x^D = 5{,}74$ kN; $P_y^D = 2{,}28$ kN.

Soil according to the borehole log: Up to 0,3 m depth: humus; from 0,3 m depth: medium sand with fine sand, silty, clayey; watertable up to the ground level; compression probing see Figure 13.25.

Steel pile: Helically-welded tube 609,6 × 10 mm, length: 10,0 m; steel cross section $A_s = 188$ cm^2; section modulus $W = 2778$ cm^3.

Pile point with 0,70 m long sides according to Figure 13.24 b; perimeter $4 \cdot 0{,}70 = 2{,}80$ m.

The compression probing shows point pressures between 8 and 18 MN/m^2 and a correlated ratio of skin friction fs to point pressure q_s of 2 to 1 %. According to Figure 13.6, the soil is sand to clayey sand, as can be seen as well from the borehole log. The soil is classified as medium-dense according to Table 13.7.

The ultimate resistance of the pile will be calculated from the recorded skin friction values following the procedure proposed in [13.13]. The first 2,0 m of the pile length are considered as non-bearing and the residual 8,0 m long section of pile divided into four parts. The expected friction forces result then from the diagram of the local skin friction data (Figure 13.25).

Depth in m	Related friction force in MN/m
2 to 4	$(0{,}60 - 0{,}20) = 0{,}40$
4 to 8	$(1{,}35 - 0{,}60) \cdot 0{,}3 = 0{,}22$
8 to 10	$(1{,}60 - 1{,}35) = 0{,}25$
Total	$0{,}87$

According to Table 13.16, the reduction coefficient will be 0,8 for a grouted hollow pile. Since in case of hollow piles the mortar grouting does not reach the intensity as in case of sheet-piling wall piles, only 90 % of the friction force are considered.

Ultimate uplift force: $0{,}87 \cdot 2{,}8 \cdot 0{,}8 \cdot 0{,}9 = 1{,}75$ MN.

Required ultimate uplift resistance: $1{,}5 \cdot 0{,}888 = 1{,}332$ MN or $2{,}0 \cdot 0{,}658 = 1{,}316$ MN. The expected ultimate uplift force is higher than the required one.

Alternatively, the uplift capacity is determined according to Figure 13.26. A skin friction $S_i = 0{,}09$ MN/m^2 results for sand at $h_m = 2{,}0 + 8{,}0/2 = 6{,}0$. For the ultimate uplift resistance 90 % of this value are considered as well. Therefore, the ultimate uplift resistance results to be $0{,}09 \cdot 2{,}80 \cdot (10 - 2) \cdot 0{,}9 = 1{,}81$ MN.

The ultimate uplift forces determined according to both procedures coincide quite well. The

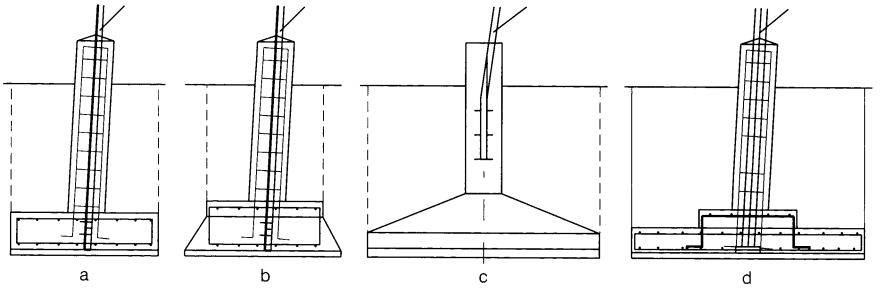

Figure 13.27: Design of steel-reinforced pad and chimney foundations

transfer of the horizontal forces can be verified as demonstrated for single pile foundations in clause 13.4.3.7 and, therefore, will not be repeated here.

13.4.4.6 Steel reinforced pad and chimney foundation

Reinforced pad and chimney foundations are characterized by a slender shaft ending in a pad. The pad can be designed with a flat upper face (Figure 13.27 a, b), an inclined upper face (Figure 13.27 c) or with a stepped block (Figure 13.27 d). The pad can be undercut into the soil, stable soil provided (Figure 13.27 b). The loads are transferred from the chimney to the pad and then to the subsoil. The chimney is adjusted to the inclination of the leg member stub, which reaches frequently into the pad. This design is statically favourable and results in a low and economic concrete volume. The chimney can as well be arranged vertically. However, its cross section needs then to be selected large enough to accommodate the anchoring elements of the leg member stub. If the leg member is bent to the vertical (Figure 13.27 c), the horizontal component of the leg member force creates an additional bending moment in the chimney, which is considerably higher than in case of an inclined design. The horizontal force increases the bearing pressure at the edges of the pad subface. A vertical arrangement of the chimney results in a less economic design than an inclined arrangement. The chimney can be designed with square or circular cross section. The circular cross section is only advisable where circular formwork elements are available; otherwise, a square cross section is to be preferred because of the simpler formwork.
The *geotechnical design* comprises the verification of stability under the action of both compression and uplift loads. Under compression loads, the resistance against compression divided by the material partial factor should be higher than the acting ultimate force or the permissible bearing pressure may not exceed under characteristic loads. The dead weight of the foundation and the weight of the soil resting vertically upon the pad need to be considered in addition to the leg member force. The horizontal forces acting on the individual footings yield to a moment in the foundation subface with the consequence of a bearing pressure distribution with maxima at the pad edges. This distribution may be mathematically represented by an inclined plane. The bearing pressure at the edges can be obtained from

$$\sigma = N/(b_x \cdot b_y) \cdot (1 + 6\,e_x/b_x + 6\,e_y/b_y) \quad , \tag{13.32}$$

where b_x and b_y are the width of the foundation subface and the eccentricities e_x and e_y follow from $e_x = M_y/b_x \leq b_x/6$ and $e_y = M_x/b_y \leq b_y/6$.
The verification of stability under uplift loads is carried out as in case of concrete block foundations. The dead weight of the soil resting upon the pad and the dead weight of the foundation is assumed to counteract the uplift force. An earth frustum may be taken into account, where the angle depends on the type of soil and the design and

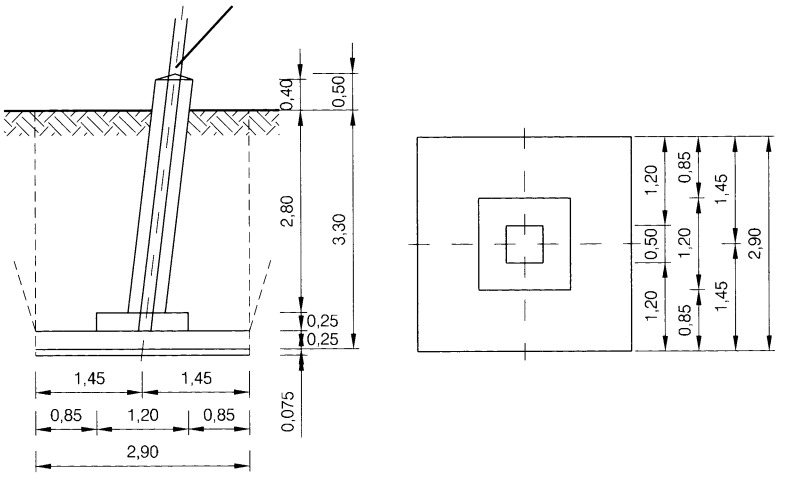

Figure 13.28: Pad and chimney foundation (example)

construction of the pad. These angles can be taken from Table 13.14 or from experience. The partial factors applied to the design resistance of the foundation depend on the loads, being characteristic of ultimate loads. These partial factors are between 1,5 in case of characteristic loads and more than 1,2 in case of ultimate loads.
The internal moments and forces need to be calculated taking into account the design loads and the material partial factors required by the relevant standard or project specification such as EN 50 341-1. The bending strain of the pad, which is prevalent for the design of the reinforcement below the upper surface, results from the weight of the soil in case of an uplift-loaded foundation. For the reinforcement close to the lower face of the pad, the bearing pressure under the compression-loaded foundation is prevalent. The shear stresses within the pad have to be verified. A *verification of punching* for the compression- or uplift-loaded foundations needs to be carried out at the transition between the chimney and the pad.

Example: A pad and chimney foundation has to be designed. The dimensions of the foundation are assumed as shown in Figure 13.28. The lowermost pad is concreted to the planking. From the static analysis of the tower, it results: Leg member tensile design force 640 kN; leg member compression design force 738 kN; horizontal design force of the bracings $P_x^{\mathrm{D}} = 34{,}8\ kN$, $P_y^{\mathrm{D}} = 35{,}7\ kN$. The equivalent characteristic loads are $S_{\mathrm{K\,up}} = 474$ kN; $S_{\mathrm{K\,comp}} = 546$ kN; $P_x^{\mathrm{D}} = 25{,}8\ kN$, $P_y^{\mathrm{D}} = 26{,}5\ kN$.
The soil characteristics result from Tables 13.13 and 13.14 for firm cohesive soil with non-cohesive additions: Specific weight of soil γ =19 kN/m^3, earth frustum angle $\beta_0 = 10 + (13 - 10)(5{,}0 - 2{,}9)/(5{,}0 - 1,\ 5) = 11{,}8°$; $\beta = 11{,}8\sqrt{2{,}9/3{,}05} = 11{,}5°$; permissible bearing pressure up to 1,5 m depth 100 kN/m^2; ultimate bearing pressure 160 kN/m^2, factor $\kappa = 3{,}0$.
Specific weight of reinforced concrete: $\gamma_{\mathrm{B}} = 24$ kN/m^3
Volume of concrete body: $V_{\mathrm{cr}} = 3{,}20 \cdot 0{,}5^2 + 0{,}25 \cdot (1{,}20^2 + 2{,}90^2) = 3{,}26$ m^3
Dead weight of concrete body: $G_{\mathrm{cr}} = 3{,}26 \cdot 24 = 78{,}3$ kN
Volume of soil body vertically upon the foundation subface: $V_{\mathrm{E}} = 2{,}90^2 \cdot 3{,}05 - 1{,}20^2 \cdot 0{,}25 - 0{,}5^2 \cdot 2{,}80 = 24{,}59$ m^3
Weight of this soil body: $G_{\mathrm{E}} = 24{,}59 \cdot 19 = 467{,}2$ kN
Width of earth frustum at ground level: $2{,}90 + 2 \cdot 3{,}05 \cdot \tan 11{,}5° = 4{,}14$ m
Volume of soil body with an earth frustum angle: $V_{\mathrm{E}} = 3{,}05/3 \cdot (4{,}14^2 + 4{,}14 \cdot 2{,}90 + 2{,}90^2) - 1{,}20^2 \cdot 0{,}25 - 0{,}5^2 \cdot 2{,}80 = 37{,}12$ m^3
Weight of earth frustum: $G_{\mathrm{E}} = 37{,}12 \cdot 19 = 705$ kN

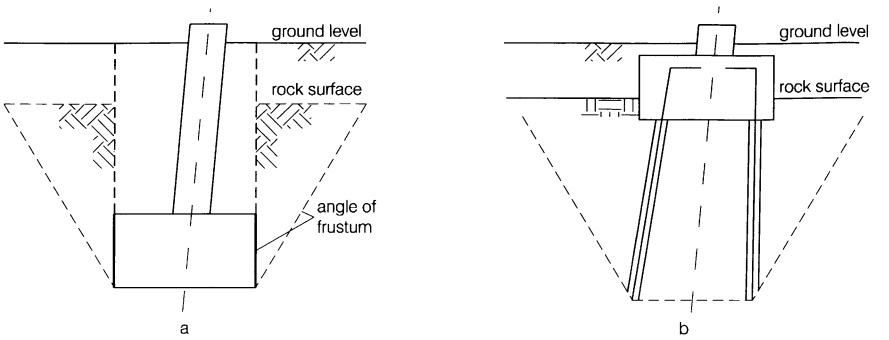

Figure 13.29: Foundations in rock: a without anchors, b with anchors

Design based on characteristic loads:
Proof of stability under compression loads:
Vertical force due to leg member compressive force, weight of concrete and soil: $N = 546 + 78{,}3 + 467{,}2 = 1092$ kN
Moments of actions: $M_x = 26{,}5 \cdot 3{,}80 = 100{,}7$ kNm; $M_y = 25{,}8 \cdot 3{,}80 = 98{,}0$ kNm
Eccentricities: $e_x = 98{,}0/1092 = 0{,}09$ m; $e_y = 100{,}7/1092 = 0{,}09$ m
Maximum soil pressure: $\sigma = 1092/2{,}90^2 \cdot (1 + 6 \cdot 0{,}09/2{,}9 + 6 \cdot 0{,}09/2{,}9) = 178$ kN/m^2 < 203 kN/m^2
The permissible bearing pressure in 3,30 m depth according to (13.4) amounts to
$\sigma_\tau = 100 + (3{,}30 - 1{,}50) \cdot 19 \cdot 3{,}0 = 203$ kN/m^2
Proof: $\sigma = 178$ kN/m^2 < $\sigma_\tau = 203$ kN/m^2
Proof of stability under uplift:
Partial factor at least 1,5
Uplift load: $S_K = 474$ kN
Weight of concrete and earth frustum $78{,}3 + 705 = 783$ kN
Proof: $783/474 = 1{,}65 > 1{,}5$

Design based on design ultimate loads:
Proof of stability under compression loads:
Partial factor for weight of concrete and soil $\gamma = 1{,}35$
Vertical force due to leg member compressive force, weight of concrete and soil: $N = 738 + 1{,}35 \cdot (78{,}3 + 467{,}2) = 1474$ kN
Moments of actions: $M_x = 35{,}7 \cdot 3{,}80 = 135{,}7$ kNm; $M_y = 34{,}8 \cdot 3{,}80 = 132{,}2$ kNm
Eccentricities: $e_x = 132{,}2/1474 = 0{,}09$ m; $e_y = 135{,}7/1474 = 0{,}09$ m
Maximum soil pressure: $\sigma = E_d = 1474/2{,}90^2 \cdot (1 + 6 \cdot 0{,}09/2{,}9 + 6 \cdot 0{,}09/2{,}9) = 241$ kN/m^2
The permissible bearing pressure in 3,30 m depth according to (13.5) amounts to
$\sigma_\tau = 160 + 1{,}6 \cdot (3{,}30 - 1{,}50) \cdot 19 \cdot 3{,}0 = 324$ kN/m^2
Partial factor of resistance $\gamma = 1{,}2$
Design bearing pressure: $R_d = 324/1{,}2 = 270$ kN/m^2
Proof: $E_d/R_d \leq 1{,}0$: $241/270 = 0{,}89 < 1{,}0$
Proof of stability under uplift:
Uplift load: $E_d = 640$ kN
Weight of concrete and earth frustum $78{,}3 + 705 = 783$ kN
Partial factor of resistance $\gamma_M = 1{,}2$
Proof: $E_d/(R_d/\gamma_M) \leq 1{,}0$: $640/(783/1{,}2) = 0{,}98 < 1{,}0$

13.4.4.7 Foundations in rock

Foundations in rock are used if the subsoil is at least moderately weathered rock corresponding to the classifications W2 defined in clause 13.3.4.2. If the rock is cleft or strongly weathered, a foundation for non-cohesive soil is used, for example a steel-reinforced pad and chimney foundation. In case of moderately weathered rock, which

can be excavated by mechanical tools, a concrete block without or with undercutting can be embedded into the rock (Figure 13.29 a). Compression forces are transferred to the rock by the pressure within the foundation subface and lateral faces. *Bearing pressures* between 1000 and 3000 kN/m^2 are permissible for rock depending on the weathering condition (Table 13.13) under the action of characteristic loads and between 1 600 and 4 800 kN/m^2 under ultimate conditions. The uplift load is prevalent for the *geotechnical design*. Size and depth of the foundation depend on the bond stress between concrete and rock; bonding should be strong enough to produce a sufficiently high ultimate resistance with respect to pulling-out of the concrete block. In addition, the shear and tensile strength of the rock should be high enough such that the concrete foundation block would not be pulled-out together with a body of rock. Potential fraction lines need to be studied for verification of the resistance. Data for ultimate or permissible shear and tensile stress are difficult to establish since these values depend on the direction of the crevice.

Anchor foundations can be adopted in solid rock which can be excavated with difficulties only (Figure 13.29 b). A concrete block is arranged upon the rock and slack, non-prestressed anchors connect the concrete blocks with the rock. The *rock anchors* can be arranged vertically or inclined. The compression load is transferred to the rock by the bearing pressure in the subface of the concrete block. The uplift load is assumed to be counteracted by the anchors only. The bonding between the grouting concrete and the rock as well as between the steel anchor and the grout determines the required number and lengths of anchors.

For the rock anchors, reinforcement steel with conventional ribs as well as with threads with a diameter of 18 to 30 mm and steel strength class S420/500 or similar grades are used. The anchoring bar is designed considering the required material partial factor. The design value of the resistance is

$$F_{t,Rd} = 0{,}9\, f_{ub} \cdot A_s/\gamma_M \quad , \tag{13.33}$$

where f_{ub} is the tensile strength, A_s the effective cross section and γ_M the partial factor to be considered, e. g. 1,25 according to EN 50 341-1.

The bonding transfers the tensile force from the anchor to the grouting concrete. The permissible *bond stress* depends on the concrete strength. According to ENV 1992-1 [13.17], for ribbed reinforcement steel the design value of the bond stress results from

$$f_{bd} = 0{,}4725 \cdot f_{ck}^{2/3}/\gamma_{cr} \quad , \tag{13.34}$$

where f_{ck} is the characteristic concrete cylinder strength and γ_{cr} the partial factor for bond, e. g. $\gamma_{cr} = 1{,}50$ according to ENV 1992-1. For grout concrete C12/15, the bond stress is f_{bd} 1,6 N/mm^2 and 2,3 N/mm^2 for grout concrete C20/25. The required *anchoring length* results, therefore, from

$$L_b = F_{t,Sd}/(\pi \cdot d_s \cdot f_{bd}) \quad , \tag{13.35}$$

where $F_{t,Sd}$ is the design tensile force of one anchor and d_s the bar diameter.

The publication [13.51] considers the application of bond stresses as used in concrete engineering as too conservative for *anchor foundations* and suggests to permit 40 % of the concrete compression strength as bond stress. This suggestion is supported by experience from tests.

To determine the bonding between the anchor and the surrounding rock, a uniform distribution of the strain along the length of the anchor is commonly adopted. However, in reality the distribution is not uniform. Details can be taken from the reference [13.52]. In case of a uniform distribution of the strain, the *resistance of the anchor* is obtained from

$$F_{bd} = \pi \cdot d_b \cdot L_b \cdot f_a \quad , \tag{13.36}$$

Table 13.18: Ultimate values for shear and compressive stress in case of anchoring steel members in concrete

Strength class of concrete	Shear stress MN/m^2	Compression stress MN/m^2
C 20/25	2,3	14,0
C 30/37	3,0	21,0

Table 13.19: Permissible bond stresses for structures anchored in concrete by adhesion

Strength class of concrete	Permissible bond stress MN/m^2
C 20/25	1,1
C 30/37	1,3

where d_b is the diameter of the borehole, L_b the length of the anchor and f_a the bond stress.

The partial factor γ_M applied on the tensile force is between 2,0 and 3,0, depending on the definition of load being characteristic or ultimate and the project specification. The bond stress between grout concrete and rock depends on the strength of rock and concrete, the structure of the borehole face, the crevice of the rock, the application of the concrete being compacted or just cast in. Bond stresses obtained from tests are given in [13.52] being between 0,3 and 5,7 N/mm^2. Therefore, this reference recommends values between 0,1 and 1,0 N/mm^2 for the practical design. According to [13.51], a value of 0,24 N/mm^2 was used for the design in case of a specific project and a resistance being twice as much verified by testing. Reliable and economic data for the bond stress to be applied are difficult to recommend because of the variations discussed. The data selected should be verified by tests to be carried out for each individual application.

The *anchoring length* should be long enough such that a pulling-out of the rock body will not be possible. The resistance against being pulled-out is formed by the dead weight of the soil and the shearing and tensile strength of the rock along the surface of the soil body considered. The weight of the rock provides the predominant portion of resistance. It is common practice to neglect the shear and tensile strength because reliable data for the encountered rock are seldom available. For solid, slightly weathered rock a frustum angle of 45° can be assumed. The partial factor γ_M should be at least 1,5 for ultimate load design.

13.4.5 Anchoring of leg member stubs

Anchoring of leg member stubs into the concrete can be carried out either using additional cleats or by bonding between the leg member stubs and the concrete alone. In most cases, anchoring elements made of commonly used angle sections or *cleats* with square or rectangular cross section are used, the latter particularly for pile foundations. The structural engineering verification of the bending between anchoring elements and concrete is carried out for the compression stress between the anchoring elements and the concrete, for the bond stress within the circumference area of the anchoring element and for the connection of the anchoring elements with the leg member stub. Design values are given in Table 13.18. The shear stress of the welding seams between the anchoring elements and the leg member is verified according to ENV 1993-1-1 [13.22]. The bending stress of the welding seams can be neglected.

If the leg members are anchored by bonding only, it should be ensured that the leg member stubs are closely encased in concrete along their total length. For angle sections or channels, the analysis may be based on the perimeter of the enclosed area, e. g. for angle sections by the leg length plus the hypotenuse. To improve the anchoring, additional cleats or the like should be provided at the leg member stubs close to the foundation subface which need not to be considered in the analysis. The leg members should end closely above to the foundation subface. Permissible bond stresses are given in Table 13.19.

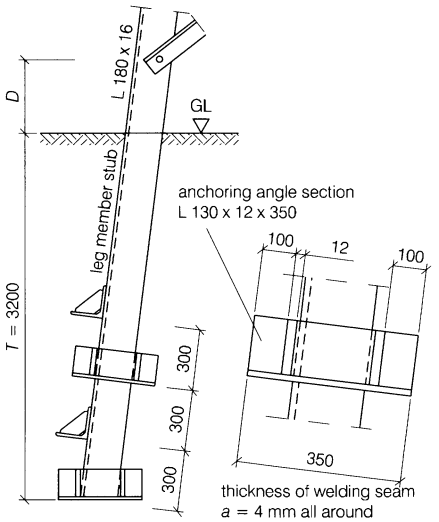

Figure 13.30: Anchoring of leg members

Example: In the following example, the leg members are anchored by means of angle sections according to Figure 13.30 into the concrete body of the stepped concrete block foundation treated in clause 13.4.4.2. According to Table 13.18, the permissible compression stress of the concrete grade C 20/25 is 14,0 MN/m^2 and the permissible bond stress is 2,3 MN/m^2. For the shear stress in the welding seam, a value of 208 N/mm^2 is permissible according to ENV 1993-1-1 [13.22].
The lowermost angle section upon the foundation subface does not contribute to the transfer of the compression forces.
Ultimate leg member compression force: 1 012 kN
Area of one anchoring angle: $0{,}35 \cdot 0{,}13 = 0{,}045$ m^2
Concrete compression stress: $\sigma_D = 1\,012/(3 \cdot 0{,}045) = 7{,}50\,\text{MN/m}^2 < 14{,}0$ MN/m^2
Perimeter of one anchoring angle: $0{,}35 + 2 \cdot 0{,}13 = 0{,}61$ m
The side of the anchoring angle directed to the leg member is not considered in the analysis since its efficiency is restricted by the leg member
Bond stress: $\tau = 1{,}012/(3 \cdot 0{,}3 \cdot 0{,}61) = 1{,}84$ MN/m$^2 < 2{,}3$ MN/m^2
Welding stress in the seam: $\tau = 1{,}012/[3 \cdot (0{,}13 + 0{,}18) \cdot 2 \cdot 0{,}004] = 136$ N/mm$^2 < 208$ N/mm^2

13.4.6 Foundation for guyed towers

13.4.6.1 Acting loads

Guyed towers, specially of the V-type, are usually provided with four guys; each of them is subjected to a pull-out load that is transferred to the relevant *guy anchor foundation.* The central foundations of the masts are subjected mainly to compression loads.

13.4.6.2 Central footings

Central footings of guyed towers, being not subjected to uplift forces, are usually shallow foundations if compared with other tower foundations (Figure 13.31). Grillage, concrete or rock footings may be used as central foundations of guyed towers and must be designed to withstand, without permanent deformation, the maximum compression forces and eventual horizontal shears originated from the specified ultimate loads for the structures.
The concrete blocks have generally the form of a stepped block or a pyramidal frustum with a widening angle towards the base of 60°, at a depth not exceeding 1,0 m. For

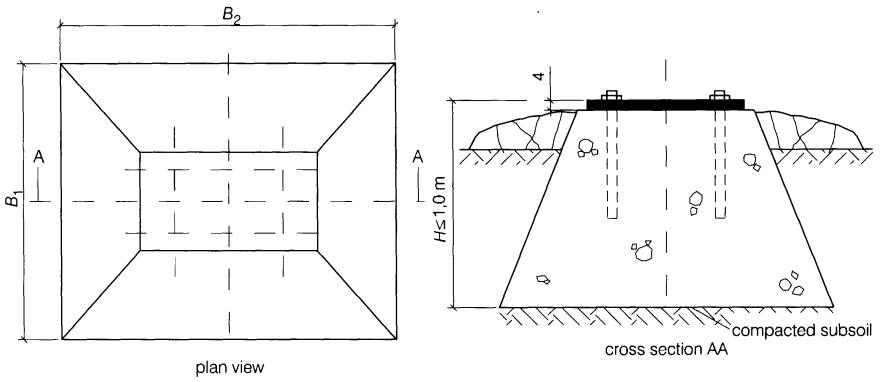

Figure 13.31: Central footing for guyed tower

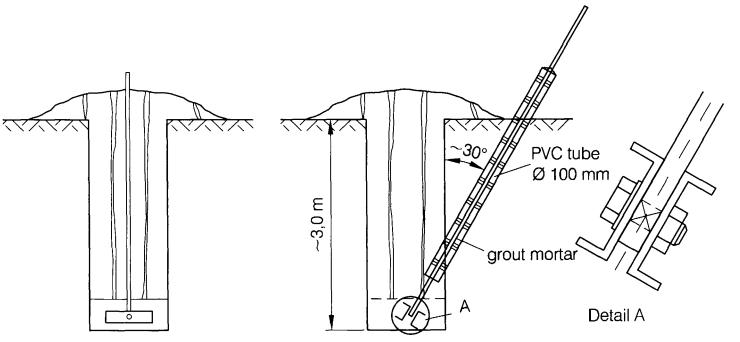

Figure 13.32: Foundation for guy wires

average or weak soils, their regeneration is admitted until 1,0 m below the subjacent layer to the block, in order to achieve the required soil pressure (see Figure 13.31).
The application of such blocks is limited to terrain with a maximum slope of 10°. For terrain with slopes higher than 10°, or if the geotechnical profile requires, that central foundation needs to be reinforced with piles or a pier foundation should be designed instead. In the latter case, for rocky soils, the option could be rock footings anchored in rocks.

13.4.6.3 Foundations for guy wires

There are several types of *foundations for guy wires* used to withstand without permanent deformation the maximum uplift forces originating from the specified structure ultimate loads. Grillage footings, concrete anchor and rock anchors have a widespread use and their choice will depend on specific characteristics of the site of installation. The subject is dealt with in [13.53].
Among the various existing methods for calculating anchor plates for guy wires, it can be mentioned: The inverted cone or pyramidal frustum method, the Biarez and Barraud's method [13.54], the Meyerhof and Adam's method [13.55]. The resistance obtained from any method should be compared with the acting load of the guy wire taking care of partial factors as well.
Usually, the guy wire and guy hardware are designed to have a certain partial factor toward the guy anchors. Some utilities specify guy wires so having an ultimate strength 1,25 to 1,50 times the guy anchor withstand. EN 50 341-3-4 requires a partial factor

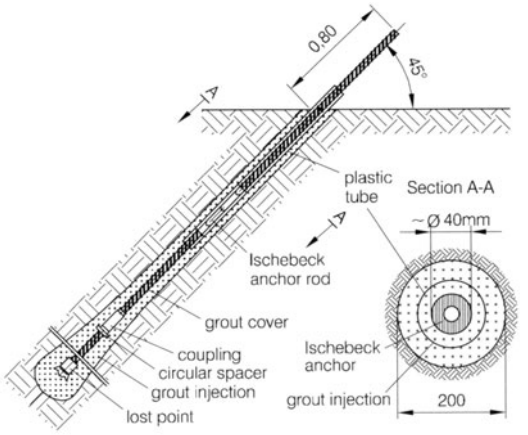

Figure 13.33: Injection anchor type Titan for terminating guy wires

$\gamma_M = 1,65$. In Figure 13.32, a typical guy anchor is shown designed for 500 kV lines. Three basic variations are considered:

- **Guy anchors for good soils**
  This type of guy anchor is applied in dry, not rocky soils, without possibility of shallow water levels, that could reach the footing. The excavation is rectangular and vertical and the minimum depth is about 2,5 m. The guy anchor bar is a forged round rod, with a diameter of about 32 mm, making with the vertical the same angle as the guy wire of about 30°.
  The anchor end is connected to two steel channel sections, that are embedded in the concrete block to help the distribution of the load into the whole block. The backfill is well compacted.
- **Guy anchors for poor soils**
  This anchor is destined to wet soils, when water or humidity is found on the bottom of the excavation. The excavation is similar to the first one, except that the depth is bigger, reaching about 3,5 m. All other characteristics are similar to the anchors for good soils, but a larger concrete volume is required. Sometimes, the earth backfill is replaced by a soil-cement backfill. For preventing corrosion, the guy anchor bars may be encapsulated with plastic tubes filled with cement paste (see Figure 13.32).
- **Rock anchors**
  For rocky terrain, the guy anchors can be inserted into sound rock and the minimum length of embedment needs to be determined (see clause 13.4.4.7).
- **Injection anchors**
  In Figure 13.33, an injection anchor type Ischebeck "Titan" [13.56] is shown. This type adopts a tube inserted of a solid bar for the anchor rod. The point of the anchor consists of a lost drilling head. The drill rod is used as grouting conduit for filling the annulus from the bottom up. The anchor is suited especially for non-cohesive soil and rock, where an ultimate resistance up to approximately 2000 kN can be achieved depending on the dimensions of the anchor tube, its length and the subsoil.

13.4.6.4 Field tests

The theoretical analysis of anchor foundations is based upon experimental methods. As a consequence, it is of paramount importance to test prototype foundations in the field, before coming to a final design of the foundations for guy wires. Several utilities

carry out field tests during the design stage.
The procedure for the final definition of guy wire foundations can be summarized as follows:

- Preliminary design is based on theoretical models.
- Field tests, comprising the main foundation types and possibly different soils, are carried out.
- Results of field tests are used as a feedback to the preliminary design and corrections are made until reaching a final design.

The main considerations to be evaluated before the final solution is found are the following:

- The withstand of the anchor foundation to uplift;
- The accommodation of the guy anchor bar inside the foundation body;
- The compaction of backfill;
- The displacement of the guy wire foundation;
- The cost of the foundations.

The tests at least validate or not the preliminary design and indicate shortcomings or overdesign. The final design can be based on the test results. The described procedure results in reliable and cost-effective guy wire foundations.

13.5 Testing of foundations

13.5.1 Definitions and object

Testing of foundations for overhead line structures is carried out to check the stability of foundations. Detailed information is given in IEC 61 773 [13.3] and [13.57]. That standard distinguishes between

- Foundations predominantly loaded by axial forces either in uplift or compression acting in the direction of the foundation central axis as discussed in clause 13.4.4.4;
- Foundations predominantly loaded by lateral forces, overturning moments or combination of both as discussed in clause 13.4.3.

The object of testing foundation is to provide information on the load-carrying capacity and the load response of the total foundation as an interaction between the foundation and the surrounding soil or rock.

13.5.2 Categories of tests

With respect to the purpose of the test, the level of investigation and the method of execution, three categories of tests can be distinguished:

- **Scientific researched tests.** Such tests are carried out under research conditions. The tests have to be designed regarding the targets of the test. No specific stipulations can be made in general.
- **Design tests.** *Design tests on foundations* are normally carried out on specially installed foundations to verify design parameters or methodologies or construction procedures, to establish geotechnical design parameters or a design methodology for a specific application; to verify compliance of foundation design with project specification; to determine the average failure load and coefficient of variation of the foundation type under specific soil conditions. Design tests should be preferably carried out with full-scale foundations. In general, design tests are carried out to at least the design load or to failure especially when a specific type was designed using the limit state approach. The level of instrumentation and of investigation should be appropriate for the purpose of the test.

In case of large dimension foundations, design tests on reduced scale foundations may be considered. The specific conditions to be complied with in this case can be taken from IEC 61 773.

- **Proof tests.** *Proof tests on foundations* are carried out on production foundations to act as a check on the quality of the installation, on the materials being used and on the absence of any major variations in the assumed geotechnical design parameters. Proof tests are taken to a specific percentage of the design load, usually 60 to 75 %, as stipulated in relevant standards or in a project specification. The proof test should not exceed the serviceability limit load. Limitations of the displacement should be stipulated and considered. The foundations tested should be fully serviceable after successfully passing the test.
  The extent of proof tests depend on the soil conditions, the type of foundation and the design approach. Proof tests should be carried out in particular on foundations where a high portion of the load is transmitted to the surrounding soil by friction.

13.5.3 Foundation installation

Proof tests are conducted on production foundations. Therefore, there should be no difference between the foundation tested and those not subjected to tests.
Design tests are generally carried out on specifically installed foundations which should be constructed using the specified materials and dimensions as close as possible to those required by design. For the purpose of design tests, the connection between the foundation and the test device requires adequate strength possible higher than that of the leg member stubs. The connection needs to be designed accordingly, however, may not alter the geotechnical characteristics of the foundation.
To ease foundation testing, the foundation may be modified so that its test axis is vertical and the loads may be applied vertically where the maximum true slope is less than 20 %. The techniques used for installation of test foundation should be as close as practical to those which are intended to be used for the production foundation. All relevant details of foundation size, construction and installation should be recorded. These records should contain details relating both to design requirements and to the actual data for the as-built test foundation. Typical record formats can be found in IEC 61 773.
A sufficient period of time should elapse between the installation of the foundation and beginning of testing to ensure adequate strength of concrete or grout. As an example, reinforced concrete foundations should be tested not before 14 days after installation. The same applies to concrete piles augered or drilled and cast-in-situ. Piles in cohesive soils should not be tested before 21 days after driving.

13.5.4 Testing equipment

The *testing equipment* and the load application mechanism should be able to mobilize the foundation capacity and overcome the design deflection criteria. The loads may be applied by a hydraulic jack, a winch system or another loading mechanism. The loads applied to the test foundation may be measured by load cells, by pressure gauge on a calibrated hydraulic jack or by dynamometers installed on the winch line. A back-up system is recommended for design tests, for example load cells and pressure gauge. Accuracy of measurement should be within five percent of the maximum test load.
The test load can be applied by

- Test loading beam and supports (see Figure 13.34).
- A fulcrum beam arrangement;
- An A-frame or
- A hydraulically operated crane.

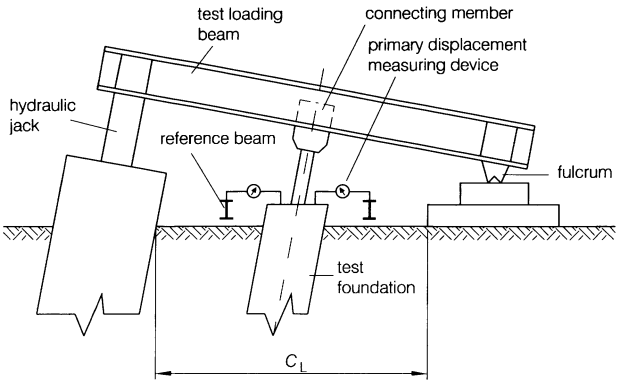

Figure 13.34: Load application by means of hydraulic jack and fulcrum beam

The minimum clear distance C_L between reaction supports (see Figure 13.34) should be chosen carefully to prevent any influence on the behaviour of the foundation. According to IEC 61 773, the minimum clearance is

$$C_L = b + 0{,}7 \cdot t \quad \text{in m} \quad , \tag{13.37}$$

where b is the width of foundation in m, t the depth of foundation in m and C_L the distance between nearest point of the reaction supports.
To *concrete piers*, *driven piles*, drilled and grouted piles, or helix anchors it applies:

$$C_L = 3 \cdot d \text{ (m) or 2 m} \quad , \tag{13.38}$$

whichever is greater. There, d is the pier or pile diameter. The clear distances between the reaction supports should be adjusted to the model of foundation design. In case of design tests, it is advisable to increase these distances.
Mechanical dial gauges with a recommended resolution of 0,01 mm or less and a recommended range of travel of 50 mm to 150 mm may be used for design and proof tests. It is recommended that the dial gauge should be clamped to the reference beam in such a manner that the gauge will expand as the load is applied, in order to prevent damage to the instrumentation in the event of a sudden failure of the foundation or equipment. Glass slides or machined plates may be fixed to test foundation to provide a smooth bearing surface for the dial gauges. For uplift and compression tests, a minimum of two gauges should be mounted equidistant from the vertical axis of the foundation and from each other. As a check on the primary measurement system, a secondary system should be used for all design tests, e. g. an optical level may be used, with a fixed benchmark and a scale.
The minimum level of measurement for proof tests should be a record of the applied load and the corresponding displacement of the foundation, using an optical level. Resolution of the optical level should be less than 0,5 mm.

13.5.5 Testing procedure

The number of tests will depend on the following factors:

- Type of test, such as design or proof;
- Significant variations in geotechnical parameters along the transmission line route;
- Proposed method of analytical review of the test results.

Wherever possible, statistical techniques should be used to evaluate the results of design tests, especially if the characteristic strength of the foundation is required (see IEC 60 826 [13.58]). By this means, the results from at least three identical foundation tests

Table 13.20: Loading schedule

Test category	Testing condition	Loading steps in % of target load according to test condition	Minimum period for maintaining loading steps
Design	design or failure load	25, 50, 70, 80, 90, 100, 0 [3]	10 min [1]
Proof	maximum proof load	50, 75, 90, 100, 0	3 min [2]

[1] In case of design tests, loading may be continued until failure occurs, subject to satisfactory provisions for sudden failure before the maximum load has been attained. The maximum load during testing may be defined as the design load or the failure load. The design load should be maintained for a minimum of 30 min to ensure that no significant movement has occurred.

[2] In case of proof tests, the maximum (proof) loads will be based on an agreed percentage of the design load and the time period that each load application is maintained will be governed by the minimum period necessary to obtain the readings and to ensure that soil conditions have stabilized.

[3] For design tests carried out to failure, further load increments of 10 % should be made beyond the design load until failure occurs. In case of cohesive soils, loading steps of 70 % and above should be maintained for at least 30 min.

in similar soil conditions, under the same test loading regime, can be satisfactorily analysed.

The number of foundations subjected to proof testing will depend on the soil type, the extent of soil investigations, the heterogeneity of subsoils, the type of foundation and the reliability of the design. Where proof tests are considered necessary, it is recommended that at least 5 % of the relevant foundations or relevant individual elements, for example piles, depending on size of population and level of confidence, should be included in a proof test program. Depending on test results, the number of tests required should be adjusted by considering the variations of subsoil, the types and dimensions of foundations, and the quality of the site supervision to be expected during installation. Some utilities carry out *proof tests* on each individual pile. This strategy leads to reliable foundations at reasonable costs since overdesigning can be avoided as well.

Testing of foundations made up of pile groups as a whole would be the ideal way of assessing the strength of the foundation, but would be technically and economically prohibitive in most cases. Alternatively, the performance of piling systems may be assessed by carrying out tests on individual piles. When evaluating the results to determine the overall capacity, the load displacement relation observed during testing, and the interaction of individual piles should be duly considered.

Table 13.20 gives typical requirements for the loading steps to be applied under both test categories and the period for maintaining the load. A preliminary stabilization cycle of up to 10 % of the test load may be required to ensure that all the test equipment has been adequately stabilized.

Each test should be recorded. A typical test recording form can be found in IEC 61 773, annex D. The record of a design test should include the following information:

(1) Soil profile and geotechnical design parameters;
(2) Plan and elevation of test foundations, reaction systems, fixed reference points for measurement of horizontal and vertical displacements;
(3) Plan and elevation of test foundation arrangement, giving dimensions and directions of movements recorded during tests;
(4) Record of environmental conditions, including ambient temperature variations, ice, wind or snow, if any, depth to water-table;
(5) Depending on the type of equipment used to measure the applied loads and the corresponding deflections, the following data should be recorded for each load or deflection measurement:
    - Time at start and end of each load application, as well as the date;

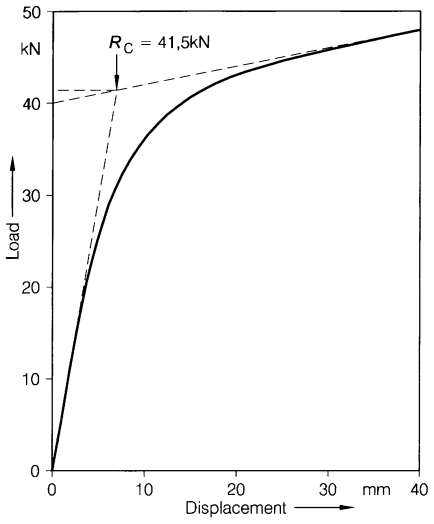

Figure 13.35: Tangent intersection method

- Applied loads;
- Displacement readings recorded at the following: At start of load cycle; at regular time intervals during load application and immediately prior to removal of load.

(6) During the execution of the test, the readings of load versus displacement should be plotted on a graph to ensure that any unexpected variations or anomalies are checked carefully.

(7) For those tests which have been taken to failure, the test report should include a brief description of the probable mechanism of failure.

For proof tests, items (2), (3), (4) and (5) are recommended.

13.5.6 Test evaluation and acceptance criteria

Test evaluation should be carried out in relation to the as-constructed conditions. The results of a design test should be either evaluated against the design parameters used, or compared with the results of similar tests in different soil conditions. If there is a marked discrepancy between the theoretical analysis and practical results, further tests may be required to identify the probable cause of the discrepancy.

Several methods are outlined in greater detail in IEC 61 773, annex E, for the evaluation of uplift or compression design tests. In Figure 13.35, the *tangent intersection method* is shown as an example. The load capacity is defined as the load related to the intersection of two tangents to the load-displacement curve, one representing the elastic range and the other the plastic range. In the example, the foundation capacity is 41,5 kN.

Results of proof tests may be evaluated against predetermined criteria according to the test method and the requirements of the design. The installation should be checked for its adequacy to fulfil its purpose. Suitable *acceptance criteria* should be established before the tests are made. Values of admissible displacements associated with applied design or proof load, including any partial factors that may apply, should be agreed upon during the design of the foundations.

The results of a design test may be deemed satisfactory if the following conditions have been fulfilled:

- The specified design load has been validated by the test;

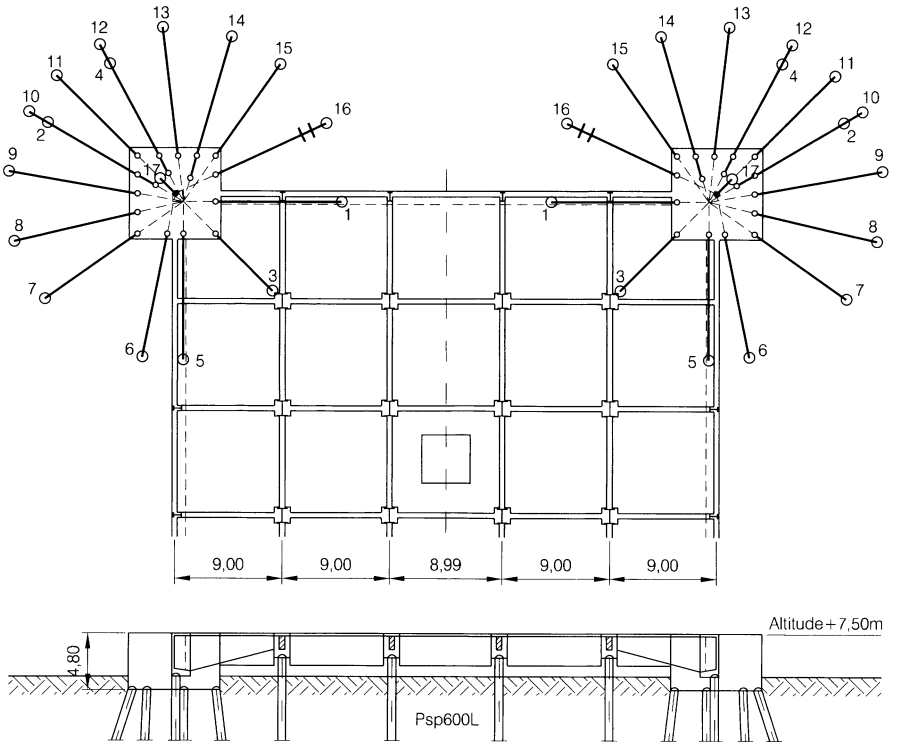

Figure 13.36: Plan view and section of suspension tower foundation adopting bare steel piles (River Elbe crossing, Germany [13.60])

- The associated displacement remains within specified limits which are compatible with the function of the structure.

If the test results do not meet these requirements, the design and/or construction procedure, soil investigation and foundation testing need to be reviewed.

The results of a proof test can be deemed satisfactory if the value of the measured displacement at the specified load is equal to or less than the limits specified. The limits depend on the ability of the structure, which is to be supported by this foundation, to absorb or to accommodate movements. If the observed displacement exceeds these specified limits, or if the assessment of the test results raises doubts about the capacity of the foundation, the following measures can be taken:

- Additional tests could be made on at least two adjacent foundations of four-legged towers to enable a statistical evaluation of the results of the first test, which can then be used to determine the acceptance of the foundation tested:
- If the results of the additional tests confirm the previous ones, the foundations must be considered as unsatisfactory;
- All foundations deemed unsatisfactory as a result of the proof test need to be strengthened or redesigned accordingly.

13.5.7 Uplift load tests on construction and test piles

Uplift load tests on test piles or more appropriately *on construction piles* of overhead lines represent a reliable and economic verification of their resistance. The verification of resistance on construction piles, therefore, is very common in Central Europe. De-

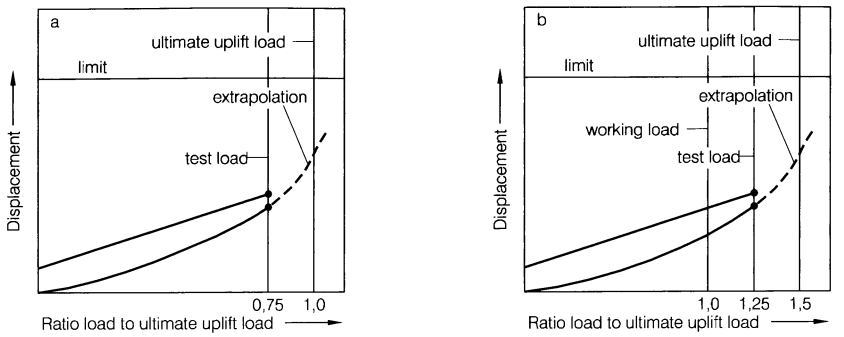

Figure 13.37: Uplift load-displacement diagram for uplift tests on piles: a test load according to EN 61 773; b test load according to EN 50 341-3-4

pending on the type of pile, the soil conditions, the construction procedure and the result of pile driving, it is a proven procedure to carry out uplift load tests at least at 5 % of the installed construction piles. Some utilities in Germany require testing of each uplift-loaded pile. After a successful test, the pile should be fully serviceable. In Figure 13.36, the foundation is shown of the 240 m tall towers for the 400 kV river Elbe crossing as described in [13.59, 13.60]. Bare hot-rolled steel piles with a cross section according to Figure 13.23 e have been used. All the approximately 35 m long steel piles were uplift tested.

According to the procedure stipulated in IEC 61 773 [13.3], the load is increased step by step up to the test load of the pile and the displacement is recorded at each load step. At each incremental step, the loads should be maintained until the increase of *uplift displacement* has settled, in any case for at least 3 minutes. The results of the tests are presented in an *uplift load/displacement diagram* (Figure 13.37). The proof of sufficient uplift resistance will be validated if the displacement does not exceed a predetermined limit and the extrapolation of the load displacement curve to the required ultimate uplift resistance is possible. *Extrapolation methods* are given in [13.3].

According to EN 50 341-3-4, the test load is 1,25 times the nominal uplift load which corresponds to the characteristic value of the uplift load of the pile. The verification of sufficient resistance is considered as successful if a displacement is measured under the test load which permits extrapolation to the uplift resistance being at least 1,5 times the nominal load and the *displacement* not exceeding the corresponding limit. After unloading, the residual displacement should also stay within limits permissible according to experience.

Uplift tests suggest that the displacements differ for the individual pile types, comparable forces and pile lengths assumed. Thus, the displacement will be a few millimetres in case of bare steel piles while some tens of millimetres can be observed in case of drilled piles. On the other hand, wide scattering of the pile resistance was observed at piles of the same design in comparable soil conditions even at the same tower site and at similar driving criteria. Therefore, no generally valid limit values for the displacement can be given. Displacements of 3 to 5 mm in case of in-situ cast concrete piles and up to 8 mm for grouted piles may be accepted as permissible if the uplift load/displacement diagram unanimously shows that the pile permits an increase of load beyond the test load up to the required ultimate uplift load. Differently from the conventional design methods, the scattering of resistance is considered in case of a *design based on probabilistic principles* [13.61].

The verification of the ultimate uplift resistance can be studied by investigating a *test pile* according to IEC 61 773 installed at the tower site but separated from the construc-

tion piles. In this case the pile is loaded up to failing. The test pile should correspond to the construction pile as far as its dimensions, its design and its characteristic construction data are concerned.
During testing the *ultimate capacity* is reached when an uplift-loaded pile is lifted perceptibly or a compression-tested pile settles down perceptibly. On the *uplift force-displacement curve* or on the *compression force-settlement curve* the resistance is determined by the point where the flat gradient, after a range of load transition with progressively increasing displacements or settlements, passes into a steeply sloping leg (Figure 13.37).

13.6 References

13.1 EN 50 341-1: Overhead electrical lines exceeding AC 45 kV. Part 1: General requirements – Common specifications. Brussels, CENELEC, 2001

13.2 DIN 4022: Subsoil and groundwater. Classification and description of soil and rock.

Part 1: Borehole logging of soil and rock not involving continuous core sample recovery. Berlin, DIN, 1987

Part 2: Borehole logging of rock. Berlin, DIN, 1987

Part 3: Borehole logging for boringin soil (loose rock) by continuous extraction of cores. Berlin, DIN, 1987

13.3 IEC 61 773: Overhead lines. Testing of foundations of supports. Geneva, IEC, 1997

13.4 DIN 1054: Subsoil; Permissible loading of subsoil. Berlin, DIN, 1976

13.5 DIN 4021: Subsoil; Ground exploration by excavation, boring and sampling. Berlin, DIN, 1990

13.6 BS 5930: Code of practice for site investigation. London, BSI, 1981

13.7 ASTM D 1452: Standard practice for soil investigation and sampling by auger borings. New York, ASTM, 1990

13.8 DIN 4094: Subsoil; Ground exploration by probes. Berlin, DIN, 1990

13.9 Grundbautaschenbuch (Soil mechanics handbook). Berlin, Wilhelm Ernst & Sohn, 3rd edition, 1980

13.10 ASTM D 1586: Standard test method for penetration test and split-barrel sampling of soils. New York, ASTM, 1999

13.11 Terzaghi, K.; Peck, R.: Bodenmechanik in der Baupraxis (Soil mechanics for civil engineering practice). Berlin, Springer-Verlag, 1961

13.12 DIN 4096: Subsoil; Vane testing; Dimensions of apparatus; Model of operation evaulation. Berlin, DIN, 1980

13.13 LGM mededelingen Laboratorium voor Grondmechanica. Delft Deel XII/XIII 1969

13.14 Schmidt, H. G.: Beitrag zur Ermittlung der horizontalen Bettungszahl für die Berechnung von Großbohrpfählen unter waagerechter Belastung (Contribution on the evaluation of the horizontal subgrade modulus with regard to drilled piers under horizontal loading). Bauingenieur 46 (1971), pp. 233 to 237

13.15 Heitfeld, K. H.: Ingenieurgeologische Probleme im Grenzbereich zwischen Locker- und Festgestein (Engineering geology issues within the transition between loose soil and rock). Berlin, Springer-Verlag, 1985

13.16 DIN 4030: Assessment of water, soil and gases for their aggressiveness to concrete;

Part 1: Principles and limiting values. Berlin, DIN, 1991

Part 2: Collection and examination of water and soil samples. Berlin, DIN, 1991

13.17 ENV 1992-1: Eurocode 2: Design of concrete structures; Part 1: General rules and rules for buildings. Brussels, CEN, 1991

13.18 DIN 4023: Borehole logging; Graphical representation of results. Berlin, DIN, 1984

13.19 EN 50 341-3: Overhead electrical lines exceeding AC 45 kV. Part 3: National Normative Aspects (NNA). Brussels, CENELEC, 2001

13.20 EN 50 341-3-4: Overhead electrical lines exceeding AC 45 kV. Part 3-4: National Normative Aspects for Germany (NNA). Brussels, CENELEC, 2001

13.21 Cigré SC22 WG07: The design of transmission line support foundations – an overview. Paris, Cigré Brochure No. 206, 2002

13.22 ENV 1993-1-1: Eurocode 3: Design of steel structures. Part 1-1: General rules and rules for buildings. Brussels, CEN, 1992

13.23 Longo, V. J. et al.: Recent advances in transmission line foundation analysis and design. Cigré Report 22-10, 1986

13.24 Lapeyre, J. L. et al.: Theoretical and experimental study of an overturning foundation for single member support. Cigré Report 22-05, 1986

13.25 Zolezzi, R.: Direct foundations by means of blocks and foundation plates in transmission lines with self-supporting towers. Comparative study. Cigré Report 22-01,1986

13.26 Grasser, E.; Thielen, G.: Hilfsmittel zur Berechnung von Schnittgrößen und Formänderungen von Stahlbetontragwerken, DAfStB – Heft 240 (Remedies to analyse internal forces and moments of steel reinforced concrete structures). DAfStB–Volumne 240). Berlin. Beuth-Verlag. 3rd edition 1991

13.27 Grundbautaschenbuch, Teil 3 (Soil mechanics handbook, Part 3). Berlin, Wilhelm Ernst & Sohn, 5th edition 1997

13.28 Sulzberger, G.: Die Fundamente der Freileitungstragwerke und ihre Berechnung (The foundations of overhead line supports and their calculation). Bull. Schweiz. Elektrotechn. Ver. 36(1945), pp. 289 to 307

13.29 Titze, E.: Über den seitlichen Bodenwiderstand bei Pfahlgründungen (On the lateral soil resistance of pile foundations). Bauingenieur Praxis, Volume 77. Berlin, Wilhelm Ernst & Sohn, 1970

13.30 Werner, H.: Biegemomente elastisch eingespannter Pfähle (Bending moments of elastically embedded piles). Beton- und Stahlbetonbau (1970) Volume 2, pp. 39 to 43

13.31 DIN 4085: Subsoil; Analysis of earth pressure; Basic principles for calculation. Berlin, DIN, 1987

13.32 Teng, W.: Foundation design. London, Prentice-Hall, 1989

13.33 Empfehlungen des Arbeitsausschusses Ufereinfassungen (Recommendations of the working group for shore reinforcements). Berlin, Wilhelm Ernst & Sohn, 1980

13.34 Blum: Wirtschaftliche Dalbenform und deren Berechnung (Economic types of piers and their analysis). Bautechnik 9 (1932), pp. 50 to 55

13.35 Schmidt, B.: Berechnung biegebeanspruchter elastisch gebetteter Pfähle (Analysis of bending-loaded elastically embedded piles). Bautechnik 62 (1985), pp. 20 to 25

13.36 Buckley, M. B.: Reliability based design of OHL foundations. Cigré Report 22-203, 1994

13.37 DIN 4124: Building pits and trenches; Slopes, working space widths, sheeting. Berlin, DIN, 1981

13.38 EN 12 699: Execution of special geotechnical work – Displacement piles. Brussels, CEN, 2000

13.39 Köhn, W.: Katalog der Ortpfahlverfahren (Catalogue of in-situ piling methods). Wiesbaden, Bauverlag, 1968

13.40 Valtinat, G.; Alt, K.; Winkler, F.: Tragverhalten von gleitfest-vorgespannten (GV)-Stößen bei Stahlrammpfählen (Performance of gliding-resistant prestressed bolted connections of driven steel piles). Elektrizitätswirtschaft 83 (1984), pp. 313 to 318

13.41 Koswig, J.; Meueler, W.; Schmidt, B.: 110-kV-Bahnstromleitung, Kreuzung der Weser bei Bremen-Mittelsbüren (110 kV traction power line, crossing of the river Weser close to Bremen). Elektrische Bahnen 78 (1980), pp. 273 to 277

13.42 Schulte, G.: Beitrag zur Ermittlung der Tragfähigkeit von Zugpfählen unter besonderer Berücksichtigung der Gründung von Hochspannungsmasten (Contribution on the determination of uplift pile resistance with particular reference to transmission line foundations). Doctorate thesis, TU München, 1970

13.43 Pätzold, G.: Der Ortbeton-Ramm-Verdrängungspfahl als Gründungselement im Freileitungsbau (The in-situ cast concrete piles used as a foundation component for transmission lines). Elektrizitätswirtschaft 74 (1975), pp. 682 to 687

13.44 Vogt, H.: Kupplungen für Stahlbeton- und Spannbetonpfähle (Couplings for steel-reinforced and prestressed concrete piles). Bautechnik 55 (1978), pp. 188 to 190

13.45 prEN 12 794: Precast concrete foundation piles. Brussels, CEN, Draft 1997

13.46 EN 1536: Execution of special geotechnical work – Bored piles. Brussels, CEN, 1999

13.47 DIN 4014: Bored cast-in-situ piles; Formation, design and bearing capacity. Berlin, DIN, 1990

13.48 DIN 1054: Subsoil; Verification of safety of earthwork and foundation. Berlin, DIN, Draft 2000

13.49 Preuss, E.: Über die Bemessung gering auf Zug belasteter Stahlpfähle im Leitungsbau (On the design of uplift-loaded steel piles used for overhead power lines). Doctorate thesis, University Braunschweig, 1967

13.50 Jelinek, R.; Ostermayer, H.: Zur Tragfähigkeit von Zugpfählen. Rechnerische Grenzbelastung und Versuchsergebnisse bei MV-Pfählen (On the capacity of uplift-loaded piles. Theoretical ultimate capacity and testing results of grouted steel piles). Felsmechanik Ingenieurgeologie, Volume 1, 1964

13.51 Vanner, M.J.: The design and construction of drilled anchor foundations and their use on a 380 kV overhead line near Riyadh. Cigré Report 22-06, 1986

13.52 Littlejohn, G.S.; Bruce, D.A.: Rock anchors – state of the art. Brentwood, Foundation Publications LTD, 1977

13.53 Gidlund, J. et al.: Foundation of 400/800 kV middle-stayed portal towers in Sweden with reference to different types, design criteria and economy. Cigré Report 22-07, 1978

13.54 Biarez, J.; Barraud, Y.: The use of soil mechanics for adapting tower foundations to soil conditions. Cigré Report 22-06, 1968

13.55 Meyerhof, G. G.; Adams, J. I.: The ultimate uplift capacity of foundations. Canadian Geotechnical Journal 1968

13.56 Titan injection anchors. Drilled and injected anchors for soil and rock. Catalogue. Ennepetal (Germany), Ischebeck GmbH, 1999

13.57 Cigré SC22 WG07: Foundation testing. Paris, Cigré Brochure No. 81, 1994

13.58 IEC/TR 60826: Loading and strength of overhead transmission lines. Geneva, IEC, 1991

13.59 Kießling, F.; Sperl, H. D.: The new 380 kV river Elbe crossing of the Nordwestdeutsche Kraftwerke AG. Siemens Power Engineering, Vol. I (1979), pp. 75 60 79

13.60 Benke, W. et al.: Die Gründung für die 380-kV-Elbekreuzung der Nordwestdeutschen Kraftwerke AG (The foundation of the 380 kV crossing over the river Elbe of Nordwestdeutsche Kraftwerke AG). Bauingenieur 54(1979)8, pp. 81 to 90

13.61 Kießling, F. et al.: Foundation design on a probabilistic basis. Cigré Report 22-11, 1986

14 Sag and tension calculations

14.0 Symbols

Symbol	Signification
a	Span length
a_{e}	Complementary span length
a_{eq}	Equivalent span length
a_ξ	Existing clearance at the position ξ
A	Conductor cross section
c	Catenary parameter
C_0, C_1, C_2	Integration constants
d_{i}	Conductor subsection length
$\mathrm{d}s$	Infinitesimal length of the conductor element s
$\mathrm{d}S$	Infinitesimal value of the conductor tensile force S
e_{el}	Elastic strain
e_{th}	Thermal strain
E	Modulus of elasticity
f	Vertical sag
f_{e}	Sag in the complementary span length
f_i	Sag within the span i
f_{Il}	Sag in case of local ice load
f_ξ	Sag at the position ξ
g	Gravitational acceleration
$G, G_1, G_2, G_i, G_j, G_n$	Concentrated load
$G_{\mathrm{A}}, G_{\mathrm{B}}$	Support force
$G_{\mathrm{K}}, G_{\mathrm{K1}}, G_{\mathrm{K2}}, G_{\mathrm{K},i}$	Weight force at the insulator set 1, 2, or i
h	Difference in height of the conductor support points
h_1, h_2, h_3	Support height
h_i	Height of conductor of attachment at support i
h_{s}	Height of conductor
H, H_1, H_2, H_i	Horizontal component of the conductor tensile force
H_0	Initial value of the conductor tensile force
$J_{\mathrm{K},i}$	Weight force of the insulator set at the support i
$K_{1\mathrm{i}}, K_{2i}, K_{3i}, K_{4i}$	Auxiliary terms
K_1, K_2, K_3, K_4	Coefficients
L, L_i	Length of the sagging curve between the support points
$L_{1,2}$	Length of sagging curve at a temperatures T_1 and T_2, respectively
$L_{0i}, L_{01,i}, L_{02,i}$	Inclined span length in the span i
L_{K}	Length of insulator set
$L_{\mathrm{K},x}$	Length of insulator set, projected into the horizontal
$m_{\mathrm{C}}, m_{\mathrm{C1}}, m_{\mathrm{C2}}$	Conductor mass per unit length
m_{CI}	Conductor mass per unit length with ice load
$m_{\mathrm{C}}g, m_{\mathrm{C1},i}g, m_{\mathrm{C2},i}g$	Conductor weight per unit length
M	Equivalent moment at support point
n	Number of spans in a tensioning section
NN_ξ	Height above sea level at the position ξ
Q_{t}	Transverse force
Q_{WC}	Wind load on conductor
s	Distance of a concentrated load to the support
s_{m}	Minimum clearance to ground
S	Conductor tensile force
T_1, T_2	Conductor temperature
u	Variable
V	Vertical component of conductor tensile force

Symbol	Signification
x	Variable
x_A, x_{Ai}, x_B	Abscissa of the sagging curve vertex
X_i	Conductor tensile force in the span i related to initial conductor force H_0
α	Opening angle of an inverted V-type insulator set
$\delta_i, \delta_{0,i}$	Horizontal insulator displacement at support i
$\Delta a, \Delta a_i$	Change of horizontal distance of conductor attachment points
Δh_i	Change of difference in height in span i
ΔL_i	Change of sagging curve length in span i
ΔS	Change of conductor tensile force
ΔT	Temperature difference
ε_T	Coefficient of thermal expansion
$\varepsilon_i, \varepsilon_{0i}$	Vertical displacement of insulator set at support i
ξ	Abscissa of a random point of the sagging curve
$\sigma, \sigma_1, \sigma_2$	Conductor tensile stress
φ	Angle between conductor in still air and in swung position
ψ	Down-strain angle, swing angle of an insulator set

14.1 Basis

If a conductor is sagged with a given tensile force between points A and B representing the attachments of the conductor at the supports, a curve, the *sagging curve* or *catenary* (Figure 14.1) will be formed due to the balance between conductor dead loads and tensile forces. The vertical distance of the conductor to the line connecting both attachment points A and B is called the *conductor sag* f.
In case of stranded conductors used for overhead power lines, it may be assumed that their dimensions and characteristics are constant at least between two adjacent supports. The *conductor mass* per unit length, the *conductor cross section* and the other characteristics do not change within a span. Since the *bending stiffness* of the conductor is relatively low tensile forces act predominantly in the conductor, therefore. At their ends, the conductors are supported rigidly but with a pivot. Therefore, no bending moments occur there. The detailed basis of conductor static is described in detail in [14.1]. Some information on sag and tension calculation is given in [14.2], [14.3] and [14.4].

14.2 Sags described by the catenary curve

To determine the sagging curve $y = f(x)$, the equilibrium conditions are established for the forces acting at a conductor element with the infinitesimal length $\mathrm{d}s$ (Figure 14.1). The conductor tensile force is divided into its vertical and horizontal component. The balance of forces in vertical direction yields

$$m_C g \, \mathrm{d}s = V + \mathrm{d}V - V \tag{14.1}$$

and because of

$$\mathrm{d}s = \sqrt{\mathrm{d}x^2 + \mathrm{d}y^2} = \mathrm{d}x\sqrt{1 + (\mathrm{d}y/\mathrm{d}x)^2}$$

it results

$$\mathrm{d}V/\mathrm{d}x = m_C g\sqrt{1 + (\mathrm{d}y/\mathrm{d}x)^2} \quad . \tag{14.2}$$

The balance of forces in horizontal direction yields

$$H + \mathrm{d}H - H = 0 \quad . \tag{14.3}$$

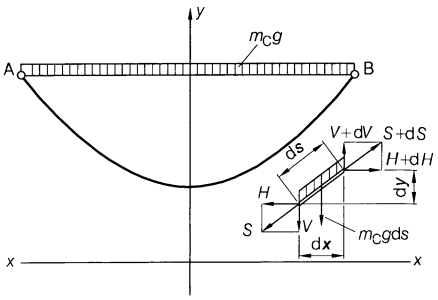

Figure 14.1: Condition of equilibrium at a conductor element

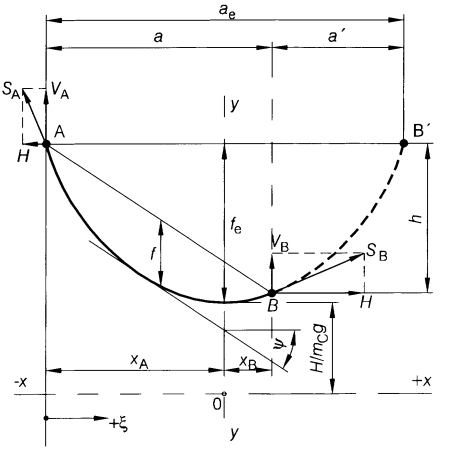

Figure 14.2: Span with supports at different altitudes

Therefore, $\mathrm{d}H = 0$ and after integration:

$$H = \text{const.} \tag{14.4}$$

The *horizontal component* H of the conductor tensile force does not change along the conductor sagging curve. The balance of moments around the centre of gravity of the conductor element results in

$$H \cdot \mathrm{d}y = V \cdot \mathrm{d}x \quad ,$$

when the effects with smaller order of magnitude are neglected or

$$V = H \cdot \mathrm{d}y/\mathrm{d}x \quad . \tag{14.5}$$

By differentiation of (14.5) to x and inserting into (14.2) the *differential equation of the sagging curve* is obtained:

$$\mathrm{d}^2y/\mathrm{d}x^2 = ((m_C g)/H)\sqrt{1 + (\mathrm{d}y/\mathrm{d}x)^2} \quad . \tag{14.6}$$

The conductor tensile stress according to $\sigma = H/A$ was not introduced in (14.6), since (14.6) applies exactly also for composite conductors for which the ratio H/A forming the equivalent tensile stress does not represent a measurable physical quantity.
To integrate the equation (14.6), this is rearranged and expanded to

$$(\mathrm{d}^2y/\mathrm{d}x^2) \cdot (\mathrm{d}y/\mathrm{d}x) \Big/ \sqrt{1 + (\mathrm{d}y/\mathrm{d}x)^2} \cdot \mathrm{d}x = (m_C g/H) \cdot (\mathrm{d}y/\mathrm{d}x) \cdot \mathrm{d}x \quad .$$

After this re-arrangement, both sides of the equation can be integrated and

$$\sqrt{1 + (\mathrm{d}y/\mathrm{d}x)^2} = m_C g \cdot y \cdot C/H = m_C g(y - y_0)/H \tag{14.7}$$

is obtained.
For the next integration step, equation (14.7) is solved to obtain $\mathrm{d}y/\mathrm{d}x$:

$$\mathrm{d}y/\mathrm{d}x = \sqrt{[m_C g(y - y_0)/H]^2 - 1} \quad .$$

By using the substitution

$$(m_C g/H)(y - y_0) = u$$

and, therefore,

$$dy/dx = (dy/du)(du/dx) = (H/(m_C g))(du/dx)$$

$du/\sqrt{u^2-1} = (m_C g/H)dx$ is obtained. Due to $\int(1/\sqrt{u^2-1})\,du = \cosh^{-1} u$ the next integration step is possible and

$$\cosh^{-1}[m_C g(y-y_0)/H] = m_C g(x-x_0)/H$$

is obtained. The function $\cosh^{-1}(y)$ represents the reverse of the *hyperbolic cosine function* $y = \cosh x = (e^x + e^{-x})/2$. Solving this equation to obtain y yields

$$y = H/(m_C g)\{\cosh[(m_C g/H)(x-x_0)] + C_0\} \quad . \tag{14.8}$$

The constant of integration y_0 was replaced by $C_0 \cdot H/m_C g$. Equation (14.8) shows that a conductor sagged between the points A and B will take the shape of a hyperbolic cosine curve. Since the same conditions apply to chains made of links, as for the conductors, this function is also valid for a freely sagged chain, being designated as *catenary curve*, therefore.

In the format (14.8), the equation for the sagging line is not well suited for practical applications. Therefore, the origin of the coordinate system is selected such that the vertex of the sagging line has the ordinates $x = 0$, $y = H/m_C g$ (Figure 14.2). Using this format for the coordinate system, the conductor ordinate for any point of the *catenary* is obtained from (14.8)

$$y = H/(m_C g)\cosh(m_C g x/H) \quad . \tag{14.9}$$

The sag of a given point at the conductor related to the connection line of the points A and B (Figure 14.2) follows to be

$$f = (h/a)(x - x_A) + (H/(m_C g))[\cosh(m_C g x_A/H) - \cosh(m_C g x/H)] \quad , \tag{14.10}$$

where x_A designates the abscissa of the fixing point A (Figure 14.2), which has still to be determined. In particular, the sag of the *vertex* S is obtained from (14.10) for $x = 0$

$$f_s = (H/(m_C g))[\cosh(m_C g x_A/H) - 1] - h \cdot x_A/a \quad . \tag{14.11}$$

In general, the span length a, the difference in height h of the attachment points, the mass per unit length and the horizontal tensile force are given for an overhead line span but not the position of the vertex expressed by the coordinate x_A. The sag will be zero for the points A and B. From (14.10) it is obtained with $x = x_B$ and $x_B - x_A = a$

$$h = [H/(m_C g)][\cosh(m_C g x_B/H) - \cosh(m_C g x_A/H)]$$

and transformed by means of the addition formulae for the hyperbolic functions to be

$$h = (2H/m_C g)\sinh[m_C g(x_A + x_B)/(2H)] \cdot \sinh[m_C g(x_B - x_A)/(2H)] . \tag{14.12}$$

The equation (14.12) can be solved explicitly regarding the variable x_A if the conductor length between the suspension points A and B is introduced:

$$L = \int_{x_A}^{x_B} \sqrt{1 + \left(\frac{dy}{dx}\right)^2}\, dx = \int_{x_A}^{x_B} \sqrt{1 + \sinh^2(m_C g x/H)}\, dx = \int_{x_A}^{x_B} \cosh(m_C g x/H)\, dx .$$

With

$$\int \cosh(m_C g x/H)\, dx = \sinh m_C g x/H$$

it is obtained

$$L = (H/(m_C g))\,[\sinh(m_C g x_B/H) - \sinh(m_C g x_A)/H)]$$

and eventually by means of the addition formulae

$$L = 2\,(H/(m_C g))\cosh[m_C g(x_A + x_B)/2H] \cdot \sinh[m_C g(x_B - x_A)/(2H)] \quad . \tag{14.13}$$

Due to $\cosh^2 x - \sinh^2 x = 1$ the *conductor length* is obtained using $x_B - x_A = a$, from (14.12) and (14.13):

$$L = \sqrt{h^2 + [(2H)/(m_C g) \cdot \sinh(m_C g \cdot a/(2H))]^2} \quad . \tag{14.14}$$

Subtracting (14.13) and (14.12) yields

$$L - h = 2\,(H/(m_C g))\sinh[(m_C g \cdot a)/(2H)] \cdot \exp[-m_C g(x_A + x_B)/(2H)] \quad .$$

Using $x_A + x_B = 2x_A + a$ and solving this formula with respect to x_A and with some transformations the *position of the vertex* is eventually obtained to be:

$$x_A = (H/(m_C g))\ln[H/(m_C g(L-h)) \cdot (1 - \exp(-m_C g \cdot a/H))] \quad . \tag{14.15}$$

If both attachment points A and B are situated at the same level, the vertex will be in the centre line of the span because of the symmetry. With $h = 0$ and $L = 2\,(H/m_C g) \cdot \sinh(m_C g \cdot a/2H)$, then $x_A = -a/2$ is obtained from (14.15). From (14.10), the *equation for the sag* in this case is obtained to be:

$$f = (H/(m_C g))\,[\cosh(m_C g \cdot a/(2H)) - \cosh(m_C g \cdot x/H)] \quad . \tag{14.16}$$

The maximum sag is obtained for $x = 0$ being

$$f_{max} = (H/(m_C g))\,[\cosh(m_C g a/(2H)) - 1] \tag{14.17}$$

In addition to the sags, the vertical forces at the attachment points and the conductor tensile force along the sagging curve is of interest. From (14.5) and (14.9), the vertical component of the conductor tensile force is obtained to be $V = H\sinh(m_C g \cdot x/H)$. This force acts against the gravitation in case of a positive sign. The *support forces* at the points A and B follow using $G = -V$ (Figure 14.2) to be:

$$G_A = -H\sinh(m_C g \cdot x_A/H) \text{ and } G_B = H\sinh(m_C g\,(a + x_A)\,/H) \quad . \tag{14.18}$$

The total tensile force is equal to the horizontal force at the vertex of the sagging curve and increases towards the suspension points according to:

$$S = \sqrt{H^2 + V^2} = H\sqrt{1 + \sinh^2(m_C g \cdot x/H)} = H\ cosh\,(m_C g \cdot x/H) \quad . \tag{14.19}$$

The mean value of the conductor tensile force can be calculated from:

$$\overline{S} = 1/a \int_{x_A}^{x_B} S\,\mathrm{d}x = H/a \int_{x_A}^{x_B} \cosh(m_C g \cdot x/H)\ \mathrm{d}x \quad .$$

Since the integral in this formula represents the length L of the conductor, it is obtained:

$$\overline{S} = H \cdot L/a \quad . \tag{14.20}$$

The *mean value of the conductor force* is equal to the conductor length divided by the span length and multiplied by the *horizontal tensile force.*

14.3 Conductor sagging curve as a parabola

With sufficient accuracy, it can be assumed for many practical applications for calculation of an overhead conductor that the gradient of the tangent to the sagging curve is small. In this case $(\mathrm{d}y/\mathrm{d}x)^2$ can be neglected compared to 1,0 in (14.2) and $\mathrm{d}^2y/\mathrm{d}x^2 = m_C g/H$ is obtained from (14.6). Neglecting the gradient of tangent corresponds to the assumption of a uniform distribution of the conductor mass along the span (Figure 14.1) and not along the sagging curve. By carrying out two integration steps, the equation for the parabola $y = m_C g/(2H)\, x^2 + C_1 \cdot x + C_2$ is obtained. Choosing the origin of the coordinate system at the vertex, yields together with $C_1 = C_2 = 0$

$$y = m_C g/(2H) x^2 \quad . \tag{14.21}$$

The *sag* of a given point of the conductor compared to the connection line of the attachment points A and B (Figure 14.2) yields

$$f = h/a\,(x - x_A) + m_C g/(2H) \cdot \left(x_A^2 - x^2\right) \quad . \tag{14.22}$$

The *position of the vertex* can be obtained from the condition that the sag f has to be zero also at the point B. With $x_B = a + x_A$, it is obtained from (14.22)

$$x_A = -a/2 + H/(m_C g) \cdot h/a \quad . \tag{14.23}$$

Moving the origin of the coordinate system to the attachment point A yields

$$f = m_C g \cdot a^2/(2H) \left(\xi/a - \xi^2/a^2\right) \quad , \tag{14.24}$$

where $\xi = x + x_A$. The sag, therefore, does not depend on the difference of heights. Its maximum value follows for $\xi = a/2$ to be

$$f_{\max} = m_C g \cdot a^2/(8H) \quad . \tag{14.25}$$

Related to the maximum sag $f_{\max}$, the sag at a given position ξ can be obtained from

$$f = 4 f_{\max}(\xi/a)\,(1 - \xi/a) \quad . \tag{14.26}$$

The maximum sag, with attachment points at the same level assumed, is obtained from (14.16) with $x = 0$ to be

$$f_{\max} = H/(m_C g)\,\{\cosh\,[m_C g \cdot a/(2H)] - 1\} \quad . \tag{14.27}$$

Developing $\cosh(x)$ to a series it results

$$f_{\max} = \frac{m_C g \cdot a^2}{8H} + \frac{(m_C g)^3 a^4}{384 H^3} + \frac{(m_C g)^5 a^6}{46\,080 H^5} + \ldots \quad . \tag{14.28}$$

Comparing this with (14.25), it can be seen that the maximum sag of the parabola is equal to the first term of the mathematical series of the catenary curve. From (14.5) the vertical component of the conductor tensile force is obtained to be $V = H \cdot \mathrm{d}y/\mathrm{d}x = m_C g \cdot x$, considering (14.21) as well. The vertical component of the conductor tensile force increases linearly with the distance from the vertex. The conductor tensile force at the suspension point A or B is given by

$$S_{A,B} = \sqrt{H^2 + (m_C g \cdot x_{A,B})^2} \quad . \tag{14.29}$$

The conductor tensile force, therefore, is given by the geometric sum of the horizontal component of the tensile force and the weight of the conductor section between the vertex and the attachment point.

The *conductor length* can be calculated from (14.14). For the parabola $y = x^2/2c$, where $c = H/(m_C g)$, the conductor length within a span with attachment points at the same level is obtained from

$$L = \int_{-(a/2)}^{a/2} \sqrt{1 + (x/c)^2}\, \mathrm{d}x \quad .$$

For cases where the sagging curve can be represented by a parabola, the expression under a square root can be developed into a series because of $(x/c)^2 \ll 1$ and integrated. It follows

$$L = \left[x + \frac{x^3}{6\,c^2}\right]\Bigg|_{x=-(a/2)}^{x=a/2} = a + \frac{a^3}{24\,c^2} = a\left[1 + \frac{(m_C g)^2 \cdot a^2}{24\,H^2}\right] . \tag{14.30}$$

Using (14.25) it is obtained

$$L = a\left[1 + (8/3)\,(f_{\max}/a)^2\right] \quad . \tag{14.31}$$

If the equation for the conductor length $L = \sinh(a/2\,c)$, resulting for the catenary curve is developed into a series and terminated after the second term, the formula (14.31) is obtained as well.
In case of differing height levels of the attachment points of the span, it is obtained from (14.14)

$$L = \sqrt{h^2 + \left\{a\left[1 + (8/3)\,(f_{\max}/a)^2\right]\right\}^2} \quad . \tag{14.32}$$

The relative error expressed in percent of the sag when replacing the exact catenary curve by the parabola curve can be calculated from (14.17) and (14.25) to be

$$\Delta f/f = \left\{\cosh\,(a/(2\,c)) - 1 - \left[(a/(2\,c))^2/2\right]\right\} / \left[(a/(2\,c))^2/2\right] \cdot 100(\%)\,, \tag{14.33}$$

where $c = H/(m_C g)$ is the *parameter of the catenary curve* and a the span length. The permissible error depends on the individual case. Where the absolute error is more than 0,10 m, the catenary curve should be used. Nowadays, sags of overhead line conductors are more or less exclusively calculated by computer programs, where the exact equations can always be adopted without any effort.

Example: An ACSR conductor 304-AL1/49-ST1A, according to EN 50182, is sagged in spans with 800 and 400 m length with a horizontal tensile force of 14 kN corresponding to a tensile stress of 40 N/mm^2. The parameter c is obtained to be

$$c = 14\,000/(1{,}235 \cdot 9{,}81) \approx 1155 \text{ m}.$$

The relative error of the parabola approximation will be 0,2 % according to (14.33) in case of 400 m span length and 1,0 % in case of 800 m span length.
The corresponding sags are calculated using the catenary curve to be

$$f_{1\,\max} = \frac{14\,000}{1{,}235 \cdot 9{,}81}\left[\cosh\left(\frac{400 \cdot 1{,}235 \cdot 9{,}81}{2 \cdot 14\,000}\right) - 1\right] = 17{,}35 \text{ m},$$

$$f_{2\,\max} = \frac{14\,000}{1{,}235 \cdot 9{,}81}\left[\cosh\left(\frac{800 \cdot 1{,}235 \cdot 9{,}81}{2 \cdot 14\,000}\right) - 1\right] = 69{,}92 \text{ m}$$

and using the parabola to be

$$f_{1\,\max} = \frac{1{,}235 \cdot 9{,}81 \cdot 400^2}{8 \cdot 14\,000} = 17{,}31 \text{ m},$$

$$f_{2\,\max} = \frac{1{,}235 \cdot 9{,}81 \cdot 800^2}{8 \cdot 14\,000} = 69{,}23 \text{ m}.$$

The errors, therefore, are 0,04 and 0,69 m, respectively. In case of span lengths up to 500 m, the calculation of the sags using the parabola is sufficient if an error of 0,1 m is accepted.

14.4 Span with differing attachment levels

The equation (14.10) applies as well for the sag in a span with differing height levels at both ends. In many cases it is advantageous for calculating to expand the span ideally, such that the attachment points have the same level in the complementary span in order to be able to apply the simpler relations for this case. Therefore, the *complementary span length* a_e in the expanded span has to be calculated. According to Figure 14.2 $a_e = 2\,|x_A|$ applies. Therefore, (14.15) yields

$$a_e = 2\,H/(m_C g)\,\ln\{[1 - \exp(-m_C g a/H)]\,/\,(L - h)\} \quad . \tag{14.34}$$

Using the parabola for the sagging line it is obtained from (14.23)

$$a_e = a + 2\,H \cdot h/(m_C g \cdot a) \quad . \tag{14.35}$$

If equation (14.16) is used for the sag in the complementary span (14.19), it applies for the conductor tensile force at the attachment point A with $\cosh m_C g \cdot a_e/(2\,H) = f_e \cdot m_C g/H + 1$

$$S_A = H + f_e \cdot m_C g \tag{14.36}$$

and at attachment point B accordingly

$$S_B = H + (f_e - h)\,m_C g \quad . \tag{14.37}$$

The conductor tensile force at the attachment point, therefore, is equal to the horizontal force increased by the product of vertical distance between the attachment point and the vertex and the conductor weight force. Using the formula for the *complementary span*, the sags can be calculated at a given point of the span in question.

14.5 Conductor state change equation

If the temperature or the loading of a conductor varies in a span, the conductor length will be expanded or contracted resulting again in a variation of the conductor tensile force (Figure 14.3). The length of the conductor in condition 2 characterized by the temperature T_2 and the loading $m_{C2}g$ results from the length in the initial condition 1 according to

$$L_2 = L_1(1 + e_{th})(1 + e_{el}) \quad , \tag{14.38}$$

where e_{th} and e_{el} designate the thermal and elastic expansion, respectively. Because of $e_{th} = \varepsilon_t \cdot \Delta T$ and $e_{el} = \Delta S/(E \cdot A)$ it is obtained

$$L_2 = L_1\,[1 + \varepsilon_t(T_2 - T_1)]\,[1 + (S_2 - S_1)/(EA)] \quad . \tag{14.39}$$

With sufficient accuracy, the parabola can be used for the sagging line since not the absolute length of the conductor but only the difference in length between the conditions 1 and 2 is considered. Therefore, L_1 and L_2 result from (14.30) to be

$$L_1 = a + a^3(m_{C1} \cdot g)^2/(24\,H_1^2) \text{ and } L_2 = a + a^3(m_{C2} \cdot g)^2/(24\,H_2^2).$$

The forces S_1 and S_2 are obtained from (14.20):

$$S_1 = H_1 \cdot (L_1/a) \text{ and } S_2 = H_2 \cdot (L_2/a) \quad .$$

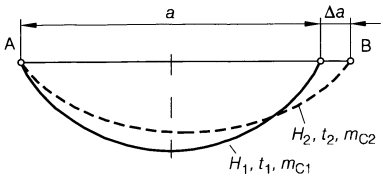

Figure 14.3: Change of the condition in a span

With acceptable accuracy, it applies $(S_2 - S_1) \sim (H_2 - H_1)$. Inserting these terms in (14.39) yields

$$\begin{aligned}
&a + a^3(m_{C2} \cdot g)^2/(24\,H_2^2) = \\
&= [a + a^3(m_{C1} \cdot g)^2/(24\,H_1^2)]\,[1 + \varepsilon_t\,(T_2 - T_1)] \cdot [1 + (H_2 - H_1)\,/EA] = \\
&= a + a\varepsilon_t(T_2 - T_1) + a(H_2 - H_1)/EA + a^3(m_{C1}g)^2/(24\,H_1^2) + \\
&\quad + a\varepsilon_t(T_2 - T_1)(H_2 - H_1)/EA + a^3(m_{C1}g)^2/(24\,H_1^2) \cdot \varepsilon_t(T_2 - T_1) + \\
&\quad + a^3(m_{C1}g)^2/(24\,H_1)^2 \cdot (H_2 - H_1)EA + \\
&\quad + a^3(m_{C1}g)^2/(24\,H_1)^2 \cdot \varepsilon_t(T_2 - T_1)(H_2 - H_1)EA\,.
\end{aligned}$$

In this equation, the last four terms are at least by two orders of magnitude lower than the others and can be neglected, therefore.
With these significations, the *conductor state change equation* is obtained:

$$H_2^2\left[H_2 - H_1 + \frac{EA(a \cdot m_{C1}g)^2}{24\,H_1^2} + EA \cdot \varepsilon_t(T_2 - T_1)\right] = \frac{EA(a \cdot m_{C2}g)^2}{24}\,. \qquad (14.40)$$

In equation (14.40), the conductor tensile forces is the unknown variable. Equation (14.40) is, therefore, correct for all conductor types, whether being single-material or composite conductors. The equivalent tensile stress $\sigma = H/A$ can be introduced and leads to

$$\sigma_2^2\left[\sigma_2 - \sigma_1 + \frac{E \cdot (a \cdot m_{C1}g)^2}{24\,\sigma_1^2 \cdot A^2} + E \cdot \varepsilon_t(T_2 - T_1)\right] = \frac{E \cdot (a \cdot m_{C2}g)^2}{24 \cdot A^2}\quad . \qquad (14.41)$$

The tensile stress can be measured physically only at single material conductors. The conductor state change equation is an algebraic equation of the 3rd degree which can be practically solved by numeric procedures available on modern pocket calculators.
If the span length is increased by the value Δa, e. g. by swinging of a suspension set, the characteristics of the conductor state will vary as well. Because of

$$L_2 = a + \Delta a + (a + \Delta a)^3 \cdot (m_{C2}g)^2/(24\,H_2^2) \approx a + \Delta a + a^3 \cdot (m_{C2}g)^2/(24\,H_2^2)$$

with the above mentioned approximation it is obtained from (14.39)

$$\begin{aligned}
&H_2^2\left[H_2 - H_1 + EA(a \cdot m_{C1}g)^2/(24\,H_1^2) + EA \cdot \varepsilon_t(T_2 - T_1) - EA\Delta a/a\right] = \\
&\qquad = EA(a \cdot m_{C2}g)^2/24\quad .
\end{aligned} \qquad (14.42)$$

An analogous format is obtained by adding the term $(-E \cdot \Delta a/a)$ to the term in the bracket on the left side of equation (14.41).
A change of the relevant conductor length can be caused by failing of an insulator string of a multiple insulator tension set, for example. The determination of the conductor tensile forces for this condition is relevant for crossings, where the verification of sufficient clearance after failing of an individual string of a multiple insulator set is required.
The *conductor state change equation* (14.40) or (14.41) can be applied to a *tensioning section* of an overhead power line with n spans, assuming that the conductor tensile

forces H_i and the loadings m_{Ci} are equal in all spans. This approximation is more precise than the assumption of rigid attachment points in each span. In a tensioning section, it applies to the total conductor lengths L_1 or L_2:

$$L_{i,1,2} = \sum_{i=1}^{n} \left[a_i + a_i^3 \cdot (m_{C1,2} g)^2 / (24\, H_{1,2}^2) \right] \quad .$$

When neglecting again the terms which are small by a higher order of magnitude, it is obtained from (14.39):

$$H_2^2 \left[H_2 - H_1 + \frac{E \cdot A (m_{C1} g)^2}{24\, H_1^2} \cdot \left(\sum_{i=1}^{n} a_i^3 \Big/ \sum_{i=1}^{n} a_i \right) + E \cdot A \cdot \varepsilon_t \, (T_2 - T_1) \right]$$

$$= \frac{E \cdot A (m_{C2} g)^2}{24} \cdot \left(\sum_{i=1}^{n} a_i^3 \Big/ \sum_{i=1}^{n} a_i \right) \quad .$$

The expression

$$a_{id} = \sqrt{\sum_{i=1}^{n} a_i^3 \Big/ \sum_{i=1}^{n} a_i} \tag{14.43}$$

is called the *equivalent span* or *ruling span* of a tensioning section. Using this term, it is obtained from equations (14.40) and (14.41)

$$H_2^2 \left[H_2 - H_1 + \frac{EA (m_{C1} g \cdot a_{id})^2}{24 H_1^2} + EA \cdot \varepsilon_t (T_2 - T_1) \right] = \frac{EA (m_{C2} g \cdot a_{id})^2}{24} \tag{14.44}$$

and

$$\sigma_2^2 \left[\sigma_2 - \sigma_1 + \frac{E \cdot (m_{C1} g \cdot a_{id})^2}{24 \sigma_1^2 \cdot A^2} + E \cdot \varepsilon_t (T_2 - T_1) \right] = \frac{E (m_{C2} g \cdot a_{id})^2}{24\, A^2} \quad . \tag{14.45}$$

As a first approximation, the conductor tensile forces in a tensioning section of an overhead line change as in a span with the equivalent span length. The sags in the individual spans can be determined under the assumption of equal conductor tensile forces in all spans.

Example: A tensioning section of a power line consists of six spans with the lengths 350, 200, 450, 275, 500 and 325 m. The conductor 304-AL1/49-ST1A (ACSR 300/50) is installed with a conductor tensile stress of 50 N/mm^2 at 10°C. The sag at 60°C in the span with 500 m length should be calculated.
The equivalent or ruling span follows from (14.43) to

$$a_{id} = \sqrt{\frac{350^3 + 200^3 + 450^3 + 275^3 + 500^3 + 325^3}{350 + 200 + 450 + 275 + 500 + 325}} = \sqrt{\frac{322{,}125 \cdot 10^6}{2100}} = 391{,}65 \text{ m} \quad .$$

For the conductor 304-AL1/49-ST1A, $A = 353{,}7$ mm^2; $m = 1{,}235$ kg/m; $E = 77\,000$ N/mm^2 and $\varepsilon_t = 18{,}9 \cdot 10^{-6}$ K^{-1} applies. The horizontal tensile force H_1 will be $353{,}7 \cdot 50 = 17685$ N. From (14.44) it is obtained

$$H_2^2 [H_2 - 17\,685 + 77\,000 \cdot 353{,}7 (1{,}235 \cdot 9{,}81)^2 \cdot 391{,}65^2 / (24 \cdot 17\,685^2)$$

$$+ 77\,000 \cdot 353{,}7 \cdot 18{,}9 \cdot 10^{-6} (60 - 10)] = 77\,000 \cdot 353{,}7 (1{,}235 \cdot 9{,}81)^2 \cdot 391{,}65^2 / 24$$

and

$$H_2^2 [H_2 + 89\,742] = 2554{,}95 \cdot 10^{10} \quad .$$

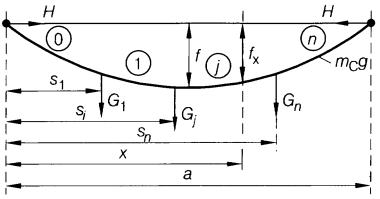

Figure 14.4: Sag with additional concentrated loads in a span

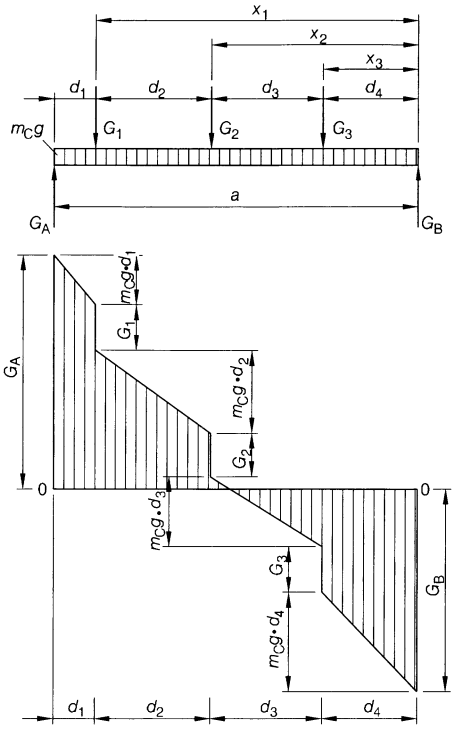

Figure 14.5: Diagram of transverse force at the equivalent beam

This equation is solved by iteration or by a modern pocket calculator:

$$
\begin{aligned}
H_{2,1} &= 16\,000 \text{ yields } H_2^2[H_2 + 89\,742] = 2707{,}00 \cdot 10^{10} \quad , \\
H_{2,2} &= 15\,500 \text{ yields } H_2^2[H_2 + 89\,742] = 2528{,}44 \cdot 10^{10} \quad , \\
H_{2,3} &= 15\,580 \text{ yields } H_2^2[H_2 + 89\,742] = 2556{,}55 \cdot 10^{10} \quad , \\
H_{2,4} &= 15\,575 \text{ yields } H_2^2[H_2 + 89\,742] = 2554{,}79 \cdot 10^{10} \quad ,
\end{aligned}
$$

$H_{2,4} = 15\,575$ N solves the conductor state change equation with sufficient accuracy. The maximum sag in the 500 m long span is obtained from equation (14.17)

$$
f = \frac{15\,575}{1{,}235 \cdot 9{,}81} \left[\cosh\left(\frac{1{,}235 \cdot 9{,}81 \cdot 500}{2 \cdot 15\,575} \right) - 1 \right] = 24{,}39 \text{ m} \quad .
$$

The application of the conductor state change equation directly on the 500 m long span would have resulted in a conductor tensile force of 16 265 N with a sag of 23,35 m. This would have resulted in a sag to be too low by 1,04 m.

14.6 Span with concentrated loads

The sag of a conductor with *concentrated loads* can be determined by making use of the equivalence between conductor sags and bending moments of an equivalent beam with equivalent loads. In this case, it applies for the sag $f = M/H$ where H is the conductor horizontal force and M is the moment. At the coordinate x according to Figure 14.4,

it is obtained for a span with n concentrated loads G_i:

$$f_x = (1/H)\left[x(a-x)\,m_C g/2 + x\sum_{i=1}^{n}(1-s_i/a)\cdot G_i - \sum_{i=1}^{j}(x-s_i)\cdot G_i\right] . \quad (14.46)$$

The maximum sag must not necessarily occur underneath a concentrated load. The horizontal tensile force H, unknown in equation (14.46), can be calculated according to a method proposed in [14.5]. This procedure starts with the definition of the conductor length. With (14.5) it is obtained, therefore,

$$L = \int_0^a \sqrt{1+(\mathrm{d}y/\mathrm{d}x)^2}\cdot \mathrm{d}x = \int_0^a \sqrt{1+(V/H)^2}\,\mathrm{d}x \quad . \quad (14.47)$$

The vertical component V can be considered as the transverse force Q_t according to Figure 14.5. Because of $(Q/H)^2 \ll 1$ the conductor length L is obtained from (14.47) as

$$L = \int_0^a \left[1 + 1/2\cdot Q^2/H^2\right]\mathrm{d}x = a + 1/(2\,H^2)\cdot\int_0^a Q^2\,\mathrm{d}x \quad . \quad (14.48)$$

The equations (14.38) and (14.39) represent the relation between the conductor lengths in the conditions 1 and 2. If the conductor length according to (14.48) is used in these equations and products of terms with small order of magnitude are neglected, it is eventually obtained

$$H_2^2\left[H_2 - H_1 + \frac{EA}{2\cdot a\cdot H_1^2}\int_0^a Q_1^2\,\mathrm{d}x + EA\varepsilon_t(T_2-T_1)\right] = \frac{EA}{2\,a}\cdot\int_0^a Q_2^2\,\mathrm{d}x\,, \quad (14.49)$$

where Q_1 is related to the condition 1, e. g. without concentrated loads, and Q_2 due to the condition 2, e. g. with concentrated loads. The integration can be carried out analytically, section by section, or with well-known approximations, e. g. with the Simpson rule. According to Figure 14.5, the integration can be carried out, section by section, whereby it applies for each section with the length d_i

$$\int_0^{d_i} Q_i^2(x)\,\mathrm{d}x = d_i/3\,(Q_{i-1}^2 + Q_i^2 + Q_{i-1}\cdot Q_i)$$

and, therefore, for the total span

$$\int_0^a Q^2(x)\,\mathrm{d}x = \sum_{i=1}^{n} d_i/3\,(Q_{i-1}^2 + Q_i^2 + Q_{i-1}\cdot Q_i) \quad . \quad (14.50)$$

For a span with only one concentrated load G acting in the middle of the span it is obtained

$$\int_0^a Q^2\,\mathrm{d}x = G^2\cdot a/4 + G\cdot(m_C g\cdot a)\,a/4 + (m_C g\cdot a)^2\cdot a/12 \quad .$$

With $G = 0$, the *conductor state change equation* (14.40) follows from (14.49).

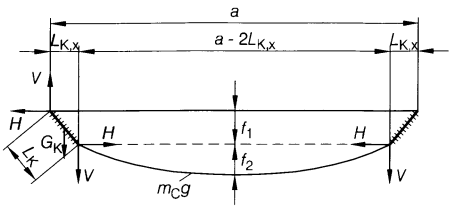

Figure 14.6: Sag taking care of weights of tension insulator sets

Example: In a 400 m long span with the conductor 264-AL1/34-ST1A and a conductor tensile stress of 50 N/mm^2 at +10°C a concentrated load of 2000 N is applied in the middle of the span. How do the conductor tensile stress and the sag change? The temperature should not change.
It applies

$$1/a \int_0^a Q^2(x) = 2000^2/4 + 2000 \cdot 0{,}998 \cdot 9{,}81 \cdot 400/4 + (0{,}998 \cdot 9{,}81 \cdot 400)^2/12$$
$$= 1 \cdot 10^6 + 1{,}958 \cdot 10^6 + 1{,}278 \cdot 10^6 = 4{,}236 \cdot 10^6$$

The equation (14.49) yields

$$H_2^2 \left[H_2 - 297{,}8 \cdot 50 + \frac{74\,000 \cdot 297{,}8 \cdot 1{,}278 \cdot 10^6}{2 \cdot (297{,}8 \cdot 50)^2} \right] = (74\,000 \cdot 297{,}8 \cdot 4{,}236 \cdot 10^6)/2$$

and

$$H_2^2 [H_2 - 14\,890 + 63\,515] = 46{,}675 \cdot 10^{12} \quad .$$

Thereof, $H_2 = 25\,152$ N or $\sigma_2 = 84{,}46$ N/mm^2 is obtained. The sag in the middle of the span can be calculated from (14.46) with $x = a/2$ and $j = 0$ to be

$$f = 1/H \left[m_C g a^2/8 + G a/4 \right] = 1/25\,152 \cdot [0{,}998 \cdot 8{,}81 \cdot 400^2/8 + 2000 \cdot 400/4]$$
$$= 15{,}74 \text{ m} \quad .$$

While the horizontal tensile force is increased by 69 % the sag increases from 13,15 m to 15,74 m only, that means by 20 %.

14.7 Span with tension insulator sets at both ends

In a span with a short length and tension insulator sets at both ends, their effect on conductor tensile forces and sags cannot be neglected. In view of adequate consideration of the insulators, a distinction is to be made between rigid and flexible insulator sets. The first case corresponds to sets consisting of one long rod insulator, the second to an insulator set made of cap-and-pin insulators or with several long rod insulators. It applies to the case of a rigid insulator set (Figure 14.6)

$$L_{K,x} = L_K \Big/ \sqrt{1 + (V/H)^2} \approx L_K \left[1 - 1/2 \, (V/H)^2 \right] \quad . \tag{14.51}$$

The equivalent vertical load is in this case

$$V = 1/2 \, [m_C g (a - 2\, L_{K,x}) + G_K] \approx 1/2 \, [m_C g (a - 2\, L_K) + G_K] \quad , \tag{14.52}$$

where G_K is the weight of the insulator set, L_K the length of the insulator set, $m_C g$ the weight of the conductor per unit length and $L_{K,x}$ the length of the insulator set projected to the horizontal line.

For determination of the conductor tensile force H_2 at a temperature T_2 and with the conductor mass per unit length $m_{C2}g$, the following formula for the *conductor state change equation* can be obtained

$$H_2^2\Big\{H_2 - H_1 + EA\cdot\varepsilon_t(T_2-T_1) + E\cdot A/H_1^2 \cdot\left[\frac{(m_{C1}g)^2(a-2L_K)(a+4L_K)}{24} + \frac{G_{K1}\cdot m_{C1}g\cdot L_K}{2} + \frac{G_{K1}^2\cdot L_K}{4(a-2L_K)}\right]\Big\}$$
$$= E\cdot A\Big\{\frac{(m_{C2}g)^2(a-2L_K)(a+4L_K)}{24} + \frac{G_{K2}\cdot m_{C2}g\cdot L_K}{2} + \frac{G_{K2}^2\cdot L_K}{4(a-2L_K)}\Big\}\,. \quad (14.53)$$

In this equation, G_{K2} represents the insulator weight with ice load. Comparison with the conductor state change equation in the usual format (14.40) shows that the term $(m_Cg)^2a^2/24$ has been replaced by

$$\frac{(m_Cg)^2(a-2\,L_K)(a+4L_K)}{24} + \frac{G_K\cdot m_Cg\cdot L_K}{2} + \frac{G_K^2\cdot L_K}{4(a-2\,L_K)}\quad .$$

The sag consists of the lowering of the insulator set and the conductor sag in the middle of the span (Figure 14.6).
With $f_1 = (V/H)L_{K,x}$ and $f_2 = [(m_Cg)/(8H)](a-2L_{K,x})^2$, the total sag in the middle of the span results

$$f = (V/H)L_K\left[1 - 1/2\,(V/H)^2\right] + m_Cg(a-2\cdot L_{K,x})^2/(8\,H)\quad . \quad (14.54)$$

A flexible insulator set can be simulated by a conductor section with a length according to the length of the insulator set L_K, where the weight force of the insulator set is assumed to be uniformly distributed. The conductor state change equation can be expressed in the following format:

$$H_2^2\{H_2 - H_1 + E\cdot A\cdot\varepsilon_t(T_2-T_1) + E\cdot A/H_1^2 \cdot[(m_{C1}g)^2a^2/24 + G_{K1}\cdot m_{C1}g\cdot L_K/2 + G_{K1}^2\cdot L_K/(3\,a)]\}$$
$$= E\cdot A[(m_{C2}g)^2a^2/24 + G_{K2}\cdot m_{C2}g\cdot L_K/2 + G_{K2}^2\cdot L_K/(3\,a)]\quad . \quad (14.55)$$

The term $(m_Cg)^2\cdot a^2/24$ of the conductor state change equation (14.44) is replaced by

$$(m_Cg)^2\cdot a^2/24 + G_K\cdot m_Cg\cdot L_K/2 + G_K^2L_K/(3a)\quad .$$

The total sag will be

$$f = 1/(2\,H)(m_Cg\cdot a^2/4 + m_Cg\cdot L_K^2 + G_K\cdot L_K)\quad . \quad (14.56)$$

Example: The sags at 40°C and −5°C with an ice load of 10 N/m should be calculated for a span of $a = 50$ m and a conductor 565-AL1/72-ST1A (ACSR 564/72). The insulator sets are assumed to be 5,0 m long and weigh 150 kg without ice load and 200 kg with ice load, respectively. The conductor tensile stress should be 10 N/mm² at 10°C. The conductor cross section is 635,5 mm², the modulus of elasticity 68 kN/mm², the coefficient of linear expansion $19{,}4\cdot10^{-6}$/K. From (14.53) it follows for the condition +40°C

$$H_2^2\{H_2 - 10\cdot635{,}5 + 68\cdot10^3\cdot635{,}5\cdot0{,}0000194\cdot30 + 68\cdot10^3\cdot635{,}5/6355^2\cdot$$
$$\cdot[(2{,}116\cdot9{,}81)^2\cdot40\cdot70/24 + 150\cdot9{,}81\cdot2{,}116\cdot9{,}81\cdot5{,}0/2$$
$$+ (150\cdot9{,}81)^2\cdot5{,}0/(4\cdot40)]\} = 68\cdot10^3\cdot635{,}5\cdot[(2{,}116\cdot9{,}81)^2\cdot40\cdot70/24$$

$$+ 150 \cdot 9{,}81 \cdot 2{,}116 \cdot 9{,}81 \cdot 5{,}0/2 + (150 \cdot 9{,}81)^2 \cdot 5{,}0/(4 \cdot 40)] \quad .$$

With $H_2' = H_2/1000$, this equation can be transferred to $H_2'^2\{H_2' - 6{,}3 + 25{,}1 + 207{,}9\} = 8396{,}5$. Solving of this equation yields $H_2 = 6005$ N, eventually. From (14.55) it is obtained $H_2 = 6005$ N as well. With $V = (2{,}116 \cdot 9{,}81 \cdot 40 + 150 \cdot 9{,}81)/2 = 1150{,}9$ N, according to (14.52), the sag in the middle of the span follows from (14.54) to be

$$f = \frac{1150{,}9}{6005} \cdot 5{,}0\left[1 - \frac{1}{2}\left(\frac{1150{,}9}{6005}\right)^2\right] + \frac{2{,}116 \cdot 9{,}81(50 - 2 \cdot 4{,}91)^2}{8 \cdot 6005} = 1{,}64 \text{ m}$$

and from (14.56) $f = 1/(2 \cdot 6005)[(2{,}116 \cdot 9{,}81 \cdot 50^2)/4 + 2{,}116 \cdot 9{,}81 \cdot 5{,}0^2 + 150 \cdot 9{,}81 \cdot 5{,}0] = 1{,}74$ m. While the conductor tensile forces are the same, the sags differ by 0,1 m. For the condition $-5°$C with ice load, the conductor tensile forces can be calculated from (14.53) and (14.55) to be 9122 N and 9099 N, respectively. The sags can be calculated from (14.54) and (14.56) to be 1,54 and 1,64 m, respectively. Also in this case, virtually the same conductor tensile forces result under both assumptions, while the sags differ to a small extent. The sags are somewhat higher in the case of flexible insulator sets, the same conditions assumed.

14.8 Conductor forces and sags in a tensioning section

14.8.1 Introduction

In clauses 14.2 to 14.7 it was assumed that the conductors are rigidly fixed at their ends. This assumption, however, is only valid for earth wires which are directly fixed to the supports and for spans with tension insulator sets at both ends. At all suspension supports of an overhead power line, the conductors are attached to suspension insulator sets which can move in conductor longitudinal direction as well as rectangular to this direction. Changes in the condition, e. g. changes of the conductor tensile force in one span, affect the conductor tensile forces in the neighbouring spans as well. The effect of a change in the temperature depends on the span length. In case of differing spans in a *tensioning section*, the total tensioning section has to be taken into consideration, therefore. This applies particularly to the case of differing ice loads in the individual spans. The verification of the sags and *clearances to crossed objects* occurring under this condition is required in several standards. In the literature, a series of methods to determine the condition of the conductor in the tensioning section of an overhead power line is given [14.6] to [14.8].

Modern methods utilize the possibilities of computer programs and have been established, accordingly. Only these methods guarantee a sufficiently exact consideration of all impact factors and deliver results which comply with up-to-date requirements on accuracy. Hereafter, the determination of the *conductor tensile forces in a tensioning section* will be described, following the procedure presented in [14.6].

Regarding design and construction of overhead contact lines, the following assumptions can be made for the conductors:

- Conductor cross section and mass are constant in the tensioning section and do not depend on the temperature.
- Ice loads are at least uniformly distributed on the sagging curve in one span.
- The bending stiffness of the conductors can be neglected. Therefore, only tensile forces occur in the conductors.
- The coefficient of linear expansion and the modulus of elasticity do not depend on the conductor temperature or the tensile stress.
- The conductors are fixed rigidly at the suspension clamps, such that conductor tensile forces in line direction can be transferred to the insulator sets.

14.8.2 Conductor state in spans with end points movable in line direction

In case of a *temperature change* or the occurrence of ice load, the length of the sagging curve changes and, therefore, the conductor tensile force and the sag change as well. In addition, these quantities depend on the current state of the conductor. If the temperature of a conductor suspended movably at its ends changes from T_1 to T_2, then the conductor length in the state 2 can be obtained from (see also (14.39))

$$L_2 = L_1[1 + \varepsilon_t(T_2 - T_1)]\left[1 + (\overline{S}_2 - \overline{S}_1)/(E \cdot A)\right] \quad . \tag{14.57}$$

All quantities which refer to the initial state are marked by the index 1, all quantities which refer to the final state by the index 2. The mean conductor tensile force $\overline{S}$ is obtained from (14.20) to be $H \cdot L/a$. Since the terms $\varepsilon_t \cdot (T_2 - T_1)$ and $(\overline{S}_2 - \overline{S}_1)/(E \cdot A)$ are small compared to 1, their product can be neglected in (14.57) and the following relation is obtained

$$L_2 \approx L_1 + L_1 \cdot \varepsilon_t(T_2 - T_1) + L_1/(E \cdot A)\,[H_2(L_2/a) - H_1(L_1/a)] \quad . \tag{14.58}$$

The length L of the catenary curve can be taken from (14.14). For further processing, the hyperbolic sine function is developed into an exponential series and squared:

$$L = L_0\sqrt{1 + \frac{a^2}{L_0^2} \cdot \left(\frac{a^2}{12c^2} + \frac{a^4}{360c^4} + \ldots\right)} \quad ,$$

where $L_0 = \sqrt{a^2 + h^2}$ and $c = H/m_C g$. Since

$$\frac{a^2}{L_0^2}\left(\frac{a^2}{12\,c^2} + \frac{a^4}{360\,c^4} + \ldots\right) \ll 1$$

the square root can be again developed into a converging exponential series because of $\sqrt{1+x} \approx 1 + x/2 - x^2/8 + \ldots$:

$$L \approx L_0\left[1 + \frac{a^2}{L_0^2}\left(\frac{a^2}{24c^2} + \frac{a^4}{720c^4}\right) - \frac{a^4}{L_0^4} \cdot \frac{a^4}{1152c^4}\right] = L_0(1 + \overline{L}) \tag{14.59}$$

where the abbreviation $\overline{L}$ was used for

$$\overline{L} = \frac{a^2}{L_0^2}\left(\frac{a^2}{24c^2} + \frac{a^4}{720c^4}\right) - \frac{a^4}{L_0^4} \cdot \frac{a^4}{1152c^4} \quad .$$

Example: The accuracy of the approximation (14.59) should be verified compared with equation (14.14) by an example with extreme conditions. For the conductor 304-AL1/49-ST1A (ACSR 300/50) sagged with 45 N/mm^2 conductor tensile stress, the conductor length will be determined with both formulae. For a span length $a = 800$ m and 200 m difference in height, the relative error is only $1{,}32 \cdot 10^{-7}$. The formula (14.59) represents the conductor length in this case with an accuracy of approximately 0,1 mm, which is sufficiently precise.

In case of a rigid termination of the conductor at the ends, the lengths L_1 and L_2 differ only in the terms $\overline{L}_1$ and $\overline{L}_2$, which are both small compared to 1. Therefore, from (14.58) and (14.59) it is obtained:

$$\overline{L}_1 - \overline{L}_2 + \frac{L_0(1 + \overline{L}_1)}{a \cdot A \cdot E}[H_2(1 + \overline{L}_2) - H_1(1 + \overline{L}_1)] + \varepsilon_t(T_2 - T_1)(1 + \overline{L}_1) = 0\,. \tag{14.60}$$

The equation (14.60) represents the *conductor state change equation* for a span with suspension points of the conductor at differing height levels. In case of the difference of height $h = 0$, the well-known format of the conductor state change equation (14.40)

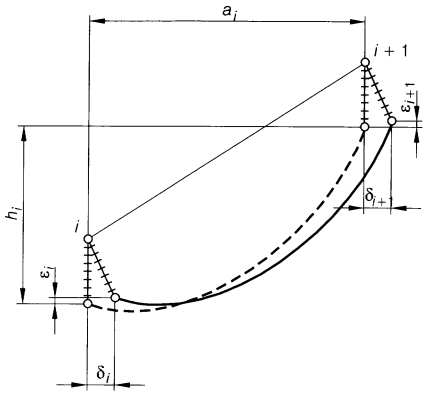

Figure 14.7: Change of the span length due to offset of the insulator set

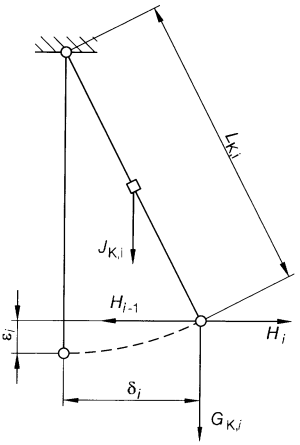

Figure 14.8: Equilibrium of forces at an insulator set

follows from (14.60), where $L_0 = a$, $\overline{L}_1$ and $\overline{L}_2$ are neglected compared to 1 and only the first term $a^2/24\,c^2$ is considered for $\overline{L}$.

In general, the conductors are adjusted at the insulator strings such that the suspension sets will hang vertically after clipping-in. The horizontal tensile forces are equal in all spans then in the condition which will be assumed as initial state in the following. Also in cases, where this assumption does not apply, the described method can be used accordingly.

If the conductor condition is changed, e. g. by an ice load in a span, the conductor tensile force is increased there with the effect that the suspension point moves into the span with the increased conductor tensile forces thus reducing the length there and increasing the length in the adjacent spans. By this procedure, the conductor tensile force is not increased to such an extent as in case of fixed attachment points. The sag, however, is increased to a larger extent. In this case, there will be a state of equilibrium between the effects of the horizontal forces in the adjacent spans and the vertical loads at the insulator set. It is the task then to calculate, for this state of equilibrium, the conductor tensile forces in the individual spans of a tensioning section considering the offset of the insulator sets. Finally, the sags can be determined from the conductor tensile forces.

The variation ΔL_i of the length L_{0i} of the line connecting the two attachment points of the span i caused by the offset of the insulator sets at the ends, is obtained from $\Delta L_i = L_{02,i} - L_{01,i} = \sqrt{(a_i + \Delta a_i)^2 + (h_i + \Delta h_i)^2} - \sqrt{(a_i)^2 + (h_i)^2}$. As an approximation hereof, it can be written:

$$\Delta L_i \approx (a_i \cdot \Delta a_i + h_i \cdot \Delta h_i)\,/L_{0i} \quad , \tag{14.61}$$

where Δa_i and Δh_i are the changes of the horizontal span length and vertical difference in height, respectively, within this span i (Figure 14.7). Between Δa_i and Δh_i, respectively, and the *offset of the insulator sets*, the following relations exist (Figure 14.7)

$$\Delta a_i = (\delta_{i+1} - \delta_{0,i+1}) - (\delta_i - \delta_{0,i}) \quad , \tag{14.62}$$

$$\Delta h_i = (\varepsilon_{i+1} - \varepsilon_{0,i+1}) - (\varepsilon_i - \varepsilon_{0,i}) \quad . \tag{14.63}$$

The values δ_i in this relations are the horizontal, the values ε_i the vertical displacements at the insulator sets. The values $\delta_{0,i+1}$ and $\varepsilon_{0,i+1}$ represent the displacements in the

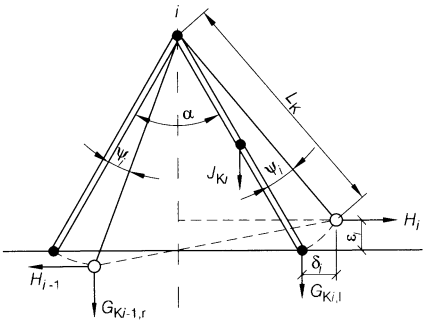

Figure 14.9: Forces and kinematics at an inverted V-insulator set

initial condition. These may be assumed to be zero in case of suspension insulator sets, while in case of tension insulator sets, they are determined by the equilibrium of the conductor tensile force and the dead weight of the insulator sets.
Due to the difference of the conductor tensile stresses in adjacent spans, the insulator sets are deflected such that there is an equilibrium of moments resulting from the vertical force at the insulator set and the horizontal components of the conductor tensile forces (Figure 14.8). From this condition, it is obtained

$$\delta_i = (H_i - H_{i-1}) \cdot L_{K,i} \,/\, \left(\sqrt{G_{K,i}^2 + (H_i - H_{i-1})^2}\right) \quad , \tag{14.64}$$

$$\varepsilon_i = \left[1 - G_{K,i} \,/\, \left(\sqrt{G_{K,i}^2 + (H_i - H_{i-1})^2}\right)\right] L_{K,i} \quad . \tag{14.65}$$

The equivalent vertical forces $G_{K,i}$ at the insulator sets consist of the vertical loadings in the adjacent spans according to (14.18) and the dead weight $J_{K,i}$ of the insulator set. For an insulator set at the support i, it applies

$$G_{K,i} = \frac{J_{K,i}}{2} + X_{i-1} H_0 \sinh\left[\frac{m_{Ci-1} g (a_{i-1} + x_{A,i-1})}{X_{i-1} H_0}\right] - X_i H_0 \sinh \frac{m_{Ci} g x_{A,i}}{X_i H_0} . \tag{14.66}$$

The horizontal conductor force H_i in the span i is expressed as a multiple of the initial horizontal force H_0: $H_i = X_i \cdot H_0$. The coordinate of the vertex $x_{A,i}$ results from (14.15) with the length of the conductor L_i from (14.14). It can be seen from (14.66) that the vertical insulator loading does not only depend on the span length and the conductor weights in the adjacent spans, but also on the difference in height between the adjacent attachment points and the conductor horizontal forces.

14.8.3 Conductor stresses and sags in case of inverted V-insulator sets

Inverted V insulator sets are sometimes used at suspension supports (Figure 14.9). This design reduces the swinging of the conductors in line direction in case of unbalanced ice loads of spans and the increase of conductor sag resulting thereof. By equipping existing supports with such insulator sets, increase of support heights can be waived that would be necessary otherwise. The kinematic and static behaviour of such arrangements differs essentially from that of conventional suspension sets. In [14.9], basic considerations are presented for determining the tensile forces and sags.
Compression forces are possible in the insulators of such sets. Therefore, the individual strings should be designed to be compression-resistant. The short conductor section between both suspension clamps leads to similar conditions as at a conductor fixed to a rigid insulator. In case of vibrations, a considerably higher strain is produced, therefore, compared with conventional suspension sets, requiring adequate vibration protection provisions.

Figure 14.9 shows the inverted V-arrangement in a swung position, too. With the symbols used in clause 14.8, it applies $\delta_i = L_K[\sin(\alpha/2 + \psi_i) - \sin\alpha/2]$ and $\varepsilon_i = L_K[\cos(\alpha/2) - \cos(\alpha/2 + \psi_i)]$. Using the addition formulae of the trigonometric functions as well as $\cos\psi_i \approx 1$; $\sin\psi_i \approx \psi_i$; then $\delta_i = L_K \cdot \psi_i \cdot \cos(\alpha/2)$ and $\varepsilon_i = L_K \cdot \psi_i \cdot \sin(\alpha/2)$ are obtained. The equilibrium of moments yields the equation for the angle ψ_i:

$$\psi_i = \frac{(H_i - H_{i-1})\cos(\alpha/2) + (G_{Ki-1,r} + G_{Ki,l})\sin(\alpha/2)}{(H_i + H_{i-1})\sin(\alpha/2) + (G_{Ki-1,r} + G_{Ki,l})\cos(\alpha/2)} \quad . \tag{14.67}$$

According to (14.66), $G_{Ki-1,r}$ and $G_{Ki,l}$ are obtained from:

$$G_{Ki-1,r} = J_{Ki}/2 + H_{i-1}\sinh[m_{Ci-1}g(a_{i-1} + x_{A,i-1})/H_{i-1}] \quad , \tag{14.68}$$

$$G_{Ki,l} = J_{Ki}/2 + H_i \sinh[m_{Ci}g \cdot x_{A,i}/H_i] \quad .$$

The values δ_i and ε_i can be inserted into equations (14.62) and (14.63) together with (14.67) and (14.68). Then, the horizontal conductor tensile forces can be calculated, as described in clauses 14.8.4 and 14.8.5.

In [14.9], the consequences of the inverted V-application are mentioned by means of an example for a 110 kV line equipped with the conductor 184-AL1/30-ST1A. Assuming an opening angle of 60° for the inverted V, a 2,42 m higher clearance to ground is obtained in case of 6,9 N/m local ice load in the span studied. The use of inverted V-insulator sets at suspension supports results in higher differences of the conductor tensile forces in the adjacent spans. With the example mentioned, this difference is 4,0 kN, compared with 1,3 kN in case of conventional suspension sets. In general, suspensions supports are designed for such unbalanced loads in ice-prone regions. The design with an opening angle of 60° represents a useful compromise between reduction of sag and limiting the load increase of the suspension supports.

14.8.4 Conductor state change equation for a tensioning section

The displacements of the insulator sets change the span lengths and the conductor condition in the adjacent spans. According to (14.58), the *conductor state change equation* for the span i can be established, assuming that, in the initial condition, all insulator sets hang vertically and, therefore, the conductor tensile forces in all spans are equal to H_0:

$$L_{02,i}(1 + \overline{L}_{2,i}) = L_{01,i}(1 + \overline{L}_{1,i}) + L_{01,i} \cdot \varepsilon_t(1 + \overline{L}_{1,i}) \cdot (T_2 - T_1) \tag{14.69}$$

$$+ \frac{L_{01,i}(1 + \overline{L}_{1,i})}{a_i \cdot E \cdot A} \cdot \left[\left(1 + \overline{L}_{2,i}\right) L_{02,i} \cdot X_i \cdot H_0 - \left(1 + \overline{L}_{1,i}\right) L_{01,i} \cdot H_0\right] \quad .$$

In (14.69), the horizontal tensile force $H_{2,i}$ in the condition 2 was expressed as $X_i \cdot H_0$ and in the condition 1 the conductor tensile force $H_{1,i}$ is equal to H_0. The difference in the span length $L_{02,i} - L_{01,i}$ is equal to the change of span lengths due to the displacement of the insulator sets and results from (14.61). For the further steps of calculation, $L_{02,i} \approx L_{01,i} \approx L_{0,i}$ can be used. Then it is obtained from (14.69):

$$(L_{1,i} - L_{2,i}) + (1 + \overline{L}_{1,i})\frac{L_{0,i}}{a_i \cdot E \cdot A}\left[X_i \cdot H_0\left(1 + \overline{L}_{2,i}\right) - H_0\left(1 + \overline{L}_{1,i}\right)\right] \tag{14.70}$$

$$+ (1 + \overline{L}_{1,i})\varepsilon_t(T_2 - T_1) - \frac{a_i \cdot \Delta a_i + h_i \cdot \Delta h_i}{L_{0,i}^2} = 0 \quad , \quad i = 1, 2, \ldots, n$$

With (14.62) to (14.65) as well as

$$\overline{L}_{2,i} = \frac{a_i^2}{L_{0,i}^2}\left[\frac{a_i^2 \cdot (m_{C2,i}g)^2}{24\,(X_i \cdot H_0)^2} + \frac{a_i^4 \cdot (m_{C2,i}g)^2}{720\,(X_i \cdot H_0)^4}\right] - \frac{a_i^4}{L_{0,i}^4}\left[\frac{a_i^4 \cdot (m_{C2,i}g)^4}{1152\,(X_i \cdot H_0)^4}\right] \tag{14.71}$$

from (14.59), a system of n equations for the conductor tensile forces $H_{2,i} = X_i \cdot H_0 (i = 1, 2, \ldots, n)$ is obtained from (14.70), where n is the number of spans within the tensioning section:

$$\left.\begin{aligned}
&X_1^4[X_1 \cdot K_{1,1}K_{2,1} - C_1(X_1, X_2)] \\
&\qquad + \left(X_1 \cdot K_{1,1} - \frac{E \cdot A}{H_0}\right) \cdot (X_1^2 \cdot K_{3,1} + K_{4,1}) \frac{a_1^2}{L_{0,1}^2} = 0, \\
&X_2^4[X_2 \cdot K_{1,2}K_{2,2} - C_2(X_1, X_2, X_3)] \\
&\vdots \qquad + \left(X_2 \cdot K_{1,2} - \frac{E \cdot A}{H_0}\right) \cdot (X_2^2 \cdot K_{3,2} + K_{4,2}) \frac{a_2^2}{L_{0,2}^2} = 0, \\
&X_i^4[X_i \cdot K_{1,i}K_{2,i} - C_i(X_{i-1}, X_i, X_{i+1})] \\
&\vdots \qquad + \left(X_i \cdot K_{1,i} - \frac{E \cdot A}{H_0}\right) \cdot (X_i^2 \cdot K_{3,i} + K_{4,i}) \frac{a_i^2}{L_{0,i}^2} = 0, \\
&X_{n-1}^4[X_{n-1} \cdot K_{1,n-1}K_{2,n-1} - C_{n-1}(X_{n-2}, X_{n-1}, X_n)] \\
&\quad + \left(X_{n-1} \cdot K_{1,n-1} - \frac{E \cdot A}{H_0}\right) \cdot (X_{n-1}^2 \cdot K_{3,n-1} + K_{4,n-1}) \frac{a_{n-1}^2}{L_{0,n-1}^2} = 0, \\
&X_n^4[X_n \cdot K_{1,n}K_{2,n} - C_n(X_{n-1}, X_n)] \\
&\qquad + \left(X_n \cdot K_{1,n} - \frac{E \cdot A}{H_0}\right) \cdot (X_n^2 \cdot K_{3,n} + K_{4,n}) \frac{a_n^2}{L_{0,n}^2} = 0.
\end{aligned}\right\} \quad (14.72)$$

In equation (14.72), the following terms are used:

$$\left.\begin{aligned}
&K_{1,i} = (1 + \overline{L}_{1,i}) \frac{L_{0,i}}{a_i} \quad , \\
&K_{2,i} = -(1 + \overline{L}_{1,i})^2 \frac{L_{0,i}}{a_i} + \frac{E \cdot A}{H_0} \overline{L}_{1,i} + \frac{E \cdot A \cdot \varepsilon_t}{H_0} (1 + \overline{L}_{1,i}) \cdot (T_2 - T_1), \\
&K_{3,i} = \frac{a_i^2 \cdot (m_{C2,i} g)^2}{24 H_0^2} \quad , \\
&K_{4,i} = \frac{a_i^4 \cdot (m_{C2,i} g)^4}{720 H_0^4} - \frac{a_i^2}{L_{0,i}^2} \cdot \frac{a_i^4 \cdot (m_{C2,i} g)^4}{1152 H_0^4} \quad , \\
&L_{1,i} = \frac{a_i^2}{L_{0,i}^2} \left(\frac{a_i^2 \cdot (m_{C1} g)^2}{24 H_0^2} + \frac{a_i^4 \cdot (m_{C1} g)^4}{720 H_0^4} \right) - \frac{a_i^4}{L_{0,i}^4} \cdot \frac{a_i^4 \cdot (m_{C1} g)^4}{1152 H_0^4} \\
&C_i(X_{i-1}, X_i, X_{i+1}) = \\
&= \frac{E \cdot A \cdot a_i}{H_0 \cdot L_{0,i}^2} \left\{ \left[\frac{X_{i+1} - X_i}{\sqrt{(G_{K,i+1}/H_0)^2 + (X_{i+1} - X_i)^2}} L_{K,i+1} - \delta_{0,i+1} \right] \right. \\
&\left. - \left[\frac{X_i - X_{i-1}}{\sqrt{(G_{K,i}/H_0)^2 + (X_i - X_{i-1})^2}} L_{K,i} - \delta_{0,i} \right] \right\} \\
&+ \frac{E \cdot A \cdot a_i}{H_0 \cdot L_{0,i}^2} \left\{ \left[\left(1 - \frac{G_{K,i+1}/H_0}{\sqrt{(G_{K,i+1}/H_0)^2 + (X_{i+1} - X_i)^2}} \right) L_{K,i+1} - \varepsilon_{0,i+1} \right] \right. \\
&\left. - \left[\left(1 - \frac{G_{K,i}/H_0}{\sqrt{(G_{K,i}/H_0)^2 + (X_i - X_{i-1})^2}} \right) L_{K,i} - \varepsilon_{0,i} \right] \right\} \quad .
\end{aligned}\right\} \quad (14.73)$$

The terms C_i, which depend in each case on the conductor tensile forces of three consecutive spans, couple the equations of (14.72). In particular (14.73) yields $C_1 = C_1 \cdot (X_1, X_2)$ with $X_0 = 0$ and $C_n = C_n(X_{n-1}, X_n)$ with $X_{n+1} = 0$. The quantities $\delta_{0,i}$; $\delta_{0,i+1}$; $\varepsilon_{0,i}$ and $\varepsilon_{0,i+1}$ represent the offsets in the initial condition. These offsets are zero

in general at the suspension supports and can be calculated for the strain supports at the begin and end of the tensioning section from (14.64) and (14.65).
The equations (14.72) form a system of coupled non-linear equations. In the equation i of the system, the relative conductor tensile force X_i in span i and the conductor tensile forces X_{i-1} and X_{i+1} in the neighbouring spans $i-1$ and $i+1$ occur. The coupling is due to the movement of the insulator sets, as can be seen from (14.72) and (14.73). The system of equations delivers the n unknown conductor tensile forces in the individual spans of a tensioning section with n spans, if the condition of the conductor changes, e. g. by variation of temperatures or due to ice loads. Analogously to the conductor state change equation (14.40) for an individual span with fixed conductor attachment points, the system of equations (14.72) represents the *conductor state change equation* for a tensioning section with movable insulator sets at the suspension supports. For a tensioning section with n spans, therefore, n non-linear coupled equations have to be solved. An explicit solution of this equation system is not possible. To determine the unknown variables X_i, numerical iteration methods are adopted. With the aid of electronic computers, the equation system can be solved with sufficient accuracy for all occurring cases.
The *Newton approximation method* with an expansion to systems of non-linear equations can be adopted [14.10] for solving the conductor state change equations (14.40) for the individual span and the system of conductor state change equations (14.72). According to this method, the solution of the system of equations

$$f_i(X_1, X_2, \ldots, X_n) = 0 \quad , \qquad (i = 1, 2, \ldots, n) \quad , \tag{14.74}$$

is to be found, where f_i are non-linear functions of the unknown variables X_1, X_2, ..., X_n. The equations (14.74) can be expressed as

$$\boldsymbol{f}(\boldsymbol{X}) = \begin{pmatrix} \boldsymbol{f}_1(\boldsymbol{X}) \\ \boldsymbol{f}_2(\boldsymbol{X}) \\ \vdots \\ \boldsymbol{f}_n(\boldsymbol{X}) \end{pmatrix} = \begin{pmatrix} \boldsymbol{f}_1(X_1, X_2, \ldots X_n) \\ \boldsymbol{f}_2(X_1, X_2, \ldots X_n) \\ \vdots \\ \boldsymbol{f}_n(X_1, X_2, \ldots X_n) \end{pmatrix} = 0 \quad . \tag{14.75}$$

The functions $\boldsymbol{f}_i$ can be differentiated in the considered range of the elements X_i of the vector $\boldsymbol{X}$ and the differentials are

$$\boldsymbol{f}_{ik}(\boldsymbol{X}) = \frac{\partial f_i(X_1, X_2, \ldots, X_n)}{\partial X_k} \qquad (i, k = 1, 2, \ldots, n) \quad . \tag{14.76}$$

The differentials can be represented by the following matrix:

$$\boldsymbol{F}(\boldsymbol{X}) = \begin{pmatrix} f_{11}(\boldsymbol{X}), & f_{12}(\boldsymbol{X}), & \ldots, & f_{1n}(\boldsymbol{X}) \\ f_{21}(\boldsymbol{X}), & f_{22}(\boldsymbol{X}), & \ldots, & f_{2n}(\boldsymbol{X}) \\ \vdots & & & \vdots \\ f_{n1}(\boldsymbol{X}), & f_{n2}(\boldsymbol{X}), & \ldots, & f_{nn}(\boldsymbol{X}) \end{pmatrix} \quad . \tag{14.77}$$

Furthermore, it can be assumed that the differentials $\boldsymbol{F}(\boldsymbol{X})$ have an inverse $[\boldsymbol{F}(\boldsymbol{X})]^{-1}$. With these symbols, the iteration process of the Newton method for a system of non-linear equations is described by:

$$\boldsymbol{X}_{\nu+1} = \boldsymbol{X}_\nu - [\boldsymbol{F}(\boldsymbol{X}_\nu)]^{-1}(\boldsymbol{f}(\boldsymbol{X}_\nu)) \quad . \tag{14.78}$$

For a given adequately selected start vector $\boldsymbol{X}_0$ with approximate values for the solutions of the equation system (14.72), values $\boldsymbol{X}_{\nu+1}$ are obtained from (14.78), improved step by step.
From (14.72), together with (14.73), (14.66), (14.14) and (14.15), it can be seen that the relation between the functions f_i and the unknown variable X_i for the condition of the

Table 14.1: Conductor states within a tensioning section of an overhead line

```
 SIEMENS AG DEPT PTDH158 TRANSMISSION LINES

COMPUTATION AND PLOT OF LONGITUTINAL PROFILE WITH CONDUCTOR

 110 kV LINE                                HT76 Fuerstenberg - Waren
 CONDUCTOR : 2*3*1 * ACSR 265/35 * 47.0 N/QMM

 LINE SECTION FROM TOWER  NO.   1                        TO TOWER NO. 4

 CONDUCTOR LEVEL 1                                                 LEFT PHASE
 ****************
 CROSS SECTION DIAMETER   WEIGHT   MOD. E   EXP.COEF. STRENGTH
   SQMM   SQMM       MM     KG/M  KN/SQMM        1/K   N/SQMM
 263.66  34.09    22.40     .998   74.000    .0000196   278.51                *

 LIMITS        TEMPERATURE    ICE LOAD    WIND LOAD       TENSION
 ******           DEGREE C         N/M         N/M         N/SQMM
                     -20.0        .000        .000         500.00             *
                      -5.0       7.240        .000         500.00             *
                      10.0        .000        .000          47.00             *

 STARTING             10.0        .000        .000          47.00 #
 CONDITION           -20.0        .000        .000          53.03
                      -5.0       7.240        .000          79.39

               TOWER POSITION  CROSSARM            INSULATOR SET
 TOWER                HEIGHT  HEIGHT      LENGTH  TYPE LENGTH WEIGHT
 NO. TYPE    STATIONS  AB.SEA          LEFT RIGHT

 1   TT+0         .00  285.50   16.00 -6.00  6.00    DA   3.00   2000          *
 2   ST+3      251.00  284.50   17.20 -4.00  4.00    DH   1.80   1000          *
 3   ST+12     676.00  261.05   26.20 -4.00  4.00    DH   1.80   1000          *
 4   TT+0      910.00  247.00   16.00 -6.00  6.00    DA   3.00   2000          *

 TOWER          PHASE EXTENSION
 NO. TYPE          LEFT  SY.-AXIS     RIGHT   CROSSARM ANGLE

 1   TT+0           .47       .00      -.47 M    105.000 GON
 4   TT+0          1.45       .00     -1.45 M    115.500 GON

 EQUIVALENT SPAN                     340.49 M

 COMPUTED CONDITION   10.0        .000         .000
 ************************************************


 TOWER  PHASE   SAG  TENSION N/SQMM     VERTEX       INSULATOR SET  WEIGHT SPAN
 NO.    LENGTH       HORIZ.SUPPORT(L/R) DIST. HEIGHT HORIZ VERT    RIGHT LEFT

 1     251.48  5.64  47.00 47.20 47.16  133.6  295.0  2.96  .48    133.6
 2     425.00 15.83  47.00 47.78 47.31  260.9  276.0   .00 1.80    260.9 117.8
 3     235.45  4.98  47.00 47.75 47.01  255.0  262.7   .00 1.80    255.0 164.1
 4                                                   -3.00  .17          -19.5

 COMPUTED CONDITION  -20.0        .000         .000
 ************************************************


 TOWER  PHASE   SAG  TENSION N/SQMM     VERTEX       INSULATOR SET  WEIGHT SPAN
 NO.    LENGTH       HORIZ.SUPPORT(L/R) DIST. HEIGHT HORIZ VERT    RIGHT LEFT

 1     251.48  4.98  53.14 53.31 53.27  134.8  295.7  2.97  .43    134.8
 2     425.00 14.11  52.74 53.47 53.00  266.9  277.6  -.05 1.80    266.9 116.7
 3     235.45  4.39  53.22 53.98 53.24  273.1  262.4   .05 1.80    273.1 158.1
 4                                                   -3.00  .11          -37.6

 COMPUTED CONDITION   40.0        .000         .000
 ************************************************


 TOWER  PHASE   SAG  TENSION N/SQMM     VERTEX       INSULATOR SET  WEIGHT SPAN
 NO.    LENGTH       HORIZ.SUPPORT(L/R) DIST. HEIGHT HORIZ VERT    RIGHT LEFT

 1     251.48  6.26  42.33 42.55 42.51  132.8  294.4  2.95  .53    132.8
 2     425.00 17.42  42.71 43.55 43.07  256.5  274.5   .05 1.80    256.5 118.7
 3     235.45  5.54  42.26 43.01 42.26  241.2  262.8  -.05 1.80    241.2 168.5
 4                                                   -2.99  .22          -5.7

 COMPUTED CONDITION   80.0        .000         .000
 ************************************************


 TOWER  PHASE   SAG  TENSION N/SQMM     VERTEX       INSULATOR SET  WEIGHT SPAN
 NO.    LENGTH       HORIZ.SUPPORT(L/R) DIST. HEIGHT HORIZ VERT    RIGHT LEFT

 1     251.48  7.06  37.58 37.82 37.79  131.9  293.6  2.94  .60    131.9
 2     425.00 19.34  38.45 39.34 38.87  252.1  272.7   .11 1.80    252.1 119.6
 3     235.45  6.26  37.43 38.18 37.43  227.1  262.7  -.12 1.80    227.1 172.9
 4                                                   -2.99  .28           8.3
```

Table 14.1: (continued)

```
COMPUTED CONDITION   -5.0       7.240         .000
**************************************************

TOWER  PHASE   SAG  TENSION N/SQMM     VERTEX       INSULATOR SET WEIGHT SPAN
NO.   LENGTH        HORIZ.SUPPORT(L/R) DIST. HEIGHT HORIZ VERT    RIGHT LEFT

1     251.48  5.80  78.86 79.21 79.14  133.8  294.9  2.97  .41    133.8
2     425.00 16.35  79.13 80.53 79.70  259.4  275.5   .02 1.80    259.4 117.6
3     235.45  5.12  78.80 80.09 78.81  249.4  262.8  -.02 1.80    249.4 165.6
4                                                   -3.00  .09          -14.0

COMPUTED CONDITION   -5.0     LOCAL ICE LOAD      3.620 N/M
**********************************************************

TOWER  PHASE   SAG  TENSION N/SQMM     VERTEX       INSULATOR SET WEIGHT SPAN
NO.   LENGTH        HORIZ.SUPPORT(L/R) DIST. HEIGHT HORIZ VERT    RIGHT LEFT

1     251.48  6.71  53.71 54.03 53.98  132.3  294.0  2.96  .51    132.3
2     425.00 16.59  61.37 62.48 61.83  258.7  275.3   .11 1.80    258.7 119.2
3     235.45  5.96  53.29 54.31 53.29  231.3  262.8   .17 1.79    231.3 166.3
4                                                   -2.99  .19           4.1

COMPUTED CONDITION   -20.0     INSULATOR FAILURE TOWER 1
**********************************************************

TOWER  PHASE   SAG  TENSION N/SQMM     VERTEX       INSULATOR SET WEIGHT SPAN
NO.   LENGTH        HORIZ.SUPPORT(L/R) DIST. HEIGHT HORIZ VERT    RIGHT LEFT

1     251.48  5.31  49.84 50.03 49.99  134.2  295.4  2.97  .46    134.2
2     425.00 14.99  49.65 50.41 49.93  263.7  276.8  -.02 1.80    263.7 117.3
3     235.45  4.69  49.88 50.64 49.89  263.4  262.5   .03 1.80    263.4 161.3
4                                                   -3.00  .14          -27.9

COMPUTED CONDITION   -20.0     INSULATOR FAILURE TOWER 4
**********************************************************

TOWER  PHASE   SAG  TENSION N/SQMM     VERTEX       INSULATOR SET WEIGHT SPAN
NO.   LENGTH        HORIZ.SUPPORT(L/R) DIST. HEIGHT HORIZ VERT    RIGHT LEFT

1     251.48  5.31  49.84 50.03 49.99  134.2  295.4  2.97  .46    134.2
2     425.00 14.99  49.65 50.41 49.93  263.7  276.8  -.02 1.80    263.7 117.3
3     235.45  4.69  49.88 50.64 49.89  263.4  262.5   .03 1.80    263.4 161.3
4                                                   -3.00  .14          -27.9

COMPUTATION OF WRIGHT-OF-WAY ZONE AND CONDUCTOR CURVE
**************************************************

COMPUTED CONDITION   TEMPERATURE   40.000 DEGREE C

SPAN LENGTH LEFT    251.48 M    SAG         6.26 M
SPAN LENGTH RIGHT   250.54 M    SAG         6.22 M

TOWER NO.                          1                  2                *
SUSPwnsion POINT HEIGHT          301.50             299.90
CROSSARM LENGTH                    6.00               4.00             *
WRIGHT-OF-WAY AT CROSA. DIR.       9.01               8.27
REQ. CLEARANCE                     3.00                                *

INS.STR.SWING ANGLE     .00 GON  49.83 GON   WIND ON INSULATO  300.00 N
CONDUCT.SWING ANGLE   56.10 GON   LEFT       WIND ON CONDUCTOR  11.87 N/M

      DISTANCE FROM        HALF    ALTITUDE    ALTITUDE
         LEFT TOWER       WIDTH   STILL AIR       SWUNG

              -.71       -8.98      301.50      301.50
               .00       -9.04      301.41      301.45
             31.38      -11.15      298.38      299.51
             62.75      -12.51      296.30      298.18
             94.13      -13.28      294.98      297.33
            115.31      -13.46      294.53      297.04
            156.88      -13.05      294.65      297.11
            188.25      -12.04      295.64      297.73
            219.63      -10.45      297.38      298.83
            251.00       -8.27      299.90      300.42

  WRIGHT-OF-WAY  AREA:      (SQUARE M)     TOTAL
                 PARABOLA                 5940.94
                 STRAIGHT LINES           6731.56
```

conductors within a tensioning section of an overhead contact line is very complicated. According to (14.72), the functions depend on the vertical forces $G_{K,i}$ at the insulator set; these again depend on the unknown variables X_i and the coordinates of the vertices $x_{A,i}$ of the sagging curves. The coordinates $x_{A,i}$ are functions of the unknown variables X_i and the conductor lengths L_i. Because of this reason, an explicit calculation of the differentials and, in the next step, the functional matrix is not advisable. Therefore, this matrix is approximated by:

$$\boldsymbol{f}_{ik}(\boldsymbol{X}) = [f_i(X_i, \ldots, X_k + p_k, \ldots, X_n) - f_i(X_i, \ldots, X_k p_k, \ldots, X_n)] / (2p_k), \quad (14.79)$$

where the quantities p_k represent the elements of a suitably selected vector $\boldsymbol{P}$ for the step widths.

14.8.5 Computer program for conductor state change in a tensioning section

The method described for determining the conductor state change in a tensioning section of an overhead line can be utilized practically, only with the aid of computers. The programming should not be explained in detail here. With the described methods, the following problems can be studied and solved:

- Influence of differences in the span length on sags and tensile stresses,
- Influence of differing conductor temperatures,
- Influence of the insulator length,
- Influence of differences in heights of the suspension points,
- Exact determination of the sags, in case of local ice loads,
- Influence of ice loads in parts of the tensioning section,
- Effects of concentrated loads,
- Line sections with inverted V-insulator sets,
- Conductor tensile forces after failure of a conductor.

In Table 14.1 results for a typical tensioning section of an overhead power line are summarized. For this calculations it was assumed that, at a temperature of 10°C, all insulator sets hang vertically, i. e. the conductor forces in the individual spans of the tensioning sections are equal. For each condition the sag, the conductor tensile stresses in the vertex and at the suspension points and the position of the vertex, as well as the offsets of the insulator sets in each span, are calculated.

14.8.6 Approximate formulae of sags at ice load in one span only

Although computer programs are available to calculate the sags precisely and without high effort in case of an *ice local load* only in one span of a tensioning section approximate values for the needed sag may help in some cases.
The relation for the sag with ice load in one span only is

$$f_{II} = K_1 \cdot K_2 \cdot K_3 \cdot K_4 \cdot f_{(-5°+m_{CI}g)} \quad , \quad (14.80)$$

where $f_{(-5°+m_{CI}g)}$ means the sag in this span with ice load $m_{CI} \cdot g$, when an ice load is present in all spans of the tensioning section. This sag can be determined by using the equivalent span of the tensioning section. The factor K_1 is obtained from

$$K_1 = \sqrt{2 \Big/ \left[1 + \left(\frac{m_C g}{m_{CI} g + m_C g}\right)^2\right]} \quad . \quad (14.81)$$

There, $m_C g$ represents the conductor dead weight per unit length. The factor K_2 takes care of the position of the crossing span, in relation to the tension towers of the tensioning section; it depends also on the conductor material and is listed in Table 14.2. The

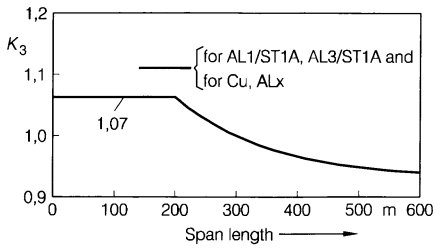

Figure 14.10: Factor K_3 depending on the span length a.

Table 14.2: Factor K_2 for the position of the crossing span within the tensioning section

	Span 1 and n	Span 2 and $n-1$	Spans 3 to $n-2$
ALx/ST1A and ALx	1,03	1,06	1,07
Aluminium	1,05	1,09	1,11

Table 14.3: Factor K_4 depending on the nominal voltage and the length of insulator sets

U_n in kV	20			110	220	380
L_K in m	0,5	0,80	1,00	1,80	3,25	5,00
K_4	0,94	0,95	0,96	1,00	1,02	1,03

factor K_3 takes care of the length of the crossing span and can be taken from Figure 14.10. Finally, the factor K_4 depends on the length of the insulator sets whereby K_4 is equal to 1,0 in case of lengths between 1,80 and 2,0 m, which are typical for 110 kV lines (Table 14.3).
The relation (14.80) delivers sufficiently exact results for ice loads $m_{CI} \cdot g$ less than 10 N/m and for conductors AL1/ST1A, ALx/ST1A and ALx, up to span lengths of 600 m, as well as for AL1 conductors up to 350 m span length. In case of spans with higher differences in the suspension heights or in lengths of adjacent spans, errors of unacceptable magnitude may occur.

Example: The sag of the last span of a tensioning section with six spans, equipped with the conductor 264-AL1/34-ST1A, span length 355 m, voltage 220 kV should be determined at $-5°C$ and local ice load. Conductor dead weight: $(m_C g) = 9{,}81 \cdot 0{,}998 = 9{,}79$ N/m, local ice load: $(m_{CI} g) = 3{,}62$ N/m.
The conductor tensile stress at $-5°C$ and 3,62 N/m ice load in the total tensioning section is assumed to be 68,0 N/mm^2.
Sag with ice load: $f_{(-5°+m_{CI}g)} = (355^2\,(9{,}79 + 3{,}62))/(8 \cdot 297{,}8 \cdot 68{,}0) = 10{,}43$ m,

$$K_1 = \sqrt{2 \Big/ \left[1 + \left(\frac{9{,}79}{13{,}41}\right)^2\right]} = 1{,}142\,,$$

$K_2 = 1{,}03$ (last span); $K_3 = 0{,}985$ for $a = 355$ m and conductor AL1/ST1A; $K_4 = 1{,}02$ (220 kV). With this data it is obtained from (14.80):

$$f_{II} = 10{,}43 \cdot 1{,}142 \cdot 1{,}03 \cdot 0{,}985 \cdot 1{,}02 = 12{,}33 \text{ m}\,.$$

14.9 Clearances to ground and to objects

14.9.1 Requirements

In clause 2.5.2.7, Table 2.23, the required minimum *clearances to ground surface* and *to crossed objects*, according to EN 50 341-1 [14.11], are given with the corresponding loading cases. For verification of compliance with these data, the clearances between the conductors and the ground or crossed objects at the maximum conductor temperature, for the sags under ice load and in case of ice load only in one span of the relevant tensioning section, have to be determined. For this purpose, at first the corresponding conductor tensile stresses have to be determined. This can be achieved by means of the methods described in clauses 14.5, 14.8.4 and 14.8.5. The practical calculation is demonstrated by means of the example of a tensioning section of a 110 kV line (Figure 15.18) hereafter.

The tensioning section consists of three spans equipped with the conductor 264-AL1/34-ST1A (ACSR 265/35), according to EN 50 182. The initial tensile stress at $T_1 = 10°C$ is assumed to be 47 N/mm^2 (everyday stress). By means of the mentioned data and the formulae given in the clauses 14.2, 14.3 and 14.8.6, the *clearance of the conductor to terrain*, to a crossed road and to a crossed overhead power line will be calculated. The differences between the results of a simplified and the exact calculation with computer programs will be demonstrated.

14.9.2 Calculation of clearance to ground

The equivalent span length results from (14.43) to be

$$a_{\mathrm{id}} = \frac{\sum a^3}{\sum a} = \sqrt{\frac{251{,}0^3 + 425{,}0^3 + 234{,}0^3}{251{,}0 + 425{,}0 + 234{,}0}} = 340{,}32 \text{ m} \quad ,$$

the horizontal tensile stress is obtained from (14.45)

$$\sigma_2^2\left[\sigma_2 - \sigma_1 + \frac{E \cdot (m_{\mathrm{C1}} g \cdot a)^2}{24 \cdot \sigma_1^2 \cdot A^2} + E \cdot \varepsilon_{\mathrm{t}}(T_2 - T_1)\right] = \frac{E \cdot (m_{\mathrm{C2}} g \cdot a)^2}{24 \cdot A^2} \quad ,$$

and the sag from (14.16) with $x = 0$

$$f_{\mathrm{id}} = \frac{\sigma \cdot A}{m_{\mathrm{C}} g} \cdot \left[\cosh\left(\frac{m_{\mathrm{C}} g\, a_{\mathrm{id}}}{2\sigma \cdot A}\right) - 1\right] \quad .$$

With the given data: $\sigma_1 = 47$ N/mm^2; $T_1 = 10°C$; $m_{\mathrm{C1}} = 0{,}998$ kg/m; $A = 297{,}8$ mm^2; $d = 22{,}4$ mm; $E = 74\,000$ N/mm^2; $\varepsilon_{\mathrm{t}} = 19{,}6 \cdot 10^{-6}$ 1/°C
it results for $T_2 = -5°C$ and $m_{\mathrm{C2}} = 0{,}998 + (5 + 0{,}1 \cdot 22{,}4)/9{,}81 = 1{,}736$ kg/m:

$$\sigma_{2,\mathrm{id}} = 79{,}38 \text{ N/mm}^2 \text{ and } f_{2,\mathrm{id}} = 10{,}44 \text{ m}$$

and for $T_2 = -20°C$ and $m_{\mathrm{C2}} = 0{,}998$ kg/m, it follows $\sigma_{2,\mathrm{id}} = 53{,}03$ N/mm^2 and $f_{2,\mathrm{id}} = 8{,}98$ m and finally for $T_2 = 80°C$ and $m_{\mathrm{C2}} = 0{,}998$ kg/m $\sigma_{2,\mathrm{id}} = 38{,}00$ N/mm^2 and $f_{2,\mathrm{id}} = 12{,}55$ m.
Since the equivalent sag at $T = 80°C$ is higher than the sag at $T = -5°C$ and ice load the first condition will prevail. With these data the clearance between conductor and ground is calculated in the span 2 (Figures 15.18 and 14.11) at the longitudinal coordinate 506,0 m. The sag in span 2, having a span length a_2, can be determined from the sag in the equivalent span:

$$f_2 = (a_2/a_{\mathrm{id}})^2 \cdot f_{\mathrm{id}} \tag{14.82}$$

For the example, the sag in middle of the span 2 (Figure 15.18) with the span length $a_2 = 425$ m has to be determined. It is obtained

$$f_2 = \left(\frac{425{,}00}{340{,}32}\right)^2 \cdot 12{,}55 \text{ m} = 19{,}58 \text{ m}.$$

The sag at the studied position ξ is obtained from (14.26) $f_\xi = 4 \cdot f_{\max}\, \xi/a\,(1 - \xi/a)$ with $\xi = 255$ m (Figure 14.11) to be $f_\xi = 18{,}80$ m.
The available clearance a_ξ at the position ξ results from

$$a_\xi = h_{oi} - (h_{oi} - h_{oi+1})\,\xi/a_{\mathrm{i}} - f_\xi - \mathrm{NN}_\xi \quad . \tag{14.83}$$

In the example, there are $h_{oi} = 299{,}9$ m, $h_{oi+1} = 285{,}45$ m and $\mathrm{NN}_\xi = 266{,}0$ m.
The available clearance is 6,43 m, therefore. According to EN 50 341-1 [14.11], a minimum clearance of $(5 + D_{\mathrm{el}})$ m with $D_{\mathrm{el}} = 1{,}0$ m is required. Therefore, the available clearance complies with this requirement. The results of the calculation are given in Table 14.4 together with the results obtained by a computer program. Although the difference in height in the span 3 is 22,45 m and the span length in span 2 is approximately 25% higher than the equivalent span, the results differ only to a small extent.

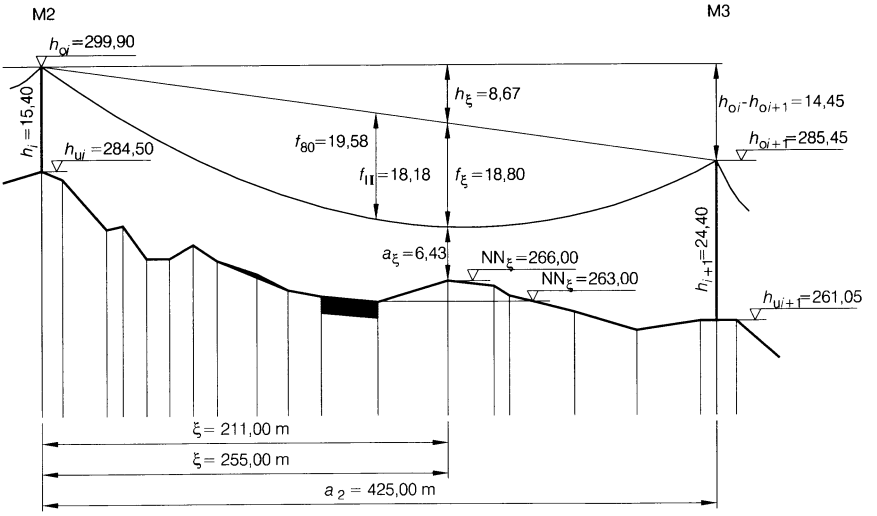

Figure 14.11: Explanations to calculation of the clearance to ground

Table 14.4: Clearances to ground

	Calculation by hand	Computer program	Difference
Equivalent span	340,32 m	340,49 m	−0,17 m
Equivalent sag at 80°C	12,55 m	12,56 m	−0,01 m
Sag at mid span at 80°C	19,58 m	19,33 m	+0,25 m
Sag location of minimum clearance at 80°C	18,80 m	18,55 m	+0,25 m
Clearance at 80°C	6,43 m	6,68 m	−0,25 m

14.9.3 Calculation of the clearance to a crossed road

According to [14.11], a minimum *clearance to the road surface* of $(6 + D_{el})$ m has to be verified in case of the maximum sag of the conductor and for local ice load in the span. As an example, the data for the local ice load according to EN 50341-3-4 [14.12] is assumed. The equivalent span, the tensile stress and sag as well as the sag at the crossing point are calculated as shown in clause 14.9.2, since the crossed road is situated in the same span.
As it can be seen from Figures 15.18 and 14.11, the shortest clearance has to be expected for the coordinate 462,0 m or $\xi = 211$ m.
With a sag $f_{max} = 19{,}58$ m at 80°C and $\xi = 211$ m, it is obtained from (14.26) $f_\xi = 19{,}57$ m and with $NN_\xi = 263$ m from (14.83)

$$a_\xi = 299{,}9 - 14{,}45\,(211{,}0/425) - 19{,}57 - 263{,}0 = 10{,}2 \text{ m}.$$

The available clearance is larger than that required.
In addition, the clearance with local ice load equal to $(5 + 0{,}1 \cdot 2{,}24)/2 = 2{,}62$ N/m in the relevant span has to be verified. Starting with the horizontal tensile stress of $\sigma_1 = 47$ N/mm^2 at 10°C in the equivalent span, the tensile stress at −5°C and ice load of 2,62 N/m has to be determined. From (14.45), a horizontal tensile stress of $\sigma_2 = 65{,}07$ N/mm^2 is obtained for this ice load and from (14.16) an equivalent sag of $f_{id} = 10{,}03$ m. Related to the actual span length of 425 m, the sag in midspan is obtained to be (Figure 14.11):

$$f_{(-5°+m_{C1}g)} = \left(\frac{425{,}0}{340{,}32}\right)^2 \cdot 10{,}03 = 15{,}65 \text{ m}.$$

The sag with local ice load follows from (14.80). The used parameters there can be taken from (14.81), Table 14.2 and 14.3, as well as from Figure 14.10:

$$K_1 = \sqrt{2/(1 + (9{,}79/13{,}41)^2)} = 1{,}142,$$

Table 14.5: Calculation of clearances to a crossed road

```
SIEMENS AG DEPT PTDH158 TRANSMISSION LINES

110 kV LINE                              HT76 Fuerstenberg - Waren
CONDUCTOR : 2*3*1 * ACSR 265/35 * 47.0 N/QMM

LINE SECTION  FROM TOWER  NO.   1                      TO TOWER NO. 4


CONDUCTOR LEVEL 1                                                LEFT PHASE
*****************
 CROSS SECTION DIAMETER   WEIGHT   MOD. E   EXP.COEF. STRENGTH
   SQMM    SQMM      MM     KG/M  KN/SQMM        1/K   N/SQMM
263.66   34.09    22.40     .998   74.000    .0000196   278.51                *

LIMITS        TEMPERATURE    ICE LOAD    WIND LOAD       TENSION
******          DEGREE C        N/M          N/M          N/SQMM
                   -20.0         .000         .000         500.00              *
                    -5.0        7.240         .000         500.00              *
                    10.0         .000         .000          47.00              *

STARTING            10.0         .000         .000          47.00 #
CONDITION          -20.0         .000         .000          53.03
                    -5.0        7.240         .000          79.39

CROSSGING CLEARANCES, LEFT PHASE
********************************
COMPUTED       1 MAX. TEMPERATURE              80.000 DEGREE C
CONDITIONS     2 LOCAL ICE LOAD                 3.620 N/M

CROSSING     NO. 01                                                          *
CROSSING OBJECT: ROAD                                                        *
*******************************************************************************
SPAN                                              M   425.00
PHASE LENGTH                                      M   425.00
DISTANCE FROM LINE AXIS TO  CROSSING POINT        M     4.00
DISTANCE FROM LEFT TOWER TO CROSSING POINT        M   211.01                  *
ALTITUDE OF LINE AXIS AT CROSSING POINT           M   263.00                  *
ANGLE OF LINE AXIS RELATIVE TO CROSSING LINE    GON   100.10                  *
ALTITUDE OF REFERENCE  POINT                      M   263.10                  *

TOWER NO.                                                2              3 *
TOWER TYPE                                             SS+3          SS+12 *
INSULATOR SET TYPE                                       DH             DH *
LENGTH OF DROPPER                                 M     .00            .00 *

WEIGHT OF INSULATOR SET WITH DROPPER              N  1000.00        1000.00 *
STATION OF TOWER POSITION                         M   251.00         676.00 *
ALTITUDE OF TOWER LOCATION                        M   284.50         261.05 *
HEIGHT LOWEST CROSSARM                            M    17.20          26.20 *
LENGTH OF INSULATOR SET WITH DROPPER              M     1.80           1.80 *
ALTITUDE OF CONDUCTOR SUSPENSION POINT            M   299.90         285.45

CONDUCTOR TEMPERATURE CONDITION                          "1"            "2"
CONDUCTOR SUSPENSION HEIGHT DIFFERENCE            M   -14.45         -14.45
ALTITUDE OF CONDUCTOR SUSPENSION POINT            M   292.73         292.73
SAG AT MIDSPAN                                    M    19.34          16.59
SAG AT CROSSING POINT                             M    19.34          16.59
ALTITUDE OF CONDUCTOR                             M   273.38         276.14
ALTITUDE OF CROSSING POINT                        M   263.01         263.01
EXISTING CLEARANCE                                M    10.37          13.13
REQUIRED CLEARANCE                                M     7.00           6.00 *
ADDITIONAL CLEARANCE (TO REQUIRED)                M     3.37           7.13
```

K_2 = 1,06 (second span, conductor AL1/ST1A),

K_3 = 0,96 (span length 425 m, conductor AL1/ST1A),

K_4 = 1,0 (110 kV insulation).

From (14.80) it is obtained in midspan $f_{II} = 1{,}142 \cdot 1{,}06 \cdot 0{,}96 \cdot 1{,}0 \cdot 15{,}65 = 18{,}19$ m and at the crossing point from (14.26) with $\xi = 211{,}0$ m, $f_\xi = f_{II} = 18{,}18$ m.
Formula (14.83) yields the available clearance:

$$a_\xi = 299{,}9 - 14{,}45 \cdot (211{,}0/425) - 18{,}18 - 263{,}0 = 11{,}25 \text{ m}.$$

Also in this case, the clearance is larger than the required. The clearances were calculated as well with the method described in clause 14.8.5. Table 14.5 shows the results and Table 14.6 the comparison with the approximations. At 80°C, the approximation and the exact calculation differ only to a small extent (10,20 m compared with 10,37 m).

Table 14.6: Clearances to a crossed road

	Calculation by hand	Computer program	Difference
Sag at crossing point			
– at 80°C	19,57 m	19,34 m	+0,23 m
– at −5°C and local ice load	18,18 m	16,59 m	+1,59 m
Clearances to road at the crossing point			
– at 80°C	10,20 m	10,37 m	−0,17 m
– at −5°C and local ice load	11,25 m	13,13 m	−1,88 m

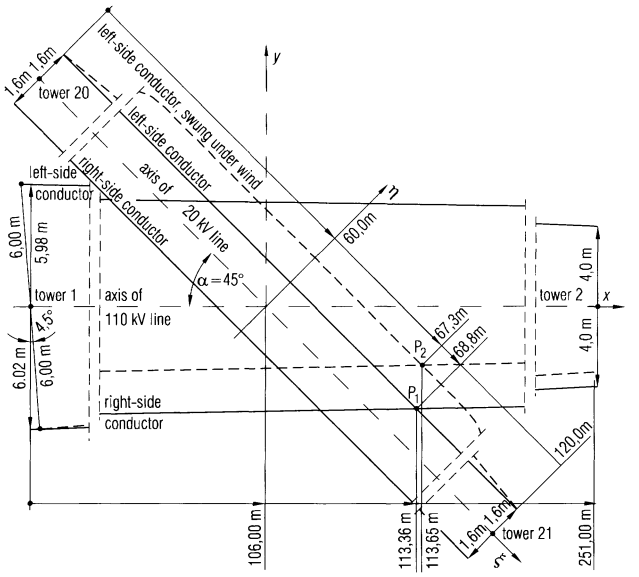

Figure 14.12: Determination of the crossing point of two overhead lines

Essential differences, however, occur for a local ice load. The exact calculation results in a clearance to the road surface of 13,13 m, while the approximation results in a value of 11,25 m only. The approximation is on the safe side in this case.

14.9.4 Calculation of clearance to a crossed line

The clearances to a crossed 20 kV line in span 1 (Figure 15.18) of the example should be calculated. According to [14.12], it has to be checked, whether the minimum clearances required according to [14.11] are complied with under the following conditions:

- **Condition 1:** Sag at maximum conductor temperature for the crossing overhead line: In this case 80°C ; conductor temperature 40°C for crossed line;
- **Condition 2:** Local ice load at crossing line; no ice load at crossed line, temperature −5°.
- **Condition 3:** Wind on the conductors of crossed line rectangular to the line direction; wind action on the overcrossing line with an aerodynamic pressure reduced by 40 %, due consideration of the angle of attack, temperature 40°C.

The crossed 20 kV line consists of three spans with 120, 148 and 133 m lengths. The relative position of both lines is shown in Figure 14.12. In principle, four points of conductor intersection have to be checked. From the position of the crossing and the sags, it can be seen, however, that the crossing of the right-side conductor of the 110 kV line with the left conductor of the 20 kV line will result in the shortest clearances.

In condition 1, the conductors do not move and the coordinates of the crossing points result from the intersection of the both straight lines which represent the conductor in the plan view: $y = 0{,}0079\,x - 5{,}98$ and $y = -x + 108{,}26$ zu $x_{P1} = 113{,}36$ m (Figure 14.12).

Table 14.7: Clearances to a crossed overhead line

	D_{pp} 110 kV	Calculation by hand	Computer program	Difference
		Clearance at the crossing point		
– condition 1	1,15 m	2,10 m	1,89 m	+0,21 m
– condition 2	1,15 m	1,50 m	1,93 m	−0,43 m
– condition 3	1,15 m	2,00 m	1,18 m	+0,82 m

With the equivalent span and the equivalent sag for 80°C, according to 14.9.2, the sag of the right-side conductor in midspan of the crossing span is obtained from (14.82):

$$f_{\max 80} = (250{,}5/340{,}3)^2 \cdot 12{,}55 = 6{,}80 \text{ m}.$$

The sag at point P_1 (Figure 14.12) in the span between tower 1 and tower 2 follows according to (14.26):

$$f_P = 6{,}80 \cdot 4\left(\frac{113{,}36 - 0{,}47}{250{,}5}\right) \cdot \left(1 - \frac{113{,}36 - 0{,}47}{250{,}5}\right) = 6{,}73 \text{ m} \quad .$$

Similarly, formula (14.83) yields the altitude of the conductor to be

$$\text{NN}_{P1} = 301{,}5 - 1{,}6 \cdot 112{,}9/250{,}5 - 6{,}73 = 294{,}0 \text{ m} \quad .$$

For the crossed line equipped with the conductor 122-AL1/20-ST1A, the sag at 40°C is 2,16 m and at −5°C without ice load 1,24 m. These values were obtained from the conductor state change equation (14.40) and the equation (14.82) (Figure 14.12). Related to the crossed line, the crossing point P_1 is situated in a distance of 68,80 m from support 20 (Figure 14.12). There, the sag is 2,11 m according to (14.26) and the height of the conductor $\text{NN}_{P2} = 294{,}0 - 2{,}1 = 291{,}9$ m. Therefore, the existing clearance is 294,0 − 291,9 = 2,10 m, for which at least a clearance of D_{pp}, in this case 1,15 m, for 110 kV is required.
Also in condition 2, the conductors stay in their position in the plan view. Therefore, the same crossing points are obtained as in condition 1. As described in clause 14.9.3, the sag of the 110 kV line at local ice load in midspan is obtained from (14.80) to be

$$f_{II} = 1{,}142 \cdot 1{,}03 \cdot 1{,}025 \cdot 1{,}00\,(250{,}5/340{,}3)^2 \cdot 10{,}03 = 6{,}55 \text{ m}$$

and at the crossing point to be $f_{PII} = 6{,}55 \cdot 4(112{,}0/250{,}5) \cdot (1 - 112{,}9/250{,}5) = 6{,}48$ m. The conductor height is, therefore, 294,3 m.
For the 20 kV line, a sag of 1,21 m results at −5°C without ice load and the corresponding conductor height will be 292,8 m. Therefore, the clearance is 1,5 m, while again a minimum value of 1,15 m is required.
In condition 3, the conductors of both lines swing under wind action. Therefore, the position of the crossing point moves from P_1 to P_2 (Figure 14.12). The wind load on the conductor 122-AL1/20-ST1A results from (6.73) for an aerodynamic pressure of $0{,}75(800 + 3{,}10) = 622$ N/m^2 at a height of 10 m above ground to be 10,3 N/m and for the conductor 264-AL1/34-ST1A at a height of 16 m above ground to be $w = 848 \cdot 1{,}0 \cdot 0{,}0224 \cdot 0{,}6 \cdot \cos^2 45 \cdot (0{,}45 + 60/250{,}5) \approx 4{,}0$ N/m.
The swinging of the conductor has to be studied for a temperature of 40°C. In midspan, the sag of the 20 kV line is 2,16 m. The swinging angle of the conductor 122-AL1/20-ST1A is calculated due to the static condition approach:

$$\psi_2 = \tan^{-1}[Q_{WC}/(m_C g)] = \tan^{-1}[10{,}3/(0{,}494 \cdot 9{,}81)] = 64{,}8° \quad .$$

For the conductor 264-AL1/34-ST1A the relevant swinging angle will reach

$$\psi_1 = \tan^{-1}[4{,}0/(0{,}998 \cdot 9{,}81)] = 22{,}2° \quad .$$

The crossing point P_2 is obtained as the intersection of both conductor curves in the plan view. The horizontal deflection of the conductor of a 110 kV line in midspan is $6{,}12 \sin 22{,}2° = 2{,}31$ m. At support 2, the suspension string swings by $1{,}8 \cdot \sin 22{,}2° = 0{,}638$ m.
For the determination of the crossing point P_2 of the swung conductors, several alternatives can be adopted:

Table 14.8: Calculation of clearances for crossing of two overhead lines

```
SIEMENS AG DEPT PTDH158 TRANSMISSION LINES

EVALUATION OF CLEARANCES FOR CROSSINGS WITH OTHER LINES

110 kV LINE                                HT76 Fuerstenberg - Waren

CROSSING NO.    OVERCROSSING LINE              UNDERCROSSING LINE
------------    -----------------------------  ---------------------------
1.0             110 KV LINE                    20 KV LINE
                Federow-Waren                  e.dis
                                               CONDUCTOR : ACSR 120/20

TOWER NO.                                   1        2                M20      M21 *
TOWER TYPE                               TT+0     ST+3               HZ-M     HZ-M *
INSULATOR SET TYPE                         DT       DS                 TK       TK *
CROSSARM LENGTH LEFT                     6.00     4.00               2.00     2.00 *
            RIGHT                        6.00     4.00               2.00     2.00 *
SYSTEM DISPLACEMENT                       .00      .00                .00      .00 *
HORIZ. ANGLE   GON                      395.00      .00             200.00   200.00 *
ALTITUDE OF TOWER LOCATION               285.50   284.50             282.00   279.00 *
CROSSARM HEIGHT                           16.00    17.20              12.40    15.40 *
INSULATOR SET LENGTH                       .00     1.80                .40      .40 *
DROPPER LENGTH                             .00      .00                .00      .00 *
CONDUCTOR SUSPENSION ALTITUDE            301.50   299.90             294.00   294.00 *
DIFF. OF SUSPENSION ALTITUDE                       1.60                        .00 *
SPAN LENGTH                        M              251.00                     120.00 *
CROSSING ANGLE                   GON               50.00                            *
LINE ANGLE UNDERCR. LINE         GON              200.00                            *
DISTANCE OF CROSSING POINT
OF AXES FROM LEFT TOWER                           106.00                      60.00 *
CONDUCTOR WEIGHT                KG/M                .998                       .494 *
WIND LOAD                        N/M               4.020                     10.300 *

SAGS, TEMPERATURES AND REQUIRED CLEARANCE FOR THREE CASES
      UPPER LINE          LOWER LINE              REQUIRED
  LEFT CENTRE RIGHT TEMP   LEFT  CENTRE RIGHT TEMP CLEARANCE
  7.06   7.03  7.01   80   2.11    2.11  2.11   40      1.15                      *
  6.71   6.69  6.66   -5   1.80    1.80  1.80   -5      1.15                      *
  6.26   6.24  6.22   40   1.90    1.90  1.90   40      1.15                      *


CALCULATION CONDITION                    AT STILL AIR              AT STILL AIR
TEMPERATURE CONDITION                     80 DEGREE C               40  DEGREE C
CRITICAL SAG AT MIDSPAN                          7.01                      2.11
SPAN LENGTH OF CRITICAL PHASE          RIGHT  250.54             RIGHT  120.00
DISTANCE OF CRIT. CROSS.PT./TO TOWER  113.45      1             69.19     M20
SAG AT CROSSING POINT                            6.95                      2.06
DIFFERENCE OF ALTITUDE AT CROSSING POINT         0.72                      0.00
CONDUCTOR ALTITUDE AT CROSSING                 293.83                    291.94
CLEARANCE EXISTING/REQUIRED/ADDITIONAL           1.89     1.15              .74

CALCULATION CONDITION                  LOCAL ICELOAD               NO ICELOAD
TEMPERATURE CONDITION                    -5 DEGREE C               -5  DEGREE C
CRITICAL SAG AT MIDSPAN                          6.66                      1.80
SPAN LENGTH OF CRITICAL PHASE          RIGHT  250.54             RIGHT  120.00
DIST. OF CRIT. CROSS.PT./TO TOWER     113.45      1             69.19     M20
SAG AT CROSSING POINT                            6.60                      1.76
DIFFERENCE OF ALTITUDE AT CROSSING POINT         0.72                      0.00
CONDUCTOR ALTITUDE AT CROSSING                 294.17                    292.24
CLEARANCE EXISTING/REQUIRED/ADDITIONAL           1.93     1.15              .78

CALCULATION CONDITION            WIND 351 GON 100 %        WIND 300 GON 100 %
TEMPERATURE CONDITION                     40 DEGREE C               40  DEGREE C
CRITICAL SAG AT MIDSPAN                          6.12                       .81
WINDLOAD              N/M                        3.69                     10.30
SWING ANGLE           GON                       11.70                     72.01
SPAN LENGTH OF CRITICAL PHASE          RIGHT  250.54             RIGHT  120.00
DIST. OF CRIT. CROSS.PT./TO TOWER     115.05      1             69.40     M20
SAG AT CROSSING POINT                            6.07                       .79
DIFFERENCE OF ALTITUDE AT CROSSING POINT         0.72                      0.00
CONDUCTOR ALTITUDE AT CROSSING                 294.70                    293.44
CLEARANCE EXISTING/REQUIRED/ADDITIONAL           1.26     1.15              .11

CALCULATION CONDITION            WIND 351 GON  60 %        WIND 300 GON 100 %
TEMPERATURE CONDITION                     40 DEGREE C               40  DEGREE C
CRITICAL SAG AT MIDSPAN                          6.18                       .81
WINDLOAD              N/M                        3.69                     10.30
SWING ANGLE           GON                        7.07                     72.01
SPAN LENGTH OF CRITICAL PHASE          RIGHT  250.54             RIGHT  120.00
DIST. OF CRIT. CROSS.PT./TO TOWER     115.53      1             70.10     M20
SAG AT CROSSING POINT                            6.14                       .79
DIFFERENCE OF ALTITUDE AT CROSSING POINT         0.72                      0.00
CONDUCTOR ALTITUDE AT CROSSING                 294.62                    293.44
CLEARANCE EXISTING/REQUIRED/ADDITIONAL           1.18     1.15              .03
```

- Both curves for the swung conductors are represented by functions, the intersection of which is calculated then;
- In the vicinity of the intersection, the swinging curves can be approximated by straight lines, the intersection of which is to be determined;
- The intersection is determined in a sketch to scale;
- Approximate formulae are used assuming that the swung conductor is in a parallel position to the conductor in still air.

For the example the approximation mentioned last will be used:

$$\chi_{P_2} = \chi_{P_1} + f_2 \sin\psi_2/\sin\alpha - (f_1 \sin\psi_1 + \Delta i)/\tan\alpha$$

and

$$\xi_{P_2} = \xi_{P_1} + f_2 \sin\psi_2/\tan\alpha - (f_1 \sin\psi_1 + \Delta i)/\sin\alpha \quad .$$

The sags f_1 and f_2 apply in this case for the point P_1 being 6,02 and 2,12 m at 40°C, respectively. Δi takes care of the horizontal displacement of the conductor due to the swinging of the insulator sets. In this case: $\Delta i = 1{,}8 \sin 22{,}2° \cdot 112{,}9/250{,}5 = 0{,}31$ m. For the 20 kV line, the insulator length is considered to be 0,4 m. The coordinates of the crossing point result, therefore, as

$$\chi_{P_2} = 113{,}36 + (2{,}12 + 0{,}5) \sin 64{,}8°/\sin 45° - (6{,}02 \sin 22{,}2° + 0{,}31)/\tan 45° \approx 114{,}1 \text{ m}$$

and

$$\xi_{P_2} = 68{,}8 + (2{,}12 + 0{,}5) \sin 64{,}8°/\tan 45° - (6{,}02 \sin 22{,}2° + 0{,}31)/\sin 45° \approx 67{,}31 \text{ m} \quad .$$

A sketch to scale confirms these values. The exact calculation results in $\chi_{P_2} = 115{,}5$ m and $\xi_{P_2} = 70{,}1$ m. The conductor height for the undercrossing line is

$$NN_{S2} = 294{,}4 - (2{,}12 + 0{,}5) \cos 64{,}8° = 293{,}3 \text{ m} \quad .$$

The conductor height for the overcrossing line follows from

$$NN_{S1} = h_{oi} - (h_{oi} - h_{oi+1})\chi_P/a_i - (f_P + l_k \cdot \chi_{P2}/a_i) \cos\psi_1 \quad ,$$

where f_P is equal to the sag of 6,02 m and the component of the insulator length at support 2 is $1{,}80 \cdot 114{,}1/250{,}5 = 0{,}82$ m. This height is

$$NN_{S1} = 301{,}5 - (301{,}5 - 301{,}7)114{,}1/250{,}5 - 6{,}84 \cdot \cos 22{,}2° = 295{,}3 \text{ m} \quad .$$

Therefore, the available clearance is 2,0 m. In Table 14.7 the results are shown. The clearances calculated by computer are represented in Table 14.8. There, the conductor positions have been determined exactly. While the clearances calculated by hand and by program coincide quite well for conditions 1 and 2, the differences are higher for condition 3. Therefore, it is recommended to check the clearances by exact computer programs.

14.10 References

14.1 Girkmann, K.; Königshofer, E.: Die Hochspannungsfreileitungen (Overhead power lines). Wien, Springer-Verlag 2nd edition, 1952

14.2 Fink, D. G.; Beaty, H. W.: Standard handbook for electric engineers. New York. McGraw-Hill, 12th edition 1987

14.3 Trash, R. et al.: Overhead conductor manual. Carrolton, Ga., Southwire, 1994

14.4 Draft IEC 61 989: Overhead electrical conductors – Guide to calculation of sag and tension. Geneva, IEC, Draft 1999

14.5 Palkowski, S.: Statik der Seilkonstruktionen (Statics of stranded wire structures). Berlin, Springer-Verlag, 1990

14.6 Kießling, F.: Berechnung des Zustandes der Seile im Abspannabschnitt einer Starkstromfreileitung (Computation of conductor state change in a tensioning section of an overhead power line). Siemens Forsch. Entwicklungsber. 1 (1972), pp. 125 to 132

14.7 Halbig, A.: Beitrag zur Durchhangsermittlung bei Hochspannungsfreileitungen (On the sag calculation of high-voltage overhead lines). ETZ-Report 10, Berlin, VDE-Verlag 1973

14.8 Schmidt, B.: Die Berechnung von Freileitungsseilen nach der Methode der finiten Elemente(Computation of overhead line conductors based on the finite element method). Elektrizitätswirtschaft 84 (1985), pp. 846 to 851

14.9 Begemann, D. et al.: Vergrößerung von Seilabständen mittels Halbverankerungsketten an Tragmasten (Increasing clearances in overhead power lines by means of inverted-V insulator sets at suspension structures). Elektrizitätswirtschaft 91 (1992), pp. 1519 to 1525

14.10 Hütte: Die Grundlagen der Ingenieurwissenschaften (Handbook of Engineering science). Berlin, Springer-Verlag, 29th edition, 1989

14.11 EN 50 341-1: Overhead electrical lines exceeding AC 45 kV. Part 1: General requirements – Common specifications. Brussels, Cenelec, 2001

14.12 EN 50 341-3-4: Overhead electrical lines exceeding AC 45 kV. Part 3-4: National Normative Aspects for Germany (NNA). Brussels, Cenelec, 2001

15 Route selection and detailed line design

15.0 Symbols

Symbol	Signification
a	Span length
a_{max}	Maximum span length
a_{min}	Minimum span length
a_{ph}	Maximum span
a_{som}	Minimum distance in air between live and earthed parts of an insulator set
b_1, b_2	Tower width
c	Calibration parameter
d_{min}	Clearance according to EN 50341-1
D_{el}	Minimum clearance in air between phase conductor and earthed elements
D_{pp}	Minimum clearance in air between phase conductors
f_C	Sag at point C
f_{max}	Maximum sag within the span
F	Reduction coefficient
$h_{1,2}$	Tower heights
h	Minimum ground clearance
H_0,H_1,H_2,H_3,H_4	Altitude of tower locations
H_I	Altitude of survey instrument
H_x	Altitude of measured point
i	Height of instrument
L, L_1, L_2	Horizontal distance
L_{p1}, L_{p2}, L_C	Distances of conductor points
m	Calibration parameter
R	Earth's radius
s	Measured inclined distance
t	Height of reflector
U_s	Highest system voltage
z, z_0, z_1, z_2	Zenith angle
α_1, α_2	Angle of crossarm axis
β_{M1}, β_{M2}, β_C	Horizontal angle
Δh	Difference of altitudes
ϕ_C	Conductor swing angle

15.1 Introduction

15.1.1 Basic information

The requirements for *route selection* and detailed line design of a high-voltage overhead line are established by the preparatory work, studies and assessments described in Chapter 1 "Overall planning". They have been developed on the basis of an electric network analysis, defining in principle the required starting and terminal point of a transmission connection taking into account the generation and consumption load centres. The *voltage level* and the required *conductor cross section* are as well determined by the existing network structure and the requirements of load flow, such that the design engineer is provided with essential parameters. The requirements on the supports to be used for a line project depend on the line voltage, number of circuits, conductor

dimensions and arrangement as well as on climatic, topographic, infrastructure or legal aspects. When selecting the support structures, the design engineer will try to utilize available designs to avoid the expenditures for a new tower family including the workshop drawings, especially in case of relatively short lines. However, the development of new supports designed to the specific line requirements can result in technical improvements and investment savings and is an often adopted and recommended practice.

The required documentation of the line route needs to be considered during *route selection*. Detailed and as far as possible commonly understandable presentation of the line project is necessary for starting the *licensing approval procedure*, as presented in clause 1.11.

The provision of suitable maps with a scale adjusted to the spatial expansion of the project to be designed is necessary for the contractor responsible for the design. *Overview maps* in a scale of 1:100 000 are commonly used for more extended projects. Multi-colour UTM-maps in a scale of 1:50 000 or 1:25 000 serve to show the affected areas close to the route. Such overview maps are usually available for existing lines at the network operators. However, the most recent edition of maps should be used for planning of new line route corridors. These maps can be acquired from companies in the internet, from the provincial surveying administrations or from local land register and surveying authorities. For determining the affected properties along the new line axis, maps with a scale of 1:5 000 are helpful. In countries without a completed land register system, ortho-photos can be used as well to determine at least crop borders which might indicate borders of plots as well. If neither maps nor aerial photos are available, contacting local authorities might be helpful for a detailed investigation of plot borders.

Before a first line route proposal will be presented to the *licensing authority* in charge, all the administrative and environmental concerns as well as the existing and planned land use have to be observed and considered. The plans for further extension of infrastructure around municipalities should be checked against the requirements of the new line corridor. In addition, this information needs to be acquired and provided within a wider corridor which may be considered as suitable for the new line. At this occasion, all the problematic areas close to the line route will be identified and assessed based on the line engineer's experience.

15.1.2 Preliminary activities

A contracting company with experience in overhead line construction or an adequate surveying company should be engaged for route selection and line design if experienced utility staff is not available within the entity planning a new line. Later on, synergy effects may be utilized because numerous contacts to land owners, authorities and other institutions established during the planning stage may not be looked for again when the line construction will start.

If surveying activities would be necessary during the search for a line route, it has to be proved as expedient to ask the involved municipalities to inform the public in order to avoid conflicts with land owners. This information will be necessary in any case when starting the *detailed surveying*.

During the search for a line route, it is necessary to acquire an overview as precise as possible on the terrain concerned by the line design to monitor all details at the most recent status. A terrain investigation to the most attentive extent by inspection on site yields partial impressions only because of the limited view in most cases. A complete overview, however, can be obtained by flying along the route and through documentation by *aerial photographs* and *laser scannings* of the investigated area. The scale of the photographs can be selected such that a sufficiently large area is recorded

and, at the same time, all necessary details are presented clearly. The tower sites of existing transmission lines get visible most clearly through the shadow at a low sun.
When *searching for a line route*, several technical aspects as well as the manifold concerns of nature and landscape, existing infrastructure, other planning entities and existing traffic routes need to be considered. It will not be possible in all cases to take care of all diverging interests without conflicts. Therefore, it is expedient just from the beginning to establish several *optional line routes* and to present them in maps. During site inspections, these optional routes can be studied in the terrain and discussed with the municipalities and other authorities concerned to minimize possible conflicts during the following *licensing procedure*.
Especially in case of more extended projects, it has proved favourable to record the specialities of the area concerned with respect to the *avifauna*; this can be done by interviewing the local bird experts and initiating even a recording of nesting and visiting birds in due time, since such a recording should be carried out during the relevant seasons. A delay of line design or licensing procedures because of missing ornithological data can be avoided thereby.
After finalizing the investigation studies for a *preliminary route*, it should be possible to establish the required documentation for the licensing procedure, considering the technical design of the line and the known concerns of entities which develop the infrastructure planning .
More or less numerous modifications of the preliminary route will result from the licensing procedure and from the *environmental impact study*, which is to assess and minimize the impacts to the nature. In the context of the line project, care should be taken regarding all conditions and guidelines resulting from these licensing processes. The modifications will be considered in the final route selection and surveying. To meet the requirements and wishes of land owners, it is expedient to agree first upon the line deflection points and then upon the sites for the suspension supports, which can be moved easier along a straight line section.
In some countries, overhead lines are not governed by the directives for approvals and supervision of civil engineering structures. There, an application for construction is not necessary and the technical documentation needs not to be approved by any authorities. However, before starting construction the utilities need to get the approval of the land owners and tenants as well as the approval for crossing roads, railway lines, shipping lanes etc., and to finalize correlated contracts and to obtain the right-of-way, if any. In most cases, the utility will arrange for the right-of-way, since official attorney is required for land acquisition and legal procedures regarding infrastructure projects. Sometimes, it might be necessary for the utility to buy the land from the owners. If an agreement is not reached, a legal decree from authority is necessary. This can delay the implementation of the project.

15.2 Route selection and licences

15.2.1 Introduction

15.2.1.1 General aspects and guidelines

Two line categories can be considered, regarding route selection, fitting lines into the terrain, line design and tower spotting, namely:

- Lines situated in highly populated regions;
- Lines predominantly located in rural areas or in regions of low population density.

For the first category of lines, the design and construction optimized with respect to technical and economic aspects will not be possible, for instance, in Central Europe, parts of North America and Asia, because of the numerous constraints on the *selection*

of support sites and line configurations. The increasing number of relevant directives and laws on national and international level forces the design engineer to accept numerous compromises already when *selecting the route* to fit the line into the environment in an as far as possible considerate manner and to get the route and its implementation approved. Regional planning and approval procedures on the basis of *environmental protection laws* are used to minimize the number of contradictions in the requirements and their consequences. A profound knowledge is necessary in line technology regarding the relations between the individual characteristics to avoid negative effects on several other parameters when modifying one parameter in a positive direction and not to lose of sight the resulting economic consequences [15.1].

However, for the second category of lines mentioned above, an overall optimization procedure is feasible. For such lines, an appropriate family of towers can be defined, a route close to a straight line can be selected and an optimum tower spotting can be implemented.

Selection of a transmission line route between two defined ends is an optimization task with the aim of minimizing the *impacts on landscape and environment* as well as the investments for implementation. Due to the manifold constraints, such an optimization is possible to a limited extent only. From the technical point of view, a line route should be selected which avoids angle points, as far as possible, since they require considerably higher efforts and investment. A tower configuration as uniform as possible and adjusted to the topography should be selected. To minimize the investment and maintenance costs, such a tower configuration can be optimized with respect to the required area for the tower sites and width of right-of-way and to the height of the towers which all together affect the expenditures for compensation, foundations and towers. Therefore, self-supporting structures have prone to be adequate when compensations are high, while guyed structures may form an interesting solution in regions without intensive use of land.

An easy *access to the tower sites* reduces the compensation for land use and maintenance costs. Tower sites on exposed points of the terrain, such as rock noses, should be avoided although they would offer advantages concerning the adjustment of the conductor catenary to the terrain. The line should be routed where less valuable land can be used. Therefore, land reserved for residential areas, very fertile agricultural terrain and forests should be avoided from the investment point of view. Areas with constraints for a line implementation such as air corridors should be by-passed at an adequate distance when selecting the route.

The investment for foundations rises with unfavourable *subsoil conditions*. So far as possible, supports should not be spotted on sites with very low-bearing soil or in swamps.

Numerous crossings with traffic routes and other lines may be necessary when implementing a new overhead power line. In these cases, small angles of intersection between the installations should be avoided since they would result in long crossing sections.

Certain industrial installations such as cement plants form a source of increased pollution which could endanger the insulation of power lines and cause corrosion at metallic elements. Therefore, lines should not be routed close to such areas since otherwise increased investment and maintenance costs have to be expected.

The increasing number of *wind energy converters* also at wind-prone inland sites has led to discussions on the required distance to overhead lines although new lines are seldom planned close to existing wind energy parks. As a pragmatic compromise, a minimum distance of three times the rotor diameter should be met between the tip of the rotor wing of a wind energy converter and the outermost conductor of a line in still air. When the line is well protected against vibration of conductors, this distance may be reduced to one rotor diameter [15.2]. This compromise takes care of the interests of operators of wind energy converters to accept distances as low as possible and to minimize the

additional investments for the connections to the network and mitigates the concerns of electric network operators on damage of conductors due to the wake of the wind energy installations, failing of rotor wings and increased hazard due to lightning.

15.2.1.2 Alternative line designs

Self-supporting lattice towers composed of angle sections have proved their suitability for transmission lines worldwide since the beginning of overhead line technology. Guyed towers form an economic alternative where enough space is available and costs for land compensation are low. Wood has been used as a structural material for lines up to 220 kV where timber is available. However, its lifetime is limited (see clause 12.1.3.5). Plastic materials have shown in studies to be less economic with respect to the high loads to be carried. They can be used for individual elements like insulating crossarms. *Round-shaped poles made of spun concrete* offer a realistic alternative up to lines of the 220 kV level and in special cases for higher voltages, if they are manufactured with prestressed steel reinforcement (see clause 12.7.2). Polygonal poles made of steel form an attractive alternative for concrete poles and *lattice towers* because of their slender aesthetic perception. Since these poles show a relatively high deflection resulting from horizontal forces, conductor cross sections and forces, line deflections, span lengths and pole heights need to be limited to avoid inadmissible deflections, inclinations of crossarms as well as unacceptably large diameters and weights of the poles. Therefore, they cannot be considered as a fully adequate substitute for rigid lattice or guyed towers. However, they are frequently used in valleys and narrow forest aisles for voltages up to 500 kV because of aesthetic reasons. Also in suburban areas, polygonal poles have revealed to be an attractive solution, due to the narrow right-of-way required and also as an economic alternative when compared to underground cables. Worldwide attempts are made to adopt new tower shapes designed according to architectural ideas and rules considering aesthetic aspects, also for extra-high voltages. The investments for such designs are considerably higher than those of conventional steel towers. Results of studies carried out by architects are presented in [15.3, 15.4]. In Figure 12.10, an example is shown. Alternative designs are presented also in [15.5].

15.2.1.3 Conversion of existing lines

When planning a new line, it should be considered alternatively, whether bundling of transmission circuits owned by different operators on the same structures is possible as far as interests of these operators are congruent. The common use of right-of-way and overhead line structures has to be settled in contracts taking care of the mutual portions on the investments [15.6].
Uprating of existing transmission lines to an increased capacity or a higher voltage level instead of constructing a new line can be considered as an alternative solution as well [15.7, 15.8]. The advantage of a legally or contractually secured right-of-way is important and valuable in densely populated or sensitive areas. Removal of an existing line and construction of a new one within the existing right-of-way is economic, since necessary additional compensations and line construction can be achieved with less problems than the acquisition of a new right-of-way.

15.2.1.4 Underground transmission

The *adoption of underground cables* is always questioned in context with overhead line projects during the approval stage and required with emphasis as well. The physical performance of overhead lines and underground cables is different (see clause 1.12), the investment for underground cables is much higher [15.9, 15.10]. Today, there is a

certain consensus to adopt preferably underground cable installations for voltage levels of 110 kV and above only, where overhead lines cannot be routed, for example in urban environments. However, short underground sections between two adjacent overhead line sections, called *intermediate underground cable sections*, should be avoided. Underground cables need larger cross sections and are not capable of withstanding overloads contrary to overhead lines. Therefore, such intermediate cable sections represent an operationally weak element. Extra-high-voltage underground cable installations are restricted to urban underground networks in large cities, such as Berlin/Germany or Copenhagen [15.11]. For their construction and operation, other standards apply than for overhead transmission networks. *Gas insulated pipelines* and cryogenic cables are on development stage now [15.12, 15.13].

15.2.2 Regulatory controls and permit procedures

15.2.2.1 Introduction

Regulatory controls for new overhead lines vary from country to country. They have their origins in the cultural, political and administrative systems of each country. Although the regulatory controls for overhead lines may differ greatly, there are some common lessons to learn from general trends. In [15.5], a summary is given on these general trends based on a questionnaire response [15.14] and a working document regarding licensing procedures and environmental impacts, that were prepared by the members of the Cigré SC22 working group.

15.2.2.2 Permits

The requirements regarding authority's approval are partly dependent on the voltage level. The lower limit varies from 1 kV to 345 kV. A typical lower limit is above 20 kV. In recent years, *Environmental Impact Assessments* (EIA) for overhead lines have been introduced in the overhead line licensing procedures in many countries. Sometimes it is incorporated in already existing procedures. Formal limits triggering an EIA have often been introduced. For example, limits on the voltage level and/or the minimum length of the line are used. The European Union (EU) has regulations concerning EIA since 1985. Under the Directive 85/337/EEC [15.15] it was left to the responsibility of individual countries to decide on the necessity for EIA on overhead lines. But with the Directive 97/11/EEE [15.16], EIA became necessary for all overhead lines of at least 220 kV and with a length of more than 15 km.
Moreover, the administrative requirements on carrying out the EIA have been tightened up concerning permissions, public hearings, assessment of alternatives, information etc. In case of work on *existing lines*, permits and EIA are normally not necessary for maintenance but they could be required for major modifications to existing lines, e. g. significant structure alterations, upratings or upgradings.

15.2.2.3 Regulations, approvals and procedures

The various kinds of permits required in different countries can be summarized as follows:

- Approval under *environmental planning* and assessment act (e. g. New South Wales [15.17], Germany [15.18];
- Approval under concessions, "electrical permits" (e. g. Netherlands, Sweden, Austria);
- Approval under regional physical planning (e. g. Denmark [15.19]);
- Approval under local physical planning (e. g. Ireland [15.20]);

- In Germany, an environment impact assessment (EIA) is mandatory for all lines longer than 15 km with a nominal voltage of 220 kV and above. For lines of 110 kV or shorter than 15 km, such an assessment may be required after a preliminary check of the individual project. In addition, a planning licensing procedure is stipulated for construction, operation and modification of lines for which an EIA is necessary [15.18];
- Approval under nature conservation acts;
- Permits for right-of-way, expropriation acts;
- Building permits.

The main issues regarding overhead lines considered in licensing procedures are:

- Justification, necessity and public interest: In most cases dealt with by the authority who is responsible for the electricity supply industry;
- Routing, including mitigation: In most cases dealt with by the physical and environmental authority;
- Construction, including mitigation: Dealt with by several authority levels;
- Compensation: Dealt with by utilities, land owners and expropriation authority.

When the necessary permits are obtained, appeals can be lodged. These appeals are dealt with by tribunals or boards and often the courts are involved.

Appeals always include a serious risk of losing licences granted. As a consequence, the whole procedure or parts of the procedure may have to start again. Therefore, it is important to minimize this risk.

The period necessary for the *permit process* including EIA and appeals varies from country to country and is indicated by 1 to 10 years in [15.5].

The uncertainty about the length of time for public consultation and negotiations with land owners on the right-of-way and on support sites are prevalent. Therefore, the attitude of many utilities is to receive a permit even if it takes a longer time to be granted, rather than suffer a quick rejection.

Besides approval by authorities, negotiations with land owners are necessary to get their approval for the right-of-way, tower sites and access roads. The utility can be obliged to buy the land affected by the line or a licence is granted and legally secured by the land register.

The *authorisation of overhead lines* is not always structured in a logical or most efficient way. Local authorities and individuals can have a determining influence on the licensing of overhead lines and can cause unacceptable delay. Although the environmental requirements for overhead lines are specified in advance, new requirements could come up during the licensing process. This is also the case for the requirements of the environmental impact studies or their methods of evaluation [15.21].

15.2.2.4 Compensations

Line owners need to compensate the land owners for the right-of-way and support sites. In most cases, this is done by paying a lump sum based on a contract. The amount of payment depends on the land use and on the value of the land. In total, the compensation can reach 20 % of the line investment.

In addition, contributions to environmental or community funds are often required, related to specific projects or other forms of environmental or community *compensation.* In some cases, the contribution of the utility is based on a percentage of the project costs, e. g. 5 % of investment in Belgium.

Few utilities grant financial compensation to local authorities. Among those that do so, such compensation takes the form of environmental enhancement programs or contributions towards them based on conditions as part of government authorisations or planning permits required for a specific project, or the regulations in force.

Installation of an overhead line may infringe the environment balance at sensitive locations. The reasons can be aesthetical or visual impacts in recreational areas, impairing of breeding and migrating birds, aisles in forests, infringement of continuous agricultural areas or approaching of residual areas.
As a first step of compensation, it is looked for adequate areas which are suited for a specific preparation to re-establish the original natural functions in the vicinity of the right-of-way. This can be achieved by reforestating, establishing bird protection areas or installation of recreational parks.
If no suitable areas can be found in the direct line vicinity, the licensing authority will decide upon, whether suitable areas without a relation to the route should be looked for or whether expedient compensations have to be paid, to enable realization of measures bundling together several projects. The scales for establishing compensation payments depend subjectively on the individual experts since any assessment approaches on scientific bases are lacking.

15.2.3 Environmental impact assessment

15.2.3.1 Outline of the process

An *environmental impact assessment* (EIA) process constitutes an *environmental impact study* and public consultations and is carried out as required by law and so, the content and method are different from country to country. In general, the EIA reports cover the following subjects:

- Need for the project;
- System alternatives;
- Proposal of line route and project;
- Environmental impact assessment comprising:
  - Environmental situation without the line project comprising hydrology and water quality, soil surface, flora and fauna, landscape and visual impact, infrastructure and cultural subjects, impacts on humans, roads and traffic;
  - Development of environment without the line;
  - Environmental impacts of the new line comprising the aspects mentioned above supplemented by electrical and magnetic fields, effects on land use, sociological considerations;
- Conclusions.

The method used for involving citizens and agencies in the process often includes written information, information displays, public workshops and land owner/occupier and community consultations. Normally, the citizens and agencies are involved early in the process by comprehensive consultation with official bodies, including government representatives, and local authorities or informal public consultation, including visits and open evenings or public presentations as well as discussion with land owners and tenants.
Out of the environmental process, the selection of an alternative project location or design could result, as well as re-evaluation of the planned network or even withdrawal of the project.
Implementation of mitigation measures can be formalized in an *environmental management plan* for the project, setting out the mechanism and responsibility for carrying out the measures and the procedure for monitoring their effectiveness. Examples of aspects monitored are soil erosion, impact on fauna and flora, impact on land use, visual impact and impact on archaeology and heritage.

15.2.3.2 Enviromental impact studies

When assessing a new line route, the environmental impacts of the planned project on the land affected by the line need to be considered especially in case of voltages above 110 kV. The aim is a line route leading to a minimum of conflicts with other projects for use of limited land resources. The *environmental impact study* (EIS) intensifies these considerations, establishes a catalogue of measures to avoid or reduce the environmental impacts and lists *compensation and substitute measures*, if any. Since the expenditures required for such measures can amount to a considerable component of investment, the design engineer, when selecting the preliminary route, should make himself acquaintance with the relevant environmental problems. For their detailed handling, experts might be engaged as far as necessary.

The frequently asked question regarding the necessary *width of the corridor* to be studied on both sides of a transmission line route cannot be answered generally. In addition to the possible infringement of third party rights and interests, the impacts depend on the visual and aesthetic impression of the line planned and, therefore, on the *topography* of the terrain in question. In a mountainous or rolling terrain, a distance results different from that in a flat terrain where the far reaching *visibility* of the line requires wider corridors to be studied. The aspect of visibility alone, however, would result in overdone widths of corridors to be studied. A reasonable distance may result from the answer to the question, how far from the line a resident or viewer would be annoyed by the line in the given surrounding. In case of agricultural terrain, some hundred meters on both sides of the route centre line result as a viewing corridor; however, this distance would be considerably wider in terrain used by tourists and for recreation depending on the subjective sensitivity.

The impact of a new overhead line cannot be assessed without conflicts. Especially, for the environmental impact studies no approved and binding procedure exists [15.22]. Verbal qualifying procedures are used in addition to numerical assessment methods. In both cases, the results can be controlled to a certain extent by the assessing scale. Special emphasis should, therefore, be put on aiming at a transparent and comprehensive assessment understandable for non-professionals as well.

In an environmental impact study, the expected impacts of an overhead line project concerning the intrusion to the situation of nature and the environment compared with the original condition, have to be presented in a summarizing assessment. Available *alternatives for the line route* are weighed comparatively and that alternative is identified, which would result in the lowest impacts on the environment. Within the studied corridor, steps for avoiding or reducing infringements are listed in a catalogue of measures, and recommendations are given for a route optimized from the environmental point of view. In addition, compensation and substitute measures are determined during the *legal procedures for nature protection*, which, as a rule, will be imposed on the line owner to be implented during construction in a more or less modified manner.

15.2.3.3 Existing environmental situation without the line project

To analyse possible *environmental impacts* of a planned line, it is necessary to record the existing situation within the planned line corridor. This environmental situation, already existing strains included, needs to be presented and assessed. Predominantly, the subjects to be protected are studied, including the following subjects:

- ***Water quality***: The documentation should contain the ground-water quality, already existing strains caused by agriculture and industry, as well as burdens by previous use, traffic etc. Water protection areas and catchment areas for *drinking-water supply* require especial investigation as well as flowing and calm waters, because an input of polluting agents might be possible during line construction.

- ***Soil surface*:** In general, only that soil function is recorded and assessed which might have some context to possible effects of construction and operation of the line. Removal or contamination of soil by construction, land use and sealing is within this category as well as the soil sensitivity to compaction, erosion caused by construction activities and possible strains by polluting agents, e. g. by organic material, heavy metal or locally by dumps.
- ***Air and climate*:** Only the *micro climate* of the region concerned might affect the environment which depends mainly on the existing terrain infrastructure. Loss of trees and coppices to a larger extent and especially aisles in forests may change the micro climate conditions while sealing of the soil at the tower foundations may have negligible effects only. Air quality and air pollution caused for instance by local emitters like traffic and industry are recorded and documented.
- ***Flora and fauna*:** Within the line corridor, the existing *vegetation biotopes* are classified and recorded mostly by means of already existing maps; the latter will be updated by inspections on site. Codes for mapping biotope types are usually available from official institutions. The infringements caused by the line project are in most cases limited to the support sites, the location of which can be adjusted. Therefore, detailing of records can be limited in most cases. Regarding the line project, the biotopes concerned are assessed with respect to their appreciation of protection and sensitivity concerning impacts during line construction.
  Regarding the *fauna*, specific studies are necessary only when forests are used for hunting and any activities carried out there could lead to economic losses. After completion of the construction activities, however, game animals will return to the site.
  The *avifauna* (bird fauna) needs detailed observation and documentation, at least in case of long lines with tall towers. Infringements of the avifauna due to installation of new lines needs to be expected if uniform landscapes are divided by the new line. It has been observed that species breeding on ground or other species prone to colliding with lines by limitation of their flight space have been displaced. Crossing of *bird migration corridors* by overhead lines might create severe problems. If such problems are expected when selecting a line route, an ornithological study is recommended. It should be carried out as early as possible. The study should record and assess the bird migration during spring and autumn, as well as birds' breeding on ground in areas close to the line route.
- ***Visual perception of a landscape*:** The *visual perception of a landscape* could lead to long-lasting discussions between experts and non-professionals. The description and the assessment of a subjectively perceived landscape, requires a high degree of the observer's objectivity when processing the numerous information. In this case, it is not dealt with a quantity to be assessed objectively because the perception of a landscape may change, depending on the site of observation and on the oberserver's sensitivity. No internationally accepted tool for the analysis and *assessment of landscape* [15.23] exists. Therefore, subjectively describing procedures will be used in most cases. The scope of analysis can be divided into units characterized by typical elements. The sensitivity of individual parts of the landscape with respect to possible changes or infringements is assessed step by step based on the manifold of existing positive stimuli in contradiction to the disturbing elements.
- ***Cultural and economic subjects*:** Since a generally accepted definition of the term *cultural subject* does not exist, any monuments concerning buildings, gardens and nature, as well as specialities of landscape can be summarized and recorded under this term following the EC Directive [15.16]. Utilization of natural resources such as all types of mines as well as protective and preferred areas for agriculture

and forestry need to be considered.

- ***Human beings***: The condition of the protected objects mentioned afore without any doubts affects at least indirectly the well-being and life quality of people living in the area concerned. Already existing burdens affect directly people which might be living in the studied area and, therefore, have to be recorded. Road and railway traffic as well as air pollution can be mentioned in this context. On the other hand, possibilities for sport activities, bike and hiking paths, as well as recreational areas, will have a positive effect and have to be recorded and assessed since they are part of the existing environmental situation [15.24].

15.2.3.4 Reference alternative

An analysis of the environmental aspects within the area to be studied, comprising a description of the existing situation to the extent as explained above, would not be complete if it didn't contain statements concerning the development of the environmental situation without the line project. When establishing the *reference alternative*, existing planning details and general development objectives, for example as a result of regional master planning, need to be considered. Eventually, an assessment has to be made on the extent to which the line project would affect the general development.

15.2.3.5 Environmental impacts of a new line

The representation and assessment of the *environmental situation* before construction of a line are followed by the assessment of possible infringements on the subjects mentioned in clause 15.2.3.1. As a rule, it is distinguished between impacts occurring during the line construction which are temporary only, and impacts during operation and maintenance. For the latter, a period of time of at least 50 years should to be considered [15.25]. However, because the maintenance methods will change during the course of time and will have to be adjusted to developing environmental requirements, such assessment contains some uncertainty. The impacts are discussed in clauses 15.2.4 and 15.2.5.

15.2.4 Route selection and line design in view of visual impact

15.2.4.1 Introduction

This clause reviews the subject of *visual impacts* of overhead lines, and how these impacts can be assessed and visualized. Some attention is given to evaluation principles and to the possibilities of minimizing visual impact in selecting the route for an overhead line and its design.

Apart from aspects of route selection, the size and shape of the overhead line supports and their components are considered as having the most significant influence on visual impacts of an overhead line. Therefore, efforts to reduce the visibility of these supports and their components or to increase their absorption by the landscape are considered most important in reducing the visual impact of a line.

Report [15.5] describes various methodologies for assessment for the visual impact of overhead lines in the landscape and has been used as a basis for preparing this clause. In recent years, a broad palette of assessment models has been produced ranging from detailed surveys supported by *photomontage graphics* to elaborate computer programmes which combine visual modelling techniques with rating methods. However, in the authors' opinion, there are doubts whether these models really contribute much to validate the placement of new overhead lines.

15.2.4.2 Conceptual approaches

A major conceptual approach at the initial planning stages is the recognition of whether the existing landscape has the capacity to absorb the proposed project. This approach establishes whether the line should be integrated, i. e. concealed within the landscape so as to make it less conspicuous or whether the line should be asserted, i. e. made a visual feature.

It is the element of scale which establishes the significance, character and identity of what is associated with various landscapes. A landscape with broad panoramic views and simple, large topographic features, would tend to be read as having greater scale than a landscape where views are restricted and there is a great diversity of elements. Thus, a desert or very open flat landscape would have greater scale associated with it than one with many hills and random placement of trees. As a result, the assessment of the visual impact of a proposed overhead line in a landscape is often the combined assembly of the many individual components which create the scale and diversity of the landscape. These components like vegetation, slope, field patterns, diversity of elements, land use are also the elements which contribute to the formation of criteria for the eventual evaluation of a power line within the landscape.

It is the interpretation of scale which is the single most important element that aids in the selection of the basic planning approach of an overhead line. This can be achieved either through asserting a power line within a landscape as an identifiable element or icon, or choosing to integrate the power line within the latent landscape character and features. Both approaches can be assessed through the use of either qualitative or quantitative techniques.

15.2.4.3 Assessment through qualitative methods

The qualitative assessment approach places importance on the quality of change in visual impression caused by the new line. This approach generally uses graphical material in association with guidelines to measure potential change. With respect to *qualitative assessment of visual impact*, numerous graphical techniques and illustrated guidelines have been produced [15.26, 15.27]. These guidelines serve as checklists for procedures or measurement that should be devised for preservation of scenic sites.

In principle, these guidelines are specific to regions and not always applicable or transferable to other regional landscapes. Recent *computer simulation* graphics are also allowing better presentation of implemented guidelines for assessment by all parties involved so as to gain an understanding of various options impacting on the visual amenity of the landscape [15.28, 15.29].

Qualitative techniques are generally the preferred techniques to be used for dealing with the public while quantitative assessment is used for in-house studies so as to verify the process of final route selection.

15.2.4.4 Assessment through quantitative methods

The *quantitative assessment* seeks to clearly define factors that can be translated into quantifiable figures and forecast specific impacts through formulae and result in objective criteria to be applied throughout the design procedure. Thus, *environmental compensation* on the preservation of landscape can more easily be applied to any administrative procedure if based on quantitative criteria [15.29, 15.30]. The *landscape units approach* [15.20] is an example of a quantitative method of assessment. The results can be easily understood and it is easy to visualize the distinctions between one landscape type and another. However, it is difficult to quantitatively evaluate the visual impact because it depends not only on objective values, but also on subjective

factors. The definition of these factors depends on personal opinions although these can be taken into account by means of suitable coefficients [15.28, 15.29]. Current approaches have not yet resolved satisfactory formulae or scoring methods which could be understood by the public.

There is no consistency in methods of quantitative assessment at present, as urban or rural communities and cultures see environments in different ways. Methods differ for both techniques and criteria while the type of models have all been developed separately in different regions. Current research indicates that landscape evaluation is still determined through a subjective basis and thus a difficulty arises in formulating an evaluation method for *visual impact assessment.* Thus, rating systems should be able to account for variable public reactions. The use of the mathematical formulae can be useful for analysing different routes, tower impact and design. However, this approach is difficult for the public to understand and, therefore, has limited effect for presenting the impact at public hearings.

15.2.4.5 Routing for minimum visual impact

Visual impact

Careful routing of an overhead line is the single most important aspect in reducing the visual impact of both line and support structures. The support structures need to be visually absorbed by *integration into* the *landscape.* Integration tries to limit the visual presence of the line through the use of natural features like forests, vegetation, backdrop of hills, selective placement of supports or camouflaging the appearance of the components through vegetation, colour, height of support structures.

The decision on asserting or integrating the proposed overhead line is followed up through the implementation of the appropriate landscape guidelines prepared by utilities to control and mitigate *visual impact* [15.31, 15.32] and on installation of a new line [15.33, 15.34, 15.35, 15.36].

Of course, routing of overhead lines must also take account of other constraints such as land use, sites of ecological, historical and archaeological interest. At such sites, it is important to mitigate the visual impact by hiding the line behind natural screening or by *camouflage of line components.*

Power corridors

Bundling of new overhead line with transportation routes or existing lines is frequently required by authorities. Therefore, *power corridors* are created with more than one power line. The lines generally run parallel with each other or are arranged on common structures. Power corridors are considered to be a land use issue, however, this choice is to control visual impact, as well. Power corridors reduce encroachment into lands as yet untouched by overhead lines or other infrastructure.

As a recommendation, lines that are put in the same area should, if possible, share the same route and avoid semi-parallel solutions. Supports of similar shape and size with tower spotting at same span lengths reduce overall visual impact.

Planning authorities require bundling of transportation corridors with overhead lines being placed beside existing infrastructure. Essentially, placement of lines within such corridors reinforces the presence of the line. Some line designer feel that this approach to line location would appear to produce the maximum visual impact by ensuring that the line is visible to all travellers and rather than integrating the line with the surrounding setting. This approach reinforces the function and scale of large engineering projects. If the visual characteristics of the landscape favour the concept of asserting an overhead line, joint use of corridors should be pursued since the problem of scarce land would be lessened. However, lines along such a corridor are harder to blend into the landscape.

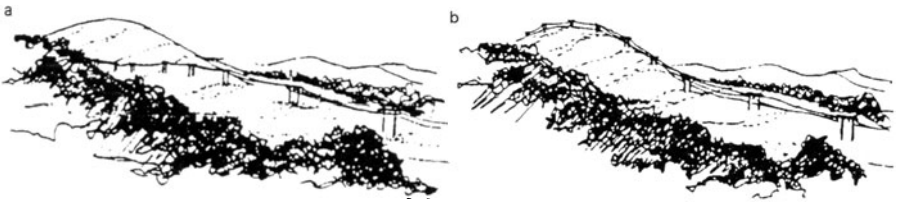

Figure 15.1: Line routing to avoid breaking the skyline. a recommended; b to be avoided

Routing guidelines

A large number and variety of guidelines have been developed with regard to routing [15.5]. Some generally applicable ones should be mentioned here.

- Avoiding natural parks and areas of high scenic, architectural or historic value. In any case, the line should be hidden, so as to minimize the visual impact.
- It is desirable to avoid open expanses of water and marshland. The overhead line should not go too close to shores of a river or natural lake. Rivers should be crossed as close to the right angle as possible.
- The most direct line with no sharp change of direction should be chosen with few angle supports only, these being placed where they are not too visible.
- In moderately open valleys with woods, the apparent height should be as low as possible and views of the line to be broken by trees minimizing the exposure of numbers of towers.
- In forested land, a sinuous cut or angle near important view points is preferable to a straight one so that people cannot see too far down the line.
- The line should follow natural lines created by topographic change, geology and vegetation that will help to minimize the visual impact.
- It is preferable to avoid breaking the skyline (see Figure 15.1).
- The towers should be placed near to the most vertical elements in the landscape, such as tree groups or hill slopes.

Structure allocation

Though technical and economic criteria are important in the selection of support heights and span lengths, evaluation of the visual impact may lead to the adoption of a different spotting of supports on the longitudinal profile of the line.

Support height has an important influence on visual impact, as the choice of taller structures will generate longer spans and reduced numbers of structures. However, taller supports have a greater presence in the landscape and are more conspicuous. Tall towers allow having the line suspended above the mature canopy height, thus avoiding the creation of corridors cutting through forests. Lower supports can be visually integrated with existing vegetation and topography as they are easier to visually absorb. However, the number of supports will increase, because span lengths need to be reduced.

Although, selection of structure sites depends on local conditions and constraints on available locations, some generally applicable guidelines can be given.

- When crossing over the top of a hill or mountain, the use of lower supports rather than higher ones should be considered (see Figure 15.2).
- When crossing a flat landscape characterized by a wide visual field and a clear organisation of land pattern, it is preferable to use taller towers with longer span lengths.
- In complex, picturesque landscapes, support heights should be adjusted to avoid intruding into the skyline and be absorbed into the background, thus the lowest tower is preferable.

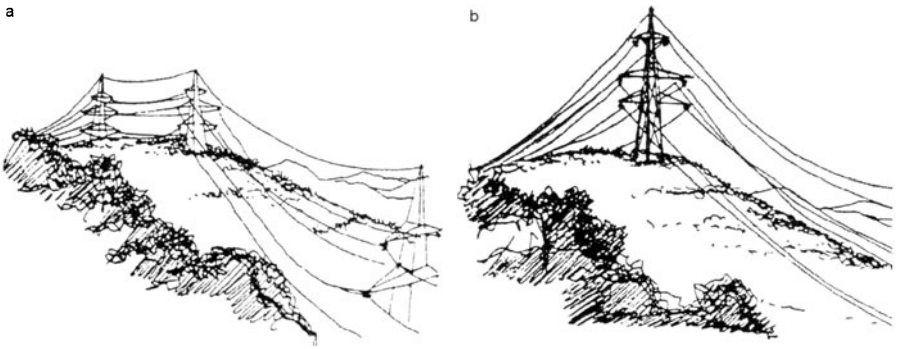

Figure 15.2: Line routing on hills. a recommended; b to be avoided

- Structures should be placed at the edge of woodlands, small groups of trees and hedgerows along the route.
- Towers should be preferably located on field boundaries rather than free standing within fields.
- Skyline interruptions by individual towers could be overcome by examining the possibility of lowering the tower height, if technical constraints do not result in additional adverse visual impacts (see Figure 15.2).

15.2.4.6 Visualization of new lines

In the following, various methods of *visual* simulation and *impact assessment* are summarized with respect to their techniques and criteria. In many cases, these techniques for *visualization of new lines* are used in combination with each other. Some techniques are best suited to assessment and verification by route planners, while others are better suited for consultancy with third party representatives or public.

Sketches

The simplest method for illustrating the potential change in a landscape setting as a result of placing a proposed overhead line, is to create freehand drawings of the potential changes generally rendered in pencil. Reproductions of photos form the base for the sketches. Simple sketches and photographs can create a sufficient understanding for the potential impact of a new line. However, the *visibility of overhead lines* is often difficult to show to the appropriate scale. In addition, this technique is often dependent upon the capability of detailed representation.

Photomontages

Photomontages provide a rather accurate future representation of proposed overhead lines as they illustrate the existing landscape with the insertion of a CAD-generated view of proposed towers and overhead lines. With this technique, it is possible to provide an accurate overhead line representation. Good quality site photographs which can be used for final presentation are the basic requirement. This technique has become the most popular method used by utilities for illustrating a new line on site. Due to time necessary to produce several single point views of a proposed project, this method is expensive and time-consuming, especially when presenting alternatives.

Digitized terrain models

Digitized terrain models represent the relief differences in the terrain. They are either produced by digitizing the contour lines on existing topographical maps, or created using aerial stereo-photogrammetry. Digital terrain models can be viewed as two-dimensional height charts or can be represented in three dimensions, i. e. in a perspective

view. Digital terrain models can be overlaid with a digital ortho-photo map of the same area, thus creating a virtual landscape.

Dynamic 3D simulation models can provide a representation of virtual landscapes so as to include realistic impressions of proposed structures. This approach allows to travel through the landscape by showing a quick succession of 3D static images, one after another. The use of manipulated geometrically corrected aerial photographs or ortho-photo maps can allow the creation of virtual 3D landscape models in which the new structures can be visualized. These techniques depend on the availability of digitized base maps which can be tied into graphical information systems (GIS). Paper [15.37] outlines how these techniques have been developed for use with the Belgium utilities.

Computergraphic methods

More sophisticated *computergraphic methods* have been developed and seem to be becoming better and better. An example is the method mentioned in [15.38], where the landscape is digitally reconstituted by using aerial photographs and a computer software programme. In fact, this is the same principle as the use of a digitized terrain model, but a picture of the landscape is superimposed on the terrain model by this method. The resulting landscape can be analysed, and an intended overhead line can be set up in a simulated form, and visualized from any point of view. It is possible to show how the line will look like from many viewpoints, either in pictures or on video film, and it is possible to analyse different routes.

Recommendations

With respect to the use of visualization techniques for presentation to the public, the following can be recommended:

- The selected method is not so important as long as the result is lifelike and understandable for most people and not only for experts.
- Photomontages are still the most suitable method for visual presentation to the public. The accuracy of the tower heights and placement within the terrain is crucial to public acceptance. They are also helpful in illustrating camouflage techniques and different designs.
- Digitized terrain models are not very effective, however, if they are overlaid with digitally reconstituted aerial photographs, a basic visual presentation can be achieved.

With respect to the use for planning and routing, the following would be the case:

- Digitized terrain models in combination with computer design of towers is fast to use and gives an indication of the visibility of the line and towers from many different points of view.
- Means of measuring potential impact are still under consideration. However, no specific system has been demonstrated to be helpful at public hearings. Thus, qualitative measurements of change are at present the most prevalent method for assessing visual impact.

15.2.4.7 Design of components to reduce visual impact

Supports

Since design of supports has an important effect on the visual line perception, some mitigation measures regarding *support design* are widely adopted according to [15.5]:

- Construction of *compact lines* with minimum clearances;
- Construction of *multi-circuit lines* with four and more circuits on common structures;
- Use of poles instead of lattice towers;
- Use of composite insulating crossarms;
- Coating of towers to camouflage the line against the background.

Adoption of different tower configurations in one line may be required to take account of the different environments crossed and of visual impacts of the line on these environments. Some of these solutions may increase the necessary investment, however, can be recommended to get a project approved.

Lattice towers

Lattice towers are still the predominant structure for transmission lines of 110 kV and above. They are usually constructed in pyramid or delta shape with the bodies and crossarms constructed from hot-rolled angle steel sections. For voltage levels above 220 kV, lattice towers are considered as having less visual impact than other structures, whereas poles are used on lower voltage levels for the same reason. Sometimes, cold-formed steel members are used to reduce the visibility of bracing in lattice towers. The use of tube sections instead of the usual angle steel members enables a reduction in the number of members in the structure due to the greater resistance to buckling of the tube sections. However, this is counterbalanced by the required greater investment and the problems regarding corrosion protection of tubes.

Poles

Poles made of wood, concrete or steel are often used on lines for voltages below 220 kV and have been introduced at higher voltages, specially for compact lines. The use of *insulating crossarms* on poles results in compacted configurations [15.4]. Camouflage or hiding of lines constructed of poles is often considered more difficult due to the supports solidity and the generally shorter spans as compared with lattice structures especially in the case of lines where the predominant views of the line are distant. For these reasons, the use of pole designs is favoured for overhead lines where the line appears in the foreground and lattice towers where lines appear in distant views.

As poles need a reduced area for their base, rights-of-way and impacts on land use can be reduced. This is balanced by shorter span lengths necessitating more supports for the line. In industrial and urban environments, these types of lines are an advantage due to the perceived reduced visual impact. *Timber poles* are used for medium voltages, mainly in Scandinavian countries, the USA, Canada, South America and Australia.

Portals and guyed structures

Portal or frame structures are typical supports for single-circuit lines. They can be made of timber, lattice or tubular steel, of concrete or a combination of these materials, being H-frames, portals or A-frames and often provided with guys. Self-supporting structures need more massive footing, whilst guyed structures result in smaller sizes of foundations but increased use of ground space due to their increased number of anchoring points. *Guyed supports* allow for considerable reduction in volumetric dimensions but increased right-of-way. Problems with farming and security sometimes prevent the use of guyed towers.

Structures without a metallic upper beam bring reductions in tower weight resulting in a lightweight appearance. The function of the missing upper beams is taken by chains of insulators. In general, portals and guyed structures do not reduce the visual impact to a perceivable extent (see clause 12.1.3.7).

Unconventional tower design

Unconventional structures have been designed by industrial architects. Some of these supports may be considered more as modern art than as overhead line supports. Several ideas are known presenting U-frame structures, egg-shape and Y-shape towers, tennis racket form (see Figure 12.4) and many others. These structures may consist of lattice steel, concrete, wood or synthetic materials and are used as single solutions, e. g. for deviations from existing lines or as eye-catcher near facilities. They do not reduce the visual impact but improve the line aesthetics. The investment significantly exceeds that for standard towers. Some examples are shown in [15.5].

Surface treatment of supports

Surface treatment of metallic supports is needed for protection against corrosion. The worldwide standard procedure is galvanizing. This zinc protection coating does not last for eternity and additional protective coating of towers on site is necessary after a lifetime of zinc protection between 10 and 30 years.

In recent times in-factory-coating of galvanized steel has become an option for long-lasting protection of steel supports. This method follows the *Duplex system* and at least doubles the period of time until an additional coating will be necessary. Coating of supports with *camouflage colours* and sometimes additional coating of conductors and fittings [15.39] was used in special cases to hide a line in a sensitive background. Special care should be taken when deciding the colour and it should be done in close cooperation with the concerned people and the authority. The line's background, predominant weather conditions, kind and duration of vegetation etc. are to be considered. Wrong decisions may turn the effect to the opposite and result in greater line visibility.

Conductors

The visual impact of conductors depends mainly on the phase arrangement, the number of subconductors and on the brilliance of the conductors. The phase arrangement is a major conditioning factor in the design of the supports, and vica versa. Vertical *phase arrangement*, associated with high supports, tends to produce a high visual impact of the line as a whole, due to the height above ground of the conductors and of the towers, resulting in a fence effect which may also increase the risk of collision for birds. On the other hand, the vertical arrangement provides the minimum right-of-way requirement. Horizontal phase arrangements produce the opposite effects. Between these two extremes, intermediate arrangements are compromise solutions as a result of the circumstances governing each specific project.

New untreated conductors exhibit a highly reflective surface; they usually achieve a matt finish after a few years, depending on the climate and degree of air pollution. Even new conductors can, however, be treated to reflect less light or to exhibit a low contrast with the background [15.39]. Low reflection conductors are either obtained by sandblasting the complete conductor, by coating with a camouflage colour or by use of special additives during the poltrusion process of the wires. Proper surface treatment allows to lower the reflectivity of a new conductor to less than half of the standard value of a new untreated aluminium conductor.

Insulators

The need to find visually less obstrusive lines, and the development of composite materials have made it possible to adopt increasingly new insulator types which in turn may influence the line visibility:

- *Horizontal V-arrangement*: The crossarm of a tensioned and a compressed insulating element rotates as a whole permitting compact tower designs.
- *Line post insulators*: The progress in the development of new composite-type materials enables their use, where the line loading is low.
- *Cross-rope or chainette arrangement*: In this concept, all the conductors are supported by a funicular polygon composed of insulating elements, strung between two vertical guyed supports.
- *Insulated crossarms*: Insulated crossarms adopting flexible composite insulators have a low visual impact.

A proper choice of insulator material, configuration and colour may reduce the visibility significantly. Use of composite insulators is advantageous in this aspect.

15.2.5 Route selection in view of people

Electric energy cannot be transported to the consumers without conflicts with interests of people, e. g. without visual impacts. Regarding this aspect, bundling of line corridors with traffic infrastructure such as railways and highways can be considered as more readily acceptable since such infrastructure corridors are unavoidable. Overhead lines are only routed to the periphery of residual areas, and underground cables distribute the energy at medium and low voltage. Frequently, line corridors situated previously in the open terrain are more and more used for constructing hauses. In some cases, the residents complain on emissions from lines, however, only contractual terms can protect the utility against requirements for line upgrading to mitigate the emissions.
Where new lines approach or traverse existing residential areas, potential infringement of people by emissions needs to be considered during route selection. Electrical and magnetic fields, audible noise and radio interference, especially under bad weather conditions should be mentioned. Line design should obey the specified limits. Limitation of emissions to harmless, acceptable levels is a matter of line design and line operation and not an aspect of line route selection.

15.2.6 Route selection and line design in view of ecological systems

15.2.6.1 Introduction

This chapter focuses on the *impacts* from overhead lines *on flora* and *fauna*, i. e vegetation and wildlife, and the interdependence between them, covering impacts on birds and wild herds and dealing with the effects on vegetation. The protection of endangered species is a matter of universal concern, and most often this involves the preservation of the habitat of rare botanical species or a dwindling colony of animals etc. The main ecological problems are the possible bird collision with the conductors or earth wires and effects of tree clearing and removal of vegetation within the right-of-way.
In the Ramsar Convention on Wetlands (UNESCO) [15.40], several countries have agreed upon the protection of wetlands of international importance especially as waterfowl habitat. The list of localities included is continuously supplemented. Most countries also have other protected areas due to regional, national or international environmental classifications. Construction of overhead lines in such areas should be avoided. A considerate route planning and use of bird flight diverters to reduce *bird collisions* are the most common mitigation measure when lines are constructed in sensitive areas.
Clearing the right-of-way may have positive ecological effects due to the increased biotic diversity in the clearing zone under the line. The positive ecological effects seem to a great extent to be a result of tree clearing in mono-cultural forested areas. Under the line, there will be many new plant species and low, narrow vegetation having a positive effect on different animals as feeding sites or places of refuge. Systematic planning and minimizing vegetation trimming may avoid the negative effects within the clearing zone (see clause 17.4.3.6).

15.2.6.2 Impacts on avifauna

Regarding the *avifauna*, bird mortality due to collision is an often discussed negative ecological impact. Mortality due to *electrocution* is mainly a problem for lower voltage lines, typically lower than 60 kV, due to the short distances between conductor and earth.
The literature on this subject is comprehensive, but it is not all easily accessible since much is found as unpublished reports and in national or regional periodicals. A review of literature regarding birds interactions with overhead lines is given in reference [15.41,

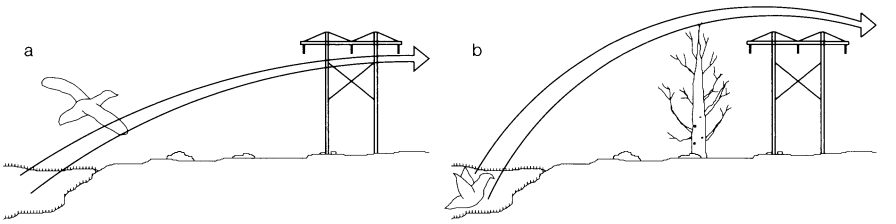

Figure 15.3: Line routing to avoid collision with birds (according to [15.5]). a not desirable, b to aspire

15.42] and [15.43]. Bird collisions and mitigation measures are dealt with in references [15.44] and [15.45].

Flight behaviour and vision are the two important biological aspects to be considered when evaluating the collision potential of a bird species. A trained ornithologist may be able to predict leading lines, *migration sectors* and flight lanes on the basis of topographical features. An overhead line located between a feeding area and a roosting site of wetland birds can be hazardous, especially when only a short distance separates them so that the birds only have to make a short flight at the critical height. Overhead lines passing near key *ornithological habitats* should be skilfully located close to the bases of near protective rows of trees, which force birds to fly over the wires (Figure 15.3). Locating a power line in the vicinity of tall buildings, bridges and other man-made structures may also reduce the collision risks, as well as locating the line along main roads where birds usually increase their flying height.

In addition to the principle of forcing an increase in flying heights, lines should, if possible, be placed parallel to major flight corridors. *Breeding areas* for different species along a line in the open terrain are devaluated because the supports are often used by predators as resting places.

Topographical, biological and meteorological aspects are important in the route planning process. Careful route planning is among the best and least expensive way of reducing bird collision. In general, ecologically sensitive areas such as wetlands, where birds congregate to nest, feed, roost, migrate or stay overwinter, should be avoided.

A reduction of collision frequency can be achieved through adjusting phase conductor height, conductor diameter, spacing, configuration and number of circuits. A flat line configuration is preferred to a vertical one. The earth wires are particularly likely to cause bird collision. The use of thicker earth wires and of *bird fly diverters*, that are balloons, spheres, spirals, plastic strips, etc. attached to phase conductors and/or earth wires are the most common mitigation measures. Several studies have found that use of diverters can be effective and decrease the number of victims by up to 90 % [15.46].

In sensitive line sections, sufficient mitigation measures should be adopted after consultation with environmental experts and the environmental authorities. Therefore, the route planning process should include *ornithologist consultation* to verify if vulnerable species can be influenced by a line and registration of primary ornithological functions of an area to consider them during line design [15.47].

15.2.6.3 Impacts on wild animals

It is general regarded that wild animals get accustomed to overhead lines, and thus their presence does not need to influence the choice of the power line route. In fact, the change in vegetation within the right-of-way in extensively forested areas will often

have a positive ecological effect for several species since this zone provides an additional source of food. In areas with wild herds, route planning and choice of construction period should be carefully discussed with wild life agencies.

15.2.6.4 Impacts on vegetation

Aisles in forests excepted, the impact on vegetation is limited to the support sites. If these sites are selected such that areas of rare and endangered plants are not infringed, *impairing the flora* can be virtually neglected, although within the right-of-way a limitation of tree heights might be necessary. If being selected skilfully regarding the topographical, forest and ecological aspects [15.48], there is little harm on vegetation. Where necessary, *vegetation control* should be preferably carried out by mechanical methods and not by application of chemical products or herbicides.

15.2.6.5 Conservation and wilderness areas

Possible construction of lines in *conservation*, recreation and *wilderness areas* is highly dependent on the legislation of each country. If avoidance of such areas is impossible, specific precautions have to be taken. The route planning and tower design need to consider the special values of the areas and make every effort to protect them. Clearing of the line corridors should be done with special care to avoid damage to the genuine natural landscape as much as possible. The undergrowth under the lines should be allowed to flourish so that the bio-diversity of the area does not suffer.

15.2.7 Route selection in view of land use

15.2.7.1 Introduction

In this section selection of power corridors is discussed in view of less conflicts with use of land under or in the vicinity of the line or on the possible future use of the different types of land over which the line is routed. Restrictions on future land use result mainly from the tower structures and conductors, or from electric safety requirements. The area of land under the tower structures is occupied by them. Restrictions in the use of land under the conductors vary, depending on their earlier use and on stipulations applicable in various countries. Especially, the required clearances limit the height of buildings to be constructed below lines [15.47].

15.2.7.2 Agricultural areas

In many regions, like Central Europe, overhead lines run predominantly in *agricultural terrain*. They do not prevent agriculture although they may impair it in particular locations. There will not be any crop loss due to the presence of the high-voltage conductors as such. The inconvenience of the lines results primarily from the tower structure. The circling of tower structures causes extra work and the tower structures may increase weeds in the fields. Safety clearances required from conductors in fields may also result in precautions in the operation of large farm machines.
Construction and maintenance of lines may cause losses of crops, compaction or rutting of soil, breakage of covered drains or fences, blocking of ditches and wear and tear on farm roads and tracks. All land damaged has to be restored to its original condition and any loss of use compensated for after completion of the works.
A line routing at the border between fields and coppices or forests proves to be favourable since infringement of agricultural use will be low. Supports should be spotted at the edge of paths or borders of plots to keep low damage to crops and infringement of agricultural use. An unrestricted use of agricultural machines is mandatory.

15.2.7.3 Forestry

Where the proportion of *forested areas* of the entire land area is small, forests are appreciated as an element of the environment more than as a raw material for the forest industry. Where forestry is a significant part of the economy, its use is natural, without forgetting the values of nature conservation.
Crossing of extended areas with larger stocks of *forests*, woods, coppices or hedges can be carried out by *passing above the forest* or by providing an *aisle*. One of these alternatives needs to be selected case by case, considering the given boundary conditions. In case of crossing above the trees, impacts on the forest will be limited to the tower sites whereby the necessary access roads need to be considered [15.49]. The wide-round visibility of tall towers forms a disadvantage in particular after cutting the trees or devastation caused by storms. The lines situated then relatively high above the terrain form a danger for birds to collide with the conductors when they stretch outside the forest scenery. When crossing above the forest, the final height of the trees has to be considered for defining the tower height. When cutting an aisle through the forest vegetation, specific directives [15.50, 15.51] and forestry aspects are important. Dependent on the specific forest aisle, its economic utilization and maintenance, a variation of the vegetation spectrum has to be expected. In addition, the adjacent *vegetation in the forest* could change because of boundary effects.
Due to certain safety considerations, the heights of trees growing in a line corridor are restricted, unless the line is constructed with adequate clearances above the tree tops. There can also exist zones where the trees can grow freely under the conductors due to the terrain, for instance when crossing valleys. Due to these restrictions, the use of overhead line corridors for normal timber production is usually not possible. It is mainly seeding stands or Christmas trees that can be grown under the lines and in the marginal zone the height of the growing timber is restricted so that a falling tree cannot touch the conductors. The compensation to be paid for the timber depends on the value of the trees and their age. The greatest loss normally comes from the area remaining permanently out of the natural cyclic growth of the forest.
As a rule, *forested areas* should be used by lines only to an extent as low as possible. When crossing forested areas, it should be agreed upon between the land owners, authorities and experts prior to further steps, whether an aisle or a crossing above the tree tops would result in minimum impacts on the interests involved.

15.2.7.4 Industrial areas and infrastructure developments

The implementation of lines in *industrial areas* does normally not cause any major problems with regard to land use if the line corridor was taken into consideration when the use of land was planned. The area under the lines can be used for storage of low height goods or for car parking, but industrial buildings can be allowed under the conductors. Landscape problems are not significant in industrial areas where other environmental impacts resulting from various activities are normally greater than those caused by the lines. In the immediate vicinity of work places near transmission lines, issues relating to electromagnetic fields may arise.
The construction of lines in areas in use for other infrastructure developments or reserved for public roads, railways, pipelines, water channels and watercourses or in their close vicinity does not change the original land use to any great extent and indeed may facilitate optimum use of a land corridor with minimized overall impact from the overhead line. The layout of tower structures and conductor ground clearances need to consider certain restrictions.
Line routing in the vicinity of certain infrastructure installations needs to take care of special requirements or will not be possible at all. Such installations are:

- **Airports and airfields:** Close to *airports*, the height of new lines will be limited by air traffic regulations and marking the structures by coating with warning colours or warning lighting during the night is required. The conductors or earth wires need to be fitted with warning spheres.
- **Mining areas:** In areas with *open-pit mining*, or with *underground mining*, routing of overhead lines has to take care of these installations. Open-pit mining may cause pollution which has to be considered when designing the insulation. Transmission lines need to be designed with cautious consideration in areas prone to cavity or earth falls. Corresponding investigations are necessary because possible settlement of terrain plays an important role when designing the foundations.
- **Military installations:** In general, overhead lines cannot be constructed within the protected area of *military installations*. Military installations which cannot be visually identified, such as pipelines, underground storage, communication installations, will be realized only during approval procedure and request often wide-space rerouting.
- **Microwave lines:** If crossing of *microwave lines* of telecommunication companies or other operators had not been known when establishing a preliminary line route, they need to be considered during the final approval procedure. Conflicts may be solved by a suitable selection of the tower sites.
- **Roads:** It is expedient to route lines in parallel to *traffic routes* following the principle of bundling between power lines and other infrastructure installations. However, overhead line supports may not be spotted in certain protective areas along motorways or highways.
- **Railways:** To crossings of *railway lines* as well as of *ropeways*, specific guidelines apply which should be considered already when selecting a preliminary route.
- **Waterways and water engineering:** When *crossing waterways* used by any kind of vessels, the clearance is stipulated by a certain gauge which needs to be agreed upon before deciding on the final line route. For the crossing of shipping lanes and other waters, as well as for support sites prone to flooding, approvals need to be applied for through the authorities in charge. Special precaution methods have to be adopted in *drinking-water protection areas* when constructing the line, to avoid any pollution.

15.2.7.5 Urban areas

As many examples demonstrate, existence of transmission lines in built-up *urban areas* does not cause any major problems for land use by the inhabitants, but restrictions will be given in planning the future land use. Change in land use within the area under the lines is not a major problem, but problems are caused by the encroachment of other developments on the line corridor resulting, for example, in the location of towers in the immediate vicinity of dwelling areas and raising the question of alleged health risks. In some countries, building of residential homes under lines is not permitted. Problems resulting from these changes in the land use can be diminished by utilizing the line corridors for various functions, such as car parking, gardening, footpaths, access corridors.

15.3 Survey on site

15.3.1 Steps of survey

Detailed maps along the selected line corridor should be available as a basis for *detailed design*. Based on these maps, a *layout of the line* is established, which the design

Figure 15.4: Total station

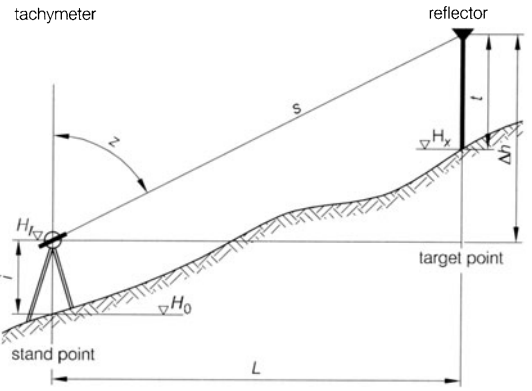

i height of instrument, t height of reflector, s measured inclined distance, z angle of zenith, H_0 altitude of the instrument site, H_I altitude of instrument, H_x altitude of the measured point in the terrain, L horizontal distance, Δh difference of altitudes

Figure 15.5: Height and distance measurement using a tachymeter

engineer uses to select the support sites and to identify the owners of the real estates concerned by the line project.
The activities on site start with the transfer of the selected route into the terrain, in particular by *fixing the angle points*. The line axis is designed as a straight connection of the line angle points. Along the line axis, *centre line beacons* are installed to identify and secure the line. This step is called *line alignment*. The *survey of the longitudinal profile* follows, whereby the terrain and all objects within the right-of-way are surveyed such as roads, water stretches, buildings and trees. The *pegging of the support sites* characterized by their centres and the *survey of diagonal profiles* at tower sites in inclined terrain complete the activities on site.

15.3.2 Survey procedures and instruments adopted

15.3.2.1 Direct survey in the terrain

In case of *direct survey*, the surveyor establishes the designed route in the terrain and carries out the profile survey there. Regarding the adopted procedures and the instruments used, considerable progress has been achieved during the recent years, contributing to rationalize the terrain activities and to permit a *continuous data flow* with computers in view of further processing of measured data. The utilization of satellite-based systems formerly reserved only for military application simplified and accelerated the activities to be carried out in the terrain. Nowadays, so-called *total stations* are mostly used for survey of overhead line routes in the terrain (Figure 15.4). These automatically recording *theodolites* equipped with a pogrammable surface process the distances measured in the terrain and the directions into point coordinates and record them in a three-dimensional coordinate system.
The coordinates of the individual points are required for the graphical output on a computer screen as used nowadays. Since the measuring tolerances for straight lines

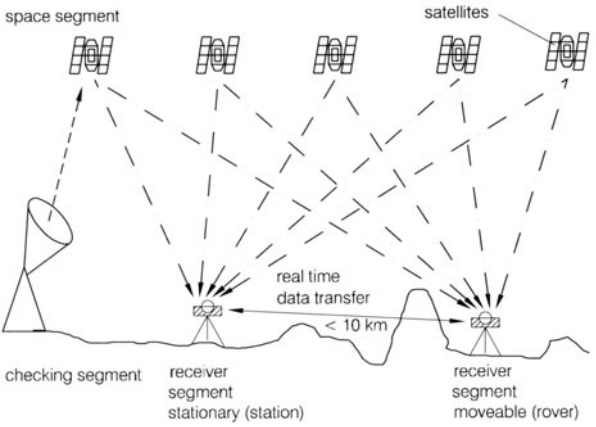

Figure 15.6: GPS device

Figure 15.7: Distance survey with GPS

are within the range of millimetres, a *mean precision of profile points* below 10 mm can be obtained related to distances up to 3 km. Automatically focussing systems, so-called *one-man stations*, where the surveyor controls the *total station* using an electronic field logger at the reflector, are not very suited for overhead lines since the activities in the terrain are oriented at straight lines and recording a high point density is not necessary. In Figure 15.5, the measured quantities i, t, s and z are shown recorded by a tachymeter in case of *height* and *distance measurements*. For each instrument, the calibration data c (addition parameter) and m (multiplication parameter) are given. When determining the trigonometric height, the reduction coefficient F has to be considered as well. This coefficient takes care of the Earth's curvature

$$F = L^2/(2\,R) \quad , \tag{15.1}$$

where $R = 6370$ km is the Earth's radius. The wanted quantities Δh, L and H_x result from

$$\Delta h = c + s \cdot m \cdot \cos z + F \quad , \tag{15.2}$$

$$L = c + s \cdot m \cdot \sin z + F \quad \text{and} \tag{15.3}$$

$$H_x = H_0 + i + \Delta h - t \quad . \tag{15.4}$$

By means of geocentrically positioned satellites, each spot on Earth can be reached by *Global Positioning Systems (GPS)*. By measuring of the wave running period between satellites and two receivers on the Earth surface, the distances are computed. As a result, three-dimensional coordinates are obtained, which can be transformed to the reference coordinate system.

The individual satellite signals experience disturbances on their way through the ionosphere and, in addition, are falsified, to some extent, by the operators of the satellite networks. The results of these facts would constitute coordinates from measurements based on one satellite only not having any acceptable accuracy in view of the overhead line survey requirements. Differential measurements by receiving simultaneously data

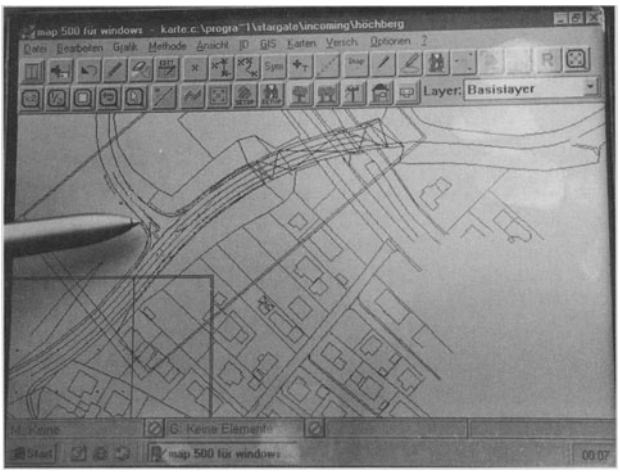

Figure 15.8: Graphical computer data logger

from several Earth orbiting satellites compensate the errors and result in data with coordinate discrepancies of a few centimetres only. For several years, real-time GPS systems have been on the market enabling measurement, correction and immediate evaluation with a high accuracy directly on site. De-activating the distorting signal by the US Department of Defence in 2000 brought the GPS system to the accuracy of *total stations*. In Figure 15.6, a GPS equipment is shown and in Figure 15.7 the arrangement of geocentric satellites and basis of distance measurements.

GPS systems are available worldwide, enabling a quick recording in the open terrain. They are, to a large extent, independent of the weather, do not require any visual connection between the stationary and the movable receiver segment, called *rover*, and need *fix points* in a distance of some kilometres only. The results of the GPS survey are three-dimensional coordinates. However, it is disadvantageous for *survey of overhead lines*, that the GPS systems do not permit direct measurement and determination of heights of crossed objects such as transmission lines, buildings etc. For this purpose, tachymeters are necessary in addition.

Total stations and real time GPS stations can store the quantity of data recorded during a whole week. As with other electronic storage systems, security copies, however, are recommended. During practical use, the devices have proved to be reliable under all measuring conditions. Direct measuring systems need a virtually complete accessibility to the line route.

To visualize the data on site and to increase the performance of survey, the data recording can be carried out on site directly using a *graphic data logger*. Graphic data loggers are computers suitable for use in the open which, due to their capacity, permit storage and presentation of land and topographical maps. Using corresponding calculation routines, each measured point can be directly checked against the designed line route on the computer display (Figure 15.8).

15.3.2.2 Indirect line survey

Indirect survey systems record the route corridor either based on photographs (aerial photogrammetry) or by signals obtained through scanning. In case of *aerial photogrammetry*, the survey corridor is flown over by a panchromatic aerial survey camera, which delivers overlapping photographs of the *terrain surface*. By means of adjustment points with known coordinates within the line corridor, the photographs are aligned and rectified. The evaluation using a digital stereograph delivers rectified aerial

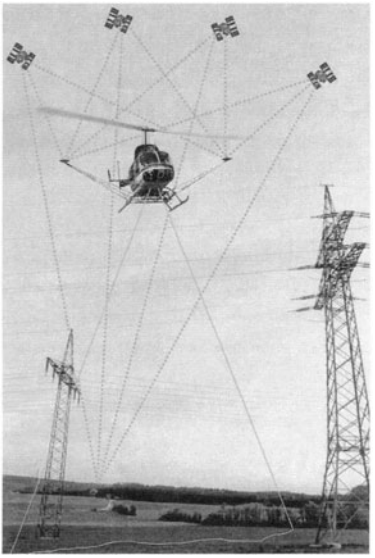

Figure 15.9: Principle of laser scanning with rotating lasers installed at a helicopter

photographs as results, being called *ortho-photographs*. From the ortho-photographs, a *three-dimensional terrain model* can be produced using computers.
The more recently developed *laser scanning* method adopts rotating lasers installed at an airplane or helicopter to scan the Earth's surface and existing installations such as overhead electrical lines (Figure 15.9). Since within the right-of-way many vertically structured objects need to be survey the arrangement of two laser devices obliquely below the helicopter has proved to be advantageous. By means of the GPS, the position of the helicopter is controlled providing continuously a three-dimensional determination of the laser positions. The helicopter flies approximately 100 m above ground with around 50 km/h. The laser scanning method enables to survey the position of any objects in three dimensions. It is possible to scan 200 km of lines per day. As results, digital profiles are obtained with the relevant information on the terrain, infrastructure and existing lines in three dimensions. The method is applicable also in forest areas under trees [15.52] if sufficient openings are given in the leafy canopy. Applications [15.53] demonstrated that this system is capable of verifying overhead line structures, finding span lengths, conductor sags and checking conductor clearances to ground as well as vegetation, residential and industrial buildings and crossed infrastructure. Airborne survey combines high productivity and relatively low costs. It displays all features of profiles and ground surface. The location of important objects within and close to the right-of-way can be determined. Utilities use the survey results to decide on and prepare refurbishment and upgrading. They improve the reliability and efficiency of maintenance as well.
When using indirect surveying systems, an approval to access the line route is not necessary. The high one-time expenses are compensated by shortening of the planning period, which might be advantageous in case of big projects. Indirect systems deliver data with an accuracy within the decimeter range; heights of objects within the line corridor can be determined. Alternative routes can be evaluated, too. However, in view of accuracy and costs, the direct surveying systems are superior to the indirect ones.

15.3.2.3 Terrain data banks

Terrain data banks have been under preparation in 2002 but available only in parts of Europe, North America and Japan. However, in future they will form the basis for planning of extended infrastructure projects. Within a few years, numerous geographic satellites will be commissioned which will provide highly-resolving photographs. These photographs will be accessible in the format of three-dimensional terrain models via internet. By input of the coordinates of the line angle points, the user can receive the wanted corridor and evaluate it. At the moment, mesh widths of 10 m are available and linear interpolation is carried out in between. Resolutions below one meter are envisaged which would be sufficient for planning of overhead line routes at all.

The decision on the system to be used depends on local conditions, the density of points within the surveyor fix point net as well as the period of time available for design and, therefore, needs to be decided upon separately for each individual project.

15.3.3 Survey of angle points and line alignment

A layout plan forms the precondition for *surveying angle points* in the terrain. It should be established on the basis of *land maps* with a scale of 1:5000 or even bigger containing the borders of real estates, as well. Such land maps can be obtained from surveying authorities or the land register either printed in island-type formats or framework maps or electronically as *automated land register maps.* They contain information on the used coordinate system as well.

If land maps are not available for all areas, then *topographical maps* with a smaller scale have to be used for defining the line route. In this case, the use of *GPS* can be recommended to define the angle points. A layout plan in a larger scale will be established in the course of the survey process. If UTM coordinates are available in the maps, the coordinates evaluated by GPS can be transferred to this system and serve as reference between planning in the map and on site.

Before deciding on and surveying of the angle points, the objects within the right-of-way, such as crossed overhead lines, buildings, railways and motorways should be surveyed. If a planned line route can be realized without conflicting with such objects, the angle points can be referenced to available fix points, boundary stones, real estate boundaries or to the coordinates of the reference net and pegged out, then. After definition of the angle points, a straight *alignment* is measured and pegged out in the terrain. If a direct vision between two adjacent angle points is given, it is recommended to peg out the centreline beacons directly by means of a total station. The exact line alignment is pegged out by precisely arranged centre mark heads on the *centre line beacons.* In many cases, the line alignment cannot be obtained directly, since distance, forests, settlements or terrain prevent a direct sight to the adjacent angle point. In this case, the centreline beacons can be pegged out using relevant coordinates without the need of a complete accessibility of the line route. Placing of the line route by means of GPS proves to be advantageous, since, in this case, survey is possible at all accessible points, also at those without a direct sight. A survey by polygons should be limited to areas where the satellite signals are shadowed. Singular obstacles in the line route can be passed by through staggering the tachymeter in parallel.

The determined right-of-way is transferred into the layout plan and handed out to the line owner for *inspection.* During inspection, the route can be visualized and critical points such as approaches and crossings be agreed upon with the line owner before starting the construction. To avoid misunderstandings, the centre line beacons for line points, angle points and tower sites should be characterized by different colours.

15.3.4 Survey of terrain profile

When using direct survey systems, the *terrain profile* along the line axis and a *parallel profile* at the edge of the right-of-way in case of laterally inclined terrain, need to be measured and recorded. During this procedure, all striking points within the terrain and crossed objects within the line corridor are recorded with their position and height. When using indirect survey systems, at first the established digital *terrain model* is restricted to the relevant line corridor. With the aid of angle point coordinates, a straight line is drawn through the digital terrain model, representing the line axis, and then a longitudinal profile is interpolated along the line axis by means of an evaluation software. In this case, the step width selected for the interpolation of the profile is of substantial importance. A longitudinal profile produced by means of a terrain model can only be such accurate as the width of meshes within the terrain models. Since the resolution of such a model amounts to some meters only, the results obtained from the terrain model should be compared with the real terrain to verify the correct line design. Critical points should be checked in the terrain.

15.3.5 Location of supports

The support sites are pegged out using direct survey systems. The use of GPS systems proved to be economic in this case. Pegging is carried out based on the calculated coordinates of the support sites and can be secured by referencing to buildings, surveying fix points or the like. Thoroughly documented *support sites* form the basis for line construction. The width of the supports at the surface is prevalent for this activity and for compensating the real estate owners.
Pegging out of the support sites has to be carried out unequivocally and durably, complying with the contract or line owner specifications. The system Feno (Figure 15.10) has proved its qualification for marking lines, because its resistance against vandalism.

15.3.6 Survey of existing lines

Survey of existing lines gained increasing importance in countries with an extended infrastructure to document the physical condition of the line network. In some member countries of the European Community, the checking intervals are legally stipulated. When surveying existing lines, the data can be recorded in such a way that they can be directly transferred into a *graphic information system* (GIS). During resurveying, the topography and the line condition can be checked. The topographical check aims at newly installed structures and modification of land use within the line corridor. The engineering check comprises the condition of foundations, support structures and insulators, as well as checking the conductor sag. From the recorded sag, it can be concluded where the stipulated safety clearances are met and where refurbishment might be necessary.
To determine the conductor position by a direct measuring system, a tachymeter position is selected on the line axis outside the span to be surveyed (Figure 15.11). At first, the width of the crossarm at tower 2 is determined from

$$b_2 = L_2 \sin \beta_{M2} / \sin(200^g - \alpha_2 - \beta_{M2}) \quad , \tag{15.5}$$

where β_{M2} and L_2 are measured. The definitions of the angles β_{M2} and α_2, as well as of the distance L_2, can be obtained from Figure 15.11. If tower 2 is a suspension tower, then $\alpha_2 = 100^g$. The determination of the distances L_{p1} and L_{p2} follows, using the cosine law:

$$L_{p1,p2} = \sqrt{L_{1,2}^2 + b_{1,2}^2 - 2 \cdot L_{1,2} \cdot b_{1,2} \cos \alpha_{1,2}} \quad . \tag{15.6}$$

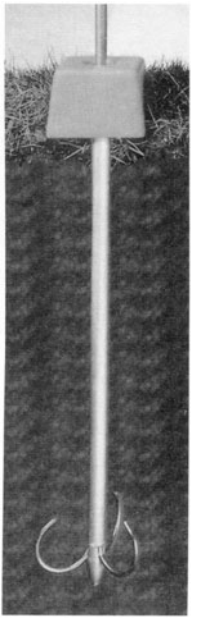

Figure 15.10: Line beacons type Feno

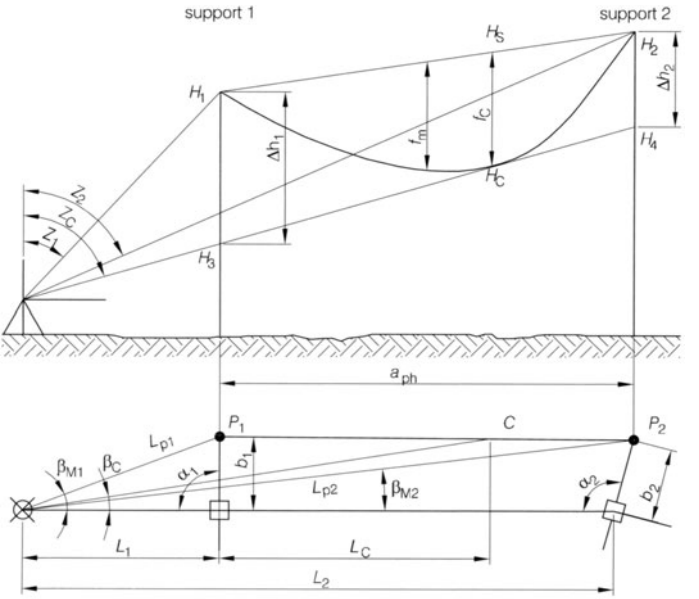

Figure 15.11: Tangential survey of sag of an existing line

In case of suspension towers, the angles α are equal to 100^g. With these data, the coordinates of points P_1 and P_2 and their distance a_{ph} can be calculated.
The determination of the heights H_1, H_2, H_3 and H_4 follows related to the position of the tachymeter. For this purpose, the zenith angles z_1, z_2 and z_C to the point of the tangent C at the conductor have to be surveyed as well as the corresponding horizontal angle β_C. The heights H_1, H_2, H_3 and H_4 are obtained from

$$H_{1,2} = L_{p1,2} \cdot \tan(100^g - z_{1,2}), \quad H_{3,4} = L_{p1,2} \cdot \tan(100^g - z_C)/\cos\beta_C . \tag{15.7}$$

The relation between the sag f_C at tangent C, the differences in heights Δh_1 and Δh_2, as well as the distances L_C and a_{ph} according to Figure 15.11, are given by

$$f_C = \Delta h_1 + L_C/a_{ph} \cdot (\Delta h_2 - \Delta h_1) \quad . \tag{15.8}$$

The ratio L_C/a_{ph} can be expressed by the measured relative heights H_1, H_2, H_3 and H_4 and their differences Δh_1 and Δh_2 by

$$L_C/a_{ph} = \sqrt{\Delta h_1/\Delta h_2} \Big/ \left(\sqrt{\Delta h_1/\Delta h_2} + 1\right) \quad , \tag{15.9}$$

where $\Delta h_1 = H_1 - H_3$ and $\Delta h_2 = H_2 - H_4$. From these quantities, the data necessary to determine the *sag at midspan* are known:

$$f_{max} = f_C/\left[4 \cdot (L_C/a_{ph}) \cdot (1 - L_C/a_{ph})\right] \quad . \tag{15.10}$$

In case of an indirect measurement (see clause 15.3.2.2), the conductor position is determined from the survey data.
As an alternative to the tangential measurement of sag, a measurement is possible from a position laterally to the line axis as well. The measurements can then be evaluated using equations (15.2) to (15.4).

Table 15.1: Minimum clearances to define approaches

Object	Load case	Clearance
Gauge or components of a railway contact line installation	wind load, sags at correlated temperature[1)]	0,5 m + D_{el}, minimum 1,5 m
Ropeway	as above	4,0 m + D_{el},
Rim of a road, motorway or shipping lane	as above	0,5 m + D_{el}, mimimum 1,5 m
Rim of a railway track	as above	4,0 m + D_{el} or 15,0 m, if electrification is planned

[1)] 40°C in Central Europe

15.4 Line design and establishing of plans

15.4.1 Clearances

Minimum clearances to the terrain surface and to crossed objects need to be complied with to protect people as well as fixed or movable objects against hazardous approach to live conductors and against discharges. The basic requirements are specified in standards, such as EN 50 341-1 [15.54] applicable for the European Community and EN 50 341-3-4 [15.55] valid for Germany and explained in detail in clause 2.5.2. According to EN 50 341-1, it is distinguished between minimum clearances to

- *Ground* in areas remote from buildings, roads, railways and navigable waterways ([15.54], Table 5.4.4);
- *Residential and other buildings* ([15.54], Table 5.4.5.2);
- *Lines crossing roads, railways and navigable waterways* ([15.54], Table 5.4.5.3.1);
- Lines adjacent to roads, railways, navigable waterways ([15.54], Table 5.4.5.3.2);
- *Other power lines or overhead telecommunication lines* ([15.54], Table 5.4.5.4) and
- *Recreational areas* ([15.54], Table 5.4.5.5).

The stipulated *minimum clearances* are presented in Table 2.22. In addition to the data in Table 2.22, an *electrical clearance* D_{el} has to be considered which depends on the insulation of the line with respect to the stresses by fast-front or slow-front overvoltages. Data obtained from experience for these distances are listed in Table 2.19, depending on the *maximum voltage for equipment* U_s. The total clearance against rigid, non-movable crossed objects, obtained as the sum of the values according to Table 2.22 and D_{el}, must at least result in 1,1 times of the shortest value of *straight line distance* a_{som} between live parts and earthed parts of the insulator strings in still air position (see clause 2.5.2.2). In principle, the minimum clearances to be met by an individual line project need to be specified separately for each line, therefore. In EN 50 341-1 [15.54], the conditions are listed under which the afore mentioned clearances have to be complied with as follows:

- At a *maximum operating temperature of the conductors*, specified for the line;
- Under specified *ice loads*, depending on the area where the line will be erected;
- Under the action of a *wind load*, having a return period of three years;
- Under the action of a wind load with a return period of 50 years. In this case, electrical clearances necessary to withstand the power frequency voltage will be sufficient;
- Under combined action of wind and ice. National standards or a project specification should stipulate the conditions to be met in this case.

In addition to these basic requirements, some standards require the verification of clearances under ice load in one or few spans only. Table 2.21 lists conductor temperatures and ice loads for checking the clearances according to [15.56]. The temperatures vary between 40 and 80°C, the ice load depends on the reference climate at the overhead

line location. As an example, the requirements according to EN 50 341-3-4 [15.55] valid for Germany should be discussed hereafter.

- A value for the maximum operating temperature is not specified. The maximum operating temperature, however, should be at least 60°C. Often, 80, 100 or 120°C are stipulated by line owners providing for *conductor creep*, as well.
- The clearances have to be verified for the ice loads specified for a line, whereby all conductors and spans of the line are loaded by the same ice load.
- In case of crossings, clearances under *local ice load* in the crossing span have to be verified, whereby a local ice load of 50 % of the specified ice load has to be assumed.
- The clearances have to be verified under action of a medium wind load, corresponding to a three year return period. This amounts to 58 % of the design wind load, whereby the minimum clearances according to EN 50 341-1 (Table 2.22) plus D_{el} need to be obeyed. The conductor position can be calculated according to sags occurring at +40°C . The *determination of swing angles* is explained in clause 2.5.2.4. In case of angle suspension towers, the radial component of the conductor tensile force acts in addition to the wind load (see clause 12.2.4).
- The clearances need not be verified under design wind load or under combined action of wind and ice loads.

In case of *crossings between two overhead lines*, the positions of the conductors of both lines vary with temperature, wind and ice load. The most unfavourable condition depends on loads, crossing angles and conductor types. Therefore, some cases are verified in practice as stipulated in the relevant standard or project specification. At least, the following three conditions should be analysed according to [15.55]:

- The maximum sag either at the maximum conductor temperature or at ice loads at −5°C of the overcrossing line and the sag of the undercrossing line at +40°C or −5°C without ice load. The conductors do not swing.
- Local ice load at the conductors of the overcrossing line and sags at −5°C without ice load of the undercrossing line. The conductors do not swing.
- Medium wind load having a three year return period perpendicularly to one of both lines with sags at +40°C and wind load on the other line multiplied by the square of the cosine of the angle of wind attack on the conductors of the other line. Thereby, the wind load has to be varied in between 100 and 60 %.

Clause 14.9.4 contains an example.

In Figure 15.12, the protective ranges are shown between a conductor and a crossed structure. There, it is also shown where specifications for *crossings* have to be met and where the situation may be considered as an approach. For the latter case, Table 5.4.5.3.2 of [15.54] lists discriminating rules which are summarized in Table 15.1. If these clearances are not met, the requirements specified for crossings apply.

In addition to the clearances explained, requirements on the *line design in crossings* are stipulated in most standards. In [15.55], these requirements refer to:

- Arrangement of conductors at *multiple insulator sets*, at least double sets;
- Clearances of $0{,}75 \cdot D_{pp}$ between conductors have to be verified also for the case that one conductor is loaded with 50 % of the design ice load while the other conductors are without ice. The values for D_{pp} can be found in Table 2.19;
- After *failing of an individual insulator string* of a multiple insulator set, a clearance between the conductors of $0{,}75 \cdot D_{pp}$ must be given at −20°C .

In recent years, *wind energy converters* have been installed in many countries. The clearances between such installations and overhead power lines were controversial discussed because of possible effects on the lines and their components. As a result, clearance requirements were provided. As an example, according to the rules applicable in Germany, the clearance to the closest conductor in still air should be:

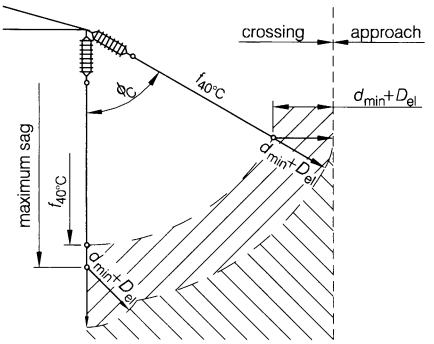

Figure 15.12: Protective ranges between conductor in still air or swinging under wind and the nearest part of a building in case of crossing of obstacles according to EN 50 341-3-4. The angle ϕ_C applies in between the conductor in still air and in a swung position under wind load; d_{min} clearance according to EN 50 341-1; D_{el} nominal air clearance depending on the operating voltage

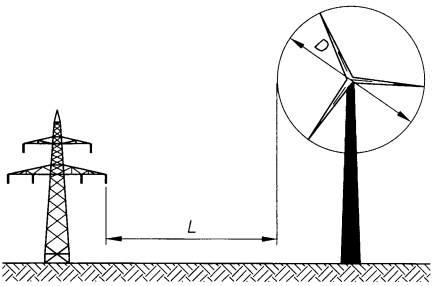

Figure 15.13: Minimum clearance between high-voltage overhead lines with nominal voltages above 30 kV and wind energy converter installations:
- without vibration protection $L \geq 3\,D$
- with vibration protection $L \geq D$

- Equal or larger than three times the rotor diameter if the conductors are not protected against aeolian vibrations or
- More than one rotor diameter if the conductors are protected against aeolian vibrations. The tips of the rotor may not project into the right-of-way of the transmission line. Figure 15.13 depicts schematically these requirements.

Between a wind energy converter and overhead lines, lower clearances than those described above, may be accepted if the transmission line is situated outside the wake of the wind energy converter (see [15.2, 15.57]).

15.4.2 Determination of support locations, tower types and heights

15.4.2.1 Evaluation of the profile survey

To obtain a *longitudinal profile* from the surveyed data, it is necessary to refer the registered data to known altitudes at the beginning and the end of the line. A data file of coordinates results from the profile survey, enabling the drawing of a longitudinal profile along the line axis with all relevant information. This longitudinal profile forms the basis for tower spotting. Where necessary, a *parallel profile* at the edge of the right-of-way is established in addition. The clearances between the respective longitudinal profile and the conductor catenary curve are used for planning of tower locations and heights.

15.4.2.2 Basis and relevant parameters

As a result of the terrain survey, a longitudinal profile (Figure 15.18) of the line route with all information relevant for the detailed line design such as type of terrain and utilization, crossed traffic roads, waters, railways is available. Within the next step, the support locations have to be defined and the support types and heights to be determined. This step decides on the visual perception of the line and affects the investment for construction as well; it is known as *tower spotting.*

Even when the route has been finally selected, there are many possibilities for designing an overhead line between two given points, e. g. a large number of low towers with short

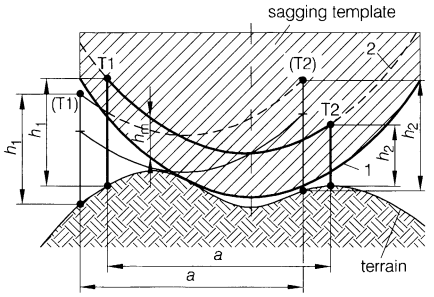

Figure 15.14: Manual tower spotting with the aid of a sagging template. 1 ground clearance curve; 2 conductor catenary curve; T1 suspension tower 1; T2 suspension tower 2; h_1 height of T1; h_2 height of T2; h_m minimum ground clearance; a span length

spans or a few tall towers with long spans. In general, the terrain, the soil characteristics and land use within an overhead corridor change to a more or less great extent. That alternative should be selected, which complies with all technological and terrain conditions and involves the lowest investment.

The angle points along the selected route are fixed points for tower locations, only the height of angle towers is to be selected at the tower spotting stage. The terrain profile along and across the route determines the necessary *tower heights*; the investments necessary for foundations depend on the soil condition; the *accessibility of the individual tower locations* affects the efforts for construction, as well as for operation. The conductor sags between the attachments at the towers change with conductor temperature and ice loads. Tower spotting must ensure that adequate clearances between the conductors themselves and to objects crossed by the line are maintained under all conditions.

The possible conductor suspension heights and permissible spans between two towers are determined by the geometrical dimensions of the available tower types and their horizontal and vertical load capacities. An optimum tower spotting requires taking into account all investments for towers, insulators, accessories and foundations as precisely as possible. The same applies to the construction expenditures particularly in projects where access to tower sites is difficult. Attention has also to be given to the expenditures associated with *land acquisition* and *compensation for tower locations* and for real estates crossed by the conductors.

15.4.2.3 Manual tower spotting

In a conventional manner, *tower spotting* is carried out manually by the design engineer. The route profile drawing and a template showing the catenary to the same scale as the profile drawings are used. This *sagging template* is produced based on the sags related to the expected equivalent span (ruling span) and the maximum conductor temperature (Figure 15.14). In parallel to the ground curve, which is represented by the edge of the template, the *conductor catenary* is shown in a distance according to the stipulated ground clearance. If the template touches the terrain, this parallel curve represents the conductor position and enables determining the conductor attachment points and checking the clearances to crossed objects.

In Figure 15.14, the sagging template is presented in a position to determine the location and height of tower 2, assuming that tower 1 is fixed at location 1. While the sagging curve starts at the conductor attachment point at tower 1, the ground clearance curve touches the ground surface. The sagging template is adjusted such that its horizontal edge runs in parallel to the abscissa of the longitudinal profile. Therefore, its centre line is perpendicular to the horizontal abscissa. It is expedient to start tower spotting at locations where constraints on the free selection of a support site exist, e. g. at important crossings, fixed tower locations, angle points etc. While carrying out tower spotting, the engineer should take care of avoiding higher differences in the span lengths

and tower heights.

After preparing a preliminary tower spotting, the compliance with all technical stipulations, such as *wind* and *weight span*, relations of wind to weight span, geometric maximum span etc. need to be checked in detail. Where applicable, compliance with permissible *electrical or magnetic field* strength below the line and at the edge of the right-of-way needs to be verified as well. If these conditions are not complied with, tower heights, tower types or the tower spotting at all need to be corrected accordingly.

The quality of manual tower spotting depends largely on the experience and care of the design engineer. He is hardly in a position to evaluate the economic consequences of all the possible tower locations, because such a comparison of possible alternatives would take too much time. Especially in long line sections, it is easy to lose sight of essential parameters during manual tower spotting. Much experience is, therefore, required to ensure that all relevant factors receive sufficient attention, and a correspondingly high quality of the tower spotting is achieved.

15.4.2.4 Tower spotting and optimization by means of data processing

Tower spotting with the aid of data processing presupposes, that the task can be performed analytically and digitally taking care of all relevant parameters. Optimizing the tower spotting can be included. In principle, the *optimization of the tower spotting* covers the whole line and can be carried out between its end points. However, optimization is also possible for specific line sections only. The quality and accuracy of the results do no longer depend on the the design engineer's experience, but solely on the extent of calculations performed.

The basic activities for preparing an optimization of tower spotting comprise the following steps:

- Definition of the tower family with tower types and heights, available body and leg extensions, characteristic parameters like wind span, weight span, maximum span;
- Determination, as accurately as possible, of associated investment for every tower type and height, taking into account the equipment like insulator sets, fittings and foundations as well as transportation to site and erection;
- A digitalized profile for input into the computer program;
- Definition of ranges which cannot be used for tower locations;
- Definition of locations mandatory for tower sites, especially for angle points, and the tower types to be adopted there;
- Input of location and height of crossed objects within the line corridor;
- Assigning additional investments to individual line ranges, where tower location is possible, however involves extra money for compensations, transportation of material and equipment, to construct foundations and erect towers. Examples are steep mountainous terrain, swampy land, low-bearing soil;
- Establishment of design parameters, line deflection angles, weight span to wind span ratios, insulator set swing angles, clearances to ground, conductor sags etc.

Tower spotting by computer program can be carried out using the *successive elimination method* [15.58, 15.59]. There, the line is divided into equidistant steps between 5 and 20 m long and each step of the profile is dealt with as a temporary end point for the purpose of tower spotting calculation. For each temporary end point, an optimum tower spotting is determined between the beginning of the line and the point currently being dealt with. Only the data of the optimum tower spotting calculated for each step need to be stored in the memory and to be given further consideration.

In Figure 15.15, the optimization process is visualized. Starting at the tower S at the begin of the line section to be spotted, each point of the profile in a distance between

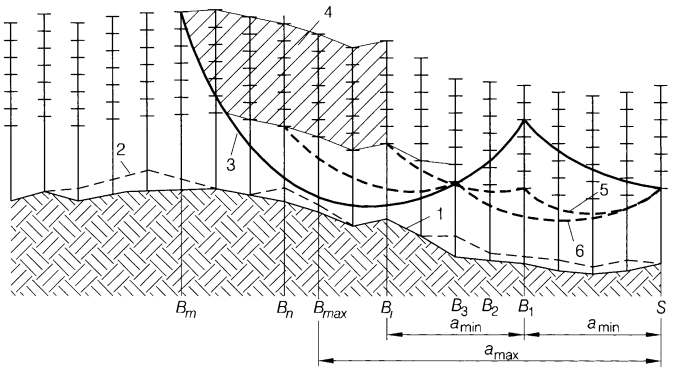

Figure 15.15: Tower spotting with location B_i considered as provisional end point. 1 centre line profile; 2 parallel profile; 3 ground curve of conductor sag, alternative with maximum tower height at location B_m; 4 range of technically possible tower locations and extensions with respect to location B_1 and height alternative 4; 5 tower spotting with one intermediate tower between S and B_i; 6 optimum tower spotting to B_n

permissible minimum and maximum span is considered as a possible tower site. The first acceptable location is B_1, situated at minimum distance a_{min} from tower S. Then a conductor catenary line is established to the lowest height alternative of tower S and the clearances to ground are checked at all intermediate profile steps between the locations S and B_1. It is obvious that for the minimum span minimum tower heights at both tower locations would be sufficient. Therefore, this solution would present the optimum and is the one kept in the memory correlated to the site B_1 and tower height considered there. All other tower extension alternatives at the location B_1 would also lead to a minimum investment in combination with the shortest tower at location S. After processing all tower height alternatives at the location B_1, the procedure continues with the location B_2. There, again the only span length alternative is to the tower at the location S and the technically acceptable and least expensive height alternative is selected. This procedure is continued until a location corresponding to the maximum permissible span a_{max} will be reached. However, if the available maximum tower extensions at locations B_i and S were not enough to provide the required clearance to ground or to obstacles, an alternative is checked with an intermediate tower location between the temporary end and S. In principle, such a solution can be implemented at location B_i in a distance of two times a_{min} from S. In this case, a tower spotting alternative assuming lowest tower heights at the involved tower locations considered would represent the lowest investment. This process is continued along the whole line section which is to be optimized. Only technically acceptable alternatives are subsequently included in the comparison of investments. For each temporary end point of the profile studied, only the solution representing the minimum investment is stored again characterized by the distance of the optimum tower site and the height there in direction of the beginning of the section to be optimized. Thus, starting from each step currently considered as line end point, the most cost-effective height alternative and distance of the next tower is selected from technically acceptable solutions. For each point of the profile considered temporarily as an end point, this process is repeated for the terrain between the specified minimum and maximum span length towards the beginning of the line section. The most economic tower spotting is then assigned to the particular tower height alternative at the tower location considered as a line end point. This procedure is continued until the end of the line section to be spotted. When arriving the end point,

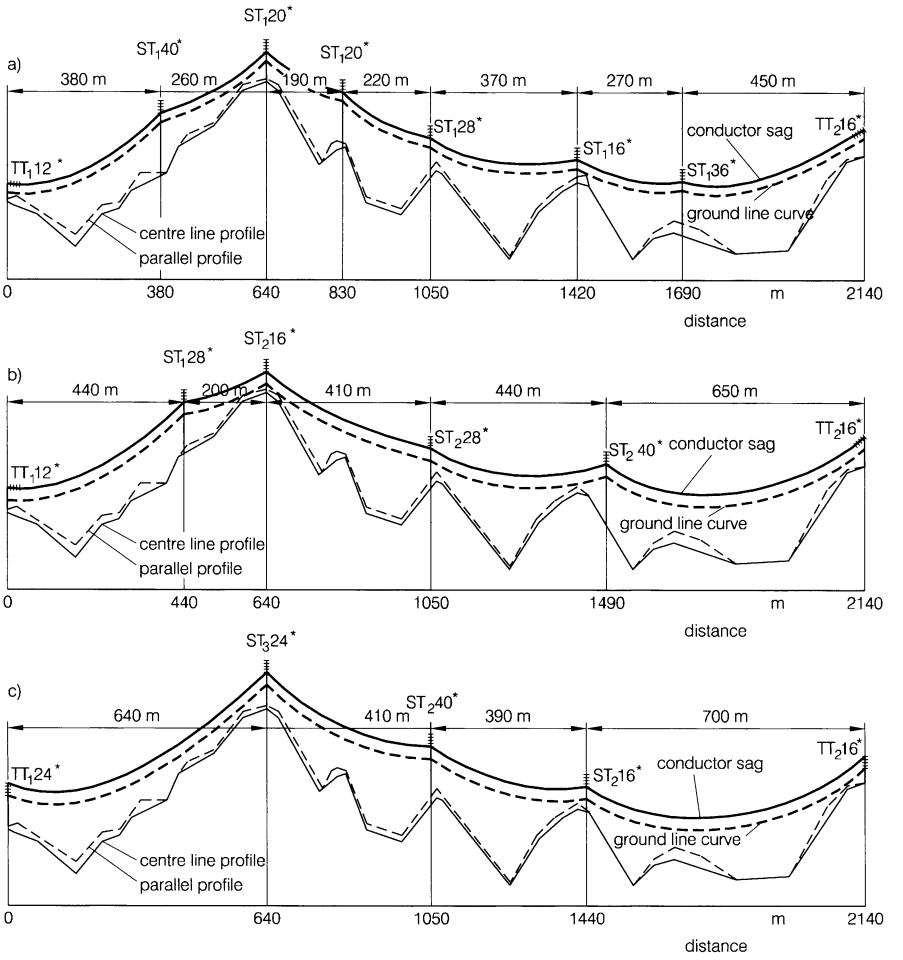

Figure 15.16: Tower spotting using several types of suspension towers. a) tower spotting with one suspension tower type; b) tower spotting with two suspension tower types; c) tower spotting with three suspension tower types; ST_1 to ST_3 suspension towers; TT_1, TT_2 angle strain towers; * height of the lowermost crossarm

the optimum tower spotting can be obtained by retracing back the chain of optimum solutions towards the start point of the line section. In Figure 15.15, the tower spotting step is demonstrated, where the location B_n is considered as the current end point of the line. From Figure 15.15 it is obvious that the most economic tower spotting starting with the lowest extension at location B_n is that with one intermediate tower at location B_3, since only one intermediate tower is necessary and the tower extensions are always the lowest possible. In Figure 15.15 this alternative is given the number 6.

Example: The design engineer should check the result of the tower spotting in view of consistence and construction requirements. He may introduce modifications of the optimum spotting by moving tower sites. The necessary modifications of other tower locations and heights can be obtained from the optimization output. Detailed design of the selected alternative, preparing profile drawings, lists of materials, clipping offsets and sagging tables, construction lists, design of crossings etc. is then carried out.

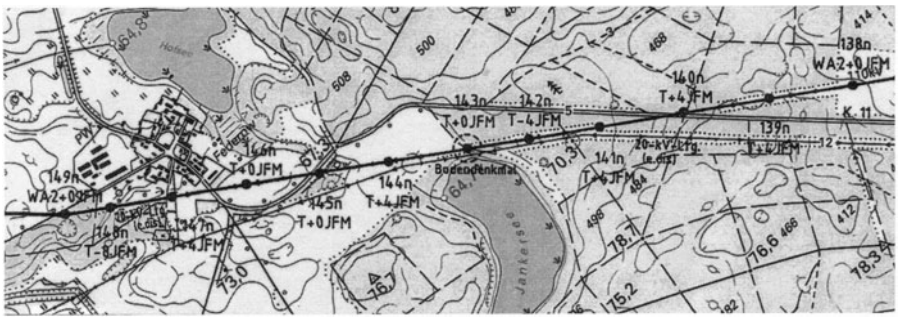

Figure 15.17: Overview plan

Other computer programs like [15.60, 15.61, 15.62] optimize the tower spotting along a line or parts of it by selecting the most economic alternative out of all feasible solutions at the end of the calculation process.
As an example for a digital tower spotting, the result of optimization is shown for a 2,1 km long line section (Figure 15.16), adopting different line data for the tower spotting. The three alternatives are the following:

- Overhead line with one type of suspension tower, with a permissible weight and wind span of 400 m. According to the optimization process, six tower locations are necessary between the assumed end points (alternative a).
- Overhead line with two types of suspension towers, with weight and wind spans of 400 and 550 m, respectively. There, four tower locations result from the optimization (alternative b).
- Overhead line with three types of suspension towers, with permissible wind and weight spans of 400, 500 and 700 m, respectively. The result of the optimization are three tower locations only (alternative c).

15.4.3 Documentation of lines

After the alignment of the line axis and the survey of the longitudinal profile, a transmission line can be technologically planned according to the project specifications. During planning, a series of drawings and lists are used for *documentation of lines*:
Overview plan: The *overview plan* (Figure 15.17) is based on topographical maps with a scale of 1:25 000 or 1:50 000 and serves to represent the line corridor in view of general planning procedures on future land use. The entities taking care of public interests receive a corresponding section of the map. The representation of the right-of-way is limited to an accuracy of ±12,5 m and ±25 m, respectively, corresponding to a mapping and reading tolerance of ±0,5 mm. The overview plan is also used to define the access to the tower sites.
Plan layout: The *plan layout* (Figure 15.19) represents the line in a scale of 1:2000 or 1:5 000 with high precision and is established based on land maps or other precise maps. The plan layout contains as well the *plot boundaries* and all *crossing objects* (other lines, roads, waterways), in the most cases with designations and additional information. The design layout establishes the basis for the detailed planning in densely populated areas. If land maps are not available, *ortho-photographs* with a scale of 1:5000 or 1:10 000 can be used for detailed line design without conflicting with other objects.
Longitudinal profile: The *longitudinal profile* (Figure 15.18) contains all parameters and data relevant for design, construction and operation of a line in a scale 1:200 to 1:500 at the vertical and 1:2000 to 1:5000 at the horizontal coordinates adjusted to the scale of the plan layout. Using the tower designation number, reference to other technological information and to documents concerning the ownership is possible. The longitudinal

profile presents the tower spotting and the clearances to terrain and to crossed objects. The *sagging curves* are shown for the final condition with data as planned.

Sagging tables: *Sagging tables* should contain initial sags with conductors in stringing blocks and final sags with conductors clipped-in depending on ambient temperatures and the period of time during which the conductors have been suspended on the stringing blocks, so to compensate creep. The offset at the suspension points needs to be listed as well (see clause 16.8.5).

Diagonal profile: The *diagonal profile* for self-supporting towers (Figure 15.20) shows the relation between terrain elevation at the individual tower legs in an inclined terrain with reference to the tower centre. Differences in elevation between the positions of leg members at the ground surface determine the required lengths of the leg extension. In case of guyed towers, the diagonal profiles of the guy wire attachment projection on the surface level and between the masts should be surveyed. Such diagonal profiles aim at defining the guy wire and mast lengths and the points where these elements need to be installed.

Tower list: In the *tower list* (Figure 15.21), all relevant data for construction are summarized: Tower numbers and designation, tower type, length coordinates, leg extensions, lengths of masts and guy ropes, type of foundation, type of insulator set and additional information, if any.

List of land owners: As a basis for compensation of land owners concerned by an overhead line, a *real estates list* is established containing the size of the part of the plot tangled by the transmission line.

15.5 Data processing for line design and administration

15.5.1 Data processing systems for planning of overhead lines

In the previous clauses, the individual steps to be taken for the *design of overhead lines* have been explained. Today, computer programs are available for all these steps, which take care of routine work.

These individual *data processing programs* have been combined to *program systems* [15.63] *for designing overhead lines* [15.60]. In Figure 15.22, the individual components and their interfaces are shown. The data recorded in the terrain (angles, distances, coordinates, characteristic parameters) are transferred from the electronic field data logger into the computer, which evaluates the *terrain* and *crossing data*, as well as the data for the towers when existing lines are surveyed. The data for conductors and supporting structures are added by input or edited from existing data files. The files produced out of this information form the basis for *establishing the longitudinal profile*, for *tower spotting*, for computation of *clearances in crossings*, for establishing the tower lists and conductor sagging tables, as well as for the determination of leg extensions, lengths of individual masts and guy wires, if necessary. The results are again logged in a data file, such that always unambiguous data are available as a basis for all kinds of documents to be produced during the line design process.

The line design program system can be linked to other independent digital computer programs, e. g. for establishing land owner lists, for conductor sagging tables and for calculation of clearances to buildings.

15.5.2 Establishing the longitudinal profile

In Figure 15.23, the necessary steps and the data flow are shown from the survey of field data to finalizing the longitudinal profile. The route data recorded by an electronic tachymeter or a GPS (Global Positioning System) station, as well as added information are stored as alphanumerically coded data files in an electronic field data logger, for

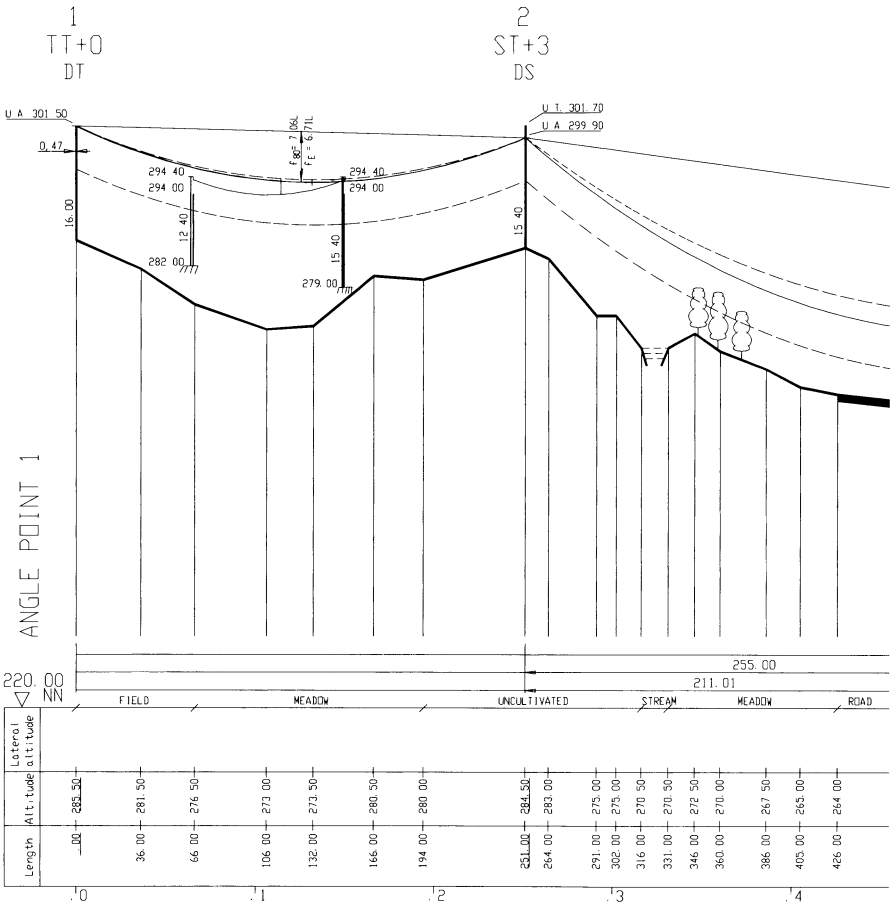

Figure 15.18: Longitudinal profile

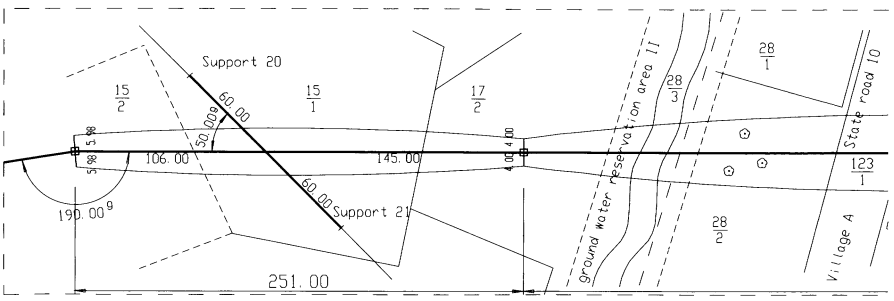

Figure 15.19: Plan layout

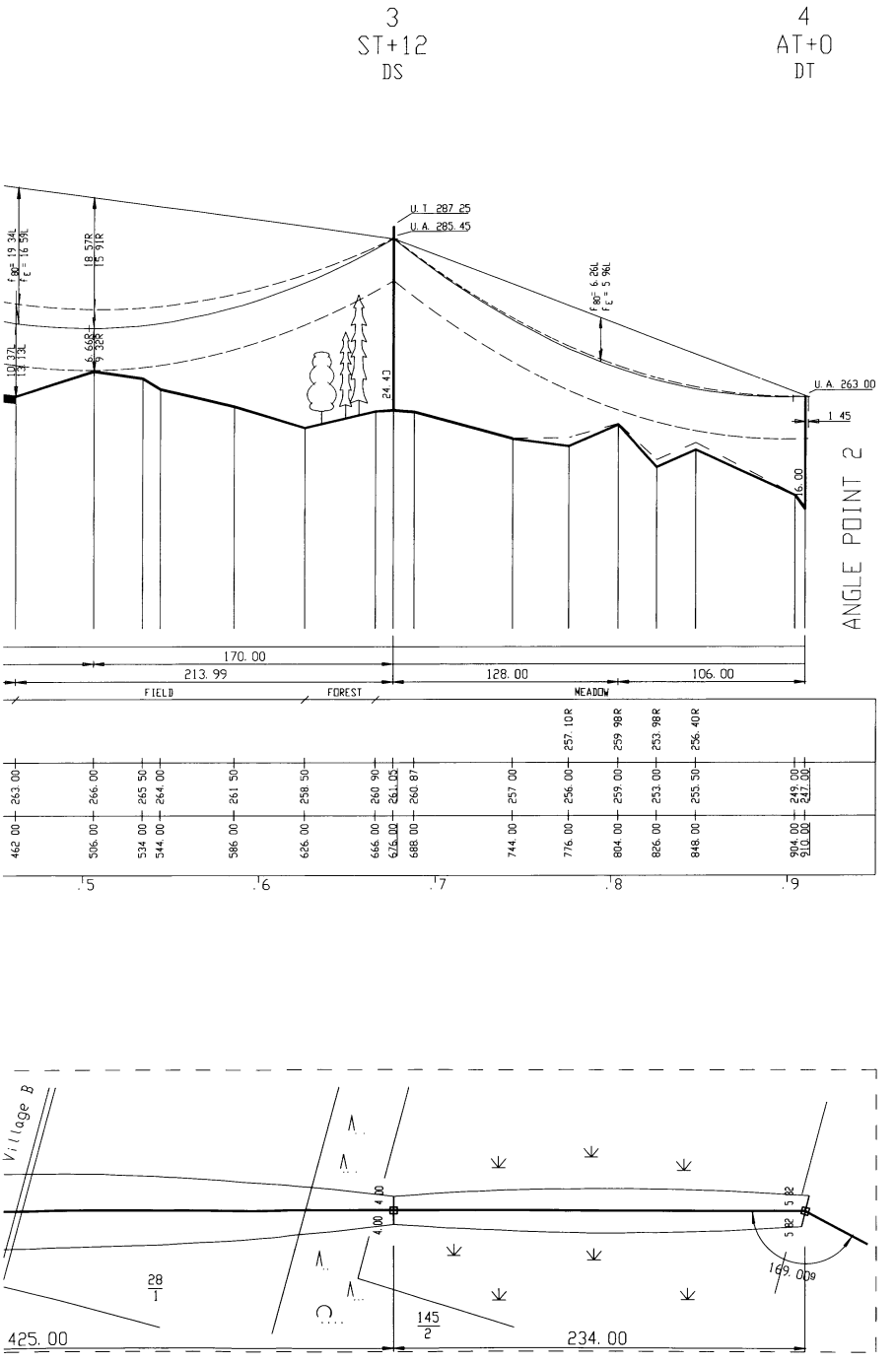
3
ST+12
DS
4
AT+0
DT
U. T. 287. 25
U. A. 285. 45
U. A. 263. 00
1. 45
6. 00
24. 43
ANGLE POINT 2
170. 00
213. 99
128. 00
106. 00
FIELD
FOREST
MEADOW
Village B
425. 00
234. 00
189. 009

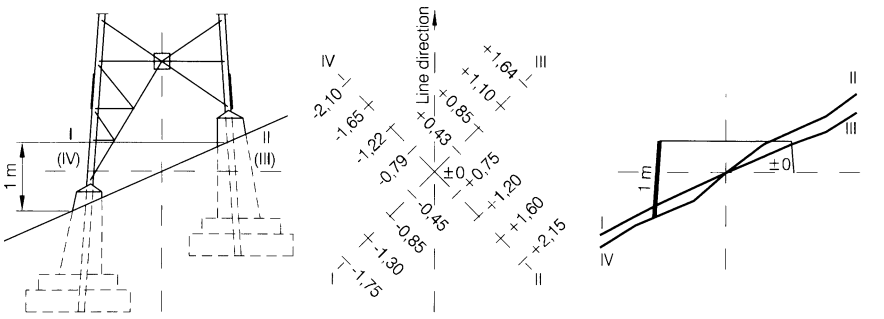

Figure 15.20: Diagonal profile in inclined terrain

which a field computer or the memory card of a tachymeter can be used. The data stored in the field data logger, given in a binary code, are transferred into ASCII data files for the use by the line design program system. Within the module called "transmission line" in Figure 15.23, the terrain data are evaluated, the *tower spotting* and the conductors related mechanical engineering calculations are carried out. As a result, a longitudinal profile is produced containing the terrain, the towers, the conductor sags and the clearances to ground and to crossed objects.

The resulting files can be processed further using CAD systems, like AutoCAD, while additional information concerning land use, protected areas, not yet surveyed or planned objects etc. can be added. The established profile can be transformed into all commonly used CAD formats, according to the specific requirements of the line owner.

Projects can also be processed in a *Graphical Information System (GIS)*. In Figure 15.24, the GIS processing used by RWE Net AG, Germany, is presented as an example. For this purpose, the terrain data are converted into the input format necessary for the GIS processing, by means of a program module designed for this porpose. The Graphical Information System is explained in clause 15.5.4.

15.5.3 Establishing the plan layout

In Figure 15.23, the steps of processing and the data flow for *establishing the plan layout* are shown. On a CAD computer working place, the *land maps* are digitalized.

Construction No.	Final No.	Tower plate	Span length (m)	Height difference (m)	Length of section (m)	Line angle 400g (gon)	Line angle 360° (degree)	Tower type: Suspension tower	Tower type: Tension tower	Tower elevation	Leg extension (m) A	B	C	D
1	2	3	4	5	6	7	8	9	10	11	12	13	14	15
1	1	-				right 190.00g	171° 0'	-	TT + 0	-	1,0	0,0	0,5	0,0
2	2	-	251.00	- 1.00				ST+3	-	-	0,0	1,0	0,0	0,0
3	3	-	425 00	- 23.45				ST+12	-	-	1,0	0,0	0,0	0,5
4	4	-	234.00	- 14.05	910.0	right 169.00g	152° 6'	-	TT + 0	-	0,0	0,0	0,0	1,0

D C A B

e. dis
Germany

SIEMENS AG
PTD H1 58

Date
as built
rev.

110 kV Line Fuerstenberg - Waren

Figure 15.21: Tower list (partly)

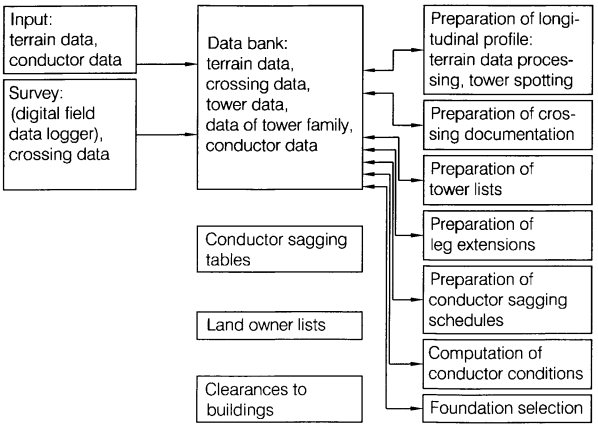

Figure 15.22: Schematic overview of a program system for design of transmission lines established by Siemens AG and FBG-Freileitungsbau GmbH, Germany

If a digital *automatically processed land map* is available from the survey authorities on a continuous basis for the terrain concerned, this map can be logged into the CAD computer working place.

To carry out data exchange concerning topography, boundaries for protected areas, data of the line route etc. with the plan layouts to be produced at the CAD working place, a transformation of digitalized land maps into the corresponding data format is required, whereby a conversion can also be carried out to requirements specified by the line owner concerning colours, layers etc. The data exchange with the plan layout can be utilized to copy the relevant section of the land map into the layout section of the longitudinal profile.

In case of the *GIS processing* of RWE Net AG, only one integrated data processing system is used according to Figure 15.24. In this case, neither during data input nor during data output, data files have to be converted. The data of the longitudinal profiles are exchanged within the system.

Type of foundation	Type of subsoil	Dropper (mm)	Type of insulator set	Crossings	Spacers	Number of dampers: conductor	Number of dampers: earth wire	Span length: wind (m)	Span length: weight (m)	Remarks
16	17	18	19	20	21	22	23	24	25	26
CONCRETE	SAND	-	DT / DT					440.0	390.6	W 1
CONCRETE	SAND		DS	20 kV LINE	3	3	1	430.0	445.6	
CONCRETE	SAND	-	DS	ROAD	3	3	1	447.5	463.4	
CONCRETE	SAND		DT / DT	GROUND	3	3	1	480.0	465.8	W 2

Name	Date	20-7.2000	Siemens AG	Tower list	Sheet 1
	Drawing	Müller			
	checked	Kliegel	from tower No. 1	to tower No. 4	Page 1
	Abt.PTD	H 1 58			

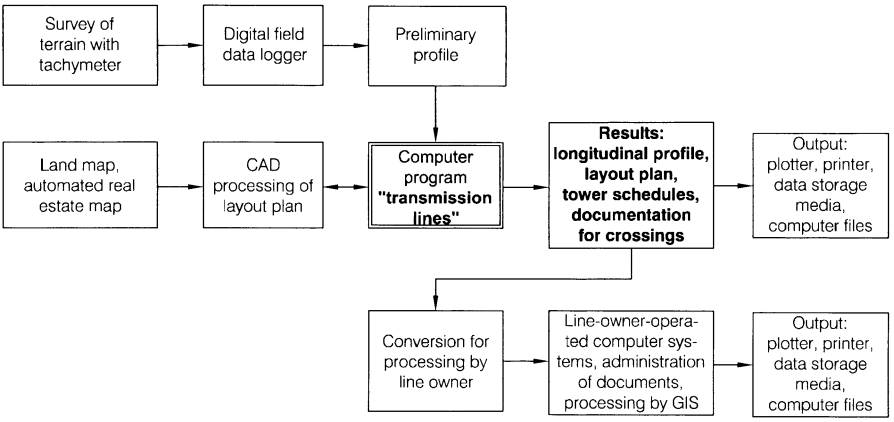

Figure 15.23: Evaluation of longitudinal profiles, establishing the longitudinal profile and processing the plan layout

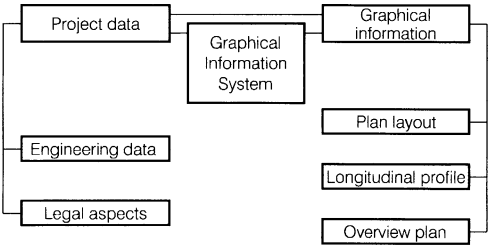

Figure 15.24: Overview of the Graphical Information System used by RWE Net AG, Germany

15.5.4 Graphical Information System with integrated data bank

In Figure 15.24, the *transmission line information system* of RWE Net AG, Germany, is represented schematically. The subsystems, called project data and graphical information, are coupled via the *Graphical Information System*, thus enabling an exchange of information and data between the systems. The layout plans are realized on a UNIX/IRIX work station with the GEO information system SICAD and an integrated Oracle data bank as software. By means of the modules developed by RWE, the following operations are carried out:

- The individual basic elements are digitalized;
- Complex elements, like real estate units, buildings, transmission lines, one-dimensional or polygonal objects, are generated;
- The objects are correlated to a *project data set* and
- The graphical data are stored in a continuous *graphical data bank* without any overlaps (GPB).

The longitudinal profile and crossing objects are generated from the measured data by means of an interface file and form the basis for establishing the longitudinal profile. Other data necessary for the completion of the longitudinal profile plan are added interactively at the computer screen. Besides other studies, alternatives can be investigated by means of masks at the screen, concerning differing conductor stresses, differing conductor attachment heights, differing span lengths etc. The program module carrying out the calculations for conductor mechanics is based on the catenary equation being exact in any case. This module is used to determine the shortest geometrical distances to spot-type, one-dimensional or two-dimensional objects as well as to overhead lines. The calculations can include concentrated loads on the conductors as well.

The partial view of plan layout correlated to the line section in progress is established based on the data available in the graphical data bank, being generated when preparing the plan layout and then added to the longitudinal profile. The finalized longitudinal profiles are stored as separate plan files.
The line design system used by RWE Net AG is based on a Graphical Information System, which does not only deliver digital information as commonly used CAD systems but also:

- Adopts precise calculation procedures;
- Establishes logical objects in different layers and
- Correlates these objects to project data, such that, in addition to digital administration of plans and lists, the manifold of possibilities of a digital data bank information system can be used.

15.5.5 Administration of plans, lists and documents

In the course of time, each line will experience modifications; changes will occur in the surrounding environment. These modifications, e. g. changed tower sites and heights, have to be followed up in line plans and documentation. Using the described program systems for line design, the necessary adjustments of all kinds of documentation can be carried out efficiently and completely. During this procedure, all the calculations concerning the line data are carried out and the documents are revised according to the latest situation. The input of the modified data into one of the files suffices to revise all the documents, like plan layout, longitudinal profile and tower list. The possibilities of *administration of plans* using computer programs represent an essential advantage together with electronic files when establishing overhead line plans with CAD systems.

15.6 References

15.1 Lomas, C. et al.: Integrating overhead lines into an environmentally sensitive world. Cigré Report 22-206, 1996

15.2 Degner, T.; Kießling, F.; Tzschoppe, J.: Mindestabstand zwischen Windenergieanlagen und Freileitungen (Clearances between wind energy converters and overhead tower lines). Elektrizitätswirtschaft 98 (1999) 7, pp. 32 to 35

15.3 Cigré SC22 WG02: The environmental impacts of high-voltage overhead transmission lines. Cigré SC 22 WG02.02, Final Draft 1986

15.4 Ammann, M. et al.: A new 400 kV line with compact towers and composite insulated crossarms. Cigré Report 22/33/36-06, 1998

15.5 Cigré SC22 WG22-14: High-voltage overhead lines. Environmental concerns, procedures, impacts and mitigation. Paris, Cigré Brochure 147, 1999

15.6 Boos, K.-V., et al.: Experience gained in the operation of mulitple-circuit high-voltage overhead lines of compact design. Cigré Report 22-12, 1986

15.7 Kießling, F.; Nefzger, P.: Umrüstung vorhandener 220-kV-Leitungen auf den 380-kV-Betrieb (Converting existing 220 kV lines for 380 kV operation). Elektrizitätswirtschaft 89 (1990), pp. 1322 to 1329

15.8 Kießling, F. et al.: Upgrading high-voltage lines to increase their capacity and mitigate environmental impacts. Cigré Report 22-208, 1998

15.9 Cigré SC 21/22: Comparison of high-voltage lines and underground cables. Report and guidelines. Paris, Cigré Brochure 110, 1997

15.10 Fricke, K. G. et al.: AC overhead and underground HV lines – Comparison and new aspects. Cigré Report 21/22-07, 1996

15.11 Andersen, et al.: Development of a 420 kV XLPE cable system for the metropolitan power project in Copenhagen. Cigré Report 21-201, 1996

15.12 Thuries, E. et al.: Underground gas-insulated transmission line. Cigré Report 21/22-05, 1996

15.13 Ryu, K. S. et al.: Development and research activities on the cryogenic power transmission cable in Corea. Cigré Report 21/22-08, 1996

15.14 Cigré SC22 WG14: Summary report on the questionnaire on the effects of regulatory controls, environmental legislation, concerns, issues and developments on OHL design routing, estimation and operation. SC 22 Meeting, Sendai, Japan 1997 power transmission cable in Corea. Cigré Report 21/22-08, 1996

15.15 Directive 85/337/EEC: Assessment of the effects of certain public and private projects on the environment. Brussels, EC, 1985

15.16 Directive 97/11/EC: Amending Directive 85/337/EEC. Brussels, EC, 1997

15.17 Fitzgerald, C. F. et al.: Community consultation and environmental assessment for high-voltage transmission line projects in New South Wales. Cigré Report 22-202, 1996

15.18 Federal Republic of Germany: Gesetz zur Umsetzung der UVP-Änderungsrichtlinie, der IVU-Richtlinie und weiterer EG-Richtlinien zum Umweltschutz (Law for implementation of EIS directive and other EC directives on environmental protection). Bundesgesetzblatt Jahrgang 2001, Teil I, Nr. 40, August 2001, pp. 1950 ff

15.19 Engsbro, L. et al.: Modernisation of the high-voltage transmission system in Denmark. Cigré Report 21/22-03, 1996

15.20 O'Luain, C. et al.: Transmission line route selection procedures for minimal environmental impact in Ireland. Cigré Report 22-203, 1996

15.21 Hickey, J.: The effect of environmental impact legislation on right-of-way utilisation. Cigré Report 22-202, 1992

15.22 Fleckenstein, K.; Palic, M.; Rhiem, W.: Räumliche Auswirkungen von Feileitungen (Spacial effects of overhead power lines). etz 113 (1992), Vol. 1, pp. 32 to 36

15.23 Wedeck, H.: Zur Bedeutung der Bündelung technisch-industrieller Strukturen bei Eingriffen in das Landschaftsbild (On the significance of bundling technical and industrial structures affecting the landscape). Raumforschung und Raumplanung 54 (1996), pp. 45 to 53

15.24 Nolasco, J. F., da Silva, J. B. G. F.: Use of rights-of-way of overhead lines in urban areas – an experience in Brazil. Cigré Report 22-204, 1992

15.25 Energieübertragung und Ökologie: Informationen zur Trassenpflege (Energy transmission and ecology: information on maintenance of right-of-way). Essen, RWE Energie AG, 1996

15.26 Switzerland, Federal Department of the Interior: Transportation of electrical energy and protection of landscape: Guidelines. Berne, 1980

15.27 O'Neill, A. M.: Criteria for the siting of power line towers. Dublin, ESBI, 1994

15.28 Takebe, T. et al.: Scenery preservation measures and evaluation methods for transmission lines. Cigré Report 22-205, 1996

15.29 D'Ajello, L. et al.: Quantitative evaluation of the visual impact of overhead lines. Cigré Report 22-210, 1996

15.30 Shoji Shintani, S.: Transmission lines and the environment – Route selection systems. Sendai, Cigré SC22 Colloquium, 1997

15.31 The National Grid Company plc. England. Guidelines for the routing of new high-voltage overhead transmission lines. The Holford rules

15.32 FERC Guidelines. Federal Energy Regulatory Commission (USA). Guidelines for the Protection of Natural, Historic, Scenic, and Recreational Values in the Design and Location of Rights-of-Way and Transmission Facilities.

15.33 Thompson, J. W.: Siting the Line. Landscape Architecture 46, August 1996

15.34 Pilegaard, M.: Local and regional related environmental issues. Environmental impact and consequences of electrification in rural areas, grid expansions and transmission lines. Paper on behalf of UNIPEDE Group 40.SYST.

15.35 Weedy, B. M.: Environmental Aspects of Route Selection for Overhead Lines in the U.S.A. Electrical Engineering Department, The University, Southhampton. Electric Power System Research, 16(1989), pp. 217 to 226

15.36 Vité, Mallet and Chambon: Comparison of Technologies for Devloping 400 kV Networks, with Consideration of their Environmental Impact. EDF, Paper from Second Conference on the Development and Operation of Interconnected Power Systems. Budapest, November 1996, Session 4: The Insertion of Interconnected Systems into the Environment.

15.37 Rogier, J. et al.: Visualization of overhead line project in Belgium. Cigré Report 22-209, 1996

15.38 Doyen-Vigvier, C. et al.: Digital simulation for better integration of overhead transmission lines in the environment. Cigré Report 22-201, 1996

15.39 3.30: Lugschitz, H.; Egger, H.: Experience with a 380 kV camouflage line. Cigré Report 22/33/36-04, 1998

15.40 UNESCO: Convention on wetlands of international importance especially as waterfowl habitat. 1971, amended 1982 and 1987

15.41 Bevanger, K.: Bird interactions with utility structures: Collision and electrocution, causes and mitigation measures. IBIS 136: pp. 312 to 425

15.42 Heijnis, R.: Vogeltod durch Drahtanflüge bei Hochspannungsleitungen (Death of bird due to collisions with overhead power lines). Ökologie der Vögel, Second Special issue 1980

15.43 Hoerschelmann, H. et al.: Verluste und Verhalten von Vögeln an einer 380-kV-Freileitung (Losses and behaviour of birds on a 380 kV overhead line). Ökologie der Vögel, (1988), pp. 85 to 103

15.44 Avian Power Line Interaction Committee (APLIC): Mitigating bird collisions with power lines: The state of the art in 1994. Washington, D.C., Edision Electric Institute, 1994

15.45 Avian Power Line Interaction Committee (APLIC): Suggested practices for raptor protection on power lines: The state of the art in 1996. Washington, D. C., Electric Institute/Raptor Research Foundation, 1996

15.46 Koops, F. B. J.: Collision victims of high tension lines in the Netherlands and effects of marking. Madrid, Technical sessions on power lines and the environment, 1994

15.47 Piper, W. et al.: Ornithologische Begleituntersuchungen zur Errichtung einer 380-kV-Leitung (Stadorf) – Lüneburg-Krümel (Ornithological studies referring to construction of a 380 kV line Stadorf-Lüneburg-Krümmel). Internal report of PreussenElektra AG prepared by INUF, 1992

15.48 VDEW: Orientierungshilfe zu Pflegemaßnahmen in Leitungstrassen (Orientating guidelines on maintenance activities in overhead line rights-of-way). Frankfurt am Main, VDEW-Verlag, 1993

15.49 Fleckenstein, K.; Rhiem, W.: Waldüberspannung und Walddurchquerung. Ökologische und landschaftspflegerische Aspekte beim Freileitungsbau (Crossing above forests or aisles through forests. Ecological and landscape aspects in case of overhead lines). Reports of ANL, 1991

15.50 Brackel, V. W.: Vegetationskundliche Untersuchung einer Stromleitungstrasse (Investigations of vegetation within the power line right-of-way). Natur und Landschaft, 64 (1989) Vol. 11

15.51 Coch, T.; Uther, D.: Biotopmanagement in walddurchquerenden Trassen von Hochspannungsleitungen (Biotope management in the right-of-way of overhead power lines through forests). Naturschutz und Landschaftsplanung 26 (1994), Vol. 3

15.52 Hoss, H.: Digitales Höhenmodell in Waldgebieten. Erfahrungen aus Laserscanner-Befliegungen (Digital height elevation model in forestal areas. Experience from laser scanning flights). Landesvermessungsamt Baden-Württemberg 1994

15.53 Mekhanoshin, B. I. et al.: Use of an airborn laser locator to improve availability and quality of maintenance of overhead lines. Cigré Report 22-204, 2000

15.54 EN 50 341-1: Overhead electrical lines exceeding AC 45 kV. Part 1: General requirements – Common specifications. Brussels, CENELEC 2001

15.55 EN 50 341-3-4: Overhead electrical lines exceeding AC 45 kV. Part 3-4: National Normative Aspects (NNA) for Germany. Brussels, CENELEC 2001

15.56 EN 50 341-3: Overhead electrical lines exceeding AC 45 kV. Part 3: National Normative Aspects. Brussels, CENELEC, 2001

15.57 VDE 0210: Planning and design of overhead power lines with rated voltages above 1 kV, amendment A4. Frankfurt am Main, DKE Draft, 1999

15.58 Dahlberg, F.; Palm, Y.: Optimum tower spotting on transmission lines by means of electronic computer. Swedish State Power Board, Blue-white series No. 33 (1963)

15.59 Kießling, F.: Optimum tower spotting for an overhead line. Siemens Power Engineering 5 (1983), pp. 34 to 38

15.60 PSLCADD: Computer program for the integrated analysis and design of a transmission line. Madison (Wi.) Power line systems, 1997

15.61 Riisio, P. J.; Kioivanta, V. M.: Computer aided design systems for line routes tower spotting and line structures in Finland. Cigré Report 22-104, 1990

15.62 Ranero, I.: Automatic minimum cost support spotting by computer. Cigré Report 22-105, 1990

15.63 Siemens program system Overhead Power Line. Establishment and administration of plans for overhead power lines using SICAD. Erlangen, Siemens AG 1987

16 Construction

16.0 Symbols

Symbol	Signification
a	Span length
a_S	Position of the sagging curve vertex
A	Cross-sectional area
c	Propagation speed
D	Vertical distance between attachment point of the conductor and the theodolite tilting axis
e	Creeping strain
$\overline{e}$	Creeping strain at everyday stress
e_{1h}	Parameter for creep strain
e_{30}	Creeping strain after 30 years
$\overline{e}_{30}$	Creeping strain at everyday stress after 30 years
E	Modulus of elasticity
f	Sag in general
f_i	Sag within span i
f_h	Sag to horizontal viewing line
$\overline{F}$	Virtual force
g	Gravitational acceleration
G_K	Dead weight force of insulator set
h	Difference in height of adjacent conductor attachment points
h_i	Difference in height of conductor attachment point in span i
h_T	Reference height above tower base
h_{si}	Difference of height of vertices in adjacent spans
H	Horizontal conductor tensile force
$H_{E,k}$	Equivalent horizontal conductor tensile force in the iteration step k
H_O	Horizontal conductor tensile force of clipped-in conductor
H_i	Horizontal conductor force in span i
$I(x)$	Moment of inertia
k_σ	Factor for creeping strain
L_i	Inclined span length i
L_o	Conductor length in span i
L_K	Length of insulator set
M	Centre of stringing blocks
m_C	Conductor mass per unit length
$M(x)$	Bending moment due to external load
$\overline{M}(x)$	Bending moment due to virtual load
$\overline{M}_\varrho$	Bending moment due to a virtual moment
n	Exponent of creeping strain
n	Number of tower sections or joints
$\overline{N}$	Axial force due to virtual load
$N(x)$	Axial force due to external load
r	Eccentricity of point of load attack
r_c	Residual eccentricity
r_{el}	Elastic bending deformation
r_m	Horizontal displacement at tower top or considered crossarm height
s_i	Distance between joint i and position, where deflection is considered
S_i, S_e	Conductor tensile force at support
t	Running time of a wave, time after first loading of a conductor, period of time
v_i	Offset of conductor at tower i
V	Vertical load at insulator
V_i	Vertical load at insulator set i

Symbol	Signification
w	Steel portion of conductor weight
α_{si}	Tilting of joint i
β	Insulator set swing angle, inclination of towers
δ	Displacement of conductor attachment point from the vertical axis
ε_T	Coefficient of thermal expansion
Δh_{si}	Difference in height of conductor vertices in spans i and $i+1$
ΔT_{id}	Virtual conductor temperature change
ϱ_{el}	Elastic deformation angle at crossarm height
$\overline{\sigma}$	Relative everyday stress
ϕ	Vertical angle for sagging

16.1 Construction planning

16.1.1 Introduction

The construction of a transmission line requires the installation and operation of a high number of individual construction sites to carry out the implementation of tower foundations, *erection of supports* and *stringing of conductors* along a line many kilometres long.

As well as the design of an overhead transmission line, the construction method needs to be adjusted to the type of terrain encountered. For carrying out the individual construction steps during installation of an overhead line, specific knowledge, craftsmanship and physical fitness of the construction staff are necessary as well as suitable equipment. A foresighted planning of the construction and an expedient site organisation are required to achieve a perfect quality, construction to schedule with infringement of the environment only to an extent as low as possible and a satisfying economic result.

During the construction period, attempts should be made to avoid any pollution of the surface or ground-water, e. g. by an appropriate selection and use of harmless substances. Pollution might be possible as a consequence of an accident. Therefore, it is recommended to use biologically *recycling oils* for hydraulic purposes. *Damage of vegetation* and disturbance of the soil surface, e. g. by compaction due to heavy vehicles, cannot always be avoided, although the support sites have been selected close to access roads and thick planks or plates are used to drive along. After ending the construction activities, such soil compactions have to be broken up again. Temporarily constructed *access roads* need to be removed appropriately and residual *excavation material* should be recycled whenever possible. A not complete removal of packing and construction material such as steel parts, conductor and wire ends, lost bolts, packing foils and wood parts may infringe the agricultural land use along the line route and did sometimes result in damage of agricultural machines or lead to loss of cattle. Damage or even loss of trees caused by construction equipment form major infringements. Annoyance to neighbouring residence by noise generated at the construction site for example by pile driving has to be expected only at a few line sections, however, should be reduced to a minimum by using insulated low-noise equipment.

A thorough investigation of the local conditions should precede the construction planning. Type of terrain, soil conditions, existence of buildings, agricultural use, infrastructure, crossing roads and other lines as well as the accessibility are of special interest.

16.1.2 Construction time schedule

Based on the number of supports and foundations as well as on the length of the line, the quantities to be installed are determined and the activities to be carried out during a given period of time will be calculated. The individual construction steps correlated to each other can be clearly presented above the construction period in a *construction*

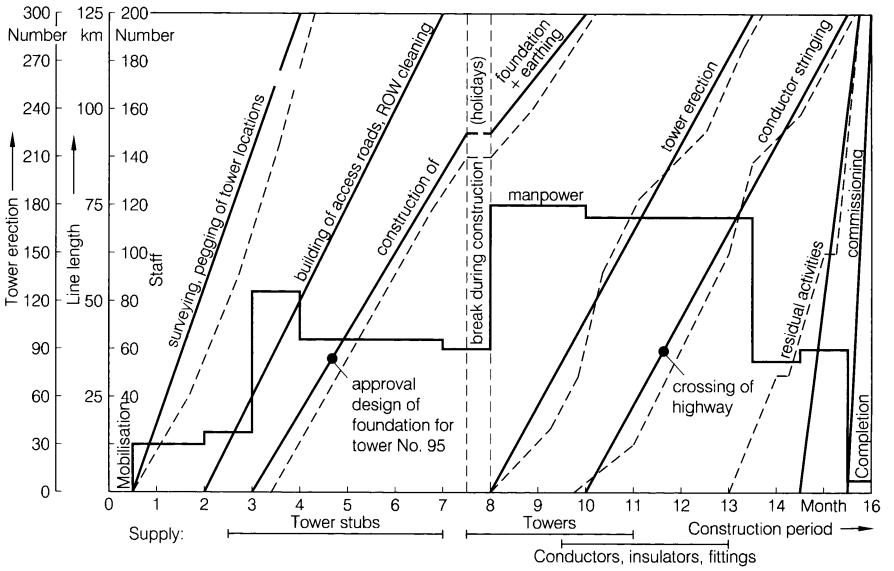

Figure 16.1: Construction time schedule
Full line: planning, broken line: actual progress of construction

time schedule (Figure 16.1). Considering the achievable progress and the correlated expenditures, the *construction methods* can be determined for each individual step and the required demand for manpower, vehicles and equipment be established for the construction gangs. From the construction time schedule, also the data for supply of tower stubs, support parts, conductors, insulators and fittings to the construction site can be realized. For more extended overhead line installations, the construction time schedule can be established as a *network diagram*. This facilitates to pursue the deadlines for material supply and construction progress to a large extent. By inserting the progress achieved into the construction time schedule, a comparison between planned and achieved milestones is possible at any time.

16.1.3 Mobilisation and stockyard

The *mobilisation of the construction site* belongs to the construction planning as well. Construction site office and stockyard should be chosen closely to the line route and need good road connections as well.

A sufficiently wide area with a solid surface usable for heavy lorries is suited as a *stockyard* for construction material, concrete formwork, shuttering and planking, parking of vehicles and for a well-structured storage of the supplied material including driven piles, reinforcement steel, tower parts, fittings, earth wire and conductor reels. In cases where the tower parts are supplied bundled item-wise, a sufficient large area should be available for sorting and warehousing parts tower by tower. The stockyard should include a hall or shelter where tools and fittings can be stored as well as cement if required for site-mixed concrete. For maintenance and repair of vehicles and tools, an accordingly equipped workshop is installed in case of larger line projects.

Activities at the stockyard include unloading, inspecting, inventing and storing all materials. Material should be inspected to conform with the shipping manifest. Damaged material should be rejected and arrangements made to expedite replacements. A determination of material requiring special protection should be made so that appropriate

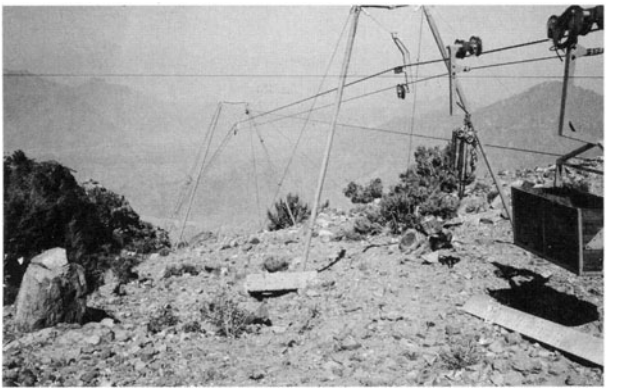

Figure 16.2: Ropeway

storage is provided. In order to reduce delays and cost overruns, all material should be on hand and in good condition before installation begins. Material stored in open area should be protected from soil with wood blocking.
Lay down areas at each site should be prearranged. A sketch showing material placement is helpful for the unloading crew. Tower material should be arranged to minimize rehandling and should be checked for shortages or damaged members. The members or tower components should be located within reach of the erection equipment. If special handling or erection procedures are to be followed, they should be outlined on the erection drawing, or appropriate sketches provided to the crews. Tower members should not be dragged across the ground. In particular, all joints should be clean of mud or other undue substances before assembly.

16.2 Transportation

16.2.1 Means of transport

Due to the extended length of a line, *transportation* gains high importance when constructing transmission lines. Concrete aggregates or ready-mixed concrete, considerable quantities of reinforcement steel, soil excavation, material for planking and shuttering and concrete formwork, driven piles, setting templates, tower parts, reels with earth wires and conductors, insulators, fittings as well as the construction equipment need to be transported to or from the individual support sites, sometimes in an undeveloped terrain without access roads. An optimum organisation of the transport, therefore, is decisive for an economically successful implementation of a project.
For construction of transmission lines, vehicles with four-wheel drive, cross-country gear and differential blocking are used in most cases: Lorries, unimog and tractors. On surface with peat or sand, the wheel diameter should be as large as possible and low pressure pneus with a large surface area should be used; for special cases, vehicles equipped with tracks are used.
In steep terrain not accessible for lorries, e. g. in high mountains, the material is transported either with *ropeways* or by *helicopters* to the individual tower sites. For ropeways, designs are used which consist of low-weight components easily to be transported, quickly installed and remaining reusable after being dismantled (Figure 16.2). The expensive but versatile usable helicopter is as well qualified for transportation of transmission line materials. However, the relatively high costs, the limited load capacity and the sensitivity on weather ask for a detailed planning of helicopter disposition.
Loading and unloading activities are predominantly carried out by cranes; in most

cases with hydraulically-operated cranes installed on the lorries. Conductor reels are transported by means of self-loading transport trailers. The hydraulic pressure for the lifting equipment is provided from a tractive engine to the trailer.

16.2.2 Access roads

Access roads should be built where necessary, taking into account the site topography and line importance, considering the following conditions:

- After the line construction, easy access to the supports is required, for maintenance purposes.
- Existing roads should be used, as far as possible.
- Rain water drainage should be built.
- Every road built should be conveniently recorded on design maps with the number of towers to be accessed, clear reference being made to highways and secondary roads to reach them.
- In special cases, preparation of existing roads (paved or unpaved) may be required for construction activities. Thereby, the steepest ramp should be less than 20 %, the minimum curvature radius 10 m and the minimum width 3 m.
- Traffic of vehicles under guy wires should be avoided and, therefore, access roads are not allowed to cross such areas. In areas subjected to traffic of agricultural machines, guy wires should be protected against being hit and conveniently signalized.

Damage to roads, paths and fields caused by transport vehicles should be avoided as far as possible; also it should be aimed at limiting the land damage caused by transportation of material to an unavoidable extent. For this purpose, the access roads and working areas at the individual tower sites need to be prepared for heavy loads. In soft terrain, reinforcing by temporary truck ways is advisable.

16.2.3 Fences, gates and cattle-guards

All existing fences that have to be opened for work needs or future maintenance should be recomposed or protected with gates, gateposts or cattle-guards, under an agreement with the owner. Fences for crossing railways or highways are to be made with the relevant criteria of the crossed ways.
In order to interrupt the electric continuity of conducting material, barbed-wire or flat-wire fences running parallel or crossing a power line have to be sectionalized and earthed before conductor stringing.

16.3 Construction of foundations

16.3.1 Introduction

The *construction of foundations* should be considered already when selecting and planning the type of foundation taking care of the soil and terrain conditions as well as of the access to the individual tower sites. The construction of foundation types typically for transmission lines will be discussed in the following clauses.

16.3.2 Concrete foundations black and slab foundations

To start the excavation of pits for *stepped concrete foundations*, *slab foundations* or *pad and chimney foundations* (see clause 13.4.4.2), the foundation pits are surveyed at the individual tower site and pegged out. Concerning excavation, the following types of soil can be distinguished:

- *Normal soil*, comprising clay, silt, sand and their combinations, including rocky fragments which are easy to be removed.
- *Decomposing rocks*, presenting pebbles or gravel and requiring pick mattock or even a big compressor for their removal.
- *Loose stones*, comprising rocky terrain whose stones have such sizes and dimensions that high gear force is required for excavation.
- *Sound rocks* which require very high gear force or explosives.
- *Soil under water* and *swamp terrain.*

Hydraulic excavators are preferably utilized for the excavation in the first category. In heavy soils of the second and third category, excavators with back-action shovels having a high gear force are adopted. To loosen rock characterized by the fourth category, pneumatic hammers, heavy excavators with hydraulic hammers or explosives are necessary. Here, anchor foundations are advantageous, requiring a minimum of excavation for the concrete muff only. In terrain of the fifth category, driven piles should be preferred which do not require excavation.

The foundation pits should be secured against collapse and inadmissible entering according to *labour safety standards* [16.1]. The protection is carried out by a vertical planking with horizontal shuttering using timber or steel. In case of steel reinforced foundations, a 50 to 100 mm thick layer of lean concrete is placed to achieve a subface keeping the reinforcement clean.

After hardening of the lean concrete, the reinforcement is installed so far as necessary according to the design drawings, and the leg member stubs or tower bodies are installed and adjusted. The concrete is placed layer by layer (see clause 16.3.7.5) and compacted. The *concrete formwork* is installed in case of stepped or pad and chimney foundations according to the progress of work. After ending the stipulated periods for concrete curing, the concrete formwork and pit shuttering can be removed and the open space of the pit is filled in by excavated soil and other material.

Before beginning the backfill, the water and mud eventually present in the pit should be removed. In general, the soil at sites where concrete foundations are installed in excavated pits, can be used for backfill. However, the backfill should be free of roots, organic material and/or waste. The backfill should be carried out and compacted at layers approximately 0,20 m thick, considering also the line owner criteria. If the excavated soil is not suitable for compaction, other material should be imported. The main target of backfill is to achieve soil characteristics close to those of the natural soil.

Compaction should preferably be made by motor-driven hammers. If they are not available, manual compaction equipment with a weight of about 20 kg is acceptable. The backfill services, once begun, should be completed up to the surface level at the same day. If this is not feasible, it is necessary to scarify the superficial layer of the existing backfill, before continuing to set new layers up to the completion of the work. Compaction of soil above concrete bases should begin not before 24 hours after placing the concrete.

Compaction should be carried out thoroughly in order to achieve characteristics of the backfill as close as possible to those of the undisturbed soil. The residual excavation material is distributed on the tower site or carried to a damp. In case of an inclined terrain, special care needs to be taken that the required soil surcharge will be achieved.

16.3.3 Augerbored foundations

Auger-bored foundations (see clause 13.4.4.3) require stable soils which can be augered. For the excavation of such foundations, earth-drilling rigs are used which are mounted on cross-country vehicles with wheels or tracks (Figure 16.3). *Earth-drilling rigs* should reach the tower sites without extreme effort. Augers or split buckets with a maximum

Figure 16.3: Earth drilling rig mounted on a crawler track chassis

Figure 16.4: Piling rig with a diesel-operated hammer

diameter of 1,50 m mounted on crawlers excavate the soil at depths up to 8,00 m. After the cylindrical borehole has reached the designed depth, an expansion in form of a truncated cone can be produced by means of an undercutting device. Augerbored foundations are equipped with reinforcement steel to provide for tensile forces and bending moments acting on the foundation when loaded by lattice towers or poles. Prior to placing the concrete, the reinforcement is installed in the borehole.
The borehole needs to be secured against collapsing. This can be achieved by a protective casing or by installing the reinforcement and placing the concrete immediately after augering the hole. In this case, the borehole is filled up with concrete to such an extent that enough space is left for installing and adjusting the tower stubs. Since the foundation pit is completely filled up with concrete, the excavated material is distributed on the tower site or carried to a damp.

16.3.4 Driven pile foundations

16.3.4.1 Common rules

Driven pile foundations (see clause 13.4.4.5) are often adopted in case of low bearing soils or a ground-water table close to the surface. The conditions of an overhead line project impose several special requirements on the *pile driving device* (Figure 16.4). Its weight should be as low as possible with respect to the mobility and cross-country suitability. On soft soil surfaces, the crawler tracks need to be equipped with wide and long tracks to attain a low soil pressure. To achieve a short period of time to move the pile driving device from one site to the next, the piling rig with the hammer should be easily erected and dismantled. The rig should permit rakes up to 250 mm/m. Its height should be tall enough such that 14 to 20 m long piles can be driven. The action weight of the drop hammer should approximately be equal to the weight of the piles to be driven.
During pile driving, the position of the pile, its deviation, distorsion and penetration as well as its rake have to be monitored and controlled. The driving process is recorded

Table 16.1: Example for a driving report
Line: 110 kV line T-off Haffeld HT35; tower no. 17H; tower type WA_2+0, type of pile: steel tube 609 × 10; length 12,5 m; diesel hammer D30-32; Date: June 25, 2000

Depth m	Number of blows for tower leg 1	2	3	4
0 to 1	10	9	8	11
1 to 2	15	12	9	13
2 to 3	19	14	12	16
3 to 4	22	18	15	19
4 to 5	38	22	19	24
5 to 6	51	33	24	31
6 to 7	72	48	37	38
7 to 8	81	57	49	44
8 to 9	90	83	55	55
9 to 10	95	91	73	76
10 to 11	108	96	88	83
11 to 12	118	105	100	97
12 to 12,5	91	83	74	61
In total	810	671	563	568
Volume of grout (m^3)	1,75	1,80	1,65	2,00
Grouting factor	0,81	0,83	0,76	0,93

in a *driving report*. The number of blows for one meter of penetration depth of the pile into the soil permits conclusions on driving resistance and on uplift load capability of the piles. A pile driving report is shown in Table 16.1. Reference [16.2] gives guidance on preparation of driving reports.

16.3.4.2 Steel piles

Box-type, tubes or H-beam sections are suited for transmission line foundations. All of them are open at their pile point (see clause 13.4.4.5, bare *steel piles*), i. e. they are driven into the soil without a specially prepared point. A pile helmet adjusted to the pile profile avoids damage of the pile heads by pile driving. Extensions of piles can be carried out by welding or fish-plating a butt joint with the additional pile length on site. The welded butt joint is reinforced by welded fishplates which can be arranged inside or outside the pile. In case of a driving resistance too high or soil layers not anymore suited for pile driving, the surplus pile length can be shortened by cutting with a blow-torch. The uplift resistance of the shortened pile should be verified by a load test.

16.3.4.3 Steel piles grouted by mortar

The steel parts having a box-type, tube or H-beam cross section are provided with a laterally protruding point for cladding the pile by grout (see clause 13.4.3.4). During pile driving, the space formed by the protruding pile point will be filled from the point up to the ground surface with concrete mortar by means of a pressuring hose guided to the pile point. A pressure of 10 bar is aimed at for the filling process. Ready-mixed grout supplied by a concrete plant should be preferred in general and pressed in by a concrete pump. However, site-mixed grout is used as well.
The ratio of the filled in mortar volume to the theoretically determined space for grouting is named *grouting factor*. It is a characteristic data expressing the extent to which the space formed by the pile point is filled up with grout. This factor is included in the *driving report* and can be used to assess the load carrying capacity of the *grouted steel pile* (see Table 16.1).

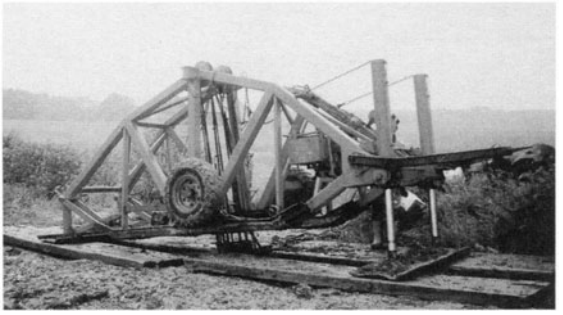

Figure 16.5: Test loading bridge

16.3.4.4 Testing

Testing of installed foundations, in particular of piles and anchors, is part of the construction. According to IEC 61 773 [16.2], *uplift proof testing* of transmission line piles in heterogeneous soils and varying soil densities is recommended. Adopting this procedure, the reliability of the foundation can be increased and the necessary investment lowered. At least 5 % of all installed piles should be proof-tested. However, tests at a group of piles or at piles with very high capacity cannot be carried out at overhead line tower sites because of the necessary equipment and reaction abutment. According to [16.2], the *proof test load* should be 60 to 75 % of the expected limit load or 125 % of the working load [16.3]. The test loads are applied by hydraulic jacks. In case of tensile testing up to loads of 1000 kN, a *test loading bridge* (Figure 16.5) is arranged above the pile to be tested such that the loading axis coincides with the pile axis. For the individual loading steps, the pile displacements are measured and recorded in a *load-displacement diagram.* Examples for test recordings are contained in [16.2]. A low displacement under load indicates a higher bearing capacity of the pile. Bare steel piles should be tested not earlier than three weeks after driving since the skin friction and the tensile capacity increase considerably after pile driving. Grouted steel piles can be tested after hardening of the mortar (see clause 13.5.3).
In Figure 16.6, *load-displacement diagrams* are shown for two routine proof tests carried out at piles which were loaded to 1,2 times the working load. The load displacement lines have been extrapolated to 1,5 times the working load. For pile 1, an extrapolated displacement of 5,2 mm is expected while pile 2 will reach a displacement of only 1,5 mm at this load. Displacements of both piles are below the limit of 6,0 mm.

16.3.5 Grillage foundations

The equipment mentioned hereafter should be available for constructing *grillage foundations* (see clause 13.4.4.4):

- Inclination and torsion templates;
- Face templates or measures determining inclinations of each face of the stubs;
- Measuring equipment or devices such as transits, optical levels, measuring tapes, plumbs, squares, bubble levels.

Before starting grillage assembly, soil regeneration should be carried out if existing soil is very weak and more resistant soil needs to be taken from another area. The construction activities comprise:

- Levelling of excavation bottom which should be covered by an approximately 0,10 m thick layer of sand.
- Positioning and levelling of grillage base profiles.
- Assembling and levelling of grillage support members or tower stubs (see clause 16.5).

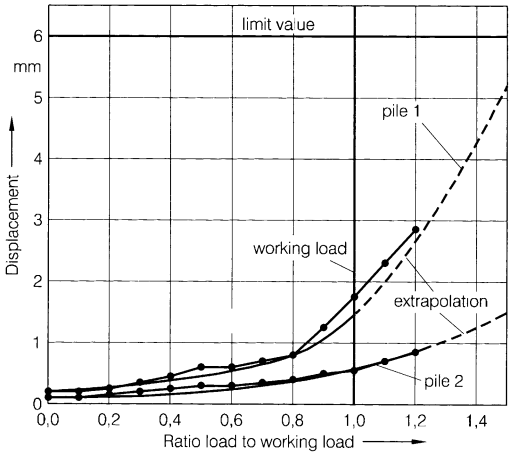

Figure 16.6: Uplift load-displacement diagram

- Filling of all voids in between grillage members with friable material, e. g. sand. Alternatively, the grillage base profiles are cast in concrete, if specified.
- Then, backfilling needs to be carried out carefully without damaging the steel parts. Therefore, mechanical backfilling is not advisable. Instead, the backfill is placed in manually.
- Compaction of backfill is carried out with a pneumatic hammer or by a compactor having a weight of at least 10 kg. It is preferable to use the same soil for backfilling as removed during excavation, if suitable. The layer thickness for backfill should be around 0,20 m.
- It is recommended to carry out the backfill until a height of about 0,30 m above the ground level, in order to avoid water accumulation around the foundation.

Grillage foundations have been successfully used for lines in less corrosive soil conditions and for towers with relatively low foundation loads.

16.3.6 Anchor foundations

Transmission line towers at sites with rock subsoil can be erected on foundations using *tensile anchors*, if the rock complies with the classifications WO and W1 according to Table 13.8 characterized as not to be loosened manually. Special anchors are adopted for the stay wires of guyed towers.

The drillings into the rock are carried out by *rock drilling rigs* which adopt rotational drilling, beat drilling or beat-rotational drilling methods. For transmission lines, the beat drilling rigs using compressed air for rinsing out the material are used. Drilling diameters up to 120 mm can be achieved.

To transfer the loads from the anchor to the subsoil, the borehole together with the installed anchor bar is cast with mortar. Mortar premixed by the producer or site-mixed mortar with admixtures can be used. The borehole diameter should be 40 mm larger than the nominal diameter of the anchor bar to achieve complete covering of the anchor bars by mortar as well as the required resistance and sufficient corrosion protection. Spacers are required to guarantee the necessary concrete covering.

The tensile strength can be tested after sufficient hardening of the mortar. When using premixed cast-in mortar or site-mixed mortar with admixtures for an early strength, testing can be carried out already after a few days. According to common practice, one anchor is tested for each individual foundation. The anchors are connected to the tower stubs by means of a steel-reinforced concrete muff.

16.3.7 Concrete for foundations

16.3.7.1 Ready-mixed and site-mixed concrete

Ready-mixed concrete supplied by a concrete plant should be preferred for foundations of overhead lines. In Europe and other industrialized countries, an area-covering supply with only short transport distances is guaranteed; in this case, the use of ready-mixed concrete is economic and provides a guaranteed quality by supervision and quality testing at the concrete plant and during transport.

In less industrialized countries and in case of non-acceptably long transport distances, the concrete needs to be mixed on site. This is the reason why the basic principles of *concrete technology* are presented here. The concrete strength class C 20/25 or at most C 30/37 according to [16.4] is sufficient for foundations of overhead lines. Experienced workmanship is necessary to prepare high-quality concrete on site.

16.3.7.2 Constituent materials

Cement

Cement is a hydraulic binder for mortar and concrete. When mixed with water, cement hardens at the air and is capable doing so under water. The hardened cement paste formed such is water resistant. The standards ENV 197 [16.5] and DIN 1164 [16.6] apply for cement. ENV 197 distinguishes between three main types:

- CEM I: Ordinary Portland cement,
- CEM II: Portland iron pulverized fuel-cement, Portland ash cement, Portland limestone cement,
- CEM III: Blast furnace cement.

Cement is offered with special features such as "LHPC" for low-heat Portland cement, "SR" for high-sulphur-resisting cement and "LA" for low alcali cement and with differing strength classes.

Ordinary Portland cement with the *strength classes* 32,5 or 42,5 is used predominantly for overhead line foundations, whereby the nominal strength after 28 days will be at least 32,5 N/mm^2 or 42,5 N/mm^2, respectively. The letter "R" (rapid) added to the strength class refers to an early strength. For ordinary Portland cement, the initial setting time may not be less than 60 minutes (at 20°C) according to [16.6] after adding the water. The concrete has to be placed within this period of time. In case of cement according to [16.5], the setting may start already after 45 minutes. The start of setting can be delayed by *admixtures*, e. g. calcium sulphate.

Cement takes up humidity and carbonic acid from the air resulting in a strength reduction. Therefore, the cement needs to be protected against these impacts during transport and storing (see [16.7], clause 2.1.3). Cement used for overhead line construction should not be older than three months.

Aggregates

For *concrete aggregates*, ENV 206 [16.4] refers to national standards or project specifications. Aggregates according to standard requirements as specified in DIN 4226-1 [16.8] are sufficient for overhead lines. The compressive strength is an essential property of the concrete. It will be achieved if the compressive strength of hardened cement paste and aggregates is higher than the *concrete compressive strength* envisaged. In practice, the compressive strength of the aggregates is higher than that of the hardened cement paste and, therefore, not decisive for the concrete strength. The compressive strength of concrete is not much affected by the strength of the aggregates unless they were very weak.

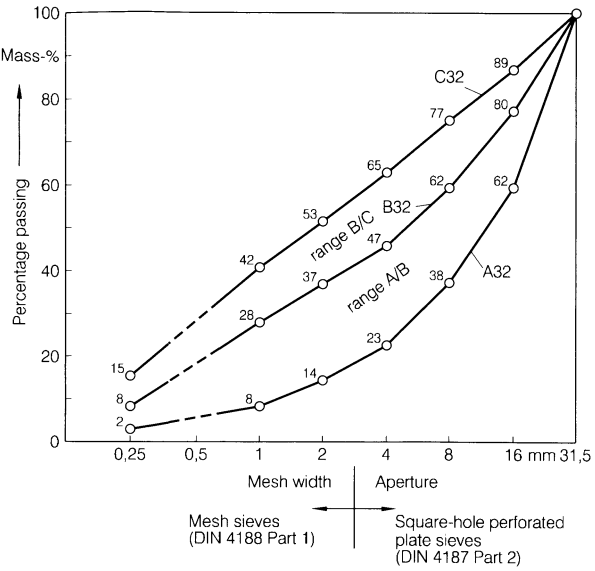

Figure 16.7: Standard grading curves for 32 mm maximum particle size according to DIN 1045

The *particle size distribution* of aggregates is characterized by *grading curves*. The proportion in mass of the individual particle sizes can be determined as a percentage of the total mass with sieves of varying mash or hole widths. The distribution of the aggregates should show a grading curve within the lines A and C (Figure 16.7) [16.7]. The shape of aggregates is usually described by items such as rounded, angular or irregular whereby longitudinally stretched and flat particles of the particle size 4/32 should be limited to below 50 % of mass proportion. The grading of aggregates determines the *water demand* and, as a consequence, the cement demand. The more fine particles the aggregate mixture contains the higher the water demand will be and, therefore, the cement demand will rise.

When designing a concrete mixture, the requirements concerning concrete properties and workability have to be complied with and the economics and possibilities of aggregate procurement to be considered as well. For several overhead power line construction sites, it might be difficult to procure gravel or crushed gravel with particle sizes above 4 mm. A high aggregate content of sand requires an increased amount of mixing water and a higher amount of cement.

The *ultra-fines content* consists of cement and the aggregates with particle size 0/0,125 mm. Ultra-fines contents are necessary for a superior adhesive performance and avoiding demixing. An ultra-fines (0/0,125) content of 350 kg/m^3 and an ultra-fines plus very fine sand (0,125/0,250) content of 420 kg/m^3 is envisaged for overhead line foundations. A too high content of ultra-fines particles increases the water demand and affects the frost resistance and the resistance to chemical attacks of the hardened concrete. The content of ultra-fines particles should be limited to an extent necessary for a smooth placing of the concrete (see [16.7, 16.9]).

Settleable solids with particle sizes below 0,063 mm reduce the bonding between the cement paste and the aggregates especially if these settleable solids are clayey; therefore, their content needs to be limited. Permissible limits are given in [16.8]. *Settleable solid particles* are predominantly combined with fine grain aggregates. For the particle size 0/4, the limit of settleable solids is 4,0 % by mass. By means of the settlement test according to DIN 4226-3 [16.10], the content can be approximately determined on the construction site together with non-soluble particles of organic origin, e. g. humus.

Any components of organic origin, sugar, sulphates and chlorides affect the concrete quality negatively in different manners and should be avoided. Reliable limits and verification methods are stipulated in [16.8] and [16.10], respectively.

Mixing water and surface water of aggregates

Mixing water is added to the concrete during the mixing procedure. Drinking water and water from any other source not adversely affecting the essential properties of the concrete can be used. Water containing oil, grease, sugar, dust, humus or peat is not suited as is water from mineral sources, too. In case of doubts, the suitability of the water should be examined.

Salty seawater could be used for plain concrete and for reinforced concrete, if the chloride contents within the concrete remained below generally accepted limits. However, numerous corrosion damage was experienced on the Arabian peninsula, where aggregates and mixing water from the ocean were used. The damage was caused by carbonizing and attack by chlorides and other salts present in the mixing water. Therefore, salty seawater or aggregates taken from the sea are no longer accepted in this area at all.

A certain amount of water resulting from the sum of free mixing water and surface water of the aggregates is necessary to achieve the desired consistence of the fresh concrete. The water content of the aggregates from which it is concluded on the surface water can be determined by a relatively cost-effective drying test. For overhead lines, values from experience or a visual assessment of the aggregates on the construction site are sufficient.

In Central Europe, an aggregate mixture with a maximum particle size of 32 mm with a grading in the range A/B contains 2,5 % of mass of water on average as *surface moisture.* In case of 1980 kg aggregates for 1 m^3 concrete, this will be 1980 kg $\cdot$ 0,025 $\approx$ 50 kg water, i. e. approximately 30 % of the required water will be supplied by the surface moisture.

Concrete admixtures

Concrete admixtures may be added to the concrete to control the properties of the fresh or hardened concrete. A certificate issued by a civil engineering supervising organisation or, at least by the supplier, is a precondition for their application. *Concrete plasticizers* improve consistence and workability without modifying the water-cement ratio. *Retarding* or accelerating *admixtures* control the setting time. For overhead lines, retarding admixtures are frequently necessary to place the concrete before initial setting in case of long transport distances or warm weather.

Admixtures for *water and damp proofing* should avoid the ingress of water into the concrete. However, expedient concrete composition and compaction achieve the same density in the most cases. The application of concrete admixtures assumes the verification of the suitability of a concrete mixture. Therefore, suitability tests or experience with comparable mixtures over many years are required.

16.3.7.3 Requirements on concrete and concrete properties

Concrete strength

The *concrete strength classes C20/25* and *C30/37* according to ENV 206 [16.4] are used for overhead line foundations. The first value refers to the compressive strength obtained by testing a cylinder with 150 mm diameter and 300 mm height and the second value to the compressive strength of a cube with 150 mm length of edge, both given in N/mm^2. Preparation and storage of *test specimens* are standardized in ISO 2736 [16.11]. Due to the uncertainties of site-mixed concrete, overhead line foundations

Table 16.2: Consistence ranges and indices for concrete

Consistence range	Spreading index (mm)	Compaction factor	Slump (mm)	Vebe time (sec)
Stiff	F1	C1	S1	V1
	up to 340	1,45–1,26	10–40	30–21
Plastic	F2	C2	S2	V2
	340 to 410	1,25–1,11	50–90	20–11
Soft	F3	C3	S3	V3
	420 to 480	1,10–1,04	100–150	10–5
Flowing	F4	—	S4	V4
	490 to 600	—	≥ 160	≤ 4

should be designed for the strength class C20/25 so far as possible. The strength class C30/37 can be used in case of ready-mixed concrete.
A correlation of the concrete strength data according to [16.4] to those specified in national standards cannot be established directly and is only possible to a limited extent. The data according to DIN 1045 refer to a cube with 200 mm length of edges and storing conditions for the specimens different from those according to [16.11].
The properties of the hardened cement paste are prevalent for the *concrete compressive strength*,. These properties depend on the strength class of the cement and on the water-cement ratio. Guideline data to determine the concrete compressive strength depending on the cement class and water-cement ratio can be obtained from Figure 16.8.
When carrying out a suitability test, a higher strength needs to be verified than the nominal strength of the concrete. E. g., the compressive strength of a 150 mm test cube should be 35 N/mm^2 in case of concrete class C20/25.

Consistence
Four consistence ranges are distinguished for fresh concrete: Stiff, plastic, soft and flowing (ISO 4103, [16.12]). The *consistence* is a summarizing property for the workability of the concrete, whereby the *consistence data* are used as measuring and assessment quantities. Four methods can be used to determine the *consistence indices*: The spreading index test [16.13], the compaction test [16.14], the Slump test [16.15] and the Vebe test [16.16]. For overhead line foundations, predominantly plastic concrete is used which can be well compacted by vibrators. Table 16.2 contains the consistence ranges and the related consistence indices according to standardized test methods.

Water and cement demand
Cement and *water demand* of concrete are closely correlated. The correlation is described by the *water-cement ratio* defined as the ratio of the weight of water to the weight of cement. In Figure 16.8, the concrete strength is shown as a function of the water-cement ratio. However, enough water is necessary to provide for good workability and compaction with the available compaction tools, e. g. vibrators. A water-cement ratio between 0,5 and 0,6 should be used when preparing plastic concrete for tower foundations. If a water-cement ratio of 0,5 is envisaged, the water demand corresponds to half of the cement weight.
There are several possibilities to determine the water and cement demand of an aggregate mixture. One of these methods is based on the *finess index*, characterizing the particle distribution of the aggregates. The finess index is a scale for the total surface of all particles and, therefore, for the water demand which depends directly on this surface. The finess index is obtained by summing up the individual test sieve residuals of a test sieve set in percent by mass and dividing this sum by 100. Details can be found in [16.7].

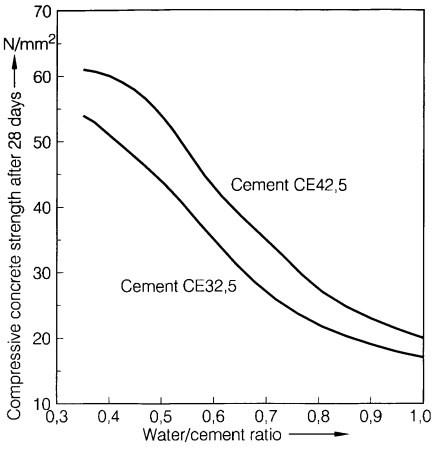

Figure 16.8: Compressive concrete strength depending on the water-cement ratio, cement classes CE 42,5 and CE 32,5, cubes with 150 mm length of edges and storage of the cubes according to ISO 2736

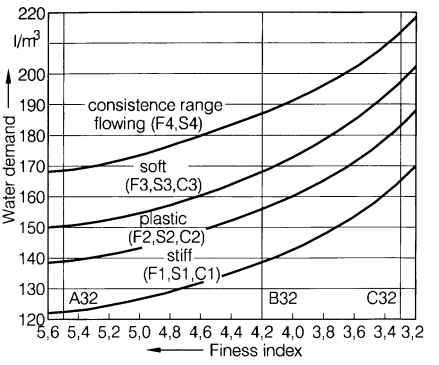

Figure 16.9: Determination of the consistence-depending water demand of aggregate mixtures by means of finess index

From Figure 16.9, the *water demand* of an aggregate mixture necessary for the envisaged consistence can be determined based on the finess index. E. g., 168 l/m^3 water will be necessary for aggregates having a grading curve B32 to achieve a plastic concrete close to the limit of soft consistence. For concrete strength class C20/25, a minimum cement content of 280 kg/m^3 is required according to Table 16.3. In case of a water-cement ratio of 0,6, a total of 168 l/m^3 water will be necessary, a result which is also obtained from Figure 16.9.

In some project specifications, a minimum cement content is stipulated, lying well above the content necessary due to concrete technology. Such stipulations take care of frequently adverse conditions and uncertainties for mixing and handling of concrete on site.

Concrete temperature

According to [16.4] and [16.9], the temperature of the fresh concrete should neither exceed 30°C nor fall below 5°C during the period between mixing and placing of the concrete. The temperature of the fresh concrete can be controlled by heating up the aggregates and the added water during cold weather. It needs to be ensured that the temperature of the concrete does not fall below 5°C before the strength has achieved at least 6 N/mm^2. In hot weather, attention should be paid to avoid heating up of aggregates and water. The water needs to be cooled in extreme climate.

Durability of concrete

Concrete should durably protect the reinforcement against corrosion and resist given environmental conditions. Standard ENV 206 [16.4], therefore, requires measures related to the following five *exposure conditions*:

- (1) Dry environment;
- (2 a/b) Humid environment without and with frost, respectively;
- (3) Humid environment with frost and effects of de-icing salts;
- (4) Attack by seawater environment;
- (5 a/b/c) Attack by chemically aggressive environment (low, medium, high).

According to ENV 206, Table 4, requirements on the composition of the concrete concerning *minimum cement content* and maximum water-cement ratio, on the type of cement, e. g. cement with sulphate resistance, and for coatings to protect the concrete in direct contact with aggressive media (exposure condition 5 c) result for the individual exposure conditions. National standards may be used until ENV 206 will be mandatory approved. According to [16.9], concrete complying with the requirements for exposure condition 2 b (concrete for external application) should be used for overhead lines.

16.3.7.4 Ready-mixed concrete

Ready-mixed concrete is prepared in a concrete plant, mixed in the plant or on a truck mixer and delivered to site in a condition ready for placing. Ready-mixed concrete presents the most economic solution for many overhead lines, complying reliably with the quality and testing requirements. In [16.4], the responsibility between the construction company (user of concrete) and the producer of the concrete is controlled with reference to the following types of order:

- **Prescribed mixture:** The concrete composition and the aggregates are specified by the construction company.
- **Design mixture:** The concrete producer selects the aggregates and determines the concrete composition.

For overhead line purposes, mostly design mixtures are selected from the concrete type list of the producer, considering the following criteria:

- *Strength classes*: C20/25 or C30/37 or others;
- *Maximum particle size of aggregates*: 32 mm or others;
- Purpose of use: Reinforced concrete, environmental conditions, exposure conditions: see clause 16.3.7.3;
- Workability: Consistence, admixtures in case of long transport distance or placing periods, ability for pumping, fresh concrete temperature;
- Type of cement: Special climatic conditions, special requirements concerning protection against chemical attack.

The construction company should check the delivering notes in view of conformity with the order and the transport period before unloading on the construction site. During unloading, the *consistence* should be checked visually or by tests in case of doubts.

16.3.7.5 Site-mixed concrete

Mixing of concrete on site requires a *mixing instruction* which can be obtained from:

- Specifications stipulated by the line owner or by project specification. These stipulations should be checked on compliance with the minimum requirements of the relevant standards.
- Use of *standard-mixed concrete*, e. g. according to DIN 1045 (Table 16.3), if this is permitted for the individual application.
- Selection of aggregates and composition of concrete according to the mix design and verification of the required properties of fresh and hardened concrete.

Mixtures stipulated by a line owner aim at achieving the desired quality without much care on economics. They take into consideration any uncertainties possibly occurring at overhead line construction sites and assume *grading curves* with high water demand which may not care enough on the particle size distribution of actually used aggregates. Concrete may be produced following prescribed mixtures without suitability tests according to [16.9]. Standard-mixed concrete should comply with the minimum requirements according to Table 16.3. The application of standard-mixed concrete is advantageous if low concrete quantities are necessary or a tight schedule requires its use.

Table 16.3: Requirements on standard-mixed concrete C20/25 depending on exposure conditions according to ENV 206 [16.4] and on concrete without suitability test according to DIN 1045 [16.9]. Maximum particle size 32 mm, cement according to strength class 32,5

ENV 206			DIN 1045				
Condition of exposure	Water/ cement ratio	Cement content kg/m³	Grading curve	Water/ cement ratio	Cement content for consistence class F1/C1/S1 kg/m³	F2/C2/S2 kg/m³	F3/C3/S3 kg/m³
2 a	0,60	280			No information		
2 b	0,55	280	A/B	0,6	300[2)]	320[2)]	350[2)]
			B/C	0,6	320[2)]	350[2)]	380[2)]
5 a	0,55	280[3)]			n. p.[1)]	n. p.[1)]	n. p.[1)]
5 b	0,50	300[3)]			n. p.[1)]	n. p.[1)]	n. p.[1)]
5 c	0,45	300[3)]			n. p.[1)]	n. p.[1)]	n. p.[1)]

[1)] Not permissible without suitability test

[2)] Concrete for external applications according to DIN 1045, 6.5.5.1 – Table 4

[3)] In case of a sulphate content above 500 mg per kg water or above 3000 mg per kg soil, sulphate resistance cement needs to be used

However, it is a prerequisite that the specifications valid for a project permits the use of standard mixtures.

A *mix design* offers the most economic solution in case of larger concrete quantities as required for overhead line construction sites. The mixture of the concrete should be specified based on suitability tests or on experience with comparable conditions. The special conditions concerning the aggregates available on the construction site need to be considered to ensure that the required characteristics of the concrete will be met.

For many overhead lines, the exposure condition 2 b (humid environment with frost) according to [16.4] is relevant. The concrete strength class C20/25 and a maximum particle size of 32 mm for the aggregates are provided for this application. For a superior workability, plastic consistence, e. g. a consistence with a spreading index of 370 to 390 mm, should be aimed at.

According to Table 16.3, a cement content of 280 kg/m³ is necessary according to ENV 206 [16.4] without any special requirements on the strength class and type of cement. The water-cement ratio may reach 0,55 at maximum according to a water demand of 280·0,55 = 154 l. The grading curve may be between the lines A32 and C32 according to Figure 16.7. According to Figure 16.8, a cube strength of 37 N/mm² can be expected under these preconditions, using a cement with the strength class 32,5. However, to achieve a consistence range F2 with a water demand of 154 l/m³, a finess index of approximately 5,0 is required according to Figure 16.9. Therefore, the grading curve needs to be within the range A/B. This can be achieved with 600 kg/m³ aggregate of the particle size 0/4, 800 kg/m³ of the particle size 4/16 and 600 kg/m³ of the particle size 16/32.

The example demonstrates that with standard mixtures according to ENV 206 the required properties cannot be securely achieved. Therefore, a verification of the stipulated properties should be carried out.

According to DIN 1045 [16.9], a standard mixture without suitability tests for the consistence range F2 and for the exposure condition 2b is required as follows (Table 16.3): Minimum cement content 320 kg/m³ with a cement strength class 32,5; water-cement ratio at maximum 0,6, that is 320 · 0,6 = 192 l water; grading curve within the range A/B.

Under these conditions, a strength of 35 N/mm² tested at cube results from Figure 16.8. In case of 192 l/m³ water, a finess index of 3,4 is required for the consistence range F2 according to Figure 16.9. For this water and cement content, all types of aggregates having grading curves within the range A/C can be used. The specified properties can

be safely achieved with the standard mixtures according to [16.9].
If no other stipulated properties require the use of cement according to the strength class 32,5, cement according to the *strength class* 42,5 should be selected. The concrete strength will be increased and the minimum cement demand can be reduced by 10 %. Cement with both strength classes is offered at the same price on the market.

16.3.7.6 Handling and placing the concrete

Placing the concrete requires a clean and so far as possible dry excavation pit. Water should be pumped out or the concrete has to be placed as under-water concrete.
The reinforcement may not be polluted by soft soil subfaces. Therefore, a *subgrade layer* of lean concrete should be provided before installing the reinforcement. Mixing of soft soil and concrete would affect the concrete quality and needs to be avoided.
The concrete formwork should withstand the expected load. It should be clean and coated with release agents not contaminating the reinforcement. The position of the reinforcement may not be dislocated when placing the concrete. To avoid such a dislocation of reinforcement, thick timber planks should be used to walk on.
Ready-mixed concrete should be placed without interruption after delivery. In case of concrete without retarding admixtures, the transport and placing period at 20°C may not exceed 60 minutes in case of cement types according to German standards or 45 minutes in case of cement types according to EN standards.
The workability of concrete depends on its consistence. Plastic concrete, e. g. according to consistence range F2, can be compacted by vibrators. During transportation and placing, the concrete may not demix, especially honey combs may not be generated. Elephant trunks, craning skips or chutes need to be used in case of falling heights above 2,0 m, column-type structural components with a cross section of 0,5 m times 0,5 m excepted.
The concrete should be placed such that after compaction no hollow spaces will be left below anchoring sections or cleats. The concrete is placed in 0,5 m thick layers and compacted by *internal vibrators*. The internal vibrator should be dipped rapidly into the concrete at distances of 0,4 to 0,8 m and pulled out slowly depending on the working principle of the vibrator. The vibrator should penetrate approximately 0,15 m into the bottom layer which was previously compacted, to achieve a sufficient bonding between the individual layers and avoid unscheduled construction joints. When pulling out the vibrator, the hole within the concrete should close itself. The vibration procedure should be stopped when no more air bubbles escape at the surface. A too long vibration process should be avoided since otherwise a watery concrete mud would be formed at the surface.
Rain as experienced in Central Europe does not affect the concrete quality to a noticeable extent. However, very heavy and enduring rainfalls may result in washing off the cement at horizontal and inclined surfaces and in demixing of concrete layers close to the surface, thus increasing the water-cement ratio. Therefore, the concrete should be adequately protected in this cases.

16.3.7.7 Curing the concrete

The concrete needs the water content for hardening, therefore a *curing of freshly placed concrete* is always necessary, e. g. to avoid drying out.
Methods of curing the concrete are:

- Continuous spraying with water;
- Application of humid covers;
- Keeping the formwork up to the end of the curing period;

- Backfilling of the excavation with slightly humid material immediately after removing of the formwork and planking;
- Spraying of curing agents which form a protecting film.

The required period for concrete curing amounts between two and ten days according to [16.4] and depends on the development of concrete strength and on the environmental conditions such as sun radiation, action of wind and air humidity. Curing the concrete may also be necessary to protect the concrete against heavy rainfall, flowing water, a too rapid cooling or freezing at low air temperatures. At temperatures of 10 to 20°C, the concrete reaches 80 % of its final strength after a period of 14 days; then the *tower erection* can start.

16.3.7.8 Methods for verification of concrete properties

Compressive strength

Standard [16.4] requires a *test series of the concrete compressive strength* according to [16.17] and [16.11] to be carried out after 28 days at 300 mm tall cylinders with 150 mm diameter or at cubes with 150 mm length of edges. The test specimens are stored under water at 18 to 22°C before testing. Standard [16.9] requires a test series according to [16.18]. The test specimens are stored seven days under water and 21 days at air with a humidity of 50 to 70 % and 15 to 22°C temperature.

The differing dimensions of the test specimens affect the testing results. For comparisons, the compressive strengths obtained from differing *test specimens* can be converted using factors gained from experience. Assuming the storing conditions according to [16.9], the following relations for the strengths apply: $\beta_{\text{cube200}} = 0{,}95\,\beta_{\text{cube150}}$; $\beta_{\text{cube200}} = 1{,}18\,\beta_{\text{cyl}}$ and $\beta_{\text{cube150}} = 1{,}24\,\beta_{\text{cyl}}$, where β_{cube200} is the *compressive strength* gained at a test cube with 200 mm length of edges, β_{cube150} that at a test cube with 150 mm length of edges and β_{cyl} that gained at a standard cylinder.

With increasing penetration of humidity, the friction forces within the texture decreases Therefore, it can be concluded that also the storing conditions affect the test results. Test results gained from the procedures according to EN or DIN standards cannot be compared directly. Test results gained from testing a cube with 200 mm length of edges and processed according to specifications given in DIN 1048 have to be reduced by a factor of 0,92 according to [16.19], page 5.6 to gain data which can be compared with compressive strengths obtained from tests on cylinders.

Consistence

To assess the *consistence*, the spreading index test according to ISO 9812, the compaction test according to ISO 4110 or the Slump test according to ISO 4109 are frequently used. Table 16.2 represents information relevant for overhead lines. The assessment of consistence according to the specified approaches does not completely coincide. That means, that the consistence range F2 is not completely equivalent to the class S2. In Central Europe, the spreading index or compaction test is given priority, while outside of Europe the Slump test is most frequently adopted.

16.3.7.9 Quality supervision and quality management

According to [16.4],*quality supervision* comprises all measures, decisions and tests which are carried out corresponding to stipulations for concrete with the aim of guaranteeing the specified requirements.

The quality supervision can be divided into:

- ***Contractor supervision*** (production supervision): *Contractor supervision* comprises checks and tests including the evaluation of the test results. The contractor

supervision needs to be carried out by the construction manager, the subcontractors and suppliers, whereby each of these entities is responsible for its range of tasks.

- ***Quality verification***: *Quality verification* comprises measures and decisions based on stipulated criteria to assess conformity with stipulated requirements. Within this group are the quality verification by independent quality control organisations and/or acceptance tests taking test specimens. For overhead lines using concrete according to the strength class C20/25, the quality verification can be carried out by the construction company, since in case of *site-mixed concrete* only negligible reliability related risks are given.

A *documentation* according to the rules is an essential part of quality supervision. Retraceable records need to be made for which the construction manager is responsible. The tests need to be recorded and approved with respect to the necessary number of tests and the compliance of the results with the stipulations. The chronological progress of the individual activities like installation of the reinforcement, placing the concrete and curing have to be documented. For this purpose, the weather conditions, unusual events and special measures, if any, to reach the stipulated concrete characteristics are recorded, e. g. protection against frost.

Suitability tests belong to the responsibility of the contractor's supervision. Prior to using the concrete, the *concrete composition* is verified which is needed to reach reliably the requirements on the concrete with the aggregates and the conditions at the construction site.

In case of *ready-mixed concrete*, the manufacturing plant verifies the suitability if concrete is delivered according to a design mixture. Delivery notes and consistence need to be checked visually when the ready-mixed concrete is delivered to site.

For *site-mixed concrete*, a series of tests concerning the constituent materials of concrete, tools and production of the concrete have to be carried out according to [16.4]. Also for production, transportation, placing, compacting, curing and quality supervision of concrete *quality management programs* are increasingly established or required. These contain requirements, measures to comply with the requirements, tests and specifications for documentation. Within these categories are:

- Requirements on constituent materials (cement and aggregates);
- Requirements on composition and properties of the concrete;
- Type, extent and documentation of tests for verification that the requirements are complied with;
- Description of methods for production, transportation, placing, compaction and curing of the concrete;
- Methods for documentation.

Quality management programs have proven their adequacy for a qualitatively convincing and economic execution of concrete works [16.20].

16.4 Installation of earthing

Where necessary, transmission line supports are equipped with earthing installations to conduct failure and induction currents as well as currents from lightning strokes into the earth (see Chapter 5). For this purpose, horizontally arranged electrodes, named *counterpoises* or earthing rods can be installed in the soil.

Horizontally arranged electrodes can be installed radial or as rings in manually or tool-assisted excavated trenches in depths between 0,6 and 1,0 m. The earthing conductor or strap is conductive connected to the tower leg members. Earthing straps should be installed endup in the trench such that the back-filled soil touches the earthing strap

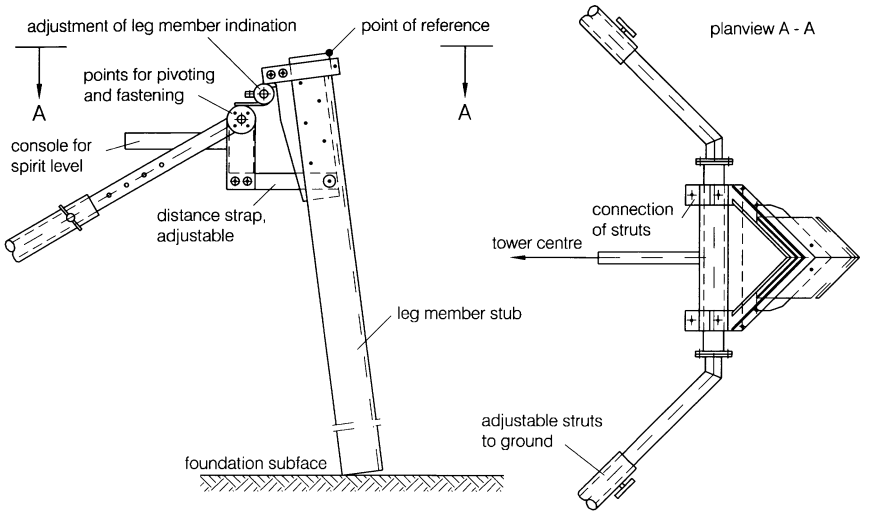

Figure 16.10: Example of an equipment for installation of individual stubs

on both sides. Low earthing resistance are achieved in cohesive soil. Stones or coarse gravel directly at the earth electrode increase the *earthing resistance*to a large extent. *Earthing rods* are driven manually or by tools as deeply as possible into the soil. In case of shallow foundations, they can be driven into the soil from the excavation pit subface before starting of concrete placing.
The earthing resistance are measured by means of an earth tester (see clause 5.11). If the required earthing resistance is exceeded, the earthing properties need to be improved by additional earth electrodes. To achieve low transition resistance, metallic bright connections between earth connectors and towers should be envisaged and supervised.

16.5 Setting of tower stubs or bases

16.5.1 Methods and tools

The stubs or bases of lattice steel towers need to be set in place before establishing the connection with the foundation. There are two procedures adopted:

- The stubs are set by means of a setting template or with the tower base.
- The stubs are set individually and independently of each other.

In case of shallow foundations, the stubs are arranged on concrete blocks in the excavation or on a layer of lean concrete. Differences in heights are balanced by placing steel plates underneath the stubs or by adjustment of bolts arranged at the lowermost cleats at the stubs.
In case of augered foundations or piles, the setting templates are supported and adjusted by jack stands. The stubs are connected to the setting templates hanging into the borehole or above the pile head. The tower axis should intersect the line axis at the tower witness pillar. The tower base or setting template can be adjusted by means of a theodolite. Reference marks at the template or tower base can ease this activity.
Setting of stubs individually has proved its qualification especially in case of wide-spread towers and towers with great differences in the level of the individual leg member foundations. Each individual leg member stub is separately adjusted to the required position and fixed there. Thereby, the efforts for manufacturing, transport and expensive installation and removing of wide and heavy setting templates can be waived. An equipment

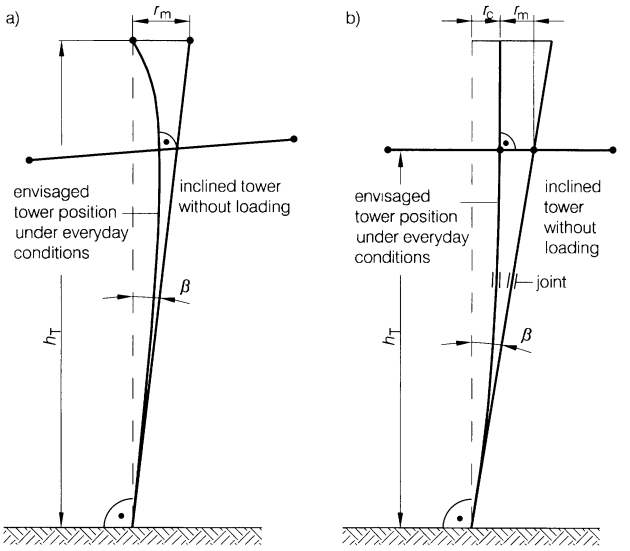

Figure 16.11: Position of towers without and with conductor everyday loads a) tower top vertically above the tower centre; b) crossarm horizontally

is schematically shown for setting stubs individually in Figure 16.10. The stubs should be carefully levelled complying with a maximum tolerance of level between the highest and lowest leg not more than approximately 6 mm.
Both methods are suited to reach the accuracy needed in view of the tower alignment. Only two days after placing the concrete, the setting template or the equipment for setting the stubs may be removed. The concrete strength achieved is decisive for this period. Since during the short period, the concrete strength does not reach its final value, any vibrations of the leg members should be avoided when removing the setting templates or equipment.

16.5.2 Inclination of angle and dead-end towers

In order to achieve a vertical position of angle, angle-section and dead-end supports, permanently loaded by conductor tensile forces after stringing, the structures need to be erected with an inclination against the direction of loading. The objective of the inclination can be either

- A position of the tower top vertically above the tower centre at the tower base (Figure 16.11 a) or
- A horizontal position of the longest crossarm since an inclined crossarm would provide a negative visual impression.

In the latter case, a vertical tangent line to the deformation curve of the tower body at the height of the crossarm connection is aimed at (Figure 16.11 b). Before stringing the conductors, the *inclination* of the tower is higher in this case than with respect to a vertical position of the tower top.
The loads under everyday conditions form the basis for the determination of the necessary inclination; in EN 50 341-3-4 the everyday condition is specified as 10°C without wind, to mention an example. In addition to the elastic deformation, the *bolt slippage* and the tilting of *slip joints* of solid wall steel poles contribute to the deformation.
When aiming at a vertical position of the reference point above the pole centre at ground, the inclination during erection is expressed by the angle β

$$\beta = \arctan\left(r_m/h_T\right) \approx r_m/h_T \quad , \tag{16.1}$$

where
r_m is the horizontal displacement at the top of the structure (Figure 16.11 a) and
h_T the reference height above the base of the structure.

The horizontal displacement follows from

$$r_m = r_{el} + \sum_{i=1}^{n} \alpha_{si} \cdot s_i \quad , \tag{16.2}$$

where
r_m is the elastic deformation of the structure at the reference height,
α_{si} the tilting angle of the joint,
i and s_i the distance between this joint and the position of the structure where the deformation is considered and
n the number of joints.

The *elastic deformation* r_{el} can be calculated according to the principle of the virtual energy assuming a virtual horizontal force $\overline{F} = 1$ at the position where the deformation is considered:

$$r_{el} = \int_0^{h_T} \frac{N(x)\overline{N}(x)}{EA(x)}\,dx + \int_0^{h_T} \frac{M(x)\overline{M}(x)}{EI(x)}\,dx \quad . \tag{16.3}$$

In this equation, there are
$N(x)$ axial member force due to external load at everyday condition;
$\overline{N}$ axial member force due to virtual load;
$A(x)$ cross-sectional member area;
$M(x)$ bending moment due to external load at everyday condition;
$\overline{M(x)}$ bending moment due to virtual load;
$I(x)$ moment of inertia;
E modulus of elasticity.

When aiming at a horizontal position of the considered crossarm after stringing, the inclination angle β of the unloaded structure should be (Figure 16.11 b):

$$\beta = \varrho_{el} + \sum_{i=1}^{n} \cdot \alpha_{si} \tag{16.4}$$

where ϱ_{el} is the elastic deformation angle at the height of the considered crossarm.
The deformation angle ϱ_{el} can be obtained according to the principle of the virtual energy assuming a virtual external moment $\overline{M}_\varrho = 1$ at the position where the deformation is considered

$$\varrho_{el} = \int_0^{h_T} \frac{M_x(x)\,\overline{M}_\varrho}{EI(x)}\,dx \quad , \tag{16.5}$$

where $\overline{M}_\varrho$ is the virtual bending moment and h_T the height of the considered crossarm above ground. Alternative approaches for calculation of deformations are described in clause 12.5.14.
When aiming at a horizontal crossarm position, an eccentricity of

$$r_c = h_T \tan\beta - r_{el} - \sum_{i=1}^{n} \alpha_{si}\, s_i \tag{16.6}$$

results after installation of conductors (Figure 16.11 b). The necessary inclination is determined for the actual load at the specific tower or pole site.
Using the method described in clause 12.5.14, the elastic deformation of lattice steel towers can be determined. Due to the great number of members, this might be time-consuming. In addition to the elastic deformation of bolted lattice steel towers, also the

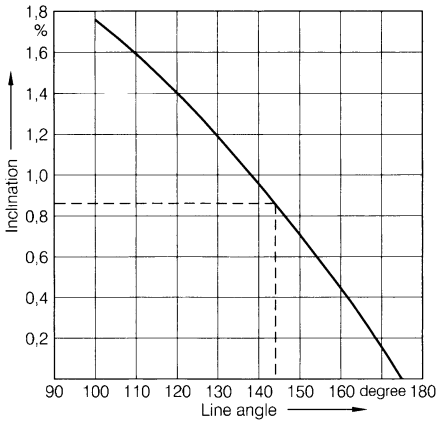

Figure 16.12: Inclination of an angle strain tower given as a percentage of the tower width (example)

tilting due to the bolt slippage within the joints should be considered. An assumption of 4 mm slip per joint has been proved as correct. An additional inclination of 0,1 to 0,2 % of the tower height takes care of visual amplification of tower inclination due to tension insulator sets and the deformation of the foundation. In Figure 16.12, the data for determination of inclination depending on the line angle are shown for a 110 kV line. The inclination is expressed as the increase in level of the compression loaded stubs relatively to the tower width at the joint above ground surface.
The diagram in Figure 16.12 applies for a tower installed in the bisectrix of the angle. From this diagram, also the necessary inclination of towers can be determined which are not arranged in the bisectrix or are loaded by differing conductor tensile forces. For this purpose, the acting forces are divided into components in parallel to both tower axes. For these components, the equivalent line angles can be determined which would lead to the same horizontal forces. For these fictitious line angles, the inclination as a percentage of the tower width can be taken from the diagram in Figure 16.12. By multiplication with the tower widths, the portions in increase of stubs of the individual tower legs can be obtained.

Example: For a line angle of 145° and a tower width of 6,30 m, the increase of stub elevation should be determined from Figure 16.12.
For 145° an inclination of 0,86 % results from Figure 16.12, yielding a difference in height of $6{,}30 \cdot 0{,}86 \cdot 1000/100 = 54$ mm.
In case of *solid wall steel poles* with slip joints, the publication [16.21] proposes to consider a tilting of 0,4° per joint at the maximum load. In [16.22], the deformation of solid wall steel poles equipped with slip joints is reported. The poles were erected with the predetermined inclinations and then checked with respect to the position of the crossarms after finalizing conductor stringing. From this study, it can be concluded that independently of the loading and the pole type a tilting of 0,3 to 0,4° should be considered for each joint. From these measurements, no conclusion on the inclination of the foundations could be drawn. Since an inclination against the tower loading seems always to be more expedient, the inclination of the foundation should be considered by an angle of at least 0,1° unless locally more unfavourable subsoil conditions would advice to adopt higher values.

Figure 16.13: Tower erection by elevation

16.6 Erection of supports

16.6.1 Introduction

The method used for erection of supports depends on design, weight and dimensions of towers or poles, accessibility of tower sites, available tools and machines and qualification of the erection staff. The method has to be selected with respect to economics as well. Assessing these aspects, lattice steel towers are erected piece by piece with preassembled walls, with preassembled sections or completely assembled on ground and lifted or tilted then.

16.6.2 Assembly and erection by elevation

Low-weight and short self-supporting lattice steel towers are frequently assembled by elevation. The activities are started by erection of the legs, continuing with the first horizontal diaphragm as base for the erection of the supports. The erection then proceeds by installing sets of preassembled or individual members. Hoisting of parts is carried out manually assisted by winches and trucks. The hoisted members are rendered to the linemen at the mounting position to insert them in due place and tighten the bolts. After completing a tower section, the assembly of the following section can start. In this phase, bolts are only partially tightened just enough to keep the structure in position. The final bolt tightening is carried out when revising the assembling. In Figure 16.13, tower *assembly by elevation method* is shown. Guyed towers as well can be erected by elevation making use of provisional guys. Here, winches are generally adopted.

16.6.3 Tower erection using a crane

Tower or pole erection by means of a *mobile crane* suitable for going cross-country is advantageous if the support sites can be accessed without difficulties at all weather conditions. Single poles made of wood, concrete or steel tubes can be lifted by a crane onto the foundation or into an excavation. By the help of a crane, lattice steel towers having heights up to 30 m and widths up to 2,5 m can be erected in one piece. A sufficiently wide space is necessary for a complete three-dimensional assembly on ground. Taller and wider towers have to be erected section by section after preassembling on ground.

16.6.4 Tower erection by means of a gin pole

16.6.4.1 Procedures

Where erection by mobile crane is not possible or uneconomic, several methods are in use where the crane is replaced by a *gin pole* in combination with a hoisting winch. A lattice steel structure made of tubes or angle sections is used as a gin pole, whereby the dimensions correspond to the required rating and the hoisting height. A gin pole made of aluminium alloy is lighter in weight, however, is more susceptible to damage and cannot be repaired by tools available on the construction site. To ease its transport, the gin pole is divided into individual parts with lengths of approximately 5 m. Therefore, the total length can be adjusted by removing or inserting individual sections. At the ends of the gin pole, foot and head components, respectively, are arranged depending on the application.

For hoisting the tower components, slowly running *drum winches* with continuously varible revolution control are used which can also be adopted for *sagging* during conductor stringing operation. The required length of rope of approximately 300 m can be perfectly winded up layer by layer on a sufficiently wide reel. Its core diameter should at least reach 20 times the rope diameter. Crane ropes available on the market are used as *hoisting ropes*, the theoretical failing load of which should be at least three times the expected tensile force. The hoisting winches are hydraulically driven. When the pressure within the hydraulic system decreases, the reel brake is automatically closed. In addition, a deadman's circuit leads to an immediate stand-still of the winch if the control stick is let go off. To be able to unwind the winch rope without any load, the reel is decoupled from the hydraulic drive. A protecting device against slacking rope prevents an unintentional decoupling under load.

The differing *erection procedures* for piecemeal tower erection are distinguished by the arrangement of the gin pole at the tower.

16.6.4.2 Erection with a gin pole outside the tower

When erecting a tower with a *gin pole arranged outside the tower body*, a bracket is fixed at the upper part of a leg member by which the gin pole is supported (Figure 16.14). The foot component of the gin pole is articulated on the bracket and fixed to the leg member. The head of the gin pole is equipped with four anchors to ground staggered at approximately 90°, the length of which can be varied from the ground surface by means of come-alongs. Therefore, it is possible to incline the gin pole into a position required for hoisting of a tower component. The hoisting rope runs from the anchored hoisting winch to the leg member, is deviated by approximately 90° upwards by means of a pulley and runs then in parallel to leg member and gin pole over pulleys at the head component to the load. The part to be hoisted being a tower section, a tower face or an individual member is guided by an anchor rope to avoid clashing to the gin pole or to the tower body already assembled.

When a tower section is completely assembled, the gin pole is lifted. For this purpose, an additional bracket is arranged at the upper end of the leg member of the tower section just assembled. The hoisting rope runs then from the winch to the pulley at the leg member stub, further to the pulley at the upper bracket and then downwards to be fixed to the foot component of the gin pole. When the winch starts pulling, the foot component can be released from the lower bracket and the gin pole is hoisted by simultaneously releasing the head anchors until the foot component can be fixed to the upper bracket.

Tower erection by means of a gin pole arranged outside the tower body requires a wide working area because of the anchors to ground. Other transmission lines, railways or

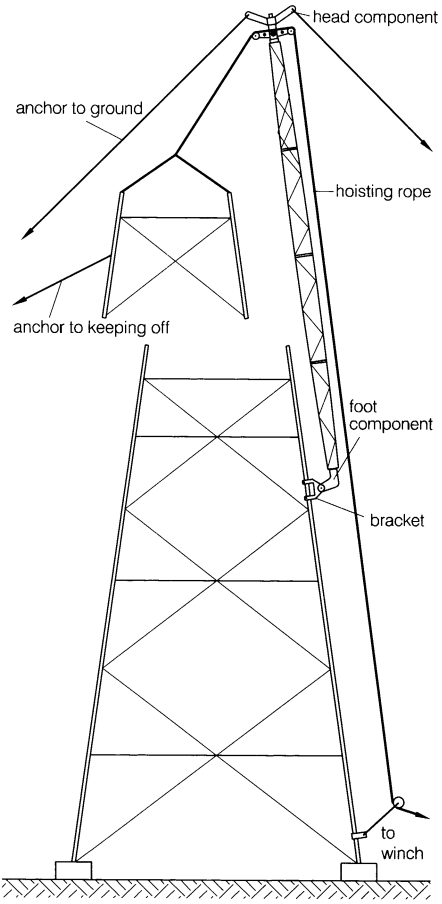

Figure 16.14: Erection with a gin pole outside the tower

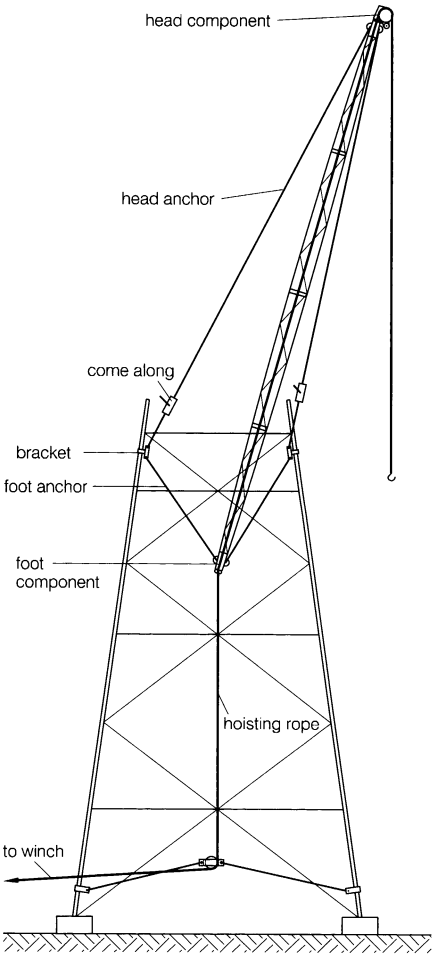

Figure 16.15: Erection with a gin pole arranged in the centre of the tower

roads in close proximity to the tower to be erected aggravate the anchoring, as do fruit-trees, vineyards or forests. Also the soil conditions may not be in favour of installing anchors, e. g. mud or rock. Under such conditions, an erection procedure should be preferred without the necessity of anchors to ground.

16.6.4.3 Erection with gin pole in the tower centre

Erection using a *gin pole arranged in the tower centre* is especially suited for towers with large widths and at tower sites with more difficult conditions since no anchors to ground are necessary.

The gin pole has in principle the same design as used for working outside the tower body and is arranged in the centre of the tower body. The foot component is supported by four equally long anchors which are carried by brackets arranged in the upper section of the leg members. Approximately two thirds of the total gin pole length protrude above the brackets. The head of the gin pole is anchored by means of four anchors to the same brackets as the foot anchors (Figure 16.15). The lengths of the head anchors can

be varied by means of come-alongs similarly as in case of gin pole arranged outside the tower. The hoisting rope is guided from the hoisting winch over a pulley installed close to the ground surface in the centre of the tower and through the gin pole and a revolving pulley at the gin pole head to the load. By this procedure, the tower components can be assembled piece by piece or face by face.
With the work progress, the gin pole must be lifted to a higher section. For this purpose, the head anchors equipped with the come-alongs are first fixed to brackets installed at the tower section just assembled. Then, the lifting of the gin pole is carried out by means of a hoisting rope fixed at the foot component of the gin pole. This hoisting rope is guided over a pulley arranged at a rope between two opposite leg members of the just assembled section. During lifting of the gin pole, the head anchors are released such to keep the gin pole in a vertical position as far as possible. When the foot anchors can be arranged to the same brackets as the head anchors, the new position of the gin pole is reached.
By means of a gin pole arranged in the centre, towers with large widths and tall heights can be erected without any anchors to the ground. Therefore, this method has gained priority during the last years, especially for erection of self-supporting towers consisting of a tower body and several crossarms. As an example the suspension towers of the 380 kV crossing over the river Elbe with a height of 227 m and approximately 1000 t weight should be mentioned [16.23]. The 40 m long gin pole had a load capacity of 100 kN.
Using the same procedure, the suspension towers of the 500 kV crossing over the Suez canal [16.24] with a weight of 710 t each and a height of 220 m as well as the suspension towers of the 380 kV crossing III over the Bosphorus [16.25] (weight 450 t, height 160 m) were erected. In Figure 16.16, the erection of a suspension tower of the crossing over the Suez canal is shown .

16.6.4.4 Erection with a gin pole in the tower at a leg member

For light-weight lattice towers with small width, the assembly using a gin pole arranged in the tower centre seems not to be expedient because of the costly handling of foot and head anchors. In such a case, erection using a*gin pole arranged inside the tower at a leg member* is more suited because neither anchors to the ground nor anchors within the tower are necessary. The gin pole is arranged articulately on a bracket fixed to the leg member inside the tower. At a height of one third of the gin pole length, a strop equipped with a chain hoist and fixed to the same leg member is adopted to move the gin pole into the desired position. An anchoring of the gin pole head to the ground surface in opposite direction of the load relieves the gin pole when heavy components are hoisted. The hoisting rope is guided through the gin pole and over a pulley at the gin pole head (Figure 16.17).
It is possible to hoist tower faces or single members. Since the gin pole is loaded on bending, special care has to be taken on avoiding any overloads. Due to their limited hoisting capacity, the gin pole and the winch can be designed relatively light and transported simply also in terrain difficult to access.

16.6.5 Erection of guyed towers

16.6.5.1 Hoisting of a crossarm using a gin pole

After the tower body has been erected completely, the crossarms are installed. For this purpose, the gin pole arranged outside the tower body is inclined to arrange its head directly above the position where the crossarm will be finally fixed to the tower body. The crossarm assembled at the ground surface is then lifted in a horizontal position

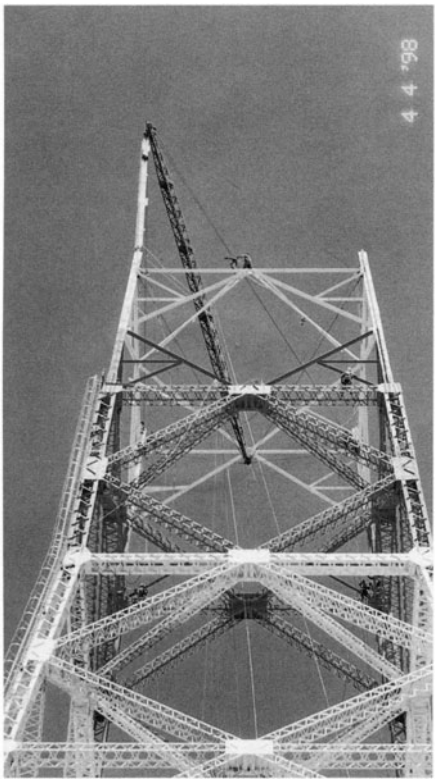

Figure 16.16: Gin pole arranged in the centre of a tower, 550 kV line across the Suez canal

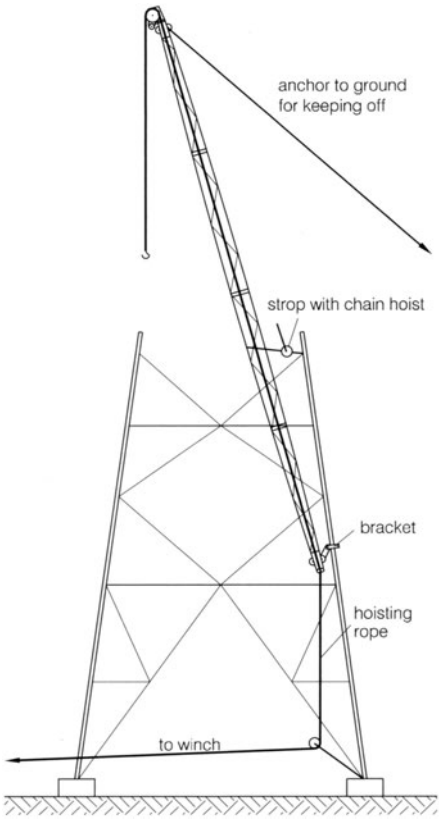

Figure 16.17: Tower erection by means of a gin pole arranged inside the tower at a leg member

and bolted to the tower body. Other crossarms arranged below can be lifted using the already installed upper crossarm. For this purpose, the hoisting rope is guided from the gin pole head to the crossarm assembled at ground, then deviated by a pulley and guided back to the crossarm already installed. According to this arrangement, the gin pole and the already installed crossarm each carry half of the loads to be hoisted .
A gin pole arranged in the centre of the tower body can be inclined to a low extent only. Therefore, the upper crossarm must be hoisted with its top directed upwards, then jointed to the tower body by means of the upper crossarm chords and tilted into the final position and bolted (Figure 16.18). The crossarms arranged underneath the first one are lifted utilizing the crossarms above.

16.6.6 Tower erection using helicopters

The use of helicopters may be advantageous when towers have to be erected within very short periods of time, lines are converted or the access is difficult, e. g. in mountainous terrain. The *use of helicopters*, however, is expensive, connected with stress for the erection staff and to a great extent weather-dependent. To achieve an economic advantage, the components of the towers are preassembled on the ground surface corresponding to the capacity of the helicopter used. A sufficiently high number of linemen is distributed simultaneously on several towers such that the helicopter can transport tower parts

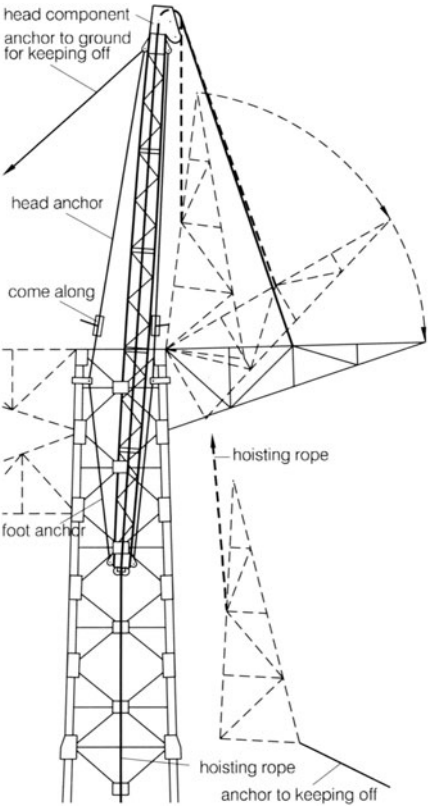

Figure 16.18: Hoisting of a crossarm

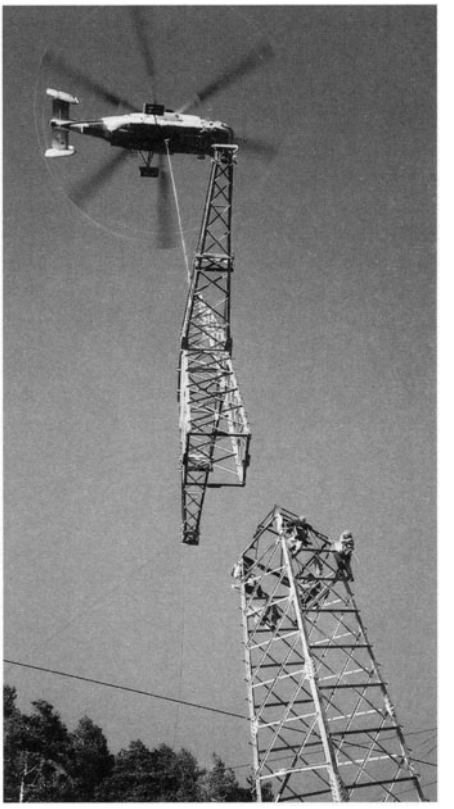

Figure 16.19: Tower erection using a helicopter

from the storage area to the tower sites where they are installed continuously without any interruption. Therefore, the linemen on the towers will be active for short periods of time only. When adopting high-performance helicopters for heavier weights necessary to erect taller towers, the wake of the rotor will become so strong that working of linemen on the towers would be risky. For this case, auxiliary erection remedies are required which provide guidance and temporarily fastening of the tower components flown in until the linemen can bolt this parts after the departure of the helicopter and the auxiliary erection remedies can be dismantled again. In Figure 16.19, tower erection by means of a helicopter is shown.

16.6.6.1 Manual method

For manual *erection of guyed towers*, the tower is assembled by elevation similarly to erection of self-supporting towers described in clause 16.6.2. Provisional guys are adopted for stability of the assembled sections.

16.6.6.2 Use of an auxiliary mast

A tubular mast composed of about 5 m long modules, sufficiently high according to the tower to be erected is used. On its upper part, an articulated support piece is fastened which lays horizontally during the erection. At the lower edge of the mast, a base is

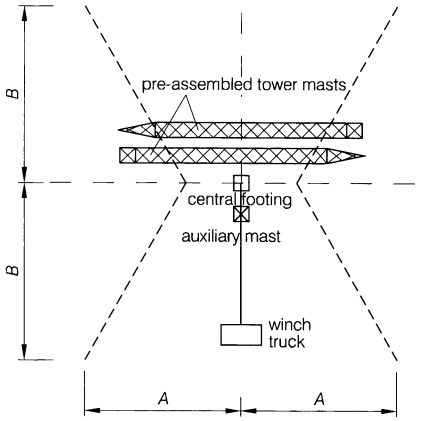

Figure 16.20: Arrangement of tower site with preassembled guyed tower

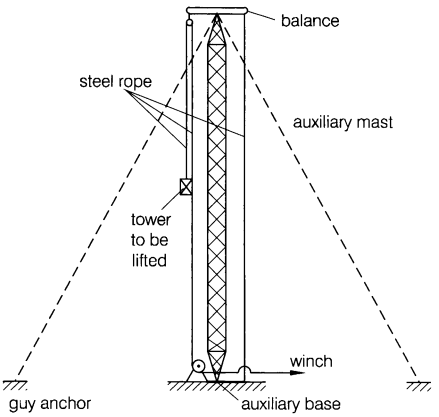

Figure 16.21: Lifting of preassembled guyed tower with auxiliary mast

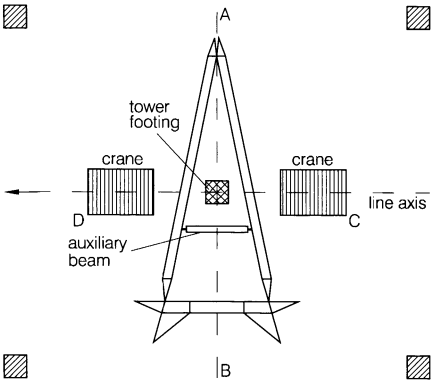

Figure 16.22: Erection of guyed tower with an auxiliary crossbeam by cranes

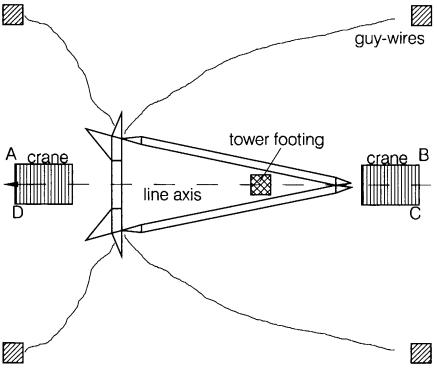

Figure 16.23: Erection of guyed tower by cranes without auxiliary crossarm

laid down for supporting the mast and transferring the compression loads to the soil. Figures 16.20 and 16.21 outline this erection method.

16.6.6.3 Erection by cranes

The quicker and usually cheaper method of erecting guyed towers is by means of cranes of adequate capacity, which picks up the assembled tower on the ground either directly at the crossarm or at an auxiliary crossbeam. In Figures 16.22 and 16.23, it is outlined how the crane method is applied for erecting towers up to 40 m high (crossarm to ground). The cranes adopted should have a capacity of approximately 500 kN and a lifting height of 45 m. Due to the reduction of lifting capacity with height, towers higher than 32 m require the use of auxiliary crossbeams. The pick-up point of the crane, as well the detailed design of the auxiliary crossbeam are made by the tower manufacturer. After erection, while the crane still holds the tower, the guy wires are provisionally tied to the guy anchors. The guy wires are then cut to appropriate lengths as a function of the terrain slopes, and with the help of two theodolites laid down at longitudinal and transverse directions, the tower is positioned at the plumb, as shown in Figure 16.24.

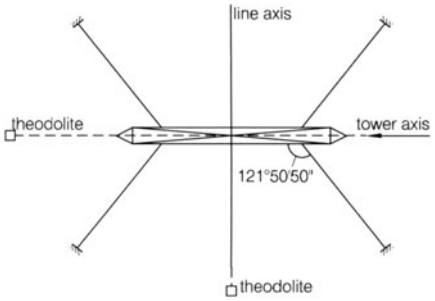

Figure 16.24: Plumbing a guyed tower

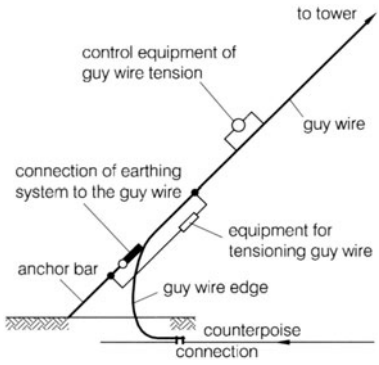

Figure 16.25: Detail of guy wire tensioning and connection

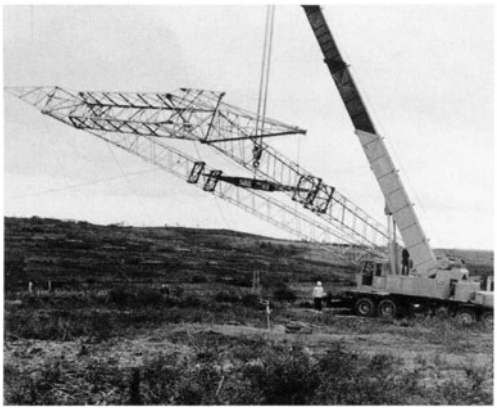

Figure 16.26: Lifting of a 500 kV guyed-V tower by means of a crane picking up the tower at an auxiliary crossbeam

A dynamometer controls the tension at one of the guy wires prescribed to be between 7 to 10 % of the rope RTS. The preformed grips are then installed and the guy wire ends are connected to the counterpoise wires, as shown in Figure 16.25. The acceptable tolerances for the tower being out of the perpendicular and torsion are 3 mm/m of tower height. In Figure 16.26, the erection of a 500 kV guyed-V tower using a crane is shown. The crane picks up the structure at an auxiliary crossbeam, since the crane height is too low for reaching the crossarm. The auxiliary crossbeam is removed after tightening of guy wires.

Erection by crane is more appropriate for flat terrain, where the environment is not disturbed essentially. For hilly terrain, the manual erection and the use of an auxiliary mast are usually preferable, because they require neither special access roads nor large terrain cuts near the assembled structure.

16.6.7 Bolts and torques

Bolts should be tightened in accordance with prescribed torques or values, as given in Table 16.4.

In some cases, the use of special torques can be required by the design. All nuts should be secured against getting loose. Frequently springer washers are used for this purpose.

Table 16.4: Torques for bolt tightening

Bolt type	M12	M16	M20	M22	M24	M27
Bolt diameter (mm)	12	16	20	22	254	27
Torque (N·m)	40 to 60	80 to 120	130 to 180	190 to 230	300 to 340	475 to 610

Alternatively, bolts should be punched on three points spaced at 120°, and protected with anti-corrosive dyes. Alternatively, other blocking systems can be used, as the employment of spring washers or special glues.

16.7 Installation of insulator sets and hardware

16.7.1 Insulator sets

The insulators are transported in standardized boxes or in crates to the installation sites and should be stored there on wood supports and adequately protected. For *assembling the insulator strings*, special care should be taken, such as:

- The insulator sets should be assembled in accordance with the design drawings.
- Pins of shackles and clamps, when installed vertically, should be inserted from top to bottom such that they cannot get lost.
- The heads of the counterkeys should be positioned such that an easy access during live-line works is possible.

The suspension insulator sets are lifted and installed before conductor stringing. Protective cradles should be used for multiple insulator sets to avoid clashing of individual strings. The stringing blocks are fixed to the insulator sets to prepare the conductor stringing. The insulator sets should be in a vertical position after the conductor sagging and the maximum tolerance towards the plumb is limited to 2 % of the string length for both transverse and longitudinal directions (see clause 16.8.5).

16.7.2 Joints

All cares recommended for the insulators are applicable to the *installation of hardware* as well. In particular, damage to the finish should be prevented, in order to minimize replacements.

Compression clamps and splices, after being made, should be accurately checked with regard to correct workmanship. In case of doubts, X-ray tests can be carried out.

Conductor splices should be at least 10 m far from the nearest structure. Depending on the project, conductor joints may not be permitted at spans crossing over highways, railways or other transmission lines. It is recommended to limit the number of joints to one per span for every conductor or subconductor. All the conductors can be jointed at the same span, but the subconductors of the same phase should be jointed only at minimum spacing of 1,5 m from one another.

16.8 Conductor stringing

16.8.1 General requirements

Conductor stringing should be handled by an experienced crew, not only to prevent damage to the conductors and earth wires but also to maintain the sags and tensions specified in the design. Correct sags are essential to give the required mechanical safety, but it is just as important that the actual sags in the line correspond to those used in the design, to ensure proper clearances to ground and to obstacles.

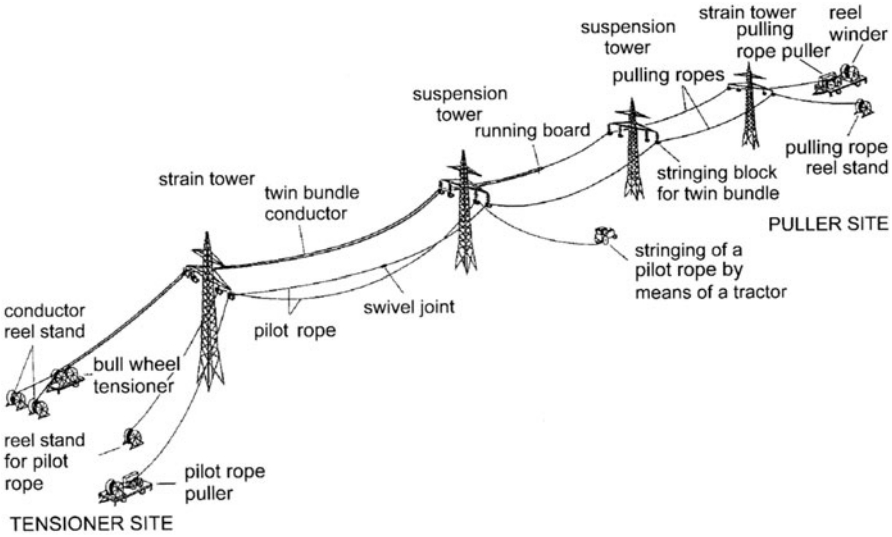

Figure 16.27: Stringing of a twin bundle conductor

To prevent dangerous overvoltages that may result from electrostatic induction by parallel energized lines, safety measures should be adequately defined during conductor stringing.

Before stringing, dynamometers, earth meggers and other equipment should be checked and adjusted.

Before conductor stringing, the contractor should present to the client, for approval, a complete plan of distribution and unwinding of the conductor and earth wire reels along the line, containing control spans, layout of stringing equipment, position of the joints, provisional anchors to ground. Attention should be given to the reel lengths, aiming at losing the least possible amount of cables. The maximum length of conductor to be strung under tension should not exceed 8 to 10 km.

16.8.2 Stringing methods

There is no international or European standard on conductor stringing. IEC 61 328 TS [16.26] deals with installation of conductors in the vicinity of live circuits. The German standard DIN 48 207-1 [16.27] is applicable for the *stringing of* overhead line *conductors*. Phase conductors and earth wires should be installed under tension without touching the ground or any obstacles. Touching ground or obstacles could cause damage of the conductors, that would infringe their mechanical and electric characteristics. Furthermore, the conductors could corrode because of chemical products potentially available on the soil. Therefore, the conductors should run over stringing blocks suspended at the supports, with sufficient tension to keep them clear of ground surface or obstacles. For this purpose, the conductor to be unwinded is connected to a pulling rope at the tensioner site and strung by a puller to the *puller site*, which can be installed some kilometres apart from the tensioner site (Figure 16.27). To guarantee enough clearance to the ground during conductor stringing, an adequate tensile force has to be applied by means of a controlled *tensioner*.

In case of long line routes with only a few angle points, it is expedient to utilize the capacity of conductor reels to their full extent with respect to the production length,

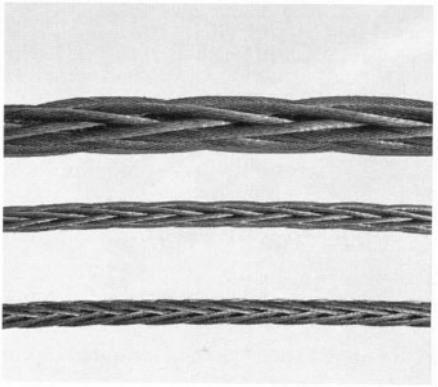

Figure 16.28: Braided pulling ropes

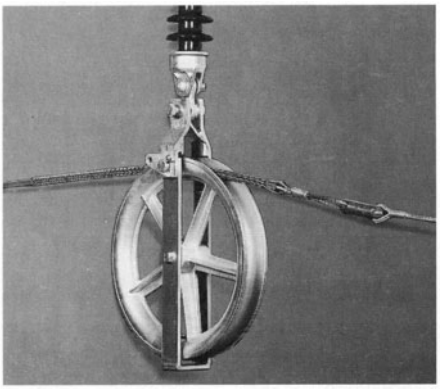

Figure 16.29: Jointing of conductor and pulling rope

stringing the conductors even over strain towers. For this stringing procedure, the same lengths are chosen for the pulling ropes as for the phase conductors. However, it is necessary to establish tensioner and puller sites regardless the terrain and the sites of the strain towers. The ends of the conductors are anchored to ground after stringing at the tensioner site as well as at the puller site. A line crew operating independently of the stringing procedure adjusts the conductors and terminates them at the strain towers. In densely populated areas like Central Europe, the terrain and the land use do rarely permit to plan and construct lines with long straight tensioning sections. There, it is more appropriate to string the conductors tensioning section by tensioning section from one strain tower to the next. Behind each strain tower at the end of a tensioning section a tensioner or puller site is installed. The stringing operation is carried out independently of the lengths of the conductors and the available pulling ropes. If the tensioning section lengths are shorter than the conductor manufacturing lengths, the conductors are cut; if they are longer, they need to be extended by tension- and current-resistant joints (see clause 10.2.4).

16.8.3 Conductor stringing equipment

16.8.3.1 Requirements

Conductor stringing requires special *pulling ropes*, *stringing blocks*, *pullers*, *tensioners* and accessories. The conductor type and cross section to be installed are decisive for the design of conductor stringing equipment. The required stringing equipment depends on the *conductor stringing force* for which the everyday stress may be assumed as maximum. For standard conductors, the everyday stress is approximately 50 N/mm^2.

16.8.3.2 Pulling ropes

Pulling ropes should be as far as possible twist-free. Their minimum failing load should be at least three times the expected stringing force. Ropes may not be used further if a given number of visible strand failures has been reached. Two pulling rope types have proved worthwhile and are mainly used:
Braided ropes made of eight or twelve plaited steel strands have low twist and are, therefore, well-suited (Figure 16.28). Loops formed during the stringing process open again automatically under tension without forming a typical sharp bend within the rope. This type of pulling rope has a relatively low filling coefficient compared with

Table 16.5: Specification of pulling ropes

Subconductor cross section mm^2	Pulling rope Diameter mm	Ultimate tensile strength kN	Standard length m
Single up to 300	11	73	3 000
Single 300 to 500	13	115	1 600
Twin bundle up to 500	16	165	1 200
Triple bundle up to 500	20	280	000
Quadruple bundle up to 600	24	380	800

stranded conductors. Therefore, braided pulling ropes are thicker than stranded ropes of the same tensile strength and need a larger winding volume on reels or winch drums. Due to their costlier production, braided ropes are more expensive than stranded ropes. *Compacted*, mostly three-plaited-strand *steel ropes* are less twist-free and, therefore, should be kept continuously under tension during the stringing procedure. The compaction of the ropes after stranding of the litzes increases their strength and the filling coefficient, thus reducing the twisting strain. Pulling ropes compacted in this manner need an essentially lower winding volume compared with braided pulling ropes, however, are more susceptible against forming of loops and cannot be spliced because of the design made of three plaited strands. Therefore, joints and thimbles have to be compressed in this cases. In Table 16.5 specifications for pulling ropes are shown.

16.8.3.3 Rope connections

During conductor stringing, *rigid connections* and *swivelling joints* are used. The first type is used for jointing conductors of the same type due to the absence of any twist, while the latter is used for jointing different conductor types to compensate the expected twist. Rigid connectors may run over the bullwheel puller, however, swivels may not be used such.

All *conductor connections* applied during stringing operations should withstand three times the maximum *stringing force* to be expected. They should be as slim as possible and designed with a diameter as low as possible to enable running over sheaves without being blocked there. Sharp edges must be avoided.

Several types of connections can be distinguished in view of conductor stringing:

- Connection of two identical pulling ropes by a rigid joint;
- Connection of two pulling ropes with differing diameter by means of a swivelling joint;
- Connection of a conductor and a pulling rope by means of *woven wire grips* with a swivel (Figure 16.29);
- Connection of two conductors by two woven wire grips with a rigid connector;
- Connection of the subconductors of a bundle with one pulling rope by means of a *running board*, which equalizes the tensile forces in the strung subconductors and stabilizes them in a horizontal position to guide the connection between pulling ropes and the subconductor over the multiple stringing block without a jerk. The pulling rope and the conductors are connected to the running board by means of swivels for this purpose. Easy mobility of the hinges and pulleys of the running board and the swivels is of particular importance (see Figure 16.30).

For ease, compression joints at the conductors can be installed on the ground surface directly behind the tensioner before continuing conductor stringing. The connector should be provided with a protector against bending when running over stringing blocks. Passing of the protector, however, requires sheaves with accordingly designed groove dimensions.

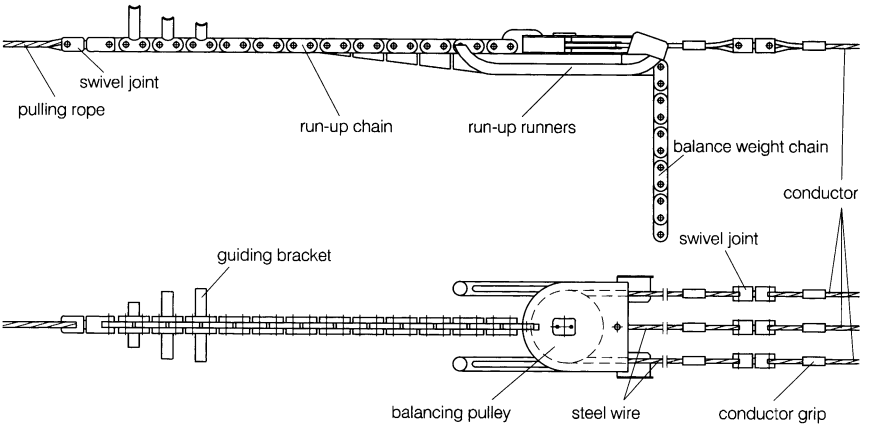

Figure 16.30: Running board for stringing of bundle conductors

Inductive or capacitive interference may occur on the conductors to be strung due to live parallel circuits which cannot be disconnected. The current to be expected, therefore, should be known in advance to select suited swivels and woven wire grips. According to DIN 48 207, Part 2 [16.28], woven wire grips made of steel can be used for currents up to 160 A. In case of a higher current, damage cannot be excluded. For this case, temporary compression joints or special clamps for an increased current capacity should be used. Application of swivels and pulling woven wire grips is standardized in [16.28] and [16.29], respectively.

16.8.3.4 Stringing blocks

The size of sheaves for stringing of overhead line conductors depends on the diameter of the conductor to be strung; the diameter of the pulleys at the groove basis should amount to at least 20 times the conductor diameter. A sufficient width of the grooves should enable an unhindered passage of temporary joints like swivels and woven wire grips. When selecting the stringing blocks, the maximum load expected due to the conductor rollover angle should be considered as well. Therefore, it is recommended to use reinforced stringing blocks at strain towers close to the tensioner and puller site. Neoprene- or perlon-lined sheaves should be used to protect the aluminium layers of the conductors. The sheaves can be combined to stringing blocks for stringing of bundle conductors, whereby the grooves of the central sheaves accommodating the pulling ropes need not to be lined.

16.8.3.5 Puller for conductor stringing

The *pullers* used nowadays for *conductor stringing* haul either pilot ropes or pulling ropes, whereby *reel-type* or *twin bullwheel pullers* are used. *Reel-type pullers* equipped with a permanently integrated drum are used to string pilot or pulling ropes for conductors with cross sections up to 300 mm^2.

For pulling conductors with higher cross sections with adequate conductor tensile forces, predominantly hydraulically driven *twin bullwheel pullers* are preferred which haul pilot and pulling rope by means of two bullwheels (Figure 16.31), designed with six to ten grooves each for running of the ropes. The wheels having a diameter of at least 30 times the rope diameter are staggered by half of the groove width to each other.

The shape of the groove is designed such that rigid connectors to be hauled will be able

Figure 16.31: Twin bullwheel puller

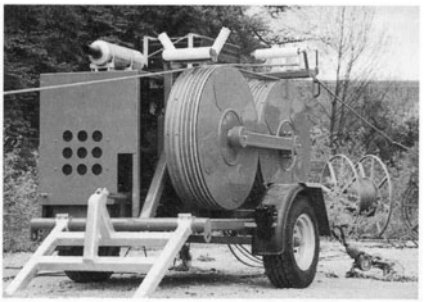

Figure 16.32: Conductor tensioner driven by an engine

to pass over the grooves. A brake working at the bullwheel and a clamping device, which closes automatically in case of a standstill or a pressure decrease within the hydraulic system, exclude gliding of the ropes.
Behind the puller the rope is winded on a reel winder equipped with changeable reels. The hydraulic drive of the reel winder keeps the rope continuously under a tensile force to exclude sliding of the rope over the bullwheels. The size of the reels is the same for all diameters of pilot and pulling ropes. The reels, therefore, can store different rope lengths depending on the rope diameter. E. g., in case of a rope with 24 mm diameter, 800 m can be wound on one reel, while in case of a rope diameter of 11 mm 3 000 m can be wound (see Table 16.5).
The lineman operating the puller controls the machine by means of a portable remote control unit. He can, therefore, chose a position where he is able to follow closely the running of the ropes over the bullwheels and onto the reel winder. He is located at sufficient distance from the puller, such that the noise generated by the drive will not impair too much the communication.
The *running velocity* depends on the load and may achieve up to 100 m/min in case of low loads and up to 50 m/mm in case of heavy bundle conductors.
Bullwheel pullers offer the following considerable advantages compared with reel-type pullers:

- Due to the separation of the winder for the ropes the weight of the bullwheel puller is lower.
- A change of the rope type is possible just by changing the rope reel without time- and cost-consuming rewinding activities.
- The total length of the rope can be expanded as necessary just by coupling the ropes stored on reels.
- When running over the bullwheels, constant stringing speed and stringing forces are achieved at the same driving intensity due to the constant wheel diameter.
- Winding off the ropes from separate reels treats them with care since the ropes are under a low pretension only and cannot cut into the rope layers on the reels with the full tensile force.

Modern bullwheel pullers are equipped with an adjustable overload control, meter counters, tachometers and instruments for recording the tensile force. *Tensioners* equipped with a driving unit, also called puller tensioner, are used to hold tension against the pulling rope and are as well suited to string pilot or pulling ropes (see 16.8.3.6).

16.8.3.6 Tensioner

The conductors to be strung run over *conductor tensioners* which are used to hold tension against the pulling rope and are designed preferably as twin bullwheel units. Alternative designs adopt one wheel only which is equipped with an endless shoe chain. The conductor is guided over two bullwheels equipped with three to six grooves and hold to tension. The diameter of the wheels should correspond at least to 30 times the conductor diameter. The dimensions of the grooves lined with neoprene are selected such that the thickest conductor for which the tensioner is provided can run with a woven wire grip or a connector over the wheel.
The tensioner should hold the conductor from standstill to the maximum stringing speed at different tensile forces continuously variable and without jerks and dissipate the braking heat generated thereby. This requirements have lead to differing designs of tensioners which will be described hereafter.

Mechanical tensioners

The bullwheels of *mechanical tensioners* are equipped with *mechanical braking units.* While in the past flexible band brakes or block brakes have been used, nowadays predominantly disc brakes with sufficiently large discs are adopted which dissipate the braking energy without artificial cooling. The required braking pressure is applied pneumatically or hydraulically by means of a pump operated by feet or hand similar to operation of disc brakes in automobiles.
A sufficiently large rotating mass of the bull wheels equalizes the running of the mechanical tensioners during starting due to overcome the higher friction coefficient at standstill (adhesive friction) than during operation (gliding friction) and ensures steady stringing of the conductor. Mechanical tensioners are characterized by noiseless running, a relatively simple design and economic advantages resulting therefrom.

Hydraulic tensioners

The bullwheels of *hydraulic tensioners* are coupled with a hydraulic pump which is driven by the wheels during braking operations. The braking effect is achieved by restraining the oil stream generated by the pump, whereby the braking force can be controlled continuously variable by means of a throttle valve. The oil will be heated by the dissipated braking energy. The heat is extracted from the oil in a radiator unit before being sent back to the hydraulic pump.

Engine-driven brakes

The bullwheels of *engine-driven tensioners* as shown in Figure 16.32 are driven hydraulically as in case of a twin bullwheel pullers. A diesel engine drives a hydraulic pump, by which the oil flow within the hydraulic system is controlled. When pulling or holding conductors, the hauling or holding force, respectively, as well as the conductor stringing speed can be adjusted by means of the running speed of the oil. To avoid overspeeding during braking, the oil flow is guided through a throttle valve and decelerated, whereby the braking energy is dissipated within the oil circuit. The oil heated up flows back to the hydraulic pump via a radiator unit.
Engine-driven tensioners can be universally used for stringing and replacing of conductors under everyday tensile stress. They are designated, therefore, as combined *puller/tensioner* and are suited for conductor sagging as well. When combined with a reel stand connected to the hydraulic system, the tensioner can also be used for dismantling conductors, whereby the conductor is permanently kept under tensile stress by the driven reel stand and wound up.

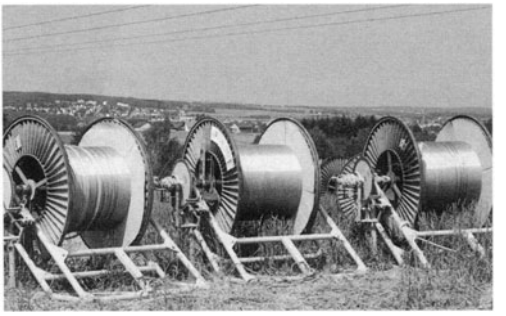

Figure 16.33: Reel stands

In addition, the puller tensioner can be used also to haul pulling or pilot ropes in connection with a hydraulically driven reel stand. By this procedure, the pilot or pulling ropes are handled with care due to the large diameter of the bullwheels and the groove lining made of plastic material.

16.8.3.7 Reel stands

The conductor reels are installed in reel stands behind the tensioner for unwinding the conductors (Figure 16.33). Depending on the design of the *reel stand*, the drums are installed by tilting or lifting using winches. The conductor reels are clamped on a shaft between adjustable cones to ensure a smooth running without jerking. The reel stands need to be equipped with brakes for the reels to pretension the conductor in front of the bullwheel tensioner to exclude slipping of the conductor over the tensioner and to avoid continuation of unwinding the drum after a sudden stop of the tensioner. For this purpose, disc brakes are used the saddle of which is operated by hand, air or hydraulic pressure from the control unit of the tensioner.
Reel stands equipped with hydraulically operated brakes are used in combination with motor-driven tensioners. In this case, the hydraulic system of the tensioner supplies the reel stand as well.

16.8.4 Conductor stringing

16.8.4.1 Preparations

Before starting *conductor stringing*, the line section between tensioner site and puller site needs to be prepared accordingly. *Scaffolds* are installed to protect crossed objects during conductor stringing. *Low-duty scaffolds* made of wood are suited to protect fences, orchards, vineyards etc. They need not to withstand the stresses due to conductor failure because the damage to objects would be limited in such an event. *Scaffolds* for protecting roads, railway lines, low- and medium-voltage lines, telephone lines etc. should withstand the loads that might occur after failure of a conductor or of a connector during stringing activities, thus excluding any contact with objects under the line. In special cases, e. g. if motorways cannot be blocked for a longer period, plastic or metallic nets are installed over the crossed object.
To prepare for conductor stringing, the fittings preassembled in the store are transported to the tower sites and assembled there with the insulators to form suspension insulator sets. The stringing blocks for the stringing of single or bundle conductors are fitted instead of the suspension clamps. The pulley for the pulling rope is provided with a light-weight, flexible finger rope for leading the pulling rope through the stringing block.
Eventually, the suspension set can be hoisted in one piece and suspended from the

crossarm. Hoisting can be carried out by hand or by means of a winch or a wheeled tractor. The use of a *lifting yoke* or cradle is recommended for double or multiple insulator sets to avoid clashing of insulators. The *finger ropes* ease leading the pulling rope over stringing blocks at the suspension supports which need not to be climbed again.
The crossarms of towers next to the tensioner or puller site are anchored during stringing operation to balance one-sided loads. The anchor ropes are arranged as lowly inclined as possible under the given local conditions. The crossarm ends are anchored to the tower top or tower body. The *tensioner site* should be installed far enough from the tower to achieve only a small downstrain angle of the conductor from the tower to the tensioner. The tensioner is adjusted in direction of the stringing block and anchored to the ground taking account of the holding force to be expected. The reel stand is placed in a distance of at least six times the reel width behind the tensioner and aligned to the tensioner intake. After placing the conductor reels in the reel stands, the reel cover is removed and a pulling grip is fitted to the conductor. Then, the conductor is guided through the grooves of the bullwheels by means of a plastic finger rope.
The *puller* is installed sufficiently far from the tower site, aligned to the stringing block and anchored taking account of the conductor stringing force.
All conductor stringing devices should be earthed precautionally to take care for possible short-circuit currents, inductive currents and atmospheric flashovers. The standing sites of the operation staff at the machines, such as steel grades, are connected with the earthing of the stringing machine for equipotential bonding. In addition, conducting connections should be installed between these earth electrodes and the closest tower as well as between stringing blocks and towers.
Before starting the conductor stringing, communication channels should be installed between all linemen active in the stringing operation.

16.8.4.2 Stringing procedure

Before *stringing the conductors*, a steel or plastic pilot rope is installed passing over the stringing blocks at the towers between puller and tensioner site. If the pulling rope for conductor stringing is too heavy to be strung directly, at first a pilot rope is installed having a lower cross section. This rope is used afterwards to string the pulling rope from the puller site to the tensioner site. The rope to prepare an initial connection across the running blocks at towers is installed either by hand, horses, tractors, caterpillars or helicopters depending on the terrain and the tower design. In any case, the rope needs to be held at tension to achieve a controlled unwinding from the storage reel or the drum of a puller. This can be achieved by reverse running of the bullwheel puller or by using a reel stand equipped with a mechanical brake. If the rope stored on a reel is not long enough, it can be connected with the rope of another reel by means of rigid connectors. At the tensioner site, the pulling rope is coupled with the conductor or conductor bundle.
At the beginning of conductor stringing process, the pulling rope puller is moderately accelerated up to the running speed envisaged. The tensioner has to hold the conductor well tuned, such that it does not touch the ground surface or any obstacles. The conductors on the reel stand are braked accordingly to achieve a sufficiently pretensioned intake of the conductors to the tensioner. After arriving of the conductor at the puller site it is connected by means of a dead-end clamp with the dead-end insulator set at the strain tower.
When the conductor on one reel is not long enough to fit between two adjacent strain supports, permanent joints need to be installed. Compression joints are used at most for this purpose. The joints are installed on ground following the manufacturer's instructions.

16.8.4.3 Sagging the conductors

The conductor can be sagged after installation of the dead-end clamps at the insulator set of the strain tower at the puller site. For this purpose, the conductor at the tensioner site is connected with a sagging winch (see 16.6.4.1) and strung to such an extent that the required *initial sag* is achieved. The determination of initial sags is described in clause 16.8.5. If the tensioner is equipped with a drive which can be used to haul the conductor into the reverse direction, an additional *sagging* winch is not necessary.
Several procedures can be used to *supervising the sags* during *conductor sagging*. If possible, horizontal sag battens are arranged at adjacent towers at heights corresponding to the initial sag. Then, the conductor tensile force is modified until the viewing line between the sag battens coincides with the lowest point of the conductor within the span. It is recommended to use field glasses with spider lines, a telescopic sight or a theodolite for sighting. To avoid sagging mistakes, it is necessary to carry out additional checking measurements in a second span especially in case of long tensioning sections.
Measurement of the wave running periods forms another possibility for checking the sag. The propagation speed of a transversal wave on a conductor is

$$c = \sqrt{H/m_C} \quad . \tag{16.7}$$

The running period of an impact wave in a span will be, therefore,

$$t = a/c = a/\sqrt{H/m_C} \quad , \tag{16.8}$$

where a is the span length, H the conductor tensile force and m_C the conductor mass per unit length.
As a first approximation, it applies for the sag:

$$f = a^2 \cdot m_C g/(8\,H) \quad , \tag{16.9}$$

from which it is obtained using (16.8)

$$f = g/8 \cdot t^2 \quad . \tag{16.10}$$

According to these formulae, the running periods of waves allow to check the sags. The wave is initiated by an impact exerted by means of a rope guided across the conductor in the vicinity of the attachment. The wave is reflected at the adjacent tower. To improve the accuracy, the wave is led to run three times between adjacent towers before the running period t is measured in seconds. The subconductors of a bundle conductor have to be checked separately. During this checking stage, no additional fittings, such as spacers or vibration dampers, should be installed. From the period t_6 measured in seconds for running six times the span length, the corresponding sag can be determined by:

$$f = 0{,}0003405 \cdot t_6^2 \quad \text{in m} \quad . \tag{16.11}$$

This method for conductor sag determination applies to span lengths and conductor tensile stresses as far as the approximation (16.9) is applicable. The method is independent of the conductor material.
In hilly terrain, *checking the conductor sag* by means of a viewing line inclined by the angle is well suited (Figure 16.34). The angle ϕ can be obtained from

$$\phi = \arctan\left(h - 4\,f + 4\sqrt{(f \cdot D)/a}\right) \quad . \tag{16.12}$$

There, ϕ is the inclination angle of the tangent at the initial sagging line ($+\phi$ above the horizon, $-\phi$ below the horizon), a the horizontal distance between the towers T_1

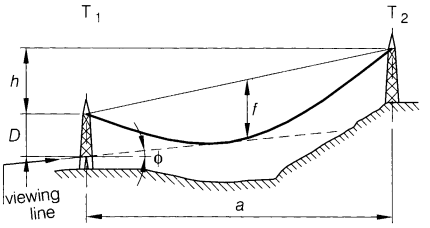

Figure 16.34: Conductor sagging by means of an inclined viewing line

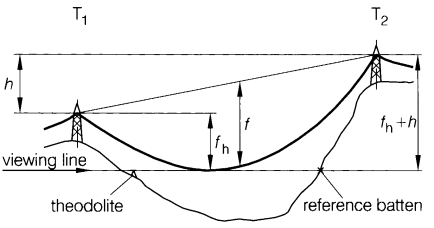

Figure 16.35: Conductor sagging by means of a horizontal viewing line

and T_2 (span length), f the initial sag according to the temperature during sagging, D the vertical distance between the conductor attachment and the inclination axis of the theodolite placed at the tower centre of tower T_1 and h the vertical distance between the conductor attachments at the towers T_1 and T_2.

During sagging, the conductor should touch the horizontal spider lines within the viewing range of the theodolite. For this purpose, the theodolite is aligned in the line direction, however, not turned laterally to the conductor. This adjustment procedure may be used only if the conductor touches the viewing line within the central third of the sagging control span.

In long spans having high differences between the attachment levels of the conductors at the towers, the sag is checked using a horizontal viewing line through the lowermost point of the conductor (Figure 16.35). The sag at this point is obtained from

$$f_h = f\,[1 + h/(4 \cdot f)]^2 - h \quad , \tag{16.13}$$

where f_h is the sag at a *horizontal viewing line*, f the target initial sag corresponding to the temperature during sagging and h the vertical distance between the attachments of the conductors. When checking the sag with a horizontal viewing line, the sag f_h is measured at a tower between the conductor attachment and the viewing line. At this point, the theodolite for the horizontal sight is arranged. A check of the viewing line is possible by installing a sag batten at the opposite tower of the span (see Figure 16.35).

16.8.4.4 Terminating the conductors

After sagging, the conductor can be terminated to the strain tower close to the tensioner site. For this purpose, the position of the dead-end clamp has to be marked on the conductor taking account of the length of the dead-end insulator set. The dead-end clamps can be installed on a working platform arranged at the tower or on ground, whereby the conductor has to be lowered again.

16.8.4.5 Clipping-in of conductors

After preparation of the dead-ends, the suspension clamps can be installed. Then the stringing blocks are removed. With respect of a vertical position of the insulator sets after *clipping-in*, the conductors are clipped-in with an offset compared to their position on the stringing blocks especially in rough terrain. The procedure to determine the offset is described in clause 16.8.5.2. For clipping-in at the appropriate position, it is necessary to mark the conductors at the position where they rest on the stringing blocks and measure from that position the offset of suspension points as calculated before (Figure 16.36). Clipping-in to suspension clamps can only be started when offsets have been marked at all suspension sets of the tensioning section or at least the positions of the conductors on the stringing blocks.

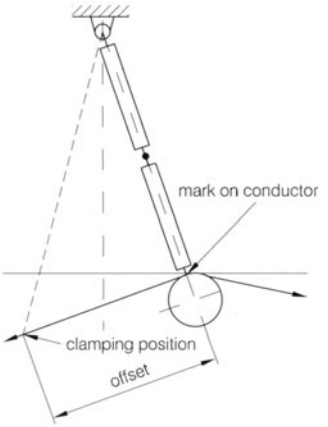

Figure 16.36: Offset of the installation position of a suspension clamp

Figure 16.37: Line car

16.8.4.6 Installation of jumper loops

At each strain tower, the corresponding ends of the conductors terminated at the insulator sets need to be connected such that they can conduct the current. In case of wedge-type tension clamps, the conductor ends extend through the clamps such that the *jumper loop* can be produced by overlapping the ends to be connected. The conductor ends overlapping on approximately one third of the jumper loop length are connected by two or three parallel groove clamps. In case of conductor terminations using compression dead-end clamps, preassembled jumper loops made of conductors of the same type are connected to the lugs at the compression clamps.
All clamping positions at the jumper loop connections should be metallically clean to ensure low electric transition resistance. For any type of jumper loops, the designed distances between adjacent loops and to the tower structure need to be obeyed also in swung conditions.

16.8.4.7 Installation of dampers and bundle spacers

The *installation of dampers and spacers* for bundle conductors completes the conductor stringing activities together with the installation of aircraft warning markers on the earth wires, if any. Light *line cars* driven manually or heavy line cars driven by engines are used (Figure 16.37) for these activities. The designed positions of dampers and distances between the bundle spacers or between markers are measured using a meter counter arranged at the line car.

16.8.4.8 Conductor replacement

Conductor replacements may be necessary for refurbishment or upgrading of existing overhead lines. A procedure has proven its qualification for this purpose, where the tensioner site is, as in case of stringing new conductors, equipped with a reel stand and a tensioner and the conductor to be replaced is used directly as pulling rope for stringing the new conductors [16.30].
Instead of a conventional puller, a motor driven tensioner (puller tensioner) is installed at the puller site hauling the conductor to be replaced. Joints possibly available on the conductor can run without difficulties over the grooves of the puller tensioner. Separable

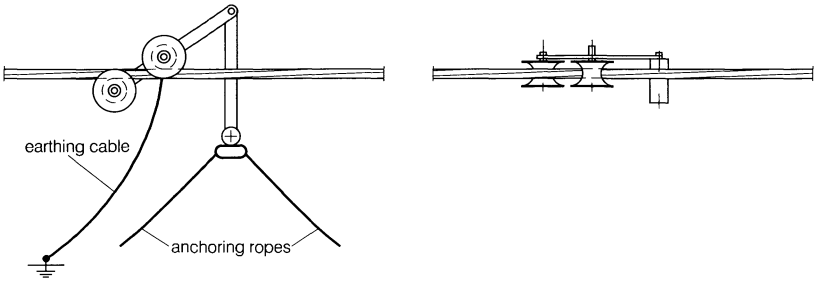

Figure 16.38: Running earthing system

reels, inserted to a reel winder equipped with brake, wind on the replaced conductors. Afterwards, the winded conductor coils can be removed from the separable reels and recycled. If the replaced conductors need to be dismantled in a reusable condition, a driven stand for standardized conductor reels is used.

16.8.4.9 Stringing conductors with optical fibres

Conductors with optical fibres or all dielectric self-supporting (ADSS) cables are frequently installed in overhead power lines. Stranded conductors with integrated fibres are adopted as earth wires (OPGW – optical ground wire) and less frequently as phase conductors. In general, the same tools and procedures are used for *stringing conductors with optical fibres* as in case of conventional conductors. For some conductors with optical fibres, the manufacturers stipulate specific limits for the stringing tensile stress. To verify the compliance with these limits, the tensile force of puller or tensioner needs to be recorded continuously, for example by means of monitoring the hydraulic pressure. In addition, the bending radii stipulated by the manufacturer and the minimum diameters of stringing blocks as given for example in DIN 48 207, Part 1 [16.27] may not be disregarded.
During the stringing procedures, the conductors with optical fibres may not be handled with conventional working grips but only with adjusted *tension-proof armor rods* (see clause 10.2.2).

16.8.4.10 Installation of conductors adjacent to or crossing energized lines

The publication IEC 61 328 [16.26] deals with precaution measures for installation of conductors in parallel to or crossing of energized lines. Their electrical and magnetic field induce voltages and currents on parallel conductors. If the conductors would not be earthed, the electrical field may induce a voltage as much as 30 % of that of the energized line voltage. Adequate earthing reduces the voltage to acceptable values. A current of several amperes will flow through the earth. If the earthing is removed, the capacitive potential is immediately re-established and linemen could be exposed to a dangerous voltage.
The energized, current-carrying conductor and the conductor being installed may be looked upon as primary and secondary windings of an air-core transformer. If the new conductor is earthed say at both ends, a circulating current will flow along and back through the earth. This current depends on the geometry and impedance of the system and on the load of the energized line. It can become large and affect the selection of equipment, such as pulling grips, swivels and earthing assemblies. At the moment of removing the last but one earth, the circulating current is being broken and a voltage appears across the gap, which can become dangerously high. The earthing sections,

therefore, should be short enough to limit the open circuit voltage.
IEC publication 61 328 contains a series of procedures on earthing of work sites. The most important ones should be summarized here:

- The automatic reclosers should be disabled on all energized lines where physical contact may occur as a result of an accident.
- The conductor stringing equipment and temporary anchors should be earthed with an earth rod having an earthing resistance less than 25 Ω and located in an area lined by an earthing mat.
- While stringing, the conductors should have running earthing systems located in front of the puller and tensioner, respectively. In Figure 16.38, a running earthing system is shown.
- The first structures in front of the puller and tensioner as well as every third support should be equipped with a stringing block earthing system.
- At the tower, where clipping-in takes place, all conductors should be earthed to a tower member or earthing point. The same applies to attaching conductors to strain structures and installation of jumper loops.
- The earthing equipment should withstand a test current of 20 kA for 0,4 s.

16.8.5 Determination of initial sags

16.8.5.1 Requirements

After stringing the conductors they are sagged so that after clipping-in they are in the position determined by the survey, planning and calculation, the suspension sets suspended vertically. When adjusting the conductors, provisions need to be taken for the permanent extension of the conductors during operation, called *conductor creep*. The conductors are sagged when they are suspended in stringing blocks. The *initial sags* should take care of the creep expected during operation and the current conductor temperature.

16.8.5.2 Position of the conductor on stringing blocks and in clamps

The mechanical behaviour of *conductors suspended on stringing blocks* (Figure 16.39) within a tensioning section differs essentially from the behaviour when the conductors are fixed to suspension clamps (Figure 16.40), if either large differences in the attachment heights of the conductors at the towers exist or if the span lengths differ to a larger extent within a tensioning section. These aspects have to be considered when determining the *conductor sagging data*.
It is the goal of the procedure described in [16.31] to determine the sags of conductors and the installation positions of the suspension clamps at the conductors resting on stringing blocks such that the sags of the conductors and the position of the insulator sets after clipping-in comply with the data established during line planning.
Since the conductors are fixed in line direction at the suspension supports, the insulator sets will assume a vertical position only if the horizontal components of the conductor tensile forces in the adjacent spans are equal. However, if the conductors rest on stringing blocks, a condition of equilibrium exists if the conductor tensile forces on both sides of the stringing blocks are equal. Then, no resulting moment acts around the block axle (Figure 16.39). The horizontal components of the tensile forces of the conductors in the adjacent spans will be equal, if there are neither differences in height between the conductor attachments nor in the span lengths. Only under this condition, the downstrain angles of the conductors on both sides of the stringing block are equal. In case of differing attachment heights of conductors or differing span lengths, differing conductor downstrain angles α exist (Figure 16.39) and differing horizontal components

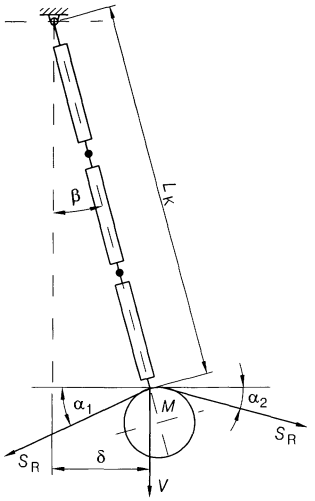

Figure 16.39: Condition of a conductor suspended by a stringing block before clamping

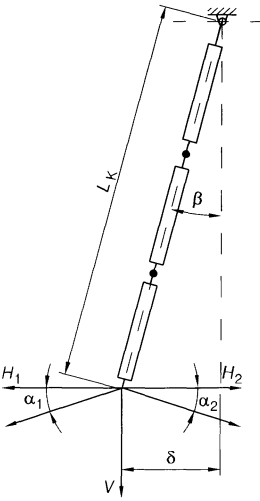

Figure 16.40: Condition of a conductor fixed by a suspension clamp

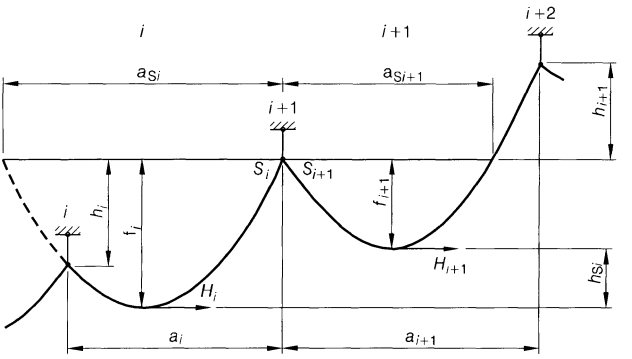

Figure 16.41: Data to determine the conductor state in spans between suspension towers

of conductor tensile forces result thereof. The differences affect a *displacement of the insulator set* in direction of the span with the lower conductor downstrain angle. The difference of horizontal tensile forces of two adjacent spans results from Figure 16.41 and [16.31] to be

$$H_{i+1} - H_i = (f_i - f_{i+1}) \cdot m_C g = h_{Si} \cdot m_C g \quad , \tag{16.14}$$

where h_{Si} is the difference of the height of the sagging line vertices of two adjacent spans. This relation describes the state of equilibrium of the conductor, when the conductors rest on stringing blocks at all suspension sets of the tensioning section. If the horizontal tensile force in the first span is given, then the value in the span i results from

$$H_i = H_1 + m_C g \sum_{j=1}^{i-1} h_{Sj} \quad . \tag{16.15}$$

If the conductors are fixed to a suspension clamp, the equilibrium of moments is complied with around the suspension pivot of the insulator set (Figure 16.40). The behaviour of conductors suspended by clamps within a tensioning section of an overhead line is dealt with in clause 14.8 in detail.

For an exact installation of the conductors, the position of the suspension clamps at each suspension tower of the tensioning section needs to be determined. The exact initial sags have to be calculated as well for the conductors suspended by stringing blocks such that the insulator strings assume a plumb position after clipping-in the suspension clamps.
The swing angle β_{i+1} at the insulator set $i+1$ can be determined from

$$\beta_{i+1} = \arctan\left[(H_{i+1} - H_i) \,/\, (V_{i+1} + G_{\mathrm{K}i+1}/2)\right] \quad , \tag{16.16}$$

where V_{i+1} is the vertical conductor load at the set $i+1$ according to

$$V_{i+1} = H_i \sinh\left(\frac{a_{\mathrm{S}i} \cdot m_{\mathrm{C}}g}{2 \cdot H_i}\right) + H_{i+1} \sinh\left(\frac{a_{\mathrm{S}i+1} \cdot m_{\mathrm{C}}g}{2 \cdot H_{i+1}}\right) \quad . \tag{16.17}$$

The signification of the variables $a_{\mathrm{S}i}$ and $a_{\mathrm{S}i+1}$ can be taken from Figure 16.41. The offset of the conductor suspension point is obtained from

$$\delta_{i+1} = L_{\mathrm{K}i+1} \cdot \sin\beta_{i+1} \quad . \tag{16.18}$$

Due to the offset of the insulator set, the theoretical lengths of the individual spans are modified according to

$$a'_i = a_i + \delta_{i+1} - \delta_i \quad . \tag{16.19}$$

The conductor length can be obtained from (14.14) for conductors on stringing blocks

$$L'_i = \sqrt{h_i^2 + \left(2\,\frac{H'_i}{m_{\mathrm{C}}g}\,\sinh\frac{a'_i \cdot m_{\mathrm{C}}g}{2\,H'_i}\right)^2} \quad . \tag{16.20}$$

The length of the clipped-in conductor in the span i is obtained from

$$L_i = \sqrt{h_i^2 + \left(2\,\frac{H_0}{m_{\mathrm{C}}g}\,\sinh\frac{a_i \cdot m_{\mathrm{C}}g}{2\,H_0}\right)^2} \quad , \tag{16.21}$$

assuming a constant horizontal tensile force H_0 in all spans. The variation of the conductor length in the span i between a suspension of conductors in stringing blocks or clipped-in results from

$$\Delta L_i = L_i - L'_i \quad . \tag{16.22}$$

From (16.22), the offsets can be determined by which the suspension clamps at each insulator set need to be displaced such that the insulator sets will be suspended vertically after installation of the suspension clamps and the horizontal forces and sags in all spans correspond to the required data. The *offset* measured approximately along the conductor at the insulator set of the tower i of a tensioning section with n spans is obtained from

$$v_i = \sum_{j=1}^{i-1} \Delta L_j = \sum_{j=1}^{i-1} (L_j - L'_j) \quad . \tag{16.23}$$

The offsets in a tensioning section are shown in Figure 16.42. In case of a positive sign of the offset v_i, the suspension clamp at tower i has to be installed in a distance v_i measured in direction to tower $i+1$.
The relations (16.20) to (16.23) enable to determine the offset v_i for any given horizontal tensile forces H_i such that the insulator sets will be suspended vertically after clipping-in and the horizontal tensile force is constant and equal to H_0 within the whole tensioning

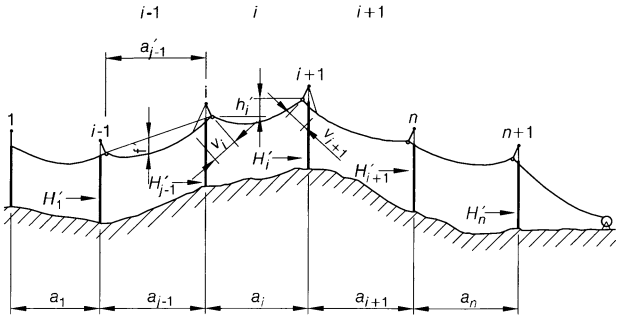

Figure 16.42: Sagging of a tensioning section, conductor resting on stringing blocks

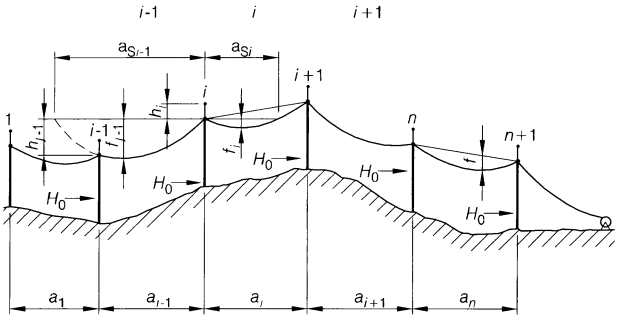

Figure 16.43: Sags and conductor tensile forces in a tensioning section after clipping-in of conductors

section. However, in this case the conductor needs to be readjusted at the strain tower at the end of the tensioning section with n spans by the value

$$v_{n+1} = \sum_{j=1}^{n} \Delta L_j = \sum_{j=1}^{n} (L_j - L'_j) \quad . \tag{16.24}$$

An optimum could be achieved if the conductor tensile stringing forces for the conductor resting in stringing blocks (Figure 16.42) were determined such that the offsets within the tensioning section are mutually compensated after the clipping-in. Then, the offset v_{n+1} at the strain tower will be zero and any readjustment would not be necessary anymore (Figure 16.43). This requirement is complied with, if the sum of conductor catenary lengths is equal for the conductors on stringing blocks and for conductors clipped-in at the suspension clamps.
With the abbreviation

$$L_{0i} = \sqrt{h_i^2 + a_i^2} \tag{16.25}$$

an approximation for the conductor catenary length can be obtained from

$$L_i \approx L_{0i} + \frac{a_i^4 \cdot (m_C g)^2}{24\, L_{0i} \cdot H_i^2} \quad . \tag{16.26}$$

The sum of the conductor catenary lengths in the tensioning section is obtained from the horizontal tensile forces H_i for conductors suspended on stringing blocks from

$$L' = \sum_{i=1}^{n} \left(L'_{0i} + \frac{a_i'^4 \cdot (m_C g)^2}{24\, L'_{0i} \cdot H_i^2} \right) \quad . \tag{16.27}$$

After clipping-in of conductors with the horizontal tensile forces H_0 in all spans from the sum of the catenary lengths will be

$$L = \sum_{i=1}^{n} \left(L_{0i} + \frac{a_i^4 \cdot (m_C g)^2}{24\, L_{0i} \cdot H_0^2} \right) \quad . \tag{16.28}$$

As assumed, the lengths L and L' should be equal. The horizontal tensile forces H_i to be selected in the stringing condition can be obtained from (16.27) and (16.28):

$$\sum_{i=1}^{n} \frac{a_i^4}{L_{0i} \cdot H_i^2} = \frac{1}{H_0^2} \cdot \sum_{i=1}^{n} \frac{a_i^4}{L_{0i}} \quad , \tag{16.29}$$

where $L'_{0i} \approx L_{0i}$ and $a'_i \approx a_i$ was assumed.
Equation (16.29) cannot be solved directly to one of the n horizontal tensile forces H_i. An iteration procedure is recommended where at first a value $H_{1,0}$ for the horizontal tensile force in the first span of a tensioning section is assumed and then the data $H_{i,0}$ within the other spans are calculated by equation (16.15). The equivalent horizontal tensile force $H_{\mathrm{E},k}$ can be computed from (16.29):

$$H_{\mathrm{E},k} = \sqrt{\sum_{i=1}^{n} \frac{a_i^4}{L_{0i}} \Big/ \sum_{i=1}^{n} \frac{1}{L_{0i}} \left(\frac{a_i^2}{H_{i,k}} \right)^2} \quad . \tag{16.30}$$

There, the index k refers to the iteration step. Using the value $H_{\mathrm{E},k}$, the tensile forces $H_{i,k+1}$ used in the following step can be determined according to

$$H_{i,k+1} = H_{i,k} + H_0 - H_{\mathrm{E},k} \quad . \tag{16.31}$$

The iteration process is continued until $H_{\mathrm{E},k}$ corresponds with sufficient accuracy to the target value H_0. A few steps are sufficient to achieve this goal.
The practical calculation needs some effort because of the necessary iterations and the large number of possible adjustment conditions which should take care of the ambient temperature during adjustment and the time schedule of conductor installation activities. Therefore, the calculation is carried out using computer programs.

16.8.5.3 Impact of conductor creep

Conductors for overhead lines, being single-material conductors made of aluminium or aluminium alloy or composite conductors made of aluminium and steel or aluminium alloy and steel, expand non-elastically under a permanent tensile load. This creep process results in a non-reversible elongation of the conductors and steadily increasing sags during overhead line operation. Planning and installation should provide for conductor creep.
A non-reversible elongation of a conductor is caused by consolidation of the conductor structure after the first loading of the stranded conductor. This phenomenon occurs already during stringing of the conductor and continues during operation especially under increased mechanical loads. Then, additional irreversible elongations are caused by metallurgical procedures within the conductor material, which is called *conductor creep*. The conductor tensile stress and the conductor temperature affect essentially the conductor creep. With rising tensile stress and temperature, the speed of creep is increased as well. To provide for the additional sag due to creep, it is necessary to estimate the non-elastic elongation to be expected during the life-cycle of the conductors. A forecast is difficult also in case where measured data for the creep behaviour of a certain conductor are available, since such a forecast would need the variations of tensile forces and temperatures during operation. However, these data are not known in advance.
Numerous measurements were carried out at overhead line conductors to determine their creep behaviour [16.32, 16.33]. An evaluation of these tests with proposals for considering the creep is given in [16.34]. The expected irreversible creep strain can be described by

$$e = e_{1\mathrm{h}} \cdot t^n \quad . \tag{16.32}$$

There, e is the *creep strain*, measured in thousandth; e_{1h} and n are parameters depending on the conductor design, conductor material and conductor cross section, the operation history, the tensile stress and the temperatures; t is the period of time elapsed after the first loading of the conductors in hours. The parameter e_{1h} represents the creep strain one hour after loading the conductor.
To determine the parameters n and e_{1h}, tests need to be carried out for each conductor under sagging conditions and an expected mean temperature. Such tests, however, need a long period of time and are costly because of the long duration and the required accuracy of the measurements. A procedure for *testing the creep behaviour* of conductors is standardized in IEC 61 395 [16.35]. In [16.34], a method and data are given which can be used to forecast the *creep strain* for practical application. The creep strain to be expected after an operation period of 30 years can be obtained from

$$e_{30} = \overline{e}_{30} \cdot k_\sigma \quad . \tag{16.33}$$

The parameter $\overline{e}_{30}$ is the non-elastic strain at everyday stress according to 20 % of the rated tensile strength (RTS) of the conductor. As an approximation, the creep elongation can be assumed as depending linearly on the steel content of the conductor weight

$$\overline{e}_{30} = 1{,}12 - 0{,}97 \cdot w/100 \quad , \tag{16.34}$$

where w is the steel content of the conductor weight, expressed in percent. As an appropriate approximation, the parameter k_σ is assumed to depend linearly on the relative everyday stress $\overline{\sigma}$.

$$k_\sigma = \overline{\sigma}/20 \quad . \tag{16.35}$$

The relative everyday stress is expressed as a percentage of the rated tensile stress.
The relations (16.34) and (16.35) apply for ACSR conductors with $\overline{\sigma} \leq 30$ %, however, they can be used for AACSR conductors as an approximation, too.
The *creep process* of the conductors starts immediately after stringing. Since the creep strain is relatively high immediately after stringing, the period between the stringing and the sagging of the conductor reaching up to several weeks should be considered when determining the sagging data. For this purpose, equation (16.32) can be used. The exponent n is gained from tests [16.35]; for some conductor types, information is given in [16.34]. Where other data are not available, $n = 0{,}25$ can be used as an approximation. The parameter e_{1h} can be obtained from (16.32) with $t = 24 \cdot 365 \cdot 30 = 2{,}628 \cdot 10^5$ h and $\overline{e}_{30}$ according to (16.34). From (16.32), the creep strain at a given time can be calculated then using the mentioned data for e_{1h} and n.
The elongation of conductors due to creep produces the same change of the conductor state as an equivalent temperature variation ΔT_{id}, which can be obtained from

$$\Delta T_{id} = e/\varepsilon_T \quad , \tag{16.36}$$

where e is the creep strain according to (16.32) and ε_T the coefficient of thermal expansion given in 1/K. To provide for creep, the conductor may not be adjusted with data for the ambient temperature during sagging, but with data for a conductor temperature which is lower by the *equivalent temperature difference* ΔT_{id}. Taking into account a constant creep strain and an equivalent temperature difference for all span lengths means, that the reduction of sag is relatively higher, the lower the span length is. The initial stress is, therefore, increased to a higher extent than in long spans, and the resistance of the structures may limit the reduction of sags.

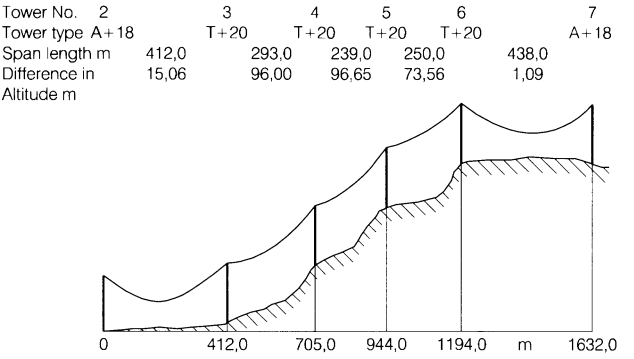

Figure 16.44: Longitudinal profile of a tensioning section in a mountainous area

Table 16.6: 110 kV line: Creep elongation, equivalent temperature difference and conductor offset

Time	12 h	24 h	7 d	14 d	30 d
Creep elongation in thousands	0,441	0,431	0,393	0,376	0,353
Temperature difference in K	23,3	22,8	20,8	19,9	18,7
Offset in cm at					
Tower No. 2	0	0	0	0	0
Tower No. 3	−6	−7	−10	−12	−13
Tower No. 4	−86	−87	−87	−88	−88
Tower No. 5	−96	−96	−97	−98	−98
Tower No. 6	−56	−57	−57	−58	−58
Tower No. 7	2	2	2	2	2

Example: For the conductor 564-AL1/72-ST1A (ACSR 564/72), which is used as a twin bundle for 400 kV lines (see [16.36]), an equivalent temperature difference of 30 K is assumed corresponding to a creep strain of approximately 0,06 % for 30 years. The final everyday stress at 10°C should be 57 N/mm^2. For a span length of 600 m, the reduction of the sag is 1,45 m equal to 5,5 % of the sag, and for 400 m span length it will be 1,30 m or 11,4 % of the sag and, finally, for 200 m span length 0,80 m or 27,5 %, respectively.

16.8.5.4 Example: Sagging data for an overhead line in a mountainous area

The longitudinal profile of an overhead line in a mountainous area is shown in Figure 16.44. Phase conductors 128-AL1/30-ST1A are used and installed with an everyday stress of 50 N/mm^2, reaching 13,7 % of the rated tensile stress of 365 N/mm^2. The conductor mass per unit length is 0,59 kg/m, having a steel content of 0,23 kg/m, reaching 39 % of the conductor mass.

From equation (16.34), the creep strain $\bar{e}_{30}$ is obtained for this condition to be 0,074 % and the parameter k_σ is calculated from (16.35) to be 0,685. The creep strain to be considered is, therefore,

$$e_{30} = 0{,}74 \cdot 0{,}68 = 0{,}051\ \% \quad .$$

The exponent n used in equation (16.32) is assumed to be 0,2 [16.33]. The parameter e_{1h} results from

$$e_{1h} = 0{,}51/(2{,}628 \cdot 10^5)^{0{,}2}\, 0{,}2 = 0{,}00420\ \% \quad .$$

It is assumed, that the conductors are sagged either 12 h, 24 h, 7 d, 14 d or 30 d after stringing. The equivalent temperature differences for which the sag is determined follow from (16.36). For this case, the creep strain expected at the time of adjustment is to be determined from (16.32) with the mentioned parameters n and e_{1h} and then to be substracted from the strain

Table 16.7: Sagging table: Sags in m and conductor tensile stresses in N/mm^2 for sagging, conductors in stringing blocks, 14 days after stringing

		Temperature during sagging °C							
		0	5	10	15	20	25	30	35
Span 1	Sag	16,36	16,64	16,92	17,19	17,47	17,74	18,01	18,27
412,0 m	Tensile stress	50,3	49,5	48,6	47,9	47,1	46,4	45,7	45,0
Span 2	Sag	8,74	8,88	9,02	9,16	9,29	9,43	9,56	9,70
293,0 m	Tensile stress	50,0	49,2	48,4	47,7	47,1	46,4	45,7	45,1
Span 3	Sag	5,70	5,79	5,87	5,96	6,04	6,12	6,20	6,28
239,0 m	Tensile stress	52,3	51,4	50,7	50,0	49,3	48,7	48,1	47,4
Span 4	Sag	5,49	5,57	5,64	5,72	5,79	5,86	5,94	6,01
250,0 m	Tensile stress	57,4	56,6	55,8	55,1	54,4	53,7	53,1	52,4
Span 5	Sag	15,23	15,44	15,65	15,86	16,07	16,27	16,47	16,66
438,0 m	Tensile stress	61,0	60,1	59,4	58,6	57,8	57,1	56,4	55,7

Table 16.8: Sags in m and conductor tensile stresses in N/mm^2 for conductors clipped-in, adjustment 14 days after stringing

	Temperature during adjustment °C							
	0	5	10	15	20	25	30	35
Tensile stress at N/mm^2	54,6	53,7	52,9	52,2	51,4	50,7	50,0	49,3
Sag in m								
Span 1 412,0 m	15,07	15,31	15,54	15,77	16,00	16,22	16,45	16,67
Span 2 293,0 m	8,01	8,13	8,25	8,38	8,50	8,62	8,74	8,85
Span 3 239,0 m	5,46	5,54	5,63	5,71	5,79	5,87	5,95	6,03
Span 4 250,0 m	5,77	5,86	5,95	6,04	6,12	6,21	6,30	6,38
Span 5 438,0 m	17,03	17,29	17,55	17,81	18,07	18,33	18,58	18,83

e_{30} applicable for an operation period of 30 years. For the conductor 128-AL1/30-ST1A, the coefficient of thermal expansion is $18{,}9 \cdot 10^{-6}$1/K.

The results of the calculation explained above are shown in Tables 16.6, 16.7 and 16.8 together with the data necessary for sagging. Table 16.7 is designated also as *sagging table*. The offset at the tower No. 5 reaches approximately one meter in this case. For other examples, especially in case of long tensioning sections, offsets reaching several meters are possible. As verified by many practical examples, conductor sagging using the described procedure leads to the designed final sags also in extreme cases. Comparison of Tables 16.7 and 16.8 allows to recognize the essential difference between the sags and conductor tensile stresses for conductors suspended in stringing blocks compared with conductors clipped-in in suspension clamps.

16.9 References

16.1 VBG 37: Bauarbeiten, Unfallverhütungsvorschrift (Construction works, safety regulations). Cologne, Berufsgenossenschaft der Feinmechanik und Elektrotechnik, 1977

16.2 IEC 61 773: Overhead lines: Testing of foundations for structures. Geneva, IEC, 1996

16.3 EN 50 341-3-4: Overhead electrical lines exceeding 45 kV. Part 3-4: National Normative Aspects (NNA) for Germany. Brussels, CENELEC, 2002

16.4 ENV 206: Concrete; attributes, production, implementation and quality evidence. Brussels, CEN, 1990

16.5 ENV 197: Concrete; composition, requirements and parameter of conformity. Brussels, CEN, 1992

16.6 DIN 1164-1: Cement; Part 1: Composition, requirements. Berlin, DIN, 1994

16.7 Betonkalender (Annual concrete report 1996), Part 1. Berlin, Ernst & Sohn

16.8 DIN 4226-1: Aggregates for concrete, aggregates with dense structures, definitions, characteristics and requirements. Berlin, DIN, 1983

16.9 DIN 1045: Reinforced concrete structures; design and constructions. Berlin, DIN, 1988

16.10 DIN 4226-3: Aggregates for concrete, aggregates with dense and porous structures. Berlin, DIN, 1983

16.11 ISO 2736: Test of concrete; preparation of test cubes, specimens taken from fresh concrete. Geneva, ISO, 1986

16.12 ISO 4013: Concrete; classification of consistence. Geneva, ISO, 1979

16.13 ISO 9812: Fresh concrete: Determining of consistence, spreading index. Geneva, ISO 1979

16.14 ISO 1411: Fresh concrete: Determining of consistence, compression test. Geneva, ISO 1979

16.15 ISO 4109: Fresh concrete: Determining of consistence, slump test. Geneva, ISO, 1991

16.16 ISO 4110: Fresh concrete: Determining of consistence; "Vebe" test. Geneva, ISO, 1991

16.17 ISO 4012: Concrete; determining of compression strength at test cubes. Geneva, ISO, 1978

16.18 DIN 1048-1: Testing concrete; testing of fresh concrete. Berlin, DIN, 1991

16.19 Schneider, K.-J.: Bautabellen für Ingenieure (Construction tables for engineers). Düsseldorf, Werner-Verlag, 13th edition 1998

16.20 Gardes, J.-L. et al.: EDF's approach to the design and constrution of foundations for the transmission network overhead lines. Cigré Report 22-104, 1994

16.21 Studiengesellschaft Stahlanwendung e.V. Stahlmaste in Vollwandbauweise (Solid wall steel towers): Project No. 152. Universität-Gesamthochschule Essen, Department Civil Engineering, 1992

16.22 Gohm, H.; Kießling, F.; Mahr, V.: Verformung von Stahlvollwandmasten mit Steckstößen beim Einsatz in Hochspannungsfreileitungen (Deformation of solid-wall steel poles with slip joint used for transmission lines). Elektrizitätswirtschaft 97 (1998)23, pp. 27 to 31

16.23 Raymond, W.; Schnakenberg, D.: Errichtung 227 m hoher Stahlgittermaste für eine Freileitungs-Flusskreuzung (Erection of 227 m high steel towers for a 380 kV transmission line river crossing). Elektrizitätswirtschaft 78 (1979), pp. 255 to 261

16.24 Fuchs, A.; Schramm, H.: 500 kV overhead transmission line across Suez Canal. Erlangen, Siemens AG PTD H2, 1999

16.25 Schramm, H. et al.: Freileitung der Superlative verbindet Europa und Asien. 420-kV/800-kV-Bosporuskreuzung III (Superlative transmission line connects Europe with Asia, 420 kV/800 kV Bosphorus Crossing III). Elektrizitätswirtschaft 99 (2000), pp. 13 to 19

16.26 IEC TS 61 328: Live working – Minimum requirements for the utilization of tools, devices and equipment. Geneva, IEC, 2000

16.27 DIN 48 207-1: Overhead lines with nominal voltage exceeding 1 kV: Methods and equipment for the installation of conductors. Part 1: Installation of conductors. Frankfurt, DKE, Draft 1999

16.28 DIN 48 207-2: Overhead lines with nominal voltage exceeding 1 kV: Methods and equipment for the installation of conductors. Part 2: Pulling grips, steel made. Frankurt, DKE, Draft 2000

16.29 DIN 48 207-3: Overhead lines with nominal voltage above 1 kV: Methods and equipment for the installation of conductors. Part 3: Swivel joints. Frankfurt, DKE, Draft 2000

16.30 Raymond, W.: Replacing conductors of high-voltage transmission lines. Siemens Power Technology 2 (1980), pp. 35 to 42

16.31 Kießling, F.: Die Verlegung der Leiter einer Hochspannungs-Freileitung (Installation of conductors for a high-voltage transmission line). Elektrizitätswirtschaft 78 (1979), pp. 712 to 719

16.32 Helms, R.; Ziebs, J.: Stand der Untersuchungen an Al/St-Freileitungsseilen mit unterschiedlichen Querschnittsverhältnissen (Status of actual investigation for ACSR conductors with different cross-sectional portions). Berlin, Bundesanstalt für Materialprüfung, Report 1967

16.33 Brandt, E.; Thomas, R.: Der Einfluss der bleibenden Seildehnung auf das Durchhangsverhalten von Freileitungen (The influence of permanent creep on sags of overhead lines). Elektrizitätswirtschaft 78 (1979), pp. 262 to 268

16.34 Cigré SC22 WG22-05: A practical method of conductor creep determination. Electra 24 (1974), pp. 105 to 137

16.35 IEC 61 395: Overhead electrical conductors. Creep test procedure for stranded conductors. Geneva, IEC, 1998

16.36 Flug, R.; Schnakenberg, D.: Überlegungen bei der Projektierung einer neuen 380-kV-Freileitung (Considerations on designing a new 380 kV transmission line). Elektrizitätswirtschaft 70 (1971), pp. 606 to 610

17 Commissioning, operation and line management

17.0 Symbols

Symbols	Signification
C_i	Annual expenditures
$E_{\mathrm{d}i}$	Deterministic costs in year i, planned expenditures
E_{f}	Costs of failure consequences
$E_{\mathrm{p}i}$	Probabilistic costs in year i, risk of failure
FEU	Forced energy unavailability
EA	Energy availability
FOR	Forced outage rate
GRC	Galloping readiness coefficient
i	Index to designated year i
$I_{\mathrm{AB}}, I_{\mathrm{AC}}, I_{\mathrm{BC}},$	Current
I_{W}	Wind gust intensity
MTBF	Mean time between failure
MTTR	Mean time to repair
n	Length of period, number of elements
NPV	Net present value
p	Probability of failure of an element
P_{f}	Probability of failure
$P_{\mathrm{f\,el}}$	Probability of electric failure
$P_{\mathrm{f\,m}}$	Probability of mechanical failure
$P_{\mathrm{f}n}$	Probability of failure in n years
$P_{x,n}$	Probability of occurrence of an event
POF	Probability of failure
P_{S}	Probability of survival
r	Discount rate
R_{A}, R_{B}, R_{C}, $R_{\mathrm{AB}}, R_{\mathrm{AC}}, R_{\mathrm{BC}}$	Resistance
R'_{A}, R'_{B}, R'_{C}, R'_{T}	Resistance per unit length measured at temperature T
R'_{20}	Resistance per unit length at 20°C
SEU	Scheduled energy unavailability
T	Temperature
T_{air}	Air temperature
T_{mean}	Mean conductor temperature
T_{D}	Dew point temperature
$T_{\mathrm{S}}, T_{\mathrm{M}}, T_{\mathrm{E}}$	Temperature measured at the beginning, middle and end of a line
T_{R}	Return period of ultimate loads
$V_{\mathrm{AB}}, V_{\mathrm{AC}}, V_{\mathrm{BC}}$	Voltage
V_{W}	Wind velocity
x	Elements of a line
α	Temperature coefficient of resistivity
δ	Angle between line and wind direction

17.1 Commissioning

17.1.1 Introduction

The high investment necessary for a new high-voltage overhead line justifies a continuous check and supervision of all planning and approval steps and of design, manufacturing and construction activities. To assure that the whole line, its components and elements will comply with the specifications and fulfil the required performance, tests

are carried out, here named as *commissioning*. In particular, a stringent *supervision of the schedule* for all steps of approval, the necessary expert studies included, is important because the begin of the construction activities depends on the approval and supply of material, so it needs to be planned and controlled just in time.
The complete procedure of a continuous supervision of approval, design, manufacturing and construction can be split in three stages, namely:

- Supervision of approval, design and manufacturing, before starting construction;
- *Supervision of construction* activities;
- *Final inspection* and *commissioning.*

After completion, each stage is subject to *acceptance procedures* corresponding to the respective activities carried out for its completion, as specified in the individual contract. Supervision can be carried out by the line owner's engineering staff or by consulting companies.

17.1.2 Supervision of approval, design and manufacturing stage

Before starting construction, the following subjects can be defined, which need a continuous supervision:

- Approval procedures, contracts with land owners;
- Environmental studies;
- Selection of conductors, aerial cables with optical fibres, earth wires, insulator sets, fittings and hardware;
- Studies on vibration damping;
- Tower outline, especially in view of required clearances, and tower analysis;
- Design of earthing system;
- Line design and survey, *tower spotting*, analysis of external clearances, especially in crossings, *longitudinal profiles* and layouts;
- *Checking of soil investigation* and probing results;
- *Selection of foundation design* with respect to feasibility and economic viability;
- *Supervision of production* of components by checks, sample tests or acceptance tests at the manufacturer's premises. Since the contractor is usually responsible for supply of material according to the contract, he uses to supervise the manufacturing and, in particular, type and acceptance tests. Line owners, however, use to supervise production of some main items like foundations and towers by on-site inspection especially in case of long lines. The line owner should reserve himself the right to carry out or observe acceptance tests.

The extent to which the individual steps need to be recorded or approved and released in detail by the line owner may be different for individual projects and should be agreed upon when placing the contract. The responsibility for design and construction activities belongs to the line designer and to the contractor, who should deliver to the line owner complete sets of documents that constitute the line design and construction planning.
When time-consuming supervision cannot or should not be carried out by the line owner's staff, it is recommended to engage line experts from consulting companies independent of the designing and construction companies. For approval procedures, the help of experienced lawyers might be necessary and advantageous.
After *supervision of design*, the line owner or its representative releases the design for manufacturing and construction. For all prototype, *sample* and *routine tests*, reports need to be issued by the manufacturer and confirmed by the line owner or contractor. The line owner or his representative will check these reports and finally approve the material for construction, so far the relevant standards and specifications have been fulfilled.

The tests to be carried out are detailed in the relevant chapters 7 to 13 of this book. All the materials composing the design should be clearly specified according to aspects of design, manufacturing, inspection and testing. Also maintenance procedures for live-line or dead-line works need to be specified.
The *quality control* applicable during manufacturing of components needs to comply with the relevant standards. All materials and elements are subjected to an appropriate quality control during the fabrication. Certified reports of *type tests* of the main line components are usually supplied by the manufacturer.

17.1.3 Supervision and acceptance of construction

During construction stage, it is important that despite the contractor's responsibilities, the line owner or his representative takes care of supervising the individual *construction* activities and steps, since modifications and corrections would be not always possible after completion of construction.

- **Information of municipalities, local residents, land owners and tenants.** The start of survey and construction activities needs to be openly announced to the public by the municipalities. However, a direct approach to the farmers and real estate owners involved has proved as advantageous. So, problems concerning access roads, damage of crops, fences or cattle can be solved by mutual understanding.
- **Obeying special conditions imposed with the approval.** Some contractors may attempt to circumvent unpleasant conditions made by authorities and excuse themselves as being not informed. Since the line owner constructing a line will be held responsible for any violation and be liable for any damage, preventive *supervisory checks* should be carried out on a scheduled basis.
- **Line route, *tower spotting* and *right-of-way clearing.*** After completion of the *right-of-way clearing*, a partial inspection should be carried out by the line owner's representative and the contractor. The basic criteria used for defining the route and right-of-way clearing will be reviewed and its achievement checked. If any, corrective measures are agreed upon.
- **Avoiding *environmental infringements.*** As in case of violation of any other conditions, an immediate removal of disturbances in close cooperation with the environmental authorities is indispensable. The tough construction work on site cannot be used as an excuse. However, many contractors attempt to contribute to environmental protection, for example by replacing the hydraulic oil in construction machinery by decomposable raps oil.
- ***Inspection of access roads* and their maintenance.** Especially during construction of overhead lines with extra-high voltages, access roads not prepared for heavy load traffic are often greatly affected. Therefore, it became usual for such projects to record the condition of the access roads together with the owner before the construction starts to avoid arguments later on. Especially under adverse weather conditions, a permanent supervision is recommended to decide in due time on measures such as filling up extra material to avoid extended damage.
- ***Installation of foundations.*** Already before starting of excavation activities, the pegging should be checked again to avoid misplacing of supports. The items to be checked from the engineering point of view are discussed in detail in chapters 13 and 16 and depend also on the type of the foundation to be installed. In particular, surplus excavation material needs to be recycled. As well, residual concrete may in no case be deposited in the close vicinity without permission. During installation of foundations, checks should be carried out comprising dimensions, backfill and recomposition of the terrain near the foundations.

- ***Assembly and erection of towers.*** Although checking of all individual parts with respect to damage and completeness is within the responsibility of the construction company, a short-coming of jointing material might be realized at the start of erection, which cannot be compensated from the material in the linemen's hand. Therefore, it can be in the line owner's interest to check the completeness of supports before erection starts. After completion of the erection activities, the vicinity of a tower site should be searched in view of lost bolts, nuts and other small parts which could otherwise damage agricultural machines to be indemnified by the line owner. In case of lines with poles, an in-time check of the correct *inclination of angle supports* has proved to be expedient.
- ***Supervision of conductor stringing.*** Also before starting the conductor stringing, the protection scaffolds, protecting nets included, should be checked with respect to an acceptable and proper installation. During stringing, it should be continuously checked that the conductors do not touch the ground or obstacles. All the fittings for aerial cables with optical fibres should be visually inspected again before installation. It is the task of the contractor to care for a perfect condition of the stringing blocks, pullers and tensioners as well as earthing when stringing conductors in the vicinity of live circuits. After completion of stringing activities, important *clearances to crossed objects* should be checked against the designed data. After conductor and shield wire stringing, the contractor should prepare tables with sag measurements in the regulating spans, tables with conductor-to-ground clearances in the critical points of the spans and tables with measurements of clearances at strain structures.
  In some cases, *recycling of packing material* and wooden pallets of insulators may create problems. However, it is not anymore permitted to fire such materials on site. With regard to live stock, any wire ends and strips must be thoroughly collected and removed from the construction site.
- **Checking of individual elements.** The line owner should check randomly the *connection of earthing*, the *installation of jumper loops*, dampers, spacers etc. Repairing of spacers which have failed due to defective installation is extraordinary time-consuming and expensive. The efficiency of earthing systems is commonly verified by *earthing and interference measurements* carried out shortly before energizing. In some cases, it might be expedient to check the earthing resistance before stringing the earth wires.
- **Calibration of telecommunication installations.** This activity can only be carried out by specially trained people after installation of splices and joints of optical fibres used on most lines.
- ***Clearing* along the line route.** It should be self-understanding that the line route is cleared after completion of construction. However, because of the enhanced sensitivity of the residents, this task needs to be carried out thoroughly and checked by the line owner. The removal of any material residuals should be scrutinized especially.
- ***Recording of damage to crops.*** It is common practice to record any damage continuously during construction to be able to locate and assess the damage as precise as possible. Damage to forests and to access roads needs again to be recorded after completion of the construction activities together with the land owners or authorities.
- ***Coating of structures.*** Coating of structures is carried out often directly after completion of construction preferably during the spring or summer season in the northern hemisphere or, in the southern hemisphere countries, in dry periods of the year, because of the favourable weather conditions. Due to the necessary de-energizing, barring and obeying of environmental correctness, coating activities

need a comprehensive permanent supervision even more intensive than during construction period itself. The line owner is responsible for violations of any standards. Stringent values for conductance apply to coating activities close to live circuits or in case of parallel lines due to the hazard of electric interference [17.1].

As agreed upon by the contract, the performed activities or checks have to be recorded in an *acceptance certificate*, which will be signed by the line owner and the contractor. Any open residual works or short-comings have to be settled according to the stipulated schedule; their completion needs to be supervised.

17.1.4 Final inspection and acceptance

As a rule, a *final inspection* is carried out after completion of all construction activities, at least with more extended projects. The line owner determines the people who participate in this inspection. Thereby, each line section is visited and all open items recorded during the construction supervision are checked and their grade of completion is recorded. An *acceptance record* is established and signed by the people participating in the inspection. The record should list all recognized short-comings and the necessary activities as well as the time for completion.

The following check list can be used for the final inspection:

Right-of-way

- Clearing and, if necessary, protection around the structures and guy wires;
- Removal of trees inside and outside the right-of-way, if they put the line security under an increased risk;
- Removal of cut vegetation to damps or recycling facilities.

Access roads

- Checking general conditions;
- Checking conservation conditions of roads, canalisation pipes, drainage etc.;
- Decisions on improvements, such as terrain cuts, protections etc. to restore the previous condition.

Terrain and foundations

- Earth embankments on the tower foundations;
- Terrain conditions that may put a risk to tower stability, such as deviation or channelling of rain waters;
- Protection of the tower legs against collision of vehicles, if necessary;
- Damage to local vegetation;
- Rebuild of terrain near the foundations.

Earthing system

- Compaction and depth of earthing rods or strips;
- Connections of earthing conductors or counterpoises;
- Check of records with foundation resistance measurements;
- Earthing of fences or other objects.

Structures

- Verticality, torsion, deflection angle and alignment;
- Completeness of members, bolts, step-bolts, washers, nuts and lock-nuts;
- Existence of damaged pieces; quality coatings;
- Tightening, position, locking and coating of the bolts;
- Numbering of the structures, arrangement of warning plates;
- Anti-climbing devices, if necessary.

Insulation, hardware and accessories

- Insulator string verticality, number of insulators, position and eventual lack of locking devices;
- Conditions of cleanness, cracks, splits and bubbles in the insulators;

- General checks of the hardware concerning bolt tightening, position, locking devices, counterweights etc.;
- Number and position of spacers and dampers;
- Installation of the armor rods, repair sleeves, arcing horns, corona rings etc.;
- Use of double and multiple insulator sets and jumper strings as per design.

Conductors and earth wires

- *Clearances conductor-to-ground* or conductor-to-obstacles at crossings, checking of the clearances with insulated rods or electronic means should be carried out at critical points;
- Minimum clearances conductor-to-earthed parts of the structures, conductor condition, broken strands, abrasion, twists, checking the clearances of parallel phases in one span;
- *Aerial warning spheres* or lights;
- Layout and arrangement of the conductor jumpers at strain towers.

17.1.5 Quality assurance

It is standard practice to apply *quality assurance* principles as required for example by EN 50 341-1 [17.2]. During design, manufacture and construction, the quality assurance should conform to the relevant requirements of ISO 9002 [17.3] and ISO 9003 [17.4] as appropriate.

The systems and procedures, which the designer and/or installation contractor will use to ensure that the project works comply with the project requirements, should be defined in the designer's and/or installation contractor's quality assurance plan for the project works. Each *quality assurance plan* should set out activities in a logical sequence and should take into account the following:

- An outline of the proposed work and program sequence;
- The structure of the organisation for the contract, both at the head office and at any other centres responsible for parts of the work;
- The duties and responsibilities assigned to staff ensuring quality of the work;
- Hold and notification points;
- Submission of engineering documents required by the project specification;
- The inspection of materials and components on receipt;
- Reference to the quality assurance procedures appropriate to each activity;
- Inspection during manufacture and construction;
- Final inspection and testing.

The quality assurance plan is part of the execution plan of a project or a project phase.

17.1.6 Performance tests

17.1.6.1 Measurements of tower earthing resistance

The *tower earthing resistance* should be measured by the construction crew before the earth wire stringing. There are several methods for measuring the ground resistance, but it is recommended to use the three-point method *(Wenner Method)*, which is the most usual one [17.5]. The high-frequency device (see [5.12]) can be used to check the earthing resistance with the earth wires connected to the tower. In case of commissioning tests, it can be decided to accept measurements carried out by construction crews or to execute additional measurements at specially selected or critical points.

17.1.6.2 Power losses and electrical resistance of conductors

Some line owners require the verification of the *power losses* as to ascertain that they are under control or warranty by the line contractor. However, direct measurement of

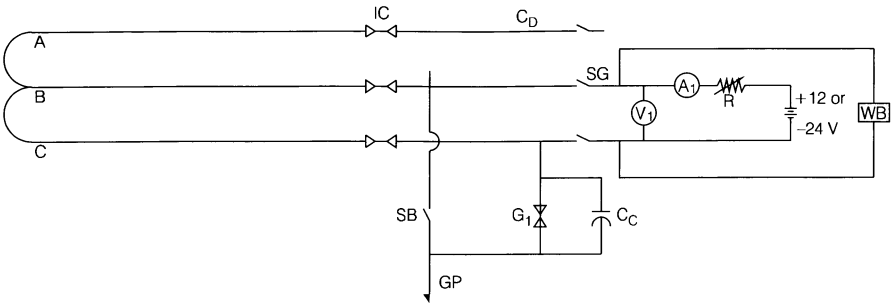

Figure 17.1: Simplified diagram for measuring of conductor resistance. A, B, C phase conductors; IC connection between measuring kit and conductors; C_C capacitor $\simeq 30\mu$ F/250 V, AC; SG general disconnecting switches AC 250 V, 60 A; R variable resistance (Rheostat); C_D insulated downcable Cu ~35 mm^2; WB Wheatstone Bridge as alternative device for checking purpose; V_1 moving coil voltmeter – 0 to 30 V scale, accuracy class 0,5 %; A_1 moving coil ampere-meter – accuracy class 0,5 %; GP Safety earthing point (grounding), G_1 sparking device (car sparking plug type); SB safety switch

power losses is usually not carried out due to the unfeasibility of installing accurate instrumentation in the field and the low precision of transducers to be installed at the sending and receiving ends of the line sections. The percent losses are practically of the same order as the accuracy of potential transformers, current transformers and measuring instruments.

In view of the unfeasibility of carrying out measurement of the power losses, it is sometimes agreed to execute *measurements of conductor resistance*, as the losses are directly proportional to the conductor resistance.

The measurements can be carried out in a complete line section, and the voltmeter-ampere-meter method is recommended with DC voltage. Viability of this measurement should be examined under the viewpoint of safety for the workers and security for the measuring equipment. In Figure 17.1, a single line diagram of a measuring arrangement is shown as employed in a practical example.

The measurement of the conductor resistance is performed in pairs of phases A–B, B–C and C–A, short-circuiting the conductor phases in one of the terminals, and measuring each set of two phases at each time. The resistance for these pairs of phases is obtained from

$$R_{AB} = R_A + R_B = V_{AB}/I_{AB} \quad , \tag{17.1}$$

$$R_{BC} = R_B + R_C = V_{BC}/I_{BC} \quad , \tag{17.2}$$

$$R_{AC} = R_A + R_C = V_{AC}/I_{AC} \quad , \tag{17.3}$$

where V_{AB}, V_{BC} and V_{AC} are the recorded voltages and I_{AB}, I_{BC} and I_{Ac} the corresponding currents. By solving equations (17.1), (17.2) and (17.3), the resistance of phases A, B and C are obtained.

$$R_A = (R_{AB} + R_{AC} - R_{BC})/2 \quad , \tag{17.4}$$

$$R_B = (R_{AB} + R_{BC} - R_{AC})/2 \quad , \tag{17.5}$$

$$R_C = (R_{AC} + R_{BC} - R_{AB})/2 \quad . \tag{17.6}$$

The approximate average temperature along the line is determined as

$$T_{mean} = (T_S + T_M + T_E)/3 \quad , \tag{17.7}$$

where T_S, T_M and T_E are measured at the beginning, at the middle and at the end of the line and T_{mean} is the average value. Then, the conductor unit resistance is calculated as a function of the measured values of the resistance divided by the conductor lengths, in km, and of the temperatures:

$$R'_{20} = R'_T/(1 + \alpha(T_{mean} - 20)) \quad , \tag{17.8}$$

where R'_T is the resistance per unit length at the measured average temperature T_{mean} and α the temperature coefficient of resistivity; for an ACSR conductor, α is equal to 0,00403 K^{-1} and R'_{20} is the conductor resistance per unit length at the reference temperature of 20°C.

Finally, the unit resistance values in Ω/km are determined and compared with the manufacturer's base or guaranteed values. For taking into account measurement errors of resistance and temperatures, a tolerance of around 5 to 10 % is usually accepted.

The induced voltages and currents, caused by parallel lines, should be estimated or preferably measured for reasons of personnel safety and equipment security. As a function of the obtained values, longer or shorter line sections should be selected for every measurement.

Example: The ohmic resistance of a 73,2 km long 220 kV line was measured with an arrangement as shown in Figure 17.1. The values obtained for each pair of phase conductors and the resulting calculations of the unit values are indicated below. The average temperature along the line was determined as $T_{mean} = 32{,}9°C$.

$R_{AB} = V_{AB}/I = 23,7/2,8 = 8,464\,\Omega$; $R_{BC} = 23,4/2,79 = 8,387\,\Omega$; $R_{AC} = 23,5/2,75 = 8,545\,\Omega$.

From equations (17.4) to (17.6) it results

$R_A = (8,464 + 8,545 - 8,387)/2 = 4,311\,\Omega$; $R_B = (8,464 + 8,387 - 8,545)/2 = 4,153\,\Omega$; $R_C = (8,545 + 8,387 - 8,464)/2 = 4,234\,\Omega$.

For calculating the resistance per unit length in Ω/km, it suffices to divide the total values by the conductor length. Assuming the catenary length is 2 % longer than the line length, the conductor length is $1,02 \cdot 73,2 = 74,66$ km.

So, the resulting unit resistance at the temperature $T_2 = 32,9°C$ will be:

$R'_A = 4,311/74,66 = 0,0577\ \Omega$/km; $R'_B = 4,153/74,66 = 0,0556\ \Omega$/km and $R'_C = 4,234/74,66 = 0,0567\ \Omega$/km.

Correction of the resistance to the reference temperature 20°C using equation (17.8) yields

$R'_{20\,A} = 0,0577/\,(1 + 0,00403(32,9 - 20)) = 0,0548\,\Omega$/km; $R'_{20\,B} = 0,0566/1,052 = 0,0528\,\Omega$/km; $R'_{20\,C} = 0,0567/1,052 = 0,0539\,\Omega$/km.

The nominal value supplied by the manufacturer was 0,0545 Ω/km and the maximum tolerance admitted was 5 %. So the measurement proved that the values were quite satisfactory and were, therefore, approved by the line owner.

17.1.6.3 Line energization test

After finalizing the construction of more important lines, especially relatively long EHV lines, it is sometimes required to carry out *line energization tests* as part of the commissioning tests. Therefore, they should be approved by the line owner or by the utility in whose system the line will be inserted.

The main purposes of such tests could be mentioned as:

- Detection of eventual *construction irregularities*, for instance insulation flaws, loose earth connections, like provisional earthing schemes not removed after stringing;
- Direct measurement of voltage elevation at the line end (Ferranti effect), measurement of switching overvoltages caused by energization;

- Application of rated voltage to the line for detection of corona effects on conductors and/or fittings;
- Measuring electrical and magnetic fields.

An example of energization test on a 400 km long 220 kV line is shown in [17.6].
For carrying out a line energization test in case of an interconnected system, it is necessary to study carefully the conditions of the system where the line will be inserted. A closing scheme should be prepared, aimed at avoiding any instability to the electric system during the test. It is especially important to define the reactive power requirements. The same is valid even for radial lines, where overvoltages by the Ferranti effect may occur. Reactors installed in the line by system reasons should be switched on during the test to prevent too high overvoltages.

17.1.6.4 Electrical and magnetic fields (EMF)

The *measurement of electrical and magnetic fields* has become a requirement in some projects. The key point is the growing concern of the public and communities on electrical and magnetic fields and their effects on the health and welfare of persons and animals. Because of that, the fulfilment of precaution values established for such fields has to be verified through adequate measurements at the commissioning stage. Electrical and magnetic fields are usually measured before line energization for commercial operation. The best time for their execution is during the line energization test as to clause 17.1.6.3.
Using instruments available on special market, measurements of electrical and magnetic fields are carried out across the right-of-way of a line to survey the profile of the fields. The results are greatly affected by the local conditions, such as topography, distortion by buildings, trees etc. since the fields are three-dimensional parameters. An accurate control of the voltages, current and phase shift angles at each phase during the measurements is important in order to make possible a coherent set of comparable values as compared with the calculated values. A previous coordination with the dispatch centre is required for keeping all the system conditions under control. After having the measurements in several points, it is possible to establish representative graphs of both electrical and magnetic fields.
Studies carried out by utilities [17.7, 17.8] revealed wide-spread effects of transmission line geometry, topography and other shielding influences greatly distorting the fields. However, investigations performed in areas not influenced by such irregularities demonstrated satisfying coherence with calculated values.

17.1.6.5 Vibration performance measurements

Vibration measurements, when made, are usually carried out after line energization for commercial operation in order not to impose major delays in the line operation. In view of that line owner and contractor should come to an agreement as far as warranty is concerned. Performing vibration measurements by the line contractor before the line is commissioned is hardly possible because of the relatively long period necessary to carry out vibration measurements which can be evaluated. However, it seems appropriate to carry out such tests lasting generally several weeks, whereby the vibrations are monitored in special points, supposedly more prone to the occurrence of vibrations after line energizing.

Aeolian vibrations

Aeolian vibrations are measured through vibration sensors installed 89 mm apart from the conductor clamp, according to Cigré [17.9] or IEEE recommendations [17.10]. Clause 11.2.8 contains details on measurements. The selected spans of a line for performing aeolian vibration measurements should be preferably located where there is a

higher probability of occurrence of laminar winds in the range of 2 to 10 m/s, as the aeolian vibration phenomenon is created predominantly in this range of wind speeds. Using the results of the measurements, the *conductor* and earth wire *lifetime* can be assessed using the method reported in [17.11] (see clause 11.2.9). The wind velocity is recorded by mechanical or ultrasonic anemometers.

Subspan oscillations

For the measurement of *subspan oscillations*, spans should be selected where high wind speeds occur, say winds higher than 10 m/s. Such measurement is performed using special vibration sensors or the same type as employed for aeolian vibration measurement. For this case, the sensible axes of the transducers should be installed in horizontal direction so as to detect horizontal oscillations of the subconductors.

17.1.7 Energization and commence of operation

After all *commissioning tests* have been performed, it is sometimes required to carry out corrections of any problems that may have been detected. In such cases, the line and/or the associated electric system usually needs to stay out of operation until all pending items have been solved. The line is finally released for *commercial operation* and is then energized and integrated with the meshed electric system to which it will belong or, in case of radial supply, it is connected with the load for which it has been built.

17.2 Operation

17.2.1 Real-time monitoring of conductor ampacity

17.2.1.1 Targets and benefits

Papers [17.12] and [17.13] provide an overview on targets, benefits and methods of *real-time monitoring of conductor conditions* and *conductor ampacities* having become a worthwhile tool for operation of transmission lines during the last decade.

The *thermal rating* of an overhead transmission line is the maximum current that a circuit can carry without exceeding the design temperature. The sag design temperature is that temperature at which the legislated height of the phase conductor above ground or obstacles is met. The thermal rating of conductors is dealt with in clause 7.2.3.

An overhead line is inherently exposed to many factors such as wind velocity and direction, intensity of solar radiation, ambient air temperature or terrain conditions, which are changing along the line. Therefore, the position of the conductor in space, i. e. the sag, is continuously changing affecting the vertical safety clearance and, subsequently, the thermal rating of the line. The variability of the parameters affecting the thermal rating is difficult to predict. This has resulted in some conservative assumptions being made in order to always ensure public safety.

The main purpose of real-time line monitoring is to assist system operators in a better *utilization of the load current capacity* of overhead lines, ensuring that the regulatory clearances above ground are always met. Real-time monitoring of relevant parameters enables the conductor position above ground or obstacles to be determined in real time or to be forecast. With real-time systems, the line is not operated at temperatures higher than designed but running at its design temperature for a longer period of time. As the line is running closer to the thermal limit, the losses will increase. Therefore, continuous running of a line close to its ampacity limit cannot be recommended.

Real-time monitoring to accurately determine the current thermal capacity of a line is often used when strengthening of a system is envisaged due to the projected load exceeding the existing thermal limit or in emergency situations with other transmission

lines out of service. In this case, it is recommended that a probabilistic approach should be used to determine the thermal rating using actual recorded weather data [17.14]. It has been found that the increase in thermal rating of lines based on real-time systems is up to 35 % [17.15] with an average of 15 %.

The *monitoring methods* can be divided into two categories, namely direct measuring the conductor temperature or tension and indirect methods using the ambient conditions and line current to calculate the conductor temperature.

17.2.1.2 Direct methods

Direct methods include clamp-on devices to measure the temperature of the conductor as well as methods to measure the conductor tensile force. *Direct temperature measurements* are performed generally by clamp-on thermal couples that transmit the temperature via radio communication to a central station [17.16, 17.17]. The recorded temperature is then compared to the design temperature and the readings can be used for thermal limit determination.

The sensors are usually located at one or a few positions only. However, the temperature varies along the span as well as between spans. To make a judgement on a few readings only can be risky since the temperature of the conductor can vary from span to span due to different wind velocities or angles of wind attack, especially if the line direction or terrain changes. Therefore, conductor temperatures should be determined in several spans and line sections allowing determination of average temperatures. Nevertheless, the temperature measured is the conductor surface temperature and not the average conductor temperature that affects sag. The conversion from the conductor surface temperature to a sag dimension is still required in order to determine the position of the conductor in real time. The accuracy of the thermal rating will depend on how precisely the relationship between temperature and sags can be established [17.13].

A load cell in the strain assembly can be used to measure the conductor tensile force [17.18]. The tension measurements can be transmitted to a station by cable or radio. The load cell is always at ground potential. Since the tensile force of a conductor in a given section of a line depends on the conductor temperature, the tension data provide information on conductor temperature.

Tension monitoring systems can be mounted on selected dead-end structures along a transmission line. The system described in [17.18] can also record the ambient and net radiation temperature (solar temperature). The *net radiation temperature* is used to determine tension-based line ratings by linking the conductor temperature with measured tensile force. The short-term current rating can be determined by knowing the difference between the present and the design temperature of the line. The rating is that current which will result in the design temperature being reached in a given period of time, e. g. within 30 minutes.

Tension monitors are solar-powered. Either cellular phone technology or the utilities telecommunication systems can be used in retrieving and sending information to the control centre. The measured tensile force is the most appropriate parameter for determining the wanted sag. Less adaptation of the readings is, therefore, required to obtain the position of the conductor. The tensile force along the tensioning section is almost constant and, therefore, takes into account the changing conditions along this section. It reflects the averaging effect of all environmental conditions including the effect of wind along this section on the conductor tensile force.

To determine the *thermal conductor rating*, a link between the net radiation solar temperature [17.19] and the sag needs to be established. This requires the characteristics of a line with tension and solar temperature measurements being taken. The sag-temperature relationship is then established.

Only lines equipped with the system can be monitored by direct methods. The thermal rating of other lines in the area cannot be determined. Direct methods for thermal rating are used by more than 50 utilities [17.13, 17.20, 17.21].
The Power Donut System installed by the Brazilian utility CEMIG is an example for real-time monitoring. It consists of:

- Conductor temperature sensors, which monitor the operating temperature through a contact thermometer installed at the line conductor while another sensor measures the current. Power sources are extracted from the monitored line. The sensors transmit the recorded data via radio link to a substation where the data are checked.
- Optional substation equipment sensors monitor interesting parameters in substations, such as transformer temperatures.
- The data are collected at a remote terminal unit, where the control is carried out.
- The data are then transmitted to the systems operation centre (*dispatch centre*) through a dedicated communication channel. Depending on the recorded data, decisions are made by the people in charge of the system operation.

17.2.1.3 Indirect methods

Indirect methods use the ambient conditions and the line current to calculate the temperature of the conductor. The temperature is then used to determine the position of the conductor. It is assumed that the safety limit could be exceeded creating a risk to the public if the design temperature is reached.
The ambient conditions to be monitored are wind speed, wind direction, solar radiation and ambient temperature. The anemometer should be able to measure wind speeds below 1 m/s. More than one line in the same area can be monitored. Additional lines can, therefore, be included without further equipment being needed. The weather data can be used as means of forecasting probable thermal limits up to 24 h in advance [17.15], thus enabling decisions on planning of generation capacities or line de-energizing for maintenance and repair.
Indirect methods may not cater for variation in parameters that could affect the conductor temperature and hence the sag. Variation in the value of the parameters can be caused by variability of the terrain, e. g. sheltering of a line by trees or buildings. In addition, wind speed and direction can differ from the point of measurement to the actual line. To mitigate the above effects, there may be a need to install a number of weather stations along the lines; associated communication problems to transmit the readings may occur together with uncertainty of the best location of weather stations. This is because the critical span for current determination could vary.
It is expedient to combine the used weather data with tension measurements getting the benefit of both methods with minimizing the drawbacks. The tension method can be used as a check to decide whether to use or not the weather data for other lines in the area that are not being monitored with load cells thus ensuring more accurate predictions.

17.2.1.4 Examples and experience

There are many examples for *application of real-time ampacity rating.* A more effective use of existing transmission lines is the goal of real-time thermal rating based on measurements from weather stations as reported in [17.22]. The short-term rating could be raised by approximately 30 %. In [17.15], a dynamic thermal rating system is presented which enables to predict the ambient temperatures 24 h in advance being useful during emergency situations, when higher capacity is needed, and for planning of line de-energizing for maintenance. An increase of ampacity up to 35 % is reported.

Paper [17.23] deals with determination of the ampacity of 400 kV lines connecting the former Yugoslavian power system with UCPTE. The comparison between measured and predicted conductor temperatures showed errors of only ± 2,5 K. Comparisons between predictions and measurements are presented in paper [17.24] as well. Paper [17.25] deals with thermal rating and uprating of existing lines.
According to [17.26], it seemed appropriate for the Norwegian grid to relate the thermal line rating to the ambient temperatures. This resulted in an improved basis for determining thermal capacities of individual lines and justified an increase by 10 % in ampacity without exceeding the specified conductor limit temperature. Other applications are summarized in [17.13].
Most transmission systems are operated based on the *(n-1) criterion*. After a disturbance, the system should return to a stable condition within typically 5 to 15 minutes. Knowing the real-time ampacity of the system, dispatch changes may not be necessary or at least delayed, benefiting from the thermal inertia of conductors [17.27].
From *real-time rating* it can be seen that ampacities vary with a daily pattern. A common finding is that at many locations the ampacity during daytime is higher than at night time due to substantially higher wind velocities during daytime than at night. Real-time monitoring can increase the line ampacity considerably. Thus, investments for line upgrading can be postponed or may not be required at all.

17.2.2 Thunderstorm monitoring and forecast

Lightning phenomena highly affect the reliability of overhead lines, especially where high lightning flash densities and high soil resistivities are prevalent along the line route. This fact justifies that utilities, other relevant public entities and research centres around the world decided to establish intensive lightning research programs, including the installation of Lightning Location Systems (LLS) for *thunderstorm monitoring* and *forecast*. Some of such systems are mentioned in Chapter 4. Besides being excellent operative tools, such systems can be useful for improving the lightning performance of the transmission system. These location systems can be isolated or operated in an integrated structure. According to experience in Germany, up to 30 % of the total amount of faults is due to lightning strokes and a higher percentage is reported from regions with high keraunic activity, e. g. 60 % in Brazil. Modern lightning location systems are described in [17.28, 17.29, 17.30]. In the latter case, there are a central station and regional stations as well, comprising great parts of a country or even several countries.
Several lightning location systems have been installed around the world, as can be seen in Chapter 4, Table 4.1; among them, one example can be mentioned from Brazil, comprising a total of 21 detection sensors installed in six Brazilian states in Central and South Brazil with three network central analysers in different points of the high-voltage system [17.28]. Due to the integration, the monitored area is expanded and recorded data are shared, leading to a better detection efficiency and a much more accurate *lightning location*. Figure 17.2 shows a flow chart of the lightning location system diagram of Brazil for processing, visualizing and storing lightning data. The technology applied is called Lightning Position and Tracking System (LPATS), developed by Global Atmospherics Inc. The central station processes data transmitted by sensors located in the detection stations, synchronized by the *Global Position System* (GPS), supplying time information with a 100 nanosecond resolution as well as its location, polarity and maximum return stroke current.
The processing unit configures, monitors, stores and processes the information of the signals received. It can store the rough data supplied by the sensors and also transmit them to a storing centre, which allows an access to visualizing software. Visualization

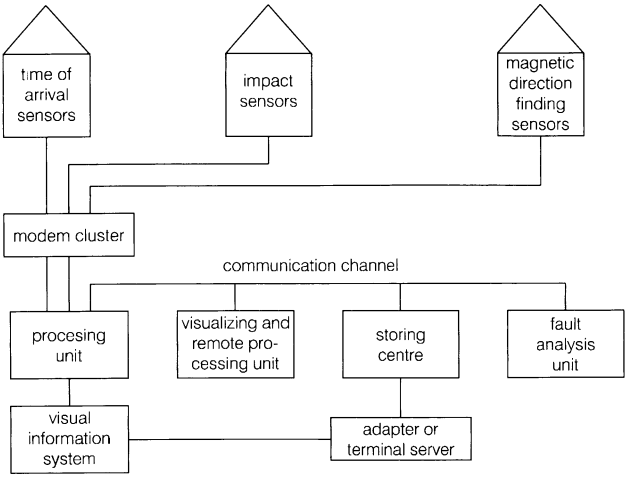

Figure 17.2: Typical diagram for processing, visualizing and storing lightning data in a lightning location system (see [17.28])

of lightning discharges can be performed through computers connected to the central processing unit or to the data bank in the storing centre.

Thirteen measuring stations all over Germany register the moment when the electromagnetic wave arrives at the receiving aerial. The high exactness of the lightning detection system is based on the time of arrival principle. The strike location is analysed by the difference of the times recorded by the different receivers. Time signals via satellites of the Global Positioning System assure a highly exact synchronization of the receivers. In case of an alarm from the protective devices a lightning stroke in the network can be determined by comparing the coordinate of the stroke location indicated by the system with the corresponding coordinates of the line or transformer station.

The German utility E.ON examined exactness and business benefits of a lightning location system. A comparison of the lightning detection system with fault locators was carried out. The deviation between the location signalized by the system and real fault location proved to be lower than in case of fault locators used previously. Therefore, the system reduces the costs for checks. The benefits are especially high in 110 kV networks with resonant earthed neutral, where faults could otherwise allocated to the electric circuit only.

The applications can be summarized as follows:

- Anticipation of thunderstorm approach and establishing preventive measures to reduce the impact on electric systems.
- Lightning strokes can be located immediately and reliably. This assists the operator to establish first fault diagnosis and to initiate line patrols fast and systematically.
- Damaged line components detected during regular controls can be traced back to lightning strokes based on data logged in the system.
- The system allows a statistical analysis of the frequency and intensity distribution of lightning strokes. On this basis, the design of new lines can be improved.
- In case of work being carried out on lines, especially live-line working, the linemen can be warned in time, thus improving safety and security of the installation.

17.2.3 Ice observations

Ice accretion on conductors causes an increase of sags and high loads on conductors, insulators and supports. Damage would result if the design ice load were exceeded to a certain extent. Therefore, *ice monitoring systems* are useful to alert the operational

staff, the dispatch centres and clients thus triggering countermeasures, e. g. establishing de-icing circuits. Icing observation systems are reported in [17.31, 17.32] and [17.18]. The paper [17.31] describes ice observations in remote areas by video detecting systems and fibre optic sensors to monitor the mechanical stress of the conductors.
According to [17.32], Hydro Quebec's *ice accretion telemonitoring system* SYGIVRE consists of a network of 20 sites distributed throughout the transmission system, where ice accretion and air temperature are measured using an icing rate meter and a thermal probe. The data are transmitted to a central computer, where they are analysed in real time 24 hours a day. For each site, each event is analysed according to the type of icing governing the site. The type of ice involved is identified as being glaze ice, rime ice or snow and the total accumulation is calculated observed during one hour.
Paper [17.18] reports on the use of load cells installed primarily for real-time ampacity rating also for observation of ice on conductors. The load cells monitor the conductor tensile stress. The ice accretion can be determined by plots of tension versus the net radiation temperature. The technical report IEC 61 774 [17.33] describes standardized *ice measurement techniques* using test stands separated from line conductors.
The scope of the report [17.34] is to provide line operators with guidelines to collect icing data from overhead lines and to evaluate these data with the goal of establishing an improved base for design of new lines or upgrading existing ones.

17.2.4 Galloping alerting system

Conductor galloping can cause severe disturbances for line operation. Therefore, the German utility VEW, since 2001 part of RWE Energy AG, developed a *galloping alerting system* to warn early when a galloping-prone climatic condition could occur. The utility would then be able to take precautions by re-arranging the energy supply thus avoiding damage due to line failures.
A total of 66 galloping cases were correlated to the climatic conditions given within a period of 72 hours before the galloping events. The study identified the wind condition, the ice accretion, the air temperature and the dew point temperature as those parameters governing the galloping probability.
The studies resulted in a *galloping readiness coefficient*

$$\mathrm{GRC} = \frac{(1 + \sin\delta) \cdot (1 + 0,5\, I_\mathrm{W}) \cdot V_\mathrm{W}}{1 + (T_\mathrm{air} - T_\mathrm{D})/2 + T_\mathrm{air}^2} \quad , \tag{17.9}$$

where
δ angle between direction of line and wind,
I_W wind gust intensity,
V_W wind velocity in m/s,
T_air air temperature in °C,
T_D dew point temperature in °C.

Using GRC = 40 as a threshold, 85 % of the galloping cases could be forecast. Experience has shown that the warning should be kept in force during a period of 10 hours after the threshold of 40 had been reached.

17.2.5 Insulator contamination and performance

The electric, mechanical and environmental *performance of overhead line insulators* is important with respect to the line life. Tools have been developed for improving and optimizing design and maintenance of the insulators.

Damaged or cracked insulators may be detected while they are in service, but suitable precautions should be followed. In general, the methods employed for faulty cap-and-pin insulator detection are based upon the measurement of the voltage gradient across the individual units of a string of suspension insulators or across the parts of multi-part pin-type insulators. For safety reasons, none of the test methods should be used in wet weather.

Faulty insulators may also be detected by special radio interference locators, consisting essentially of a sensitive battery-operated receiver coupled to either a directional loop antenna or a whip antenna. The latter type may be attached to a hot-line stick to enable close investigation of the insulator under test; infra-red techniques are also employed.

According to [17.35], the *energized insulator tester* [17.36] represents a spark-gap voltmeter which is safe to use and gives high accuracy in measuring potentials in the field of live-line insulators.

The equipment consists of a micrometer spark-gap in series with a capacitor and a special telephone-type headset to listen to gap sparkovers. The degree of defect in the tested disc is indicated by the size of the maximum gap at which a noise is heard in the tester, as compared with the size of a maximum gap for a good disc in the same position in a string. A totally dead disc gives no sound, irrespective of the gap setting. In practice, one gap length is fixed in advance and used for all units of the string. The operator judges if a unit is defective from the noise heard in the headset.

The live-line insulator tester can also detect defective insulators, either multi-part pin-type or suspension, by comparing the measured voltage distribution over insulators or insulator strings in service with characteristic curves plotted for good insulators of the same type.

Long rod insulators do not require any tests to detect faulty units since they are puncture-proof. In-service testing is completely unknown with these insulators.

Non-ceramic insulators, due to presence of organic materials in their structure, may suffer long-term degradation. This motivates the establishment of condition assessment methods being able to detect the evolution of defects before they become critical for the dielectric withstand of the line. During the tests, external defects are applied along the insulator surface by means of thin conductive foils having 5 mm width and variable length. The sound insulator length, for which a 50 % flashover probability is determined, is called critical defect length. The *critical defect length* in a configuration representative of live-line working conditions can be used for assessment. Results of dielectric tests carried out in 145 and 420 kV configurations have shown critical defect lengths between 35 and 40 % of the design length; that means, by simulating external defects along the insulator surface, insulation failures occurred in conditions of live-line work when the insulator reduction reached around 60 to 70 %: Switching impulse and power frequency stresses, combined with environmental conditions. Reference [17.37] deals with assessment of non-ceramic insulators.

In [17.38], other methods are described for checking residual performance of non-ceramic insulators especially composite insulators. The electrical field distribution measurement and the *infra-red thermography* are among the most widely used and sensitive to detect faulty insulators in the early stage of degradation. Paper [17.38] concludes that non-ceramic insulators can have potential advantages as compared to other insulator designs; however, the presence of polymeric material in their structures rises the possibility of long-term defects under the different design stresses. Diagnostic methods are, therefore, necessary to check periodically their operating conditions.

17.3 Asset management

17.3.1 Definitions

In the context of *line asset management*, the following definitions as per [17.39] are used:

***Availability*:** The state of an item being able to perform its required function.

***Capability*:** The product of *capacity* and its *availability*.

***Capacity* (electric):** The product of nominal values of voltage and current in a circuit.

***Capacity* (mechanical):** The maximum rated mechanical strength of a component or element.

***Chance*:** The potential for the occurrence of an event.

***Conductor assembly*:** All current carrying elements, overhead earth wires and fibre optic cables including conductor clamps, spacers, dampers and other attachments.

***Component*:** A part of a transmission line, i. e. insulator string assembly, conductor assembly, support assembly or foundation.

***Consequence*:** Result of an *event*.

***Defect*:** Imperfection in the state of an item, which increases the probability of failure of itself, or another item.

***Design working life*:** Assumed period for which an item is to be used for its required function with anticipated maintenance but without substantial repair being necessary.

***Event*:** Occurrence of a set of circumstances.

***Failure*:** The termination of the ability of an item to perform a required function.

***Inspection*:** The total process of detecting, measuring or estimating those properties and characteristics or symptoms, that contribute to the physical condition of an item, using either non-destructive or destructive methods to enable the production of an inspection report.

***Life extension*:** Extensive renovation or repair of an item without restoring their original design working life.

***Maintenance*:** Total set of activities performed during the design working life of an item to maintain its purpose. It includes routine conservation and small or local repair.

***Outage*:** The state of a circuit being unable to perform its required function.

***Outage duration*:** The period during which a circuit is incapable of performing its required function within a specified period of time.

***Predictable event*:** An event that has a well defined probability of occurrence at a given location, and whose probability of occurrence and/or consequences can be economically reduced with proactive measures.

***Proactive measure*:** Measure or action taken prior to the occurrence of an *event* in order to reduce the probability of *failure*.

***Reactive measure*:** Measure or action that become effective after the occurrence of an *event*, i. e. they do not reduce the probability of failure but reduce the *consequences of failure*.

***Refurbishment*:** Extensive renovation or repair of an *item* to restore their intended design working life.

***Reliability*:** Probability of an item to perform a *required function* under a set of conditions for a specified period of time achieved by appropriate design. It is thus a measure of the success of an *item* in accomplishing its *required function*.

***Restoration*:** Repair of a failed *item*, so that it may perform a *required function*.

***Required function*:** Specific performance function.

***Risk*:** Combination of the chance of an event and its consequences. *Risk* is product of the annual probability of occurrence of failure of an item and the totality of resulting consequences expressed in monetary terms.

***Risk increase*:** Actions increasing the chance, negative consequences, or both, of a particular *risk* for possible gain.
***Risk reduction*:** Actions taken to lessen the chance, negative *consequences*, or both, of a particular risk.
***Unpredictable event*:** An event whose *risk* is managed by reactive measures since its probability of occurrence cannot be economically reduced with proactive measures.
***Upgrading*:** Increasing the original mechanical strength of an item due to, for example, a requirement for higher meteorological actions. Upgrading will decrease the probability of failure.
***Uprating*:** Increasing the electric characteristics of a line due to, for example, a requirement for higher electric capacity, or larger electrical clearances. Uprating will increase the electric capacity of a line, thereby, potentially increasing the consequences of a failure.

17.3.2 Introduction and targets

In the past, decisions on the *management of existing overhead lines* were frequently based on the qualitative judgement of experienced individuals. In [17.39], guidance is provided on quantitative assessment. There, methods for estimating costs and risks are given associated with actions required for proper management of an overhead line asset. These management actions are based on adequate *inspections* of the transmission line *components*, cost factors, safety, regulatory and environmental considerations. Due to their complexity, extent and bold exposure to the elements of overhead power lines are vulnerable to *degradation* and possible failure from a wide variety of initiating events. Since it is becoming increasingly difficult to acquire new *rights-of-way* and to build new lines, utilities are seeking ways to get the most from their existing overhead line assets. To increase the *availability* of an overhead line, there should be a clear understanding of the negative and positive risks resulting from management decisions.

17.3.3 Risk management of line assets

Future management decisions concerning line assets may be based on maximizing the *return on investment* of these assets and/or minimizing expenditures for maintaining these assets. Other factors that need to be considered are: *availability*, *reliability*, *system operation* and environment. A model for line management should be able to qualitatively include all of these factors. An overhead line may be degraded to a lower level of reliability or it may be upgraded or uprated to a higher level of reliability or electric capacity.
Inspection and repair activities are conducted to prevent *degradation* beyond a desired performance level. The time to perform these *maintenance activities* to achieve a desired performance level of the overhead line is a critical question. Although failure of an overhead line is not desirable, total elimination of this risk may not be economically justifiable.
Failures are dependent on the physical characteristics of the overhead line and can result from external influences such as either predictable causal events e. g. infrequent high winds and ice loads or unpredictable causal events such as natural disasters, human error or sabotage. An overhead line is considered to have failed when it cannot transmit power from one end to the other.
Since overhead lines are subject to a wide range of environmental factors, management decisions will always have to be made under conditions of risk and uncertainty [17.40]. It is the knowledge and understanding of various options and their associated risk that will allow to choose the most appropriate option.

17.3.4 Net present value of annual expenditures

It is assumed that the goal of any management decision is to minimize the net present value (NPV) of the annual expenditures over a predetermined investment period. In order to get comparable results, future costs are discounted to the present. In general terms:

$$\mathrm{NPV} = \sum_{i=0}^{i=n} C_i/(1+r)^{\mathrm{i}} \quad , \tag{17.10}$$

where NPV is the *net present value* of the annual expenditures, n the period of years taken into consideration, r the discount rate and C_i the annual expenditures in year i, with

$$C_i = E_{\mathrm{d}i} + E_{\mathrm{p}i} \quad , \tag{17.11}$$

where $E_{\mathrm{d}i}$ are the deterministic costs or planned expenditures in year i, and $E_{\mathrm{p}i}$ the probabilistic costs associated with risk of failure in year i. For an overhead line asset all relevant deterministic and probabilistic cost factors have to be taken into consideration during the investment period. The deterministic cost factors are called *planned expenditures* ($E_{\mathrm{d}i}$). They consist of normal operation and maintenance costs, planned outages and investment costs accounted for in the year or at the time they are incurred. These costs are discussed in clause 17.3.5.

The probabilistic cost factor is called *risk of failure* ($E_{\mathrm{p}i}$). In general terms, risk is defined as the product of chance and consequence. Chance is usually expressed as a probability of an event. In common usage, the event is undesirable and the consequences are adverse.

When the event is an overhead line failure, the chance is the probability of occurrence of the event initiating failure, and the consequences are the totality of resulting consequences. This *risk of failure* ($E_{\mathrm{p}i}$) can be stated in its simplest form as:

$$E_{\mathrm{p}i} = \mathrm{POF} \cdot E_{\mathrm{f}} \quad , \tag{17.12}$$

where E_{f} is the cost of consequences.

Risk of failure during a time interval may be defined in economic terms, such as net present value NPV. It is a function of time since both the probability of failure and the consequences will vary as a function of time. From equation (17.12), it is obvious that risk can be controlled by either the likelihood of occurrence of the failure initiating event, or the magnitude of the resulting consequences. In general, the risk of failure ($E_{\mathrm{p}i}$) is a function of planned expenditures $E_{\mathrm{d}i}$. Risk of failure, the probability of failure and their resulting consequences are discussed in clause 17.3.6.

17.3.5 Planned expenditures

Planned expenditures include costs of normal operations and costs of investments, namely:

- *Costs of investments*;
- *Energy and capacity losses* depending on the conductors and the load;
- Costs of planned outages;
- *Operation* and *maintenance costs.* Regular inspections and patrols are necessary and the conditions of the components and elements need to be checked. Recoating, tree trimming and smaller interventions are performed regularly.
- Costs for collecting information and maintaining a data base for management of the overhead line asset.

Table 17.1: Comparison of predictable and unpredictable events

	Failure due to	
	Predictable events	Unpredictable events
Probability	relatively high	relatively low
Economic way to avoid failure	exists	does not exist
Proactive action	can be taken economically	not economically
Properly designed line	will survive	will not survive
Reactive actions	are possible	may reduce the risk

17.3.6 Risk of failure

The risk of failure of an overhead line is defined as the probability of failure multiplied by the totality of resulting consequences. The event causing failure may be predictable or unpredictable, and the consequences of the failure may be expressed qualitatively or quantitatively. The consequences of a predictable event may be different from the consequences of an unpredictable event. The following sections will briefly describe failure probabilities and list the possible consequences [17.41].
Under the simple laws of statistics, there are two outcomes to an event: Failure or survival. The annual probability of survival P_S is the complement of the annual probability of failure P_f or

$$P_S = 1 - P_f \quad . \tag{17.13}$$

The probability of survival is over an extended length of time such as n years of service life, or an investment period of n years:

$$(P_{S1} \cdot P_{S2} \cdot P_{S3} \cdot \ldots \cdot P_{Sn}) = (P_S)^n \quad , \tag{17.14}$$

provided the probability of survival remains constant over the period of n years. Then, the probability of failure P_{fn} over n years of service life is:

$$P_{fn} = 1 - (P_S)^n \quad . \tag{17.15}$$

For example, if the components of an overhead line have the strength to withstand a predictable fifty-year storm, resulting in an annual probability of survival $P_S = 1 - 1/50 = 0,98$, the overhead line still has a $(1 - 0,98^5) \cdot 100 = 9,6$ % predictable chance of failure within the next five years.
Failures due to *predictable events* can be forecast by analytical analysis of the mechanical capability of the line components and the least reliable component can be identified. Depending on the type of component, the line damage after an initial failure can be assessed.
The term *unpredictable event* is used to represent events that are managed by reactive measures, since their probability of occurrence cannot be economically reduced with proactive measures. Certain events such as natural disasters, sabotage or human error will occur; however, the nature of the event precludes taking proactive correctives to reduce the probability of failure of the event. Natural disasters such as hurricanes, cyclones or typhoons, tornadoes, massive ice storms, floods, earthquakes and earth slides fortunately occur infrequently. When they do, these disasters can cause total destruction of the overhead line and can cause the total outage for a long period. In Table 17.1, predictable and unpredictable events are assessed.

17.3.7 Consequences of a failure

Overhead lines may provide different functions:

- Transmit power between points A and B continuously;

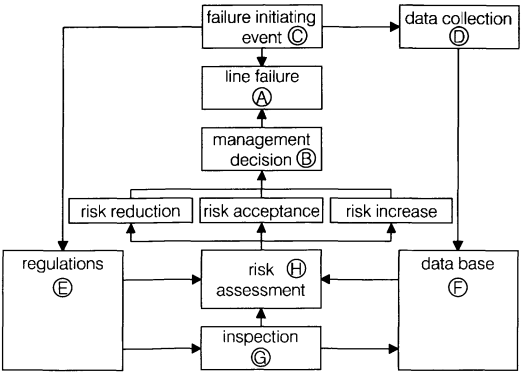

Figure 17.3: Process or model for management of existing overhead line assets

- Transmit power between points A and B if another line failed;
- Increase stability margin without continuous transportation of power.

Therefore, the consequences would be different, should the overhead line fail. Consequences resulting from an extended outage of an overhead line are site- and function-specific and can be considerable and *monetary losses* can occur to the overhead line owner.

The following costs may be associated to overhead line failures:

- In the worst case, injuries or death may occur, mainly in urban areas and at crossings. The line owner has to pay compensation as far as not covered by insurance. The responsible persons will be cited to the court and the line owner may have negative publicity.
- Serious damages to the environment caused by line failures have a similar, but less critical effect on the line owner than mentioned above.
- Frequent failures can create negative publicity for the company even if there is little or no direct effect on the public or on the line customers. It can have a major economic impact on the line owner because of the potential loss of major customers and other factors such as looking for new right-of-way, or public pressure to put overhead lines underground.
- Some failures can lead to the collapse of a part of the electric system or limitation of supply in the system.
- Energy losses generally increase because of the failed line.
- Sometimes, more expensive generation must be used during the failure period because of the separation of a power plant from the network or because of thermal or stability limits in the network.
- Revenues and profits will be lost if customers are not supplied.
- Depending on contracts for delivering energy, penalties may have to be paid in case of supply interruptions.
- Sometimes, regulators set requirements concerning reliability of the lines and penalties must be paid in case of too many failures.
- Cost of repairing the line that had failed.

17.3.8 Overhead line asset management process

To present to the management appropriate options that minimize the net present value of annual expenditures over an investment period, a management process needs to be implemented. In Figure 17.3, an idealized process or model of the activities leading to management decisions for an overhead line asset is shown. This *management process* presents the activities as described in [17.39].

Table 17.2: Management options and their consequences

Management decision	Planned expenditures	Change of failure probability	Change of failure consequences
Proactive risk reduction			
Maintenance	increase in annual costs	decrease	no
Refurbishment	increase in investment	decrease	no
Life extension	increase in investment	decrease	no
Upgrading	increase in investment	decrease	no
Decommissioning	decrease in annual costs	zero	local consequences
Reactive risk reduction			
Fast restoration	increase in investment	no	yes, mainly system consequences decrease
Insurance	increase in annual costs	no	decrease
System development [1)]	increase in investment	no	decrease
Risk acceptance			
Do nothing	no change	no	no
Risk increase			
Reduce maintenance	decrease in annual costs	increase	no
Uprating without upgrading	increase in investment	increase	increase

[1)] Installation of new lines

There is no fixed starting point in this process. However, it could begin by examining the process after an overhead line failure (A) (see Figure 17.3). Line failures cannot be completely excluded, however, management may decide to achieve an acceptable *rate of failures* due to certain events which are consistent with management goals (B). Failures may also be due to outside failure events (C) beyond the management's control.
When an overhead line *failure event* occurred, data must be taken to determine the cause of the failure (D), as described in clause 17.4.4. Without this data collection, improvements to the management decision making process will be difficult if not impossible. Ideally, a useful *data base*, as described in [17.39], will be established (F). This data base could contain information on the overhead line, its components and its critical elements.
The overhead line must be patrolled and inspected (G) in order to update information on the degradation of right-of-way and overhead line components and elements. This information is supplied to the data base and used to determine the line's present capabilities (H) including residual electric or mechanical strength, and the remaining life of the covered component or element. Then, the risk can be calculated for various management options and used as a basis for management decisions (B).
The cost and benefit of each management option is considered and accounted for in the net present value calculations. Various options and management initiatives are outlined and described in clause 17.3.10. Management can then select the best option consistent with company goals. Although the names used in Figure 17.3 for management options might give the impression that one type of decision is better than the other, this is not true. All types are equally appropriate based on the risk assessment (H). In addition, failure events may initiate a re-evaluation of specifications (E) with a feed back on risk assessment and inspection practice.

17.3.9 Data base

An inventory of the line components or *line data base* is necessary for the quantification of the management options as well as the organization of daily maintenance. The data base is a source of information about:

- The original physical composition of the line and the components by an as-built documentation.
- The modifications of the line and the components: Exchanged parts, alterations, life extension, re-coating, refurbishment, upgrading, uprating etc.
- Service experience with the line and the components: Forced outages, defects, failures, availability and reliability.
- The actual physical condition of components and elements: Wear, ageing, etc.

Management may need data giving an overview of the overhead line assets. *Maintenance* activities, including reliability centred refurbishment, need detailed information about each individual component.

If a defect is found in a component or element, the assessment of these components or elements may require their detailed history. Such a detailed history, i. e. statistical data on their original strength, history of failures or location of critical components or elements, would be invaluable in estimating their probability of failure. Other information such as system related costs might need to be obtained from other sources.

The data base must be designed to fulfil all needs, within cost limitations. From a failure assessment point of view, the raw data on all elements should be kept for possible future processing, since it may not be known which element is critical or important for many years. In [17.39], suggestions for design and handling of an overhead line data base are made. Keeping a data base updated needs a thorough, continuous and consequent handling of inputs and care over long periods. Therefore, considerable efforts are required to guarantee that the data base reflects correctly the life history of a line.

17.3.10 Management options

Management options may be grouped in three basic categories: *Risk reduction*, *risk acceptance* and *risk increase*. The three types are equally appropriate based on the *risk assessment*. If the risk is deemed acceptable, no action or decision is appropriate. When risk is deemed too low, risk may be increased with an opportunity for gain by decreasing planned expenditures. If risk seems to be too high, it can be decreased by increasing planned expenditures. When the risk due to predictable events is deemed too high, generally proactive decisions are appropriate. When the risk is too high due to unpredictable events, generally reactive decisions are appropriate. If the potential consequences are too high, both proactive and reactive decisions may be appropriate in order to reduce risk.

Proactive actions tend to decrease the probability of failure as well. The proactive options are maintenance, refurbishment, upgrading and decommissioning. Their effects on planned expenditures, probability of failure and consequence of failure can be seen in Table 17.2.

Reactive actions tend to decrease the consequences of failure. The reactive options are fast restoration, insurance and system development. Their effects on planned expenditures, probability of failure and consequence of failure can be seen in Table 17.2.

Risk acceptance means that the present state is acceptable and there is no reason to take any special action. No change is planned in the present maintenance practice. Increasing risk may mean that the present status is too good and there is a potential for economic gain through less planned expenditure and allowing greater risk. Costs can be saved by building less robust lines in the future or by less maintenance on the existing lines. Increased risk may also occur if overhead lines are uprated without also being upgraded. The effects of *risk increase* on planned expenditures, probability of failure and consequence of failure can be seen in Table 17.2.

Table 17.3: Basic data for risk management of a 110 kV line (see [17.39])

Transmission line		
Voltage	110	kV
Length	10	km
Number of towers	50	
Number of insulators	168	
Resistance of conductor	0,5	Ω/phase
Number of crossings	1	
Load		
Continuous load for 8 700 hours/year	100	MW
Load can be supplied from medium voltage in emergency	60	MW
Loss of load (penalties to be paid for)	40	MW
Annual probability of failures of an element		
Failure of a single tower (times per year)	0,0001	
Failure of a single insulator (times per year)	0,0002	
Time of repair		
Tower failure	240	hours
Insulator failure	5	hours
Costs, penalties and losses		
Management and headquarters costs	10 000	EUR/year
Penalty for not delivering energy	1 000	EUR/MWh
Cost of losses	25	EUR/MWh
Cost of tower repair	20 000	EUR
Cost of changing failed insulator	1 500	EUR
Cost of doubling insulator	1 000	EUR
Principal costs for human injuries and damage at railway crossing	100 000 000	EUR
Cost of upgrading with higher reliability insulators	700	EUR
Cost of one emergency tower	20 000	EUR
Cost of a new line	1 000 000	EUR

17.3.11 Example on management of risk of failure

17.3.11.1 Basic data

A 10 km long 110 kV radial transmission line has 50 towers, 168 long rod insulators, 44 suspension and 6 tension towers. Resistance of conductor is 0,5 Ω/phase. There is one railway crossing. The load is continuously 100 MW. If the line failed, 60 MW could be supplied from the medium voltage network but 40 MW load would not be covered. The basic data can be seen in Table 17.3.

17.3.11.2 Calculation of planned expenditures and risks

The failures are supposed to be independent from each other and the time of repair is negligible. The probability $P_{x,n}$ of occurrence of the event that x elements will fail from n elements when p is the failure probability for an individual element is obtained from

$$P_{x,n} = (1-p)^{n-x} p^x \left[\frac{n!}{x!(n-x)!} \right] \quad , \tag{17.16}$$

The results of risk and cost calculation are presented in Table 17.4.
The loss in case of a tower failure is 240 hours · 40 MW · 1 000 EUR/MWh = 9 600 000 EUR.
The loss in case of an insulator failure is 5 hours · 40 MW· 1 000 EUR/MWh = 200 000 EUR.
Risks are calculated by multiplying annual probabilities and annual losses (see Table 17.4). System risk of tower failures is 48 000 EUR, system risk of insulator failure is 6 720 EUR in one year. The line risk comprises the costs connected to repair.
The risk connected to the railway crossing is separately presented. Probability of failure of one or more towers and insulators is calculated as previously. Principal losses are known from basic data. Risk of tower failure is 19 999 EUR, risk of insulator failure is 119 940 EUR in a year.
Other costs are management and headquarters and energy losses, being 10 000 EUR in one year. Energy loss is calculated from the load, the voltage and the resistance. The current is

Table 17.4: Risk and cost calculation in EUR

Number of failed towers or insulators	Annual probability of tower failures	Annual loss (EUR)	Risk (EUR)	Annual probability of insulator failures	Annual loss (EUR)	Risk (EUR)	Total
System risk							
0	0,99501223	0	0,00	0,966954961	0	0,00	
1	0,00497556	9 600 000	47 765,36	0,032496186	200 000	6 499,24	
2	1,21913E-05	19 200 000	234,07	0,000542795	400 000	217,12	
3	1,95008E-08	28 800 000	0,56	6,00813E-06	600 000	3,60	
4	2,29243E-11	38 400 000	0,00	4,9577E-08	800 000	0,04	
5	2,10925E-14	48 000 000	0,00	3,2529E-10	1 000 000	0,00	
6	1,58209E-17	57 600 000	0,00	1,76776E-12	1 200 000	0,00	
7	9,94558E-21	67 200 000	0,00	8,18386E-15	1 400 000	0,00	
Total risk			48 000,00			6 720,00	54 720
Line risk							
0	0,99501223	0	0,00	0,966954961	0	0,00	
1	0,004975559	20 000	99,51	0,032496186	1 500	48,74	
2	1,21913E-05	40 000	0,49	0,000542795	3 000	1,63	
Subtotal			100,00			50,40	150
Risk at crossing							
	0,00019999	100 000 000	19 999,00	0,0011994	100 000 000	119 940,00	
Line risk			20 099,00			119 990,40	140 089
Total risk			68 099,00			126 710,40	194 809
Costs							
Management and headquarters							10 000
Losses							90 089
Total planned annual costs							100 089
Total risk plus cost							294 898

$I = 100 \cdot 10^6/(110 \cdot 10^3 \cdot \sqrt{3}) = 525$ A. The energy loss is $3 \cdot 525^2 \cdot 0,5 = 0,413$ MW, the yearly loss $8\,700 \cdot 0,413 = 3\,600$ MW, its value is 90 089 EUR in one year. Therefore, the planned annual costs are 100 089 EUR. The value of all costs and risks is 294 898 EUR in one year.

17.3.11.3 Management options and assessment

The options examined in this example are

- Do nothing but follow present maintenance activities (1).
- Selectively upgrade by doubling insulators at the railway crossing (2).
- Upgrade by changing all insulators to a more reliable design having a 5 times less probability of failure (3).
- Fast restoration of a tower failure with emergency towers (4).
- System development by installing a second transmission line (5).
- Combined action by doubling insulators at crossing and buying emergency towers (6).

The expenses of these activities in year 0 can be seen in Table 17.5. The costs of the following years will be determined by the activities in year 0. It is supposed that inflation is zero and there is no change in the conditions of the line or in the system. 5, 10 and 20 years are taken into consideration. The discount rate is 5 % in the whole period. The costs are as follows:

- Do nothing column is the collection of numbers from Table 17.4. Net present value for 20 years is 3 675 089 EUR.
- Selective upgrading by doubling insulators at railway crossing will decrease local risks at the crossing. It is supposed that failures in a double chain are independent from each other. There is an additional advantage by reducing system risk, however, this is neglected. So the sum of costs and risks is about 174 982 EUR. Net present value for 20 years is 2 186 670 EUR.
- Upgrading insulators will decrease system risk caused by the insulators. System risks and crossing risks caused by insulators are 5 times less than previously. Net present value is 2 529 415 EUR.

Table 17.5: Options and evaluation

	Option					
	Do nothing	Selective upgrade	Upgrade	Fast restor-ation	System develop-ment	Combined action
	(1)	(2)	(3)	(4)	(5)	(6)
	Absolute EUR	Change in EUR compared to "do nothing"				
Investment at beginning		6 000	117 600	20 000	1 000 000	26 000
System risk of tower	48 000	0	0	-38 400	-48 000	-38 400
System risk of insulator	6 720	0	-5 367	0	-6 720	0
Local risk of tower	100	0	0	0	100	0
Local risk of insulator	50	0	-40	0	50	0
Local risk of tower/crossing	19 999	0	0	0	0	0
Local risk of insulator/crossing	119 940	-119 916	-95 952	0		-119 916
Planned annual costs						
Management	10 000	0	0	0	10 000	0
Energy loss	90 089	0	0	0	-45 044	0
Sum of changes compared to "do nothing"	0	-119 916	-101 368	38 400	-89 614	-158 316
Annual costs and risks	294 898	174 982	193 530	256 498	205 284	136 582
Net present value (20 years)	3 675 089	2 186 670	2 529 415	3 216 540	3 556 566	1 728 122
Net present value (10 years)	2 277 129	1 357 169	1 611 989	2 000 614	2 584 133	1 080 654
Net present value (5 years)	1 276 756	763 583	955 485	1 130 504	1 888 266	617 331

- Fast restoration will decrease system risk of tower failure from 48 000 to 9 600 EUR because time will decrease from 240 to 48 hours. Net present value is 3 216 540 EUR.
- System development with a second transmission line will diminish system risks practically. It will decrease energy losses to the half of the original value. Management costs and local risk costs of repair will be doubled. It is supposed that there is no crossing through this line at all. Net present value for 20 years is 3 556 566 EUR.
- Combined action is the combination of insulator doubling at crossing and emergency tower utilization. This is a reasonable action because these risks are independent and these are the greatest risks. Net present value for 20 years is 1 728 121 EUR.

All the actions seem reasonable for the long run. However, the 20 years net present value of system development is very close to that of the same period with no action and its 5 years value is much higher. As circumstances may change in the future, this action seems to be a rather risky investment. The combined action is the best solution for the long term and for the short run as well. Risks can be decreased substantially without huge investment.

17.4 Maintenance

17.4.1 Introduction

Effective *maintenance of a system* is as essential to superior service as is excellent engineering design. In fact, a well designed system may fall short of its service requirements owing to faulty maintenance. Aside from switching lines promptly to meet load conditions of the system, maintenance consists not only in restoring service immediately after an interruption, but also in predicting, detecting, removing and replacing faulty components, thus actually preventing the development of faults or long-term outages. The power utility or the line owner is, therefore, also concerned about preserving the integrity of the line components during the life of the line, especially in a market-driven electricity industry [17.42].

According to DIN 31 051 [17.43], the term *maintenance* describes measures aiming at the preservation and/or restoration of the desired condition and at the ascertainment and assessment of the actual condition of the engineering components of a system.

Maintenance comprises
- Inspection;
- Servicing;
- Repair.

Inspection means the ascertainment and objective of the actual condition of assets, comprising:
- Preparation of inspection implementation.
- Implementation of the inspection, mainly the quantitative recording of parameters defined in the plan and the assessment by means of component-specific criteria.
- Reviewing of the inspection results.
- Qualitative assessment of the inspection results to define the actual condition.
- Decision on measures based on the maintenance strategies.
- Documentation of inspection.

Service activities, in general, are measures aiming at keeping the function of components, which do not concern the planning strategy. Servicing is not required for overhead power lines.

Repairs comprise measures aiming at the restoration of the desired condition of components, which are to be coordinated with the management options. These measures comprise:
- Definition of the content of work to be performed, tendering and contracting.
- Preparation of implementation of the measure: Cost evaluation, time scheduling, coordination with external and internal parties concerned, assignment of in-house and/or external personnel and material, and preparation of measures.
- Documentation of measures.
- Final assessment and cost accounting.

To achieve the targets of inspections and repairs, experienced and skilful linemen are necessary, who have an understanding of function and the design criteria of supports, conductors, insulators and other components. They should be able to immediately recognize any deviations from the desired condition like broken strands or insulators, missing bolts or components.

The necessity of periodical maintenance of electric transmission and distribution networks does not only result from engineering and economic requirements. In many countries, a regularity framework for the energy sector comprising a series of laws exists from which the maintenance requirements can be derived.

17.4.2 Inspection

17.4.2.1 Reasons and procedures for inspections

Utilities or line owners usually have an established *maintenance inspection program* conducted at defined frequencies. Aerial inspection by helicopter should be supplemented with ground inspection, as well as with climbing inspection programs to check the structures and other components.

Under a broad classification, inspections can be preventive or corrective, the former one being considered as the most important because they have the objective of assessing the conditions of equipment and of detecting problems at an initial phase; thus, it is possible to provide for the correction or replacement of faulty components before they cause major damage or longer outages to the lines.

So, *periodic inspections* are normally programmed for all lines, with the frequency of inspections depending on the terrain traversed, type of structures (metallic, concrete or wood), line age, line performance and importance. In some densely settled areas, more frequent patrols may be considered necessary, whereas important lines in remote areas do not require inspection more than once a year. *Corrective* or *special inspections*

Table 17.6: Inspection program depending on support material, example from South America

Year	1	2	3	4	5	6	7	8	9	10	11
Wood	SI1	RI+PI	PI	RI	RI+PI	RI+SI3	LI+RI	RI+PI	RI	RI	PI+SI2
Metallic	SI1	RI	PI	–	RI	PI+SI3	PI	RI	–	CI	RI+SI2
Concrete	SI1	RI	PI	–	RI	PI+SI3	PI	RI	–	CI	RI+SI2

SI1 Inspection by commissioning crew; SI2 Inspection of conductors and earth wires; RI Routine inspection; PI Preventive inspection; SI3 Inspection of earthing system; LI Tower leg inspection; CI Corrosion inspection.

should be carried out after heavy storms or other events probably having affected an overhead power line.

Patrols may cover the line on foot, on horseback, by motorcycle, by automobile or by helicopter, depending upon the characteristics of the right-of-way. Close and accurate patrolling is not obtained by one person in an automobile, in general, even when the line follows a highway. Helicopter patrol is by far the best over mountainous and sparsely settled terrain. An efficiency of up to 300 km a day can be covered readily. The helicopter can fly as slowly and as close to the line as necessary, and it has the great advantage that the patroller is looking down on the line instead of up against the bright sky as background. Tower and wood-pole structure numbers should be fastened to the tops of the supports in such a manner that they can be read without trouble by the person in the helicopter. *Helicopter patrol* cannot be used over urban or congested industrial areas because of restrictions on height of flight. Patrols on foot are best in such areas. Horseback patrol are nowadays rarely used but they can be best in cattle-range terrain, if aerial patrol is not available. Motorcycle patrols have had growing use in rough terrain instead of horseback or automobile patrols, because they are faster, more efficient and less costly.

Landslides, washouts, loose timber or anything else should be reported as a potential danger to the line, such as piles of brush, straw or sugarcane plants which, if burned, could cause hot gases to flashover the line. Of course, the persons on patrol should closely look out for damaged conductors, insulators, fittings and structures.

Emergency crews are stationed at locations always available by telephone or radio so that every important section of the transmission line can be reached by a crew within a reasonable short period of time. Depending on the distances, small storage houses containing spare parts, such as insulators, lengths of conductors and cables, clamps, repair sleeves etc. should be located at intermediate and accessible points along the line in sparsely settled regions.

17.4.2.2 Inspection classification and frequency

Following South-American practice, the main types of inspections and their frequencies are illustrated in Table 17.6 comprising mainly:

Preventive inspections (PI) are carried out at all structures of a line and comprise basically the climbing at the structures to perform the following activities:

- Verification of loose or missing bolts and their tightening, fatigue or weathering problems, damage to members or bolt finish; verticality of the structures; guy wire tensions etc.
- *Vandalism* including insulators, hardware or conductor damage and collision damage, signs of vibration damage at conductors, hardware or insulator metallic parts, wear of fittings. This kind of inspection has usually a biennial or quadrennial frequency after the second year of the start of line operation for wood-pole structures, and quadrennial frequency after the third year for lines with metallic or concrete structures.

Routine inspections (RI) are *visual inspections* carried out along the lines, without compulsory climbing the structures. Such inspections are performed using binoculars for verifying the high parts of the structures, conductors and earth wires. This type of inspection can be carried out efficiently with helicopters, from which the detection of failures becomes much easier. Local patrols come afterwards to defective spots identified by the helicopter crew. Climbing might be necessary for a local and careful verification. Routine inspections usually have an annual frequency for lines with wood structures, and a triennial frequency, starting in the second year of line operation, for lines with metallic or concrete structures.

Tower leg inspections (LI) are usually performed in lines with wood structures, with excavations around the poles and a preservative treatment of affected areas. This inspection is carried out every eight to ten years continued with routine inspections.

Corrosion inspections (CI) are sampling inspections, performed to evaluate the corrosion state at grillages or legs of steel structures. Its frequency depends on the extent of corrosion that has been detected at a line. After the tenth year of operation, about 10 % of the steel structures should be inspected annually. If corrosion is detected, the remaining structures should be examined as well.

Special inspections (SI)

- **Approval inspections (SI1)** performed by the commissioning crew after the completion of line construction or its upgrading and/or uprating.
- **Inspections of conductors (SI2)** and earth wires is an aperiodic inspection to verify the existence of vibration problems, fatigue signs, damages near spacers etc. Its frequency depends chiefly on the past occurrences of conductor damages due to vibrations, pollution etc.
- **Earthing system inspection (SI3)** comprises checking the state of counterpoise and other earthing schemes, measuring earth resistance etc. Excavation for checking the earthing rods or counterpoises may be required.
- **Inspections through electronic systems** are based on electrical field distortions caused by defective components under voltage, such as the so called "Corona System" and the "Net Spy System" [17.44]. It operates as a function of the electrical field emitted by energized parts and its eventual distortion by a failed component. It doesn't require load but only that the rated voltage be applied. Some utilities consider it as quite efficient for detecting *insulation flaws* (shivers in the glass skirts, defects in the pins, shells), bad joints, scratches on conductor surfaces, *broken strands* in the conductors, loose dampers or spacers.
- **Thermographic or infra-red process (thermovision)** operates as a function of the temperature of the inspected components. Some manufacturers have equipment that directly indicate the temperature. This process requires a conductor load of at least 60 % of the full load. In such case it detects *overheating problems*. It is affected by solar radiation and in several cases a high intense level of radiation forces the interruption of the inspections.

In Table 17.6, an illustrative example is shown of the frequency of different inspection types according to the practice in a utility. Some particularities shown in the example are for instance: Wood pole lines should be submitted to preventive inspection much more frequently than concrete poles or metallic structures. It is recommended to submit concrete and metallic structures to a corrosion inspection after 10 years of operation. A special earthing system inspection is proceeded in lines having metallic or concrete supports after 5 years of operation. Conductors and earth wires should be inspected closely after 10 years.

Utilities in Central Europe carry out inspections by air or by patrolling along the lines. Air inspection by helicopter is carried out approximately once a year. Good flying weather conditions are a precondition. The average flying speed is approximately

20 km/h and normally includes a short stop at every tower. The flight crew consists of two staff members having knowledge on the topography and right-of-way. Every line is flown along in just one direction. If there are more than two circuits per tower, the circuits are shared out among the crew and inspected. In the next year, the same line is flown along on the other side of the towers.

Patrolling inspections of the line route and checking of the line by binoculars, basically without climbing the towers, is carried out once a year on an average, as well. Especially the following issues are to be paid attention to:

- Vegetation along the route; climbing of the towers might be advantageous to assess the height of vegetation;
- Building activities within right-of-way along the route and in the vicinity;
- Foundations;
- Tower structures;
- Suspension and dead-end insulator sets;
- Tilted bundles, loose or damaged bundle spacers;
- Conductors, earth wires and OPGW.

Independent of annual inspections, in-depth inspections are carried out approximately every ten years comprising:

- Tower sites and foundations;
- Climbing of towers in order to ascertain condition of crossarms, corrosion, insulators and fittings, suspensions, line conductors, earth wires, optical ground wires.

The findings of the inspections are documented in standardized formats [17.45].

Additional inspections combined with tests are performed on a condition-oriented or random sample basis, either as a result of regular inspection showing specific shortcomings or on occasion of special events, e. g. extreme weather conditions or lightning strokes.

17.4.2.3 Foundations and stubs

For the majority of foundations, constructed using appropriate materials and installation workmanship, there are no significant modes of degradation. Poor workmanship and design deficiency however, give rise to potentially serious problems. Uplift failures, where the foundation body remains in the ground, can occur if the stub is insufficiently encased in the body or the cleating is inadequate. Corrosion of the tower steel stub can occur when moisture and oxygen are present.

The main factors, which affect the rate at which the tower stub can corrode, are:

- Foundation construction quality – continuity of concrete, interface quality, concrete thickness;
- Soil types – clay, alluvial soils are worst due to water retention;
- Ground-water levels and frequency of change in level.

Inspection of foundations is described in detail in [17.46]. There is no general applicable strategy and method for foundation inspection due to the heterogeneous nature of the soil, changing environmental conditions causing potential degradation of foundations, wide reliability in the quality of construction and the potential number of different types of foundations available. Therefore, an appropriate inspection strategy should be selected by the line operator considering the individual conditions.

According to [17.46], the inspection can be carried out on four levels.

Level 1 inspections are mainly of the visual nature and designed to form a basis for more complex inspections. This type of inspection is carried out on all foundations under consideration and is normally part of a complete inspection of a transmission line. It should establish the type of foundation, so far as not exactly known, determi-

nation of the surrounding land use and vegetation, profile of the terrain surrounding the foundation and the soil cover, present pollution, surface conditions shortcomings in concrete making, damaged edges, gaps between tower stub steel work in concrete, corrosion of foundation steel parts, previous modifications or repairs. The main object is to identify those foundations requiring more detailed inspections.

Level 2 inspections aim at identifying foundation types, extent of deterioration, re-establishing of geotechnical parameters. The evaluation of level 2 inspections should indicate those foundations, where *refurbishment* or *upgrading* might be necessary.

The main aim of level 3 inspection is to provide the data for determining the geotechnical strength of the foundation and the degree of deterioration of individual elements in order to plan refurbishment. Paper [17.47] describes an example for the verification of pad and chimney foundations. In case of grillage foundations, excavations should be made until the water level, if any, to verify the existence of corroded coatings. Where the corrosion infringes the strength of the grillage, the change of the grillage would be necessary. Since this is a rough and onerous work not worthwhile to be carried out, the replacement of the grillage by a concrete footing should be considered instead.

At level 4 inspection, in [17.46] full scale testing of existing foundations is recommended to determine the load capacity, in addition to inspections as per level 3.

17.4.2.4 Supports including corrosion protection

The main factors, which affect the rate and onset of steel corrosion, can be categorised into effects caused by environment such as prevalent weather conditions, climate, fertilisers and pollution levels and effects by shortcomings of protection such as workmanship and coating policy.

In most circumstances, it will be a combination of two or more factors causing corrosion. Any combination of the above factors will lead to a variety of support steel conditions. If the first coating is delayed until significant loss of galvanizing has occurred and the steelwork has become corroded, extensive preparation may be required before coating. This work may involve grit blasting or replacement of certain tower members. Inevitably, this will reduce the overall life of supports. Most supports are constructed using galvanized steel members, which may be coated prior to erection or coated some time after erection.

During *support inspection*, the following verifications should be carried out regarding the state of metallic supports:

- Loose or lacking bolts;
- Existence of bird nests or bee hives;
- Loose or unattached guy wires of guyed towers;
- Corrosion vestiges at the guy anchors and anchor rods;
- Loose or lacking stepbolts;
- Finish state of coatings; measuring of paint and galvanizing thickness;
- Torsion at the structures;
- Deformation of members.

The *strength of concrete* or of *steel structures* is affected by various of the above mentioned parameters, beside the ageing or defects of the steel or concrete as well as by corrosion of the steel grillage foundations or of the reinforcing steel in case of concrete structures [17.47].

In non-aggressive environment, experience has shown that galvanized and coated steel structures and steel foundations are resistant to corrosion after being many years in service. However, in industrial areas, especially near chemical industries, several premature corrosion problems have been detected in the super-structure, depending also on the frequency of corrective coating. The necessity of coating refurbishment depends

on the condition of a line in total and its residual life time. E. g. a line which will be decommissioned in some years needs not to be coated although being in bad condition. I aggressive soils, steel foundations or steel components of concrete foundations may be subject to an early corrosion attack.
Regarding the tools employed for checking steel properties, hardness tests can be easily done on site. However, the execution of laboratory analysis in samples taken from the steel or concrete is more recommended.
Corrosion and connection problems are still better detected by *visual inspection.* Since corrosion does not attack a support uniformly, there are difficulties to assess their strength based on spot checks. Paper [17.45] summarizes experience on steel structure inspections.
For the purposes of *visual inspection by climbing*, each support is subdivided into zones according to the height and design of the support. Steelwork condition is assessed against standard photographs showing steelwork at various stages of deterioration. Each zone is then given a score accordingly.
Thickness measurement of non-ferrous metal paints (e. g. chromium, copper, zinc, etc.) or plastic coatings on steel, can be carried out by means of instruments using magnetic induction. With paint or plastic coating, or on non-ferrous structures, measurements are possible using instruments, which employ eddy currents. This technique can also be used for the measurement of ferrous and non-ferrous metal coating on steel. The thickness of protective coatings and the individual layers can be reliably measured using a *paint inspection gauge* (PIG), also called thickness cutter.
Stay wires are subjected to elongation due to oscillations whilst under tension. These oscillations result in mechanical fatigue of the wires, causing minor separation of the strands and thus, a relaxation and/or lengthening of the cable, which can result in mechanical damage to the support. It is, therefore, necessary to verify the tension of the stays on a regular basis and in some cases, to carry out retensioning.
Measurement of the tension related to the pressure measured on jacks fixed to the stays anchorage devices allows simultaneous retensioning if required.
Measurement of the perpendicular effort required to initiate a calibrated deflection between two points enables calculation of the corresponding tension in the stay. The equipment is light and easy to operate.
Devices based on magnetic induction process record the variation of the magnetic flux at the defect locations of stay wires. These variations are identified on the signal records and then compared to signals related to typical defects of various magnitudes due to corrosion or broken strands.

17.4.2.5 Conductors

Inspection of conductors aims at detecting broken strands, loose spacers, defective joints and clamps as well as spots showing increased corona.
Two basic electronic tools are available for *inspecting components* of high-voltage overhead lines: The first one requires the application of voltage to the line and uses the distortion caused by some faulty components on the electronic field produced by the conductors or energized components of the line. The second method is based on the application of current to the line and uses the *temperature increase* caused by heating of joints or any elements through which the current flows.
The first method can be used either for inspecting a line before the start-up of the commercial operation at the commissioning phase, as well as for routine inspection. Some systems are commercially known such as the *corona system inspection* or the *net spy system* [17.44]. Such electronic equipment is installed in a helicopter that flies at a safe distance to the line conductors, at a maximum speed of around 50 km/h,

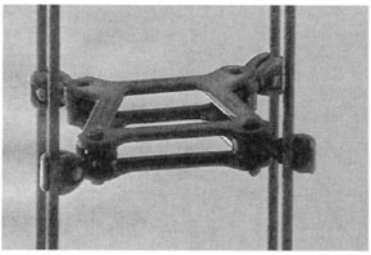

Figure 17.4: Spacer with a loose grip connection detected by electronic equipment (Courtesy from Grid Services GmbH, Karlsruhe, Germany)

enough to detect any distortions in the electrical field caused by any energized faulty component of the line. Detection of anomalies in connectors, splices, joints, insulators etc. is possible.

A normal corona pattern is adjusted in an oscillograph being part of the equipment. Any *distortion of the electrical field* is shown through a change in the corona pattern. A calibration carried out in the laboratory forecasts different types of distortions as caused by various faulty components. The fault indication is afterwards analysed in the office. *Corrective actions* are then programmed. When an apparently prominent failure is detected, the helicopter can fly around the probable defective point to permit a closer spotting of it.

The *net spy system*, developed from the same principle, but operating digitally, enables to examine and analyse in real time from the helicopter the surrounding electrical field of each high-voltage transmission line starting from 10 kV, based on high-frequency disturbances. Such disturbances are caused mainly by sparks or *partial discharges*, which are originated from local increased intensity of the electrical field strength at defective points. The measurement procedure complies with the distances of the visual control method and the flight speed is at 50 km/h maximum. *High-frequency disturbances* are signalized to the operator graphically and acoustically by the measurement equipment. When the measurement spots a defective point, the flight is immediately stopped and the operator tries to locate the source of the disturbances from the helicopter with a digital video camera. Likewise, the disturbance is digitally recorded and the global positioning system data is entered. If it is not possible to localize the source immediately, a later more exact analysis of the recorded signal is performed in the office and it is decided whether the point should be submitted to a more accurate control from the ground with a telescope or should be checked live-line. All relevant defects are listed in a report. In Figure 17.4 a photograph of a spacer damper is shown with a loose connection that was spot by this system, what would not be possible by naked eye. In multi-circuit lines, locating defected faults seem to be less effective, according to experience. The systems based on electrical field monitor distortions produced by bad connections, cracked insulators or other abnormalities.

The *thermal image test*, also called *thermovision*, is used for inspecting energized lines to assess the condition of components which carry the current. The test results are reliable and reflect the actual condition.

Infra-red thermography allows the inspector to see thermal patterns that correspond to severe problems. Normal current flow, for example, through a loose or corroded

connection, results in elevated temperatures as a consequence of increased electrical resistance. Before the temperature is high enough to cause a damage or an outage, the patterns can easily be examined through an infra-red imaging camera. Similarly, a video camera converts thermal radiation into a visible picture. Surface temperature differences as small as 0,3°C can be displayed in black and white or colour temperature maps. Infra-red survey is not suitable to detect conductor corrosion unless there is a large number of broken strands in the conductor.

The thermal image test operates on the flow of current and the corresponding overheating produced if the connection is not well executed. The thermal image inspection requires at least 50 to 60 % of the full load for an adequate performance.

Internal corrosion of *zinc coating* is caused principally by industrial and sea salt pollution in the presence of moisture. Original conductor grease levels, together with condition and thickness of the galvanizing coating of the steel, will determine the rate of corrosion. Corrosion of the zinc coating is temperature dependent and has a maximum between 60 and 70°C. Above this temperature, the rate of corrosion decreases.

When contacting unprotected steel, e. g. after the loss of zinc or aluminium cladding, the aluminium will be sacrificial. The *rate of aluminium corrosion* is high when there are marine and industrial pollutants present. The aluminium and its corrosion products eventually cause the conductor to bulge. Reduction in the aluminium section leads to a loss of mechanical strength and electric conductivity. In severe cases, this causes a transfer of current to the steel and subsequent failure due to overheating. It is possible that all the outside strands of the conductor appear intact whilst inner aluminium wires have severed [17.48].

It is possible in non-polluted areas, for the *unprotected steel* to act as the anode, resulting in loss of section of the steel without loss of aluminium section. No external indication of this process of deterioration will be visible until the conductor fails in tension. *Visual inspection* will not detect corrosion at an early stage. As corrosion becomes more advanced, an experienced line inspector will detect the conductor bulging due to the corrosion products being several times the volume of the aluminium and possible discolouration of several strands.

The *eddy current corrosion detector* [17.49] works in an indirect manner by detecting the loss of galvanizing from the steel strands of the conductor. Loss of galvanizing can be detected by inducing eddy currents into the conductor from a coil that clips around the conductor. The resultant magnetic field is measured with a second coil that is sufficiently sensitive to detect the disturbed field in conductor sections where the galvanizing has been attacked. This detector can be used for ALx/STyz conductors but not where an optical cable has been wrapped on the earth wire.

It can also be used on earth wires made of galvanized steel by adding a plastic shell to the sensing head with adequate number of aluminium wires fitted in it.

The steel core corrosion detector detects a loss in steel cross-sectional area. This area is measured by generating and receiving 2 000 pulses per second: The highest amplitude of every 20 pulses received is recorded on the built-in computer, which compiles the data at 100 points per second. This information can be printed later by the computer's graphic plot program.

Sulphurous pollutants cause *external corrosion* of *aluminium conductors*, i. e. pitting, of the surface where solid impurities are deposited on the outer surface of the conductor. Small corrosion cells are then set up when moisture is present. Normally, this type of corrosion is evenly spread on the outside of the conductor and does not reduce the strength to the same extent as internal corrosion.

Overhead lines are affected by *wind induced oscillation* in form of *aeolian vibration*, *subconductor oscillation*, and *galloping*. In general, the damage can be seen as:

- Drooping/missing/slipped vibration dampers;

- Missing nuts from suspension clamps or hardware;
- Split pins missing or displaced from normal positions in cotter (clevis) pins, etc.;
- Corona rings or insulator strings displaced from their proper positions;
- Broken outer conductor strands, usually emanating from the ends of the suspension clamps;
- Aircraft warning markers moved or missing from conductors or support wires;
- Loose or broken tower members;
- Severe wear of suspension hardware.

In summary, wind induced motions may cause one or more of the following damage to conductors: Fretting, fatigue or abrasion.

The main problem, as with conductor corrosion, is the identification of susceptible line sections to be inspected for incipient damage in due time. The first steel breaks in conductors occur under clamps and spacers and are not detectable by any practical techniques tried to date. However, in good conditions it may be possible to detect broken conductor strands protruding from the clamp by use of visual inspection.

The worn surfaces of fittings are usually very difficult to see from the ground and may even be missed in a climbing or helicopter inspection. In due time, this wear can be sufficient to reduce the remaining strength of the supporting hardware to dangerous levels and to allow the conductor to drop.

Instead of examination by the staff and recording findings on the site, the use of a video camera is reported as a suitable method to survey a line from a helicopter and examine all fittings in a relatively short period. Pictures taken at a long distance allow the majority of components to be examined. The images are recorded and can be analysed later. Broken strands, wear of fittings, defective or loosened spacers and missing or drooping dampers can be detected by this method. This method gives less satisfying results for multi-circuit lines.

Earth wires are installed at the top of high-voltage lines to protect the conductors from lightning strokes. However, although they are designed to have a good level of resistance to lightning impact, phase conductors may suffer *damage from lightning strikes* during particularly severe strokes. The damage varies from pitting of the outer surface, to melting and breakage of outer strands with consequent reduction of the mechanical strength of the conductor. Detection of damage is possible using one of the above mentioned methods.

17.4.2.6 Joints and fittings

Inspection of fittings and *joints* is carried out to prepare corrective measures. Among the fittings used in overhead line conductors, one of the most vital components are the *conductors'* full *tension joints.* To assess the joint condition and its remaining life, a number of inspection methods have been proposed, some of them are difficult if not impractical to apply as they sometimes require work at live line, such as *X ray imaging, infra-red techniques* and *resistance measurements.* The last method is recommended and applied with success according to [17.50] through a technique developed in Sweden. The resistance is obtained indirectly from the temperature of the joint, which is measured with a high accuracy. The resistance is calculated through the AC voltage drop over each half of the joint, current through the conductor and the temperatures of the joint and the conductor.

Papers [17.50] and [17.51] consider the joints as the most critical component that operates in series with the conductor and, therefore, is permanently submitted to full mechanical tensile load. The use of thermography is in this case proposed. Systematic laboratory evaluation of this method has indicated sufficient accuracy. Other conclusions of such experimental investigation are that critical conditions are already reached

when the joint resistance becomes two or three times the resistance of a conductor section of equal length.

Most joints used on ALx/STyz conductors have been of the compression type, although bolted joints are used in jumpers. Overheating of these joints arises from incorrectly constituted compression along the length of the joint, mainly due to either poor design or installation problems. This will allow moisture penetration and results in oxidation of the internal aluminium surfaces between the joint and conductor. The resistive aluminium oxide reduces the paths for current flow and may cause micro arcing within the joint. In cases of malfunction, there is an increase in the contact resistance between the aluminium layers and the aluminium sleeve of the joint giving rise to an increase of the joint temperature. This can be detected using infra-red thermography, being used either from a helicopter or from the ground. It provides evidence for further action and justification for accurate measurement of joint resistance. Over a period of time, the joint resistance will increase, resulting in excess current flowing in the steel core of the conductor, leading to overheating and rupture.

Joints in jumpers are typically bolted parallel groove or compression type or wedge type clamps. Overheating of these joints occurs primarily due to improper preparation and installation of the joint. Under normal conditions, the temperature of the joints will be lower than that of the conductors due to the lower resistance per unit length and to the larger amount of surface area to dissipate the heat generated by the current. To obtain a better assessment of the actual condition of the joint, especially with low currents and/or high wind speeds, it is advisable to record load and wind data and make allowance for operation under standard conditions. Infra-red survey should be carried out at times of adequate thermal loads.

Various devices of joint resistance measurers are available which can be used with live-line or dead-line circuits. The technology used is more direct than infra-red thermography and is not subject to radiation, weather, current loading and background conditions. The lightweight live-line devices are designed to be attached directly to the high-voltage line by the use of an insulated stick and read the resistance of any joint directly in micro-ohms. They can also be designed to simply indicate good or bad for a given joint [17.50] and [17.51].

All the articulated connections in a line experience tear and wear during operation. The wear is high at suspension sets and, in particular, at the suspensions of earth wires and OPGW. The wear may be expected to be further increased in line sections running perpendicular to the main wind direction and at supports with a low vertical load only. The fittings subject to such condition need special attention during inspection.

17.4.2.7 Insulators

Damaged or cracked *cap-and-pin insulators* may be detected while they are in service but suitable precautions should be followed. Maintenance of insulators can distinguish among the following insulator types involved and their behaviour:

- *Glass cap-and-pin insulators* usually present more problems during the first years of operation. The occurrence of insulator units with bubbles and splinters is a common manufacture deficiency which can lead insulators to fail in the beginning of their operational existence. Bubbles usually cause the glass insulators, even when provided with a convenient toughening, to explode when submitted to varying climatic variations. Splinters in their turn are a kind of superficial defects that in most cases are acceptable to a certain extent without causing major failures. However, vandalism cases excepted, glass insulators tend to stabilize and even improve their performance with ageing.

  Glass cap-and-pin insulators are usually inspected by naked eye or telescope,

from a helicopter or from the ground. Electronic systems based on electrical field distortion, such as corona system or net spy system, are also an efficient tool for detecting glass insulator abnormalities, as broken shells, pin reduction etc.

- *Porcelain cap-and-pin insulators* have a different behaviour. Usually they present few failures during the first periods of operation. However, ageing acts in a growing rate as the insulators are submitted to long periods of outdoor operation. Porcelain usually degrades more rapidly than glass, especially in areas with low temperature, so that the rate of insulation defects increases with time.
  The main cause of failure to suspension and tension *cap-and-pin porcelain insulators* is corrosion of the steel pin in the cap and the pin assembly. Surface leakage currents are concentrated at the pin, causing a higher current density in this area and consequent dry band formation around the pin base. Partial discharges bridge these dry bands resulting in severe spark erosion and after rapid removal of the galvanizing, natural corrosion of the pin occurs until the remaining cross-sectional area can no longer support the load. Additionally, the expansive corrosion products create a tensile, hoop stress, which leads to radial cracks in the porcelain. Defective insulators will be more susceptible to failure during a pollution or lightning flashover as the arc passes through the cap of the punctured unit causing it to split open and precipitate a line drop. Most failures of this type have occurred at the live end of suspension strings where the voltage across the shells is highest.
  Incipient radial cracks that occur in porcelain insulator shells and which can initiate tensile fracture, can be detected from ground level using an *insulator voltage drop measurer* by application of a 30 or 50 kV test voltage. This requires extensive outage duration of 1 to 10 hours. Meters have been developed for testing in-situ, dead-line or live-line. This method is time consuming and the reliability of the results is dependent upon the weather, pollution and humidity levels.
  Also *infra-red thermography*, operated from a helicopter or from the ground, can be used to identify defective insulators. The technique can identify defects under favourable conditions where head cracks result in warmer insulator caps. However, the differentiation between warm insulators and cracked insulators is not always great enough to be completely reliable and, therefore, this method should be used in conjunction with the electrical field or voltage drop measurer.
- *Long rod insulators* are electrically puncture-proof. Therefore, they do not require a periodical check of their electric performance. That is economically advantageous. During scheduled line patrol, long rod insulators are checked visually regarding possible mechanical damage of sheds caused by vandalism or arcing. Insulators are replaced if the damage is important. Ageing of modern long rod insulators made of alumineous porcelain is not known.
- *Composite insulators.* Degradation of composite insulators can occur through premature ageing or internal manufacturing defects. It is not possible, using current technology, to choose a single technique that will detect all types of defective insulators with a satisfactory degree of confidence. A combination of two or more techniques has been proved in practice to be the most effective means of identifying defective composite insulators in service [17.52].

17.4.2.8 Clearances

The preservation of safe clearances along the line is an important point to be observed by the patrols, especially in more sensitive areas, such as crossings with other lines or with highways. The patrolling crew needs to be provided with plans for the crossings and tables showing the clearances depending on the conductor temperature in order to

check the conductor position by direct sight. Eventually, during *inspection of clearances*, the patrollers can make measurements with electronic infra-red devices, so as to certify that the minimum design clearances are still kept. Using of scanning technology can also precisely measure clearances but the process is more expensive (see clause 15.3.2.2).

17.4.3 Corrective maintenance

17.4.3.1 Strategy

In addition to the findings on the line conditions based on inspection, an assessment of the future line function in the network is required. Safety-relevant defects need to be repaired immediately. However, other refurbishment activities will depend on the asset owner's decisions. E. g., in a line having a residual life time of some years only, partially worn-out fittings need not to be replaced. Corrective maintenance should be reported in the owner's files. Utilities operate computer data bases for these activities.
Maintenance of the line documentation such as longitudinal profiles, plan layouts, crossing clearances, tower lists etc. is part of the owner's commitments.
Replacements of damaged elements are accomplished either when the line is energized (live-line) or de-energized (dead-line). The line crew should notify the dispatching centre when a particular line or section is desired for maintenance, either under live line or de-energized work. For the latter case, the line should then not be merely cleared through the circuit breaker but opened by disconnectors as well. Automatic reclosing device should be set inactive. If it is to be out of service for an extended period and there is a danger of lightning, the line should be earthed at its terminals for safety reasons. According to some national standards, earthing of circuits to be subjected to maintenance is mandatory [17.53].

17.4.3.2 Refurbishment and upgrading of foundations

Refurbishment and upgrading *of foundations* are dealt within [17.46]. The corrective measures regarding foundations comprise the following processes:

- The treatment of grillage foundations or of metallic elements of foundation types is carried out after cleaning by sand jetting or by hydraulic means, consisting first in applying an epoxy resin or coal tar type paint; in some cases, *cathodic protection* is then applied to impair the corrosion process.
- The structures which have already lost more than 10 % of the steel cross sections need to be replaced because they are considered as being in failure state.
- Those structures which have lost up to 10 % of the cross sections are considered to be able of repair work through mass deposit (electric weld). After such recovery, the foundation is coated as in the latter case and sometimes cathodically protected. ASTM E 376 [17.49] gives basic recommendations for the installation of cathodic protection.

17.4.3.3 Renewal of coating, replacement of tower components

Renewal of coating is necessary in intervals between 10 and 20 years depending on the environmental conditions. It should aim at protecting the galvanization subjected to corrosion to a considerable extent. Galvanization is the basic protection guaranteeing a long life of steel structures. The repair of aerial corrosion is carried out at the following manner:

- Cleaning and painting all components which have lost the galvanizing coating;
- Replacing components which have lost more than 10 % of their mass;
- Restoring with electric weld components which material loss is up to 10 %, since this process is considered as more viable than the replacement.

Table 17.7: Minimum sound cap-and-pin U70BL, U100BL or U120B insulators per string

Voltage kV	500	380	345	230	138	110	69
Usual number of insulators	24 to 26	19 to 21	17	14	9	8	5
Minimum number of sound insulators	15	13	11	7	5	4	2

- Reinforcing of components by bolting plates or angle sections to restore the full load resistance. Frequently, prestressed or fitted bolts are used.

17.4.3.4 Repair of conductors

The following cases are considered:

- Conductors having broken strands are repaired through the application of *conductor repair sleeves*, mainly armor patch rods;
- Conductors with the steel core corroded need to be totally replaced.

Paper [17.54] reports on replacing ACSR having corroded steel cores. Replacing of conductors or earth wires is often carried out in parallel to live conductors. Therefore, the provisions given in clause 16.8.4.10 should be obeyed.

17.4.3.5 Replacement of insulators, fittings, dampers and spacers

17.4.3.5.1 Tasks and priorities

Cap-and-pin porcelain insulators need to be replaced either live-line or dead-line when there are broken shells or corroded metallic parts (pins and sheds). For *insulator replacements*, the minimum number of sound cap-and-pin units per string is shown in Table 17.7 as a function of the voltage level according to practice in South America. This table shows the minimum number of sound units required for safe live-line work. Glass insulators are replaced when they are broken but keeping their mechanical function.

Live-line replacement has been not necessary for long rod insulators, because there are practically no failures of sheds or bodies and the system permits to switch off a circuit keeping the service through other lines. However, live-line replacement of old defective long rod insulators could be carried out where required.

Replacement of fittings, dampers and spacers is always total, i. e. no part thereof is changed separately. For replacing spacers and spacer dampers and installing repair joints, e. g. patch rods on damaged conductors, line cars are used where possible in view of labour safety.

The priority of performing a certain replacement task is related to the urgency of the repair. Worse problems should have priority over problems of lower severity. The classification of the priority should take into account the component where the problem was detected, as well as the importance of the line, the main loads supplied and the performance required. The priorities of the repair or maintenance services can be classified in four groups, namely:

- Priority U: Urgent repair
- Priority A: Immediate repair
- Priority B: Repair less than one year
- Priority C: Repair in more than one year

The method adopted for the replacement of components is important because it defines the tools and equipment required, the agreement with operating personnel for line outages etc. It is preferable to carry out replacements on de-energized lines, since it permits to carry out the tasks most effectively. Live-line techniques may be adopted where switching off is not feasible or would be expensive.

Table 17.8: Clearances to linemen for live-line working

Voltage kV	36,0	72,5	145	245	362	525	765
Minimum clearances m	0,70	0,92	1,10	1,55	2,20	3,60	4,60

17.4.3.5.2 Dead-line work

Dead-line work requires that the line should be switched off and earthed. Beside the earthing made at the line terminals in the substations, each working crew should install its own temporary and clearly visible earthing system aiming at protecting the electricians against accidental energization, induced voltages, atmospheric overvoltages etc. For accomplishing temporary earthings, heavy extra-flexible copper cables are specified, being attached by means of hot-line tools and clamps; the line is considered to be hot until the earthing system is applied.

17.4.3.5.3 Live-line work

To carry out diagnostics, repairs and replacements without switching off a circuit methods and tools for *live-line work* have been developed. Papers [17.55] and [17.56] give a good account of the state of the art. According to [17.57], four categories are distinguished:

- Contact or *barehand work*, in which the lineman and the equipment, for example the helicopter, are energized at the phase potential and fully insulated from other energized parts and earth. This category is used on the highest voltage systems. Details are given in [17.56].
- At-a-distance or *hot-stick work*, in which the lineman uses insulating (fibreglass) sticks to perform work on energized parts. This category is used on intermediate voltage systems.
- *Insulated glove work*, in which the lineman is fully insulated from all energized parts by the use of insulating gloves, sleeves and cover-up equipment. This category is used on systems below 60 kV.
- *De-energized work*, in which work is performed only after the system is de-energized. This category of work is also considered as live working for the following three reasons:
  - The parts that will be handled by the linemen may be at non-zero potential just prior to earthing;
  - The parts that will be handled by the linemen may be at non-zero potential immediately after earthing connections are removed;
  - Significant potentials may appear at the worksite in case of accidental energization of the system.

Some care must be taken when a live-line work is performed among which the following should be mentioned:

- Safety clearances according to [17.51], determined as a function of some voltage levels prescribed in IEC 60 071-1 [17.58] and IEC 61 472 [17.59] are shown in Table 17.8.
- *Live-line tools* and equipment such as sticks, ladders and ropes must be rigorously clean and should be tested before beginning every service to ascertain that their insulation is perfect. Such equipment should be stored in stoves to prevent the absorption of moisture.
- Atmospheric conditions need to be obeyed. No live-line work should be performed when the weather is rainy, snowy, heavily clouded or subjected to lightning strokes.
- Operative conditions require agreements made with operating personnel and must warrant that reclosing of circuit breakers, either manually or automatically, be

prevented. If the line is switched off, reclosing can only be performed after the authorization by the maintenance crew. All the personnel involved in live-line work must be able to perfectly master the working techniques. The methods used in each service should be previously studied and examined to avoid improvisations.
- For every job, a specific instruction is developed, listing the tools which will be used, the number of linemen required and the job stages, step by step. The loads to which every tool will be submitted during all phases of the work need to be carefully analysed.

17.4.3.6 Clearing of right-of-way, trimming of trees

Right-of-way clearing is carried out according to a planned schedule. The lines or parts of long lines are split in separate groups and each group is cleared in one year so that at the end of the scheduled cycle the complete network has been cleared. The cycle depends on the climate and vegetation. In tropical countries, the frequency may be three years, in moderate climate five to ten years. In this work, the trimming of trees is performed and the vegetation is selectively cleared so as to keep the necessary safety clearances. Special attention should be paid to sugarcane plantations, e. g. because of the high possibility of firing and, therefore, line switching off due to the exhausted gases. It should be aimed at avoiding chemical clearing due to the possible environmental damages to crops, fauna and flora. In Central Europe and other regions, this method is not anymore accepted but may be permitted elsewhere under certain limitations. Tree gangs whose sole duty is to remove brush, trim trees and remove danger timber have been found to be advantageous by large utilities.

As an example for right-of-way management, the procedures introduced by RWE in Germany should be mentioned here [17.60]. RWE is presently the largest private utility in Europe; its power line system exceeds 25 000 km. RWE considers ecological planning of right-of-way management important now. Scientific studies suggest that several successive years of clear-cutting and tree-trimming can improve the ecological situation because such successive processes are rather rare in open cultivated landscapes as well as in forested areas. From an ecological point of view, the following activities are recommended:

- Selective advancement of small and low-growing plant species to minimize the effects of separating the right-of-way;
- Developing vegetation which stabilizes the edge of the forest;
- Realization of vegetation maintenance techniques appropriate for specific sections;
- No service in tree- and shrub-free primary sites;
- Preservation of natural ground reliefs;
- Mowing, if necessary, at long-term intervals.

Forests in Central Europe have been affected by intensive human use for more than 1 000 years. Accordingly, natural forests are rare nowadays. In the course of time, all utility companies have turned away from complete clear-cutting and the application of herbicides in the right-of-way through forests. The main objective today is to optimize the right-of-way maintenance ecological, economic and technical framework. One important step towards achieving this goal is support of slow-growing species with heights ending far below the lines. The aim of these measures is to develop a stepped structure across the corridor to the edge of the forest as shown in Figure 17.5. This decreases vegetation maintenance costs and improves ecologically the right-of-way. It also helps to ensure the reliability of electric systems by stabilizing the adjoining forest stand.

The restructuring of vegetation systems has to be planned and realized continuously by long-term programs. Before planning activities can start, the following basic information is required:

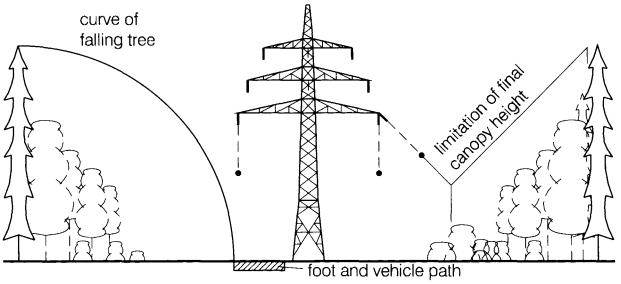

Figure 17.5: Developing a stepped structure across the line corridor in forests (RWE Net AG, Germany

- Extent and exact location of nature reserves, i. e. forest, water and soil;
- Owner of the property;
- Ecological importance of the area;
- Recording and description of the ecological system.

Based on this information, a concept for future maintenance has been developed. Besides meeting all technical requirements, control procedures for certain parts of the corridor are defined by determining the method, scale and interval. This process helps to ensure that, as a first step, each right-of-way is optimized according to the ecological possibilities. The final optimization process depends on economic and safety perspectives. Corrective actions will be realized if needed. The different maintenance activities are recorded in operation maps. In order to ensure the sustainability of the actions, the biotope management planning procedure is coordinated by competent authorities, nature conservation organisations and property owners.

Right-of-way maintenance in developed areas and in open cultivated landscape is different to that in forests. The control procedures, in contrast to forested areas, have to take care of a large number of isolated shrubs and trees on wayside, in fields, gardens and parks. There, it is essential that all actions should be carried out with great respect to the sensibility of individual land owners. To improve the maintenance procedure outside forests, RWE has developed a data base management system which documents hundreds of independent actions. The basic information, such as procedure of maintenance, landowner and nature preserve, is collected, documented and transferred to a land register data bank.

The physical *vegetation control* procedures are carried out either by utility staff or by contractors. In both cases, it has to be ensured that all control procedures will be performed correctly, according to requirements of the competent authorities and internal entrepreneurial guidelines. Therefore, the relevant knowledge, including modified theoretical background information and requirements by authorities, are imparted by training and practical introductions. Each predefined step of action is followed by quality control measures, which are also useful for controlling and optimizing costs of maintenance. Acquired information is used to assist future planning activities.

Today, electric utility companies like RWE endeavour to develop new strategies for right-of-way maintenance that fulfil ecological and economic requirements. The proposed concept for a long-term oriented vegetation management program, performed without the application of herbicides, helps to take into account the different interests of the competent authorities, property owners and the public.

There are several strategies adopted by RWE depending on the vegetation encountered along the right-of-way. The right-of-way area is divided in several plots forming a chess board or a fishbone pattern (Figure 17.6) and vegetation is controlled successively in one group of plots in one year and maintenance carried out on other plots on the

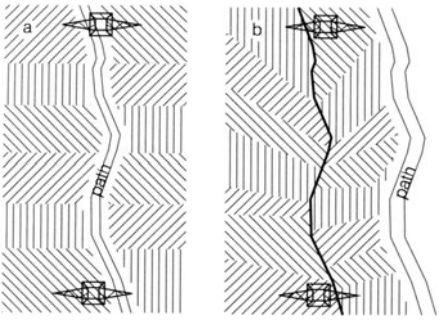

Figure 17.6: Division of right-of-way in vegetation control zones. a chess board pattern; b fishbone pattern (RWE Net AG, Germany)

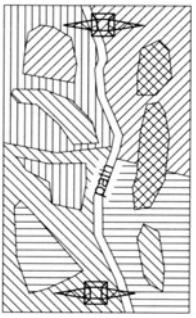

Figure 17.7: Right-of-way management through vegetation islands (RWE Net AG, Germany)

following years. If there is a natural structure of the right-of-way formed by vegetation islands, the management follows this structure by carrying out activities on certain islands according to a regular schedule (Figure 17.7).

17.4.3.7 Access roads

The *maintenance of the access roads* to the towers is of high importance for lines in remote areas and is reported to present some problems at individual lines. When support failures occur, it has been observed that the access to the tower sites is sometimes impractical because the access roads were damaged or even totally destroyed. Agreements with land owners should be kept regarding a minimum preservation of access roads.

17.4.3.8 Earthing

Earthing installations, essential to keep the lightning performance and safety of the line as designed, and any protective measures against inadmissible touch voltages need to be repaired where necessary as a result of inspection or measurements. The same principles apply as to earthing installation at new lines (see Chapter 5).

17.4.4 Investigation of line failures

17.4.4.1 General

Line failures occur infrequently; however, these failures provide a valuable opportunity to increase the understanding of transmission line behaviour. A systematic investigation can provide information which may be used to improve design criteria or the investigation may reveal that the conditions were extraordinarily rare and in excess of design criteria and no modification of the criteria seems justified. Consequently, the goal of any failure investigation is to establish the cause of the failure and determine what change to design criteria and installation is appropriate, if any.

17.4.4.2 Causes of failure

The *causes of line failures* can be grouped as follows:

***Natural phenomena* exceeding design conditions**

- Extreme wind;
- Extreme ice loads;
- Combined wind and ice loads;

- Lightning strokes;
- Conductor vibrations and galloping;
- Avalanches;
- Landslides;
- Flooding.

External effects

- Sabotage, vandalism, theft of members and bolts;
- Damage caused by equipment and vehicles, airplanes, cranes, etc.

Structural deficiency

- Design inadequacies of structures;
- Missing members or bolts caused by vibration or vandalism;
- Misfabricated members resulting in incorrect size, length or grade of steel;
- Inadequate foundations concerning concrete quality;
- Bad workmanship.

Conductor, earth wire and hardware deficiencies

- Improper wire splices due to design and installation;
- Faulty or inadequate hardware;
- Fatigue failure of wire or hardware components;
- Puncture of insulators.

Construction related causes

- All kinds of installation deficiency not detected during final inspection;
- Excess vertical load during stringing;
- Excess longitudinal load during stringing, e. g. caused by running board hanging up in the stringing block or by anchoring;
- Residual stresses caused by overloading during construction;
- Improper stringing sequence during reconductoring.

Operation related causes

- Overvoltages;
- Pollution.

17.4.4.3 Investigation procedures

The first principle for *investigation procedures* consists in avoiding premature judgements as to a failure cause until a thorough investigation is completed. At first it should be attempted to eliminate events that may not have happened. Then, several failure scenarios should be postulated and the data examined to see which one, if any, is supported by the data. When possible, a team approach should be used in the investigation. Members of the team can complement one another, and possibly supply valuable theories and pieces of information which might be overlooked by an individual. Prior to visiting the site, a review should be carried out on the plan and profile, construction data, stringing manual and other pertinent design information. The equipment useful for field investigations should be arranged, such as pocket scale, cloth measuring tape, micrometer, notebooks, markers, identification tags, safety gear, pocket tape recorders, binoculars, photographic equipment with standard and teleobjective lens etc. If the line crews have already arrived at the site for starting repair operations, the necessary period of time should be obtained for a *visual inspection* of the damaged line section. An overall picture of the site and of details may provide information which could be lost after the repair activity has started. The first impression on site should be recorded as it can result in a multitude of ideas about the failure.

Sketches and notes should be prepared of the damaged portion of the line, showing position of conductors, insulators, towers, guy anchors, foundations and any indication of the conductors having been pulled across the ground. A reference coordinate system

can be helpful in identifying the location and orientation of displayed parts of the structure. Each photograph should be indicated on a sketch. Interviews with individuals living in the area of the failed line should be made as an additional source of information. If the wind is suspected as the cause of failure, damage to surrounding trees, buildings etc. should be looked for. The use of the Beaufort Scale (see clause 6.3.2) can provide valuable information as to the approximate wind velocity. Report [17.61] gives information on ice observations in Canada and [17.34, 17.62] provide guidelines to collect ice data on overhead power lines.

Any attempt should be made to determine the *trigger mechanism* that initiated the line failures. Signs of rust on sheared surfaces indicate that the bolt or member may have partially failed previously; burn marks on the conductor or tower indicate initial point of discharge to ground; missing or loose bolts may give hints to sabotage. If hardware, insulators, conductors or overhead earth wires are broken, they may have contributed to the failure, some severed specimens should be retrieved. It may be desirable to remove tower steel from selected tower members for material tests.

A search for design inadequacies should be done such as: Conductor weaker than towers, combined loading producing critical member stress not previously considered, premature foundation failures. Weather data from nearest weather station should be asked for. The field data need to be studied carefully, trying to match field data with postulated cause of failure. If the structure appears to have failed below the design loads, a more detailed analysis may be initiated, taking into account secondary stresses due to bending and non-linearities. Conductor behaviour and its potential effect on the transmission line system should be examined.

An initial *failure report* should be prepared detailing the investigation and outlining the resulting conclusions. These should cover the following information:

- Line tripped out of service due to structure failure: Did the tower or foundations fail completely? Were adjacent towers affected?
- Line remained in service even with damaged structure: Has the line to be taken out of service to repair damage?
- The conclusions should define if the damage was initiated by foundation, structure, conductor or hardware failure.

The utilities legal staff should review the initial report and determine if there are any legal problems involved. The initial report should be circulated to other utilities, comments should be solicited. All the information gained during the investigation process should be incorporated into a final report.

17.4.4.4 Experience on line failures

An investigation was carried out by Cigré through a questionnaire in the period 1991 to 1996, regarding *transmission line failures* that occurred around the world [17.63]. The investigation documented in this project aimed at compiling *failures of towers* and foundations and trying to analyse them inside a statistical approach. A total of around 300 failures was surveyed, involving more than 1 700 towers. In Table 17.9, a summary is presented of the events reported. Some common observations and realistic conclusions could be extracted:

- A total sample of around 50 000 km of overhead lines, involving more than 100 000 towers, during an average period of 15 years, experienced the failures analysed in this project. The sample is statistically big enough to permit deductions and conclusions herein presented.
- The great majority of the failures documented were originated from causes that can be statistically treated: Wind, ice or wind plus ice, although such treatment had not been used in the original project design.

Table 17.9: Summary of line failures as per origin

Cause of failure	HV lines, voltage ≤ 240 kV			EHV lines, voltage > 240 kV		
	Events	Towers failed	Special aspects	Events	Towers failed	Special aspects
Wind	94	606	high wind, cyclone, thunderstorm, cascading effect	45	240	high wind, tornado, thunderstorm, inadequate design
Ice	28	205	cascading effect	9	469	wet snow, ice, cascading effect
Wind and ice	65	122	snow and wind	16	21	no information
Broken conductor or shield wire	4	16	–	–	–	–
Hardware failure	4	4	insulator hardware or clamp failure, corrosion	6	6	bolt or hardware breakage, stress corrosion
Vandalism	1	1	bolt removal, theft	3	4	sabotage, bolt removal, theft
Impact of vehicles	3	3	farming tractor, airplane	–	–	farming tractor
Soil sliding, overflow	8	17	overflow, avalanche	2	5	mud sliding
Others	8	8	flood, fire	1	1	airplane clashing
Total	215	982		84	749	

- The use of *statistical methods* to evaluate climatic loads would have prevented some of the failures, of course, if enough statistical data had been available at the time of the projects. However, a better knowledge of such phenomena, obtained through measurements, would have led the line designer to increase their design loads in regions prone to higher winds or ice accretions. On the other hand, line designs in regions of milder wind or ice activities would have led to more economic lines. This point emphasized the recommendations to install more *measurement stations* for climatic variables to improve the statistical data.
- Among all the events of which some information or a more detailed description had been received, a very low percentage of *foundation failures* was reported, as compared with *tower failures*. Thus, the extension of the probabilistic approach to the foundation design, even with a reliability level higher than the one used for the supports, could result in more economic foundations and, therefore, in global cost savings.
- Examining the failures under the viewpoint of strength coordination, a few comments can be made on the suggestions made in IEC 60 826 [17.64]: Suspension towers proved to be really the weakest component, as compared with angle towers, dead-end towers and conductors. The *strength coordination* within major components is seemingly tower, hardware, foundations, the foundations seem to be the last component to fail. Within the conductor system, the observed coordination seems to be insulators, hardware, conductors, that is, the conductors are the strongest component. Thus, it seems that failures due to conductor failure could be taken as an indication that security loads were not adequately considered.
  In general, it can be concluded that the strength coordination set up by [17.64] seems to be the most adequate and, therefore, be kept as it is. Line designers keep in mind making the low-cost components, insulators and hardware, stronger than the high-cost conductors.
- The great majority of the failures occurred in lines which were only deterministically treated. In few cases, the use of *probabilistic methods* was reported, not for

the original line design itself but for the redesign or repair of the failed towers, especially. Often the *design criteria* for new lines were amended, based on the statistical re-evaluation of the failures. In one case, the feasibility and advantage of using the probabilistic approach turned out evident. Thus, the reappraisal of the lines after failures under a statistical approach proved to be an efficient way to establish a certain reliability level for that line henceforth. A clear conclusion is that when a failure occurs in a line, the statistical evaluation of the loads as a function of the real spans and tower heights, can result in significant savings on the required reinforcements.

- Due to the failure descriptions, high costs incurred in the repairs, both direct costs and lost-energy costs. Such high costs of repairs show the importance of correctly choosing the reliability level for a line, as a low *reliability level* means generally a low initial investment but higher maintenance and repair costs in the future and vice-versa. A true *line optimization* has to take this point into account.
  Concerning the silhouettes and construction types of the failed towers, no reference is made in [17.63] to concrete poles. Just one failed wood pole line was described. Among the metallic towers, there is a wide variation of types involved in the failures, self-supporting and guyed structures, steel poles etc., with no apparent advantage of one design type over the others.
- The change of *design criteria*, especially regarding ice loads, has occurred frequently, as a consequence of failures. It seems that ice load criteria have been often defined in the past without having enough climatic measurements or experience. As the time passed, the occurrence of failures and the execution of more ice measurements have permitted the improvement of the design criteria regarding ice loads. In [17.65] suggestions are made for design ice loads in Germany based on the evaluation of line failures.
- The occurrence of high-wind events known as *transverse cascades* or cyclonic winds resulting in tower failures has been also reported, showing that they are not a rare phenomenon. These can require other design assumptions, as not yet considered in existing lines.

17.5 Reliability and availability

17.5.1 Introduction and definitions

Reliability and *availability* of the overhead lines have become of growing interest in the exchange of electric energy after the *deregulation process* of the electric systems. Private suppliers and line owners assess electric systems under a set of new market conditions, in which the *continuity of services* of the electric supply is of paramount importance. It is not possible to design a power system with hundred percent reliability. However, power system managers and engineers strive to obtain the highest possible system reliability within their socio-economic constraints. In addition to the terms listed in clause 17.3.1, the list below shows basic definitions of some main items directly or indirectly related to line performance, reliability and availability (see also [17.66]).

***Absolute unavailability* (%):** *Total unavailable time* divided by *period duration* and multiplied by 100.

***Forced energy unavailability* (FEU):** It is an index that measures the percent ratio between the number of forced unavailable hours of a line during one year divided by the total number of hours of one year.

***Forced outage*:** The outage due to unscheduled putting out of service of a circuit. It refers to automatic or emergency de-energizing of a circuit.

***Forced outage frequency* (1/100 km·a):** Number of forced outages divided by kilometer and years.

***Forced outage rate* (FOR):** Ratio between the mean time to repair and the number of hours per year.

***Forced unavailable time* (h):** Elapsed time (hours) required to completely restore the circuit to service after a forced outage.

Kilometer–year (km·a): Summation of the product of line or circuit length (km) and the period duration (years) for the lines or circuits.

***Maintainability*:** The ability of a component or element to be retained in or to be restored to a state in which it can perform a *required function* when *maintenance* is performed using the required resources following stated procedures.

***Mean time between failures* (MTBF):** Index that measures the average time elapsed between two consecutive failures.

***Mean time to repair* (MTTR) (h/a):** Average time for repairing the non-scheduled failures, expressed in hours per year.

***Mean unavailability duration* (h):** Total unavailable times (hours) divided by the number of forced outages.

Number of forced outages: Number of circuit related forced outages during the period duration.

***Outage duration*:** The time during which a circuit was incapable of performing its required function within a specified period of time.

***Period duration* (a):** Number of years of observation of forced outages.

***Planned* or scheduled *outage*:** The outage due to the programmed taking out of service of a circuit.

Relative unavailability (%/100 km): *Total unavailability time (years)* divided by kilometer-years (100 km·a) and multiplied by 100. The relative unavailability is equal to the product of forced outage frequency (1/(100 km·a) and period duration (a) multiplied by 100 or absolute unavailability times 100 divided by the line length.

***Safety*:** The ability of an overhead line not to cause injuries to humans and animals or loss of lives.

***Scheduled energy unavailability* (SEU):** Index that measures the percent ratio between the number of unavailable hours of a line in one year divided by the total number of hours of one year (8760).

***Security*:** The ability of an overhead line to be protected from a major collapse (cascading effect) if a failure is triggered in a given component.

***Sustained forced outage*:** Forced outage of which the outage duration is one minute or more.

***Total unavailable time* (h):** Summation of forced unavailable times (hours) of a circuit during the period duration.

***Transient forced outage*:** Forced outage when outage duration is less than one minute.

***Unavailability*:** The state of a component being unable to perform its required function.

***Unreliability*:** Complement to *reliability* or the probability of occurrence of a *component or element failure.*

17.5.2 Energy availability, general description and guidelines

17.5.2.1 Availability

The *availability* is measured in number of hours that an electric system is able to perform its function. It depends on the individual availability of every major component, such as transformers, circuit breakers, instrument transformers, bus bars and overhead lines. Here, only the availability of the overhead lines is dealt with, considering both mechanical and electrical availability. The *mechanical availability* of the line is defined on the base of the following assumptions:

- Risk of outage of the line caused by mechanical failure of towers is computed according to [17.64] by
$$P_{fl} = 1/(2\,T_r) \quad , \tag{17.17}$$
where P_{fl} is the yearly failure probability and T_r the return period of ultimate loads.
- Risk of outage of the line caused by mechanical failure of other mechanical components is generally taken as an empirical value at the order of 30 % of the risk of a tower failure.

The *electric unavailability* of a line relates to failures comprising three main sources, namely:

- The failure rate of the line as a consequence of lightning discharges on the line that may cause overvoltages and flashovers with the following line outage. This kind of failures is measured with the index *forced outages/(100 km · a)*;
- Flashovers caused by switching overvoltages that may exceed the line insulation. Its consequences are usually measured in terms of *flashover probability* (POF) and its order of magnitude is usually small and in the range of one outage per 100 to 1 000 switching operations. This index is usually small and can be neglected when determining line unavailability;
- Flashovers caused by power frequency overvoltages.

The summation of the mechanical and of the electrical unavailability of a line composes the total *unavailability* of the line. The availability of the line is, therefore, the complement to 100 % of the unavailability.

The mechanical portion of *forced energy unavailability (FEU)* of a transmission line is mainly based on the probability of mechanical failures of the weakest link, considered to be the suspension tower, according to IEC 60826 [17.64]. It depends on the assumed return period of the climatic loads causing the design stress. The failures of all the other components such as conductors, insulators, foundations, can add not more than about 30 % to the tower failures in order to compose the mechanical unavailability.

The electric portion of the forced energy unavailability (FEU) of a transmission line depends predominantly on the probability of electric failures produced by lightning overvoltages. The risk of permanent outages associated with lightning flashovers, that result in unsuccessful reclosing operation of the line, is considered as an average of around 35 % of the total lightning flashovers determining the number of line outages/(100 km·a) as obtained by different line performance assessment methods. The *average time to repair* of the above mentioned fault is assumed to be between two and four hours, according to utility experience.

As a second cause, it should be considered the occurrence of failures due to power frequency flashovers associated with different causes, such as vegetation burning underneath the line, branches of trees touching on the conductors, non-restorable flashovers, associated with breaking of insulator shells. This component accounts in average to 0,3 events per year according to utilities' experience. The average time to repair the above failure can be assumed to be about eight hours.

All maintenance operations that require switching off an overhead line are considered in the calculation of the scheduled time while the line must be out. The determination of the *scheduled energy unavailability (SEU)* and its reduction to a minimum should take into account several measures such as:

- A rigorous program of *routine maintenance* on the line components should be established. So it will be important to predict, detect, remove and replace faulty components, thus actually preventing the development of permanent faults or long-lasting line outages.
- A minimum of *spare components* supplied and stored in conveniently located places along the line, so as to speed up emergency restorations.
- Live-line maintenance, either by the stick-rod method or by the bare-hand method could be programmed for the line [17.67], if permitted and adquate.
- The maintenance crews should be planned to be sited so as to reach failure areas or components inside not more than few hours after the occurrence of a failure having the consequence of an unscheduled outage.
- The *lightning performance* is predicted to be about one outage/(100 km·a) (see clause 4.4.4). A convenient *reclosing scheme* can avoid that about 65 % of such outages degenerate into permanent outages. To keep that performance, it is important that the number of broken insulators per string be kept the lowest possible through an adequate preventive maintenance program.

17.5.2.2 Determination of energy availability, example

The main indices of availability and reliability as described and defined above will be presented by means of an example. A 500 kV line, 350 km long, will be considered in this example, and the number of line outages due to lightning will be taken as 1/(100 km·a), resulting in an average number of 3,5 outages/a.

The proposed unavailability to be expected can be determined as follows:

- Mechanical unavailability of the towers follows from (17.17) assuming a return period of 150 a for ultimate loads and considering an average failure duration of 7 days. According to [17.62], the line length above 100 km may be considered by increasing the probability of extreme load and associated failures in relation to the length of a line. For the line in question, the return period of the ultimate load would be $150 \cdot (100/350) \approx 43$ a. Hence, forced unavailable time is $(1/(43 \cdot 2)) \cdot 24 \cdot 7 \sim 2,0$ h/a or $P_{\mathrm{f1m}} = 2,0 \cdot 100/8760 = 0,022$ %.
- Mechanical unavailability of other components is considered not to exceed 30 % of the unavailability of the towers

  $$P_{\mathrm{f2m}} = 0,3 \cdot 0,022 = 0,007\ \% \quad .$$

Therefore, the mechanical unavailability is 0,029 % in total.

- The *electric unavailability* is due to unsuccessful reclosing operations and to failures at power frequency voltage. In the first case, it is considered that 35 % of the operations are not successful and that every line outage lasts two hours in average:

  $$P_{\mathrm{f1\,el}} = 0,35 \cdot 3,5 \cdot 2 = 2,45\ \mathrm{h/a} \quad \text{or}$$

  $$P_{\mathrm{f1\,el}} = 2,45/8760 \cdot 100 = 0,028\ \% \quad .$$

  From adverse weather conditions during power frequency voltage, 0,3 events per year are assumed lasting on average eight hours:

  $$P_{\mathrm{f2\,el}} = 0,3 \cdot 8 = 2,4\ \mathrm{h} \quad \text{or}$$

  $$P_{\mathrm{f2\,el}} = 2,4/8760 \cdot 100 = 0,027\ \% \quad .$$

Therefore, the total electrical unavailability is 0,055 %.

The summary of the predicted unavailability for the example is: Mechanical unavailability: 0,029 %, electrical unavailability: 0,055 %. Therefore, the *forced energy unavailability (FEU)* is 0,084 %.

The scheduled unavailability for the transmission lines is based on approximately three outages/year, with an average duration of eight hours per outage reaching a scheduled unavailability of

$$\mathrm{SEU} = 3 \cdot 8 \cdot 100/8760 = 0,27\ \%.$$

The scheduled energy unavailability is much higher than the forced unavailability.
The *energy availability (EA)* is defined by

$$EA = 100 - (FEU + SEU) \quad .$$

With the data determined above, it is obtained for the example

$$EA = 100 - (0,084 + 0,27) \quad \text{or} \quad EA = 99,65\ \% \quad .$$

The index EA determined above refers to transmission line scheduled and forced unavailability. However, in order to determine the index EA, valid for the whole electric system, all other unavailability indices, related to other components of the system, should also be calculated and added to the line unavailability index. Then, the complement to 100 % should be determined. According to the calculations already performed, the sum of the forced outages considering both lightning and power frequency events are $3,5 + 0,3 = 3,8$ failures per year. The period corresponding to these failures is $2,45 + 2,4 = 4,85$ hours (rounded value 5 hours). The *mean time between failure* will be, therefore, for the example

$$MTBF = 8760/3,8 - 5 = 2303 \text{ hours.}$$

If all outage periods of the line are duly added, it results for the *mean time to repair*:

MTTR = 5,6 hours per year (rounded value MTTR 6 hours).

The *forced outage rate (FOR)* relates to forced outages and is the ratio between the mean time to repair and the number of hours per year. For the example, this index will be:

$$FOR = 6 \cdot 100/8760 = 0,068\ \% \quad .$$

17.6 Line refurbishment, upgrading and uprating

17.6.1 Definitions

The need of new lines, also adopting higher voltages, to increase the transmission capacity of existing trunks has existed permanently, as the load growth and system development continue to be significant. However, obtaining new servitude and corridors becomes increasingly difficult and expensive.
Therefore, taking advantage of existing overhead lines and improving their transmission capacities, has been an extensively used tool. Then, new servitude are not required.
The increased use of existing lines and rights-of-way can be achieved by three methods:

- Increasing the power transmitted by the line through increasing the conductor design temperature, or alternatively, by replacing conductors or by increasing the voltage, or both, defined as *uprating*;
- Increasing the reliability of the line, defined as *upgrading* and
- Repair of damaged components or restoring their capacities, defined as *refurbishment*.

The first method – *uprating* – can be practically accomplished by increasing the design temperature of the existing conductors if they are not to be changed, or by using bigger conductor cross sections, or other types with higher current rating.
Another type of uprating consists in increasing the insulation levels, if feasible, or compacting the line, that will eventually operate with lower insulation levels from thereon if the compaction would not be viable by keeping insulation on the original level.
The second method – *upgrading* – refers to the line components such as towers, conductors, foundations so as to increase the line reliability level, for instance by reducing the annual risk of failure from $2 \cdot 10^{-2}$ to level $10^{-2,5}$
The third method – *refurbishment* – consists simply in renovating the deteriorated or weathered line components, so restoring their ability to a sound operation without upgrading or uprating.

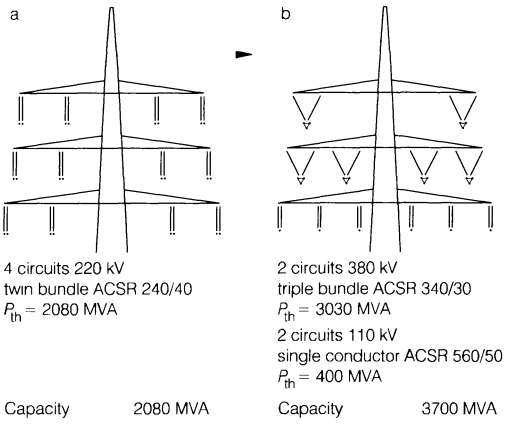

Figure 17.8: Conversion of a 220 kV four-circuit line to a line with two circuits 380 kV and two circuits 110 kV
a before conversion;
b after conversion

17.6.2 Uprating

17.6.2.1 Current uprating

If the voltages and the conductors are to be kept, the current can be increased by amending the line for a higher conductor temperature. If a line was plotted using 50°C as the conductor temperature and it is intended to increase the conductor temperature to 80°C, what would correspond to about 30 % more power, a complete redesign of the line should be carried out, in order to solve clearance-to-ground and clearance-to-obstacles problems which may arise at the new conductor temperature. The activities required are usually as follows:

- Direct measurement of *conductor temperatures* and clearances of conductor to ground or to obstacles. A field check is also recommended of the span lengths, tower heights, conductor tensions, etc. Eventually, a new topographic survey may be required. Modern tools have been developed in the recent years for surveying exactly the existing conditions of a line by laser scanning (see clause 15.3.2.2).
- Using measurements or a new survey (see clause 15.3.6) together with the original design data, if available, the line should be redesigned so that the least and cheapest modifications are required, only.
- Agreement should be made between operating and maintenance personnel about the schedule of works required at the line, so that working procedures either at live-line or dead-line can be established, with no or minimum line outages.

Common modifications for this kind of current uprating of an existing line are:

- Replacement of existing structures by higher structures in order to increase conductor heights and, therefore, clearances of conductor to ground and to obstacles. This activity usually requires some line outages, unless a provisional parallel line section is built.
- Insertion of structures at midspan position to increase conductor heights. As in the latter case, this work requires some hours of line outages.
- Restringing of conductors and earth wires, to increase conductor heights. This job requires some line outages as well. The mechanical resistance of the structures should be checked as higher longitudinal loads will be applied to them. Eventually field tests on components, such as structures or foundations, may be necessary.

17.6.2.2 Uprating by reconductoring or voltage increase

Voltage increase or *reconductoring* may impose a new set of load conditions to the supports. Thus, the structural design should be re-evaluated for new transverse, lon-

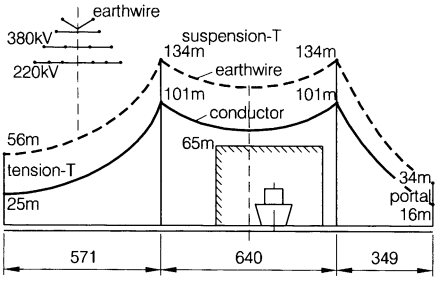

Figure 17.9: Profile of the 220/380 kV river Weser crossing

gitudinal and vertical loads. In [17.68], some examples for uprating are represented. A four-circuit line in Germany installed in 1965 and situated in the highly-industrialized Ruhr area, had been equipped with four circuits of twin bundle 243-AL1/39-ST1A. Closing of a 380 kV ring was only possible using this existing right-of-way and maintaining the sites for 22 tension and 13 suspension towers. During the approval procedures, an agreement was achieved with the authorities to transfer a parallel 110 kV distribution line to the line under construction and to abandon this right-of-way. Due to the high number of residential areas along the right-of-way, no tower site could be moved and the width of the right-of-way and tower heights not be changed. The selected tower top geometry (Figure 17.8) takes into account this requirements.

To arrive at the planning target of 3 300 MW transmission capacity, a decision had to be made on the 380 kV circuits to use a quadruple bundle 264-AL1/34-ST1A or a triple bundle 382-AL1/49-ST1A. In view of the more favourable swinging properties, the triple bundle was finally selected. The total capacity was increased approximately by 1 600 MW.

In order to comply with the stipulations concerning clearances, sags and widths of right-of-way, conductor tensile forces varying by ± 7,5 % within the individual line sections were adopted. New tower tops with adjusted insulation, new conductors and reinforcement of foundations and tower bodies were necessary for the implementation of the modifications.

17.6.2.3 Replacement of earth wire by optical cables (OPGW)

Another kind of modification that has become very common in existing overhead lines is the replacement of one or two conventional earth wires by OPGW. The optical cables are aimed at transmitting telecommunication signals and the use of overhead lines for such purposes has turned out advantageous (see Chapter 8).

17.6.3 Upgrading

17.6.3.1 Introduction

According to the definition given in clause 17.3.1, *upgrading* means increasing the original mechanical or electric strength of a line or a component, e. g. to adjust the line to higher meteorological actions. In this case, it should be aimed at reducing the probability of failure by one order of magnitude, e. g. from $2 \cdot 10^{-2}$ to $2 \cdot 10^{-3}$ because of the uncertainties in the basic data.

17.6.3.2 Upgrading of a 380/220 kV river crossing in Germany

In 1968, a transmission line comprising two 380/220 kV circuits with triple bundle 434-AL1/56-ST1A and two 220 kV circuits with single 434-AL1/56-ST1A was constructed across the river Weser in Germany. The two suspension towers reached a height of

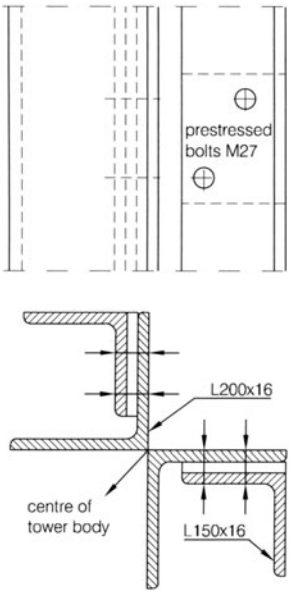

Figure 17.10: Reinforcement of a leg member

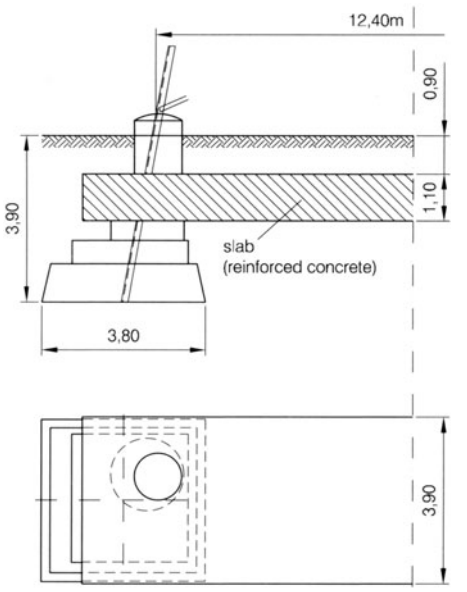

Figure 17.11: Upgrading a tension tower foundation (380/110 kV line Kastenweiher-Hausen, Germany)

134 m (Figure 17.9). The line has been in operation without any problems since commissioning.

The line had been designed according to the German standard valid at the time of construction. More recently, the utility in charge decided to analyse the reliability of the crossing under amended load assumptions and, if indicated, to upgrade strength with the aim of reducing the risk of failure by one order of magnitude.

At the reference height of 70 m, the ultimate wind pressure at design was 1 600 N/m^2 while 2 080 N/m^2 was used for upgrading. Assuming a gust factor of 2,6 according to [17.64], the reference 10 min wind velocities 10 m above ground were obtained to be 31,3 m/s and 36,0 m/s.

The reference wind velocity 10 m above ground is 32,0 m/s having a return period of 50 a. Therefore, the wind load for which the line had been originally designed would be expected every 35 years and that used for redesign every 300 years.

The suspension towers of the crossing had leg members consisting of two cruciform high-tensile angle sections L200x16. The characteristic compression load was 2 350 kN and reached 2 965 kN under the modified load assumptions. The reinforcement was a challenging task in this case and was solved by adding two additional high-tensile sections L150x60 (Figure 17.10). Existing and new leg member sections were connected by batten plates at distances of 700 mm adopting prestressed high-tensile bolts.

This example proves that lattice steel towers made of open hot-rolled angle sections, in contrast to other support types, can be reinforced for higher loads with acceptable investment.

17.6.3.3 Upgrading of a 380/110 kV line in view of increased ice loads

The line had originally been designed for a characteristic ice load on conductors of 8,2 N/m which corresponds to a limit ice load of 38 N/m. The assumption adopted for

conversion increased the limit ice load to 60 N/m. According to icc load observations, these loads may be expected every 20 and 200 years, respectively [17.65], thus complying with the target of reducing the risk of failure by one order of magnitude.
Towers and foundations were found not to be strong enough for the increased loads and were upgraded. As an example, upgrading of foundation should be described here. The concrete block foundations of five tension towers received loads increased by 320 kN. Upgrading was achieved by arranging flat reinforced concrete slabs between the two permanently uplift-loaded foundations (Figure 17.11). The increase of strength capacity was obtained from the dead weight of the concrete slab and the soil while the uplift capacity of the remaining concrete blocks can be used as long as it will not be affected by the upgrading measures.

17.7 References

17.1 DIN VDE 0105-100: Operation of electrical installations. Berlin, DKE, 2000

17.2 EN 50 341-1: Overhead electrical lines exceeding AC 45 kV. Part 1: General requirements – Common specifications; Brussels, CENELEC, 2001

17.3 ISO 9002: Quality systems. Model for quality assurance in production, installation and servicing. Geneva, ISO, 1998

17.4 ISO 9003: Quality systems. Model for quality assurance in final inspection and tests. Geneva, ISO, 1998

17.5 Wenner, F.: A method of measuring soil resistivity. Scientific papers of the Bureau of Standards 285 (1917), pp. 469 to 478

17.6 Nolasco, J. F.: 220 kV lines Aguaytia – Tingo Maria – Paramonga: Summary of the project and engineering studies. Lima, University 1996

17.7 Sendaula, M. et al.: Analysis of electric and magnetic fields. IEEE Transactions on Power Apparatus and Systems, Vol. 103, No. 2, 1984

17.8 Cigré SC22 WG 09: Electromagnetic fields – Electric fields of overhead transmission lines – Relation between electric field and overhead transmission line costs. Working Group Report, 1991

17.9 Cigré SC22 WG22-11: Guide to vibration measurements on overhead lines. Electra 163 (1995), pp. 125 to 137

17.10 IEEE Paper 31 CP 65-156: Standardization of conductor vibration measurements. IEEE Transactions on Power Apparatus and Systems, Vol. 85, No. 1, 1965

17.11 Cigré SC22 WG22-04: Endurance capability of conductors – Final report. Paris, 1988

17.12 Cigré SC22 WG12: Real-time monitoring. Electra No. 197(2002), pp. 33 to 47

17.13 Cigré SC22 WG12: Description of state of the art methods to determine thermal rating of lines in real-time and their application in optimizing power flow. Cigré Report 22-304, 2000

17.14 Cigré SC22 WG12: Probabilistic determination of conductor current ratings. Electra 164(1996), pp. 103 to 117

17.15 Cibulka, L. et al.: PG & E's transmission line dynamic thermal rating system. Cigré Report 22-102, 1992

17.16 Davis, M. W.: The real-time thermal rating system for strategic overhead transmission lines. Part 1. IEEE Transactions on Power Apparatus and Systems, Vol. 96, 1977

17.17 Foss, S. D. et al.: Conductor temperature sensor and laboratory field test evaluation. IEEE Transactions on Power Apparatus and Systems, Vol. 102(1983), pp. 1865 to 1873

17.18 Seppa, T. O. et al.: Use of on-line tension monitoring systems for real-time ratings, ice loads and other environmental effects. Cigré Report 22-102, 1998

17.19 Seppa, T. O. et al.: Accurate ampacity determination: Temperature-sag model for operational real-time ratings. IEEE Transactions on Power Apparatus and Systems, Vol. 10(1995), pp. 1460 to 1470

17.20 Seppa, T. O. et al.: Application of real-time thermal ratings for optimizing transmission line investment and operation decisions. Cigré Report 22-301, 2000

17.21 Douglass, D. A. et al.: IEEE's approach for increasing transmission line ratings in North America. Cigré Report 22-302, 2000

17.22 Soto, F. et al.: Increasing the capacity of overhead lines in the 400 kV Spanish transmission network: Real-time thermal ratings. Cigré Report 22-211, 1998

17.23 Muftic, D. et al.: Overhead lines ampacity in the European interconnection. Cigré Report 22-104, 1992

17.24 Palazuelos, E. et al.: Conductor thermal rating, methodology and analysis. Cigré Report 22-105, 1992

17.25 Stephen, R.; Muftic, D.: Determination of the thermal rating and uprating methods for existing lines. Cigré Report 22-305, 2000

17.26 Vognild, L. H.; Fikke, S. M.: Utilizing meteorological data for peak load reference temperature and ambient temperature for conductor ratings in system planning and operation. Cigré Report 22-103, 1992

17.27 Seppa, T. O.: Improving asset utlization of transmission lines by real-time rating. IEEE SPM Edmonton, 1999

17.28 Cherchiglia, L. C. L. et al.: CEMIG experience in improving transmission line lightning performance using a lightning location system. Cigré Report 33-207, 2002

17.29 Bernstein, R. et al.: Lightning detection network averts damage and speeds restoration. IEEE Computer Application in Power 9(1996)2, pp. 12 to 17

17.30 Kappemann, J. G.; van House, D. L.: Location-centred mitigation of lightning-caused disturbances. IEEE Computer Applications in Power 9(1996)4, pp. 36 to 40

17.31 Fikke, S. M. et al.: Remote monitoring of environmental impacts on transmission line in Norway. Cigré Report 22-103, 1998

17.32 Hardy, C. et al.: Monitoring the effect of environmental factors on Hydro Quebec's overhead line. Cigré Report 22-101, 1998

17.33 IEC 61774/TR: Meteorological data for assessing climatic loads. Geneva, IEC, 1998

17.34 Cigré SC22 WG06: Guidelines for observation and measurement of ice loadings on overhead power lines. Paris, Cigré Brochure No. 179, 2001

17.35 Fink, D. G.; Beaty, H. W.: Standard handbook for electrical engineers. New York, Mc Graw-Hill, 12th edition 1987

17.36 Doble, F. C.: Progress in field testing of insulators. Electrical World, Vol. 81(1923), pp. 1397

17.37 de Tourreil, C; Ishiwari, M.: Assessment of the state of insulators on live transmission lines. Cigré Report 01-04, 2000

17.38 De Nigris, M. et al.: Diagnostic methods of non-ceramic insulators for HV lines. Cigré Report 22-207, 2000

17.39 Cigré SC22 WG13: Management of existing overhead transmission lines. Paris, Cigré Brochure No. 175, 2001

17.40 Drucker, P. F.: Management: Tasks, responsibilities, practices. N.N., Harper & Row, 1973

17.41 Pohlman, J. C. et al.: Practical steps for increasing availability of existing overhead transmission lines. Cigré Report 22-105, 2000

17.42 Carter, C. N. et al.: Working in a market-driven electricity supply industry: Modifications to UK overhead transmission line working practice. Cigré Report 22-201, 2000

17.43 DIN 31051: Physical assets maintenance; definitions and actions. Berlin, DIN, 1985

17.44 Grid Services: Corona net spy system. Catalogue. Karlsruhe, Grid Services GmbH, 2001

17.45 Kohlmeyer, A.; Pohlmann, H.: Condition of old lattice steel towers – Evaluation of damages, description of reconstruction concepts. Cigré Report 22-301, 1994

17.46 Cigré SC22 WG07: Refurbishment and upgrading of foundations. Paris, Cigré Brochure No. 141, 1999

17.47 Chone, F. et al.: Assessment of existing overhead transmission lines and solutions for extending their residual lifetime. Cigré Report 22-201, 2000

17.48 Maddock, B. J. et al.: Some investigation of the ageing of overhead lines. Cigré Report 22-09, 1988

17.49 ASTM E 376: Measuring coating thickness by magnetic field or eddy-current (electromagnetic) test methods. New York, ASTM, 1976

17.50 Pirovano, G. et al.: Diagnostics of compression joints of conductors for HV overhead lines. Cigré Report 22-206,1998

17.51 Örmin, J.; Bartsch, J.: Hot-line inspection and control of joints. Cigré Report 22-203, 1998

17.52 Cigré SC22 WG03: An in-service diagnostic testing of composite insulators. Electra 169(1996), pp. 105 to 119

17.53 Delree, X. et al.: Inspection policy of existing overhead lines and assessment methodology based on practical experience. Cigré Report 22-302, 1994

17.54 Raymond, W.: Replacing conductors on a high-voltage overhead transmission line. Siemens Power Engineering (1990), pp. 91 to 94

17.55 Thione, L.: An overview of live-line diagnostic techniques. Cigré Report P1-02, 2000

17.56 Gela, G.: Live working and maintenance techniques. Cigré Report P1-03, 2000

17.57 IEC 60743: Terminology for tools and equipment to be used in live working. Geneva, IEC, 1995

17.58 IEEE: Recommendation for safety in live-line maintenance. IEEE Transaction on Power Apparatus and Systems, Vol. 57 (1999)

17.59 IEC 61472: Live working, minimum approach distances; method of calculation. Geneva, IEC, 1998

17.60 Draxler, R. et al.: New aspects of right-of-way management for high-voltage power lines. New Orleans, EPRI, the sixth international symposium on environmental concerns in rights-of-way management, 1997

17.61 Bell, N.; et al.: Increasing the reliability of transmission lines rebuilt after the January 1998 ice storm. Cigré Report 22-106, 2000

17.62 Cigré SC22 WG06: Probabilistic design of overhead transmission lines. Paris, Cigré Brochure No. 178, 2001

17.63 Cigré SC22 WG06: Review of IEC 60 826 Loading and strength of overhead power lines. Paris, Cigré Brochure No. 109, 1996

17.64 IEC 60 826: Loading and strength of overhead transmission lines. Geneva, IEC, 1991

17.65 Kießling, F.; Ruhnau, J.: Ice loads and their effects on reliability and design of overhead line. 6th International Workshop on Atmospheric Icing of Structures. Budapest, 1993

17.66 Billington, R. et al.: Power system reliability calculations. Massachussets and London, The MIT Press, 1973

17.67 Thione, L.: An overview of live-line working and maintenance techniques. Cigré Report P01-01, 2000

17.68 Kießling, F. et al.: Upgrading high-voltage lines for increase their capacity and mitigate environmental impacts. Cigré Report 22-208, 1998

Index